STUDY OF ARTERIALIZED VENOUS FLAPS IN THE EXPERIMENTAL MODEL OF THE WISTAR RAT AND IN THE HUMAN CADAVER

ESTUDO DE RETALHOS VENOSOS ARTERIALIZADOS NO MODELO EXPERIMENTAL DE RATO WISTAR E NO CADÁVER HUMANO

Diogo André de Abreu Esteves Bogalhão do Casal

Setembro de 2017

STUDY OF ARTERIALIZED VENOUS FLAPS IN THE EXPERIMENTAL MODEL OF THE WISTAR RAT AND IN THE HUMAN CADAVER

ESTUDO DE RETALHOS VENOSOS ARTERIALIZADOS NO MODELO EXPERIMENTAL DE RATO WISTAR E NO CADÁVER HUMANO

Autor:

Diogo André de Abreu Esteves Bogalhão do Casal

Orientadores:

Professor Doutor Diogo de Freitas Branco Pais, Professor Associado da Nova Medical School | Faculdade de Ciências Médicas da Universidade Nova de Lisboa

Professor Doutor João Erse Goyri O'Neill, Professor Catedrático da Nova Medical School | Faculdade de Ciências Médicas da Universidade Nova de Lisboa

Co-orientadora:

Professora Doutora Paula Alexandra Quintela Videira, Professora Auxiliar da Faculdade de Ciências e Tecnologia da Universidade Nova de Lisboa

Tese para obtenção do grau de Doutor em MEDICINA na Especialidade de CIRURGIA E MORFOLOGIA HUMANA (CIRURGIA) na Faculdade de Ciências Médicas | NOVA Medical School da Universidade Nova de Lisboa

Setembro de 2017

“STUDY OF ARTERIALIZED VENOUS FLAPS IN THE EXPERIMENTAL MODEL OF THE WISTAR RAT AND IN THE HUMAN CADAVER”

“ESTUDO DE RETALHOS VENOSOS ARTERIALIZADOS NO MODELO EXPERIMENTAL DE RATO WISTAR E NO CADÁVER HUMANO”

Dedicatória

À minha mulher Raquel e à nossa filha Laura, porque tudo só faz sentido com elas e para elas.

Ao meu pai, que me tem apoiado incondicionalmente todos os dias da minha vida.

Ao meu irmão Gonçalo, sempre presente.

À memória da minha mãe e da minha avó, que me despertaram para o prazer de estudar.

À memória da Professora Doutora Maria Angélica Almeida Roberto, cujos exemplos de cirurgiã e investigadora têm sido uma inspiração.

Agradecimentos

O trabalho que aqui apresento só foi possível porque nele colaboraram muitas pessoas, de diversas áreas e em diversos momentos, entusiasmadas com a ideia de poderem contribuir de alguma forma para o avanço da Ciência. Seria impossível, ou pelo menos muito pouco prático, nomear todas estas pessoas. Por isso, gostaria antecipadamente de pedir sinceras desculpas e simultaneamente agradecer a quem não me refiro neste momento, mas que contribuiu de alguma forma para este trabalho.

Em primeiro lugar, gostaria de penhoradamente agradecer a todos os dadores anónimos que altruisticamente doaram em vida o seu corpo à Ciência, para contribuírem para o ensino e progresso da Medicina. Sem eles, grande parte deste trabalho não teria sido possível.

Em seguida, gostaria de agradecer ao Professor Doutor Diogo de Freitas Branco Pais, brilhante anatomista e pedagogo, pela amizade de quase duas décadas, bem como pelo companheirismo e pelo exemplo de trabalho e rigor que põe em tudo o que faz. Os seus conselhos, comentários, críticas e contínuo incentivo foram imprescindíveis para a finalização desta tese.

Ao Professor Doutor João Erse de Goyri O'Neill, estou muito grato pelo seu exemplo de dinamismo, pelo seu entusiasmo contagiante pela inovação e progresso na Anatomia, pelo seu apoio incondicional aos trabalhos de investigação no Departamento que dirige e pelo estímulo que sempre deu para a concretização deste trabalho. O seu exemplo como professor, médico e anatomista são para mim e para todos aqueles que tiveram o privilégio

de ser seus alunos uma referência. Nunca esquecerei que foi a seu convite que no dia 14/07/1998 comecei a colaborar no Departamento de Anatomia da então designada Faculdade de Ciências Médicas. Foi aí que começou uma das fases mais gratas da minha vida!

À Professora Doutora Paula Alexandra Quintela Videira, agradeço pela acessibilidade e pela disponibilidade imediata em ser co-orientadora desta tese. Não posso deixar de realçar, de uma forma muito especial, as palavras de ânimo e de confiança que sempre me ofereceu e os múltiplos conselhos prestados ao longo destes trabalhos. Estes conselhos permitiram ultrapassar muitas das dificuldades técnicas com que nos deparámos.

Às minhas indefetíveis colegas de laboratório, Mestre Inês Raquel Iria e Mestre Eduarda Mota Silva, companheiras de vários anos de experiências, gostaria de agradecer a sua amizade, paciência e tenacidade. Partilhámos a monotonia, as frustrações e as vitórias de milhares de registos, medições, análises e repetições… Sem elas, grande parte do trabalho que aqui é apresentado não existiria.

À Professora Doutora Valentina Vassilenko, agradeço a amizade e o pronto interesse em colaborar connosco em diversos projetos multidisciplinares. Estou particularmente grato pela sua preciosa ajuda em diversas das técnicas usadas neste trabalho, nomeadamente na realização de termografias, dinamometrias e avaliações electroneurofisiológicas.

À Professora Doutora Maria Alexandre Bettencourt Pires, à Professora Doutora Maria Assunção O'Neill e ao Professor Carlos Godinho, estimados mestres, amigos e colegas do Departamento de Anatomia da Nova Medical School, gostaria de agradecer o

companheirismo e constantes palavras de entusiasmo e ânimo, incitando-me a terminar este trabalho.

À minha muito estimada Senhora Teresa Sousa, secretária do Departamento de Anatomia da Nova Medical School gostaria de agradecer a sua ajuda inigualável na gestão de grande parte da logística associada à realização da parte prática deste trabalho. Agradeço-lhe também muito a sua simpatia e amizade de muitos anos.

Ao meu amigo Carlos Lopes, técnico experiente do Departamento de Anatomia, gostaria de expressar a minha admiração e o meu agradecimento pela forma generosíssima como me passou inúmeros ensinamentos de técnicas e procedimentos para preparação de material anatómico e histológico, coligidos em dezenas de anos de intensa atividade.

Ao Sr. Octávio Jordão Chaveiro, técnico de Microscopia Eletrónica, de competência notável, afabilidade e disponibilidade inigualáveis, pelos seus ensinamentos no processamento e interpretação do material para observação em microscopia eletrónica de varrimento.

Ao Sr. Marco Costa, assistente técnico do Laboratório de Anatomia Experimental, agradeço a infatigável colaboração na dissecção do material cadavérico usado nesta tese. Foram muitas as horas passadas juntos a preparar os cadáveres, a dissecá-los, a fazer fotografias e medições. Muitas vezes, este trabalho decorreu com prejuízo do seu descanso, nos intervalos ou depois das aulas práticas, à noite e/ou ao fim de semana. Por tudo isto, estou muito grato.

À Mestre Ana Farinho gostaria de expressar a minha gratidão pela sua preciosa ajuda na obtenção e preparação das peças biológicas para observação em microscopia de fluorescência.

Ao Senhor Nuno Folque, desenhador do Departamento de Anatomia da Faculdade de Ciências Médicas, gostaria de agradecer por várias das figuras que fazem parte desta tese. Apesar de já não estar entre nós, o seu trabalho perdurará e será um tributo indelével à sua qualidade como artista.

Ao Mestre Filipe Franco gostaria de expressar a minha gratidão pela maior parte das ilustrações incluídas nesta tese. O seu talento, a sua experiência e a sua paciência em nos escutar e incluir vários pormenores que nos pareceram relevantes permitiram a elaboração de ilustrações de grande qualidade estética e, esperamos nós, científica.

Aos colegas do Departamento de Anatomia Patológica do Centro Hospitalar de Lisboa Central, em particular Dr. Luís Mascarenhas Lemos, ao Dr. Carlos Pontinha, ao Dr. Mário Ferraz Oliveira, aos Mestres José Martins Ferreira, Sara Alves e Cláudia Pen, gostaria de expressar o meu agradecimento pela preparação histológica das várias centenas de amostras biológicas envolvidas neste trabalho.

Aos Mestres David Tanganho, Teresa Cunha e ao Dr. Nuno Silva agradeço a colaboração e o voluntarismo na recolha dos dados dos artigos usados nas revisões sistemáticas efetuadas neste trabalho.

Gostaria de agradecer a inestimável colaboração do meu amigo Senhor Alberto Severino, técnico de Audiovisuais, na edição de muitas das imagens e vídeos contidos neste trabalho.

A todos os meus colegas do Centro Hospitalar de Lisboa Central, agradeço pela amizade, apoio e pelo entusiasmo que me expressaram desde que decidi abarcar este projeto. Gostaria de agradecer em particular aos diretores de Serviço, nomeadamente à Professora Doutora Maria Angélica Almeida e ao Dr. José Videira e Castro, por todo o entusiasmo e interesse que sempre colocaram nos meus projetos e na minha formação.

À minha chefe, colega e amiga, Dra. Maria Manuel Mouzinho, insigne Cirurgiã Plástica e destacadíssima Cirurgiã da Mão, queria expressar o meu agradecimento pelo seu incentivo, pela sua ajuda e conselhos técnicos que generosamente sempre me disponibilizou ao longo da realização desta tese. Estou-lhe muito reconhecido pela preciosa ajuda que me deu na concretização deste trabalho.

Gostaria de agradecer em especial ao meu tutor no internato de Cirurgia Plástica e Reconstrutiva, Dr. Gerardo Ordiales Millan, pela generosidade e paciência com que me ensinou, tolerou os meus erros e foi corrigindo muitas das minhas imperfeições técnicas. O seu entusiasmo pela descoberta, pela inovação e pela melhoria contínua são para todos os que com ele contactam uma inspiração. Devo-lhe ainda o facto de ter colmatado com o seu trabalho algumas das tarefas que deixei de executar no Centro Hospitalar de Lisboa Central para poder terminar esta tese. Por tudo isto, um “Muito Obrigado”!

Gostaria ainda de agradecer ao meu amigo Dr. Pedro Martins, experiente microcirurgião, que no início das cirurgias experimentais deste trabalho se disponibilizou a ajudar-me, passando algumas tardes no laboratório, ensinando-me a executar com proficiência algumas das técnicas cirúrgicas que vim a aplicar.

Ao Sr. Virgílio Moreno, carpinteiro do Centro Hospitalar de Lisboa Central, pela disponibilidade em desenhar vários dos sistemas de teste e fisioterapia usados nas experiências com roedores.

Ao Instituto Gulbenkian Ciência em Oeiras, agradeço a disponibilização de vários microscópicos que permitiram a obtenção de imagens fulcrais para a realização de várias partes deste estudo.

Ao Instituto Superior Técnico por nos ter deixado usar a sua unidade de Microscopia Eletrónica de Varrimento, permitindo obter imagens de grande qualidade técnica, o que foi útil para várias partes deste trabalho.

Ao Programa Gulbenkian Formação Médica Avançada, do qual fui aluno, agradeço a oportunidade que me deram. Graças a este programa, pude interromper o internato de Cirurgia Plástica e Reconstrutiva durante seis meses e contactar com múltiplos vultos da Ciência, de várias áreas. Esta experiência permitiu-me colher ensinamentos e perspetivas que dificilmente adquiriria de outra forma.

Finalmente, gostaria de agradecer à Nova Medical School e a todos os que nela trabalharam, por terem permitido, de várias formas, a realização deste trabalho.

Abstract

Introduction: Unconventional perfusion flaps (**UPFs**) are reconstructive options characterized by being perfused exclusively by veins. In UPFs at least one of the afferent veins of the flap is anastomosed to a feeding vessel. Usually, this feeding vessel is an artery, and the UPF is called an arterialized venous flap (**AVF**). If the feeding vessel is a vein, the UPF is called a venous flap (**VF**). The efflux of blood is ensured in most cases by the continuity of one or more of the UPF's veins with neighboring veins. Although UPFs present several potential advantages relatively to conventional perfusion flaps, they have rarely been mentioned in the clinical literature, due to reported high necrosis rates, particularly in the presence of infection, and due to a poor understanding of their underlying physiologic mechanisms.

Methods: We performed systematic reviews and meta-analyses on the clinical and experimental used of UPFs. Followingly, we studied in detail the vascular anatomy of the ventrolateral aspect of the rat's abdomen. Using this knowledge, we improved a model of a conventional flap (**CF**) harvested from the epigastric region of the fat. Subsequently, we developed an optimized a model of AVF in the abdomen of the rat. We, then, evaluated the effect of transfecting the optimized model with human beta defensin genes (**BD-2** and **BD-3**) to increase flap survival in the presence of *Pseudomonas aeruginosa* infection and of a foreign body. Moreover, we compared the efficacy of arterialized neurovenous flaps (**ANVFs**) with other nerve conduits to reconstruct a 10-mm-long median nerve gap in an ischemic environment in a rat model. Followingly, we performed cadaveric studies to assess pertinent aspects of the anatomy and histology of anatomical regions commonly used to harvest UPFs. Finally, we used some of the information gathered to treat a teenager with an ulnar artery and nerve composite defect at the forearm level.

Results: We estimated an overall survival rate of UPFs of 89.5% in the clinical context and of 90.8% in the experimetal setting. Clinically, there was a positive correlation between the

rate of postoperative infection and the need of a new flap (Pearson coefficient 0.405; p=0.001). Blood supply to the abdominal integument of the rat was more dependent on axial vessels, comparatively to humans. Venous valves were clearly observed in this region. The free epigastric CF and the homologous optimized AVF presented survival rates of nearly 100%, and 76.86 ± 13.67%, respectively. Transfecting the AVF model with BD-2 and BD-3 increased flap survival, and decreased biofilm formation. ANVFs produced more complete and faster recovery than nerve grafts, for most of the parameters used to assess nerve regeneration. Anatomical and histological studies revealed that large subcutaneous veins were surrounded by doublings of the superficial fascia. Moreover, veins were placed at different depths, with the largest ones being deeply placed and the smallest more superficially placed. Finally, it was noted that superficial cutaneous nerves, routinely used as autologous nerve grafts, were closer to sizeable superficial veins than to arteries and respective *comitante* veins of significant caliber. UPFs could be tailored to specific defects by including either skin, subcutaneous tissue, tendons, nerves, muscle fascia and/or bone in variable combinations. The used of an ANVF in a teenager allowed the successful reconstruction of both the arterial and nerve defects.

Conclusion: Although many question remain to be answered relatively to UPFs physiology, optimization, and indications, there seems to be enough evidence to support their use in the realm of integumentary and nerve reconstruction.

Resumo

Introdução: Os retalhos de perfusão não convencionais (UPFs) são opções reconstrutivas caracterizadas por serem perfundidas exclusivamente por veias. Nos UPFs, pelo menos uma das veias aferentes do retalho é anastomosada a um vaso de alimentação. Normalmente, este vaso de alimentação é uma artéria, e o UPF é chamado de retalho venoso arterializado (AVF). Se o vaso de alimentação for uma veia, o UPF é chamado de retalho venoso (VF). O fluxo de sangue é assegurado na maioria dos casos pela continuidade de uma ou mais veias do UPF com veias vizinhas. Embora os UPFs apresentem várias vantagens potenciais em relação aos retalhos de perfusão convencionais (CFs), raramente são mencionados na literatura, devido às altas taxas de necrose relatadas, particularmente na presença de infeção, e devido a uma má compreensão de seus mecanismos fisiológicos subjacentes.

Métodos: Realizámos revisões sistemáticas e metanálises sobre o uso clínico e experimental dos UPFs. Seguidamente, estudamos detalhadamente a anatomia vascular do aspecto ventrolateral do abdômen do rato. Com esse conhecimento, melhoramos o modelo de um retalho convencional colhido na região epigástrica. Posteriormente, desenvolvemos um modelo otimizado de AVF no abdómen do rato. Avaliamos o efeito de transfectar este modelo otimizado com genes de beta defensina humana (BD-2 e BD-3) para aumentar a sobrevivência do retalho na presença de infecção por *Pseudomonas aeruginosa* e de um corpo estranho. Além disso, comparamos a eficácia dos retalhos neurovenosos arterializados (ANVFs) com outros condutos nervosos com o intuito de reconstruir um hiato de 10 mm no nervo mediano do rato num ambiente de isquémia local. Seguidamente, realizamos estudos cadavéricos para avaliar os aspetos pertinentes da anatomia e histologia das regiões anatômicas comumente usadas para colher UPFs. Finalmente, usamos algumas das informações coletadas para tratar um adolescente com um defeito do pedículo vásculo-nervoso ulnar ao nível do antebraço.

Resultados: Estimámos uma taxa de sobrevivência global de UPFs de 89,5% no contexto clínico e de 90,8% em condições experimentais. Clinicamente, houve uma correlação

positiva entre a taxa de infeção pós-operatória e a necessidade de um novo retalho (coeficiente de Pearson 0,405; p = 0,001). O fornecimento de sangue ao tegumento abdominal do rato era sobretudo dependente dos vasos axiais, contrastando com o que acontece no Homem. Válvulas venosas foram claramente observadas nesta região. O retalho convencional epigástrico livre e o AVF otimizada homólogo apresentaram taxas de sobrevivência de quase 100% e 76,86 ± 13,67%, respectivamente. Transfectando-se o modelo de AVF com BD-2 e BD-3, observou-se aumento da sobrevivência do retalho e diminuição da formação de biofilmes. Os ANVFs produziram uma recuperação mais completa e mais rápida do que os enxertos nervosos, para a maioria dos parâmetros utilizados para avaliar a regeneração nervosa. Estudos anatómicos e histológicos revelaram que as veias subcutâneas de maiores dimensões encontravam-se envolvidas por desdobramentos da fáscia superficial. Além disso, as veias encontravam-se em profundidades diferentes, estando as maiores colocadas profundamente e as mais pequenas localizadas mais superficialmente. Finalmente, observou-se que os nervos cutâneos superficiais, rotineiramente utilizados como enxertos de nervos autólogos, estavam mais próximos das veias superficiais do que das artérias e respetivas veias comitantes com calibre significativo. Os UPFs podem ser adaptados a defeitos específicos, incluindo pele, tecido celular subcutâneo, tendões, nervos, fáscia muscular e / ou osso em combinações variáveis. O uso de um ANVF no referido adolescente permitiu a reconstrução dos defeitos arterial e nervoso com sucesso.

Conclusão: Apesar de muitas questões continuarem por responder em relação à fisiologia, otimização e indicações dos UPFs, parece haver evidência suficiente para apoiar seu uso no âmbito da reconstrução tegumentar e nervosa.

Résumé

Introduction: Les lambeaux de perfusion non conventionnels (UPF) sont des options de reconstructives caractérisées par une perfusion exclusive pour le veines. Dans les UPF, il ya au moins une des veines afférentes du Lambeau qui est anastomosée à un vase d'alimentation. Habituellement, ce vaisseau d'alimentation est une artère, et l'UPF s'appelle un lambeau veineux arterialisé (AVF). Si le vaisseau est une veine, l'UPF s'appelle un lambeau veineux (VF). L'effusion de sang est assurée dans la plupart des cas par la continuité d'une ou plusieurs veines de l'UPF avec des veines voisines. Bien que les UPF présentent plusieurs avantages potentiels par rapport aux lambeaux de perfusion conventionnels, ils ont rarement été mentionnés dans la littérature clinique, en raison des taux élevés de nécrose reportés, en particulier en présence d'une infection, et en raison d'une mauvaise compréhension de leurs mécanismes physiologiques.

Méthodes: Nous avons procédé à deux analyses systématiques et méta-analyses sur l'utilisation clinique et expérimentale des UPFs. Nous avons étudié en détail l'anatomie vasculaire de l'aspect ventral de l'abdomen du rat. À l'aide de cette connaissance, nous avons amélioré un modèle de lambeau conventionnel (CF) récolté dans la région épigastrique de l'abdomen. Par la suite, nous avons développé un modèle optimisé d'AVF dans l'abdomen du rat. Nous avons ensuite évalué l'effet de la transfection du modèle optimisé avec les gènes de la beta-defensine humaine (BD-2 et BD-3) pour augmenter la survie des lambeaux en présence d'une infection pour *Pseudomonas aeruginosa* et d'un corps étranger. Nous avons aussi comparé l'efficacité des lambeaux neurovenous arterialisés (ANVF) avec d'autres conduits nerveux pour reconstruire un hiatus nerveux de le nerf médian de 10 mm de longueur dans un environnement ischémique dans le modèle de le rat Wistar. Par la suite, nous avons effectué des études cadavériques pour évaluer les aspects pertinents de l'anatomie et de l'histologie des régions anatomiques couramment utilisées pour récolter des UPFs. Enfin, nous avons utilisé une partie des informations

recueillies pour traiter un adolescent souffrant d'un défaut composite de l'artère ulnaire e de le nerf ulnaire au niveau de l'avant-bras.

Résultats: Nous avons estimé un taux global de survie des UPF de 89,5% dans le contexte clinique et de 90,8% dans le contexte expérimental. Cliniquement, il y avait une corrélation positive entre le taux d'infection postopératoire et la besoin d'un nouveau lambeau (coefficient de Pearson 0,405; p = 0,001). L'approvisionnement en sang du tégument abdominal du rat dépendait davantage des vaisseaux axiaux, comparativement aux humains. Les valves veineuses ont été clairement observées dans cette région. Le lambeau épigastrique conventionnel livre et l'AVF homologue optimisée ont présenté des taux de survie de près de 100% et 76,86 ± 13,67%, respectivement. Transféction de le modèle AVF optimisée avec BD-2 et BD-3 augmenté la survie du lambeau et la formation de biofilm a été diminuée. Les ANVF ont produit une récupération plus complète et plus rapide que les greffes nerveuses, pour la plupart des paramètres utilisés pour évaluer la régénération nerveuse. Des études anatomiques et histologiques ont révélé que les grandes veines sous-cutanées étaient entourées de doublures du fascia superficiel. De plus, les veines ont été placées à différentes profondeurs, les plus grandes étant profondément placées et les plus petites placées plus superficiellement. Enfin, il a été noté que les nerfs cutanés superficiels, habituellement utilisés comme greffes autologues, étaient plus proches des veines superficielles importantes que des artères et des veines comitantes respectives de calibre significatif. Les UPF pourraient être adaptés à des défauts spécifiques en incluant la peau, le tissu sous-cutané, les tendons, les nerfs, le fascia musculaire et / ou l'os dans des combinaisons variables. L'utilisation d'un ANVF chez un adolescent a permis la reconstruction réussie des défauts artériels et nerveux.

Conclusion: Bien que beaucoup de questions restent à répondre par rapport à la physiologie, à l'optimisation et aux indications de l'UPF, il semble y avoir suffisamment des preuves scientifiques pour favoriser leur utilisation dans le domaine de la reconstruction de l'integument et des les nerfs.

Index of Contents

2 Casal D, Cunha T, Pais D, Videira P, Coloma J, Zagalo C, Angelica-Almeida M, O'Neill JG. Systematic Review and Meta-Analysis of Unconventional Perfusion Flaps in Clinical Practice. Plastic and reconstructive surgery 2016;138:459-79

3 Casal D, Tanganho D, Cunha D, Mota-Silva E, Iria I, Pais D, Videira PA, Videira-e-Castro J, Goyri-O'Neill J. Unconventional perfusion flaps in the experimental setting: a systematic review and meta-analysis *[submitted]*

4 Casal D, Pais D, Iria I, Videira PA, Mota-Silva E, Alves S, Mascarenhas-Lemos L, Pen C, Vassilenko V, Goyri-O'Neill J. Blood Supply to the Integument of the Abdomen of the Rat: A Surgical Perspective *[in press]*

5 Casal D, Pais D, Iria I, Mota-Silva E, Almeida M-A, Alves S, Pen C, Farinho A, Mascarenhas-Lemos L, Ferreira-Silva J, Ferraz-Oliveira M, Vassilenko V, Videira PA, Goyri-O'Neill J. A Model of Free Tissue Transfer: The Rat Epigastric Free Flap. Journal of Visualized Experiments 2017:e55281

6 Casal D, Mota-Silva E, Pais D, Iria I, Videira PA, Tanganho D, Alves S, Mascarenhas-Lemos L, J. M-F, Ferraz-Oliveira M, Vassilenko V, Goyri-O'Neill J. Optimization of an arterialized venous fasciocutaneous flap in the abdomen of the rat. PRS Global Open 2017 *[in press]*

7 Casal D, Iria I, Ramalho JS, Alves S, Mota-Silva E, Mascarenhas-Lemos L, Pontinha C, Cabral MG, Ferreira-Silva J, Ferraz-Oliveira M, Vassilenko V, Goyri-O'Neill J, Pais D, Videira PA. BD-2 and BD-3 increase skin flap survival in a rat model of ischemia and *Pseudomonas aeruginosa* infection in the presence of a foreign body *[submitted]*

8 Casal D, Mota-Silva E, Iria I, Alves S, Farinho A, Pen C, Silva N, Mascarenhas-Lemos L, Ferreira-Silva J, Ferraz-Oliveira M, Vassilenko V, Videira PA, Goyri-O'Neill J, Pais D. Reconstruction of a 10-mm-long median nerve gap in an ischemic environment using different vascularized nerve grafts: a comparative study in the rat *[submitted]*

9 Casal D, Pais D, Mota-Silva E, Iria I, Videira PA, Alves S, Mascarenhas-Lemos L, Pen C, Vassilenko V, Goyri-O'Neill J. Surgical anatomy of common regions used to harvest arterialized venous flaps: a cadaveric dissection study and nomenclature update *[submitted]*

10 Casal D, Pais D, Toscano T, Bilhim T, Rodrigues L, Figueiredo I, Aradio S, Angelica--Almeida M, Goyri-O'Neill J. A rare variant of the ulnar artery with important clinical implications: a case report. BMC Res Notes 2012;5:660

11 Casal D, Pais D, Angélica-Almeida M, Bilhim T, Santos A, Goyri-O'Neill J. Morphometric analysis of the extensor tendons of the hallux and potential implications for tendon grafting. European Journal of Anatomy 2010;1:11-8

12 Casal D, Pais D, Mota-Silva E, Pelliccia, Iria I, Videira P, Mendes MM, Goyri-O'Neill, Mouzinho MM. Reconstruction of a long defect of the ulnar artery and nerve with an arterialized neurovenous free flap in a teenager: a case report and literature review *[submitted]*

Index of Figures

Chapter 5 – BLOOD SUPPLY TO THE INTEGUMENT OF THE ABDOMEN OF THE RAT: A SURGICAL PERSPECTIVE

Chapter 6 – THE RAT EPIGASTRIC FREE FLAP: A MODEL OF FREE TISSUE TRANSFER

Chapter 7 – OPTIMIZATION OF AN ARTERIALIZED VENOUS FASCIOCUTANEOUS FLAP IN THE ABDOMEN OF THE RAT

Chapter 8 – BD-2 AND BD-3 INCREASE SKIN FLAP SURVIVAL IN A RAT MODEL OF ISCHEMIA AND *PSEUDOMONAS AERUGINOSA* INFECTION IN THE PRESENCE OF A FOREIGN BODY

Chapter 9 – RECONSTRUCTION OF A 10-MM-LONG MEDIAN NERVE GAP IN AN ISCHEMIC ENVIRONMENT USING AUTOLOGOUS CONDUITS WITH DIFFERENT PATTERNS OF BLOOD SUPPLY: A COMPARATIVE STUDY IN THE RAT

Chapter 10 – SURGICAL ANATOMY OF COMMON REGIONS USED TO HARVEST UNCONVENTIONAL PERFUSION FLAPS: A CADAVERIC DISSECTION STUDY

Chapter 11 – A RARE VARIANT OF THE ULNAR ARTERY WITH IMPORTANT CLINICAL IMPLICATIONS: A CASE REPORT

Chapter 12 – MORPHOMETRIC ANALYSIS OF THE EXTENSOR TENDONS OF THE HALLUX AND POTENTIAL IMPLICATIONS FOR TENDON GRAFTING

Chapter 13 – RECONSTRUCTION OF A LONG DEFECT OF THE ULNAR ARTERY AND NERVE WITH AN ARTERIALIZED NEUROVENOUS FREE FLAP IN A TEENAGER: A CASE REPORT AND LITERATURE REVIEW

Index of Tables

Abbreviations

AMP - antimicrobial peptide

ANVF - arterialized neurovenous flap

AUC - area under the curve

AVA - arterialized venous arterial flap

AVF - arterialized venous flap

BD – β defensin

BD-2 - human β-defensin 2

BD-2 IH - immunohistochemical staining with anti-human β-defensin 2)

BD-3 - human β-defensin 3

BD-3 IH - immunohistochemical staining with anti-human β-defensin 3)

cDNA - complementary deoxyribonucleic acid

CF - conventional flap

CFU - colony forming unit

CMAP - compound muscle action potential

CNF - conventional nerve flap

CPF - conventional perfusion flap

DEFB103A - defensin beta 103A

DEFB4A - defensin beta 4A

DIEP - deep inferior epigastric artery perforator

DNA - deoxyribonucleic acid

DRG - dorsal root ganglion

DSCI - deep circumflex iliac artery

EHB - extensor hallucis brevis tendon

EHLa - accessory extensor hallucis longus tendon

EHLp - extensor hallucis longus tendon

ENMG – electroneuromyography

EOMA - external oblique myocutaneous artery perforator

EPA - external pudendal artery

EPV - external pudendal vein

FCR - flexor carpi radialis

gDNA - genomic deoxyribonucleic acid

GFP - Green Fluorescent Protein

HE - Hematoxylin-Eosin

HPRT - hypoxanthine phosphoribosyltransferase

IOVAAR - integument over the ventrolateral aspect of the abdomen of the rat

IRT - infra-red thermography

LB - Luria-Bertani

LT – lateral thoracic

LV-GFP - green fluorescent protein coding lentivirus

LY - Lucifer Yellow

MN - median nerve

MN - median nerve

MT - Masson's Trichrome

NG – nerve graft

PBS - phosphate buffered saline

pcDNA - plasmidium complementary deoxyribonucleic acid

PNFs – prefabricated nerve flaps

RA - radial artery

rDNA - ribosomal deoxyribonucleic acid

SCEV - superficial caudal epigastric vein

SCEVs - superficial caudal epigastric vessels

SCIA - superficial circumflex iliac artery

SCM - sternocleidomastoid

SEM - scanning electron microscopy

SIEA - superficial caudal epigastric artery (rat)/ superficial inferior epigastric artery (human)

SIEV - superficial caudal epigastric vein

SuBUA - superficial brachioulnar artery

TB – True Blue

TRAM - transverse rectus abdominis myocutaneous

UPF - unconventional perfusion flap

VF - venous flap

VRAM - vertical rectus abdominis myocutaneous

Preambule

Anatomy has been ancestrally related to Plastic and Reconstructive Surgery genesis and development.[1] Being an anatomist and a plastic and reconstructive surgeon, I have always been a firm supporter of the synergy between these two disciplines.

Some of the problems I currently encountered as a plastic and reconstructive surgery, and for which I could not find a clear solution either in the medical literature and/or in talking to my peers, led me to formulate **the central hypothesis of this thesis: arterialized venous flaps use could be improved with human cadaveric studies and experimental studies in the Wistar rat.**

To tackle this working hypothesis, I collaborated with various people, of different areas, conducting several sets of literature reviews and experiments that comprise the bulk of the practical component of this thesis. In addition, I have used this knowledge to treat a challenging traumatic *sequela* of a teenager.

These reviews and experiments have led to 1 electronic book chapter, 6 published/accepted papers, and 5 submitted papers. **Table 1** synthesizes the publications resulting from the experimental work done in the thesis.

Thesis Chapter	Reference	Type of scientific communication	Publication status
1 - Introduction	Casal D, Carvalho S, Pais D, Mota-Silva E, Iria I, Vieira P, Goyri-O'Neill J. **Unconventional Perfusion Flaps.** In: Casal D, ed. Flap Surgery: AvidScience; 2017:2-41.	Book chapter	**Published**
3- Systematic Review and Meta-Analysis of Unconventional Perfusion Flaps in Clinical Practice	Casal D, Cunha T, Pais D, Videira P, Coloma J, Zagalo C, Angelica-Almeida M, O'Neill JG. **Systematic Review and Meta-Analysis of Unconventional Perfusion Flaps in Clinical Practice**. Plastic and reconstructive surgery 2016;138:459-79	Paper	**Published**
4- Unconventional perfusion flaps in the experimental setting: a systematic review and meta-analysis	Casal D, Tanganho D, Cunha D, Mota-Silva E, Iria I, Pais D, Videira PA, Videira-e-Castro J, Goyri-O'Neill J. **Unconventional perfusion flaps in the experimental setting: a systematic review and meta-analysis**	Paper	Submitted
5- Blood Supply to the Integument of the Abdomen of the Rat: A Surgical Perspective	Casal D, Pais D, Iria I, Videira PA, Mota-Silva E, Alves S, Mascarenhas-Lemos L, Pen C, Vassilenko V, Goyri-O'Neill J. **Blood Supply to the Integument of the Abdomen of the Rat: A Surgical Perspective.** Plastic and Reconstructive Surgery Global Open *[in press]*	Paper	**Accepted**
6- A Model of Free Tissue Transfer: The Rat Epigastric Free Flap	Casal D, Pais D, Iria I, Mota-Silva E, Almeida M-A, Alves S, Pen C, Farinho A, Mascarenhas-Lemos L, Ferreira-Silva J, Ferraz-Oliveira M, Vassilenko V, Videira PA, Goyri-O'Neill J. **A Model of Free Tissue Transfer: The Rat Epigastric Free Flap**. Journal of Visualized Experiments 2017:e55281	Paper	**Published**
7- Optimization of an arterialized venous fasciocutaneous flap in the abdomen of the rat	Casal D, Mota-Silva E, Pais D, Iria I, Videira PA, Tanganho D, Alves S, Mascarenhas-Lemos L, J. M-F, Ferraz-Oliveira M, Vassilenko V, Goyri-O'Neill J. **Optimization of an arterialized venous fasciocutaneous flap in the abdomen of the rat**. PRS Global Open 2017; in press.	Paper	**Accepted**
8- BD-2 and BD-3 increase skin flap survival in a rat model of ischemia and *Pseudomonas aeruginosa* infection in the presence of a foreign body	Casal D, Iria I, Ramalho JS, Alves S, Mota-Silva E, Mascarenhas-Lemos L, Pontinha C, Cabral MG, Ferreira-Silva J, Ferraz-Oliveira M, Vassilenko V, Goyri-O'Neill J, Pais D, Videira PA. **BD-2 and BD-3 increase skin flap survival in a rat model of ischemia and *Pseudomonas aeruginosa* infection in the presence of a foreign body** *[submetido]*	Paper	Submitted
9- Reconstruction of a 10-mm-long median nerve gap in an ischemic environment using different vascularized nerve grafts: a comparative study in the rat	Casal D, Mota-Silva E, Iria I, Alves S, Farinho A, Pen C, Silva N, Mascarenhas-Lemos L, Ferreira-Silva J, Ferraz-Oliveira M, Vassilenko V, Videira PA, Goyri-O'Neill J, Pais D. **Reconstruction of a 10-mm-long median nerve gap in an ischemic environment using different vascularized nerve grafts: a comparative study in the rat**	Paper	Submitted
10- Surgical anatomy of common regions used to harvest unconventional perfusion flaps: a cadaveric dissection study	Casal D, Pais D, Mota-Silva E, Iria I, Videira PA, Alves S, Mascarenhas-Lemos L, Pen C, Vassilenko V, Goyri-O'Neill J. **Surgical anatomy of common regions used to harvest arterialized venous flaps: a cadaveric dissection study**	Paper	Submitted
11- A rare variant of the ulnar artery with important clinical implications: a case report	Casal D, Pais D, Toscano T, Bilhim T, Rodrigues L, Figueiredo I, Aradio S, Angelica--Almeida M, Goyri-O'Neill J. **A rare variant of the ulnar artery with important clinical implications: a case report.** BMC Res Notes 2012;5:660	Paper	**Published**
12- Morphometric analysis of the extensor tendons of the hallux and potential implications for tendon grafting	Casal D, Pais D, Angélica-Almeida M, Bilhim T, Santos A, Goyri-O'Neill J. **Morphometric analysis of the extensor tendons of the hallux and potential implications for tendon grafting.** European Journal of Anatomy 2010;1:11-8	Paper	**Published**
13- Reconstruction of a long defect of the ulnar artery and nerve with an arterialized neurovenous free flap in a teenager: a case report and literature review	Casal D, Pais D, Mota-Silva E, Pelliccia, Iria I, Videira P, Mendes MM, Goyri-O'Neill, Mouzinho MM. **Reconstruction of a long defect of the ulnar artery and nerve with an arterialized neurovenous free flap in a teenager: a case report and literature review**	Paper	Submitted

Table 1 - Synthesis of the publications that resulted from the experimental work done in this thesis.

References

1. Santoni-Rugiu P, Sykes PJ. The anatomical foundations of surgery. In: Schröder G, ed. A history of plastic surgery. First ed. Berlin: Springer-Verlag; 2007:1-37.

Chapter 1

INTRODUCTION

Authors: Diogo Casal[1,2], Sara Carvalho[2], Diogo Pais[1], Eduarda Mota Silva[3], Inês Iria[4], Paula Videira[5], João Goyri O'Neill[1]

Affiliations:

1- Anatomy Department, NOVA Medical School, Universidade NOVA de Lisboa, Lisbon, Portugal

2- Plastic and Reconstructive Surgery Department and Burn Unit, Centro Hospitalar de Lisboa Central – Hospital de São José, Lisbon, Portugal

3- LIBPhys, Physics Department; Faculdade de Ciências e Tecnologias, Universidade NOVA de Lisboa, Caparica, Portugal

4- Molecular Microbiology and Biotechnology Unit | Drug Discovery Area; Faculdade de Farmácia, Universidade de Lisboa, Lisbon, Portugal

5- UCIBIO, Life Sciences Department, Faculty of Sciences and Technology, Universidade NOVA de Lisboa, Caparica, Portugal

ABSTRACT

Integumentary defects, either isolated or combined with loss of other tissues, are frequently encountered clinically, and their reconstruction is often vexing and imperfect.

Unconventional perfusion flaps (UPFs) are reconstructive options characterized by being perfused exclusively by veins. They were first introduced in the clinical literature by Vaubel in 1976 and further elaborated experimentally in 1981 by Nakayama. In UPFs at least one of the afferent veins of the flap is anastomosed to a feeding vessel. Usually, this feeding vessel is an artery, and the UPF is called an arterialized venous flap (AVF). If the feeding vessel is a vein, the UPF is called a venous flap (VF). The efflux of blood is ensured in most cases by the continuity of one or more of the UPF's veins with neighboring veins.

UPFs present several potential advantages relatively to conventional perfusion flaps, namely: faster and easier dissection; thinness and pliability; minimal morbidity in the donor zone; and can be harvested from most regions of the body.

Despite all these advantages, UPFs have rarely been mentioned in the clinical literature, probably because some authors report high necrosis rates, particularly in the presence of infection, and because the underlying physiologic mechanisms remain poorly understood.

Notwithstanding, there is considerable evidence to suggest the usefulness of these reconstructive options in integumentary reconstruction, particularly in regions where a thin and pliable covering is desirable. Moreover, UPFs may be useful for bridging nerve defects. However, further studies are needed to certify the efficacy of UPFs in this context.

Unconventional perfusion flaps in the context of plastic and reconstructive surgery

There is ample evidence that from the dawn of times human beings have sustained injuries to all regions of the body.[1, 2] In fact, even human ancestors' remains show skeletal evidence of violent blows from as early as the beginning of the Paleolithic period.[3] From these injuries a wide variety of defects presumably resulted, the most well documented being fractures and fractures' complications, such as osteomyelitis.[4]

When these injuries did not result in the death of those affected, functional disability and/or deformity resulted. The latter, in turn, devalued individuals both familiarly, socially, and economically, curtailing the potential of the individuals affected. Even today, apart from the obvious consequences of functional impairment, disfigurement has been shown to be associated with low self-esteem, to greatly depreciate one's value in society, and to exert a major toll in one's love life [5-9]. From another perspective, the importance attributed to beauty throughout times has led people from all parts of the world to seek numerous procedures to boost external appearance. The contemporary corollary of this prevailing trend is the hype for aesthetic surgery worldwide [10, 11]

As a result of these ancestral worries, tales of body parts transfers between individuals, frequently from different species, are found in many of the most ancient civilizations from all over the globe.[12] More than three millennia ago, local flaps with reconstructive purposes were described in the Edwin Smith papyrus.[12] However, the strategies available to reconstruct faulty or missing parts of the body were limited for a great part of the human history by an insufficient knowledge of physiology.[13-15]

It was only in 1628, when William Harvey provided an accurate description of the blood circulation in the human body, that it was known that systemic arteries deliver blood rich in oxygen and nutrients to tissues for their maintenance, while systemic veins drain carbon dioxide and metabolic wastes from these tissues back to the right atria of the heart.[16] This knowledge, published for the first time in "*Exercitatio Anatomica de Motu Cordis et Sanguinis in Animalibus*", commonly quoted as "*de Motu Cordis*", truly revolutionized all fields of Medicine. It laid the foundations for understanding tissue transfers, such as grafts and flaps, in what much later become known as Plastic and Reconstructive Surgery.[13, 17]

In contemporary times, integumentary defects, either isolated or combined with loss of other tissues, such as tendon, bone, vessels and/or nerve, can result from a great deal of situations such as trauma, including burns; tumor extirpation; infection; radiotherapy and/or auto-immune conditions.[18] These defects can thus be rather diverse in nature and clinical implications. However, in most circumstances optimal aesthetical and functional results are difficult to attain. Generally speaking, the following surgical options are available in increasing order of complexity: grafts, local flaps, regional flaps and free flaps.[18]

A **graft** is defined as the transference of a tissue or a combination of tissues with no blood supply of their own initially to another place in the body. The potential viable volume and thickness of grafts are therefore limited, as during the first 2 to 3 days after grafting tissues will be forced to survive through a process of “plasmatic imbibition”. This process consists in direct exchanges of oxygen, carbon dioxide, water, metabolites and catabolites

between the engrafted tissues and the wound bed through direct diffusion.[18] For this process to occur, it is mandatory that the wound bed and neighboring tissues are adequately perfused, until neoangiogenesis provides the graft with a blood supply of its own.[19]

There are references to skin grafts being performed as far back as in ancient Indian scrolls more than 2500 years ago.[20] Apart from the anecdotal report of Leonardo Fioravanti replantation of an avulsed nasal tip of a Spanish soldier in 1570 as a skin graft, this technique was all but forgotten until the work of Barionio's work on skin grafts in sheep.[21] This work was published in 1804 with the title "*On grafting in animals*". Notwithstanding, skin grafting only became current clinical practice after the description of pinch skin grafts by Reverdin in 1869.[12] Ollier and Thiersch further expanded the application of skin grafts by the introduction of partial thickness skin grafts in 1872 and 1886, respectively.[22] The introduction of large full-thickness skin grafts is generally attributed to Wolfe and Krause in 1875 and 1893, respectively.[20] In 1964, Tanner described the mesh skin graft, permitting the expansion of skin grafts up to nine times their original surface. Arguably, this further revolutionized plastic surgery, and in particular the treatment of burned patients, saving countless lives.[23, 24] Building on these milestones, numerous advances were made, leading to contemporary grafting procedures, now encompassing numerous structures besides the skin, such as mucosa, tendon, bone, cartilage, nerve, and fat alone or in multiple combinations.[12, 25-30]

A **flap** is a composite block of tissues with a blood supply of its own. The flap can be **pedicled** if its original vascular connections are left in place. The flap's pedicle then

becomes the pivotal point around each the tissue transfer can be performed. In a **free flap**, the original blood supply is sectioned and subsequently its vessels are microvascularly sutured to vessels in the recipient zone. In large and/or complex tissue defects, free flaps are frequently the only reconstructive option, allowing the replacement of vessels, nerves, tendons, ligaments, bone, cartilage, muscle and/or joints.[18, 31-35] Despite the inherent technical difficulties in performing the microvascular anastomoses and the non-negligible risk of pedicle vessel thrombosis, free flaps have become increasingly common in the past decades, with numerous different flaps and variations of these flaps being described.[17, 36] Nowadays, free flaps solve otherwise untreatable situations or cases whose prior treatment was clearly insufficient. [31-35, 37, 38]

Most free flaps used in contemporary clinical practice are based on a vascular pedicle composed of, at least, one artery and one vein. These flaps can be considered **conventional flaps** (**CFs**). In order to obtain arteries of sufficient length and caliber to adequately perform vascular anastomoses at the recipient site, CFs arteries are usually painstakingly dissected below muscular fascias, often demanding a deep, technically challenging and time-consuming dissection. As a corollary, CFs tend to be relatively thick, even after debulking the flap, and the donor site morbidity is not always insignificant. Unfortunately, thick CFs are not always ideal to reconstruct regions where the integument is shallow, such as the head and neck regions, the dorsum of the hand, the foot or the external genitalia. Additionally, the harvesting of a CF demands the sacrifice of significant anatomical structures in the donor zone, as it entails at least the recruitment of a large enough deep artery and eventually of a deep vein, on which the CF is based.[39]

In the past two decades, in an effort to minimize these shortcomings of CFs, some surgeons have advocated the resort to **supermicrosurgery** techniques, in which flaps are pedicled on very fine vessels, less than 1 mm in diameter, with resort to special surgical instruments and techniques.[40] Although supermicrosurgery does preclude, in many cases, the need to dissect and sacrifice CP vessels bellow muscular fascia, it has not gained widespread acceptance, as it is technically very demanding, requires special and expensive equipment, flaps' pedicles are often short and difficult to inset, and flaps are, according to many authors, prone to thrombosis, due to the tiny size of flaps' vessels.[17, 40, 41]

Unconventional perfusion flaps (UPFs) are characterized by being perfused solely through their venous system. They were first introduced in the clinical literature in 1976 by Vaubel to reconstruct the dorsum of the hand with a forearm fasciocutaneous flap.[42, 43] In 1981, Nakayama *et al.* described a fasciocutaneous UPF in the ventrolateral aspect of the rat's abdomen.[44] In UPFs at least one of the afferent veins of the flap is anastomosed to a feeding vessel at the recipient site. Usually, this feeding vessel is an artery, and the UPF is called an **arterialized venous flap** (**AVF**). If the feeding vessel is a vein, the UPF is called a **venous flap** (**VF**).[43] In UPFs the efflux of blood is ensured in most cases by the continuity of one or more of the flap's veins with neighboring veins (**Fig. 1**).

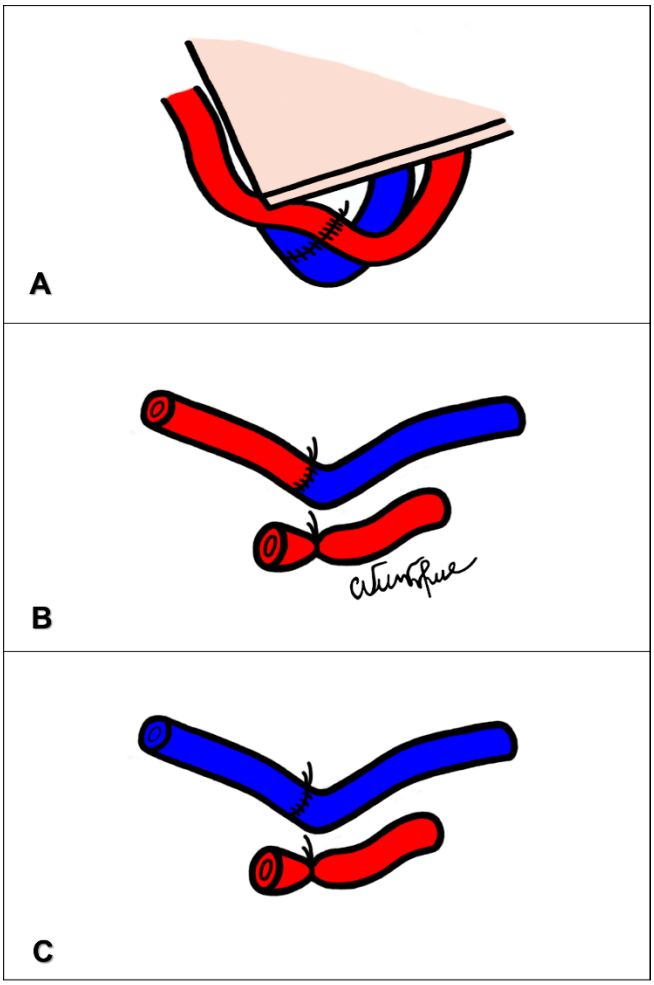

Figure 1 - Schematic representation of the basic vascular architecture at the afferent side of the flap of a conventional perfusion flap (A), of a venous arterialized flap (B), and of a venous flap (C).

Red vessels represent arteries and blue vessels symbolize veins.

A, In a conventional flap, here exemplified by a conventional free flap, the artery and vein that normally supply the three-dimensional block of tissues that compose the flap are anastomosed to a vein and artery at the reception zone. Blood perfusion through the flap occurs as in the rest of the body.

B, In an arterialized venous flap, the three-dimensional block of tissues that constitute the flap is completely deprived of any arteries and thus become entirely dependent on the venous system for blood flow. At least one of the flap's veins is connected to one recipient site's artery. One or more veins are usually anastomosed to recipient site's veins in order to permit flap outflow (not shown).

C, In venous flaps, the tissues that make up the flap also rely initially completely on perfusion through the venous system. Venous anastomoses are performed at the recipient site at the inflow and outflow regions of the flap (the latter are not shown).

In rare circumstances, the draining vein of the flap is surgically connected to an adjacent artery, usually to satisfy the double purpose of draining the UPFs blood efflux and to reconstruct a missing artery segment. These latter UPFs are called **flow through AVFs**.[45, 46]

Advantages of unconventional perfusion flaps

Being based solely on the venous system, UPFs can be easily tailored around the superficial venous system. These flaps can include any tissues' neighboring veins. Hence, they can include skin, subcutaneous tissue, fascia, nerves, fascia, and even bone and/or cartilage in various combinations.[43, 47] Consequently, UPFs present several potential advantages relatively to CFs, namely:

- UPFs are faster and easier to dissect, as the superficial venous system is readily observed and accessible above muscle fascia;

- UPFs avoid the need to resort to ancillary image examinations, making them excellent options when expedite reconstruction is necessary, particularly in trauma cases

- UPFs can be very thin and pliable, being ideal to reconstruct similar regions of the integument;

- UPFs are associated with minimal morbidity in the donor zone, as their dissection does not require going deeper to the muscle fascia;

- UPFs can be harvested from most regions of the body, allowing to choose inconspicuous donor zones where the integument is redundant, such as in the anteromedial aspect of the limbs, in order to facilitate direct closure of the secondary defect.[43, 48, 49]

For all these reasons, there has been some enthusiasm with the use of these flaps in the reconstruction of multiple types of defects, namely in deep burns [50-54], defects of

the hands and fingers [49, 50, 55-60], including congenital or acquired defects of the nail complex [61, 62], as well as in the reconstruction of other limb defects [63, 64], and in defects resulting from the excision of head and neck tumors.[48, 65, 66]

In the cases of burns to the face and hands, UPFs seem particularly promising, as they allow the reconstruction of aesthetic and functional areas with thin, pliable and homogenous skin. In this way, they reportedly ensure a better functional and aesthetical outcome compared to grafts in these burns.[50, 53]

Despite all these advantages, UPFs have been reported in relatively few papers, which describe in most cases small series of patients.[43, 67] Three main reasons have been proposed to explain this limited use. One is that some authors report high necrosis rates with these flaps, particularly in the presence of infection.[43, 49] Another reason is that the physiologic mechanisms that allow UPFs to survive are still poorly understood.[48, 49, 68] Finally, although a myriad of experimental models of UPFs has been described in various animal species, no one has stood out as ideal. Therefore, overall, there is lack of uniformity in the literature on UPFs regarding the best methodologies to improve survival of these flaps.[46, 69, 70]

Physiology of unconventional perfusion flaps

There is no consensus in the literature regarding UPFs' mechanisms of survival, nor on the best vascular patterns for their vascular design and transplantation.[46, 70, 71]

Among the multiple mechanisms proposed to justify the early survival of UPFs, the following are repeatedly mentioned as being the most significant in the short term and are schematically illustrated in **Figure 2**:

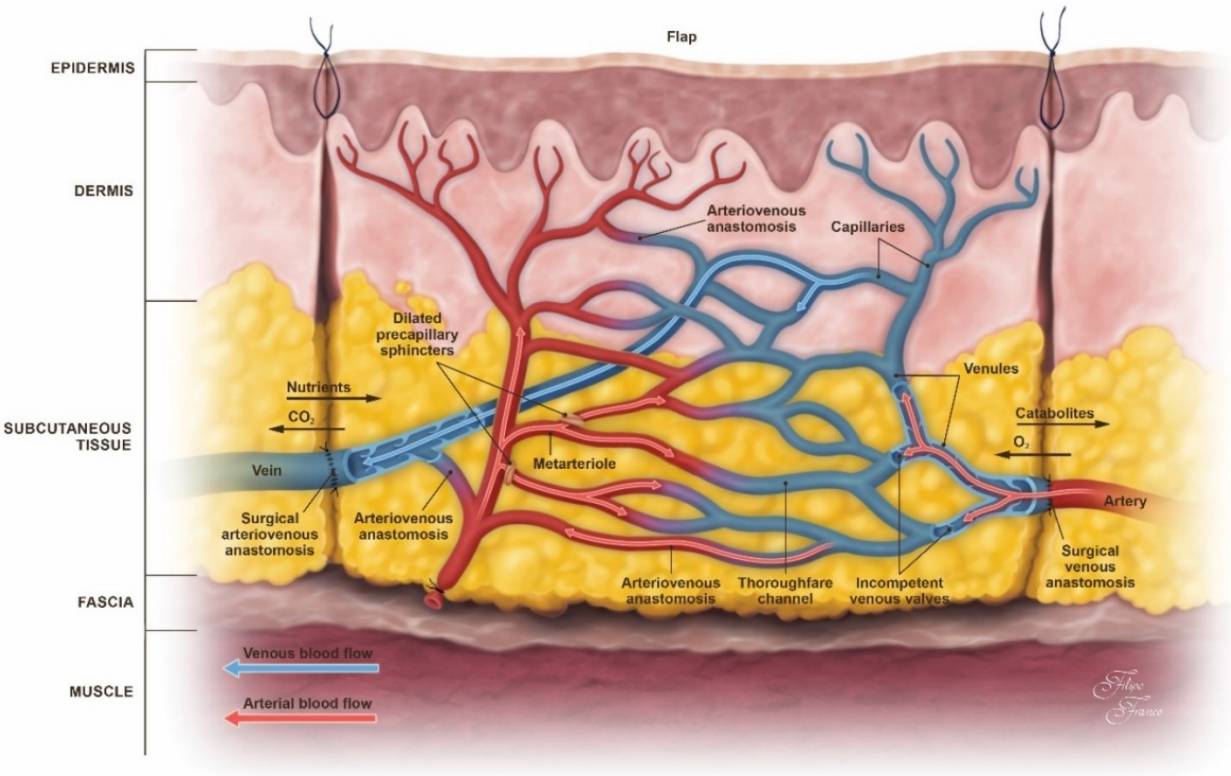

Figure 2 - Schematic representation of an unconventional perfusion flap (arterialized venous flap) and its blood supply illustrating the putative physiologic mechanisms that allow its survival during the first 3 to 4 days after flap transfer. Plasmatic imbibition, venous valve incompetency, microvascular arterio-venous shunting, and the Bohr effect are considered the main mechanisms.

Red vessels represent the original arterial system of the flap. Blue vessels represent the original venous system of the flap.

Red arrows indicate the direction of arterial blood flow. Blue arrows indicate the direction of venous blood flow.

The drawing is not to scale.

- During the first 3 to 4 days, plasmatic imbibition from the wound bed and adjacent margins allows the diffusion of oxygen, water and metabolites from the wound to the flap, as well as the elimination of carbon dioxide and catabolites in the opposite direction.[72-78]
- The arterial blood flowing into the venous system renders most venous valves incompetent, allowing antidromic blood perfusion within the flap.[48, 49]
- The ischemic condition of the UPF promotes the relaxation of the precapillary sphincters and of the thick muscular walls of the arterio-venous anastomoses' permitting antidromical blood flow from the venous component of capillaries and from venules into the arterial component of capillary networks and into arterioles, respectively. From there blood percolates the proximal arterial tree, creating multiple microvascular shunts and functional arterio-venous shunts. For this mechanism to be efficient, a sufficiently extensive venous network must be present.[48, 49, 68, 79-83]
- The ischemic and acidic environment of the flap facilitates oxygen uptake from hemoglobin at the precapillary, capillary and postcapillary levels due to the Bohr effect.[73, 84-88]

In the long term, the survival of UPFs seems to be mainly dependent on vertical neoangiogenesis from the wound bed into the flap, as well as on horizontal neoangiogenesis from the wound margins into the flap (**Fig. 3**). Neoangiogenesis within the flap itself, increasing its collateral circulation, also seems to play a pivotal role.[49, 70, 89, 90]

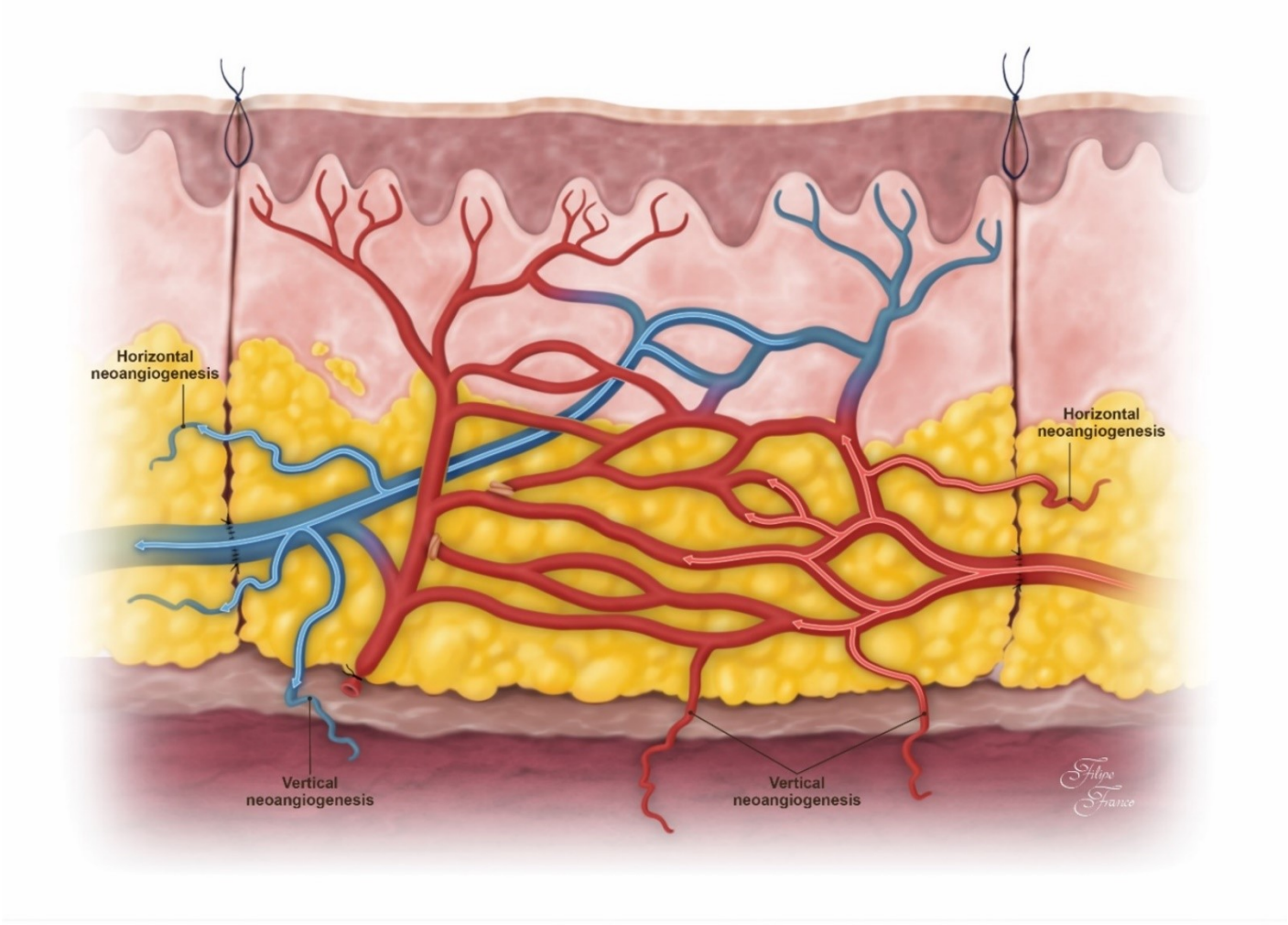

Figure 3 - Schematic representation of an unconventional perfusion flap (arterialized venous flap) and its blood supply illustrating the putative physiologic mechanisms that allow its survival after the first 3 to 4 days after flap transfer. Vertical and horizontal neoangiogenesis are considered the prevailing mechanisms.

Red vessels represent the arterial system of the flap (original arteries of the flap and the original veins that have suffered a process of arterialization). Blue vessels represent the venous system of the flap.

Red arrows indicate the direction of arterial blood flow. Blue arrows indicate the direction of venous blood flow.

The drawing is not to scale.

Despite intensive research on the mechanisms explaining the viability of unconventional perfusion, there are several reports of UPFs' high necrosis rates both experimentally and clinically.[91-94] Multiple strategies have been proposed to increase UPFs' viability, namely delay procedures [95-100], pre-arterialization [100-102], surgical expansion [51, 75], growth factor application [103, 104], arterio-venous shunt restriction (i.e., ligation of large and direct communications between the afferent and efferent sides of the flap, in order to force blood flow into the periphery of the flap)[105] and choice of specific vascular patterns.[49, 89, 102] Until now, there is no clear evidence of the efficacy of these measures.

Unconventional perfusion flaps and nerve repair

One of the main limitations in the reconstruction of extensive nerve defects, such as brachial plexus injuries, is the limited number of nerve sources available for nerve repair.[106, 107] Moreover, there is growing experimental and clinical evidence that nerve flaps are superior to nerve grafts for bridging long and thick nerve defects.[108] However, currently, nerve grafts are the most commonly used options for bridging nerve defects in the clinical context.[109-113]

Nerve flaps, having a blood supply of their own, have been shown experimentally to be more efficient than nerve grafts in promoting the invasion by macrophages, the removal of myelin fragments in the degenerating nerve fibers, and the survival of Schwann cells.[114, 115] Overall, nerve flaps are less prone to central necrosis, fibrosis and histological derangement relatively to nerve grafts, particularly in conditions of local ischemia.[116, 117] In fact, nerve grafts are initially entirely dependent on plasmatic imbibition and diffusion from the local medium, until neoangiogenesis occurs. If the local environment is mostly deprived of oxygen and nutrients and/or too far from the inner portion of the graft, nerve graft necrosis and failure of nerve repair will ensue.[109, 118-121]

These experimental data have been supported by some empirical clinical data. In fact, it has been shown clinically that an adequate blood supply to the proximal and distal nerve stumps is associated with better functional results after peripheral nerve repair. [122] The influence of an adequate blood supply to the zone of peripheral nerve repair is

particularly evident in cases of concomitant radiotherapy (as it happens in the context of tumor extirpation and administration of adjuvant therapy), or in areas of marked fibrosis, such as those present after extensive local trauma.[111, 112, 123]

All the data mentioned above refers to “conventional nerve flaps” (**CNFs**), These can be defined as nerve segments with an arterial and venous blood supply. However, CNFs are seldom used clinically because there are only a few dispensable nerve segments (i.e., whose extirpation will not result in a significant deficit in the donor zone) that present a blood supply that allows harvesting them as CNFs.[120] The sural nerve, the saphenous nerve, the lateral cutaneous nerve of the thigh, and the sensory branch of the radial nerve to the dorsum of the hand are the most commonly used CNFs, while the ulnar nerve flap has been used in cases of extensive brachial plexus lesions.[109, 122, 124, 125]

Another reason that hinders the clinical application of CNFs is that they entail laborious harvesting dissections and technically vexing anastomoses of small sized vessels. Moreover, due to anatomical constraints, CNFs cannot always be raised.[126] To try to surpass these limitations of CNFs, Townsend and Taylor in 1984 proposed concept of “arterialized neurovenous flaps” (**ANVFs**).[127] These flaps are composed of nerve segments pedicled exclusively on their accompanying veins. When insetted in the recipient zone, at least one of the ANVF’s veins is connected to a local artery, whereas at least one of its veins is anastomosed to a recipient site’s vein.[127] The use of these flaps greatly expands the choice of nerve flaps for reconstructing peripheral nerve defects. As peripheral nerves and the venous system develop in a synchronous fashion, with multiple levels of

molecular cross-talk in their origin, differentiation, and elongation until reaching their target organs, they remain in close anatomical proximity since the end of the fetal period.[128] Consequently, there are numerous places where the superficial venous system is in the vicinity of expendable superficial nerves that thus can be raised as ANVFs.[128, 129]

However, since their original description, ANVFs' use in the clinical context has been reported only rarely and these reports have been limited to case reports and small case series.[43] This may be partly justified by the fact that there are only two papers on the functional, histological and electrophysiological outcome of ANVFs in peripheral nerve repair in the experimental context.[130, 131] These studies describe femoral nerve repairs in rats followed during relatively short periods of time. Therefore, further experimental and clinical studies with ANVFs are definitely warranted.

Contemporary limitations in the knowledge of unconventional perfusion flaps

As alluded above, there are several significant hiatuses in the knowledge of UPFs, that have been deterring many surgeons to use them in the clinical context. From the authors' perspective, the following are among the most pressing questions to address in this realm:

1- Systematically review and analyze the somewhat disperse and often contradictory literature on the experimental and clinical use of UPFs, in order to infer patterns that could maximize the efficacy of these flaps.

2- Establish standardized experimental models of UPFs in order to facilitate comparison of interventions, and results, as well as to allow surgical training by novices in the field.

3- Thoroughly evaluate the experimental and clinical usefulness of using ANVFs for bridging nerve defects in situations where local perfusion was either preserved or compromised

4- Assess the surgical anatomy of UPFs in different regions of the body, in order to facilitate the choice of particular vascular patterns of UPFs in specific clinical circumstances.

CONCLUSION

Despite some current limitations in the knowledge of UPFs, there is considerable experimental and clinical evidence to suggest the usefulness of these reconstructive options. Most frequently, these flaps have been used in integumentary reconstruction, particularly in regions where a thin and pliable covering is desirable. In these circumstances, UPFs seem to present several advantages compared to CPFs. Moreover, there is some evidence that UPFs may be useful for bridging nerve defects, especially when local ischemia is present. However, further studies are needed to certify the efficacy of UPFs in this context.

ACKNOWLEDGEMENTS

The authors would like to thank Mr. Nuno Folque for producing the drawings contained in figure 1 and Mr. Filipe Franco for the drawings contained in figures 2 and 3.

References

1. Roberts C. Recording and analysis of data: palaeopathology. In: Roberts C, editor. Human remains in Archaeology: a handbook. Second ed. Great Britain: Council for British Archaelogy; 2012. p. 153-90.

2. Roberts C, Manchester K. Trauma. In: Roberts C, Manchester K, editors. The archaelogy of disease. Third ed. Great Britain: The History Press; 2010. p. 84-131.

3. A.C. A, Rogriguez-Martin C. Traumatic conditions. In: A.C. A, Rogriguez-Martin C, editors. The Cambridge encyclopedia of human paleopathology. 1. First ed. United Kingdom: Cambridge University Press; 2011. p. 19-50.

4. A.C. A, Rogriguez-Martin C. Bacterial infections: osteomyelitis. In: A.C. A, Rogriguez-Martin C, editors. The Cambridge encyclopedia of human paleopathology. 1. First ed. United Kingdom: Cambridge University Press; 2011. p. 172-81.

5. Etcoff N. Introduction: The nature of beauty. In: Etcoff N, editor. The survival of the prettiest: the science of beauty. 1. First ed. USA: Random house; 1999. p. 1-28.

6. Thompson A, Kent G. Adjusting to disfigurement: processes involved in dealing with being visibly different. Clinical psychology review. 2001;21(5):663-82.

7. Cooke Macgregor F. Facial disfigurement: problems and management of social interaction and implications for mental health. Aesthetic plastic surgery. 1990;14(1):249-57.

8. Ellis K. A Brief Overview of the Effect of War Injuries on Sexual Health and Intimacy. Intimacy Post-Injury: Combat Trauma and Sexual Health. 2016:1.

9. Low C, Fullarton M, Parkinson E, O'brien K, Jackson S, Lowe D, et al. Issues of intimacy and sexual dysfunction following major head and neck cancer treatment. Oral oncology. 2009;45(10):898-903.

10. Gilman SL. Judging by appearances. In: Gilman SL, editor. Making the body beautiful: a cultural hystory of aesthetic surgery. 1. First ed. United Kingdom: Princeton Umiversity Press; 2001.

11. Teitelbaum S. Enthusiasm versus data: how does an aesthetic procedure become "hot"? : The Oxford University Press; 2006.

12. Bettencourt-Pires MA, Casal D, Arrobas-da-Silva F, Ritto IC, Furtado IA, Pais D, et al. ANATOMY AND GRAFTS - From Ancient Myths, to Modern Reality. Archives of Anatomy. 2014;1(1):88-107.

13. Santoni-Rugiu P, Sykes PJ. The anatomical foundations of surgery. In: Schröder G, editor. A history of plastic surgery. 1. First ed. Berlin: Springer-Verlag; 2007. p. 1-37.

14. Barker CF, Markmann JF. Historical overview of transplantation. Cold Spring Harb Perspect Med. 2013;3(4):a014977. doi: 10.1101/cshperspect.a014977. PubMed PMID: 23545575; PubMed Central PMCID: PMCPMC3684003.

15. Evans LA. A historical, clinical, and ethical overview of the emerging science of facial transplantation. Plast Surg Nurs. 2011;31(4):151-7. doi: 10.1097/PSN.0b013e31822f6611. PubMed PMID: 22157604.

16. Ribatti D. William Harvey and the discovery of the circulation of the blood. Journal of Angiogenesis Research. 2009;1:3-. doi: 10.1186/2040-2384-1-3. PubMed PMID: PMC2776239.

17. Kocher MS. History of replantation: From miracle to microsurgery. World Journal of Surgery. 1995;19(3):462-7. doi: 10.1007/bf00299192.

18. Mathes S, Hansen S. Flap Classification and Applications. In: Mathes S, Hentz V, editors. Plastic Surgery General Principles. Second ed. Philadelphia: Saunders Elsevier; 2006. p. 365-481.

19. Paletta C, Pokorny J, Rumbolo P. Skin Grafts. In: Mathes S, Hentz V, editors. Plastic Surgery General Principles. Second ed. Philadelphia: Saunders Elsevier; 2006. p. 293-316.

20. Johnson TM, Ratner D, Nelson BR. Soft tissue reconstruction with skin grafting. Journal of the American Academy of Dermatology. 1992;27(2):151-65.

21. Miller PJ, Hertler C, Alexiades G, Cook TA. Replantation of the amputated nose. Archives of otolaryngology--head & neck surgery. 1998;124(8):907-10. Epub 1998/08/26. PubMed PMID: 9708718.

22. Smahel J. The healing of skin grafts. Clin Plast Surg. 1977;4(3):409-24. PubMed PMID: 328215.

23. Tanner JC, Jr., Vandeput J, Olley JF. THE MESH SKIN GRAFT. Plastic and reconstructive surgery. 1964;34:287-92. Epub 1964/09/01. PubMed PMID: 14209177.

24. Singh M, Nuutila K, Collins KC, Huang A. Evolution of skin grafting for treatment of burns: Reverdin pinch grafting to Tanner mesh grafting and beyond. Burns : journal of the International Society for Burn Injuries. doi: 10.1016/j.burns.2017.01.015.

25. Chick LR. Brief History and Biology of Skin Grafting. Annals of plastic surgery. 1988;21(4):358-65. PubMed PMID: 00000637-198810000-00011.

26. Hauben DJ, Baruchin A, Mahler D. On the History of the Free Skin Graft. Annals of plastic surgery. 1982;9(3):242-6.

27. Mahmoudi N, Eslahi N, Mehdipour A, Mohammadi M, Akbari M, Samadikuchaksaraei A, et al. Temporary skin grafts based on hybrid graphene oxide-natural biopolymer nanofibers as effective wound healing substitutes: pre-clinical and pathological studies in animal models. Journal of materials science Materials in medicine. 2017;28(5):73. doi: 10.1007/s10856-017-5874-y. PubMed PMID: 28361280.

28. Fox JD, Baquerizo-Nole KL, Van Driessche F, Yim E, Nusbaum B, Jimenez F, et al. Optimizing Skin Grafting Using Hair-derived Skin Grafts: The Healing Potential of Hair Follicle Pluripotent Stem Cells. Wounds. 2016;28(4):109-11. PubMed PMID: 27071137.

29. Achora S, Muliira JK, Thanka AN. Strategies to promote healing of split thickness skin grafts: an integrative review. J Wound Ostomy Continence Nurs. 2014;41(4):335-9; quiz E1-2. doi: 10.1097/WON.0000000000000035. PubMed PMID: 24988511.

30. van der Eerden PA, Verdam FJ, Dennis SC, Vuyk H. Free cartilage grafts and healing by secondary intention: a viable reconstructive combination after excision of nonmelanoma skin cancer in the nasal alar region. Arch Facial Plast Surg. 2009;11(1):18-23. doi: 10.1001/archfacial.2008.501. PubMed PMID: 19153288.

31. Morain WD. Historical Perspectives. In: Mathes SJ, editor. Plastic Surgery. 1. Second ed. Philadelphia: Saunders; 2006. p. 27-34.

32. Christoforou D, Alaia M, Craig-Scott S. Microsurgical management of acute traumatic injuries of the hand and fingers. Bull Hosp Jt Dis (2013). 2013;71(1):6-16. Epub 2013/09/17. PubMed PMID: 24032578.

33. Santoni-Rugiu P, Sykes PJ. Skin flaps. In: Santoni-Rugiu P, Sykes PJ, editors. A History of Plastic Surgery. First ed. Germany: Springer; 2007. p. 79-119.

34. Tamai S. The history of microsurgery. In: Tamai S, Usui M, Yoshizu T, editors. Experimental and Clinical Reconstructive Microsurgery. First ed. Tokyo: Springer-Verlag; 2003. p. 3-24.

35. Bettencourt-Pires MA, Casal D, Arrobas-da-Silva F, Ritto IC, Furtado IA, Pais D, et al. ANATOMY AND GRAFTS – From Ancient Myths, to Modern Reality. Archives of Anatomy. 2014;2(1):88-107.

36. Casal D, Pais D, Iria I, Mota-Silva E, Almeida M-A, lica, et al. A Model of Free Tissue Transfer: The Rat Epigastric Free Flap. Journal of Visualized Experiments. 2017;(119):e55281. doi: doi:10.3791/55281.

37. Casal D, Gomez MM, Antunes P, Candeias H, Almeida MA. Defying standard criteria for digital replantation: A case series. International journal of surgery case reports. 2013;4(7):597-602. doi: 10.1016/j.ijscr.2013.03.033. PubMed PMID: 23702366; PubMed Central PMCID: PMCPMC3679422.

38. Gomez MM, Casal D. Reconstruction of large defect of foot with extensive bone loss exclusively using a latissimus dorsi muscle free flap: a potential new indication for this flap. J Foot Ankle Surg. 2012;51(2):215-7. doi: 10.1053/j.jfas.2011.07.008. PubMed PMID: 21945400.

39. Wei F, Suominen S. Principles and Techniques in Microvascular Surgery. In: Mathes S, Hentz V, editors. Plastic Surgery General Principles. Second ed. Philadelphia: Saunders Elsevier; 2006. p. 507-38.

40. Park JE, Chang DW. Advances and Innovations in Microsurgery. Plastic and reconstructive surgery. 2016;138(5):915e-24e. doi: 10.1097/PRS.0000000000002715. PubMed PMID: 27783011.

41. Shurey S, Akelina Y, Legagneux J, Malzone G, Jiga L, Ghanem AM. The rat model in microsurgery education: classical exercises and new horizons. Archives of plastic surgery. 2014;41(3):201-8. Epub 2014/06/03. doi: 10.5999/aps.2014.41.3.201. PubMed PMID: 24883268; PubMed Central PMCID: PMC4037763.

42. Hussmann J, Bahr C, Steinau HU, Vaubel E. [Indications for arterialization of tissue]. Langenbecks Arch Chir Suppl Kongressbd. 1996;113:1164-6. Epub 1996/01/01. PubMed PMID: 9101806.

43. Casal D, Cunha T, Pais D, Videira P, Coloma J, Zagalo C, et al. Systematic Review and Meta-Analysis of Unconventional Perfusion Flaps in Clinical Practice. Plastic and reconstructive surgery. 2016;138(2):459-79. doi: 10.1097/PRS.0000000000002390. PubMed PMID: 27465169.

44. Nakayama Y, Soeda S, Kasai Y. Flaps nourished by arterial inflow through the venous system: an experimental investigation. Plastic and reconstructive surgery. 1981;67(3):328-34. Epub 1981/03/01. PubMed PMID: 7232566.

45. Fukui A, Inada Y, Maeda M, Tamai S, Mizumoto S, Yajima H, et al. Pedicled and "flow-through" venous flaps: clinical applications. J Reconstr Microsurg. 1989;5(3):235-43. Epub 1989/07/01. doi: 10.1055/s-2007-1006873 [doi]. PubMed PMID: 2769627.

46. Goldschlager R, Rozen WM, Ting JW, Leong J. The nomenclature of venous flow-through flaps: updated classification and review of the literature. Microsurgery.

2012;32(6):497-501. Epub 2012/03/22. doi: 10.1002/micr.21965. PubMed PMID: 22434451.

47. Borumandi F, Higgins JP, Buerger H, Vasilyeva A, Benlidayi ME, Sencar L, et al. Arterialized Venous Bone Flaps: An Experimental Investigation. Scientific reports. 2016;6.

48. Kovacs AF. Comparison of two types of arterialized venous forearm flaps for oral reconstruction and proposal of a reliable procedure. Journal of cranio-maxillo-facial surgery : official publication of the European Association for Cranio-Maxillo-Facial Surgery. 1998;26(4):249-54. Epub 1998/10/20. PubMed PMID: 9777504.

49. Woo SH, Kim KC, Lee GJ, Ha SH, Kim KH, Dhawan V, et al. A retrospective analysis of 154 arterialized venous flaps for hand reconstruction: an 11-year experience. Plastic and reconstructive surgery. 2007;119(6):1823-38. Epub 2007/04/19. doi: 10.1097/01.prs.0000259094.68803.3d [doi]

00006534-200705000-00029 [pii]. PubMed PMID: 17440363.

50. Woo SH, Seul JH. Optimizing the correction of severe postburn hand deformities by using aggressive contracture releases and fasciocutaneous free-tissue transfers. Plastic and reconstructive surgery. 2001;107(1):1-8. Epub 2001/02/15. PubMed PMID: 11176593.

51. Woo SH, Seul JH. Pre-expanded arterialised venous free flaps for burn contracture of the cervicofacial region. Br J Plast Surg. 2001;54(5):390-5. Epub 2001/06/29. doi: 10.1054/bjps.2001.3597 [doi]

S0007122601935970 [pii]. PubMed PMID: 11428768.

52. Agarwal P, Kumar A, Sharma D. Feasibility of type III venous flap in coverage of hand defects following trauma and burns. J Clin Orthop Trauma. 2016;7(Suppl 2):150-3. doi:

10.1016/j.jcot.2016.11.001. PubMed PMID: 28053377; PubMed Central PMCID: PMCPMC5197441.

53. Iglesias M, Butron P, Chavez-Munoz C, Ramos-Sanchez I, Barajas-Olivas A. Arterialized venous free flap for reconstruction of burned face. Microsurgery. 2008;28(7):546-50. Epub 2008/08/08. doi: 10.1002/micr.20525 [doi]. PubMed PMID: 18683867.

54. Ueda Y, Mizumoto S, Hirai T, Doi Y, Fukui A, Tamai S. Two-stage arterialized flow-through venous flap transfer for third-degree burn defects on the dorsum of the hand. J Reconstr Microsurg. 1997;13(7):489-96. Epub 1997/11/14. doi: 10.1055/s-2007-1006429 [doi]. PubMed PMID: 9353700.

55. Takeuchi M, Sakurai H, Sasaki K, Nozaki M. Treatment of finger avulsion injuries with innervated arterialized venous flaps. Plastic and reconstructive surgery. 2000;106(4):881-5. Epub 2000/09/28. PubMed PMID: 11007404.

56. Inoue G, Suzuki K. Arterialized venous flap for treating multiple skin defects of the hand. Plastic and reconstructive surgery. 1993;91(2):299-302; discussion 3-6. Epub 1993/02/01. PubMed PMID: 8430145.

57. Iwasawa M, Ohtsuka Y, Kushima H, Kiyono M. Arterialized venous flaps from the thenar and hypothenar regions for repairing finger pulp tissue losses. Plastic and reconstructive surgery. 1997;99(6):1765-70. Epub 1997/05/01. PubMed PMID: 9145155.

58. Woo SH, Jeong JH, Seul JH. Resurfacing relatively large skin defects of the hand using arterialized venous flaps. J Hand Surg Br. 1996;21(2):222-9. Epub 1996/04/01. PubMed PMID: 8732406.

59. Yokoyama T, Tosa Y, Hashikawa M, Kadota S, Hosaka Y. Medial plantar venous flap technique for volar oblique amputation with no defects in the nail matrix and nail bed. Journal of plastic, reconstructive & aesthetic surgery : JPRAS. 2010;63(11):1870-4. Epub 2010/01/26. doi: 10.1016/j.bjps.2009.11.042. PubMed PMID: 20096658.

60. Park JU, Kim K, Kwon ST. Venous Free Flaps for the Treatment of Skin Cancers of the Digits. Ann Plast Surg. 2014. Epub 2014/07/09. doi: 10.1097/01.sap.0000449793.38397.c2. PubMed PMID: 25003463.

61. Nakayama Y, Iino T, Uchida A, Kiyosawa T, Soeda S. Vascularized free nail grafts nourished by arterial inflow from the venous system. Plastic and reconstructive surgery. 1990;85(2):239-45; discussion 46-7. Epub 1990/02/01. PubMed PMID: 2300629.

62. Patradul A, Ngarmukos C, Parkpian V, Kitidumrongsook P. Arterialized venous toenail flaps for treating nail loss in the fingers. J Hand Surg Br. 1999;24(5):519-24. Epub 1999/12/22. doi: 10.1054/jhsb.1999.0254 [doi]

S0266-7681(99)90254-1 [pii]. PubMed PMID: 10597923.

63. Koshima I, Soeda S, Nakayama Y, Fukuda H, Tanaka J. An arterialised venous flap using the long saphenous vein. Br J Plast Surg. 1991;44(1):23-6. Epub 1991/01/01. doi: 0007-1226(91)90171-F [pii]. PubMed PMID: 1993230.

64. Chavoin JP, Rouge D, Vachaud M, Boccalon H, Costagliola M. Island flaps with an exclusively venous pedicle. A report of eleven cases and a preliminary haemodynamic study. Br J Plast Surg. 1987;40(2):149-54. Epub 1987/03/01. PubMed PMID: 3567447.

65. Safak T, Akyurek M. Cephalic vein-pedicled arterialized anteromedial arm venous flap for head and neck reconstruction. Ann Plast Surg. 2001;47(4):446-9. Epub 2001/10/17. PubMed PMID: 11601584.

66. Park SW, Heo EP, Choi JH, Cho HC, Kim SH, Xu L, et al. Reconstruction of defects after excision of facial skin cancer using a venous free flap. Ann Plast Surg. 2011;67(6):608-11. Epub 2011/03/05. doi: 10.1097/SAP.0b013e318209a77f. PubMed PMID: 21372670.

67. Jabir S, Frew Q, El-Muttardi N, Dziewulski P. A systematic review of the applications of free tissue transfer in burns. Burns : journal of the International Society for Burn Injuries. 2014;40(6):1059-70. Epub 2014/02/13. doi: 10.1016/j.burns.2014.01.008. PubMed PMID: 24518305.

68. Nichter LS, Jazayeri MA. The physiologic basis for nonconventional vascular perfusion. Plastic and reconstructive surgery. 1995;95(2):406-12. Epub 1995/02/01. PubMed PMID: 7824625.

69. Garlick JW, Goodwin IA, Wolter K, Agarwal JP. Arterialized venous flow-through flaps in the reconstruction of digital defects: case series and review of the literature. Hand (N Y). 2015;10(2):184-90. Epub 2015/06/03. doi: 10.1007/s11552-014-9684-0. PubMed PMID: 26034428.

70. Yan H, Brooks D, Ladner R, Jackson WD, Gao W, Angel MF. Arterialized venous flaps: a review of the literature. Microsurgery. 2010;30(6):472-8. Epub 2010/03/20. doi: 10.1002/micr.20769 [doi]. PubMed PMID: 20238385.

71. Yan H, Zhang F, Akdemir O, Songcharoen S, Jones NI, Angel M, et al. Clinical applications of venous flaps in the reconstruction of hands and fingers. Arch Orthop Trauma

Surg. 2011;131(1):65-74. Epub 2010/05/13. doi: 10.1007/s00402-010-1107-2 [doi]. PubMed PMID: 20461524.

72. Ueda K, Harada T, Nagasaka S, Oba S, Inoue T, Harashina T. An experimental study of delay of flow-through venous flaps. Br J Plast Surg. 1993;46(1):56-60. Epub 1993/01/01. PubMed PMID: 8431742.

73. Fukui A, Inada Y, Maeda M, Mizumoto S, Yajima H, Tamai S. Venous flap-its classification and clinical applications. Microsurgery. 1994;15(8):571-8. Epub 1994/01/01. PubMed PMID: 7830540.

74. Inada Y, Fukui A, Tamai S, Maeda M, Mizumoto S. An experimental study of the venous flap: investigation of the recipient vein. J Reconstr Microsurg. 1990;6(2):123-8. Epub 1990/04/01. doi: 10.1055/s-2007-1006811 [doi]. PubMed PMID: 2352219.

75. Mutaf M, Tasaki Y, Fujii T. Expansion of venous flaps: an experimental study in rats. Br J Plast Surg. 1998;51(5):393-401. Epub 1998/10/15. doi: S000712269790151X [pii]. PubMed PMID: 9771368.

76. Hyza P, Vesely J, Novak P, Stupka I, Sekac J, Choudry U. Arterialized venous free flaps - a reconstructive alternative for large dorsal digital defects. Acta Chir Plast. 2008;50(2):43-50. Epub 2008/09/24. PubMed PMID: 18807390.

77. Fukui A, Inada Y, Murata K, Tamai S. "Plasmatic imbibition" in the rabbit flow-through venous flap, using horseradish peroxidase and fluorescein. J Reconstr Microsurg. 1995;11(4):255-64. Epub 1995/07/01. doi: 10.1055/s-2007-1006541 [doi]. PubMed PMID: 7562717.

78. Fukui A, Maeda M, Tamai S, Inada Y. "Plasmatic imbibition" in the rat musculocutaneous pedicled venous flap: enzymatic proof using horseradish peroxidase. Microsurgery. 1993;14(2):114-9. Epub 1993/01/01. PubMed PMID: 7682275.

79. Galumbeck MA, Freeman BG. Arterialized venous flaps for reconstructing soft-tissue defects of the extremities. Plastic and reconstructive surgery. 1994;94(7):997-1002. Epub 1994/12/01. PubMed PMID: 7972487.

80. Woo SH, Kim SE, Lee TH, Jeong JH, Seul JH. Effects of blood flow and venous network on the survival of the arterialized venous flap. Plastic and reconstructive surgery. 1998;101(5):1280-9. Epub 1998/04/07. PubMed PMID: 9529214.

81. Roberts AP, Cohen JI, Cook TA. The rat ventral island flap: a comparison of the effects of reduction in arterial inflow and venous outflow. Plastic and reconstructive surgery. 1996;97(3):610-5. Epub 1996/03/01. PubMed PMID: 8596793.

82. Inada Y, Fukui A, Tamai S, Mizumoto S. The arterialised venous flap: experimental studies and a clinical case. Br J Plast Surg. 1993;46(1):61-7. Epub 1993/01/01. PubMed PMID: 8431743.

83. Fukui A, Inada Y, Murata K, Ueda Y, Tamai S. A method for prevention of arterialized venous flap necrosis. J Reconstr Microsurg. 1998;14(1):67-74. Epub 1998/04/02. doi: 10.1055/s-2007-1006904. PubMed PMID: 9524006.

84. Dvir E, Hickey MJ, Hurley JV, Morrison WA. A histological and carbon perfusion study of cephalic and saphenous venous flaps in the dog. Br J Plast Surg. 1994;47(4):263-7. Epub 1994/06/01. PubMed PMID: 8081615.

85. Liu C, Lu K, Wu W. [The causes of necrosis of arteriovenous flap and its modification]. Zhonghua Zheng Xing Shao Shang Wai Ke Za Zhi. 1994;10(3):173-7. Epub 1994/05/01. PubMed PMID: 7834517.

86. Masquelet AC. [Venous return in the flap with retrograde arterial flow]. Annales de chirurgie plastique et esthetique. 1994;39(3):327-9. Epub 1994/06/01. PubMed PMID: 7717667.

87. Smith RJ, Fukuta K, Wheatley M, Jackson IT. Role of perivenous areolar tissue and recipient bed in the viability of venous flaps in the rabbit ear model. Br J Plast Surg. 1994;47(1):10-4. Epub 1994/01/01. PubMed PMID: 8124559.

88. Suzuki Y, Suzuki K, Ishikawa K. Direct monitoring of the microcirculation in experimental venous flaps with afferent arteriovenous fistulas. Br J Plast Surg. 1994;47(8):554-9. Epub 1994/12/01. PubMed PMID: 7697283.

89. Yan H, Zhang F, Akdemir O, Songcharoen S, Jones NI, Angel M, et al. Clinical applications of venous flaps in the reconstruction of hands and fingers. Arch Orthop Trauma Surg. 2010. Epub 2010/05/13. doi: 10.1007/s00402-010-1107-2 [doi]. PubMed PMID: 20461524.

90. Yan H, Kolkin J, Zhao B, Li Z, Jiang S, Wang W, et al. The effect of hemodynamic remodeling on the survival of arterialized venous flaps. PloS one. 2013;8(11):e79608. Epub 2013/11/23. doi: 10.1371/journal.pone.0079608. PubMed PMID: 24265782; PubMed Central PMCID: PMC3827173.

91. Germann GK, Eriksson E, Russell RC, Mody N. Effect of arteriovenous flow reversal on blood flow and metabolism in a skin flap. Plastic and reconstructive surgery. 1987;79(3):375-80. Epub 1987/03/01. PubMed PMID: 3823213.

92. Sakai S. Arterialised venous groin flap: case report. Br J Plast Surg. 1996;49(2):90-2. Epub 1996/03/01. PubMed PMID: 8733346.

93. Yucel A, Bayramicli M. Effects of hyperbaric oxygen treatment and heparin on the survival of unipedicled venous flaps: an experimental study in rats. Ann Plast Surg. 2000;44(3):295-303. Epub 2000/03/29. PubMed PMID: 10735222.

94. Atabey A, Gezer S, Vayvada H, Kirkali G, Menderes A, Karaca C, et al. Ischemia/reperfusion injury in flow-through venous flaps. Ann Plast Surg. 1998;40(6):612-6. Epub 1998/06/26. PubMed PMID: 9641279.

95. Cho BC, Byun JS, Baik BS. Dorsalis pedis tendocutaneous delayed arterialized venous flap in hand reconstruction. Plastic and reconstructive surgery. 1999;104(7):2138-44. Epub 2001/01/10. PubMed PMID: 11149781.

96. Cho BC, Lee JH, Byun JS, Baik BS. Clinical applications of the delayed arterialized venous flap. Ann Plast Surg. 1997;39(2):145-57. Epub 1997/08/01. PubMed PMID: 9262768.

97. Lalkovic M, Kozarski J, Panajotovic L, Visnjic M, Djurdjevic D, Djordjevic B, et al. Surface enlargement of a new arterialised venous flap by the surgical delay method. Vojnosanitetski pregled Military-medical and pharmaceutical review. 2014;71(6):547-53. Epub 2014/07/22. PubMed PMID: 25039108.

98. Ueda K, Nuri T, Akamatsu J, Sugita N, Otani K. Clinical trial of delay of the venous island flap. Plastic and reconstructive surgery. 2010;126(2):104e-5e. Epub 2010/08/04. doi: 10.1097/PRS.0b013e3181de2563. PubMed PMID: 20679811.

99. Ueda K, Nuri T, Akamatsu J, Sugita N, Otani K, Yamada A. Delay of the reverse pedicled venous island flap: clinical applications. Journal of plastic surgery and hand surgery. 2013;47(5):350-4. Epub 2013/05/29. doi: 10.3109/2000656X.2013.767822. PubMed PMID: 23710795.

100. Yan H, Brooks D, Jackson WD, Angel MF, Akdemir O, Zhang F. Improvement of prearterialized venous flap survival with delay procedure in rats. J Reconstr Microsurg. 2010;26(3):193-200. Epub 2010/02/02. doi: 10.1055/s-0030-1247715. PubMed PMID: 20119898.

101. Alexander G. Multistage type III venous flap or 'pre-arterialisation of an arterialised venous flap'. Br J Plast Surg. 2001;54(8):734. Epub 2001/12/01. doi: 10.1054/bjps.2001.3699 [doi]

S0007122601936999 [pii]. PubMed PMID: 11728126.

102. Wungcharoen B, Santidhananon Y, Chongchet V. Pre-arterialisation of an arterialised venous flap: clinical cases. Br J Plast Surg. 2001;54(2):112-6. Epub 2001/02/24. doi: 10.1054/bjps.2000.3513. PubMed PMID: 11207119.

103. Zhang F, Brooks D, Chen W, Mustain W, Chen MB, Lineaweaver WC. Improvement of venous flap survival by application of vascular endothelial growth factor in a rat model. Ann Plast Surg. 2006;56(6):670-3. Epub 2006/05/25. doi: 10.1097/01.sap.0000203998.37851.57. PubMed PMID: 16721083.

104. Pittet B, Quinodoz P, Alizadeh N, Schlaudraff KU, Mahajan AL. Optimizing the arterialized venous flap. Plastic and reconstructive surgery. 2008;122(6):1681-9. Epub 2008/12/04. doi: 10.1097/PRS.0b013e31818cbef1. PubMed PMID: 19050520.

105. Lin YT, Henry SL, Lin CH, Lee HY, Lin WN, Wei FC. The shunt-restricted arterialized venous flap for hand/digit reconstruction: enhanced perfusion, decreased congestion, and improved reliability. J Trauma. 2010;69(2):399-404. Epub 2010/04/09. doi: 10.1097/TA.0b013e3181bee6ad. PubMed PMID: 20375918.

106. Kakinoki R, Ikeguchi R, Nakayama K, Nakamura T. Functioning transferred free muscle innervated by part of the vascularized ulnar nerve connecting the contralateral cervical seventh root to themedian nerve: case report. J Brachial Plex Peripher Nerve Inj. 2007;2:18. Epub 2007/09/22. doi: 1749-7221-2-18 [pii]

10.1186/1749-7221-2-18. PubMed PMID: 17883873; PubMed Central PMCID: PMC2080628.

107. Engin MS, Demirtas Y, Neimetzade T, Ayas B, Aksakal IA, Karacalar A. A vascularized nerve graft substitute generated in a chamber bioreactor-A preliminary report. Hand and Microsurgery. 2016;5(2):62-9.

108. Friedman AH. An eclectic review of the history of peripheral nerve surgery. Neurosurgery. 2009;65(4 Suppl):A3-8. Epub 2009/12/16. doi: 10.1227/01.NEU.0000346252.53722.D3. PubMed PMID: 19927076.

109. Trehan SK, Model Z, Lee SK. Nerve Repair and Nerve Grafting. Hand clinics. 2016;32(2):119-25. Epub 2016/04/21. doi: 10.1016/j.hcl.2015.12.002. PubMed PMID: 27094885.

110. Wood MJ, Johnson PJ, Myckatyn TM. Anatomy and physiology for the peripheral nerve surgeon. In: Mackinnon SE, Yee A, editors. Nerve Surgery. 1. First ed. New York: Thieme; 2015. p. 1-40.

111. Brandt J, Dahlin LB, Lundborg G. Autologous tendons used as grafts for bridging peripheral nerve defects. J Hand Surg Br. 1999;24(3):284-90. Epub 1999/08/05. doi: 10.1054/jhsb.1999.0074

S0266-7681(99)90074-8 [pii]. PubMed PMID: 10433437.

112. Millesi H. Bridging defects: autologous nerve grafts. Acta Neurochir Suppl. 2007;100:37-8. Epub 2007/11/08. PubMed PMID: 17985542.

113. D'Arpa S, Claes KEY, Stillaert F, Colebunders B, Monstrey S, Blondeel P. Vascularized nerve "grafts": just a graft or a worthwhile procedure? Plastic and Aesthetic Research. 2015;2(4):183-94.

114. Koshima IH, K. Experimental studies on vascularized nerve grafts in rats. J Microsurg. 1981;2:225-6.

115. Donzelli R, Capone C, Sgulo FG, Mariniello G, Maiuri F. Vascularized nerve grafts: an experimental study. Neurological research. 2016;38(8):669-77. doi: 10.1080/01616412.2016.1198527. PubMed PMID: 27349271.

116. Breindenbach WT, JK. The anatomy of free vascularized nerve grafts. Clin Plast Surg. 1984;11:65-71.

117. Burnett MG, Zager EL. Pathophysiology of peripheral nerve injury: a brief review. Neurosurgical focus. 2004;16(5):1-7.

118. Sinis N, Kraus A, Papagiannoulis N, Werdin F, Schittenhelm J, Meyermann R, et al. Concepts and developments in peripheral nerve surgery. Clinical neuropathology. 2009;28(4):247-62. Epub 2009/08/01. PubMed PMID: 19642504.

119. Desouches C, Alluin O, Mutaftschiev N, Dousset E, Magalon G, Boucraut J, et al. [Peripheral nerve repair: 30 centuries of scientific research]. Revue neurologique. 2005;161(11):1045-59. Epub 2005/11/17. PubMed PMID: 16288170.

120. Terzis JK, Skoulis TG, Soucacos PN. Vascularized nerve grafts. A review. International angiology : a journal of the International Union of Angiology. 1995;14(3):264-77. Epub 1995/09/01. PubMed PMID: 8919247.

121. Taylor GI, Pan WR. The angiosome concept. In: Dodwell P, editor. The angiosome concept and tissue transfer. 1. First ed. Florida: Quality Medical Publishing, Inc.; 2014. p. 354-95.

122. Jabaley ME. Primary Nerve Repair. In: Peripheral Nerve Surgery: Practical Applications in the Upper Extremity. Editores: Slutsky, D.J.; Hentz, V.R. Churchill Livingstone. 2006:23-38.

123. Iida T, Nakagawa M, Asano T, Fukushima C, Tachi K. Free vascularized lateral femoral cutaneous nerve graft with anterolateral thigh flap for reconstruction of facial nerve defects. J Reconstr Microsurg. 2006;22(5):343-8. Epub 2006/07/18. doi: 10.1055/s-2006-946711. PubMed PMID: 16845615.

124. Battiston B, Papalia I, Tos P, Geuna S. Chapter 1: Peripheral nerve repair and regeneration research: a historical note. International review of neurobiology. 2009;87:1-7. Epub 2009/08/18. doi: 10.1016/S0074-7742(09)87001-3. PubMed PMID: 19682630.

125. Breidenbach WC, Terzis JK. Vascularized nerve grafts: an experimental and clinical review. Ann Plast Surg. 1987;18(2):137-46. Epub 1987/02/01. PubMed PMID: 3566101.

126. Hong MK, Taylor GI. Angiosome territories of the nerves of the upper limbs. Plastic and reconstructive surgery. 2006;118(1):148-60. Epub 2006/07/04. doi: 10.1097/01.prs.0000221075.91038.08. PubMed PMID: 16816688.

127. Townsend PL, Taylor GI. Vascularised nerve grafts using composite arterialised neuro-venous systems. Br J Plast Surg. 1984;37(1):1-17. Epub 1984/01/01. PubMed PMID: 6692051.

128. Carmeliet P. Blood vessels and nerves: common signals, pathways and diseases. Nature Reviews Genetics. 2003;4(9):710-20.

129. Chuang DC. Adult brachial plexus reconstruction with the level of injury: review and personal experience. Plast Reconstr Surg. 2009;124(6 Suppl):e359-69. Epub 2010/01/09. doi: 10.1097/PRS.0b013e3181bcf16c

00006534-200912001-00010 [pii]. PubMed PMID: 19952704.

130. Vargel I, Demirci M, Erdem S, Firat P, Surucu HS, Tan E, et al. A comparison of various vascularization-perfusion venous nerve grafts with conventional nerve grafts in rats. J Reconstr Microsurg. 2009;25(7):425-37. Epub 2009/05/28. doi: 10.1055/s-0029-1223852. PubMed PMID: 19472105.

131. Vargel I. Impact of vascularization type on peripheral nerve microstructure. J Reconstr Microsurg. 2009;25(4):243-53. Epub 2008/12/17. doi: 10.1055/s-0028-1104557. PubMed PMID: 19085817.

Chapter 2

THESIS AIMS

Taking in consideration the current limitations in the knowledge of unconventional perfusion flaps, which were discussed in the Introduction Section (**Chapter 1**), the following are the general and specific aims of this thesis.

GENERAL AIMS

1- Review the literature on the use of arterialized venous flaps (**Phase I**)

2- Characterize an experimental model of a fasciocutaneous arterialized venous flap in the rat (**Phase II**)

3- Study the possibility of increasing the survival of the experimental model described above in the presence of a bacterial infection by transducing this flap with two antimicrobial peptides (**Phase III**)

4- Study the usefulness of using an arterialized neurovenous flap to bridge a peripheral nerve gap associated with local ischemia in the rat model (**Phase IV**)

5- Study in the human cadaver the surgical anatomy and histology of regions commonly used to raise arterialized venous flaps (**Phase V**)

6- Evaluate the possibility of applying arterialized venous flaps in the clinical context (**Phase VI**)

SPECIFIC AIMS

1- Perform a systematic review and meta-analysis of unconventional perfusion flaps in clinical practice (**Phase I; Chapter 3**).

2- Perform a systematic review and meta-analysis of unconventional perfusion flaps in the experimental setting (**Phase I; Chapter 4**).

3- Describe in a detailed fashion and from a surgical perspective the macro and microvascular blood supply to the integument of the ventrolateral aspect of the abdomen of the rat (**Phase II; Chapter 5**).

4- Characterize a model of a conventional fasciocutaneous free flap in the ventrolateral aspect of the abdomen of the rat (**Phase II; Chapter 6**).

5- Characterize a model of an arterialized venous fasciocutaneous flap in the ventrolateral aspect of the abdomen of the rat (**Phase II; Chapter 7**).

6- Transduce the arterialized venous fasciocutaneous flap described above with two human beta defensin genes (BD-2 and BD-3) to increase flap survival in the presence of *Pseudomonas aeruginosa* infection and of a foreign body (**Phase III; Chapter 8**).

7- Compare the efficacy of arterialized neurovenous flaps with other nerve conduits to reconstruct a 10-mm-long median nerve gap in an ischemic environment in a rat model (**Phase IV; Chapter 9**).

8- Study the surgical relevant anatomy and histology of regions commonly used to harvest arterialized venous flaps (**Phase V; Chapters 10, 11** and **12**).

9- Explore the possibility of applying the data obtained in the previous experiments to maximize the clinical application of arterialized venous flaps (**Phase VI; Chapter 13**).

Chapter 3

SYSTEMATIC REVIEW AND META-ANALYSIS OF UNCONVENTIONAL PERFUSION FLAPS IN CLINICAL PRACTICE

Authors: Diogo Casal, M.D.[1,2,3], Teresa Cunha, M.Sc. [1], Diogo Pais, M.D., PhD[2], Paula Videira, PhD[4], Joana Coloma, R.N., MSPH[5], Carlos Zagalo, M.D., PhD[6], Maria Angélica-Almeida, M.D., PhD.[1,2], João Goyri O'Neill, M.D., PhD.[2]

Affiliations:

1- Plastic and Reconstructive Surgery Department and Burn Unit; Centro Hospitalar de Lisboa Central, Lisbon, Portugal

2- Anatomy Department; Nova Medical School, Faculdade de Ciências Médicas da Universidade Nova de Lisboa, Lisbon, Portugal

3- Centre for Chronic Diseases (CEDOC); Nova Medical School, Faculdade de Ciências Médicas da Universidade Nova de Lisboa, Lisbon, Portugal

4- Department of Life Sciences, Faculdade de Ciências e Tecnologia, Universidade NOVA de Lisboa

5- Global Health and Tropical Medicine; Nova Medical School, Faculdade de Ciências Médicas da Universidade Nova de Lisboa, Lisbon, Portugal

6- Head and Neck Surgery Department; Lisbon delegation of the Portuguese Institute of Oncology, Lisbon, Portugal

ABSTRACT

Background: Unconventional perfusion flaps (**UPFs**) are in clinical use since 1975, presenting numerous potential advantages over conventional perfusion flaps. However, many surgeons are still deterred from using UPFs due to some reports of high necrosis rates. The main goal of this work was to determine the survival rate of UPFs.

Methods: We performed a systematic review and meta-analysis of all the articles written in English, French, German, Spanish and Portuguese on the clinical use of UPFs and indexed to PubMed since 1975 until 15th July 2015. For each article, data on patient and flap characteristics, and clinical results were analyzed.

Results: A total of 134 studies were found, encompassing 1445 patients. The estimated survival rate of UPFs was 89.5% (87.3-91.3%; 95% confidence interval [CI]; p<0.001). Ninety two per cent of UPFs (89.9-93.7%; CI 95%; p<0.001) presented complete or near complete survival. Most defects mandating UPFs reconstruction were caused by trauma (63.6%), especially of the hand and fingers (75.1%). The main complication of all types of UPFs was a variable degree of necrosis (7.5% of all UPFs presented marginal necrosis; 9.2% and 5.5% had significant and complete necrosis, respectively). There was a positive correlation between the rate of postoperative infection and the need of a new flap (Pearson coefficient 0.405; p=0.001). UPFs used to reconstruct the upper limb showed better survival than those transferred to head and neck or to the lower limb (p<0.001).

Conclusions: UPFs show high survival rates and should probably be used more liberally, particularly in the realm of upper limb reconstruction.

INTRODUCTION

Forty years have passed since Vaubel first executed an arterialized venous flap (**AVF**) to cover a defect on the dorsum of the hand. (1) This marked the birth of the so called unconventional perfusion flaps (**UPFs**). UPFs can be defined as composite blocks of tissues perfused solely through their venous system. They comprise AVFs and venous flaps (**VFs**). AVFs receive an arterial inflow at one end of their venous system, and drain their blood through another portion of their venous system. VFs receive venous blood through one end of their venous system and drain their blood into a venous outflow. (2-5)

Since Vaubel's first description in 1975, the use of UPFs has been mainly sporadic, due largely to some reported high necrosis rates (6-10), and also due to a still incompletely understood physiology and ill-defined clinical indications. (2-5)

In particular, various papers have described higher partial and complete necrosis rates when UPFs are placed over chronically infected open wounds or ischemic wound beds, or when large flaps are used. (2, 3, 11-14) Moreover, several authors have advocated the use of particular vascular patterns for reconstructing specific types of defects. (2-4, 11, 12) However, these indications and vascular constructions have not been submitted to proper literature comparison and statistical scrutiny.

In spite of a few excellent narrative reviews regarding the use of UPFs, no systematic reviews and meta-analyses are available. (2-4, 15) Furthermore, German literature has been largely neglected in these reviews. Finally, a literature wide review

and subsequent statistical analysis of the factors associated with UPFs success or failure are direly needed.

The primary objective of this work was to comprehensively review the literature on UPFs in order to estimate the global survival rate of these flaps. The secondary aim of this paper was to determine the relation between several patient and wound parameters and UPFs survival.

METHODS

On the 15th July 2015, the authors searched the PubMed data base, regarding the clinical application of UPFs (**Fig. 1**). The following terms were used: “arterialized venous flap"; “arterialised venous flap”; "unconventional flap", "unconventional perfusion flap"; "venous flap". The search terms were combined with the Boolean operators ‘‘AND” and “OR”. Only articles referring to human studies and written in English, French, Spanish, German and Portuguese were selected. Studies written in different languages from those mentioned above or papers referring exclusively to animal or dissection studies were excluded.

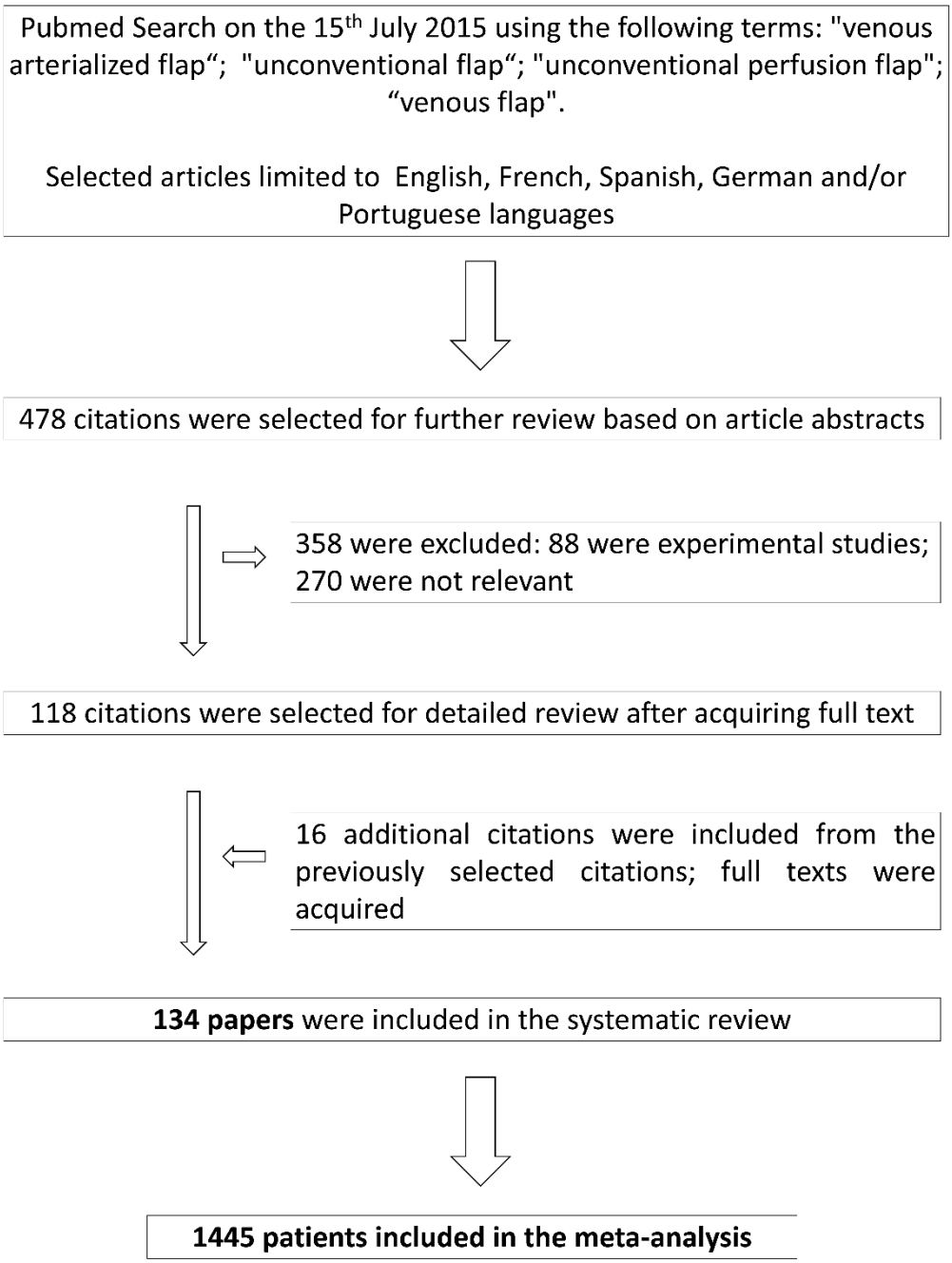

Figure 1 - Data collection from the literature. A total of 134 papers was obtained, corresponding to data from 1445 individual patients.

The title and abstract of all identified studies were examined independently by two reviewers (DC and TC). In cases where suitability of a given study for inclusion in the review was unclear, the entire article was obtained and assessed for appropriateness. Next, the references contained in these papers were scanned by the two independent reviewers to obtain further articles that were missed in the first round search. All papers were obtained in their full text version and read independently by the two reviewers.

For each study the following parameters were assessed: year of publication; nationality; patients' age; gender proportion; defect location and etiology; flap size; flap donor site; flap composition; flap insetting vascular architecture; percentage of flaps that presented *complete survival* (defined as 100% survival area or superficial necrosis with self-healing of the flap's surface within the first 15 days after surgery), *nearly complete survival* (considered 90 to 100% flap survival or unspecified inconsequential "marginal necrosis"), *significant necrosis* (> 10% flap necrosis) and *complete necrosis* (100% flap necrosis or "non-surviving flaps"); presence of infection prior to flap insetting; wound bed status prior to flap placement (*well vascularized* if the flap was placed over viable muscle, fascia, fat, synovial tissue, epitenon or granulation tissue; *poorly vascularized*, if the flap was placed over an irradiated area, scar tissue or tendon; and *non-vascularized*, if the flap was placed over bone, cartilage or prosthetic material); and presence and nature of complications (epidermolysis, flap congestion and venous insufficiency by themselves were not considered complications, as they were uniformly present in the first few days after surgery). *Epidermolysis* was considered to be present when there was only evidence of the epidermis being loosely attached to the dermis, readily exfoliating or forming blisters. (16) If the damage to the skin was deeper than the epidermis, flap necrosis was considered to be present, as described above.

The quality of evidence of each article was assessed using the modified GRADE quality assessment criteria (17) (all series with less than 3 patients were considered to be composed of sparse data and to have a significant probability of reporting bias, and thus were attributed a “Very Low Quality of Evidence Score. When estimating effect sizes for the entire population, the authors only included studies with at least a “Low Quality of Evidence Score” according to the modified GRADE quality assessment criteria. (17) Whenever individual patient data were present in papers, they were used for individual patient data meta-analysis. For the sake of individual case analysis the data from the two papers of Hussmann, which referred to the same series, were considered coincidental. (18, 19)

The data were retrieved from the available literature, each parameter at a time, from each report separately. Finally, the data were inserted in an Excel data base. When discrepancies were found in data retrieval, the articles were re-analyzed by the two reviewers independently.

Qualitative variables were expressed as percentages. Quantitative variables were expressed as means ± standard deviation. The Comprehensive Meta-analysis 2.0 ® software was used to estimate population summary effects and to produce forest plots using random-effects models. The SPSS 21.0 ® software was used for descriptive and inferential statistical analysis. The Kolmogorov-Smirnov test was used to assess if variables were normally distributed. ANOVA and t-Student test were used to compare averages in normally distributed data. Kruskal-Wallis and Mann-Whitney tests were used to compare means in non-normally distributed data. Proportions were analyzed

with the Chi-square test or Fisher's exact test. Dichotomous variables were compared with the binomial test. A two tailed $p<0.05$ was considered to be statistically significant.

RESULTS

A total of 134 studies were found regarding the clinical application of UPFs, encompassing 1445 patients (**Fig. 1**). **Table 1** summarizes the information present in these studies.

Author	Year	Country	n	Age (years)		M:F	Defect location	Defect origin	Flap survival rate (%)	Categorical flap survival %				Complications		Flap size (cm^2)		Flap type	Flap(s) donor site(s)	Flap composition
				mean	**min-max**					**CS**	**NC**	**SN**	**CN**	**%**	**% Type**	**mean**	**min-max**			
Vaubel (1)	1975	Germany	1	66	66	1:0	HF	Tr	100	100	0	0	0	0	0	35	35	4	F	S
Honda (38)	1984	Japan	5	n/a	20-51	4:1	HF	Tr	100	0	100	0	0	100	60% SpN; 40% MN	n/a	10-12	5	Ft	S
Townsend (39)	1984	Australia	7	33.2	20-54	4:3	HN; F; HF	Tu; B; Tr	100	n/a	n/a	n/a	0	0	0	n/a	n/a	8	L	Sne
Gu (40)	1985	China	14	30.8	20-54	10:4	F	Tr	85.7	0	0	0	0	14	7.1% FTN; 7.1% SpN+I	n/a	n/a	8	L	Sne
Mimoun (41)	1986	France	1	50	50	1:0	L	I	100	0	100	0	0	100	100% FTN+SpN	48	48	1	F	S
Chavoin (42)	1987	France	11	42.8	70-13	10:1	HN; L; HF	Tu; B; Tr; O	100	81.8	18	0	0	18	18.2% SpN	7.3	5-20	7	Ft; HF; HN	S
Thatte (43)	1987	India	2	n/a	n/a	0:2	F; L	B; Tr	100	100	0	0	0	0	0	22.5	21-24	7	F	S
Tsai (8)	1987	USA	15	n/a	n/a	13:2	HF	Tr	73.3	73.3	0	0	27	33	26.7% FTN; 6.7% I	7.9	14-6	5	F; Ft; HF	S
Yoshimura (44)	1987	Japan	13	37.5	21-60	n/a	HF	n/a	100	92.3	7.7	0	0	8	7.7% SpN	5.9	4-10	0	F	S
Amarante (45)	1988	Portugal	2	17.5	16-19	2:0	HF	B	100	100	0	0	0	50	50% AR	n/a	n/a	6	F	S
Chia (46)	1988	China	1	24	24	0:1	L	SC	100	100	0	0	0	100	100% I+MN+AR	144	144	3	T	S
Foucher (47)	1988	France	23	45.2	1-66	n/a	HF	B; Tr; I; SC	95.7	82.6	8.7	4.4	4.4	26	8.7% SpN; 8.7% FTN; 8.7% I	3.2	1-12	5	HF	S
Inoue (13)	1988	Japan	15	38	7-64	11:4	F; Ft	Tr; I	80	60	6.7	13	20	40	40% FTN	21.6	3.8-43.8	0; 8	F; L	S
Fukui (48)	1989	USA	11	44.8	24-64	3:1	F; HF	B; Tr	100	50	25	25	0	50	9.1% SpN; 9.1% AR+FTN	19.8	2-40	5; 7	F; L; HF	S
Gu (49)	1989	China	4	29.8	17-54	3:1	F; L; HF	SC	75	75	0	0	25	25	25% FTN	136.8	48-240	8	F; L	S; sne
Nishi (50)	1989	USA	7	30.6	17-51	5:2	HF	Tr	100	71.4	14	14	0	28.6	14.3% SpN; 14.3% FTN	5.3	1-13.5	8	F; Ft	S
Rose (51)	1989	USA	1	38	38	1:0	HF	SC	100	n/a	n/a	n/a	0	0	0	5.2	5.2	5	n/a	S; sne
Rose (52)	1989	USA	14	29	18-55	9:1	HF	Tr	100	n/a	n/a	n/a	0	0	0	n/a	n/a	8	Ft	Sne
Thatte (53)	1989	India	8	23.4	8-35	2:6	F	B; Tr	87.5	87.5	6.7	0	0	13	12.5% FTN	53.6	21-105	7	F	S
Thatte (6)	1989	India	8	32.4	14-60	6:2	L	B; Tr	87.5	62.5	13	13	13	38	25% FTN; 12.5% MN	73.1	40-112.5	7	L	S
Inoue (54)	1990	Japan	22	40	7-68	17:5	HF	n/a	95.5	77.3	0	18	4.6	23	22.7% FTN	n/a	1-36	0; 8	F	S
Nakayama (55)	1990	Japan	3	22	21-23	1:2	HF	B; Tr; CM	100	n/a	n/a	n/a	0	33	33.3% AR	n/a	n/a	3	Ft	S
Chen (56)	1991	Taiwan	28	27	10-42	19:9	HF	B; Tr	96.4	89.3	0	7.1	3.6	11	10.7% FTN	n/a	n/a	0; 5; 6; 8	n/a	n/a
Inada (57)	1991	Japan	6	41.5	15-72	5:1	HF	Tr; SC	100	66.7	33.3	0	0	0	33.3% SpN	5.4	3.8-6	11	HF	S
Inoue (58)	1991	Japan	4	42	31-67	4:0	HF	Tr	100	50	25	25	0	50	25% FTN; 25% MN	8.4	2-21	0; 8	F	St
Inoue (59)	1991	Japan	16	30	12-55	13:3	Ft	O	81.3	43.8	13	25	19	56	56.2% FTN	n/a	28-72	0	L; Ft	S
Koshima (60)	1991	Japan	3	57	45-78	2:1	HN; HF; Ft	Tu; Tr; SC	100	100	0	0	0	0	0	51	36-77	0	L	S; sb
Iwasawa (61)	1992	Japan	1	39	39	1:0	HF	Tr	100	n/a	n/a	n/a	0	0	0	n/a	n/a	3	Ft	S
Morris (62)	1992	Australia	1	33	33	0:1	HN	Tr	100	0	100	0	0	100	100% MN	150	150	0	HN	S
Ohtsuka (63)	1992	Japan	1	54	54	1:0	L	Tr	100	n/a	n/a	n/a	0	0	0	96	96	0	F	S
Fasika (64)	1992	UK	2	32	32	1:0	HF	B; Tr	100	100	0	0	0	0	0	6	6	8	F	S
Fukui (65)	1993	Japan	7	59.9	35-85	6:1	F	Tr	100	14.3	57	29	0	86	57.1% SpN; 28.6% FTN	270.6	164-390	7; 11	HF	S

Author	Year	Country	n	Age (years)		M:F	Defect location	Defect origin	Flap survival rate (%)	Categorical flap survival %				Complications		Flap size (cm^2)		Flap type	Flap(s) donor site(s)	Flap Composition
				Mean	**min-max**					**CS**	**NC**	**SN**	**CN**	**%**	**% Type**	**mean**	**min-max**			
Takeuchi (99)	2000	Japan	2	23.5	21-26	2:0	HF	Tr	100	100	0	0	0	0	0	47.8	35-60.5	0; 1	Ft	Sne
Alexander (100)	2001	India	1	n/a	n/a	n/a	Ft	n/a	100	100	0	0	0	0	0	60.8	60.8	0	L	S
Chia (101)	2001	Singapore	1	26	26	1:0	HF	Tr	100	100	0	0	0	0	0	12	12	8	F	S
Murata (102)	2001	Japan	7	39	20-57	6:0	HF	Tr	100	85.7	14	0	0	14	14.2% SpN	12.3	6.3-42	6	HF	S; sne
Safak (103)	2001	Turkey	1	45	45	1:0	HN	B	100	100	0	0	0	0	0	180	180	10	F	S
Woo (104)	2001	Korea	4	n/a	n/a	n/a	HF	B	100	n/a	n/a	n/a	0	0	0	n/a	n/a	4	F; L	n/a
Woo (105)	2001	Korea	3	29	22-36	3:0	HN	B	100	100	0	0	0	0	0	146.7	120-180	3	F	S
Wungcharoen (106)	2001	Egypt	8	40.1	20-67	7:1	F; L; Ft	Tu; B; Tr; O	100	75	25	0	0	25	25% FTN	53.1	16-90	1	F; L	S
Brooks (107)	2002	USA	1	20	20	1:0	HF	Tr	100	0	100	0	0	100	100% FTN	54	54	1	HF	S
De Lorenzi (108)	2002	Netherlands; Belgium	40	32	3-66	36:4	HF	B; Tr	92.5	57.5	0	35	7.5	43	42.5% FTN	n/a	36-45	0	F; L	S
Kushima (109)	2002	Japan	25	32	5-63	15:7	HF	Tr	96	84	0	12	4	16	16% FTN	6.2	3-10	0; 8	F; HF	S
Aoki (110)	2003	Japan	1	70	70	0:1	Hf	I	100	100	0	0	0	0	0	1	1	7	Ft	S
Hussmann (19)	2003	Germany	70	47.4	7-78	n/a	HN; F; L; HF	Tu; B; Tr; CM	94.3	81.4	0	13	5.7	19	18.6% FTN	n/a	1-150	0; 3; 4; 14	F; L; Ft	S; stnb; sc
Zhu (7)	2003	USA	5	37	18-56	3:2	L; Ft	B; Tr; O	20	20	0	0	80	80	20% FTN+AR; 60% FTN	67.2	20-110	5	L	S
Cheng (111)	2004	Taiwan	1	22	22	1:0	Ft	Tr	100	100	0	0	0	0	0	26.3	26.3	1	F	S
Koch H (112)	2004	Austria	13	33.9	19-47	9:4	L; HF	B; Tr	100	84.6	7.7	7.7	0	15	15.4% FTN	20.8	1-77	3	F	S; st
Kopp (113)	2004	Germany	6	32.5	n/a	5:1	F; HF	Tr	100	n/a	n/a	n/a	n/a	n/a	n/a	n/a	n/a	4	F	S
Lin (114)	2004	Taiwan	18	35	16-64	10:2	HF	Tr	100	94.4	0	5.5	0	6	5.6% FTN	n/a	n/a	0	F	St
Nakazawa (115)	2004	Japan	4	41	20-71	n/a	L	CM	100	100	0	0	0	0	0	101.8	65-153	4	L	S; sne
Nakazawa (116)	2004	Japan	1	23	26	1:0	HF	Tr	100	100	0	0	0	0	0	32	32	8	F	S
Titley (117)	2004	UK	2	47	46-48	1:1	HF	Tr	100	100	0	0	0	50	50% I	13	12.5-13.5	8	F	S
Deune (118)	2005	USA	1	50	50	1:0	F	Tu	100	0	100	0	0	100	100% FTN	24	24	8	HF	S
Hyza (119)	2005	Czech Republic	1	17	17	0:1	HF	Tr	100	100	0	0	0	0	0	10	10	1	F	S
Kopp (120)	2006	Germany	1	82	82	0:1	HF	Tr	100	100	0	0	0	0	0	80	80	4	F	S
Mureau (121)	2006	Netherlands	1	82	82	0:1	HN	Tu	100	100	0	0	0	0	0	n/a	n/a	0	L	B
Pellini (122)	2006	Italy	11	56	51-61	n/a	HN	O	100	100	0	0	0	0	0	n/a	n/a	5	F	S
Yokoyama (123)	2006	Japan	6	54	34-73	6:0	HF	Tr	100	100	0	0	0	0	0	3.6	2-6.75	0	Ft	S
Woo (20)	2007	Korea	154	35.7	16-65	112:40	HF	B; Tr	98.1	92.9	3.3	2	2	7	7.1% FTN	22.1	6.5-47.6	0; 1; 2; 3; 4	F; L; Ft; HF	S; st; sne
Brooks (124)	2008	USA	8	n/a	27-38	8:0	HF	Tr	100	100	0	0	0	0	0	6	4-8	8	F	S
Hyza (125)	2008	Czech Republic	13	n/a	n/a	n/a	HF	Tr	100	76.9		23	0	23	7.7% FTN;15.4% AR	n/a	n/a	0; 1; 4; 5	F	S; st
Iglesias (126)	2008	Mexico	1	25	25	1:0	HN	B	100	0	100	0	0	100	100% FTN+I	322	322	4	F	S

Table 1 - Summary of the studies on unconventional perfusion flaps included in the meta-analysis

Legend:

n, number of patients in each series

M, male; **F**, female

Categorical flap survival: CS, complete survival; **NC**, nearly complete survival; **SN**, significant necrosis; **CN**, complete necrosis; **n/a**, non-available.

Defect location and flap donor site: F, forearm; **G**, groin; **L**, leg; **Ft**, foot; **HN**, head and neck; **HF**, hand and fingers; **T**, thigh.

Defect origin: B, burn and its sequelae; **I**, infection; **CM**, congenital malformation; **SC**, scar contracture; **Tr**, trauma; **Tu**, tumor; **VU**, venous ulcer; **O**, others.

Complications: AR, anastomosis revision; **FTN**, full thickness necrosis; **I**, infection; **MN**, marginal necrosis; **SpN**, superficial necrosis.

Flap type (2, 20)**:** "0", type Ia arterialized venous flap according to Woo classification; "1", type Ib arterialized venous flap according to Woo classification; "2", type IIa arterialized venous flap according to Woo classification; "3", type IIb arterialized venous flap according to Woo classification; "4", type III arterialized venous flap according to Woo classification; "5", type I venous flap according to Chen classification; "6", type IIa venous flap according to Chen classification; "7", type IIb venous flap according to Chen classification; "8", Arterialized venous arterial (**AVA**) flow through flap; "9", AVA flow through flap with ≥ 1 additional discontinuous efferent veins; "10", pedicled arterialized venous flap; "11", sliding venous flap; "12", unspecified type venous arterialized flap; "13", type I arterialized venous flap according to Woo classification; "14", single vein venous flap; "15", multiple types of arterialized venous flap.

Flap composition: b, bone; **s**, skin with its appendages and subcutaneous tissue; **sb**, skin and bone; **sc**, skin and cartilage; **sne**, skin and nerve; **st**, skin and tendon; **stnb**, skin, tendon, nerve and bone.

All studies were clinical observational studies. The average number of patients included in each study was 11.3 ± 17.7. The most common countries where these studies

were conducted were, in decreasing order of frequency: Japan (25.9%), USA (12.6%), China/Taiwan (10.4%), South Korea and Turkey (8.1% each), and Germany (6.7%). According to the GRADE quality assessment criteria, the quality of these studies was "low" in 48.9% and "very low" in 50.4% of cases. The largest series was that presented by Woo *et al.* in 2007, corresponding to 154 cases of AVFs. (20) The different types of UPFs and their main clinical applications are illustrated in **Figure 2**.

Vascular patterns referred in the literature		General description		First description	Classifications	Main clinical indications
	Venous arterialized flaps	"Arterialized venous flow-through flaps" Orthodromic blood flow (blood flows in the same direction as venous valves open)	Straight venous pattern akin to a standard vein graft	Yoshimura 1987 (37)	IA (Woo) III (Chen)	Small, long and narrow defects (19) Can be used for simultaneous vascular reconstruction (19)
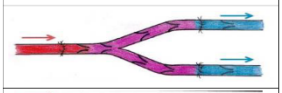			Y-shaped pattern	Mimoun 1986 (34)	IB (Woo) III (Chen)	
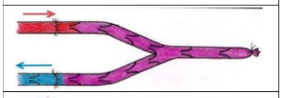		Antidromic blood flow (blood flows in the opposite direction of venous valves opening in the afferent vein)	Y-shaped pattern	Kovacs 1998 (6)	IIA (Woo)	Medium-sized defects (19) Can be used for simultaneous vascular reconstruction (19)
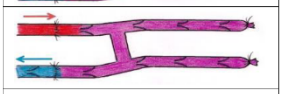			H-shaped pattern	Chia 1988 (39)	IIB (Woo)	
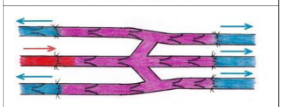		Anti and orthodromic blood flow (mixed pattern of through and against-valve blood flow)		Vaubel 1975 (1)	III (Woo)	Large-sized defects (19) Can be used for simultaneous vascular reconstruction (19)
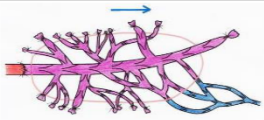		Pedicled arterialized venous flap (blood enters the flap antidromically and leaves orthodromically through preserved efferente veins)		Kayikcioglu 1998 (84)	-	Medium-sized limb defects defects (84)
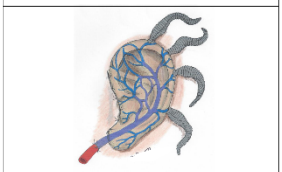		Single vein arterialized venous flap (blood enters the flap through a single vessel; usually venous drainage is ensured by medical leeches)		Hussman 1996 (17)	-	Reported in cases of replantation of body parts in which a single vein can be used for vascular anastomosis (17, 18)
	Venous flaps	Free venous flow through flap (the flap is nourished exclusively by venous blood flowing orthodromically)		Honda 1984 (31)	I (Chen)	Can be used for simultaneous vascular reconstruction (31)
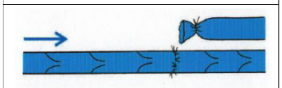		Distally pedicled based venous flap		Amarante 1988 (38)	IIA (Chen)	Upper and lower limb defects small and medium defects (38)
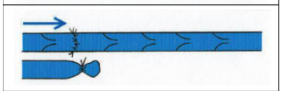		Proximally pedicled venous flap		Chavoin 1987 (35)	IIB (Chen)	Upper and lower limb defects small and medium defects (35)
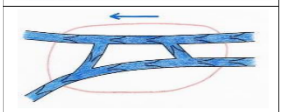		Sliding venous flap (the flap is transposed based exclusively on the dissected venous network)		Inada 1991 (50)	-	Useful for mobilizing adjacent tissues in areas where the superficial venous network is well developed, such as the dorsum of fingers and toes (50)
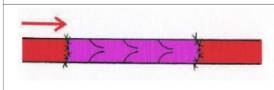	Arterialized venous arterail flap	Arterialized venous arterial (AVA) flow through flap		Townsend 1984 (32)	IA (Woo) IV (Chen)	Can be used for simultaneous vascular reconstruction Can incorporate long nerve segments (32)
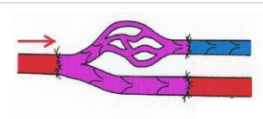		Arterialized venous arterial (AVA) flow through flap with ≥ 1 additional discontinuous efferent veins		Rozen 2012 (136)	IV (Chen)	Can be used for simultaneous vascular reconstruction (19)

Figure 2 - Schematic representation of the different types of unconventional perfusion flaps described in the literature, their respective classification and reported clinical applications.

Red area represents arterial blood flow. Blue and purple regions stand for venous and mixed arterial and venous blood, respectively. The arrows indicate the direction of blood flow. The curved lines inside the vessels represent venous valves. The drawings are not to scale.

There were more males than females being submitted to UPFs reconstruction (76.26% vs. 23.74%; p<0.001). Patients' average age was 37.10 ± 16.69 years (n=629), varying between 1 and 86 years. Flap size varied between 1.0 to 390.0 cm^2, presenting an average size of 27.36 ± 42.52 cm^2 (n=795).

Most defects mandating UPF reconstruction were caused by trauma (63.6%). However, defects also resulted from tumor extirpation (13.5%), burns (8.7%), congenital malformations (1.8%), infections (1.2%), Dupuytren's disease treatment and/or scar contracture release (4.6%), and venous ulcer coverage (0.1%). These defects were distributed by the following anatomical regions: head and neck (8.5%), arm and forearm (4.4%), hand and fingers (75.1%), leg (2.6%), trunk and genitals (4.7%), and foot (4.7%). As shown in **Figure 3**, type I AVFs were the most commonly used UPFs for reconstructing the head, neck, hand, fingers, and foot ($p < 0.05$). "Arterialized venous arterial" flow through flaps were the most frequent UPFs employed in the reconstruction of the arm and forearm ($p < 0.05$). For reconstructing leg defects VFs were preferred ($p < 0.05$).

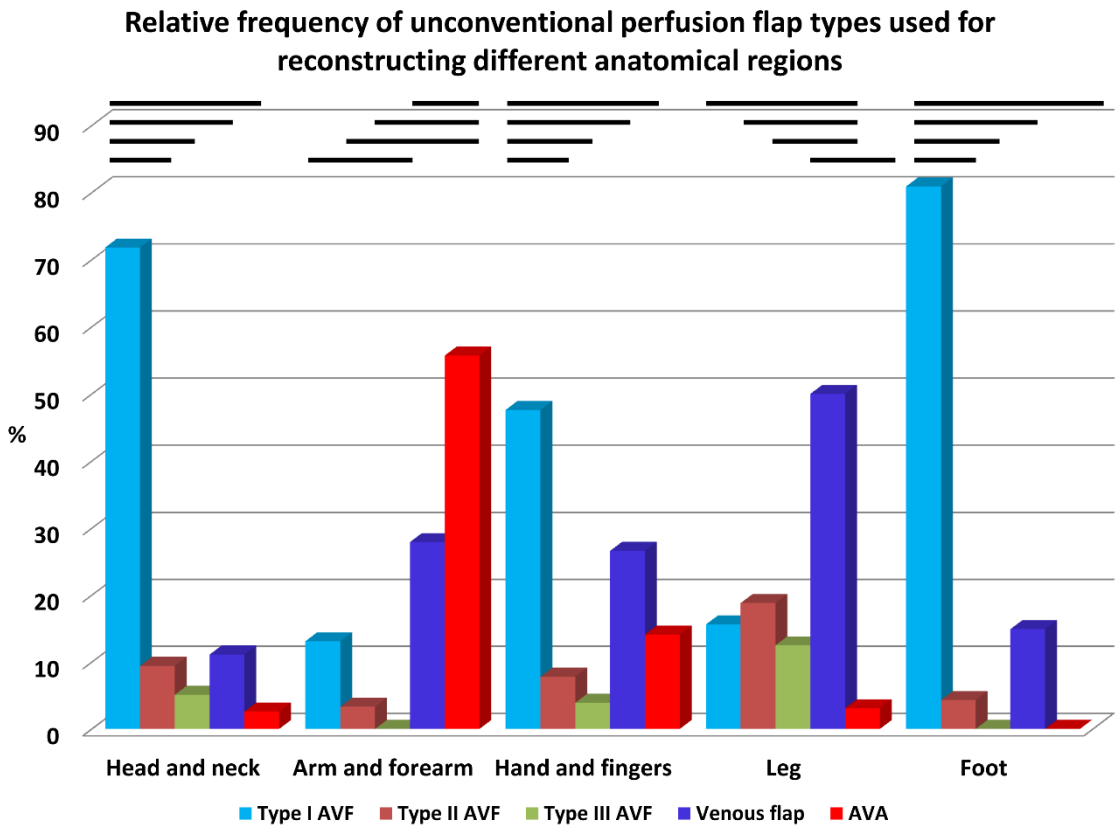

Figure 3 - Bar chart depicting the relative frequency of unconventional perfusion flap types used for reconstructing different anatomical regions. The lines on top of the bars indicate statistically significant differences in the relative frequency of major unconventional perfusion flap types ($p < 0.05$)

AVF, arterialized venous flap; **AVA**, arterialized venous arterial flap.

The most common donor sites were, in decreasing frequency: the forearm (61.8%), the hand and fingers (18.9%), foot and toes (9.8%), lower leg (8.4%), thigh (0.4%), and groin (0.2%).

UPFs composition was rather heterogeneous: skin, skin appendages and subcutaneous fat (87.3%); skin, subcutaneous fat and subcutaneous nerves (8.1%); skin,

subcutaneous fat and tendon(s) (3.5%); skin, tendon(s), nerve(s) and bone (0.6%); skin and cartilage (0.3%); skin, subcutaneous fat and bone (0.1%); and bone (0.1%).

Meta-analysis of the survival rate of UPFs using the CMA 2.0 software and a random effects model, estimated an overall survival rate of 89.5% (87.3-91.3%; 95% confidence interval [CI]; p<0.001). Using the same methodology, 92.0% UPFs (89.9-93.7%; CI 95%; p<0.001) were estimated to present complete or near complete survival, whereas only 7.5% (5.9-9.5%; CI 95%; p<0.001) UPFs presented complete or near complete necrosis (**Fig. 4**). This pattern of most flaps presenting complete or near complete survival was observed in all types of UPFs ($p \leq 0.003$).

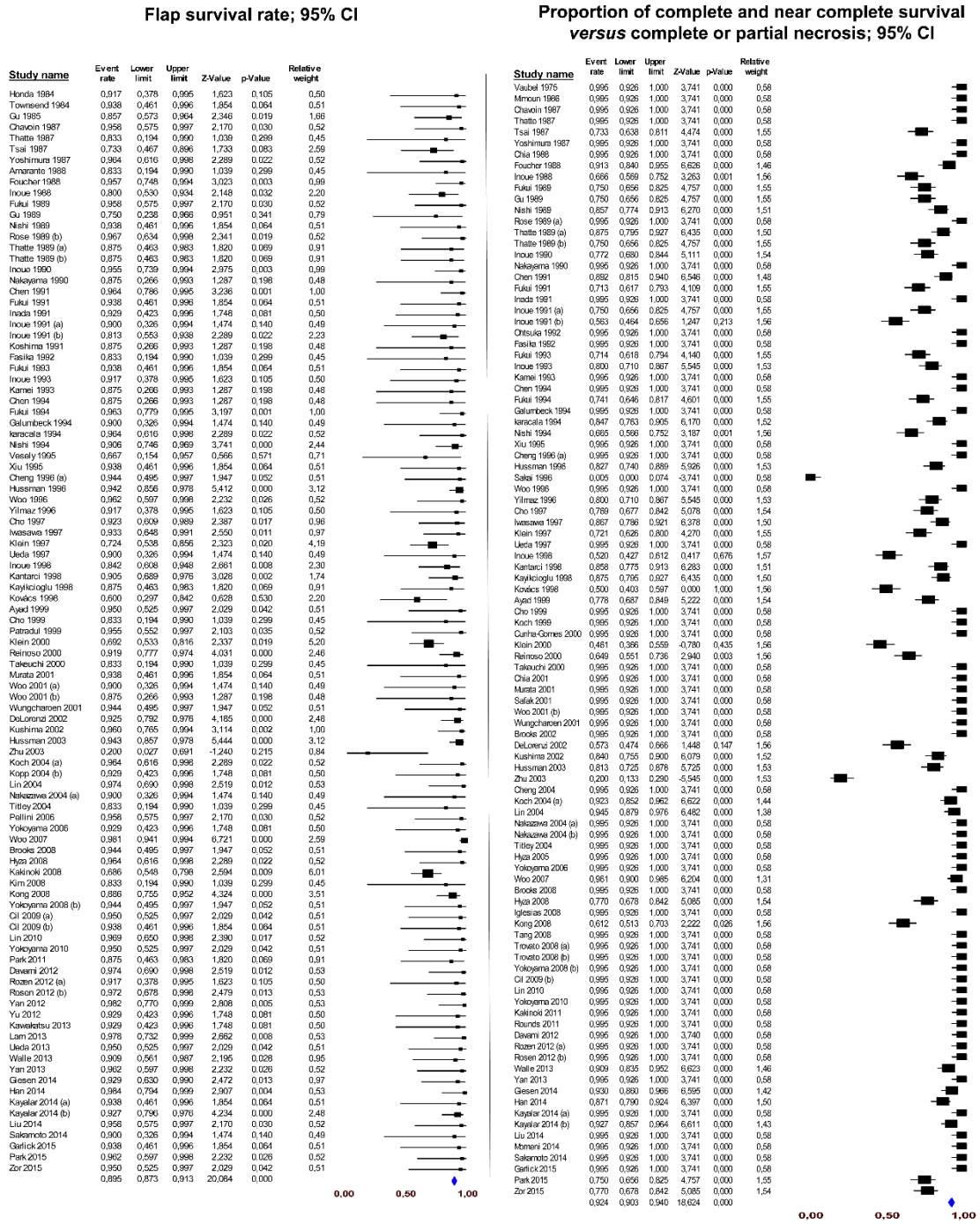

Figure 4 - Forest plots of all case series reporting unconventional perfusion flaps (**UPFs**) reviewing survival rate and proportion of complete and near complete survival *versus* complete or partial necrosis. A random effects model was used. Meta-analysis of the survival rate of UPFs using the CMA software and random effects model, revealed an overall survival rate of 89.5%; p<0.001 ([87.3-91.3%]; 95% CI). Using the same

methodology, 92.0% (90.3-94.0%; CI 95%) UPFs showed complete or near complete survival (p<0.001), whereas only 8.8% UPFs presented complete or near complete necrosis.

CI, confidence interval.

The survival and complications of the different types of UPFs is illustrated in **Table 2** and in **figures 5** and **6**. The main complication of all types of UPFs was a variable degree of necrosis. Globally, 7.5% of flaps presented marginal necrosis; 9.2% and 5.5% had significant and complete necrosis, respectively. Less common complications included need of anastomoses revision (1.2%), infection (0.9%), and hematoma formation (0.5%) (**Figs. 7** and **8**).

Type of unconventional perfusion flap (n)	**Complete survival** % (n)	**Nearly complete survival** % (n)	**Significant necrosis** % (n)	**Complete Necrosis** % (n)	**Complications other than necrosis**			
					None % (n)	**Infection** % (n)	**Hematoma** % (n)	**Need of anastomosis revision** % (n)
Type IA AVF (n = 285)	76.5% (n = 218)	4.9% (n = 14)	11.6% (n = 33)	7.0% (n = 20)	72.4% (n = 181)	0.4% (n = 1)	0.8% (n = 2)	0.8% (n = 2)
Type IB AVF (n = 107)	78.5% (n = 84)	12.1% (n = 13)	5.6% (n = 6)	3.7% (n = 4)	76.6% (n = 82)	0.0% (n = 0)	0.0% (n = 0)	3.7% (n = 4)
Type IIA AVF (n = 24)	100.0% (n = 24)	0.0% (n = 0)	0.0% (n = 0)	0.0% (n = 0)	95.8% (n = 23)	0.0% (n = 0)	0.0% (n = 0)	0.0% (n = 0)
Type IIB AVF (n = 60)	75.0% (n = 45)	8.3% (n = 5)	11.7% (n = 7)	5.0% (n = 3)	73.0% (n = 46)	1.6% (n = 1)	0.0% (n = 0)	1.6% (n = 1)
Type III AVF (n = 31)	83.9% (n = 26)	12.9% (n = 4)	0.0% (n = 0)	3.2% (n = 1)	83.9% (n = 26)	3.2% (n = 1)	0.0% (n = 0)	0.0% (n = 0)
Type I VF (n = 127)	69.3% (n = 88)	15.0% (n = 19)	6.3% (n = 8)	9.4% (n = 12)	68.4% (n = 93)	2.2% (n = 3)	0.0% (n = 0)	2.2% (n = 3)
Type IIA VF (n = 40)	95.0% (n = 38)	2.5% (n = 1)	0.0% (n = 0)	2.5% (n = 1)	78.3% (n = 18)	0.0% (n = 0)	0.0% (n = 0)	4.3% (n = 1)
Type IIB VF (n = 73)	63.0% (n = 46)	16.4% (n = 12)	17.8% (n = 13)	2.7% (n = 2)	54.0% (n = 34)	0.0% (n = 0)	3.2% (n = 2)	0.0% (n = 0)
Type IV AA P0 (n = 114)	77.2% (n = 88)	8.8% (n = 10)	8.8% (n = 10)	5.3% (n = 6)	79.1% (n = 106)	1.5% (n = 2)	0.8% (n = 1)	0.0% (n = 0)
Type IV AA P1 (n = 17)	94,1% (n = 16)	5.9% (n = 1)	0.0% (n = 0)	0.0% (n = 0)	94.1% (n = 16)	0.0% (n = 0)	0.0% (n = 0)	0.0% (n = 0)
Pedicled AVF (n = 13)	76.9% (n = 10)	15.4% (n = 2)	0.0% (n = 0)	7.7% (n = 1)	76.9% (n = 10)	0.0% (n = 0)	0.0% (n = 0)	0.0% (n = 0)
Sliding VF (n = 7)	71,4% (n = 5)	28.6% (n = 2)	0.0% (n = 0)	0.0% (n = 0)	71.4% (n = 5)	0.0% (n = 0)	0.0% (n = 0)	0.0% (n = 0)
Single vein AVF (n = 3)	100.0% (n = 3)	0.0% (n = 0)	0.0% (n = 0)	0.0% (n = 0)	100.0% (n = 3)	0.0% (n = 0)	0.0% (n = 0)	0.0% (n = 0)

Type I AVF (includes types IA AVF and IB AVF) (n = 460)	76.0% (n = 327)	6.3% (n = 27)	11.4% (n = 49)	6.3% (n = 27)	72.9% (n = 288)	0.3% (n = 1)	0.5% (n = 2)	1.5% (n = 6)
Type II AVF (includes types IIA AVF and IIB AVF) (n = 84)	82.1% (n = 69)	6.0% (n = 5)	8.3% (n = 7)	3.6% (n = 3)	79.3% (n = 69)	1.1% (n = 1)	0.0% (n = 0)	1.1% (n = 1)
Type III AVF (n = 31)	83.9% (n = 26)	12.9% (n = 4)	0.0% (n = 0)	3.2% (n = 1)	83.9% (n = 26)	3.2% (n = 1)	0.0% (n = 0)	0.0% (n = 0)
Venous flaps (n = 247)	71.7% (n = 177)	13.8% (n = 34)	8.5% (n = 21)	6.1% (n = 15)	65.5% (n = 150)	1.3% (n = 3)	0.9% (n = 2)	1.7% (n = 4)
Type IV AA (n = 131)	79.4% (n = 104)	8.4% (n = 11)	7.6% (n = 10)	4.6% (n = 6)	80.8% (n = 122)	1.3% (n = 2)	0.7% (n = 1)	0.0% (n = 0)
Flap area < 6 cm^2 (n = 114)	87.7% (n = 100)	4.4% (n = 5)	7.0% (n = 8)	0.9% (n = 1)	82.4% (n = 89)	1.9% (n = 2)	0.9% (n = 1)	0.9% (n = 1)
Flap area 6-20 cm^2 (n = 374)	81.8% (n = 306)	6.1% (n = 23)	5.3% (n = 20)	6.7% (n = 25)	72.5% (n = 198)	0.7% (n = 2)	0.4% (n = 1)	1.1% (n = 3)
Flap area > 20 cm^2 (n = 242)	71.9% (n = 174)	13.6% (n = 33)	7.9% (n = 19)	6.6% (n = 16)	65.4% (n = 134)	1.5% (n = 3)	1.0% (n = 2)	1.5% (n = 3)
All groups (n = 1445)	77.8% (n = 958)	7.5% (n = 92)	9.2% (n = 113)	5.5% (n = 68)	71.2% (n = 723)	0.9% (n = 9)	0.5% (n = 5)	1.2% (n = 12)

Table 2 - Survival rates and complications of different unconventional perfusion flaps calculated from individual patient data extracted from the different articles.

Legend: AVF, arterialized venous flap; **VF**, venous flap

Complete survival was defined as 100% survival area or superficial necrosis with self-healing of the flap's surface within the first 15 days after surgery). Nearly complete survival (considered 90 to 100% flap survival or unspecified inconsequential "marginal necrosis"). Significant necrosis was defined as more than 10% of flap necrosis. Finally, complete necrosis was defined as 100% flap necrosis.

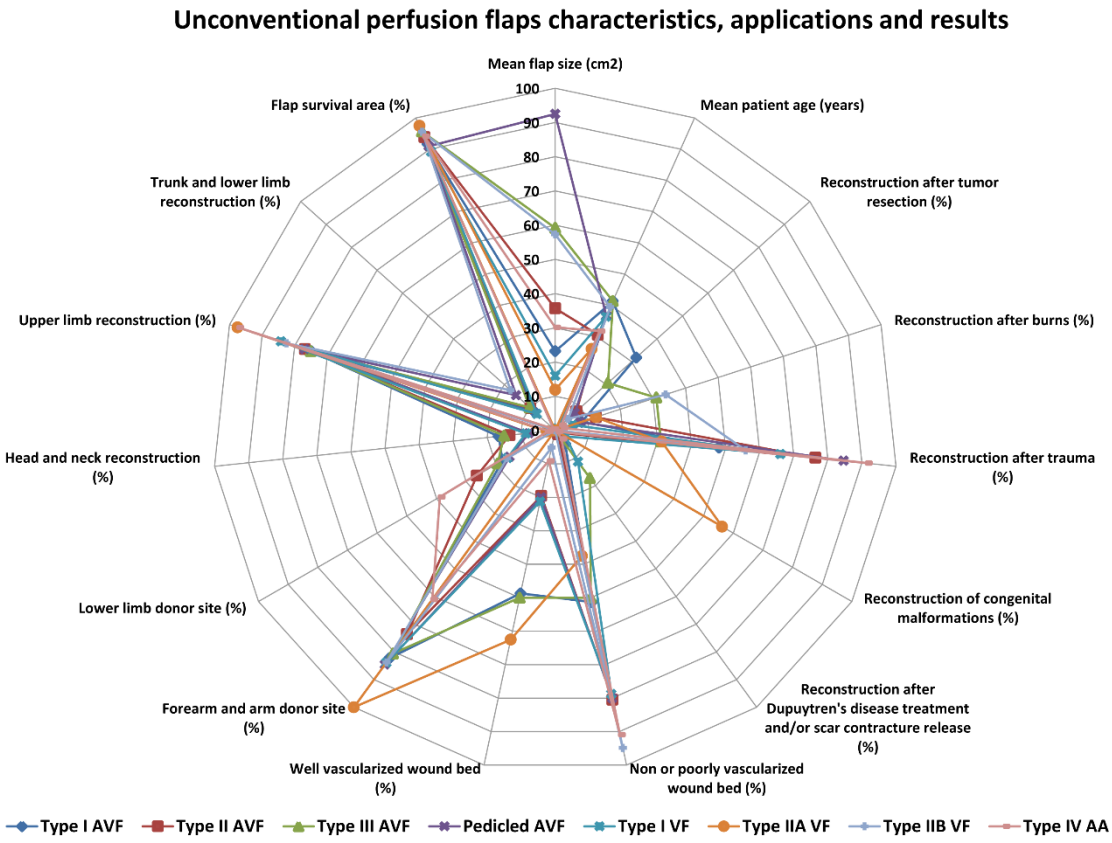

Figure 5 - Star plot illustrating unconventional perfusion flap characteristics, applications and clinical results.

AVF, arterialized venous flap; VF, venous flap; AA, arterialized venous arterial flap.

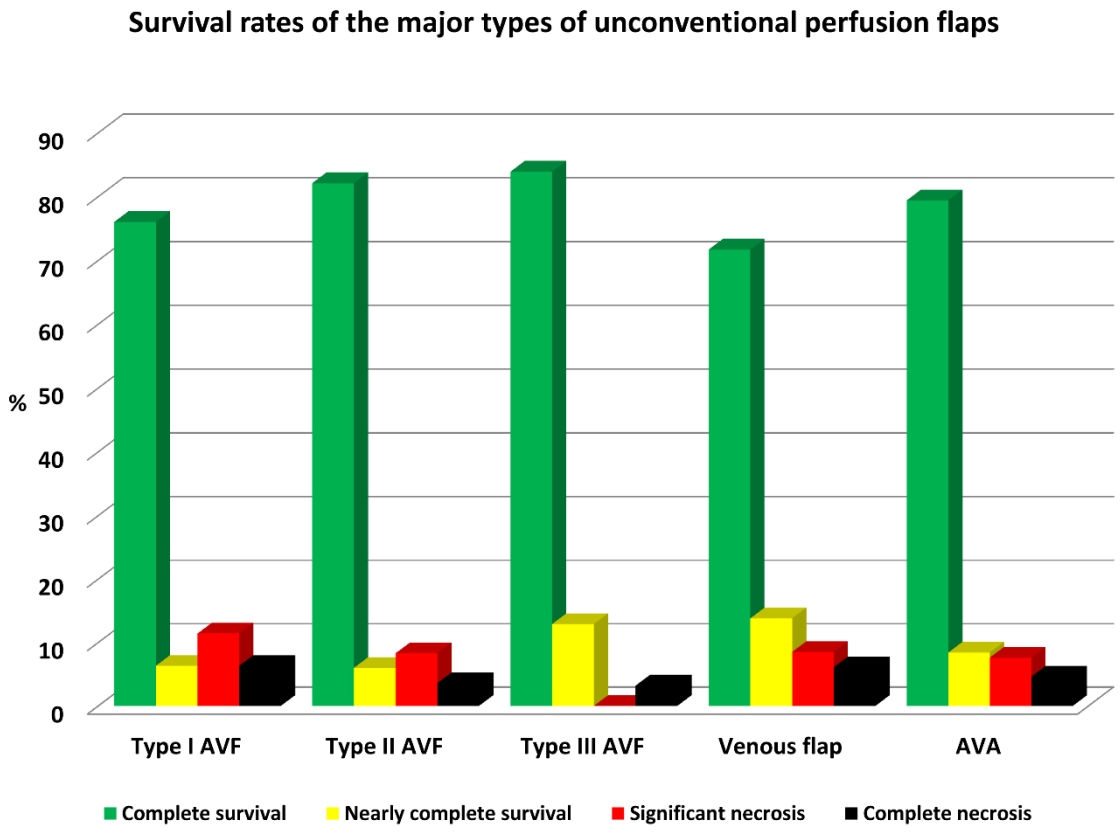

Figure 6 - Bar charts illustrating the survival of the most common types of unconventional perfusion flaps.

AVF, arterialized venous flap; **AVA**, arterialized venous arterial flap.

There were no statistically significant differences between the different types of unconventional perfusion flaps ($p < 0.05$).

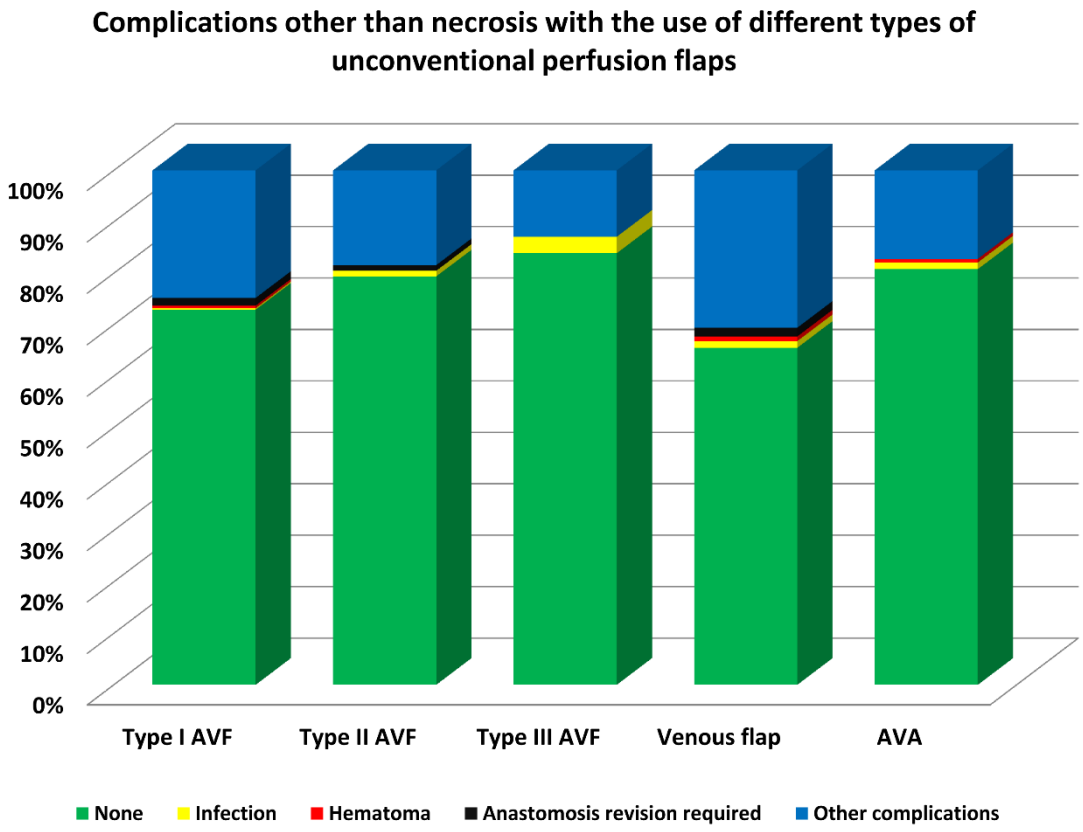

Figure 7 - Stacked column chart illustrating complications other than necrosis with the use of different types of unconventional perfusion flaps. The group *other complications* includes wound dehiscence, delayed healing, prolonged venous stasis, and significant flap congestion.

AVF, arterialized venous flap; **AVA**, arterialized venous arterial flap.

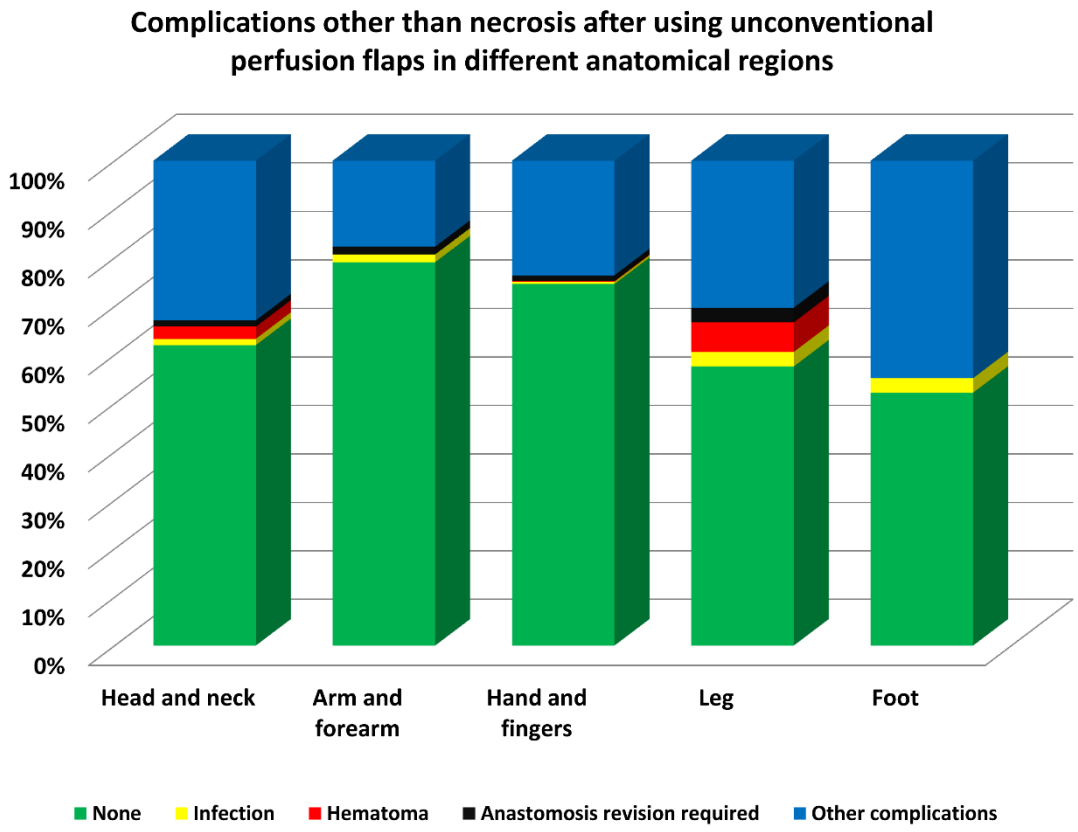

Figure 8 - Stacked column chart illustrating complications other than necrosis with the use of unconventional perfusion flaps in different anatomical regions.

AVF, arterialized venous flap; **AVA**, arterialized venous arterial flap.

The group *other complications* includes wound dehiscence, delayed healing, prolonged venous stasis, and significant flap congestion.

Figure 5 illustrates the characteristics of the major types of UPFs, as well as their main applications and results. Overall, there was a negative correlation between flap size and complete flap survival (Pearson coefficient -0.354; $p<0.001$). Additionally, there was a positive correlation between average flap size and the following variables: presence of significant necrosis (Pearson coefficient 0.263; $p=0.028$); average rate of complications (Pearson coefficient 0.441; $p<0.001$); presence of epidermolysis (Pearson

coefficient 0.270; p=0.028); rate of postoperative infection (Pearson coefficient 0.663; p<0.001); and need of new flap (Pearson coefficient 0.373; p=0.003). Flaps with an area over 20 cm^2 were not correlated with higher necrosis rates than smaller flaps, after stratifying for flap type. No statistically significant differences were found between the different types of UPFS regarding overall survival rates, categorical flap survival, or complications rates (**Figs. 7, 8 and 9**).

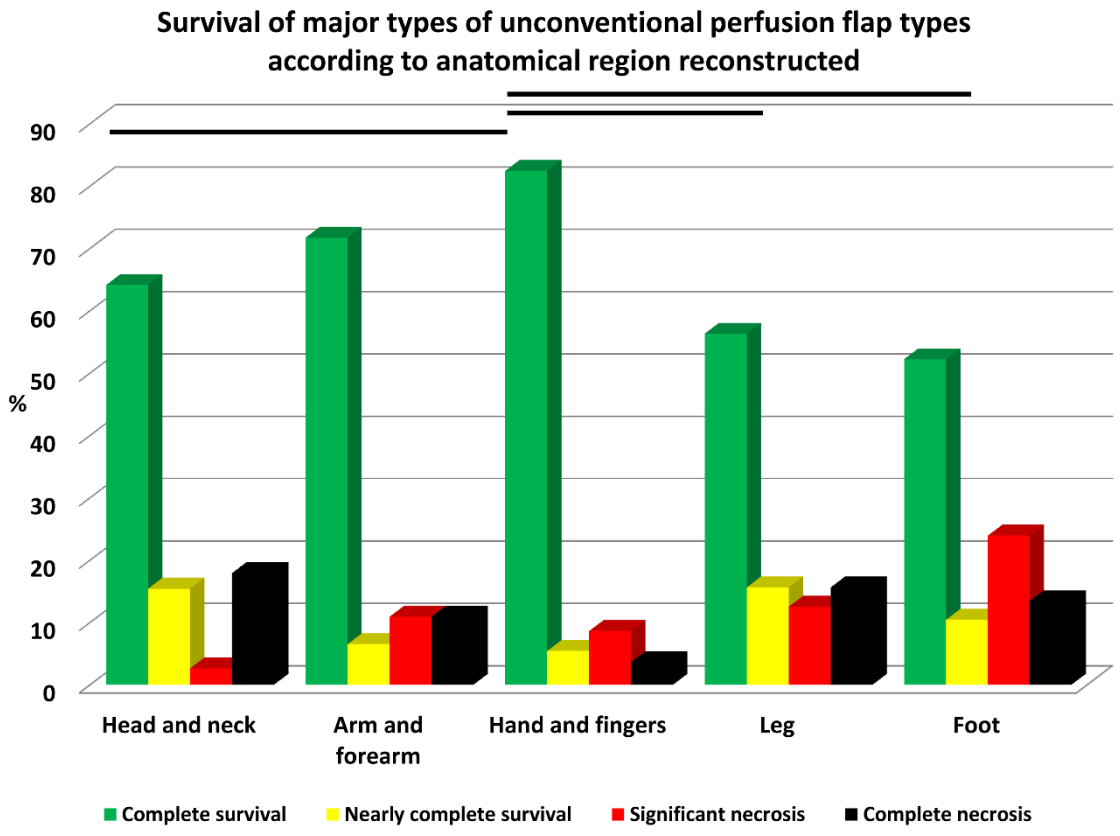

Figure 9 - Bar charts illustrating the survial of the major types of unconventional perfusion flaps according to anatomical region reconstructed.

AVF, arterialized venous flap; **AVA**, arterialized venous arterial flap.

The lines on top of the bars indicate statistical significant differences in the relative frequency necrosis rates for each anatomical region ($p < 0.05$).

The rate of postoperative infection was 3.79 ± 17.57 %. The need of a new flap after a UFP was observed in 7.90 ± 21.46 % of cases. There was a positive correlation between the rate of postoperative infection and the need of a new flap (Pearson coefficient 0.405; p=0.001). When clinically significant postoperative infection was noted, UPF loss requiring a new flap occurred in 50% of cases (n=4; p<0.001).

No association was found between wound bed blood supply and UPF survival.

Flap overall survival rate was 82.93 ± 37.86 % in the head and neck (n=82); 91.94 ± 27.45 % in the arm and forearm (n=62); 95.33 ± 21.10 % in the hand and fingers (n=1050); 84.85 ± 36.41 % in the leg (n=33); and 86.57 ± 34.36 % in the foot (n=67). UPFs used to reconstruct the upper limb showed better overall survival rates than those transferred to head and neck or to the lower limb (p<0.001) (**Fig. 8**). No difference was found in the survival rate of UPFs used for reconstructing defects of different origin.

Digital replantation as AVFs showed complete survival in all cases reported (n=3) (19). The single vein AVF also showed a survival rate of 100% in three cases of ear replantation. (19, 21, 22)

Comparing study results before and after the 2007 Woo *et al.'s* paper (20), several significant differences were noted: the average UPFs' survival area increased from 91.10 ± 16.83 cm^2 to 97.65 ± 1.68 cm^2 (p=0.01); the proportion of UFPs with complete survival increased from 74.22 ± 29.48 % to 87.85 ± 20.83 % (p=0.16); the percentage of UPFs undergoing complete necrosis decreased from 6.24 ± 12.75 to 1.76 ± 3.87 (p=0.009); and the proportion of flaps implanted on non-perfused wound beds increased from 43.84 ± 35.56 % to 71.56 ± 35.61 % (p=0.043).

DISCUSSION

Some of the lingering questions behind the use of UPFs are related to their survival rate, their clinical efficacy, and their overall usefulness relatively to the increasingly diverse, tailor-made, and thin conventional flaps. (2-4, 15) According to the present study, the estimated survival rate of UPFs is 89.5% (87.3-91.3%; 95% CI; $p<0.001$). Moreover, 92.2% (90.1-93.9%; CI 95%; $p<0.001$) of these flaps are estimated to present complete or near complete survival, whereas only 7.5% (5.9-9.5%; CI 95%; $p<0.001$) will show complete or near complete necrosis. This means that not only do UPFs survive in most cases, but also that in most instances their survival is complete or near complete. However, in 7.90 ± 21.46 % of cases, it was necessary to perform a new flap to reconstruct the defect not solved by the initial UPF. In fact, it may be argued that the mentioned rate of 89.5% of UPFs survival is still lower than the frequently reported 95% to 100% survival rate of most conventional free flaps. (23-25) In addition, conventional flaps seldom present significant areas of necrosis, making them overall more reliable. (23-25) Notwithstanding, UPFs still have unique advantages relatively to conventional flaps, namely their ease of dissection, not requiring the sacrifice of major arteries at the donnor site, their thinness and pliability, and their potential to include missing tissues other than skin, namely tendons, nerves, and even bone. (23-25) As they can be fabricated from any combination of tissues abutting the venous system, they show a remarkable versatily in the reconstructing of multiple defects, as it is summarized in Figure 2.

In addition, UPFs are important options to consider in replantation of severed body parts, such as digits, for two distinct reasons. On the one hand, as stated above, completely avulsed digits, with no useable artery in the amputated segment that were replanted as purely AVFs showed complete survival in all cases reported (n=3). (19) On the other hand, according to the literature on digital replantation, UPFs are frequently used to bridge skin defects in the amputation zone, fulfilling the double purpose of reconstructing vascular and skin defects in amputated segments that are otherwise replantated in a conventional fashion. (20, 23-26) In summary, the literature suggests that even in the context of trauma and eventually prolonged ischemia commonly associated with digital amputation, UPFs may be useful options to bear in mind.

Interestingly, the single vein AVF also showed a survival rate of 100% in three cases of ear replantation. (19, 21, 22) This latter finding is somewhat counter-intuitive, as it is a necessary condition for blood to flow in any given capillary network that there is a pressure gradient between the afferent and the efferent side. However, in 2 of the 3 studies referring to single vein AVF ear replantation, medical leeches were used, which probably created a venous outflow that allowed flap blood perfusion. (19, 21, 22)

Noteworthily, UPFs used to reconstruct the upper limb showed better viability than those transferred to head and neck or to the lower limb ($p<0.001$). To the best of the authors' knowledge, this has not been reported before, and thus deserves further study. One reason for this difference in UPFs' viability in distinct anatomical areas may be related to the diverse venous pressures in these areas. (27) One may argue that the relatively low venous pressure in the head and neck region may lead to rapid blood flow in the central veins of the flap, making the peripheral region of the flap more prone to

critical ischemia and necrosis. On the contrary, in the lower limb, the higher venous pressure may diminish the gradient between the inflow and outflow veins, making global flap perfusion less efficient. However, these hypotheses lack further experimental and clinical validation.

There was a positive correlation between average flap size and the following variables: presence of significant necrosis (Pearson coefficient 0.263; p=0.028); average rate of complications (Pearson coefficient 0.441; p<0.001); presence of epidermolysis (Pearson coefficient 0.270; p=0.028); rate of postoperative infection (Pearson coefficient 0.663; p<0.001); and need of new flap (Pearson coefficient 0.373; p=0.003). This suggests that, as a general rule, UPFs should be kept relatively small and thin, as has been proposed by several authors. (20, 23-26) However, regarding categorical flap size, flaps with an area over 20 cm^2 were not correlated with higher complete necrosis rates. This may be partly explained by publication bias, as authors are less likely to report large or very later UPFs that suffered complete necrosis.

Contrarily to what has been reported by some authors, no association was found between poorly or non-perfused wound beds and flap failure. However, there was a positive correlation between the rate of postoperative infection and the need of a new flap (Pearson coefficient 0.405; p=0.001). Moreover, when clinically significant postoperative infection was noted, UPF loss requiring a new flap occurred in 50% of cases (n=4; p<0.001). This may explain why several authors avoid using UPFs when dealing with infected wound beds.(12)

It is interesting to note that the 2007 paper published by Woo *et al.*, based on their large experience of over 150 AVFs, marks a turning point in the literature on UPFs,

probably by help clarifying the physiology, vascular architecture and clinical application of these flaps.(20) In fact, comparing study results before and after this seminal work, several differences were noted: the average UPFs survival area increased from 91.10 ± 16.83 cm^2 to 97.65 ± 1.68 cm^2 (p=0.01); the proportion of UFPs with complete survival increased from 74.22 ± 29.48 % to 87.85 ± 20.83 % (p=0.16); the percentage of UPFs undergoing complete necrosis decreased from 6.24 ± 12.75 to 1.76 ± 3.87 (p=0.009); and the proportion of flaps implanted on non-perfused wound beds increased from 43.84 ± 35.56 % to 71.56 ± 35.61 % (p=0.043). In this paper, Woo *et al.* classified AVFs into three major types, taking into account blood flow direction inside the venous system and its orientation relatively to the venous valves, the venous architecture inside the flap, and the number of recipient veins (Fig. 2). (20) In addition, clear indications regarding the size and ideal clinical applications of each flap type were given in that paper, which may have helped optimize their use. (20) A similar attempt at systematizing the various types of venous flaps has been made by Chen, Tang, Noordhoff and Goldschlager (Fig. 2). (2)

Noteworthy, 71.8% of all reported studies on UPFs were conducted in 7 countries alone (Japan, USA, China, Taiwan, South Korea, Turkey, and Germany). These data suggest that these flaps are not yet routinely performed worldwide, and that they are probably more common in countries with a longer microsurgical tradition.

The authors concede that, as happens in all systematic reviews, the present systematic review and meta-analysis may be affected by several types of bias, particularly publication bias. (28, 29) The latter is related to the fact that positive results are much more likely to be published than negative ones. The most efffective way to

minimize this type of error in meta-analysis is to perform a truly comprehensive review of the literature in a given period, as the authors did in the present study. (28, 29) As far as we could determine the present work is the most extensive review on the subject of UPFs, including not only the English literature, but also the French, German, Spanish and Portuguese literature. The inclusion of the German literature brought to light, for example, that, contrarily to what is frequently stated, it was not Nakayama who described for the first time a AVF in 1981. (30) In fact, in 1975 Vaubel had already reported an AVF to reconstruct the integumentary defect resulting from the excision of a tumor on the dorsum of the hand. (1)

As in all meta-analyses, the data were retrieved from the available literature, each parameter at a time, from each report separately. As expected, not all articles provided information for all variables. Therefore, the data extracted from the individual papers and from the individual patient data were not coincidental for all variables. As a consequence, the statistical inferences made from these data using specific statistical techniques and software to extrapolate the values of each variable to the general population were not always completely overlapping. (31) This is the reason why, for example, we observed an apparent 2.5% discrepancy in the estimated UPFs' overall survival and the proportion of UPFs that presented complete or near complete survival. However, we would like to point out that the estimated survival rate of UPFs was 89.5%, but the 95% confidence interval of this estimate was 87.3-91.3%. Furthermore, the estimated proportion of UPFs that presented complete or near complete survival was 92.0%, but the 95% confidence interval of this estimate was 89.9-93.7%. Therefore, although these variables were not absolutely coincidental there was an overlap in the estimated 95% confidence interval of 89.9-91.3% ($p<0.001$) These confidence intervals

reflect the inherent uncertainty in producing estimates for the general population, describing a range of values within wich we can reasonably expect the true value to be. (32)

Another limitation of the present work is that all studies included are composed of case series and case reports, which are merely observational studies. According to the GRADE quality assessment criteria, the quality of evidence in these studies was "low" in 48.9% and "very low" in 50.4% of cases. This proportion is similar to those reported in many systematic reviews and meta-analyses in the field of Plastic Surgery. (33) In order to diminish the effect of biases due to small series inclusion, when estimating the average flap survival rate and the proportion of complete and near complete survival *versus* complete or partial necrosis, the authors only included studies with "Low Quality of Evidence Score" (Fig. 3). Figure 3 shows that the effect sizes are reasonably constant from study to study, which suggests that it is appropriate to compute summary effect sizes with these data for these two variables. (32, 34)

Finally, it is well known that in technically demanding procedures, such as those involved in planning and executing UPFs, heterogeneity of surgeons and patients alike, in different centers in various parts of the world, may yield substantial different results in apparently similar circumstances. (35)

Hence, due to the possibility that the results herein presented may be somewhat affected by these biases and limitations, prospective studies comparing conventional and UPFs are still warranted to better assess the true survival rate and advantages of the latter.

According to the available literature, UPFs, conventional free flaps and local conventional flaps each present potential advantages and disadvantages (**Table 3**). For example, most UPFs and all conventional free flaps require microsurgical skills and instruments. In addition, they are associated with larger operating times. Hence, these two types of flaps may be precluded in patients with significant comorbidities in whom prolonged surgery would be too risky. In this context, local pedicled flaps may be advantageous. Notwithstanding, it shoud be noted the latter type of flaps may be limited by the quality and quantity of local tissues. Moreover, due to frequent anatomical variations, local and free conventional flaps often require preoperative imagiological and/or ultrasound evaluation. (36) On the contrary, UPFs can often be raised after visual inspection of the venous system, without the need for these ancilliary examinations. In addition, UPFs provide the significant advantage of allowing a natural thin and pliable covering of integumentary defects, namely in hands, feet and genitalia. (3, 37)

Type of flap	Unconventional perfusion flaps (UPFs)	Conventional free flaps	Conventional local flaps
Advantages	Thin and pliable Easy to plan and to harvest Can include different structures abutting the flap's venous system (e.g., tendons, nerves, cartilage, bone, etc.) Can be easily tailored to reconstruct small to large vascular defects Minimal donor site morbidity (often can be programmed to allow primary closure of the donor region; do not require sacrificing an arterial source) Can be used as rescue flaps in the absence of arteries in	Can be tailored to include multiple tissues in various geometrical arrangements Can be used to transfer distant tissues with high metabolic rates such as muscle and bowel Minimal or no necrosis in the majority of cases Easy and standardized postoperative monitoring in most cases	Usually do not require microsurgical skills Tissue transfer is relatively easy and fast, which is important in patients in whom prolonged surgery is not advisable Allow reconstruction with similar neighboring tissues Flap thickness is usually similar to that of the neighboring defect Minimal or no necrosis in the majority of cases Easy and standardized postoperative monitoring

	amputated segments (e.g. digits or ear parts)		
Disadvantages	Difficult postoperative monitoring Some degree of unpredictability Frequent epidermolysis, congestion and marginal necrosis More prone to necrosis in the presence of infection Often requires microsurgical skills Longer operating times than local flaps	Usually bulkier Thinning the flap through perforator dissection requires advanced microsurgical expertise Affected by unpredictable anatomical variation, often demanding pre-operative imagiological or ultrasound evaluation Greater donor site morbidity (demands the sacrifice of a donor site artery) Always requires microsurgical skills Usually more laborious and time consuming to harvest than UPFs	Choices limited by type, quality and quantity of local tissues Add an additional injury to an already damaged body segment When large local flaps are harvested, additional flaps or grafts are required to reconstruct the secondary defect Perforator flaps are based on perforator vessels which are highly variable in number, location, caliber and relationship with surrounding structures, often demanding pre-operative imagiological or ultrasound evaluation

Table 3 - Comparison of the advantages and disadvantages of unconventional perfusion flaps, conventional free flaps and conventional local flaps in the clinical setting.

This systematic review showed that some degree of flap congestion and epidermolysis was invariably described with UPFs' use. This may make the postoperative surveillance of these flaps more difficult compared to that of conventional flaps. (2-4, 15)

CONCLUSION

According to this meta-analysis the estimated survival rate of UPFs is 89.5% (87.3-91.3%; 95% CI; $p<0.001$). Hence, these flaps are safe in most circumstances, and should probably be used more liberally, particularly in the realm of upper limb reconstruction.

ACKNOWLEDGEMENTS

The authors are very grateful to Mr. Nuno Folque for producing all the drawings contained in this paper.

References

1. Vaubel, W. Indikationen und Technik des arterialisierten Lappens zur Deckung großer Defekte im Handbereich. *Hefte Unfallheilkd* 1975;126:381.

2. Goldschlager, R., Rozen, W. M., Ting, J. W., Leong, J. The nomenclature of venous flow-through flaps: updated classification and review of the literature. *Microsurgery* 2012;32:497-501.

3. Yan, H., Brooks, D., Ladner, R., Jackson, W. D., Gao, W., Angel, M. F. Arterialized venous flaps: a review of the literature. *Microsurgery* 2010;30:472-478.

4. Yan, H., Zhang, F., Akdemir, O., et al. Clinical applications of venous flaps in the reconstruction of hands and fingers. *Arch Orthop Trauma Surg* 2010.

5. Jabir, S., Frew, Q., El-Muttardi, N., Dziewulski, P. A systematic review of the applications of free tissue transfer in burns. *Burns : journal of the International Society for Burn Injuries* 2014;40:1059-1070.

6. Thatte, R. L., Thatte, M. R. The saphenous venous flap. *Br J Plast Surg* 1989;42:399-404.

7. Zhu, C., Zhang, F., Lei, M. P., Oswald, T., Lineaweaver, W. C. Clinical case experience using microsurgical venous flaps for soft-tissue coverage of the lower extremity. *J Reconstr Microsurg* 2003;19:173-177.

8. Tsai, T. M., Matiko, J. D., Breidenbach, W., Kutz, J. E. Venous flaps in digital revascularization and replantation. *J Reconstr Microsurg* 1987;3:113-119.

9. Klein, C. [Experiences with an arterialized venous flap for intraoral defect reconstruction]. *Zentralbl Chir* 2000;125:51-55.

10. Kovacs, A. F. Comparison of two types of arterialized venous forearm flaps for oral reconstruction and proposal of a reliable procedure. *Journal of cranio-maxillo-facial surgery : official publication of the European Association for Cranio-Maxillo-Facial Surgery* 1998;26:249-254.

11. Garlick, J. W., Goodwin, I. A., Wolter, K., Agarwal, J. P. Arterialized venous flow-through flaps in the reconstruction of digital defects: case series and review of the literature. *Hand (N Y)* 2015;10:184-190.

12. Woon, C. Y., Lee, J. Y., Teoh, L. C. Flap resurfacing of postinfection soft-tissue defects of the hand. *Plast Reconstr Surg* 2007;120:1922-1929.

13. Inoue, G., Maeda, N. Arterialized venous flap coverage for skin defects of the hand or foot. *J Reconstr Microsurg* 1988;4:259-266.

14. Brooks, D. The "reliably unreliable" venous flap. *J Hand Surg Am* 2009;34:1361-1362; author reply 1362.

15. Yan, H., Fan, C., Zhang, F., Gao, W., Li, Z., Zhang, X. Reconstruction of large dorsal digital defects with arterialized venous flaps: our experience and comprehensive review of literature. *Ann Plast Surg* 2013;70:666-671.

16. Epidermolysis. In B. Werner ed., *Stedman's medical dictionary*, 27th ed. USA: Lippincott Williams and Wilkins, 2000:604.

17. Guyatt, G. H., Oxman, A. D., Vist, G. E., et al. GRADE: an emerging consensus on rating quality of evidence and strength of recommendations. *BMJ* 2008;336:924-926.

18. Hussmann, J., Bahr, C., Steinau, H. U., Vaubel, E. [Indications for arterialization of tissue]. *Langenbecks Arch Chir Suppl Kongressbd* 1996;113:1164-1166.

19. Hussmann, J., Bahr, C., Russell, R. C., Steinau, H. U., Vaubel, E. Experimentelle und klinische Erfahrungen mit der Stromumkehr. *Journal der Deutschen Gesellschaft für Plastische und Wiederherstellungschirurgie* 2003:24.

20. Woo, S. H., Kim, K. C., Lee, G. J., et al. A retrospective analysis of 154 arterialized venous flaps for hand reconstruction: an 11-year experience. *Plast Reconstr Surg* 2007;119:1823-1838.

21. Trovato, M. J., Agarwal, J. P. Successful replantation of the ear as a venous flap. *Ann Plast Surg* 2008;61:164-168.

22. Momeni, A., Parrett, B. M., Kuri, M. Using an unconventional perfusion pattern in ear replantation - arterialization of the venous system. *Microsurgery* 2014;34:657-661.

23. Khouri, R. K., Cooley, B. C., Kunselman, A. R., et al. A prospective study of microvascular free-flap surgery and outcome. *Plast Reconstr Surg* 1998;102:711-721.

24. Bui, D. T., Cordeiro, P. G., Hu, Q. Y., Disa, J. J., Pusic, A., Mehrara, B. J. Free flap reexploration: indications, treatment, and outcomes in 1193 free flaps. *Plast Reconstr Surg* 2007;119:2092-2100.

25. Nakatsuka, T., Harii, K., Asato, H., et al. Analytic review of 2372 free flap transfers for head and neck reconstruction following cancer resection. *J Reconstr Microsurg* 2003;19:363-368; discussion 369.

26. Casal, D., Gomez, M. M., Antunes, P., Candeias, H., Almeida, M. A. Defying standard criteria for digital replantation: A case series. *International journal of surgery case reports* 2013;4:597-602.

27. Fukui, A., Maeda, M., Inada, Y., Tamai, S., Mine, T. An investigation of venous pressure and oxygen tension in human extremities: an experimental study of survival in pedicled venous flaps. *J Reconstr Microsurg* 1991;7:217-221; discussion 223-214.

28. Borenstein, M., Hedges, L. V., Higgins, J. P., Rothstein, H. R. Publication bias. In M. Borenstein ed., *Introduction to Meta-analysis*, First ed. United Kingdom: Wiley and Sons; 2009:277-292.

29. Sterne, J. A., Egger, M., Mother, D. Addressing reporting biases. In J. P. Higgins, S. Green eds., *Cochrane handbook for systematic review of interventions*, First ed. United Kingdom: Wiley-Blackwell; 2009:297-333.

30. Nakayama, Y., Soeda, S., Kasai, Y. Flaps nourished by arterial inflow through the venous system: an experimental investigation. *Plast Reconstr Surg* 1981;67:328-334.

31. Higgins, J. P. T., Deeks, J. J. Selecting studies and collecting data. In J. P. T. Higgins, S. Green eds., *Cochrane handbook of systematic reviews of interventions*, First ed. USA: Wiley-Blackwell; 2009:151-185.

32. Schünemann, H. J., Oxman, A. D., Vist, G. E., et al. Interpreting results and drawing conclusions. In J. P. T. Higgins, S. Green eds., *Cochrane handbook of systematic reviews of interventions*, First ed. USA: Wiley-Blackwell; 2009:359-387.

33. Margaliot, Z., Chung, K. C. Systematic Reviews: A Primer for Plastic Surgery Research. *Plastic and Reconstructive Surgery* 2007;120:1834-1841.

34. Borenstein, M., Hedges, L. V., Higgins, J. P. T., Rothstein, H. R. Why perform a meta-analysis. In M. Borenstein ed., *Introduction to Meta-Analysis*, First ed. USA: Wiley; 2009:9-14.

35. Lu, X. W., Idu, M. M., Ubbink, D. T., Legemate, D. A. Meta-analysis of the clinical effectiveness of venous arterialization for salvage of critically ischaemic limbs. *European*

journal of vascular and endovascular surgery : the official journal of the European Society for Vascular Surgery 2006;31:493-499.

36. Cil, Y., Yapici, A. K., Kocman, A. E., Ozturk, S. Distally based venous flap for proximal phalangeal soft tissue burn defect and web space burn contracture. *J Burn Care Res* 2009;30:643-647.

37. Yan, H., Zhang, F., Akdemir, O., et al. Clinical applications of venous flaps in the reconstruction of hands and fingers. *Arch Orthop Trauma Surg* 2011;131:65-74.

38. Honda, T., Nomura, S., Yamauchi, S., Shimamura, K., Yoshimura, M. The possible applications of a composite skin and subcutaneous vein graft in the replantation of amputated digits. *Br J Plast Surg* 1984;37:607-612.

39. Townsend, P. L., Taylor, G. I. Vascularised nerve grafts using composite arterialised neuro-venous systems. *British journal of plastic surgery* 1984;37:1-17.

40. Kakinoki, R., Ikeguchi, R., Nankaku, M., Nakamua, T. Factors affecting the success of arterialised venous flaps in the hand. *Injury* 2008;39 Suppl 4:18-24.

41. Mimoun, M., Baux, S., Kirsch, J. M., Fahed, I. [An original flap: the arterialized venous flap]. *Ann Chir Plast Esthet* 1986;31:219-224.

42. Chavoin, J. P., Rouge, D., Vachaud, M., Boccalon, H., Costagliola, M. Island flaps with an exclusively venous pedicle. A report of eleven cases and a preliminary haemodynamic study. *Br J Plast Surg* 1987;40:149-154.

43. Thatte, R. L., Thatte, M. R. Cephalic venous flap. *Br J Plast Surg* 1987;40:16-19.

44. Yoshimura, M., Shimada, T., Imura, S., Shimamura, K., Yamauchi, S. The venous skin graft method for repairing skin defects of the fingers. *Plast Reconstr Surg* 1987;79:243-250.

45. Amarante, J., Reis, J. Reverse-flow island flap: clinical report and venous drainage. *Plast Reconstr Surg* 1988;81:137.

46. Chia, S. L., Cheng, H. H., Mao, L. Free transplantation of venous network pattern skin flap. *Plast Reconstr Surg* 1988;82:892-895.

47. Foucher, G., Norris, R. W. The venous dorsal digital island flap or the "neutral" flap. *Br J Plast Surg* 1988;41:337-343.

48. Fukui, A., Inada, Y., Maeda, M., et al. Pedicled and "flow-through" venous flaps: clinical applications. *J Reconstr Microsurg* 1989;5:235-243.

49. Gu, Y. D., Zhang, G. M., Chen, D. S., Yan, J. G., Cheng, X. M. Arterialized free flap. Report of four cases. *Chin Med J (Engl)* 1989;102:140-144.

50. Nishi, G., Shibata, Y., Kumabe, Y., Hattori, S., Okuda, T. Arterialized venous skin flaps for the injured finger. *J Reconstr Microsurg* 1989;5:357-365.

51. Rose, E. H. Small flap coverage of hand and digit defects. *Clin Plast Surg* 1989;16:427-442.

52. Rose, E. H., Kowalski, T. A., Norris, M. S. The reversed venous arterialized nerve graft in digital nerve reconstruction across scarred beds. *Plast Reconstr Surg* 1989;83:593-604.

53. Thatte, M. R., Kumta, S. M., Purohit, S. K., Deshpande, S. N., Thatte, R. L. Cephalic venous flap: a series of 8 cases and a preliminary report on the use of 99mTc labelled RBCs to study the saphenous venous flap in dogs. *Br J Plast Surg* 1989;42:193-198.

54. Inoue, G., Maeda, N., Suzuki, K. Resurfacing of skin defects of the hand using the arterialised venous flap. *Br J Plast Surg* 1990;43:135-139.

55. Nakayama, Y., Iino, T., Uchida, A., Kiyosawa, T., Soeda, S. Vascularized free nail grafts nourished by arterial inflow from the venous system. *Plast Reconstr Surg* 1990;85:239-245; discussion 246-237.

56. Chen, H. C., Tang, Y. B., Noordhoff, M. S. Four types of venous flaps for wound coverage: a clinical appraisal. *J Trauma* 1991;31:1286-1293.

57. Inada, Y., Fukui, A., Tamai, S., Kakihana, T., Maeda, M. The sliding venous flap for covering skin defects with poor blood supply on the lateral aspects of fingers. *Br J Plast Surg* 1991;44:368-371.

58. Inoue, G., Tamura, Y. One-stage repair of both skin and tendon digital defects using the arterialized venous flap with palmaris longus tendon. *J Reconstr Microsurg* 1991;7:339-343.

59. Inoue, G., Maeda, N., Suzuki, K. Closure of big toe defects after wrap-around flap transfer using the arterialized venous flap. *J Reconstr Microsurg* 1991;7:1-8.

60. Koshima, I., Soeda, S., Nakayama, Y., Fukuda, H., Tanaka, J. An arterialised venous flap using the long saphenous vein. *Br J Plast Surg* 1991;44:23-26.

61. Iwasawa, M., Furuta, S., Noguchi, M., Hirose, T. Reconstruction of fingertip deformities of the thumb using a venous flap. *Ann Plast Surg* 1992;28:187-189.

62. Morris, S. F., MacGill, K. A., Taylor, G. I. Scalp replantation by arterialised venous network flow-through. *Br J Plast Surg* 1992;45:187-192.

63. Ohtsuka, H., Ohtani, K. A free arterialized venous loop flap. *Plast Reconstr Surg* 1992;89:965-967.

64. Fasika, O. M., Stilwell, J. H. Arterialized venous flap for covering and revascularizing finger injury. *Injury* 1993;24:67-68.

65. Fukui, A., Maeda, M., Tamai, S., Inada, Y. The pedicled venous flap. Clinical applications. *Br J Plast Surg* 1993;46:68-71.

66. Inada, Y., Fukui, A., Tamai, S., Mizumoto, S. The arterialised venous flap: experimental studies and a clinical case. *Br J Plast Surg* 1993;46:61-67.

67. Inoue, G., Suzuki, K. Arterialized venous flap for treating multiple skin defects of the hand. *Plast Reconstr Surg* 1993;91:299-302; discussion 303-296.

68. Kamei, K., Ide, Y. The pedicled arterialized venous flap. *J Reconstr Microsurg* 1993;9:287-291.

69. Chen, C. L., Chiu, H. Y., Lee, J. W., Yang, J. T. Arterialized tendocutaneous venous flap for dorsal finger reconstruction. *Microsurgery* 1994;15:886-890.

70. Fukui, A., Inada, Y., Maeda, M., Mizumoto, S., Yajima, H., Tamai, S. Venous flap--its classification and clinical applications. *Microsurgery* 1994;15:571-578.

71. Galumbeck, M. A., Freeman, B. G. Arterialized venous flaps for reconstructing soft-tissue defects of the extremities. *Plast Reconstr Surg* 1994;94:997-1002.

72. Karacalar, A., Ozcan, M. Free arterialized venous flap for the reconstruction of defects of the hand: new modifications. *J Reconstr Microsurg* 1994;10:243-248.

73. Nishi, G. Venous flaps for covering skin defects of the hand. *J Reconstr Microsurg* 1994;10:313-319.

74. Webster, H. R., Inglefield, C. J. Closure of the second toe transfer donor site without disruption of the deep transverse metatarsal ligament. *Microsurgery* 1994;15:802-804.

75. Xiu, Z. F., Chen, Z. J. Clinical applications of venous flaps. *Ann Plast Surg* 1995;34:518-522.

76. Yilmaz, M., Menderes, A., Karaca, C., Barutcu, A. Free arterialized venous forearm flap. *Ann Plast Surg* 1995;34:88-91.

77. Vesely, J., Kucera, J. Immediate free flap reconstruction of traumatic defects. *Acta Chir Plast* 1995;37:7-11.

78. Bolitho, D. G., Hudson, D. A. The superficial temporal venous island flap for eyebrow reconstruction. *European Journal of Plastic Surgery* 1996;19:103-104.

79. Cheng, S. L., Wong, S. S. Salvage of superficial palmar avulsion. *J Trauma* 1996;40:22-26.

80. Cheng, T. J., Chen, H. C., Tang, Y. B. Salvage of a devascularized digit with free arterialized venous flap: a case report. *J Trauma* 1996;40:308-310.

81. Inoue, G., Tamura, Y., Suzuki, K. One-stage repair of skin and tendon digital defects using the arterialized venous flap with palmaris longus tendon: an additional four cases. *J Reconstr Microsurg* 1996;12:93-97.

82. Sakai, S. Arterialised venous groin flap: case report. *Br J Plast Surg* 1996;49:90-92.

83. Woo, S. H., Jeong, J. H., Seul, J. H. Resurfacing relatively large skin defects of the hand using arterialized venous flaps. *J Hand Surg Br* 1996;21:222-229.

84. Yilmaz, M., Menderes, A., Karatas, O., Karaca, C., Barutcu, A. Free arterialised venous forearm flaps for limb reconstruction. *Br J Plast Surg* 1996;49:396-400.

85. Cho, B. C., Lee, J. H., Byun, J. S., Baik, B. S. Clinical applications of the delayed arterialized venous flap. *Ann Plast Surg* 1997;39:145-157.

86. Iwasawa, M., Ohtsuka, Y., Kushima, H., Kiyono, M. Arterialized venous flaps from the thenar and hypothenar regions for repairing finger pulp tissue losses. *Plast Reconstr Surg* 1997;99:1765-1770.

87. Klein, C., Kovacs, A., Stuckensen, T. Free arterialised venous forearm flaps for intraoral reconstruction. *Br J Plast Surg* 1997;50:166-171.

88. Ueda, Y., Mizumoto, S., Hirai, T., Doi, Y., Fukui, A., Tamai, S. Two-stage arterialized flow-through venous flap transfer for third-degree burn defects on the dorsum of the hand. *J Reconstr Microsurg* 1997;13:489-496.

89. Inoue, G., Maeda, N. Complications in wrap-around-flap donor sites after reconstruction using an arterialized venous flap. *J Reconstr Microsurg* 1998;14:377-380; discussion 380-371.

90. Kantarci, U., Cepel, S., Gurbuz, C. Venous free flaps for reconstruction of skin defects of the hand. *Microsurgery* 1998;18:166-169.

91. Kayikcioglu, A., Akyurek, M., Safak, T., Ozkan, O., Kecik, A. Arterialized venous dorsal digital island flap for fingertip reconstruction. *Plast Reconstr Surg* 1998;102:2368-2372; discussion 2373.

92. Ayad, H. Free arterialized venous flap. *Annals of burns and fire disasters* 1999;12:158-163.

93. Cho, B. C., Byun, J. S., Baik, B. S. Dorsalis pedis tendocutaneous delayed arterialized venous flap in hand reconstruction. *Plast Reconstr Surg* 1999;104:2138-2144.

94. Koch, H., Moshammer, H., Spendel, S., Pierer, G., Scharnagl, E. Wrap-around arterialized venous flap for salvage of an avulsed finger. *J Reconstr Microsurg* 1999;15:347-350.

95. Patradul, A., Ngarmukos, C., Parkpian, V., Kitidumrongsook, P. Arterialized venous toenail flaps for treating nail loss in the fingers. *J Hand Surg Br* 1999;24:519-524.

96. Cunha-Gomes, D., Bhathena, H., Kavarana, N. M. Case report: a free arterialized venous flap for intraoral cancer reconstruction. *Acta Chir Plast* 2000;42:13-15.

97. Klein, C. Erfahrungen mit arterialisierten Venenlappen zur intraoralen Defektdeckung. *ZENTRALBLATT FUR CHIRURGIE* 2000;125:51-55.

98. Reynoso, R., Haddad, J. L., Sastre, N. A few considerations regarding enhancement of arterialized skin flap survival. *Microsurgery* 2000;20:176-180.

99. Takeuchi, M., Sakurai, H., Sasaki, K., Nozaki, M. Treatment of finger avulsion injuries with innervated arterialized venous flaps. *Plast Reconstr Surg* 2000;106:881-885.

100. Alexander, G. Multistage type III venous flap or 'pre-arterialisation of an arterialised venous flap'. *Br J Plast Surg* 2001;54:734.

101. Chia, J., Lim, A., Peng, Y. P. Use of an arterialized venous flap for resurfacing a circumferential soft tissue defect of a digit. *Microsurgery* 2001;21:374-378.

102. Murata, K., Inada, Y., Fukui, A., Tamai, S., Takakura, Y. Clinical application of the reversed pedicled venous flap containing perivenous areolar tissue and/or nerve in the hand. *Br J Plast Surg* 2001;54:615-620.

103. Safak, T., Akyurek, M. Cephalic vein-pedicled arterialized anteromedial arm venous flap for head and neck reconstruction. *Ann Plast Surg* 2001;47:446-449.

104. Woo, S. H., Seul, J. H. Optimizing the correction of severe postburn hand deformities by using aggressive contracture releases and fasciocutaneous free-tissue transfers. *Plast Reconstr Surg* 2001;107:1-8.

105. Woo, S. H., Seul, J. H. Pre-expanded arterialised venous free flaps for burn contracture of the cervicofacial region. *Br J Plast Surg* 2001;54:390-395.

106. Wungcharoen, B., Santidhananon, Y., Chongchet, V. Pre-arterialisation of an arterialised venous flap: clinical cases. *Br J Plast Surg* 2001;54:112-116.

107. Brooks, D., Buntic, R., Buncke, H. J. Use of a venous flap from an amputated part for salvage of an upper extremity injury. *Ann Plast Surg* 2002;48:189-192.

108. De Lorenzi, F., van der Hulst, R. R., den Dunnen, W. F., et al. Arterialized venous free flaps for soft-tissue reconstruction of digits: a 40-case series. *J Reconstr Microsurg* 2002;18:569-574; discussion 575-567.

109. Kushima, H., Iwasawa, M., Maruyama, Y. Recovery of sensitivity in the hand after reconstruction with arterialised venous flaps. *Scandinavian journal of plastic and reconstructive surgery and hand surgery* 2002;36:362-367.

110. Aoki, M., Watanabe, K., Kura, S.-j., Yamashita, T. Flag flap for coverage of a skin defect caused after debridement of chronic osteomyelitis of the proximal phalanx of the 5th toe. *The Foot* 2003;13:171-173.

111. Cheng, T. J., Chen, Y. S., Tang, Y. B. Use of a sequential two-in-one free arterialised venous flap for the simultaneous reconstruction of two separate defects on the foot. *Br J Plast Surg* 2004;57:685-688.

112. Koch, H., Scharnagl, E., Schwarzl, F. X., Haas, F. M., Hubmer, M., Moshammer, H. E. Clinical application of the retrograde arterialized venous flap. *Microsurgery* 2004;24:118-124.

113. Kopp, J., Bach, A., Loos, B., et al. [Use of vacuum therapy during defect coverage of the upper extremity with microsurgically grafted arterialized venous flaps]. *Zentralbl Chir* 2004;129 Suppl 1:S82-84.

114. Lin, C. H., Wei, F. C., Lin, Y. T., Chen, C. T. Composite palmaris longus-venous flap for simultaneous reconstruction of extensor tendon and dorsal surface defects of the hand--long-term functional result. *J Trauma* 2004;56:1118-1122.

115. Nakazawa, H., Nozaki, M., Kikuchi, Y., Honda, T., Isago, T. Successful correction of severe contracture of the palm using arterialized venous flaps. *J Reconstr Microsurg* 2004;20:527-531.

116. Nakazawa, H., Kikuchi, Y., Honda, T., Isago, T., Morioka, K., Itoh, H. Use of an arterialised venous skin flap in the replantation of an amputated thumb. *Scand J Plast Reconstr Surg Hand Surg* 2004;38:187-191.

117. Titley, O. G., Chester, D. L., Park, A. J. A-a type, arterialized, venous, flow-through, free flap for simultaneous digital revascularization and soft tissue reconstruction-revisited. *Ann Plast Surg* 2004;53:185-191.

118. Deune, E. G., Rodriguez, E., Hatef, D., Frassica, F. Arterialized venous flow-through flap for simultaneous reconstruction of a radial artery defect and palmar forearm soft-tissue loss from sarcoma resection. *J Reconstr Microsurg* 2005;21:85-91.

119. Hyza, P., Vesely, J., Stupka, I., Cigna, E., Monni, N. The bilobed arterialized venous free flap for simultaneous coverage of 2 separate defects of a digit. *Ann Plast Surg* 2005;55:679-683.

120. Kopp, J., Bach, A. D., Kneser, U., Loos, B., Horch, R. E. [Use of vacuum therapy in a huge arterialized venous flap to reconstruct a complete avulsion of a thumb]. *Zentralbl Chir* 2006;131 Suppl 1:S3-6.

121. Mureau, M. A., Flood, S. J., Hofer, S. O. Total peroneal artery occlusion during fibula free flap harvesting: salvage using the venous flow-through principle. *Plast Reconstr Surg* 2006;117:101e-106e.

122. Pellini, R., Pichi, B., Ruggieri, M., Ruscito, P., Spriano, G. Venous flow-through flap as an external monitor for buried radial forearm free flap in head and neck reconstruction

J Plast Reconstr Aesthet Surg 2006;59:1217-1221.

123. Yokoyama, T., Hosaka, Y., Kusano, T., Morita, M., Takagi, S. Finger palmar surface reconstruction using medial plantar venous flap: possibility of sensory restoration without neurorrhaphy. *Ann Plast Surg* 2006;57:552-556.

124. Brooks, D., Buntic, R. F., Taylor, C. Use of the venous flap for salvage of difficult ring avulsion injuries. *Microsurgery* 2008;28:397-402.

125. Hyza, P., Vesely, J., Novak, P., Stupka, I., Sekac, J., Choudry, U. Arterialized venous free flaps--a reconstructive alternative for large dorsal digital defects. *Acta Chir Plast* 2008;50:43-50.

126. Iglesias, M., Butron, P., Chavez-Munoz, C., Ramos-Sanchez, I., Barajas-Olivas, A. Arterialized venous free flap for reconstruction of burned face. *Microsurgery* 2008;28:546-550.

127. Kakinoki, R., Ikeguchi, R., Nankaku, M., Nakamua, T. Factors affecting the success of arterialised venous flaps in the hand. *Injury* 2008;39:18-24.

128. Kim, J. S., Choi, T. H., Kim, N. G., et al. Flow-through arterialised venous free flap using the long saphenous vein for salvage of the upper extremity. *Scand J Plast Reconstr Surg Hand Surg* 2008;42:218-223.

129. Kong, B. S., Kim, Y. J., Suh, Y. S., Jawa, A., Nazzal, A., Lee, S. G. Finger soft tissue reconstruction using arterialized venous free flaps having 2 parallel veins. *J Hand Surg Am* 2008;33:1802-1806.

130. Tang, W. R., Varkey, P., Girotto, R., Tan, N. C., Rose, V., Chen, H. C. The venous flap - a safe alternative to the simple vein graft in a special situation. *J Plast Reconstr Aesthet Surg* 2008;61:434-437.

131. Trovato, M. J., Brooks, D., Buntic, R. F., Buncke, G. M. Simultaneous coverage of two separate dorsal digital defects with a syndactylizing venous free flap. *Microsurgery* 2008;28:248-251.

132. Yokoyama, T., Cardaci, A., Hosaka, Y., Revol, M., d'Alcontres, F. S., Servant, J. M. Location of communicating veins for medial plantar venous flap. *Ann Plast Surg* 2008;61:99-104.

133. Yokoyama, T., Hosaka, Y., Servant, J. M., Takagi, S., Cardaci, A. A simplification for harvesting medial plantar venous flap with communicating veins: usefulness of preoperative ultrasound imaging. *Ann Plast Surg* 2008;60:379-385.

134. Cil, Y., Kocman, A. E., Yapici, A. K. Distally based venous flap: a new technique for the correction of syndactyly without skin graft in adult patients. *Chir Organi Mov* 2009;93:123-129.

135. Ueda, K., Nuri, T., Akamatsu, J., Sugita, N., Otani, K. Clinical trial of delay of the venous island flap. *Plast Reconstr Surg* 2010;126:104e-105e.

136. Yokoyama, T., Tosa, Y., Hashikawa, M., Kadota, S., Hosaka, Y. Medial plantar venous flap technique for volar oblique amputation with no defects in the nail matrix and nail bed. *J Plast Reconstr Aesthet Surg* 2010.

137. Park, S. W., Heo, E. P., Choi, J. H., et al. Reconstruction of defects after excision of facial skin cancer using a venous free flap. *Ann Plast Surg* 2011;67:608-611.

138. Rounds, K., Buntic, R., Brooks, D. Artery-vein-artery venous flap for simultaneous soft-tissue repair and radial artery reconstruction: case report. *J Hand Surg Am* 2011;36:1339-1342.

139. Davami, B., Arasteh, E., Pourkhamene, G. Versatility of venous flap for coverage of proximal and middle phalanges of fingers. *Techniques in hand & upper extremity surgery* 2012;16:23-26.

140. Rozen, W. M., Ting, J. W., Gilmour, R. F., Leong, J. The arterialized saphenous venous flow-through flap with dual venous drainage. *Microsurgery* 2012;32:281-288.

141. Yan, H., Gao, W., Zhang, F., Li, Z., Chen, X., Fan, C. A comparative study of finger pulp reconstruction using arterialised venous sensate flap and insensate flap from forearm. *J Plast Reconstr Aesthet Surg* 2012;65:1220-1226.

142. Kawakatsu, M., Ishikawa, K., Sawabe, K. Free arterialised flow-through venous flap with venous anastomosis as the outflow (A-A-V flap) for reconstruction after severe finger injuries. *Journal of plastic surgery and hand surgery* 2013;47:66-69.

143. Lam, W., Lin, W., Bell, D., Higgins, J., Lin, Y., Wei, F. The physiology, microcirculation and clinical application of the shunt-restricted arterialized venous flaps for the reconstruction of digital defects. *Journal of Hand Surgery (European Volume)* 2012:1753193412468632.

144. Ueda, K., Nuri, T., Akamatsu, J., Sugita, N., Otani, K., Yamada, A. Delay of the reverse pedicled venous island flap: clinical applications. *Journal of plastic surgery and hand surgery* 2013;47:350-354.

145. Walle, L., Vollbach, F., Fansa, H. [Arterialized venous free flaps for resurfacing hand and finger defects]. *Handchirurgie, Mikrochirurgie, plastische Chirurgie: Organ der Deutschsprachigen Arbeitsgemeinschaft fur Handchirurgie: Organ der*

Deutschsprachigen Arbeitsgemeinschaft fur Mikrochirurgie der Peripheren Nerven und Gefasse: Organ der V 2013;45:160-166.

146. Giesen, T., Forster, N., Kunzi, W., Giovanoli, P., Calcagni, M. Retrograde arterialized free venous flaps for the reconstruction of the hand: review of 14 cases. *J Hand Surg Am* 2014;39:511-523.

147. Han, S. K., Kim, S. Y., Gu, J. H., Jeong, S. H., Kim, W. K. Influence of the pedicle orientation and length on viability of unipedicled venous island flaps. *Microsurgery* 2014;34:197-202.

148. Kayalar, M., Levent, K., Sugun, T. S., Gurbuz, Y., Savran, A., Kaplan, I. Syndactylizing arterialized venous flaps for multiple finger injuries. *Microsurgery* 2014.

149. Kayalar, M., Kucuk, L., Sugun, T. S., Gurbuz, Y., Savran, A., Kaplan, I. Clinical applications of free arterialized venous flaps. *J Plast Reconstr Aesthet Surg* 2014.

150. Liu, Y., Jiao, H., Ji, X., et al. A comparative study of four types of free flaps from the ipsilateral extremity for finger reconstruction. *PloS one* 2014;9:e104014.

151. Sakamoto, N., Matsumura, H., Komiya, T., Imai, R., Niyaz, A., Watanabe, K. Syndactyly correction using a venous flap with the plantar cutaneous venous arch. *Ann Plast Surg* 2014;72:643-648.

152. Park, J. U., Kim, K., Kwon, S. T. Venous free flaps for the treatment of skin cancers of the digits. *Ann Plast Surg* 2015;74:536-542.

Chapter 4

UNCONVENTIONAL PERFUSION FLAPS IN THE EXPERIMENTAL SETTING: A SYSTEMATIC REVIEW AND META-ANALYSIS

Authors: Diogo Casal, M.D.[1,2,3], David Tanganho M.D.[1,2], Teresa Cunha, M.D. [1,2], Eduarda Mota-Silva, M.Sc.[1,2,4], Inês Iria, M.Sc.[5], Diogo Pais, M.D., PhD[2], Paula Antunes Videira, PhD[3], José Videira e Castro, M.D.[1], João Goyri O'Neill, M.D., PhD.[2]

Affiliations:

1- Plastic and Reconstructive Surgery Department and Burn Unit; Centro Hospitalar de Lisboa Central, Lisbon, Portugal

2- Anatomy Department; Nova Medical School, Lisbon, Portugal

3- UCIBIO, Departamento de Ciências da Vida, Faculdade de Ciências e Tecnologias, Universidade NOVA de Lisboa, Caparica, Portugal

4- LIBPhys – Physics Department, Faculdade de Ciências e Tecnologias, Universidade NOVA de Lisboa, Caparica, Portugal

5- Molecular Microbiology and Biotechnology Unit|Drug Discovery Area; Faculdade de Farmácia, Universidade de Lisboa, Lisbon, Portugal

ABSTRACT

Background: Unconventional perfusion flaps (**UPFs**) offer multiple potential advantages compared to traditional flaps. Although there are numerous experimental papers on UPFs, the multiple animal species involved, the myriad vascular constructions used, and the frequently conflicting data reported makes synthesis of this information challenging. The main aim of this paper was to perform a systematic review and meta-analysis of the literature on the experimental use of UPFs, in order to identify the best experimental models proposed as well as to estimate their global survival rate.

Methods: We performed a systematic review and meta-analysis of all the articles written in English, French, Italian, Spanish and Portuguese on the experimental use of UPFs and indexed to PubMed since 1981 until the 1st February 2017.

Results: A total of 68 studies were found, corresponding to 86 optimized experimental models and to 1073 UPFs. Overall UPF survival rate was 90.8% (95% CI, 86.9% to 93.6%; $p<0.001$). The estimated proportion of experimental UPFs presenting complete survival or nearly complete survival was 74.4% (95% CI, 62.1% to 83.7%; $p<0.001$). The most commonly reported animal species in the literature were the rabbit (57.1%), the rat (26.4%), and the dog (14.3%). No significant differences were found in survival rates among these species, nor among the diverse vascular patterns used.

Conclusions: These data do not differ significantly from those reported regarding the use of UPFs in human medicine, suggesting that rabbit, rat and canine experimental UPF models may adequately mimic the clinical application of UPFs.

INTRODUCTION

Unconventional perfusion flaps (**UPFs**) have been increasingly used in the clinical setting for the past four decades, offering multiple advantages relatively to traditional flaps.(1) Being composite blocks of tissues perfused solely through their venous system, their dissection is relatively simple, expeditious and not associated with major donor site morbidity. Moreover, these flaps, which comprise arterialized venous flaps (**AVFs**) and venous flaps (**VFs**), are intrinsically thin and pliable. These last features are potentially highly advantageous for reconstructing shallow defects particularly in mobile regions where the integument is thin, namely in the upper limb, in the face and the external genitalia.(1-5) Finally, as they are usually tailored around the superficial venous system, which is often visible through the skin, their harvesting precludes the need of ancillary pre-operative tests. Consequently, UPFs are particularly useful for emergent reconstruction in the realm of trauma cases.

Even though there are several clinical and experimental papers on UPFs, the multiple animal species involved, the myriad vascular constructions used, and the frequently conflicting data reported makes synthesis of this information challenging. For this reason, even today many surgeons and researchers are discouraged from using these flaps in either the clinical or the experimental settings.(1-6) Thus, it would be of paramount importance to find patterns in the available literature on UPFs, with the goal to facilitate knowledge acquisition by novices in the field, and to aid in future experimental works.

Hence, the main aim of this paper was to perform a systematic review and meta-analysis of the literature on the experimental use of UPFs, in order to identify the best

experimental models proposed as well as to estimate their global survival rate. Secondarily, this paper aimed at estimating the UPF survival rate for each animal species and vascular patterns used in these optimized experimental models.

METHODS

On the 1st February 2017, the authors searched the PubMed database concerning experimental animal models of UPFs (**Fig. 1**). The following terms were used: “arterialized venous flap”; “arterialised venous flap”; “unconventional flap”; “unconventional perfusion flap”; “non-conventional flap”; “non-conventional perfusion flap”; “venous flap” and “venous perfusion flap”. These search terms were combined with the Boolean operators ‘‘OR” and “AND”.

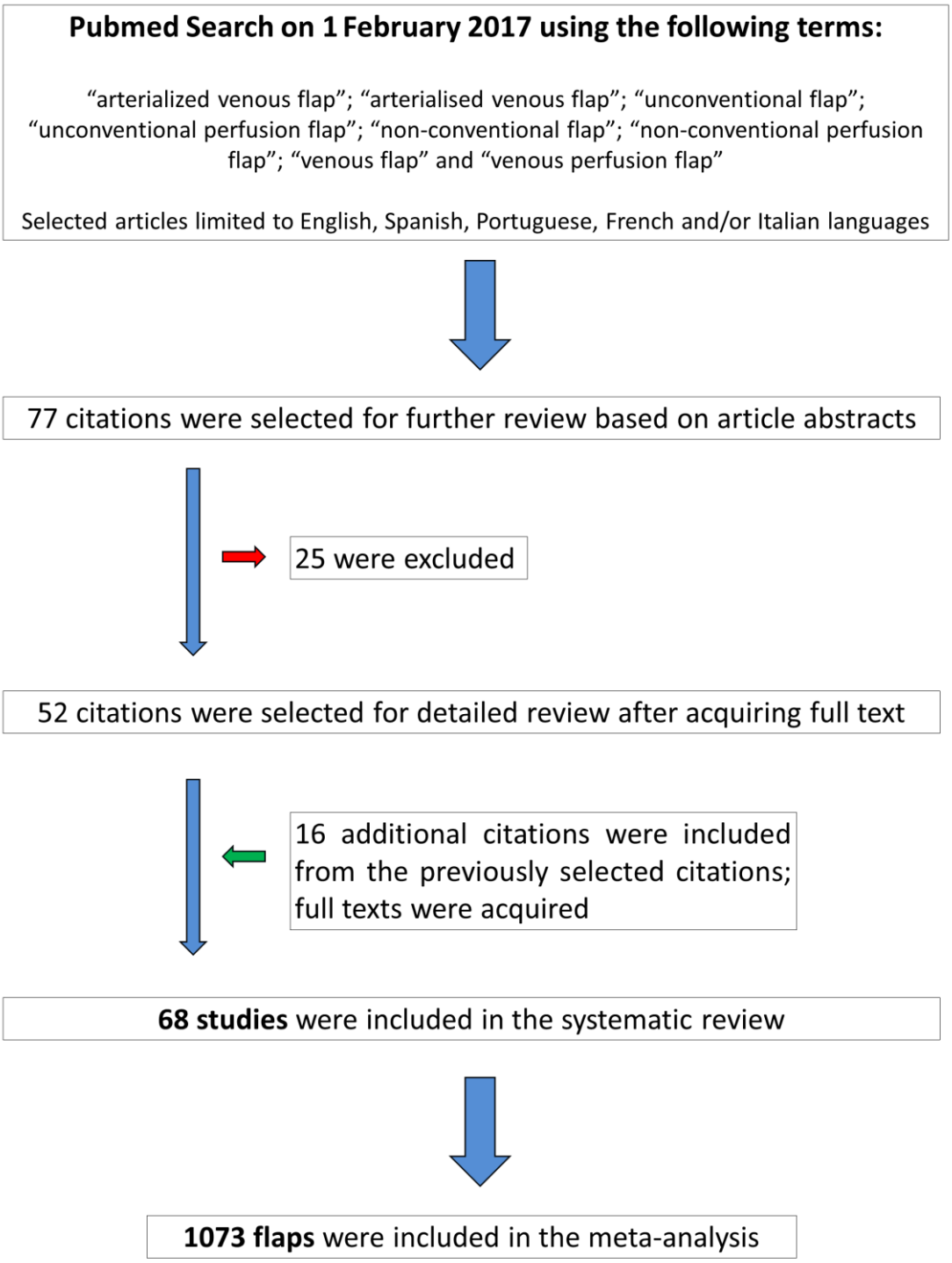

Figure 1 - Data collection from the literature. A total of 68 studies were retrieved from the literature, corresponding to data from 1073 individual unconventional perfusion flaps.

Inclusion Criteria

All articles reporting experimental animal studies, written in English, Spanish, Portuguese, French or Italian, and describing qualitatively and/or quantitatively flap survival and/or necrosis were selected.

Exclusion Criteria

The following articles/experimental models were excluded from the analysis:

1 - Studies written in different languages from those mentioned above;

2- Articles referring exclusively to human or dissection studies;

3- Studies/experimental models addressing solely histological features or pharmacological and/or genetic manipulation of flaps with no information regarding quantitative or qualitative evaluation of flap necrosis or survival;

4- Studies/experimental models whose flap vascular network included total blood flow reversal at the expense of one major artery without apparent potential clinical benefit;

5- Studies/experimental models addressing revascularization of the extremities by reverse circulation;

6- Papers/experimental models describing exclusively pre-fabricated flaps with arteriovenous fistulas, since these flaps tend to behave similarly to conventional perfusion flaps.(7, 8)

In each paper included for analysis, individuals whose vascular anastomoses presented thrombosis were excluded from the analysis.

The title and abstract of all identified studies were examined independently by three reviewers (D.C., D.T. and T.C.). In cases where suitability of a given study for inclusion in the review was not clear, the entire article was obtained and evaluated for appropriateness. Furthermore, the references contained in the retrieved articles were scanned by the three independent reviewers, in order to obtain further articles that were missed in the first-round search. All articles were acquired in their full-text version and read independently by the three reviewers.

For each study, the following variables were recorded: year of publication; nationality; animal species, and strains used, as well as experimental animal gender. When a study reported more than one vascular construction, the one or ones with a better flap survival rate ($p<0.05$) was/were chosen as **optimized experimental models**. These models were used as individual units for the sake of subsequent statistical analysis.

For each experimental model, the following parameters were assessed: number of animals used; anatomical region of the UPF donor site; vascular pattern used to perfuse the flap (1) (when considering rabbit ears, the authors took into consideration that the largest veins [central vein, anterior marginal vein and posterior marginal vein] are devoid of venous valves (9, 10)); vascularization of the recipient wound bed (*well vascularized* if the flap was placed over viable muscle, fascia, fat, synovial tissue, epitenon or granulation tissue; and *non-vascularized*, if the flap was placed over bone, cartilage or prosthetic material); application of an impermeable barrier between the flap and the recipient bed (to prevent diffusion of oxygen and nutrients and/or neoangiogenesis from the wound to the deep aspect of the flap); resort to flap delay procedures; flap composition; flap innervation; flap survival rate; percentage of flaps

that presented *complete survival* (defined as 100% survival area or superficial necrosis with self-healing of the flap's surface at its latest evaluation), *nearly complete survival* (considered 85 to 100% flap survival or unspecified inconsequential "marginal necrosis"), *significant necrosis* (> 15% flap necrosis) and *complete necrosis* (100% flap necrosis or "non-surviving flaps"). If in doubt, a higher necrosis category was considered for each experimental model. The numeric values of necrosis considered were always those reported on the last day of the experiments described in each individual article.

The presence and nature of complications were also recorded (epidermolysis, flap congestion and venous insufficiency by themselves were not considered complications, as they were reportedly present in the first few days after surgery according to most authors). *Epidermolysis* was considered to be present when there was only evidence of the epidermis being loosely attached to the dermis, readily exfoliating or forming blisters.(11) If the damage to the skin extended deeper than the epidermis, flap necrosis was considered to be present, as described above.

When estimating effect sizes for the entire population, the authors only included studies with at least 3 animals, to minimize publication bias. Whenever individual animal data were present in papers, they were used for individual data meta-analysis. (12)

The data were retrieved from the available literature, each parameter at a time, from each paper in turn. Finally, the data were inserted into an Excel database (Microsoft Corp., Redmond, Wash.®). When discrepancies were found in data retrieval, the articles were reanalyzed by the three reviewers independently.

Statistical Analysis

Quantitative variables were expressed as means ± standard deviation. Qualitative variables were expressed as percentages. IBM SPSS Version 21.0 software (IBM Corp., Armonk, N.Y.®) was used for descriptive and inferential statistical analysis.

The Kolmogorov-Smirnov test was used to assess whether variables were normally distributed. Analysis of variance and *t-student* tests were used to compare averages in normally distributed data. Kruskal-Wallis and Mann-Whitney tests were used to compare means in non-normally distributed data. Proportions were analyzed with the Chi-square test or Fisher's exact test. Dichotomous variables were compared with the binomial test. Association between numerical variables was assessed using Pearson's correlation coefficient.

The Comprehensive Meta-Analysis 2.0 software (Biostat, Englewood, N.J.®) was used to estimate population summary effects and to produce forest and funnel plots using random-effects models. Studies heterogeneity for each parameter was assessed using Cochran's Q test, I-squared and Tau-squared statistics.(13) Evidence of publication bias was investigated through evaluation of funnel plot symmetry and by application of the Egger's test.(14, 15)

A two-tail value of $p < 0.05$ was considered to be statistically significant.

RESULTS

The systematic review of the literature allowed the identification of 68 studies on the experimental use of UPFs in the experimental setting (**Fig. 1**). Overall, this corresponded to a total of 1073 flaps. Among these studies, it was possible to identify 86 optimized experimental models of UPFs. The features of these models are summarized in **Table 1**.

First Author	Year	Country	Optimized experimental animal model	Species	Strain	Gender	n	Flap donor site	Flap vascular pattern	Wound bed blood supply	Delayed flap	Flap composition	Flap innervation preserved	Flap survival rate (%)	Categorical flap survival (%)				Necrotic flap area (%)		
															CS	NCS	SN	CN	Average	Min.	Max.
Nakayama (16)	1981	Japan	1	Rat	n/a	M	5	T/A	6	WV	Yes	FC	n/a	100	100	0	0	0	0	0	0
			2	Rat	n/a	M	10	T/A	6	WV	No	FC	n/a	100	n/a	n/a	0	0	2	0	2.7
			3	Rat	n/a	M	20	T/A	4	WV	No	FC	n/a	100	n/a	n/a	n/a	0	7	0	21
Voukidis (17)	1982	UK	4	Rat	SD	M+F	10	A/G	3	IB	Yes	FC	No	100	n/a	n/a	n/a	0	n/a	n/a	n/a
Mundy (18)	1984	USA	5	Rabbit	n/a	n/a	5	E	1	B/C	Yes	FC	No	n/a	n/a	n/a	n/a	n/a	13	n/a	n/a
			6	Rabbit	n/a	n/a	5	E	1	B/C	No	FC	No	n/a	n/a	n/a	n/a	n/a	24	n/a	n/a
Ji (19)	1984	China	7	Rabbit	n/a	M+F	33	E	1	B/C	No	FC	No	100	90.9	0	9.1	0	n/a	0	n/a
Beehary (20)	1984	France	8	Rat	n/a	n/a	5	A/G	3	WV	No	FC	n/a	100	100	0	0	0	0	0	0
Baek (21)	1985	South Korea	9	Dog	M	n/a	36	H	10	WV	No	FC	No	100	100	0	0	0	0	0	0
			10	Dog	M	n/a	10	H	10	IB	No	FC	No	100	100	0	0	0	0	0	0
			11	Dog	M	n/a	2	H	7	WV	No	FC	No	100	100	0	0	0	0	0	0
Nichter (10)	1985	USA	12	Rabbit	NZ	M	10	E	2	SE	No	B/C	No	100	n/a	n/a	n/a	0	n/a	n/a	n/a
Thatte (22)	1987	India	13	Dog	M	M+F	14	H	10	WV	No	FC	No	91.7	n/a	n/a	n/a	8.33	n/a	n/a	100
Germann (23)	1987	Germany	14	Pig	Y	M	12	H	5	WV	No	FC	Yes	0	0	0	0	100	100	100	100
Amarante (24)	1988	Portugal	15	Dog	n/a	n/a	5	H	10	WV	No	FC	Yes	100	100	0	0	0	0	0	0
			16	Dog	n/a	n/a	5	H	9	WV	No	FC	Yes	100	100	0	0	0	0	0	0
			17	Dog	n/a	n/a	4	H	7	WV	No	FC	Yes	100	100	0	0	0	0	0	0
Fukui (25)	1988	Japan	18	Rabbit	n/a	n/a	20	E	10	B/C	No	FC	No	100	90	10	0	0	n/a	0	n/a
Sasa (26)	1988	USA	19	Dog	M	M+F	8	F	10	WV	No	FC	No	75	0	75	0	25	n/a	n/a	100
Inada (27)	1989	Japan	20	Rabbit	n/a	n/a	20	E	10	B/C	No	FC	No	100	90	0	10	0	n/a	0	n/a
			21	Rabbit	n/a	n/a	21	E	1	B/C	No	FC	No	100	85.7	0	14.3	0	n/a	0	n/a
Yuen (28)	1991	China	22	Rat	W	M	10	A/G	9	WV	No	FC	n/a	90	80	n/a	n/a	10	n/a	0	100
			23	Rat	W	M	10	A/G	9	IB	No	FC	n/a	100	90	n/a	n/a	0	n/a	0	n/a
Noreldin (29)	1992	USA	24	Rat	W	M	20	A/G	10	WV	No	FC	n/a	90	75	n/a	n/a	10	n/a	0	100
Takato (30)	1992	Canada	25	Rabbit	NZ	F	18	A/G	3	WV	No	FC	No	100	66.7	33.3	0	0	2.4	0	10
Chow (31)	1992	China	26	Rat	SD	n/a	20	A/G	3	WV	No	FC	n/a	n/a	n/a	n/a	n/a	n/a	39.6	n/a	n/a
Angel (32)	1992	USA	27	Dog	n/a	n/a	6	H	10	WV	No	FC	No	100	n/a	n/a	n/a	0	n/a	n/a	n/a
Inada (33)	1992	Japan	28	Rabbit	n/a	n/a	10	E	10	B/C	No	FC	Yes	100	0	0	100	0	56	30	78
Inada (34)	1993	Japan	29	Rabbit	J	n/a	18	E	1	B/C	No	FC	n/a	100	n/a	n/a	0	0	n/a	n/a	n/a
			30	Rabbit	J	n/a	17	E	2	B/C	No	FC	n/a	100	n/a	n/a	0	0	n/a	n/a	n/a
Matsushita (35)	1993	USA	31	Rabbit	NZ	M+F	6	T/A	10	WV	No	FC	Yes	100	83.3	n/a	n/a	0	n/a	0	n/a
Gençosmanoglu (36)	1993	Turkey	32	Rabbit	n/a	n/a	10	T/A	10	WV	No	FC	Yes	100	80	20	0	0	n/a	0	n/a
Ueda (37)	1993	Japan	33	Rabbit	n/a	n/a	15	E	10	SE	Yes	B/C	Yes	100	n/a	n/a	n/a	0	n/a	n/a	n/a
Fukui (38)	1993	Japan	34	Rat	F	M	28	D	10	WV	No	MFC	Yes	85.7	85.7	0	0	14.3	14.3	0	100
Takato (39)	1993	Japan	35	Rabbit	NZ	M	5	A/G	10	IB	No	FC	n/a	100	0	0	100	0	74.8	67.6	79.7
Thatte (40)	1993	India	36	Rat	W	M	5	A/G	10	WV	No	FC	n/a	100	n/a	n/a	n/a	0	n/a	n/a	n/a
Lenoble (41)	1993	France	37	Rat	W	M+F	15	A/G	10	WV	No	FC	Yes	26.7	0	20	6.7	73.3	77	10	100
Smith (42)	1994	USA	38	Rabbit	NZ	n/a	10	E	10	B/C	No	FC	n/a	100	70	n/a	n/a	0	18.1	0	n/a
Dvir (43)	1994	Australia	39	Dog	M	n/a	6	F	10	WV	No	FC	n/a	66.7	33.3	0	33.3	33.3	41.7	0	100
			40	Dog	M	n/a	6	F	1	WV	No	FC	n/a	66.7	33.3	16.7	16.7	33.3	41.7	0	100
			41	Dog	M	n/a	6	F	4	WV	No	FC	n/a	66.7	50	0	16.7	33.3	46.7	0	100
Suzuki(44)	1994	Japan	42	Rabbit	J	M	6	E	1	B/C	No	FC	Yes	100	n/a	n/a	n/a	0	n/a	n/a	n/a
Wolff (45)	1995	Germany	43	Rat	W	M	7	A/G	4	WV	No	FC	n/a	100	14.3	57.1	28.6	0	7	0	16
Byun (46)	1995	USA	44	Rabbit	NZ	M	8	E	3	SE	Yes	B/C	Yes	100	0	100	0	0	5.9	n/a	n/a
Xiu (47)	1996	China	45	Rabbit	n/a	n/a	20	T/A	10	WV	No	FC	n/a	n/a	n/a	n/a	n/a	n/a	7.68	n/a	n/a
Pittet (48)	1996	USA	46	Rabbit	NZ	n/a	16	E	1	B/C	No	FC	No	100	100	0	0	0	0	0	1
Adamo (49)	1996	Italy	47	Rat	W	n/a	10	T/A	10	WV	No	FC	n/a	100	n/a	n/a	40	0	n/a	n/a	n/a
			48	Rat	W	n/a	10	T/A	10	IB	No	FC	n/a	100	n/a	n/a	30	0	n/a	n/a	70
Xiu (50)	1996	China	49	Rabbit	n/a	n/a	40	T/A	10	WV	No	FC	No	n/a	n/a	n/a	n/a	n/a	31.3	0	100
Miles (51)	1997	Canada	50	Rat	SD	M	4	T/A	5	WV	No	FC	n/a	n/a	n/a	n/a	n/a	n/a	43	n/a	n/a
Yilmaz (52)	1997	Turkey	51	Rabbit	NZ	n/a	12	E	10	SE	No	B/C	No	83.3	41.7	n/a	n/a	16.7	24.2	0	100
Fukui (53)	1998	Japan	52	Rabbit	n/a	n/a	22	E	1	WV	Yes	FC	No	100	54.6	n/a	n/a	0	n/a	0	n/a
Woo (54)	1998	South Korea	53	Dog	M	M+F	12	H	4	IB	No	FC	n/a	n/a	n/a	n/a	n/a	n/a	3.8	n/a	n/a
Yuan (55)	1998	China	54	Rabbit	NZ	n/a	38	E	10	SE	No	B/C	No	100	n/a	n/a	n/a	0	n/a	n/a	n/a
Atabey (56)	1998	Turkey	55	Rabbit	NZ	n/a	10	T/A	10	WV	No	FC	No	30.0	30	0	0	70	30	0	100
Cho (57)	1998	South Korea	56	Rabbit	NZ	M	7	E	1	SE	Yes	B/C	Yes	100	0	0	100	0	40.3	22	56
Mutaf (58)	1998	Japan	57	Rat	L	n/a	10	T/A	10	IB	Yes	FC	n/a	n/a	n/a	n/a	n/a	n/a	37.4	n/a	n/a
Yilmaz (59)	1999	Turkey	58	Rabbit	NZ	n/a	12	E	1	IB	No	B/C	No	83.3	58.3	n/a	n/a	16.7	22	0	100
Murata (60)	1999	Japan	59	Rabbit	n/a	n/a	10	E	10	WV	No	FC	Yes	100	10	n/a	n/a	0	17.5	0	100
Yücel (61)	2000	Turkey	60	Rat	SD	M	32	A/G	10	WV	No	FC	No	0	0	0	0	100	100	100	100
Tang (62)	2000	Taiwan	61	Rabbit	NZ	n/a	30	T/A	10	WV	No	MFC	No	100	n/a	n/a	n/a	0	n/a	0	n/a
Wungcharoen (63)	2001	Thailand	62	Rat	W	M	9	T/A	3	IB	Yes	FC	No	n/a	n/a	n/a	n/a	n/a	2.5	n/a	n/a
Saray (64)	2002	Turkey	63	Rabbit	n/a	n/a	10	E	10	IB	No	FC	No	100	n/a	n/a	n/a	0	41.9	n/a	n/a
Chang (65)	2003	China	64	Rabbit	NZ	n/a	10	H	8	IB	No	FC	Yes	100	50	50	0	0	5.5	0	n/a
Coruh (66)	2004	Turkey	65	Rabbit	NZ	M	10	E	10	B/C	No	FC	No	100	0	0	100	0	40	26.0	77.6
			66	Rabbit	NZ	M	10	E	10	B/C	No	FC	No	100	0	0	100	0	42	19.7	55.4
Lin (67)	2004	Taiwan	67	Rabbit	NZ	n/a	13	E	10	SE	No	B/C	No	100	n/a	n/a	n/a	0	6.6	0	55.6
Baser (68)	2005	Turkey	68	Rat	SD	n/a	6	D	10	WV	Yes	FC	n/a	100	16.7	0	83.3	0	37.5	0	46
Zhang (69)	2006	USA	69	Rat	SD	M	10	A/G	10	WV	No	FC	No	n/a	n/a	n/a	n/a	n/a	61	n/a	n/a
Özyazgan (70)	2007	Turkey	70	Rabbit	NZ	n/a	7	E	10	B/C	No	FC	No	n/a	n/a	n/a	n/a	n/a	44	n/a	n/a
Özyazgan (71)	2007	Turkey	71	Rabbit	NZ	M	14	E	10	B/C	No	FC	No	n/a	n/a	n/a	n/a	n/a	39	n/a	n/a
Pittet (72)	2008	Switzerland	72	Rabbit	NZ	n/a	15	E	1	WV	No	FC	No	100	n/a	n/a	0	0	0.6	0	n/a
			73	Rabbit	NZ	n/a	19	E	1	WV	No	FC	No	100	n/a	n/a	6	0	5.3	n/a	n/a
			74	Rabbit	NZ	n/a	14	E	1	IB	No	FC	No	100	n/a	n/a	8	0	6.5	n/a	n/a
Tan (73)	2009	Singapore	75	Rabbit	NZ	M+F	10	T/A	3	IB	No	FC	No	80.0	40	0	40	20	55.5	0	100
Yan (74)	2010	USA	76	Rat	SD	M	8	A/G	4	WV	Yes	FC	n/a	100	0	100	0	0	2	n/a	n/a
Lalkovic (75)	2010	Serbia	77	Rabbit	BC	n/a	10	E	3	SE	No	B/C	No	100	n/a	n/a	n/a	0	1.7	n/a	n/a
Iglesias (76)	2013	Mexico	78	Rabbit	NZ	M+F	12	E	1	SE	No	B/C	n/a	100	91.7	8.3	0	0	1.2	0	15
Yan (77)	2013	China	79	Rabbit	J	M+F	6	T/A	3	WV	No	FC	n/a	100	0	n/a	n/a	0	40.8	n/a	n/a
Yan (78)	2013	China	80	Rabbit	J	M+F	12	T/A	3	WV	Yes	FC	n/a	100	0	n/a	n/a	0	40.8	n/a	n/a
Ceylan (79)	2014	Turkey	81	Rat	W	M	6	A/G	9	WV	No	FC	n/a	100	0	16.7	83.3	0	28.7	6.2	54.8
			82	Rat	W	M	6	A/G	9	WV	Yes	FC	n/a	100	0	83.3	16.7	0	12.1	8.0	18.2
Lalkovic (80)	2014	Serbia	83	Rabbit	BC	M	10	E	1	SE	Yes	B/C	No	100	0	100	0	0	8.7	4.1	15.4
Borumandi (81)	2016	Austria	84	Pig	n/a	n/a	6	H	4	WV	No	B/C	No	100	n/a	n/a	n/a	n/a	n/a	n/a	n/a
Weng (82)	2017	China	85	Rabbit	J	M+F	11	A/G	6	WV	No	FC	n/a	n/a	n/a	n/a	n/a	n/a	28.1	n/a	n/a
			86	Rabbit	J	M+F	12	A/G	5	WV	No	FC	n/a	n/a	n/a	n/a	n/a	n/a	26.7	n/a	n/a

Table 1 - Summary of the studies on unconventional perfusion flaps in experimental animal models identified in the systematic review and included in the meta-analysis. For each study, the optimized experimental animal model is identified, as well as its characteristics. These experimental models were those which presented better flap survival rates in each published paper ($p<0.05$).

n, number of flaps in each optimized experimental model; **n/a**, information non-available; **Min.**, minimum; **Max.**, maximum

Categorical flap survival: CN, complete necrosis; **CS**, complete survival; **NCS**, nearly complete survival; **SN**, significant necrosis

Strain: BC, Big Chinchilla rabbit; **F**, Fischer rat; **J**, Japanese white rabbit; **L**, Lewis rat; **M**, Mongrel dog; **NZ**, New Zealand white rabbit; **SD**, Sprague Dawley rat; **W**, Wistar rat; **Y**, Yorkshire pig

Gender: F, female; **M**, male; **M + F**, both males and females

Flap donor site: A/G, abdomen and/or groin; **D**, dorsum; **E**, ear; **F**, forelimb; **H**, hindlimb; **T/A**, thorax and abdomen

Flap vascular pattern (1): "**1**", type Ia arterialized venous flap according to Woo classification; "**2**", type Ib arterialized venous flap according to Woo classification; "**3**", type IIa arterialized venous flap according to Woo classification; "**4**", type IIb arterialized venous flap according to Woo classification; "**5**", type III arterialized venous flap according to Woo classification; "**6**", pedicled arterialized venous flap; "**7**", type I venous flap according to Chen classification; "**8**", type IIa venous flap according to Chen classification; "**9**", type IIb venous flap according to Chen classification; "**10**", sliding venous flap

Wound bed blood supply: B/C, bone or cartilage; **IB**, impermeable barrier underneath the flap; **SE**, skeletonized ear; **WV**, well vascularized

Flap composition: B/C, includes bone and/or cartilage (other than skin with its appendages and subcutaneous tissue); **FC**, fasciocutaneous (skin with its appendages and subcutaneous tissue); **MFC**, myofasciocutaneous (skin with its appendages, subcutaneous tissue and muscle/portion of muscle)

Studies publication spanned from 1981 to 2017. Half of the identified papers were published until 1994, and three quarters of these were published until 2003. Studies were performed in 20 different countries (**Table 1**). By decreasing order of frequency, the countries with the greater number of studies were: Japan (19.8%), Turkey (14.3%), China and the USA (13.2% each), and Canada and South-Korea (both corresponding to 5.5%). The most commonly used animal species was the rabbit (57.1%), followed by the rat (26.4%), the dog (14.3%), and the pig (2.2%). Mice models were not reported in the literature. Amongst rabbits, the most commonly used strain was the White New Zealand rabbit (55.8%), followed by the White Japanese rabbit (9.6%), and the Big Chinchilla rabbit (3.8%). The most commonly strain of rat was the Wistar rat (45.8%), followed by the Sprague-Dawley rat (29.2%), and the Lewis and Fischer strains (4.2% each). Almost all the studies made in dogs were performed in mongrel dogs (96.2%). Concerning the two pig studies, one reported the use of the Yorkshire pig strain, while the other used an unspecified variety of pigs.

On average, each optimized experimental model was developed based on the dissection of 12.14 ± 8.01 UPFs (ranging from 2 to 40). Regarding animal gender, most studies were conducted on male animals (26.4%), or using both male and female animals (15.4%). Only 3.3% of studies reported studies exclusively on female animals. However, the majority of the studies did not specify the gender of experimental animals (54.9%). Concerning anatomical location, most UPFs models were performed in the ear (36.3%).

In decreasing order of frequency, the next most common anatomical regions used were the abdomen and/or groin (25.3%), the thorax and the abdomen (18.7%), the hindlimb (13.2%), the forelimb (4.4%), and the dorsum (2.2%). The most common anatomical regions used in each species to produce UPFs were as follows: the ear in the rabbit (63.5%), the abdomen and/or groin in the rat (58.3%), the hindlimb in the dog (69.2%), and in the pig (100%).

The different vascular patterns reported in the literature are detailed in **Figures 2** and **3**.

The most common vascular patterns were in decreasing order of frequency: sliding VFs (40.7%), type IA AVFs (20.9%), type IIA AVFs (8.8%), pedicled AVFs (6.6%), and both type IIB AVFs and proximally pedicled VFs (5.5% each). Infrequent vascular patterns included type IB AVFs (4.4%), type III AVFs (3.3%), free venous flow through (2.2%), and distally based VFs (1.1%).

Vascular patterns referred in the literature	General description			Additional Information
	"Arterialized venous flow-through flaps" Orthodromic blood flow (blood flows in the same direction as venous valves open)	Straight venous pattern akin to a sttandard vein graft	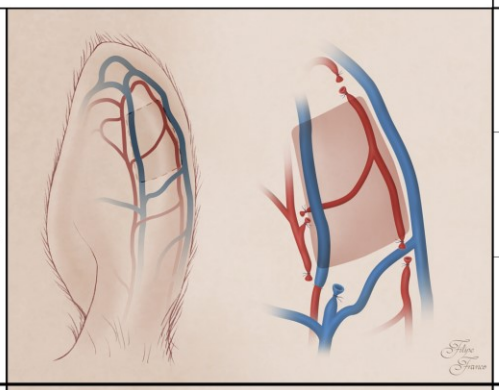	**First Discription** Mundy 1984 [18] **(E)** **Classifications** IA (Woo) III (Chen) **Number of papers and Flaps Analized** **Rabbits**: 12 papers; 215 flaps **Dog:**1 paper; 6 flaps
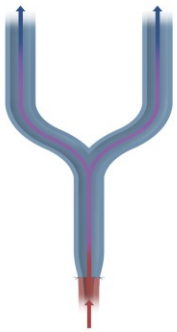		Y-shaped pattern	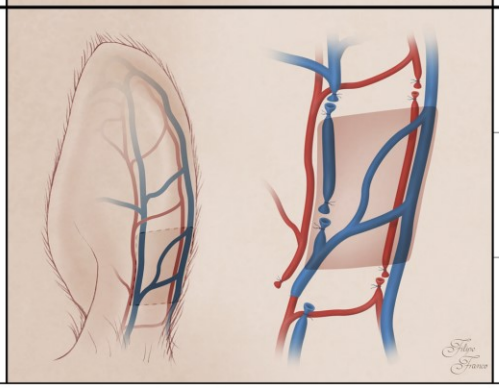	**First Discription** Nichter 1985 [10] **(E)** **Classifications** IB (Woo) III (Chen) **Number of papers and Flaps Analized** **Rabbits**: 2 papers; 27 flaps

Figure 2A

Vascular patterns referred in the literature	General description			Additional Information
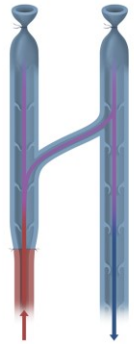	Antidromic blood flow (blood flows in the opposite direction of venous valves opening in the afferent vein)	Y-shaped pattern	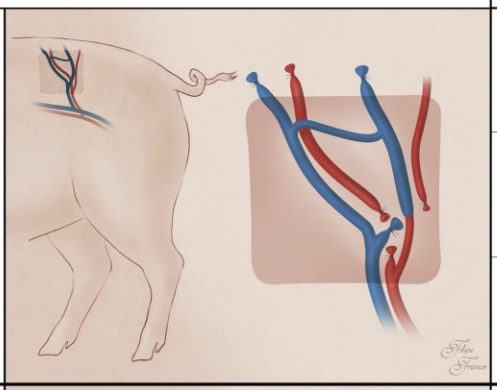	**First Discription** Voukidis 1982 [17] **(E)** **Classifications** IA (Woo) **Number of papers and Flaps Analized** **Rabbits**: 6 papers; 64 flaps **Rat:** 4 paper; 44 flaps
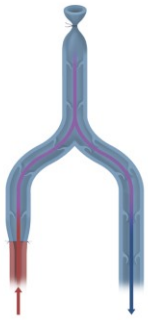		H-shaped pattern	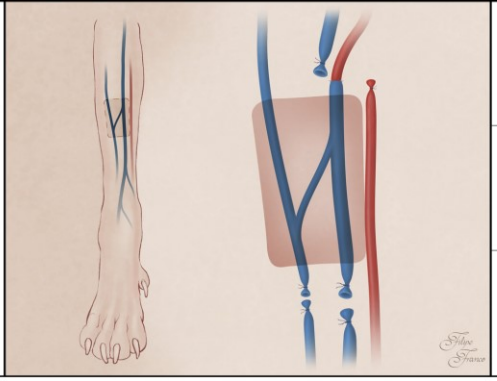	**First Discription** Nakayama 1981 [16] **(E)** **Classifications** IB (Woo) **Number of papers and Flaps Analized** **Rat**: 3 papers; 35 flaps **Dog**: 2 papers; 18 flaps; **Pig**: 1 paper; 6 flaps

Figure 2B

Vascular patterns referred in the literature	General description		Additional Information
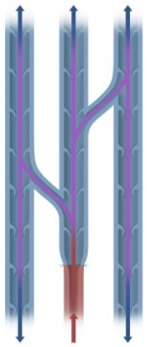	Anti and orthodromic blood flow (mixed pattern of through and against-valve blood flow)	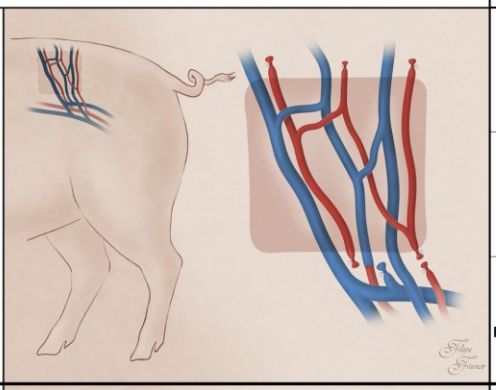	**First Discription** Germann 1987 [23] **(E)** **Classifications** III (Woo) **Number of papers and Flaps Analized** **Rabbits**: 1 paper; 12 flaps **Pig:** 1 paper; 12 flaps; **Rat:** 4 paper; 44 flaps
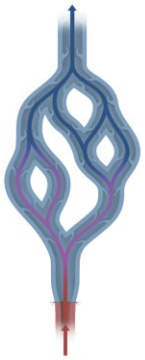	Pedicled arterialized venous flap (blood enters the flap antidromically and leaves orthodromically through preserved efferent veins)	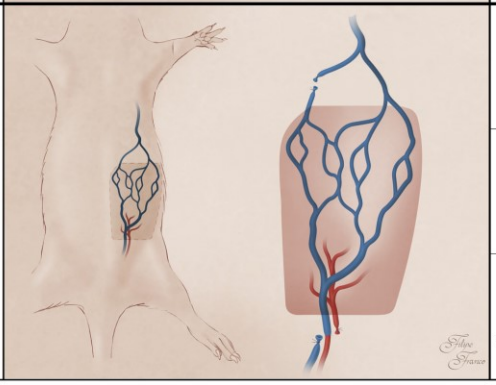	**First Discription** Nakayama 1981 [16] **(E)** **Classifications** - **Number of papers and Flaps Analized** **Rat**: 1 paper; 15 flaps **Rabbit:** 1 paper; 11 flaps

Figure 2C

Figures 2A, 2B and 2C - Schematic representation of the different types of arterialized venous flaps (**AVFs**) performed in experimental models according to the literature.

AVFs receive arterial blood through one or more of their veins. AVFs venous drainage occurs through one or more veins to neighboring veins and/or arteries.

Red areas represent arterial blood flow. Blue and purple regions denote venous and mixed arterial and venous blood, respectively. The arrows specify the direction of blood flow. The curved lines inside the vessels illustrate venous valves.

First description: in cases where the first description of the type of unconventional pattern was not performed in the experimental setting (E), the description in the clinical setting (C) is also indicated.

Classifications: The classifications used were those proposed by Woo (96), and by Chen, Tang, and Noordhoff (2).

The drawings are not to scale.

Vascular patterns referred in the literature	General description		Additional Information
	Free venous flow through flap (the flap is nourished exclusively by venous blood flowing orthodromically)	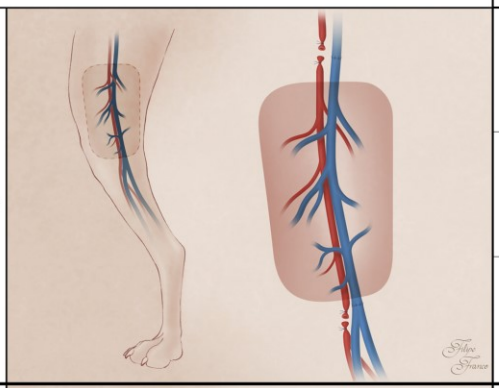	**First Discription** Baek 1985 [21] **(E)** Honda 1984-[95] **(C)** **Classifications** I (Chen) **Number of papers and Flaps Analized** **Dog:** 2 papers; 6 flaps
	Distally pedicled based venous flap	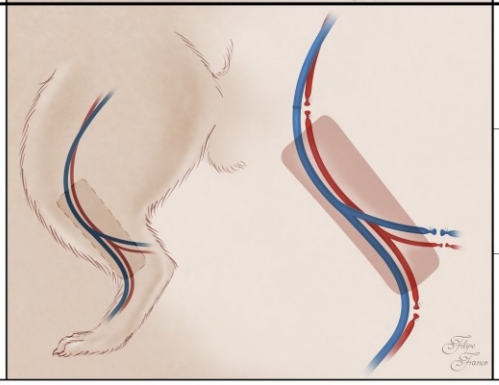	**First Discription** Chang 2003 [65] **(E)** Amarante 1988 [24] **(C)** **Classifications** IIA (Chen) **Number of papers and Flaps Analized** **Rabbit:** 1 paper; 10 flaps

Figure 3A

Vascular patterns referred in the literature	General description		Additional Information
	Proximally pedicled venous flap	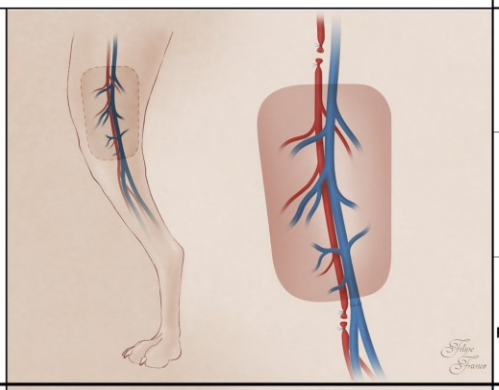	**First Discription** Amarante 1988 [24] **(E)** Chavoin 1987 [93] **(C)** **Classifications** IIB (Chen) **Number of papers and Flaps Analized** **Rabbit:** 2 papers; 32 flaps **Dog:** 1 paper; 5 flaps
	Sliding venous flap (the flap is transposed based exclusively on the dissested venous network)	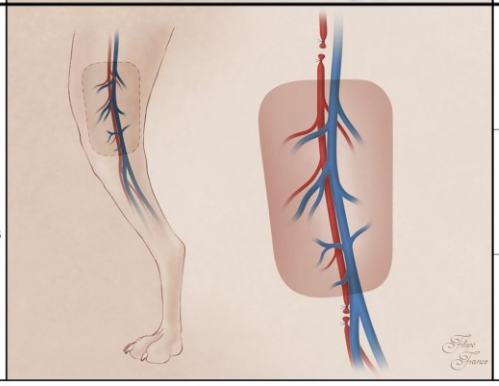	**First Discription** Baek 1985 [21] **(E)** **Classifications** - **Number of papers and Flaps Analized** **Rabbit:** 21 papers; 320 flaps **Rat:** 9 papers; 146 flaps **Dog:** 6 papers; 85 flaps

Figure 3B

Figures 3A and 3B - Schematic representation of the different types of venous flaps (**VFs**) performed in experimental models according to the literature.

These flaps receive venous blood through one or more of their veins. VFs venous drainage occurs through one or more veins to neighboring veins.

Red areas represent arterial blood flow. *Blue* and *purple* regions denote venous and mixed arterial and venous blood, respectively. The *arrows* specify the direction of blood flow. The curved lines inside the vessels illustrate venous valves.

First description: in cases where the first description of the type of unconventional pattern was nor performed in the experimental setting (**E**), the description in the clinical setting (**C**) is also indicated.

Classifications: The classifications used were those proposed by Woo (96), and by Chen, Tang, and Noordhoff (2).

The drawings are not to scale.

Figure 4 shows the relative proportion of the different vascular patterns in the different animal species. This figure also highlights the main features of the optimized experimental models in the different animal species.

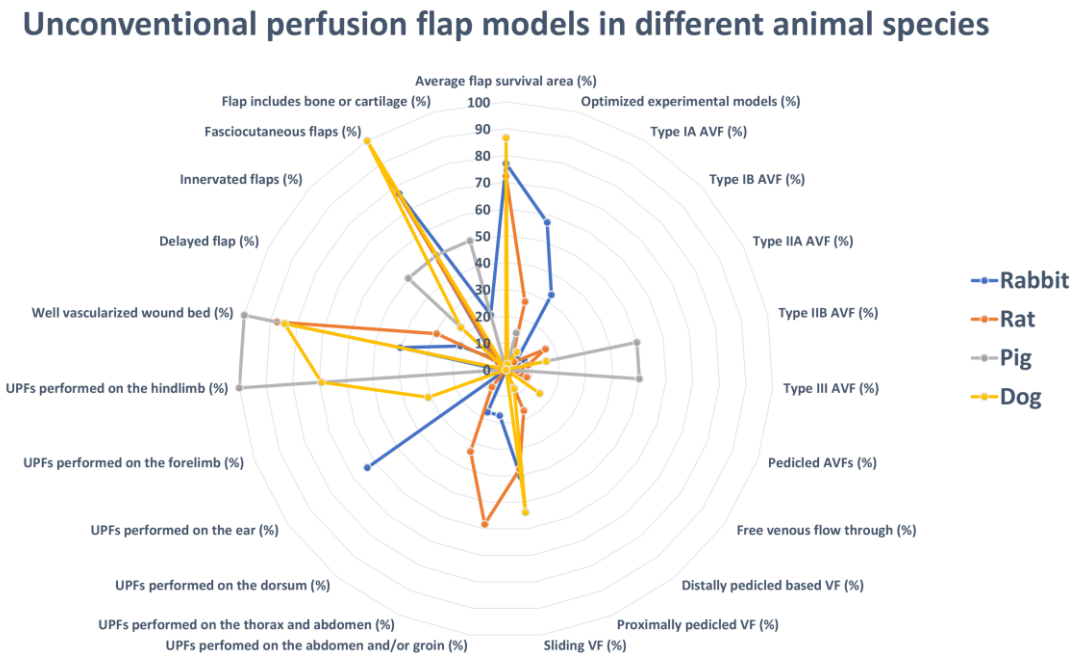

Figure 4 - Star plot illustrating unconventional perfusion flap models' features in different animal species. **AVF**, arterialized venous flap; **VF**, venous flap; **UPF**, unconventional perfusion flap.

In the majority of cases (54.7%), flaps were placed over well-perfused wound beds. In 18.6% of cases, flaps were placed over bare bone or cartilage. In 15.6% of the models an impermeable barrier was placed under the UPF to prevent flap nutrition or gas exchanges from the wound bed. When rabbits were used, UPFs were frequently based on skeletonized ears or ear segments. In these cases (11.6% of all experimental models) the flap was also completely dependent on its own vascular pedicle, not being

able to depend on a vascularized wound bed. In 18.7% of cases some sort of surgical delay procedure was performed prior to flap elevation to increase flap survival.

Concerning flap composition, most UPFs were fasciocutaneous (85.7%; p<0.001). Flaps included bone and/or cartilage in 13.2% of cases. There was only one study reporting a myofasciocutaneous flap, corresponding to 1.1% of all optimized experimental models.(38) In almost all cases, UPFs were non-innervated (91.2%; p<0.001).

Meta-analysis of experimental UPFs using a random effects model estimated an overall flap survival rate of 90.8% (95% CI, 86.9% to 93.6%; p<0.001) [**Fig. 5**]. Study heterogeneity assessment for this parameter was as follows: Cochran-Q value 134.98; p<0.001; I-squared 47.40; Tau-squared 1.24. The funnel plot of the studies used to produce this estimate suggested there was evidence of publication bias regarding this parameter (**Fig. 6**). Publication bias was further supported by Egger's test (p<0.001).

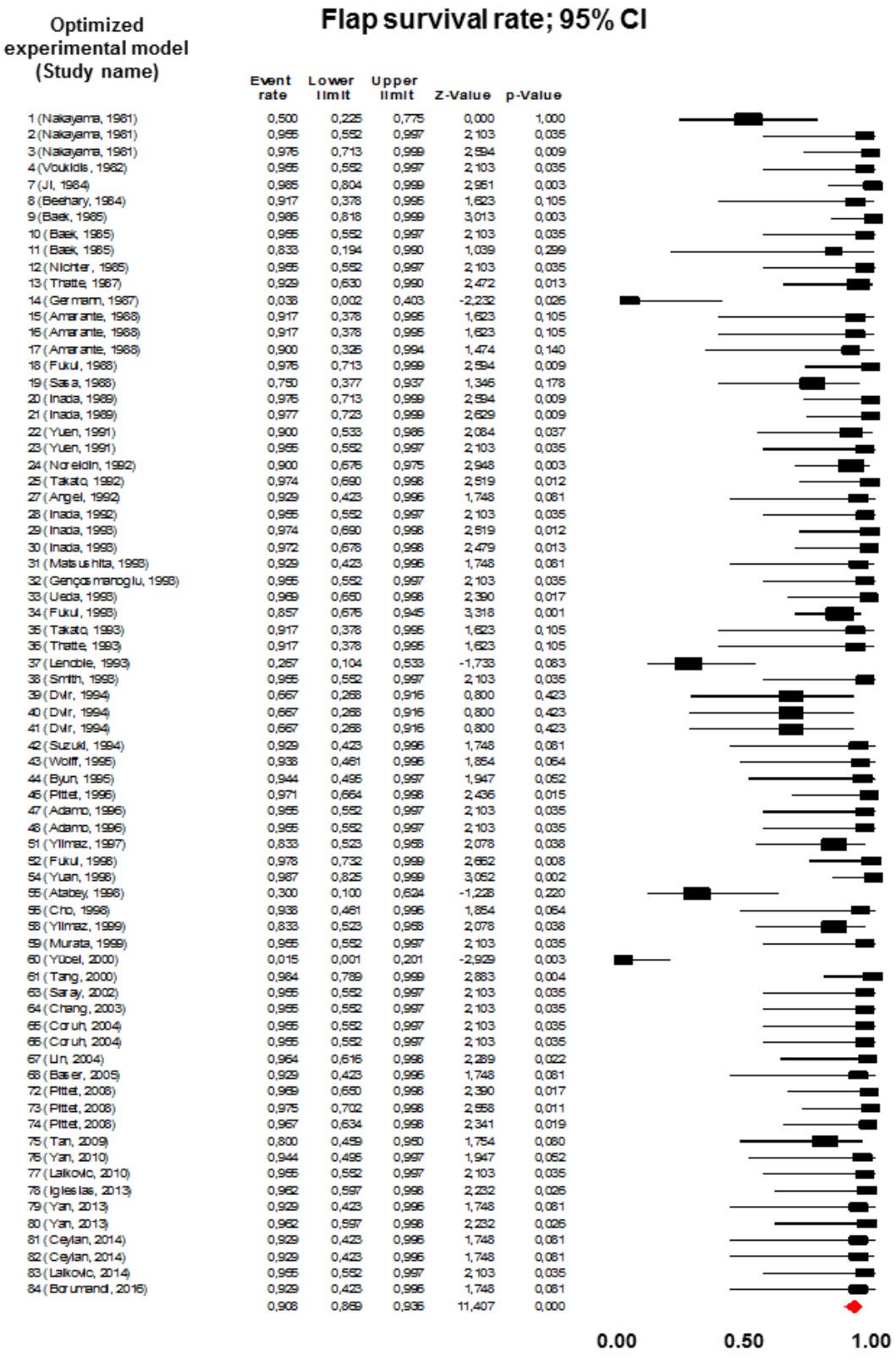

Figure 5 - Forest plot of all studies reporting unconventional perfusion flap (**UPFs**) survival rates. Meta-analysis of experimental UPFs using a random effects model estimated an overall flap survival rate of 90.8% (95% CI, 86.9% to 93.6%; p<0.001)

CI, confidence interval.

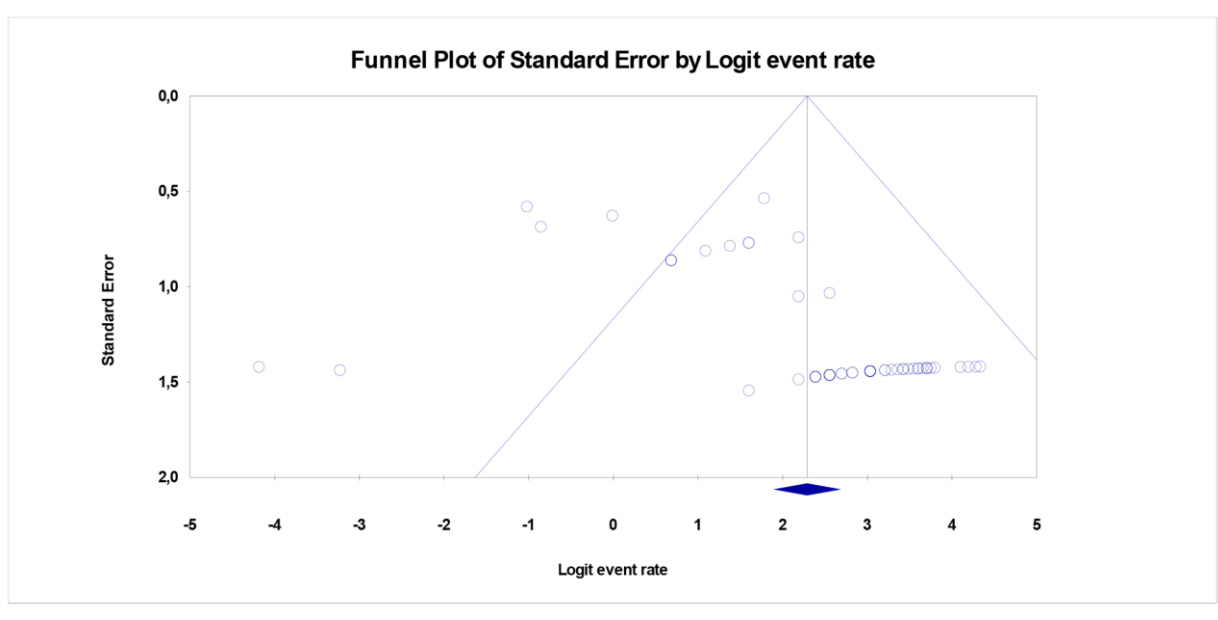

Figure 6 - Funnel plot of the studies used to estimate the survival rate of the experimental unconventional perfusion flaps. This graphic suggests there is publication bias. This was confirmed by the application of the Egger's test (p<0.001).

Study heterogeneity assessment for this parameter was as follows: Cochran-Q value 134.98; p<0.001; I-squared 47.40; Tau-squared 1.24.

The estimated proportion of experimental UPFs presenting complete survival or nearly complete survival was 74.4% (95% CI, 62.1% to 83.7%; p<0.001) [**Fig. 7**]. Evaluation of studies heterogeneity regarding this variable was: Cochran-Q value 162.77; p<0.001; I-squared 71.74; Tau-squared 2.58. The funnel plot regarding the estimation of this parameter suggested the presence of publication bias (**Fig. 8**). However, Egger's test failed to support this assumption (p=0.342).

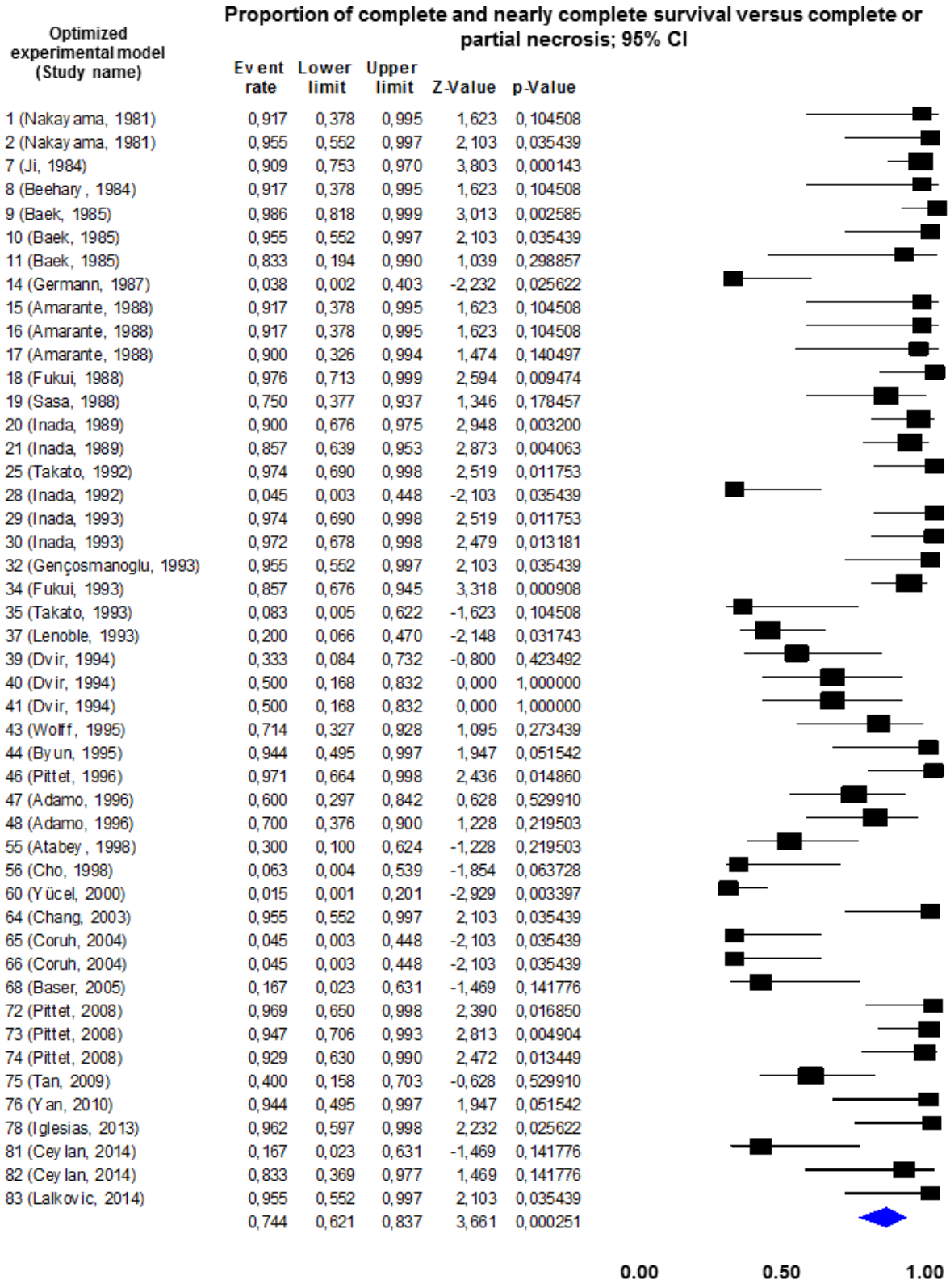

Figure 7 - Forest plot of all studies describing the proportion of unconventional perfusion flaps (**UPFs**) presenting complete survival or nearly complete survival

The estimated proportion of experimental UPFs presenting complete survival or nearly complete survival was 74.4% (95% CI, 62.1% to 83.7%; p<0.001).

CI, confidence interval.

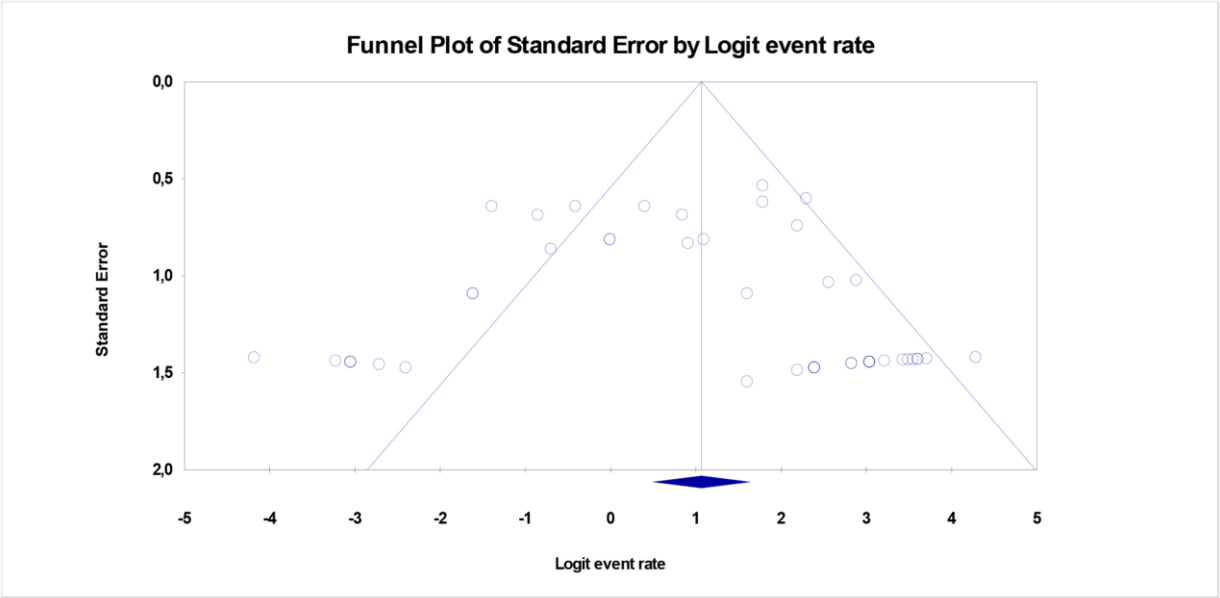

Figure 8 - Funnel plot of the studies used to estimate proportion of experimental UPFs that presented complete survival or nearly complete survival. This graphic might suggest there is publication bias. However, Egger's test failed to confirm this assumption (p=0.342).

Evaluation of studies heterogeneity regarding this variable was: Cochran-Q value 162.77; p<0.001; I-squared 71.74; Tau-squared 2.58.

In all animal species except the pig, most flaps presented complete or nearly complete survival (**Fig. 9**). In the pig, there was only one study using a type III AVF fasciocutaneous flap. In this model all flaps suffered complete necrosis.(23) No significant differences were found between UPFs necrosis rates among the other animal species. In the same way, no significant differences were found between survival rates

of the different vascular patterns (**Fig. 9**). Similarly, no differences were found in UPFs survival rates regarding: gender; anatomical location where the flap was produced; wound bed blood supply, including the placement or not of an impermeable barrier underneath the flap; resort to surgical delay procedures; UPF histological composition and/or innervation.

All articles addressing UPF's clinical features described flap congestion, edema, venous engorgement, blister formation and/or epidermolysis as constant findings in the first days after surgery.

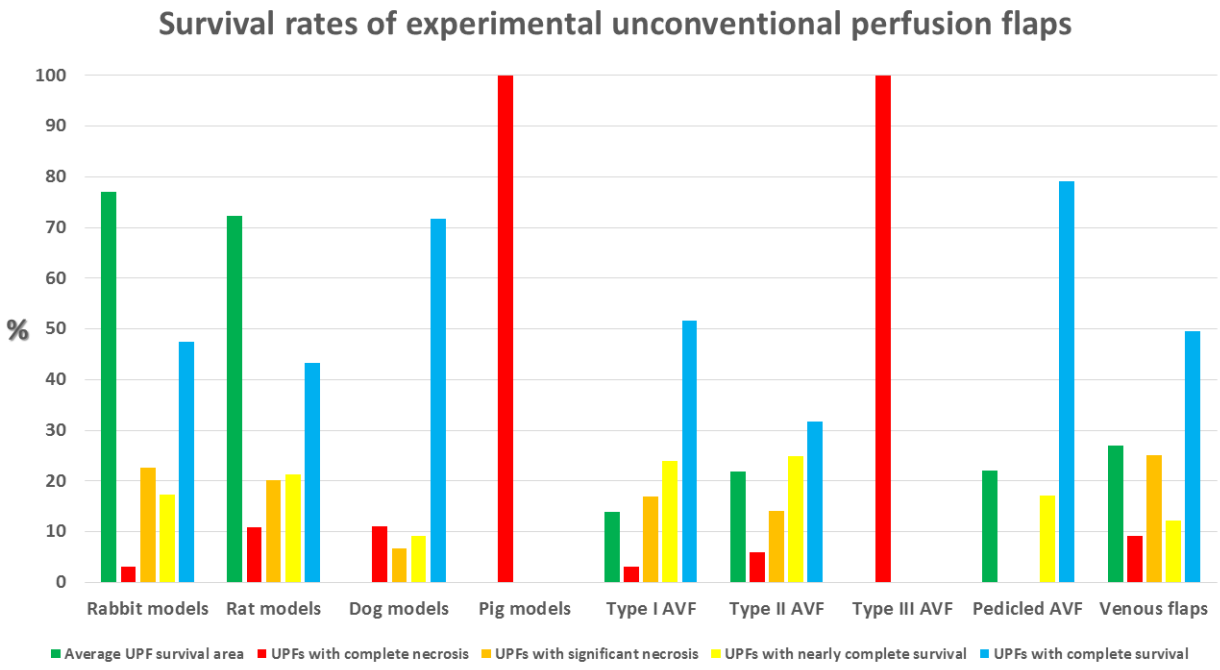

Figure 9 - Bar charts illustrating the survival of the most common types of unconventional perfusion flaps according to animal species and vascular pattern employed.

AVF, arterialized venous flap; **UPF**, unconventional perfusion flap.

There were no statistically significant differences between the different types of unconventional perfusion flaps ($p < 0.05$).

DISCUSSION

As far as the authors could determine, this paper is the first systematic review and meta-analysis on the experimental use of UPFs. Using a random effects model, the authors estimated UPF survival rate to be 90.8% (95% CI, 86.9% to 93.6%; p<0.001) [**Fig. 5**]. Moreover, using a similar methodology the estimated proportion of UPFs that survive completely or nearly completely was 74.4% (95% CI, 62.1% to 83.7%; p<0.001) [**Fig. 6**]. These data indicate that, according to the available literature, the majority of UPFs performed in the experimental setting survived, although a significant fraction of these flaps presented a variable degree of necrosis.

Interestingly, the estimated overall UPF survival rate in the experimental setting [90.8% (95% CI, 86.9% to 93.6%; p<0.001)] was similar to that reported by the authors on a previous meta-analysis addressing the clinical application of UPFs [89.%; 95% CI, 87.3 to 91.3; p < 0.001)].(1)

In contrast, the estimated proportion of UPFs presenting complete or nearly complete survival was 74.4% (95% CI, 62.1% to 83.7%; p<0.001) in the experimental setting, compared to 92.0% (95% CI, 89.9% to 93.7%; p<0.001) in the clinical context.(1) However, in both meta-analyses the majority of UPFs presented complete or nearly complete survival. The differences observed may be partially explained by the different vascular patterns used in the experimental and clinical contexts. In the experimental setting, the most common vascular constructs were in decreasing order of frequency: sliding VFs (40.7%), type IA AVFs (20.9%), and type IIA AVFs (8.8%). In the clinical context, the patterns most frequently reported were: type IA AVFs (33.5%), type IV arterialized venous arterial flaps (14.8%), and type I VF (12.5%).(1, 83)

The most commonly used animal species to produce UPFs was the rabbit (57.1%), followed by the rat (26.4%), the dog (14.3%), and the pig (2.2%). Mice were not used for this purpose. This contrasts with the majority of the literature on experimental flap surgery, which indicates the rat as the most widely used animal model.(84) This is certainly due to the fact that rabbits and rats are easy to obtain and keep, they are relatively inexpensive, and they have a large enough size to perform microvascular procedures.(84-86) Although dogs and pigs have larger-sized vessels, they are more expensive to obtain and to maintain. In addition, the use of these animal species has been submitted to increasingly stringent control by ethical committees and animal welfare bodies.(87-89) Noteworthily, there were no significant differences in UPF survival rates in the most commonly used animal species (rabbit, rat, and dog) [**Fig. 7**].

Regarding animal gender, most studies were conducted on male animals (26.4%), or on both male and female animals (15.4%). Only 3.3% of studies used exclusively female animals. Several authors defend the choice of male animals for experimental flap studies based on the lesser variability of the hormonal *milieu* in the latter gender, and based on the fact that female sex hormones are associated with increased proclivity to vascular anastomoses' thrombosis.(40) However, in the present meta-analysis, the authors failed to observe statistically significant differences in UPFs related to experimental animal gender.

Concerning flap composition, the majority of UPFs were fasciocutaneous (85.7%). Flaps included bone and/or cartilage in 13.2% of cases. It was possible to identify a single study reporting myofasciocutaneous flaps, corresponding to 1.1% of all experimental models.(38) This adds strength to the widely held belief that

unconventional perfusion is most adequately suited to perfuse tissues with low metabolic needs, such as those composing the integument, cartilage and/or bone.(1-6)

The authors feel that care must be used when extrapolating the results of this meta-analysis for the clinical setting, since there are important differences between the UPFs performed experimentally and those performed in humans. For example, one of the main discrepancies relates to the disparate vessel and flap sizes across species.(1) Another important difference is that in almost experimental studies vascular anastomoses are performed locally between similarly sized vessels. In opposition, clinically, UPFs are mostly transferred to distant places.(1) This makes vessel caliber incongruence more probable in the latter setting. In addition, vessels' twisting or traction are more likely in distant tissue transfers. These, in turn, may potentiate vascular thrombosis.

Moreover, the blood supply to the integument of various experimental animals has been shown to vary substantially to that reported in humans.(90, 91) For example, Taylor *et al.* have shown that in loose-skinned animals, such as the rabbit, the rat or the dog, there is a preponderance of the direct cutaneous vessels, compared to the dominance of the musculocutaneous vessels in humans and pigs.(90, 91) Furthermore, experimental animals, particularly those with loosely draped skin possess a layer of smooth muscle in the deep aspect of the integument known as panniculus carnosus, which is associated with vascular plexuses of its own.(85, 92) In humans, this layer is virtually absent in the majority of the body, being represented mostly by the platysma and the palmaris longus muscles. In pigs, the panniculus carnosus layer is present in most of the integument. However, it is firmly adherent to overlying skin and to the underlying muscle fascia, making pig skin apparently a more suitable model for

comparison with the human integument.(93, 94) Despite all these data, the only study conducted on the pig's hindlimb to produce a type III arterialized venous fasciocutaneous flap revealed complete necrosis of all flaps.(23) This may be explained by the larger thickness of the pig's integument relatively to that of the other experimental animal species, and even to that of humans in the usual locations where these flaps are harvested in this latter species.(1, 93) In fact, according to most authors, UPFs depend, at least initially, on gas exchanges in the vicinity of the venous system of the flap, which could help explain why thin flaps present the best results in the clinical setting.(1, 95-97)

Table 2 summarizes the main features of the different animal species used to produce experimental UPFs.

	Rabbit	Rat	Dog	Pig
Availability	Easy to acquire	Easy to acquire	Requires special facilities and more stringent evaluation by ethical committees	Requires special facilities and more stringent evaluation by ethical committees
Acquisition cost	Moderate	Low	High	High
Maintenance cost	Low	Low	Moderate	High
Handling and maintenance facilities and skills	Requires special facilities and training	Commonly available	Requires special facilities and training	Requires special facilities and training
Integumentary similarity to the human integument	Significant differences in integument composition and blood supply	Significant differences in integument composition and blood supply Smaller vessels than those most commonly employed clinically	Significant differences in integument composition and blood supply	Similar to humans in terms of blood supply architecture and vessel sizes Differs from humans due to the presence of a well-developed panniculus carnosus and due to the relatively thick integument
Proportion of UPFs experimental models in the literature	57.1%	24.6%	14.3%	2.2%

Table 2. Comparison of the different animal species used for producing experimental unconventional perfusion flaps (UPFs.)

Study Limitations

The present study may be affected by several types of bias, as happens in all meta-analyses, particularly retrospective meta-analysis, as this one.(98, 99)

One of the problems of including UPFs performed in different animal species using multiple vascular patterns is that there is a variable degree of inherent heterogeneity. In fact, this heterogeneity was confirmed for both population estimates using the Cochran-Q test ($p<0.001$). The authors tried to partially circumvent this problem by using random effects models for estimating population parameters.(13)

Another major potential caveat of the present study was the effect of publication bias. The latter bias reflects the observation that positive results are more likely to be published compared to neutral or negative ones. The Egger's test supported the presence of this type of bias for the estimate of overall UPF survival, while failing to support it in the estimation of the proportion of UPFs whose survival was complete or near complete. It is widely accepted that the most efficacious way to downplay the effect of publication bias is to perform a systematic and comprehensive review of the literature, as it was performed in the present study.(98, 99) Additionally, the authors have strictly adhered to the widely accepted PRISMA checklist for systematic reviews and meta-analysis, as shown in the **Table 3**, to minimize the risk of committing methodological mistakes.(100, 101)

Section/topic	#	Checklist item	Reported on page #
TITLE			
Title	1	Identify the report as a systematic review, meta-analysis, or both.	1

ABSTRACT			
Structured summary	2	Provide a structured summary including, as applicable: background; objectives; data sources; study eligibility criteria, participants, and interventions; study appraisal and synthesis methods; results; limitations; conclusions and implications of key findings; systematic review registration number.	2
INTRODUCTION			
Rationale	3	Describe the rationale for the review in the context of what is already known.	5
Objectives	4	Provide an explicit statement of questions being addressed with reference to participants, interventions, comparisons, outcomes, and study design (PICOS).	5
METHODS			
Protocol and registration	5	Indicate if a review protocol exists, if and where it can be accessed (e.g., Web address), and, if available, provide registration information including registration number.	6-9
Eligibility criteria	6	Specify study characteristics (e.g., PICOS, length of follow-up) and report characteristics (e.g., years considered, language, publication status) used as criteria for eligibility, giving rationale.	6
Information sources	7	Describe all information sources (e.g., databases with dates of coverage, contact with study authors to identify additional studies) in the search and date last searched.	6
Search	8	Present full electronic search strategy for at least one database, including any limits used, such that it could be repeated.	6,7
Study selection	9	State the process for selecting studies (i.e., screening, eligibility, included in systematic review, and, if applicable, included in the meta-analysis).	6-8
Data collection process	10	Describe method of data extraction from reports (e.g., piloted forms, independently, in duplicate) and any processes for obtaining and confirming data from investigators.	6-8
Data items	11	List and define all variables for which data were sought (e.g., PICOS, funding sources) and any assumptions and simplifications made.	7,8
Risk of bias in individual studies	12	Describe methods used for assessing risk of bias of individual studies (including specification of whether this was done at the study or outcome level), and how this information is to be used in any data synthesis.	9
Summary measures	13	State the principal summary measures (e.g., risk ratio, difference in means).	9
Synthesis of results	14	Describe the methods of handling data and combining results of studies, if done, including measures of consistency (e.g., I^2) for each meta-analysis.	9

Table 3 - Application of the PRISMA checklist in the present work, in order to minimize methodological mistakes. (100, 101)

Finally, the authors believe that although this paper has the significant merit of providing a synthesis of the available literature regarding the use of experimental UPFs, it contributes only modestly to understanding the mechanisms underlying the survival or necrosis of these flaps, making further studies in this field warranted. Ideally, a large animal study in primates could help to elucidate more perfectly the mechanisms of UPF perfusion, viability, and overall survival in humans. However, such a study would be logistically vexing and expensive to conduct.

CONCLUSIONS

According to the present data, the majority of UPFs performed in the experimental setting survive (90.8%; 95% CI, 86.9% to 93.6%; p<0.001). Furthermore, survival is complete or nearly complete in an estimated 74.4% of cases (95% CI, 62.1% to 83.7%; p<0.001). The rabbit, the rat and the dog were the most commonly used animal species for producing UPFs. No significant differences were found in survival rates among these species, nor among the diverse vascular patterns used.

These data do not differ significantly from those reported in a similar study performed on the UPFs in human medicine.(1) This suggests that the available rabbit, rat and canine experimental UPF models can adequately mimic the clinical application of UPFs.

ACKNOWLEDGEMENTS

The authors are very grateful to Mr. Filipe Franco for producing all the drawings contained in this paper.

References

1. Casal, D., Cunha, T., Pais, D., et al. Systematic Review and Meta-Analysis of Unconventional Perfusion Flaps in Clinical Practice. *Plastic and reconstructive surgery* 2016;138:459-479.

2. Goldschlager, R., Rozen, W. M., Ting, J. W., Leong, J. The nomenclature of venous flow-through flaps: updated classification and review of the literature. *Microsurgery* 2012;32:497-501.

3. Yan, H., Brooks, D., Ladner, R., Jackson, W. D., Gao, W., Angel, M. F. Arterialized venous flaps: a review of the literature. *Microsurgery* 2010;30:472-478.

4. Yan, H., Zhang, F., Akdemir, O., et al. Clinical applications of venous flaps in the reconstruction of hands and fingers. *Arch Orthop Trauma Surg* 2011;131:65-74.

5. Jabir, S., Frew, Q., El-Muttardi, N., Dziewulski, P. A systematic review of the applications of free tissue transfer in burns. *Burns : journal of the International Society for Burn Injuries* 2014;40:1059-1070.

6. Weng, W., Zhang, F., Zhao, B., et al. The complicated role of venous drainage on the survival of arterialized venous flaps. *Oncotarget* 2017.

7. Guo, L., Pribaz, J. J. Clinical flap prefabrication. *Plastic and reconstructive surgery* 2009;124:e340-350.

8. Abbase, E. A., Shenaq, S. M., Spira, M., el-Falaky, M. H. Prefabricated flaps: experimental and clinical review. *Plastic and reconstructive surgery* 1995;96:1218-1225.

9. Haines, P., Nichter, L. S., Morgan, R. F., Horowitz, J. H., Edgerton, M. T. A digit replantation model. *Microsurgery* 1985;6:70-72.

10. Nichter, L. S., Haines, P. C. Arterialized venous perfusion of composite tissue. *Am J Surg* 1985;150:191-196.

11. Epidermolysis. In B. Werner ed., *Stedman's medical dictionary*, 27th ed. USA: Lippincott Williams and Wilkins, 2000:604.

12. Korevaar, D. A., Hooft, L., ter Riet, G. Systematic reviews and meta-analyses of preclinical studies: publication bias in laboratory animal experiments. *Laboratory animals* 2011;45:225-230.

13. Borenstein, M., Hedges, L. V., Higgins, J. P., Rothstein, H. R. Identifying and quantifying heterogeneity. In M. Borenstein, L. V. Hedges, J. P. Higgins, H. R. Rothstein eds., *Introduction to Meta-analysis*, First ed. United Kingdom: Wiley; 2009:107-125.

14. Sterne, J. A., Sutton, A. J., Ioannidis, J. P., et al. Recommendations for examining and interpreting funnel plot asymmetry in meta-analyses of randomised controlled trials. *BMJ* 2011;343:d4002.

15. Egger, M., Davey Smith, G., Schneider, M., Minder, C. Bias in meta-analysis detected by a simple, graphical test. *Bmj* 1997;315:629-634.

16. Nakayama, Y., Soeda, S., Kasai, Y. Flaps nourished by arterial inflow through the venous system: an experimental investigation. *Plastic and reconstructive surgery* 1981;67:328-334.

17. Voukidis, T. An axial-pattern flap based on the arterialised venous network: an experimental study in rats. *Br J Plast Surg* 1982;35:524-529.

18. Mundy, J. C., Panje, W. R. Creation of free flaps by arterialization of the venous system. *Arch Otolaryngol* 1984;110:221-223.

19. Ji, S. Y., Chia, S. L., Cheng, H. H. Free transplantation of venous network pattern skin flap: an experimental study in rabbits. *Microsurgery* 1984;5:151-159.

20. Beehary, S., Hoang, P., Foucher, G. L'artérialisation des lambeaux veineux. *Annales de chirurgie plastique et esthetique* 1985;30:95-97.

21. Baek, S. M., Weinberg, H., Song, Y., Park, C. G., Biller, H. F. Experimental studies in the survival of venous island flaps without arterial inflow. *Plastic and reconstructive surgery* 1985;75:88-95.

22. Thatte, R. L., Thatte, M. R. A study of the saphenous venous island flap in the dog without arterial inflow using a non-biological conduit across a part of the length of the vein. *Br J Plast Surg* 1987;40:11-15.

23. Germann, G. K., Eriksson, E., Russell, R. C., Mody, N. Effect of arteriovenous flow reversal on blood flow and metabolism in a skin flap. *Plastic and reconstructive surgery* 1987;79:375-380.

24. Amarante, J., Costa, H., Reis, J., Soares, R. Venous skin flaps: an experimental study and report of two clinical distal island flaps. *Br J Plast Surg* 1988;41:132-137.

25. Fukui, A., Inada, Y., Tamai, S., Mizumoto, S., Yajima, H., Sempuku, T. Skin graft including subcutaneous vein: experimental study and clinical applications. *J Reconstr Microsurg* 1988;4:223-231.

26. Sasa, M., Xian, W. Q., Breidenbach, W., Tsai, T. M., Shibata, M., Firrell, J. Survival and blood flow evaluation of canine venous flaps. *Plastic and reconstructive surgery* 1988;82:319-327.

27. Inada, Y., Fukui, A., Tamai, S., Masuhara, K. Experimental studies of skin flaps with subcutaneous veins. *J Reconstr Microsurg* 1989;5:249-261.

28. Yuen, Q. M., Leung, P. C. Some factors affecting the survival of venous flaps: an experimental study. *Microsurgery* 1991;12:60-64.

29. Noreldin, A. A., Fukuta, K., Jackson, I. T. Role of perivenous areolar tissue in the viability of venous flaps: an experimental study on the inferior epigastric venous flap of the rat. *Br J Plast Surg* 1992;45:18-22.

30. Takato, T., Zuker, R. M., Turley, C. B. Viability and versatility of arterialized venous perfusion flaps and prefabricated flaps: an experimental study in rabbits. *J Reconstr Microsurg* 1992;8:111-119.

31. Chow, S. P., Chen, D. Z., Gu, Y. D. A comparison of arterial and venous flaps. *J Hand Surg Br* 1992;17:359-364.

32. Angel, M. F., Knight, K. R., Dvir, E., Mellow, C. G., Morrison, W. A., O'Brien, B. M. Biochemical analysis of the venous flap in the dog. *J Surg Res* 1992;53:24-29.

33. Inada, Y., Hirai, T., Fukui, A., Omokawa, S., Mii, Y., Tamai, S. An experimental study of the flow-through venous flap: investigation of the width and area of survival with one flow-through vein preserved. *J Reconstr Microsurg* 1992;8:297-302.

34. Inada, Y., Fukui, A., Tamai, S., Mizumoto, S. The arterialised venous flap: experimental studies and a clinical case. *Br J Plast Surg* 1993;46:61-67.

35. Matsushita, K., Firrell, J. C., Ogden, L., Tsai, T. M. Blood flow and tissue survival in the rabbit venous flap. *Plastic and reconstructive surgery* 1993;91:127-135; discussion 136-127.

36. Gencosmanoglu, R., Ulgen, O., Yaman, C., Songur, E., Akin, Y., Cagdas, A. Mechanisms of viability in rabbit flank venous flaps. *Ann Plast Surg* 1993;30:60-66.

37. Ueda, K., Harada, T., Nagasaka, S., Oba, S., Inoue, T., Harashina, T. An experimental study of delay of flow-through venous flaps. *Br J Plast Surg* 1993;46:56-60.

38. Fukui, A., Tamai, S., Maeda, M., Inada, Y., Mii, Y., Mine, T. The pedicled venous flap. An experimental study. *Br J Plast Surg* 1993;46:116-121.

39. Takato, T., Komuro, Y., Yonehara, H., Zuker, R. M. Prefabricated venous flaps: an experimental study in rabbits. *Br J Plast Surg* 1993;46:122-126.

40. Thatte, M., Healy, C., McGrouther, D. Laser Doppler and microvascular pulsed Doppler studies of the physiology of venous flaps. *European Journal of Plastic Surgery* 1993;16:134-138.

41. Lenoble, E., Lavau, L., Foucher, G., Voisin, M. C., Goutallier, D. [Influence of the anatomy of the pedicle on the survival of venous vascularized flaps. Experimental study on the rat]. *Annales de chirurgie plastique et esthetique* 1993;38:612-620.

42. Smith, R. J., Fukuta, K., Wheatley, M., Jackson, I. T. Role of perivenous areolar tissue and recipient bed in the viability of venous flaps in the rabbit ear model. *Br J Plast Surg* 1994;47:10-14.

43. Dvir, E., Hickey, M. J., Hurley, J. V., Morrison, W. A. A histological and carbon perfusion study of cephalic and saphenous venous flaps in the dog. *Br J Plast Surg* 1994;47:263-267.

44. Suzuki, Y., Suzuki, K., Ishikawa, K. Direct monitoring of the microcirculation in experimental venous flaps with afferent arteriovenous fistulas. *Br J Plast Surg* 1994;47:554-559.

45. Wolff, K. D., Telzrow, T., Rudolph, K. H., Franke, J., Wartenberg, E. Isotope perfusion and infrared thermography of arterialised, venous flow-through and pedicled venous flaps. *Br J Plast Surg* 1995;48:61-70.

46. Byun, J. S., Constantinescu, M. A., Lee, W. P., May, J. W., Jr. Effects of delay procedures on vasculature and survival of arterialized venous flaps: an experimental study in rabbits. *Plastic and reconstructive surgery* 1995;96:1650-1659.

47. Xiu, Z. F., Chen, Z. J. The microcirculation and survival of experimental flow-through venous flaps. *Br J Plast Surg* 1996;49:41-45.

48. Pittet, B., Chang, P., Cederna, P., Cohen, M. B., Blair, W. F., Cram, A. E. The role of neovascularization in the survival of an arterialized venous flap. *Plastic and reconstructive surgery* 1996;97:621-629.

49. Adamo, C., Rubino, C. Venous flaps and perivenous areolar tissue: an experimental study in rats. *J Reconstr Microsurg* 1996;12:179-181.

50. Xiu, Z., Chen, Z. The effect of glutathione, superoxide dismutase and adenosine triphosphate on venous flap survival. *European Journal of Plastic Surgery* 1996;19:170-173.

51. Miles, D. A., Crosby, N. L., Clapson, J. B. The role of the venous system in the abdominal flap of the rat. *Plastic and reconstructive surgery* 1997;99:2030-2033.

52. Yilmaz, M., Menderes, A., Vayvada, H., Karaca, C., Barutcu, A. Effects of the number of pedicles on perfusion and survival of venous flaps: an experimental study in rabbits. *Ann Plast Surg* 1997;39:278-286.

53. Fukui, A., Inada, Y., Murata, K., Ueda, Y., Tamai, S. A method for prevention of arterialized venous flap necrosis. *J Reconstr Microsurg* 1998;14:67-74.

54. Woo, S.-H., Kim, S.-E., Lee, T.-H., Jeong, J.-H., Seul, J.-H. Effects of Blood Flow and Venous Network on the Survival of the Arterialized Venous Flap. *Plastic and reconstructive surgery* 1998;101:1280-1289.

55. Yuan, R., Shan, Y., Zhu, S. Circulating mechanism of the "pure" venous flap: direct observation of microcirculation. *J Reconstr Microsurg* 1998;14:147-152.

56. Atabey, A., Gezer, S., Vayvada, H., et al. Ischemia/reperfusion injury in flow-through venous flaps. *Ann Plast Surg* 1998;40:612-616.

57. Cho, B. C., Lee, M. S., Lee, J. H., Byun, J. S., Baik, B. S. The effects of surgical and chemical delay procedures on the survival of arterialized venous flaps in rabbits. *Plastic and reconstructive surgery* 1998;102:1134-1143.

58. Mutaf, M., Tasaki, Y., Fujii, T. Expansion of venous flaps: an experimental study in rats. *Br J Plast Surg* 1998;51:393-401.

59. Yilmaz, M., Menderes, A. Investigation of metabolism and perfusion in arterialized venous replantation: experimental study in rabbits. *Ann Plast Surg* 1999;43:67-73.

60. Murata, K., Tamai, S., Inada, Y., Fukui, A., Miyamoto, S. Transfer of a pedicled venous flap containing perivenous areolar tissue and nerve: an experimental study. *Br J Plast Surg* 1999;52:223-229.

61. Yucel, A., Bayramicli, M. Effects of hyperbaric oxygen treatment and heparin on the survival of unipedicled venous flaps: an experimental study in rats. *Ann Plast Surg* 2000;44:295-303.

62. Tang, Y. B., Simchon, S., Chen, H. C. Microcirculation of a venous flap: an experimental study with microspheres in rabbits. *Scand J Plast Reconstr Surg Hand Surg* 2000;34:207-212.

63. Wungcharoen, B., Pradidarcheep, W., Santidhananon, Y., Chongchet, V. Pre-arterialisation of the arterialised venous flap: an experimental study in the rat. *Br J Plast Surg* 2001;54:621-630.

64. Saray, A., Can, B., Sevin, K. Effects of methylprednisolone on the viability of experimental flow-through venous flaps. *J Reconstr Microsurg* 2002;18:615-622.

65. Chang, S. M., Gu, Y. D., Li, J. F. Comparison of different managements of large superficial veins in distally based fasciocutaneous flaps with a veno-neuro-adipofascial pedicle: an experimental study using a rabbit model. *Microsurgery* 2003;23:555-560.

66. Coruh, A., Abaci, K., Gunay, G. K. Effect of topical nitroglycerine on the survival of ischemic flow-through venous flaps in rabbits. *J Reconstr Microsurg* 2004;20:261-266.

67. Lin, C. H., Wei, F. C., Mardini, S., Ma, S. F. Microcirculation study of rabbit ear arterial and venous flow-through flaps using a window chamber model. *J Trauma* 2004;56:894-900.

68. Baser, N. T., Silistreli, O. K., Sisman, N., Oztan, Y. Effects of surgical or chemical delaying procedures on the survival of proximal predicled venous island flaps: an experimental study in rats. *Scand J Plast Reconstr Surg Hand Surg* 2005;39:197-203.

69. Zhang, F., Brooks, D., Chen, W., Mustain, W., Chen, M. B., Lineaweaver, W. C. Improvement of venous flap survival by application of vascular endothelial growth factor in a rat model. *Ann Plast Surg* 2006;56:670-673.

70. Ozyazgan, I., Tuncer, A., Yazici, C., Gunay, G. K. Reactive oxygen species in experimental ischemic flow-through venous flaps and effects of antioxidants on reactive oxygen species and flap survival. *Ann Plast Surg* 2007;58:661-666.

71. Ozyazgan, I., Ozkose, M., Baskol, G. Nitric oxide in flow-through venous flaps and effects of L-arginine and nitro-L-arginine methyl ester (L-NAME) on nitric oxide and flap survival in rabbits. *Ann Plast Surg* 2007;59:550-557.

72. Pittet, B., Quinodoz, P., Alizadeh, N., Schlaudraff, K. U., Mahajan, A. L. Optimizing the arterialized venous flap. *Plastic and reconstructive surgery* 2008;122:1681-1689.

73. Tan, M. P., Lim, A. Y., Zhu, Q. A novel rabbit model for the evaluation of retrograde flow venous flaps. *Microsurgery* 2009;29:226-231.

74. Yan, H., Brooks, D., Jackson, W. D., Angel, M. F., Akdemir, O., Zhang, F. Improvement of prearterialized venous flap survival with delay procedure in rats. *J Reconstr Microsurg* 2010;26:193-200.

75. Lalković, M., Kozarski, J., Panajotović, L., et al. The new experimental design of arterialized venous flap on the rabbit ear model. *Acta veterinaria* 2010;60:633-640.

76. Iglesias, M., Fonseca-Lazcano, J. A., Moran, M. A., Butron, P., Diaz-Morales, M. Revascularization of Arterialized Venous Flaps through a Total Retrograde Reverse Blood Flow: Randomized Experimental Trial of Viability. *Plastic and reconstructive surgery Global open* 2013;1:e34.

77. Yan, H., Kolkin, J., Zhao, B., et al. The effect of hemodynamic remodeling on the survival of arterialized venous flaps. *PloS one* 2013;8:e79608.

78. Yan, H., He, Z., Li, Z., et al. Large prefabricated skin flaps based on the venous system in rabbits: a preliminary study. *Plastic and reconstructive surgery* 2013;132:372e-380e.

79. Ceylan, R., Kaya, B., Caydere, M., Terzioglu, A., Aslan, G. Comparison of ischaemic preconditioning with surgical delay technique to increase the viability of single pedicle island venous flaps: an experimental study. *Journal of plastic surgery and hand surgery* 2014;48:368-374.

80. Lalkovic, M., Kozarski, J., Panajotovic, L., et al. Surface enlargement of a new arterialised venous flap by the surgical delay method. *Vojnosanitetski pregled Military-medical and pharmaceutical review* 2014;71:547-553.

81. Borumandi, F., Higgins, J. P., Buerger, H., et al. Arterialized Venous Bone Flaps: An Experimental Investigation. *Scientific reports* 2016;6.

82. Weng, W., Zhang, F., Zhao, B., et al. The complicated role of venous drainage on the survival of arterialized venous flaps. *Oncotarget* 2017;8:16414-16420.

83. Chen, H. C., Tang, Y. B., Noordhoff, M. S. Four types of venous flaps for wound coverage: a clinical appraisal. *J Trauma* 1991;31:1286-1293.

84. Dunn, R. M., Mancoll, J. Flap models in the rat: a review and reappraisal. *Plastic and reconstructive surgery* 1992;90:319-328.

85. Casal, D., Pais, D., Iria, I., et al. A Model of Free Tissue Transfer: The Rat Epigastric Free Flap. *Journal of Visualized Experiments* 2017;1:e55281.

86. Mapara, M., Thomas, B. S., Bhat, K. M. Rabbit as an animal model for experimental research. *Dental Research Journal* 2012;9:111-118.

87. Swindle, M. M., Smith, A. C., Laber-Laird, K., Dungan, L. Swine in Biomedical Research: Management and Models. *ILAR Journal* 1994;36:1-5.

88. Tanaka, H., Kobayashi, E. Education and research using experimental pigs in a medical school. *Journal of Artificial Organs* 2006;9:136-143.

89. Hasiwa, N., Bailey, J., Clausing, P., et al. Critical evaluation of the use of dogs in biomedical research and testing in Europe. *Altex* 2011;28:326-340.

90. Taylor, G. I., Minabe, T. The angiosomes of the mammals and other vertebrates. *Plastic and reconstructive surgery* 1992;89:181-215.

91. Taylor, G. I., Pan, W. R. The angiosome concept. In P. Dodwell ed., *The angiosome concept and tissue transfer*, Vol. 1, First ed. Florida: Quality Medical Publishing, Inc.; 2014:354-395.

92. Pearl, R. M., Johnson, D. The vascular supply to the skin: an anatomical and physiological reappraisal--Part II. *Annals of plastic surgery* 1983;11:196-205.

93. Rose, E. H., Vistnes, L. M., Ksander, G. A. The panniculus carnosus in the domestic pig. *Plastic and reconstructive surgery* 1977;59:94-97.

94. Kerrigan, C. L., Zelt, R. G., Thomson, J. G., Diano, E. The pig as an experimental animal in plastic surgery research for the study of skin flaps, myocutaneous flaps and fasciocutaneous flaps. *Laboratory animal science* 1986;36:408-412.

95. Kovacs, A. F. Comparison of two types of arterialized venous forearm flaps for oral reconstruction and proposal of a reliable procedure. *Journal of cranio-maxillo-facial surgery : official publication of the European Association for Cranio-Maxillo-Facial Surgery* 1998;26:249-254.

96. Woo, S. H., Kim, K. C., Lee, G. J., et al. A retrospective analysis of 154 arterialized venous flaps for hand reconstruction: an 11-year experience. *Plastic and reconstructive surgery* 2007;119:1823-1838.

97. Wharton, R., Creasy, H., Bain, C., James, M., Fox, A. Venous flaps for coverage of traumatic soft tissue defects of the hand: a systematic review. *The Journal of hand surgery, European volume* 2017:1753193417712879.

98. Borenstein, M., Hedges, L. V., Higgins, J. P., Rothstein, H. R. Publication bias. In M. Borenstein ed., *Introduction to Meta-analysis*, First ed. United Kingdom: Wiley and Sons; 2009:277-292.

99. Sterne, J. A., Egger, M., Mother, D. Addressing reporting biases. In J. P. Higgins, S. Green eds., *Cochrane handbook for systematic review of interventions*, First ed. United Kingdom: Wiley-Blackwell; 2009:297-333.

100. Liberati, A., Altman, D. G., Tetzlaff, J., et al. The PRISMA statement for reporting systematic reviews and meta-analyses of studies that evaluate health care interventions: explanation and elaboration. *PLoS medicine* 2009;6:e1000100.

101. Panic, N., Leoncini, E., de Belvis, G., Ricciardi, W., Boccia, S. Evaluation of the endorsement of the preferred reporting items for systematic reviews and meta-analysis (PRISMA) statement on the quality of published systematic review and meta-analyses. *PloS one* 2013;8:e83138.

Chapter 5

BLOOD SUPPLY TO THE INTEGUMENT OF THE ABDOMEN OF THE RAT: A SURGICAL PERSPECTIVE

Authors: Diogo Casal, MD[1,2,3,4]; Diogo Pais, MD, PhD[2]; Inês Iria, MSci[4,5]; Paula A. Videira, PhD[3,4,6]; Eduarda Mota-Silva, MSci.[7]; Sara Alves, MSci[8]; Luís Mascarenhas-Lemos, MD[8]; Cláudia Pen, MSci[8]; Valentina Vassilenko, PhD[7]; João Goyri-O'Neill, MD, PhD[2]

Affiliations:

1- Plastic and Reconstructive Surgery Department and Burn Unit; Centro Hospitalar de Lisboa Central, Lisbon, Portugal

2- Anatomy Department; Nova Medical School, Lisbon, Portugal

3- UCIBIO, Departamento de Ciências da Vida, Faculdade de Ciências e Tecnologia, Universidade NOVA de Lisboa, Caparica, Portugal

4- CEDOC, NOVA Medical School, Universidade NOVA de Lisboa, Lisbon, Portugal

5- iMed - Research Institute for Medicines, Faculdade de Farmácia Universidade Lisboa, Lisbon, Portugal

6- CDG & Allies – Professionals and Patient Associations International Network (CDG & Allies – PPAIN), Caparica, Portugal

7- LIBPhys, Physics Department, Faculdade de Ciências e Tecnologias, Universidade NOVA de Lisboa, Lisbon, Portugal

8- Pathology Department; Centro Hospitalar de Lisboa Central, Lisbon, Portugal

ABSTRACT

Background: Many fundamental questions regarding the blood supply to the integument of the rat remain to be clarified, namely the degree of homology between rat and humans. The aim of this work was to characterize in detail the macro and microvascular blood supply to the integument covering the ventrolateral aspect of the abdominal wall of the rat.

Methods: Two hundred and five Wistar male rats weighing 250 to 350 grams were used. They were submitted to: gross anatomical dissection after intravascular colored latex injection (n=30); conversion in modified Spalteholz cleared specimens (n=10); intravascular injection of a Perspex® solution, and then corroded, in order to produce vascular corrosion casts of the vessels in the region (n=5); histological studies (n=20); scanning electron microscopy of vascular corrosion casts (n=10); surgical dissection of the superficial caudal epigastric vessels (n=100); and to thermographic evaluation (n=30).

Results: The ventrolateral abdominal wall presented a dominant superficial vascular system, which was composed mainly of branches from the superficial caudal epigastric artery and vein in the caudal half. The cranial half still received significant arterial contributions from the lateral thoracic artery in all cases, and from large perforators coming from the intercostal arteries, and from the deep cranial epigastric artery.

Conclusions: These data show that rats and humans present a great deal of homology regarding the blood supply to the ventrolateral aspect of the abdominal integument.

However, there are also significant differences that must be taken into consideration when performing and interpreting experimental procedures in rats.

INTRODUCTION

The rat is arguably the most commonly used animal model for training and research in plastic surgery.(1-11) Its abdominal wall is frequently employed in tissue perfusion and transference studies.(12-18) Oddly, anatomical and histological studies concerning the blood supply to the integument over the ventrolateral aspect of the abdomen of the rat (**IOVAAR**) are scant and are based on small series of animals.(19) Hence, many fundamental questions remain to be clarified, namely the degree of homology between it and that of humans.(19) The aim of this work was to characterize in detail the macro and microvascular blood supply to the IOVAAR.

METHODS

This study focused on the blood supply to the IOVAAR, defined by the region ventral to the dorsal axillary lines. Two hundred and five Wistar male rats weighing 250-350 grams were used.

All the animals were housed under standard environmental conditions and given nothing by mouth six hours before surgical procedures.

All *in vivo* studies were performed in strict accordance with the recommendations in the Guide for Proper Conduct of Animal Experiments and Related Activities in Academic Research and Technology, 2006.

The protocol was approved by the Institutional Animal Care and Use Committee and Ethical Committee at the authors' institution (08/2012/CEFCM).

Gross Anatomical Dissection

In 30 rats a 22G catheter was introduced in the left ventricle and another in the right ventricle. A volume of 180-200 ml/Kg of a red colored latex solution (Robbialac®) was introduced in the left ventricle and a volume of 300-350 ml/Kg of a blue colored latex solution (Robbialac®) was introduced in the right ventricle, until good peripheral contrast perfusion was noted. Subsequently, the rats were submitted to abdominal wall dissection in order to characterize the origin of the supplying vessels. This technique allows to highlight the vessels as they are normally observed during surgical procedures.(20)

In 10 rats subjected to a similar procedure the IOVAAR was converted into modified Spalteholz cleared specimens.(21) This technique creates transparent three-dimensional specimens, while preserving vascular and perivascular structure.(22)

Five rats were submitted to a left ventricular injection of a Perspex® solution, and then corroded, in order to produce vascular corrosion casts of the vessels in the IOVVAR. Vascular corrosion casts produce a faithful replica of vascular beds, allowing detailed three-dimensional morphological analysis of even small vessels.(23)

All identified perforator vessels were plotted on a Cartesian grid centered on the pubic symphysis.

Microscopic Anatomical Study – Optical Microscopy

Ten rats were submitted to surgical collection of the IOVAAR which was fixed in 10% paraformaldehyde, and prepared for histological examination, using hematoxylin-eosin and Masson's trichrome stains, as well as immunohistochemistry for CD31 for staining the endothelium(24-26), and for neurofilaments for staining nerves.(27) Rats were submitted to axial sections in the caudal, middle and cranial aspect of both sides of the abdomen. Ten additional rats were subjected to the preparation just described and their largest integumentary veins were sectioned longitudinally for evaluation of venous valves.

Microscopic Anatomical Study – Scanning Electron Microscopy (SEM) of Vascular Corrosion Casts

Ten rats were submitted to intravascular injection of a resin cast (Mercox®) and latter corroded.(28) The vascular casts were processed and examined using two scanning electron microscopes (acceleration voltage of 2-30kV): a JEOL JSM-5410, for histomorphometric analysis, and a JEOL JSM-7001F, for obtaining high quality images. Vascular casts were interpreted according to Aharinejad and Lametschwandtner.(28)

Surgical anatomy of the superficial caudal epigastric vessels

In 100 rats used for surgical training and experiments, the origin of the superficial caudal epigastric vessels (**SCEVs**) was registered on the left side of the abdomen.

The specimens were photographed using adequate microscopes. Vessels' dimensions were determined using the ImageJ® software.

Thermographic evaluation

In 30 rats, thermographic assessment of the IOVAAR was performed with a FLIR® E6 camera placed 25 cm above the abdomen. Evaluations were done after the rats were anesthetized intraperitoneally with a mixture of ketamine and diazepam, and placed on their backs for 10 minutes. The day before the evaluation, animals were lightly anesthetized and the hair of the abdominal area removed using a depilatory cream.

Evaluations were performed at a constant room temperature (22 ºC) and humidity (50%).(29)

Statistical Analysis

Qualitative variables were expressed as percentages. Quantitative variables were expressed as means ± standard deviation. The SPSS 21.0® software was used for statistical analysis. The Kolmogorov-Smirnov test was used to assess normality. ANOVA and t-Student test were used to compare averages in normally distributed data. Kruskal-Wallis and Mann-Whitney tests were used to compare means in non-normally distributed data. Proportions were analyzed with the Chi-square test or Fisher's exact test.

A cluster analysis was performed using a two-step clustering procedure based on the Schwarz Bayesian criteria to determine the overall distribution of all significant cutaneous perforators.

A two-tailed $p<0.05$ was considered to be statistically significant.

RESULTS

Gross Anatomy

Figure 1 summarizes the most common disposition found of the main vessels supplying the IOVAAR. This region presented a dominant superficial vascular system (**Figs. 2** to **4**). In the caudal half, this system was composed mainly of branches from the superficial caudal epigastric artery (**SIEA**) and vein (**SIEV**), which are the equivalent to the human superficial inferior epigastric artery and vein (for the purpose of simplicity, these structures will be referred to as SIEA and SIEV in both species throughout this article). The cranial half also received significant arterial contributions from the lateral thoracic (**LT**) artery in all cases, and from one (64.4%), two (26.7%) or three (8.9%) large perforators coming from the intercostal arteries, and from the deep cranial epigastric artery, forming, in this latter case, the superficial cranial epigastric artery (present in 95.6% of cases on the right side and 93.3% of cases on the left side). Most of the lateral and cranial aspects of the IOVAAR drained into the tributaries of the large LT vein (thoracoepigastric vein). In all cases, the lateral branch of the SIEV and the branches that originated the LT vein were anastomosed in the lateral aspect of the midportion of the abdomen (**Fig. 3**).

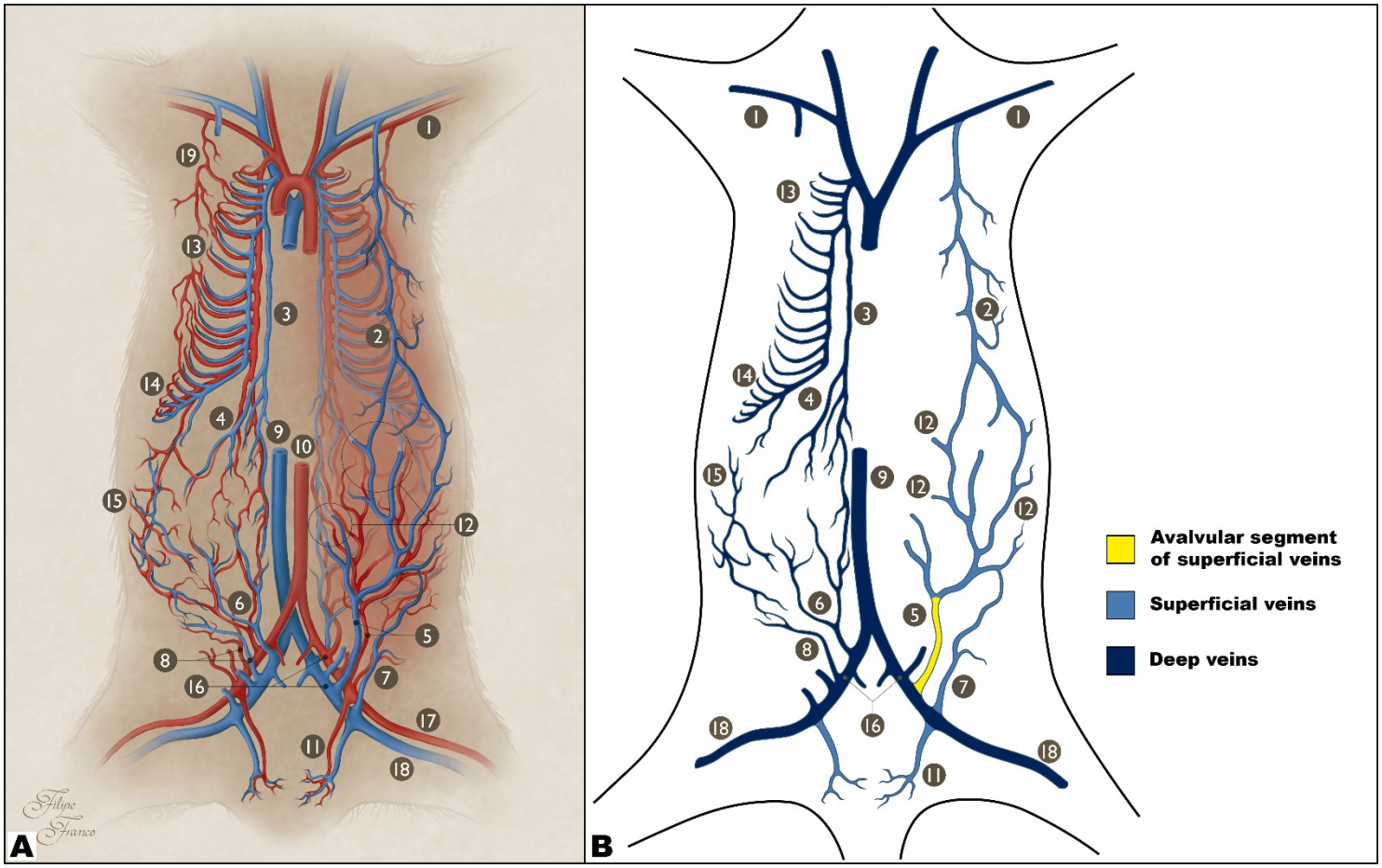

Figure 1 - Macrovascular blood supply to the integument over the ventrolateral aspect of the abdomen of the rat.

A, Schematic drawing illustrating the major vessels supplying integument over the ventrolateral aspect of the abdomen of the rat. On the right side of the picture, the superficial vessels (superficial to the muscle fascia) are represented in full. On this side, the deeper vessels (deep to the muscle fascia) are represented in a lighter color. On the left side of the picture, only the deeper vessels (deep to the muscle fascia) are represented.

Blue structures represent veins. Red structures represent arteries.

B, Schematic drawing illustrating the major veins draining the integument over the ventrolateral aspect of the abdomen of the rat, as represented in 1A. On the left side of the picture are represented the deep veins (deep to the muscle fascia), whereas on the right side of the picture are represented the superficial veins. The valvular and avalvular segments are shown.

1, Axillary artery and vein; 2, Lateral thoracic (Thoracoepigastric) vein; 3, Internal thoracic artery and vein; 4, Cranial epigastric artery and vein; 5, Superficial caudal epigastric artery and vein; 6, Deep caudal epigastric artery and vein; 7, Superficial circumflex iliac artery and vein; 8, Deep circumflex iliac artery and vein; 9, Caudal vena cava; 10, Abdominal aorta; 11, Superficial external pudendal artery and vein; 12, Perforator arteries and veins; 13, Cranial intercostal arteries and veins; 14, Caudal intercostal arteries and veins; 15, Lumbar (or Iliomumbar) arteries and veins; 16, External iliac artery and vein; 17, Femoral artery; 18, Femoral vein; 19, Lateral thoracic artery.

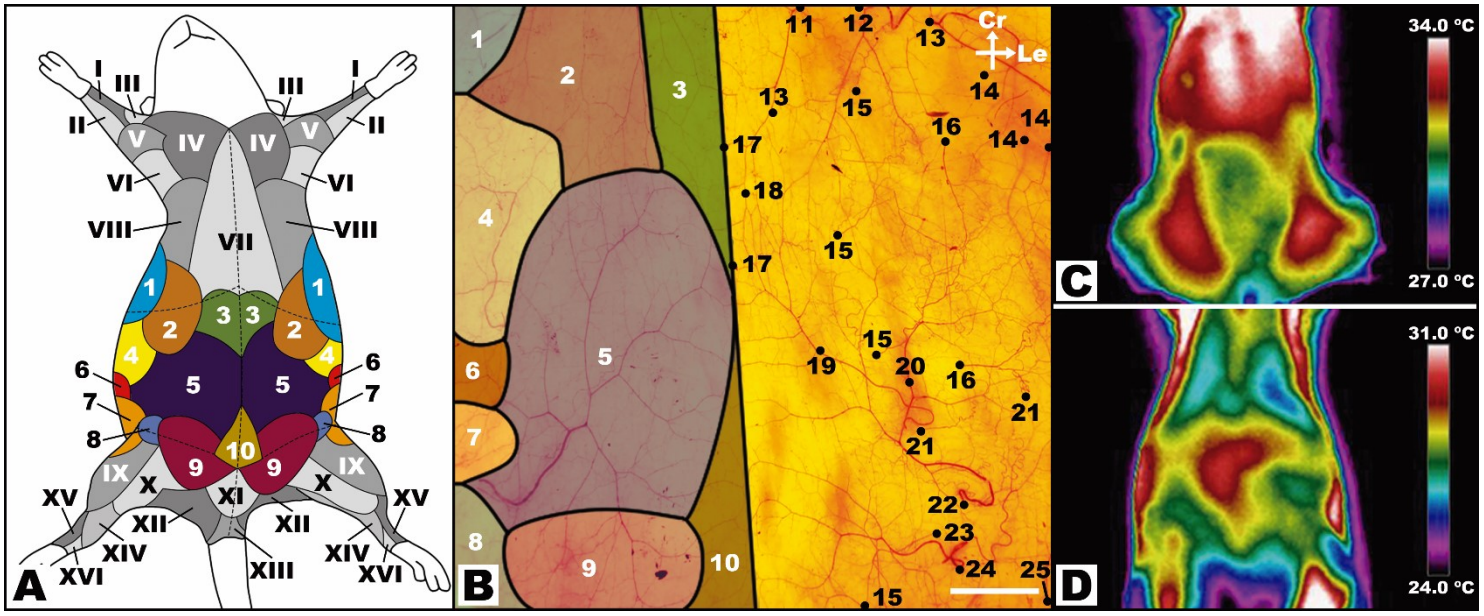

Figure 2 - Macrovascular blood supply to the ventrolateral aspect of the rat's abdominal wall.

A, Schematic representation of the angiosomes of the ventrolateral aspect of the rat. The angiosomes of the abdomen studied in the present study are represented are numbered in arabic numerals and represented in different colors. The adjacent angiosomes are numbered in roman numerals and highlighted in different levels of gray. These angiosomes have been represented according to Taylor *et al* (32, 33) and Kochi *et al.*(40).

B, Photograph of the integument covering the ventrolateral aspect of the abdomen of the rat after processing by the modified Spalteholz technique showing the suppling vessels and respective angiosomes. The top limit of the photograph corresponds to the lower limit of the rib cage, the lower limit to a

transverse line abutting the pubic symphysis; the lateral limits of the photograph correspond to the dorsal axillary lines.

C and D, Representative infra-red thermography images of the ventrolateral aspect of the abdomen of the rat. C, Direct infra-red thermography with hotspots in the region of the dominant axial vessels (the caudal superficial epigastric vessels); D, Infra-red thermography after cooling of the rat's surface, by placing a silicone gel bag at a temperature of approximately 21 ºC for 2 minutes. This image shows the location of the dominant perforator vessels in the central and cranial aspect of the abdomen. The thermograms were taken for a period of 5 minutes with 30-second intervals.

Ca, Caudal; Cr, cranial; Le, left; La, lateral; M, medial

I, Median angiosome; II, Ulnar angiosome; III, Deep brachial angiosome; IV, Transverse cervical angiosome; V, Dorsal circumflex humeral angiosome; VI, Circumflex scapular angiosome; VII, Internal thoracic angiosome; VIII, Cranial intercostal perforators angiosome; IX, Lateral circumflex femoral angiosome; X, Medial circumflex femoral angiosome; XI, Superficial external pudendal angiosome; XII, Caudal gluteal angiosome; XIII, Internal pudendal angiosome; XIV, Saphenous angiosome; XV, Fibular angiosome; XVI, Anterior tibial angiosome.

1, Thoracodorsal angiosome; 2, Lateral thoracic angiosome; 3, Cranial epigastric angiosome; 4, Caudal intercostal perforators angiosome; 5, Superficial caudal epigastric angiosome; 6, Lumbar (or Iliolumbar) perforators angiosome; 7, Deep circumflex iliac angiosome; 8, Deep external pudendal angiosome; 9, Superficial external pudendal angiosome; 10, Deep caudal epigastric angiosome; 11, Cranial deep epigastric artery perforator; 12, Lateral thoracic artery; 13, Thoracodorsal artery perforator; 14, Intercostal perforators; 15, Perforators from the medial branch of the deep caudal and cranial epigastric arteries; 16, Perforators from the lateral branch of the deep caudal and cranial epigastric arteries; 17, Choke vessels between the two superficial caudal epigastric angiosomes; 18, Anastomoses between the superficial caudal epigastric arteries and the lateral thoracic arteries; 19, Medial branch of the superficial caudal epigastric artery; 20, Lateral branch of the superficial caudal epigastric artery; 21, Lumbar perforators; 22, Superficial caudal epigastric artery; 23, Superficial external pudendal artery; 24, Deep external pudendal artery; 25, Deep circumflex iliac artery.

Calibration bar = 10 mm.

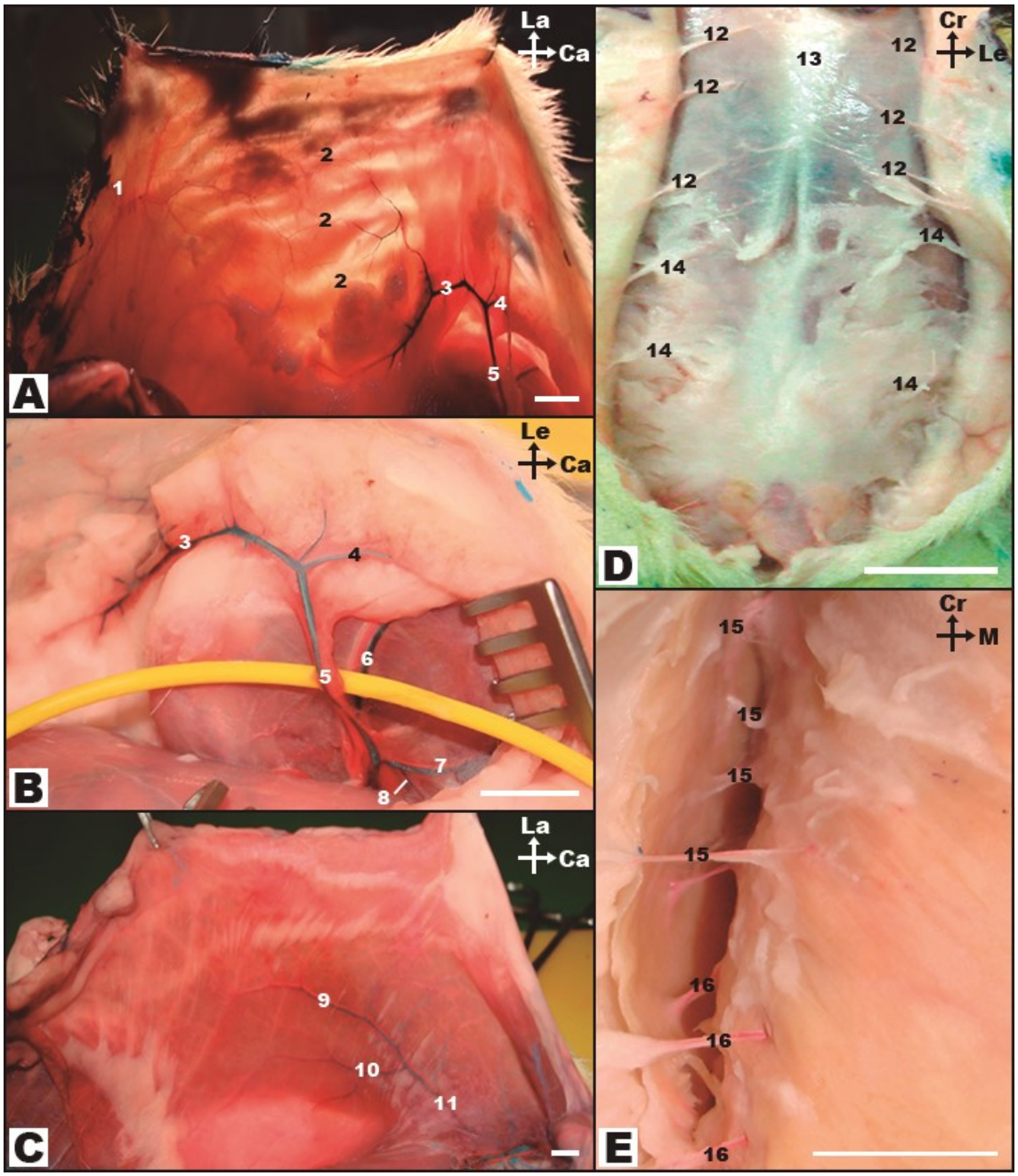

Figure 3 - Macrovascular blood supply to the ventrolateral aspect of the rat's abdominal wall. A, Photograph under transillumination of the integument covering the left side of the abdomen sowing its largest vessels. B, Photograph of the left groin region showing the origin of the superficial caudal epigastric vessels from the femoral vessels; C, Photograph of the deep surface of the left rectus abdominis muscle, showing the deep caudal epigastric vessels suppling this muscle; D, Photograph of the integument of the ventral region of the abdomen of the rat, after midline incision and partial lateral retraction, showing multiple perforators supplying this region coming off the deep cranial and caudal epigastric vessels; E,

Photograph of the right flank of the abdomen showing multiple lateral perforators supplying the lateral aspect of the integument of the rat in this region.

Ca, Caudal; Cr, cranial; Le, left; La, lateral; M, medial

1, Lateral thoracic artery; 2, Anastomoses between the superficial caudal epigastric arteries and the lateral thoracic arteries; 3, Lateral branch of the superficial caudal epigastric artery; 4, Medial branch of the superficial caudal epigastric artery; 5, Superficial caudal epigastric artery; 6, Femoral vessels and nerve; 7, Deep external pudendal artery; 8, Superficial external pudendal artery; 9, Medial branch of the deep caudal epigastric artery; 10, Lateral branch of the deep caudal epigastric artery; 11, Deep caudal epigastric vessels; 12, Cranial deep epigastric artery perforator; 13, Xyphoid process; 14, Perforators from the medial branch of the deep caudal and cranial epigastric arteries; 15, Intercostal perforators; 16, Lumbar perforators

Calibration bar = 10 mm.

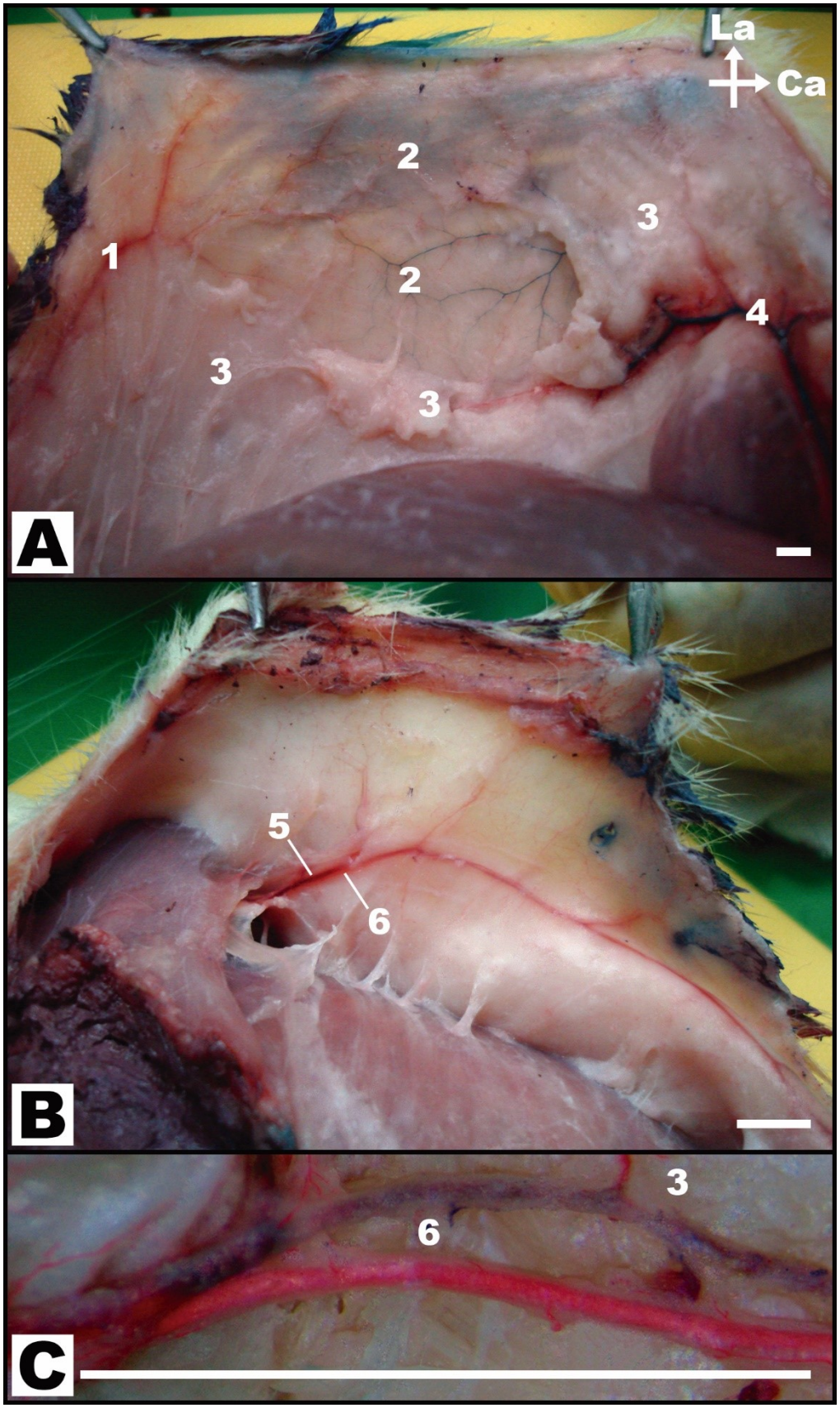

Figure 4 - Lateral thoracic vessels and their anatomical relations.

A, Photograph of a medial view of the left region of the integument of the ventrolateral aspect of the thorax of the rat showing the lateral thoracic vessels. The lateral thoracic vein is seen draining to the axillary region into the axillary vein (not shown). The lateral thoracic which is of smaller caliber is seen escorting the homonymous vein after its origin in the axilla.

B, Photograph of a medial view of the left region of the integument of the ventrolateral aspect of the abdomen of the rat showing the lateral thoracic vessels coursing superficial to the panniculus carnosus layer. The branches of the lateral thoracic vessels present numerous anastomoses with the superficial caudal epigastric vessels.

C, Photograph of a high magnification view of the lateral thoracic vessels immediately after the origin the lateral thoracic vein.

Ca, caudal; La, lateral;

1, Lateral thoracic vein; 2, Lateral thoracic artery; 3, Panniculus carnosus; 4, Lateral thoracic vessels; 5, Superficial caudal epigastric vessels; 6, Anastomoses between the lateral thoracic vessels and the superficial caudal epigastric vessels.

Calibration bar = 10 mm.

The IOVAAR received relatively minor contributions from the comparatively diminutive deep inferior epigastric system, from the terminal branches of the last 6 intercostal vessels and lumbar/iliolumbar vessels, from the thoracodorsal vessels, from the deep and superficial circumflex iliac vessels, and from the external pudendal vessels.

The angiosomes of the IOVAAR are represented in **Figure 2**.

The SCEVs presented numerous variations (**Fig. 5**). In most cases (71.7%), the SIEA and the external pudendal artery (**EPA**) originated from a common trunk called pudendoepigastric arterial trunk. In only 28.3% of cases did the SIEA and the superficial

external pudendal artery arise as isolated vessels. The SIEA and the EPA were each accompanied by a comitant vein that had a parallel course, draining either into the pudendoepigastric venous trunk or into the femoral vein.

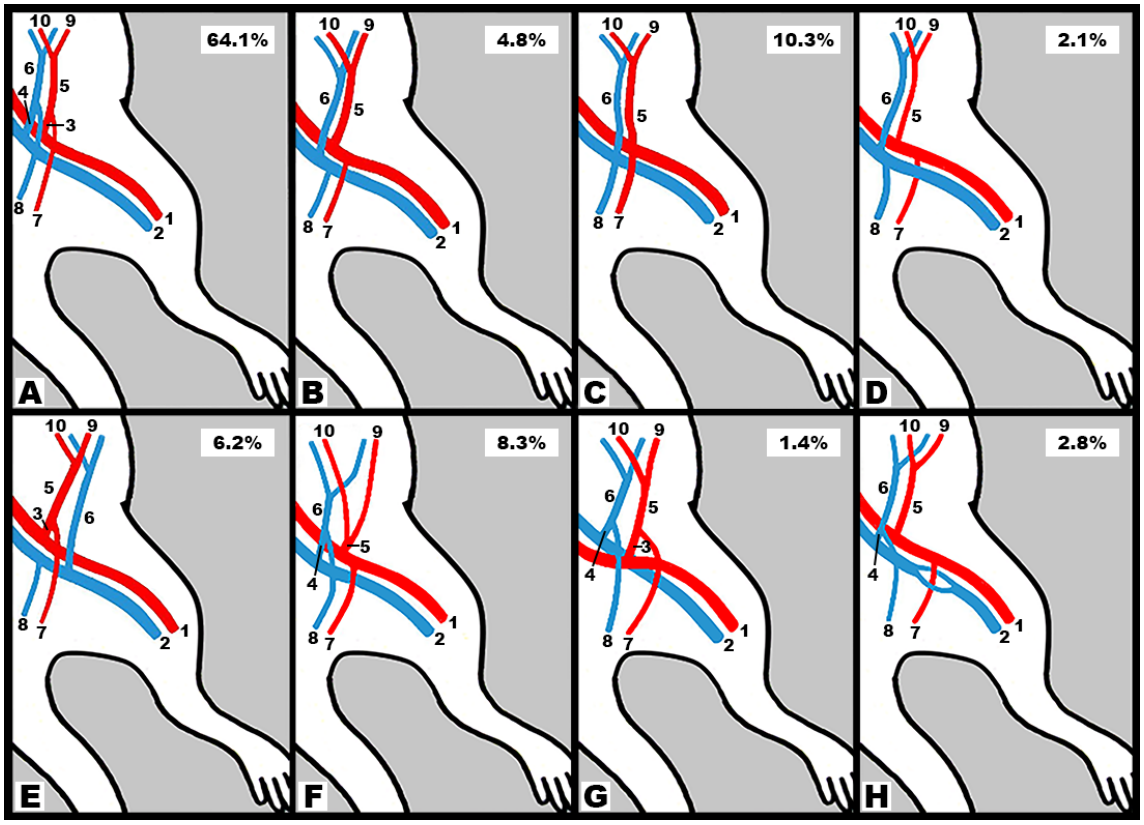

Figure 5- Schematic representation of the variations in the origin, termination and distribution of the superficial caudal epigastric artery and vein (**SIEA** and **SIEV**, respectively), and the external pudendal artery (**EPA**) and vein (**EPV**) on the left side of the rat. The frequency of each variation is shown at the top right hand corner of each drawing. The total number of rats analyzed was 185.

A, The most common pattern, with a common origin of the SIEA and EPA from a common pudendoepigastric arterial trunk and a common termination of the SIEV and EPV into a common pudendoepigastric venous trunk; B, The SIEA, EPA and accompanying veins had an independent origin and termination; C, The SIEA and EPA originated independently from a common point in the femoral artery, and analogously the SIEV and EPV terminated independently into the same region of the femoral vein; D, Similar to that shown in B, with the exception that the external pudendal artery crossed beneath the

femoral vein; E, The arteries show the most common pattern, whereas the SIEV and EPV terminate independently; F, There is a short independent SIEA that originates its two branches soon after its origin; G, Similar to the most common pattern (A), but the femoral artery is medially placed relatively to the homonymous vein at the proximal aspect of the thigh to later cross over the femoral vein; H, The EPA originates independently and crosses through a doubling of the femoral vein.

1, Femoral artery; 2, Femoral vein; 3, Pudendoepigastric arterial trunk; 4, Pudendoepigastric venous trunk; 5, Superficial caudal epigastric artery; 6, Superficial caudal epigastric vein; 7, External pudendal artery; 8, External pudendal vein; 9, Lateral branch of the superficial caudal epigastric artery; 10, Medial branch of the superficial caudal epigastric artery.

After its origin, the SIEA moved obliquely in the direction of the axilla. In all cases, this artery divided into two branches, being followed in its trajectory towards the axilla by its lateral branch. The lateral branch of the SIEA was larger than its medial counterpart in nearly all cases (94.5% of cases on the right side, and 95.6% on the left side). The lateral branch anastomosed with the terminal branches of the LT artery and with the dominant perforators originating from the intercostal vessels. The medial branch of the SIEA anastomosed with the superficial cranial epigastric artery and/or with perforators of the deep cranial epigastric artery (**Figs. 2** to **4**).

The large LT vein could be found in a line drawn from the rat's hip to the ipsilateral axilla (**Figs. 3** and **4**). This vein originated at the level of the costal margin from the convergence of three veins that drained the medial, central and lateral portion of the cranial aspect of the IOVAAR.

The SIEA and the SIEV were accompanied by a sizeable branch of the saphenous nerve – the caudal epigastric nerve (**Fig. 6**). At its origin, the diameter of this nerve was 0.33 ± 0.17 mm. It divided into 2, 3 or 4 branches in the proximal third of the SIEA in

60.6%, 13.1%, and 26.2% of cases, respectively. These branches traveled with the SIEA from its origin and in turn provided multiple twigs throughout the territory of the SCEVs, and also to the medial aspect of the thigh.

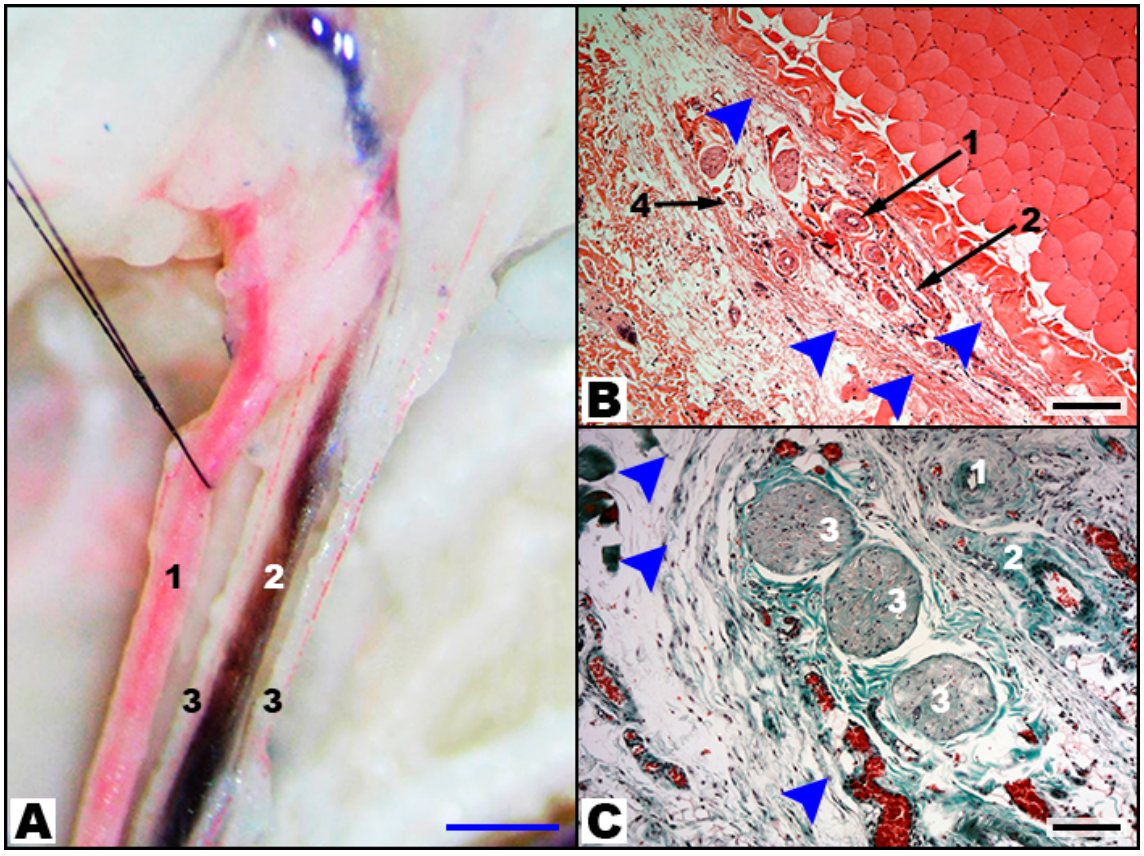

Figure 6 - Superficial caudal epigastric neurovascular bundle and its branches.

A, Photograph of the superficial caudal epigastric neurovascular bundle after intra-arterial and intra-venous injection with a red and blue solution, respectively. B, Microphotograph of a hematoxylin-eosin stained section of a transverse section of the caudal superficial epigastric neurovascular bundle. C, Microphotograph of a Masson's trichrome stained section of a transverse section of the caudal superficial epigastric neurovascular bundle.

1, Superficial caudal epigastric artery; 2, Superficial caudal epigastric vein; 3, Branches of the caudal epigastric nerve; 4, Superficial caudal epigastric lymphatic vessels.

Arrow heads indicate the sheath involving the superficial caudal epigastric neurovascular bundle.

Calibration bar in A = 1000 µm; Calibration bars in B and C = 100 µm.

Musculocutaneous Perforators

Multiple sizeable perforator vessels were seen piercing the muscles and muscular fascia and supplying the IOVAAR (**Figs. 2** to **4** and **7**). These perforators were most commonly seen arising from the rectus abdominis fascia in the central aspect of the abdomen (**Fig. 8**). In this region, the superficial vascular system was less dense (**Fig. 2**). The largest central abdominal perforators derived mainly from the deep epigastric vessels, and particularly from the cranial deep epigastric vessels. On each side, there were on average 6.52 ± 3.64 perforators on the right side, and 6.56 ± 3.67 perforators on the left side, ranging between 2 and 15.

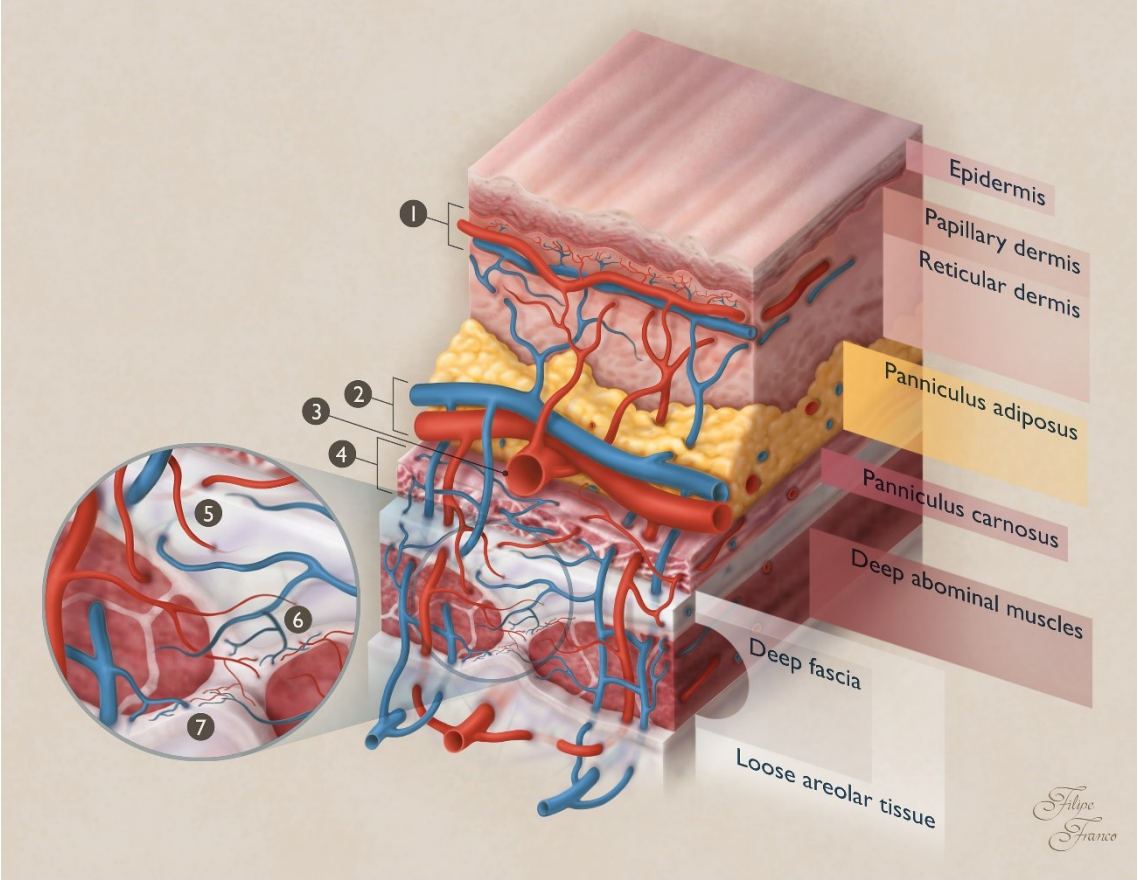

Figure 7 - Schematic drawing of the blood supply to the different layers of the integument of the ventrolateral aspect of the abdomen of the rat.

The integument of the rat is composed of the skin, a fatty layer known as panniculus adiposus, and beneath this latter layer of a sheath of loose connective tissue associated with white adipose tissue and smooth muscle forming a layer known as panniculus carnosus. This layer is located just above the abdominal wall muscles and muscle fascias. There is a loose areolar tissue beneath the panniculus carnosus and the muscle fascia.

The integument presented the following plexuses:

- A loose and thin **prefascial plexus** in the prefascial areolar tissue;
- A dense and thin **panniculus carnosus plexus** encompassing the entire thickness of this layer and mostly dependent on the direct cutaneous axial vessels. This plexus was mostly composed of third-order arterioles and venules, as well as capillaries;

- A loose **panniculus adiposus plexus**, mainly composed of obliquely disposed ascending and descending first-order arterioles and venules, respectively, supplying the overlying layers and the adjacent fatty tissue;
- A **subdermal plexus** at the upper portion of the panniculus adiposus, immediately beneath the skin, composed of second-order arterioles and venules with a horizontal orientation;
- A **reticular dermal plexus** composed of vertically arranged third-order ascending and descending arterioles and venules, respectively, as well as their terminal branches, which formed capillary networks around sebaceous dermal glands and the papillae of hair follicles;
- A **subpappilary dermal plexus**, at the dermal-epidermal interface, composed of capillary loops with a predominantly horizontal disposition interspersed with occasional vertical capillary loops. These capillaries were in continuity with the vertical arterioles and venules of the reticular plexus.

Blue structures represent veins. Red structures represent arteries.

1, Subpapillary vascular plexus; 2, Subdermal vascular plexus; 3, Superficial arteriole in the panniculus adiposus; 4, Panniculus carnosus vascular plexus; 5, Arterioles and venules supplying the prefascial vascular plexus in the prefascial areolar tissue; 6, Fascial vascular plexus; 7, Subfascial vascular plexus.

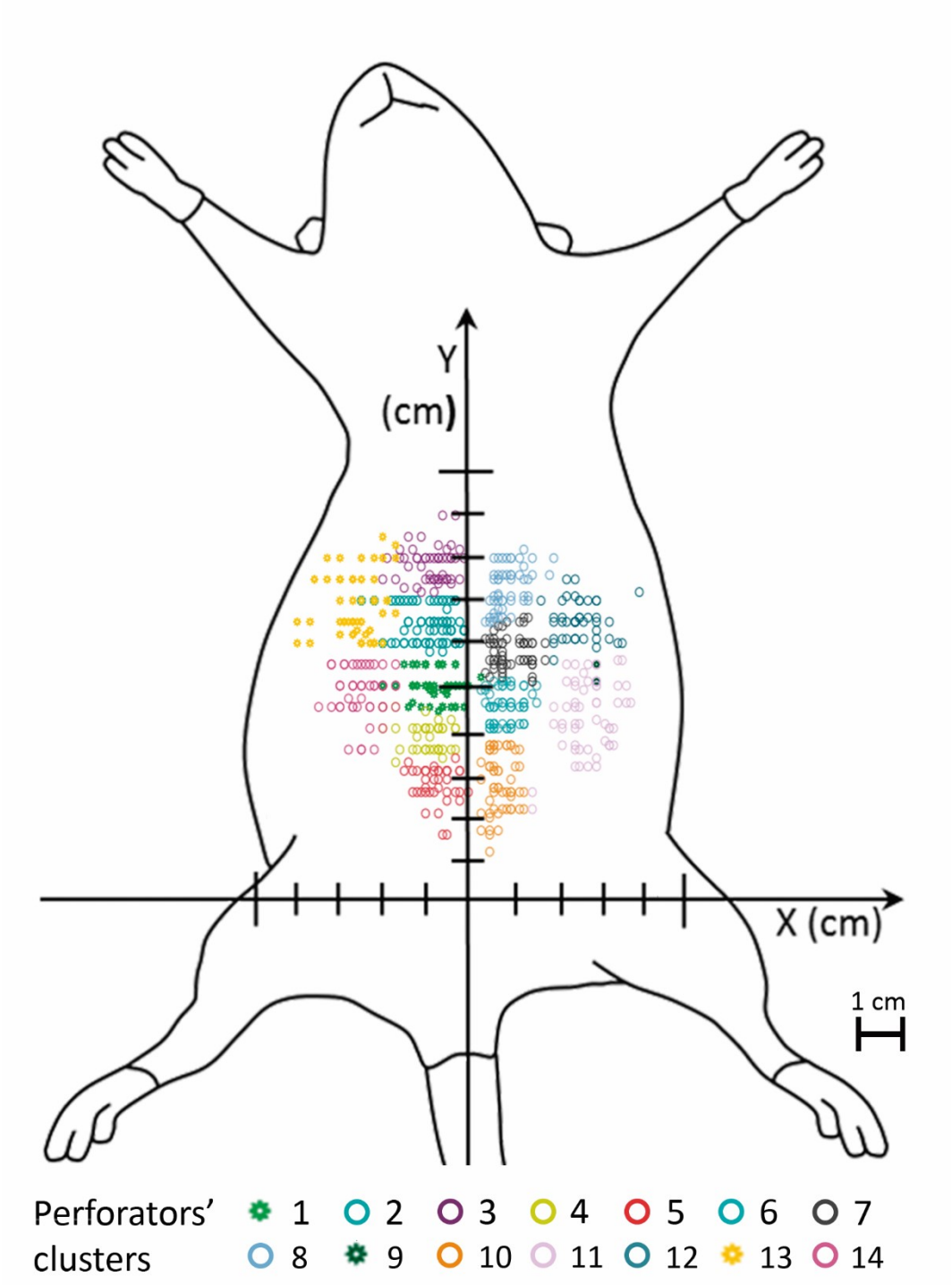

Figure 8 - Dot plot graph drawn over a schematic drawing of the ventrolateral surface of the rat showing the location of the abdominal perforator arteries in the anterior and lateral aspect of the abdominal wall. A two-step cluster analysis based on the Schwarz Bayesian criteria allowed the identification of 7 perforator clusters on each side of the abdomen.

Overall, 79.1% of perforators originated in the deep epigastric system, while 28.1% originated in the segmental vessels that supplied the abdominal wall (last 6 intercostal, lumbar/iliolumbar, and the deep circumflex iliac vessels). This difference was statistically significant ($p<0.05$). Perforators were more common in the cranial half of the abdomen (**Fig. 8** and **Fig. 9**), that is to say in the region were the axial vessels were inexistent or of a smaller caliber ($p<0.05$). A two-step cluster analysis based on the Schwarz Bayesian criteria allowed the identification of 7 musculocutaneous perforator clusters on each side of the abdomen (**Fig. 8**).

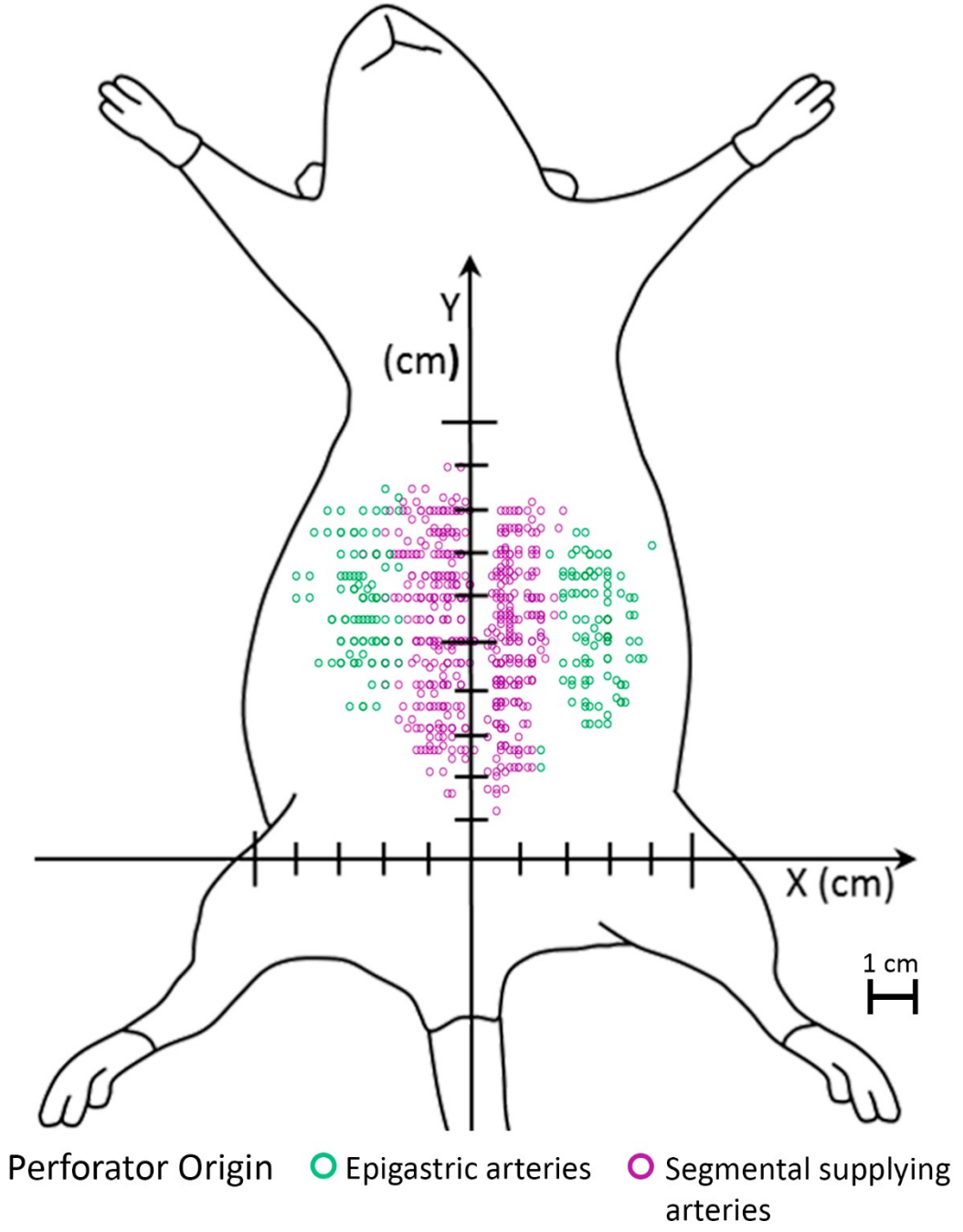

Figure 9 - Dot plot graph drawn over a schematic drawing of the ventrolateral surface of the rat showing the location of the abdominal perforator arteries in the anterior and lateral aspect of the abdominal wall and their origin from the paramedian arteries (cranial and caudal deep epigastric arteries), and from the segmental vessels (intercostal, lumbar/iliolumbar arteries).

Table 1 summarizes the main histomorphometric features of the largest vessels supplying the IOVAAR. No statistical significant differences were found between the right and left sides of the body.

Vessel	Length‡ (cm)	Caliber‡‡ (mm)	Wall Thickness‡‡‡ (µm)
Superficial caudal epigastric artery	1.45 ± 0.22	0.32 ± 0.13	479.07 ± 27.37
Superficial caudal epigastric vein	1.61 ± 0.19	0.65 ± 0.24	183.05 ± 15.63
First divisions of the superficial caudal epigastric artery	0.72 ± 0.16	0.13 ± 0.08	288.19 ± 31.72
First divisions of the superficial caudal epigastric vein	0.92 ± 0.18	0.18 ± 0.05	128.24 ± 43.53
Second divisions of the superficial caudal epigastric artery	0.60 ± 0.12	0.08 ± 0.03	202.38 ± 87.34
Second divisions of the superficial caudal epigastric vein	0.85 ± 0.20	0.16 ± 0.09	102.63 ± 65.71
Thoracoepigastric vein	4.13 ± 1.59	0.47 ± 0.17	41.67 ± 15.67
First divisions of the thoracoepigastric vein	1.63 ± 0.47	0.17 ± 0.04	0.11 ± 0.09

Second divisions of the thoracoepigastric vein	0.96 ± 0.54	0.14 ± 0.05	0.09 ± 0.08

Table 1 - Histomorphometric evaluation of the major arteries and veins supplying the ventrolateral region of the integument of the abdomen of the rat. Values are expressed as average values ± standard deviation.

[ŧ] Length determination was based on Spalteholz cleared specimens (n=10).

[ǂ] Caliber determination was based on Spalteholz cleared specimens (n=10), on transverse histological sections stained with CD 31 (n=10), and on the scanning electron microscopy observation of the vascular corrosion casts (n=10).

[ǂǂ] Wall thickness determination was based on transverse histological sections stained with Masson's Trichrome (n=10).

Noteworthily, the large direct cutaneous vessels described above were present in areas where the integument was laxer, whereas the musculocutaneous perforators were placed more densely in the region where the IOVAAR was more adherent to the underlying muscle fascia. Moreover, the perforator vessels were longer in the lateral aspect of the abdomen compared to those that were more centrally placed in the region of the rectus abdominis muscles. Interestingly, on each side of the abdomen, there was a triangular region, lateral to the lateral branch of the SCEVs where large vessels were absent (**Fig. 10**).

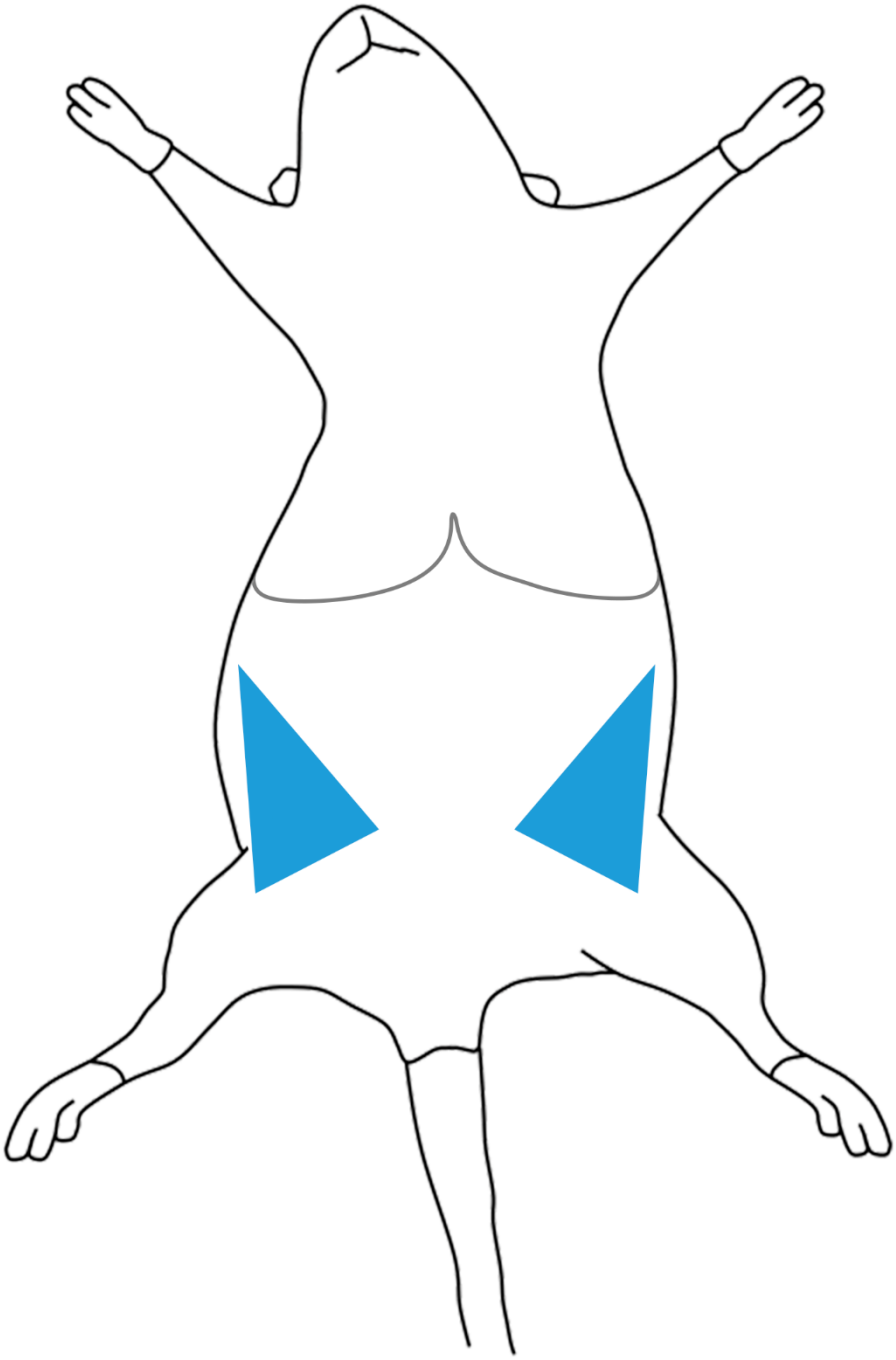

Figure 10 - Schematic diagram illustrating the safe zones (blue) for subcutaneous and intraperitoneal injections in the ventrolateral abdomen of the rat due to the relative scarcity of large vessels in these areas.

Microscopic Anatomy

The IOVAAR was composed of multiple layers, including a sheath of loose connective tissue associated with white adipose tissue and smooth muscle known as panniculus carnosus (**Fig. 7** and **Fig. 11**). Soon after their origin, the large nominated vessels with an axial pattern were found in the panniculus adiposus, immediately superficial to the panniculus carnosus layer. These vessels gave ascending branches to all layers of the IOVAAR, including to the panniculus carnosus. The musculocutaneous perforator vessels originated arterioles and received venules to and from the muscular subfascial, fascial and epifascial plexuses. Additionally, in their ascending trajectory towards the skin they gave branches to all the layers of the IOVAAR. Overall, integumentary vessels formed fine interconnecting meshworks of predominantly horizontal arrangement, establishing the following vascular plexuses: prefascial plexus; panniculus carnosus plexus; panniculus adiposus plexus; subdermal plexus; reticular dermal plexus; and subpappilary dermal plexus (**Figs. 3, 4, 6** to **8, 11** and **12**).

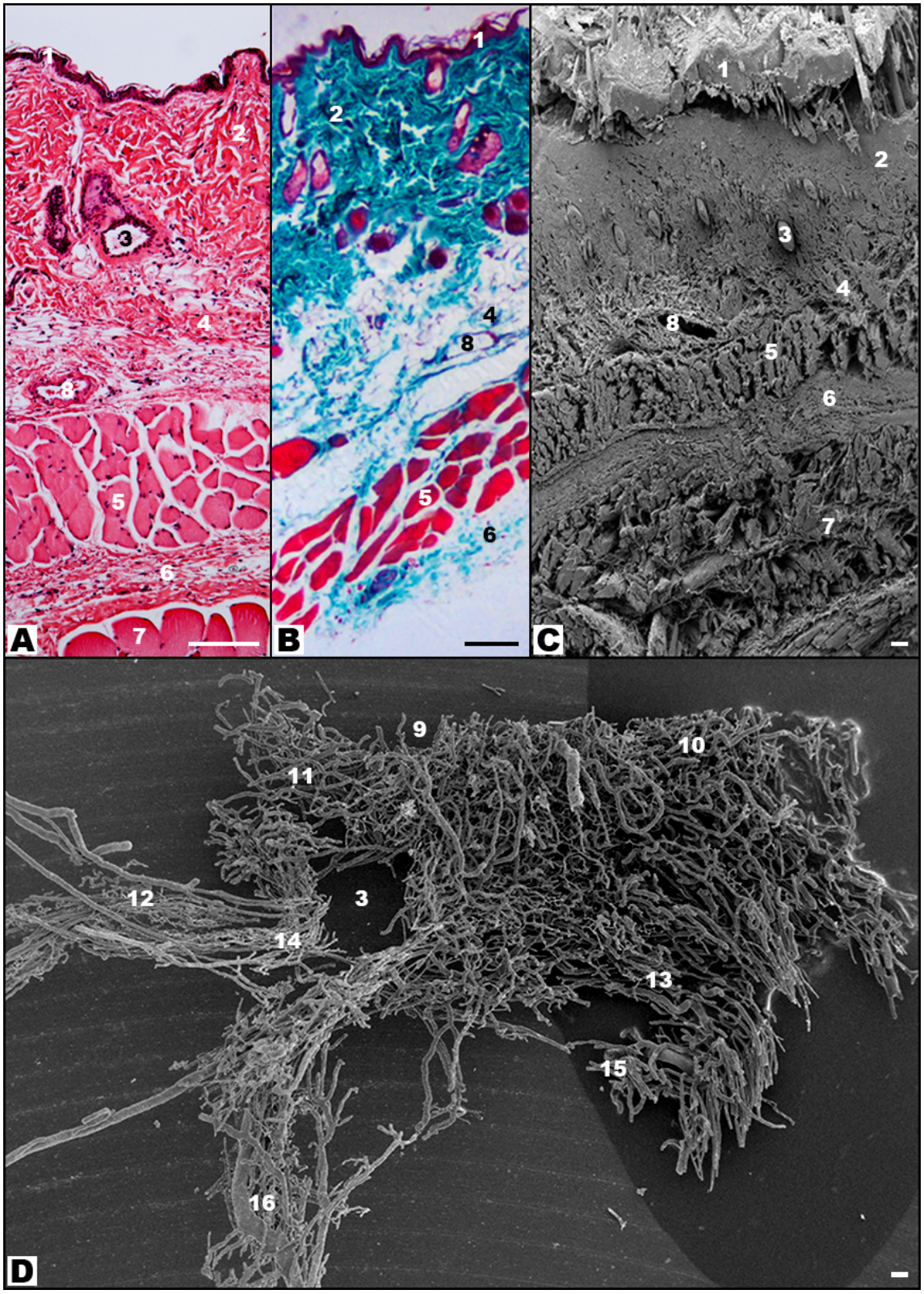

Figure 11 - General view of the blood supply to the different layers of the ventrolateral aspect of the abdominal wall of the Wistar rat.

A, Photograph of a hematoxylin-eosin stained transverse section on the integument over the ventrolateral aspect of the abdominal wall of the Wistar rat; B, Photograph of a Masson's trichrome stained transverse section on the integument over the ventrolateral aspect of the abdominal wall of the Wistar rat;

C, Scanning electron microscope image of a critical point drying of a transverse section of the ventrolateral aspect of the abdominal wall of the Wistar rat; D, Scanning electron microscope image of a corrosion vascular cast of the vessels supplying the integument over the ventrolateral aspect of the abdomen of the rat.

1, Epidermis; 2, Dermis; 3, Hair follicle; 4, Panniculus adiposus; 5, Panniculus carnosus; 6, Deep muscle fascia; 7, Deep abdominal wall muscles; 8, Superficial vein (thoracoepigastric vein); 9, Subpapilary vascular plexus; 10, Deep dermal plexus; 11, Subdermal plexus; 12, Superficial vessels in the panniculus adiposus; 13, Panniculus carnosus' vascular plexus; 14, Fascial plexus; 15, Subfascial plexus; 16, Perforator vessels.

Calibration bar = 100 µm.

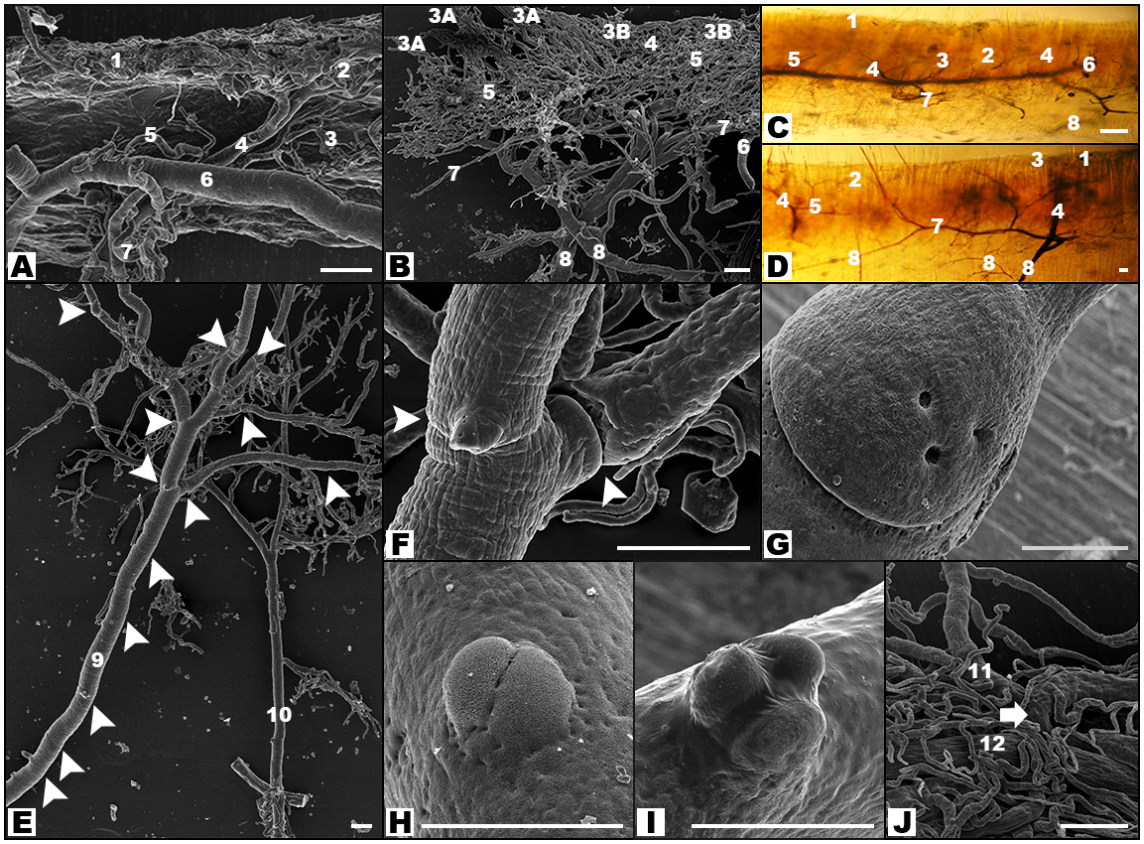

Figure 12- Relevant details of the blood supply to the different layers of the ventrolateral aspect of the abdominal wall of the Wistar rat.

A, Scanning electron microscope image of a partially corroded vascular cast at the skin and panniculus adiposus level showing a large subdermal vein with no venous valves; B, Scanning electron microscope image of a corrosion vascular cast at the level of the skin and panniculus adiposus showing the large first degree arterioles and venules at the level of this latter layer, as well as the subdermal, reticular dermal and subpapilary plexuses in the former layer. In this image, it is clear that the capillary loops in the subpapilary plexus have a predominantly horizontal arrangement. C and D, Photographs of longitudinal section of specimens processed through the modified Spalteholz technique showing the longitudinal disposition of the large subdermal vessels contrasting with the predominantly vertical arrangement of the vessels in the panniculus adiposus and in the reticular dermal plexuses. E to J, Scanning electron microscope images of corrosion vascular casts. E, Cranial deep epigastric musculocutaneous perforators. It is possible to observe numerous venous valves in the perforator vein and its tributaries. F, A magnification view of a venous valve in one of the branches of origin of the vein shown in E; G, Venous valve of vein of the panniculus adiposus; H, Bicuspid venous valve in a tributary of a subdermal vein; I, Tricuspid venous valve in a tributary of a subdermal vein; J, Arteriovenous anastomosis at the subdermal plexus.

1, epidermis; 2, capillary loops of the dermal papilae; 3, subpapillary plexus; 3A, vertically arranged subpapillary capillary loops; 3B, horizontally arranged subpapillary capillary loops; 4, ascending arterioles; 5, reticular dermal plexus; 6, subdermal venule; 7, subdermal plexus; 8, panniculus adiposus vascular plexus; 9, musculocutaneous perforator venule; 10, musculocutaneous perforator arteriole; 11, subdermal venule; 12, subdermal arteriole.

Arrow heads, venous valves. Arrow, arteriovenous anastomosis at the subdermal plexus.

Calibration bar = 100 µm.

At the subdermal and the subpapillary vascular plexuses, scattered and rare arteriovenous anastomoses were found. Pre-capillary sphincters were frequent findings

at the subdermal and reticular dermis plexuses. Multiple venous valves were found in all layers of the integument, from the reticular dermis plexus until the major nominated veins. However, the first-order subdermal veins presented large segments devoid of valves. Venous valves were almost always bicuspid, although a few tricuspid valves were observed. All the nominated veins and their tributaries presented venous valves, with the exception of the SIEV itself, which presented no valves in all specimens studied (**Figs. 11 to 14**).

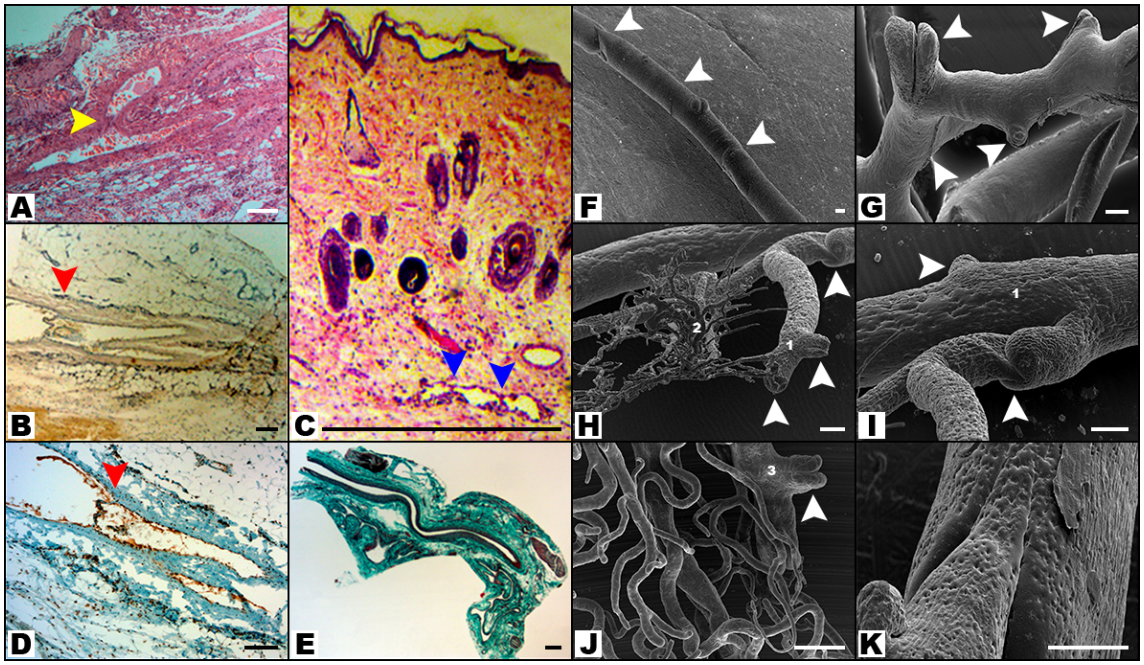

Figure 13 - Venous drainage of the integument of the ventrolateral abdomen of the rat.

A, Microphotograph of a hematoxylin eosin stained longitudinal section of the superficial epigastric vein close to its origin showing venous valves at the confluence of its branches of origin; B, Microphotograph of a CD31 stained longitudinal section of the superficial epigastric vein close to its origin showing venous valves at the confluence of its originating branches; C, Microphotograph of a hematoxylin eosin stained transverse section of the lateral thoracic vein close to its origin showing venous valves at the confluence of its originating branches; D, Microphotograph of a CD31 stained longitudinal section of the superficial

epigastric vein at its middle portion showing a venous valve; E, Microphotograph of a Masson's trichrome stained longitudinal section of the superficial epigastric vein showing absence of venous valves; F, Scanning electron microscope image of the lateral thoracic vein showing numerous venous valves throughout its course and at the ending of its tributaries; G, Scanning electron microscopy image of a tributary vein of the lateral afferent of the superficial caudal epigastric vein; the former presented venous valves at the ending of its tributary veins; H, Scanning electron microscope image of a reticular dermis venule draining the subpapilary venous plexus; I, Scanning electron microscope image of the reticular dermis venule shown in H draining into a panniculus adiposus vein; J, Image of a superficial reticular venule; K, Scanning electron microscope image of one of the afferents of the superficial caudal epigastric vein showing the typical aspect of the venous valves of the veins of the panniculus adiposus at the place of the termination of its afferents.

Arrow heads indicate the presence of venous valves.

1, Deep reticular dermis vein; 2, Subpapillary venous plexus; 3, Panniculus adiposus vein; 4, Superficial reticular dermis vein

Calibration bar = 100 μm.

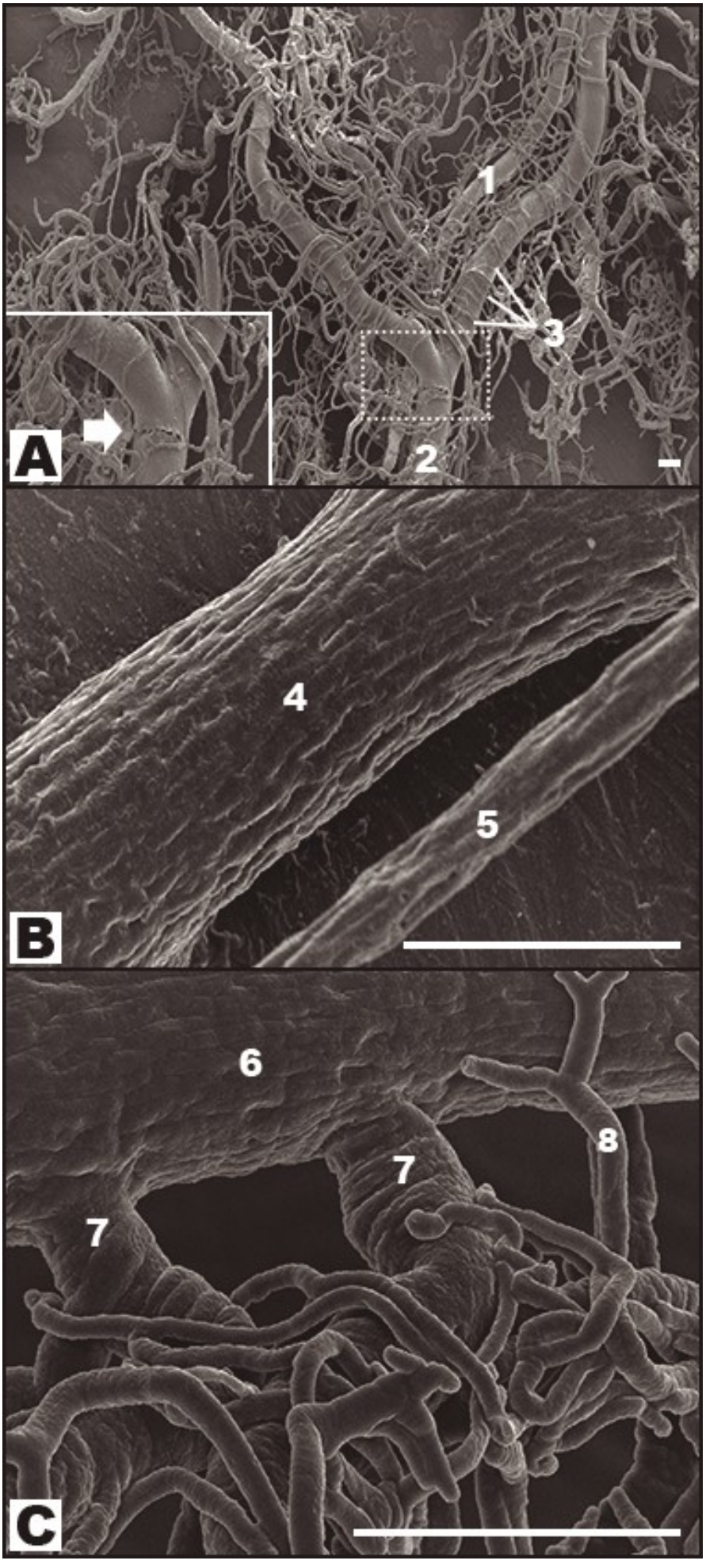
1
2
3
A
4
5
B
6
7
7
8
C

Figure 14 - Details of the microvascular blood supply to the integument covering the ventrolateral aspect of the abdomen of the rat.

A, Scanning electron microscope image of a vascular corrosion cast of the superficial caudal epigastric vessels; the box demonstrates a high magnification view of the superficial caudal epigastric vein showing a slit corresponding to a venous valve; B, Scanning electron microscope image of a vascular corrosion cast of the lateral thoracic artery and vein; C, Scanning electron microscope image of a vascular corrosion cast of a reticular dermis arteriole and its capillaries branches and their pre-capillary sphincters.

1, Superficial caudal epigastric artery; 2, Superficial caudal epigastric vein; 3, *Vasa vasorum* of the superficial epigastric vessels; 4, Lateral thoracic vein; 5, Lateral thoracic artery; 6, Subdermal second-order arteriole; 7, Pre-capillary sphincter; 8, capillaries.
The arrow indicates the slit marking the presence of a venous valve at the confluence of the lateral and medial branches of the superficial caudal epigastric vein.

Calibration bar = 100 µm.

Each of the branches of the caudal epigastric nerve presented a monofascicular pattern (**Fig. 6**). The average number of nerve fibers in the proximal portion of this nerve was 1093.00 ± 88.32 on the right side and 1051.50 ± 107.39 on the left side, being overall 1072.20 ± 97.80. The difference between sides was not statistically significant.

Thermographic Results

Figure 2 illustrates the typical infra-red thermographic images of the IOVAAR obtained directly and post cooling of the rat's surface. In all cases, direct thermography showed a region of higher temperature corresponding to the territory of the SCEVs and the LT vessels. Post cooling thermography, used to highlight perforator vessels, showed a region of higher temperatures in the central and cranial aspect of the abdomen.

DISCUSSION

The IOVAAR has been used regularly for training and research purposes since at least 1967 when the rat epigastric flap was described.(30) Surprisingly, few studies have addressed the macroscopic vascular anatomy of this region.(4, 7, 31-37) Furthermore, the literature on the microvascular blood supply to the rat's integument is even scarcer, being restricted to the paw and tail regions.(28, 38) As far as the authors could determine, the present series, comprising 205 rats, is the largest on the macroscopic and microscopic anatomy of the vascular blood supply to the IOVAAR.

Numerous doubts persist regarding the extent of similarity between the blood supply to this region in humans and rats. Some authors state that the blood supply is relatively similar(31), whereas others argue that it is substantially different.(32) **Table 2** summarizes the main differences found in the present study. Overall, although there are some strong analogies between rats and the humans, namely a common vascular framework (**Figs. 1** and **7**), there are also some noteworthy differences.

	Humans	Rat
Dominant arteries	Musculocutaneous (*in particular the deep inferior epigastric artery*)	Direct cutaneous (*in particular the superficial caudal epigastric artery/ superficial inferior epigastric artery*)
Dominant veins	Superficial and deep veins (*in particular the deep inferior epigastric veins and the superficial inferior epigastric vein*)	Superficial veins (*in particular the lateral thoracic vein/thoracoepigastric vein and the superficial caudal epigastric vein/superficial inferior epigastric vein*)
Superficial inferior epigastric artery	Frequently absent or hypoplasic	Always present and with a sizeable caliber
Perforator vessels	Major role in the normal perfusion More numerous More abundant laterally and below the umbilicus	Less important role in integumentary perfusion Less numerous Mostly located in an area cranially to the umbilicus
Venous valves	Uniformly present in the superficial and deep venous systems	More abundant in the deep venous system and in the cranial aspect of the superficial venous system
Panniculus carnosus	Absent	Well-developed and associated with a vascular plexus

Nerves accompanying major vessels	Intercostal nerves 7 to 12 accompanying the homonymous vessels	Intercostal nerves 7 to 12 accompanying the homonymous vessels Caudal epigastric nerve/inferior epigastric nerve is a sizeable and constant nerve that is part of the superficial caudal epigastric neurovascular bundle

Table 2 - Main differences between the usual blood supply to the integument of the ventrolateral aspect of the abdomen of humans (33, 58) and rats.

The most striking difference refers to the preponderance of the direct cutaneous vessels in the rat, compared to the dominance of the musculocutaneous vessels in humans. Taylor attributed this difference to the fact that in loose-skinned animals, like the rat, the integument is more mobile relative to the underlying muscles due to the presence of a loose areolar tissue layer between the muscular fascia and the panniculus carnosus (**Fig. 7**). (32, 33) The corollary of this is a greater dependence on direct cutaneous vessels in loose-skinned animals compared to humans.(32, 33) Interestingly, in the present study the greater number of perforators was in fact found close to the midline, an in particular in the cranial half of the abdomen, precisely where the integument of the rat was more adherent to the underlying muscle fascia (**Fig. 8**). In this region, the superficial vascular system was less dense (**Fig. 1**).

Another important difference found in this work relative to humans is that central abdominal perforators in the rat were derived mostly from the deep cranial epigastric artery, and not from the deep inferior epigastric vessels as in the former species.(34) These findings are supported by the two other articles that systematically evaluated the number and location of musculocutaneous perforators of the rat's abdomen.(34, 37) Hence, perforator flaps in the IOVAAR seem to be substantially different from those in humans, in terms of vascular homology.

An additional difference relative to humans is the importance of the vessels in the panniculus carnosus of the rat for integumentary perfusion. This had already been hinted by the greater survival of flaps that included this layer, comparatively to flaps that excluded it.(39) In fact, we observed that, soon after their origin, the major subcutaneous vessels coursed in the panniculus adiposus immediately superficial to panniculus carnosus. In addition, the panniculus carnosus was provided with a vascular plexus of its own that was connected with the deep vascular system through anastomoses with branches of the musculocutaneous perforators (**Figs. 7, 11 and 12**).

Interestingly, the SCEVs in the rat presented numerous anatomical variations (**Fig. 5**). This had already been demonstrated in mice and humans. (40-42)

Our data showed that in nearly all cases the lateral branch of the SIEA was dominant relative to its medial counterpart. This is in accordance with the observations of Petry and Wertham who suggested that part of the survival variance of the rat epigastric flap could be explained by the inconsistent incorporation of this branch.(4)

To the best of the authors' knowledge, the fascial envelope surrounding the superficial caudal epigastric neurovascular bundle and determining a specific

compartment had not been described before. Notwithstanding, it is well known that when dissecting the superficial caudal epigastric pedicle, one has to tease away or to cut a delicate tissue sleeve that surrounds these structures. The superficial caudal epigastric fascia resembles the saphenous fascia that surrounds the saphenous veins in the lower limbs.(43) Acknowledging this fascial envelope may facilitate dissection of flaps in this region, particularly by novices in microsurgery.

An interesting information provided by this study was the identification of a triangular zone on each side of the IOVAAR where large vessels were absent (**Fig. 10**). These zones are probably safer for performing abdominal injections. As far as the authors could determine, these safe zones had not been described before.

Our thermographic analysis suggested that the most important perforators physiologically were located in the central and cranial aspect of the abdomen (**Fig. 2**). This information concurred with the anatomical dissection studies performed in the present studies and with those described by other authors.(34, 35) Moreover, our thermographic examination also favored the notion that in normal conditions the superficial vessels were more important for supplying blood to the integument in the caudal and lateral aspects of the IOVAAR, whereas the perforator vessels were more important in the central and cranial aspects. Additionally, these data lend support to the use of thermography as a good technique for evaluating the most important perforator vessels in rats, as it had already been shown in humans by other authors.(29)

The presence of valves in the veins of the IOVAAR has been a matter of debate.(19) Our data show that multiple venous valves are found in all layers of the integument, from the reticular dermis plexus until the major nominated veins (**Figs. 11**

to 14). However, the subdermal first-order venules presented large segments devoid of valves, which probably facilitate oscillating or bidirectional blood flow.(44) All the nominated veins and their tributaries presented venous valves, with the exception of the SIEV (**Fig. 1B**). Valdatta *et al.* also failed to observe valves inside this vein.(19) SEM of vascular corrosion casts of human tissues revealed valves in in superficial veins as small as 20 µm in diameter in different regions of the integument, and in particular in the lower limb, the anterior and posterior walls of the trunk.(45) The major difference between humans and rats regarding venous valves in these regions is, thus, the relative paucity of venous valves in the caudal aspect of the dominant venous system of rats, namely in the SIEV. This difference should be born in mind, for example, when using rats in experimental studies of tissue perfusion, namely in unconventional perfusion flaps and in particular in arterialized venous flaps.(46, 47)

Human microcirculatory studies have shown that the skin subpapillary plexus presents an abundance of vertically arranged capillary loops, coinciding with the dermal papillae. These loops are more pronounced and numerous in body regions were the skin is thicker and subject to intense forces, namely in weight bearing regions or the palm of the hands. (48) However, in our study and contrarily to what has been described in the skin in the footpad of the rat (48, 49), vertical capillary loops in the subpapillary plexus were relatively scarce. Capillaries were more frequently disposed in a horizontal manner in this region. These findings may be due to the fact that this region of the skin of the rat is thinner, has fewer dermal papillae, and it is not usually submitted to intense vertical forces (**Figs. 11 and 12**).

In concordance with other microcirculatory studies performed in the skin covering the abdomen of humans, the authors found that there were few arteriovenous

anastomoses in the IOVAAR.(48, 50) This suggests that this region probably does not play a primordial role in thermoregulation.(50)

This study also lends support to the use of the epigastric flap as sensate flap, as proposed by Hirigoyen et al. (**Fig. 6**) (51). This construction has a similar anatomical rationale to that of using the 12th intercostal nerve in the human species to tailor a neurosensible fasciocutaneous SIEA flap.(51) However, a major difference between rats and humans is that in the former the SIEA and the caudal epigastric nerve are proportionally larger and are always present. Additionally, it should be noted that there is no exact human equivalent to the caudal epigastric nerve.(51)

One of the main limitations of the present work is that the histomorphometric data presented probably understimates vessels' size, since optical microscopy images, as well as SEM images are known to be associated with vessels' shriking during processing, resulting in understimation of vessels' size of up to 30%.(28, 52)

Finally, we believe that the anatomical study herein described helps to better plan, execute and interpret the evolution of the multiple flaps performed in the IOVAAR for teaching, training and research purposes (**Figs. 15 and 16**). (2, 7, 30, 35, 53-57)

Figure 15 - Vascular pedicle of common flaps raised on the ventrolateral surface of the abdomen of the rat.

Some of the most common flaps performed in this region are the Transverse Rectus Abdominis Myocutaneous (**TRAM**) flap based on the cranial epigastric vessels; the Superficial Circumflex Iliac Artery (**SCIA**) flap (also known as iliofemoral flap) based on the superficial circumflex iliac vessels; the Deep Inferior Epigastric Artery Perforator (**DIEP**) flap based on the perforator vessels originating from the deep cranial epigastric vessels; the Deep Circumflex Iliac Artery (**DSCI**) flap (also known as iliac osteocutaneous flap) based on the deep circumflex iliac vessels; the Superficial Inferior Epigastric Artery (**SIEA**) flap (also known as groin flap) based on the superficial caudal epigastric vessels; the External Oblique Myocutaneous Artery (**EOMA**) perforator flap based on the perforators originating from the 6 last intercostal vessels or from the lumbar vessels; and the Vertical Rectus Abdominis Myocutaneous (**VRAM**) flap, based on either the cranial epigastric vessels or the deep caudal epigastric vessels.

1, TRAM (Transverse Rectus Abdominis Myocutaneous) flap based on the cranial epigastric vessels;

2, SCIA (Superficial Circumflex Iliac Artery) or Iliofemoral flap based on the superficial circumflex iliac vessels;

3, DIEP (Deep Inferior Epigastric Artery Perforator) flap based on the perforator vessels originating from the deep cranial epigastric vessels;

4, DSCI (Deep Circumflex Iliac Artery) or iliac osteocutaneous flap based on the deep circumflex iliac vessels;

5, SIEA (Superficial Inferior Epigastric Artery) or groin flap based on the superficial caudal epigastric vessels;

6, EOMA (External Oblique Myocutaneous Artery perforator) flap based on the perforators originating from the last 6 caudal intercostal vessels or from the ilo-lumbar vessels;

7, VRAM (Vertical Rectus Abdominis Myocutaneous) flap, based on either the cranial epigastric vessels or the deep caudal epigastric vessels.

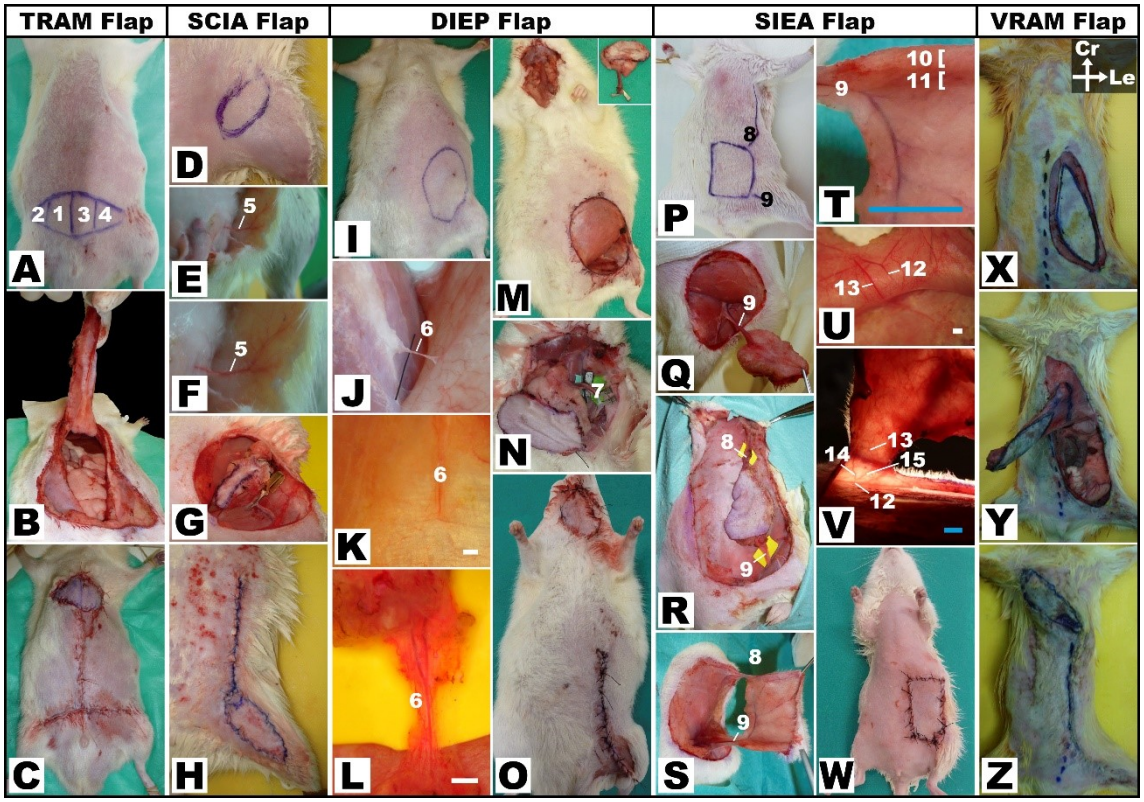

Figure 16 - Photographs illustrating the surgical anatomy of a few common flaps made on the ventrolateral aspect of the abdomen of the rat based on nominated vessels.

A, A right TRAM flap is drawn with its 4 perfusion zones (34); B, The TRAM flap being raised including the right abdominis muscle; C, Flap insetting in the neck region; D, A SCIA is drawn on the left groin; E and F, The undersurface of the SCIA flap showing its vascular pedicle (the superficial circumflex iliac vessels); G, The SCIA flap fasciocutaneous flap after incision of its margins; H, Flap insetting after rotating the SCIA

90º caudally; I, A left DIEP is drawn on the left side; J, The DIEP flap is elevated on a perforator pedicle from the cranial epigastric vessels; K, Operating microscope view of the perforator pedicle piercing the rectus abdominis muscle fascia (arrow head); L, Operating microscope view of the perforator pedicle after muscle fascia opening and partial intramuscular dissection; M, The DIEP flap after harvesting and receptor site dissection; N, Microsurgical anastomoses are performed between the superficial caudal epigastric vessels and the common carotid artery and the external jugular vein; O, The DIEP flap in the ventral aspect of the neck after completion of the anastomoses and closure of the surgical wounds; P, Skin markings of the potential limits of the SIEA flap, as well as of the skin projection of the superficial caudal epigastric vessels and the lateral thoracic vessels; Q, The SIEA flap after incision of boundaries and pedicle release; R, The SIEA flap territory pedicled on the superficial caudal epigastric vessels and the lateral thoracic vessels; S, The deep surface of the SIEA flap. Through the panniculus carnosus it is possible to observe the superficial caudal epigastric vessels and the lateral thoracic vessels and their anastomoses in the central portion of the abdomen; S, Amplified view of the undersu; T and U, The deep surface of the cranial aspect of the undersurface of the SIEA flap. Through the panniculus carnosus it is possible to see the lateral thoracic artery and vein; V, Transillumination of the cranial aspect of the SIEA flap showing the medial and lateral branches of the lateral thoracic vein and the lateral thoracic artery crossing between them; W, The SIEA flap after elevation and wound suture; X, VRAM flap after incision of its boundaries; Y, VRAM flap transposition; Z, VRAM flap insetting in the thoracic region,

TRAM, Transverse Rectus Abdominis Myocutaneous flap based on the cranial epigastric vessels; SCIA, Superficial Circumflex Iliac Artery or Iliofemoral flap based on the superficial circumflex iliac vessels; DIEP, Deep Inferior Epigastric Artery Perforator flap based on the perforator vessels originating from the deep cranial epigastric vessels; SIEA, Superficial Inferior Epigastric Artery or groin flap based on the superficial caudal epigastric vessels; VRAM, Vertical Rectus Abdominis Myocutaneous flap.

1, 2, 3, 4 – perfusion zones of TRAM flap; 5- Superficial circumflex iliac vessels; 6- Perforator vessels from the cranial epigastric vessels; 7, Anastomoses between the superficial caudal epigastric vessels and the common carotid artery and the external jugular vein; 8, Lateral thoracic vessels; 9, Superficial caudal epigastric vessels; 10, Panniculus adiposus; 11, Panniculus carnosus; , Lateral thoracic vein; 13, Lateral thoracic artery; 14, Medial branch of the lateral thoracic vein; 15, Lateral branch of the lateral thoracic vein

White calibration bar = 1 mm

Blue calibration bar = 10 mm

CONCLUSION

The data presented in this paper show that rats and humans present a great deal of homology regarding the blood supply to the ventrolateral aspect of the abdominal integument. However, there are also significant differences that must be taken into consideration when performing and interpreting experimental procedures in rats.

ACKNOWLEDGEMENTS

The authors are very grateful to Mr. Filipe Franco and to Mr. Nuno Folque for producing the drawings contained in this paper.

The authors are very thankful to Prof. Maria Angélica Almeida and Dr. José Videira e Castro for their advice in all steps of the research project. The authors would also like to acknowledge the role of Mr. José Ferreira Silva and that of Dr. Mário Ferraz Oliveira in the supervision of the histological specimens.

References

1. Miles, D. A., Crosby, N. L., Clapson, J. B. The role of the venous system in the abdominal flap of the rat. *Plastic and reconstructive surgery* 1997;99:2030-2033.

2. Oksar, H. S., Coskunfirat, O. K., Ozgentas, H. E. Perforator-based flap in rats: a new experimental model. *Plastic and reconstructive surgery* 2001;108:125-131.

3. Ozgentas, H. E., Shenaq, S., Spira, M. Development of a TRAM flap model in the rat and study of vascular dominance. *Plastic and reconstructive surgery* 1994;94:1012-1017; 1025-1016 discussion.

4. Petry, J. J., Wortham, K. A. The anatomy of the epigastric flap in the experimental rat. *Plastic and reconstructive surgery* 1984;74:410-413.

5. Roberts, A. P., Cohen, J. I., Cook, T. A. The rat ventral island flap: a comparison of the effects of reduction in arterial inflow and venous outflow. *Plastic and reconstructive surgery* 1996;97:610-615.

6. Sano, K., Hallock, G. G., Rice, D. C. The relative importance of the deep and superficial vascular systems for delay of the transverse rectus abdominis musculocutaneous flap as demonstrated in a rat model. *Plastic and reconstructive surgery* 2002;109:1052-1057; discussion 1058-1059.

7. Strauch, B., Murray, D. E. Transfer of composite graft with immediate suture anastomosis of its vascular pedicle measuring less than 1 mm. in external diameter using microsurgical techniques. *Plastic and reconstructive surgery* 1967;40:325-329.

8. Kayano, S., Hallock, G. G., Rice, D. C., Nakagawa, M. Instructional models for dissection techniques of perforator flaps. In P. Blondeel, S. F. Morris, G. G. Hallock, P. C.

Neligan eds., *Perforator flaps: anatomy, technique and clinical applications* Vol. 1, Second ed. Italy: Quality medical publishing, Inc.; 2013:97-107.

9. Shurey, S., Akelina, Y., Legagneux, J., Malzone, G., Jiga, L., Ghanem, A. M. The rat model in microsurgery education: classical exercises and new horizons. *Archives of plastic surgery* 2014;41:201-208.

10. Lee, S. Historical events on development of experimental microsurgical organ transplantation. *Yonsei Med J* 2004;45:1115-1120.

11. Siemionow, M. Z. Microsurgery models. In M. Z. Siemionow ed., *Plastic and Reconstructive Surgery: Experimental models and research designs*, First ed. London: Springer - Verlag; 2015:3-67.

12. Fukui, A. Microvascular anastomoses in the rat. In S. Tamai, M. Usui, T. Yoshizu eds., *Experimental and Clinical Reconstructive Microsurgery*, First ed. Japan: Springer-Verlag; 2004:35-43.

13. Hirase, Y. Skin and muscle flaps in the rat. In S. Tamai, M. Usui, T. Yoshizu eds., *Experimental and Clinical Reconstructive Microsurgery*, First ed. Japan: Springer-Verlag; 2004:111-114.

14. Morain, W. D. Historical Perspectives. In S. J. Mathes ed., *Plastic Surgery*, Vol. 1, Second ed. Philadelphia: Saunders; 2006:27-34.

15. Santoni-Rugiu, P., Sykes, P. J. Skin flaps. In P. Santoni-Rugiu, P. J. Sykes eds., *A History of Plastic Surgery*, First ed. Germany: Springer; 2007:79-119.

16. Tamai, S. The history of microsurgery. In S. Tamai, M. Usui, T. Yoshizu eds., *Experimental and Clinical Reconstructive Microsurgery*, First ed. Tokyo: Springer-Verlag; 2003:3-24.

17. Michaels, J. t., Levine, J. P., Hazen, A., et al. Biologic brachytherapy: ex vivo transduction of microvascular beds for efficient, targeted gene therapy. *Plastic and reconstructive surgery* 2006;118:54-65; discussion 66-58.

18. Lao, W. W., Wang, Y.-L., Ramirez, A. E., Cheng, H.-Y., Wei, F.-C. A new rat model for orthotopic abdominal wall allotransplantation. *Plastic and reconstructive surgery Global open* 2014;2.

19. Valdatta, L., Congiu, T., Thione, A., Buoro, M., Faga, A., Dall'Orbo, C. Do superficial epigastric veins of rats have valves? *Br J Plast Surg* 2001;54:151-153.

20. Fukui, A. Tecnhique of microangiography. In S. Tamai, M. Usui, T. Yoshizu eds., *Experimental and Clinical Reconstructive Microsurgery*, First ed. Japan: Springer-Verlag; 2004:55-56.

21. Sempuku, T. Technique for making a Spalteholz cleared specimen. In S. Tamai, M. Usui, T. Yoshizu eds., *Experimental and Clinical Reconstructive Microsurgery*, First ed. Japan: Springer-Verlag; 2004:59-60.

22. Steinke, H., Wolff, W. A modified Spalteholz technique with preservation of the histology. *Ann Anat* 2001;183:91-95.

23. Sempuku, T. Technique for making a vascular corrosion cast. In S. Tamai, M. Usui, T. Yoshizu eds., *Experimental and Clinical Reconstructive Microsurgery*, First ed. Japan: Springer-Verlag; 2004:57-58.

24. Fischer, A. H., Jacobson, K. A., Rose, J., Zeller, R. Hematoxylin and eosin staining of tissue and cell sections. *Cold Spring Harbor Protocols* 2008;2008:pdb. prot4986.

25. Foot, N. C. The Masson trichrome staining methods in routine laboratory use. *Stain Technology* 1933;8:101-110.

26. Pusztaszeri, M. P., Seelentag, W., Bosman, F. T. Immunohistochemical expression of endothelial markers CD31, CD34, von Willebrand factor, and Fli-1 in normal human tissues. *Journal of Histochemistry & Cytochemistry* 2006;54:385-395.

27. Raimondo, S., Fornaro, M., Di Scipio, F., Ronchi, G., Giacobini-Robecchi, M. G., Geuna, S. Chapter 5: Methods and protocols in peripheral nerve regeneration experimental research: part II-morphological techniques. *International review of neurobiology* 2009;87:81-103.

28. Aharinejad, S. H., Lametschwandtner, A. Identification and Interpretation of Cast Vessel Structures In S. H. Aharinejad, A. Lametschwandtner eds., *Microvascular corrosion casting in scanning electron microscopy: Tecnhiques and applications*, First ed. New York: Springer-Verlag; 1992:103-115.

29. Sheena, Y., Jennison, T., Hardwicke, J. T., Titley, O. G. Detection of perforators using thermal imaging. *Plastic and reconstructive surgery* 2013;132:1603-1610.

30. Gurunluoglu, R., Siemionow, M. Z. The microsurgical groin skin flap in the rat model. In M. Z. Siemionow ed., *Plastic and Reconstructive Surgery: Experimental models and research designs*, First ed. London: Spronger; 2015:53-62.

31. Dunn, R. M., Mancoll, J. Flap models in the rat: a review and reappraisal. *Plastic and reconstructive surgery* 1992;90:319-328.

32. Taylor, G. I., Minabe, T. The angiosomes of the mammals and other vertebrates. *Plastic and reconstructive surgery* 1992;89:181-215.

33. Taylor, G. I., Pan, W. R. The angiosome concept. In P. Dodwell ed., *The angiosome concept and tissue transfer*, Vol. 1, First ed. Florida: Quality Medical Publishing, Inc.; 2014:354-395.

34. Hallock, G. G., Rice, D. C. Physiologic superiority of the anatomic dominant pedicle of the TRAM flap in a rat model. *Plastic and reconstructive surgery* 1995;96:111-118.

35. Hallock, G. G., Rice, D. C. Cranial epigastric perforator flap: a rat model of a true perforator flap. *Ann Plast Surg* 2003;50:393-397.

36. Ozkan, O., Coskunfirat, O. K., Ozgentas, H. E., Dikici, M. B. New experimental flap model in the rat: free flow-through epigastric flap. *Microsurgery* 2004;24:454-458.

37. Ozkan, O., Koshima, I., Gonda, K. A supermicrosurgical flap model in the rat: a free true abdominal perforator flap with a short pedicle. *Plastic and reconstructive surgery* 2006;117:479-485.

38. Aharinejad, S. H., Lametschwandtner, A. The peripheral sense organs. The integument. In S. H. Aharinejad, A. Lametschwandtner eds., *Microvascular corrosion casting in scanning electron microscopy: Tecnhiques and applications*, First ed. New York: Springer-Verlag; 1992:354-360.

39. Pearl, R. M., Johnson, D. The vascular supply to the skin: an anatomical and physiological reappraisal--Part II. *Annals of plastic surgery* 1983;11:196-205.

40. Kochi, T., Imai, Y., Takeda, A., et al. Characterization of the arterial anatomy of the murine hindlimb: functional role in the design and understanding of ischemia models. *PloS one* 2013;8:e84047.

41. Gagnon, A., Blondeell, P. Deep and superficial inferior epigastric artery perforator flaps. *Cirugía Plástica Ibero-Latinoamericana* 2006;32.

42. Fathi, M., Hatamipour, E., Fathi, H. R., Abbasi, A. The anatomy of superficial inferior epigastric artery flap. *Acta Cirurgica Brasileira* 2008;23:429-434.

43. Abu-Hijleh, M. F., Roshier, A. L., Al-Shboul, Q., Dharap, A. S., Harris, P. F. The membranous layer of superficial fascia: evidence for its widespread distribution in the body. *Surgical and radiologic anatomy : SRA* 2006;28:606-619.

44. Blondeel, P. N., Morris, N. J., Hallock, G. G., Neligan, P. C. Vascular territories of the integument. In P. N. Blondeel, N. J. Morris, G. G. Hallock, P. C. Neligan eds., *Perforator flaps: anatomy, techique and clinical implications*, Vol. 1, Second ed. St. Louis, Missouri: Quality Medical Publishing, Inc.; 2013:26-52.

45. Caggiati, A., Phillips, M., Lametschwandtner, A., Allegra, C. Valves in small veins and venules. *European journal of vascular and endovascular surgery* 2006;32:447-452.

46. Casal, D., Cunha, T., Pais, D., et al. Systematic Review and Meta-Analysis of Unconventional Perfusion Flaps in Clinical Practice. *Plastic and reconstructive surgery* 2016;138:459-479.

47. Koyama, T., Sugihara-Seki, M., Sasajima, T., Kikuchi, S. Venular valves and retrograde perfusion. In H. M. Swartz, D. K. Harrison, D. F. Bruley eds., *Oxygen transport to tissue XXXVI*, Vol. 1. New York, USA: Springer; 2014:317-323.

48. Aharinejad, S. H., Lametschwandtner, A. Microangioarchitecture of selected organ systems: the integument. In S. H. Aharinejad, A. Lametschwandtner eds., *Microvascular corrosion casting in scanning electron microscopy: Tecnhiques and applications*, First ed. New York: Springer-Verlag; 1992:354-360.

49. Imayama, S. Scanning and transmission electron microscope study on the terminal blood vessels of the rat skin. *The Journal of investigative dermatology* 1981;76:151-157.

50. Walløe, L. Arterio-venous anastomoses in the human skin and their role in temperature control. *Temperature* 2016;3:92-103.

51. Hirigoyen, M. B., Rhee, J. S., Weisz, D. J., Zhang, W. X., Urken, M. L., Weinberg, H. Reappraisal of the inferior epigastric flap: a new neurovascular flap model in the rat. *Plastic and reconstructive surgery* 1996;98:700-705.

52. Millington, P. F., Wilkinson, R. The skin in depth: dermal vasculature. In R. J. Harrison, R. M. McMinn eds., *Biologic structure and function of the skin: Skin*, Vol. 1, First ed. United Kingdom: Cambridge University Press; 1983:69-72.

53. Syed, S. A., Tasaki, Y., Fujii, T., Hirano, A., Kobayashi, K. A new experimental model: the vascular pedicle cutaneous flap over the dorsal aspect (flank and hip) of the rat. *Br J Plast Surg* 1992;45:23-25.

54. Özkan, Ö., Akyürek, M., Safak, T., Kaykçoglu, A., Güler, G., Erk, Y. A new flap model in rats: iliac osteomusculocutaneous flap. *Ann Plast Surg* 2001;47:161-167.

55. Nasır, S. New Modification of the Oldest Flap in Rats to Increase Antigenicity of Transplanted Skin: The Extended Groin Flap Model. *Plastic and reconstructive surgery*: Springer; 2015:227-236.

56. Dunn, R. M., Huff, W., Mancoll, J. The Rat Rectus Abdominis Myocutaneous Flap: A True Myocutaneous Flap Model. *Ann Plast Surg* 1993;31:352-357.

57. Dunn, R. M., Mancoll, J. Flap models in the rat: a review and reappraisal. *Plastic and reconstructive surgery* 1992;90:319-328.

58. Taylor, G. I., Watterson, P. A., Zelt, R. G. The vascular anatomy of the anterior abdominal wall: The basis for flap design. *Perspectives in Plastic Surgery* 1991;5:1-28.

Chapter 6

THE RAT EPIGASTRIC FREE FLAP: A MODEL OF FREE TISSUE TRANSFER

Authors: Diogo Casal[1-4], Diogo Pais[1], Inês Iria[3,4], Eduarda Mota-Silva[5], Maria-Angélica Almeida[2], Sara Alves[6], Cláudia Pen[6], Ana Farinho[4], Luís Mascarenhas-Lemos[1,6], José Ferreira-Silva[6], Mário Ferraz-Oliveira[6], Valentina Vassilenko[5], Paula A. Videira[3,4], João Goyri O'Neill[1,5]

Affiliations:

1 - Anatomy Department, NOVA Medical School, Universidade NOVA de Lisboa, Lisbon, Portugal

2- Plastic and Reconstructive Surgery Department and Burn Unit, Centro Hospitalar de Lisboa Central – Hospital de São José, Lisbon, Portugal

3- UCIBIO, Life Sciences Department, Faculty of Sciences and Technology, Universidade NOVA de Lisboa, Caparica, Portugal

4- CEDOC, NOVA Medical School, Universidade NOVA de Lisboa, Lisbon, Portugal

5- LIBPhys, Physics Department, Faculty of Sciences and Technology, Lisbon, Portugal

6- Pathology Department, Centro Hospitalar de Lisboa Central – Hospital de São José, Lisbon, Portugal

ABSTRACT

Free tissue transfer has been increasingly used in clinical practice since the 1970s, allowing reconstruction of complex and otherwise untreatable defects resulting from tumor extirpation, trauma, infections, malformations or burns. Free flaps are particularly useful for reconstructing highly complex anatomical regions, like those of the head and neck, the hand, the foot and the perineum. Moreover, basic and translational research in the area of free tissue transfer is of great clinical potential. Notwithstanding, surgical trainees and researchers are frequently deterred from using microsurgical models of tissue transfer, due to lack of information regarding the technical aspects involved in the operative procedures. The aim of this paper is to present the steps required to transfer a fasciocutaneous epigastric free flap to the neck in the rat.

This flap is based on the superficial epigastric artery and vein, which originates from and drain into the femoral artery and vein, respectively. On average the caliber of the superficial epigastric vein is 0.6 to 0.8 mm, contrasting with the 0.3 to 0.5 mm of the superficial epigastric artery. Histologically, the flap is a composite block of tissues, containing skin (epidermis and dermis), a layer of fat tissue (*panniculus adiposus*), a layer of striated muscle (*panniculus carnosus*), and a layer of loose areolar tissue.

Succinctly, the epigastric flap is raised on its pedicle vessels that are then anastomosed to the external jugular vein and to the carotid artery on the ventral surface

of the rat's neck. According to our experience, this model guarantees the complete survival of approximately 70 to 80% of epigastric flaps transferred to the neck region. The flap can be evaluated whenever needed by visual inspection. Hence, the authors believe this is a good experimental model for microsurgical research and training.

INTRODUCTION

Free tissue transfer has been increasingly used in clinical practice for reconstructing missing tissues since the 1970s. [1-5] This has allowed reconstruction of complex and otherwise untreatable defects resulting from tumor extirpation, trauma, infections, malformations or burns. [1-7] Free flaps of this kind are particularly useful for reconstructing highly complex anatomical regions, like those of the head and neck, the hand, the foot, and the perineum. [1,4]

However, even today surgical trainees are frequently daunted by the complexity of several steps involved in raising, transferring and insetting a free flap with the use of microsurgical techniques and instruments.[8,9] In addition, it is widely accepted that to become a proficient microsurgeon, extensive experimental practice in an animal model is mandatory.[4,8-13]

Moreover, basic and translational research in the area of free tissue transfer is of great clinical potential. [8,14-16] Notwithstanding, researchers are frequently deterred from using microsurgical models of tissue transfer due to lack of information regarding the technical aspects involved in the operative procedures.[4,8-14] The rat is a good animal model for microsurgical research and training, as it is relatively inexpensive, easy to keep, and amenable to frequent manipulation. [8,11,13,14,17,18]

Although several free bone, muscle and skin flaps have been described in the rat [18-24], the free epigastric fasciocutaneous flap is the most widely used for teaching purposes [9,12,13,18,25]. This free flap was first described in 1967 by Strauch and Murray and has gained increasing popularity ever since, due to several factors, namely constant vascular anatomy, relative ease of dissection, sizeable nutrient vessels, and redundancy of skin in the donor zone, which allows primary closure of the defect resulting from flap's elevation. [4,9-11,13,17,18,25-28]

Flap Anatomy and Histology

The epigastric flap is supplied by the superficial epigastric artery and vein (**Fig. 1**). These vessels originate from and drain into the femoral artery and vein, respectively. On average the caliber of the superficial epigastric vein is 0.6 to 0.8 mm, contrasting with the 0.3 to 0.5 mm of the superficial epigastric artery (**Fig. 2**). [17,18] The superficial epigastric artery gives off two main branches: a lateral and a medial branch that in turn divide multiple times, originating capillary networks that supply most of the integument of the epigastric region. These capillaries drain into the tributaries of the superficial epigastric veins that have a parallel course to the arterial tree (**Fig. 2**). [13,17,18] The diagram in **Figure 3** represents the region of the ventrolateral abdominal wall supplied by the superficial epigastric vessels that can be mobilized in the epigastric flap. This flap can be up to 5 cm in length and 3 cm in width. [13,17,18]

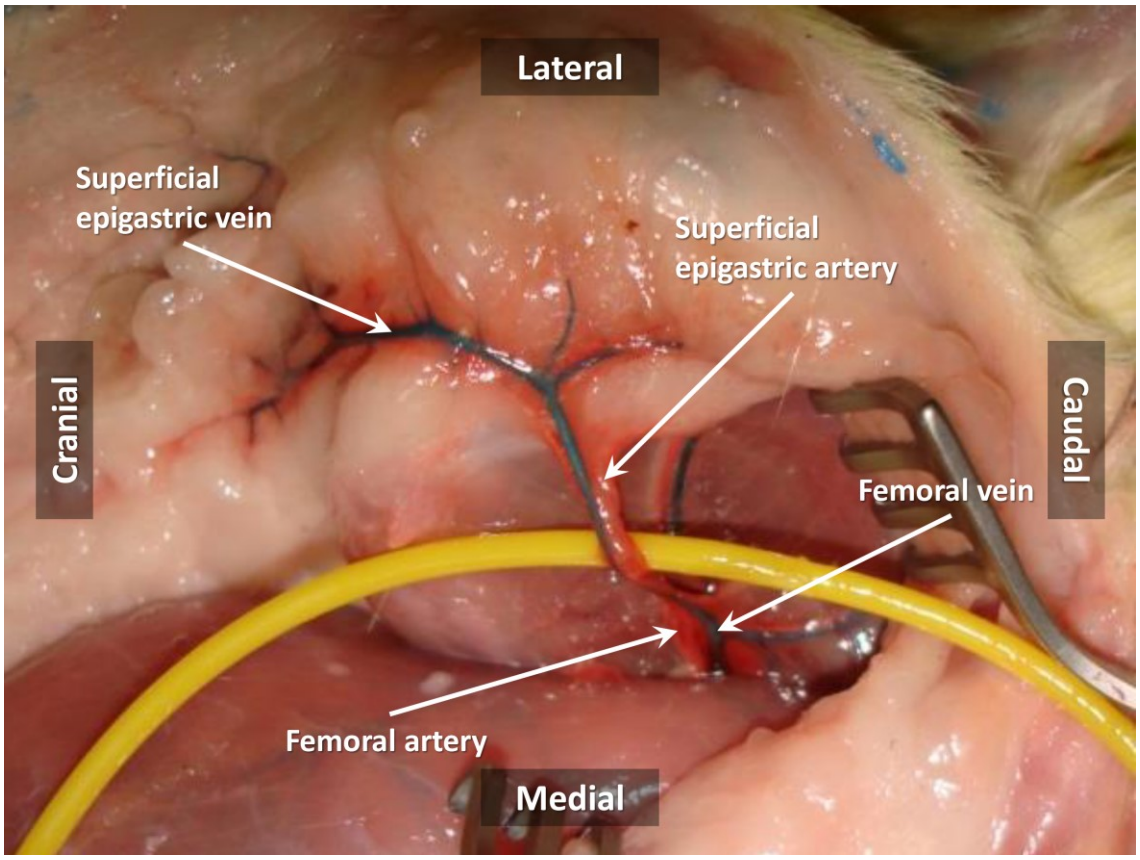

Figure 1 - Vascular anatomy of the epigastric free flap.

This photograph shows the left epigastric region of a rat previously injected with a red latex solution in the arterial system and with a blue latex solution in the venous system.

It is possible to observe that the epigastric region receives an axial blood supply from the superficial epigastric artery and vein. These vessels originate from and drain into the femoral artery and vein, respectively.

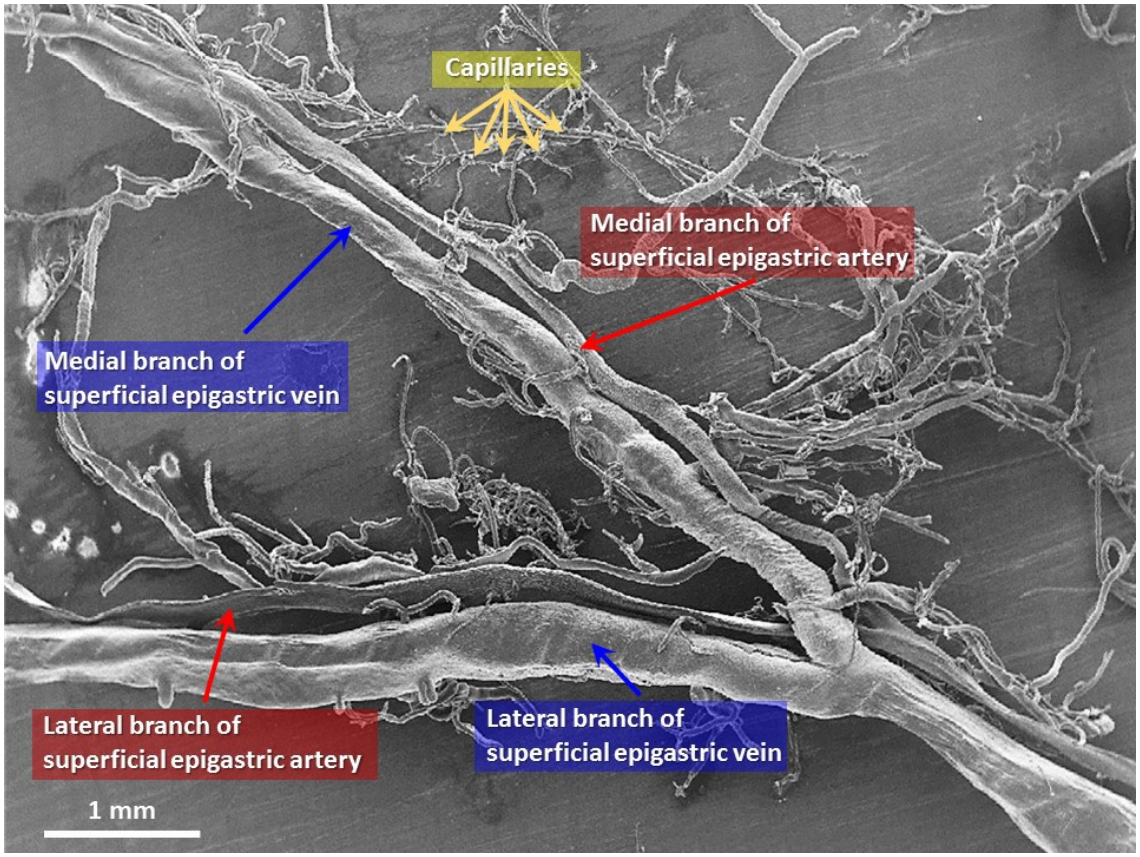

Figure 2 - Scanning electron microscopy image of a corrosion cast of the superficial epigastric vessels showing the microscopic vascular blood supply to the epigastric free flap.

This scanning electron microscopy image of a corrosion cast of the superficial epigastric vessels of the rat shows that the vein has a larger caliber that the artery. On average the caliber of the superficial epigastric vein is 0.6 to 0.8 mm, compared with the 0.3 to 0.5 mm of the superficial epigastric artery. This image also shows that the superficial epigastric artery originates two main branches: a lateral and a medial branch that in turn divide multiple times, originating capillary networks that supply most of the epigastric region. These capillaries drain into the tributaries of the superficial epigastric vein that have a parallel course to the arterial tree.

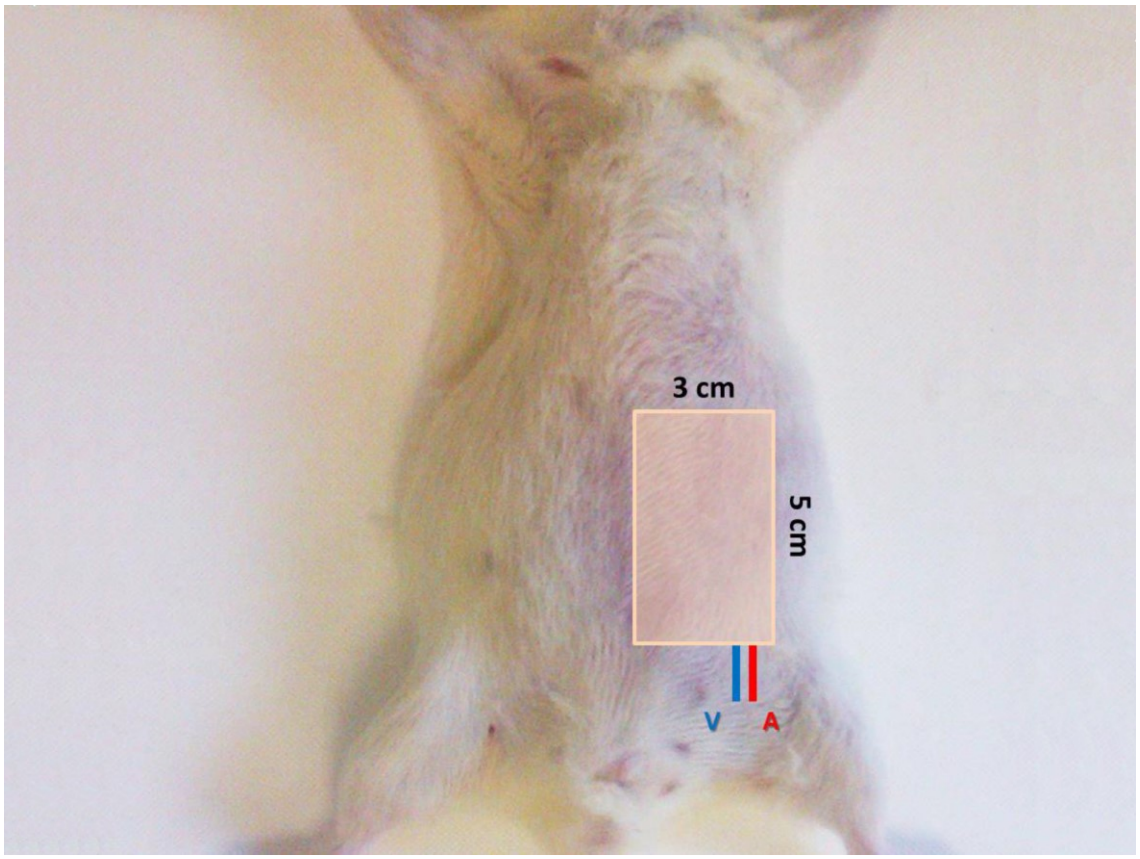

Figure 3 - Potential area of a left epigastric free flap in the rat.

This diagram represents the region of the abdominal wall supplied by the superficial epigastric vessels and that can be mobilized in the epigastric flap. This flap can be up to 5 cm in length and 3 cm in width.

Histologically, the flap is composed of the integument that covers the ventrolateral abdominal wall muscles (**Fig. 4**). [13,17,18] It contains a superficial layer of skin, formed by the dermis and epidermis. Beneath the skin there is a layer of fat tissue named *panniculus adiposus*. Below this layer there is another layer of striated muscle known as *panniculus carnosus*. [18,28,29] Below the *panniculus carnosus* there is loose areolar tissue which is superficial to the deep fascia that covers the larger abdominal muscles. Hence, the flap is a composite block of tissues, containing all these layers, except for the deep muscle fascia (**Fig. 5**). [13,17,18,27-31]

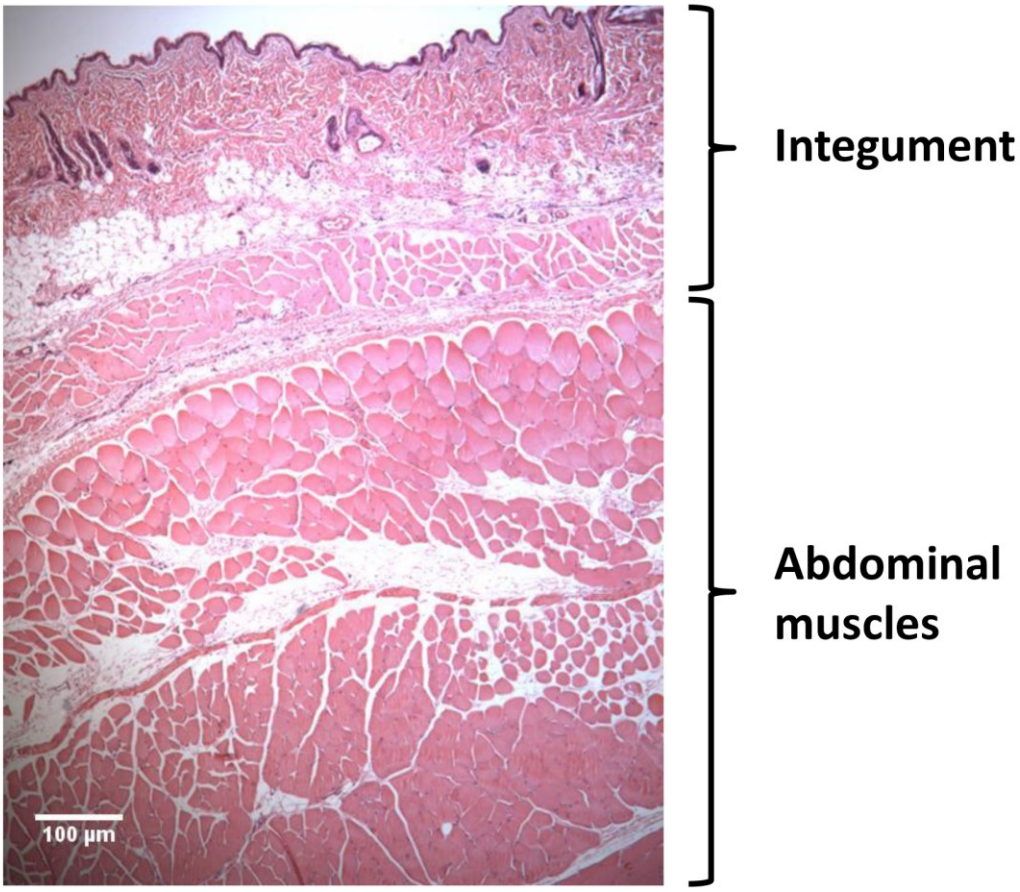

Figure 4 - Photograph of a hematoxilin-eosin stained section of the epigastric flap.

This hematoxilin-eosin stained section of the epigastric region shows that the epigastric flap is composed of the integument of this region that covers the abdominal wall muscles.

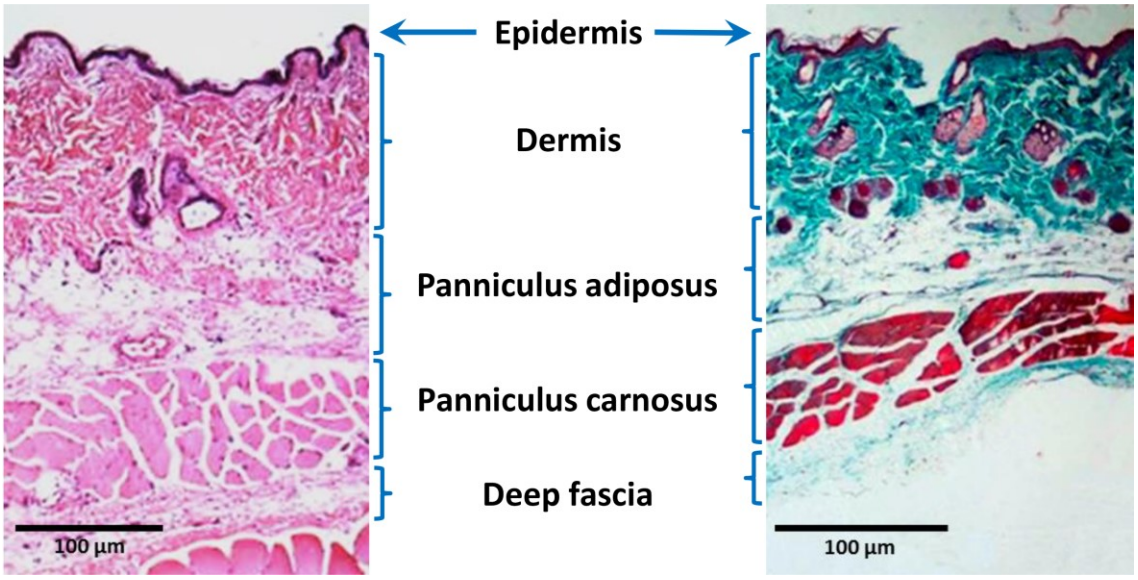

Figure 5 - Histological composition of the epigastric flap.

The photograph on the left side represents a hematoxilin-eosin stained section of an epigastric flap, whereas the photograph on the right side was obtained from a Masson's trichrome section of this flap. These two pictures illustrate that the epigastric flap of the rat is a composite block of tissues. It contains a superficial layer of skin, formed by the dermis and epidermis. Beneath the skin there is a layer of fat tissue named *panniculus adiposus*. Below this layer there is layer of striated muscle known as *panniculus carnosus*. Below the *panniculus carnosus* there is a deep fascia that covers the larger and deeper abdominal muscles.

PROTOCOL

All procedures involving animal subjects were approved by the Institutional Animal Care and Use Committee and Ethical Committee at Nova University Medical School, Lisbon, Portugal (08/2012/CEFCM).

1. **Surgical Procedure Set-up Notes**

1.1. Use adult Wistar rats weighing 250 to 350 grams.

1.2. Keep the rats with food and water ad libitum with 12-hour light-dark cycles 7 days prior to surgery.

1.3. Weigh the rat in order to determine the amount of anesthetic required.

1.4. Autoclave all surgical instruments before surgery.

1.5. Layout all the surgical supplies and instruments needed for the procedure (see the Table of Specific Surgical Instruments).

1.6. Perform the surgery under an operating microscope using conventional and microsurgical instruments.

1.7. Position the homeothermic blanket, rectal probe, and heat lamp.

1.8. Place one 20-mL sterilized vial containing 0.9% saline in a water bath warmed to 37 ºC.

1.9. Wear sterilized gloves to disinfect all surfaces of the operating setting with an

alcoholic solution. Remove the gloves.

1.10. Place a scrub cap and mask.

1.11. Disinfect hands with water and soap and wear another pair of sterilized gloves.

1.12. Wear a sterile surgical gown.

2. Anesthesia and Skin Preparation

Note: Have an assistant help with the following four steps, as a sterile gown and gloves are worn.

2.1. Anesthetize the rat with a mixture of Ketamine and Diazepam given intraperitoneally. The dose is 5 mg/kg ketamine and 0.25 mg/kg diazepam. Judge the depth of anesthesia by toe pinch and by observance of respiration rate throughout the entire procedure. [8,14,15,32]

2.2. Apply an ophthalmic gel over the anterior surface of the eyes to avoid corneal abrasion.

2.3. Remove the hair over the ventral surface of the abdomen with a depilatory cream. After hair removal, the depilatory cream should be removed with warm saline.

2.4. Spray a substantial amount of alcoholic solution (Cutasept F®) over the operative site. Leave the product act in the operative site and do not wipe it off. Wait at least 15 seconds. Repeat the application 3 times. Leave a contact time of at least 2 minutes before proceeding with the surgery. Other research units use other protocols to prevent surgical site infection.

2.5. Wearing sterilized gloves, place 2 surgical drapes on both sides of the rat.

3. Donor Site Surgical Procedure

3.1. Set the boundaries of an epigastric flap ranging approximately 5 cm in length and 3 cm width.

3.1.1. Using a surgical skin marker, draw a line from the xiphoid process of the sternum to the pubic symphysis, in order to mark the midline over the ventral surface of the rat's abdomen.

3.1.2. On the left side of the rat, using a surgical skin marker, draw two perpendicular lines to the first line: one crossing immediately caudal to the thoracic cage, and another one, parallel to the latter and just cranial to the groin fold (**Figs. 3** and **6**).

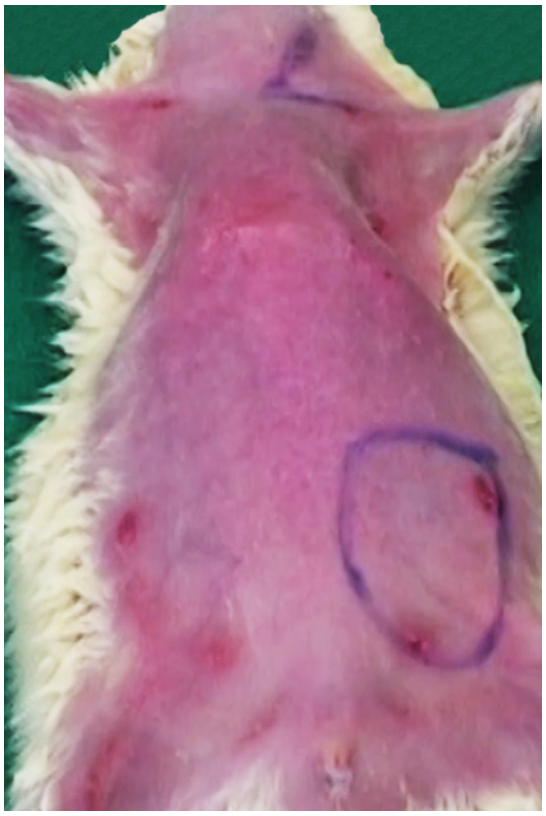

Figure 6 - Pre-operative skin markings on the ventral surface of the rat prior to surgery.

This photograph illustrates the skin markings for the incisions used to raise the left epigastric flap and subsequently to inset this flap in the ventral aspect of the left cervical region.

3.1.3. Mark the lateral incision with a surgical skin marker with a line parallel to the midline and around 3 cm apart from it.

3.2. Flap harvesting

3.2.1. Incise the skin with a number 15 scalpel blade until reaching the *panniculus carnosus* layer.

3.2.2. Deeper to the *panniculus carnosus* plane make the incision with an electric cautery

until reaching the muscle fascia.

3.2.3. Raise the flap from medial to lateral and from cranial to caudal, exposing the flap's pedicle.

3.2.4. Carefully ligate and divide the perforating vessels coming up from the deep muscle layer and going into the flap's deep surface.

3.2.5. Place a retractor in the caudal aspect of the flap and dissect the flap's pedicle cautiously by gently teasing away the loose surrounding tissues (**Fig. 7**).

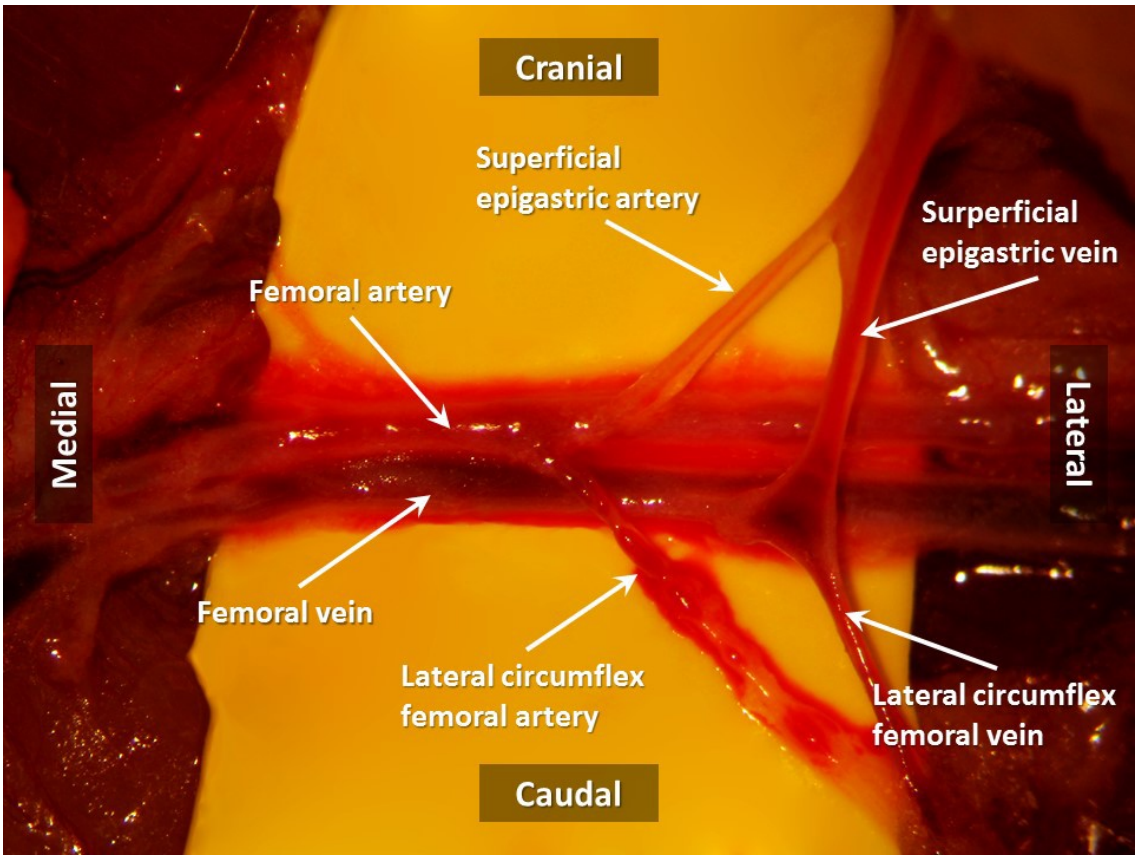

Figure 7 - Surgical anatomy of the epigastric flap's nutrient vessels under the operating microscope (10x magnification).

This photograph shows the superficial epigastric artery and vein originating from and draining into the femoral artery and vein, respectively. The lateral femoral circumflex artery usually arises from the caudal aspect of the superficial epigastric artery. The lateral femoral circumflex vein has a similar path and usually terminates into the superficial epigastric vein.

3.2.6. Ligate and divide the lateral femoral circumflex artery and vein using 9/0 Nylon for the ligatures.

3.2.7. Isolate the femoral artery and vein. When present, ligate (using 9/0 Nylon) and divide branches of these vessels to adjacent muscles.

3.2.8. Firstly, use a double vascular clamp to clamp the proximal aspect of the femoral vein. Subsequently clams its distal aspect. Then, clamp the distal aspect of the femoral artery and finally its proximal aspect.

3.2.9. Clamp the distal aspect of the femoral artery and finally its proximal aspect.

3.2.10. Place a single vascular clamp in the superficial epigastric vein and another one in the superficial epigastric artery. Use a pair of straight microsurgery scissors to cut the superficial epigastric artery and vein at their origin and termination, respectively.

3.2.11. Copiously irrigate the lumen of these vessels with heparinized normal saline 10 IU/mL, until no blood or debris are seen inside the vessels' lumen. [33]

3.2.12. Pull and trim a cuff of adventitia close to the vascular section sites.

3.2.13. Transfer the epigastric flap to the neck using Addison's forceps (**Fig. 8**).

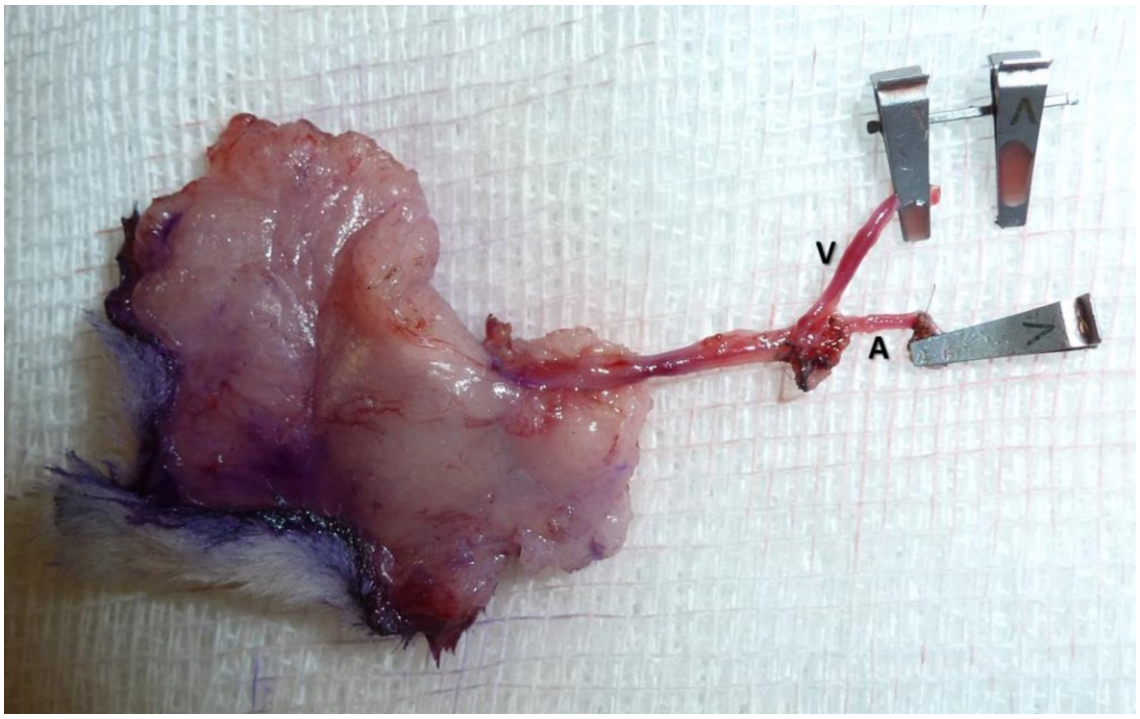

Figure 8 - The epigastric flap *ex vivo* pedicled on its nutrient vessels (the superficial epigastric artery and vein – A, V, respectively).

3.2.14. Close the donor site with subcuticular interrupted 5/0 absorbable stitches.

3.2.15. Close the skin with interrupted 5/0 Nylon stitches.

4. Recipient Site Surgical Procedure

4.1. Exposure of Recipient Site Vessels

4.1.1. Using a surgical skin marker, draw a line over the medial border of the left sternocleidomastoid (**SCM**) muscle.

4.1.2. Using a surgical skin marker, draw another line immediately cranial and parallel to

the left clavicle. These two lines must converge at the left sternoclavicular joint.

4.1.3. Incise the skin using a number 15 scalpel blade.

4.1.4. Use an electric cautery to cut through the subcutaneous tissue.

4.1.5. Use a pair of dissecting scissors to skeletonize the external jugular vein lateral to the SCM muscle.

4.1.6. Isolate and ligate the tributaries of the external jugular in this (**Fig. 9**).

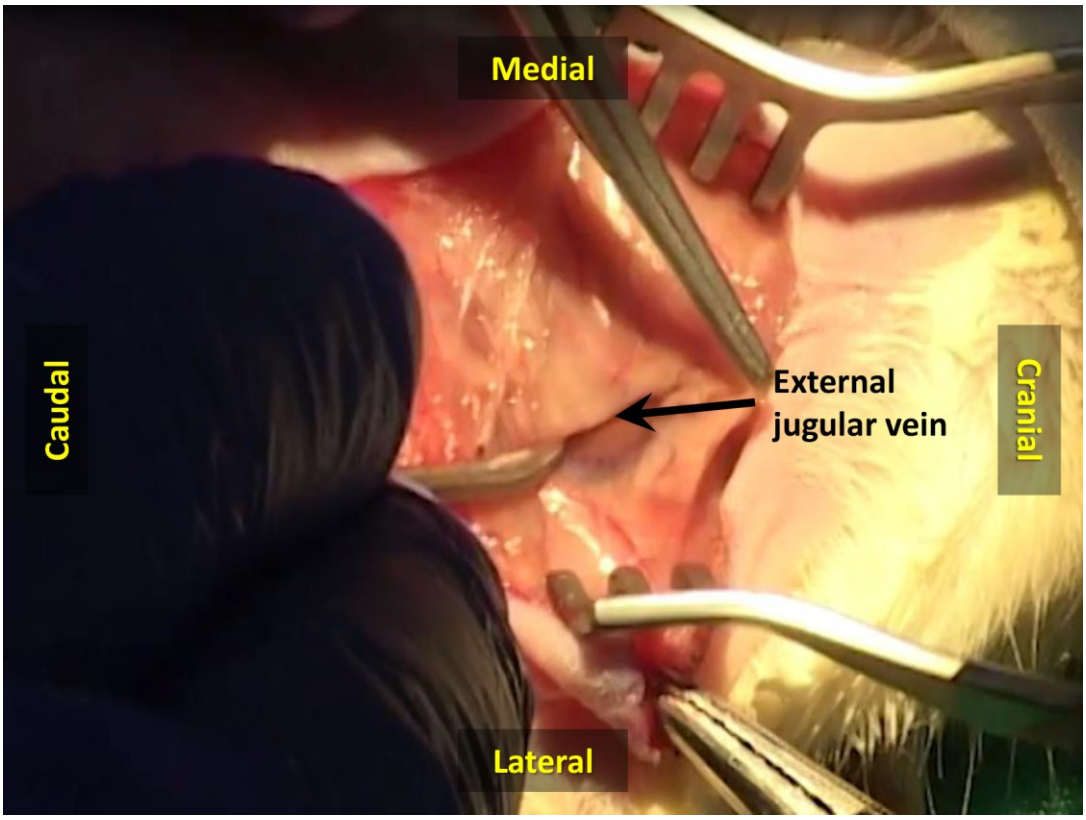

Figure 9 - Operating view of the dissection of the recipient vein, i.e., the external jugular vein, on the left side of the neck (6x magnification).

It is possible to observe the subcutaneous course of the external jugular vein lateral to the sternocleidomastoid muscle.

4.1.7. Ligate the external jugular vein just below the mandible with a 9/0 Nylon suture.

4.1.8. Place a single venous clamp beneath the latter ligation and cut the external jugular vein using a pair of straight microsurgery scissors.

4.1.9. Wash the lumen of the vein with heparinized normal saline in a concentration of 10 IU/mL.

4.1.10. Isolate the medial margin of the SCM muscle and retract this muscle laterally, thus exposing the carotid artery and the vagus nerve (**Fig. 10**).

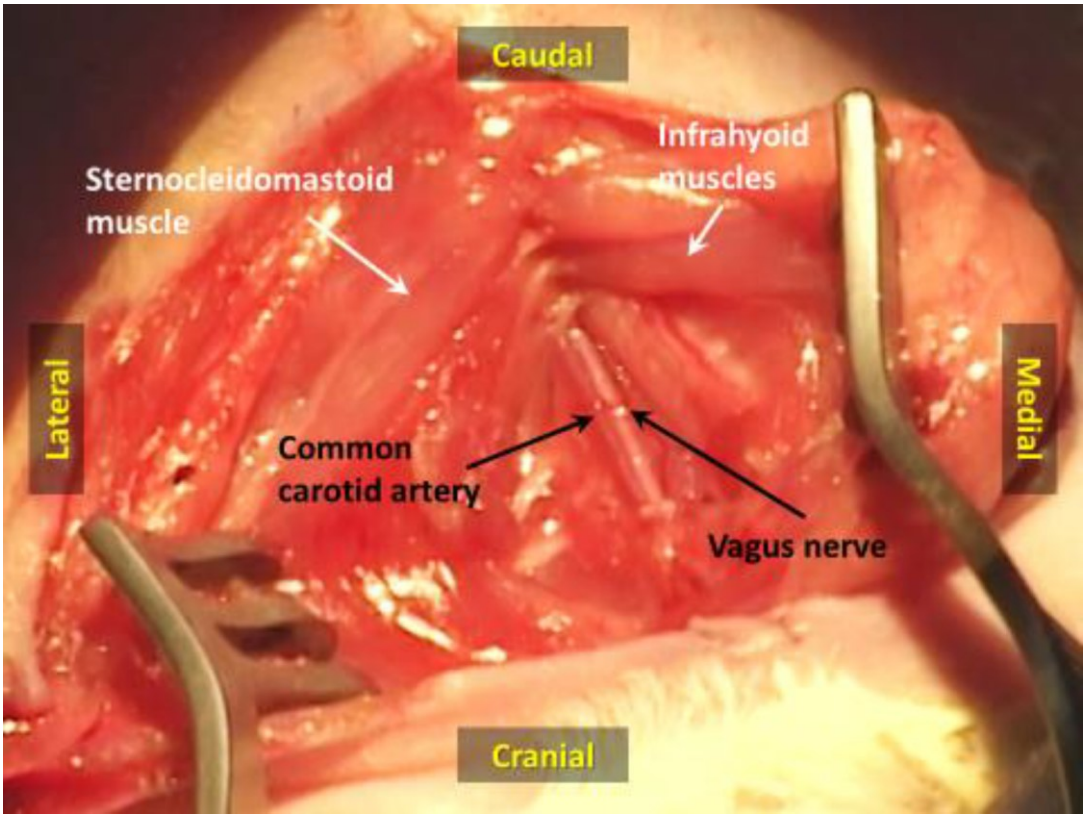

Figure 10 - Operating view of the dissection of the donor artery, i.e., the common carotid, on the left side of the neck (10x magnification).

The artery and accompanying vagus nerve are exposed after retracting the sternocleidomastoid and the infrahyoid muscles, as shown.

4.1.11. Make a transverse incision in the middle third of the SCM muscle using the electric cautery.

4.1.12. Place a retractor between the deep surface of the SCM muscle and the strap

muscles.

4.1.13. Tease away the vagus nerve from the carotid artery, taking care not to damage these structures.

4.2. Vascular anastomoses

4.2.1. Position a double arterial clamp in the carotid artery.

4.2.2. Place a 9/0 Nylon stitch in the lateral aspect of the carotid artery, and use this stitch to pull this part of the vessel wall.

4.2.3. Use a pair of straight microsurgery scissors to produce an opening in this region of vessel wall.

4.2.4. Using interrupted 10/0 Nylon sutures perform a termino-lateral anastomosis between the superficial epigastric artery of the flap and the carotid artery at the level of the recently created carotid opening.

4.2.5. Approach the proximal stump of the external jugular vein and the superficial epigastric vein and inspect the caliber of these two veins.

4.2.5.1. If the discrepancy in size is slight to moderate, dilate the lumen of the cut

end of the superficial epigastric vein using dilation forceps.

4.2.5.2. If the caliber difference is very pronounced, in addition to forceps dilation, bevel the end of the superficial epigastric vein in a 30 to 45° angle.

4.2.5.3. Perform the venous anastomosis, using interrupted 11/0 Nylon sutures.

4.2.6. Remove the single clamps placed onto the flap's vessels.

4.2.7. Remove the double clamp positioned in the femoral vein.

4.2.8. Remove the double clamp placed in the femoral artery.

4.3. Assess patency and competency of anastomoses

4.3.1. Verify if the flap's artery and vein are fully dilated and no significant bleeding is observed after 3 minutes of removing the vascular clamps (**Fig. 11**).

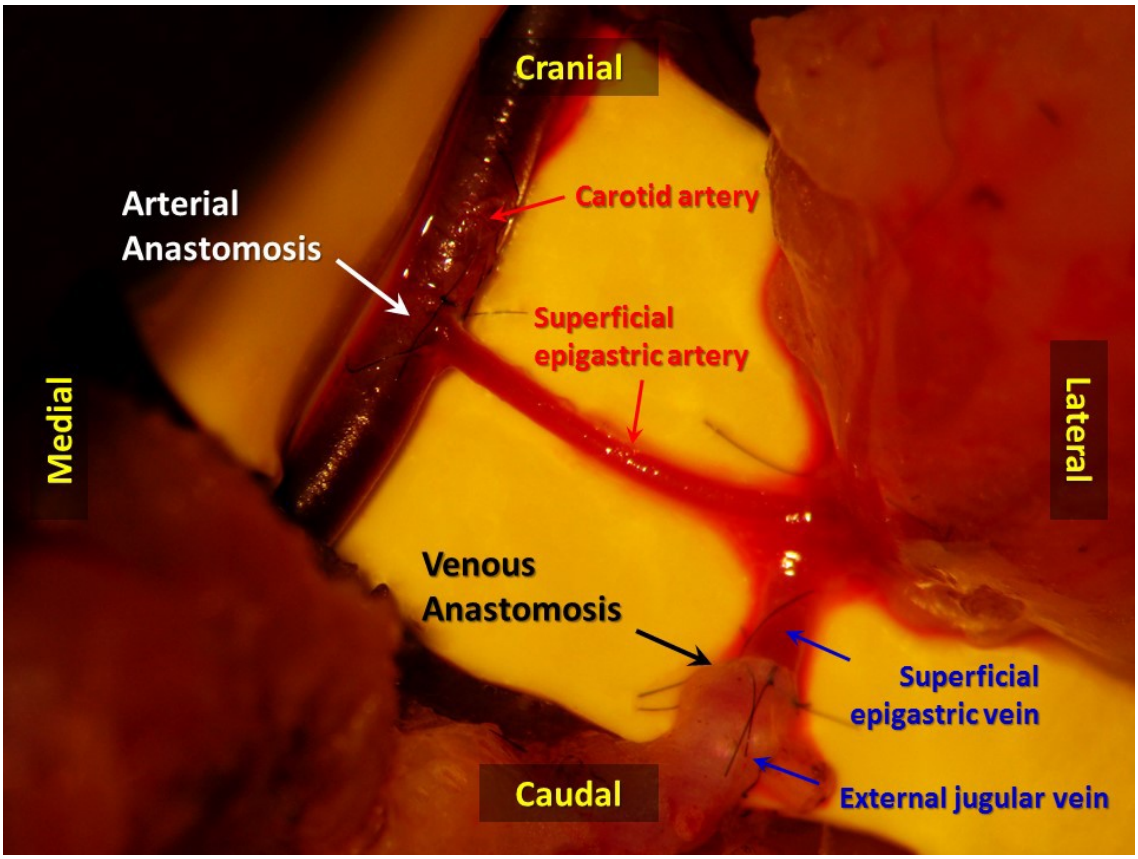

Figure 11 - Photograph of the vascular anastomoses between the flap's vessels and the recipient vessels in the neck, as seen under the operating microscope (10x magnification).

This photograph shows the termino-lateral anastomosis between the common carotid and the superficial epigastric arteries. It is also possible to observe the termino-terminal anastomosis between the superficial epigastric and the external jugular veins.

4.3.1.1. If there is bleeding during this period place a moist saline gauze over the anastomosis and apply gentle pressure.

4.3.1.2. If bleeding from anastomoses does not stop after 3 minutes, perform additional 11/0 Nylon interrupted sutures, after vascular clamp placement, as needed.

4.3.2. Wait 10 minutes with the flap connected to the neck vessels and wrapped by a gauze moistened in warm saline.

4.3.3. Assess flap's perfusion and neck wound hemostasis. Inspect the anastomoses for signs of hemorrhage, thrombosis or excessive traction.

4.3.4. Secure the flap in the recipient site starting with 5/0 subcuticular interrupted sutures.

4.3.5. Close the skin with 5/0 Nylon interrupted sutures (**Fig. 12**).

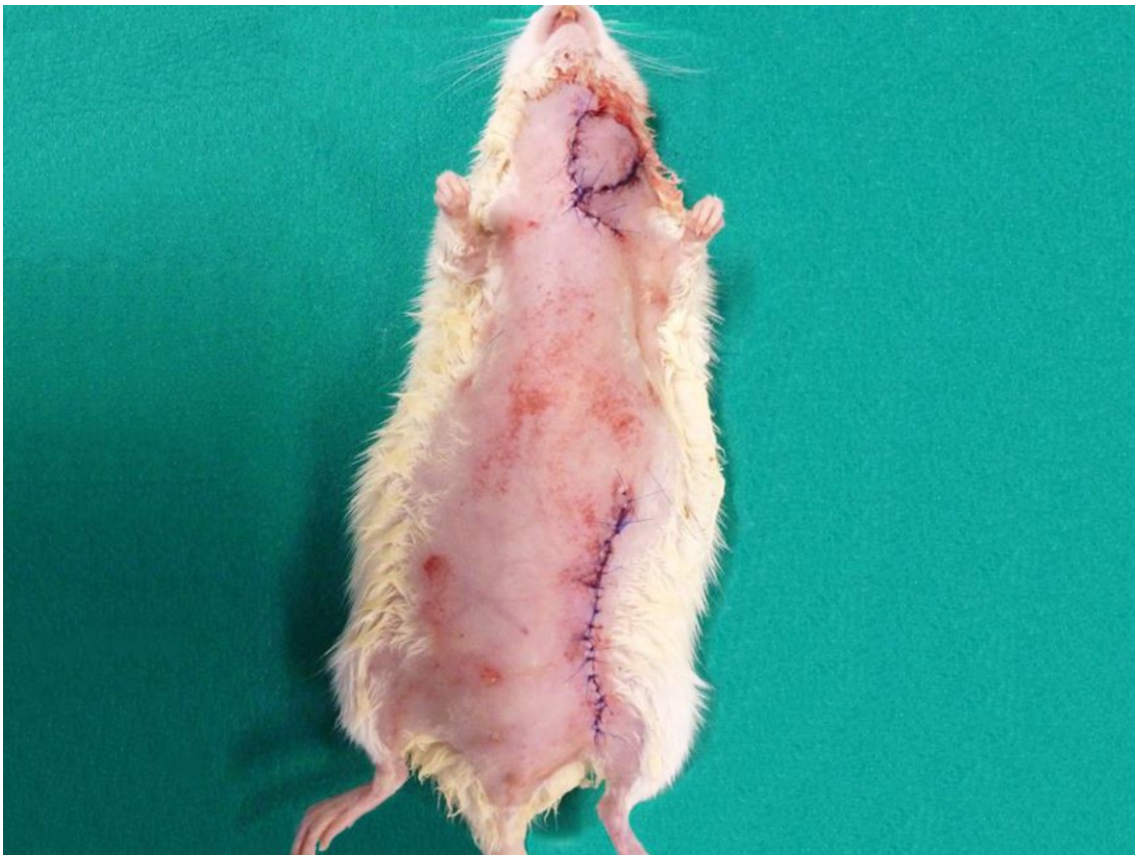

Figure 12 - Photograph of ventral aspect of the rat immediately after the surgery.

Notice that the donor zone is easily closed primarily.

5. Post-operative Care

5.1. Leave the rat to recover inside its individual cage in the right lateral decubitus position. Keep the cage warm by placing an electric heat pad set on low beneath. Place a light cloth between the cage and the electric heat pad to avoid hyperthermia.

5.2. Watch the animal continuously turning it to the opposite lateral decubitus every 5 minutes, until it resumes sternal recumbency and it is able to ambulate.

5.3. House the rats individually until removing the surgical stitches two weeks after the

surgical procedure.

5.4. Give Meloxicam Metacam® 1 mg/kg subcutaneously once a day for the 3 days following surgery, for postoperative analgesia.

6. Flap Assessment

6.1. Present a food treat over the head of the rat and assess flap's viability by visual inspection.

6.2. If exposure is insufficient using the previous step, have an assistant applying gentle touch over the interscapular region of the rat, while you examine the flap.

6.3. Use digital photography and ImageJ software to quantitatively evaluate the areas of wound dehiscence, flap epidermolysis, hyperemia, congestion and/or necrosis, as explained in detail by Trujillo et al. [15]

REPRESENTATIVE RESULTS

According to the authors' experience of more than ten years using the epigastric free flap as a model of free tissue transfer both in the context of microsurgery courses and for research purposes, the rate of flap survival depends somewhat on the dexterity and experience of the surgeon. Generally speaking, if the technical aspects described above are taken into consideration, a nearly complete survival rate (<10% of flap necrosis) of around 70% of flaps is to be expected. Around 10% of flaps present partial necrosis (10 to

50%). About 20% of flaps suffer complete necrosis. An 80% nearly complete survival rate was obtained in the last 20 procedures performed by the first author (D.C.) (**Fig. 13**).

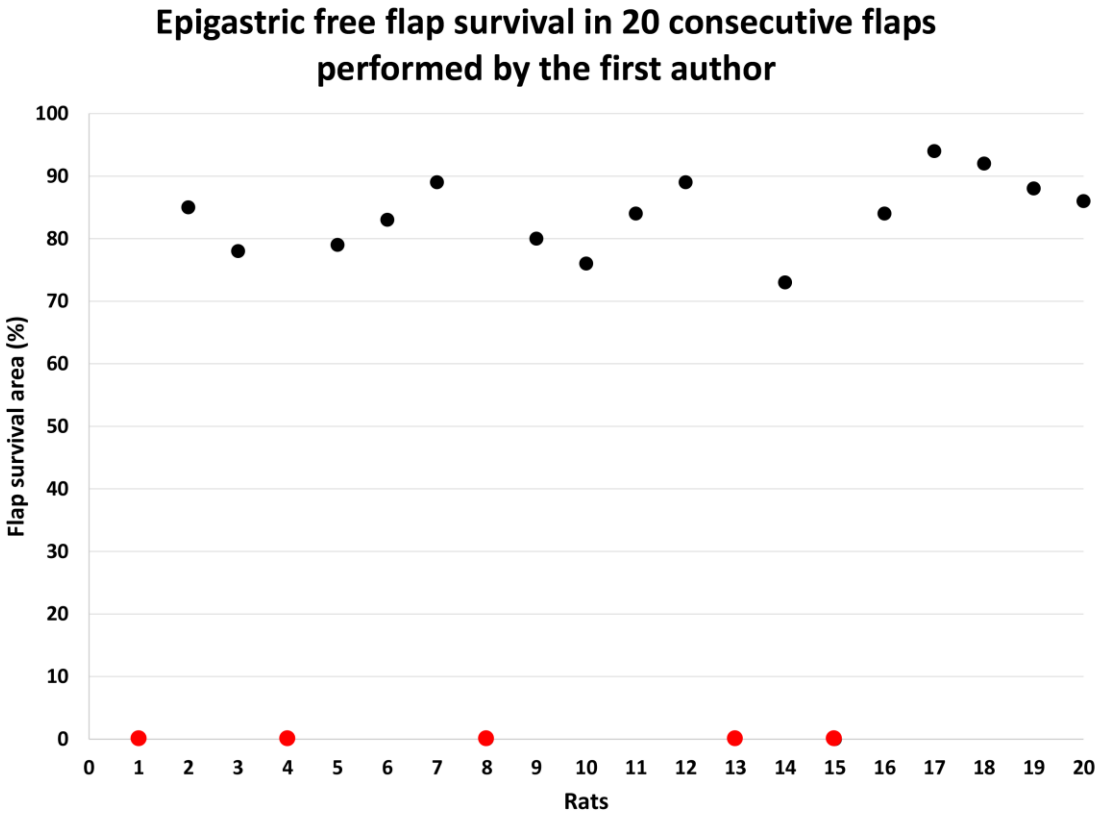

Figure 13 - Epigastric free flap survival in 20 consecutive rats operated on by the first author (D.C.). Five rats (20%) presented complete flap necrosis (cases 1, 4, 8, 13 and 15, represented by the red dots). Areas of flap necrosis were determined using the free software Image J®, as explained in detail by Trujillo et al. [15]

During the first two days postoperatively, the free epigastric flap is often edematous and presents some degree of venous congestion. These usually both subside gradually between 3 and 5 days after surgery. Typically, during the first week, the rat removes most external stitches and part of the subcuticular sutures, often resulting in scattered areas of slight wound dehiscence (**Fig. 14**). After day 10, the hair slowly starts to

grow on the flap's surface. At the end of the first month after surgery, the flap is usually covered with slightly shorter hair than the adjacent skin. Two months postoperatively, the presence of the flap is heralded by a slight lump, and by a relatively inconspicuous scar around the flap's margins (**Fig. 14**).

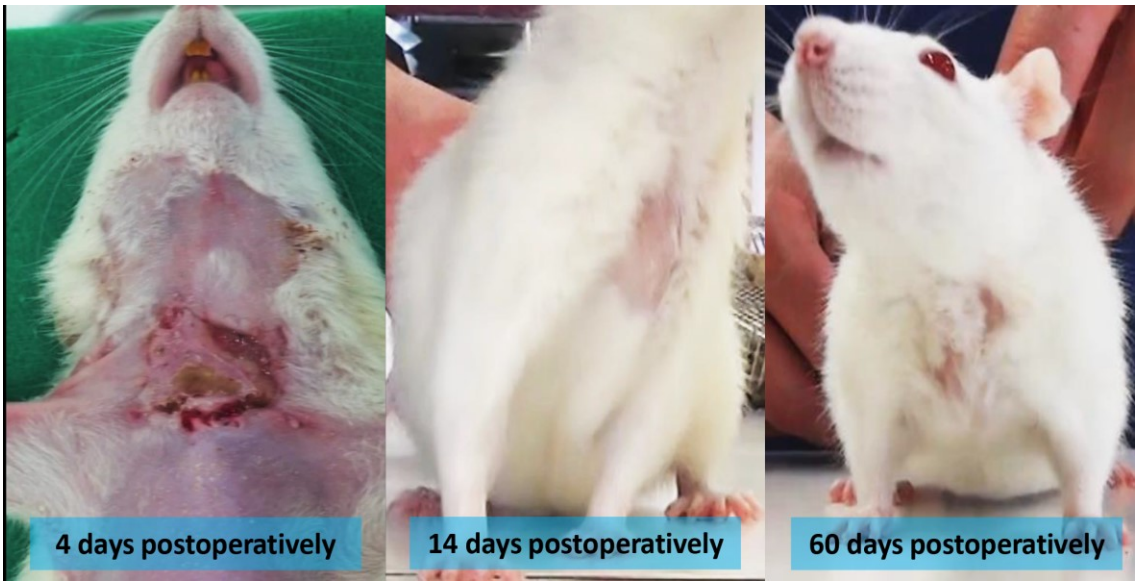

Figure 14 - Photographs of the epigastric flap placed on the ventral aspect of the neck 4, 14 and 60 days postoperatively.

Four days after surgery, there is typically some wound dehiscence, as the rat removes the stitches. However, the flap usually remains in place. It is possible to examine the flap daily by simple visual inspection.

Auto cannibalism of the flap is an infrequent finding that, in the authors' experience, occurs almost exclusively in cases of total flap necrosis.

DISCUSSION

The most important aspect to obtain consistent flap survival is paying attention to detail in various steps of the microsurgical technique. For example, to obtain good visualization of the vessels, of the surgical instruments and of the fine suture lines, it is very helpful to place underneath the vessels, a sterilized colored plastic background. As many researchers, we prefer to use sterilized fragments of yellow or green balloons (**Figs. 7** and **11**). This background provides the additional advantage of minimizing adherence of suture lines to the adjacent structures, which sometimes leads to the need of pulling the suture line with too much tension, which may in turn lead to vascular tearing. Finally, the use of a background has the additional advantage of decreasing the probability of inadvertently dragging potential thrombogenic tissue debris to the anastomosis site.

Considering that the flap's vessels are very fine and fragile, it is important not to pinch the entire width of the vessels, in order to avoid intimal lesion that, in turn, will lead to intravascular thrombosis and flap failure. To prevent inadvertent injury to both the flap's vessels and to the recipient site's vessels, it is safer to liberally ligate and divide neighboring tributaries, which will allow an easier manipulation of these vessels.

Before starting the anastomoses, it is vital to place the vessels in their definitive position, striving to prevent vascular kinking or torsion of the flap's pedicle. Given the small caliber and delicate consistency of the vessels, these are often difficult to exclude

unequivocally. One helpful trick is to secure the flap in its final position with 3 stitches placed away from the site of the anastomoses. Next, if in doubt, temporarily open the vascular clamps placed at the flap's pedicle, and fill the vessels' lumen with heparinized normal saline in a concentration of 10 IU/mL until they become engorged. This leads vessels to assume the configuration they will present after being perfused by blood, as when the clamps are removed after anastomoses completion.

Moreover, it is of paramount importance to detect any air bubbles, even if small, inside the vessels during the entire procedure and particularly before tying the final stitches. If these bubbles are distant from the vascular section, the vessels can be milked gently with microsurgical forceps. If they are located close to the anastomotic sites, simple irrigation leads the less dense bubbles to be easily expelled from the vascular lumen. Failure to acknowledge the presence of air bubbles can cause irreversible flap ischemia and necrosis, no doubt due to the fine caliber of the flap vessels.

Additionally, it cannot be overemphasized the need for meticulous care while passing and tying the stitches, in order to:

- include the three layers of the vessels (intima, media and adventitia);
- obtain good vessel eversion to ensure adequate intimal contact, which is vital to anastomosis sealing and endothelial regrowth;
- avoid loose vascular contact, which will result in anastomotic incompetence, i.e., bleeding;
- avoid grabbing too much vascular tissue, which will lead to anastomosis

stenosis and proclivity to thrombosis, which in turn will result in venous congestion or poor flap perfusion, if the vein or artery are involved, respectively.

Finally, it is essential to ensure perfect hemostasis, during the entire procedure, especially when raising the flap in its deep surface. Otherwise hematoma formation and rat death are likely to ensue.

Modifications and troubleshooting of the technique

The authors observed that making a transverse incision in the middle portion of the SCM using an electric cautery, not only allows a better exposure of the carotid artery, but also minimizes the risk of undue tension over the future arterial anastomosis.

Another important technical tip is to start the anastomosis from the vessels' back wall, in order to minimize the risk of unwillingly catching this wall when placing the stitches in the more easily exposed front wall. If the back wall is sutured to the anterior aspect of the anastomosis, lack of vascular patency will almost invariably result either immediately due to mechanical reasons or after only a few hours as a result of thrombosis.[8]

If the anastomoses of the epigastric vessels of the rat are considered too technically challenging due to the small caliber of these vessels, the femoral vessels can be ligated distal to the origin of the epigastric vessels and used as the vascular pedicle of the

epigastric flap. In this way, larger vessels will be used (the femoral artery has a caliber of 1.0 to 1.2 mm; and the femoral vein has a caliber of 1.2 to 1.5 mm). Moreover, by dissecting and ligating the other tributaries of the femoral vessels, a vascular pedicle length of over 2 cm can be obtained, which will facilitate flap insetting. [18,34,35]

Reproducibility

Our experience of more than ten years of using this flap for teaching and research purposes strongly suggests that the rat epigastric flap is a reproducible model of free tissue transfer. [11,13,17,18,26] It can be easily incorporated in microsurgical courses, as it is a good teaching and training model for microsurgery trainees. [11,13,17,18,26] In our experience, although technically challenging in the beginning for the novice in microsurgery, after some training, the free epigastric flap can be successfully transferred to the neck of the rat with minimal to no subsequent necrosis in 70 to 80% of cases. These results concur with those generally reported in the literature. [13,18,36]

Significance with respect to existing methods

Numerous free flaps have been described in the rat. [10,16,18,37-39] The most commonly used for teaching and research purposes have been the transverse *rectus abdominis* myocutaneous flap, the *latissimus dorsi* and *serratus anterior* muscle flaps, the hind limb replantation model, and the epigastric (groin) flap. [18,35] These flaps have been favored, due to their consistent anatomy and sizeable vascular pedicle. The epigastric flap is arguably the one associated with lesser donor site morbidity, as it dissected above the

muscle fascia. [18] Moreover, the epigastric flap, described in 1967, was the first flap to be described in rats. [34,35] This occurred only 4 years after the first description of an experimental flap in an animal by Goldwyn. Interestingly, this flap was a groin flap in the dog. [34]

Limitations of the technique

The two main limitations of this model are the need for microsurgical skills in order to carry out the surgery, and the presence of significant necrosis in 20 to 25% of cases, according to different authors. [13,18,36] Another potential limitation of the model herein presented is the auto cannibalism of the flap. However, as the authors above, this is an infrequent finding that almost only occurs in cases of total flap necrosis.

Future applications of the technique

The rat epigastric free flap can be used in experimental studies of tissue perfusion, tissue repair and surgical wound infection. [40,41] Its nutrient vessels are particularly suitable for intravascular injection of solutions containing substances of interest, namely drugs, viral vectors or liposomes, that will mostly produce a local or regional effect. [30,31] In addition, beneath the flap, pathogens, foreign bodies, radioactive seeds or chemicals can also be placed, mimicking several disease processes and potential treatments. [30,31]

ACKNOWLEDGMENTS

The authors would like to thank the technical help of Mr. Alberto Severino in filming and editing the video. The authors are also grateful to Mr. Octávio Chaveiro, Mr. Marco Costa and Mr. Carlos Lopes for their help in preparing the animal specimens presented in this paper.

Finally, the authors would like to thank Ms. Gracinda Menezes for her help in all the logistical aspects pertaining to animal acquisition and maintenance.

REFERENCES

1 Morain, W. D. in *Plastic Surgery* Vol. 1 (ed S.J. Mathes) 27-34 (Saunders, 2006).

2 Christoforou, D., Alaia, M. & Craig-Scott, S. Microsurgical management of acute traumatic injuries of the hand and fingers. *Bull Hosp Jt Dis (2013).* **71** (1), 6-16 (2013).

3 Santoni-Rugiu, P. & Sykes, P. J. in *A History of Plastic Surgery* eds P. Santoni-Rugiu & P.J. Sykes) Ch. 3, 79-119 (Springer, 2007).

4 Tamai, S. in *Experimental and Clinical Reconstructive Microsurgery* eds S. Tamai, M. Usui, & T. Yoshizu) Ch. 1, 3-24 (Springer-Verlag, 2003).

5 Bettencourt-Pires, M. A. *et al.* ANATOMY AND GRAFTS – From Ancient Myths, to Modern Reality. *Archives of Anatomy.* **2** (1), 88-107 (2014).

6 Casal, D., Gomez, M. M., Antunes, P., Candeias, H. & Almeida, M. A. Defying standard criteria for digital replantation: A case series. *Int J Surg Case Rep.* **4** (7), 597-602, doi:10.1016/j.ijscr.2013.03.033 (2013).

7 Gomez, M. M. & Casal, D. Reconstruction of large defect of foot with extensive bone loss exclusively using a latissimus dorsi muscle free flap: a potential new indication for this flap. *J Foot Ankle Surg.* **51** (2), 215-217, doi:10.1053/j.jfas.2011.07.008 (2012).

8 Plenter, R. J. & Grazia, T. J. Murine heterotopic heart transplant technique. *J Vis Exp.* (89), doi:10.3791/51511 (2014).

9 Pichierri, A. *et al.* How to set up a microsurgical laboratory on small animal models: organization, techniques, and impact on residency training. *Neurosurg Rev.* **32** (1), 101-110; discussion 110, doi:10.1007/s10143-008-0154-4 (2009).

10 Klein, I., Steger, U., Timmermann, W., Thiede, A. & Gassel, H. J. Microsurgical

training course for clinicians and scientists at a German University hospital: a 10-year experience. *Microsurgery.* **23** (5), 461-465, doi:10.1002/micr.10180 (2003).

11 Fukui, A. in *Experimental and Clinical Reconstructive Microsurgery* eds S. Tamai, M. Usui, & T. Yoshizu) Ch. 1, 35-43 (Springer-Verlag, 2004).

12 Ad-El, D. D., Harper, A. & Hoffman, L. A. Digital replantation teaching model in rats. *Microsurgery.* **20** (1), 42-44 (2000).

13 Ruby, L. K., Greene, M., Risitano, G., Torrejon, R. & Belsky, M. R. Experience with epigastric free flap transfer in the rat: technique and results. *Microsurgery.* **5** (2), 102-104 (1984).

14 Edmunds, M. C., Wigmore, S. & Kluth, D. In situ transverse rectus abdominis myocutaneous flap: a rat model of myocutaneous ischemia reperfusion injury. *J Vis Exp.* (76), doi:10.3791/50473 (2013).

15 Trujillo, A. N., Kesl, S. L., Sherwood, J., Wu, M. & Gould, L. J. Demonstration of the rat ischemic skin wound model. *J Vis Exp.* (98), doi:10.3791/52637 (2015).

16 Siemionow, M. Z. in *Plastic and Reconstructive Surgery: Experimental models and research designs* (ed M.Z. Siemionow) Ch. 1-7, 3-67 (Springer - Verlag, 2015).

17 Petry, J. J. & Wortham, K. A. The anatomy of the epigastric flap in the experimental rat. *Plast Reconstr Surg.* **74** (3), 410-413 (1984).

18 Hirase, Y. in *Experimental and Clinical Reconstructive Microsurgery* eds S. Tamai, M. Usui, & T. Yoshizu) Ch. 6, 111-114 (Springer-Verlag, 2004).

19 Zhang, F. *et al.* Microvascular transfer of the rectus abdominis muscle and myocutaneous flap in rats. *Microsurgery.* **14** (6), 420-423 (1993).

20 Tonken, H. P. *et al.* Microvascular transplant of the gastrocnemius muscle in rats. *Microsurgery.* **14** (2), 120-124 (1993).

21 Miyamoto, S. *et al.* Free pectoral skin flap in the rat based on the long thoracic vessels: a new flap model for experimental study and microsurgical training. *Ann Plast Surg.* **61** (2), 209-214, doi:10.1097/SAP.0b013e318157a6ea (2008).

22 Nasir, S., Aydin, A., Kayikcioglu, A., Sokmensuer, C. & Cobaner, A. New experimental composite flap model in rats: gluteus maximus-tensor fascia lata osteomuscle flap. *Microsurgery.* **23** (6), 582-588, doi:10.1002/micr.10212 (2003).

23 Coskunfirat, O. K., Islamoglu, K. & Ozgentas, H. E. Posterior thigh perforator-based flap: a new experimental model in rats. *Ann Plast Surg.* **48** (3), 286-291 (2002).

24 Ozkan, O. *et al.* A new flap model in rats: iliac osteomusculocutaneous flap. *Ann Plast Surg.* **47** (2), 161-167 (2001).

25 Padubidri, A. N. & Browne, E., Jr. Modification in flap design of the epigastric artery flap in rats--a new experimental flap model. *Ann Plast Surg.* **39** (5), 500-504 (1997).

26 Strauch, B. & Murray, D. E. Transfer of composite graft with immediate suture anastomosis of its vascular pedicle measuring less than 1 mm. in external diameter using microsurgical techniques. *Plast Reconstr Surg.* **40** (4), 325-329 (1967).

27 Green, C. E. *Anatomy of the Rat.* First edn, 124-153 (Hafner Publishing Company, 1968).

28 Greene, E. C. Anatomy of the rat. New York, Hafner. (1959).

29 Langworthy, O. R. A morphological study of the panniculus carnosus and its genetical relationship to the pectoral musculature in rodents. *American Journal of*

Anatomy. **35** (2), 283-302 (1925).

30 Popesko, P., Ratjová, V. & Horák, J. in *A Colour Atlas of the Anatomy of Small Laboratory Animals* Vol. 2 13-104 (Saunders, 1992).

31 Brown, S. H., Banuelos, K., Ward, S. R. & Lieber, R. L. Architectural and morphological assessment of rat abdominal wall muscles: comparison for use as a human model. *J Anat.* **217** (3), 196-202, doi:10.1111/j.1469-7580.2010.01271.x (2010).

32 Harder, Y. *et al.* Ischemic tissue injury in the dorsal skinfold chamber of the mouse: a skin flap model to investigate acute persistent ischemia. *J Vis Exp.* (93), e51900, doi:10.3791/51900 (2014).

33 Cox, G. W., Runnels, S., Hsu, H. S. & Das, S. K. A comparison of heparinised saline irrigation solutions in a model of microvascular thrombosis. *Br J Plast Surg.* **45** (5), 345-348 (1992).

34 Gurunluoglu, R. & Siemionow, M. Z. in *Plastic and Reconstructive Surgery: Experimental models and research designs* (ed M.Z. Siemionow) Ch. 6, 53-62 (Spronger, 2015).

35 Nasır, S. in *Plast Reconstr Surg* 227-236 (Springer, 2015).

36 Parsa, F. D. & Spira, M. Evaluation of anastomotic techniques in the experimental transfer of free skin flaps. *Plast Reconstr Surg.* **63** (5), 696-699 (1979).

37 Dunn, R. M., Huff, W. & Mancoll, J. The Rat Rectus Abdominis Myocutaneous Flap: A True Myocutaneous Flap Model. *Ann Plast Surg.* **31** (4), 352-357 (1993).

38 Özkan, Ö. *et al.* A new flap model in rats: iliac osteomusculocutaneous flap. *Ann Plast Surg.* **47** (2), 161-167 (2001).

39 Ozkan, O., Koshima, I. & Gonda, K. A supermicrosurgical flap model in the rat: a free true abdominal perforator flap with a short pedicle. *Plast Reconstr Surg.* **117** (2), 479-485, doi:10.1097/01.prs.0000197215.94170.b8 (2006).

40 Dorsett-Martin, W. A. Rat models of skin wound healing: a review. *Wound Repair Regen.* **12** (6), 591-599, doi:10.1111/j.1067-1927.2004.12601.x (2004).

41 Ghali, S. *et al.* Treating chronic wound infections with genetically modified free flaps. *Plast Reconstr Surg.* **123** (4), 1157-1168, doi:10.1097/PRS.0b013e31819f25a4 (2009).

Chapter 7

OPTIMIZATION OF AN ARTERIALIZED VENOUS FASCIOCUTANEOUS FLAP IN THE ABDOMEN OF THE RAT

Authors: Diogo Casal, MD[1,2,3]; Eduarda Mota-Silva, MSc[4]; Diogo Pais, MD, PhD[2]; Inês Iria, MSc[5]; Paula A. Videira, PhD[5]; David Tanganho, MD[1,2]; Sara Alves, MSc,[6]; Luís Mascarenhas-Lemos, MD[6]; José Martins Ferreira, BSc[6]; Mário Ferraz-Oliveira, MD[6]; Valentina Vassilenko, PhD[4]; João Goyri-O'Neill[2]

Affiliations:

1- Plastic and Reconstructive Surgery Department and Burn Unit, Centro Hospitalar de Lisboa Central, Lisbon, Portugal;

2- Anatomy Department, Nova Medical School, Lisbon, Portugal;

3- Glycoimmunology, CEDOC, NOVA Medical School, Lisbon, Portugal;

4- LIBPhys, Physics Department, Faculdade de Ciências e Tecnologias, Universidade NOVA de Lisboa, Caparica, Portugal;

5- Department of Life Sciences, Faculdade de Ciências e Tecnologias, Universidade NOVA de Lisboa, Caparica, Portugal; and

6- Pathology Department, Centro Hospitalar de Lisboa Central, Lisbon, Portugal.

ABSTRACT

Background: Although numerous experimental models of arterialized venous flaps (**AVFs**) have been proposed, no single model has gained widespread acceptance. The main aim of this work was to evaluate the survival area of AVFs produced with different vascular constructs in the abdomen of the rat.

Methods: Fifty-three male rats were divided into 4 groups. In **group I** (n=12) a 5 cm long and 3 cm wide conventional epigastric flap was raised on the left side of the abdomen. This flap was pedicled on the superficial caudal epigastric vessels caudally and on the lateral thoracic vein cranially. In groups II, III and IV a similar flap was raised but the superficial epigastric artery was ligated. In these groups AVFs were created using the following arterial venous anastomosis (**AVA**) at the caudal end of the flap: **group II** (n=13) a 1 mm long side-to-side anastomosis was performed between the femoral artery and vein laterally to the ending of the superficial caudal epigastric vein (**SCEV**). In **group III** (n=14) in addition to the procedure described for group II, the femoral vein was ligated medially. Finally, in **group IV** (n=14), the SCEV was cut from the femoral vein with a 1 mm long ellipse of adjacent tissue and an end-to-side AVA was established between it and the femoral artery.

Results: Seven days postoperatively, the percentage of flap survival was 98.89±1.69, 68.84±7.36, 63.84±10.38, 76.86±13.67 in groups I to IV, respectively.

Conclusions: An optimized AVF can be produced using the vascular architecture described for group IV.

INTRODUCTION

More than thirty years have passed since Vaubel's 1975 description of an arterialized venous flap (**AVF**) to reconstruct the dorsum of the hand, and the highly-cited Nakayama's 1981 paper on the creation of an experimental AVF model in the abdomen of the rat.(1, 2) Initially, there was great enthusiasm with AVFs, since they allowed the transference of composite blocks of tissues based exclusively on the venous system. This in turn allowed the creation of thin, pliable and versatile flaps, that could be tailored rapidly and with minimal morbidity in the donor zone.(3) However, reports of high necrosis rates and a poorly understood physiology have been deterring many surgeons of using AVFs in clinical practice.(3-8)

Although numerous experimental models of AVFs have been proposed, no model has gained widespread acceptance, which hinders comparison of observations on the physiology and interventions on these flaps. Additionally, lack of a standardized model of AVF can be an obstacle for the novice in microsurgery while preparing to execute these flaps in a training environment.(9) Therefore, the main aim of this work was to evaluate the flap survival area of AVFs produced with different vascular constructs in the abdomen of the rat. Secondary endpoints were determination of the time required to produce the flap, animal mortality and surgical complications, as well as thermographic, histological, and microvascular characterization of the different constructs. The ultimate goal of all these evaluations was to define an optimized model of AVF that could be easily replicated for research and teaching purposes.

METHODS

Fifty-three male rats weighing 250-350 g were used. Only male rats were used to prevent potential confounding effects of cyclical hormonal changes in female rats.(10) All the animals were housed under standard environmental conditions and given nothing by mouth six hours before surgical procedures. No antibiotic prophylaxis was given.

Rats were anesthetized with a mixture of ketamine (5 mg/kg) and diazepam (0.25 mg/kg) given intraperitoneally. The depth of anesthesia was evaluated by toe pinch and by observance of respiration rate throughout the entire procedure. Supplementary doses of the anesthetic mixture were provided as needed.(11)

After shaving the abdomen and placing the animals on the operation table, the skin was disinfected with an antiseptic solution (Cutasept®). Hypothermia was avoided by placing the rat over an heating pad for the duration of the surgery.

Under a surgical operating microscope, a 5 cm long and 3 cm wide fasciocutaneous flap was raised on the left side of the rat's abdomen immediately deep to the panniculus carnosus layer (**Fig. 1**). This flap was initially pedicled on the superficial caudal vessels caudally and on the lateral thoracic vein cranially. All other vessels were carefully ligated.(9, 11)

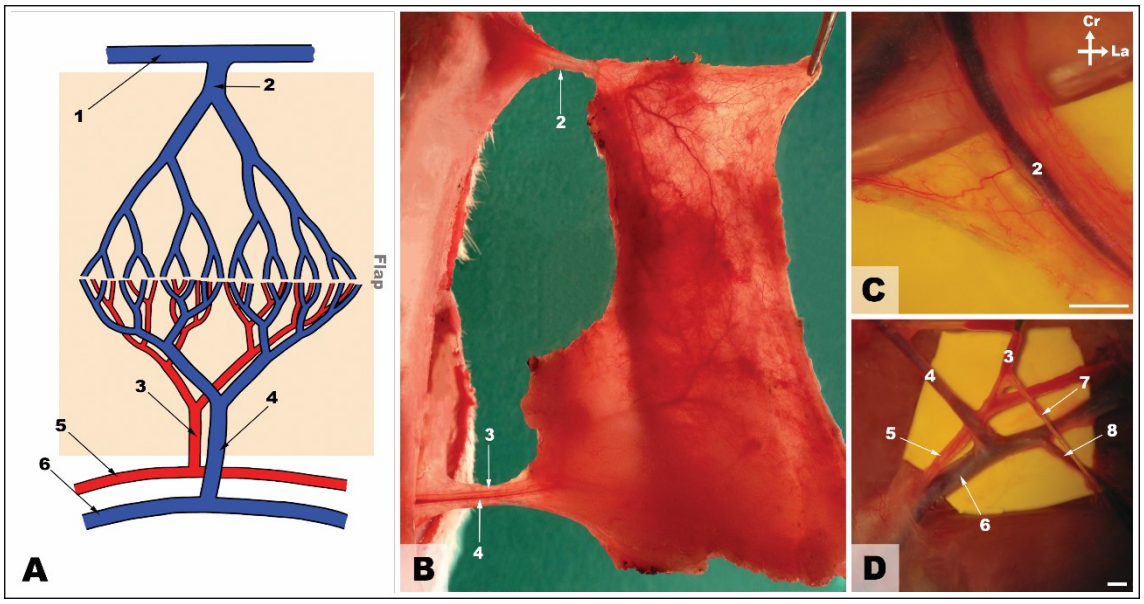

Figure 1 - Epigastric flap surgical anatomy.

A. Schematic drawing of the blood supply to the rat's epigastric flap. The shaded area represents the flap.

B. Photograph under transillumination of the flap's deeps surface raised on the left side of the abdomen showing its largest vessels.

C. High amplification photograph of the lateral thoracic vein before being dissected from the surrounding loose areolar tissue.

D. Photograph showing the origin of the superficial caudal epigastric vessels from the femoral vessels.

Cr, cranial; La, lateral.

1, Axillary vein; 2, Lateral thoracic vein; 3, Superficial caudal epigastric artery; 4, Superficial caudal epigastric vein; 5, Femoral artery; 6, Femoral vein; 7, Superficial external pudendal artery; 8, Superficial external pudendal vein.

Calibration bar = 1 mm.

Rats were then randomly assigned to the following groups (**Fig. 2**):

In **group I** (n=12), a conventional perfusion flap (**CPF**) was raised as described above.

In groups II, III and IV the superficial epigastric artery was ligated with an 8/0 Nylon suture. In these groups AVFs were created using the following arterial venous anastomosis (**AVA**) at the caudal end of the flap:

In **group II** (n=13), a 1 mm long side-to-side anastomosis was performed between the femoral artery and vein laterally to the ending of the superficial caudal epigastric vein (**SCEV**) in the femoral vein. The AVA was performed after making a 1 mm long ostium in adjacent flanks of the femoral artery and vein. A monofilament Nylon 11/0 interrupted suture was used for the vascular anastomosis.(12)

In **group III** (n=14), in addition to the procedure described for group II, the femoral vein was ligated immediately medial to the ending of the SCEV, in order to increase blood flow through the AVA.

Finally, in **group IV** (n=14), the SCEV was cut from the femoral vein with a 1 mm long ellipse of adjacent femoral vein tissue. The ostium in the femoral vein was closed with a monofilament Nylon 11/0 continuous suture. The same suture line was used to perform a side-to-end AVA between the SCEV and the ventral flank of the femoral artery through a 1 mm long ostium previously created in the latter vessel. Interrupted stitches were used for this anastomosis.

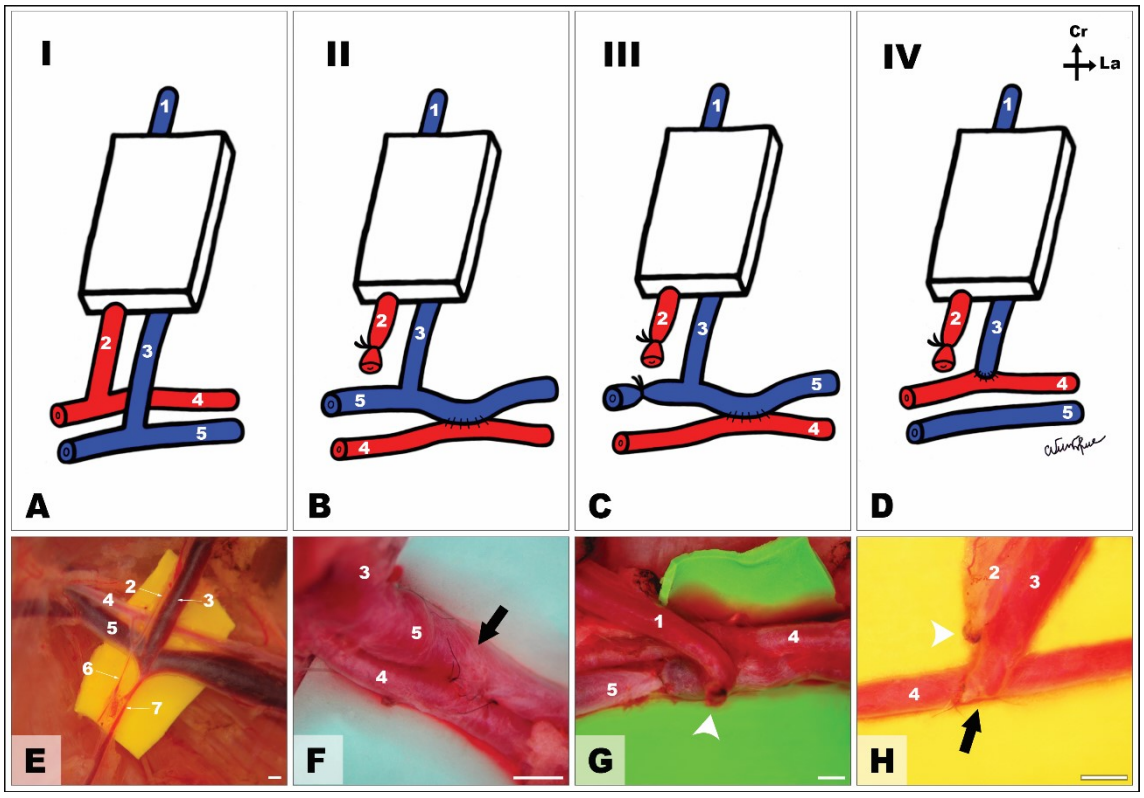

Figure 2 - Schematic representation and surgical operating view of the vascular patterns in the different experimental groups.

A. Group I (Conventional perfusion flap).

B. Group II (Arterialized venous flap produced by femoral side-to-side anastomosis).

C. Group III (Arterialized venous flap produced by femoral side-to-side anastomosis and proximal ligation of the femoral vein).

D. Group IV (Arterialized venous flap produced by terminal-lateral anastomosis of the epigastric vein to the femoral artery).

E, F, G, H. Surgical operating view of the inflow vessels of the flap in groups I, II, III and IV, respectively. Cr, cranial; La, lateral.

Arrows indicate place of arteriovenous anastomosis. Arrow heads indicate vessel ligation.

Calibration bar = 1 mm.

Surgical wounds were closed with 5/0 Nylon stitches. No anticoagulants were administered pre, intra or postoperatively.

After surgery, rats were kept in solitary rat cages and offered rat chow and water *ad libitum*.

Seven days after the surgery, rats were anesthetized as described above and AVA patency was noted. Only animals with patent AVAs were included in the study.

All surgical procedures were performed under aseptic conditions by the same microsurgeon (D.C.), in order to minimize inter-surgeon variability. The operative time was registered in all animals by a blinded observer.

One hour postoperatively, 2 rats in each group were submitted to infra-red thermography with a FLIR® E6 camera placed 25 cm above the abdomen. Rats were placed on their backs for 10 minutes prior to this evaluation. Thermographic measurements were made at a constant room temperature (22±0.05 ºC) and humidity (50%).(13)

Rats were assessed daily by the same researcher, in order to reduce inter observer bias and variability.(8) The following parameters were evaluated: animal wellbeing, flap viability, flap ischemia and presence of complications. Objective measurement of flap survival was performed on the 3rd and 7th days postoperatively based on digital photographs, which were later analyzed by a blinded observer using the free Image J® software.(11) AVF survival was expressed as a percentage of the total flap surface area.(14)

Half of the rats in each group were prepared for conventional histological examination, whereas the other half was submitted to processing in order to obtain vascular corrosion casts for scanning electron microscopy (**SEM**) evaluation. For

histological processing, rats were submitted to axial sections in the caudal, middle and cranial aspect of the AVF that were later stained using hematoxylin-eosin and Masson's trichrome. These rats were euthanized by exsanguination after dividing the neck vessels under sedation.

The rats destined to SEM analysis were submitted to intravascular injection of a resin cast (Mercox®) and latter processed.(15) SEM images were obtained using a JEOL JSM-7001F with an acceleration voltage of 2-30kV. Vascular cast interpretation of microvascular findings was made according to Aharinejad and Lametschwandtner.(15) These rats were euthanized by exsanguination after left and right ventricular catheterization.

All *in vivo* studies involving rats were carried out in strict accordance with the recommendations in the Guide for Proper Conduct of Animal Experiments and Related Activities in Academic Research and Technology.(16)

The protocol was approved by the Institutional Animal Care and Use Committee and Ethical Committee at the authors' institution (CEFCM/08/2012).

Statistical Analysis

Qualitative variables were expressed as percentages. Quantitative variables were expressed as means ± SD. IBM SPSS Version 21.0® software was used for descriptive and inferential statistical analysis. The Kolmogorov-Smirnov test was used to assess whether variables were distributed normally. Analysis of variance and t test were used to compare averages in normally distributed data. Kruskal-Wallis and Mann-Whitney tests were used to compare means in non-normally distributed data.

Proportions were analyzed with the chi-square test or Fisher's exact test. Kaplan Meier survival analysis was performed to identify differences in mortality between groups.

A two-tail value of $p<0.05$ was considered to be statistically significant.

RESULTS

Contrarily to CPFs (group I), all AVFs presented venous congestion, marked edema, epidermolysis and areas of necrosis (**Fig. 3**). Most of the necrotic areas were clearly defined on the third day after surgery (**Figs. 3** to **5**). On this day, the percentage of flap survival was 99.16 ± 1.46, 71.48 ± 7.80, 68.01 ± 12.39 and 83.21 ± 11.36 for groups I, II, III and IV, respectively. Seven days postoperatively, the percentage of flap survival in these groups was 98.89 ± 1.69, 68.84 ± 7.36, 63.84 ± 10.38, 76.86 ± 13.67. Necrotic areas were more extensive in the caudal third of the flap (**Fig. 3**). Flap survival was higher in the CPF group than in any of the AVF groups ($p<0.01$). Among AVFs, group IV presented a higher flap survival than groups II and III ($p<0.05$). There were no statistically significant differences between groups II and III.

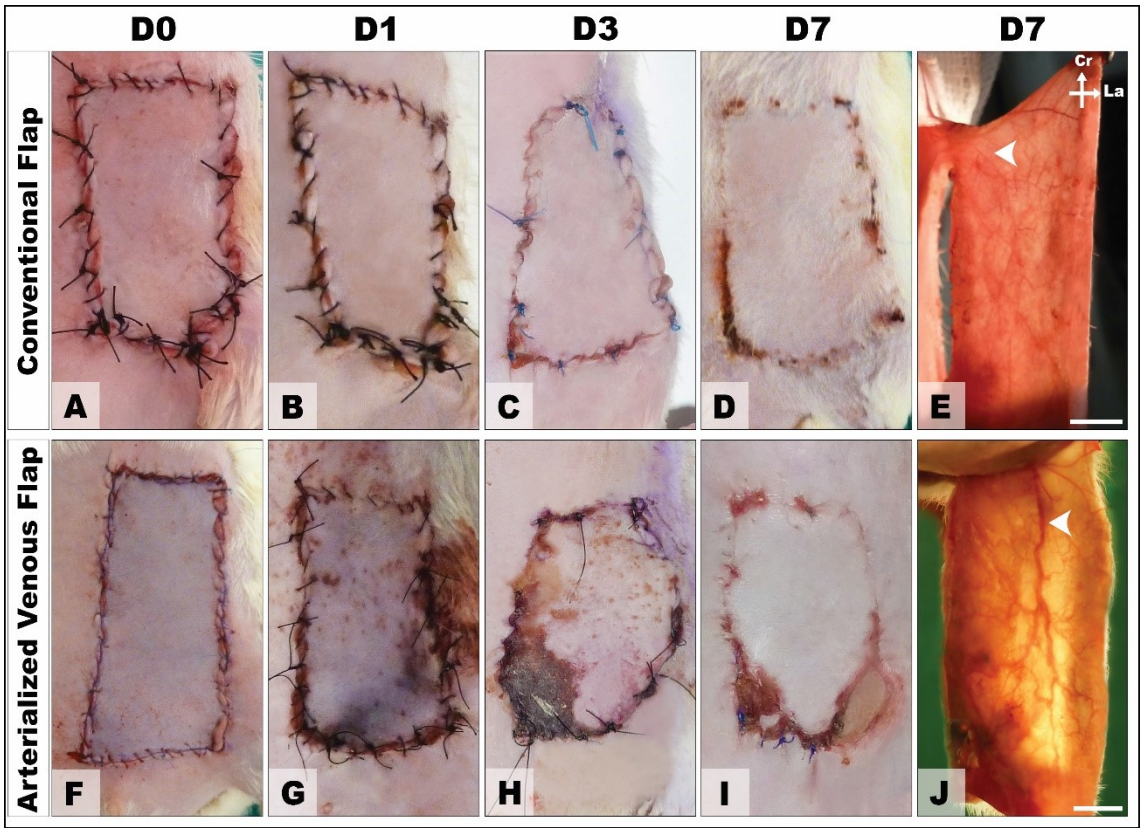

Figure 3 - Representative photographs of conventional perfusion flaps and arterialized venous flaps from the end of surgery to the 7th postoperative day.

D0, one hour after surgery; D1, one day postoperatively; D3, three days postoperatively; D7, seven days postoperatively.

A-D and F-I are photographs taken perpendicularly to the flap's skin surface.

E. Photograph under transillumination of the conventional perfusion flap's deep showing multiple small vessels.

J. Photograph under transillumination of the arterialized venous flap's deep showing an engorged venous system, especially in the territory of the lateral thoracic vein.

The arrow indicates the location of the lateral thoracic vein.

Cr, cranial; La, lateral.

Calibration bar = 10 mm.

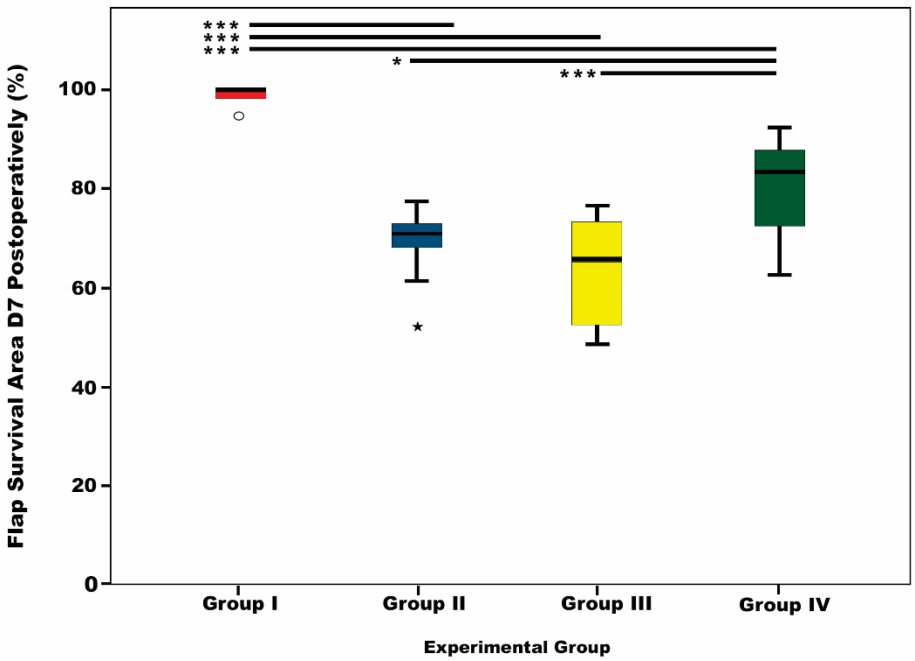

Figure 4 - Box plots graphics illustrating flap survival in the different experimental groups 7 days postoperatively. Horizontal lines over boxplots indicate statistically significant differences.

*, $p<0.05$;

**, $p<0.01$;

***, $p<0.001$.

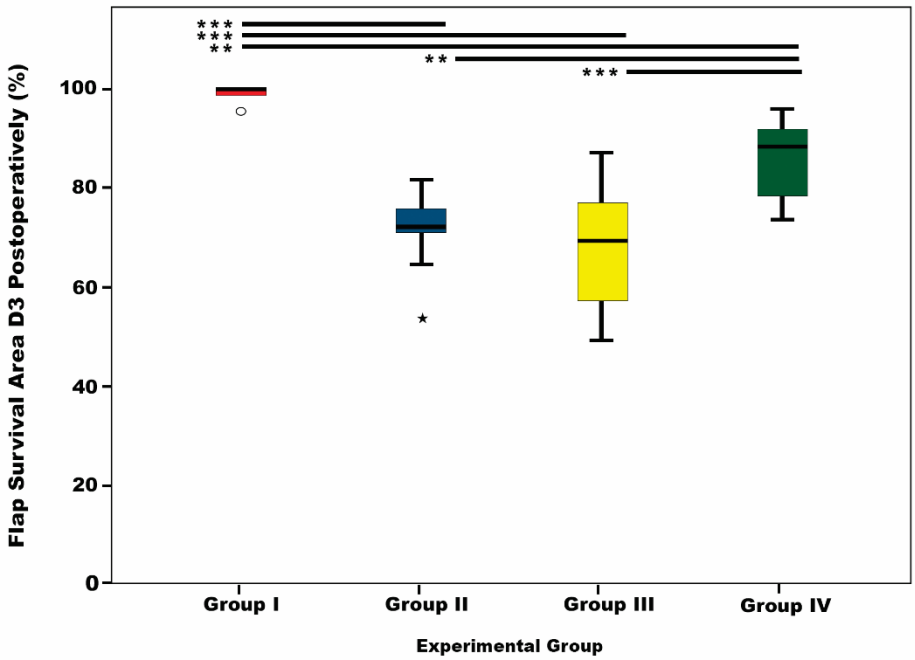

Figure 5 - Box plots graphics illustrating flap survival in the different experimental groups 3 days postoperatively. Horizontal lines over boxplots indicate statistically significant differences.

**, p<0.01;

***, p<0.001.

Average operating time was increasing longer in groups I, II, III and IV (**Table 1**; p<0.0001). On average, it took twice the time to produce a group IV AVF compared to a CPF (group I).

		Group I Conventional Perfusion Flap (n=12)	Group II Arterialized Venous Flap produced by side-to-side anastomosis (n=13)	Group III Arterialized Venous Flap produced by side-to-side anastomosis and femoral vein ligation (n=14)	Group IV Arterialized Venous Flap produced by terminal-lateral anastomosis (n=14)	Statistically significant differences
Average operating time (min)		43.0 ± 5.4	72.2 ± 10.0	75.1 ± 9.4	89.9 ± 10.1	I<II<III<IV p<0.0001
Rat mortality (%)		16.7	23.1	28.6	21.4	None
Surgical Complications (%)	**Arteriovenous anastomosis thrombosis**	0	0	0	7.1	None
	Arteriovenous anastomosis aneurysm	0	0	7.1	0	None
	Hematoma	8.3	23.1	21.4	14.3	None
	Hind limb ischemia	0	0	35.7	0	Larger in group III (p=0.002)
	Complications other than necrosis	8.3	23.1	42.8	21.4	None
Technical difficulty		Easy	Moderate	Moderate	Challenging	N/A

Table 1 - Comparison of the different vascular constructs for producing arterialized venous fasciocutaneous epigastric flaps in the rat. A two-tail value of $p < 0.05$ was considered to be statistically significant.

N/A, non-applicable.

There were no statistically significant differences in rat mortality rates among the different groups (**Table 1**).

The most common complication was hematoma, which occurred in 8.3, 23.1, 21.4 and 14.3 percent of cases of groups I, II, II and IV, respectively. Five rats (35.7%) in group III developed venous congestion and a swollen left hind limb. Four of these rats died within the first 48 hours after surgery. At the end of the experiment, surgical inspection of the AVA revealed an aneurysm in one of the rats in group III and thrombosis in one of the rats in group IV. No infections were noted. Overall, complications were more common in group III, although this difference was not statistically significant.

Thermographic evaluation revealed that all flaps, including CPFs, presented a lower temperature than the contralateral non-operated region (**Fig. 6**). However, the temperature difference was higher in the AVFs, being of at least of 2 °C in these flaps. In all AVFs, temperature was lower in the caudal third of the flap. No significant difference was found among the different AVF groups.

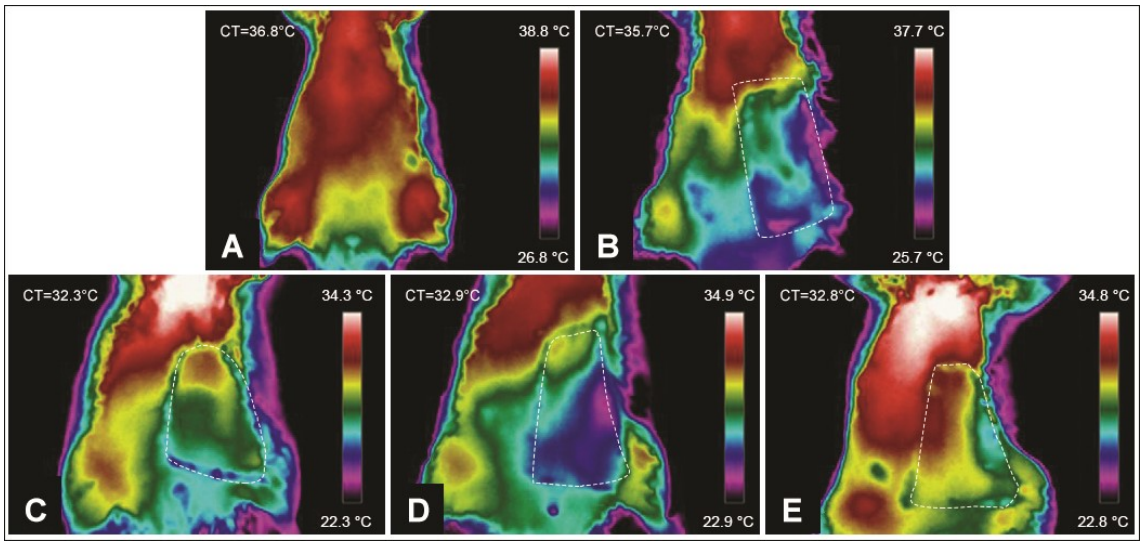

Figure 6 - Representative direct infra-red thermography images of the ventrolateral aspect of the abdomen of the rat 1 hour postoperatively. Flap boundaries are highlighted with the interrupted lines.

A. Rats prior to surgery. This image shows the location of the dominant perforator vessels in the central and cranial aspect of the abdomen.

B. Group I (Conventional Flap).

C. Group II (Arterialized venous flap produced by femoral lateral-lateral anastomosis).

D. Group III (Arterialized venous flap produced by femoral latero-lateral anastomosis and proximal ligation of the femoral vein).

E. Group IV (Arterialized venous flap produced by terminal-lateral anastomosis of the epigastric vein to the femoral artery).

CT, rat core temperature.

Histological and SEM evaluation of vascular corrosion casts revealed great morphological homogeneity among the different AVFs (**Figs. 7** and **8**). In fact, the authors were not able to identify distinctive morphological patterns for any of the AVFs groups, based on qualitative and/or quantitative features. Nevertheless, from a histological standpoint, comparatively to CPFs, AVFs presented greater flap edema,

epidermolysis, loss of skin appendages, venous congestion and rupture, subcutaneous hematoma, and necrosis. In AVFs there were regions of necrosis scattered throughout all integumentary layers. These histological features were more prominent in sections taken from the caudal third of AVFs. Moreover, all AVFs presented signs of SCEV arterialization and significant increment of the lumen diameter of the lateral thoracic vein (**Fig. 7**).

Histological Region	Conventional Perfusion Flap (CPF)	Arterialized Venous Flap (AVF)	Main diferences between CPF and AVF
Flap general outlook	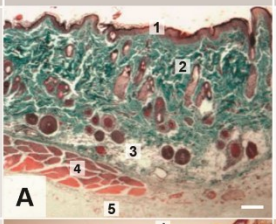	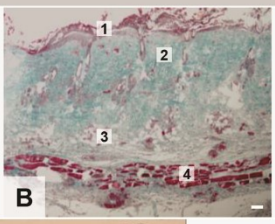	Greater flap edema, venous congestion and necrosis in AVFs
Epidermis	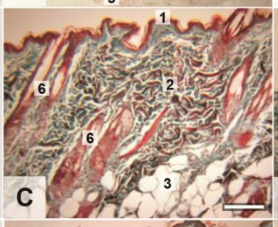	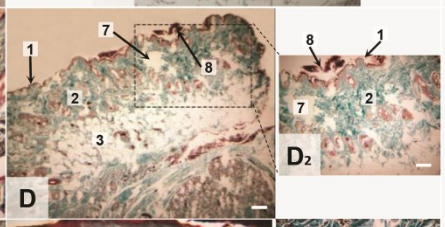	Greater epidermolysis and focal necrosis in AVFs
Dermis	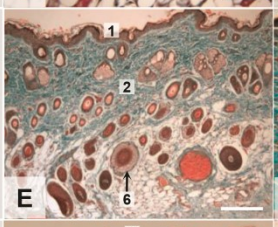	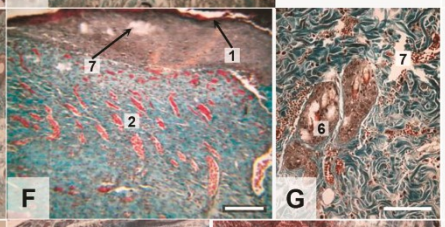	Dermal vascular congestion and rupture, edema, focal necrosis and loss of skin appendages in AVFs
Panniculus adiposus	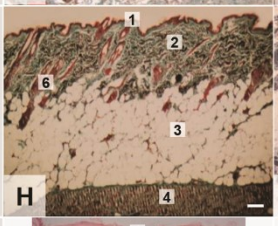	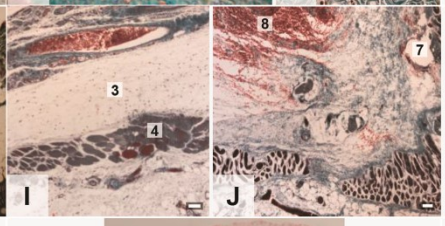	Steatonecrosis, vascular congestion, rupture and haematoma formation in AVFs
Panniculus carnosus	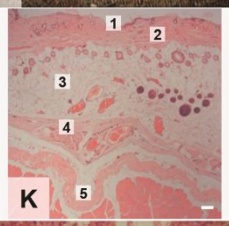	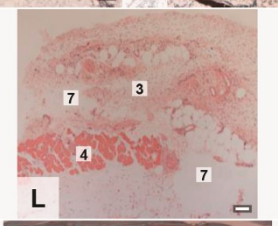	Areas of panniculus carnosus necrosis and segmental interruption in AVFs
Superficial caudal epigastric vessels	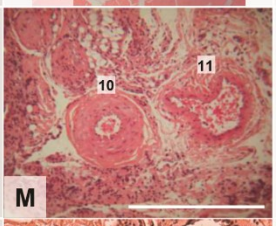	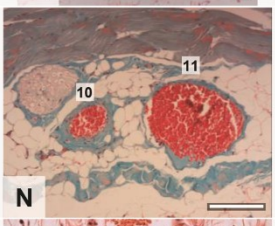	Arterialization of the vein in AVFs
Lateral thoracic vein	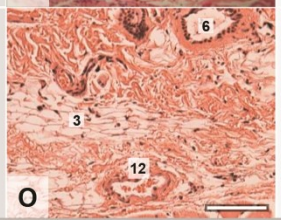	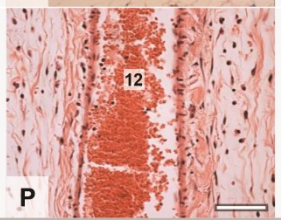	Significant luminal increment

Figure 7 - Comparison of the histological features of arterialized venous flaps (**AVFs**) compared to the conventional perfusion flaps (**CPF**) controls.

A-J and N, Masson's Trichrome stained axial sections of the flap.

D2, High magnification view of the epidermis and dermis in the region of D included in the interrupted rectangle.

K, L, M and O, hematoxylin eosin stained axial sections of the flap.

P, Hematoxylin stained longitudinal section of the flap in the region of the lateral thoracic vein.

1, epidermis; 2, dermis; 3, panniculus adiposus; 4, panniculus carnosus; 5, prefascial loose areolar tissue; 6, hair follicles; 7, necrosis; 8, red blood cell extravasation; 9, granulation tissue; 10, superficial caudal epigastric artery; 11, superficial caudal epigastric vein; 12, lateral thoracic vein.

Calibration bar = 100 μm

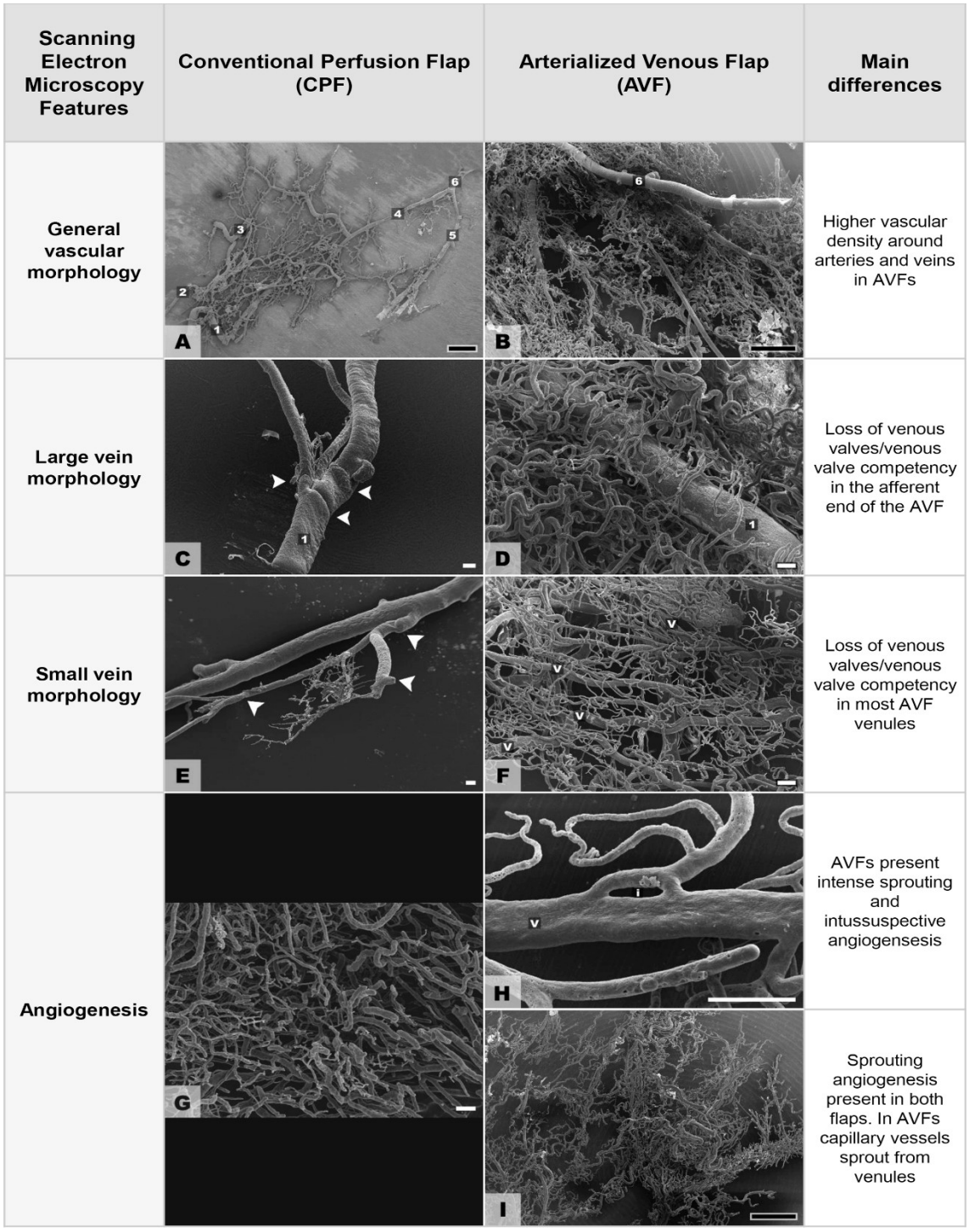

Figure 8 - Comparison of the microvasculature of the conventional flap and the arterialized venous flap using scanning electron microscope images of vascular corrosion casts.

Arrow heads identify venous valves. V, venules; i, Area of intussusceptive angiogenesis

1, Superficial caudal epigastric vein; 2, Superficial caudal epigastric artery; 3, Perforator vein; 4, Medial branch of the lateral thoracic vein; 5, Lateral branch of the lateral thoracic vein; 6, Lateral thoracic vein

White calibration bar = 100 µm

Black calibration bar = 1000 µm

The study of the microvasculature through SEM vascular corrosion casts revealed higher vascular density in AVFs. In addition, these flaps also presented loss of venular valves and/or venous valve incompetency particularly in the caudal half of the flap. Signs of sprouting angiogenesis were present in both CPFs and AVFs, although more markedly in the latter group. In AVFs capillary vessels sprouted more commonly from venules, whereas in CPFs new capillary vessels sprouted mostly from neighboring capillaries. In AVFs it was also frequent to find evidence of intussuspective angiogenesis (**Fig. 8**).

DISCUSSION

Average flap survival area of the best AVF model in this work (group IV) was 76.86 ± 13.67%. This value is slightly inferior to that reported on a recent systematic review and meta-analalysis on the clinical apllication of AVFs. In fact, it was estimated that the survival area of unconventional perfusion flaps used in the clinical context varies between 87.30 to 91.30 percent ($p<0.001$).(3) However, as the cited authors mention, this estimation may be affected by several biasses associated with any meta-analysis, namely publication bias, which tend to overstimate positive outcomes.(3)

AVF survival in the present work was worse than that described in the early description of Nakayama *et al*. These authors described a mean area of survival of 98% in non delayed AVFs. However, they left a superior skin pedicle that no doubt contributed arterial axial and random perfusion to the flap.(2) Nevertherless, the results herein presented concerning AVF survival are similar to those reported by other authors in the rat.(17-20)

The impact of different anastomotic layouts in flap survival had already been tested in CPFs.(21, 22) In these flaps it was shown that side-to-end and end-to-end arterial anastomoses of similarly sized arteries guaranteed comparable survivals.(21) However, as far as the authors could determine, this is the first time that the impact of microvascular anastomotic type on the survival of AVFs is studied. In the present work the vascular layout used in group IV (side-to-end AVA) proved to be superior regarding AVF survival than that used in groups II and III (side-to-side AVAs). Many authors have used side-to-side AVAs of the femoral rats to obtain AVFs of the rat's abdomen. In this way, they avoid the technical challenging AVAs of very small vessels such as the SCEV

and the homonymous artery, which are considerably prone to thrombosis.(12) Moreover, Nakayama *et al.* had already demonstrated in a pilot study that direct end-to-end AVA of the femoral artery and SCEV was associated with significant hemodynamic disturbance and death of 13 out of 15 rats.(2)

The data herein presented suggest that the incorporation of a 1 mm ellipse of the femoral vein adjacent to the drainning point of the SCEV (group IV) allows a safe AVA. This pattern probably ensures a more direct blood flow into the SCEV and thus greater venous valves' incompetency, in comparison to AVAs in groups II and III. Furthermore, it is reasonable to expect that after removing the vascular clamps, the AVA in group IV is pulled by the distension of walls of the femoral artery, resulting in radial distraction of the SCEV. This, in turn, will further lead to venous valve incompetency in the later vessel, thus facilitating the entry of blood through the afferent vein of the group IV AVF.

Interestingly, mathematical modelling using Laplace's law has suggested that the fine structure of venules under 100 μm in diameter renders the valves in these vessels readily incompetent in the presence of venous arterialization of ischemic lower limbs in humans.(23) Our SEM data give empirical support to this assertion in the rat model, as in all AVFs groups there were signs of loss valve competency particularly in venules located in the afferent half of the flap (**Fig. 8**). Similar findings have been reported by other authors.(12)

Multiple examples of intussusceptive angiogenesis in the vascular molds of AVFs were observed in the present study. These may be justified by the fact that increases in blood pressure inside small vessels have been shown to be associated with transluminal tissue pillar formation and subsequent vascular splitting and neovessel formation.(24)

This mechanism has been largely neglected in the literature and may have a pivotal role in AVF hemodynamic adaptation.(12)

To the best of the authors' knowledge, thermography imaging had never been employed before to study perfusion of AVFs. Notwithstanding, skin temperature has been used as surrogate marker of perfusion in hindlimb vein arterialization in rats. The rationale for this is that skin temperature is proportional to integumentary perfusion.(25) Our study lends support to the use of infra-red thermography imaging for AVF perfusion evaluation, since it confirmed an inferior temperature in these flaps comparatively to CPFs and to the contralateral side of the abdomen. Additionaly, in all AVFs, temperature was lower in the caudal third of the flap, where necrosis was more commonly found.

Recently, it has been shown that this region of the abdomen of the rat can be used to produce axial flaps simulating arterial ischemia or venous congestion, readily observed macroscopically by a pale and dark violet color, respectively.(14) Remarkably, in the present study all AVFs groups presented a dark bluish color suggestive of venous congestion (**Fig. 3**). Another common finding in these two studies was that necrotic areas were clearly defined in both CPFs and AVFs on the third postoperative day.(14) This information may be of great interest for future research works using similar flaps in this region of the rat.

Rats were chosen in the present study because they have been the most widely used animal model in the realm of experimental flap surgery. (26) This is certainly due to the fact they are readily available in most countries, they are easy to keep, and they are amongst the cheapest animals to obtain and to maintain. (26) Nonetheless, it should be noted that AVFs performed in humans are usually based on vessels of a larger

caliber.(3) Hence, extrapolation of data obtained with the AVFs used in this paper to humans must be done with this limitation in mind. In fact, it would be interesting to study the various vascular constructions described in these paper in other animal species, where larger flaps could be produced.

Furthermore, it is well known that in loose-skinned animals the well-developed panniculus carnosus in the deep aspect of the integument leads to significant contraction of wounds and flaps.(27) To tackle this problem multiple strategies have been devised, namely choosing anatomical sites where the integument is firmly adherent to the deep structures (e.g., rabbit ear) or using various devices or splints to fixate the integumentary layer and the surgical flaps.(27) Despite, these limitations, in plastic surgery experimental research, it is customary to consider flap's survival and necrosis as a percentage of flap's total area, as the authors did in the present article.(9, 11, 14, 26) However, this difference in flap and wound behavior between rodents and humans should be taken into consideration when generalizing the data presented in this article to the clinical scenario.

Finally, the authors believe that the AVFs in group IV represent an optimized model of unconventional perfusion flap that can be easily replicated for research and teaching purposes. However, further studies are warranted to confirm or dismiss their usefulness in these contexts.

CONCLUSION

An optimized AVF can be reliably produced in the ventrolateral aspect of the abdomen of the rat by performing an end-to-side AVA between the femoral artery and the SCEV including the adjacent portion of the femoral vein, in order to produce a 1 mm wide afferent vein. This model presented an average flap survival area of 76.86 ± 13.67%.

ACKNOWLEDGEMENTS

The authors are very grateful to Mr. Carlos Lopes and Mr. Octávio Chaveiro for their help in producing and observing the SEM specimens.

The authors would also like to thank Mr. Nuno Folque for producing all the drawings contained in this paper.

References

1. Vaubel, W. Indikationen und Technik des arterialisierten Lappens zur Deckung großer Defekte im Handbereich. *Hefte Unfallheilkd* 1975;126:381.

2. Nakayama, Y., Soeda, S., Kasai, Y. Flaps nourished by arterial inflow through the venous system: an experimental investigation. *Plastic and reconstructive surgery* 1981;67:328-334.

3. Casal, D., Cunha, T., Pais, D., et al. Systematic Review and Meta-Analysis of Unconventional Perfusion Flaps in Clinical Practice. *Plastic and reconstructive surgery* 2016;138:459-479.

4. Goldschlager, R., Rozen, W. M., Ting, J. W., Leong, J. The nomenclature of venous flow-through flaps: updated classification and review of the literature. *Microsurgery* 2012;32:497-501.

5. Yan, H., Brooks, D., Ladner, R., Jackson, W. D., Gao, W., Angel, M. F. Arterialized venous flaps: a review of the literature. *Microsurgery* 2010;30:472-478.

6. Yan, H., Zhang, F., Akdemir, O., et al. Clinical applications of venous flaps in the reconstruction of hands and fingers. *Arch Orthop Trauma Surg* 2010.

7. Yan, H., Fan, C., Zhang, F., Gao, W., Li, Z., Zhang, X. Reconstruction of large dorsal digital defects with arterialized venous flaps: our experience and comprehensive review of literature. *Ann Plast Surg* 2013;70:666-671.

8. Weng, W., Zhang, F., Zhao, B., et al. The complicated role of venous drainage on the survival of arterialized venous flaps. *Oncotarget* 2017.

9. Hirase, Y. Skin and muscle flaps in the rat. In S. Tamai, M. Usui, T. Yoshizu eds., *Experimental and Clinical Reconstructive Microsurgery*, First ed. Japan: Springer-Verlag; 2004:111-114.

10. Thatte, M., Healy, C., McGrouther, D. Laser Doppler and microvascular pulsed Doppler studies of the physiology of venous flaps. *European Journal of Plastic Surgery* 1993;16:134-138.

11. Casal, D., Pais, D., Iria, I., et al. A Model of Free Tissue Transfer: The Rat Epigastric Free Flap. *Journal of Visualized Experiments* 2017:e55281.

12. Wungcharoen, B., Pradidarcheep, W., Santidhananon, Y., Chongchet, V. Pre-arterialisation of the arterialised venous flap: an experimental study in the rat. *Br J Plast Surg* 2001;54:621-630.

13. Sheena, Y., Jennison, T., Hardwicke, J. T., Titley, O. G. Detection of perforators using thermal imaging. *Plastic and reconstructive surgery* 2013;132:1603-1610.

14. Matsumoto, N. M., Aoki, M., Nakao, J., et al. Experimental Rat Skin Flap Model That Distinguishes between Venous Congestion and Arterial Ischemia: The Reverse U-Shaped Bipedicled Superficial Inferior Epigastric Artery and Venous System Flap. *Plastic and reconstructive surgery* 2017;139:79e-84e.

15. Aharinejad, S. H., Lametschwandtner, A. Identification and Interpretation of Cast Vessel Structures In S. H. Aharinejad, A. Lametschwandtner eds., *Microvascular corrosion casting in scanning electron microscopy: Tecnhiques and applications*, First ed. New York: Springer-Verlag; 1992:103-115.

16. National Research Council (U.S.). Committee for the Update of the Guide for the Care and Use of Laboratory Animals., Institute for Laboratory Animal Research (U.S.), National Academies Press (U.S.). Guide for the care and use of laboratory animals. 8th ed. Washington, D.C.: National Academies Press,, 2011:xxv, 220 p.

17. Baser, N. T., Silistreli, O. K., Sisman, N., Oztan, Y. Effects of surgical or chemical delaying procedures on the survival of proximal predicled venous island flaps: an experimental study in rats. *Scand J Plast Reconstr Surg Hand Surg* 2005;39:197-203.

18. Chow, S. P., Chen, D. Z., Gu, Y. D. A comparison of arterial and venous flaps. *J Hand Surg Br* 1992;17:359-364.

19. Miles, D. A., Crosby, N. L., Clapson, J. B. The role of the venous system in the abdominal flap of the rat. *Plastic and reconstructive surgery* 1997;99:2030-2033.

20. Mutaf, M., Tasaki, Y., Fujii, T. Expansion of venous flaps: an experimental study in rats. *Br J Plast Surg* 1998;51:393-401.

21. Miyamoto, S., Takushima, A., Okazaki, M., Ohura, N., Minabe, T., Harii, K. Relationship between microvascular arterial anastomotic type and area of free flap survival: comparison of end-to-end, end-to-side, and retrograde arterial anastomosis. *Plastic and reconstructive surgery* 2008;121:1901-1908.

22. Parsa, F. D., Spira, M. Evaluation of anastomotic techniques in the experimental transfer of free skin flaps. *Plastic and reconstructive surgery* 1979;63:696-699.

23. Koyama, T., Sugihara-Seki, M., Sasajima, T., Kikuchi, S. Venular valves and retrograde perfusion. In H. M. Swartz, D. K. Harrison, D. F. Bruley eds., *Oxygen transport to tissue XXXVI*, Vol. 1, First ed. New York, USA: Springer; 2014:317-323.

24. Makanya, A. N., Hlushchuk, R., Djonov, V. G. Intussusceptive angiogenesis and its role in vascular morphogenesis, patterning, and remodeling. *Angiogenesis* 2009;12:113-123.

25. Sasajima, T., Kikuchi, S., Ishikawa, N., Koyama, T. Skin temperature in lower hind limb subjected to distal vein arterialization in rats. In H. M. Swartz, D. K. Harrison,

D. F. Bruley eds., *Oxygen transport to tissue XXXVI*, Vol. 1, First ed. New York, USA: Springer; 2014:361-368.

26. Dunn, R. M., Mancoll, J. Flap models in the rat: a review and reappraisal. *Plastic and reconstructive surgery* 1992;90:319-328.

27. Davidson, J. M., Yu, F., Opalenik, S. R. Splinting Strategies to Overcome Confounding Wound Contraction in Experimental Animal Models. *Advances in Wound Care* 2013;2:142-148.

Chapter 8

BD-2 AND BD-3 INCREASE SKIN FLAP SURVIVAL IN A RAT MODEL OF ISCHEMIA AND *PSEUDOMONAS AERUGINOSA* INFECTION IN THE PRESENCE OF A FOREIGN BODY

Authors: Diogo Casal[1-4 ¶ *], Inês Iria[3,4,#a,#b ¶], José S. Ramalho[4], Sara Alves[5], Eduarda Mota-Silva[6], Luís Mascarenhas-Lemos[1,5], Carlos Pontinha[1,5], Maria Guadalupe Cabral[4], José Ferreira-Silva[5], Mário Ferraz-Oliveira[5], Valentina Vassilenko[6], João Goyri-O'Neill[1], Diogo Pais[1], Paula A. Videira[3,4]

Affiliations:

1- Anatomy Department, NOVA Medical School, Universidade NOVA de Lisboa, Lisbon, Portugal

2- Plastic and Reconstructive Surgery Department and Burn Unit, Centro Hospitalar de Lisboa Central – Hospital de São José, Lisbon, Portugal

3- UCIBIO, Departamento de Ciências da Vida, Faculdade de Ciências e Tecnologia, Universidade NOVA de Lisboa, Caparica, Portugal

4- CEDOC, NOVA Medical School, Faculdade de Ciências Médicas, Universidade NOVA de Lisboa, Lisbon, Portugal

5- Pathology Department, Centro Hospitalar de Lisboa Central – Hospital de São José, Lisbon, Portugal

6- LIBPhys, Physics Department, Faculdade de Ciências e Tecnologias, Universidade NOVA de Lisboa, Caparica, Portugal

#a- Molecular Microbiology and Biotechnology Unit, iMed, ULisboa, Faculty of Pharmacy, Universidade de Lisboa, Lisbon, Portugal

#b- INESC, MN – Microsystems and Nanotechnologies, Instituto Superior Técnico, Universidade de Lisboa, Lisbon, Portugal

¶ These authors contributed equally to this work.

ABSTRACT

Pseudomonas aeruginosa is one of the major culprits of nosocomial infections, particularly of prosthetic material, due to its ability to produce biofilms, and to thrive in poorly perfused tissues. The main aim of this work was to study the usefulness of human β-defensins 2 (**BD-2**) and 3 (**BD-3**) in the treatment of infected ischemic skin flaps. We investigated the effect of transducing rat ischemic skin flaps with lentiviral vectors encoding human BD-2, BD-3, or both BD-2+BD-3, to increase flap survival in the context of a *P. aeruginosa* infection associated with a foreign body. The secondary endpoints assessed were: bacterial counts, and biofilm formation on the surface of the foreign body.

Arterialized venous flaps of the left epigastric region of rats were intentionally infected by placing two catheters under the flap with 10^5 colony-forming units (**CFUs**) of *P. aeruginosa* before the surgical wound was hermetically closed.

Flap biopsies were performed 3 and 7 days post-operatively, and the specimens submitted to immunohistochemical analysis for BD-2 and BD-3, as well as bacterial quantification. Subsequently, the catheter segments were analyzed with scanning electron microscopy (**SEM**).

Ischemia and infection development were successfully confirmed by thermography and bacterial counting. Flaps transduced with BD-2 and BD-3 showed a successful expression of these defensins and presented increased flap survival. Moreover, rats transduced with BD-3 presented a net reduction in the number of *P. aeruginosa* on the surface of the foreign body and lesser biofilm formation. Flap survival was better correlated

with SEM findings on the surface of the foreign body than with other bacterial quantification methods.

This study demonstrates for the first time a model of ischemic flaps with infection and the usefulness of human BD-2 and BD-3 lentiviral vectors to clear infection in this context. Defensin gene therapy may be a suitable approach to treat nosocomial surgical infections.

INTRODUCTION

Multi-resistant bacteria are on the rise all over the world, leading many to proclaim an imminent post-antibiotic era, in which common infections and surgeries could become life threatening conditions.[1-3] For instance, several authors have shown that a leg ulcer lasting for one month will have on average at least one isolated multi-drug resistant organism at that time.[4] Hence, it comes as no surprise that multiple new strategies to tackle bacterial infections are actively being sought [1-3, 5] and alternatives to conventional antibiotics are direly needed.[6]

In this context, antimicrobial peptides (**AMPs**) become particularly appealing as a new way to target one of the last "Achilles' heels" of bacteria.[5, 7-13] AMPs are small cationic peptides that have pleotropic bactericidal effects. They are divided in multiple chemical classes, of which the most studied and populated are the cathelicidins, the defensins, the histatins, and the dermcidins.[5] Defensins have been indicated as one of the most promising AMP classes for potential therapeutic used based on *in vitro* essays.[13-15] Defensins, similarly to other AMPs, act mainly by disrupting the structure of gram-positive and gram-negative bacterial cell membrane. These AMPs also inhibit bacterial deoxyribonucleic acid (**DNA**) replication, transduction and translation, disturbing bacterial homeostasis (**Fig. 1**). The resulting byproducts trigger the activation of the complement system and inflammatory processes that further help clearing bacterial infections (**Figs. 1** and **2**).[7, 10, 16] Moreover, it has been shown that due to its peculiar action in the cell membrane, seldom are bacteria able to develop resistance to defensins.[5, 17, 18]

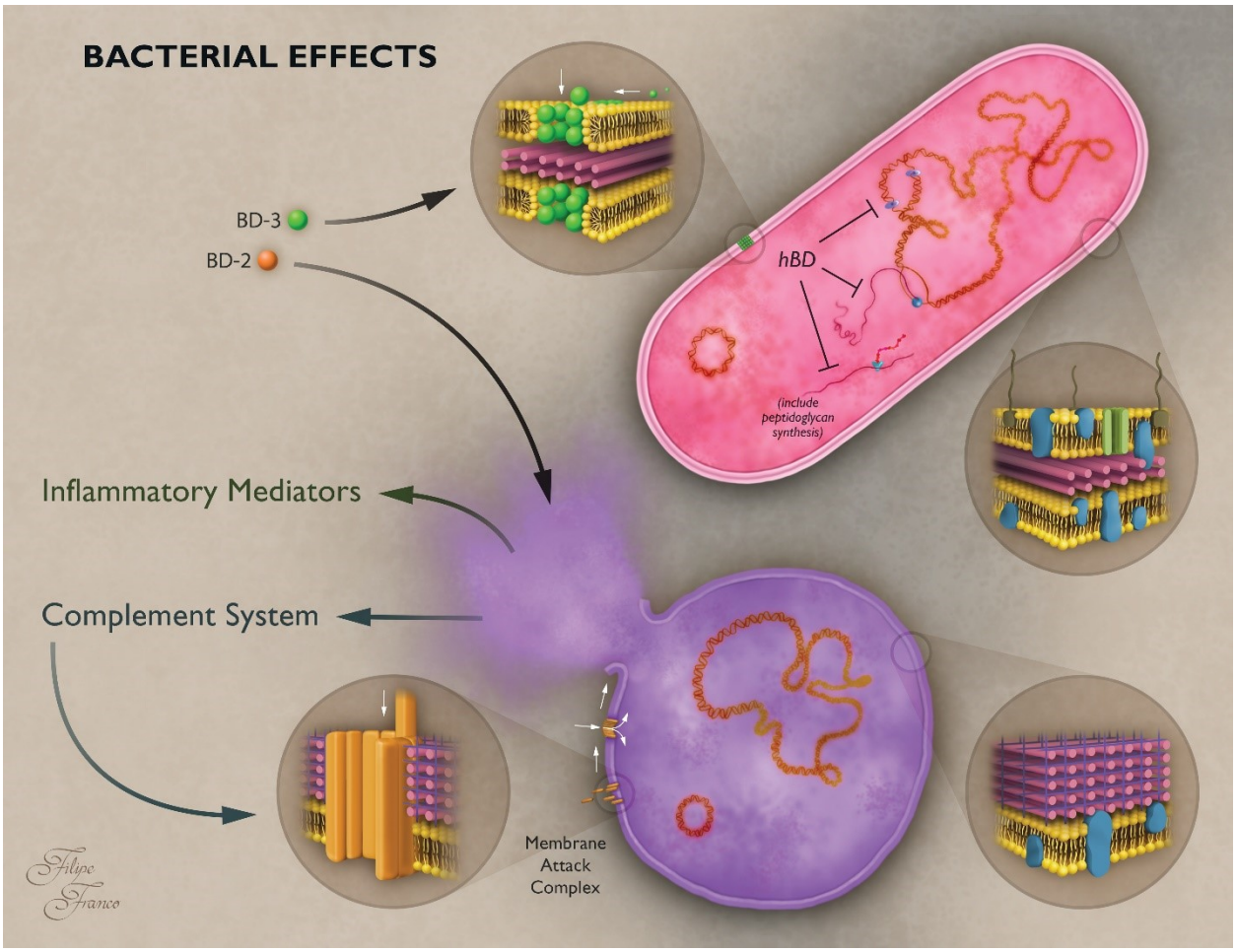

Figure 1 - Schematic representation of some of the known effects of human β-defensins 2 and 3 on bacteria. Typical gram-negative bacteria are represented by the pink-red rod. Typical gram-positive bacteria are depicted by the violet coccus. Defensins intercalate into bacterial cell membrane and form pores through bacteria walls promoting osmotic imbalance and bacterial membrane rupture. This, in turn, promotes activation of the alternative pathway of the complement system leading to the formation of membrane attack complexes that further promote bacterial lysis and complement activation. Byproducts of complement activation and bacterial cell rupture act as chemotactic factors promoting the recruitment of inflammatory cells that will enhance bacterial clearance.[7, 82] Intracellularly, defensins inhibit bacterial DNA replication, transduction and translation, disturbing bacterial homeostasis.

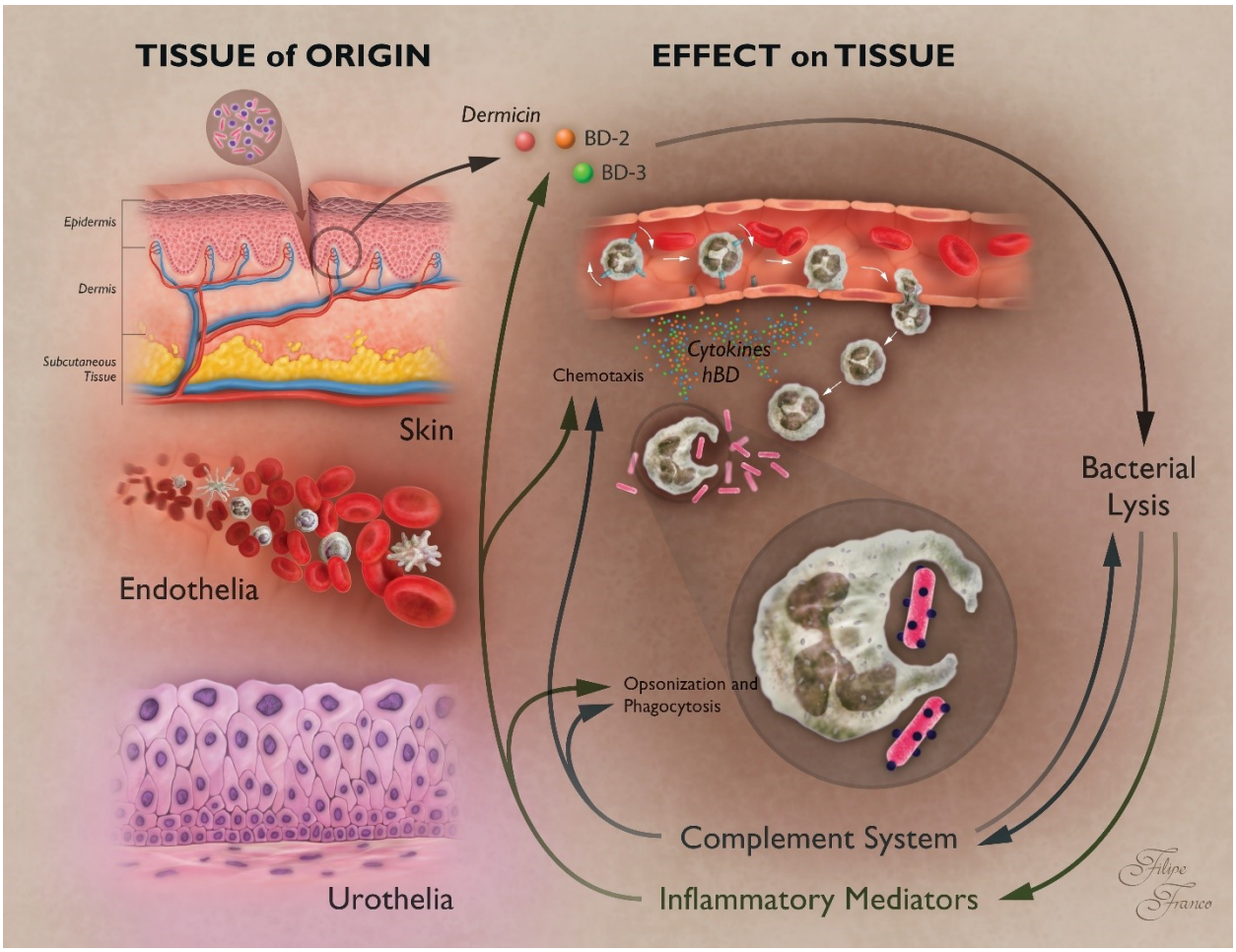

Figure 2 - Schematic representation of some of the known effects of human β-defensin 2 and 3 on the immune system and their role in the destruction of bacteria. Gram-negative bacteria are represented by pink-red rods, whereas gram-positive bacteria are depicted by violet cocci.

Antimicrobial peptides, including defensins, are part of the innate resistance against bacterial invasion. Defensins are secreted by multiple epithelia, namely those lining skin, endothelia, gut, airways and the genitourinary tract, as well as by leucocytes and platelets. Microbial components, such as lipopolysaccharide, and other pro-inflammatory stimuli are strong inducers of the expression and secretion of defensins. Defensins, in turn, act as potent chemotactic agents, activate the complement system, promote opsonization and phagocytosis of bacteria, and concomitantly lead to the release of oxygen reactive species and of further pro-inflammatory factors. All these phenomena lead to positive feedback mechanisms that collectively facilitate resolution of bacterial infections.[19, 82]

BD-2, human β-defensin 2; **BD-3**, human β-defensin 3; **hBD**, human β-defensin

Defensins, of which 15 isoforms are currently identified in humans, are remarkably widely secreted in multiple epithelia, leucocytes and platelets (**Fig. 2**).[14, 19, 20] Apart from their role in the innate immunity, it has been recognized that they are instrumental in immune regulation and to initiate, mobilize, and amplify acquired immunity.[5]

Among the most commonly encountered multi-resistant bacteria, *Pseudomonas aeruginosa* stands out as one of the major culprits of nosocomial infections worldwide, being associated with significant morbidity, mortality, and increased health costs. *P. aeruginosa* frequently causes antibiotic-refractory infections of prosthetic material, due to its ability to produce biofilms, and to its intrinsic, acquired and adaptive resistance mechanisms to multiple antibiotics.[2, 21, 22] Noteworthy, *P. aeruginosa* is known to thrive in poorly perfused tissues, as in ischemic wounds or limbs, such as those of many diabetic patients, as well as in chronic wounds or around prosthetic material.[4, 6, 23, 24]

Although numerous AMPs have shown microbicidal activity against *P. aeruginosa in vitro* [16, 25-27], as far as the authors could determine, there are no studies using β-defensins (**BDs**) to treat *P. aeruginosa* infections in *in vivo* models.[26, 27] This is unfortunate, since BDs have shown to be efficient against multi-resistant *P. aeruginosa in vitro*.[26, 27] Moreover, amongst BDs, BD-2 has been shown to be particularly effective against Gram-negative bacteria and some fungi, although relatively less potent against Gram-positive bacteria. Furthermore, BD-3 is reportedly a powerful antimicrobial agent

with a broad range of activity toward yeast, Gram-negative and Gram-positive bacteria, including the vancomycin-resistant *Enterococcus faecium*.[25, 26]

Despite these interesting *in vitro* results, there are several reports stating that defensins, being cationic, have hampered bactericidal activity *in vivo* due to the presence of neutralizing anionic compounds in living tissues.[26, 28, 29]

Hence, the main aim of this work was to study the usefulness of transducing an ischemic skin flap in the rat with two human BDs (**BD-2** and **BD-3**) to increase skin flap survival in the context of a *P. aeruginosa* infection in the presence of a foreign body. The secondary endpoints assessed were: reduction in bacterial counts, reduction in biofilm formation, and increase in rat survival rates. Interestingly, we observed that BD-2 and BD-3 increased skin flap survival in our model. Moreover, rats transduced with BD-3 presented a net reduction in the number of *P. aeruginosa* on the surface of the foreign body and lesser biofilm formation.

Figures 3 and **4** summarize the experiments done in this work.

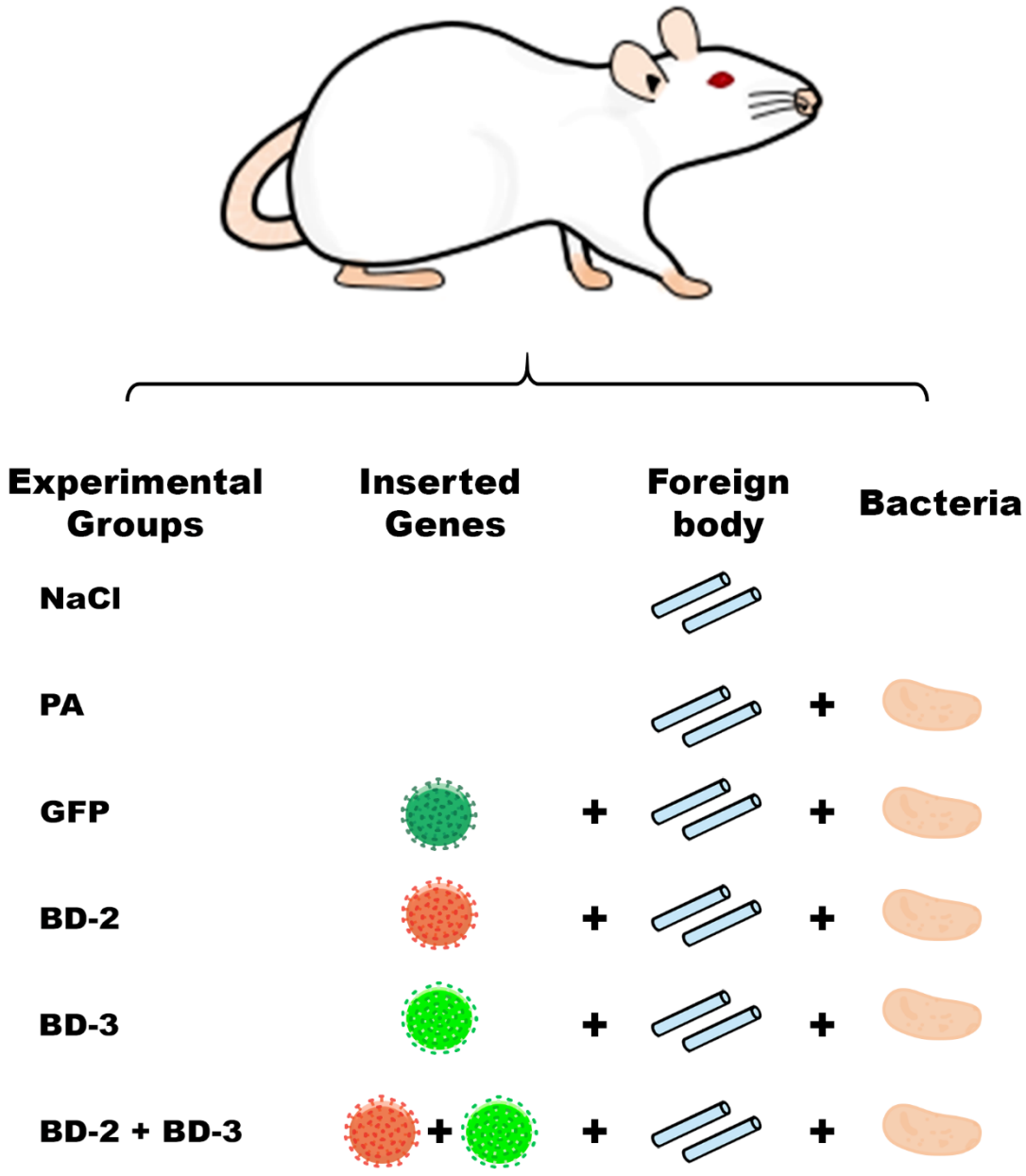

Figure 3 - Diagram illustrating the experimental groups used in this work.

NaCl group - In this group, flaps were intravascularly injected with a 100-µl solution of recombinant rat Vascular Endothelial Growth Factor-A that was left to act for 90 min. Before closing the surgical wounds, one

milliliter of a 0.9% sodium chloride solution was instilled under the flap into the vicinity of the silicone catheter segments.

PA group - In this group, flaps were intravascularly injected with a 100-µl solution of recombinant rat Vascular Endothelial Growth Factor-A that was left to act for 90 min. Before closing the surgical wounds, one milliliter of a 0.9% sodium chloride solution containing 10^5 CFU *Pseudomonas aeruginosa* was instilled under the flap into the vicinity of the silicone catheter segments.

GFP group - In this group, flaps were intravascularly injected with a 100-µl milliliter solution of recombinant rat Vascular Endothelial Growth Factor-A and a Green Fluorescent Protein coding lentivirus. This solution was left to act for 90 min. Before closing the surgical wounds, one milliliter of a 0.9% sodium chloride solution containing 10^5 CFU *P. aeruginosa* was instilled under the flap into the vicinity of the silicone catheter segments.

BD-2 group - In this group, flaps were intravascularly injected with a 100-µl solution of recombinant rat Vascular Endothelial Growth Factor-A and a human β-defensin 2 coding lentivirus. This solution was left to act for 90 min. Before closing the surgical wounds, one milliliter of a 0.9% sodium chloride solution containing 10^5 CFU *P. aeruginosa* was instilled under the flap into the vicinity of the silicone catheter segments.

BD-3 group - In this group, flaps were intravascularly injected with a 100-µl solution of recombinant rat Vascular Endothelial Growth Factor-A and a human β-defensin 3 coding lentivirus. This solution was left to act for 90 min. Before closing the surgical wounds, one milliliter of a 0.9% sodium chloride solution containing 10^5 CFU *P. aeruginosa* was instilled under the flap into the vicinity of the silicone catheter segments.

BD-2 + BD-3 group - In this group, flaps were intravascularly injected with a 100-µl solution of recombinant rat Vascular Endothelial Growth Factor-A and human β-defensin 2 and 3 coding lentivirus. This solution was left to act for 90 min. Before closing the surgical wounds, one milliliter of a 0.9% sodium chloride solution containing 10^5 CFU *P. aeruginosa* was instilled under the flap into the vicinity of the silicone catheter segments.

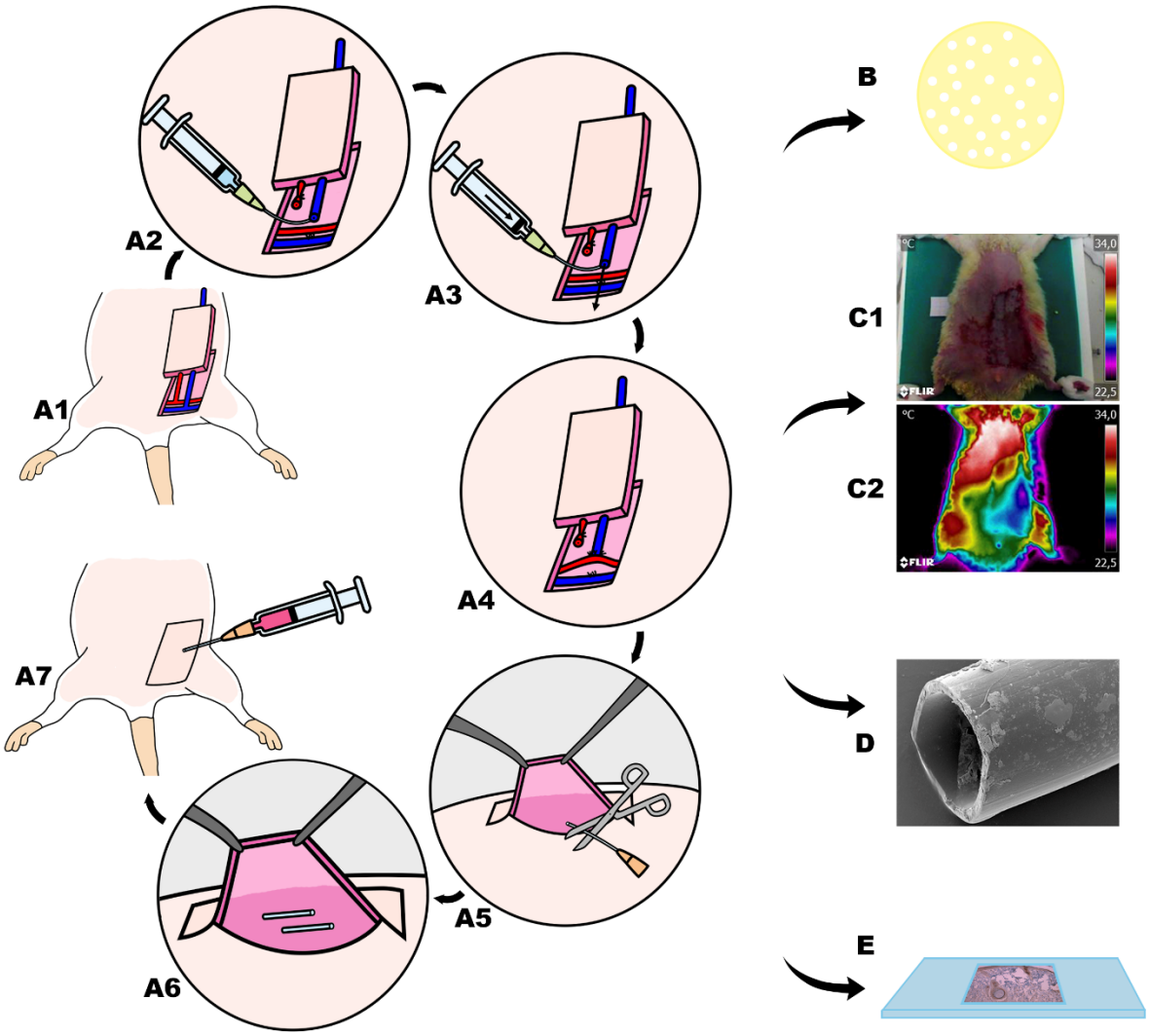

Figure 4 - Diagram illustrating the main steps in the production of the rodent model of ischemia, *Pseudomonas aeruginosa* infection associated with a foreign body, lentiviral delivery of antimicrobial peptides, and evaluation of flap progression. From (A1) to (A7), a summary of the steps involved in the model of foreign body infection underneath an ischemic fasciocutaneous flap is represented.

(A1) A variant of the rat abdominal arterialized venous flap was used as model of ischemic flap.[37, 38] In all animals, under a surgical operating microscope, a 5 cm long and 3 cm wide fasciocutaneous flap was raised

on the left side of the rat's abdomen. Cranially, the flap was connected exclusively to the skeletonized lateral thoracic vein. This vein was temporarily clamped. Caudally, the superficial caudal epigastric artery was ligated.

(A2) The SCEV was cannulated with a 27-gauge ophthalmic cannula.

(A3) The SCEV was perfused with 100 µl solution of the following solutions: **NaCl Group** (VEGF); **PA Group** (VEGF); **GFP Group** (VEGF + GFP coding lentivirus); **BD-2 Group** (VEGF + BD-2 coding lentivirus); **BD-3 Group** (VEGF + BD-3 coding lentivirus); **BD-2 + BD-3 Group** (VEGF + BD-2 + BD-3 coding lentivirus). The SCEV was then immediately clamped for 90 min, in order to leave the injected solution in contact with the flap's vascular system.

(A4) Clamps were removed and the SCEV was arterialized by connecting it to the femoral artery. In order to achieve this the SCEV was cut from the femoral vein with a 1-mm long cuff of adjacent femoral vein tissue. The ostium in the femoral vein was closed with a continuous Nylon 11/0 suture. The same suture line was used to perform a side-to-end arteriovenous anastomosis between the SCEV and the ventral flank of the femoral artery through a 1-mm long ostium previously created in the latter vessel. Interrupted stitches were used for this anastomosis. The lateral thoracic vein was preserved cranially to ensure outflow from the arterialized venous flap.

(A5) Two 1-cm segments of sterile 14-gauge silicone catheters (Mediplus™) were placed in the central aspect of the surgical wound, underneath the flap.

(A6) Surgical wounds were closed with a running 5/0 Nylon suture.

(A7) Immediately before closing the lateral aspect of the skin wound, a 1-ml of a 0.9% sodium chloride solution was instilled under the flap into the vicinity of the silicone catheter segments using a 18-gauge silicone catheter (Mediplus™). In all groups except the NaCl group, the injected solution also contained 10^5 CFU *Pseudomonas aeruginosa*. The running suture was closed immediately after injection, in order to avoid any spilling to the area adjacent to the flap. A transparent Tegaderm™ transparent film dressing was applied over the flap and adjacent skin.

(B), Flap biopsies were collected on the third and seventh day postoperatively to determine bacterial counts after bacterial culture.

(C), Flap survival and perfusion was assessed by clinical inspection and with resort to direct infrared thermography.

(D), Bacterial numbers and disposition were assessed on the surface of foreign bodies using scanning electron microscopy.

(E), Flap transduction with the BD-2 and/or BD-3 genes was evaluated by immunohistochemical evaluation of flap biopsies 3 and 7 days after surgery.

BD-2, human β-defensin 2; **BD-3**, human β-defensin 3; **CFU**, colony forming units; **GFP**, green fluorescent protein; **SCEV**, superficial caudal epigastric vein; **VEGF**, vascular endothelial growth factor

Bacterial growth

All bacteria were inoculated in Luria-Bertani (**LB**) broth and grown at 37 °C on a rotary shaker at 250 rpm, overnight. Exceptions were performed and are properly indicated.

Plasmids production

Competent *Escherichia coli* DH5α were transformed by heat-shock with pMD2.G and psPAX vectors, while competent *E. coli* Stbl3 were transformed with pLenti6.BD-2 and pLenti6.BD-3. Posteriorly, bacteria were grown in LB media, at optimal temperature in ampicillin presence, at 37 and 30 °C, respectively.

Pseudomonas aeruginosa – infection model

P. aeruginosa CECT 110^{+} strain, that was kindly provided by Professor Isabel Sá Correia (Instituto Superior Técnico, Lisbon, Portugal), was grown until the mid-exponential phase and it was serially diluted in 0.01 M PBS at a OD_{600nm} of 0.0001 corresponding at

1.0x10^5 CFU/ml. At all times, to confirm the *P. aeruginosa* CFUs, spreadings of bacteria were performed in LB agar dishes and colonies were counted after overnight incubation at 37 °C.

Before performing the antimicrobials assays in the animal model of ischemia, tests were conducted to determine the ideal bacterial concentration. The concentrations initially used were: 10^3; 10^4; 10^5; 10^6 and 10^7 CFU/ml. We selected the concentration of 10^5 CFU/ml, since this concentration systematically resulted in clinically significant infection and partial flap necrosis in our model. Higher concentrations led to complete or nearly complete flap necrosis (10^6 CFU/ml; n=2) and animal's death (10^7 CFU/ml; n=3), whereas lower concentrations (10^3 and 10^4 CFU/ml; n=3 for each concentration) did not produce clinically recognizable infection.

Lentivirus preparation

The defensin beta 4A (***DEFB4A***) and defensin beta 103A (***DEFB103A***) **cDNA** (complementary deoxyribonucleic acid) sequences, which code for the BD-2 and BD-3 proteins, respectively, were synthetized by GenScript Corporation® (New Jersey, USA) and cloned into **pcDNA** (plasmidium complementary deoxyribonucleic acid) ENTR BP, using *Xho*I/*EcoR*I (*DEFB4A*) and *Sal*I/*Kpn*I (*DEFB103A*). This expression vector was generated by inserting a polylinker, previously chemically synthetized, containing several restriction sites into pcDNA6.2GW/Em-GFP, a mammalian expression Gateway® (Invitrogen) previously digested with DraI/XhoI. The defensins coding sequences were transferred into pLenti6 (Invitrogen®) by LR recombination.[30]

Lentivirus particles were produced according to ViraPower™ Lentiviral Expression Systems (ThermoFisher®) recommendations, using HEK293 cells. Recombinant BD-2 and BD-3 expression in HEK293 was confirmed by RT-PCR. The total RNA of cells lines was extracted using the GenElute™ Mammalian Total RNA Miniprep Kit (Sigma-Aldrich®), according to the manufacturer's instructions. In order to remove any genomic DNA contamination, a RNase-Free DNase Set (Qiagen®) was used. The SuperScript® III First-Strand Synthesis System (Invitrogen™) was used to perform the reverse transcription, following the manufacturer's instructions. PCR amplification was performed using primers for each gene *DEFB4A* (*sense* – ATGAGGGTCTTGTATCTCCT, *antisense* – TCATGGCTTTTTGCAGCATT), *DEFB103A* (*sense* – TCATGGCTTTTTGCAGCATT, *antisense* – TTATTTCTTTCTTCGGCAGC) and *HPRT1* (encoding **HPRT** (hypoxanthine phosphoribosyltransferase)) (sense – ATCACAT TGTAGCCCTCTGTGTGCTCAAGG, antisense – GTCTGGAATTTCAAATCCAACAAA GTCTGGC).

Ethics statement

All procedures involving animal subjects were approved by the Institutional Animal Care and Use Committee and Ethical Committee at our institution (08/2012/CEFCM). All *in vivo* studies involving rats were carried according or exceeding the recommendations in the Guide for Proper Conduct of Animal Experiments and Related Activities in Academic Research and Technology.[31]

Animals

One hundred and two male adult Wistar rats weighing 250 to 350 grams were used. All the animals were housed under standard environmental conditions and given nothing by mouth six hours before surgical procedures. No antibiotic prophylaxis was given.

Rats were anesthetized with a mixture of ketamine (5 mg/kg) and diazepam (0.25 mg/kg) given intraperitoneally. The depth of anesthesia was evaluated by toe pinch and by observance of respiration rate throughout the entire procedure.[32-35] Supplementary doses of the anesthetic mixture were provided throughout the surgical procedures as needed.[36] An ophthalmic gel was applied over the anterior surface of the eyes to avoid corneal abrasion. The hair over the ventral surface of the abdomen was removed with a depilatory cream (Veet®). After hair removal, the depilatory cream was cleaned from the abdomen with warm saline. After shaving the abdomen and placing the animals on the operation table, body temperature was recorded with a rectal thermometer and the rats were kept on a heating pad (Skaldo, Ardes ™), in order to maintain a constant body temperature. A substantial amount of an alcoholic solution (Cutasept F®, Hartmann ™) was sprayed over the operative site. The product was left in the operative site for at least 15 seconds. Application was repeated 3 times. After the last application, the disinfectant solution was left in contact with the operating field for at least 2 min before proceeding with the surgery. All surgical procedures were performed in strict sterility conditions.

Surgical Model

Succinctly, a variant of the rat abdominal arterialized venous flap was used as model of ischemic flap (**Fig. 4**).[37, 38] This flap was transduced with an *ex vivo* infusion of a 100 µl solution containing approximately $4.7x10^9$ plaque-forming-units of recombinant lentiviruses coding for Green Fluorescent Protein (GFP) or BD-2 and/or BD-3.[39, 40] This model was combined with an adapted version of the rat foreign body infection model (**Fig. 3**).[41]

In all animals, under a surgical operating microscope, a 5 cm long and 3 cm wide fasciocutaneous flap was raised on the left side of the rat's abdomen.[38] Cranially, the flap was connected exclusively to the skeletonized lateral thoracic vein. This vein was temporarily clamped. Caudally, the superficial caudal epigastric artery was ligated with an 8/0 Nylon suture. The superficial caudal epigastric vein (SCEV) was cannulated with a 27-gauge ophthalmic cannula (BD Bioscience™). It was then perfused with a 100-µl solution whose composition varied amongst the experimental groups (**Figs. 3** and **4**). In all cases the solution contained 5 µg of recombinant rat Vascular Endothelial Growth Factor A (VEGF; Immunotools®) in DMEM, in order to increase transduction efficiency. [39] The composition of the solution injected in the flap's venous system was as follows: **NaCl Group** (VEGF); **PA Group** (VEGF); **GFP Group** (VEGF + GFP coding lentivirus); **BD-2 Group** (VEGF + BD-2 coding lentivirus); **BD-3 Group** (VEGF + BD-3 coding lentivirus); **BD-2 + BD-3 Group** (VEGF + BD-2 + BD-3 coding lentivirus) (**Fig. 3**). After injection, SCEV was immediately clamped for 90 min, in order to leave the injected solution in contact with the flap's vascular system.[39]

Subsequently, vascular clamps were removed and the SCEV was arterialized by connecting it to the femoral artery. In order to achieve this, the SCEV was cut from the femoral vein with a 1-mm long cuff of adjacent femoral vein tissue. The ostium in the femoral vein was closed with a continuous Nylon 11/0 suture. The same suture line was used to perform a side-to-end arteriovenous anastomosis between the SCEV and the ventral flank of the femoral artery through a 1-mm long ostium previously created in the latter vessel. Interrupted stitches were used for this anastomosis. The lateral thoracic vein was preserved cranially to ensure outflow from this arterialized venous flap.[38]

Two 1-cm segments of sterile 14-gauge silicone catheters (Mediplus™) were placed in the central aspect of the surgical wound. Surgical wounds were closed with a running 5/0 Nylon suture. Just before closing the lateral aspect of the skin wound, 1-ml of a 0.9% sodium chloride solution was instilled under the flap into the vicinity of the silicone catheter segments using an 18-gauge silicone catheter (Mediplus™). In all groups except the NaCl group, the latter solution contained 10^5 CFU of *P. aeruginosa*. The running suture was closed immediately after injection, in order to avoid any spilling to the area adjacent to the flap (**Fig. 4**).

No anticoagulants were administered pre, intra or postoperatively. All surgical procedures were performed by the same surgeon (D.C.), in order to minimize inter-surgeon variability.

Thermography

One hour after flap reperfusion, the rat abdomen was submitted to infrared thermography with a FLIR® E6 camera placed 25 cm above the abdomen. This evaluation intended to confirm the flap's relative ischemia compared to the contralateral side. Rats were placed on their backs for 10 min prior to this evaluation. Thermographic measurements were made at a constant room temperature (22 ºC) and humidity (50%).[38, 42]

Post-operative care and assessment

After thermographic evaluation was completed, a transparent Tegaderm™ (3M Deustschland GmbH®) transparent film dressing was applied over the flap and adjacent skin. Following surgery, rats were kept in solitary rat cages and offered rat chow and water *ad libitum*.

Rats were assessed daily by the same blinded researcher, in order to reduce inter observer bias and variability.[43] The following parameters were evaluated: animal wellbeing, flap viability, and presence of complications.

On the third and seventh days postoperatively, rats were anesthetized as described above. Objective measurement of flap survival was performed on these days based on digital photographs, which were later analyzed by a blinded observer using the free Image J® software.[36, 44] Flap survival was expressed as a percentage of the total flap surface area.

After disinfecting the rat's abdomen as described above, on the third postoperative day, a sample measuring approximately 1 cm in length and 0.5 cm in width was surgically excised from the most lateral aspect of the caudal third of the viable flap. These specimens were subjected to histological analysis, as well as bacterial counts by both culture and real-time PCR. The integumentary defect created by the biopsy was submitted to hemostasis and closure with a continuous 5/0 Nylon suture taking part of the integumentary redundancy in this region. A transparent Tegaderm™ (3M Deustschland GmbH®) transparent film dressing was again applied over the flap and adjacent skin.

On the seventh day after the first surgery, the lateral aspect of the flap was elevated, thus exposing the underlying catheter segments. These were then carefully removed, taking care not to touch the rat's skin and immediately immersed in the fixative solution.

The flap was then removed for histological analysis, as well as bacterial counts by culture and real-time PCR.

Evaluation of flap transduction by fluorescence microscopy

Four rats were submitted to the procedures described above for the GFP group with the exception that no bacteria were instilled. Seven days after the surgery, the skin flap was harvested, fresh-frozen and observed under the fluorescence microscope. Two rats were submitted to an analogous the procedure, but no lentiviruses were used to transduce the flaps in these animals.

Quantification of BD-2 and BD-3 expression by quantitative real-time PCR

Total RNA from flap biopsies weighing (45- 50 mg) collected on the 7th day postoperatively was extracted using the GenElute^{TM} Mammalian Total RNA Miniprep Kit (Sigma-Aldrich). The RNase-Free DNase Set (Qiagen®) was used to eliminate genomic DNA, according to the manufacturer's instructions. RNA concentrations were measured and only samples with A260/A280 ratios between 1.8 and 2.1 were considered further. Five hundred nanograms of total RNA was reverse transcribed with random primers using the High Capacity cDNA Reverse Transcription Kit (Applied Biosystems^{TM}), according to the manufacturer's instructions. Real-time PCR was performed in a Rotor-Gene 6000 (Corbett Life Science) using TaqMan® Fast Universal PCR Master Mix (Applied Biosystems^{TM}). The assay IDs were provided by the manufacturer, being the following: *β-actin* (4352931E); *DEFB4B* (Hs00175474_m1) and *DEFB103A* (Hs00218678_m1) (Applied Biosystems^{TM}). Each reaction was performed in triplicate. Thermal cycling conditions were 95 for 20 seconds followed by 55 cycles of 95 for 3 seconds and 60 for 30 seconds. The gene expression was normalized to the endogenous control β-actin, which is known to have significant basal expression.[45] Gene relative expression was calculated using the $2^{-\Delta CT}\times 1000$ formula, an adaptation of the $2^{-\Delta\Delta Ct}$ method described by Livak and Schmittgen.[46-48] This allows us to calculate the number of mRNA molecules of the gene of interest per 1000 molecules of the endogenous control (β-actin).

Viable bacterial cell counts

Biopsies were collected in sterility and cut in small pieces (between 0.05 and 0.10 mm of maximum diameter). Next, they were macerated in 0.9 %(w/v) NaCl (Merck®) at 100 mg/mL concentration for 5 min with a Pellet pestle (Sigma-Aldrich®). Serial dilutions were performed from the supernatant in 0.9 %(w/v) NaCl (between 10^{-1} and 10^{-5}) and were spread on LB dishes in duplicated. The dishes were incubated at 37 °C during 14 h followed by quantification of CFUs. The CFUs counted were verified by running a series of tests, namely, Gram stain (Merck®); MacConkey growth (Carl Roth®) and *Oxidase* test (BioMérieux®) according to the manufacturers' instructions.

***P. aeruginosa* quantification by real-time PCR**

Biopsies were collected in sterility, were immediately immersed in RNAlater® (Sigma-Aldrich®), and incubated overnight at 4 °C. On the following day, the biopsies were cut in small pieces (between 0.05 and 0.10 mm) and stored at -80 °C.

Forty-five to 50 mg of excised tissue was used to extract genomic DNA by NZY Tissue **gDNA** (genomic deoxyribonucleic acid) Isolation Kit (Nzytech®) according to the manufacturer's instructions.

Universal primers were used for 16S **rDNA** (ribosomal deoxyribonucleic acid): *forward* 5'-GTGSTGCAYGGYTGTCGTCA and *reverse* 5´-ACGTCRTCCMCACCTTCCTC [49], to quantify *P. aeruginosa*. The real-time PCR was performed using Applied Biosystems 7500 real-time PCR System (Thermo Fisher Scientific®). The reaction mixture (10 µl) contained 2x

SYBR Green PCR Master Mix (Thermo Fisher Scientific®), 0.1 nmol/µl of *forward* and *reverse* primers each and 5 ng/µl of *P. aeruginosa* gDNA.

Thermo-cycling program was 40 cycles of 95 °C for 20 s, 60 °C for 30 s and 72 °C for 40 s with an initial cycle at 50 °C for 2 min and 95 °C for 10 min. Next, a dissociation curve was performed at 95°C for 15 s and a range between 60 to 95 °C.

Histological processing

Flap biopsies were collected from the lateral aspect of the surgical flap of the rat 3 and 7 days postoperatively, as described above. Specimens were incubated in 10% (v/v) Formalin. After paraffinization (VWR®), specimens were cut on the microtome (Leica®) as 3 µm thick slices. These slices were stained with Hematoxylin-Eosin (**HE**) and Masson's Trichrome (**MT**), according to the manufacturers' indications.[50, 51] For immunohistochemical staining with anti-BD-2 and -BD-3, slices were obtained in the same manner, although for this purpose slices were 4 µm thick.

Immunohistochemistry processing for BD-2 and BD-3

Imunohistochemistry was performed by BenchMark ULTRA - Automated IHC/ISH slide staining system (Ventana®, Roche®). Summarily, the slides were heated at 80 °C for 15 min, deparaffinized with EZ prep (Ventana®, Roche®) for 8 min. Antigen retrieval was performed with a ULTRA CC2 (Ventana®, Roche®) at 95 °C for 8 min (for BD2 staining) and ULTRA CC1 (Ventana®, Roche®) at 95 °C for 20 min (for BD3 staining). Endogenous peroxidase was blocked with 3% (v/v) Hydrogen Peroxide (UltraView Universal DAB

Inhibitor, Ventana®, Roche®) for 4 min. The following primary monoclonal antibodies were used at 37 °C: anti-BD-2 (β-defensin 4 [L13-10-D1]: sc-59496; Santa Cruz Biotechnology, inc.®) [1:50] for 40 min; and anti-BD-3 (BD-3 human (SRP4524), Sigma Aldrich®) [1:2], for 32 min. Amplification was accomplished with the UltraView Universal HRP Multimer (Ventana®, Roche®) for 8 min. Revelation was performed with the UltraView Universal DAB Chromogen and the UntraView Universal DAB H_2O_2 for 8 min (Ventana®, Roche®) followed by intensification with the UltraView Universal DAB Copper (Ventana®, Roche®) for 4 min. The nuclear contrast was performed with Hematoxylin and Bluing (Ventana®, Roche®) for 4 min each.

Finally, the slides were washed in water and detergent, dehydrated with increasing concentrations of Ethanol (75, 90 and 99% (v/v)) for 1 min each, cleared in Xylene (VWR®) and mounted with Synthetic Mounting Medium (Quick-D M-Klinipath®).

Catheter processing for SEM

The catheters were introduced in mounting pins to incubate at 4 °C, overnight in a solution of 2 %(v/v) Glutaraldehyde (Sigma-Aldrich®) in 0.05 M Sodium Phosphate Buffer (pH = 7.4) (Merck®) to fixate the specimens. Catheters were washed 3 times in 0.15 M Sodium Phosphate Buffer (pH = 7.4). Post fixation was performed in a solution of 1 %(v/v) Osmium Tetroxide (Sigma®) in 0.12 M sodium cacodylate Buffer (pH = 7.4) (Merck®) during 2 h at room temperature. The catheters were rinsed in deionized water and were dehydrated in increasing concentrations of ethanol for analysis (10, 25, 40, 60, 95, 100 %) (Merck®) for 20 min for each incubation. Next, they were maintained in Acetone Pro-Analise

(Merck®) overnight. Critical Point (Polaron® E3100) was executed within a range of pressure and temperature of 78-80 Bar and 28-30 °C, respectively. Three purges using CO_2 (Gains®) were performed with an interval of 1 h between each. SPI Flash-Dry™ Silver Paint (SPI Supplies®) was used to mount the catheters to the stubs (Agar Scientific®). Catheters were metalized (Polaron® SC502) with Gold in the presence of Argon (Airliquide®) at a pressure between 1 and 4 Pa and a current of 0.015 A. Four metallization cycles were performed. The specimens were examined with two scanning electron microscopes: a JEOL JSM-5410, with acceleration voltage of 0.015-0.030 V, for quantification purposes, and a JEOL JSM-7001F, with acceleration voltage of 0.015-0.030 V, for obtaining high quality images of selected specimens.

Histological and immunohistochemistry analysis

Each sample was independently reviewed by two blinded researchers. HE and MT staining were used to evaluate epidermolysis and necrosis. BD-2 and BD-3 expression was semi quantitatively assessed by a staining intensity score (0, negative; 1, weak; 2, moderate; 3, strong) in the skin and perivascular regions.[52] When differences were found, specimens were again reviewed by the two researchers until a consensus was reached.

SEM analysis of catheters' surface

Bacteria, leucocytes and phagocytes were identified on the surface of catheters as described by van Gennip *et al*, Polliack and Saint-Guillain *et al*, respectively.[53-55] Only catheters whose rats had survived the entire experiment (7 days) were used for counting

purposes. Average bacterial density on the surface of the catheter was based on manual counting in 20 random SEM fields at a 7500X magnification on each of the two catheter segments in each rat by a blinded researcher. When only one catheter segment could be retrieved, average bacterial density was done analogously using 40 random SEM fields at 7500X magnification. When more than 300 bacteria were found in a given SEM field, bacteria were considered uncountable. Using the same methodology, the disposition of bacteria in each SEM field was recorded as planktonic, biofilm or mixed.

Average leucocyte density on the surface of the catheter was performed in a similar fashion, with the exception that SEM fields used were obtained at 750X magnification. The average phagocyte density on the surface of catheters was determined in the same way. Phagocytes were defined as those leucocytes that showed evidence of pseudopods in direct contact with bacteria and/or biofilm.

Bacteria and leucocyte were included in counts only if the top upper edge of the cell was in the SEM field.[56, 57] SEM fields with clots or largely occupied by biofilms were discarded, as bacteria were not accessible to counting using the methodology employed.

Statistical analysis

Qualitative variables were expressed as percentages. Quantitative variables were expressed as means ± standard deviation. The SPSS 21.0 ® software was used for descriptive and inferential statistical analysis. The Kolmogorov-Smirnov test was used to assess if variables were normally distributed. ANOVA and t-Student test were used to compare averages in normally distributed data. Kruskal-Wallis and Mann-Whitney tests were used to

compare means in non-normally distributed data. Wilcoxon rank-sum test was used to compare ordinal data. Proportions were analyzed with the Chi-square test or Fisher's exact test. Association between numerical variables was assessed using Pearson's correlation coefficient. Relationship between ordinal variables was evaluated with resort to Spearman Rank Correlation Coefficient. Differences in survival in the different experimental groups was tested with the log rank test. A two-tailed $p<0.05$ was considered to be statistically significant.

RESULTS

Inoculation of arterialized venous flaps results in a model of persistent ischemic flap infection

In order to obtain a rat model of ischemia and *P. aeruginosa* infection in the presence of a foreign body, we followed the steps summarized in **Figure 4**. Ischemia was obtained by using a variant of the rat abdominal arterialized venous flap, established by our group.[38] Infection was obtained by inoculating *P. aeruginosa* and two 1-cm segments of sterile 14-gauge silicone catheters were used to simulate foreign body.

Serial *P. aeruginosa* concentrations (10^3; 10^4; 10^5; 10^6 and 10^7 CFU/ml) were tested in the mentioned model. A target concentration of 10^5 CFU/ml was selected, since it caused no rat mortality within 7 days and systematically resulted in clinically significant infection and partial flap necrosis. Higher concentrations led to complete or nearly complete flap necrosis (10^6 CFU/ml; n=2) and animal's death (10^7 CFU/ml; n=3), whereas lower concentrations (10^3 and 10^4 CFU/ml; n=3 for each concentration) did not produce identifiable infection.

By thermography analysis, one hour after surgery, the average difference between the flap surface's temperature and the temperature of the surface of the homologous contralateral region was 2.34 ± 1.06 ºC ($p<0.001$). **Fig. 5** shows the typical thermographic appearance of the flap one hour after surgery, illustrating the lower temperature of the flap compared to the contralateral side.

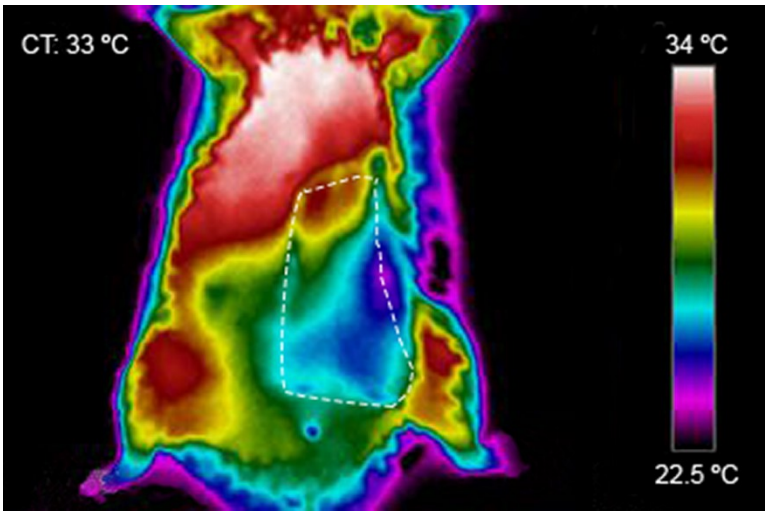

Figure 5 - Representative direct infrared thermography image of the ventrolateral aspect of the abdomen of the rat 1 hour postoperatively. Flap boundaries are highlighted with the interrupted lines. This image illustrates that the temperature of the flap's surface is inferior to the contralateral side, due to the flap's relative ischemia, which results from its unconventional pattern of perfusion.

CT, rat's core temperature.

Overall our data shows that a model of ischemia, infection and foreign body can be successfully obtained by adapting our previous established model of the rat abdominal arterialized venous flap, following inoculation with *P. aeruginosa* and introduction of silicone catheters.

BD-2 and BD-3 increase flap survival rates

We then assessed whether overexpression of BDs in the flaps could improve survival and reduce infection. For this purpose, we performed a set of experiments in rats that included flaps' transduction with lentiviruses containing the BD-2 and BD-3 genes, as represented in **Figures 3** and **4**.

Of the 102 operated rats, 19 died in the immediate postoperative period (<24 hours), and were not included in the study. The following number of rats was included in each experimental group: 12 in the NaCl control group; 13 in the *P. aeruginosa* group; 14 in the GFP group; 15 in the BD-2 transduced group; 15 in the BD-3 transduced group, and 14 in the BD-2 + BD-3 transduced group. There were no statistically significant differences between the different experimental groups regarding survival throughout the experiment. To certify the inoculation dose of *P. aeruginosa*, the effective average bacterial inoculation dose under the flap was determined by bacterial growth and found to be (9.735 ± 0.120) X 10^4 CFU, which was similar to the initial inoculation concentration of 10^5 CFU/ml. There were no statistically significant differences between the initial bacterial inoculum in the different experimental groups.

To confirm transduction efficiency, seven days after surgery, flaps from rats transduced with GFP were analyzed by fluorescence microscopy. As shown in **Figure 6**, flaps from GFP lentivirus-transduced rats showed GFP expression. The expression was greater in endothelia and in the epidermis (**Fig. 6**). Quantification of BD-2 mRNA expression by real-time PCR seven days after transduction, revealed 591.12x10^6% ± 894.00x10^6% relative expression of BD-2 in transduced flaps versus 3.53x10^6% ± 11.35x10^6% relative expression in non-transduced flaps (p=0.014) (**Fig. 7**). Analogously, the relative BD-3 expression determined in a similar fashion was 253.09x10^6% ± 354.61x10^6% in transduced flaps and 25.94x10^6% ± 87.44x10^6% for non-transduced flaps (p=0.018) (**Fig. 7**). Using the same methodology, no statistically significant differences were found in the relative expression

of BD-2 in the BD-2 and in the BD-2 + BD-3 groups, nor in the relative expression of BD-3 in the BD-3 and in the BD-2 + BD-3 groups.

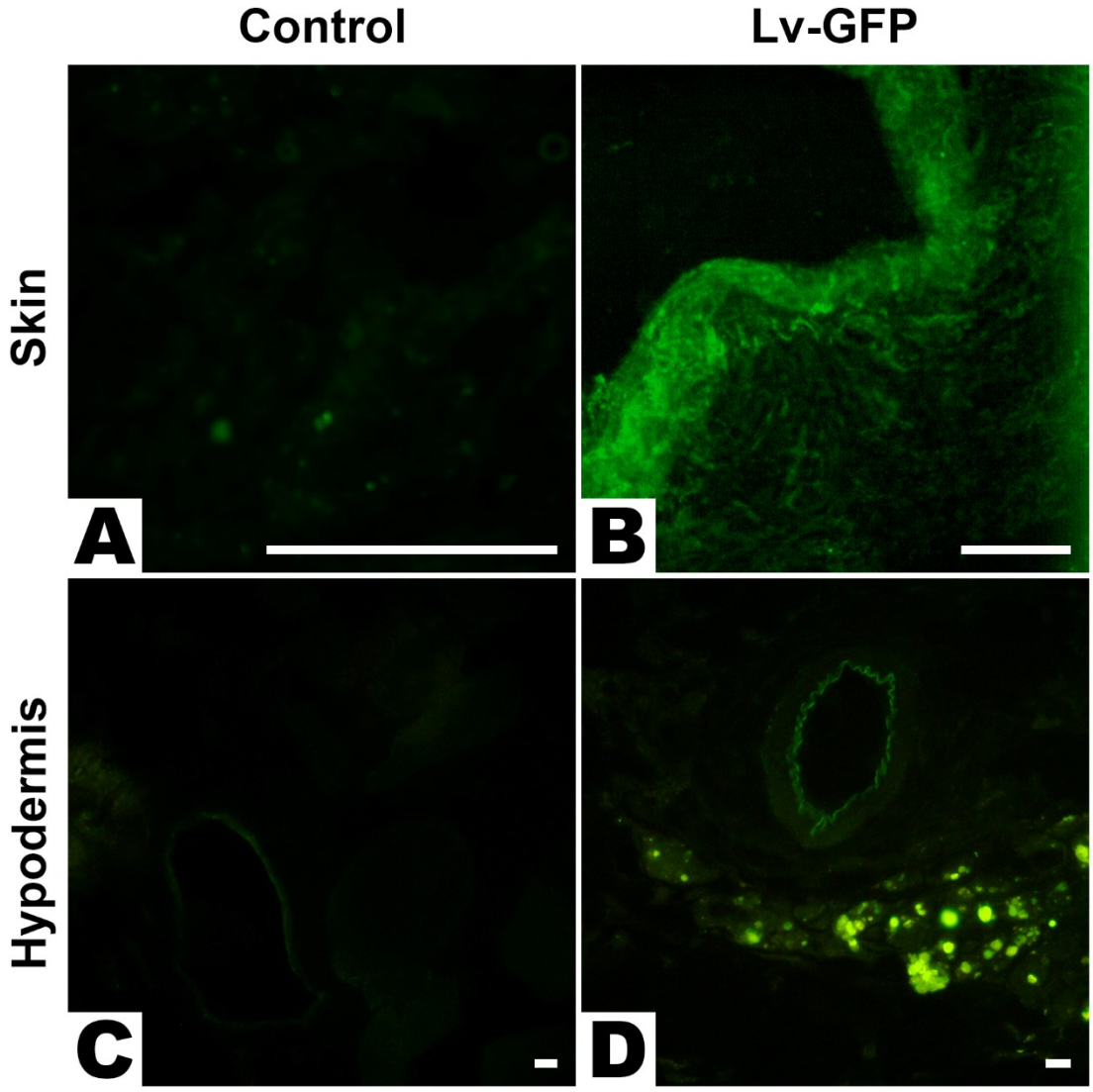

Figure 6 - Typical fluorescence image photographs of the skin and hypodermis of the flap of a rat transduced with a Green Fluorescent Protein coding lentivirus (**LV-GFP**) and those of the flap of a non-transduced rat (**Control**) seven days after surgery. These photographs demonstrate transduction of flaps by the virus. Calibration bar = 100 µm

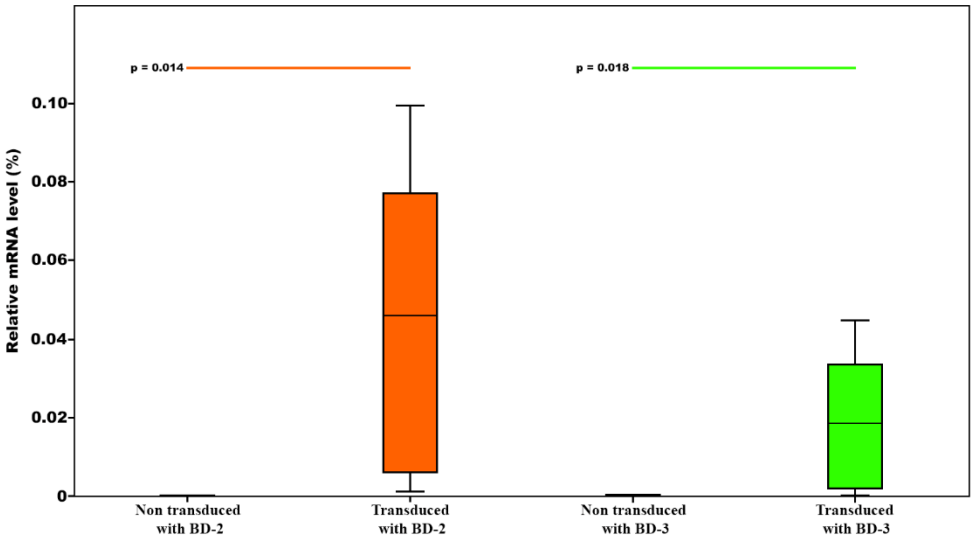

Figure 7 - Analysis of the BD-2 and BD-3 mRNA (messenger ribonucleic acid) **expression in rat flaps.** Box plots represent the relative mRNA expression level of human β-defensins 2 and 3 (**BD-2** and **3**) analyzed in transduced flaps compared to non-transduced flaps on the seventh post-operative day relatively to the expression of the β-actin in these flaps using real-time PCR. The relative mRNA levels of each gene are expressed as the percentage of the β-actin mRNA levels.

Horizontal lines in the upper portion of the figure indicate statistically significant differences between groups ($p<0.05$).

Figure 8 summarizes the main clinical, optical microscopy and SEM findings in the different experimental groups. On the third postoperative day, the average area of necrotic flap was higher in the *P. aeruginosa* (61.98% ± 18.52%) and GFP (67.39% ± 20.67%) groups than in the groups BD-2 (37.16% ± 9.04%), BD3 (17.79% ± 5.48%) and BD-2 + BD-3 (35.09% ± 9.43%) ($p\leq0.001$). The necrotic area was the smallest in the NaCl (11.07% ± 5.72%) and in the BD-3 groups. There was no statistically significant difference between these two groups ($p=0.836$) (**Fig. 9**).

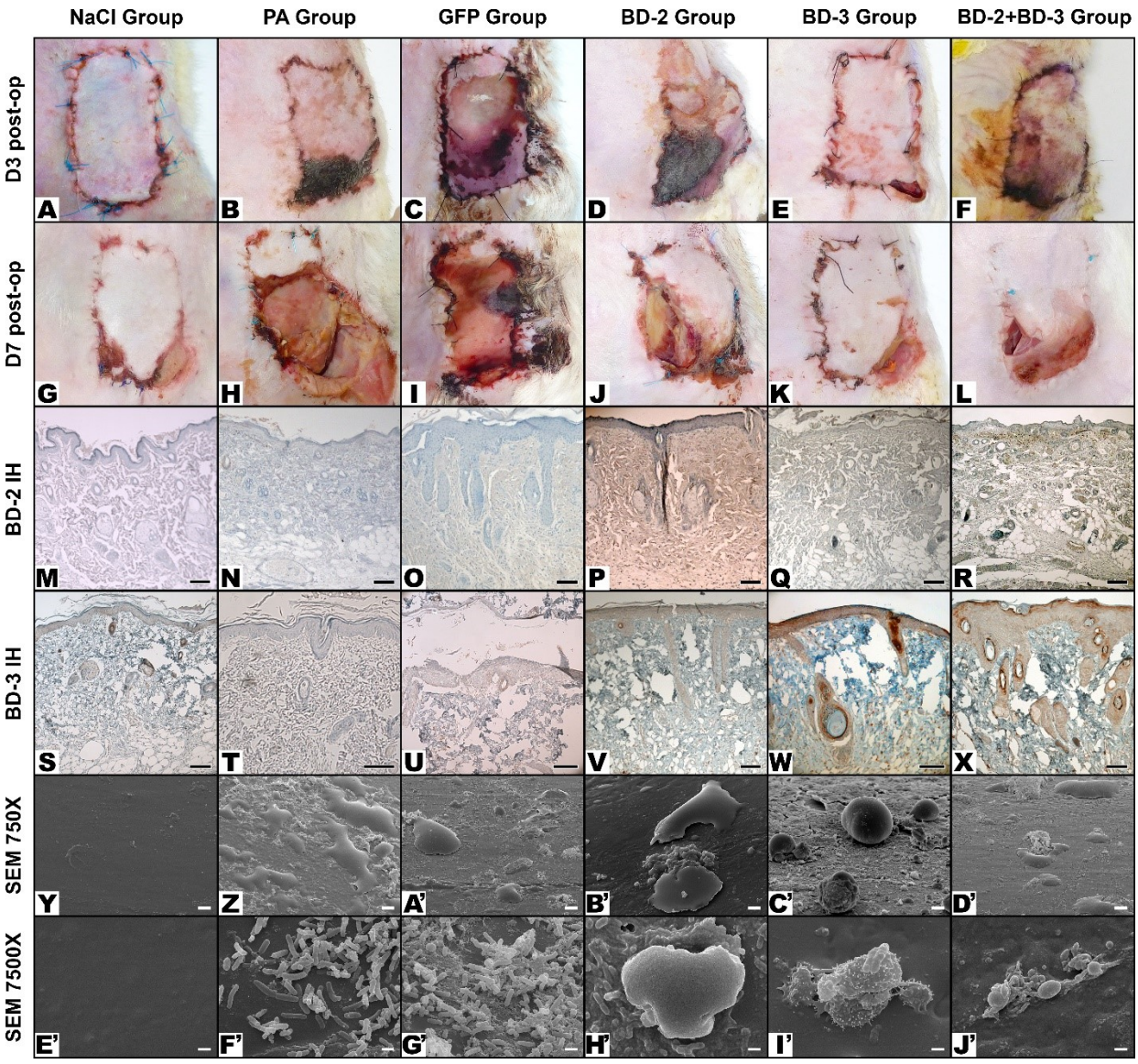

Figure 8 - Typical macroscopic and microscopic features of flaps in the different experimental groups. Macroscopic images were taken on the third day post-operatively (D3 Post-op), and seven days post-operatively (D7 Post-op). Microscopic images were taken with immunohistochemical staining with anti-BD-2 (**BD-2 IH**), or anti-BD-3 (**BD-3 IH**) antibodies of flap biopsies performed on the seventh day after the surgery. Scanning electron microscopy (**SEM**) images were taken at 750X or 7500X amplification,

Calibration bar = 100 µm (M, N, P-T, V-X); 25 µm (O, U); 10 µm (Y-D'); 1 µm (E' - J')

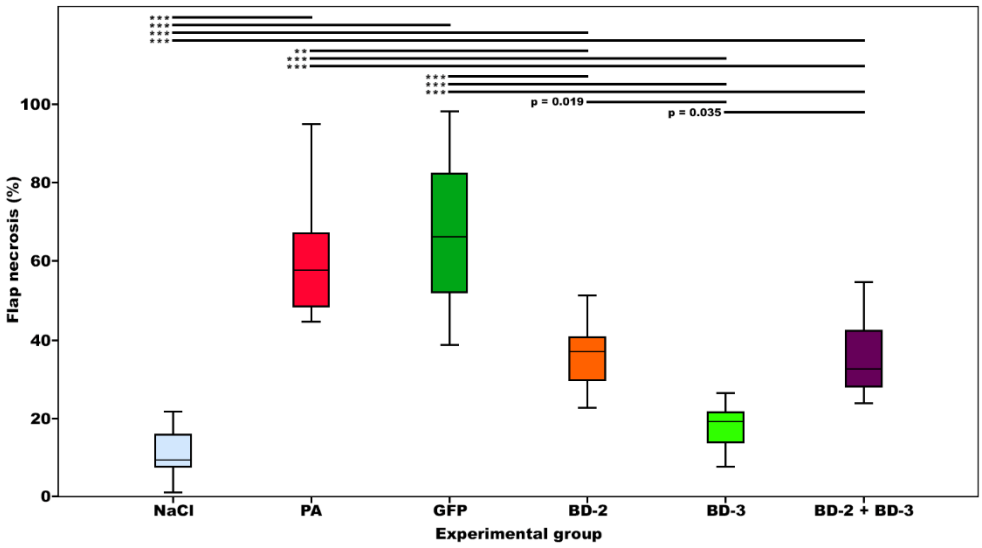

Figure 9 - Bar graphs representing the skin flap necrosis rate on the third postoperative day in the different experimental groups. Horizontal lines in the upper portion of the figure indicate statistically significant differences between groups ($p<0.05$).

Error bars indicate 95% confidence intervals.

**, $p<0.01$. ***, $p<0.001$

On the seventh postoperative day, lower average flap necrosis rates were also found in the NaCl (20.88% ± 9.94%), BD-2 (42.81% ± 13.56%), BD-3 (25.39% ± 8.50%) and BD-2 + BD-3 (49.97% ± 11.37%) groups than in the *P. aeruginosa* (74.30% ± 16.43%) and GFP (82.53% ± 19.73%) groups ($p<0.001$). Although slightly higher, the average necrosis rates of groups BD-2 and BD3 was not significantly different from that of the NaCl group. However, the average necrosis rate of BD-2 + BD-3 was higher than that of the NaCl group ($p=0.049$) (**Fig. 10**).

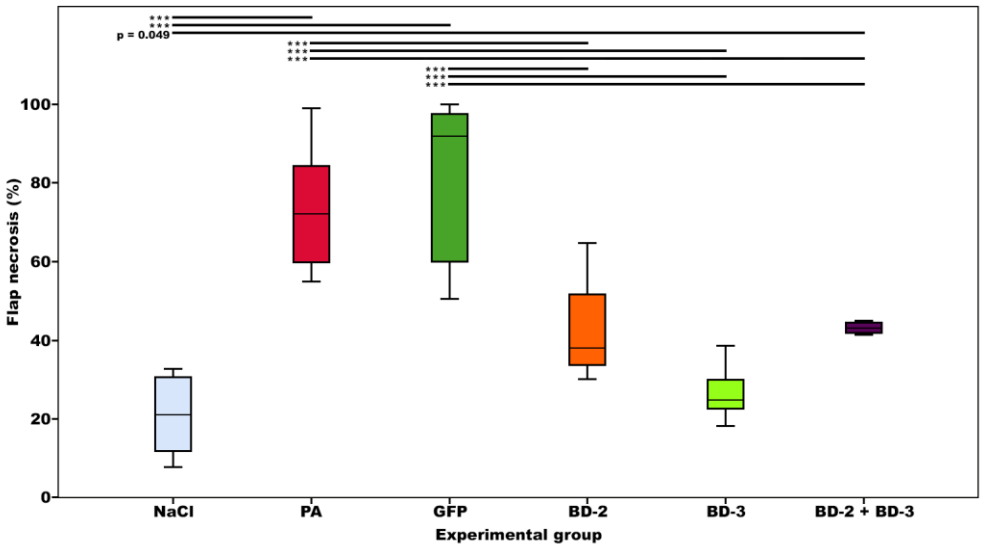

Figure 10 - Bar graphs representing the skin flap necrosis rate on the seventh postoperative day in the different experimental groups. Horizontal lines in the upper portion of the figure indicate statistically significant differences between groups ($p<0.05$).

Error bars indicate 95% confidence intervals.

***, $p<0.001$

In summary, our results demonstrate that transduction of flaps with BD-2 or BD-3 improves infected flap survival at day 7 following surgery, by decreasing tissue necrosis.

Evidence of flap ischemia and defensin expression by histology and immunohistochemistry

Histological analysis of the flaps revealed signs of venous congestion, marked edema, epidermolysis and areas of necrosis in all experimental groups. However, these changes were more pronounced in the *P. aeruginosa* and GFP groups (**Fig. 8**). Immunohistochemistry confirmed expression of BD-2 and BD-3 in the transduced rats (**Fig. 8**). BD-2 expression occurred mainly in endothelia and perivascular tissues, although it was also observed in fibroblasts and in the epidermis. BD-3 expression was strongest in the epidermis and skin appendages (**Fig. 8**). Using the mentioned semi-quantitative score for immunohistochemistry staining [52], BD-2 expression was as follows: 0.25 ± 0.45 for the NaCl group; 0.23 ± 0.44 for the PA group; 0.36 ± 0.50 for the GFP group; 2.07 ± 0.59 for the BD-2 group; 0.13 ± 0.35 for the BD-3 group; 1.64 ± 0.50 for the BD2 + BD-3 group. Proceeding in a similar way, BD-3 expression in the different experimental groups was the following: 0.67 ± 0.49 for the NaCl group; 0.69 ± 0.48 for the PA group; 0.79 ± 0.70 for the GFP group; 0.27 ± 0.59 for the BD-2 group; 2.80 ± 0.41 for the BD-3 group; 2.50 ± 0.52 for the BD2 + BD-3 group. BD-3 expression was stronger than BD-2 expression. However, this difference did not reach statistically significance.

BD-2 and BD-3 decrease bacterial numbers and biofilms on the surface of foreign bodies

We then assessed the number of bacteria on the surface of the foreign body in the different experimental groups. At the end of the experiment, it was possible to retrieve 56

catheters that were distributed as follows: 8 in the NaCl group, 6 in the PA group, 12 in the GFP group, 9 in the BD-2 group, 11 in the BD-3 group, and 10 in the BD-2 + BD-3 group.

In all rats, infection was confirmed by growth in *P. aeruginosa* MacConkey agar, Gram stain and positive oxidase reaction. **Table 1** summarizes bacterial counts determined by different methods on the 7^{th} day postoperatively in the different experimental groups.

Experimental Group	Viable bacteria cultured from skin flap biopsy (CFU/mg)	Real-time PCR from skin flap biopsy (ng/µl)	Bacteria on the surface of the foreign body (n/SEM field)
NaCl	$2.42x10^{5} \pm 5.87x10^{5}$	$1.23x10^{-5} \pm 2.06x10^{-5}$	7.74 ± 8.18
PA	$6.98x10^{6} \pm 1.17x10^{7}$	$1.26x10^{-1} \pm 1.17x10^{7}$	71.70 ± 47.4
GFP	$9.46x10^{5} \pm 6.46x10^{5}$	$7.22x10^{0} \pm 1.36x10^{1}$	92.75 ± 35.9
BD-2	$8.06x10^{5} \pm 8.59x10^{5}$	$5.52x10^{-1} \pm 7.97x10^{-1}$	67.08 ± 42.4
BD-3	$2.51x10^{5} \pm 5.88x10^{5}$	$1.13x10^{-5} \pm 1.39x10^{-5}$	19.37 ± 16.3
BD-2 + BD-3	$3.55x10^{5} \pm 4.52x10^{5}$	$1.94x10^{-3} \pm 2.92x10^{-3}$	54.04 ± 41.6
Statistical analysis summary	No significant differences were found	No significant differences were found	NaCl < PA; p=0.013 NaCl < GFP; p<0.001 NaCl < BD-2; p=0.010 PA > BD-3; p=0.042 GFP > BD-3; p<0.001 BD-2 > BD-3; p=0.035

Table 1 - Average values of bacterial counts determined by different methods on the 7th day postoperatively in the different experimental groups.

For each rat, the average number of bacteria on the surface of catheters was based on manual counting bacterial cells on 20 SEM fields at 7500X magnification on each of the two catheter segments, or, when only one catheter segment could be retrieved, on counts performed on 40 SEM fields of that catheter segment. A scanning electron microscopes JEOL JSM-5410, with acceleration voltage of 0.015-0.030 V, was used for quantification purposes.

Values are expressed as average ± standard deviation.

CFU, colony forming units; **SEM**, Scanning electron microscopy

As shown in **Table 1**, significant differences were found in the number of bacteria on the surface of the foreign body (**Fig. 11**). The number of bacteria on the surface of catheters was lower in the NaCl, BD-3, and BD-2 + BD-3 groups. There were no statistically significant differences between these 3 groups. The BD-3 group presented a smaller number of bacteria on the surface of catheters than the *P. aeruginosa* ($p<0.042$), GFP ($p<0.001$) and BD-2 ($p=0.035$) groups.

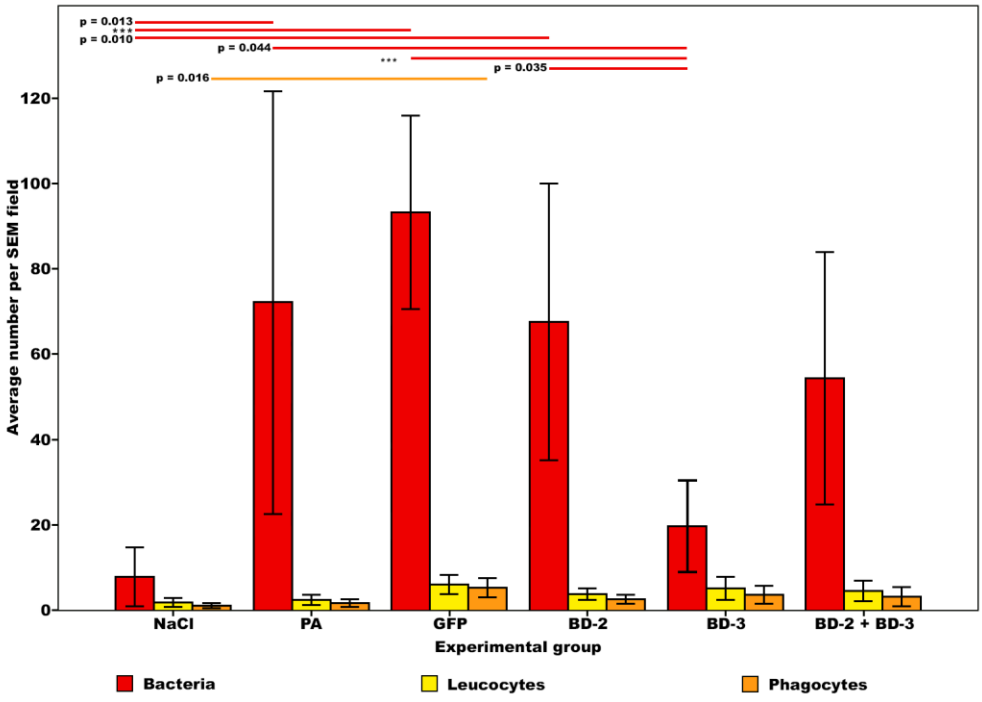

Figure 11 - Bar graphs representing the average number of bacteria, leucocytes and phagocytes on the surface of the catheter segments placed underneath the flaps per scanning electron microscopy (SEM) field. For each rat, the average number of bacteria on the surface of catheters was based on manual counting bacterial cells on 20 SEM fields at 7500X magnification on each of the two catheter segments, or, when only one catheter segment could be retrieved, on counts performed on 40 SEM fields of that catheter segment.

Average leucocyte and phagocyte density on the surface of the catheter was performed in a similar way, with the exception that SEM fields used were at obtained 750X magnification. A scanning electron microscope JEOL JSM-5410, with acceleration voltage of 0.015-0.030 V, was used for quantification purposes.

Horizontal lines in the upper portion of the figure indicate statistically significant differences between groups ($p<0.05$).

Error bars indicate 95% confidence intervals.

***, $p<0.001$

Concerning the distribution of bacteria on the surface of catheters (**Figs. 12** to **14**), the NaCl group presented the largest percentage of SEM fields without bacteria (42.81% ± 28.36%; $p<0.001$), followed by the BD-3 group (12.72% ± 17.87%), the BD-2 group (6.39% ± 12.32%), and the BD-2 + BD-3 group (2.75% ± 6.17%) (**Fig. 13**). The percentage of SEM fields without evidence of biofilm formation were also more numerous in the NaCl (99.06% ± 1.86%), BD-2 (74.44% ± 22.63%), BD-3 (88.59% ± 12.40%), and BD-2 + BD-3 (73.50% ± 17.72%) groups compared to the control groups *P. aeruginosa* (50.83% ± 23.06%) and GFP (39.38% ± 25.30%). This difference in biofilm presence of the former four groups compared to the GFP control group was statistically very significant ($p\leq0.002$) (**Fig. 13**).

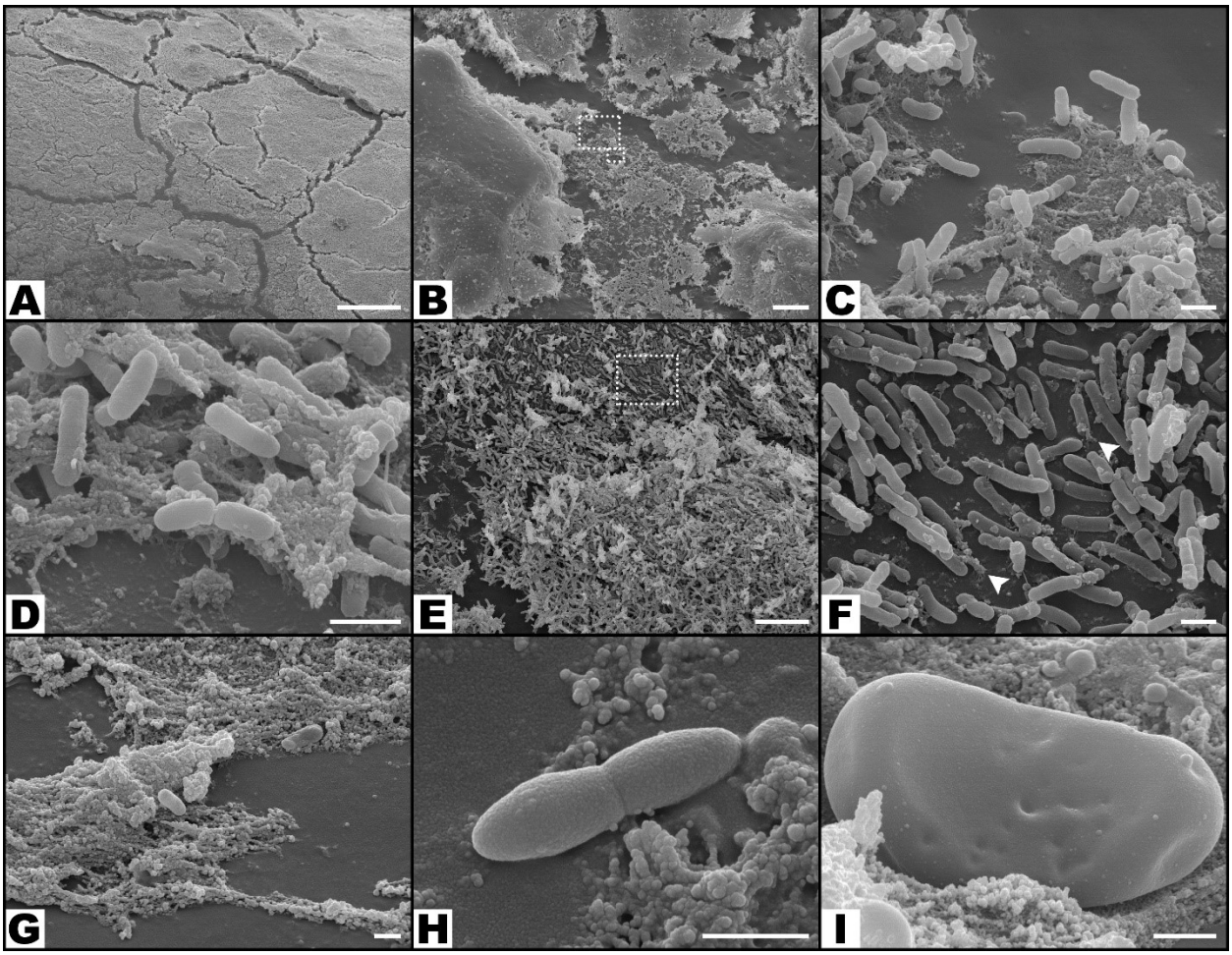

Figure 12 - Morphological features of bacteria on the surface of the foreign body in increasing magnifications by scanning electron microscopy. (A and B) Flat biofilm on the surface of a catheter segment. (C) Magnification of the large rectangular area in the center of (B) showing *Pseudomonas aeruginosa* and associated biofilm. (D) Magnification of the small rectangular area in the center of (B) showing *Pseudomonas aeruginosa* bacterial cells dividing in the biofilm. (E) Mushroom-shaped biofilm with uncountable bacterial cells. (F) Higher magnification view of the rectangular dotted area in the center of (E) showing bacterial division and adherence to the surface of the catheter (arrow heads). (G) Biofilm covering most of *P. aeruginosa* cells. (H) High magnification view of a *P. aeruginosa* cell dividing on the surface of the catheter. (I) High magnification image of a single *P. aeruginosa* cell on the surface of the biofilm showing the irregularities of the bacterial wall surface.

Calibration bar = 100 µm (A); 10 µm (B, E); 1 µm (C, D, F to I)

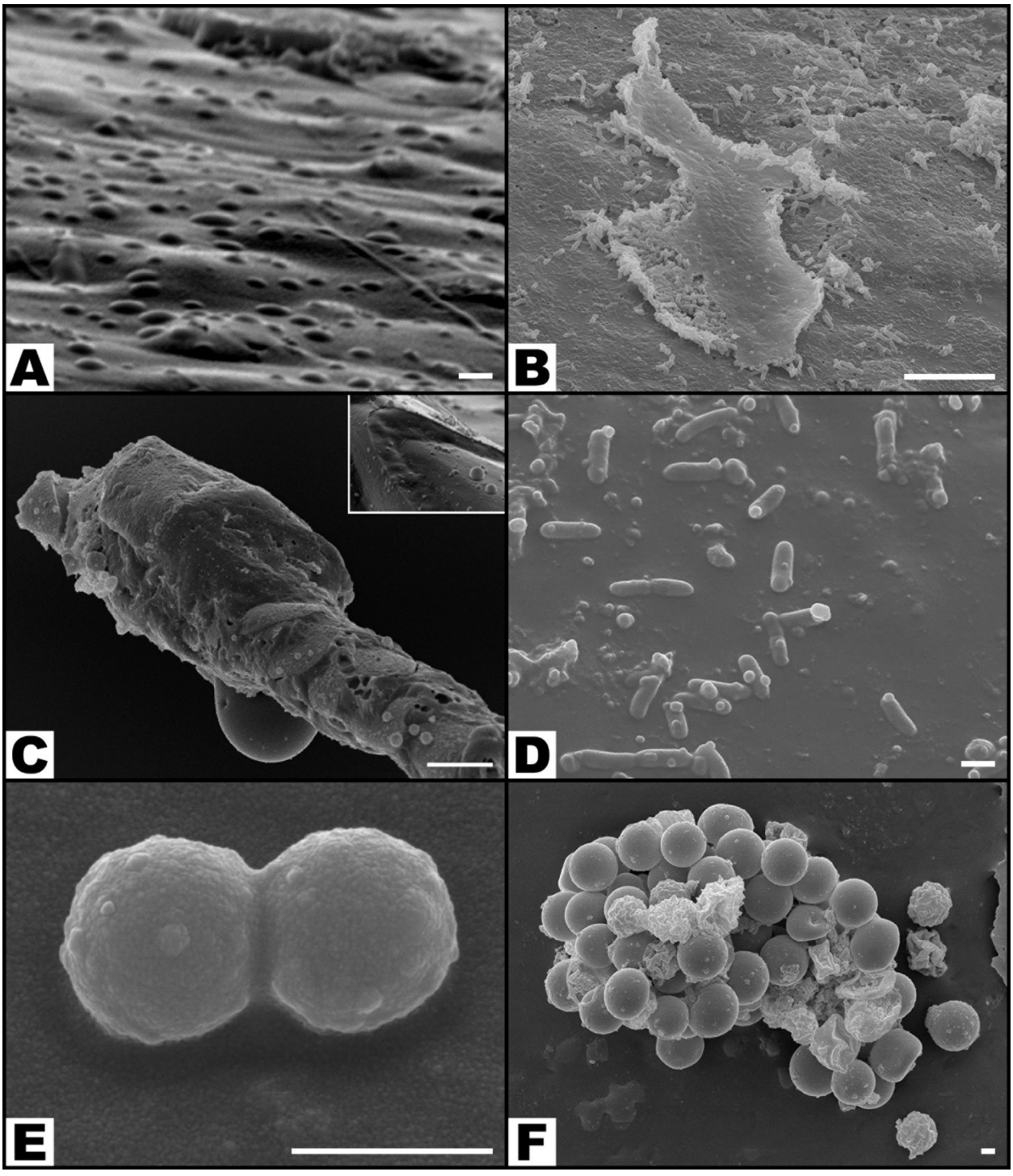

Figure 13 - Typical scanning electron microscopy images of the surface of catheters showing the variable distribution of bacteria. (A) *Pseudomonas aeruginosa* in the planktonic form; (B) *P. aeruginosa* are seen forming a large flat biofilm in the central portion of the image; (C) Small cocci (contamination) are seen on the

surface of an hair shaft that contaminated the surgical wound; the box represents an higher amplification view of the middle portion of the hair shaft (D) *P. aeruginosa* cells are seen scattered on the surface of the catheter; some of these cells are dividing; amongst *P. aeruginosa*, it is possible to observe cocci; (E) Diplococcus; (F) Staphylococcus.

Calibration bar = 1 µm (A, D, E, F); 10 µm (B, C)

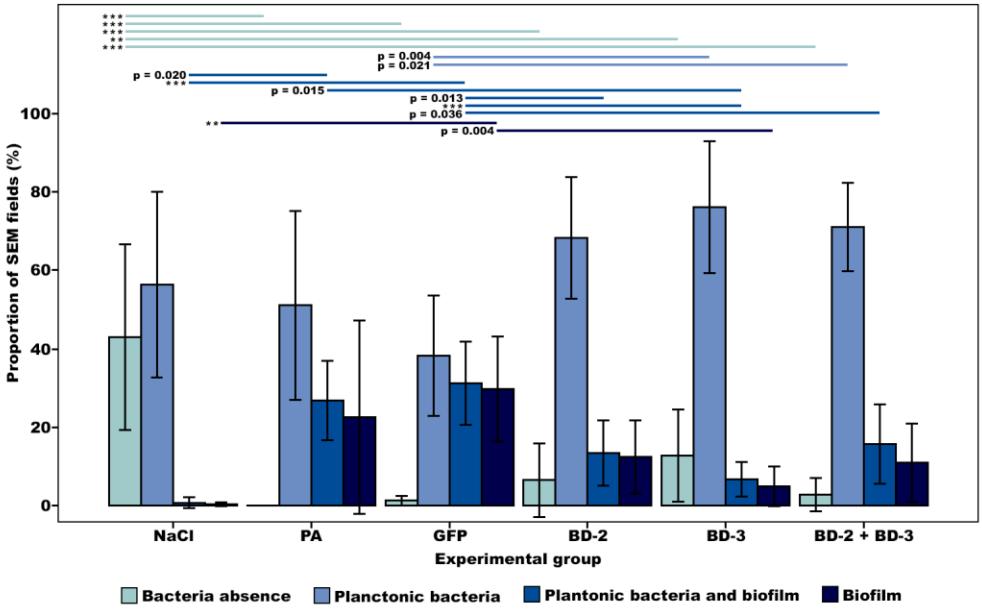

Figure 14 - Bar graphs representing the proportion of scanning electron microscopy (SEM) fields in the different experimental groups with no bacteria, with planktonic bacteria, with both planktonic bacteria and biofilm, and only with biofilm. For each rat, observations were made on 20 random SEM fields at 7500X magnification on each of the two catheter segments, or, when only one catheter segment could be retrieved, on 40 random SEM fields of that catheter segment.

Horizontal lines in the upper portion of the figure indicate statistically significant differences between groups ($p<0.05$).

Error bars indicate 95% confidence intervals.

**, $p<0.01$

***, $p<0.001$

Numerous leucocytes could be observed on the surface of catheters in all groups. (**Figs. 8, 11** and **15**). Apart from the average number of leucocytes being superior in the GFP group (4.92 ± 3.68 leucocytes/SEM field) than in the NaCl group (0.75 ± 0.93 leucocytes/SEM field; p=0.016), no other statistically significant differences were found in leucocytes' and phagocytes' numbers on the surface of catheters in the remaining experimental groups (**Fig. 11**).

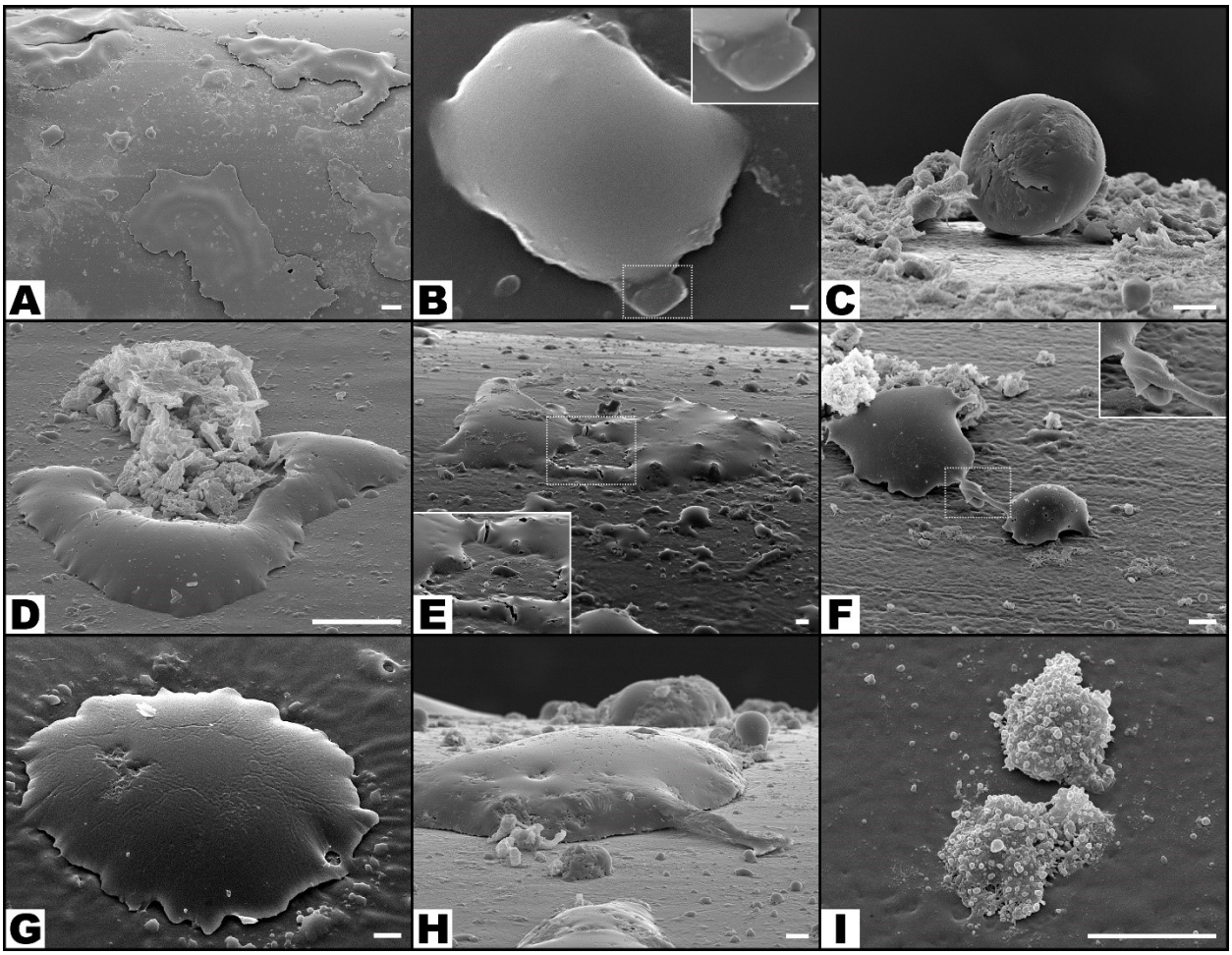

Figure 15 - Typical scanning electron microscopy images of the surface of catheters showing multiple features of leucocyte morphology and interaction with the surrounding environment. (A) Low magnification

view of the surface of the catheter showing giant leucocytes interspersed with smaller leucocytes. (B) Leucocyte engulfing a *Pseudomonas aeruginosa* cell in the area highlighted with the interrupted line box; on the top right corner of the picture there is a higher amplification view of this interaction. (C) Leucocyte adhering to the catheter's surface. (D) A leucocyte phagocytosing a region with biofilm. (E) and (F) leucocytes interacting on the surface of the catheter (dotted boxes highlight amplified views of these interactions). (G) Large leucocyte engulfing adjacent biofilm. (H) In the central portion of the image there is a large leucocyte extending a pseudopod into adjacent *P. aeruginosa*. (I) Three leucocytes with multiple vesicles on their surface.

Calibration bar = 100 µm (A); 1 µm (B); 10 µm (C to I).

Bacterial contamination with cocci were observed in 8.92% ± 22.21% of SEM fields (**Fig. 13**). There were no statistically significant differences between the different experimental groups.

Overall, data shows that in the model used the surface of foreign bodies presents significant numbers of bacteria. Flap transduction with either BD-2 or BD-3, and in particular with the latter, remarkably lowers bacterial numbers on the surface of foreign bodies.

Bacterial counts and biofilms on the surface of the foreign body were correlated with flap necrosis

We then assessed whether bacteria accumulation on the surface of the foreign body was correlated with flap necrosis. **Table 2** synthetizes the most relevant correlations in the data obtained in this study.

Variable	Variable	Pearson's correlation factor	P value
Flap necrosis rate on the 3rd postoperative day	**Flap necrosis rate on the 7th day**	0.922	p<0.001
	Average number of bacteria per SEM field	0.609	p<0.001
	Percentage of SEM fields with biofilm	0.596	p<0.001
	Percentage of SEM fields with planktonic bacteria	- 0.409	p=0.004
	Percentage of SEM fields without bacteria	- 0.426	p=0.003
	Percentage of SEM fields without biofilm	- 0.681	p<0.001
	***P. aeruginosa* counts on the 3rd postoperative day determined by culture of flap biopsies**	0.287	p=0.041
Flap necrosis rate on the 7th postoperative day	**Average number of bacteria per SEM field**	0.626	p<0.001
	Percentage of SEM fields with biofilm	0.563	p=0.001
	Percentage of SEM fields with planktonic bacteria	- 0.379	p=0.03
	Percentage of SEM fields without bacteria	- 0.462	p=0.007
	Percentage of SEM fields without biofilm	- 0.674	p<0.001
	***P. aeruginosa* counts on the 3rd postoperative day determined by culture of flap biopsies**	0.395	p=0.016
Average number of bacteria per SEM field	**Average number of leucocytes per SEM field**	0.276	p=0.041
	Average number of phagocytes per SEM field	0.401	p=0.002

Table 2 - Synthesis of the most relevant correlations in the data obtained in this study.

SEM, scanning electron microscopy

Flap necrosis rates on the 3rd and 7th day postoperatively were highly correlated (Pearson's correlation factor = 0.922; p<0.001). Flap necrosis was also correlated with several features of catheters' surface. In fact, flap necrosis rate on the third postoperative day was positively correlated with the average number of bacteria per SEM field and the percentage of SEM fields with biofilm (Pearson's correlation factor = 0.609; p<0.001 and 0.596; p<0.001, respectively). It was negatively correlated with the following variables: percentage of SEM fields with planktonic bacteria. In percentage of SEM fields without bacteria; percentage of SEM fields without biofilm (Pearson's correlation factor = - 0.409, p=0.004; - 0.426, p=0.003 and - 0.681; p<0.001, respectively).

Analogously, flap necrosis on the seventh day postoperatively was positively correlated with the following findings: average number of bacteria per SEM field (Pearson's correlation factor = 0.626; p<0.001) and the percentage of SEM fields with biofilm (Pearson's correlation factor = 0.563; p=0.001). Moreover, flap necrosis rate on the seventh day after surgery was significantly negatively correlated with the percentage of SEM fields with planktonic bacteria, without bacteria and without biofilm (Pearson's correlation factor = - 0.379, p=0.03; - 0.462, p=0.007; - 0.674, p<0.001, respectively).

The average number of bacteria per SEM field was also positively correlated with the number of leucocytes (Pearson's correlation factor = 0.276; p=0.041); and phagocytes per SEM field (Pearson's correlation factor = 0.401; p=0.002).

P. aeruginosa counts on the 3rd postoperative day determined by culture of flap biopsies, were correlated with flap necrosis on that day (Pearson's correlation factor = 0.287; p=0.041) and on the seventh day after surgery (Pearson's correlation factor = 0.395;

p=0.016) (**Fig. 16**). However, there were no statistically significant correlations between *P. aeruginosa* counts after flap biopsy on the seventh day after surgery and flap necrosis either on the 3rd or 7th postoperative days. (**Fig. 17**).

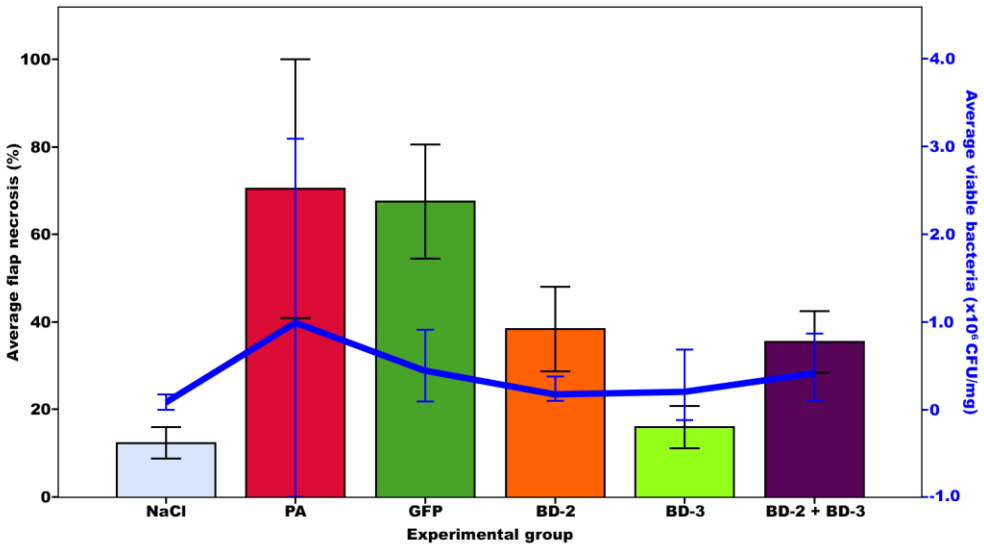

Figure 16 - Graphic representation of the relation between the proportion of flap necrosis (expressed as percentage of flap's initial area) and bacterial counts after flap biopsy on the third day after surgery in the different experimental groups.

On the third postoperative day, flap necrosis and bacterial counts were lower in the animals expressing human β-defensins 2 and 3.

Error bars indicate 95% confidence intervals.

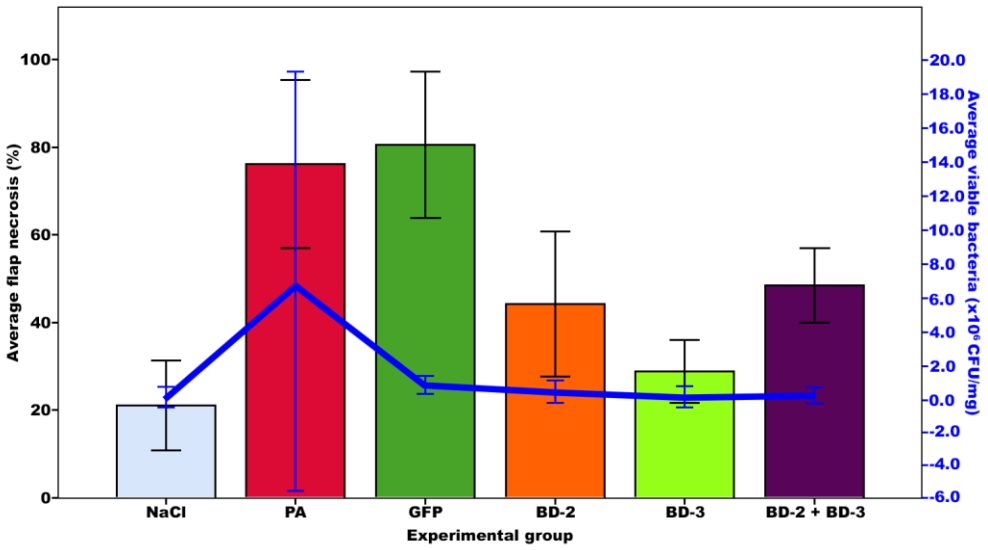

Figure 17 - Graphic representation of the relation between the proportion of flap necrosis (expressed as percentage of flap's initial area) and bacterial counts after flap biopsy on the seventh day after surgery in the different experimental groups.

On the seventh postoperative day, flap necrosis and bacterial counts were lower in the animals expressing human β-defensins 2 and 3.

Error bars indicate 95% confidence intervals.

There were no statistically significant correlations between bacterial quantification after flap biopsy and culture or real-time PCR, on the one hand, and SEM bacterial counts on the other hand.

In conclusion, our data shows that the bacterial counts on the surface of the foreign body and biofilm formation were correlated with flap necrosis.

DISCUSSION

Our study showed that transducing an ischemic skin flap in the rat with human β-defensins, the BD-2 and BD-3 genes, increased skin flap survival in the context of a *P. aeruginosa* infection in the presence of a foreign body. In addition, BD-2 and particularly BD-3 transduction reduced *P. aeruginosa* numbers and biofilm formation on the surface of the foreign body. Other authors had already shown that BD-2 and BD-3 are overexpressed in the presence of *P. aeruginosa* keratitis in mice and that overexpression was associated with diminished *P. aeruginosa* numbers in the eyes of affected mice.[14, 58]

However, as far as the authors could determine, this is the first description of the transduction of BDs genes to treat a *P. aeruginosa* infection *in vivo*.[13] It is also the first time that the transduction of an AMP gene is performed with the intent to treat an infection taking place in a poorly perfused region, simulating local ischemia. This scenario is frequent in the clinical setting, occurring after trauma, radiotherapy or in ischemic regions of the body, namely in the lower limbs of atherosclerotic and/or diabetic patients.[59, 60] This study describes for the first time the morphometric features of the bacteria on the surface of a foreign body and thoroughly compares them with the clinical evaluation of the overlying skin flap, and with bacterial quantification using microbiological cultures of skin biopsy and real-time PCR. Other authors had already shown the possibility of treating a *Staphylococcus aureus* infection transducing a normally perfused flap with the AMP cathelicidin LL-37.[39]

The fact that the groups treated with BDs presented less biofilm, suggest that *in vivo* these AMPs are able to prevent the formation of biofilms, which are one of the most common causes of clinical persistent infection.[61-66] This adds to the knowledge of BD physiology, as most papers in this field refer to the action of AMPs *in vitro*, not addressing the role of these substances *in vivo*.[67]

Flap necrosis rates on the 3rd and 7th day postoperatively were highly correlated (Pearson's correlation factor = 0.922; $p<0.001$). This suggests that, in this rodent model, the ongoing *P. aeruginosa* infection associated with the foreign body led to continuous breakdown of the overlying integument.[62] This had already been amply observed in clinical practice.[62, 68] Interestingly, in this work, flap necrosis was significantly correlated with several features of catheters' surface, namely bacterial numbers and biofilm presence. In opposition, in the present study, flap necrosis rates in the different groups was not correlated with bacterial determination by real-time PCR of flap biopsies. Moreover, only bacterial counts of microbiological cultures of biopsies of the flap performed on the third post-operative day correlated, and even then only poorly, with flap necrosis rates on the third (Pearson's correlation factor = 0.287; $p=0.041$) and seventh (Pearson's correlation factor = 0.395; $p=0.016$) days after surgery. This lends support to the notion that in bacteria capable of producing biofilms, such as *P. aeruginosa*, the protracted release of bacterial cells from the biofilm medium is one of the main determinants of continuous tissue damage to the overlying tissues.[41, 53, 62-64] In fact, a recent meta-analysis demonstrated that biofilms are present in more than three quarters of chronic wounds, increasing their extension or preventing their closure.[63]

All these data suggest that the model herein used adequately mimics clinically relevant skin ulcers and infections. Noteworthy, a similar model had already been described by Van Wijngaerden *et al*, who introduced a catheter in the back of the rat to test antibiotic efficacy. Furthermore, other authors, have also placed a catheter under a well perfused flap in the groin region of the rat. Notwithstanding, these authors did not used SEM to evaluate the surface of the catheter used as a foreign body. It was only recently that van Gennip *et al.* emphasized the potential advantages of studying the morphology and interaction of bacteria and immune cells on the surface of foreign bodies with SEM. However, these latter authors placed the foreign body inside the peritoneal cavity.[53]

We believe that our model presents the additional advantage of simulating an ischemic environment surrounding the foreign body. In fact, as shown in **Figure 5**, one hour after surgery, the average temperature difference between the flap and the contralateral side was 2.34 ± 1.06 ºC ($p<0.001$). These data confirm that the surgical skin flap placed over the foreign body was ischemic, since skin temperature is known to be proportional to integumentary perfusion.[69]

One of the limitations of the present methodology was the impossibility to precisely differentiate between leucocytes types.[53, 70-74] Although immunological methods have been proposed to distinguish leucocyte types using SEM, it has been shown that these methods may significantly affect leucocyte adhesion and morphology, making interpretation of data difficult.[75] In future works, it would be interesting to characterize with other techniques leucocyte numbers and cell types both on the surface of the foreign body and in the surrounding tissues.

Another limitation of this study was the presence of contamination of the wound by bacteria other than *P. aeruginosa*, namely by cocci, in 8.92 ± 22.21% of SEM fields (**Fig. 13**). This contamination affected all experimental groups equally. It is no doubt related to the ischemic nature of the skin flap used, leading to partial flap necrosis, surgical wound dehiscence and contamination with saprophytic flora. Hence, studies similar to this one but with normally perfused flaps are, therefore, warranted, in order to minimize contamination with other bacterial species.

The authors must concede that multiple other delivery methods of the BDs genes could have been employed.[76, 77] Many of the other available vectors have potential advantages and disadvantages. For example, it has been shown that intradermal delivery of the transgenes might be superior to intravascular perfusion using lentivirus vectors in skin flaps.[78] Consequently, further studies are warranted in this field, namely to test the superiority of other vectors, as well as the susceptibility of other bacteria species, particularly bacteria resistant to conventional antibiotics. Furthermore, it would be interesting to assess if BDs could be used to reverse established biofilm on the surface of foreign bodies.

Finally, the authors would like to note that although the potential clinical merits of AMPs have been extoled for the past two decades, their clinical application has been tardy and incipient, due to potential systemic toxicity, susceptibility to proteases, and high cost of peptide production.[9, 10, 12, 13, 79, 80] Controlled local production of a specific AMP by a flap placed over a difficult wound (for example, osteomyelitis in a mangled extremity) may theoretically allow to eradicate a bacterial infection and thus allow wound closure.[39]

If the introduction of the AMP sequence was to cause oncogenesis, the flap could be simply removed and replaced by another flap or eventually by a skin graft.[39, 81]

ACKNOWLEDGEMENTS

The authors would like to thank Mr. Filipe Franco for the drawings contained in this article.

The authors are deeply thankful to the unfaltering help of Mr. Octávio Chaveiro in the acquisition of the thousands SEM images.

References

1. Alanis AJ. Resistance to antibiotics: are we in the post-antibiotic era? Archives of medical research. 2005;36(6):697-705.

2. Falagas ME, Bliziotis IA. Pandrug-resistant Gram-negative bacteria: the dawn of the post-antibiotic era? International journal of antimicrobial agents. 2007;29(6):630-6.

3. Aminov RI. A brief history of the antibiotic era: lessons learned and challenges for the future. Frontiers in microbiology. 2010;1:134.

4. Mendes JJ, Marques-Costa A, Vilela C, Neves J, Candeias N, Cavaco-Silva P, et al. Clinical and bacteriological survey of diabetic foot infections in Lisbon. Diabetes research and clinical practice. 2012;95(1):153-61. Epub 2011/10/25. doi: 10.1016/j.diabres.2011.10.001. PubMed PMID: 22019426.

5. Peters BM, Shirtliff ME, Jabra-Rizk MA. Antimicrobial peptides: primeval molecules or future drugs? PLoS pathogens. 2010;6(10):e1001067. Epub 2010/11/10. doi: 10.1371/journal.ppat.1001067. PubMed PMID: 21060861; PubMed Central PMCID: PMC2965748.

6. Lipsky BA. Diabetic foot infections: Current treatment and delaying the 'post-antibiotic era'. Diabetes/metabolism research and reviews. 2016;32(S1):246-53.

7. Zasloff M. Antimicrobial peptides of multicellular organisms. Nature. 2002;415(6870):389-95. Epub 2002/01/25. doi: 10.1038/415389a. PubMed PMID: 11807545.

8. Fjell CD, Hiss JA, Hancock RE, Schneider G. Designing antimicrobial peptides: form follows function. Nature reviews Drug discovery. 2012;11(1):37-51.

9. Seo M-D, Won H-S, Kim J-H, Mishig-Ochir T, Lee B-J. Antimicrobial peptides for therapeutic applications: a review. Molecules. 2012;17(10):12276-86.

10. Nakatsuji T, Gallo RL. Antimicrobial peptides: old molecules with new ideas. The Journal of investigative dermatology. 2012;132(3 Pt 2):887-95. Epub 2011/12/14. doi: 10.1038/jid.2011.387. PubMed PMID: 22158560; PubMed Central PMCID: PMC3279605.

11. Sweeney IR, Miraftab M, Collyer G. A critical review of modern and emerging absorbent dressings used to treat exuding wounds. International wound journal. 2012;9(6):601-12. Epub 2012/01/18. doi: 10.1111/j.1742-481X.2011.00923.x. PubMed PMID: 22248337.

12. Shang D, Li X, Sun Y, Wang C, Sun L, Wei S, et al. Design of potent, non-toxic antimicrobial agents based upon the structure of the frog skin peptide, temporin-1CEb from Chinese brown frog, Rana chensinensis. Chemical biology & drug design. 2012;79(5):653-62. Epub 2012/02/22. doi: 10.1111/j.1747-0285.2012.01363.x. PubMed PMID: 22348663.

13. Zasloff M. Antimicrobial peptides: do they have a future as therapeutics. In: Harder J, Schroder JM, editors. Antimicrobial peptides: role in human health and disease. First ed. London: Springer; 2016. p. 147-54.

14. Gordon YJ, Romanowski EG, McDermott AM. A review of antimicrobial peptides and their therapeutic potential as anti-infective drugs. Current eye research. 2005;30(7):505-15. Epub 2005/07/16. doi: 10.1080/02713680590968637. PubMed PMID: 16020284; PubMed Central PMCID: PMC1497874.

15. Marr AK, Gooderham WJ, Hancock RE. Antibacterial peptides for therapeutic use: obstacles and realistic outlook. Current opinion in pharmacology. 2006;6(5):468-72. Epub 2006/08/08. doi: 10.1016/j.coph.2006.04.006. PubMed PMID: 16890021.

16. Wiesner J, Vilcinskas A. Antimicrobial peptides: the ancient arm of the human immune system. Virulence. 2010;1(5):440-64. Epub 2010/12/24. doi: 10.4161/viru.1.5.12983. PubMed PMID: 21178486.

17. Peschel A, Sahl H-G. The co-evolution of host cationic antimicrobial peptides and microbial resistance. Nature Reviews Microbiology. 2006;4(7):529-36.

18. Yeaman MR, Yount NY. Mechanisms of antimicrobial peptide action and resistance. Pharmacological reviews. 2003;55(1):27-55. Epub 2003/03/05. doi: 10.1124/pr.55.1.2. PubMed PMID: 12615953.

19. Hemshekhar M, Anaparti V, Mookherjee N. Functions of Cationic Host Defense Peptides in Immunity. Pharmaceuticals. 2016;9(3):40. doi: 10.3390/ph9030040. PubMed PMID: PMC5039493.

20. Yamaguchi Y, Ouchi Y. Antimicrobial peptide defensin: identification of novel isoforms and the characterization of their physiological roles and their significance in the pathogenesis of diseases. Proceedings of the Japan Academy Series B, Physical and biological sciences. 2012;88(4):152-66. Epub 2012/04/14. PubMed PMID: 22498979; PubMed Central PMCID: PMC3406309.

21. Breidenstein EB, de la Fuente-Nunez C, Hancock RE. Pseudomonas aeruginosa: all roads lead to resistance. Trends in microbiology. 2011;19(8):419-26. Epub 2011/06/15. doi: 10.1016/j.tim.2011.04.005. PubMed PMID: 21664819.

22. Chatterjee M, Anju CP, Biswas L, Anil Kumar V, Gopi Mohan C, Biswas R. Antibiotic resistance in Pseudomonas aeruginosa and alternative therapeutic options. International journal of medical microbiology : IJMM. 2016;306(1):48-58. Epub 2015/12/22. doi: 10.1016/j.ijmm.2015.11.004. PubMed PMID: 26687205.

23. Ge Y, MacDonald D, Hait H, Lipsky B, Zasloff M, Holroyd K. Microbiological profile of infected diabetic foot ulcers. Diabetic medicine : a journal of the British Diabetic Association. 2002;19(12):1032-4. Epub 2003/03/22. PubMed PMID: 12647846.

24. Schirmer S, Ritter R-G, Fansa H. Vascular surgery, microsurgery and supramicrosurgery for treatment of chronic diabetic foot ulcers to prevent amputations. PloS one. 2013;8(9):e74704.

25. Pazgier M, Hoover DM, Yang D, Lu W, Lubkowski J. Human beta-defensins. Cellular and molecular life sciences : CMLS. 2006;63(11):1294-313. Epub 2006/05/20. doi: 10.1007/s00018-005-5540-2. PubMed PMID: 16710608.

26. Maisetta G, Batoni G, Esin S, Florio W, Bottai D, Favilli F, et al. In vitro bactericidal activity of human beta-defensin 3 against multidrug-resistant nosocomial strains. Antimicrobial agents and chemotherapy. 2006;50(2):806-9. Epub 2006/01/27. doi: 10.1128/AAC.50.2.806-809.2006. PubMed PMID: 16436752; PubMed Central PMCID: PMC1366902.

27. Tai KP, Kamdar K, Yamaki J, Le VV, Tran D, Tran P, et al. Microbicidal effects of α- and θ-defensins against antibiotic-resistant Staphylococcus aureus and Pseudomonas aeruginosa. Innate immunity. 2015;21(1):17-29. doi: 10.1177/1753425913514784. PubMed PMID: PMC4062604.

28. Huang LC, Redfern RL, Narayanan S, Reins RY, McDermott AM. In vitro activity of human β-defensin 2 against Pseudomonas aeruginosa in the presence of tear fluid. Antimicrobial agents and chemotherapy. 2007;51(11):3853-60.

29. Raschig J, Mailander-Sanchez D, Berscheid A, Berger J, Stromstedt AA, Courth LF, et al. Ubiquitously expressed Human Beta Defensin 1 (hBD1) forms bacteria-entrapping nets in a redox dependent mode of action. PLoS pathogens. 2017;13(3):e1006261. Epub 2017/03/23. doi: 10.1371/journal.ppat.1006261. PubMed PMID: 28323883; PubMed Central PMCID: PMCPMC5376342.

30. Casalou C, Seixas C, Portelinha A, Pintado P, Barros M, Ramalho JS, et al. Arl13b and the non-muscle myosin heavy chain IIA are required for circular dorsal ruffle formation and cell migration. Journal of cell science. 2014;127(Pt 12):2709-22. Epub 2014/04/30. doi: 10.1242/jcs.143446. PubMed PMID: 24777479.

31. National Research Council (U.S.). Committee for the Update of the Guide for the Care and Use of Laboratory Animals., Institute for Laboratory Animal Research (U.S.), National Academies Press (U.S.). Guide for the care and use of laboratory animals. Washington, D.C.: National Academies Press,; 2011. Available from: http://www.ncbi.nlm.nih.gov/books/NBK54050.

32. Edmunds MC, Wigmore S, Kluth D. In situ transverse rectus abdominis myocutaneous flap: a rat model of myocutaneous ischemia reperfusion injury. Journal of visualized experiments : JoVE. 2013;(76). Epub 2013/06/19. doi: 10.3791/50473. PubMed PMID: 23770929.

33. Harder Y, Schmauss D, Wettstein R, Egana JT, Weiss F, Weinzierl A, et al. Ischemic tissue injury in the dorsal skinfold chamber of the mouse: a skin flap model to investigate acute persistent ischemia. Journal of visualized experiments : JoVE. 2014;(93):e51900. Epub 2014/12/10. doi: 10.3791/51900. PubMed PMID: 25489743.

34. Plenter RJ, Grazia TJ. Murine heterotopic heart transplant technique. Journal of visualized experiments : JoVE. 2014;(89). Epub 2014/07/22. doi: 10.3791/51511. PubMed PMID: 25046118.

35. Trujillo AN, Kesl SL, Sherwood J, Wu M, Gould LJ. Demonstration of the rat ischemic skin wound model. Journal of visualized experiments : JoVE. 2015;(98). Epub 2015/04/14. doi: 10.3791/52637. PubMed PMID: 25866964.

36. Casal D, Pais D, Iria I, Mota-Silva E, Almeida M-A, Alves S, et al. A Model of Free Tissue Transfer: The Rat Epigastric Free Flap. Journal of Visualized Experiments. 2017;1(119):e55281. doi: doi:10.3791/55281.

37. Wungcharoen B, Pradidarcheep W, Santidhananon Y, Chongchet V. Pre-arterialisation of the arterialised venous flap: an experimental study in the rat. Br J Plast Surg. 2001;54(7):621-30. Epub 2001/10/05. doi: 10.1054/bjps.2001.3675. PubMed PMID: 11583500.

38. Casal D, Mota-Silva E, Pais D, Iria I, Videira PA, Tanganho D, et al. Optimization of an arterialized venous fasciocutaneous flap in the abdomen of the rat. PRS Global Open. 2017;in press.

39. Ghali S, Bhatt KA, Dempsey MP, Jones DM, Singh S, Aarabi S, et al. Treating chronic wound infections with genetically modified free flaps. Plastic and reconstructive surgery.

2009;123(4):1157-68. Epub 2009/04/02. doi: 10.1097/PRS.0b013e31819f25a4. PubMed PMID: 19337084.

40. Ghali S, Dempsey MP, Jones DM, Grogan RH, Butler PE, Gurtner GC. Plastic surgical delivery systems for targeted gene therapy. Ann Plast Surg. 2008;60(3):323-32. Epub 2008/04/30. doi: 10.1097/SAP.0b013e31806917b0. PubMed PMID: 18443515.

41. Van Wijngaerden E, Peetermans WE, Vandersmissen J, Van Lierde S, Bobbaers H, Van Eldere J. Foreign body infection: a new rat model for prophylaxis and treatment. The Journal of antimicrobial chemotherapy. 1999;44(5):669-74. Epub 1999/12/20. PubMed PMID: 10552984.

42. Sheena Y, Jennison T, Hardwicke JT, Titley OG. Detection of perforators using thermal imaging. Plastic and reconstructive surgery. 2013;132(6):1603-10.

43. Weng W, Zhang F, Zhao B, Wu Z, Gao W, Li Z, et al. The complicated role of venous drainage on the survival of arterialized venous flaps. Oncotarget. 2017. doi: 10.18632/oncotarget.14845. PubMed PMID: 28145882.

44. Trujillo AN, Kesl SL, Sherwood J, Wu M, Gould LJ. Demonstration of the rat ischemic skin wound model. Journal of visualized experiments : JoVE. 2015;(98):e52637. Epub 2015/04/14. doi: 10.3791/52637. PubMed PMID: 25866964; PubMed Central PMCID: PMCPMC4401402.

45. Bas A, Forsberg G, Hammarstrom S, Hammarstrom ML. Utility of the housekeeping genes 18S rRNA, beta-actin and glyceraldehyde-3-phosphate-dehydrogenase for normalization in real-time quantitative reverse transcriptase-polymerase chain reaction analysis of gene expression in human T lymphocytes. Scandinavian journal of immunology.

2004;59(6):566-73. Epub 2004/06/09. doi: 10.1111/j.0300-9475.2004.01440.x. PubMed PMID: 15182252.

46. Livak KJ, Schmittgen TD. Analysis of relative gene expression data using real-time quantitative PCR and the 2(-Delta Delta C(T)) Method. Methods (San Diego, Calif). 2001;25(4):402-8. Epub 2002/02/16. doi: 10.1006/meth.2001.1262. PubMed PMID: 11846609.

47. Silva M, Fung RKF, Donnelly CB, Videira PA, Sackstein R. Cell-Specific Variation in E-Selectin Ligand Expression among Human Peripheral Blood Mononuclear Cells: Implications for Immunosurveillance and Pathobiology. J Immunol. 2017;198(9):3576-87. Epub 2017/03/24. doi: 10.4049/jimmunol.1601636. PubMed PMID: 28330896; PubMed Central PMCID: PMCPMC5426364.

48. Carrascal MA, Severino PF, Guadalupe Cabral M, Silva M, Ferreira JA, Calais F, et al. Sialyl Tn-expressing bladder cancer cells induce a tolerogenic phenotype in innate and adaptive immune cells. Molecular oncology. 2014;8(3):753-65. Epub 2014/03/25. doi: 10.1016/j.molonc.2014.02.008. PubMed PMID: 24656965; PubMed Central PMCID: PMCPMC5528624.

49. Maeda H, Fujimoto C, Haruki Y, Maeda T, Kokeguchi S, Petelin M, et al. Quantitative real-time PCR using TaqMan and SYBR Green for Actinobacillus actinomycetemcomitans, Porphyromonas gingivalis, Prevotella intermedia, tetQ gene and total bacteria. FEMS Immunology & Medical Microbiology. 2003;39(1):81-6.

50. Fischer AH, Jacobson KA, Rose J, Zeller R. Hematoxylin and eosin staining of tissue and cell sections. Cold Spring Harbor Protocols. 2008;2008(5):pdb. prot4986.

51. Foot NC. The Masson trichrome staining methods in routine laboratory use. Stain Technology. 1933;8(3):101-10.

52. Kesting MR, Stoeckelhuber M, Holzle F, Mucke T, Neumann K, Woermann K, et al. Expression of antimicrobial peptides in cutaneous infections after skin surgery. The British journal of dermatology. 2010;163(1):121-7. Epub 2010/03/30. doi: 10.1111/j.1365-2133.2010.09781.x. PubMed PMID: 20346023.

53. van Gennip M, Christensen LD, Alhede M, Qvortrup K, Jensen PO, Hoiby N, et al. Interactions between polymorphonuclear leukocytes and Pseudomonas aeruginosa biofilms on silicone implants in vivo. Infection and immunity. 2012;80(8):2601-7. Epub 2012/05/16. doi: 10.1128/IAI.06215-11. PubMed PMID: 22585963; PubMed Central PMCID: PMC3434577.

54. Polliack A. The contribution of scanning electron microscopy in haematology: its role in defining leucocyte and erythrocyte disorders. Journal of microscopy. 1981;123(Pt 2):177-87. PubMed PMID: 7035677.

55. Saint-Guillain ML, Vray B, Hoebeke J, Leloup R. SEM morphological studies of phagocytosis by rat macrophages and rabbit polymorphonuclear leukocytes. Scanning electron microscopy. 1980;(Pt 2):205-12. Epub 1980/01/01. PubMed PMID: 6999599.

56. West MJ. Estimating object number. In: West MJ, editor. Basic stereology for biologists and neuroscientists. 1. First ed. New York: Cold Spring Harbor Laboratory Press; 2012. p. 31-58.

57. Geuna S. The revolution of counting "tops": two decades of the disector principle in morphological research. Microscopy research and technique. 2005;66(5):270-4. Epub 2005/06/09. doi: 10.1002/jemt.20167. PubMed PMID: 15940681.

58. Wu M, McClellan SA, Barrett RP, Zhang Y, Hazlett LD. β-defensins 2 and 3 together promote resistance to Pseudomonas aeruginosa keratitis. The Journal of Immunology. 2009;183(12):8054-60.

59. Morton LM, Phillips TJ. Wound healing and treating wounds: Differential diagnosis and evaluation of chronic wounds. Journal of the American Academy of Dermatology. 2016;74(4):589-605; quiz -6. Epub 2016/03/17. doi: 10.1016/j.jaad.2015.08.068. PubMed PMID: 26979352.

60. Armstrong DG, Lipsky BA. Diabetic foot infections: stepwise medical and surgical management. International wound journal. 2004;1(2):123-32. Epub 2006/05/26. doi: 10.1111/j.1742-4801.2004.00035.x. PubMed PMID: 16722884.

61. Costerton JW, Stewart PS, Greenberg EP. Bacterial Biofilms: A Common Cause of Persistent Infections. Science. 1999;284(5418):1318-22. doi: 10.1126/science.284.5418.1318.

62. Barker JC, Khansa I, Gordillo GM. A Formidable Foe Is Sabotaging Your Results: What You Should Know about Biofilms and Wound Healing. Plastic and reconstructive surgery. 2017;139(5):1184e-94e. Epub 2017/04/27. doi: 10.1097/prs.0000000000003325. PubMed PMID: 28445380; PubMed Central PMCID: PMCPMC5407389.

63. Malone M, Bjarnsholt T, McBain AJ, James GA, Stoodley P, Leaper D, et al. The prevalence of biofilms in chronic wounds: a systematic review and meta-analysis of

published data. J Wound Care. 2017;26(1):20-5. doi: 10.12968/jowc.2017.26.1.20. PubMed PMID: 28103163.

64. Mihai MM, Holban AM, Giurcaneanu C, Popa LG, Oanea RM, Lazar V, et al. Microbial biofilms: impact on the pathogenesis of periodontitis, cystic fibrosis, chronic wounds and medical device-related infections. Curr Top Med Chem. 2015;15(16):1552-76. PubMed PMID: 25877092.

65. Ramos-Gallardo G. Chronic Wounds in Burn Injury: A Case Report on Importance of Biofilms. World J Plast Surg. 2016;5(2):175-80. PubMed PMID: 27579274; PubMed Central PMCID: PMCPMC5003954.

66. Scali C, Kunimoto B. An update on chronic wounds and the role of biofilms. J Cutan Med Surg. 2013;17(6):371-6. doi: 10.2310/7750.2013.12129. PubMed PMID: 24138971.

67. Kostakioti M, Hadjifrangiskou M, Hultgren SJ. Bacterial biofilms: development, dispersal, and therapeutic strategies in the dawn of the postantibiotic era. Cold Spring Harb Perspect Med. 2013;3(4):a010306. doi: 10.1101/cshperspect.a010306. PubMed PMID: 23545571; PubMed Central PMCID: PMCPMC3683961.

68. Snyder RJ, Bohn G, Hanft J, Harkless L, Kim P, Lavery L, et al. Wound Biofilm: Current Perspectives and Strategies on Biofilm Disruption and Treatments. Wounds. 2017;29(6):S1-s17. Epub 2017/07/07. PubMed PMID: 28682297.

69. Sasajima T, Kikuchi S, Ishikawa N, Koyama T. Skin temperature in lower hind limb subjected to distal vein arterialization in rats. In: Swartz HM, Harrison DK, Bruley DF, editors. Oxygen transport to tissue XXXVI. 1. First ed. New York, USA: Springer; 2014. p. 361-8.

70. POLLIACK A. Surface Features of Normal and leukemic lymphocytes by SEM. Clinical Immunology and Immunopathology. 1975;3:412-30.

71. Polliack A, Lampen N, Clarkson BD, De Harven E, Bentwich Z, Siegal FP, et al. Identification of human B and T lymphocytes by scanning electron microscopy. The Journal of experimental medicine. 1973;138(3):607-24. Epub 1973/09/01. PubMed PMID: 4542254; PubMed Central PMCID: PMC2139412.

72. Mian R, Westwood D, Stanley P, Marshall JM, Coote JH. Acute systemic hypoxia and the surface ultrastructure and morphological characteristics of rat leucocytes. Experimental physiology. 1993;78(6):839-42. Epub 1993/11/01. PubMed PMID: 8311950.

73. Pugh CW, MacPherson GG, Steer HW. Characterization of nonlymphoid cells derived from rat peripheral lymph. The Journal of experimental medicine. 1983;157(6):1758-79. Epub 1983/06/01. PubMed PMID: 6854208; PubMed Central PMCID: PMC2187049.

74. MacRae EK, Pryzwansky KE, Cooney MH, Spitznagel JK. Scanning electron microscopic observations of early stages of phagocytosis of E. coli by human neutrophils. Cell and tissue research. 1980;209(1):65-70. Epub 1980/01/01. PubMed PMID: 7000363.

75. Marino F, Schembri L, Rasini E, Pinoli M, Scanzano A, Luini A, et al. Characterization of human leukocyte-HUVEC adhesion: Effect of cell preparation methods. Journal of immunological methods. 2017;443:55-63. Epub 2017/02/09. doi: 10.1016/j.jim.2017.01.013. PubMed PMID: 28167274.

76. Kim TK, Eberwine JH. Mammalian cell transfection: the present and the future. Analytical and bioanalytical chemistry. 2010;397(8):3173-8. Epub 2010/06/16. doi:

10.1007/s00216-010-3821-6. PubMed PMID: 20549496; PubMed Central PMCID: PMC2911531.

77. Warnock JN, Daigre C, Al-Rubeai M. Introduction to viral vectors. In: Merten OW, Al-Rubeai M, editors. Viral vectors for gene therapy. 1. First ed. London: Humana Press; 2011. p. 1-25.

78. Leto Barone AA, Zhou ZY, Hughes MW, Park R, Schulman RM, Lee S, et al. Lentiviral transduction of face and limb flaps: implications for immunomodulation of vascularized composite allografts. Plastic and reconstructive surgery. 2012;129(2):391-400. Epub 2012/01/31. doi: 10.1097/PRS.0b013e31823aeaeb. PubMed PMID: 22286422.

79. Yang D, Chertov O, Bykovskaia SN, Chen Q, Buffo MJ, Shogan J, et al. Beta-defensins: linking innate and adaptive immunity through dendritic and T cell CCR6. Science. 1999;286(5439):525-8. Epub 1999/10/16. PubMed PMID: 10521347.

80. Stanfield RL, Westbrook EM, Selsted ME. Characterization of two crystal forms of human defensin neutrophil cationic peptide 1, a naturally occurring antimicrobial peptide of leukocytes. The Journal of biological chemistry. 1988;263(12):5933-5. Epub 1988/04/25. PubMed PMID: 3356711.

81. C Rennert R, Sorkin M, W Wong V, C Gurtner G. Organ-level tissue engineering using bioreactor systems and stem cells: implications for transplant surgery. Current stem cell research & therapy. 2014;9(1):2-9.

82. Sorensen OE. Antimicrobial peptides in cutaneous wound healing. In: Harder J, Schroder JM, editors. Antimicrobial peptides: rele in human health and disease. First ed. London: Springer; 2016. p. 1-15.

Chapter 9

RECONSTRUCTION OF A 10-MM-LONG MEDIAN NERVE GAP IN AN ISCHEMIC ENVIRONMENT USING AUTOLOGOUS CONDUITS WITH DIFFERENT PATTERNS OF BLOOD SUPPLY: A COMPARATIVE STUDY IN THE RAT

Authors: Diogo Casal[1-4*], Eduarda Mota-Silva[5*], Inês Iria[4], Sara Alves[6], Ana Farinho[4], Cláudia Pen[6], Nuno Lourenço-Silva[4], Luís Mascarenhas-Lemos[1,6], José Silva-Ferreira[6], Mário Ferraz-Oliveira[6], Valentina Vassilenko[5], Paula Alexandra Videira[3,4], João Goyri-O'Neill[1], Diogo Pais[1]

Affiliations:

1- Anatomy Department, NOVA Medical School, Universidade NOVA de Lisboa, Lisbon, Portugal

2- Plastic and Reconstructive Surgery Department and Burn Unit, Centro Hospitalar de Lisboa Central – Hospital de São José, Lisbon, Portugal

3- UCIBIO, Life Sciences Department, Faculty of Sciences and Technology, Universidade NOVA de Lisboa, Caparica, Portugal

4- CEDOC, NOVA Medical School, Universidade NOVA de Lisboa, Lisbon, Portugal

5- LIBPhys, Physics Department, Faculdade de Ciências e Tecnologias, Universidade NOVA de Lisboa, Lisbon, Portugal

6- Pathology Department, Centro Hospitalar de Lisboa Central – Hospital de São José, Lisbon, Portugal

- DC and EMS contributed equally

ABSTRACT

The aim of this study was to evaluate in the Wistar rat the efficacy of various autologous nerve conduits with various forms of blood supply in reconstructing a 10-mm-long gap in the median nerve (**MN**) under conditions of local ischemia.

A 10-mm-long median nerve defect was created in the right arm. A loose silicone tube was placed around the nerve gap zone, in order to simulate a local ischemic environment. Rats were divided in the following experimental groups (each with 20 rats): the nerve Graft (**NG**) group, in which the excised MN segment was reattached; the conventional nerve flap (**CNF**) and the arterialized neurovenous flap (**ANVF**) groups in which the gap was bridged with homonymous median nerve flaps; the prefabricated nerve flap (**PNF**) group in which the gap was reconstructed with a fabricated flap created by leaving an arteriovenous fistula in contact with the sciatic nerve for 5 weeks; and the two control groups, Sham and Excision groups. In the latter group, the proximal stump of the MN nerve was ligated and no repair was performed. The rats were followed for 100 days. During this time, they did physiotherapy. Functional, electroneuromyographic and histological studies were performed.

The CNF and ANVF groups presented better results than the NG group in the following assessments: grasping test, nociception, motor stimulation threshold, muscle weight, and histomorphometric evaluation. Radial deviation of the operated forepaw was more common in rats that presented worse results in the other outcome variables.

Overall, CNFs and ANVFs produced a faster and more complete recovery than NGs in the reconstruction of a 10-mm-long median nerve gap in an ischemic environment in the Wistar rat. Although, results obtained with CNFs were in most cases were better than ANVFs, these differences were not statistically significant for most of the outcome variables.

INTRODUCTION

Although bold surgeons such as Paul d'Argine were reportedly performing nervous sutures 600 AD, even today, despite numerous surgical and technical developments, the results with peripheral nerve repair are still disappointing.[1-3] Results are particularly unsatisfactory in cases of long nerve defects, being frequent not to obtain useful recovery in the involved nerve territory.[1-3] In 1870, Philipeaux and Vulpian proposed the use of nerve grafts (**NGs**) (devoid of intrinsic blood flow until neoangiogenesis from neighboring tissues occurs) to promote axonal regeneration through nerve defects.[4] Since then, NGs have become the gold standard for the reconstruction of peripheral nerve defects.[5] Even today, the multiple modern techniques of tubulization, using artificial nerve conduits, are generally discouraged for reconstructing defects over 5 to 6 cm in length.[1-3, 6-9] Additionally, experimental data suggests that autologous NG may yield superior motor recovery compared to nerve conduits, and to processed nerve allografts.[10]

From their inception, it was realized that the results obtained with NGs were far from perfect. Consequently, in 1921, Ney proposed the use of vascularized nerve segments, based on a conventional blood supply with an arterial and venous blood supply.[11] These conventional nerve flaps (**CNF**s) were further developed by Strange and Seddon in 1947.[12, 13] However, all these authors described pedicled CNFs, whose usefulness was limited because they could only be mobilized locally. Only in 1976 was the concept of free CNF introduced by Taylor.[14] Still, these free CNFs are based on

very small-sized nourishing vessels, making their dissection laborious and the vascular anastomoses at the recipient site difficult. Additionally, due to anatomical variations, they cannot always be raised.[15] Finally, there is a limited number of available CNFs.[16-18]

In order to circumvent these problems, in 1984, Taylor and Townsend proposed the use of arterialized neurovenous flaps (**ANVFs**).[19] These nerve flaps are based on the anatomical proximity of the venous system to multiple nerves, particularly in the subcutaneous tissue.[20, 21] ANVFs are thus composed of expendable nerve segments and adjoining veins.[20] Usually, one end of the vein is anastomosed to a recipient site artery and the other end is connected to a recipient site vein.[21] ANVFs can be harvested easily from multiple places of the body, particularly from the limbs, having a relatively expedite dissection. Furthermore, superficial veins have a large enough caliber to allow relatively easy vascular anastomoses.[19] Occasionally, the vascular architecture of ANVFs can be used to simultaneously reconstruct adjacent vascular and nerve defects.[21]

CNFs seem to guarantee better functional results than NGs for bridging nerve defects, particularly in conditions of local ischemia or fibrosis, as they are less likely to undergo central necrosis and histological disorganization.[22-24] In fact, contrarily to NGs, CNFs do not depend on plasmatic imbibition during the first 3 to 4 days after transfer for survival.[24-29]. Other authors argue that nerve flaps are not necessarily advantageous, as nerve grafts rapidly regain a new blood supply in several experimental

models.[30] Some authors add that, although recovery tends to be faster with CNFs, the end functional results are similar with CNFs and NGs.[24, 30]

Currently, as far as the authors could determine, the evidence of the efficacy of ANVFs for bridging nerve defects is limited to two articles on the reconstruction of femoral nerve defects in the rat.[28, 29]

Cavadas *et al.* suggested prefabrication of nerve flaps by placing an arteriovenous fistula in contact with nerve segments.[31] Theoretically, this could allow the creation of nerve flaps in virtually any place of the body, solving many of the problems with CNFs. Additionally, there is one study reporting that these prefabricated nerve flaps (**PNFs**) present superior results than NGs in the reconstruction of nerve defects in conditions of local compromise of circulation.[32] Yet, PNFs are not routinely used in clinical practice, in great part due to lack of supporting evidence of their usefulness.[33]

One of the reasons why conclusive evidence is difficult to obtain in the realm of peripheral nerve gap reconstruction is that different researchers have used different animal species, anatomical regions, reconstructive strategies and follow-up times. Furthermore, authors have also used variable outcome variables to assess nerve regeneration. These methodological differences make information synthesis challenging.[30] Finally, even though there are a few side-to-side comparisons of different gap reconstruction methods in the rat hindlimb, using the sciatic nerve, as far as the authors could determine, there is no similar study using the rat forelimb.[10, 22,

34] This is unfortunate, since clinically most peripheral nerve lesions occur in the upper extremity.[3, 35]

Therefore, the aim of this study was to evaluate in the Wistar rat the efficacy of various autologous nerve conduits with various forms of blood supply in reconstructing a 10-mm-long gap in the median nerve (**MN**) under conditions of local ischemia.

METHODS

Animal well-being and ethical committee's approval

All *in vivo* studies involving rats were carried out in strict accordance with or exceeding the recommendations in the Guide for Proper Conduct of Animal Experiments and Related Activities in Academic Research and Technology.[36, 37]

The experimental protocol was approved by the Institutional Animal Care and Use Committee and Ethical Committee at the authors' institution (CEFCM/08/2012).

Pre-operative training and accommodation

Three weeks before the surgery, rats were accustomed to being handled by the researchers. In addition, they were familiarized with the different functional tests used in the postoperative assessment that are described below. During this period the rats were manipulated daily.[38, 39] Pre and post-operatively the rats were maintained in an enriched environment. They were kept in customized cages of 60 X 30 X 90 cm, each with four stages, three ladders, a suspended rope and a training wheel. Each cage contained 5 to 6 rats. This environment intended to mimic the usual physiotherapy that peripheral nerve patients are typically offered postoperatively.[40]

Perioperative care of experimental animals

All the animals were housed under standard environmental conditions and fasted six hours before surgical procedures. No antibiotic prophylaxis was given.

Rats were anesthetized with a mixture of ketamine (5 mg/kg) and diazepam (0.25 mg/kg) given intraperitoneally. The depth of anesthesia was evaluated by toe pinch and by observance of respiration rate throughout the entire procedure. Supplementary doses of the anesthetic solution were provided as needed.[41]

After shaving the surgical sites and placing the animals on the operation table, the surgical field was disinfected with an antiseptic solution (Cutasept®), and draped. All surgical procedures were performed under strict antiseptic procedures. Surgeries were performed by the same author (D.C.), in order to avoid inter-surgeon variability. Surgical procedures were performed under a stereotaxic operating microscope (Leica® M651) and using microsurgical instruments. Hypothermia was avoided by placing the rat over a heating pad during surgical procedures and in the postoperative period.

Surgical model of nerve gap and ischemia in the rat's forelimb

A surgical model of ischemia surrounding a 10-mm-long median nerve defect was used (**Fig. 1**).[29, 39, 42-45] As other authors, we have used a loose silicone tube with a 5-mm-wide inner diameter, and of 15-mm-length (Fortune Medical Inst. Corp.®; Reference 2011-0035) around the nerve repair zone, in order to simulate a local ischemic environment.[29, 42] This tube was sectioned longitudinally, so that it could be opened and subsequently be used to isolate the region of the reconstructed nerve segment (**Fig. 1H**). When vascularized nerve segments were used, the longitudinal opening in the silicone tube was left wide enough to accommodate the *vasa nervorum* supplying the nerve conduit, while isolating the reconstructed nerve segment from the

surrounding vascularized tissues. At the end of the procedure a simple 5/0 Nylon stitch was placed at each end of the tube, passing both sides of the slit, to prevent migration of the silicone tube.

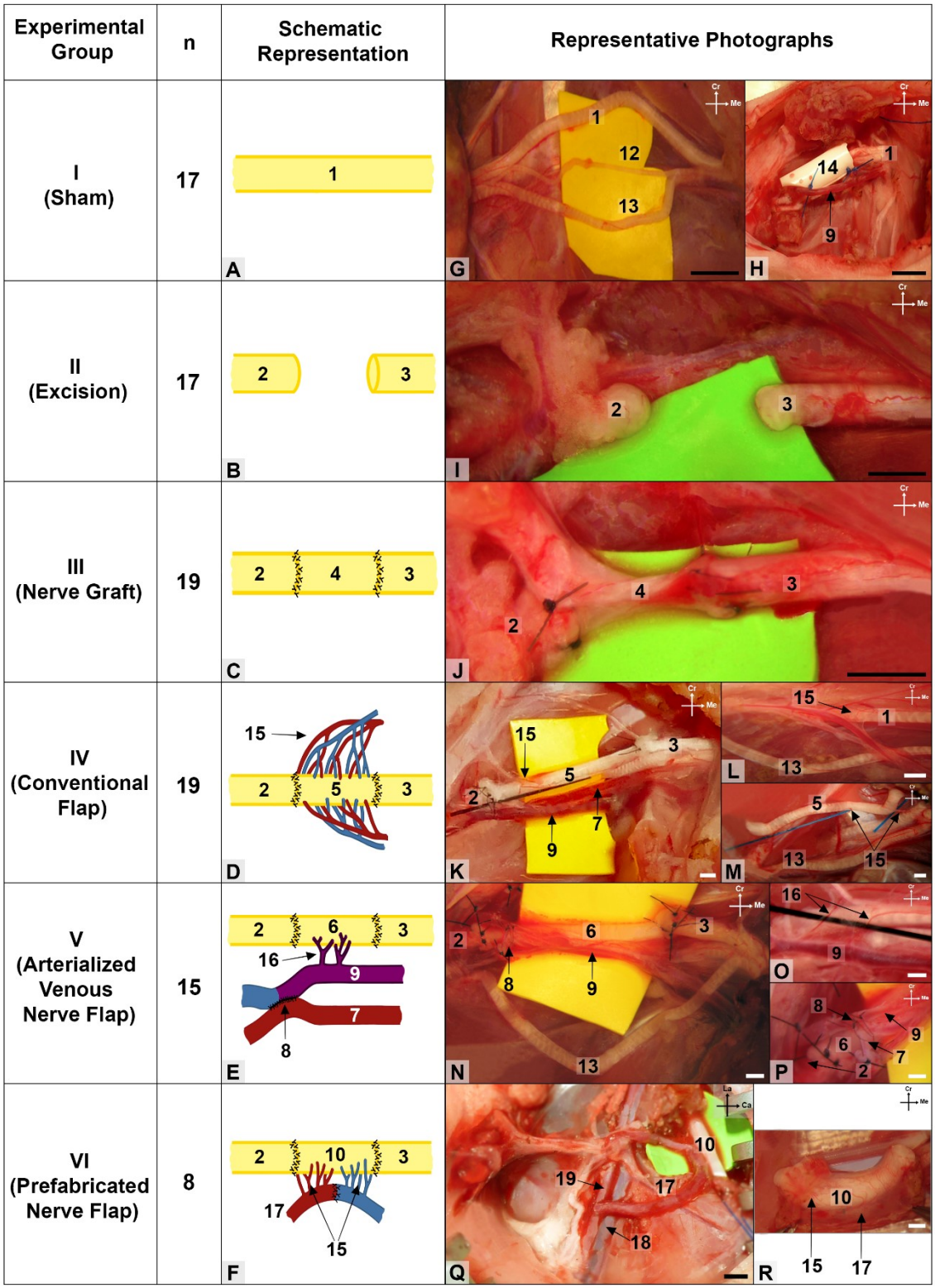

Figure 1 - Experimental groups' schematic representation and representative photographs. A to F, Schematic drawings of the different methods of bridging the median nerve gap in the various

experimental groups. G to R, photographs of representative intra-operative images. All images represent the right forelimb with the exception of Q, which represents the left groin region.

1, median nerve; 2, distal stump of the median nerve; 3, proximal stump of the median nerve; 4, autologous median nerve graft; 5, median nerve conventional flap; 6, arterialized neurovenous flap; 7, brachial artery; 8, arterio-venous anastomosis; 9, brachial vein; 10, prefabricated nerve flap; 11, arterio-venous fistula used to produce the prefabricated nerve flap; 12, medial antebrachial nerve; 13, ulnar nerve; 14, silicone rod place around the nerve gap to simulate an ischemic environment; 15, *vasa nervorum* to median nerve flap; 16, *vena nervorum*; 17, arteriovenous loop; 18, femoral vein; 19, femoral artery

Ca, Caudal; **Cr**, Cranial; **La**, Lateral; **Me**, Medial.

Calibration bar = 1 mm

One hundred and twenty female Wistar rats, aged 4 to 6 months, and weighing between 200 and 250 grams, were randomly allocated in one of the following experimental groups in equal numbers (n=20):

Sham group: a longitudinal incision was made until the subfascial plane throughout the entire medial aspect of the right arm. A myotomy of the lateral portion of the sternal head of the pectoralis major muscle was then performed, in order to expose the MN. This nerve was gently teased away from the surrounding structures in the arm region, becoming pedicled in its segmental blood supply from the brachial vessels.[46] The mentioned 15-mm-long silicone tube was placed around the nerve

preserving its local feeding branches. The skin wound was sutured with interrupted 5/0 Nylon stitches in all the experimental groups (**Fig. 1A, G** and **H**).

Excision group: After exposing the right median nerve as detailed above, a 10-mm-long segment in the central portion of the MN in the arm was marked with a surgical ruler and a surgical marker. The region of the median nerve proximal and distal to this marked region was tagged with 10/0 Nylon stitches. The marked region was cut sharply with a pair of straight microsurgery scissors. The excised segment was discarded. The proximal stump of the median nerve was ligated with an 8/0 Nylon stitch. The stumps of the median nerve were place inside both endings of the silicone tube (**Fig. 1B** and **I**).[47]

Nerve graft (NG) group: Following the excision of the 10-mm-long segment of the right MN as described above, the nerve segment was placed in its original. The nerve segment was not placed in an inverted position, as it is normally recommended, to facilitate comparison with the remaining experimental groups (**Fig. 1C** and **J**). Nerve repair was performed using four to six interrupted 10/0 epineural Nylon stitches in all the experimental groups using conduits.[48]

Conventional nerve flap (CNF) group: The 10-mm-long nerve segment was dissected and excised as detailed above, leaving it pedicled on its epineural arteries and veins in the brachial region (**Fig. 1D, K, L** and **M**).[42]

Arterialized neurovenous flap (ANVF) group: After isolating and cutting the 10-mm-long nerve segment as described for the CNF group, all epineural arteries were carefully cauterized, leaving the nerve conduit pedicled solely on the epineural veins in the brachial region. Immediately proximally to the terminal division of the brachial artery, the brachial artery and accompanying vein were anastomosed lateral-laterally after performing a 1.5-mm-long incision the adjoining flanks of these two vessels. The anastomosis was performed with interrupted 12/0 Nylon stitches. Consequently, an arterial venous anastomosis was created in the distal aspect of the arm, leading to the creation of an arterialized neurovenous conduit, which was used to bridge the MN gap (**Fig. 1E, N, O** and **P**).

Pre-fabricated nerve flap (PNF) group: In this group, a conventional nerve flap was fabricated around the left sciatic nerve of the rat using the technique described by Cavadas and Vera-Sempere (**Figs. 1F, Q** and **R**).[31] Succinctly, an arterial-venous fistula is created in the ventral aspect of the left thigh using the superficial caudal epigastric veins, which are connected to the femoral artery (**Fig. 2**). This fistula was maintained in contact with the left sciatic nerve for 5 weeks. This leads to the fabrication of a conventional perfusion flap including a segment of the left sciatic nerve. Subsequently,

this PNF was transferred to the right arm to reconstruct the median nerve defect (**Figs. 1F, Q** and **R**; and **Fig. 2**). The arterial end of the arterial-venous fistula was terminal-laterally anastomosed to the distal portion of the brachial artery and the venous end of the fistula was terminal-laterally anastomosed to the proximal aspect of the brachial vein using interrupted 12/0 Nylon stitches (**Fig. 2B**).

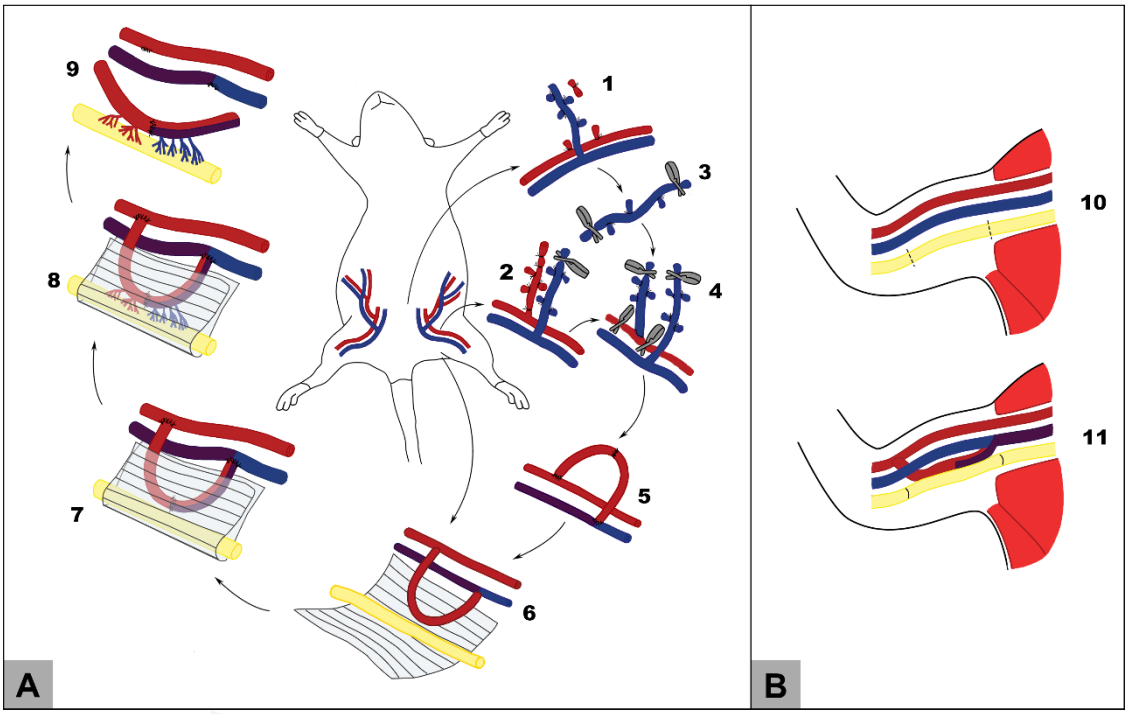

Figure 2 - Conventional flap pre-fabrication and transfer.

A. Prefabrication of the flap in the left thigh.

B. Insetting of the flap in the recipient area in the right arm.

1. An inverted "T" incision is performed in the most caudal aspect of the ventral region of the abdomen of the rat, with the axial portion crossing immediately cranial to the pubic symphysis and with the longitudinal component extending from this point cranially for 3 cm.

2. The right superficial caudal epigastric vein is dissected from the homonymous artery and the caudal epigastric nerve during its entire length, including also part of the its lateral afferent vein.

3. The venous segment is harvested and its origin and termination sites are ligated with interrupted 9/0 Nylon stitches.

4. The venous conduit is inverted and its terminal-laterally anastomosed to the left femoral artery using an interrupted 11/0 Nylon suture.

5. The two epigastric veins are terminal-terminally anastomosed with interrupted 11/0 Nylon stitches, producing and arterial-venous fistula;

6. The left sciatic nerve is exposed through a ventral approach in the medial aspect of the thigh, in the space between the gracilis muscle, placed laterally, and the semimembranosus muscle, located medially. The medial femoral circumflex vessels are ligated and divided. The arterial-venous fistula is placed over the ventrally exposed left sciatic nerve. A silicon sheath is placed around the nerve and the arterial-venous fistula.

7. The silicone sheath is folded on itself and maintained in place with interrupted 5/0 Nylon stitches. The surgical wounds are closed with interrupted 5/0 Nylon stitches.

8. The sciatic nerve and fistula are maintained in contact for 5 weeks, allowing the development of vascular connections between the fistula and the sciatic nerve.

9. After five weeks, a conventional flap including a segment of the sciatic nerve measuring approximately 15 mm has been fabricated.

10. A 10-mm-long segment of the right median nerve is excised.

12. The prefabricated nerve flap is inset in the region of the median nerve defect. Excessive neural tissue is trimmed at both ends. The arterial end of the arterial-venous fistula was terminal-laterally anastomosed to the distal portion of the brachial artery and the venous end of the fistula was terminal-laterally

anastomosed to the proximal aspect of the brachial vein using interrupted 12/0 Nylon stitches. Neural anastomoses were performed using interrupted epineural 11/0 Nylon sutures.

Postoperative Evaluation

Rats were assessed daily regarding general activity, grooming, signs of wound infections or dehiscence, as well as for signs of autotomy.[49-51] They were maintained in the recommended cycles of light and darkness. Animals were provided food and water *ad libitum*.[40]

Rats were followed for 100 days (**D**) after MN reconstruction.

Every 15 days (D15, D30, D45, D60, D75, D90), they were submitted to the following evaluations: grasping test; nociception evaluation; running velocity; walking track analysis. On D90, after being subjected to these evaluations, they were anesthetized as described above, and submitted to injection of retrogradely labelling neuronal markers. On D100, rats were submitted to infra-red thermography (**IRT**) of the palmar aspect of the forepaws, electroneuromyography (**ENMG**), and strength evaluation after direct MN stimulation. Subsequently, a median ventral thoracotomy was performed, and the left and right ventricles were catheterized with 20G silicone catheters. The rats were submitted to exsanguination and replacement of blood volume by heparinized saline injected through the left ventricle, followed by 300 ml of 4% paraformaldehyde in 0.1M PBS (pH 7.40).[52] Finally, both flexor carpis radialis muscles were harvested and weighted, and nerve tissue was collected for histomorphometrical

analysis using conventional stains, immunohistochemistry and fluorescence microscopy.[45]

Grasping Test: This test was used to assess motor recovery of the muscles controlled by the MN.[53] The rat was suspended by its tail over a grid, which it reflexively tried to grab. The rat was gently pulled by its tail with increasing strength until it loosened its grip. The rat was able to grab the grid only if the MN was functioning. Grasping strength was graded as follows: 0 – no grasping movement; 1- slight flexion of fingers, but with no significant grasping strength; 2- minimal grasping strength; 3- significant grasping strength but still inferior to the unaffected contralateral side; 4- normal grasping strength (equal to the contralateral, non-affected, limb).[53, 54]

Pin prick test: This test was used to evaluate nociception.[49, 55] In this test, the rats were placed on an elevated plastic platform with a 4x4 mm square grid pattern with 1.9 mm of length each. This grid was supported by a metallic frame that was 21-cm-tall. The grid was covered with a transparent plastic box with the following dimensions of 15.5x15.5x11cm.[49, 55] For each rat and evaluation point, rats were left on the platform covered by the plastic box for a few minutes until the exploratory and major grooming activities subsided. Subsequently, a number 4 Von Frey hair (bending force of 25g) was inserted through the mesh to poke the palmar aspect of the forepaw in its radial aspect, corresponding to the skin territory of the MN. The evaluation was considered correct only if the Von Frey filament bended.[56] Forepaws were evaluated

in turn, when the rat was stationary and standing on the four paws. A few seconds mediated each evaluation to minimize apparent behavioral responses to the previous stimulus. Ambulation and biting the filament were considered ambiguous responses, and in such cases the stimuli were repeated. Five measurements were made for each paw. Each time the following score was used: 0 – no response; 1 – the rat slowly takes the paw away from the Von Frey hair; 2 – the rat vigorously removes the forepaw from the Von Frey hair and/or licks the paw. Consequently, for each rat and time point, a nociceptive score was calculated as the sum of the responses to the five stimuli. This originated a value that ranged from 0 (no response for all noxious stimuli) to 10 (high response for all noxious stimuli).[39, 47, 49, 57-60]

Ladder rung walking test: This test was used to assess forelimb strength, stepping, placing, and co-ordination.[61] Rats were trained to run an inclined ladder of 120x9x2cm dimensions with 18 steps, of 1.5-cm-thickness and spaced 4 cm. The ladder was positioned with and inclination of approximately 10 degrees and led to a 13.20x11cm opening on a dark wooden box with 31.5x35x35cm of internal dimensions.

The rats were conditioned to run the ladder and enter the dark box on several training sessions that consisted of 5 trials each. In the first trials, the rats were positioned close to the box's door and guided in. For the subsequent 3 sessions, rats were progressively positioned further away from the box opening in each trial and persuaded to get in the box by gentle touching and/or pulling of tail's tip. Once inside the box, the sliding door closed the entrance and the rat was given a food treat. For the last trials,

rats would only receive a snack, if they walked through the ladder without stopping or hesitating. Finally, for the last 5 sessions performed before surgery, the time to complete the task was recorded. The examiner started the timer (precision of 1/100sec JUNSD®) once the animal started walking at the beginning of the ladder and stopped the timer when the rat's snout crossed the box's entrance. The test was considered valid, if the animal did not stop and did not hesitate during the task. After surgery, each evaluation session consisted of five trials, each separated by at least a one-minute interval. The time taken to complete each run was recorded.[45, 49, 55, 62]

Walking track analysis: This test was used to evaluate forelimb motor recovery.[63, 64] The experimental apparatus consisted of a confined walkway with 16.5 cm in height, 8.7 cm in width and 43 cm in length. This walkway lead to a rectangular opening with 8.8x8.2cm in one of the walls of a black wooden box with the dimensions of 23x36x28 cm. The box's entrance could be closed rapidly by a vertical sliding door. The box had a removable top that could be used to retrieve the rat. [63, 64]

Before the surgery, rats were trained to walk through the walkway until reaching the inside of the box. Particular attention was given to familiarize the rats with the noise of closing the sliding door. To positively condition rats, a food treat was given once the task was completed successfully. For the evaluations, the floor of the walkway was paved with graph paper (Ambar®). Rats forepaws were stained with methylene blue 1% W/V (Merck ®) with a painting brush. The rats were then led into the corridor. This test was done on every evaluation day and repeated as many times as needed until a representative print of both forepaws was obtained. [63, 64]

The following parameters were assessed for typical consecutive imprints of both forepaws (**Fig. 3**) [63]:

Stance factor: paw impression area on the paper sheet.

Print length factor: longest length of the paw impression.

Finger spread factor: widest width of the paw impression.

Intermediate finger spread factor: widest width between the second and third fingers.

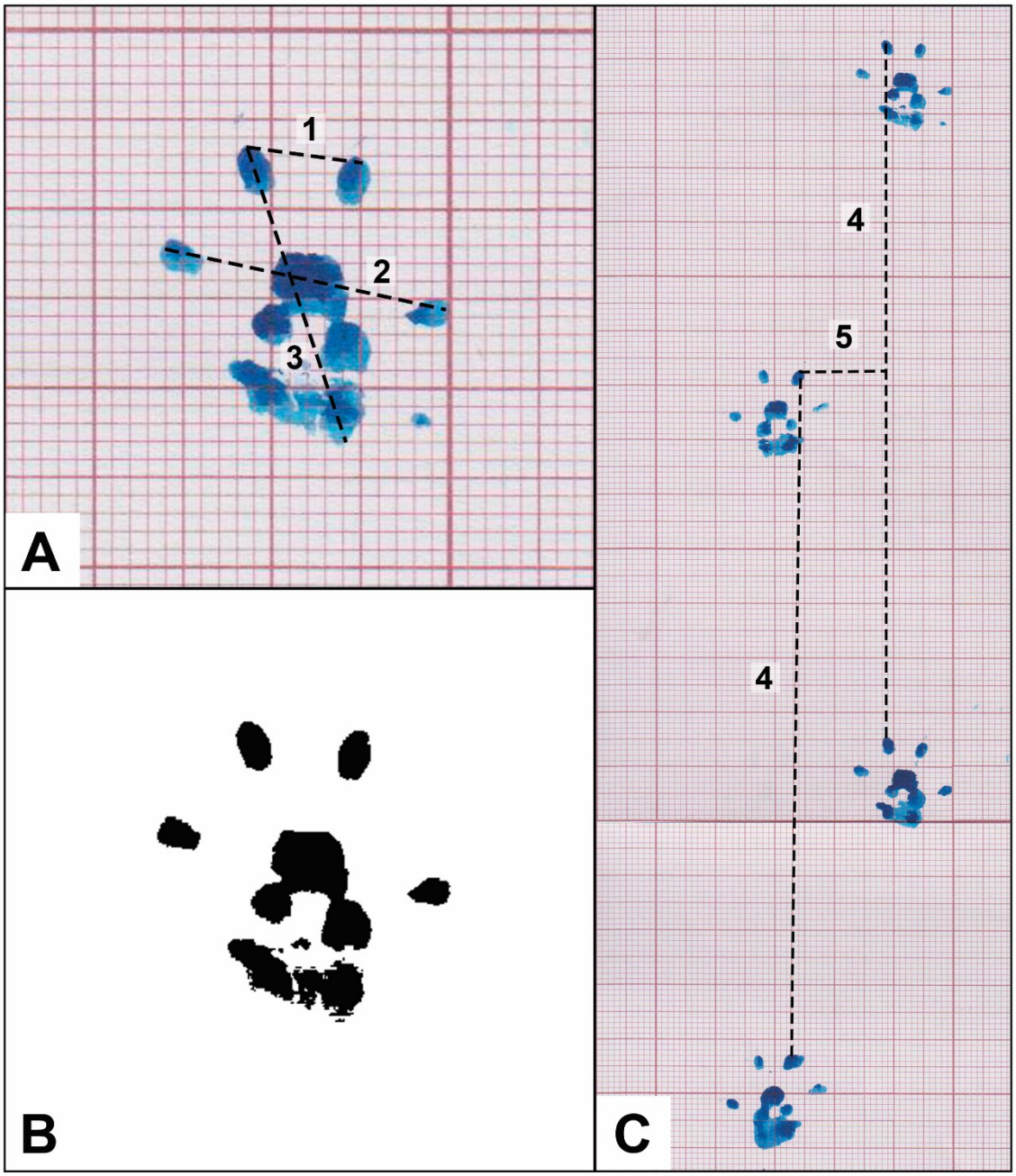

Figure 3 - Walking tracks measurements using forepaw impressions.

A. Photograph of a typical print of the left forepaw (uninjured).

B. Contrast-enhanced image of the photograph in Figure 3A, using the software Fiji®. Similar images were used for measurement purposes, namely of determination of the stance factor (paw impression area on the paper sheet)

C. Typical forepaw prints of a rat in the nerve graft group.

1, Intermediate finger spread factor: widest width between the second and third fingers; 2, Finger spread factor: widest width of the paw impression; 3, Print length factor: longest length of the paw impression; 4, Stride length: distance between homologous points of successive paw impressions on a given side; 5, Base of support: perpendicular distance between the central portion of the paw impression and the direction of movement.

Additionally, the following parameters were assessed in the two pairs of representative sequential bilateral paw impressions (**Fig. 3**) [63]:

Stride length: distance between homologous points of sequential paw impressions on a given side.

Base of support: perpendicular distance between the central portion of the paw impression and the direction of movement.[39, 49, 63]

Walking track analysis parameters were measured using the free software FIJI®.

Infra-red thermography (IRT) of the cutaneous territory of the median nerve: Thermography was used as a non-invasive surrogate marker of cutaneous denervation in the territory of the MN.[65-67] This assessment method was performed in the plantar territory of the MN on D100 after anesthetizing the rat.

The following aspects were taken into consideration before performing IRT:

- A room with a constant temperature, between 18ºC to 25ºC and without significant heat sources (such as computers or refrigerators). The room temperature and humidity was registered using a normal digital hydro-thermometer (TFA®) with a thermal resolution of 0.1º C.

- The animals were brought to the room where the acquisitions were going to be performed 2 hours prior to the evaluation to allow acclimatization to occur. After being anesthetized, rats were placed on a clean and stable surface away from reflective materials and other possible sources of artefacts. The rat's central temperature was also monitored during all evaluation using a digital thermometer (Electro® DH SA) with a thermal resolution of 0.1º C inserted 2 cm inside the rectum.

The temperature was assessed using a FLIR® E6 camera, which has an accuracy of ± 2º C within the ambient temperature range and a thermal sensitivity of <0.06° C. An IR resolution of 160 x 120 pixels interpolated on 320 x 240 resolution within the camera electronics. The camera was switched on 15 minutes before acquisition and was not switched off during the experiment. The emissivity parameter was set on the camera for that of the skin, ε=0.98.

Each rat was gently laid on its dorsum on a polyethylene sponge, and its forepaws carefully fixed in supination with double face glue tape. After 3 minutes, the camera was held at 90º angle and 30 cm distance from the rat, focusing the animal's body on the camera. Then, three acquisitions were made, spaced 30 seconds apart. In the end, the rectal thermometer was removed.

The acquired thermograms were transferred to a computer and analyzed using the free software FLIR Tools+ ®. The temperature of the plantar surface of both forepaws was measured defining a rectangular region of interest of 9 X 11 pixels in the plantar territory of the MN. The mean, maximum and minimal temperature values were exported to a ".CSV" document and later added to an Excel (Microsoft Office®) and SPSS 21.0 (IBM Statistics®) databases.

ENMG: This assessment was performed on D100 on both forelimbs. The authors ensured that rats were deeply anesthetized before starting the acquisition, to minimize variability associated with voluntary and/or involuntary movements autonomously produced by the experimental animal.[68] The evaluations were always performed by the two senior authors (D.C. and E.M.S), in the same room, and under the same controlled environmental conditions.[7, 68, 69]

The experimental setting was composed of BIOPAC MP35® hardware and a BSLM Stimulator®. The electrodes used for stimulation and recording were made by taping a pair of disposable acupuncture needles (0.25x25 mm Shenzhou® Acupuncture Needles) with a distance of 25 mm between them. The compound muscle action potentials (**CMAPs**) were recorded using the BSL PRO 3.7® software, adjusting settings to create an optimized template. The stimulator and electrodes were connected to the BIOPAC MP35. The channels were set up as follows: CH1 - Stimulator BSLSM to 0-10Volts); and CH2 - EMG to 30-1000 Hz. The signal was acquired at a sample rate of 50 kHz, at a

duration of 40.000 ms, amplified 1000X and filtered using a 30-1000 Hz band. The stimulation output was set for a single pulse with a duration of 1 ms.[7, 68, 69]

Under the surgical microscope and with the rat in dorsal decubitus, the MN was dissected free from the silicone rod and from the surrounding tissues. The flexor digitorum sublimis muscle was exposed on both forearms with a ventral longitudinal incision. The signal ground plug was connected by inserting the ground needle in the quadriceps femoris muscle of the left hindlimb. Starting with the right forepaw, the recording electrodes were put into the flexor digitorum sublimis muscle belly and the stimulation electrode hold proximally in the MN. Both electrodes were moistened with saline (Basi®). Initially, a stimulation amplitude of 10 mV was chosen by adjusting the stimulator knot and the CMAP was recorded. During the evaluation, the amplitude of stimulation was increased gradually in 10 mV steps until reaching 2000 mV. The same procedure was then repeated on the left forepaw.[7, 68, 69]

The following parameters were measured from CMPAs using measurement tools from the BSLPro 3.7® software:

- **Neurological Stimulation Threshold** - the minimum stimulus amplitude value to evoke a reproducible, stimulus correlated CMAP.

- **Motor Stimulation Threshold** - the minimum stimulus amplitude value to evoke a reproducible, stimulus correlated muscle contraction.

These last two parameters evaluate nerve regeneration, as there is a minimal number of nerve fibers required to produce either a CMAP or a visible muscle contraction.[70]

A minimal value of stimulation voltage after which the amplitude of CMAP did not increase further was registered for each rat. This value was increased by 20%, resulting in the supramaximal stimulation value. After this value was determined and the correspondent stimulus applied, the next CMAPs parameters were recorded:

- **Latency** – the time interval from the time of the electric stimulus to the first deviation from the baseline; assesses nerve conduction velocity in the fastest nerve fibers, that is to say the largest myelinated fibers.[69]
    - **Neuromuscular transduction velocity** – the quotient between electrode distance and latency
- **CMAP Amplitude** – the highest difference between the largest CMAP oscillation and baseline. This value evaluates the number of reinnervated motor units [64]
- **CMAP duration** - the interval of time during which the CMPA occurs. It assesses synchrony of muscle innervation, which is dependent on the degree of muscle reinnervation and myelination of the innervating motor fibers.[69, 71]

Wrist Flexion Strength Assessment: As wrist flexion is predominantly dependent on the MN, this evaluation was used on D100 to assess strength in this nerve's territory.

To assess wrist flexion strength the mentioned BIOPAC MP35®, BSLMA stimulator software® and stimulation electrodes were used to stimulate the MN. Using BSL PRO 3.7® software, the following parameters were adjusted to create a template for stimulation: the input channel CH1 was set as Stimulator-BSLSTM (0-10 Volts) and the output settings were selected for stimuli duration of 30 seconds with pulses of 1 ms duration and 1 Hz frequency. The amplitude of the pulses was adjusted on the stimulator knot for 1.5 V or 3 V according to the evaluation moment. A dynamometer, Sauter® FH 5, with a resolution of d=0.001 N was linked to a computer. The AFH-01® software was installed on the computer and linked to FH 5 dynamometer allowing real time visualization of data by building a plot of force per time (N/sec). This data was later imported to an excel sheet (Microsoft Office®) for analysis.[62]

With the rat anesthetized, a silk 5/0 stitch was passed through the second interosseous space. This stitch was associated with a 5-cm-long loop. The rat was put on its back and a self-retaining retractor used to expose the nerve. Starting with the right forepaw, the suture loop was placed in the dynamometer's hook and the forepaw aligned with the dynamometer, without putting too much strain on the suture line. The contralateral paw was fixed with tape to avoid extra movement interferences in the dynamometer readings. The stimulating electrodes were put proximally in the MN and wetted with saline (Basi®). The dynamometer was set to zero and the stimulator adjusted to a supramaximal amplitude stimulation of 1.5 V for 30 seconds. The same steps were done on the left forepaw. The data thus recorded with the AHF1 software® were imported into an Excel® (Microsoft Office™) datasheet. Maximum and average

force values and the area under the curve (**AUC**) for the strength X time graph were calculated for each evaluation.

Flexor carpi radialis (FCR) muscle weight: Being innervated exclusively by the MN, this muscle's weight was used to assess motor reinnervation in the territory of the MN. After euthanizing the rats as described above, the muscle was harvested on both sides from its origin until its distal tendon insertion. Both muscles were weighed using a precision scale, KERN770®, which had a precision of 0.1 mg.[45, 47]

Histological evaluation: The MN distally to the repair site and the middle portion of the nerve conduit used to bridge the defect were harvested after euthanasia. The specimens were fixed in 10% paraformaldehyde, and prepared for histological examination, using hematoxylin-eosin and Masson's trichrome stains, as well as immunohistochemistry for neurofilaments, peripherin and acetylcholinesterase (**Table 1**).[72-75]

Nerve fiber		Numerical classification of nerve fibers	Innervated structures / function	Nerve fiber diameter (µm)	Myelination	Conduction velocity (m/s)[76]
type	subtype					
A	α	Ia	Muscle spindle annulospiral receptor (main responsible for proprioception) Extrafusal skeletal muscle fibers (voluntary motor control)	12 - 22	Thickly myelinated	70 - 120
A		Ib	Golgi tendon organ (contractile force)	12 - 22	Thickly myelinated	70 - 120
A	β	II	Pressure, touch and vibration receptors of the skin (cutaneous mechanoreceptors sensibility) Muscle spindle flower spray receptors (secondary responsible for proprioception)	5 - 12	Thickly myelinated	30 - 70
A	γ	II	Intrafusal skeletal muscle fibers (muscle tone control)	2 - 8	Thickly myelinated	15 - 30
A	δ	III	Some nociceptors (sharp pain), cold receptors, most hair receptors (touch and pressure), some visceral receptors	1 - 5	Thinly myelinated	5 - 30
B	-	-	Preganglionic autonomic efferents	< 3	Thinly myelinated	3 - 15
C	-	IV	Most nociceptors (dull, aching pain), warmth receptors, some mechanoreceptors, itch receptors, some visceral receptors, postganglionic autonomic efferents	0.1-1.3	Nonmyelinated	0.6 - 2.0

Table 1 - Staining of the different types of nerve fibers using immunohistochemistry for neurofilaments (blue areas), acetylcholinesterase (red areas) and peripherin (yellow areas).[49, 77-80] Neurofilament staining marks virtually all nerve fibers. Acetylcholinesterase staining highlights mostly motor nerve fibers.[81] Most sympathetic nerve fibers are marked by peripherin staining. Fibers that do not stain by acetylcholinesterase and peripherin are predominantly myelinated sensory fibers.[79] The combination of these immunohistochemical methods roughly allows to functionally dissect peripheral nerves.[72]

Histomorphometric evaluation was performed independently by two blinded observers, using the software Fiji®. In cases of discrepancies superior to 5%, the histological sections were reviewed by the two observers. The following parameters were determined in the MN section immediately distal to the repaired nerve gap: cross section area in a transverse section, total number of nerve fibers (neurofilament positive), number of acetylcholinesterase positive nerve fibers, number of peripherin positive nerve fibers, number of acetylcholinesterase – and peripherin negative fibers. Furthermore, the vascular density in the middle of the reconstructed segment was also determined. Vascular density inside the reconstructed median nerve segment was determined based on counts of the vessels inside the epineurium, as the vessels over the epineurium mixed with the surrounding tissues in an indistinct manner, making the establishment of boundaries between the epineurium and surrounding tissues frequently impossible. [72, 82]

The number of structures inside nerve segments was calculated by the product of the cross-section area of the respective nerve segment (assessed on 4X amplification) and of the density of the structure of interest. Density was determined by counting the

average number of structures in 3 random 20X amplification fields and dividing this value by the area of that field. To avoid under or overestimation of structures number, structures included in counts only if the top upper edge of the structure was included in the microscopic field.[83, 84]

Retrograde neuron marking and fluorescence microscopy evaluation

On D90, after performing the functional examinations described above, and with the rat under anesthesia, 12 µl of 5% True Blue Diaceturate (**TB**, Sigma®) e 12 µl of 3% of Lucifer Yellow Dilithium salt (**LY**, Sigma®) were injected intradermally in the skin territory of the MN in the right hand (at the level of the radial hand pads) and in the right flexor carpis radialis muscle, respectively, using 27-gauge intradermic needles (BD Bioscience™).[40, 52, 85] This allowed to morphologically evaluate the sensory and motor reconstruction of the MN across the nerve gap.[40, 47, 86, 87]

On D100, after euthanizing the rat, the following structures were removed: MN proximal to the reconstructed MN, the C7 spinal cord segment in continuity with the dorsal and ventral C7 spinal nerve roots, and including the C7 dorsal root ganglion (**DRG**) on both sides. A left parasagittal section was made in the ventral surface of the spinal cord segment, in order to convey information on laterality. These nerve structures were immersed in 4% paraformaldehyde and 10% sucrose in 0.1 M phosphate buffered saline (**PBS**) at pH 7.4 for 48 hours for fixation. After fixation, the specimens were transferred into increasing concentrations of sucrose in PBS for at least 15 hours for each concentration (15% and 30%). The specimens were then frozen in liquid nitrogen.

Subsequently, transverse cryostat sections were cut at 20 µm for the DRG and the MN and at 50 µm for the spinal cord segments. These sections were then thaw-mounted on polylysine-coated glass slides.[88, 89]

Specimens were observed by epifluorescence under a fluorescence microscope.

The number of marked nerve fibers in the proximal aspect of the MN was assessed as described above. For each DRG, the number of True Blue labelled cells was semi quantitatively assessed by counting the fluorescent cells on what appears to be the largest cross section. For each C7 spinal cord, the region with greatest fluorescence in the ventral horn was searched with a 4X amplification. In this area, the average number of Lucifer Yellow stained cells was determined based on counts done in 3 random 20X-amplification fields.[40, 44]

Statistical analysis

Qualitative variables were expressed as percentages. Quantitative variables were expressed as means ± SD. IBM SPSS Version 21.0® software was used for descriptive and inferential statistical analysis. The Kolmogorov-Smirnov test was used to assess whether variables were distributed normally. Analysis of variance and t test were used to compare averages in normally distributed data. Kruskal-Wallis and Mann-Whitney tests were used to compare means in non-normally distributed data. Proportions were analyzed with the chi-square test or Fisher's exact test. Association between numerical variables was investigated using Pearson's correlation coefficient. Relationship between ordinal variables was evaluated with resort to Spearman Rank Correlation Coefficient. Kaplan Meier survival analysis was performed to identify differences between groups regarding time to recovery of a positive grasping test.

A two-tail value of $p<0.05$ was considered to be statistically significant.

RESULTS

Rat mortality was higher in the PNF group:

The total number of rats reaching the end of the experiment was 87. These animals were distributed in the experimental groups as follows: 17 in the Sham group; 17 in the Excision group; 10 in the NG group; 20 in the CNF group; 15 in the ANVF group; and 8 in the PNF group (**Table 2**). All rats died in the perioperative period (<48 hours after surgery). Mortality rate was higher in the PNF group than in the remaining experimental groups (60% versus 21%; $p<0.05$). In the former group, 10 deaths occurred in the first 24 hours after the first surgery, and the remaining 2 deaths in the day after the second surgery. In all the deceased animals in all experimental groups, necropsy examination revealed signs of hematoma and hypovolemia.

Daily observation of rats did not reveal signs of distress:

General health and behavior of the experimental animals was adequate throughout the experiment. All rats presented moderate to high levels of activity, grooming themselves regularly. None of the animals presented autophagy or self-mutilation. The surgical wounds healed uneventfully. Skin ulcers were not observed on the operated paws.

Animal weight gain did not vary significantly among the experimental groups:

At the end of the experiment, the average weight gain was 79.4% ± 4.9% for the Sham group; 74.2% ± 3.8% for the Excision group; 83.3% ± 6.2% for the NG group; 74.0% ± 6.8% for the CNF group; 75.3% ± 7.6% for the ANVF group; and 79.9% ± 6.1% for the PNF group. These differences were not statistically significant (**Table 2**).

Parameter		Sham group	Excision group	NG group	CNF group	ANVF group	PNF group	Relevant findings
Mortality		15%	15%	50%	0%	25%	60%	Mortality rate was higher in the NG and the PNF groups than in the remaining experimental groups ($p<0.05$)
Animal weight gain (%)		79.4 ± 4.9	74.2 ± 3.8	83.3 ± 6.2	74.0 ± 6.8	75.3 ± 7.6	79.9 ± 6.1	No significant differences
Time to recovery of grasping (days)		0 (immediately after surgery)	87.31 ± 4.41	75.00 ± 5.86	45.75 ± 2.98	34.00 ± 2.30	97.50 ± 1.53	Fastest recovery of grasping was observed in the CNF and ANVF groups ($p<0.001$)
	D30	4.00 ± 0.00	0.00 ± 0.00	0.00 ± 0.00	0.60 ± 0.82	0.67 ± 0.62	0.00 ± 0.00	On D90, grasping

Average grasping strength	**D45**	4.00 ± 0.00	0,06 ± 0.24	0.00 ± 0.00	1.10 ± 1.02	1.60 ± 0.51	0.00 ± 0.00	strength was greater in the CFN and ANVF than in the Excision, Nerve graft and PNF groups
	D60	4.00 ± 0.00	0.18 ± 0.39	0.60 ± 0.70	2.30 ± 1.13	2.60 ± 1.05	0.00 ± 0.00	
	D75	4.00 ± 0.00	0.29 ± 0.47	0.80 ± 0.63	3.00 ± 1.01	2,80 ± 1.01	0.00 ± 0.00	
	D90	4.00 ± 0.00	0.35 ± 0.49	1.30 ± 0.95	3.80 ± 0.41	3.80 ± 0.41	1.50 ± 1.20	
Running Velocity in the ladder (cm/s)	**D30**	57.17 ± 31.02	21.10 ± 6.17	15.29 ± 13.14	32.06 ± 13.30	31.81 ± 9.93	15.51 ± 6.24	On D90 there were no statistical significant differences between sham and the CNF, the ANVF and the PNF groups
	D45	58.74 ± 37.33	21.65 ± 6.57	15.32 ± 4.76	29.54 ± 7.22	34.12 ± 4.80	28.08 ± 9.85	
	D60	60.26 ± 39.96	21.56 ± 4.85	29.42 ± 12.97	40.96 ± 10.60	35.76 ± 8.62	39.66 ± 17.53	
	D75	64.63 ± 36.08	23.48 ± 4.86	30.91 ± 22.98	43.13 ± 8.36	48.88 ± 11.61	35.06 ± 7.23	
	D90	63.34 ± 31.58	23.30 ± 5.05	39.83 ± 14.33	54.46 ± 19.13	56.71 ± 10.21	39.23 ± 14.05	
Pin Prick test (%)	**D30**	97.05 ± 4.70	5.88 ± 9.39	21.71 ± 12.10	39.18 ± 44.54	75.06 ± 18.74	2.50 ± 4.63	On D90, the best results were observed in the Sham, CNF and the ANVF groups ($p<0.001$)
	D45	107.67 ± 9.12	18.69 ± 21.89	19.11 ± 16.82	69.86 ± 27.93	82.17 ± 13.80	24.17 ± 22.51	
	D60	102.21 ± 4.91	13.33 ± 4.46	20.44 ± 6.73	93.89 ± 20.12	83.33 ± 14.80	35.07 ± 3.17	
	D75	93.33 ± 5.09	16.74 ± 7.90	40.00 ± 29.06	93.00 ± 4.70	94.01 ± 8.28	37.57 ± 27.04	
	D90	100.20 ± 6.47	7.84 ± 10.95	42.00 ± 18.14	87.24 ± 17.63	107.03 ± 29.20	48.21 ± 29.81	

Table 2 - Mortality, weight gain, grasping test, ladder running test and pin prick test results throughout the experiment.

NG, nerve graft; **CNF**, conventional nerve flap; **ANVF**, arterialized neurovenous flap; **PNF**, prefabricated nerve flap

D, day after the beginning of the experiment

Average grasping strength was evaluated semi quantitatively using a scale of 0 to 4 (0, no grasping; 1, flexes fingers only without opposition; 2, flexes fingers against minimal opposition; 3, flexes fingers against opposition but with less strength than the contralateral limb; 4, flexes fingers with the same strength as the contralateral limb.

Pin prick test results are expressed as percentages of the average contralateral values.

Numeric variables are expressed as average ± standard deviation.

The Grasping Test revealed faster and more complete motor recovery in the CNF and in the ANVF groups than in the NG group:

Recovery of grasping occurred in the immediate postoperative period in all rats in the Sham Group. In all other groups, no grasping was observed immediately after surgery (**Fig. 4**). Fastest recovery of grasping was observed in the CNF and ANVF groups ($p<0.001$). At the end of the experiment, grasping strength was greater in the CFN and ANVF than in the Excision, Nerve graft and PNF groups (**Fig. 5**). In fact, on D90, there were no statistically significant differences between the CNF, ANVF and the Sham groups (**Fig. 5**).

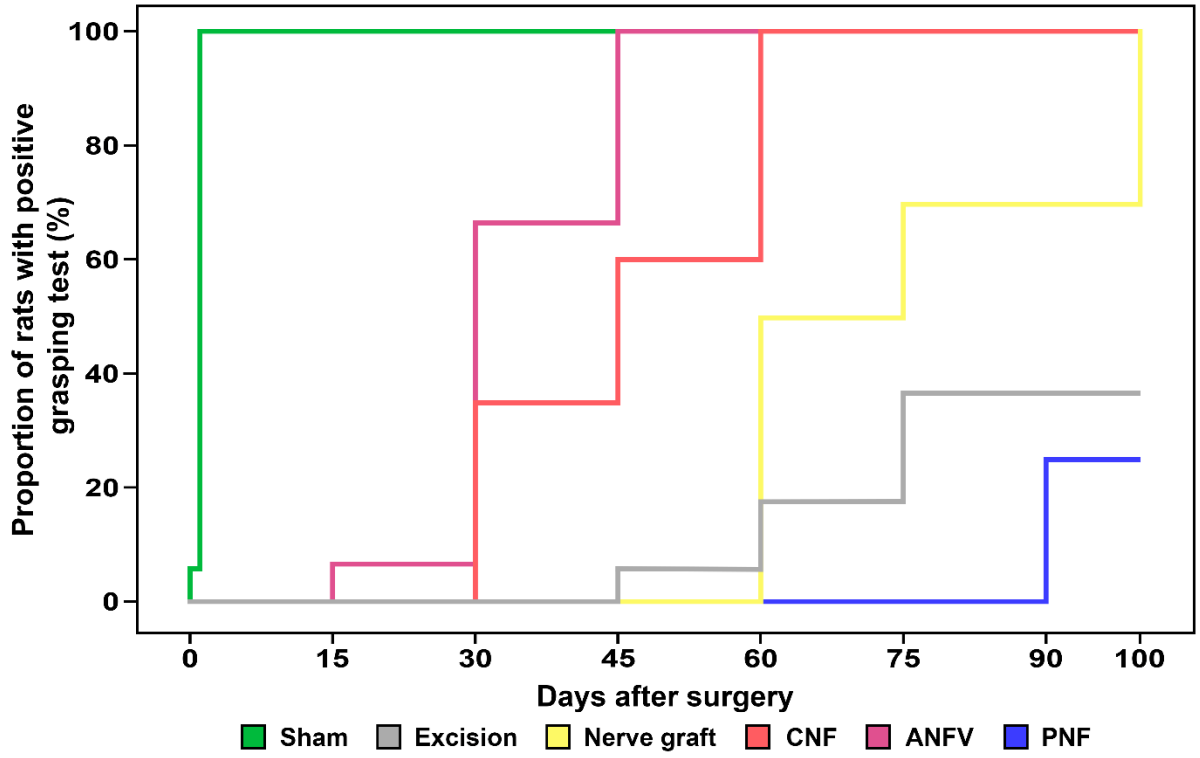

Experimental Group	Time to recovery of grasping in days (average ± standard deviation)
Sham	0 (immediately after surgery)
Excision	87.31 ± 4.41
Nerve Graft	75.00 ± 5.86
Conventional Nerve Flap (CNF)	45.75 ± 2.98
Arterialized Neurovenous Flap (ANF)	34.00 ± 2.30
Prefabricated Nerve Flap (PNF)	97.50 ± 1.53

Figure 4 - Time to recovery of grasping in the operated limb.

Fastest recovery of grasping was observed in the CNF and ANVF groups ($p<0.001$).

CNF, conventional nerve flap; **ANVF**, arterialized neurovenous flap

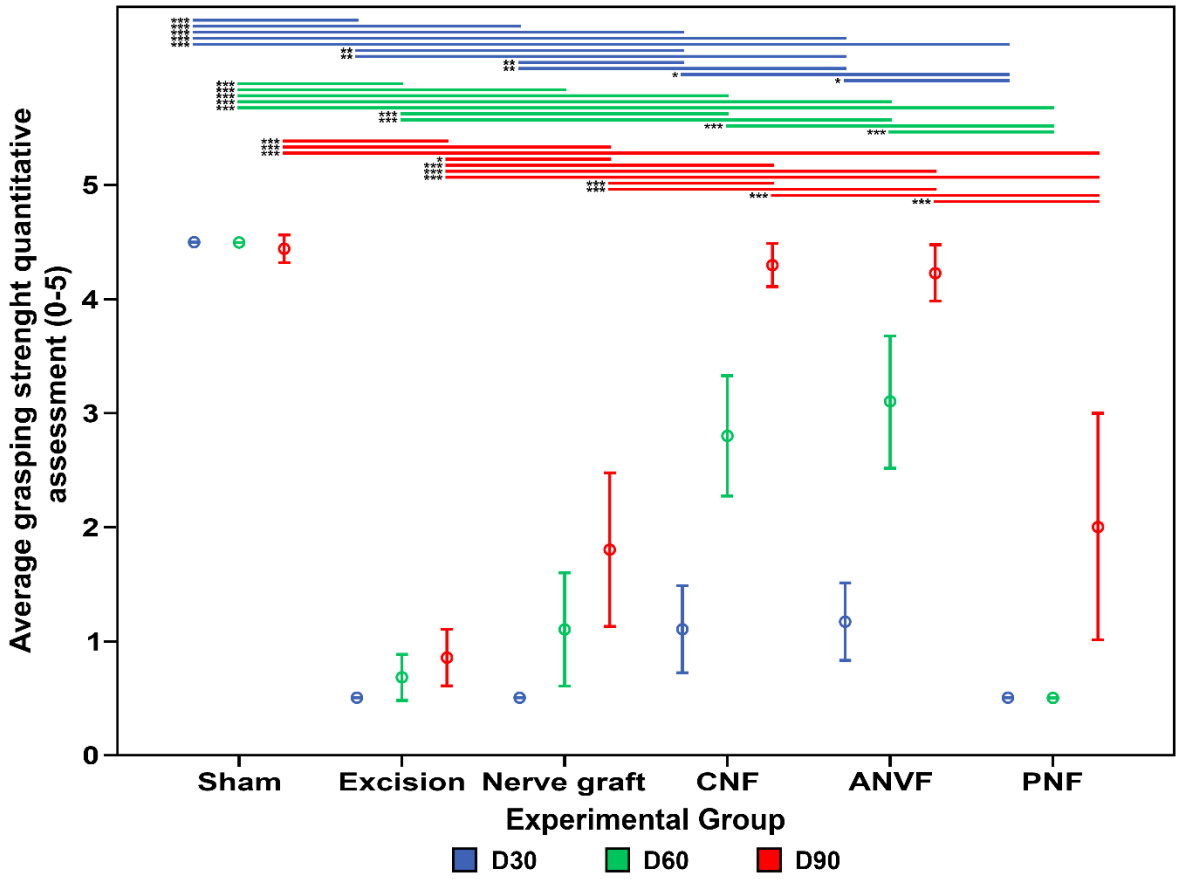

Figure 5 - Qualitative assessment of grasping strength in the operated limb in the different experimental groups 30, 60 and 90 days after the reconstruction of the median nerve gap. Vertical bars represent 95% confidence intervals.

Horizontal lines in the upper portion of the figure indicate statistically significant differences between groups ($p<0.05$).

*, $p<0.05$; **, $p<0.01$; ***, $p<0.001$

Running Ladder Test revealed comparable velocities at the end of the experiment between the Sham group and the CNF, the ANVF, and the PNF:

On D15, the average velocity in the running ladder test was greater in the Sham group than in all other groups ($p<0.01$; **Fig. 6**; **Table 2**). The superiority of this group was maintained until D60. From this time on, there was no statistical difference between this group and the CNF and PNF groups. On D90 there were no statistical significant differences between sham and the CNF, the ANVF and the PNF groups. At the end of the experiment, the CNF and ANVF groups presented better average velocities than the NG group but these differences were not statistically significant (**Fig. 6**).

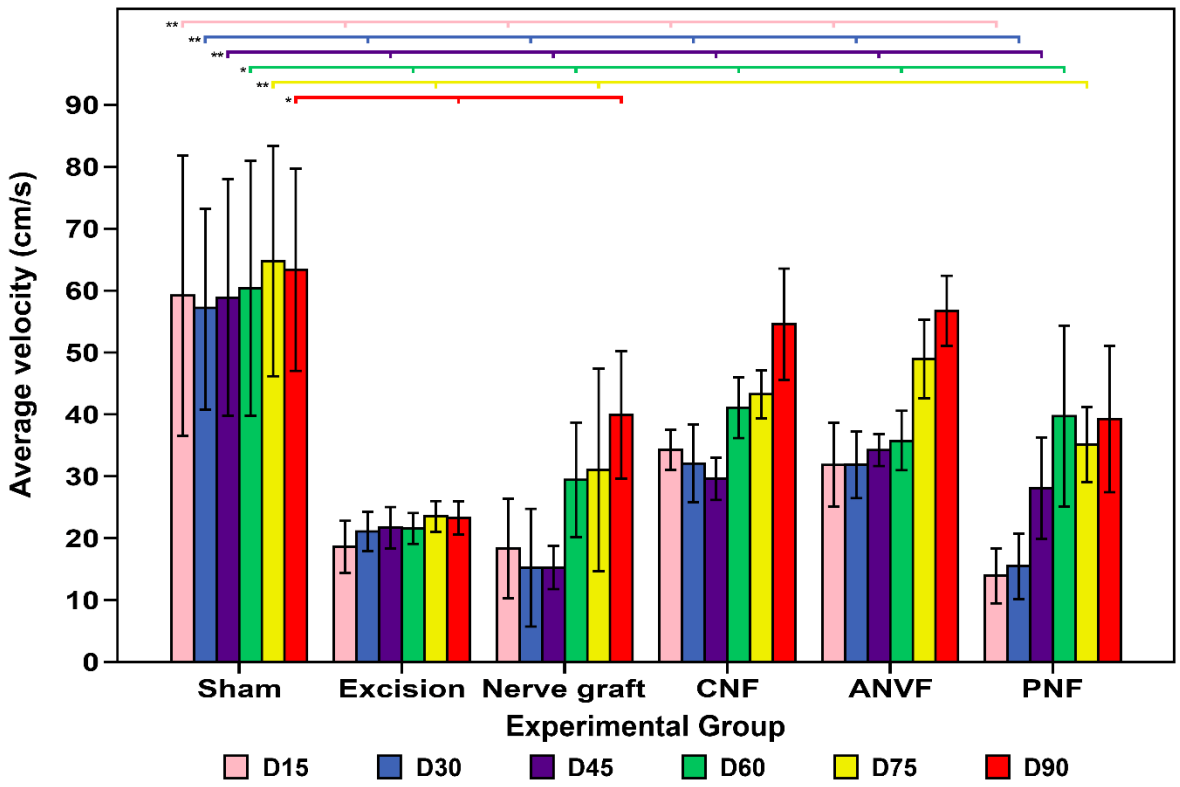

Figure 6 - Average velocity in the ladder running test in the different experimental groups during the experiment.

Vertical bars represent 95% confidence intervals.

Horizontal lines in the upper portion of the figure indicate statistically significant differences between groups on the 90^{th} day postoperatively ($p<0.05$).

*, $p<0.05$; **, $p<0.01$; ***, $p<0.001$

Pin prick test revealed better nociceptive recovery in the CNF and ANVF groups:

Thirty days after surgery, the ANVF group presented the best average sensory recovery in the Pin Prick test, showing no statistical significant difference relatively to the Sham group (**Fig. 7**; **Table 2**). On D60 and D90, the best results were observed in the Sham, CNF and the ANVF groups. The latter two groups presented average scores significantly superior to those observed in the NG and PFN groups ($p<0.001$; **Fig. 7**).

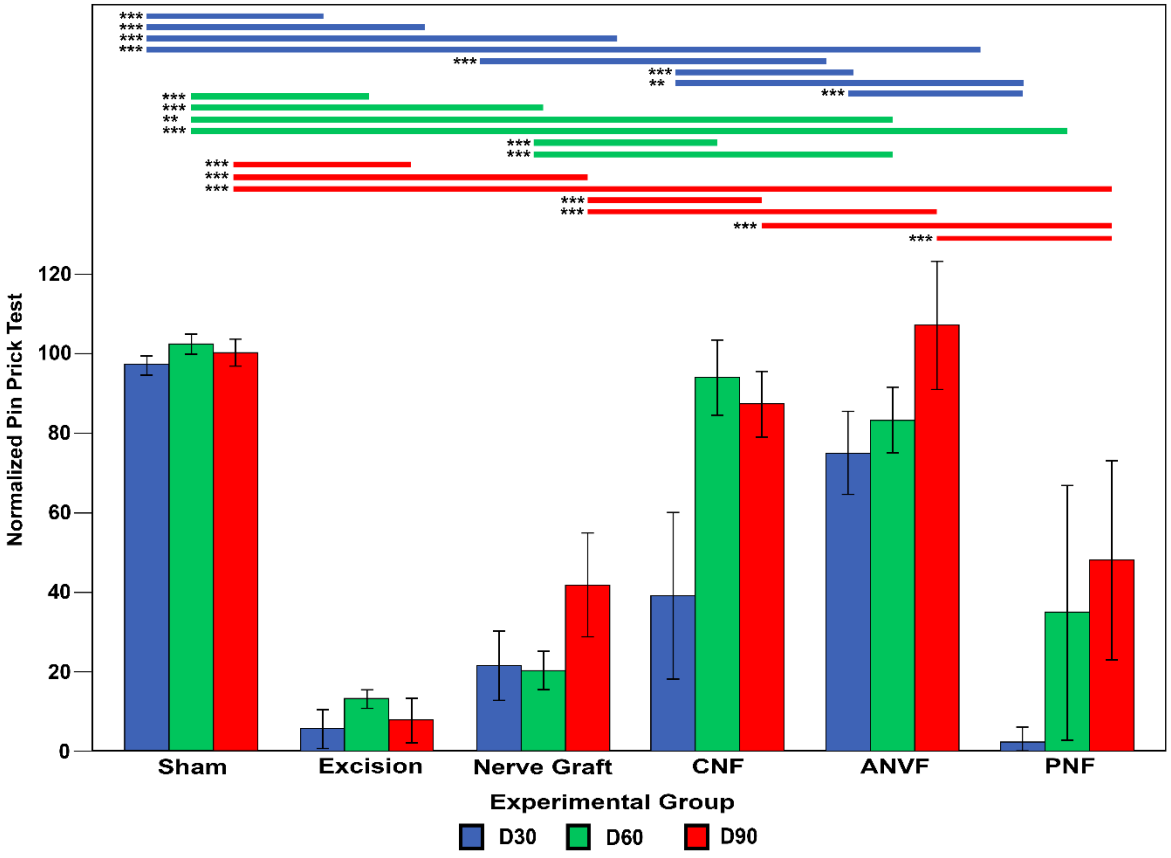

Figure 7 - Nociceptive evaluation using cumulative pin prick test results in the operated forelimb normalized to the contralateral limb in the different experimental groups throughout the experiment. Vertical bars represent 95% confidence intervals.

Horizontal lines in the upper portion of the figure indicate statistically significant differences between experimental groups ($p<0.05$).

**, $p<0.01$; ***, $p<0.001$.

Walking Track Analysis revealed that the rate of radial deviation was lower in groups in which a vascularized nerve conduit was used:

On D30 the CNF group presented a better normalized stance factor than the excision, NG and PNF groups ($p<0.001$; **Fig. 8A**; **Table 3**). Subsequently, no statistically significant differences were found between groups. The average normalized print length in the operated limb was higher in the CNF, ANVF and PNF than in the NG on D30. On D60 no differences were found between groups. On D90, CNF and PNF presented better results than the ANVF group regarding the normalized print length (**Fig. 8B**). Pertaining to normalized finger spread and intermediate finger spread, on D30, better results were observed in the groups using vascularized conduits compared to the NG group ($p<0.05$; **Figs. 8C** and **D**). However, at the end of the experiment these differences were no longer visible. Finally, stride analysis failed to reveal meaningful differences between the different groups (**Figs. 8E** and **8F**).

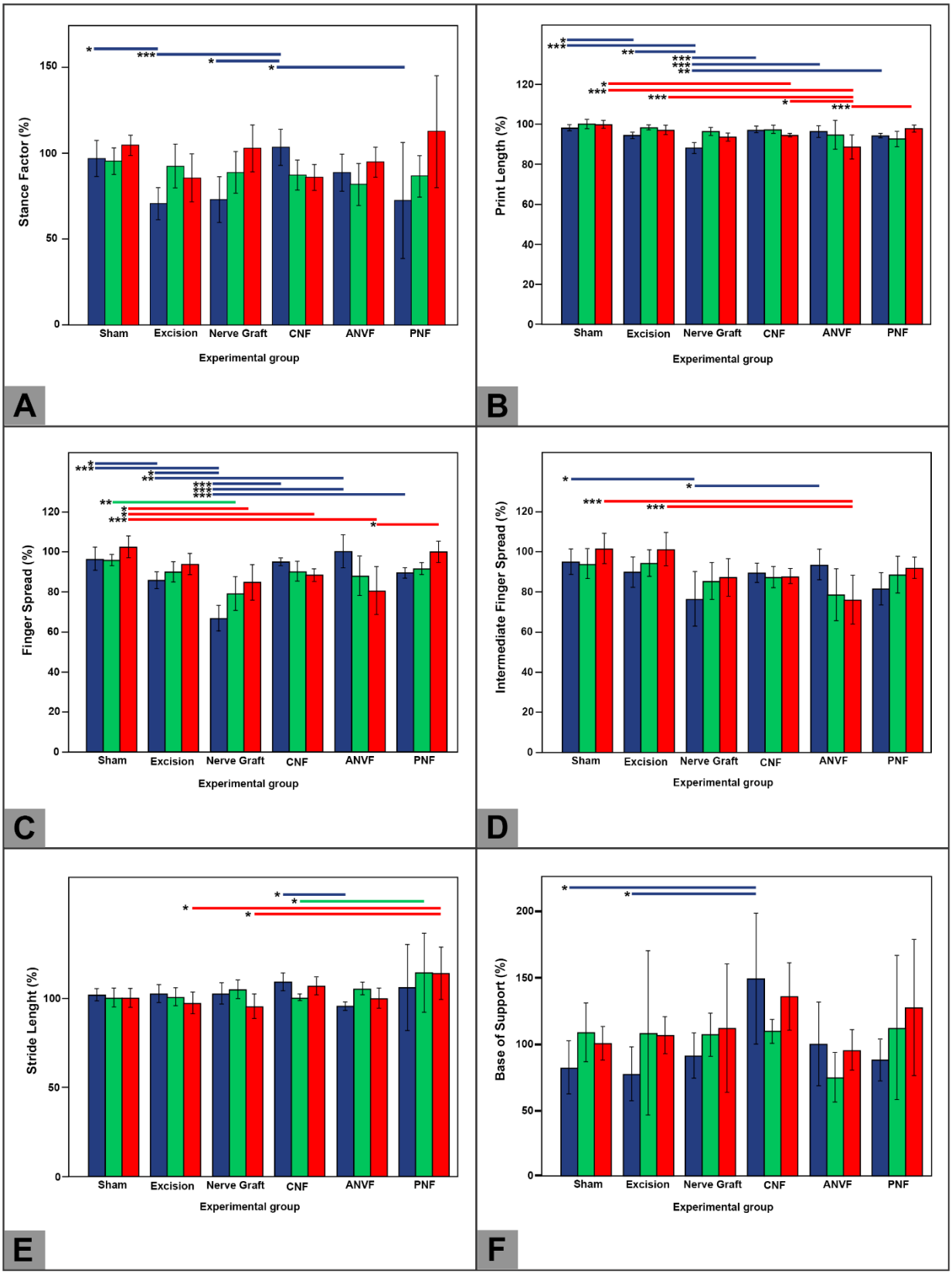
A
Stance Factor (%)
0
50
100
150
Sham
Excision
Nerve Graft
CNF
ANVF
PNF
Experimental group
B
Print Length (%)
0
20
40
60
80
100
120
Sham
Excision
Nerve Graft
CNF
ANVF
PNF
Experimental group
C
Finger Spread (%)
0
20
40
60
80
100
120
Sham
Excision
Nerve Graft
CNF
ANVF
PNF
Experimental group
D
Intermediate Finger Spread (%)
0
20
40
60
80
100
120
Sham
Excision
Nerve Graft
CNF
ANVF
PNF
Experimental group
E
Stride Lenght (%)
0
50
100
Sham
Excision
Nerve Graft
CNF
ANVF
PNF
Experimental group
F
Base of Support (%)
0
50
100
150
200
Sham
Excision
Nerve Graft
CNF
ANVF
PNF
Experimental group
D30
D60
D90

Figure 8 - Walking track analysis of the right forelimb (operated paw) of rats in the different experimental groups throughout the experience. Values are expressed as percentages of averages normalized to the contralateral side.

A, Stance factor. B, Print length; C, Finger spread factor; D, Intermediate finger spread factor; E, Stride length; F, Base of support.

Vertical bars represent 95% confidence intervals.

Horizontal lines in the upper portion of the figure indicate statistically significant differences between experimental groups ($p<0.05$).

*, $p<0.05$; **, $p<0,01$; ***, $p<0.001$

Parameter		Sham group	Excision group	NG group	CNF group	ANVF group	PNF group	Relevant findings
Stance factor (%)	D30	97.02 ± 20.42	70.57 ± 18.01	70.91 ± 18.64	103.34 ± 22.69	88.72 ± 19.44	72.39 ± 40.35	On D30 the CNF group presented a better normalized stance factor than the excision, NG and PNF groups ($p<0.001$)
	D45	100.65 ± 14.18	120.18 ± 40.80	77.85 ± 28.34	114.91 ± 21.08	100.93 ± 15.61	106.07 ± 10.93	
	D60	95.37 ± 14.98	87.47 ± 20.83	88.79 ± 16.99	88.79 ± 16.99	81.82 ± 22.12	86.66 ± 14.66	
	D75	98.75 ± 16.03	92.59 ± 24.66	77.08 ± 35.73	77.08 ± 35.73	87.24 ± 25.43	86.70 ± 17.38	
	D90	104.56 ± 11.47	85.63 ± 27.23	102.87 ± 19.10	85.77 ± 16.12	94.79 ± 15.80	112.55 ± 38.97	
Print length (%)	D30	98.24 ± 2.95	94.41 ± 3.31	88.18 ± 3.84	97.45 ± 3.45	93.38 ± 5.19	94.35 ± 5.19	On D30 print length was higher in the CNF, ANVF and PNF groups than in the NG group on D30 ($p<0.01$)
	D45	99.19 ± 5.21	97.15 ± 5.36	91.11 ± 2.19	96.59 ± 3.02	95.52 ± 13.62	99.56 ± 4.00	
	D60	100.16 ± 4.44	98.45 ± 2.45	96.40 ± 2.85	97.46 ±4.39	94.79 ± 12.94	92.72 ± 4.55	
	D75	99.98 ± 5.19	97.21 ± 5.10	95.64 ± 3.21	95.29 ± 2.86	88.66 ± 16.80	98.93 ± 4.21	
	D90	100.00 ± 4.00	97.18 ± 4.49	93.63 ± 2.80	94.51 ± 1.92	88.70 ± 10.85	97.88 ± 2.13	
Finger spread (%)	D30	96.16 ± 10.83	85.58 ± 8.05	66.72 ± 8.75	94.71 ± 4.20	99.98 ± 14.70	89.15 ± 3.24	On D30 the CNF, ANVF, and PNF groups presented better results than the NG group ($p<0.05$)
	D45	94.21 ± 4.06	90.20 ± 9.69	79.64 ± 7.01	87.96 ± 7.68	95.87 ± 21.38	98.35 ± 10.43	
	D60	95.61 ± 5.28	89.70 ± 9.74	78.94 ± 11.59	89.99 ± 10.54	87.75 ± 19.14	91.37 ± 3.60	
	D75	111.47 ± 38.51	106.03 ± 45.96	86.89 ± 5.78	87.87 ± 7.67	86.31 ± 26.29	95.13 ± 5.03	
	D90	102.07 ± 10.52	93.57 ± 10.37	84.57 ± 12.18	88.11 ± 6.71	80.42 ± 23.16	99.63 ± 6.74	

Parameter		Sham group	Excision group	NG group	CNF group	ANVF group	PNF group	Relevant findings
Intermediate finger spread (%)	D30	94.58 ± 12.14	89.42 ± 14.37	76.13 ± 18.89	89.09 ± 10.04	93.15 ± 13.70	81.21 ± 9.56	On D30 the CNF, ANVF, and PNF groups presented better results than the NG group ($p<0.05$)
	D45	89.93 ± 8.65	88.23 ± 14.16	77.92 ± 15.33	87.89 ± 14.93	91.15 ± 24.47	96.22 ± 8.38	
	D60	95.61 ± 5.28	89.70 ± 9.74	78.94 ± 11.59	89.99 ± 10.54	78.22 ± 24.92	88.14 ± 10.83	
	D75	102.32 ± 10.46	80.44 ± 26.49	85.18 ± 7.51	87.74 ± 15.62	78.67 ± 31.31	94.30 ± 12.43	
	D90	102.07 ± 10.52	93.57 ± 10.37	84.57 ± 12.18	88.11 ± 6.71	93.63 ± 6.34	91.53 ± 6.37	
Stride length (%)	D30	102.11 ± 6.80	102.86 ± 9.79	102.93 ± 8.39	109.47 ± 10.52	95.86 ± 4.09	106.26 ± 29.08	No significant differences between experimental groups
	D45	105.44 ± 12.32	103.59 ± 10.12	109.39 ± 14.56	116.24 ± 13.17	111.60 ± 32.18	101.15 ± 5.96	
	D60	100.66 ± 10.50	101.05 ± 9.82	105.18 ± 7.52	100.69 ± 3.95	105.63 ± 6.43	114.53 ± 26.66	
	D75	100.14 ± 7.62	95.74 ± 12.45	100.67 ± 15.26	102.40 ± 12.81	99.84 ± 8.70	111.28 ± 11.85	
	D90	100.40 ± 10.31	97.58 ± 12.05	95.74 ± 9.62	107.22 ± 10.75	100.37 ± 10.35	114.25 ± 17.68	
Base of support (%)	D30	82.16 ± 38.70	77.42 ± 39.42	91.22 ± 23.90	149.03 ± 10.49	99.97 ± 56.78	87.93 ± 18.65	No significant differences between experimental groups
	D45	74.38 ± 26.77	131.15 ± 58.52	82.24 ± 13.51	123.14 ± 47.25	108.52 ± 25.71	105.10 ± 47.60	
	D60	108.78 ± 42.96	108.13 ± 20.38	107.00 ± 22.48	109.57 ± 18.87	75.00 ± 33.74	112.26 ± 64.79	
	D75	87.68 ± 32.12	70.16 ± 26.24	138.07 ± 75.83	84. 88 ± 20.40	173.19 ± 87.47	135.91 ± 84.45	
	D90	100.63 ± 24.07	106.52 ± 27.14	111.80 ± 67.69	135.57 ± 53.80	95.20 ± 28.02	127.17 ± 61.37	
Presence of radial deviaion (%)	D30	0	94.1	100	40	13.3	0	For each time point, the rate of radial
	D45	0	100	100	20	13.3	0	

	D60	0	100	100	0	20	0	deviation was lower in groups in which a vascularized nerve conduit was used compared to the NG group ($p<0.001$)
	D75	0	100	70	0	20	0	
	D90	0	100	30	0	20	0	

Table 3 - Walking track analysis results throughout the experiment.

NG, nerve graft; **CNF**, conventional nerve flap; **ANVF**, arterialized neurovenous flap; **PNF**, prefabricated nerve flap

D, day after the beginning of the experiment

Numeric variables are expressed as average ± standard deviation.

Radial deviation of the operated forepaw print was present on D30 in 94.1% of the rats in the Excision group, 100% of the rats in the NG group, 40% of those in the CNF group, and 13.3% in ANVF (**Figs. 9A** and **9B**). On D60, 100% of the rats in the Excision and the NG groups presented radial deviation, while only 20% of the rats in the ANVF group presented radial deviation. From D60 on, no radial deviation was observed in the CNF group. On D90, radial deviation was observed in 100% of the Excision group, 30% of the NG group, and 20% of the ANVF group (**Fig. 9C**). Radial deviation was never observed in the animals in the Sham and in the PNF groups. For each assessment day, the rate of radial deviation was lower in the groups in which a vascularized nerve conduit was used compared to the NG group ($p<0.001$).

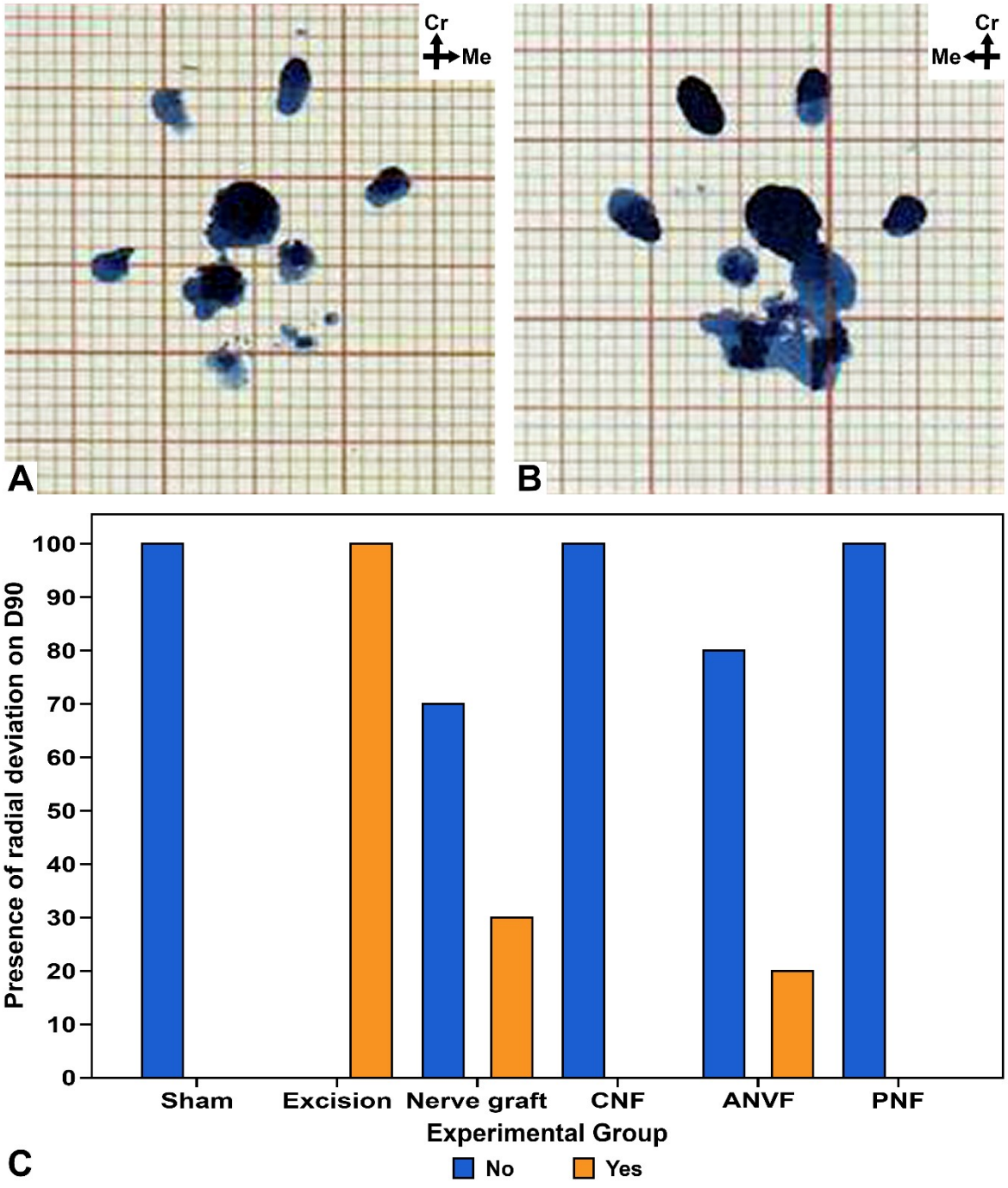

Figure 9 - Presence of radial deviation in the walking tracks of the operated forepaws in the different experimental groups at the end of the experiment. A, Left forepaw print of a rat in the nerve graft group, showing a normal

impression. B, Right forepaw print of the same rat, showing radial deviation of the paw. C, Bar graph showing the proportion of rats with radial deviation of the operated forepaws at the end of the experiment.

Thermographic assessment failed to show differences between groups:

IRT of the skin of the MN territory in the right forepaw revealed an average normalized temperature of 99.4% ± 5.9%; 101.7% ± 7.1%; 104.9% ± 13.7%; 101.8% ± 8.0%; 103.6% ± 7.2%; and 109.0% ± 10.8% in the Sham, Excision, NG, CNF, and PNF groups, respectively, compared to the contralateral side (**Fig. 10; Table 4**). These differences were not statistically significant. Analogously, no differences were found pertaining to the maximal and minimal temperatures on the surface of the forepaws (**Table 4**).

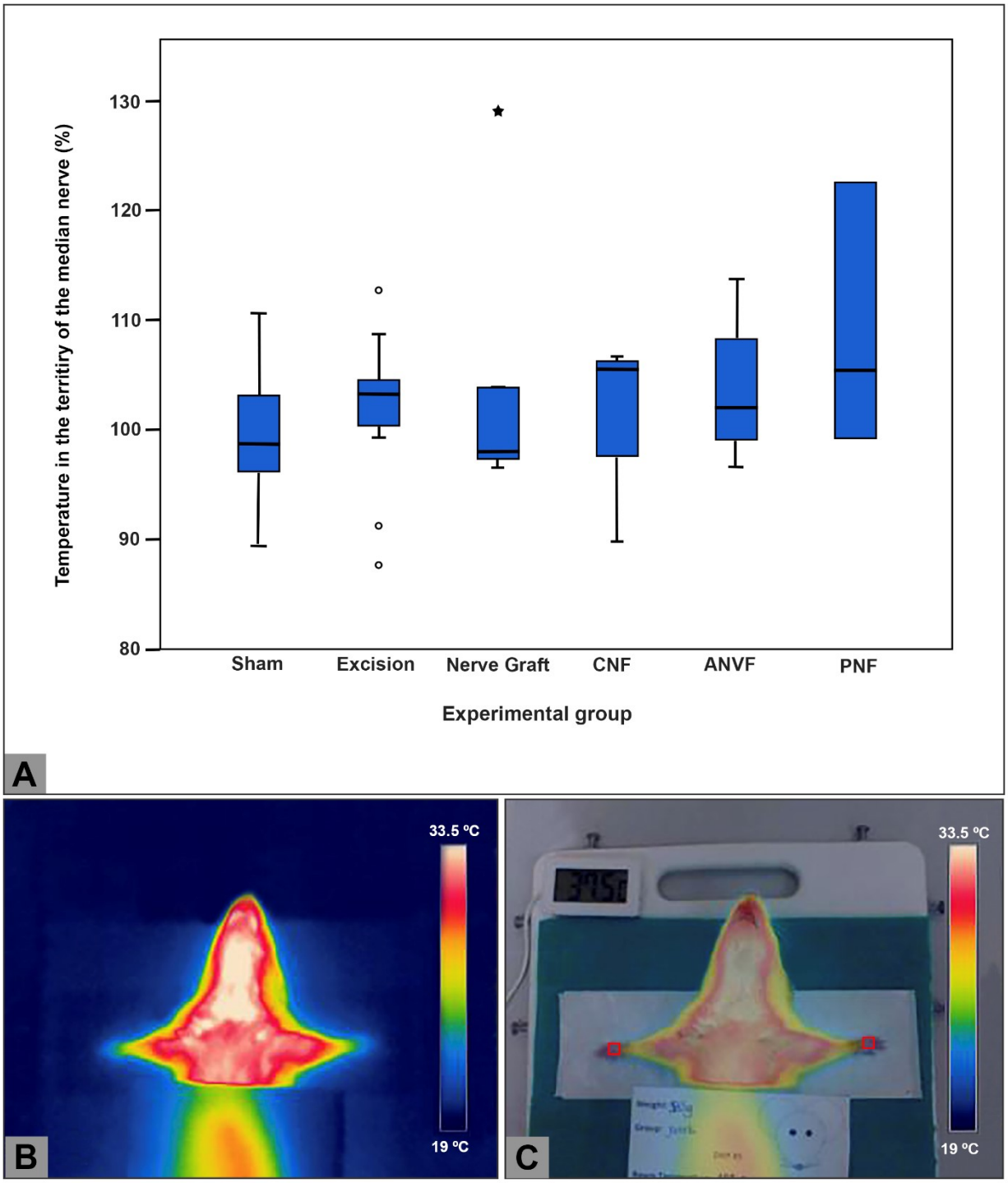

Figure 10 - Temperature on the surface of the skin territory of the median nerve.

A. Boxplot graphic illustrating the average temperature in the skin territory of the right median nerve relatively to that of the contralateral side. Temperature measurements were made using infra-red thermography.

B. Typical thermography image.

C. Image resulting from the overlap of the thermography image and of the digital photographic image. This allows to evaluate the temperature in the territory of the median nerve.

Parameter	Sham group	Excision group	NG group	CNF group	ANVF group	PNF group	Relevant findings
Forepaw average temperature (%)	99.4 ± 5.9	101.7 ± 7.1	104.9 ± 13.7	101.8 ± 8.0	103.6 ± 7.2	109.0 ± 10.8	No significant differences between experimental groups
Forepaw minimal temperature (%)	100.45 ± 5.49	102.25 ± 7.04	105.47 ± 14.34	102.45 ± 8.39	104.36 ± 7.83	108.61 ± 11.58	No significant differences between experimental groups
Forepaw maximal temperature (%)	98.86 ± 6.43	99.97 ± 6.41	101.44 ± 6.94	100.42 ± 6.74	100.63 ± 3.17	107.03 ± 5.04	No significant differences between experimental groups

Table 4 - Infra-red thermography evaluation of the region of the forepays innervated by the median nerve 90 days postoperatively.

NG, nerve graft; **CNF**, conventional nerve flap; **ANVF**, arterialized neurovenous flap; **PNF**, prefabricated nerve flap

D, day after the beginning of the experiment

Numeric variables are expressed as average ± standard deviation.

Electroneuromyographic assessment revealed a lower motor stimulation threshold in the CNF and ANVF than in the NG group:

On D90, the normalized neurological stimulation threshold was significantly higher in the Excision group than in the remaining groups ($p<0.001$; **Fig. 11A; Table 5**). In fact, no reproducible CAMP was obtained in the former group. No other differences were found relatively to normalized neurological stimulation threshold in the other groups. However, regarding the normalized motor stimulation threshold, the lowest values were obtained in the Sham group ($p<0.01$; **Fig. 11B**). Lower values were obtained in the CNF and the ANVF groups than in the NG group ($p<0.001$; **Fig. 11B**). No statistically significant differences were found in the latency and neuromuscular transduction parameters between the Sham group and the groups submitted to nerve gap reconstruction (**Figs. 11 C** and **D**). Pertaining to the CMAP amplitude, higher values were obtained in the Sham group (110.63% ± 45.66%) than in the other groups submitted to nerve gap reconstruction ($p<0.05$; **Fig. 11E**). These values were higher in the CNF group (69.53% ± 13.80%), in the ANVF group (73.34% ±22.86%) and the PNF group (71.68% ± 23.56%) than in the NG group (41.60% ± 24.4%). However, these differences did not meet statistical significance. Apart from a longer CMAP duration in the CNF group compared to the ANVF ($p<0.001$), no other significant differences were found between groups (**Fig. 11F**). **Figure 12** shows the typical morphology of the CMAPs in the different experimental groups. The ENMG pattern in the NG group tended to be similar to that of the Sham group or to that of the contralateral non-operated side of all rats, apart from having a smaller amplitude (**Figs. 12 A** and **B**). The ENMG pattern in the CNF, ANVF and in the PNF groups was invariably polyphasic, and showed a tendency to be of

a longer duration but of a slightly lesser amplitude compared to the non-operated side (**Figs. 12 C** to **E**). In the Excision group, no CMAPs were observed after applying an electrical stimulus to the MN.

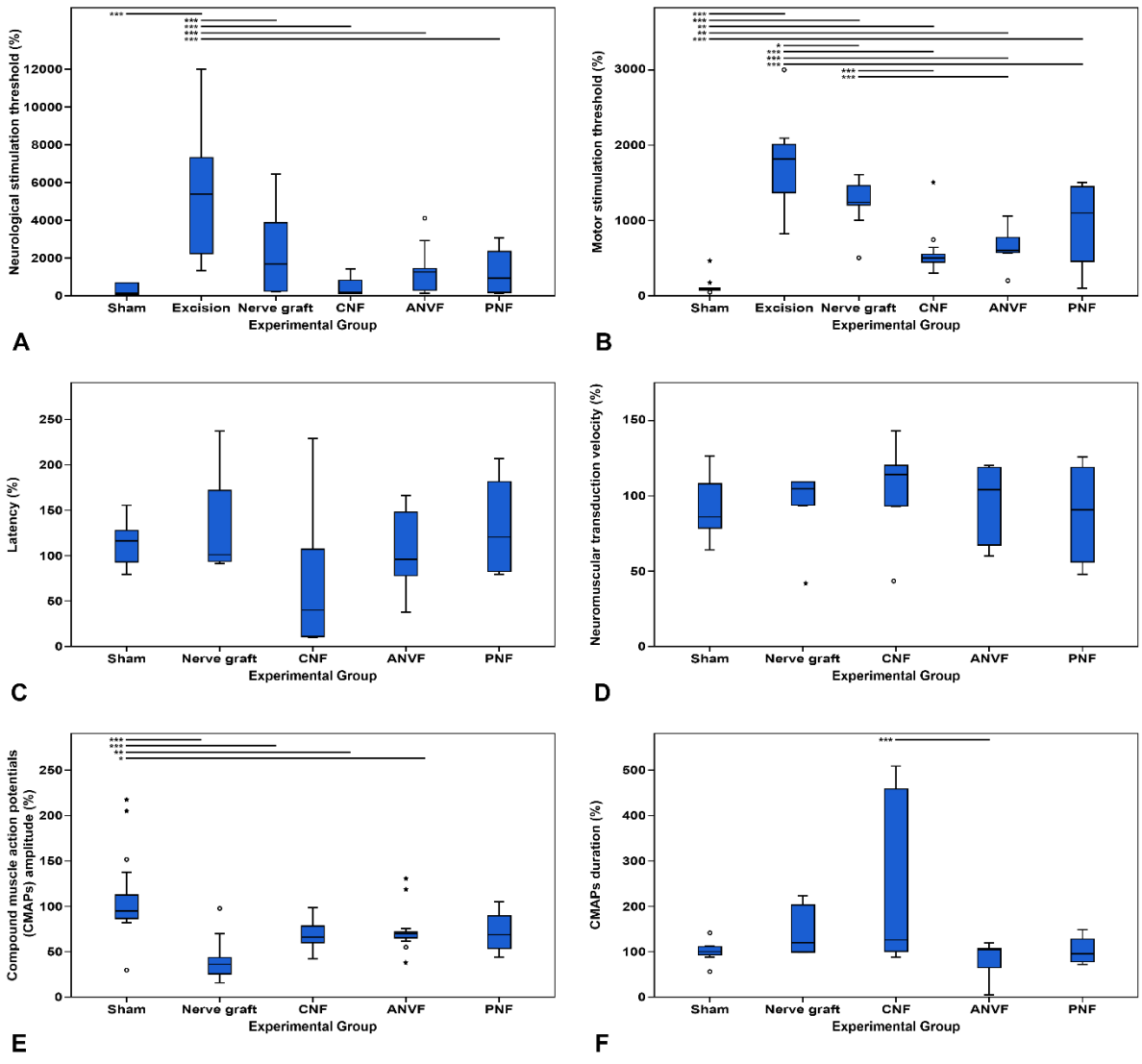

Figure 11 - Electroneuromyographic assessment of the right forelimb (operated paw) of rats in the different experimental groups throughout the experience. Values are expressed as percentages of averages normalized to the homologous contralateral side average values.

A, Neurological stimulation threshold; B, Motor stimulation threshold; C, Latency; D, Neuromuscular transduction velocity; E, Compound muscle action potentials (**CMAPs**) amplitude; F, CMAPs duration.

Vertical lines represent 95% confidence intervals.

Horizontal lines in the upper portion of the figure indicate statistically significant differences between experimental groups ($p<0.05$).

*, $p<0.05$; **, $p<0,01$; ***, $p<0.001$

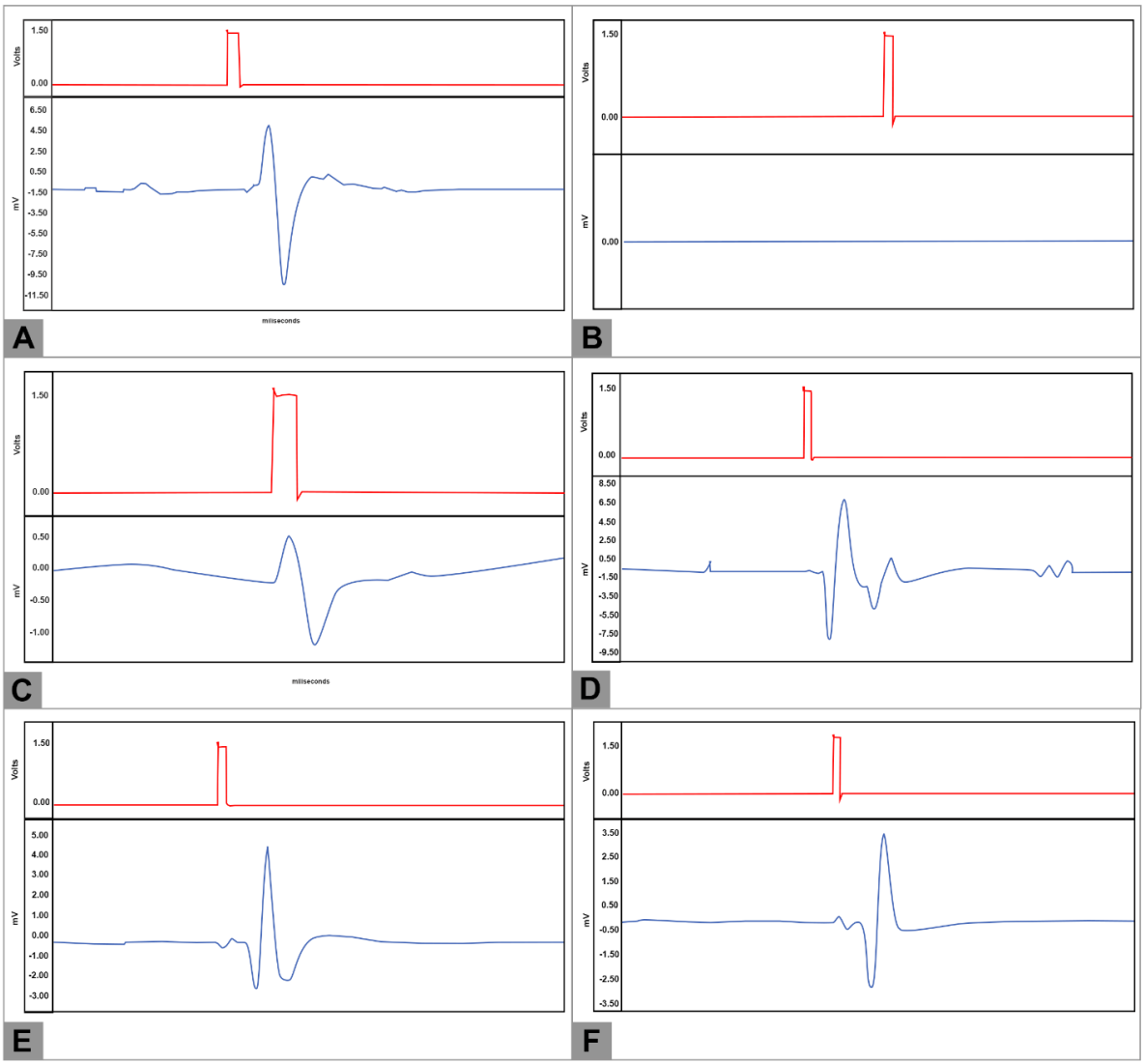

Figure 12 - Typical compound muscle action potentials patterns in the different experimental groups.

A. Sham group and left paw of the rats in the other experimental groups

B. Nerve graft group

C. Conventional nerve flap group

D. Arterialized neurovenous flap group

E. Prefabricated nerve flap group

Parameter	Sham group	Excision group	NG group	CNF group	ANVF group	PNF group	Relevant findings
Neurological stimulation threshold (%)	281.63 ± 271.65	5359.98 ± 3466.52	2108.12 ± 2115.13	428.45 ± 472.87	1063.00 ± 807.61	1270.30 ± 482.72	On D90, this parameter was significantly higher in the Excision group than in the remaining groups ($p<0.001$)
Motor stimulation threshold (%)	462.52 ± 118.91	1694.10 ± 503.24	1249.50 ± 503.24	535.38 ± 253.15	619.46 ± 264.36	948.57 ± 592.41	Lower values were obtained in the CNF and the ANVF groups than in the NG group ($p<0.001$
Latency (%)	113.55 ± 25.04	N/A	132.80 ± 69.95	72.82 ± 84.87	105.28 ± 52.41	131.97 ± 56.46	No significant differences between experimental groups
Neuromuscular transduction velocity (%)	92.01 ± 20.88	N/A	91.30 ± 26.51	100.06 ± 31.26	94.05 ± 26.33	88.15 ± 34.77	No significant differences between experimental groups
CMAPs amplitude (%)	110.63 ±45.66	N/A	41.60 ± 24.84	69.53 ± 13.80	73.34 ± 22.86	71.68 ± 23.56	No significant differences between experimental groups

CMAPs duration (%)	101.12 ± 23.92	N/A	151.06 ± 54.52	242.17 ± 185.97	82.87 ± 36.69	103.13 ± 31.24	Longer CMAP duration in the CNF group compared to the ANVF group (p<0.001)

Table 5 - Electroneuromyographic assessment at the end of the experiment

NG, nerve graft; **CNF**, conventional nerve flap; **ANVF**, arterialized neurovenous flap; **PNF**, prefabricated nerve flap

CMAPs, compound muscle action potential.

N/A, non-applicable

All parameters are expressed as percentages of the average contralateral values.

Numeric variables are expressed as average ± standard deviation.

Muscle Strength was inferior in the NG group, although the differences did not meet statistically significance:

Normalized maximum isometric tetanic wrist flexion on the operated limb on D90 was 141.00% ± 75.55% in the Sham group, 35.67% ± 46.51% in the NG, 60.56% ± 27.59% in the CNF group, 63.05% ± 12.95% in the ANVF group, and 52.61% ± 18.73% in the PNF group. This value was significantly higher in the Sham group than in the other groups ($p<0.001$; **Fig. 13A**). The normalized area under the curve during a 30-second interval and supra-tetanic stimulation was 112.54% ± 19.43% in the Sham group, 58.81% ± 29.63% in the NG group, 63.12% ± 12.43% in the CNF, 69.80% ± 31.67% in the ANVF group, and 93.61% ± 34.91% in the PNF group. Once again, the Sham group presented a better result in this parameter than all the other experimental groups, except for the PNF group ($p<0.001$; **Fig. 13B**).

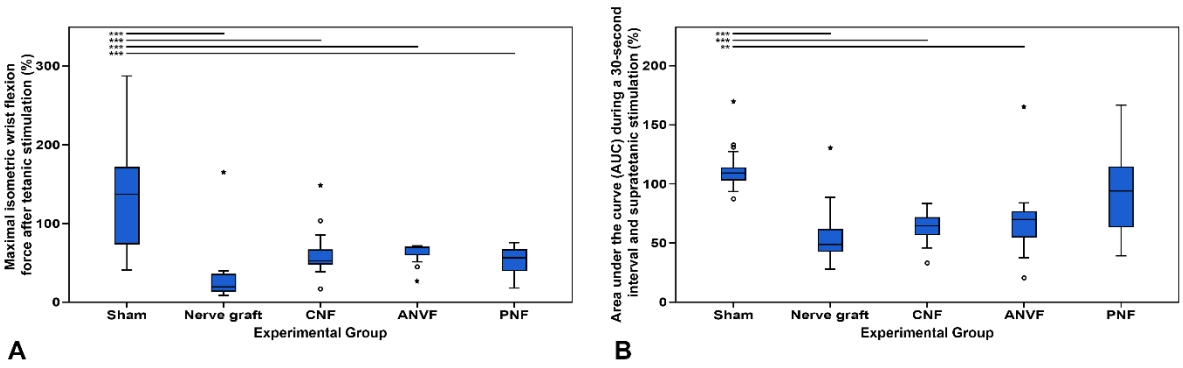

Figure 13 - Muscle strength evaluation at the end of the experiment in the operated forelimb in the different experimental groups.

A. Maximal isometric wrist flexion force after tetanic stimulation.

B. Area under the curve (**AUC**) during a 30-second interval and supratetanic stimulation

Values are expressed as percentages of averages normalized to the homologous contralateral side average values.

Vertical lines represent 95% confidence intervals.

Horizontal lines in the upper portion of the figure indicate statistically significant differences between experimental groups ($p<0.05$).

**, p<0,01; ***, p<0.001

Muscle Weight was inferior in the NG and in the PNF groups:

The normalized results for FCR muscle weight at the end of the experiment were 101.15% ± 8.14% for the Sham group, 30.24% ± 7.23% for the Excision group, 47.14% ±14.72 for the NG group, 80.29 ± 14.29% for the CNF group, 82.24% ±10.64% for the ANVF group, and 62.71% ± 11.12% for the PNF group (**Figs. 14** and **15**). The Sham group presented a higher muscle weight than any of the other experimental groups ($p<0.001$). Among the groups using nerve conduits the CNF and the ANVF presented a better muscle weight than the NG and the PNF ($p<0.01$). The difference between these latter two groups was not statistically significant, although the PNF presented a higher average value.

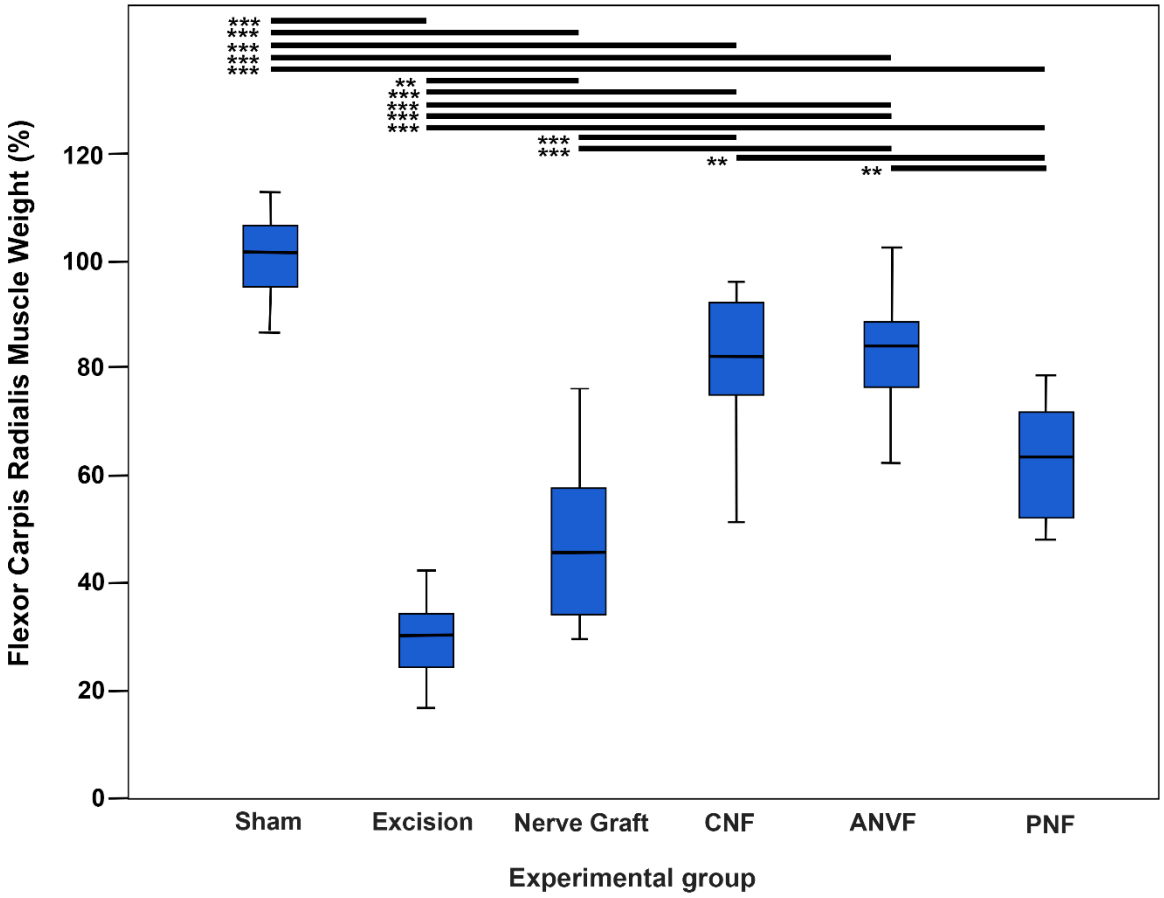

Figure 14 - Flexor carpis radialis muscle weight of the right forelimb (operated paw) of rats in the different experimental groups. Values are expressed as percentages of averages normalized to the homologous contralateral side average values.

Vertical lines represent 95% confidence intervals.

Horizontal lines in the upper portion of the figure indicate statistically significant differences between experimental groups ($p<0.05$).

p<0,01; ***, p<0.001

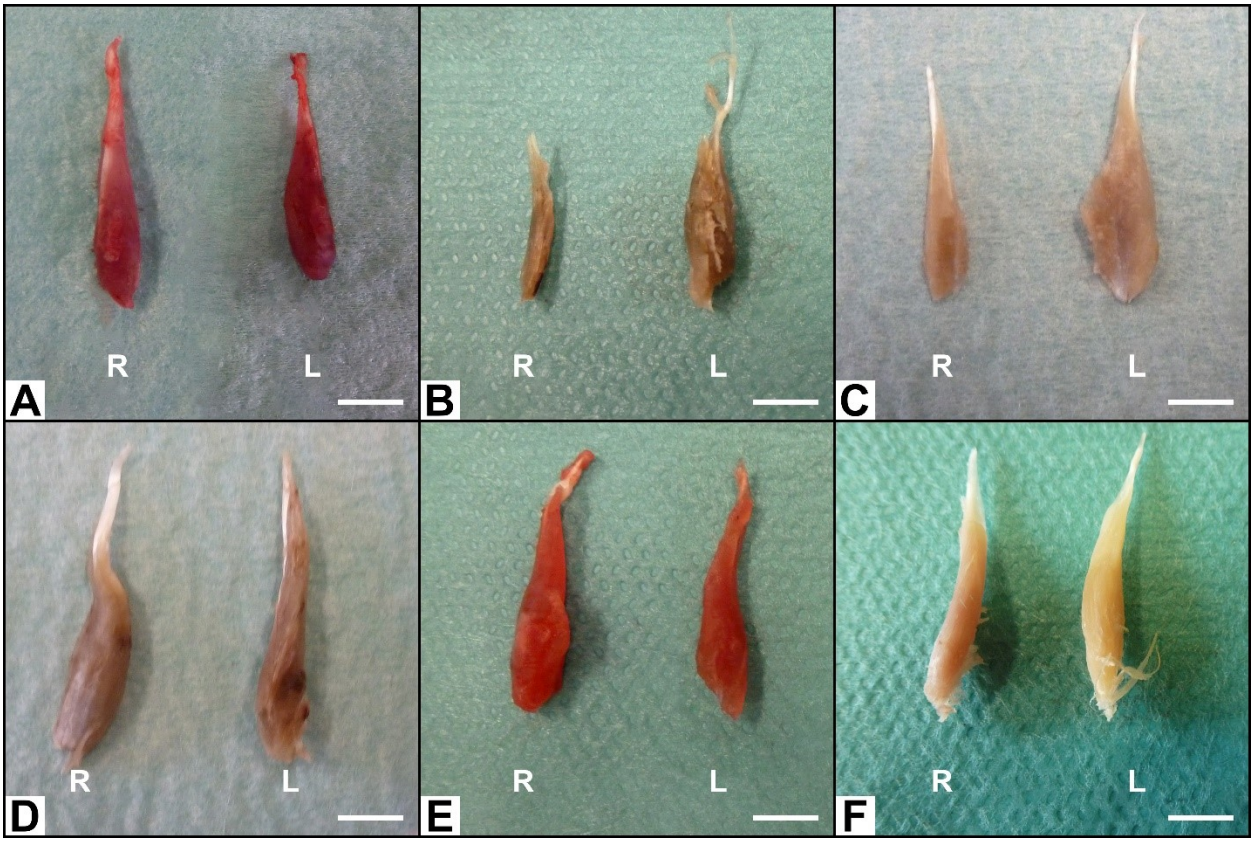

Figure 15 - Photographs of the flexor carpis radialis muscle illustrating muscle gross appearance in the different experimental groups on the operated side (**R**, right) and on the non-operated side (**L**, left).

A. Excision group

B. Nerve graft group

C. Conventional nerve flap group

D. Arterialized neurovenous flap group

E. Prefabricated nerve flap group

Histomorphometrical evaluation of the distal aspect of the median nerve showed a tendency to worse results in the NG group:

Histological examination of the median nerve distally to the reconstructed nerve segment revealed an inferior average cross section area in the Excision group (**Figs. 16 A**, and **17**; **Table 6**). Among the groups using nerve conduits, the NG presented an inferior area. However, this difference was statistically significant only between the NG and the PNF groups ($p<0.05$).

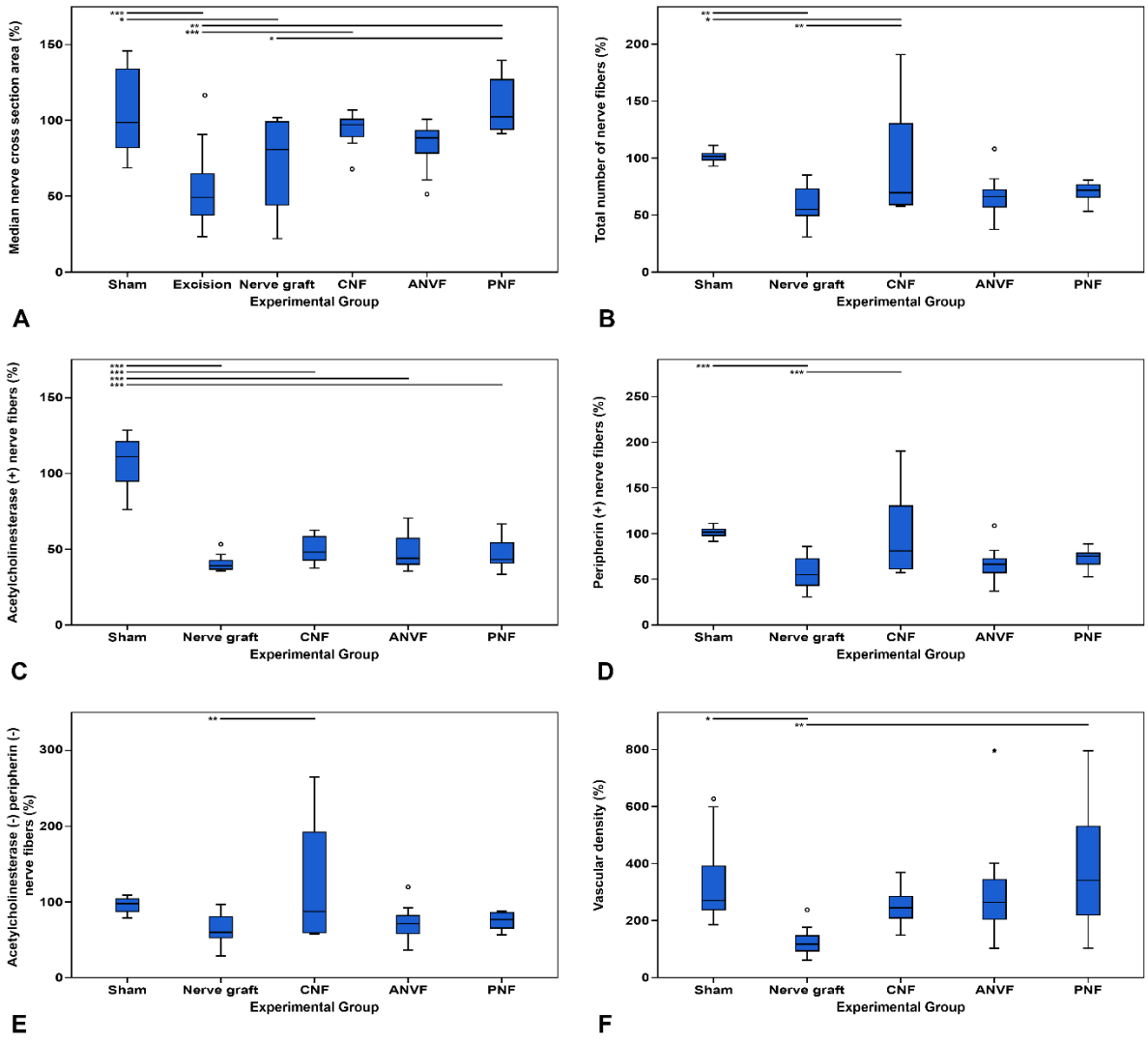

Figure 16 - Histomorphometric evaluation of the right median nerve distally to the repair zone in the different experimental groups. Results are expressed as a percentage of the normal, contralateral side and are given as the mean.

A. Median nerve cross section area distally to the repair zone.

B. Total number of fibers (stained for neurofilaments) distally to the repair zone.

C. Acetylcholinesterase positive (+) nerve fibers distally to the repair zone.

D. Peripherin positive (+) nerve fibers distally to the repair zone.

E. Acetylcholinesterase negative (-) and peripherin negative (-) nerve fibers distally to the repair zone.

F. Vascular density in a cross section of the middle portion of the reconstructed nerve defect.

Vertical lines represent 95% confidence intervals.

Horizontal lines in the upper portion of the figure indicate statistically significant differences between experimental groups ($p<0.05$).

*, $p<0.05$; **, $p<0,01$; ***, $p<0.001$

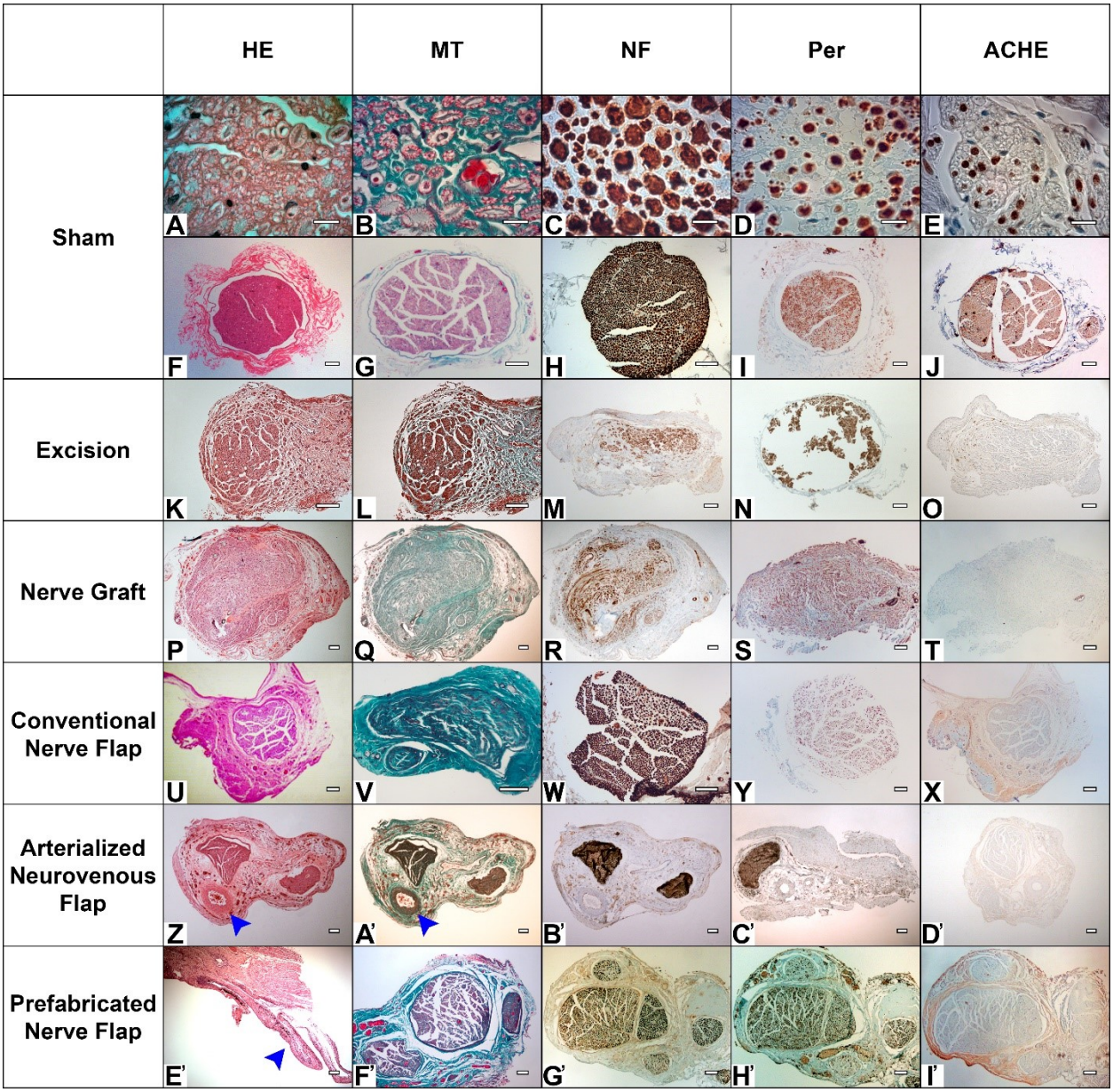

Figure 17 - Representative histological features of the different experimental groups.

HE, hematoxylin-eosin staining; **MT**, Masson's trichrome staining; **NF**, neurofilament immunohistochemical staining; **Per**, peripherin immunohistochemical staining; **ACHE**, acetylcholinesterase immunohistochemical staining.

Calibration bar (A to E) = 10 µm

Calibration bar (F to I') = 100 µm

Parameter	Sham group	Excision group	NG group	CNF group	ANVF group	PNF group	Relevant findings
Cross section area (%)	106.59 ± 27.45	54.67 ± 26.55	72.42 ± 30.28	93.38 ± 10.87	82.44 ± 15.77	109.42 ± 19.86	Higher in the PNF group than in the NG group ($p<0.05$)
Total number of fibers (%)	101.76 ± 5.30	N/A	56.88 ± 17.85	97.91 ± 50.72	67.71 ± 18.58	70.33 ± 9.31	Higher in the CNF group than in the NG group ($p<0.01$)
Acetylycholinesterase positive nerve fibers (%)	106.94 ± 17.65	N/A	40.90 ± 5.54	49.67 ± 8.61	49.67 ± 8.61	47.07 ± 10.82	No significant differences between experimental groups
Peripherin positive nerve fibers (%)	101.64 ± 5.53	N/A	56.90 ± 17.83	101.45 ± 49.23	101.45 ± 49.23	73.03 ± 11.49	Numbers of peripherin positive and acethyl-cholinesterase negative and peripherin negative fibers were higher in the CNF and in the Sham groups than in the NG group ($p<0.001$)
Acethylcholinesterase negative and peripherin negative nerve fibers (%)	95.58 ± 10.76	N/A	61.02 ± 21.59	126.28 ± 78.51	73.20 ± 22.36	75.03 ± 11.61	
Vascular density in the middle portion of the	335.98 ± 155.89	N/A	126.70 ± 50.92	249.67 ± 62.73	310.51 ± 188.86	385.04 ± 225.80	Higher in the PNF group than in the NG

reconstructed nerve segment (%)							group ($p<0.05$)

Table 6 - Histomorphometric evaluation of the right median nerve distally to the repair zone and of the vascular density in the middle portion of the reconstructed nerve defect in the different experimental groups

NG, nerve graft; **CNF**, conventional nerve flap; **ANVF**, arterialized neurovenous flap; **PNF**, prefabricated nerve flap

N/A, non-applicable

All parameters are expressed as percentages of the average contralateral values.

Numeric variables are expressed as average ± standard deviation.

Regarding the internal structure of the distal portion of the MN, the total number of nerve fibers was significantly higher in the CNF than in the NG ($p<0.01$; **Fig. 16 B**). No other differences were found between the groups using conduits. The number of acetylcholinesterase positive fibers was higher in the Sham control group than in the remaining experimental groups ($p<0.001$; **Fig. 16C**). Concerning this type of fibers, no differences were found in the latter groups. The average number of peripherin positive fibers was higher in the CNF and in the Sham groups than in the NG group ($p<0.001$; **Fig. 16D**). Finally, the average number of acetylcholinesterase negative and peripherin negative fibers was once again higher in the CNF group than in the NG group ($p<0.001$; **Fig. 16E**). Vascular density in the reconstructed nerve segment was lower in the NG group than in either the Sham or the PNF groups ($p<0.05$; **Fig. 16 F**). No statistically significant differences were found between the CNF, ANVF and the PNF groups.

Histological characterization of the nerve conduits revealed greater architectural disorganization in the nerve graft conduit:

Histological examination of the nerve conduits used to bridge the MN defect revealed preservation of the normal nerve architecture in the Sham group (**Figs. 17A** to **17J**). In the Excision group, the distal stump of the MN showed clear signs of Wallerian degeneration in all the rats, as well as a proximal stump neuroma (**Figs. 17K** to **17T**). In all rats in the NG group, there was a significant degree of fibrosis among the reconstituted nerve fibers. These fibrous septa divided the nerve structure in irregular bundles (**Figs. 17P** to **17T**). In the CNF, the ANVF and the PNF groups, the reconstructed segment presented a single nerve fascicle (CNF and ANVF groups) or two nerve fascicles (PNF) whose fibers were disposed in a cohesive fashion (**Figs. 17T** to **I'**). In all the histological specimens in the ANVF group the brachial vein showed clear signs of arterialization. In addition, large tortuous veins could be seen in the proximity of the nerve segment (**Figs. 17Z** and **17A'**). No clear signs of thrombosis were observed in the vein supplying flap in the ANVF group. In the histological sections of the PNF group it was also possible to observe arterialization of the venous fistula used to recruit the sciatic nerve segment (**Fig. 17E'**). There was a greater density of large sized arterioles and venules in the epineurial region of these nerve segments than in any of the nerve conduits used in the other groups (**Fig. 17F'**). Analogously, there is no evidence of vascular thrombosis of the vascular construct used to mobilize the nerve conduit. The primitive internal structure of the sciatic nerve was preserved until the most distal aspect of the nerve conduit in the PNF group (**Figs. 17G'** to **I'**).

Retrograde axonal tracing using fluorescent markers showed anatomical restoration in all the groups using conduits:

Lucifer Yellow and True Blue were seen reaching the proximal MN, the C7 dorsal root ganglion and the ventral horn of the C7 spinal cord segment in all rats in the Sham, NG, CNF, ANVF and PNF groups (**Figs. 18** and **19**). In the Excision group, although there was some degree of auto fluorescence, no clear intracytoplasmic markers were observed. Semi quantitative evaluation revealed a higher number of stained cells in the Sham group in all the regions studied (**Fig. 20A** to **D; Table 7**). The CNF group presented a higher expression of fluorescent markers at all these locations than the NG group. However, this difference was statistically significant only for the Lucifer Yellow staining of the cells in the ventral horn of the spinal cord ($p=0.045$; **Fig. 20D**). There were no significant differences between the NG group and the ANVF and the PNF groups regarding fluorescence staining.

Experimental Group	Right Median Nerve	C7 Spinal Cord Segment	Right Dorsal Root Ganglion
I (Sham)	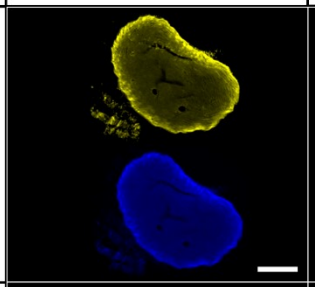	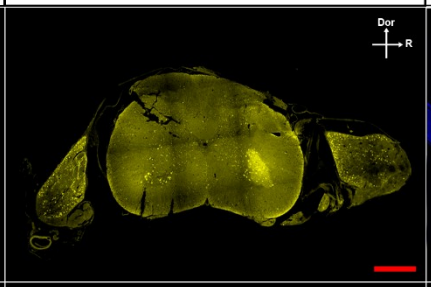	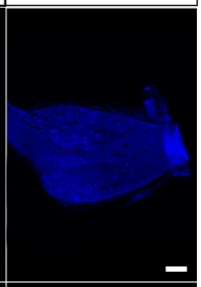
II (Excision)	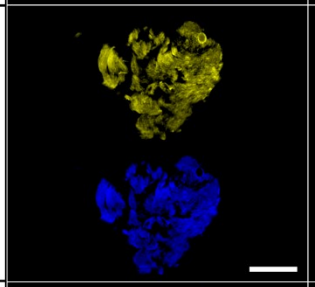	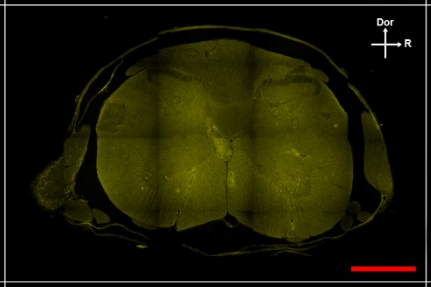	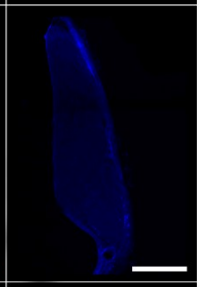
III (Nerve Graft)	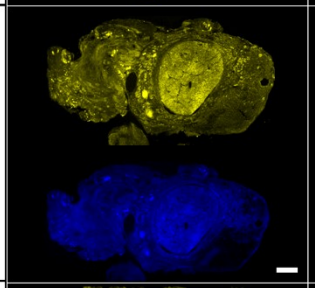		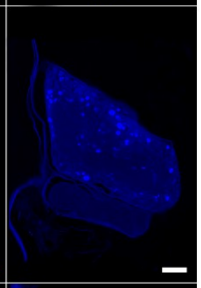
IV (Conventional Flap)	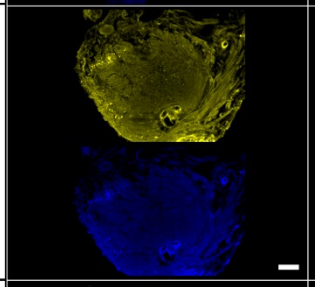		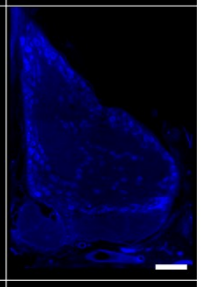
V (Arterialized Venous Flap)	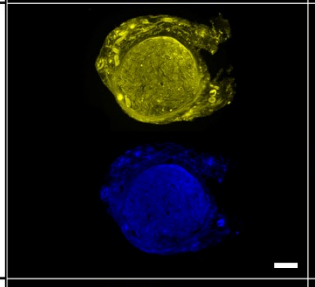	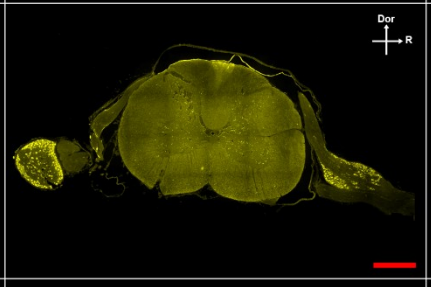	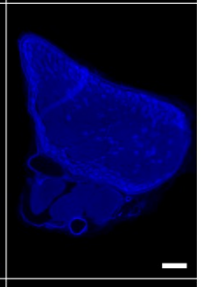
VI (Prefabricated Nerve Flap)	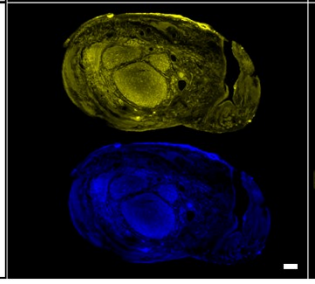	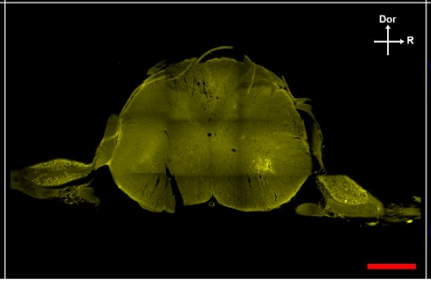	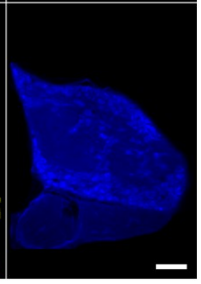

Figure 18 - Fluorescence microscopy photographs of cross sections of the right median nerve proximally to the lesion, of the C7 spinal cord segment, and of the C7 the right dorsal root ganglion in the different experimental groups.

Dor, dorsal; **R**, right

Red calibration bar = 1 mm

White calibration bar = 100 µm

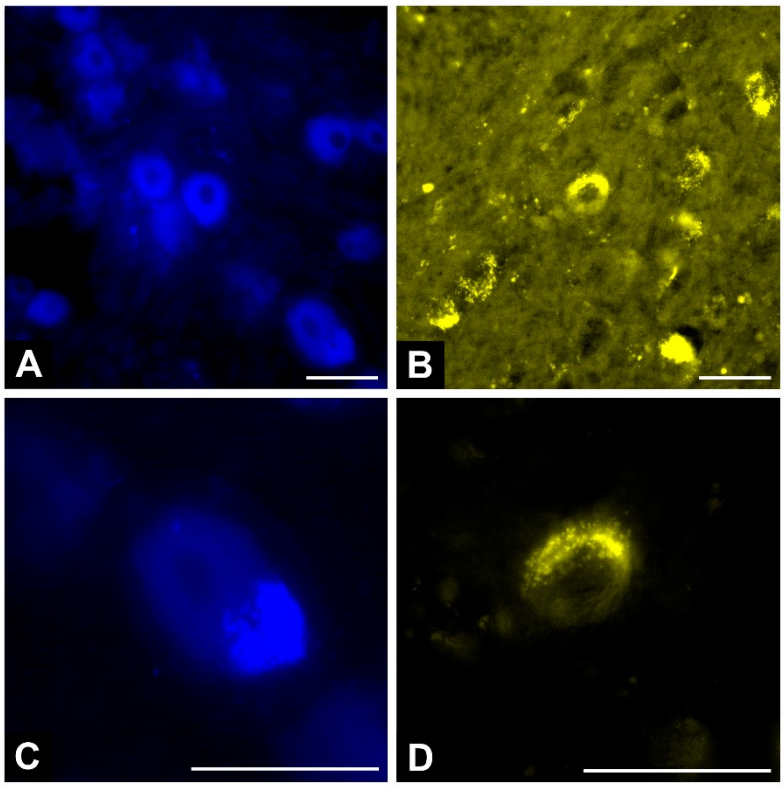

Figure 19 - Typical high amplification fluorescence microscopy photographs of cross sections of the C7 the right dorsal root ganglion (**A** and **C**) showing ganglion cells stained with the True Blue® (**TB**)tracer and of motoneurons in the ventral horn of the spinal cord stained with the lucifer yellow (**LY**) ® tracer (**B** and **D**). Intracytoplasmic inclusions of these two markers are clearly visible in a rat of the Sham group.

Calibration bar = 100 µm

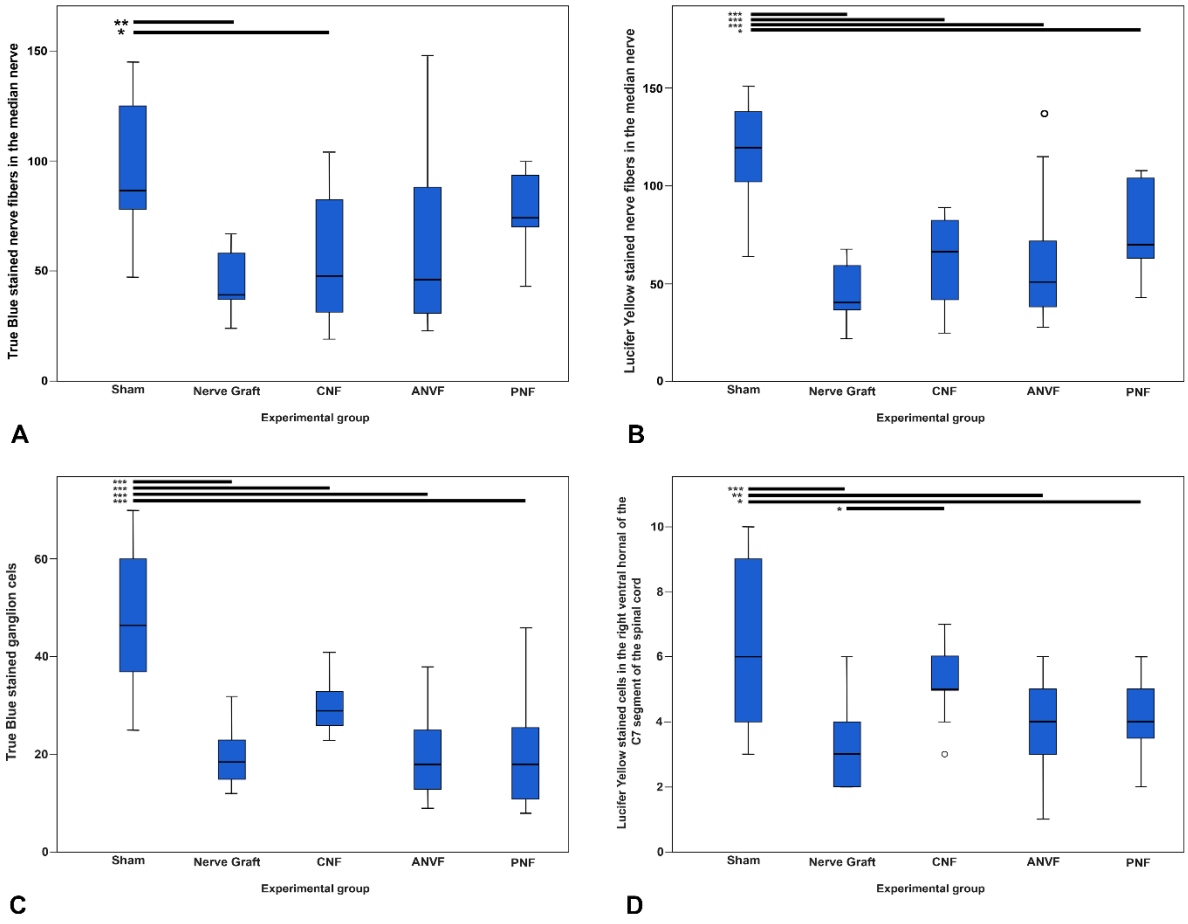

Figure 20 - Semi quantitative evaluation of retrograde marking of the right median nerve proximally to the lesion site, of the right C7 dorsal ganglion and of the right ventral horn of the spinal cord at the C7 level in the different experimental groups.

A. Average number of True Blue diaceturate stained fibers in the right median nerve proximally to the repair site.

B. Average number of Lucifer Yellow CH dilithium stained fibers in the right median nerve proximally to the repair site.

C. Average number of True Blue diaceturate stained ganglion cells in the right C/ dorsal ganglion.

D. Average number of Lucifer Yellow CH dilithium stained cells in the ventral horn of the C7 spinal cord segment.

Vertical lines represent 95% confidence intervals.

Horizontal lines in the upper portion of the figure indicate statistically significant differences between experimental groups ($p<0.05$).

*, $p<0.05$; **, $p<0,01$; ***, $p<0.001$

Parameter	Sham group	NG group	CNF group	ANVF group	PNF group	Relevant findings
True Blue stained axons in the median nerve	96.10 ± 30.70	44.00 ± 14.29	55.58 ± 30.06	61.93 ± 40.55	77.25 ± 18.50	Higher average value in the Sham group than in the NG and CNF groups ($p<0.05$)
Diamidino Yellow stained axons in the median nerve	115.70 ± 28.49	45.10 ± 14.40	63.58 ± 21.88	63.07 ± 33.22	78.12 ± 24.19	No significant differences in the experimental groups
Stained ganglion cells	48.20 ± 13.95	19.60 ± 6.36	29.92 ± 5.19	20.13 ± 8.49	20.38 ± 12.47	No significant differences in the experimental groups
Stained ventral horn cells	6.50 ± 2.59	3.20 ± 1.23	5.25 ± 1.14	3.80 ± 1.47	4.12 ± 1.25	The CNF group presented a higher average value than the NG group ($p=0.045$)

Table 7 - Evaluation of retrograde marking of the right median nerve proximally to the lesion site, of the right C7 dorsal ganglion and of the right ventral horn of the spinal cord at the C7 level.

NG, nerve graft; **CNF**, conventional nerve flap; **ANVF**, arterialized neurovenous flap; **PNF**, prefabricated nerve flap; **N/A**, non-applicable

All parameters are expressed as percentages of the average contralateral values.

Numeric variables are expressed as average ± standard deviation.

Multiple correlations were found between functional motor variables and neurophysiological and histomorphometric variables:

Time to recovery of grasping in the operated limb was positively correlated with the neurological threshold (Pearson's correlation coefficient = 0.484; p<0.001), and with the motor threshold (Pearson's correlation coefficient = 0.735; p<0.001). Time to recovery of grasping was negatively correlated with the following parameters: CMAP Amplitude (Pearson's correlation coefficient = -0.611; p<0.001); FCR weight (Pearson's correlation coefficient = -0.769; p<0.001); maximal isometric wrist flexion strength (Pearson's correlation coefficient = -0.571; p<0.001); AUC in the strength x time graph (Pearson's correlation coefficient = -0.324; p=0.003); number of MN nerve fibers (Pearson's correlation coefficient = -0.464; p<0.001); number of MN acetylcholinesterase positive fibers (Pearson's correlation coefficient = -0.718; p<0.001); number of MN peripherin positive fibers (Pearson's correlation coefficient = -0.393; p=0.004); number of Lucifer Yellow positive fibers in the MN (Pearson's correlation coefficient = -0.409; p=0.002); number of True Blue marked DRG cells (Pearson's correlation coefficient = -0.511; p<0.001); and

number of Lucifer Yellow marked neurons in the ventral horn of the spinal cord (Pearson's correlation coefficient = -0.393; p=0.004).

Similarly, FCR weight was positively correlated with the following variables: maximal isometric wrist flexion strength (Pearson's correlation coefficient = 0.548; p<0.001); AUC in the strength x time graph (Pearson's correlation coefficient = 0.288; p=0.009); CMAP amplitude (Pearson's correlation coefficient = 0.724; p<0.001); MN nerve area cross sectional area (Pearson's correlation coefficient = 0.486; p<0.001); number of MN nerve fibers (Pearson's correlation coefficient = 0.644; p<0.001); number of MN acetylcholinesterase positive fibers (Pearson's correlation coefficient = 0.624; p<0.001); number of MN peripherin positive fibers (Pearson's correlation coefficient = 0.454; p=0.001); number of MN acetylcholinesterase negative and peripherin negative fibers (Pearson's correlation coefficient = 0.294; p=0.038); vascular density in the reconstructed nerve gap (Pearson's correlation coefficient = 0.337; p=0.019); number of Lucifer Yellow positive fibers in the MN (Pearson's correlation coefficient = 0.356; p=0.008); number of True Blue stained DRG cells (Pearson's correlation coefficient = 0.418; p=0.002); and number of Lucifer Yellow marked neurons in the ventral horn of the spinal cord (Pearson's correlation coefficient = 0.352; p=0.008)

In opposition, FCR weight was negatively correlated with the neurological threshold (Pearson's correlation coefficient = -0.617; p<0.001), and with the motor threshold (Pearson's correlation coefficient = -0.803; p<0.001).

Additionally, maximal isometric wrist flexion strength was positively correlated with the following variables: CMAP Amplitude (Pearson's correlation coefficient = 0.434; $p<0.001$); MN area cross sectional area (Pearson's correlation coefficient = 0.292; $p=0.024$); number of MN nerve fibers (Pearson's correlation coefficient = 0.378; $p=0.003$); number of MN acetylcholinesterase positive fibers (Pearson's correlation coefficient = 0.639; $p<0.001$); number of Lucifer Yellow stained fibers in the MN (Pearson's correlation coefficient = 0.357; $p=0.007$); number of True Blue marked DRG cells (Pearson's correlation coefficient = 0.396; $p=0.003$); and number of Lucifer Yellow positive neurons in the ventral horn of the spinal cord (Pearson's correlation coefficient = 0.521; $p<0.001$).

Maximal isometric wrist flexion strength was negatively correlated with the neurological threshold (Pearson's correlation coefficient = -0.324; $p=0.003$); and with the motor threshold (Pearson's correlation coefficient = -0.511; $p<0.001$).

AUC in the strength x time graph was positively correlated with CMAP Amplitude (Pearson's correlation coefficient = 0.428; $p<0.001$); the number of MN acetylcholinesterase positive fibers (Pearson's correlation coefficient = 0.458; $p=0.001$); the number of Lucifer Yellow stained fibers in the MN (Pearson's correlation coefficient = 0.305; $p=0.023$), and with the number of True Blue marked DRG cells (Pearson's correlation coefficient = 0.312; $p=0.021$).

AUC in the strength evaluation graph was negatively correlated with the motor threshold (Pearson's correlation coefficient = -0.321; $p=0.003$).

Velocity in the inclined ladder on D90 was positively correlated with the following assessments: FCR weight (Pearson's correlation coefficient = 0.547; $p<0.001$); Maximal isometric wrist flexion strength (Pearson's correlation coefficient = 0.248; $p<0.024$); CMAP Amplitude (Pearson's correlation coefficient = 0.428; $p<0.001$); MN cross sectional area (Pearson's correlation coefficient = 0.302; $p=0.012$); number of MN nerve fibers (Pearson's correlation coefficient = 0.474; $p<0.001$); number of MN acetylcholinesterase positive fibers (Pearson's correlation coefficient = 0.434; $p=0.002$); number of MN peripherin positive fibers (Pearson's correlation coefficient = 0.334; $p=0.012$); and number of True Blue positive fibers in the MN (Pearson's correlation coefficient = 0.305; $p=0.012$)

Rats that did not present radial deviation in the walking tracks fared better that rats did present radial deviation in the following parameters: FCR weight (37.59% ± 16.27% vs. 84.25% ± 18.72%; $p<0.001$), maximal isometric flexion force (87.75% ± 62.36% vs. 27.47% ± 13.35%; $p<0.001$), MN cross section area (98.79% ± 22.10% vs. 66.79% ± 29.42%; $p<0.001$), total number of MN nerve fibers (87.43% ± 33.14% vs. 23.40% ± 37.77%; $p<0.001$); and number of peripherin stained fibers (88.08% ± 33.03% vs. 53.57% ± 41.28%; $p=0.021$).

Multiple correlations were found between nociception assessment and functional motor, neurophysiological and histomorphometric variables:

Nociception evaluation by the pin prick test on D90 was positively correlated with velocity in the inclined ladder on D90 (Pearson's correlation coefficient = 0.550; $p<0.001$); with CMAP Amplitude (Pearson's correlation coefficient = 0.589; $p<0.001$); with MN cross section area (Pearson's correlation coefficient = 0.422; $p=0.001$); with the number of MN nerve fibers (Pearson's correlation coefficient = 0.614; $p<0.001$); with the number of MN acetylcholinesterase positive fibers (Pearson's correlation coefficient = 0.316; $p=0.011$); with the number of MN peripherin positive fibers (Pearson's correlation coefficient = 0.348; $p=0.012$); with the number of True Blue stained fibers in the MN (Pearson's correlation coefficient = 0.295; $p=0.029$); with the number of Lucifer Yellow stained fibers in the MN (Pearson's correlation coefficient = 0.293; $p=0.030$); with the number of stained DRG cells (Pearson's correlation coefficient = 0.274; $p=0.043$); and even with the number of Lucifer Yellow positive neurons in the ventral horn of the spinal cord (Pearson's correlation coefficient = 0.339; $p=0.011$).

Finally, nociception evaluation by the pin prick test on D90 was negatively correlated the neurological threshold (Pearson's correlation coefficient = -0.561; $p=0.003$).

DISCUSSION

The authors believe that of the main merits of the present work was to apply in a same model of peripheral nerve gap and local ischemia, various autologous reconstructive techniques, in order to obtain more homogenous results. In fact, it is commonly accepted that it is difficult to conciliate the highly diverse experimental evidence, due to the various animal species tested, the multiple anatomical regions used, the inclusion or not of local ischemia, the different parameters evaluated, and the heterogenous follow-up time.[30] Additionally, to the best of the authors' knowledge, this is the largest series in the literature comparing different autologous techniques of MN gap reconstruction in the rat, in the presence of local ischemia.[90-92]

Overall, the results of this article seem to lend to support to the notion that vascularized nerve conduits in an ischemic environment lead to a more rapid and complete recovery. In fact, for all the parameters assessed, the groups using vascularized nerve conduits presented at least as good result of NG, and, in many circumstances, they ensured a better result that the latter option. For example, the Grasping Test revealed faster and more complete motor recovery in the CNF and in the ANVF groups than in the NG group. Likewise, the Pin prick test showed better nociceptive recovery in the CNF and ANVF groups than in the NG group. Walking Track Analysis revealed that the rate of radial deviation was lower in groups in which a vascularized nerve conduit was used. ENMG assessment revealed a lower motor stimulation threshold in the CNF and ANVF than in the NG group. Moreover, CNF and the ANVF presented better FCR muscle

weight than the NG group. Additionally, histomorphometric evaluation of the distal aspect of the MN showed a tendency to worse results in the NG group. In fact, CNF presented a higher MN cross section area, higher total number of nerve fibers, as well as higher number of peripherin positive and acetylcholinesterase negative and peripherin negative nerve fibers. Finally, histological characterization of the nerve conduits revealed greater architectural disorganization in the nerve graft conduit. The CNF group presented a higher expression of fluorescent markers at all these locations than the NG group.

Koshima *et al.* in 1985 had demonstrated that in the sciatic nerve of rats, CNFs yielded better results than NGs in reconstructing nerve defects in scarred regions after previous burns.[93, 94] Gu *et al.* in 1985 presented a study on New Zealand rabbits showing that CNFs were superior to nerve grafts for reconstructing a 20-mm MN defect even in favorable local conditions.[95] These data were soon validated in experiments performed in the same species by different authors.[96] However, subsequently, other authors concluded that nerve flaps did not benefit in reconstructing nerve defects in the context of normal perfusion in a rabbit model, suggesting that nerve flap reconstruction may be more beneficial in conditions of local ischemia.[30]

Notwithstanding, there is experimental evidence that CNFs, having a blood supply of its own, guarantee a better survival of Schwann cells, and are more efficiently permeated by macrophages, which will remove myelin fragments from degenerated axons.[97] Overall, these processes maintain a better architecture of the nerve conduit, promoting nerve regeneration.[22, 96-98] Blood supply to nerve conduits seems to be particularly critical in

conditions of local ischemia, namely in regions of intense fibrosis, or prior radiotherapy.[22, 96-98] These experimental findings have been corroborated clinically. In fact, it is well established that good perfusion of the nerve repair zone is mandatory to ensure a good functional outcome.[2, 3, 99, 100]

Interestingly, in this work, CNFs and ANVFs were, for most of the assessed variables, comparable.[95] Vargel *et al.* using a femoral nerve model of ischemia in the rat showed that ANVFs presented superior results to NGs in nerve gap reconstruction.[28, 29] In fact, Townsend *et al.* had already demonstrated a faster rate of axonal elongation in ANVFs executed in the hindlimb of 15 greyhound dogs compared to NGs.[19]

The PNF group did not present as good results as the CNF and the ANVF groups. This may be due to the fact that the sciatic nerve not only is larger than the MN, but it is also polyfascicular, composed of motor, sensory and mixed fascicles.[46, 47, 101] The MN of the rat is, at the arm level, monofascicular (**Fig. 17**).[102] These morphometric differences may have led to a poor correspondence between motor and sensory axons, which, in turn, may have been responsible for inferior results in the PNF group comparatively to the other groups using vascularized nerve conduits.[103] These data contrast with those presented in the report of Karcher *et al.*, in which an arteriovenous fistula was used to produce a PNF involving the femoral nerve of the rat. This PFN provided better results in the reconstruction of a fascicle of the sciatic nerve of the rat than those obtained with an homologous NG.[32]

No significant differences were observed in the thermographic pattern of the different experimental groups 100 days after surgery (**Fig. 10**). Several authors have reported higher skin temperature in the territory of recently severed nerves, putatively related to the loss of activity of the sympathetic fibers contained in these nerves, leading to cutaneous vasodilation and consequently local increase in blood supply and, ultimately higher temperature.[67, 104, 105] However, this association has not been demonstrated in cases of longstanding lesions.[106] For example, Sacharuk *et al.* have demonstrated a normalization of skin temperature in the hindlimb 21 days after a crush injury to the sciatic nerve.[106]

Interestingly, in this work multiple correlations were found between functional tests and neurophysiological and histomorphometric variables. In particular, an interesting finding of this study was the identification of radial deviation in forepaw prints of the rats with poorer outcomes in the following variables: FCR, maximal isometric flexion force, MN cross section area, total number of MN nerve fibers, and number of peripherin stained fibers. Thus, radial deviation of forepaws imprints may be of interest as surrogate marker of MN lesion. The underlying mechanism for radial deviation may be the denervation of the intrinsic muscles of the forepaw of the rat innervated by the MN, generating a situation similar to the median claw hand observed in humans.[107, 108] However, further studies are required to confirm or dismiss this hypothesis. In particular, it would have been interesting to study the histology of the muscles of rats presenting radial deviation and comparing these findings with those of rats without radial deviation.

Study Limitations Section

The trends in motor and sensory recovery between the different experimental groups were not homogenous for all the outcome variables assessed. However, the underlying mechanisms of peripheral nerve recovery are known to be complex and time-dependent, involving many issues affecting neuron survival, proximal axon regeneration, synaptogenesis, recovery of the denervated motor and sensory targets, as well as cerebral plasticity.[10, 100, 109, 110]

Apart from radial deviation, walking track analysis failed to provide consistent differences between groups. However, other authors have also found that single MN lesions in the rat frequently do not produce consistent changes in the walking pattern.[44] Moreover, other authors have argued that pawprint analysis is more useful for crushing nerve lesions than for segmental nerve defect reconstruction.[10] Moreover, it has also been shown that walking track analysis do not always correlate with muscle recovery.[111]

Regarding the choice of animal model, the rat sciatic nerve is arguably the most used nerve in peripheral nerve research.[112, 113] Notwithstanding, in this work the authors decided to use the rat MN, as the latter may present various advantages relatively to the former.[44, 45] In fact, MN lesions seem to be associated with lesser incidence of joint contractures and auto-mutilation of the affected limb.[44] Overall, rat welfare is more preserved with MN lesions than with sciatic nerve lesions.[113, 114] In addition, as the MN is shorter than the sciatic nerve, nerve recovery is observed sooner.[44, 112, 115-118] On top of this, most peripheral nerve lesions in

the human species occur in the upper limb, further validating the use of this nerve in the rat.[3, 35, 119] Moreover, fine movement coordination in hand and finger movements is remarkably similar in rats and humans.[113, 120] Finally, recently, multiple standardized strategies have been introduced to assess motor and sensory recovery in the rat MN model, permitting an easier comparison of results.[38, 39, 43, 45, 46, 62, 111, 113, 121]

Regarding the induction of a local ischemic environment, other authors have used a silicone barrier around the nerve repair zone in order to simulate a local ischemic medium.[29, 42] However, it may be argued that this model is not perfect, as silicone rods have been successfully used to reconstruct nerve defects in substitution of autologous conduits.[122, 123]

Also, the authors must concede that a major caveat of the present work is that rat peripheral nerves have much smaller cross-sectional areas than the homologous human structures. Theoretically, this should facilitate nerve revascularization, and promote better overall results in rats comparatively to humans.[29] In this sense, it would be useful to try to replicate the study herein described in larger animals. Furthermore, it is well established that reinnervation and functional recovery is more likely when nerve targets are closer to the repair zone.[109] The reasons for these are multiple: atrophy and fatty replacement of chronically denervated muscle, chronically denervated Schwann cells being less able to support regenerating axons, distal nerve histological disorganization increasing the likelihood of regenerating axons going into inappropriate endoneurial tubes and target organs (e.g. motor axons growing into endoneurial tubes connected to skin sensory organs or sensory axons growing into endoneurial tubes destined to motor plates).[109, 124] Moreover, under optimal conditions, in mammals,

axonal elongation occurs at a rate of approximately 1-3 mm/day, limited by slow anterograde axonal transport.[3, 100, 109] This means that rats and humans have similar nerve regeneration speeds. However, rat's nerves end organs are much closer to the place of nerve repair than in Man. Hence, the results of nerve repair are much faster in rats, which is convenient from an experimental point of view.[7, 93, 125, 126] Nevertheless, nerve recovery will probably be more complete than that observed in humans in similar circumstances.[3, 100, 127] To curb these biases, in the present study, the authors have restricted follow-up to 100 days. In fact, such follow-up time is used by most other researchers, in order to mitigate the effect of the exceptional neuroregenerative potential of rats.[90, 92] However, for all these reasons, the extrapolation of our results to the clinical setting should be made with caution. It would therefore be useful to try to replicate our findings in larger animals.

Another technical aspect that should be born in mind when comparing the results presented in this paper with those of other authors is that in the present work the excised MN segment was not inverted, as it is customary.[44, 48] The inversion of the nerve segment minimizes distal dispersion of the growing axons, maximizing the odds of these axons reaching their target organs, and ultimately leading to better functional recovery.[44, 48] In spite of this, the need of obtaining vascularized nerve conduits in this work precluded MN inversion. However, this variable was the same in all experimental groups, maintaining internal consistency of results.

Additionally, rat sexual dimorphism in nerve regeneration should be taken into account.[113] Female rats present better nerve regeneration, presumably because of the beneficial effects of sex hormones.[113, 128-130] This fact leads many researchers to use female

rats in peripheral nerve regeneration to maximize differences between experimental groups.[113] However, in humans, most injuries occur in males.[35, 131]

As other authors, in the present work we have used a morphological assessment of the blood supply to the reconstructed nerve segment, which was the *vasa nervorum* density.[132] However, it would be interesting to precisely evaluate the perfusion in each of the nerve conduits used using other methods in future studies.[133] Quantitative microelectrode hydrogen clearance polarography, laser doppler flowmetry, autoradiography employing radionuclides, and microsphere embolization would be viable alternatives.[132]

The arterio-venous fistula used to produce PNFs could have been applied in the contralateral forelimb, to produce a PNF involving a MN segment homologous to the nerve defect. This could potentially have facilitated comparison of the different vascular patterns used in nerve flaps. However, this option was not favored in the present study, as it would be technically vexing, and it would cause a major motor limitation in both forepaws, potentially compromising rats' abilities to conduct their daily activities, such as feeding or grooming.

In this study, only the most commonly described unconventional perfusion nerve flap was used, the ANVF. However, venous flow-through NFs have been shown to yield similar results to those obtained with ANVFs in a rat femoral nerve model.[28, 29] Further studies are warranted to confirm or dismiss this findings in the model used in the present study. Finally, it would have been interesting to include in this work a group using a rat MN allograft, as these conduits have been gaining increasing popularity in clinical practice.[9, 10, 23, 123] Noteworthily, Giusti *et al.*

have recently demonstrated in a rat sciatic nerve model that blocking allograft vascularization from surrounding tissues was detrimental for motor recovery.[23] Thus, further studies are warranted in this field.

CONCLUSION

CNFs and ANVFs produced a faster and more complete recovery than NGs in the reconstruction of a 10-mm-long median nerve gap in an ischemic environment in the Wistar rat. Although results obtained with CNFs were in most cases better than those of ANVFs, these differences were not statistically significant for most of the outcome variables.

ACKNOWLEDGEMENTS

The authors would like to thank Mr. Filipe Franco and Mr. Nuno Folque for the drawings contained in this article.

References

1. Desouches C, Alluin O, Mutaftschiev N, Dousset E, Magalon G, Boucraut J, et al. [Peripheral nerve repair: 30 centuries of scientific research]. Revue neurologique. 2005;161(11):1045-59. Epub 2005/11/17. PubMed PMID: 16288170.

2. Boyd KU, Fox IK. Nerve repair and grafting. In: Mackinnon SE, editor. Nerve surgery. 1. First ed. New York: Thieme; 2015. p. 75-100.

3. Wood MJ, Johnson PJ, Myckatyn TM. Anatomy and physiology for the peripheral nerve surgeon. In: Mackinnon SE, Yee A, editors. Nerve Surgery. 1. First ed. New York: Thieme; 2015. p. 1-40.

4. Philipeaux J, Vulpian A. Note sur des essais de greffe d'un troncon du nerf lingual entre les deux bouts du nerf hypoglosse, apres excision d'un segment de ce dernier nerf. Arch Physiol Norm Pathol. 1870;3:618-20.

5. Friedman AH. An eclectic review of the history of peripheral nerve surgery. Neurosurgery. 2009;65(4 Suppl):A3-8. Epub 2009/12/16. doi: 10.1227/01.NEU.0000346252.53722.D3. PubMed PMID: 19927076.

6. Geuna S, Tos P, Titolo P, Ciclamini D, Beningo T, Battiston B. Update on nerve repair by biological tubulization. Journal of brachial plexus and peripheral nerve injury. 2014;9(1):3. Epub 2014/03/13. doi: 10.1186/1749-7221-9-3. PubMed PMID: 24606921; PubMed Central PMCID: PMC3953745.

7. M.A. F, Wilbourn AJ. The electrodiagnostic examination with peripheral nerve injuries. In: Mackinnon SE, editor. Nerve surgery. 1. First ed. New York: Thieme; 2015. p. 59-74.

8. Rinker B, Zoldos J, Weber RV, Ko J, Thayer W, Greenberg J, et al. Use of Processed Nerve Allografts to Repair Nerve Injuries Greater Than 25 mm in the Hand. Ann Plast Surg. 2017;78(6S Suppl 5):S292-s5. Epub 2017/03/23. doi: 10.1097/sap.0000000000001037. PubMed PMID: 28328632.

9. Safa B, Buncke G. Autograft Substitutes: Conduits and Processed Nerve Allografts. Hand clinics. 2016;32(2):127-40. Epub 2016/04/21. doi: 10.1016/j.hcl.2015.12.012. PubMed PMID: 27094886.

10. Giusti G, Willems WF, Kremer T, Friedrich PF, Bishop AT, Shin AY. Return of motor function after segmental nerve loss in a rat model: comparison of autogenous nerve graft, collagen conduit, and processed allograft (AxoGen). The Journal of bone and joint surgery American volume. 2012;94(5):410-7. Epub 2012/03/09. doi: 10.2106/jbjs.k.00253. PubMed PMID: 22398734.

11. Ney KW. TECHNIC OF NERVE SURGERY. Annals of surgery. 1921;74(1):37-60. Epub 1921/07/01. PubMed PMID: 17864490; PubMed Central PMCID: PMCPMC1399588.

12. Seddon H. The use of autogenous grafts for the repair of large gaps in peripheral nerves. British Journal of Surgery. 1947;35(138):151-67.

13. Strange F. An operation for nerve pedicle grafting. Preliminary communication. British Journal of Surgery. 1947;34(136):423-5.

14. Taylor GI, Ham FJ. The free vascularized nerve graft. A further experimental and clinical application of microvascular techniques. Plastic and reconstructive surgery. 1976;57(4):413-26. Epub 1976/04/01. PubMed PMID: 1273122.

15. Hong MK, Taylor GI. Angiosome territories of the nerves of the upper limbs. Plastic and reconstructive surgery. 2006;118(1):148-60. Epub 2006/07/04. doi: 10.1097/01.prs.0000221075.91038.08. PubMed PMID: 16816688.

16. Breidenbach WC, Terzis JK. The blood supply of vascularized nerve grafts. J Reconstr Microsurg. 1986;3(1):43-58. Epub 1986/10/01. doi: 10.1055/s-2007-1007038. PubMed PMID: 3795195.

17. Chuang DC. Adult brachial plexus reconstruction with the level of injury: review and personal experience. Plast Reconstr Surg. 2009;124(6 Suppl):e359-69. Epub 2010/01/09. doi: 10.1097/PRS.0b013e3181bcf16c

00006534-200912001-00010 [pii]. PubMed PMID: 19952704.

18. Kakinoki R, Ikeguchi R, Nakayama K, Nakamura T. Functioning transferred free muscle innervated by part of the vascularized ulnar nerve connecting the contralateral cervical seventh root to themedian nerve: case report. J Brachial Plex Peripher Nerve Inj. 2007;2:18. Epub 2007/09/22. doi: 1749-7221-2-18 [pii]

10.1186/1749-7221-2-18. PubMed PMID: 17883873; PubMed Central PMCID: PMC2080628.

19. Townsend PL, Taylor GI. Vascularised nerve grafts using composite arterialised neuro-venous systems. Br J Plast Surg. 1984;37(1):1-17. Epub 1984/01/01. PubMed PMID: 6692051.

20. Casal D, Carvalho S, Pais D, Mota-Silva E, Iria I, Vieira P, et al. Unconventional Perfusion Flaps. 2017. In: Flap Surgery [Internet]. AvidScience; [2-41]. Available from: http://www.avidscience.com/wp-content/uploads/2017/08/unconventional-perfusion-flaps.pdf.

21. Casal D, Cunha T, Pais D, Videira P, Coloma J, Zagalo C, et al. Systematic Review and Meta-Analysis of Unconventional Perfusion Flaps in Clinical Practice. Plastic and reconstructive surgery. 2016;138(2):459-79. doi: 10.1097/PRS.0000000000002390. PubMed PMID: 27465169.

22. ANGÉLICA-ALMEIDA M, CASAL D, MAFRA M, MASCARENHAS-LEMOS L, SILVA E, FARINHO A, et al. Evaluation of the efficacy of different conduits to bridge a 10 millimeter defect in the rat sciatic nerve in the presence of an axial blood supply. Archives of Anatomy. 2014;2:8-30.

23. Giusti G, Lee JY, Kremer T, Friedrich P, Bishop AT, Shin AY. The influence of vascularization of transplanted processed allograft nerve on return of motor function in rats. Microsurgery. 2016;36(2):134-43. Epub 2015/01/06. doi: 10.1002/micr.22371. PubMed PMID: 25557845.

24. D'Arpa S, Claes KEY, Stillaert F, Colebunders B, Monstrey S, Blondeel P. Vascularized nerve "grafts": just a graft or a worthwhile procedure? Plastic and Aesthetic Research. 2015;2(4):183-94.

25. Brandt J, Dahlin LB, Lundborg G. Autologous tendons used as grafts for bridging peripheral nerve defects. J Hand Surg Br. 1999;24(3):284-90. Epub 1999/08/05. doi: 10.1054/jhsb.1999.0074

S0266-7681(99)90074-8 [pii]. PubMed PMID: 10433437.

26. Millesi H. Bridging defects: autologous nerve grafts. Acta Neurochir Suppl. 2007;100:37-8. Epub 2007/11/08. PubMed PMID: 17985542.

27. Hems TEJ, Glasby MA. Comparison of different methods of repair of long peripheral nerve defects: an experimental study. British journal of plastic surgery. 1992;45(7):497-502. doi: http://dx.doi.org/10.1016/0007-1226(92)90141-J.

28. Vargel I. Impact of vascularization type on peripheral nerve microstructure. J Reconstr Microsurg. 2009;25(4):243-53. Epub 2008/12/17. doi: 10.1055/s-0028-1104557. PubMed PMID: 19085817.

29. Vargel I, Demirci M, Erdem S, Firat P, Surucu HS, Tan E, et al. A comparison of various vascularization-perfusion venous nerve grafts with conventional nerve grafts in rats. J Reconstr Microsurg. 2009;25(7):425-37. Epub 2009/05/28. doi: 10.1055/s-0029-1223852. PubMed PMID: 19472105.

30. Donzelli R, Capone C, Sgulo FG, Mariniello G, Maiuri F. Vascularized nerve grafts: an experimental study. Neurological research. 2016;38(8):669-77. doi: 10.1080/01616412.2016.1198527. PubMed PMID: 27349271.

31. Cavadas PC, Vera-Sempere FJ. Prefabrication of a vascularized nerve graft by vessel implantation: preliminary report of an experimental model. Microsurgery. 1994;15(12):877-81. Epub 1994/01/01. PubMed PMID: 7535881.

32. Karcher H, Kleinert R. Regeneration in vascularized and free nerve grafts. A comparative morphological study in rats. Journal of maxillofacial surgery. 1986;14(6):341-3. Epub 1986/12/01. PubMed PMID: 3467003.

33. Guo L, Pribaz JJ. Clinical flap prefabrication. Plastic and reconstructive surgery. 2009;124(6 Suppl):e340-50. Epub 2010/01/09. doi: 10.1097/PRS.0b013e3181bcf094. PubMed PMID: 19952702.

34. Shin RH, Friedrich PF, Crum BA, Bishop AT, Shin AY. Treatment of a segmental nerve defect in the rat with use of bioabsorbable synthetic nerve conduits: a comparison of commercially available conduits. J Bone Joint Surg Am. 2009;91(1):2194-204.

35. Rosberg HEeLD. Epidemiology of hand injuries in a middle-sized city in southern Sweden - a retrospective study with an 8-year interval. Scand J Plast Rec Surg Hand Surg. 2004;(38):347-55.

36. National Research Council (U.S.). Committee for the Update of the Guide for the Care and Use of Laboratory Animals., Institute for Laboratory Animal Research (U.S.), National Academies Press (U.S.). Guide for the care and use of laboratory animals. Washington, D.C.: National Academies Press,; 2011. Available from: http://www.ncbi.nlm.nih.gov/books/NBK54050.

37. Havenaar Rea. Biology and husbrandry of laboratoy animals. In: Principles of Laboratory Animal Science. Editores: Van Zutphen, L.F.M.; Baumans, V.; Beynen, A.C.. Elsevier. 2001:29-32.

38. Bertelli JAM, J.C. Behavioural evaluating methods in the objective clinical assessment of motor function after experimental brachial plexus reconstruction in the rat. Journal of neuroscience methods. 1993;46:203-8.

39. Dijkstra JR, et al. . Methods to evaluate functional nerve recovery in adult rats: walking track analysis, video analysis and the withdrawal reflex. Journal of neuroscience methods. 2000;96(2):89-96.

40. Rupp A, Dornseifer U, Rodenacker K, Fichter A, Jutting U, Gais P, et al. Temporal progression and extent of the return of sensation in the foot provided by the saphenous nerve after sciatic nerve transection and repair in the rat - implications for nociceptive assessments. Somatosensory & motor research. 2007;24(1-2):1-13. Epub 2007/06/15. doi: 10.1080/08990220601116329. PubMed PMID: 17558918.

41. Casal D, Pais D, Iria I, Mota-Silva E, Almeida M-A, Alves S, et al. A Model of Free Tissue Transfer: The Rat Epigastric Free Flap. Journal of Visualized Experiments. 2017;1(119):e55281. doi: doi:10.3791/55281.

42. Matsumine H, Sasaki R, Takeuchi Y, Miyata M, Yamato M, Okano T, et al. Vascularized versus nonvascularized island median nerve grafts in the facial nerve regeneration and functional recovery of rats for facial nerve reconstruction study. Journal of reconstructive microsurgery. 2014;30(02):127-36.

43. Bertelli JAM, J.C. The grasping test: a simple behavioral method for objective quantitative assessment of peripherla nerve regeneration in the rat. Journal of neuroscience methods. 1995;58(1-2):151-5.

44. Bontioti EKM, Dahlin LB. Regeneration and functional recovery in the upper extermity of rats after various types of nerve injuries. Journal of the Peripheral Nervous System. 2003;8:159-68.

45. Galtrey CM, Fawcett JW. Characterization of tests of functional recovery after median and ulnar nerve injury and repair in the rat forelimb. J Peripher Nerv Syst. 2007;12(1):11-27. Epub 2007/03/22. doi: 10.1111/j.1529-8027.2007.00113.x. PubMed PMID: 17374098.

46. Angelica-Almeida M, Casal D, Mafra M, Mascarenhas-Lemos L, Martins-Ferreira J, Ferraz-Oliveira M, et al. Brachial plexus morphology and vascular supply in the wistar rat. Acta Med Port. 2013;26(3):243-50. Epub 2013/07/03. PubMed PMID: 23815839.

47. Bertelli JA, Taleb M, Saadi A, Mira JC, Pecot-Dechavassine M. The rat brachial plexus and its terminal branches: an experimental model for the study of peripheral nerve regeneration. Microsurgery. 1995;16(2):77-85. Epub 1995/01/01. PubMed PMID: 7783609.

48. Yanase Y. Micronerve suture and graft in the rat. In: Tamai S, Usui M, Yoshizu T, editors. Experimental and Clinical Reconstructive Microsurgery. First ed. Japan: Springer-Verlag; 2004. p. 44-51.

49. Geuna S, Varejao AS. Evaluation methods in the assessment of peripheral nerve regeneration. Journal of neurosurgery. 2008;109(2):360-2; author reply 2. Epub 2008/08/02. doi: 10.3171/JNS/2008/109/8/0360. PubMed PMID: 18671655.

50. Ronchi G, Nicolino S, Raimondo S, Tos P, Battiston B, Papalia I, et al. Functional and morphological assessment of a standardized crush injury of the rat median nerve. Journal of neuroscience methods. 2009;179(1):51-7. Epub 2009/05/12. doi: 10.1016/j.jneumeth.2009.01.011. PubMed PMID: 19428511.

51. Ronchi G, Raimondo S, Varejao AS, Tos P, Perroteau I, Geuna S. Standardized crush injury of the mouse median nerve. Journal of neuroscience methods. 2010;188(1):71-5. Epub 2010/01/29. doi: 10.1016/j.jneumeth.2010.01.024. PubMed PMID: 20105442.

52. Kobbert C, Apps R, Bechmann I, Lanciego JL, Mey J, Thanos S. Current concepts in neuroanatomical tracing. Progress in neurobiology. 2000;62(4):327-51. Epub 2000/06/17. PubMed PMID: 10856608.

53. Bertelli JAM, J.C. The grasping test: a simple behavioral method for objective quantitative assessment of peripheral nerve regeneration in the rat. Journal of neuroscience methods. 1995;58(1-2):151-5.

54. Papalia I, Tos P, Stagno d'Alcontres F, Battiston B, Geuna S. On the use of the grasping test in the rat median nerve model: a re-appraisal of its efficacy for quantitative assessment of motor function recovery. Journal of neuroscience methods. 2003;127(1):43-7. Epub 2003/07/17. PubMed PMID: 12865147.

55. Costa LM, Simoes MJ, Mauricio AC, Varejao AS. Chapter 7: Methods and protocols in peripheral nerve regeneration experimental research: part IV-kinematic gait analysis to quantify peripheral nerve regeneration in the rat. International review of neurobiology. 2009;87:127-39. Epub 2009/08/18. doi: 10.1016/s0074-7742(09)87007-4. PubMed PMID: 19682636.

56. Howard RF, Hatch DJ, Cole TJ, Fitzgerald M. Inflammatory pain and hypersensitivity are selectively reversed by epidural bupivacaine and are developmentally regulated. Anesthesiology. 2001;95(2):421-7. PubMed PMID: 11506116.

57. de Sousa MV, Ferraresi C, de Magalhaes AC, Yoshimura EM, Hamblin MR. Building, testing and validating a set of home-made von Frey filaments: A precise, accurate and cost effective alternative for nociception assessment. Journal of neuroscience methods. 2014;232:1-5. Epub 2014/05/06. doi: 10.1016/j.jneumeth.2014.04.017. PubMed PMID: 24793398.

58. Lambert GA, Mallos G, Zagami AS. Von Frey's hairs--a review of their technology and use--a novel automated von Frey device for improved testing for hyperalgesia. Journal of neuroscience methods. 2009;177(2):420-6. Epub 2008/12/02. doi: 10.1016/j.jneumeth.2008.10.033. PubMed PMID: 19041344.

59. Blackburn-Munro G. Pain-like behaviours in animals - how human are they? Trends in pharmacological sciences. 2004;25(6):299-305. Epub 2004/05/29. doi: 10.1016/j.tips.2004.04.008. PubMed PMID: 15165744.

60. Pitcher GM, Ritchie J, Henry JL. Paw withdrawal threshold in the von Frey hair test is influenced by the surface on which the rat stands. Journal of neuroscience methods. 1999;87(2):185-93. Epub 2001/03/07. PubMed PMID: 11230815.

61. Metz GA, Whishaw IQ. Cortical and subcortical lesions impair skilled walking in the ladder rung walking test: a new task to evaluate fore-and hindlimb stepping, placing, and co-ordination. Journal of neuroscience methods. 2002;115(2):169-79.

62. Hadlock TA, et al. A comparison of assessments of functional recovery in the rat. J Peripher Nerv Syst. 1999;4(3-4):258-64.

63. Brown CJ, Mackinnon SE, Evans PJ, Bain JR, Makino AP, Hunter DA, et al. Self-evaluation of walking-track measurement using a Sciatic Function Index. Microsurgery. 1989;10(3):226-35. Epub 1989/01/01. PubMed PMID: 2796719.

64. Hruska RE, Kennedy S, Silbergeld EK. Quantitative aspects of normal locomotion in rats. Life sciences. 1979;25(2):171-9.

65. Ludwig N, Formenti D, Gargano M, Alberti G. Skin temperature evaluation by infrared thermography: Comparison of image analysis methods. Infrared Physics & Technology. 2014;62:1-6.

66. Bennett GJ, Ochoa J. Thermographic observations on rats with experimental neuropathic pain. Pain. 1991;45(1):61-7.

67. Wakisaka S, Kajander KC, Bennett GJ. Abnormal skin temperature and abnormal sympathetic vasomotor innervation in an experimental painful peripheral neuropathy. Pain. 1991;46(3):299-313.

68. Wu Y, Martínez MÁM, Balaguer PO. Overview of the Application of EMG Recording in the Diagnosis and Approach of Neurological Disorders. In: Turker H, editor. Electrodiagnosis in New Frontiers of Clinical Research. Rijeka: InTech; 2013. p. Ch. 01.

69. Werdin F, Grussinger H, Jaminet P, Kraus A, Manoli T, Danker T, et al. An improved electrophysiological method to study peripheral nerve regeneration in rats. Journal of neuroscience methods. 2009;182(1):71-7. Epub 2009/06/10. doi: 10.1016/j.jneumeth.2009.05.017. PubMed PMID: 19505504.

70. Manoli T, Werdin F, Gruessinger H, Sinis N, Schiefer JL, Jaminet P, et al. Correlation analysis of histomorphometry and motor neurography in the median nerve rat model. Eplasty. 2014;14:e17. Epub 2014/06/07. PubMed PMID: 24904711; PubMed Central PMCID: PMC3984537.

71. Navarro X, Udina E. Chapter 6: Methods and protocols in peripheral nerve regeneration experimental research: part III-electrophysiological evaluation. International review of neurobiology. 2009;87:105-26. Epub 2009/08/18. doi: 10.1016/s0074-7742(09)87006-2. PubMed PMID: 19682635.

72. Raimondo S, Fornaro M, Di Scipio F, Ronchi G, Giacobini-Robecchi MG, Geuna S. Chapter 5: Methods and protocols in peripheral nerve regeneration experimental research: part II-morphological techniques. International review of neurobiology. 2009;87:81-103. Epub 2009/08/18. doi: 10.1016/s0074-7742(09)87005-0. PubMed PMID: 19682634.

73. World I. Neurofilament Antibody Staining Protocol for Immunohistochemistry [16/09/2017]. Available from: http://www.ihcworld.com/_protocols/antibody_protocols/neurofilament_chemicon.htm.

74. Holland SK, Hessler RB, Reid-Nicholson MD, Ramalingam P, Lee JR. Utilization of peripherin and S-100 immunohistochemistry in the diagnosis of Hirschsprung disease. Mod Pathol. 2010;23(9):1173-9.

75. Rakonczay Z, Brimijoin S. Monoclonal antibodies to rat brain acetylcholinesterase: comparative affinity for soluble and membrane-associated enzyme and for enzyme from different vertebrate species. Journal of neurochemistry. 1986;46(46).

76. Ikeda M, Oka Y. The relationship between nerve conduction velocity and fiber morphology during peripheral nerve regeneration. Brain and Behavior. 2012;2(4):382-90. doi: 10.1002/brb3.61. PubMed PMID: PMC3432961.

77. Afifi AK, Bergman RA. Neurohistology. In: Afifi AK, Bergman RA, editors. Functional Neuroanatomy: text and atlas. Second ed. United States of America: McGraw-Hill; 2005. p. 3-23.

78. Nolte J. Sensory receptors and the peripheral nervous system. In: Nolte J, editor. The human brain: an introduction to its functional anatomy. Fifth ed. Tucson, Arizon: Mosby; 2002. p. 197-222.

79. Riley DA, Sanger JR, Matloub HS, Yousif NJ, Bain JLW, Moore GH. Identifying motor and sensory myelinated axons in rabbit peripheral nerves by histochemical staining for carbonic anhydrase and cholinesterase activities. Brain Research. 1988;453(1):79-88. doi: http://dx.doi.org/10.1016/0006-8993(88)90145-X.

80. Zochodne DW. The intact peripheral nerve tree. In: Zochodne DW, editor. Neurobiology of peripheral nerve regeneration. 1. First ed. United Kingdom: Cambridge; 2008. p. 8-38.

81. Szabolcs MJ, Windisch A, Koller R, Pensch M. Axon typing of rat muscle nerves using a double staining procedure for cholinesterase and carbonic anhydrase. The journal of histochemistry and cytochemistry : official journal of the Histochemistry Society. 1991;39(12):1617-25. Epub 1991/12/01. doi: 10.1177/39.12.1719070. PubMed PMID: 1719070.

82. Geuna S, Tos P, Guglielmone R, Battiston B, Giacobini-Robecchi MG. Methodological issues in size estimation of myelinated nerve fibers in peripheral nerves. Anatomy and embryology. 2001;204(1):1-10. Epub 2001/08/17. PubMed PMID: 11506429.

83. West MJ. Estimating object number. In: West MJ, editor. Basic stereology for biologists and neuroscientists. 1. First ed. New York: Cold Spring Harbor Laboratory Press; 2012. p. 31-58.

84. Geuna S. The revolution of counting "tops": two decades of the disector principle in morphological research. Microscopy research and technique. 2005;66(5):270-4. Epub 2005/06/09. doi: 10.1002/jemt.20167. PubMed PMID: 15940681.

85. Puigdellivol-Sanchez A, Prats-Galino A, Molander C. On regenerative and collateral sprouting to hind limb digits after sciatic nerve injury in the rat. Restorative neurology and neuroscience. 2005;23(2):97-107. Epub 2005/07/02. PubMed PMID: 15990416.

86. Daly WT, Yao L, Abu-rub MT, O'Connell C, Zeugolis DI, Windebank AJ, et al. The effect of intraluminal contact mediated guidance signals on axonal mismatch during peripheral nerve repair. Biomaterials. 2012;33(28):6660-71. doi: 10.1016/j.biomaterials.2012.06.002. PubMed PMID: 22738778.

87. Sarikcioglu L, Oguz N. Exercise training and axonal regeneration after sciatic nerve injury. The International journal of neuroscience. 2001;109(3-4):173-7. Epub 2001/11/09. PubMed PMID: 11699329.

88. Jivan S, Novikova LN, Wiberg M, Novikov LN. The effects of delayed nerve repair on neuronal survival and axonal regeneration after seventh cervical spinal nerve axotomy in adult rats. Experimental brain research Experimentelle Hirnforschung Experimentation cerebrale.

2006;170(2):245-54. Epub 2005/12/06. doi: 10.1007/s00221-005-0207-7. PubMed PMID: 16328277.

89. Rupp A. Functional, electrophysioologic and morphometric evaluation of peripheral nerve regeneration after bridging a 14 mm gap in the rat sciatic nerve. Munich: Ludwig-Maximilians; 2007.

90. Angius D, Wang H, Spinner RJ, Gutierrez-Cotto Y, Yaszemski MJ, Windebank AJ. A systematic review of animal models used to study nerve regeneration in tissue-engineered scaffolds. Biomaterials. 2012;33(32):8034-9. Epub 2012/08/15. doi: 10.1016/j.biomaterials.2012.07.056. PubMed PMID: 22889485; PubMed Central PMCID: PMCPMC3472515.

91. Evans GR. Peripheral nerve injury: a review and approach to tissue engineered constructs. Anat Rec. 2001;263(4):396-404.

92. Myckatyn TM, Mackinnon SE. A review of research endeavors to optimize peripheral nerve reconstruction. Neurol Res. 2004;26(1):124-38.

93. Koshima I, Harii K. Experimental study of vascularized nerve grafts: Multifactorial analyses of axonal regeneration of nerves transplanted into an acute burn wound. The Journal of hand surgery. 1985;10(1):64-72. doi: http://dx.doi.org/10.1016/S0363-5023(85)80249-5.

94. Koshima I, Harii K. Experimental study of vascularized nerve grafts: multifactorial analyses of axonal regeneration of nerves transplanted into an acute burn wound. The Journal of hand surgery. 1985;10(1):64-72. Epub 1985/01/01. PubMed PMID: 3968406.

95. Gu YD, Wu MM, Zheng YL, Li HR, Xu YN. Arterialized venous free sural nerve grafting. Ann Plast Surg. 1985;15(4):332-9. Epub 1985/10/01. PubMed PMID: 4083733.

96. Breidenbach WC, Terzis JK. Vascularized nerve grafts: an experimental and clinical review. Ann Plast Surg. 1987;18(2):137-46. Epub 1987/02/01. PubMed PMID: 3566101.

97. Koshima IH, K. Experimental studies on vascularized nerve grafts in rats. J Microsurg. 1981;2:225-6.

98. Breindenbach WT, JK. The anatomy of free vascularized nerve grafts. Clin Plast Surg. 1984;11:65-71.

99. Jabaley ME. Primary Nerve Repair. In: Peripheral Nerve Surgery: Practical Applications in the Upper Extremity. Editores: Slutsky, D.J.; Hentz, V.R. Churchill Livingstone. 2006:23-38.

100. Dahlin LB. Nerve injury and repair: from molecule to Man. In: Slutsky DJ, Hentz VR, editors. Peripheral Nerve Surgery: Practical Applications in the Upper Extremity. Philadelphia: Elsevier; 2006. p. 1-22.

101. ANGÉLICA-ALMEIDA M, CASAL D, MAFRA M, MASCARENHAS-LEMOS L, MARTINS-FERREIRA J, FERRAZ-OLIVEIRA M, et al. Angiomorphological comparison of the sciatic nerve of the rat and the human median nerve: implications in experimental procedures. Archives of Anatomy. 2014;2:31-51.

102. Santos AP, Suaid CA, Fazan VP, Barreira AA. Microscopic anatomy of brachial plexus branches in Wistar rats. Anat Rec (Hoboken). 2007;290(5):477-85. doi: 10.1002/ar.20519. PubMed PMID: 17436315.

103. Nichols CM, Brenner MJ, Fox IK, Tung TH, Hunter DA, Rickman SR, et al. Effects of motor versus sensory nerve grafts on peripheral nerve regeneration. Experimental neurology. 2004;190(2):347-55. doi: http://dx.doi.org/10.1016/j.expneurol.2004.08.003.

104. Bennett K, Heywood W, Di WL, Harper J, Clayman GL, Jayakumar A, et al. The identification of a new role for LEKTI in the skin: The use of protein 'bait' arrays to detect defective trafficking of dermcidin in the skin of patients with Netherton syndrome. Journal of proteomics. 2012;75(13):3925-37. Epub 2012/05/17. doi: 10.1016/j.jprot.2012.04.045. PubMed PMID: 22588119.

105. Ochoa JL, Yarnitsky D, Marchettini P, Dotson R, Cline M. Interactions between sympathetic vasoconstrictor outflow and C nociceptor-induced antidromic vasodilatation. Pain. 1993;54(2):191-6. Epub 1993/08/01. PubMed PMID: 8233533.

106. Sacharuk VZ, Lovatel GA, Ilha J, Marcuzzo S, Pinho ASd, Xavier LL, et al. Thermographic evaluation of hind paw skin temperature and functional recovery of locomotion after sciatic nerve crush in rats. Clinics. 2011;66(7):1259-66.

107. Kilinc A, Ben Slama S, Dubert T, Dinh A, Osman N, Valenti P. [Results of primary repair of injuries to the median and ulnar nerves at the wrist]. Chirurgie de la main. 2009;28(2):87-92. Epub 2009/02/28. doi: 10.1016/j.main.2009.01.001. PubMed PMID: 19246233.

108. Chan RK. Splinting for peripheral nerve injury in upper limb. Hand surgery : an international journal devoted to hand and upper limb surgery and related research : journal of the Asia-Pacific Federation of Societies for Surgery of the Hand. 2002;7(2):251-9. Epub 2003/02/22. PubMed PMID: 12596288.

109. Sulaiman W, Gordon T. Neurobiology of peripheral nerve injury, regeneration, and functional recovery: from bench top research to bedside application. Ochsner J. 2013;13(1):100-8. PubMed PMID: 23531634; PubMed Central PMCID: PMCPMC3603172.

110. Vincent R. Adult and obstetrical brachial plexus injuries. In: Peripheral Nerve Surgery: Practical applications in the upper extremity. Editores: Slutsky DJ, Hentz VR. Churchill Livingstone. 2006:299-317.

111. Urbancheck MSea. Rat walking tracks do not reflect maximal muscle force capacity. J Reconstr Microsurg. 1999;15(2):143-9.

112. Bontioti E. End-to-side nerve repair. A study in the forelimb of the rat. Tese de Doutoramento. Faculdade de Medicina da Universidade de Lund. Suécia. 2005:36-41.

113. Tos P, Ronchi G, Papalia I, Sallen V, Legagneux J, Geuna S, et al. Chapter 4: Methods and protocols in peripheral nerve regeneration experimental research: part I-experimental models. International review of neurobiology. 2009;87:47-79. Epub 2009/08/18. doi: 10.1016/s0074-7742(09)87004-9. PubMed PMID: 19682633.

114. Papalia I, Tos P, Scevola A, Raimondo S, Geuna S. The ulnar test: a method for the quantitative functional assessment of posttraumatic ulnar nerve recovery in the rat. Journal of neuroscience methods. 2006;154(1-2):198-203. Epub 2006/02/10. doi: 10.1016/j.jneumeth.2005.12.012. PubMed PMID: 16466801.

115. Bodine-Fowler SCea. Inaccurate projection of rat soleus motoneurons: a comparison of nerve repair techniques. Muscle & nerve. 1997;20(1):29-37.

116. Valero-Cabre AN, X. H reflex restitution and facilitation after different types of peripheral nerve injury and repair. Brain Res. 2001;919(2):302-12.

117. Wall PD, et al. Autotomy following peripheral nerve lesions: experimental anaesthesia dolorosa. Pain. 1979;7(2):103-11.

118. Bertelli JAS, A; Pecot-Dechavassine, M. The rat brachial plexus an its terminal branches: an experimental model for the study of peripheral nerve regeneration. Microsurgery. 1995;16:77-85.

119. Murovic JA. Upper-extremity peripheral nerve injuries: a Louisiana State University Health Sciences Center literature review with comparison of the operative outcomes of 1837 Louisiana State University Health Sciences Center median, radial, and ulnar nerve lesions. Neurosurgery. 2009;65(4 Suppl):A11-7. Epub 2009/12/16. doi: 10.1227/01.neu.0000339130.90379.89. PubMed PMID: 19927055.

120. Nichols CM, Myckatyn TM, Rickman SR, Fox IK, Hadlock T, Mackinnon SE. Choosing the correct functional assay: a comprehensive assessment of functional tests in the rat. Behavioural brain research. 2005;163(2):143-58. Epub 2005/06/28. doi: 10.1016/j.bbr.2005.05.003. PubMed PMID: 15979168.

121. Bertelli JAG, M.F. Concepts of Nerve Regeneration and Repair Applied to the Brachial Plexus Reconstruction. Microsurgery. 2006;26:230-44.

122. Battiston B, Geuna S, Ferrero M, Tos P. Nerve repair by means of tubulization: literature review and personal clinical experience comparing biological and synthetic conduits for sensory

nerve repair. Microsurgery. 2005;25(4):258-67. Epub 2005/06/04. doi: 10.1002/micr.20127. PubMed PMID: 15934044.

123. Isaacs J, Browne T. Overcoming short gaps in peripheral nerve repair: conduits and human acellular nerve allograft. Hand (N Y). 2014;9(2):131-7. doi: 10.1007/s11552-014-9601-6. PubMed PMID: 24839412; PubMed Central PMCID: PMCPMC4022952.

124. Fu SY, Gordon T. Contributing factors to poor functional recovery after delayed nerve repair: prolonged denervation. The Journal of neuroscience : the official journal of the Society for Neuroscience. 1995;15(5 Pt 2):3886-95. Epub 1995/05/01. PubMed PMID: 7751953.

125. Guth L. Regeneration in the mammalian peripheral nervous system. Physiological reviews. 1956;36(4):441-78. Epub 1956/10/01. PubMed PMID: 13370345.

126. Strasberg JE, Strasberg S, Mackinnon SE, Watanabe O, Hunter DA, Tarasidis G. Strain differences in peripheral-nerve regeneration in rats. J Reconstr Microsurg. 1999;15(4):287-93. Epub 1999/06/11. doi: 10.1055/s-2007-1000103. PubMed PMID: 10363552.

127. Kaplan HM, Mishra P, Kohn J. The overwhelming use of rat models in nerve regeneration research may compromise designs of nerve guidance conduits for humans. Journal of materials science Materials in medicine. 2015;26(8):226. Epub 2015/08/25. doi: 10.1007/s10856-015-5558-4. PubMed PMID: 26296419; PubMed Central PMCID: PMCPMC4545171.

128. Melcangi RC, Giatti S, Calabrese D, Pesaresi M, Cermenati G, Mitro N, et al. Levels and actions of progesterone and its metabolites in the nervous system during physiological and pathological conditions. Progress in neurobiology. 2014;113:56-69. Epub 2013/08/21. doi: 10.1016/j.pneurobio.2013.07.006. PubMed PMID: 23958466.

129. Roglio I, Bianchi R, Gotti S, Scurati S, Giatti S, Pesaresi M, et al. Neuroprotective effects of dihydroprogesterone and progesterone in an experimental model of nerve crush injury. Neuroscience. 2008;155(3):673-85. Epub 2008/07/16. doi: 10.1016/j.neuroscience.2008.06.034. PubMed PMID: 18625290.

130. Kovacic U, Sketelj J, Bajrovic FF. Sex-related difference in collateral sprouting of nociceptive axons after peripheral nerve injury in the rat. Experimental neurology. 2003;184(1):479-88. Epub 2003/11/26. PubMed PMID: 14637117.

131. Frazier WH, et al. Hand injuries: incidence and epidemiology in an emergency service. Jacep. 1978;7(7):265-8.

132. Zochodne DW. Regeneration and the vasa nervorum. In: Zochodne DW, editor. Neurobiology of peripheral nerve regeneration. 1. First ed. United Kingdom: Cambridge; 2008. p. 153-69.

133. Wang Y, Tang P, Zhang L, Guo Y, Wan W. Quantitative evaluation of the peripheral nerve blood perfusion with high frequency contrast-enhanced ultrasound. Academic radiology. 2010;17(12):1492-7.

Chapter 10

SURGICAL ANATOMY OF COMMON REGIONS USED TO HARVEST UNCONVENTIONAL PERFUSION FLAPS: A CADAVERIC DISSECTION STUDY

Authors: Diogo Casal, MD[1,2,3,4]; Diogo Pais, MD, PhD[2]; Eduarda Mota-Silva, MSci[5]; Inês Iria, MSci[6]; Sara Alves, MSci[8]; Luís Mascarenhas-Lemos, MD[7]; Cláudia Pen, MSci[7]; Mário Ferraz-Oliveira, MD[7]; Paula A. Videira, PhD[3,4,8]; João Goyri-O'Neill, MD, PhD[2]

Affiliations:

1- Plastic and Reconstructive Surgery Department and Burn Unit; Centro Hospitalar de Lisboa Central, Lisbon, Portugal

2- Anatomy Department; Nova Medical School, Lisbon, Portugal

3- UCIBIO, Departamento de Ciências da Vida, Faculdade de Ciências e Tecnologia, Universidade NOVA de Lisboa, Caparica, Portugal

4- CEDOC, NOVA Medical School, Universidade NOVA de Lisboa, Lisbon, Portugal

5- LIBPhys, Physics Department, Faculdade de Ciências e Tecnologias, Universidade NOVA de Lisboa, Lisbon, Portugal

6- iMed - Research Institute for Medicines, Faculdade de Farmácia Universidade Lisboa, Lisbon, Portugal

7- Pathology Department; Centro Hospitalar de Lisboa Central, Lisbon, Portugal

8- CDG & Allies – Professionals and Patient Associations International Network (CDG & Allies – PPAIN), Caparica, Portugal

ABSTRACT

Background: Unconventional perfusion flaps (**UPFs**) have shown promising results for the reconstruction of otherwise difficult to treat defects. The literature is particularly scant regarding articles specifically addressing the surgical anatomy of UPFs. Hence the main aim of this paper was to perform a cadaveric dissection study to characterize the relevant anatomy and histology of these areas, from the point of view of the surgeon interested in harvesting UPFs.

Methods: Twenty-six freshly frozen adult human cadavers were used for anatomical and histological studies.

Results: In all the regions studied the superficial cutaneous nerves were closer to sizeable superficial veins than to arteries of significant caliber and to their respective *comitante* veins. The largest veins in each region were placed deeper than smaller veins. The largest veins were enveloped by relatively thick doublings of the superficial fascia, which formed fascial sheaths around these superficial veins. The thinnest flaps were the dorsal foot (2.97 ± 1.69 mm), and the anterior antebrachial flaps (4.76 ± 0.73 mm). These UPFs presented an integumentary thickness similar to that of the eyelid and that of the penis. The sural flap was the one associated with a larger single nerve (4.32 ± 0.83 mm) followed by the saphenous (3.89 ± 1.53 mm), and the medial brachial (2.87 ± 0.49) flaps.

Conclusions: In multiple anatomical regions, the superficial venous system was consistently found in close proximity to expendable superficial nerves, tendons, and even bone segments. This knowledge helps to set the ground to tailor composite UPFs for different purposes.

INTRODUCTION

Loss of significant amounts of tissue occurs frequently after trauma, tumor excision, infections, radiotherapy and/or auto-immune diseases.[1] Unconventional perfusion flaps (**UPFs**) have shown promising results for the reconstruction of otherwise difficult to treat defects.[2-4] UPFs can be defined as blocks of tissues transferred solely on their venous system.[2, 3] If at the recipient site, one side of the venous system of this type of flaps is connected to an artery, the flap is called “arterialized venous flap” (**AVF**). If both sides of the flap are connected to recipient site’s veins, the flap receives the name of “venous flap” (**VF**).[2, 3, 5]

Among the most prominent potential advantages of UPFs, are the fact that they can potentially include nerve segments, allowing the reconstruction of nerve defects with vascularized nerve segments.[2, 3, 6] This could be potentially very advantageous, as nerve flaps have been associated experimentally to better results than the traditional nerve grafts.[7-10] Moreover, the number of conventional nerve flaps (**CNF**), that is nerve segments with at least one artery and one vein of their own, is limited. Furthermore, frequently, it is technically difficult to isolate the feeding vessels of CNFs.[11, 12]

It has been largely assumed that, being UPFs usually based on the visible superficial venous system, anatomical and histological studies of these flaps are not necessary. In fact, the literature is particularly scant regarding articles specifically addressing the surgical anatomy of UPFs. Arguably, this is one of the main factors that has been limiting the clinical application of these flaps.[2] Another limiting factor is the

significant inconsistency in the surgical literature regarding the terminology used to nominate the superficial veins on which these flaps are based.[2, 13-17]

According to a recent systematic review and meta-analysis on UPFs, clinically the most common donor sites of these flaps are, in decreasing frequency, the forearm and arm (61.8%), the foot (9.8%), and the lower leg (8.4%). Hence the main aim of this paper was to perform a cadaveric dissection study to characterize the relevant anatomy and histology of these areas, from the point of view of the surgeon interested in harvesting UPFs.

Secondarily, the authors present schematic representations of the most commonly encountered superficial veins in these regions, in order to facilitate planning and execution of UPFs.

METHODS

Twenty-six freshly frozen adult human cadavers, embalmed according to a technique developed at our institution, were used.[18] Sixteen cadavers were female (61.5%), and 10 were male (38.5%). The average age of the specimens was 75.1 ± 10.5 years. Cadavers had no prior history or evidence of lower limb pathology.

In 15 cadavers, a tourniquet was placed at the proximal aspect of each thigh and upper arm. Subsequently, each cadaver was submitted to intravenous injection of a blue latex solution (Robbialac ®) in the superficial dorsal digital veins of the toes and fingers, using 22-gauge catheters. The injection was stopped when all the superficial veins in a given segment became engorged. In another cadaver, in addition to the procedure just described, a red latex solution (Robbialac ®) was injected in the common femoral arteries, until subungual perfusion of toes was noted. Cadavers were then kept at 4º C temperature for 24 hours. [19]

After this period, each region of interest was carefully dissected using 6X-magnification operating loupes (Design for Vision®). Relevant structures were measured and photographed. Their position was registered relatively to constant landmarks (joints and bone extremities).

The middle portion of each flap's region was biopsied and submitted to histological processing.

In 10 other cadavers subjected to a similar procedure, flap regions were converted into modified Spalteholz cleared specimens.[20] This technique creates

transparent three-dimensional specimens, while preserving vascular and perivascular structure.[21]

In order to compare the nerve components of flaps with frequently injured nerves, the following nerves were retrieved from two cadavers: facial nerve at the posterior aspect of the parotid gland; hypoglossal nerve at the base of the tongue; masseteric nerve at the sigmoid notch; collateral digital nerve of the index finger at the proximal phalanx level; median nerve at the distal third of the arm; anterior division of the C7 spinal nerve.[22-25]

To compare the thickness of the integument of two regions considered difficult to reconstruct with the thickness of UPFs, in two male cadavers, biopsies were performed of the upper eyelid and of the penis.[2, 3]

Specimens were prepared for histological observation using hematoxylin-eosin and Masson's trichrome stains, as well as immunohistochemistry for neurofilaments for staining nerves.[26-29] Histological sections were observed and photographed using a Leica DMLB-2® microscope. Representative images were selected for histomorphometric evaluation using the Fiji® software.

This study's protocol was approved by the Ethical Committee at the authors' institution (08/2012/CEFCM).

Statistical analysis

Qualitative variables were expressed as percentages. Quantitative variables were expressed as means ± SD. IBM SPSS Version 21.0® software was used for descriptive and inferential statistical analysis. The Kolmogorov-Smirnov test was used to assess whether variables were distributed normally. Analysis of variance and t test were used to compare averages in normally distributed data. Kruskal-Wallis and Mann-Whitney tests were used to compare means in non-normally distributed data. Proportions were analyzed with the chi-square test or Fisher's exact test. A two-tail value of $p<0.05$ was considered to be statistically significant.

RESULTS

Common anatomical and histological features of all anatomical regions studied

In all the regions studied the superficial cutaneous nerves were closer to sizeable superficial veins than to arteries of significant caliber and to their respective *comitante* veins (**Fig. 1**). Of interest, sizeable superficial veins of the limbs were not placed at the same depth. In fact, the largest veins in each region were placed deeper than smaller veins. Intermediate-sized veins were placed at an intermediate depth (**Figs. 2, 3** and **4**). The largest veins, namely the great saphenous vein, the short saphenous vein, the cephalic and basilic veins travelled close to the muscle fascia and they were enveloped by relatively thick doublings of the superficial fascia, which formed fascial sheaths around these superficial veins. Although the largest veins and superficial nerves shared common sheaths, histologically they were separated by fascial septa (**Fig. 2**).

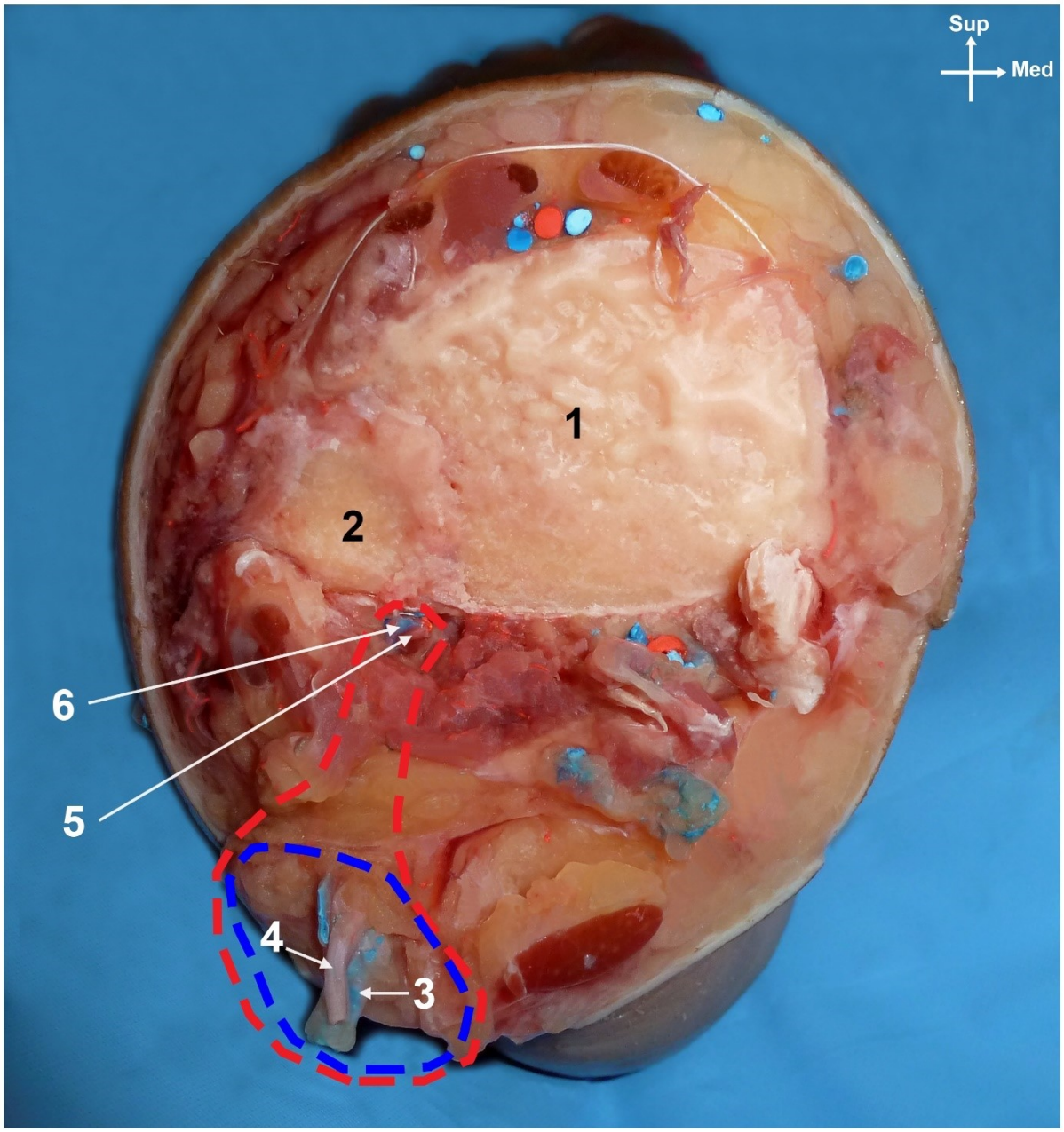

Figure 1 - Photograph of an axial section through the upper third of a left leg showing the thickness of a sural nerve flap raised as a conventional flap (red dotted line) or as an unconventional perfusion flap (blue dotted line). The cadaver was injected with a red latex solution in the arterial system and with a blue latex solution in the venous system.

1, tibial bone; 2, fibula; 3, small saphenous vein; 4, sural nerve; 5, fibular artery; 6, fibular vein

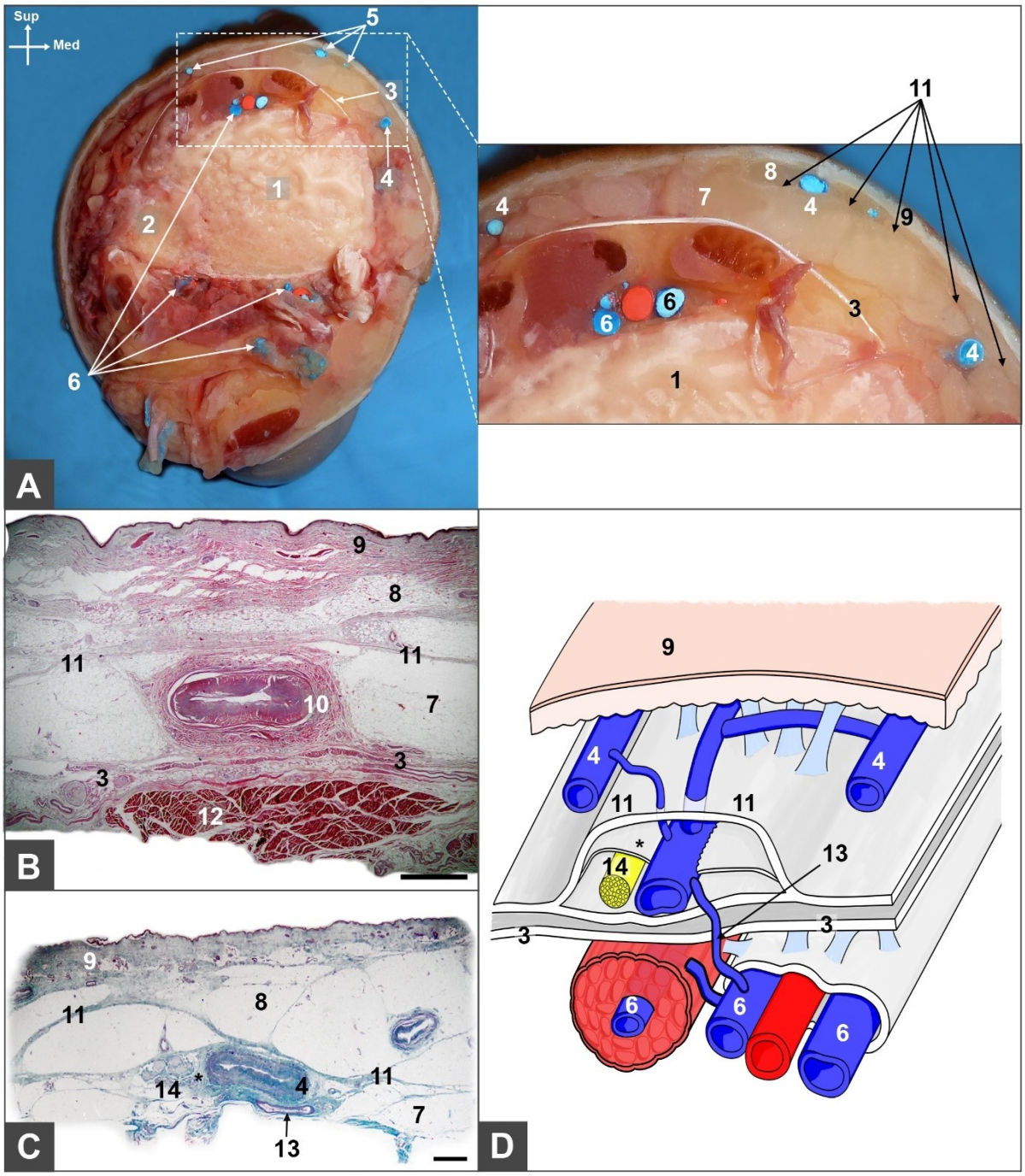

Figure 2 - Relationship between the superficial veins and nerves and the superficial fascia.

(A) Photograph an axial section of the upper third of a left leg in a cadaver previously injected with colored latex solutions showing the relative disposition of the superficial veins to adjoining fascial sheaths. (box on the right) Higher magnification view of the area highlighted in the dotted region of (A), exemplifying the position of superficial veins in different depths. (B) Microphotograph of a hematoxylin-eosin stained

axial section of an anterior antebrachial flap illustrating the relation of an anterior median antebrachial vein with the surrounding fascias. (C) Photograph of a Masson's Trichrome stained axial section of a saphenous flap illustrating the relation of superficial veins in this region with the superficial fascias. (D) Schematic representation of the location of the different superficial veins.

1, tibia; 2, fibula; 3, muscle fascia; 4, great saphenous vein; 5, other superficial veins; 6, deep veins; 7, deep fatty layer of the subcutaneous tissue; 8, superficial fatty layer of the subcutaneous tissue; 9, skin paddle; 10, median antebrachial vein; 11, superficial fascia; 12, palmaris longus muscle; 13, communicating vein; 14, saphenous nerve

Sup, Superior; Med, Medial

Arrow heads indicate the superficial fascia; the asterisk indicates the fascial septum that separates the great saphenous vein from the saphenous nerve.

Calibration bar = 1 mm

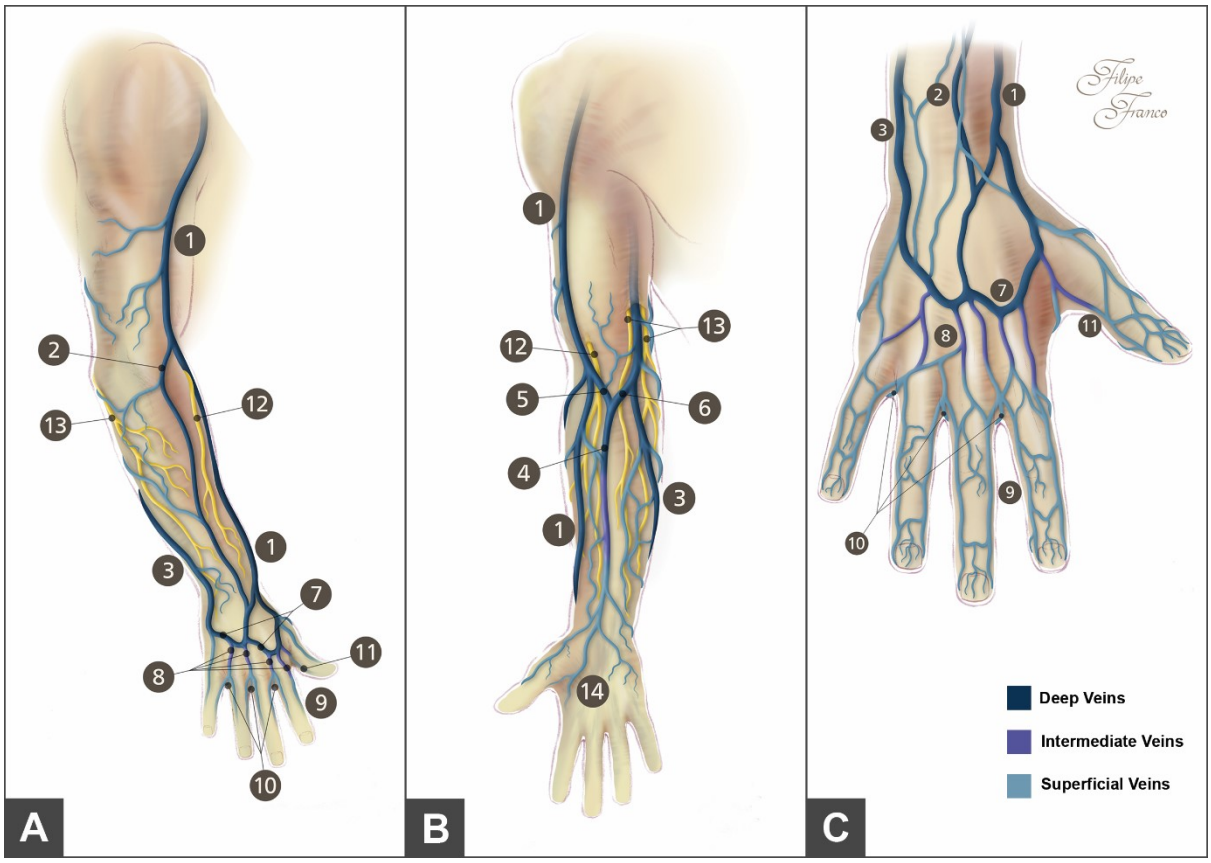

Figure 3 - Graphical representation of the most common disposition of the superficial veins of the upper limbs and their main anatomical relations with neighboring superficial nerves. These veins are placed at different depths.

1, cephalic vein; 2, accessory cephalic vein; 3, basilic vein; 4, median antebrachial vein; 5, lateral median antebrachial vein; 6, medial median antebrachial vein; 7, dorsal venous arch of the hand; 8, dorsal metacarpal veins; 9, dorsal digital veins; 10, intercapitular veins; 11, cephalic vein of the thumb; 12, lateral antebrachial nerve; 13, medial antebrachial nerve; 14, superficial palmar venous network

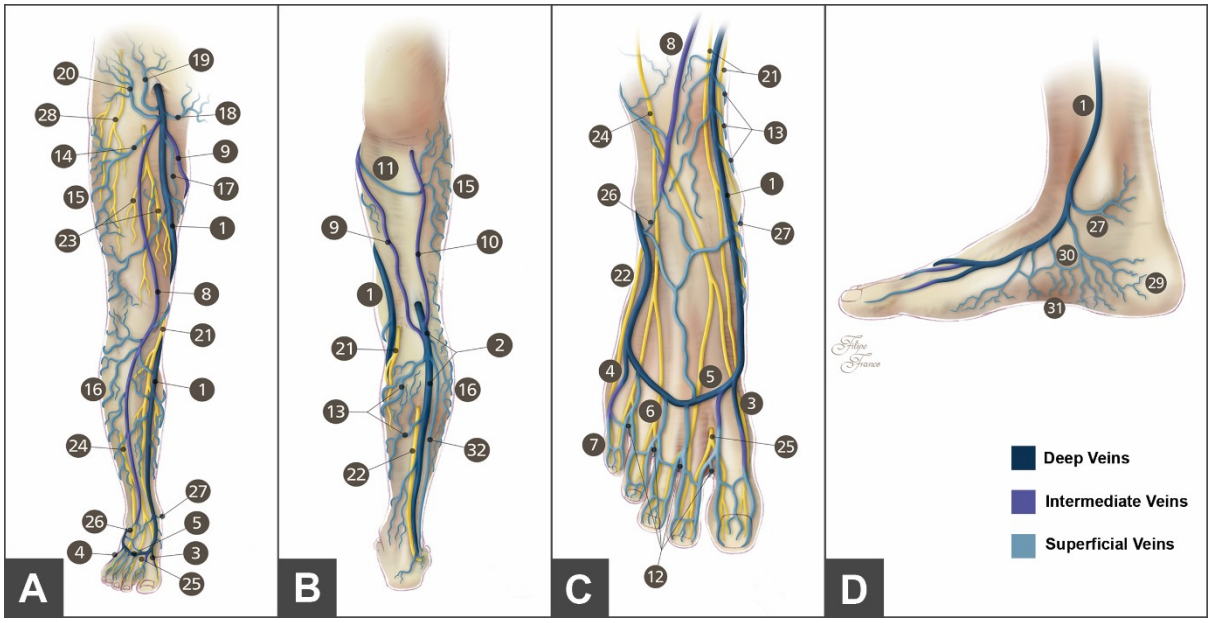

Figure 4 - Graphical representation of the most common disposition of the superficial veins of the lower limbs and their main anatomical relations with neighboring superficial nerves. These veins are placed at different depths.

1, great saphenous vein; 2, small saphenous vein; 3, medial marginal vein; 4, lateral marginal vein; 5, dorsal venous arch of the foot; 6, superficial dorsal metatarsal veins; 7, superficial dorsal digital veins; 8, anterior accessory great saphenous vein; 9, posterior accessory great saphenous vein; 10, cranial extension of the small saphenous vein; 11, posterior thigh circumflex vein or Giacomini vein; 12, intercapitular veins; 13, intersaphenous veins; 14, anterior thigh circumflex vein; 15, lateral venous plexus of the thigh; 16, lateral venous plexus of the leg; 17, superficial accessory great saphenous vein; 18, superficial external pudendal vein; 19, superficial epigastric vein; 20, superficial circumflex iliac vein; 21, saphenous nerve; 22, sural nerve; 23, anterior femoral cutaneous nerve; 24, superficial fibular nerve; 25, medial branch of the deep fibular nerve; 26, lateral malleolar vein; 27, medial malleolar vein; 28, lateral femoral cutaneous nerve of the thigh; 29, calcaneal veins; 30, peri-scaphoid venous circle; 31, superficial venous network of the plant of the foot; 32, superficial accessory small saphenous vein

The superficial fascial divided the subcutaneous fat into a superficial and a deep fatty layer. The former layer was significantly thinner than the latter (**Fig. 2**).

Medial brachial flap

In the distal half of the medial region of the arm, the basilic vein was the dominant superficial vein (**Fig. 5**). This vein was accompanied by the medial antebrachial cutaneous nerve which pierced the muscle fascia through the same foramen through which the basilic vein reached the vasculo nervous bundle of the arm. In the most superficial portion of this flap's region, there were branches of the medial antebrachial cutaneous nerve that supplied the skin of this region. In the deeper aspect, soon after reaching the subcutaneous compartment, the medial antebrachial cutaneous nerve divided into a larger anterior branch that escorted the basilic vein and a smaller posterior branch that travelled to the posteromedial aspect of the forearm. The basilic vein and the anterior branch of the medial antebrachial cutaneous nerve could be raised as a unit in all the specimens dissected. The nerve was placed deep to the vein in all cases.

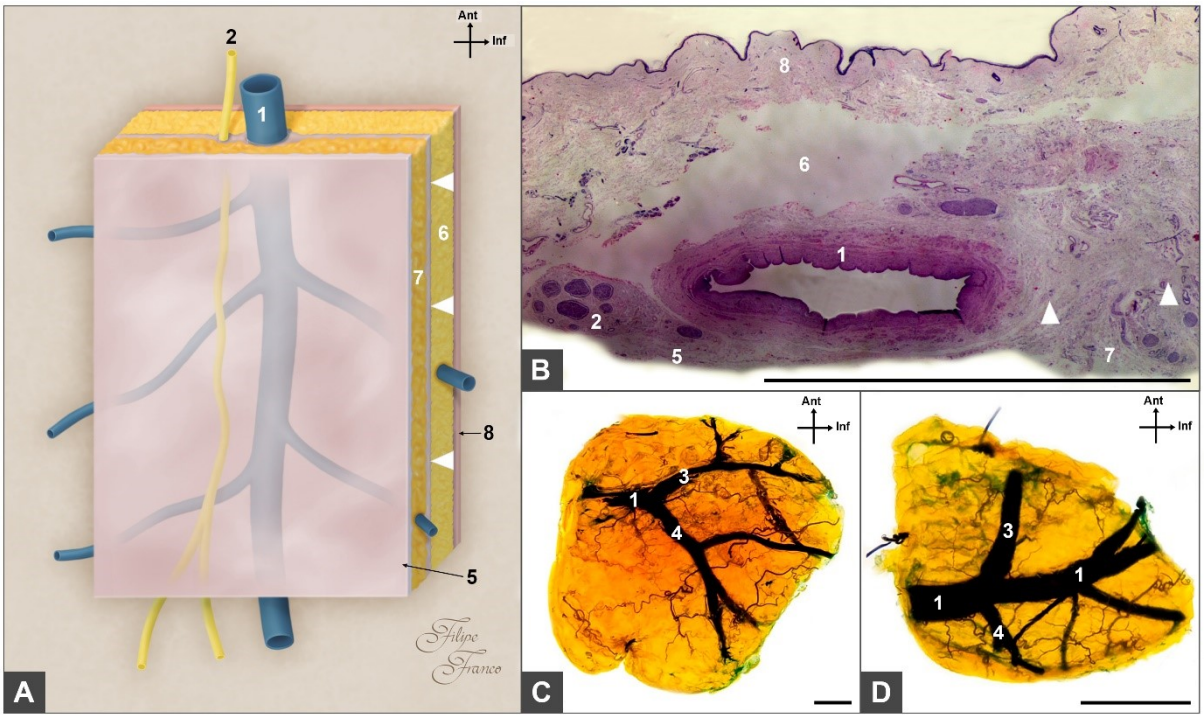

Figure 5 - Anatomy and histology of the medial brachial flap.

(A) Schematic representation of the medial venous brachial flap; (B) Photograph of a Masson's trichrome stained axial section of the middle portion of the flap; (C and D) Photographs of the flap after processing by the modified Spalteholz technique showing the venous network.

1, basilic vein; 2, medial antebrachial nerve; 3, medial median antebrachial vein; 4, medial antebrachial vein; 5, muscle fascia; 6, superficial fatty layer of the subcutaneous tissue; 7, deep fatty layer of the subcutaneous tissue; 8, skin paddle

Ant, Anterior; **Inf**, Inferior

Arrow heads indicate the superficial fascia

Calibration bar = 1 cm

Anterior antebrachial flap

The distal third of the anterior aspect of the forearm was covered with a thin and pliable integument (**Fig. 6**). In this region, the dominant veins were the affluent veins of the median antebrachial veins, which were interconnected by oblique and transverse anastomoses (**Fig. 6B**). There were small branches to the skin originating from the anterior branches of the medial antebrachial cutaneous nerve and from the lateral antebrachial cutaneous nerve. The palmaris longus tendon was present in this region in 88% of cases. The muscle fascia was placed relatively close to the superficial veins and skin, suggesting that these tissues could easily be mobilized *en bloc* as an UPF (**Fig. 6C**).

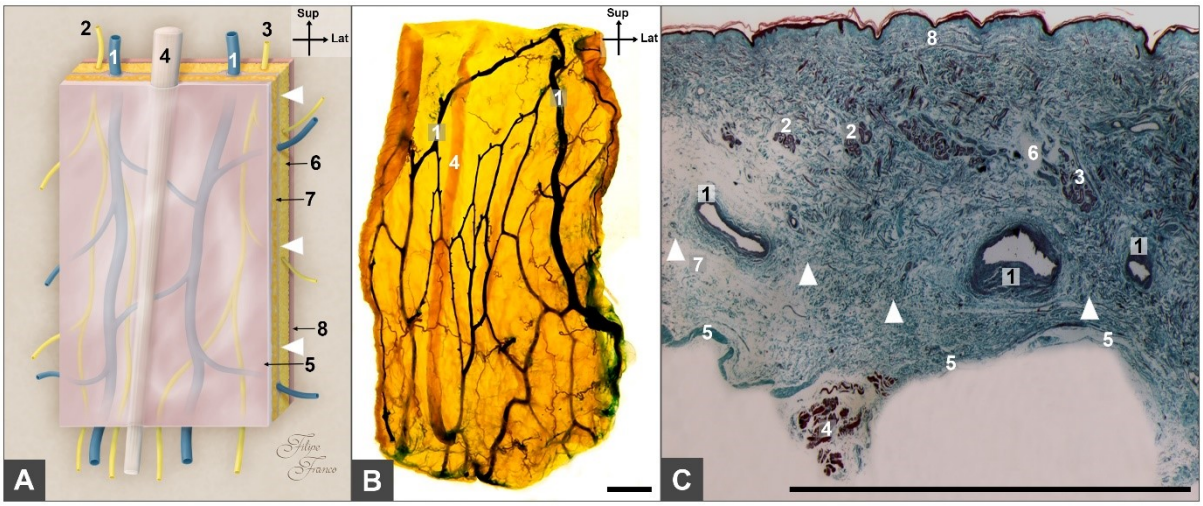

Figure 6 - Anterior forearm flap anatomy and histology.

(A) Schematic representation of the flap observed from its deep aspect; (B) Photograph of the anterior venous flap after processing by the modified Spalteholz technique showing the venous network and the palmaris longus tendon; (C) Photograph of a Masson's trichrome stained axial section of the middle third of the flap showing the flap's histology.

1, median antebrachial veins; 2, anterior branch of the medial cutaneous antebrachial nerve; 3, anterior branch of the lateral cutaneous antebrachial nerve; 4, palmaris longus tendon; 5, muscle fascia; 6, superficial fatty layer of the subcutaneous tissue; 7, deep fatty layer of the subcutaneous tissue; 8, skin paddle

Sup, Superior; **Lat**, Lateral

Arrow heads indicate the superficial fascia

Calibration bar = 1 cm

Sural flap

In the inferior three quarters of the posterior aspect of the leg, the sural nerve and the short saphenous vein were in close proximity and presented a significant caliber in all cadavers (**Fig. 7**). These structures followed a line that crossed from the space between the two bellies of the gastrocnemius muscle to the lateral aspect of the calcaneal tendon in all cases. In all specimens, both the sural nerve(s) and the short saphenous vein presented a significant diameter and could be harvested as a flap for a length of at least 25 cm (**Fig. 7B**). The sural nerve abandoned the posterior compartment of the leg in the transition between the upper third and the lower three quarters of the leg. In two cadavers (8%) the two roots of the sural nerve remained distinct throughout the entire usual course of the nerve originating two sural nerves. In the remaining cases, the sural nerve originated from two main roots derived from the common fibular and from the tibial nerves, being the latter root the dominant one. In all cases, the sural nerve(s) divided in its terminal branches in the vicinity of the lateral malleolus' tip. In 68% of cases, there was a superficial accessory small saphenous vein in the lateral aspect of the distal two thirds of the leg, travelling superficially and laterally to the short

saphenous vein, until ending as one of the tributaries of the latter vein (**Fig. 4B**). The short saphenous vein penetrated the muscular fascia in the popliteal space. This vein was anastomosed with the posterior thigh circumflex vein (also known as Giacomini vein) and with the posterior accessory great saphenous vein in 72% and 52% of cases (**Fig. 4B**). The integument of this region was significantly thicker in the upper third of the leg than in the remaining lower two thirds (**Fig. 7C** to **7E**).

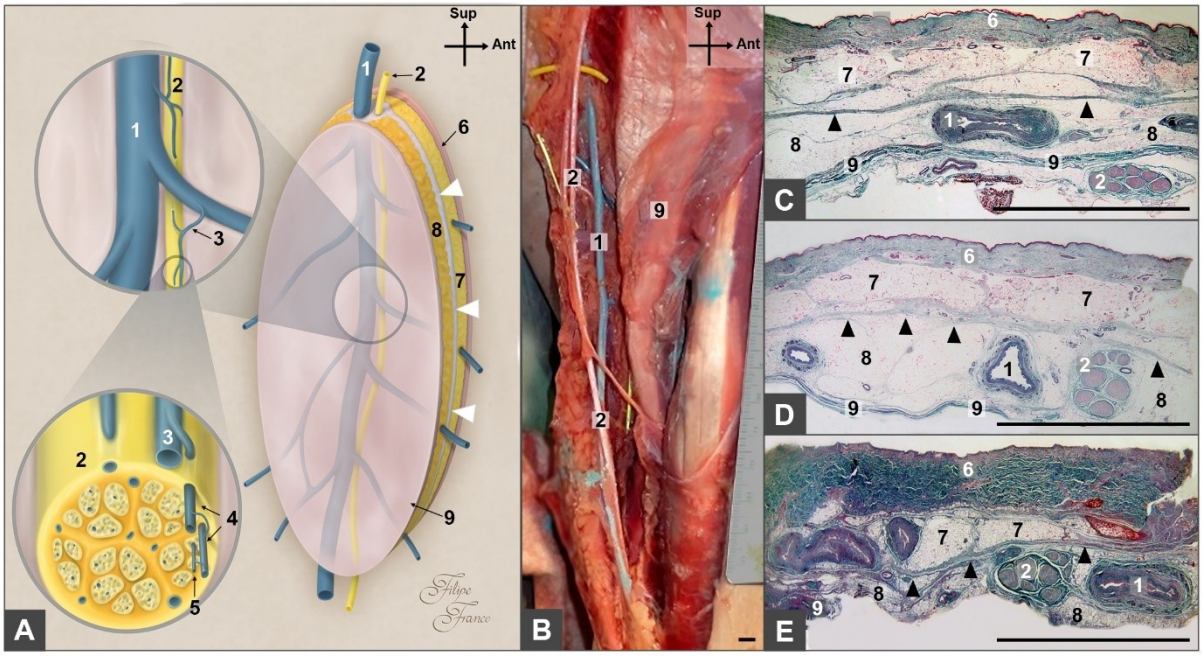

Figure 7 - Sural flap anatomy and histology.

(A) Schematic representation of the sural venous flap; (B) Photograph of a cadaveric dissection of the lateral aspect of a right leg showing the flap's neurovenous pedicle; (C) Photograph of a Masson's trichrome stained axial section of the upper third of the leg showing the flap's histology; (D) Photograph of a Masson's trichrome-stained axial section of the middle third of the leg showing the flap's histology; (E) Photograph of a Masson's trichrome stained axial section of the lower third of the leg showing the flap's histology.

1, short saphenous vein; 2, sural nerve; 3, epineurial veins; 4, perineurial veins; 5, endoneurial veins; 6, skin paddle; 7, superficial fatty layer of the subcutaneous tissue; 8, deep fatty layer of the subcutaneous tissue; 9, muscle fascia

Sup, Superior; **Ant**, Anterior

Arrow heads indicate the superficial fascia

Calibration bar = 5 mm

Saphenous flap

The great saphenous vein was located deep in the thick subcutaneous fat in the thigh. In this region, this vein was located at a significant distance from the subcutaneous nerves, namely from the saphenous nerve, which was sub aponeurotic throughout much of the thigh. This nerve became superficial only after leaving the adductor canal in the distal fifth of the thigh. Therefore, in the thigh, the great saphenous vein did not show an anatomy favorable to the elaboration of UPFs.

Below the knee, the great saphenous vein and the saphenous nerve presented a parallel path from the posterior aspect of the medial condyle of the femur to the anterior aspect of the medial malleolus (**Fig. 8**). The vein presented a sizeable caliber in all cases. In the lower leg, an anterior accessory great saphenous vein was observed superficially and laterally to the great saphenous vein on both sides in 3 cadavers (12%; **Fig. 4A**). The former vein presented a fascial sheath of its own similar to that of the great saphenous vein, until terminating in the latter vein in the thigh. In all circumstances, either through the anterior accessory great saphenous vein or through a direct tributary of the great saphenous vein, the distal two thirds of the medial aspect of the tibial bone presented venous effluents to the great saphenous vein system (**Fig. 8C**). The saphenous

nerve gave off several branches to the anterior and posterior aspects of the inner side of the leg, becoming composed of multiple thin branches in the distal aspect of the leg.

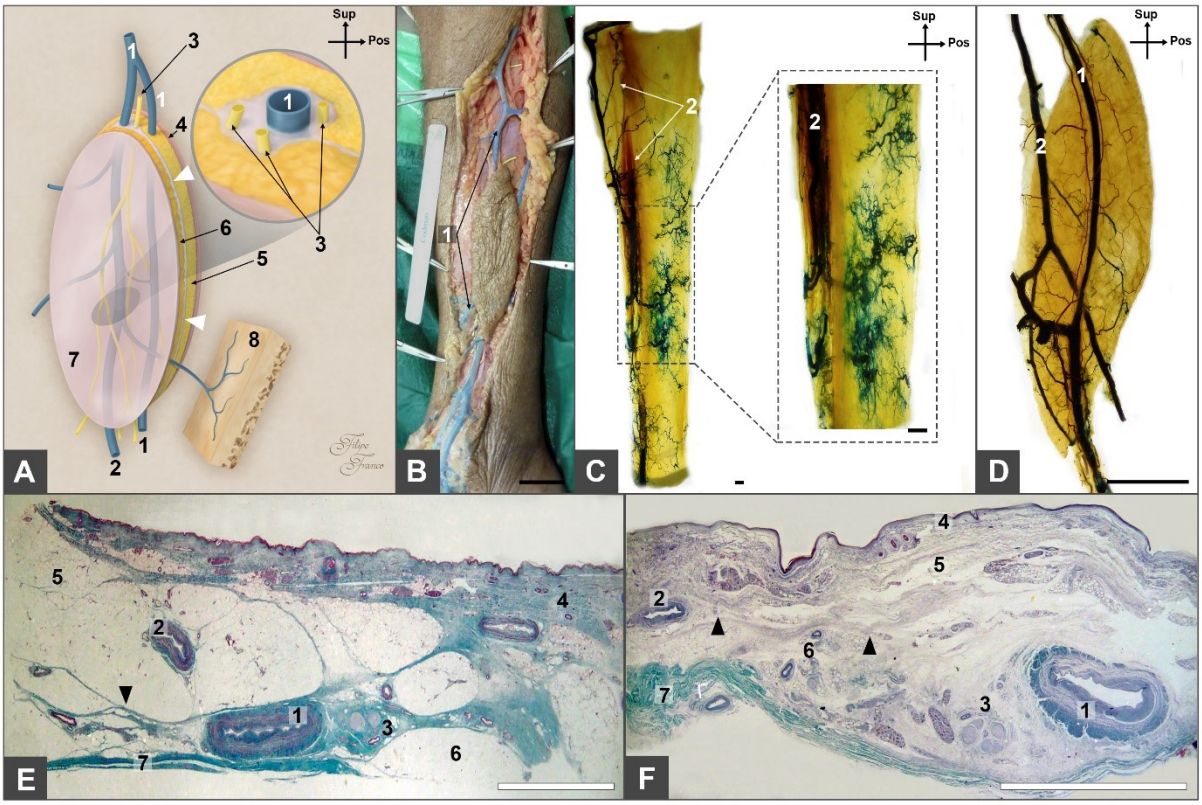

Figure 8 - Saphenous flap anatomy and histology.

(A) Schematic representation of the saphenous venous flap; (B) Photograph of a cadaveric dissection of the medial aspect of a right leg showing the flap's neurovenous pedicle; (C and D) Photographs of the flap after processing by the modified Spalteholz technique showing the venous network over the medial aspect of the tibial bone (C) and that under the skin paddle (D); (E) Photograph of a Masson's trichrome stained axial section of the upper third of the leg showing the flap's histology; (F) Photograph of a Masson's trichrome stained axial section of the distal third of the leg showing the flap's histology.

1, great saphenous vein; 2, anterior accessory great saphenous vein; 3, saphenous nerve branches; 4, skin paddle; 5, superficial fatty layer of the subcutaneous tissue; 6, deep fatty layer of the subcutaneous tissue; 7, muscle fascia; 8, medial cortex of the tibial bone

Sup, Superior; **Pos**, Posterior

Arrow heads indicate the superficial fascia

Black calibration bar in C = 1 cm

Black calibration bar in D = 5 cm

White calibration bar = 5 mm

In all the cutaneous nerves analyzed, including the saphenous and the sural nerves, a well-developed epineurial venous plexus was observed. This venous plexus drained into multiple small veins and venules that joined the adjacent superficial veins (**Fig. 9**).

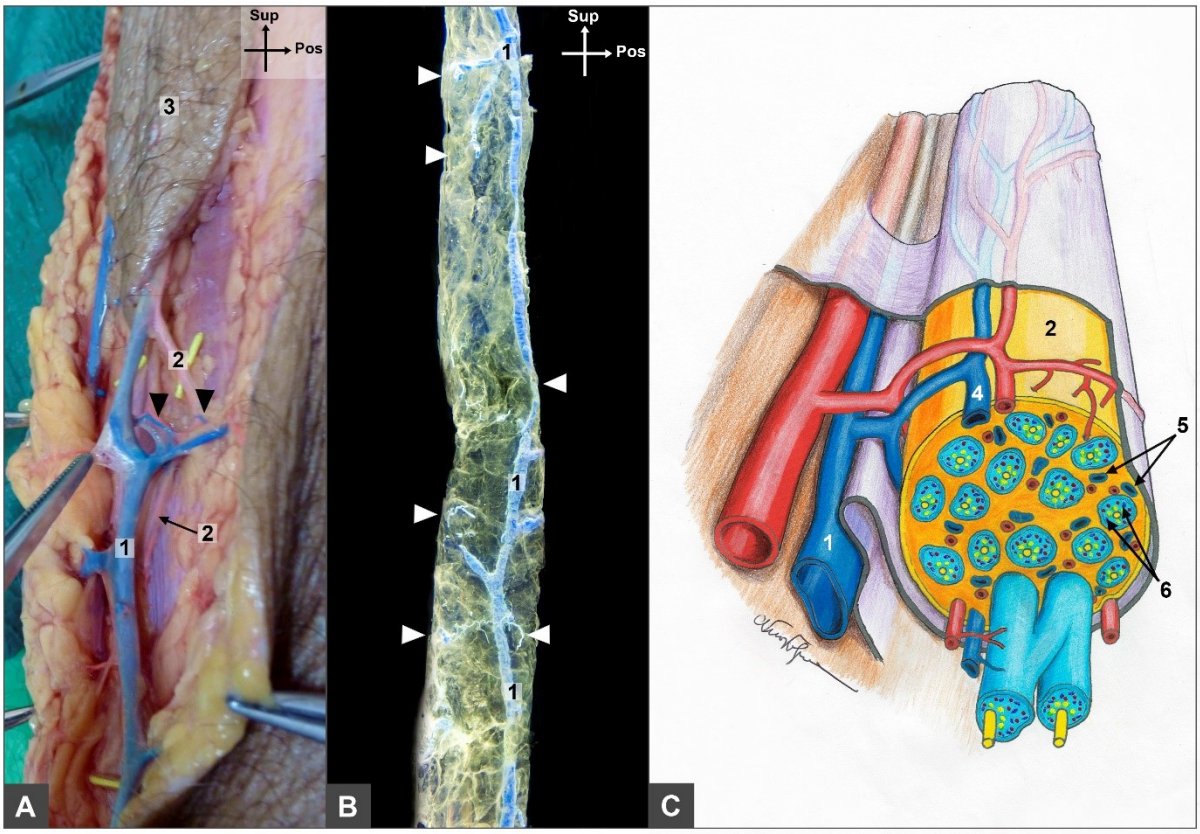

Figure 9 - Anatomical relationship between superficial veins and adjacent superficial nerves.

(A) Photograph of a cadaveric dissection of the inferior portion of a left saphenous venous flap, showing the proximity of the great saphenous vein and the saphenous nerve branches, as well as the venous branches coming from the epineurial venous plexus to the tributaries of the great saphenous vein. The cadaver had been previously injected with a blue latex solution in the venous system and with a red latex solution in the arterial system. (B) Photograph of the great saphenous vein and accompanying saphenous nerve in the lower leg after processing by the modified Spalteholz technique of a lower limb previously injected with a blue latex solution in the venous system. It is possible to observe multiple small tributary veins originating in the region of the saphenous nerve and draining into the great saphenous vein. (C) Schematic representation of the blood supply to superficial nerves from adjacent superficial arteries and veins.

1, great saphenous vein; 2, saphenous nerve branches; 3, skin paddle of the saphenous venous flap; 4, epineurial veins; 5, perineural veins; 6, endoneurial veins

Sup, Superior; **Pos**, Posterior

Arrow heads indicate veins draining the epineurial venous plexus in the adjoining superficial vein.

Dorsal foot flap

This flap's region was dominated by two large venous structures: the medial and lateral marginal veins (**Fig. 10**). These two veins were interconnected by the dorsal venous arch of the foot, which, in turn, received in its distal convexity the superficial dorsal digital veins. From the concavity of the dorsal venous arch of the foot there was a variable number of veins that drained most frequently into the territory of the great saphenous vein or less frequently to the anterior accessory great saphenous vein (12%). There were multiple venous anastomoses between all the major superficial veins of the dorsum of the foot (**Fig. 10 F**). Beneath the major veins, the medial dorsal and the intermediate dorsal cutaneous nerves of the foot could be found in all cases. Beneath these nerves, the relatively thin dorsal fascia of the foot covered the underlying extensor tendons, namely the accessory extensor hallucis longus tendon, and the extensor hallucis brevis tendon, which were present in 88% and 100% of cadavers, respectively. The integument in this region was very thin and pliable, particularly close to the proximal aspect of the toes (**Fig. 10**).

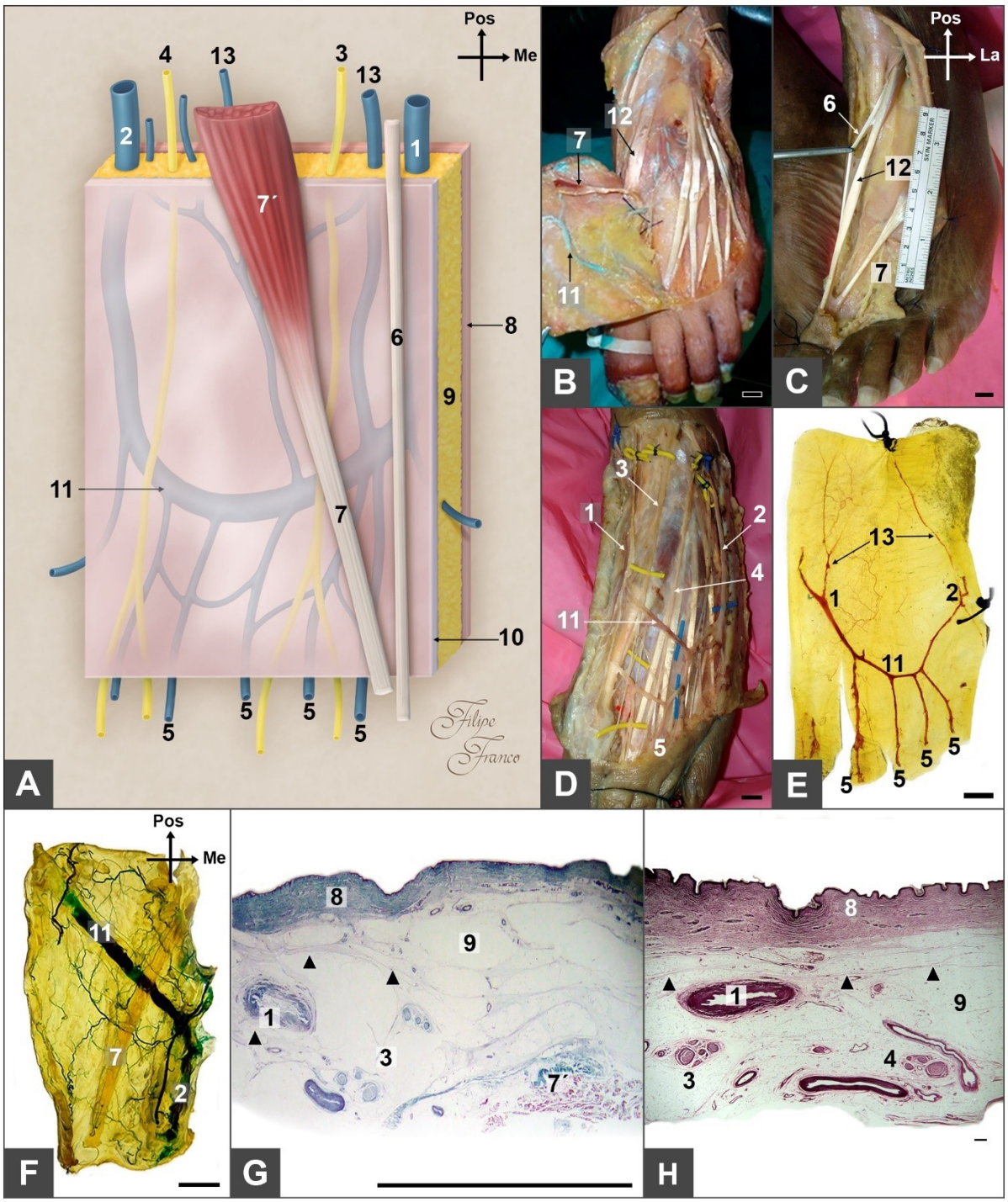

Figure 10 - Anatomy and histology of the dorsal flap of the foot.

(A) Schematic representation of the dorsal venous flap of the foot; (B to C) Photographs of cadaveric dissections of the dorsum of the left foot. In (B) it is possible to observe the inclusion of the extensor hallucis brevis tendon. In (C) it is possible to observe the intimate relation of the deep aspect of the flap

with the accessory extensor hallucis longus tendon and with the extensor hallucis brevis tendon. In (D) it is possible to observe the medial and intermediate dorsal nerves of the foot that can be included in the flap. (E and F) Photograph of the dorsal venous flap of the foot after processing by the modified Spalteholz technique showing the venous network from a superficial perspective. In (E) it is possible to observe the affluents and effluents of the dorsal venous arch of the foot. In (F) the intimate connection between the extensor hallucis brevis and the dorsal venous arch of the foot can be appreciated. (G and H) Photograph of a Masson's trichrome stained axial section of the proximal and distal half of the flap, respectively. It is possible to observe that the flap is significantly thinner close to the toes.

1, medial marginal vein; 2, lateral marginal vein; 3, medial dorsal cutaneous nerve of the foot; 4, intermediate dorsal cutaneous nerve of the foot; 5, superficial dorsal digital veins; 6, accessory extensor hallucis longus tendon; 7, extensor hallucis brevis tendon; 7´, extensor hallucis brevis muscle belly; 8, skin paddle; 9, subcutaneous fat; 10, muscle fascia; 11,dorsal venous arch of the foot; 12 extensor hallucis longus tendon, 13, superficial dorsal metatarsal veins;
Pos, Posterior; Me, Medial; La, Lateral.

Calibration bar = 1 cm

Medial plantar flap

This region presented a well-developed venous plexus surrounding the scaphoid tubercule (**Figs. 4D** and **11**). This plexus drained into the calcaneal veins, which, in turn, drained into the medial marginal vein. This region received numerous diminutive nerve branches from the terminal portion of the saphenous nerve.

The integumentary layer presented some noteworthy specificities. The skin was relatively thick and ridged, being similar to that found in the palmar aspect of the hand. The subcutaneous tissue was relatively scant and presented numerous fibrous septa

connecting the underlying muscle fascia to the deep aspect of the reticular dermis (**Fig. 11C**).

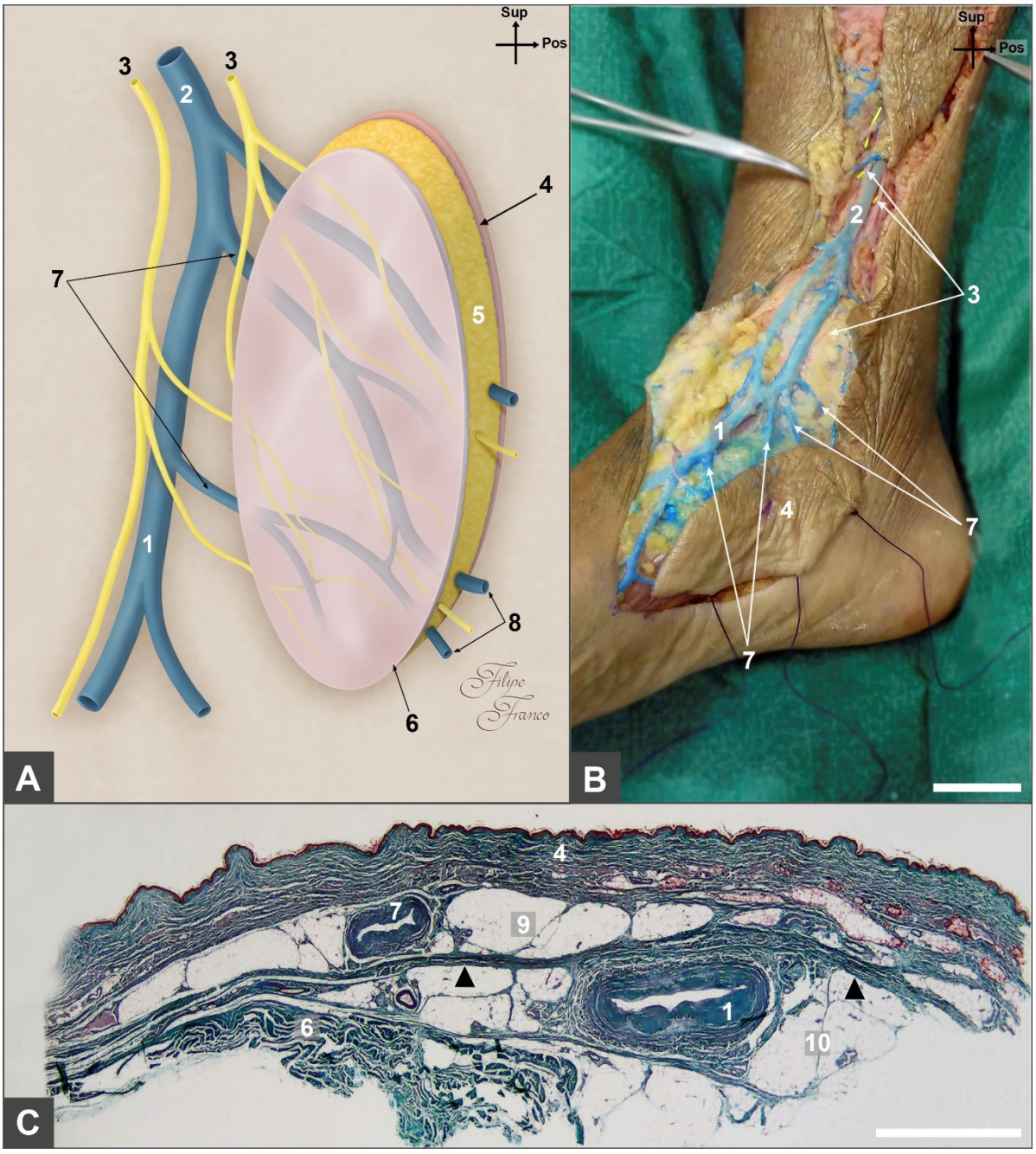

Figure 11 - Anatomy and histology of the medial plantar flap.

1, medial marginal vein; 2, great saphenous vein; 3, saphenous nerve branches; 4, skin paddle; 5, subcutaneous fat; 6, muscle fascia; 7, calcaneal veins; 8, peri-scaphoid veins; 9, superficial fatty layer of the subcutaneous tissue; 10, deep fatty layer of the subcutaneous tissue

Sup, Superior; **Pos**, Posterior

Arrow heads indicate the superficial fascia

Calibration bar = 1 cm

Morphometric features of the UPFs

The thinnest flaps were the dorsal foot (2.97 ± 1.69 mm), and the anterior antebrachial flaps (4.76 ± 0.73 mm) [**Table 1**].

Unconventional Perfusion Flap	Potential composition	Maximal thickness (mm)	Diameter of dominant structures (mm)		Some potential specific clinical applications based on anatomical features
			Veins (v)	Nerves (n)	
Medial brachial	Skin + fat + nerve	10.72 ± 1.90	Basilic v.:	Medial antebrachial n.	• Flow-through flap • Intermediate-sized nerve reconstruction
			9.02 ± 1.68	2.87 ± 0.49	
Anterior antebrachial	Skin + fat + tendon + nerve	4.76 ± 0.73	Lateral antebrachial v.	Anterior branch of the lateral antebrachial n.	• Coverage of regions where the integument is thin • Small nerve reconstruction • Tendon or ligament reconstruction
			2.48 ± 0.79	0.79 ± 0.33	
			Median antebrachial v.	Anterior branch of the medial antebrachial n.	
			1.87 ± 0.57	0.83 ± 0.47	
Sural	Skin + fat + nerve	12.62 ± 2.18	Small saphenous v.	Sural n.	• Flow-through flap • Large nerve reconstruction
			6.44 ± 0.89	4.32 ± 0.83	
Saphenous	Skin + fat + nerve + bone	11.68 ± 3.06	Great saphenous v.	Saphenous n.	• Flow-through flap • Intermediate-sized nerve reconstruction • Bone reconstruction
			8.94 ± 1.48	3.89 ± 1.53	
Dorsal foot	Skin + fat + nerve + tendon	2.97 ± 1.69	Medial marginal v.	Medial dorsal cutaneous n. of the foot:	• Ideal for types II and III AVFs[3] • Coverage of regions where the integument is thin, such as digits • Tendon and/or ligament reconstruction • Small nerve reconstruction
			4.70 ± 1.15	1.16 ± 0.67	
			Lateral marginal v.	Intermediate dorsal cutaneous n. of the foot:	
			2.89 ± 0.74	1.01 ± 0.53	
Medial plantar	Skin + fat + nerve	5.79 ± 1.97	Medial marginal v. diameter	Branches of the saphenous nerve	

			4.98 ± 1.27	0.89 ± 0.37	• Coverage of palmar skin (sturdy and sensitive skin)

Table 1 - Synthesis of surgical pertinent morphometric features of the unconventional perfusion flaps studied and their clinical corollary.

Values are expressed as averages ± standard deviation.

The thickest UPFs were the medial brachial (10.72 ± 1.90mm), the sural (12.62 ± 2.18 mm), the saphenous (11.68 ± 3.06 mm), and the medial plantar (5.79 ± 1.97 mm) flaps. The thinnest UPFs presented an integumentary thickness similar to that of the eyelid and that of the penis (**Fig. 12**).

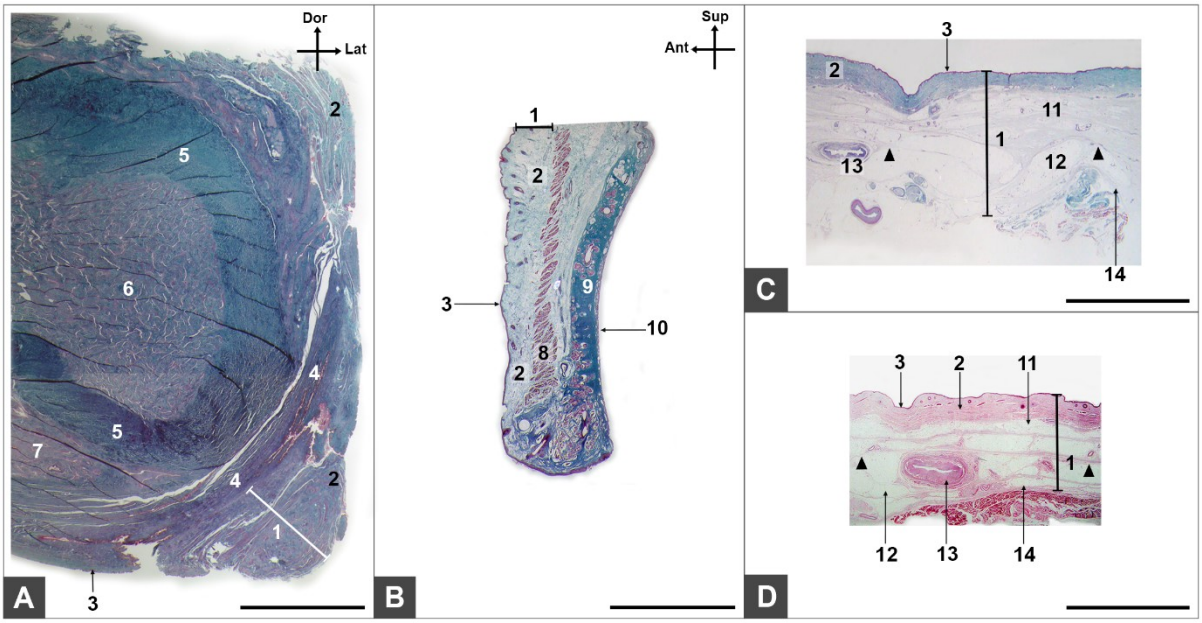

Figure 12 - Comparison of the integument thickness in the upper eyelid, in the penis, in the dorsal venous flap, and in the anterior forearm venous flap using photographs of histological sections.

(A) Photograph of a Masson's trichrome stained axial section of the left half of a penis; (B) photograph of a Masson's trichrome stained parasagittal section of an upper eyelid; (C) photograph of a Masson's

trichrome stained axial section of an anterior antebrachial venous flap; (D) photograph of a hematoxylin-eosin stained axial section of the venous flap of the dorsum of the foot.

1, integumentary layer; 2, dermis; 3, epidermis; 4, deep penile fascia; 5, albuginea layer of the penis; 6, corpus cavernosum; 7, corpus spongiosum; 8, orbicularis oculi muscle; 9, tarsal plate; 10, conjuntiva; 11, superficial fatty layer of the subcutaneous tissue of the limbs; 12, deep fatty layer of the subcutaneous tissue of the limbs; 13, superficial vein; 14, muscle fascia;

Ant, anterior; Sup, superior; Dor, dorsal; Lat, lateral

Arrow heads indicate the superficial fascia of the limbs

Calibration bar = 1 cm

The flaps with the largest associated veins were in decreasing order: the medial brachial (9.02 ± 1.68 mm), the saphenous (8.94 ± 1.48 mm), and the sural (6.44 ± 0.89 mm) flaps.

The sural flap was the one associated with a larger single nerve (4.32 ± 0.83 mm; **Fig. 13**), followed by the saphenous (3.89 ± 1.53 mm), and the medial brachial (2.87 ± 0.49) flaps.

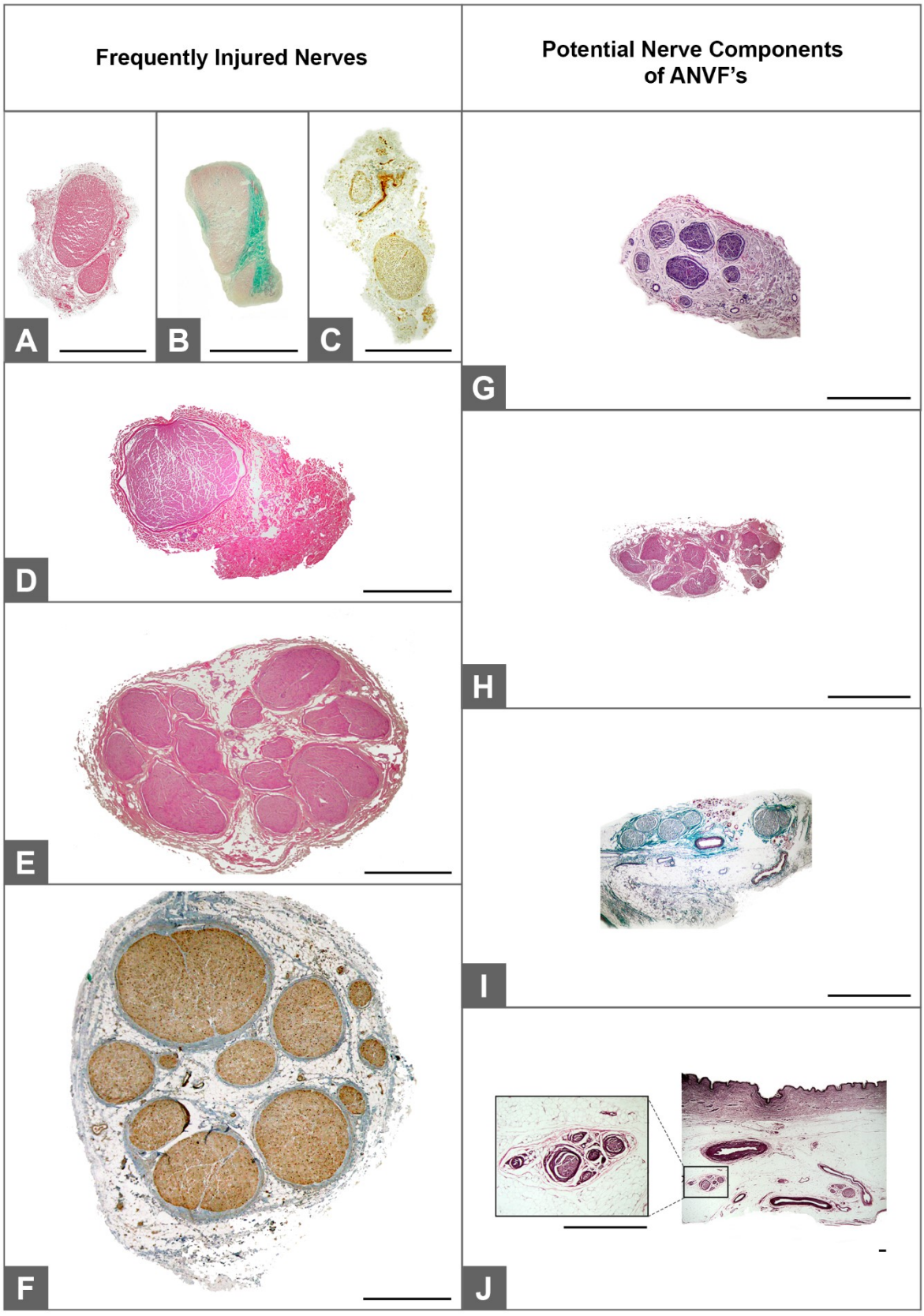
Frequently Injured Nerves
Potential Nerve Components of ANVF's
A
B
C
D
E
F
G
H
I
J

Figure 13 - Optical microscopy photographs with the same magnification showing the relative size and internal structure of commonly injured nerves (A to F), and of potential nerve components of arterialized venous flaps (**ANVFs**).

(A), facial nerve at the posterior aspect of the parotid gland; (B), hypoglossal nerve at the base of the tongue; (C), masseteric nerve at the sigmoid notch; (D), collateral radial digital nerve of the index finger at the proximal phalanx level; (E), median nerve at the distal third of the arm; (F), anterior division of the C7 spinal nerve; (G), anterior branch of the medial antebrachial cutaneous nerve at the elbow crease (medial brachial flap); (H), sural nerve in the middle third of the leg (sural flap); (I), saphenous nerve in the proximal third of the leg (saphenous flap); (J), medial dorsal cutaneous nerve of the foot (dorsal foot flap).

Calibration bar = 1 cm

DISCUSSION

The description of the surgical anatomy of the veins draining the integument has been performed by other authors, namely by Ian Taylor's group.[30, 31]

However, as far as the authors could determine, the study herein presented, being composed of 26 cadaveric dissections, represents by far the largest series on the anatomy and histology of UPFs. Townsend and Taylor, in 1984, wrote a seminal paper on the subject, succinctly describing the anatomical proximity between the sural nerve and the short saphenous vein, and between the saphenous nerve and the great saphenous vein.[4, 6, 32-35] These anatomical studies set the basis for the clinical application of arterialized neurovenous flaps (**ANVFs**). However, they were based exclusively on 13 cadaveric dissections, not including the histological characterization of these regions. Subsequently, Taylor's group described in great detail the venossomes of the nerves of the upper and lower limbs, based on very meticulous dissections of 2 and 3 cadavers, respectively.[30, 36-38] Recently, Taylor *et al* amplified their series with an additional studying involving 20 lower limb cadaveric dissections.[39]

In 1999, Caggiati and Ricci recognized that the great saphenous vein and some of its tributaries were enclosed by the superficial fascia. This, in fact, explained the typical "Egyptian eye" sign observed on ultrasound examination of these structures. Therefore, they coined the term saphenous fascia, which was validated at a consensus meeting in Rome in 2002.[17, 40-42] In 2006, Abu-Hijleh *et al* noted that this pattern of distribution of the superficial fascia around superficial veins, forming vasculo nervous sheaths could be found in other parts the body.[43] However, their study was based exclusively on the dissection and histological characterization of six embalmed adult

cadavers, along with ultrasound imaging on four living subjects. Our data further lend support to their findings.

Additionally, in the present study, it was clearly noted that superficial veins were placed at different depths in the subcutaneous tissue. This knowledge is often neglected in many anatomy and surgery textbooks.[2, 31, 34, 35, 44] However, it is of potential great clinical interest when designing UPFs, as the use of more superficial veins allows the elaboration of thinner flaps. Besides the obvious morphometric implications, thinner flaps may be associated with greater survival of certain types of UPFs.[2, 4, 32-35]

This work has shown that in multiple anatomical regions the superficial venous system is consistently found in close proximity to expendable superficial nerves, tendons, and even bone segments. This information helps to set the ground to fabricate composite UPFs for different purposes (**Fig. 4**; **Table 1**). The strong tendency for colocalization of superficial veins and nerves may be explained by the fact that these structures develop synchronically, with multiple levels of cross-talk in their origin, differentiation, and elongation until reaching their target organs. As a consequence, they remain in close anatomical proximity since the end of the fetal period.[31, 45] The practical corollary is that there are numerous places where the superficial venous system is in the vicinity of expendable superficial nerves that thus could be raised as ANVFs.[36, 45, 46] Interestingly, in all the regions studied, the superficial cutaneous nerves were closer to sizeable superficial veins than to arteries and respective *comitante* veins of significant caliber (**Fig. 1**). Thus, to harvest a nerve segment as a CNF a deeper dissection would be required than to harvest a homologous ANVF. Moreover, CNFs would tend to be bulkier than the corresponding ANVFs.

However, although there is some evidence that ANVFs may be superior to nerve grafts, ANVFs and their anatomy are frequently neglected even in contemporary textbooks.[47, 48] Notwithstanding, it should also be noted that experimental studies in rats have shown that sensory nerves used as a grafts have yielded inferior motor recovery compared with autologous motor or mixed (sensory and motor) nerve grafts.[49, 50] This may theoretically limit the usefulness of ANVFs incorporating sensory nerves as the ones described in this article for reconstructing motor nerves in the clinical context. However, presently, sensory autologous nerve grafts remain the gold standard for peripheral nerve reconstruction in the clinical context.[51-53]

The present study suggests it is anatomically possible to include a bone segment of the medial aspect of the tibial bone in a AVF or in ANVF tailored around the great saphenous vein. As far as the authors could determine, an osteocutaneous AVF involving the medial aspect of the tibia has been performed in the clinical setting only once.[3] This flap was executed by Koshima *et al.* to successfully reconstruct a defect of the carpal region associated with osteomyelitis. This flap's design was based on the intra-operative observation that the tibial bone cortex was draining its blood to the great saphenous vein.[54] The present study lends support to this architecture of the saphenous UPF. Interestingly, recently, in a pig model, it was shown that large pieces of corticocancellous bone were kept viable on an arterialized venous type perfusion, showing better viability than equivalent bone grafts.[55]

The inclusion of bone in UPFs, eventually associated with a skin paddle, and nerve segments, may further increase the potential use of these flaps for reconstruction of complex head and neck and limb defects, further increasing the reconstructive surgeon's armamentarium.

The authors believe that the anatomical data herein presented may help to decide the best region to use for UPF harvesting in specific circumstances (**Table 1**). Venous caliber and morphological pattern, flap thickness, skin quality, nerve disposition and caliber, as well as the potential for including other structures, such as bone and/or tendon are some of the factors to take in consideration in the decision process.

For example, the dorsal venous flap of the foot is a potential good candidate for digital reconstruction, namely for ring finger avulsion. In fact, its venous pattern make it a preferred option for tailoring antidromic AVFs, which seem to be most suited to cover large areas.[3] Moreover, its integument is thin and pliable, such as that of the fingers (Table 1). Finally, it can easily include the accessory extensor hallucis longus tendon which was found in the majority of cases, as well as the extensor hallucis brevis tendon, allowing for simultaneous skin, nerve, and tendon/ligament reconstruction.[56]

Study limitations

The illustrations of the most common disposition of the superficial veins and nerves of the superior and inferior limbs (**Figs. 3** and **4**) do not take into the account the multiple possible variations of these structures.[31, 57-61] However, in the present work the authors strove to show the most common patterns encountered, rather than focusing on anatomical variations of specific structures that are addressed in detail elsewhere.[31, 57-61]

Although in the present study the authors did not find any large superficial arteries, these anatomical variants, particularly in the upper limb, should always be born in mind, in order to avoid iatrogeny when raising UPFs.[62-64]

The morphometric data presented in this paper may be underestimating the true size of the structures, since histological processing is known to lead to around 20% of volume shrinking.[65, 66]

Another limitation of this work is that it focussed on the regions that, according to the literature, are the more frequently used to raise UPFs.[2, 3, 32, 34, 35] Other regions should be studied.

Finally, the theoretical considerations formulated in the discussion section, although plausible, need empirical validation.

CONCLUSION

In multiple anatomical regions, the superficial venous system is consistently found in close proximity to expendable superficial nerves, tendons, and even bone segments. This knowledge helps to set the ground to tailor composite UPFs for different purposes.

References

1. Pomahac B, Hirsch T, Eriksson E. Wound management. In: Chung KC, Disa JJ, Gosain AK, Kinney BM, Rubin JP, editors. Plastic Surgery Indications and Practice. 1. First ed. Chicago, USA: Saunders Elsevier; 2009. p. 27-32.

2. Casal D, Carvalho S, Pais D, Mota-Silva E, Iria I, Vieira P, et al. Unconventional Perfusion Flaps. 2017. In: Flap Surgery [Internet]. AvidScience; [2-41]. Available from: http://www.avidscience.com/wp-content/uploads/2017/08/unconventional-perfusion-flaps.pdf.

3. Casal D, Cunha T, Pais D, Videira P, Coloma J, Zagalo C, et al. Systematic Review and Meta-Analysis of Unconventional Perfusion Flaps in Clinical Practice. Plastic and reconstructive surgery. 2016;138(2):459-79. doi: 10.1097/PRS.0000000000002390. PubMed PMID: 27465169.

4. Wharton R, Creasy H, Bain C, James M, Fox A. Venous flaps for coverage of traumatic soft tissue defects of the hand: a systematic review. The Journal of hand surgery, European volume. 2017:1753193417712879. Epub 2017/06/14. doi: 10.1177/1753193417712879. PubMed PMID: 28605949.

5. Casal D, Mota-Silva E, Pais D, Iria I, Videira PA, Tanganho D, et al. Optimization of an arterialized venous fasciocutaneous flap in the abdomen of the rat. PRS Global Open. 2017;in press.

6. Townsend PL, Taylor GI. Vascularised nerve grafts using composite arterialised neuro-venous systems. Br J Plast Surg. 1984;37(1):1-17. Epub 1984/01/01. PubMed PMID: 6692051.

7. ANGÉLICA-ALMEIDA M, CASAL D, MAFRA M, MASCARENHAS-LEMOS L, SILVA E, FARINHO A, et al. Evaluation of the efficacy of different conduits to bridge a 10

millimeter defect in the rat sciatic nerve in the presence of an axial blood supply. Archives of Anatomy. 2014;2:8-30.

8. Giusti G, Lee JY, Kremer T, Friedrich P, Bishop AT, Shin AY. The influence of vascularization of transplanted processed allograft nerve on return of motor function in rats. Microsurgery. 2016;36(2):134-43. Epub 2015/01/06. doi: 10.1002/micr.22371. PubMed PMID: 25557845.

9. D'Arpa S, Claes KEY, Stillaert F, Colebunders B, Monstrey S, Blondeel P. Vascularized nerve "grafts": just a graft or a worthwhile procedure? Plastic and Aesthetic Research. 2015;2(4):183-94.

10. Iida T, Nakagawa M, Asano T, Fukushima C, Tachi K. Free vascularized lateral femoral cutaneous nerve graft with anterolateral thigh flap for reconstruction of facial nerve defects. J Reconstr Microsurg. 2006;22(5):343-8. Epub 2006/07/18. doi: 10.1055/s-2006-946711. PubMed PMID: 16845615.

11. Brandt J, Dahlin LB, Lundborg G. Autologous tendons used as grafts for bridging peripheral nerve defects. J Hand Surg Br. 1999;24(3):284-90. Epub 1999/08/05. doi: 10.1054/jhsb.1999.0074

S0266-7681(99)90074-8 [pii]. PubMed PMID: 10433437.

12. Millesi H. Bridging defects: autologous nerve grafts. Acta Neurochir Suppl. 2007;100:37-8. Epub 2007/11/08. PubMed PMID: 17985542.

13. Reich-Schupke S, Stucker M. Nomenclature of the veins of the lower limbs - current standards. Journal der Deutschen Dermatologischen Gesellschaft = Journal of the German Society of Dermatology : JDDG. 2011;9(3):189-94. Epub 2010/11/10. doi: 10.1111/j.1610-0387.2010.07548.x. PubMed PMID: 21059172.

14. Kachlik D, Pechacek V, Musil V, Baca V. Information on the changes in the revised anatomical nomenclature of the lower limb veins. Biomedical papers of the Medical Faculty of the University Palacky, Olomouc, Czechoslovakia. 2010;154(1):93-7. Epub 2010/05/07. PubMed PMID: 20445717.

15. Kachlik D, Pechacek V, Baca V, Musil V. The superficial venous system of the lower extremity: new nomenclature. Phlebology. 2010;25(3):113-23. Epub 2010/05/21. doi: 10.1258/phleb.2009.009046. PubMed PMID: 20483860.

16. Kachlik D, Baca V, Bozdechova I, Cech P, Musil V. Anatomical terminology and nomenclature: past, present and highlights. Surgical and radiologic anatomy : SRA. 2008;30(6):459-66. Epub 2008/05/20. doi: 10.1007/s00276-008-0357-y. PubMed PMID: 18488135.

17. Caggiati A, Bergan JJ, Gloviczki P, Eklof B, Allegra C, Partsch H. Nomenclature of the veins of the lower limb: extensions, refinements, and clinical application. Journal of vascular surgery. 2005;41(4):719-24. Epub 2005/05/06. doi: 10.1016/j.jvs.2005.01.018. PubMed PMID: 15874941.

18. Goyri-O'Neill J, Pais D, Freire de Andrade F, Ribeiro P, Belo A, O'Neill A, et al. Improvement of the embalming perfusion method: the innovation and the results by light and scanning electron microscopy. Acta Med Port. 2013;26(3):188-94. Epub 2013/07/03. PubMed PMID: 23815830.

19. Fukui A. Tecnhique of microangiography. In: Tamai S, Usui M, Yoshizu T, editors. Experimental and Clinical Reconstructive Microsurgery. First ed. Japan: Springer-Verlag; 2004. p. 55-6.

20. Sempuku T. Technique for making a Spalteholz cleared specimen. In: Tamai S, Usui M, Yoshizu T, editors. Experimental and Clinical Reconstructive Microsurgery. First ed. Japan: Springer-Verlag; 2004. p. 59-60.

21. Steinke H, Wolff W. A modified Spalteholz technique with preservation of the histology. Ann Anat. 2001;183(1):91-5. doi: 10.1016/S0940-9602(01)80020-0. PubMed PMID: 11206989.

22. Murovic JA. Upper-extremity peripheral nerve injuries: a Louisiana State University Health Sciences Center literature review with comparison of the operative outcomes of 1837 Louisiana State University Health Sciences Center median, radial, and ulnar nerve lesions. Neurosurgery. 2009;65(4 Suppl):A11-7. Epub 2009/12/16. doi: 10.1227/01.neu.0000339130.90379.89. PubMed PMID: 19927055.

23. Rosberg HEeLD. Epidemiology of hand injuries in a middle-sized city in southern Sweden - a retrospective study with an 8-year interval. Scand J Plast Rec Surg Hand Surg. 2004;(38):347-55.

24. Kouyoumdjian JA. Peripheral nerve injuries: a retrospective survey of 456 cases. Muscle & nerve. 2006;34(6):785-8. doi: 10.1002/mus.20624. PubMed PMID: 16881066.

25. Ciaramitaro P, Mondelli M, Logullo F, Grimaldi S, Battiston B, Sard A, et al. Traumatic peripheral nerve injuries: epidemiological findings, neuropathic pain and quality of life in 158 patients. J Peripher Nerv Syst. 2010;15(2):120-7. Epub 2010/07/16. doi: 10.1111/j.1529-8027.2010.00260.x. PubMed PMID: 20626775.

26. Raimondo S, Fornaro M, Di Scipio F, Ronchi G, Giacobini-Robecchi MG, Geuna S. Chapter 5: Methods and protocols in peripheral nerve regeneration experimental research: part II-morphological techniques. International review of neurobiology.

2009;87:81-103. Epub 2009/08/18. doi: 10.1016/S0074-7742(09)87005-0. PubMed PMID: 19682634.

27. Fischer AH, Jacobson KA, Rose J, Zeller R. Hematoxylin and eosin staining of tissue and cell sections. Cold Spring Harbor Protocols. 2008;2008(5):pdb. prot4986.

28. Foot NC. The Masson trichrome staining methods in routine laboratory use. Stain Technology. 1933;8(3):101-10.

29. Pusztaszeri MP, Seelentag W, Bosman FT. Immunohistochemical expression of endothelial markers CD31, CD34, von Willebrand factor, and Fli-1 in normal human tissues. Journal of Histochemistry & Cytochemistry. 2006;54(4):385-95.

30. Taylor GI, Caddy CM, Watterson PA, Crock JG. The Venous Territories (Venosomes) of the Human Body: Experimental Study and Clinical Implications. Plastic and reconstructive surgery. 1990;86(2):185-213. PubMed PMID: 00006534-199008000-00001.

31. Sangari SK. Veins of the lower limb. In: Tubbs RS, Shoja MM, Loukas M, editors. Bergman's comprehensive encyclopedia of human anatomic variation. 1. First ed. New Jersey: Wiley Blackwell; 2016. p. 900-9.

32. Garlick JW, Goodwin IA, Wolter K, Agarwal JP. Arterialized venous flow-through flaps in the reconstruction of digital defects: case series and review of the literature. Hand (N Y). 2015;10(2):184-90. Epub 2015/06/03. doi: 10.1007/s11552-014-9684-0. PubMed PMID: 26034428.

33. Giesen T, Forster N, Kunzi W, Giovanoli P, Calcagni M. Retrograde arterialized free venous flaps for the reconstruction of the hand: review of 14 cases. The Journal of hand surgery. 2014;39(3):511-23. Epub 2014/02/25. doi: 10.1016/j.jhsa.2013.12.002. PubMed PMID: 24559628.

34. Goldschlager R, Rozen WM, Ting JW, Leong J. The nomenclature of venous flow-through flaps: updated classification and review of the literature. Microsurgery. 2012;32(6):497-501. Epub 2012/03/22. doi: 10.1002/micr.21965. PubMed PMID: 22434451.

35. Yan H, Brooks D, Ladner R, Jackson WD, Gao W, Angel MF. Arterialized venous flaps: a review of the literature. Microsurgery. 2010;30(6):472-8. Epub 2010/03/20. doi: 10.1002/micr.20769 [doi]. PubMed PMID: 20238385.

36. Taylor GI, Pan WR. The angiosome concept. In: Dodwell P, editor. The angiosome concept and tissue transfer. 1. First ed. Florida: Quality Medical Publishing, Inc.; 2014. p. 354-95.

37. Hong MK, Taylor GI. Angiosome territories of the nerves of the upper limbs. Plastic and reconstructive surgery. 2006;118(1):148-60. Epub 2006/07/04. doi: 10.1097/01.prs.0000221075.91038.08. PubMed PMID: 16816688.

38. Suami H, Taylor GI, Pan WR. Angiosome territories of the nerves of the lower limbs. Plastic and reconstructive surgery. 2003;112(7):1790-8. Epub 2003/12/10. doi: 10.1097/01.PRS.0000091161.95599.D8. PubMed PMID: 14663222.

39. Gascoigne AC, Ian Taylor G, Corlett RJ, Briggs C, Ashton MW. The Relationship of Superficial Cutaneous Nerves and Interperforator Connections in the Leg: A Cadaveric Anatomical Study. Plastic and reconstructive surgery. 2017;139(4):994e-1002e. Epub 2017/03/30. doi: 10.1097/prs.0000000000003157. PubMed PMID: 28350683.

40. Caggiati A. The saphenous venous compartments. Surgical and radiologic anatomy : SRA. 1999;21(1):29-34. PubMed PMID: 10370990.

41. Caggiati A. Fascial relations and structure of the tributaries of the saphenous veins. Surgical and radiologic anatomy : SRA. 2000;22(3-4):191-6. PubMed PMID: 11143312.

42. Caggiati A, Bergan JJ, Gloviczki P, Jantet G, Wendell-Smith CP, Partsch H, et al. Nomenclature of the veins of the lower limbs: an international interdisciplinary consensus statement. Journal of vascular surgery. 2002;36(2):416-22. PubMed PMID: 12170230.

43. Abu-Hijleh MF, Roshier AL, Al-Shboul Q, Dharap AS, Harris PF. The membranous layer of superficial fascia: evidence for its widespread distribution in the body. Surgical and radiologic anatomy : SRA. 2006;28(6):606-19. Epub 2006/10/25. doi: 10.1007/s00276-006-0142-8. PubMed PMID: 17061033.

44. Woo SH, Kim KC, Lee GJ, Ha SH, Kim KH, Dhawan V, et al. A retrospective analysis of 154 arterialized venous flaps for hand reconstruction: an 11-year experience. Plastic and reconstructive surgery. 2007;119(6):1823-38. Epub 2007/04/19. doi: 10.1097/01.prs.0000259094.68803.3d [doi]

00006534-200705000-00029 [pii]. PubMed PMID: 17440363.

45. Carmeliet P. Blood vessels and nerves: common signals, pathways and diseases. Nature Reviews Genetics. 2003;4(9):710-20.

46. Chuang DC. Adult brachial plexus reconstruction with the level of injury: review and personal experience. Plast Reconstr Surg. 2009;124(6 Suppl):e359-69. Epub 2010/01/09. doi: 10.1097/PRS.0b013e3181bcf16c

00006534-200912001-00010 [pii]. PubMed PMID: 19952704.

47. Sabapathy SR, Venkatramani H. Harvest of extraplexal donor nerves for transfer or grafting. In: Dy CJ, Isaacs J, editors. American Society for Surgery of the Hand surgical anatomy: nerve reconstruction. 1. First ed. Chicago, USA: American Society for Surgery of the Hand; 2017. p. 161-86.

48. Boyd KU, Fox IK. Nerve repair and grafting. In: Mackinnon SE, editor. Nerve surgery. 1. First ed. New York: Thieme; 2015. p. 75-100.

49. Nichols CM, Brenner MJ, Fox IK, Tung TH, Hunter DA, Rickman SR, et al. Effects of motor versus sensory nerve grafts on peripheral nerve regeneration. Experimental neurology. 2004;190(2):347-55. doi: http://dx.doi.org/10.1016/j.expneurol.2004.08.003.

50. Moradzadeh A, Borschel GH, Luciano JP, Whitlock EL, Hayashi A, Hunter DA, et al. The impact of motor and sensory nerve architecture on nerve regeneration. Experimental neurology. 2008;212(2):370-6. doi: http://dx.doi.org/10.1016/j.expneurol.2008.04.012.

51. Siemionow M, Uygur S, Ozturk C, Siemionow K. Techniques and materials for enhancement of peripheral nerve regeneration: a literature review. Microsurgery. 2013;33(4):318-28. Epub 2013/04/10. doi: 10.1002/micr.22104. PubMed PMID: 23568681.

52. Sulaiman W, Gordon T. Neurobiology of peripheral nerve injury, regeneration, and functional recovery: from bench top research to bedside application. Ochsner J. 2013;13(1):100-8. PubMed PMID: 23531634; PubMed Central PMCID: PMCPMC3603172.

53. Sinis N, Kraus A, Papagiannoulis N, Werdin F, Schittenhelm J, Meyermann R, et al. Concepts and developments in peripheral nerve surgery. Clinical neuropathology. 2009;28(4):247-62. Epub 2009/08/01. PubMed PMID: 19642504.

54. Koshima I, Soeda S, Nakayama Y, Fukuda H, Tanaka J. An arterialised venous flap using the long saphenous vein. Br J Plast Surg. 1991;44(1):23-6. Epub 1991/01/01. doi: 0007-1226(91)90171-F [pii]. PubMed PMID: 1993230.

55. Borumandi F, Higgins JP, Buerger H, Vasilyeva A, Benlidayi ME, Sencar L, et al. Arterialized Venous Bone Flaps: An Experimental Investigation. Scientific reports. 2016;6.

56. Casal D, Pais D, Angélica-Almeida M, Bilhim T, Santos A, Goyri-O'Neill J. Morphometric analysis of the extensor tendons of the hallux and potential implications for tendon grafting. European Journal of Anatomy. 2010;1(14):11-8.

57. Vazquez T, Sanudo J. Veins of the upper limb. In: Tubbs RS, Shoja MM, Loukas M, editors. Bergman's comprehensive encyclopedia of human anatomic variation. 1. First ed. New Jersey: Wiley Blackwell; 2016. p. 826-31.

58. Eid EM, Hegazy AM. Anatomical variations of the human sural nerve and its role in clinical and surgical procedures. Clin Anat. 2011;24(2):237-45. Epub 2010/10/16. doi: 10.1002/ca.21068. PubMed PMID: 20949489.

59. Ramakrishnan PK, Henry BM, Vikse J, Roy J, Saganiak K, Mizia E, et al. Anatomical variations of the formation and course of the sural nerve: A systematic review and meta-analysis. Annals of anatomy = Anatomischer Anzeiger : official organ of the Anatomische Gesellschaft. 2015;202:36-44. Epub 2015/09/06. doi: 10.1016/j.aanat.2015.08.002. PubMed PMID: 26342158.

60. Mahan MA, Spinner RJ. Nerves of the upper extremity. In: Tubbs RS, Shoja MM, Loukas M, editors. Bergman's comprehensive encyclopedia of human anatomic variation. 1. First ed. New Jersey: Wiley Blackwell; 2016. p. 1068-112.

61. Apaydin N. Lumbosacral plexus. In: Tubbs RS, Shoja MM, Loukas M, editors. Bergman's comprehensive encyclopedia of human anatomic variation. 1. First ed. New Jersey: Wiley Blackwell; 2016. p. 1113-29.

62. Casal D, Pais D, Toscano T, Bilhim T, Rodrigues L, Figueiredo I, et al. A rare variant of the ulnar artery with important clinical implications: a case report. BMC Res Notes. 2012;5:660. doi: 10.1186/1756-0500-5-660. PubMed PMID: 23194303; PubMed Central PMCID: PMCPMC3529700.

63. Rodriguez-Niedenfuhr M, Vazquez T, Nearn L, Ferreira B, Parkin I, Sanudo JR. Variations of the arterial pattern in the upper limb revisited: a morphological and statistical study, with a review of the literature. J Anat. 2001;199(Pt 5):547-66. Epub 2002/01/05. PubMed PMID: 11760886; PubMed Central PMCID: PMCPMC1468366.

64. Patel A. Lower limb arteries. In: Tubbs RS, Shoja MM, Loukas M, editors. Bergman's comprehensive encyclopedia of human anatomic variation. 1. First ed. New Jersey: Wiley Blackwell; 2016. p. 741-51.

65. Millington PF, Wilkinson R. The skin in depth: dermal vasculature. In: Harrison RJ, McMinn RM, editors. Biologic structure and function of the skin: Skin. 1. First ed. United Kingdom: Cambridge University Press; 1983. p. 69-72.

66. Chatterjee S. Artefacts in histopathology. J Oral Maxillofac Pathol. 2014;18(Suppl 1):S111-6. doi: 10.4103/0973-029X.141346. PubMed PMID: 25364159; PubMed Central PMCID: PMCPMC4211218.

Chapter 11

A RARE VARIANT OF THE ULNAR ARTERY WITH IMPORTANT CLINICAL IMPLICATIONS: A CASE REPORT

Authors: Diogo Casal[1,2], Diogo Pais[3], Tiago Toscano[4], Tiago Bilhim[5], Luís Rodrigues[6], Inês Figueiredo[1], Sónia Aradio[1], Maria Angélica-Almeida[6], João Goyri-O'Neill[7]

Affiliations:

1- Anatomy Instructor, Department of Anatomy, Faculty of Medical Sciences, New University of Lisbon, Lisbon, Portugal

2- Plastic and Reconstructive Surgery Resident, São José Hospital

3- Associate Professor of Anatomy, Department of Anatomy, Faculty of Medical Sciences

4- Plastic and Reconstructive Surgery Resident, Hospital Santa Maria

5- Radiologist and Professor of Radiology, Faculty of Medical Sciences, New University of Lisbon

6- Head of the Plastic and Reconstructive Surgery Department and Burn Unit, Hospital São José

7- Chairman and Professor of Anatomy, Faculty of Medical Sciences, New University of Lisbon, Department of Anatomy, Faculty of Medical Sciences, New University of Lisbon

ABSTRACT

Background: Variations in the major arteries of the upper limb are estimated to be present in up to one fifth of people, and may have significant clinical implications.

Case Presentation: During routine cadaveric dissection of a 69-year-old fresh female cadaver, a superficial brachioulnar artery with an aberrant path was found bilaterally. The superficial brachioulnar artery originated at midarm level from the brachial artery, pierced the brachial fascia immediately proximal to the elbow, crossed superficial to the muscles that originated from the medial epicondyle, and ran over the pronator teres muscle in a doubling of the antebrachial fascia. It then dipped into the forearm fascia, in the gap between the flexor carpi radialis and the palmaris longus. Subsequently, it ran deep to the palmaris longus muscle belly, and superficially to the flexor digitorum superficialis muscle, reaching the gap between the latter and the flexor carpi ulnaris muscle, where it assumed is usual position lateral to the ulnar nerve.

Conclusion: As far as the authors could determine, this variant of the superficial brachioulnar artery has only been described twice before in the literature. The existence of such a variant is of particular clinical significance, as these arteries are more susceptible to trauma, and can be easily confused with superficial veins during medical and surgical procedures, potentially leading to iatrogenic distal limb ischemia.

INTRODUCTION

A sound knowledge of the vascular anatomy of the upper limb is of paramount importance, since this is a site of frequent injury and of various surgical and invasive procedures [1, 2]. Normally, the arterial supply to the upper limb is provided by the axillary artery that originates the brachial artery, which, in turn, at the elbow originates the ulnar and radial arteries [3]. These two are placed between the forearm muscles, and give rise at the wrist level to the arteries that form the superficial and deep arterial palmar arches [3]. Usually, the ulnar artery gives off the common interosseous artery that divides into the anterior and posterior interosseous arteries [3].

It has been increasingly recognized that variations in the major arteries of the upper limb are common, being found in up to one fifth of individuals [1, 4, 5]. Among these, variants of the ulnar and radial arteries are the most common [1, 3, 4]. Particularly, the presence of superficial radial or ulnar arteries is of utmost clinical significance, as these arteries are most susceptible to trauma, and can be easily confused with superficial veins [1, 2]. One variant of superficial ulnar arteries is the superficial brachioulnar artery (**SuBUA**), which is defined as an ulnar artery with a high origin in the arm that progresses over the superficial muscles of the forearm. The prevalence of the SuBUA varies widely in different studies [3]. For example, Adachi, in 1928, in an impressive series of 1198 upper limb dissections, identified only 8 cases of SuBUA, corresponding to a 0,7% prevalence of this variant [6]. In contrast, in 1844, Quain, had found 7% of SuBUA in 429 specimens

dissected [7]. According to a recent review by Rodriguez-Niedenfuhr et al., the overall prevalence of this variant in the literature is estimated to be around 2,7% [3].

The authors report the case of a cadaver in which a bilateral SuBUA with an unusual path was identified bilaterally. The clinical implications of this anatomical variation are undoubtedly of great significance [3, 5, 8], and are described briefly in the Discussion Section.

CASE PRESENTATION

During routine dissection of a 69-year-old fresh female cadaver at the Department of Anatomy at our institution, variations in the arterial system of both upper limbs were noted. There was no history or evidence of any invasive procedure in the upper limbs of that person.

On both sides, the brachial artery in the middle third of the arm originated a SuBUA (**Figs. 1** and **2**). This artery penetrated the brachial fascia in the lower third of the arm, crossed anteriorly to the bicipital aponeurosis and to the muscles that originated from the medial epicondyle, and ran over the pronator teres muscle in a doubling of the antebrachial fascia (**Fig. 2**). In the elbow region, the SuBUA was in intimate contact with the superficial structures, namely the medial antebrachial nerve and the subcutaneous veins (**Fig. 1**). It then dipped into the forearm fascia, passed through a gap between the palmaris longus and the flexor carpi radialis, ran deep to the palmaris longus muscle belly, and superficially to the flexor digitorum superficialis muscle, reaching the gap between the latter and flexor carpi ulnaris muscle (**Fig. 2**). In the middle third of the forearm the SuBUA was positioned lateral to the ulnar nerve.

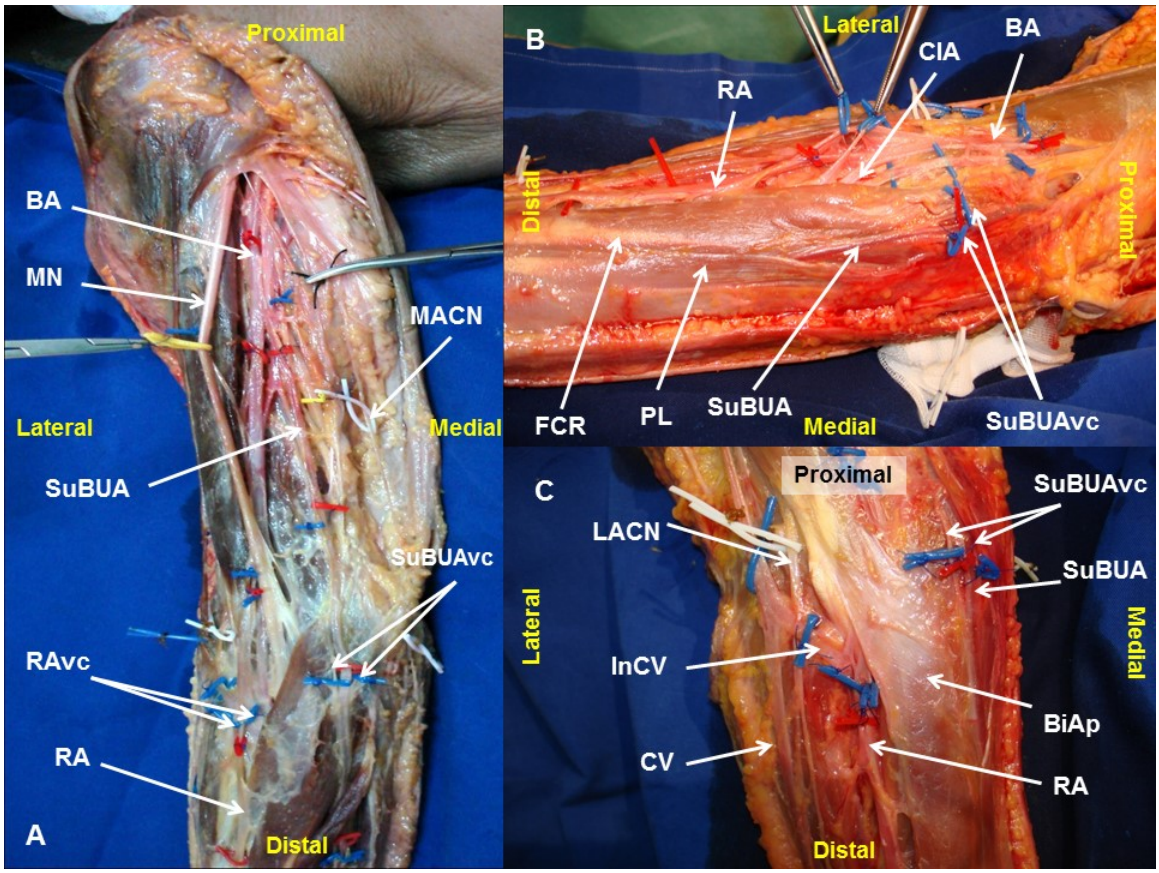

Figure 1 - Right upper limb dissection photographs showing the origin and path of the superficial brachioulnar artery, and their neighbor structures at the arm and elbow.

A – Upper arm and proximal forearm; B – Medial aspect of the elbow region; C- Anterior aspect of the elbow region.

RA, radial artery; **SuBUA**, superficial brachioulnar artery; **BA**, brachial artery; **CIA**, common interosseous artery; **CV**, cephalic vein; **InCV**, Intermediate cephalic vein; **RAvc**, radial artery venae comitantes; **SuBUAvc**, superficial brachioulnar artery venae comitantes; **LACN**, lateral antebrachial cutaneous nerve; **MACN**, medial antebrachial cutaneous nerve; **MN**, median nerve; **PL**, palmaris longus muscle; **FCR**, flexor carpi radialis muscle; **BiAp**, bicipital aponeurosis.

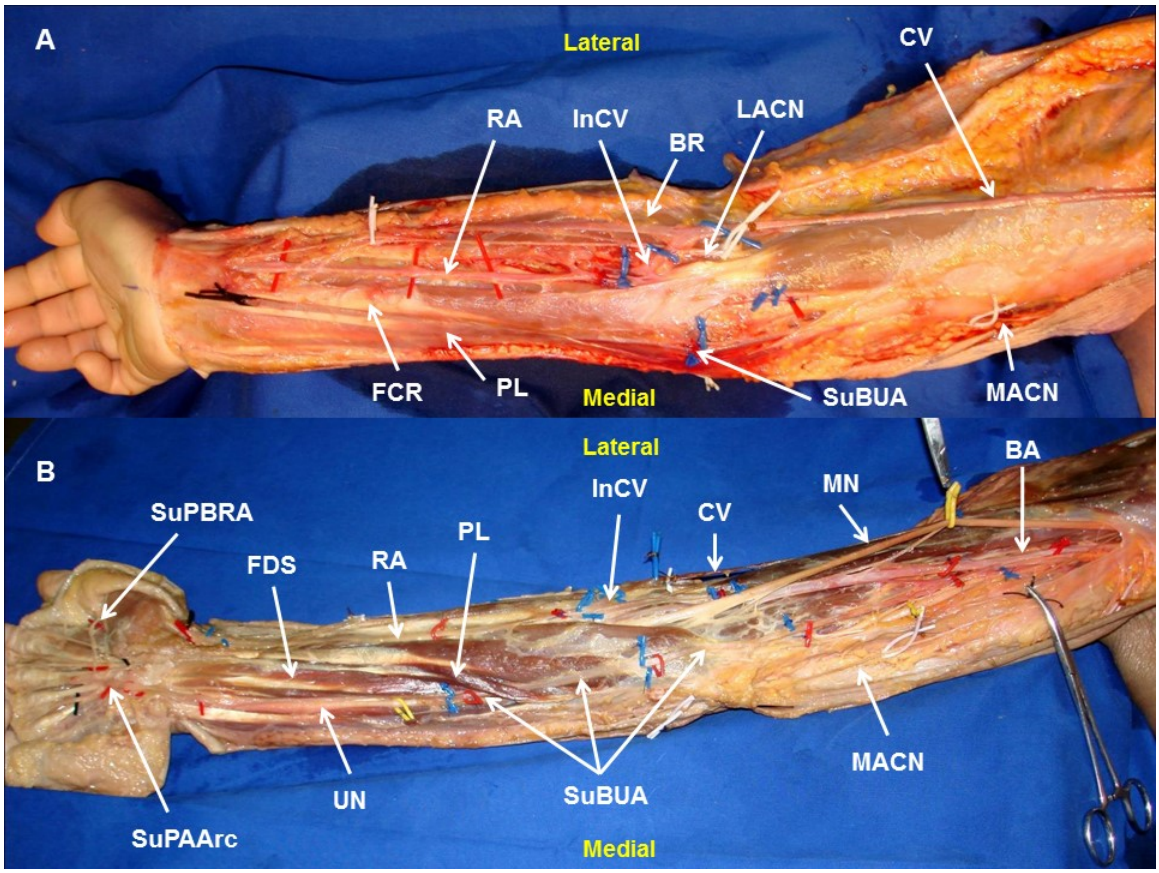

Figure 2 - Right upper limb showing the anomalous course of the superficial brachioulnar artery in an above fascia (A) and a deeper to fascia (B) dissection.

RA, radial artery; **SuBUA**, superficial brachioulnar artery; **BA**, brachial artery; **CIA**, common interosseous artery; **CV**, cephalic vein; **InCV**, intermediate cephalic vein; **RAvc**, radial artery venae comitantes; **LACN**, lateral antebrachial cutaneous nerve; **MACN**, medial antebrachial cutaneous nerve; **MN**, median nerve; **PL**, palmaris longus muscle; **FCR**, flexor carpi radialis muscle; **FDS** , flexor digitorum superficialis muscle.

The brachial artery continued through the radial artery (**RA**), which followed its usual course. In the upper third of the forearm, the RA gave off the common interosseous artery. This latter artery branched into the anterior and the posterior

interosseous arteries (**Fig. 1**). The anterior interosseous artery had a large caliber and originated branches to most of the anterior compartment muscles. The radial recurrent artery emanated from the radial artery, and the anterior ulnar recurrent artery was a branch of the common interosseous trunk.

In the distal third of the forearm and in the wrist region, the RA and the SuBUA divided in the same manner as the radial and ulnar arteries usually distribute [3], originating the superficial and deep palmar arterial arches. **Figure 3** schematically portrays the distribution of the RA and the SuBUA in the cadaver herein described.

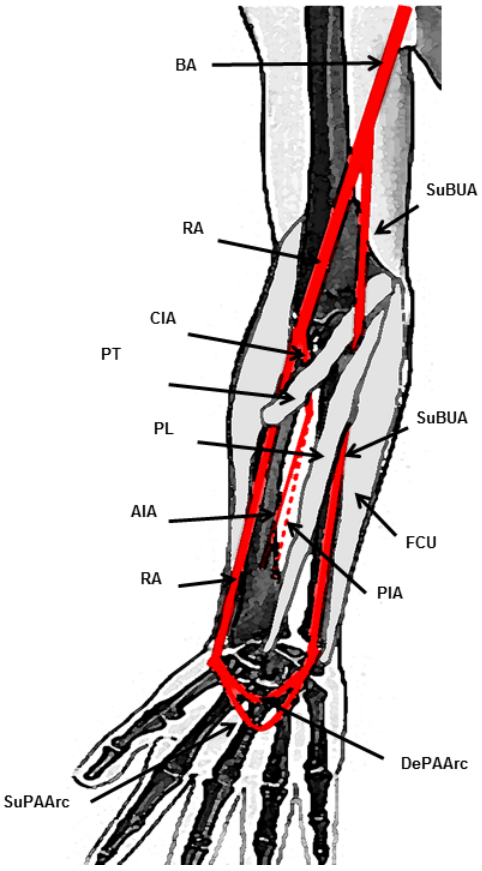

Figure 3 - Schematic drawing of the origin and distribution of the superficial brachioulnar artery and its relation with the medial epicondyle muscles.

RA, radial artery; **SuBUA**, superficial brachioulnar artery; **BA**, brachial artery; **CIA**, common interosseous artery; **AIA**, anterior interosseous artery; **PIA**, posterior interosseous artery; **SUPAArch**, superficial palmar arterial arch; **DePAArc**, deep palmar arterial arch; **PL**, palmaris longus muscle; **BR**, brachioradialis muscle; **PT**, pronator teres muscle; **FCU**, flexor carpi ulnaris muscle.

DISCUSSION

Rodriguez-Niedenfuhr et al., have recently proposed a system of classification of upper limb arterial variations, based on their extensive experience of almost 400 upper limb dissections, and based on a thorough literature review on the subject [3, 8, 9]. This terminology, which recently has been taken up by several authors [5], considers each arterial variation as an individual entity along its full extension in the upper limb [3]. Furthermore, this classification divides upper limb arterial variants in three broad groups based on their location in the arm, the arm and forearm, or the forearm. These three groups are further subdivided in several different categories, depending on the absence or duplication of arteries, and on whether these variants adopt a superficial or usual course in the forearm [3].

The variations found exclusively in the forearm are the **superficial brachial artery** and the **accessory brachial artery**. The former represents a brachial artery coursing in front of the median nerve, instead of being placed behind it. The accessory brachial artery is characterized by the existence of 2 brachial arteries that rejoin before giving off the forearm arteries. The accessory brachial artery originates from the main brachial artery [3].

The variations located at the level of both the arm and forearm are the **SuBUA**, the **brachioulnar**, the **brachioradial**, the **superficial brachioradial**, the **brachiointerosseous**, the **superficial brachiomedian**, and the **superficial brachioulnoradial arteries** [3].

The SuBUA is characterized by an ulnar artery that originates higher than usual and that courses over the forearm flexor muscles. In this setting, there is a whole arterial pattern, with a brachial or superficial brachial artery branching into the radial and common interosseous arterial trunk, or more rarely into the radial and ulnar arteries [3].

The brachioulnar artery corresponds to a high origin of the ulnar artery from the brachial artery, with the latter branching branching into the radial artery and the common interosseous arterial trunk [3].

The brachioradial artery represents a high origin of the radial artery from the brachial or superficial brachial artery that in turn branches into the ulnar artery and the common interosseous arterial trunk [3].

The superficial brachioradial artery consists of a high origin of the radial artery coursing over the brachioradialis muscle or the tendons that limit the snuffbox. In these circumstances the brachial artery usually originates the ulnar artery and the common interosseous arterial trunk [3].

The brachiointerosseous artery is defined by a high origin of the interosseous arterial trunk, in the context of a whole arterial pattern of the upper limb, with a brachial artery that divides into the radial and ulnar arteries [3].

The superficial brachiomedian artery is characterized by a high origin of the median artery that courses above the superficial flexor muscles and by a brachial artery that divides into the radial and ulnar arteries [3].

Finally, the superficial brachioulnoradial artery represents a superficial brachial artery that at the level of the elbow branches into the radial and ulnar arteries, which in turn will course over the superficial forearm flexor muscles. In this variant, the superficial brachial artery coexists with a normal brachial artery that ends in the common interosseous arterial trunk [3].

The variations found exclusively at the forearm level include the **superficial radial artery**, the **duplication of the radial arteries**, and the **absence of the radial or ulnar arteries** [3].

The superficial radial artery consists of a radial artery coursing above the tendons limiting the snuffbox. The absence of either the radial or ulnar arteries is considered very rare, as is the true duplication of the radial artery [3].

Therefore, considering Rodriguez-Niedenfuhr's classification, our case most closely resembles a SuBUA variant [3]. This variant corresponds to a brachial artery originating a superficial ulnar artery high up in the arm, whereas the radial artery is a continuation of the brachial artery [3]. The origin of the interosseous arteries from the radial artery, as recorded in the present case, is considered common in cases of ulnar arteries arising in the arm [3].

According to most authors, the SuBUA most frequently courses posteriorly to the bicipital aponeurosis, and not anteriorly as it was observed in our dissection (**Figs. 1C** and **2A**) [3]. In addition, in the work conducted by Rodriguez-Niedenfuhr et al., in all cases the SuBUA coursed anteriorly to all the flexor muscles of the forearm, and then placed itself in the lateral border of the flexor carpi ulnaris to adopt its position in the

lateral aspect of the ulnar nerve at the level of the middle third of the forearm [3]. As far as the authors could determine, a SuBUA variant similar to the one we observed, with a path deep to the palmaris longus muscle, has just been reported twice in the literature. Quain found it in 2 cases while dissecting 429 upper limbs [7], and Hazlet once in 188 limbs [10].

Upper limb vascular variations are presently thought to result from a stochastic process of persistence, enlargement and differentiation of parts of the initial capillary network which would normally remain as capillaries or even regress [5, 11]. The precise mechanisms that lead to the higher frequency of certain variants over others, remain to be elucidated [5, 11]. Interestingly, Rodriguez-Niedenfuhr et al., identified a SuBUA in 4,7% of 150 upper limbs of embryos, which is a value superior to that reported by most authors in the general adult population [11].

The clinical importance of the superficial variations of the arteries of the upper limb are increasingly being recognized [1]. For example, by being superficial, they can be easily mistaken for subcutaneous veins, leading to inadvertent artery cannulation, with the potential risk of distal limb ischemia [1, 12, 13]. In addition, the superficial position of the radial or ulnar arteries makes them more vulnerable to trauma [1]. Moreover, the possibility of a SBUR variant should always be born in mind when using the arm or forearm as a source or as a recipient of microvascular flaps, or when using the radial artery as vascular graft [14-16].

Clinically, the presence of superficial forearm arteries can be suspected in the absence of palpable ulnar or radial pulses in their usual location, when superficial

pulsatile vessels are found, or when patients complain of intermittent forearm or hand pain [1].

CONCLUSION

The ulnar artery can present several anatomical variations. In this paper we describe a bilateral superficial brachioulnar artery that, instead of travelling over the anterior aspect of the forearm muscles, as is usually the case in this variant of the ulnar artery, coursed under the palmaris longus muscle, before reaching the lateral aspect of the flexor carpi ulnaris muscle and becoming part of the ulnar neurovascular bundle. This rare variant of the ulnar artery should always be born in mind when addressing the vessels of this region clinically.

REFERENCES

1. Claassen H, Schmitt O, Werner D, Schareck W, Kroger JC, Wree A: Superficial arm arteries revisited: brother and sister with absent radial pulse. Ann Anat 2010, 192:151–155.

2. Jacquemin G, Lemaire V, Medot M, Fissette J: Bilateral case of superficial ulnar artery originating from axillary artery. Surg Radiol Anat 2001, 23:139–143.

3. Rodriguez-Niedenfuhr M, Vazquez T, Nearn L, Ferreira B, Parkin I, Sanudo JR: Variations of the arterial pattern in the upper limb revisited: a morphological and statistical study, with a review of the literature. J Anat 2001, 199:547–566.

4. Claassen H, Schmitt O, Wree A: Large patent median arteries and their relation to the superficial palmar arch with respect to history, size consideration and clinic consequences. Surg Radiol Anat 2008, 30:57–63.

5. Shen S, Hong MK: A rare case of bilateral variations of upper limb arteries: brief review of nomenclature, embryology and clinical applications. Surg Radiol Anat 2008, 30:601–603.

6. Adachi B: In Das Arteriensystem der Japaner. Volume 1. Kyoto: Maruzen; 1928:285–356.

7. Quain R: In Anatomy of the Arteries of the Human Body. London: Taylor & Walton; 1844:326–337.

8. Rodriguez-Baeza A, Nebot J, Ferreira B, Reina F, Perez J, Sanudo JR, Roig M: An anatomical study and ontogenetic explanation of 23 cases with variations in the main pattern of the human brachio-antebrachial arteries. J Anat 1995, 187(Pt 2):473–479.

9. Rodriguez-Niedenfuhr M, Sanudo JR, Vazquez T, Nearn L, Logan B, Parkin I: Median artery revisited. J Anat 1999, 195(Pt 1):57–63.

10. Hazlett JW: The superficial ulnar artery with reference to accidental intraarterial injection. Can Med Assoc J 1949, 61:289–293.

11. Rodriguez-Niedenfuhr M, Burton GJ, Deu J, Sanudo JR: Development of the arterial pattern in the upper limb of staged human embryos: normal development and anatomic variations. J Anat 2001, 199:407–417.

12. Mayhew JF, Mohiuddin S: Inadvertent median artery cannulation. Paediatr Anaesth 2005, 15:1149. author reply 1149–1150.

13. Dearlove OR, Perkins R: Inadvertent median artery cannulation. Paediatr Anaesth 2005, 15:439–440.

14. Porter CJ, Mellow CG: Anatomically aberrant forearm arteries: an absent radial artery with co-dominant median and ulnar arteries. Br J Plast Surg 2001, 54:727–728.

15. Acarturk TO, Tuncer U, Aydogan LB, Dalay AC: Median artery arising from the radial artery: its significance during harvest of a radial forearm free flap. J Plast Reconstr Aesthet Surg 2008, 61:e5–e8.

16. Kumar MR: Multiple arterial variations in the upper limb of a South Indian female cadaver. Clin Anat 2004, 17:233–235.

Chapter 12

MORPHOMETRIC ANALYSIS OF THE EXTENSOR TENDONS OF THE HALLUX AND POTENTIAL IMPLICATIONS FOR TENDON GRAFTING

Authors: Diogo Casal[1,2]; Diogo Pais[1]; Maria Angélica-Almeida[2]; Tiago Bilhim[1]; António Santos[1]; João Goyri-O'Neill[1]

Affiliations:

1. Anatomy Department; Medical Sciences Faculty, New University of Lisbon, Portugal
2. Plastic and Reconstructive Surgery Department, São José Hospital, Lisbon, Portugal

ABSTRACT

Although several tendon sources are available for reconstructive surgical procedures, all have one or more shortcomings. The aim of this work was to evaluate if the extensor tendons of the hallux showed anatomical characteristics that could make them an additional source for tendon grafting procedures.

The authors performed a detailed morphometric analysis of the extensor tendons of the hallux in 26 lower limbs, in order to evaluate the putative association of anatomical variants with hallux valgus, and to try to assess the feasibility of using part of the extensor apparatus of the hallux as a source of tendon for grafting procedures.

An accessory extensor hallucis longus tendon was found in 92,3% of cases. Extensor hallucis brevis tendon length was 10,5 ± 0,6 cm, its width was 0,5 ± 0,1 cm, and its thickness varied between 1-2 mm, making it a potentially good candidate as a source of tendon grafts. Several anatomical variations were observed, namely the fusion of the tendons of the extensor hallucis brevis and the accessory extensor hallucis longus muscles in the distal part of the foot.

This new therapeutic option, if implemented, would possibly increase the supply of autogenous donor tissue for reconstructive procedures, thereby enhancing the reconstructive surgeon's armamentarium.

INTRODUCTION

Tendon grafts are often needed in reconstructive surgery, either in the realm of Orthopedics, Plastic Surgery, Maxillofacial Surgery, Burn Surgery, or even in Heart Surgery [1-3]. These tendon grafts can be used for reconstructing tendon or ligament defects, stabilizing joints and maintaining soft tissues in position [4]. Recently, the use of plantaris tendon was even proposed for atrioventricular valve repair [5].

Redundancy in the function of certain tendons has been known for decades [6], allowing for several alternatives for tendon harvesting to become perfectly established. However, when a patient sustains extensive injuries, it is not uncommon for autologous tendons to be insufficient to reconstruct all the missing structures [7]. In addition, all tendon options currently in use for grafting procedures have one or more of several limitations, namely: inconstancy; their removal results in a variable deficit in the donor region; and the surgical incisions required to perform their extirpation are placed in body areas where healing is known to be suboptimal and thus result in conspicuous scars [7,8]. Therefore, any new alternative that would increase the supply of autologous tendons for reconstructive procedures would be invaluable.

Supernumerary tendons in the hallucal extensor apparatus have been known well documented for more than 125 years [9-12]. In 1976, Tate and Pachnik described an accessory tendon of the extensor hallucis longus in the majority of individuals [13]. Kaneff, Andreev and Stephanoff in the 1980s studied in detail the extensor tendons in the first ray of foot, reporting several accessory tendons and over 20 distinct variations [14-17]. More recently, these findings have been reproduced by several authors [18-24].

Notwithstanding the reported high frequency of these accessory tendons, their clinical importance has been considered relatively minor, and their description is even omitted from many modern, comprehensive clinical anatomy textbooks [20,25]. Moreover, the extensor tendons of the foot have not been, as far as the authors know, used as sources of tendon grafts [8,26].

Furthermore, recently, certain authors have associated certain variations in the extensor apparatus of the hallux to hallux valgus [21], which is a common condition in which there is lateral deviation of the big toe, at the metatarso-phalangeal joint [27]. However, these findings were not replicated by others and are still a matter of debate [19].

Therefore, in this work, the authors studied the extensor tendons of the hallux in human cadaveric specimens, in order to evaluate the potential of any of these tendons as source of tendon grafts, and to assess if there was any association between the morphometric features of these tendons and the presence of hallux valgus.

MATERIALS AND METHODS

The study was performed on 26 lower extremities of freshly frozen adult human cadavers that were used for routine gross anatomical dissections at the Medical Sciences Faculty in Lisbon, Portugal. Age at death was mostly between 60 and 85 (average 72,3) years. There were 7 men (53,8%) and 6 women (46,2%). They had had no prior surgical procedures in the leg or foot regions.

The dorsum of the foot and lower leg were carefully dissected, exposing the extensor tendons of the hallux from their origin to their insertion. Their origin, length, width, thickness and type of insertion were recorded, as well as the occurrence of hallux valgus. Mean width of each tendon was calculated based on the average of the widths measured at three points: tendon origin, middle portion of the tendon, and immediately before insertion, in the most distal place where it would be surgically possible to section the tendon for harvesting.

This research required no specific permission from the ethics committee of our institution, and conformed to the provisions of the Declaration of Helsinki (1995; revised 2000).

Statistical analysis was performed using the Statistical Analysis Software PASWO 18.0 (IBM®). Chi-Square test was used to compare proportions, while t-Student test and ANOVA were used for comparing means. A p value under 0,05 was considered statistically significant. Mean values are represented by their numeric value ± standard deviation.

RESULTS

In all cases, the extensor apparatus of the hallux was composed of the extensor hallucis longus tendon (**EHLp**) and the extensor hallucis brevis tendon (**EHB**). An accessory extensor hallucis longus tendon (**EHLa**) was found in 92,3% of cases. **Figure 1** portrays the usual composition of the extensor tendons of the hallux. The EHLa originated from the same muscular belly as the EHLp in all cases (**Fig. 1).** When present, the EHLa was placed medially to the EHLp (91,7%) since its origin to its termination. Only in two feet, in the same cadaver, was the EHLa absent (**Fig. 2A**). In the two feet of one cadaver (8,3%) the EHLa was placed laterally to the EHLp and terminated in the medial portion of the EHB (**Fig. 2B**). In one foot, there were two separate EHLa, one of them with normal diameter, but the other much thinner, that inserted separately in the base of the distal phalanx. These two separate EHLa were placed laterally to the EHLp.

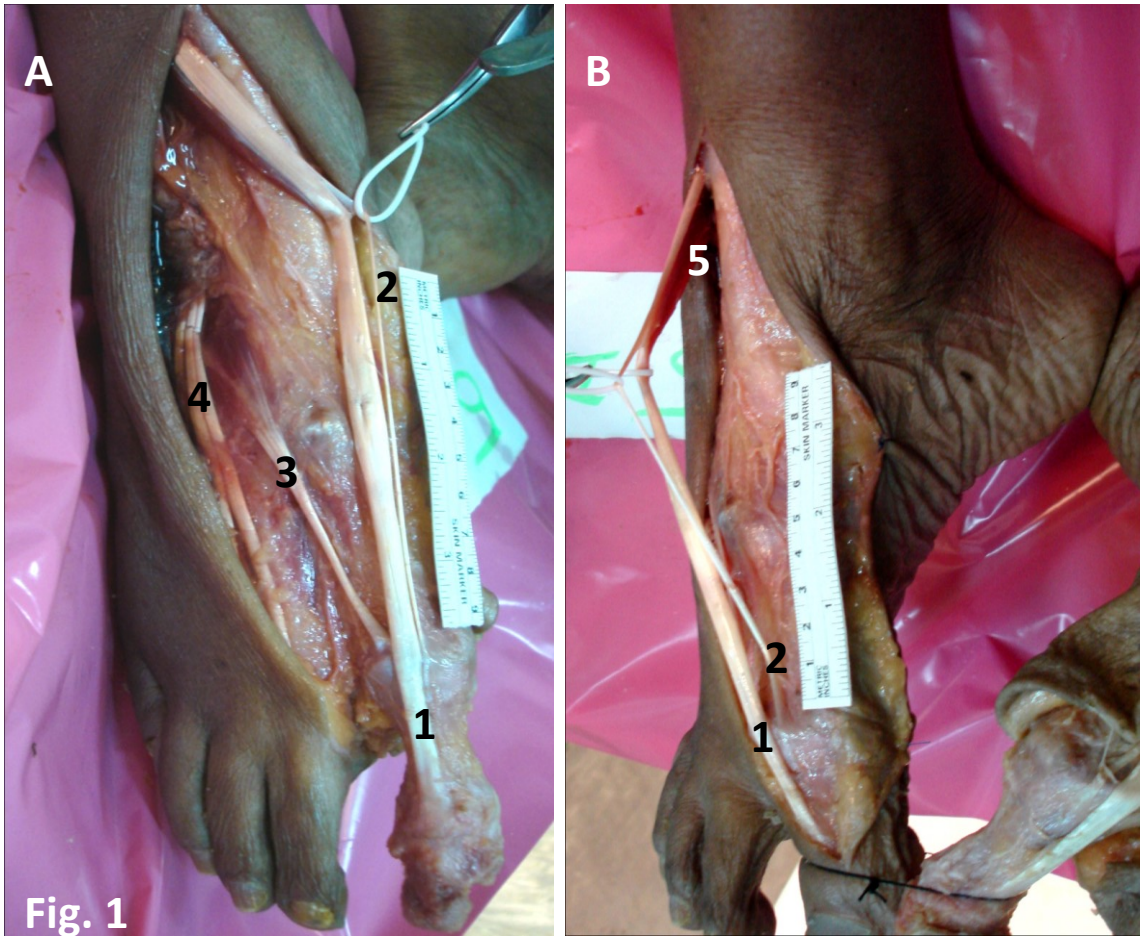

Figure 1 - Dorsal (A) and medial (B) views of the right foot showing the extensor tendons of the hallux.

1- Extensor hallucis longus tendon; 2- Accessory extensor hallucis longus tendon; 3- Extensor hallucis brevis tendon; 4- Extensor digitorum longus tendons; 5- Common muscle belly of the extensor hallucis longus muscle giving off the extensor hallucis longus tendon and its accessory tendon.

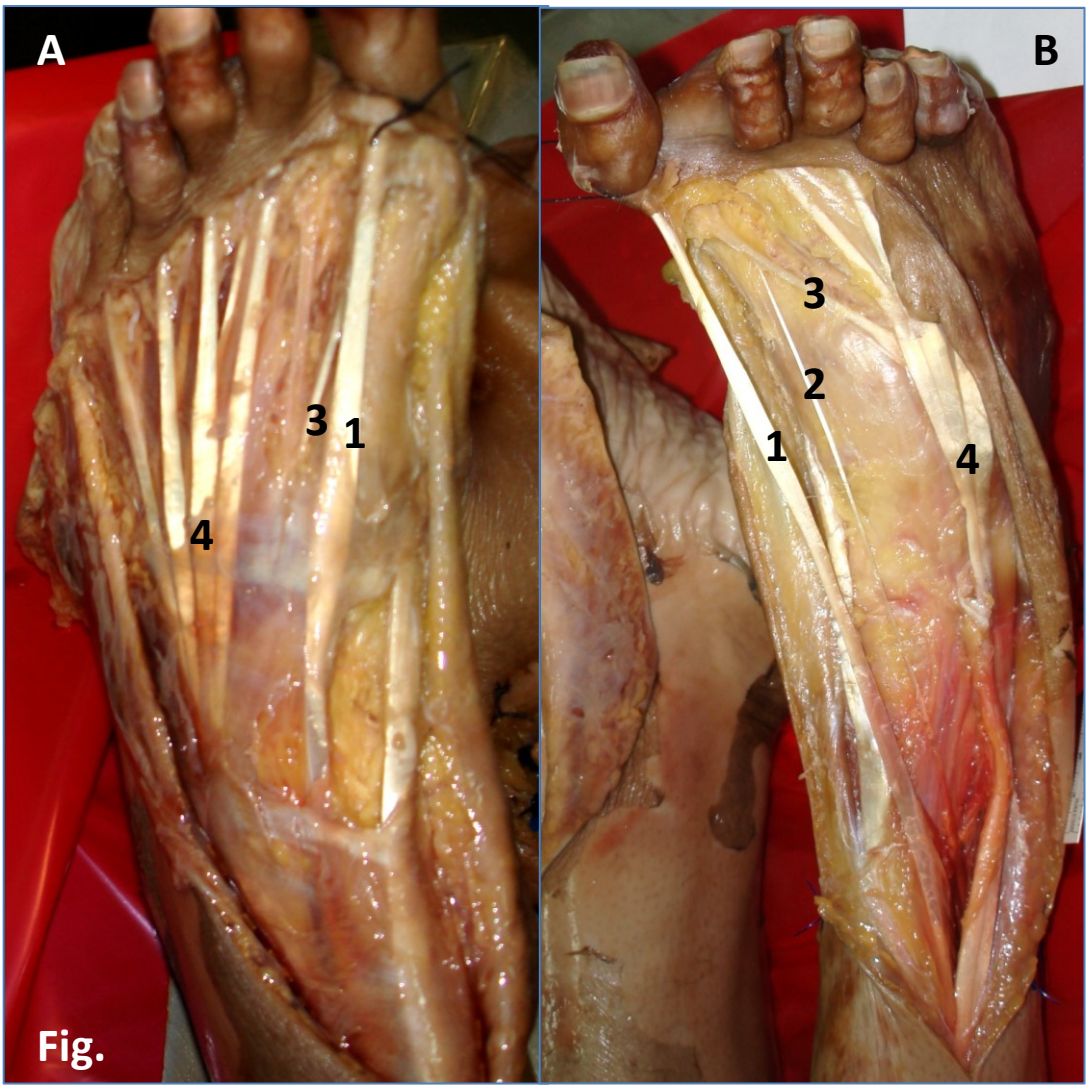

Figure 2 - Dorsal view of the left (A) and right (B) feet in two different cadavers, showing anatomical variations in the extensor tendons of the hallux. In Figure 2A there is no accessory extensor hallucis longus tendon. In Figure 2B the accessory extensor hallucis longus tendon is placed laterally to the main extensor hallucis longus tendon and fuses with the extensor hallucis brevis tendon.

1- Extensor hallucis longus tendon; 2- Accessory extensor hallucis longus tendon; 3- Extensor hallucis brevis tendon; 4- Extensor digitorum longus tendons.

Table 1 summarizes the results obtained globally, as well as those obtained after stratifying for sex and height. The EHLa mean width (0,3 ± 0,1 cm) was significantly lower

than that of the EHLp (1,0 ± 0,2 cm), corresponding to approximately one third. However, in one cadaver this EHLa had a mean width of 0,5 mm bilaterally, that is to say half of the mean width of the EHLp itself in that case. There were no statistically significant differences between tendons' length and width in the right and left sides.

			<1,75 m in Height (n=13)		>1,75 m in Height (n=13)		Overall n=26
			Male n=3	Female n=10	Male n=11	Female n=2	
EHLp	Length (cm)		24,5 ± 1,3 [23,5-26,0]	23,6 ± 0,6 [23,0-24,5]	26,5 ± 1,1 [25,0-28,0]	23,5 ± 0,1 [23,4-23,6]	24,9 ± 1,7 [23,0-28,0]
	Mean Width (cm)		0,9 ± 0,1 [0,8-1,1]	0,9 ± 0,1 [0,8-1,1]	1,1 ± 0,2 [0,7-1,3]	1,0 ± 0,1 [0,9-1,1]	1,0 ± 0,2 [0,7-1,3]
EHLa	Frequency		100%	90%	90,9%	100%	92,3% (24/26)
	Length (cm)		22,3 ± 1,9 [21,0-24,5]	21,4 ± 0,6 [21,0-22,5]	23,9 ± 0,7 [23,0-25,0]	22,0 ± 0,0 [22,0-22,1]	22,6 ± 1,4 [21,0-25,0]
	Mean Width (cm)		0,2 ± 0,0 [0,2-0,3]	0,3 ± 0,1 [0,2-0,4]	0,3 ± 0,1 [0,2-0,5]	0,3 ± 0,0 (0,3)	0,3 ± 0,1 [0,2-0,5]
	Position relatively to EHLp when present	Medial	100%	100%.	80%	100%	91,7%
		Lateral	0%	0%	20%	0%	8,3%
EHB	Length (cm)		10,3 ± 0,8 [9,5-11,0]	10,1 ± 0,7 [9,0-11,0]	10,9 ± 0,2 [10,5-11,0]	10,0 ± 0,1 [9,9-10,1]	10,5 ± 0,6 [9,0-11,0]
	Mean Width (cm)		0,5 ± 0,1 [0,4-0,5]	0,4 ± 0,1 [0,4-0,6]	0,5 ± 0,1 [0,4-0,6]	0,4 ± 0,1 [0,4-0,6]	0,5 ± 0,1 [0,4-0,6]
Pattern of Insertion	I		0%	0%	9,1%	0%	3,8% (1/26)
	II		100%	90%	90,9%	100%	92,3% (24/26)

	III	**0%**	**10%**	**0%**	**0%**	**3,8% (1/26)**
Frequency of Hallux Valgus		**100%**	**60%**	**27,3%**	**100%**	**42,3%**

Table 1 - Morphometric features of the extensor tendons of the hallux in 26 feet[35].

EHLp- extensor hallux longus proprius tendon; **EHLa** - extensor hallux longus accessorius tendon; **EHB** - extensor hallux brevis tendon. Pattern of insertion of the extensor apparatus is divided in three classes according to Al-sagaff (Al-saggaf 2003). Values between [ ] represent the limits of variation of each variable.

EHB mean length was 10,5 ± 0,6 cm, and its mean width was 0,5 ± 0,1 cm, that is to say, half of the EHLp. The average thickness of the EHLp, EHLa, and of the EHB were remarkably constant, being approximately 3-4 mm, 0,5-1 mm, and 1-2 mm, respectively.

The EHB terminated in the dorsal and medial aspect of the base of the proximal phalanx of the hallux in all cases. The pattern of insertion of the EHLp and the EHLa, on the other hand, was variable. In the majority of cases (92,3%), the tendons terminated separately: the EHLp in the base of the distal phalanx of the hallux, and the EHLa in the medial aspect of the dorsum of the base of the proximal phalanx of the big toe. In the one cadaver in which there was no EHLa, the EHLp terminated in the usual fashion in the base of the distal phalanx. In one case in which there were two EHLa, these two tendons and the EHLp terminated isolatedly in the base of the proximal and distal phalanx, respectively. Therefore, following Al-Sagaff classification of the insertion of the extensors of the hallux, type I pattern was found in 92,4% of cases, whereas patterns I and III were found in 3,8% each [21].

Hallux valgus was more frequent in females (72,7%) than in males (27,3%), being this difference statistically significant (p=0,02). No other associations between the presence of hallux valgus and other parameters, namely type of insertion, was found.

DISCUSSION

The composition of the extensor tendons of the hallux in our series didn't differ significantly from what has been described in the literature, except for the prevalence of EHLa, which was 92,3% in our series, that is to say, much higher than that originally by Kaneff and Al-Sagaff, who reported a value of 48,88% and 35%, respectively [15,21]. However, our value is not significantly higher than that described recently by other authors, who described an EHLa in 70-87% of cases [13,18,20,28]. It is plausible that the differences found between different authors may be due to populational differences. However, given that our series of 26 specimens is relatively small (**Table 2**), we believe that further studies are warranted to test this hypothesis.

Author(s)	Number of specimens studied
(Sarrafian and Topouzian, 1969)	30
(Kaneff, 1986)	151
(Denk et al., 2002)	63
(Al-saggaf, 2003)	60
(Bibbo et al., 2004)	32
(Boyd et al., 2006)	81
(Aktekin et al., 2008)	90

Table 2 - Sample sizes of the largest studies on the extensor hallux tendons published in the last 40 years[35-41].

Al-saggaf postulated that the presence of a supernumerary tendon of the extensor hallucis longus could be a predisposing factor for the development of hallux valgus [21]. However, this association was not replicated in subsequent investigations [19]. Similarly, we also failed to identify any statistical significant association between the presence of EHLa or any other morphometric feature and the presence of hallux valgus.

We found several anatomical variations regarding the EHLa. In 7,7% of cases this supernumerary tendon was absent. In addition, although it was almost always placed medially to the EHLp (91,7%) it could also be placed lateral to it (8,3%). Interestingly, in one case, the EHLa was placed laterally to the EHLp and terminated in the medial portion of the EHB, that in turn terminated in the usual fashion, in the dorsal and medial aspect of the base of the proximal phalanx of the hallux. This variation was described for the first time recently by Denk and Oznur et al., and corresponds, as far as the authors know, to the second case reported in the literature [18].

Interestingly, by performing a morphometric analysis of the extensor tendons of the hallux, we observed that the EHLa and the EHB had, on average, a width that was one third and one half of that of the EHLp, respectively. This observation was not mentioned in the literature review we conducted, and may be of great interest to a better understanding of the functional aspects of the foot and their correlation with clinical findings. This knowledge could, for example, help explain why conservative treatment may suffice in a substantial number of cases of EHLp section or rupture, as the EHB and the EHLa will probably maintain the cut ends of the EHLp tendon close together, allowing tendon repair to occur spontaneously and avoiding the need for surgery [29].

In addition, this study unequivocally suggests that the relatively large width and thickness of the EHB, as well as its significant length and constancy, make EHB an excellent candidate as a source of tendon grafts. Moreover, this tendon fulfills all the other criteria currently accepted for donor tendons for tendon or ligament repair, namely: it isn't placed too deeply, in order to facilitate harvesting; no significant donor site loss would result from its harvesting; and its cross sectional diameter is not too large to hamper revascularization, while still being sufficient to provide enough autologus material for reconstruction [7]. Another potential advantage of using this tendon as a graft would be that the surgical incision that would be necessary to harvest it would be placed in the dorsum of the forefoot, which corresponds to a place of the body where wounds usually heal inconspicuously and where scars are not easily visible [30]. This is a major advantage relatively to other donor sites, like the forearm and the leg, where scars are frequently more noticeable [30].

Functionally, there is strong evidence to suggest that harvesting this tendon wouldn't result in any significant clinical deficit, as the tendon is, for example, routinely incorporated in the dorsalis pedis flap without any resulting impairment of the extension of the hallux [31]. In fact, it is unanimously accepted that the EHB main function is only to aid the EHLp in extending the great toe at the metatarso-phalangeal joint [25].

Additionally, the EHB compares favorably to the tendons commonly used in clinical practice in terms of certain anatomical characteristics. The palmaris longus tendon, for example, which is the most commonly used donor tendon in Hand Surgery[7], is only a slighter longer (10 to 12 cm), and has a similar width and thickness: 3-5 mm and 1-2 mm, respectively [32]. Moreover, whereas the EHB is generally considered to be

constant, the palmaris longus muscle is known to be absent in up to 12 to 25% of the limbs [7,25,33]. The plantaris tendon, which is also commonly used in reconstructive procedures, is also absent in 18% of limbs [7].

In spite of all these potential advantages, the use of the EHB has been overlooked as a potential tendon donor site in Reconstructive Surgery [7,8,26,33]. We believe this is quite unfortunate, as the EHB would be particularly well suited to: repair torn ligaments of the hand, like the collateral ligaments of the metacarpal-phalangeal joint of the thumb [4]; to reconstruct the A2 and A4 pulleys associated with the flexor tendons of the hand [34]; and, eventually, in some facial reconstructive procedures, to contribute to soft tissue suspension [3]. This proposal, if implemented, would increase the supply of autologous donor tissue for reconstructive procedures, thereby enhancing the surgeon's armamentarium.

ACKNOWLEDGEMENTS

The authors appreciate the proficiency of all Technical Staff members of the Department of Anatomy, in particular that of Mr. Carlos Lopes and of Mr. Marco Costa.

References

1. Wehbe MA. Tendon graft anatomy and harvesting. Orthop Rev 1994;23:253-6.

2. Schenk S, Meizer R, Kramer R, Aigner N, Landsiedl F, Steinboeck G. Resection arthroplasty with and without capsular interposition for treatment of severe hallux rigidus. Int Orthop 2009;33:145-50.

3. Terzis JK, Kyere SA. Minitendon graft transfer for suspension of the paralyzed lower eyelid: our experience. Plast Reconstr Surg 2008;121:1206-16.

4. Breek JC, Tan AM, van Thiel TP, Daantje CR. Free tendon grafting to repair the metacarpophalangeal joint of the thumb. Surgical techniques and a review of 70 patients. J Bone Joint Surg Br 1989;71:383-7.

5. Shuhaiber JH, Shuhaiber HH. Plantaris tendon graft for atrioventricular valve repair: a novel hypothetical technique. Tex Heart Inst J 2003;30:42-4; discussion 4.

6. Brand PW. Tendon grafting. THE JOURNAL OF BONE AND JOINT SURGERY 1961;43B:444-53.

7. Williamson DG, Richards RS. Flexor tendon injuries and reconstruction. In: Mathes SJ, ed. Plastic Surgery. Philadelphia: Saunders; 2006:383-6.

8. Tang JB. Flexor tendons. In: Chung KC, Disa JJ, Gosain AK, Kinney BM, Rubin JP, eds. Plastic Surgery: Indications and Practice. 1st ed. China: Saunders; 2009:1124-5.

9. Macalister A. Additional observations on muscular anomalies in human anatomy. Trans R Ir Acad Sci 1875;25:1-130.

10. Gray H. Anatomy of the Human Body. Philadelphia

Lea & Febiger; 1918.

11. Gruber W. Über die Varietäten des Musculus extensor hallucis longus. Arch Anat Physiol Wissen Med 1875:565-89.

12. Sarrafian SK, Topouzian LK. Anatomy and physiology of the extensor apparatus of the toes. J Bone Joint Surg Am 1969;51:669-79.

13. Tate R, Pachnik RL. The accessory tendon of extensor hallucis longus: its occurrence and function. J Am Podiatry Assoc 1976;66:899-907.

14. Kaneff A. Die Aufrichtung des Menschen und die morphologische Evolution der Musculi extensores digitorum pedis unter dem Gesichtspunkt der evolutiven Myologie. Teil I. Gegenbaurs Morphol Jahrb 1986;132:375-419.

15. Kaneff A. Die Aufrichtung des Menschen und die morphologische Evolution der Musculi extensores digitorum pedis unter dem Gesichtspunkt der evolutiven Myologie. Teil III. Gegenbaurs Morphol Jahrb 1986;132:681-722.

16. Kaneff A, Andreev D. Über die organogenetische Entwicklung des M. extensor hallucis longus beim Menschen. Anat Anz 1983;154:237–44.

17. Kaneff A, Stephanoff A. Vergleichend-anatomische Untersuchung des M. extensor hallucis longus beim Menschen. Gegenbaurs Morphol Jahrb 1982;128:690–701.

18. Denk CC, Oznur A, Surucu HS. Double tendons at the distal attachment of the extensor hallucis longus muscle. Surg Radiol Anat 2002;24:50-2.

19. Bibbo C, Arangio G, Patel DV. The accessory extensor tendon of the first metatarsophalangeal joint. Foot Ankle Int 2004;25:387-90.

20. Hill RV, Gerges L. Unusual accessory tendon connecting the hallucal extensors. Anat Sci Int 2008;83:298-300.

21. Al-saggaf S. Variations in the insertion of the extensor hallucis longus muscle. Folia Morphol (Warsz) 2003;62:147-55.

22. Bergman RA, Afifi AK, Miyauchi R. Illustrated encyclopedia of human anatomic variations.

23. Boyd N, Brock H, Meier A, Miller R, Mlady G, Firoozbakhsh K. Extensor hallucis capsularis: frequency and identification on MRI. Foot Ankle Int 2006;27:181-4.

24. Aktekin M, Uzmansel D, Kurtoglu Z, Sanli EC, Kara AB. Examination of the accessory tendons of extensor hallucis longus muscle in fetuses. Clin Anat 2008;21:713-7.

25. Moore KL, Dalley AF. Lower Limb. Clinically Oriented Anatomy. 5th ed. Philadelphia: Lippincott Williams and Wilkins; 2006:554-724.

26. Chang P. Repair and grafting of tendon. In: Mathes SJ, ed. Plastic Surgery. 2nd ed. Philadelphia: Saunders; 2006:599.

27. Prosche H, Fuhrmann R, Linb W, Fröber R. The postoperative stability of the first metatarsal. Eur J Anat 2004;8:55-9.

28. Bibbo C, Anderson RB, Davis WH. Injury characteristics and the clinical outcome of subtalar dislocations: a clinical and radiographic analysis of 25 cases. Foot Ankle Int 2003;24:158-63.

29. Scaduto AA, Cracchiolo A, 3rd. Lacerations and ruptures of the flexor or extensor hallucis longus tendons. Foot Ankle Clin 2000;5:725-36, x.

30. Parkhouse N, Cubison TCS, Humzah MD. Scar Revision. In: Mathes SJ, Hentz VR, eds. Plastic Surgery. 2nd ed. Philadelphia: Saunders; 2006:235-67.

31. Furlow LT. Dorsalis Pedis Flap. In: Strauch B, Vasconez LO, Hall-Findlay EJ, Lee BT, eds. Encyclopedia of Flaps. 3rd ed. Philadelphia: Lippincott Williams and Wilkins; 2009:1483-8.

32. Chui DTW, Edgerton BW. Repair and grafting of tendon. In: McCarthy JG, ed. Plastic Surgery. 1st ed. Philadelphia: Saunders; 1990:527-45.

33. Neumeister MW, Wilhelmi BJ. Flexor Tendon Repair. In: McCarthy JG, Galiano RD, Boutros SG, eds. Current Therapy in Plastic Surgery. 1st ed. Philadelphia: Saunders; 2006:525-30.

34. Pederson WC, Stevanovic M, Zalavras CL, Sherman R. Reconstructive Surgery: Extensive Surgery to the Upper Limb. In: Mathes SJ, ed. Plastic Surgery. 2nd ed. Philadelphia: Saunders; 2006:322.

35. Al-saggaf, S. (2003). "Variations in the insertion of the extensor hallucis longus muscle." Folia Morphol (Warsz) 62(2): 147-155.

36. Aktekin, M., Uzmansel, D., Kurtoglu, Z., Sanli, E. C., Kara, A. B. 2008. Examination of the accessory tendons of extensor hallucis longus muscle in fetuses. Clin Anat, 21, 713-7.

37. Bibbo, C., Arangio, G., Patel, D. V. 2004. The accessory extensor tendon of the first metatarsophalangeal joint. Foot Ankle Int, 25, 387-90.

38. Boyd, N., Brock, H., Meier, A., Miller, R., Mlady, G. & Firoozbakhsh, K. 2006. Extensor hallucis capsularis: frequency and identification on MRI. Foot Ankle Int, 27, 181-4.

39. Denk, C. C., Oznur, A., Surucu, H. S. 2002. Double tendons at the distal attachment of the extensor hallucis longus muscle. Surg Radiol Anat, 24, 50-2.

40. Kaneff, A. 1986. Die Aufrichtung des Menschen und die morphologische Evolution der Musculi extensores digitorum pedis unter dem Gesichtspunkt der evolutiven Myologie. Teil III. Gegenbaurs Morphol Jahrb, 132, 681-722.

41. Sarrafian, S. K., Topouzian, L. K. 1969. Anatomy and physiology of the extensor apparatus of the toes. J Bone Joint Surg Am, 51, 669-79.

Chapter 13

RECONSTRUCTION OF A LONG DEFECT OF THE ULNAR ARTERY AND NERVE WITH AN ARTERIALIZED NEUROVENOUS FREE FLAP IN A TEENAGER: A CASE REPORT AND LITERATURE REVIEW

Authors: Diogo Casal, M.D.[1,2]; Diogo Pais, M.D., PhD[1,2]; Eduarda Mota-Silva[3], M.Sci.; Giovanni Pelliccia, M.D. [1;2]; Inês Iria, M.Sci.[4]; Paula A. Videira, M.Sci., PhD[5]; Maria Manuel Mendes, M.D.[1]; João Goyri-O'Neill, M.D., PhD[2]; Maria Manuel Mouzinho, M.D.[1]

Affiliations:

1- Plastic and Reconstructive Surgery Department and Burn Unit; Centro Hospitalar de Lisboa Central, Lisbon, Portugal

2- Anatomy Department; NOVA Medical School, Universidade NOVA de Lisboa, Lisbon, Portugal

3- LIBPhys, Physics Department, Faculdade de Ciências e Tecnologia, Caparica, Portugal

4- Molecular Microbiology and Biotechnology Unit|Drug Discovery Area; Faculdade de Farmácia, Universidade de Lisboa, Portugal

5- UCIBIO, Life Sciences Department, Faculdade de Ciências e Tecnologia, Universidade NOVA de Lisboa, Caparica, Portugal

ABSTRACT

There is evidence that nerve flaps are superior to nerve grafts for bridging long nerve defects. Moreover, arterialized neurovenous flaps (**ANVFs**) have multiple potential advantages over traditional nerve flaps in this context. This paper describes a case of reconstruction of a long defect of the ulnar artery and nerve with an arterialized neurovenous free flap and presents a literature review on this subject.

A 16-year-old boy sustained a stab wound injury to the medial aspect of the distal third of his right forearm. The patient was initially observed and treated at another institution where he was diagnosed with a flexor carpis ulnaris muscle and an ulnar artery section. The artery was ligated and the muscle was sutured. Four months later, the patient was referred to our institution with complaints of ulnar nerve damage, as well as hand pain and cold intolerance. Physical examination and ancillary tests supported the diagnosis of ulnar artery and nerve complete section. Surgery revealed an 8-cm hiatus of the ulnar artery and a 5-cm defect of the ulnar nerve. These gaps were bridged with a flow through ANVF containing the sural nerve and the lesser saphenous vein. The postoperative course was uneventful. Two years postoperatively, the patient had regained normal trophism and M5 strength in all previously paralyzed muscles according to the Medical Research Council Scale. Thermography revealed good perfusion in the right ulnar angiosome.

The ANVF may be an expedite, safe and efficient option to reconstruct a long ulnar nerve and artery defect.

INTRODUCTION

Vascular and nerve injuries to the upper limb are relatively frequent.[1-5] However, functional results after peripheral nerve repair are far from perfect, especially for late repairs or in cases of long nerve defects.[1,5,6] This, in turn, often results in permanent and significant social and economic devaluation of those affected.[3,6-8]

There is mounting experimental and clinical evidence that nerve flaps are superior to nerve grafts for bridging long nerve defects.[5,9] In fact, nerve flaps, having a blood supply of their own since the moment of nerve transfer, are less prone to central necrosis, fibrosis and histological disorganization compared to nerve grafts, which depend initially on diffusion and subsequently on neoangiogenesis for survival.[5,10-13]

Most literature refers to "conventional nerve flaps" (**CNFs**), that is to say to nerve segments pedicled on a given arterial and venous pedicle. However, CNFs entail laborious dissections, and sometimes cannot be raised due to local anatomical constraints.[14] To circumvent these limitations, in 1984, Townsend and Taylor suggested a new way of transferring nerve segments pedicled exclusively on their accompanying veins. In these nerve flaps, at least one of the veins was connected to a recipient site's artery, whereas at least one of the other veins drained the flap's venous blood. These flaps were named "arterialized neurovenous flaps" (**ANVFs**).[15] However, since then, ANVFs have been reported clinically only a few times in case reports or small case series.[16]

In this paper, the authors describe a case report in which deferred reconstruction of a composite long arterial and nervous defect was performed with an ANVF in a teenage boy with an excellent functional outcome. Furthermore, the authors conducted a literature review on the use of ANVFs employed in the reconstruction of

similar defects.

CASE REPORT

A 16-year-old right-handed Portuguese teenage boy sustained a broken glass injury to the medial aspect of the distal third of his right forearm when the patient was inadvertently pushed against a window at school. The patient was initially observed and treated at another institution where the patient was diagnosed with a flexor carpis ulnaris muscle and an ulnar artery section. The artery was ligated and the muscle was sutured with horizontal 3/0 Vicryl® mattress sutures.

Four months later, the patient was referred to our institution for observation in the Plastic and Reconstructive Surgery outpatient clinic. The patient complained of hypoesthesia and paresthesia in the territory of the right ulnar nerve. Moreover, the patient referred exertional pain, as well as cold intolerance in the affected hand. Physical examination, revealed an ulnar claw, with paralysis and wasting of the intrinsic hand muscles dependent on the ulnar nerve (**Fig. 1**). Allen's test revealed a poorly perfused hand when pressing the radial artery at wrist level. Electroneuromyography was consistent with chronic ulnar neurotmesis at the distal forearm.

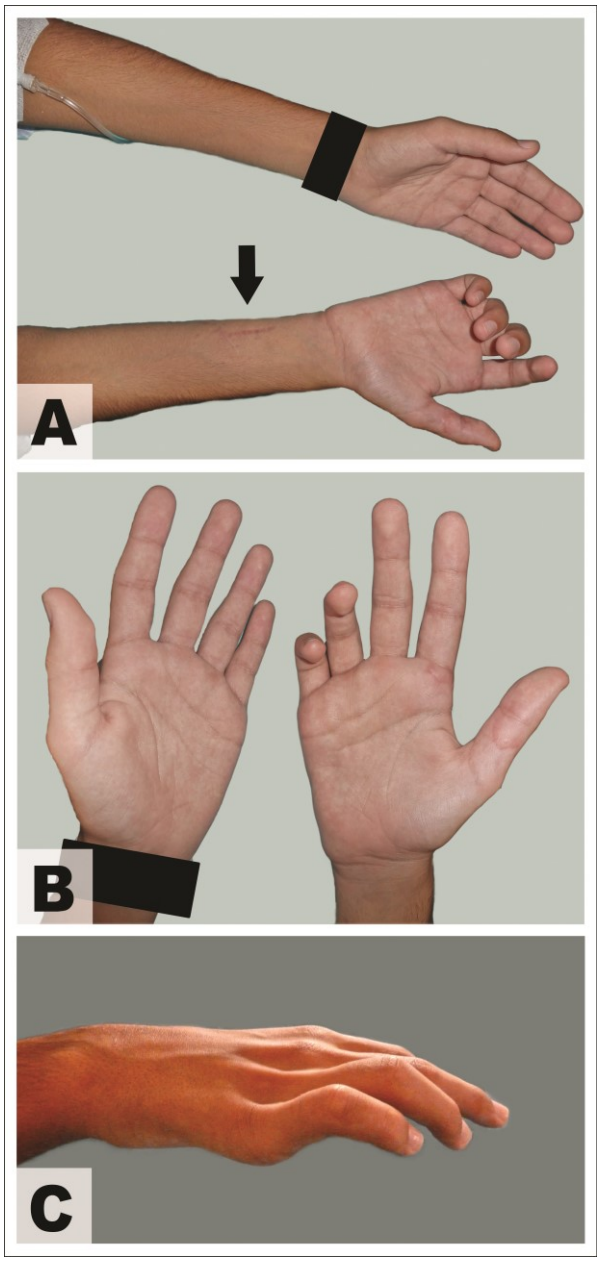

Figure 1 - Photographs showing the preoperative appearance.

A. A scar in the medial aspect of the distal third of the right forearm was visible (arrow) corresponding to the site of injury.

B. Comparison of the hands showed marked atrophy of the right hand intrinsic muscles, particularly in the medial palmar region.

C. An ulnar claw was evident due to atrophy of the intrinsic muscles supplied by the ulnar nerve.

Surgical exploration of the lesion under tourniquet control, revealed interruption of the ulnar nerve and artery (**Fig. 2A**). After debriding the fibrous tissue

and removing the proximal stump's neuroma using surgical magnifying loops, there was an 8-cm hiatus of the ulnar artery and a 5-cm defect of the ulnar nerve (**Fig. 2A**).

These gaps were bridged with a flow through ANVF raised from the left lower leg (**Fig 2B**). This flap was composed of the sural nerve and of the lesser saphenous vein (**Fig. 2C**). The flap comprised two branches of the sural nerve that were used to reconstruct the ulnar nerve according to its internal topographical anatomy at the distal forearm level (**Figs. 2D** and **Fig. 3**). It was assumed that the motor component is medially placed whereas the sensory component is in the lateral aspect of the nerve.[9,17] The ulnar artery hiatus was reconstructed with an inverted segment of the lesser saphenous vein included in the flap. Hence, blood flow in the ANVF was orthodromic. Vascular and neural anastomoses were performed with interrupted 9/0 Nylon stitches under the operating microscope.

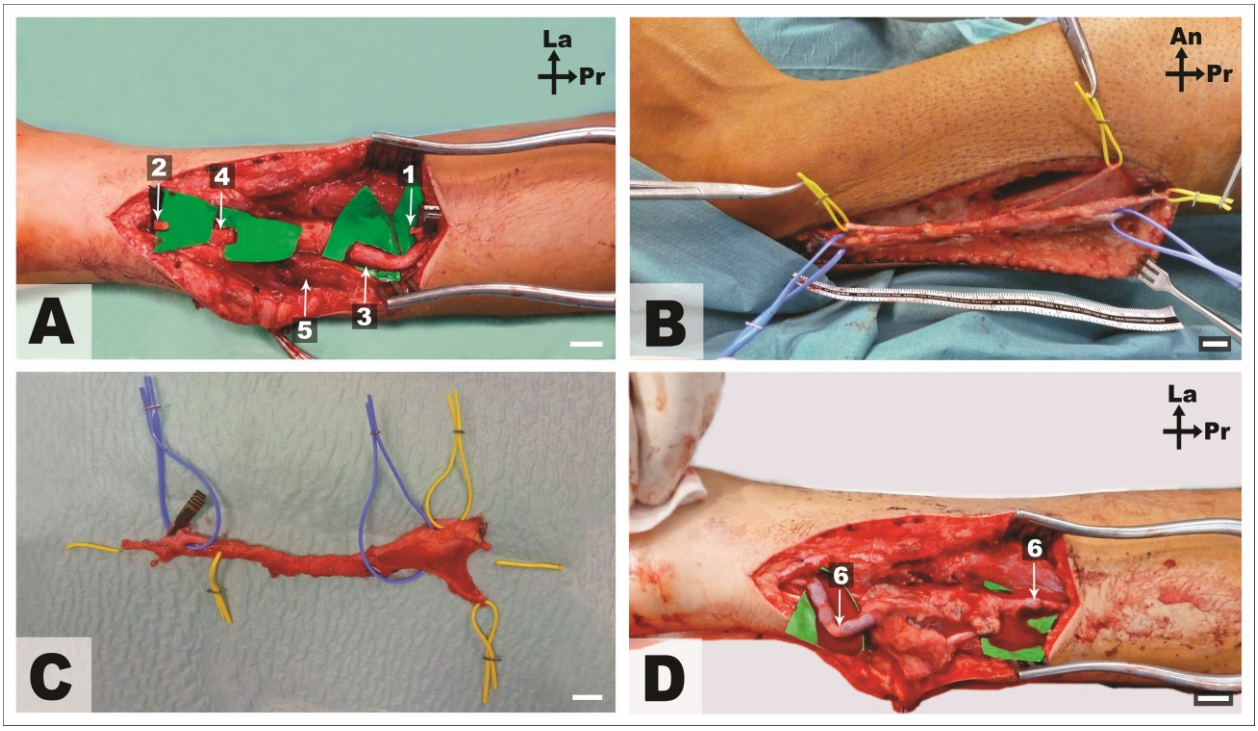

Figure 2 - Photographs of the surgery.

Scale bar = 1 cm

Pr, Proximal; **Lat**, Lateral; **An**, Anterior

1, Proximal stump of the ulnar artery; 2, Distal stump of the ulnar artery; 3, Proximal stump of the ulnar nerve; 4, Distal stump of the ulnar nerve; 5, Flexor carpis ulnaris muscle.

The yellow vessel loops were placed around two terminal branches of the sural nerve. The blue vessel loops were placed around the lesser saphenous vein.

A, Intraoperative view of the ulnar neurovascular bundle after removing the fibrotic tissue and the proximal stump neuroma; B, View of the lesser saphenous/sural neurovenous flap *in situ* after dissection; C, Detailed *ex vivo* view of the lesser saphenous/sural neurovenous flap prior to insetting into the defect; D, View of the arterialized neurovenous flap after insetting the flap and performing the neural and vascular anastomoses.

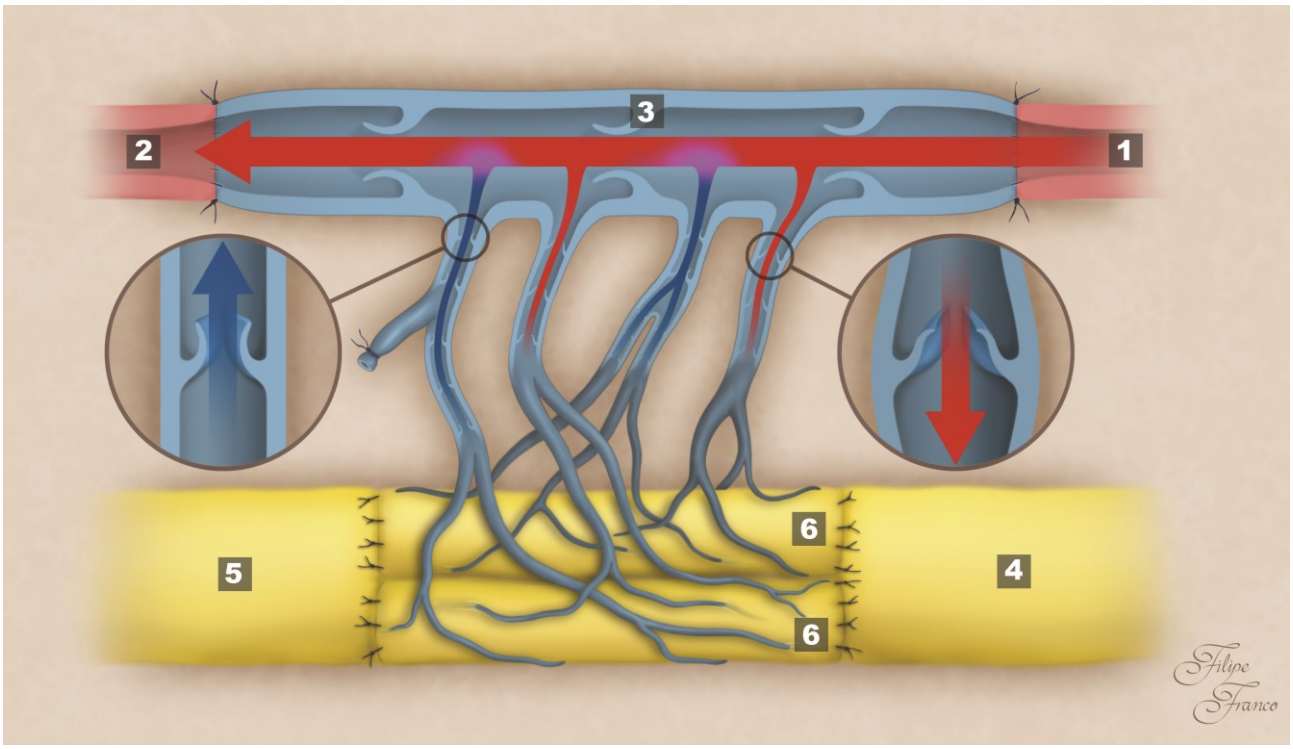

Figure 3 - Schematic representation of the composition and vascular architecture of the lesser saphenous/sural neurovenous flap used to bridge the long arterial and nerve defect. The arrows indicate the direction of blood flow.

1, Proximal segment of the ulnar artery; 2, Distal segment of the ulnar artery; 3, Lesser saphenous vein in an inverted position used to bridge the vascular gap; 4, Proximal stump of the ulnar nerve; 5, Distal stump of the ulnar nerve; 6, Sural nerve cables used for the somatotopic reconstruction of the ulnar nerve.

In the flap's donor zone, the proximal stump of the sural nerve was stitched with a 6⁄0 Nylon suture to the belly of the lateral gastrocnemius muscle after creating a small window in the muscle fascia. The surgical wounds were closed in anatomical layers. The surgery's duration was 242 minutes.

After surgery, the patient's wrist was splinted for 15 days to prevent maximal extension and thus excessive tension on the vascular and nerve repairs. The patient was allowed to ambulate and freely use the patient's fingers immediately after surgery. The patient was discharged home 3 days after surgery. Postoperatively, the patient underwent an intensive physiotherapy program for one year. The patient was followed regularly at the outpatient clinic for 2 years. Five months after surgery, Tinel's sign could be observed at the wrist level. Intrinsic muscles innervated by the ulnar nerve started to show voluntary contraction at 8 months post-operatively. The patient referred gain of sensibility in the ulnar aspect of his hand 6 months after the surgical procedure. At the last follow up visit, the patient had regained normal trophism and M5 strength in all previously paralyzed muscles according to the Medical Research Council Scale, i.e. muscle strength was no different from that observed in the opposite side (**Figs. 4A, 4C** and **4D**). Furthermore, according to this scale, his sensory recovery was S3 in the territory of the ulnar nerve, i.e. return of superficial cutaneous pain and tactile sensibility without over-response.[18] Two years after the last surgery, two-point discrimination in the hypothenar region was 5 mm and 7 mm in the palmar aspect of the fifth finger. At this time, the patient presented a relatively inconspicuous scar in the donor zone, as well as absence of limb edema (**Fig. 4E**).

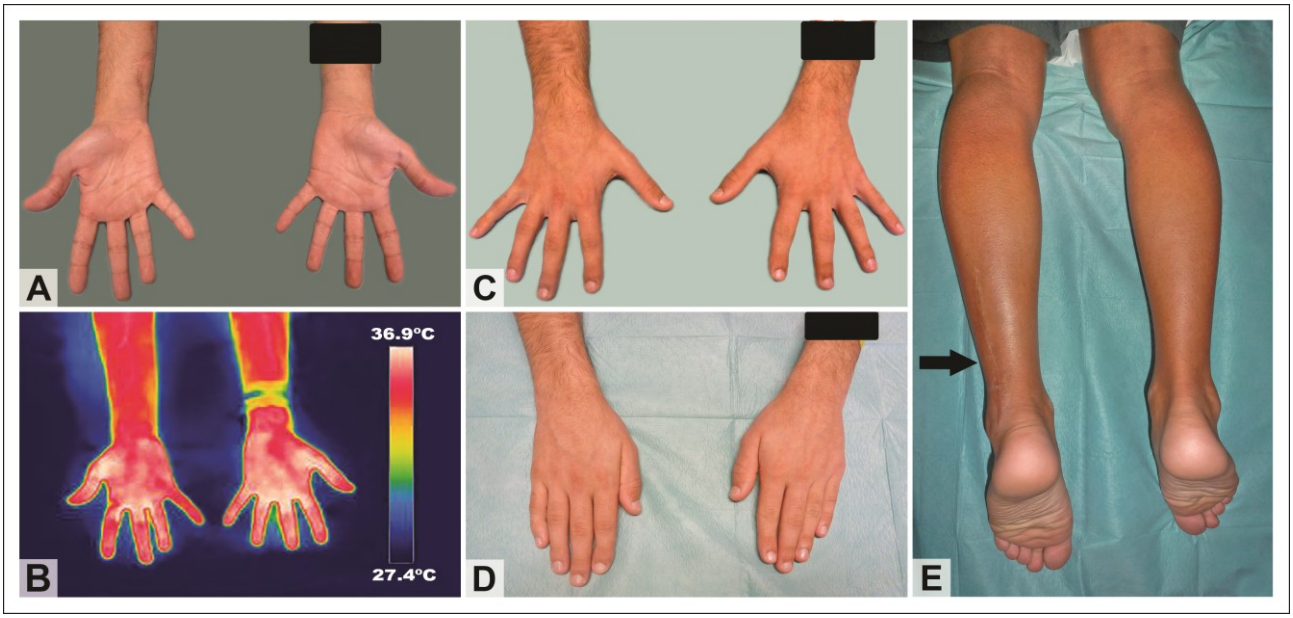

Figure 4 - Appearance of the recipient and donor zones two years after surgery.

A. Anterior view of the distal aspect of the upper limbs showed no evidence of atrophy of hand muscles.

B. Infra-red thermography of the anterior aspect of the forearms and hands showed good perfusion of the ulnar aspect of the right hand.

C. Posterior view of the forearms and hands showed absence of ulnar claw in the right hand, as well as good finger abduction.

D. Posterior view of the hands demonstrated adequate finger adduction.

E. Posterior view of the lower legs and feet showed a relatively inconspicuous scar in the donor zone (arrow), as well as absence of limb edema.

Since the last surgery, the patient denied either cold intolerance or exertional fatigue in the affected hand. Two years after this surgery, thermographic examination of the upper limbs was performed with a FLIR® E6 camera placed 25 cm above the hands.[19] This exam revealed a symmetrical pattern with good perfusion throughout, including in the territory of the right ulnar angiosome (**Fig. 4A**).

Two years after the last surgery, electroneuromyography confirmed reinnervation in the territory of the ulnar nerve.

DISCUSSION

Oddly, although potentially advantageous, the reconstruction of nerve defects using ANVFs is rarely mentioned in the literature (**Table 1**).[16] Townsend *et al* pioneered this field in 1984 with a seminal paper describing 13 lower limb cadaveric dissections, an histological study in the greyhound dog comparing axonal elongation in nerve grafts and ANVFs, and 7 clinical cases.[15] In this series, 5 combined nerve and arterial defects of the upper limb and 2 facial nerve lesions were successfully reconstructed using ANVFs.[15] The next year, Gu *et al* described 14 clinical cases in which upper limb nerve defects over 10 cm in length associated with vascular injuries were reconstructed using ANVFs.[20] Most of these patients presented good results, although there were 2 vascular thrombosis of the ANVFs and there were 2 cases of absence of neurological recovery in patients with longstanding lesions.[20] Since 1989, there were multiple papers describing the simultaneous reconstruction of nerve and skin defects using ANVFs associated with a skin paddle.[16,21-23] In that same year, Rose *et al* presented a series of 14 ANVFs fabricated from the medial fibular nerve and from the dorsalis pedis venae comitantes that were effectively used to bridge digital nerve defects associated with significant local fibrosis.[24]

Author	Year	n	Age (years)		M:F	Defect location	Defect origin	Flap(s) donor site(s)	Flap composition
			mean	min-max					
Townsend [15]	1984	7	33.2	20-54	4:3	HN; F; HF	Tu; B; Tr	L	Sne
Gu [21]	1985	14	30.8	20-54	10:4	F	Tr	L	Sne
Gu [22]	1989	4	29.8	17-54	3:1	F; L; HF	SC	F; L	S; sne
Rose [23]	1989	1	38	38	1:0	HF	SC	n/a	S; sne
Rose [24]	1989	14	29	18-55	9:1	HF	Tr	Ft	Sne
Karacalar [25]	1994	13	23.9	12-35	11:2	HF	n/a	F	S; st; sne
Hussman [26]	1996	69	47	n/a	n/a	HN; F; L; HF	B; CM; Tr; Tu	F; L; Ft	S; stnb; sc
Woo [27]	1996	12	36.2	18-59	11:1	HF	B; Tr; SC	F; L	S; sne
Kayikcioglu [28]	1998	8	28.4	19-41	8:0	HF	Tr	HF	S; sne
Patradul [29]	1999	10	25.3	6-47	4:5	HF	Tr	Ft	S; stnb
Takeuchi [30]	2000	2	23.5	21-26	2:0	HF	Tr	Ft	Sne
Murata [31]	2001	7	39	20-57	6:0	HF	Tr	HF	S; sne
Hussmann [32]	2003	70	47.4	7-78	n/a	HN; F; L; HF	Tu; B; Tr; CM	F; L; Ft	S; stnb; sc
Nakazawa [33]	2004	4	41	20-71	n/a	L	CM	L	S; sne
Woo [34]	2007	154	35.7	16-65	112:40	HF	B; Tr	F; L; Ft; HF	S; st; sne
Davami [35]	2012	18	30.6	15-40	18:0	HF	Tr	HF	Sne
Yan [36]	2012	27	n/a	n/a	n/a	HF	Tr	F	S; sne
Yu [37]	2012	6	24.5	n/a	5:1	HF; Ft	B; Tr	Ft	S; sne
Giesen [38]	2014	14	37.1	16-58	11:3	HF	Tu; Tr; I; O	F	S; st; sne
Liu [39]	2014	11	31	17-44	7:4	HF	Tr	F	Sne

Table 1 - Summary of the studies reporting unconventional perfusion flaps including nerves for reconstructive purposes.

Legend:

n, number of patients in each series

M, male; **F**, female

AVF, arterialized venous flap

Defect location and flap donor site: F, forearm; L, leg; Ft, foot; HN, head and neck; HF, hand and fingers; T, thigh.

Defect origin: B, burn and its sequelae; I, infection; CM, congenital malformation; SC, scar contracture; Tr, trauma; Tu, tumor; O, others.

Flap composition: nv, nerve and vein; s, skin with its appendages and subcutaneous tissue; sb, skin and bone; sc, skin and cartilage; sne, skin and nerve; st, skin and tendon; stnb, skin, tendon, nerve and bone.

Complications: AR, anastomosis revision; FTN, full thickness necrosis; I, infection; MN, marginal necrosis; SpN, superficial necrosis.

Since then, multiple papers have been published describing the use of ANVFs in virtually all anatomical regions. The largest of these series describe the use of several ANVFs to simultaneous reconstruct composite vascular and nerve defects of the upper limb, either occurring proximally at the arm level, or distally at the finger level.[25-27] Multiple variations in the composition of ANVFs were introduced, including tendon[25,28], deep fascia[29], bone[23,30] and/or the nail complex[30]. However, only a few authors have reported the use of ANVFs similar to that described in this paper for the reconstruction of arterial and nerve defects at the forearm level.[15,16,25,31] Moreover, all these reconstructions were performed in adults. Consequently, as far as the authors could determine, this is the first report of an ANVF being used to reconstruct a composite long nerve and arterial defect in a pediatric patient. One reason to justify this may be that extensive vascular and nerve damage is increasingly rare in children and teenagers in most countries.[32,33] Moreover, these lesions are frequently associated with damage to other structures, namely the integumentary system, mandating reconstruction of concomitant tissue injuries with flaps containing muscle and/or skin paddles. Finally, having an incompletely understood physiology, ANVFs are often not the first reconstructive option for most surgeons.[5,16]

Comparatively to CNFs, ANVFs, as the one used in this patient, have the significant merit of being easy to raise and tailor due to the constant proximity of superficial veins to superficial nerves.[5,13] Furthermore, the architecture of the ANVF used in this case, also allowed the simultaneous reconstruction of the ulnar artery and nerve (**Fig. 3).** The inclusion of two terminal branches of the sural nerve made possible to reconstruct the ulnar nerve in a somatotopic fashion. It is well established that in the distal aspect of the forearm, the ulnar nerve is composed of a motor branch centrally

located between the ulnarly-placed dorsal cutaneous branch and the radially-placed palmar sensory component.[17] This topographical nerve reconstruction may have played a significant role in the full recovery presented by the patient. This is stark contrast with the poor results generally observed with ulnar nerve reconstruction even in the distal portion of the upper limb.[5,13,34,35] Nevertheless, the authors must concede that one of the factors responsible for the good functional outcome was the young age of the patient.[5]

The patient presented a positive Tinnel's sign at the wrist level five months after surgery. Roughly, this corresponded to an average axonal growth of 1.3 mm/day (i.e., the fastest axons elongated around 200 mm in approximately 150 days). This value is similar to that generally reported in ideal conditions with nerve grafts and conventional nerve flaps at the patient's age.[36-38] In fact, it has been estimated that in optimal repair conditions axonal growth can occur at a speed of 1 to 3 mm per day.[36-38]

Similarly to what has been described by other authors, no significant donor site morbidity was observed in this patient.

CNFs are generally considered superior to nerve grafts for reconstructing long and thick nerve defects, particularly in regions of relative ischemia, such after radiotherapy, intense fibrosis subsequent to extensive trauma or in the particular case of prior deep burns.[5,9,13,39] However, the utility of ANVFs in these situations is still based on scarce experimental data, anecdotal case reports and small case series. The good results obtained in this case report lend support to the use of ANVFs for reconstructing long nerve defects in teenagers. Notwithstanding, further experimental and clinical studies are warranted to confirm or dismiss these findings.

Overall, this case report suggests that the arterialized sural nerve/lesser saphenous neurovenous flap may be an expedite, safe and efficient option to

reconstruct a long ulnar nerve and artery defect in the forearm of teenagers.

DECLARATIONS

Consent for publication

Written informed consent was obtained from the patient for publication of this case report and any accompanying images. A copy of the written consent is available for review by the Editor-in-Chief of this journal.

ACKNOWLEDGEMENTS

The authors are very grateful to Mr. Filipe Franco for the illustrative drawing in Figure 3.

References

1. Slutzky DJH, V.R. Peripheral Nerve Surgery: Practical Applications in the Upper Extremity. Churchill Livingstone. Elsevier. 2006.

2. Rosberg HEeLD. Epidemiology of hand injuries in a middle-sized city in southern Sweden - a retrospective study with an 8-year interval. Scand J Plast Rec Surg Hand Surg 2004(38):347-355.

3. Rosberg HE, et al. Injury to the human median and ulnar nerves nerves in the forearms - analysis of costs for treatment and rehabilitation of 69 patients in southern Sweden. J Hand Surg [Br] 2005;1(30):35-39.

4. Jabaley ME. Primary Nerve Repair. In: Peripheral Nerve Surgery: Practical Applications in the Upper Extremity. Editores: Slutsky, D.J.; Hentz, V.R. Churchill Livingstone. 2006:23-38.

5. Trehan SK, Model Z, Lee SK. Nerve Repair and Nerve Grafting. Hand clinics 2016;32(2):119-125.

6. Dahlin LB. Nerve injury and repair: from molecule to Man. In: Slutsky DJ, Hentz VR, editors. Peripheral Nerve Surgery: Practical Applications in the Upper Extremity. Philadelphia: Elsevier; 2006. p 1-22.

7. Broback LG, et al. Clinical and socio-economical aspects of hand injuries. Acta Chir Scand 1978;7-8(144):455-461.

8. Rosberg HESCDLB. Prospective analysis of costs, arm function and health status using DASH and SF36 in patients with and forearm trauma of varying severity (HISS). Scand J Plast Rec Surg Hand Surg 2004:2004.

9. Wood MJ, Johnson PJ, Myckatyn TM. Anatomy and physiology for the peripheral nerve surgeon. In: Mackinnon SE, Yee A, editors. Nerve Surgery. First ed. Volume 1. New York: Thieme; 2015. p 1-40.

10. Sinis N, Kraus A, Papagiannoulis N, Werdin F, Schittenhelm J, Meyermann R, Haerle M, Geuna S, Schaller HE. Concepts and developments in peripheral nerve surgery. Clinical neuropathology 2009;28(4):247-262.

11. Desouches C, Alluin O, Mutaftschiev N, Dousset E, Magalon G, Boucraut J, Feron F, Decherchi P. [Peripheral nerve repair: 30 centuries of scientific research]. Revue neurologique 2005;161(11):1045-1059.

12. Terzis JK, Skoulis TG, Soucacos PN. Vascularized nerve grafts. A review. International angiology : a journal of the International Union of Angiology 1995;14(3):264-277.

13. Taylor GI, Pan WR. The angiosome concept. In: Dodwell P, editor. The angiosome concept and tissue transfer. First ed. Volume 1. Florida: Quality Medical Publishing, Inc.; 2014. p 354-395.

14. Hong MK, Taylor GI. Angiosome territories of the nerves of the upper limbs. Plastic and reconstructive surgery 2006;118(1):148-160.

15. Townsend PL, Taylor GI. Vascularised nerve grafts using composite arterialised neuro-venous systems. Br J Plast Surg 1984;37(1):1-17.

16. Casal D, Cunha T, Pais D, Videira P, Coloma J, Zagalo C, Angelica-Almeida M, O'Neill JG. Systematic Review and Meta-Analysis of Unconventional Perfusion Flaps in Clinical Practice. Plastic and reconstructive surgery 2016;138(2):459-479.

17. Davidge KM, Boyd KU. Ulnar nerve entrapment and injury. In: Mackinnon SE, editor. Nerve surgery. First ed. Volume 1. New York: Thieme; 2015. p 251-288.

18. Wang Y, Sunitha M, Chung KC. How to measure outcomes of peripheral nerve surgery. Hand clinics 2013;29(3):349-361.

19. Sheena Y, Jennison T, Hardwicke JT, Titley OG. Detection of perforators using thermal imaging. Plastic and reconstructive surgery 2013;132(6):1603-1610.

20. Gu YD, Wu MM, Zheng YL, Li HR, Xu YN. Arterialized venous free sural nerve grafting. Ann Plast Surg 1985;15(4):332-339.

21. Gu YD, Zhang GM, Chen DS, Yan JG, Cheng XM. Arterialized free flap. Report of four cases. Chin Med J (Engl) 1989;102(2):140-144.

22. Rose EH. Small flap coverage of hand and digit defects. Clin Plast Surg 1989;16(3):427-442.

23. Hussmann J, Bahr C, Steinau HU, Vaubel E. [Indications for arterialization of tissue]. Langenbecks Arch Chir Suppl Kongressbd 1996;113:1164-1166.

24. Rose EH, Kowalski TA, Norris MS. The reversed venous arterialized nerve graft in digital nerve reconstruction across scarred beds. Plastic and reconstructive surgery 1989;83(4):593-604.

25. Woo SH, Kim KC, Lee GJ, Ha SH, Kim KH, Dhawan V, Lee KS. A retrospective analysis of 154 arterialized venous flaps for hand reconstruction: an 11-year experience. Plastic and reconstructive surgery 2007;119(6):1823-1838.

26. Hussmann J, Bahr C, Russell RC, Steinau HU, Vaubel E. Experimentelle und klinische Erfahrungen mit der Stromumkehr. Journal der Deutschen Gesellschaft für Plastische und Wiederherstellungschirurgie 2003:24.

27. Yan H, Gao W, Zhang F, Li Z, Chen X, Fan C. A comparative study of finger pulp reconstruction using arterialised venous sensate flap and insensate flap from forearm. Journal of plastic, reconstructive & aesthetic surgery : JPRAS 2012;65(9):1220-1226.

28. Karacalar A, Ozcan M. Free arterialized venous flap for the reconstruction of defects of the hand: new modifications. J Reconstr Microsurg 1994;10(4):243-248.

29. Liu Y, Jiao H, Ji X, Liu C, Zhong X, Zhang H, Ding X, Cao X. A comparative study of four types of free flaps from the ipsilateral extremity for finger reconstruction. PloS one 2014;9(8):e104014.

30. Patradul A, Ngarmukos C, Parkpian V, Kitidumrongsook P. Arterialized venous toenail flaps for treating nail loss in the fingers. J Hand Surg Br 1999;24(5):519-524.

31. Bullocks J, Naik B, Lee E, Hollier L, Jr. Flow-through flaps: a review of current knowledge and a novel classification system. Microsurgery 2006;26(6):439-449.

32. Lad SP, Nathan JK, Schubert RD, Boakye M. Trends in median, ulnar, radial, and brachioplexus nerve injuries in the United States. Neurosurgery 2010;66(5):953-960.

33. Ciaramitaro P, Mondelli M, Logullo F, Grimaldi S, Battiston B, Sard A, Scarinzi C, Migliaretti G, Faccani G, Cocito D. Traumatic peripheral nerve injuries: epidemiological findings, neuropathic pain and quality of life in 158 patients. J Peripher Nerv Syst 2010;15(2):120-127.

34. Meek MF, Coert JH, Robinson PH. Poor results after nerve grafting in the upper extremity: Quo vadis? Microsurgery 2005;25(5):396-402.

35. Barrios C, Amillo S, de Pablos J, Canadell J. Secondary repair of ulnar nerve injury. 44 cases followed for 2 years. Acta orthopaedica Scandinavica 1990;61(1):46-49.

36. Sulaiman W, Gordon T. Neurobiology of peripheral nerve injury, regeneration, and functional recovery: from bench top research to bedside application. Ochsner J 2013;13(1):100-108.

37. M.A. F, Wilbourn AJ. The electrodiagnostic examination with peripheral nerve injuries. In: Mackinnon SE, editor. Nerve surgery. First ed. Volume 1. New York: Thieme; 2015. p 59-74.

38. Boyd KU, Fox IK. Nerve repair and grafting. In: Mackinnon SE, editor. Nerve surgery. First ed. Volume 1. New York: Thieme; 2015. p 75-100.

39. D'Arpa S, Claes KEY, Stillaert F, Colebunders B, Monstrey S, Blondeel P. Vascularized nerve "grafts": just a graft or a worthwhile procedure? Plastic and Aesthetic Research 2015;2(4):183-194.

Chapter 14

DISCUSSION

In the prior chapters, a contextualization of relevant background, gaps in knowledge and rationale for performing the various parts of this experimental work were already provided. Similarly, most of the technical limitations and shortcomings of the various reviews and experiments performed in this thesis have already been addressed in detail in each of the preceding chapters.

In this chapter, I shall strive to highlight in a succinct fashion the potential contributes to scientific knowledge of each of the phases and tasks of the present research work.

PHASE I (REVIEW THE LITERATURE ON THE USE OF ARTERIALIZED VENOUS FLAPS)

1st Aim: Perform a systematic review and meta-analysis of unconventional perfusion flaps in clinical practice (**Chapter 3 – "*Systematic review and meta-analysis of unconventional perfusion flaps in clinical practice"*)

Although unconventional perfusion flaps (**UPFs**), including arterialized venous flaps (**AVFs**) and venous flaps (**VFs**), had been used for nearly four decades, there was no safe estimate of their survival rate.[1-4] In fact, despite their multiple potential advantages, the use of UPFs was mainly sporadic, due largely to some reports of high necrosis rates [5-9], and also to a still poorly understood physiology, and ill-defined clinical indications.[1-4] In particular, various papers had described higher partial and complete necrosis rates when UPFs were placed over chronically infected, open wounds or ischemic wound beds, or when large flaps were used. [1,2,10-13] Moreover, several authors had advocated the use of particular vascular patterns for reconstructing specific types of defects. [1-3,10,11] However, these **indications and vascular constructions had not been submitted to proper literature comparison and statistical scrutiny**.

In spite of a few excellent narrative reviews regarding the use of UPFs, not a single systematic review and meta-analysis was available.[1-3,14] Furthermore, German literature had been largely neglected in these reviews, which was unfortunate because there are several papers on this subject in German. Therefore, a wide literature review and subsequent statistical analysis of the factors associated with UPFs success or failure were direly needed.

In this sense, the primary goal of this work was to comprehensively review the literature on UPFs in order to estimate the global survival rate of these flaps. Secondarily, this paper aimed to determine the relation between several patient and wound parameters and UPFs survival.

We found 134 papers in the literature regarding the clinical application of UPFs, encompassing 1445 patients. Most defects mandating reconstruction with UPFs were caused by trauma (63.6%), especially of the hand and fingers (75.1%). The main complication of all types of UPFs was a variable degree of necrosis (7.5% of all UPFs presented marginal necrosis; 9.2% and 5.5% had significant and complete necrosis, respectively).

We estimated an overall survival rate of UPFs of 89.5% (87.3-91.3%; 95% confidence interval [CI]; p<0.001), **which was only slightly inferior to what has been reported in most series regarding conventional perfusion flaps (CPFs).** [15-17]

Interestingly, **there was a positive correlation between the rate of postoperative infection and the need of a new flap** (Pearson coefficient 0.405; p=0.001). **UPFs used to reconstruct the upper limb showed better survival rates than those transferred to the head and neck or to the lower limb** (p<0.001).

Contrarily to what had been reported by some authors, **no association was found between poorly or non-perfused wound beds and flap failure.**

The inclusion of the German literature brought to light that, **in opposition to what had been frequently stated, it was not Nakayama who described for the first time an arterialized venous flap in 1981.[18] In fact, in 1975 Vaubel had already reported an AVF to**

reconstruct the defect resulting from the excision of a tumor of the dorsum of the hand. [19]

This paper allowed us to conclude that **UPFs show high survival rates and should probably be used more liberally, particularly in the realm of upper limb reconstruction.**

In addition, in order to facilitate a better grasp of the numerous classifications of the multiple vascular configurations of UPFs, as well as their respective clinical indications, according to the literature, **we have produced professionally drawn diagrams that that synthesize information, enabling an easier and quicker understanding for anyone with an interest in the field**.[20]

PHASE I (REVIEW THE LITERATURE ON THE USE OF ARTERIALIZED VENOUS FLAPS)

2nd Aim: Perform a systematic review and meta-analysis of unconventional perfusion flaps in the experimental setting (Chapter 4 – "*Unconventional perfusion flaps in the experimental setting: a systematic review and meta-analysis*")

Since Nakayama's first description of an arterialized venous flap on the rat in 1981, UPFs had been regularly researched using multiple experimental models.[1,2,18,21]

Although there are numerous clinical and experimental papers on UPFs, the multiple animal species involved, the myriad of vascular constructions used, and the frequently conflicting data reported, with necrosis rates varying between 100% and 0%, made synthesis of this information challenging.[18,22,23] Thus, it was of paramount importance to find patterns in the available literature on UPFs.

The main aim of this paper was to perform a systematic review and meta-analysis of the literature on the experimental use of UPFs, in order to estimate the global survival rate of the best experimental models proposed. Additionally, in the attempt to systematize all the scattered data available, we **presented professionally-drawn figures that clearly illustrate all the vascular patterns reported in the literature. This synthesis allows a rapid and sound understanding of the literature on experimental models of UPFs.**

We identified 68 studies on the use of UPFs in the experimental setting, corresponding to a total of 1073 flaps. **The rabbit, the rat and the dog were the most commonly used animal species for producing UPFs**. Using a random effects model, **we estimated UPFs survival rate to be 90.8%** (95% CI, 86.9% to 93.6%; p<0.001). Interestingly,

the estimated overall UPFs survival rate in the experimental setting was similar to that reported by us on a previous meta-analysis addressing the clinical application of UPFs [89.%; 95% CI, 87.3 to 91.3; $p < 0.001$)].[20] **This suggests that the available rabbit, rat and canine experimental UPF models can adequately mimic the application of UPFs.**

PHASE II (CHARACTERIZE AN EXPERIMENTAL MODEL OF A FASCIOCUTANEOUS ARTERIALIZED VENOUS FLAP IN THE RAT)

3rd Aim: Describe in a detailed fashion and from a surgical perspective the macro and microvascular blood supply to the integument of the ventrolateral aspect of the abdomen of the rat (Chapter 5 – *"Blood supply to the integument of the abdomen of the rat: a surgical perspective"*).

The rat is the most commonly used experimental animal in Plastic and Reconstructive Surgery.[24-34] More specifically and as demonstrated in the previous task, the rat is the most frequently used species in experimental research in the realm of UPFs.

This study contributes substantially to anatomy and plastic and reconstructive surgery knowledge for four main reasons:

1- As far as the authors could determine, this represents by far the **largest anatomical study performed to date on the blood supply of the abdominal wall of the rat, comprising 205 specimens**. Moreover, these rats were analyzed with resort to multiple different and complimentary techniques (classical anatomical dissection of rats submitted to colored vascular injections; Spalteholz cleared specimens; vascular resin injection and subsequent corrosion for macroscopic evaluation; histological evaluation with the traditional hematoxylin-eosin (**HE**) and Masson's Trichrome staining, CD 31 and Neurofilament staining for vascular and nerve highlights; scanning electron microscopy of vascular corrosion casts; and infra-red thermography). These multisource data were used

as the basis for elaborating **the most detailed diagrams of the rat's abdominal wall vasculature in the literature to date**.

2- This work provided a solid anatomical basis for the multiple teaching and research activities using the abdominal wall of rat. The importance of the vessels in raising multiple axial and perforator flaps in this region of the rat was illustrated in an original diagram. **To facilitate comparison of the vascular anatomy of this region of the rat with that of humans, the authors have included a table comparing the data obtained in this study with that described in the literature**. This will certainly facilitate planning and interpretating experimental studies in this region.

3- **This study helps settle the question of whether there are venous valves in the veins that drain the skin in the abdominal region of the rat.**[35,36] Our data and scanning electron microscopy images **unequivocally showed the presence of venous valves throughout the integument of the rat's abdomen**. These data will **help understand the physiology of flaps in this region of the rat, namely those highly dependent on the venous system, such as UPFs**. [20,37] Additionally, it contributes to a better understanding of hemodynamics in specific veins of the abdomen of the rat. For example, **it helps predict the behavior of superficial veins of the rat's abdomen, which are commonly used to produce arteriovenous fistulas in experimental procedures**.[38,39]

4- Finally, this work **permitted the identification of a safe zone on each side of the abdomen for giving injections** (either subcutaneous or intraperitoneal), due to its relative paucity of large vessels. As far as the authors could determine, these zones have never been described before and will certainly be of great interest not only for researchers

working with rats in general, namely in the field of plastic surgery, but also for surgical trainees in general.

PHASE II (CHARACTERIZE AN EXPERIMENTAL MODEL OF A FASCIOCUTANEOUS ARTERIALIZED VENOUS FLAP IN THE RAT)

4th Aim: Characterize a model of a conventional fasciocutaneous free flap in the ventrolateral aspect of the abdomen of the rat (Chapter 6 – "*A Model of Free Tissue Transfer: The Rat Epigastric Free Flap"*).

In this work, we **presented a model of free flap transfer in the rat**.[40] In particular, we described in detailed fashion the steps required to transfer a fasciocutaneous abdominal free flap to the neck in the Wistar rat. **We based this description in our group's 10-year experience with the use of this flap for both teaching and research purposes.** To make this subject accessible to a wider audience, we **have included an anatomical and histological introduction to the flap, which was not easily available in anatomy and experimental surgery related literature.**[41-47]

We believe this work was of great interest, as **free flaps are the mainstay of contemporary reconstructive surgery** in the realm of complex and otherwise untreatable defects resulting from tumor extirpation, trauma, infections, malformations or burns.[48,49] Free flaps are particularly pertinent in the reconstruction of highly complex anatomical regions, like those of the head and neck, the hand, the foot, and the perineum. [48-54] Moreover, basic and translational research in the area of free tissue transfer is undeniably of great clinical potential and has recently been receiving great attention worldwide. Notwithstanding, surgical trainees and researchers are still frequently deterred from using

microsurgical models of tissue transfer, due to lack of information regarding the technical aspects involved in the operative procedures.

In fact, as far as we could determine, **there was no other paper describing and illustrating in a video, step by step, all the details and tips for a successful free flap transfer in the rat**. Hence, we strongly believe that this paper has significant teaching value.

PHASE II (CHARACTERIZE AN EXPERIMENTAL MODEL OF A FASCIOCUTANEOUS ARTERIALIZED VENOUS FLAP IN THE RAT)

5th Aim: Characterize a model of an arterialized venous fasciocutaneous flap in the ventrolateral aspect of the abdomen of the rat (Chapter 7 – *"Optimization of an arterialized venous fasciocutaneous flap in the abdomen of the rat"*).

Although numerous experimental models of AVFs had been proposed in the literature, no single model had gained widespread acceptance, which had been hampering comparison of observations on the physiology and interventions on these flaps.[55-58] Additionally, lack of a standardized model of AVF could be an obstacle for the novice in microsurgery while preparing to execute these flaps in a training environment.[43]

Hence, **the main aim of this work was to evaluate the survival area of AVFs produced with different vascular constructs in the abdomen of the rat, in order to produce an optimized model.** Additionally, we assessed the time required to produce the flap, rat mortality and surgical complications. Finally, we performed a detailed thermographic, histological, and microvascular characterization of the different AVFs constructs.[59]

We concluded that an optimized AVF can be reliably produced in the ventrolateral aspect of the abdomen of the rat by performing an end-to-side_arterial venous anastomosis between the superfical caudal epigastric vein (including a 1-mm-long ellipse of adjacent tissue from the femoral vein) **and the femoral artery.**

This **model presented an average flap survival area of 76.86 ± 13.67%, which was not significantly different from that reported in many clinical case series using AVFs**.[20]

We strongly believe that **this optimized model of AVF can be easily replicated for research and teaching purposes**.

PHASE III (STUDY THE POSSIBILITY OF INCREASING THE SURVIVAL OF THE EXPERIMENTAL MODEL DESCRIBED ABOVE IN THE PRESENCE OF A BACTERIAL INFECTION BY TRANSDUCING THIS FLAP THE WITH TWO ANTIMICROBIAL PEPTIDES)

6th Aim: Transduce the arterialized venous fasciocutaneous flap described above with two human beta defensin genes (BD-2 and BD-3) to increase flap survival in the presence of Pseudomonas aeruginosa infection and of a foreign body (Chapter 8 – "*BD-2 and BD-3 increase skin flap survival in a rat model of ischemia and Pseudomonas aeruginosa infection in the presence of a foreign body*").

It was well known that *Pseudomonas aeruginosa* is one of the major culprits of nosocomial infections, particularly of prosthetic material, due to its ability to produce biofilms, and to thrive in poorly perfused tissues. Moreover, it is frequently resistant to conventional antibiotics. Despite some papers suggesting the efficacy of two antimicrobial peptides [human beta defensins 2 (**BD-2**) and 3 (**BD-3**)] against *P. aeruginosa in vitro*, as far as we could determine, no studies had been performed *in vivo*.

Hence, **the main aim of this work was to study the usefulness of transducing an ischemic skin flap in the rat with BD-2, BD-3, and BD-2 + BD-3, to increase skin flap survival in the context of a *P. aeruginosa* infection associated with a foreign body**. The secondary endpoints assessed were: bacterial counts and biofilm formation on the surface of the foreign body, as well as rat survival.

The optimized model of AVF described in the previous task was used.[59] Under the flap two 1-cm long 14 gauge catheters were placed and 10^5 colony forming units (**CFUs**) of *P. aeruginosa* were inoculated. The surgical wound was hermetically closed.

Rats were followed for 7 days. Flap biopsies were performed on the 3rd and 7 th days post-operatively. Flap transduction was confirmed with Real-Time and immunohistochemical evaluation of BD-2 and BD-3 in flap biopsies. These biopsies also allowed bacterial quantification by culture and Real Time PCR. At the end of the experiment the catheter segments were quantitatively analyzed, regarding the presence of bacteria, resorting to scanning electron microscopy (**SEM**).

Interestingly, **we observed that BD-2 and BD-3 transduction increased skin flap survival in our model**. Moreover, **rats transfected with BD-3 presented a net reduction in the number of *P. aeruginosa* on the surface of the foreign body and less biofilm formation.** There was no impact on rat survival. Finally, flap survival was better correlated with SEM findings on the surface of the foreign body than with other bacterial quantification methods.

We believe that this study had the following merits:

1- It was the **first description of transduction of BDs genes to treat a *P. aeruginosa* infection *in vivo***.[60]

2- It was also the **first time that the transduction of an antimicrobial peptide (AMP) was performed with the intent to treat an infection developing in a poorly perfused region, simulating local ischemia**. These scenarios are

frequent in the clinical setting, occurring after trauma, radiotherapy or in ischemic regions of the body, namely in the lower limbs of atherosclerotic and/or diabetic patients.

3- As far as we could determine, **this paper analyzes in detail, for the first time in the literature, the morphometric features of the bacteria on the surface of a foreign body and thoroughly compares them with the clinical evaluation of the overlying skin flap,** as well as with bacterial quantification, using microbiological cultures of tissue biopsy, and Real-Time PCR.

4- The fact that the **groups treated with BDs presented less biofilm, suggests that, *in vivo*, these AMPs are able to prevent the formation of biofilms,** which are one of the most common and important causes of persistent clinical infection.[61,62] This undoubtedly adds to the knowledge of BD physiology, as most papers in this field refer to the action of AMPs *in vitro*, not addressing the role of these substances *in vivo*.[63]

5- **The methodology employed in this paper appeared to adequately mimic clinically relevant wounds and bacterial infections associated with foreign bodies and local ischemia**. This will certainly be of great use to other researchers who intend to study bacterial infections in these circumstances.

6- Finally, overall, **this study raised many possibilities, that may boost similar works in the field**, namely for testing the superiority of other vectors, and other AMPs, as well as the susceptibility of other bacteria species, particularly bacteria resistant to conventional antibiotics.

PHASE IV (STUDY THE USEFULNESS OF USING AN ARTERIALIZED NEUROVENOUS FLAP TO BRIDGE A PERIPHERAL NERVE GAP ASSOCIATED WITH LOCAL ISCHEMIA IN THE RAT MODEL)

7th Aim: Compare the efficacy of arterialized neurovenous flaps with other nerve conduits to reconstruct a 10-mm-long median nerve gap in an ischemic environment in a rat model (Chapter 9 – "*Reconstruction of a 10-mm-long median nerve gap in an ischemic environment using autologous conduits with different patterns of blood supply: a comparative study in the rat*").

To this day, few injuries create as much angst in both patients and doctors as the loss of neurological function. The patient must deal with paralysis, paresthesias, pain, and a prolonged and uncertain recovery. In fact, despite numerous surgical and technical developments, the results with peripheral nerve repair are still disappointing.[64-66] The available therapeutic options are complex, technically demanding, often unfulfilling, and frustratingly unpredictable.[67] Results are particularly unsatisfactory in cases of long nerve defects and in the presence of local ischemia. In these circumstances, it is frequent not to obtain useful recovery in the involved nerve territory.[64-66] **One of the longest debates in this field is the role of vascularized nerve grafts (i.e. nerve flaps) in the context of peripheral nerve defects associated with ischemia**.[68-71] Apparently, nerve flaps would be superior to nerve grafts. However, they are difficult to raise, adding substantially to the technical difficulty of the surgery.[72] Moreover, only a few options for tailoring nerve flaps

exist.[68,69,71] Furthermore, while some authors have reported better results with nerve grafts than nerve flaps [71,73,74], others have found no significant differences.[70,71]

Overall, no conclusive evidence existed to settle this debate. This is due to the fact that different researchers have used different animal species, anatomical regions, reconstructive strategies and follow-up times. Furthermore, authors have also used several outcome variables to assess nerve regeneration. These methodological differences make information synthesis difficult.[70] Finally, even though there are a few side-to-side comparisons of different gap reconstruction methods in the rat's hindlimb, using the sciatic nerve, as far as the authors could determine, there is no similar study using the rat's forelimb.[73,75,76] This is unfortunate, since clinically most peripheral nerve lesions occur in the upper extremity.[66,70,77]

Therefore, **the aim of this study was to evaluate, on the Wistar rat, the efficacy of various autologous nerve conduits with various forms of blood supply in reconstructing a 10-mm-long gap in the median nerve (MN), under conditions of local ischemia**.

A 10-mm-long median nerve defect was created in the right arm. A loose silicone tube was placed around the nerve gap zone, in order to simulate a local ischemic environment. Rats were divided in the following experimental groups (each with 20 rats): nerve graft (**NG**) group, in which the excised MN segment was reattached; conventional nerve flap (**CNF**) and arterialized neurovenous flap (**ANVF**) groups in which the gap was bridged with homonymous median nerve flaps; prefabricated nerve flap (**PNF**) group in which the gap was reconstructed with a fabricated flap created by leaving an arteriovenous fistula in contact with the sciatic nerve for 5 weeks; and the two control groups, **Sham** and

Excision groups. In the latter group, the proximal stump of the MN nerve was ligated and no repair was performed. The rats were followed for 100 days. During this time, a series of devices were used to simulate physiotherapy. A thorough battery of functional, electroneuromyographic and histological studies was performed.

For most of the analyzed variables, **CNFs and ANVFs produced a faster and more complete recovery** than NGs in the reconstruction of a 10-mm-long median nerve gap in an ischemic environment in the Wistar rat. Although results obtained with CNFs were in most cases better than those of ANVFs, these differences were not statistically significant for most of the outcome variables.

Additionally, to the best of the authors' knowledge, **this is the largest series in the literature comparing different autologous techniques of MN gap reconstruction in the rat, in the presence of local ischemia**.[78-80]

All **this data suggests that nerve flaps may be superior options compared to the traditionally used NGs for bridging peripheral nerve defects in the upper limb in the presence of local ischemia**, as occurs after major trauma, and/or radiotherapy, and/or in the presence of limb ischemia. This information is unquestionably of great clinical interest.

Another interesting finding of this study was the identification of radial deviation in forepaw prints of the rats with poorer outcomes in the following variables: flexor carpi radialis weight, maximal isometric flexion force, MN cross section area, total number of MN nerve fibers, and number of peripherin stained fibers. **Thus, radial deviation of forepaws imprints may be of interest as a surrogate marker of MN lesion.** The underlying mechanism for radial deviation may be the denervation of the intrinsic muscles of the forepaw of the

rat innervated by the MN, generating a situation similar to the median claw hand observed in humans.[81,82] However, further studies are required to confirm or dismiss this hypothesis.

For all these reasons, undoubtedly, **this paper contributed to expand the knowledge on peripheral nerve repair**, especially pertaining to nerve reconstruction using nerve flaps.

PHASE V (STUDY THE SURGICAL ANATOMY AND HISTOLOGY OF REGIONS COMMONLY USED TO RAISE ARTERIALIZED VENOUS FLAPS)

8th Aim: Study the surgical relevant anatomy and histology of regions commonly used to harvest arterialized venous flaps (Chapter 10 – "*Surgical anatomy of common regions used to harvest unconventional perfusion flaps: a cadaveric dissection study*").

It had been largely assumed that, being UPFs usually based on the visible superficial venous system, anatomical and histological studies of these flaps were not necessary. In fact, the literature is particularly scant regarding articles specifically addressing the surgical anatomy of UPFs. Arguably, this is one of the main factors that has been limiting the clinical application of these flaps.[83]

Therefore, **the main aim of this paper was to perform a cadaveric dissection study to characterize the relevant anatomy and histology of these areas, from the point of view of the surgeon interested in harvesting UPFs**.

Secondarily, **we presented professionally drawn schematic representations of the most commonly encountered superficial veins in these regions, in order to facilitate planning and execution of UPFs**.

Twenty-six freshly frozen adult human cadavers were used for anatomical and histological studies. **This series represents by far the largest series on the anatomy and histology of UPFs.**

Some of the **main findings of this study** were:

- Large **subcutaneous veins were surrounded by doublings of the superficial fascia**.
- Subcutaneous **veins were placed at different depths**, with the largest ones being deeply placed and the smallest more superficially placed.
- The **superficial cutaneous nerves, routinely used as autologous nerve grafts, were closer to sizeable superficial veins than to arteries and respective *comitante* veins of significant caliber**. Thus, to harvest a nerve segment as a CNF, a deeper dissection would be required than to harvest a homologous UPF. Moreover, CNFs would tend to be bulkier than the corresponding UPFs.
- The **UPF associated with the great saphenous vein could include a portion of corticocancellous bone** from the medial aspect of the tibia. The inclusion of bone in UPFs, eventually associated with a skin paddle, and nerve segments, may further increase the potential use of these flaps for reconstruction of complex head and neck and limb defects, further increasing the reconstructive surgeon's armamentarium.

In order to systematize these important findings, in addition to the **schematic drawings and illustrative cadaveric dissection and histology photographs**, the authors have added a **table synthesizing the main anatomical and morphometric features of each**

flap. This table will certainly be of great use for anyone deciding on which UPF to use to reconstruct a given defect.

PHASE V (STUDY THE SURGICAL ANATOMY AND HISTOLOGY OF REGIONS COMMONLY USED TO RAISE ARTERIALIZED VENOUS FLAPS)

8th Aim: Study the surgical relevant anatomy and histology of regions commonly used to harvest arterialized venous flaps (Chapter 11 – *"A rare variant of the ulnar artery with important clinical implications: a case report"*).

In this article, **we described a superficial brachioulnar artery with an aberrant path found bilaterally during cadaveric dissection**. This artery originated at midarm level from the brachial artery, pierced the brachial fascia immediately proximal to the elbow, crossed superficially to the muscles that originated from the medial epicondyle, and ran over the pronator teres muscle. It then dipped into the forearm fascia, in the gap between the flexor carpi radialis and the palmaris longus muscles. Subsequently, it ran deep to the palmaris longus muscle belly, and superficially to the flexor digitorum superficialis muscle, reaching the gap between the latter and the flexor carpi ulnaris muscle, where it assumed its usual position, lateral to the ulnar nerve. **As far as the authors could determine, this variant of the superficial brachioulnar artery crossing deep to the palmaris longus muscle belly has only been described twice before in the literature**. Quain found it in 2 cases while dissecting 429 upper limbs [84], and Hazlet once in 188 limbs [85].

It is well known that the presence of superficial radial or ulnar arteries, as the one described, is of particular clinical significance, as these arteries are more prone to trauma, and can be easily mistaken for superficial veins during medical procedures, potentially leading to iatrogenic distal limb ischemia. In addition, the possibility of such a variant should

always be born in mind when using the arm or forearm as a source or as a recipient of microvascular flaps, or when using the radial artery as vascular graft.

Hence, **knowledge of this variant and similar ones, should always be kept in mind when raising UPFs.**

PHASE V (STUDY THE SURGICAL ANATOMY AND HISTOLOGY OF REGIONS COMMONLY USED TO RAISE ARTERIALIZED VENOUS FLAPS)

8th Aim: Study the surgical relevant anatomy and histology of regions commonly used to harvest arterialized venous flaps (Chapter 12 – "*Morphometric analysis of the extensor tendons of the hallux and potential implications for tendon grafting*").

Tendon transfers are often needed in clinical practice to reconstruct lost tendons and/or ligaments.[86,87] Tendon harvesting is based on the redundancy in the function of certain tendons, which has been known for decades [88], allowing for several alternatives for tendon harvesting to become perfectly established. However, in extensive injuries, it is not uncommon for autologous tendons to be insufficient to reconstruct all the missing structures [86]. In addition, all tendon options currently in use for grafting procedures have one or more of several drawbacks, namely: inconstancy; their removal results in a variable deficit in the donor region; and the surgical incisions required to perform their extirpation are placed in body areas where healing is known to be suboptimal and thus result in conspicuous scars [86,87]. Therefore, any new alternative that would increase the supply of autologous tendons for reconstructive procedures would be invaluable.

In addition, **it would be convenient to have potential tendon donor sites in the vicinity of venossomes commonly used to produce UPF**.

Although several tendon sources are available for reconstructive surgical procedures, all have one or more shortcomings. **The aim of this work was to evaluate if the**

extensor tendons of the hallux showed anatomical characteristics that could make them an additional source for tendon grafting procedures.

The authors performed a detailed morphometric analysis of the extensor tendons of the hallux in 26 lower limbs, in order to evaluate the putative association of anatomical variants with hallux valgus, and to try to assess the feasibility of using part of the extensor apparatus of the hallux as a source of tendon for grafting procedures.

An accessory extensor hallucis longus tendon was found in 92,3% of cases. Extensor hallucis brevis tendon length was 10,5 ± 0,6 cm, its width was 0,5 ± 0,1 cm, and its thickness varied between 1-2 mm, making it a potentially good candidate as a source of tendon grafts. Several anatomical variations were observed, namely the fusion of the tendons of the extensor hallucis brevis and the accessory extensor hallucis longus muscles in the distal part of the foot.

This new therapeutic option, if implemented, would possibly **increase the supply of autogenous donor tissue for reconstructive procedures, namely for incorporating UPF harvested from the dorsum of the foot, thereby enhancing the reconstructive surgeon's armamentarium.**

PHASE V (STUDY THE SURGICAL ANATOMY AND HISTOLOGY OF REGIONS COMMONLY USED TO RAISE ARTERIALIZED VENOUS FLAPS)

9th Aim: Explore the possibility of applying the data obtained in the previous experiments to maximize the clinical application of arterialized venous flaps (Chapter 13 – "*Reconstruction of a long defect of the ulnar artery and nerve with an arterialized neurovenous free flap in a teenager: a case report and literature review*").

In this article, **we describe the clinical application of an ANVF for the simultaneous reconstruction of the ulnar artery and ulnar nerve defect of a 16-year-old boy**. This teenager had sustained an ulnar nerve and artery section four months previously. He was initially treated at another institution where the ulnar artery was ligated and the ulnar nerve lesion was not diagnosed. When he was referred to our institution he presented signs of complete ulnar nerve section, as well as a poorly perfused hand. In fact, not only did he present an ulnar claw, but he also complained of exertional pain and cold intolerance in the affected hand.

Surgery revealed an 8 cm hiatus of the ulnar artery and a 5 cm defect of the ulnar nerve. These gaps were bridged with a flow through ANVF containing two terminal branches of the sural nerve and the lesser saphenous vein. The inverted lesser saphenous vein was used to reconstruct the arterial defect and to perfuse the nerve cables. The latter were in turn used to reconstruct the ulnar nerve in a somatotopic fashion. **The architecture of the reconstruction is represented in a professional quality drawing**.

Two years postoperatively, the patient presented nearly normal strength and sensibility in the affected territory. **Thermography revealed good perfusion in the right ulnar angiosome**.

Although there are a few reports on the use of ANVF, as far as the authors could determine, **this is the first report of an ANVF being used to reconstruct a composite long nerve and arterial defect in a pediatric patient.**

To better support this assertion, **the authors have performed a literature review.** This table includes a summary of the papers cited on PubMed® up to the 1st March 2017 reporting the use of ANVFs in the English, German, Spanish, and French literature.

One reason to justify this being the first case of an ANVF being used to reconstruct a composite long nerve and arterial defect in a pediatric patient may be that extensive vascular and nerve damage is increasingly rare in children and teenagers in most countries. Moreover, these lesions are frequently associated with damage to other structures, namely the integumentary system, mandating reconstruction of concomitant tissue injuries with flaps containing muscle and/or skin paddles. Finally, having an incompletely understood physiology, ANVFs are not often the first reconstructive option for most surgeons.[20,68]

The authors believe that **this case report eloquently demonstrates that the arterialized sural nerve/lesser saphenous neurovenous flap is an expedite, safe and efficient option to reconstruct long composite arterial and nerve defects in pediatric patients.**

References

1. Goldschlager R, Rozen WM, Ting JW, Leong J. The nomenclature of venous flow-through flaps: updated classification and review of the literature. Microsurgery 2012;32:497-501.

2. Yan H, Brooks D, Ladner R, Jackson WD, Gao W, Angel MF. Arterialized venous flaps: a review of the literature. Microsurgery 2010;30:472-8.

3. Yan H, Zhang F, Akdemir O, Songcharoen S, Jones NI, Angel M, Brook D. Clinical applications of venous flaps in the reconstruction of hands and fingers. Arch Orthop Trauma Surg 2010.

4. Jabir S, Frew Q, El-Muttardi N, Dziewulski P. A systematic review of the applications of free tissue transfer in burns. Burns : journal of the International Society for Burn Injuries 2014;40:1059-70.

5. Thatte RL, Thatte MR. The saphenous venous flap. Br J Plast Surg 1989;42:399-404.

6. Zhu C, Zhang F, Lei MP, Oswald T, Lineaweaver WC. Clinical case experience using microsurgical venous flaps for soft-tissue coverage of the lower extremity. J Reconstr Microsurg 2003;19:173-7.

7. Tsai TM, Matiko JD, Breidenbach W, Kutz JE. Venous flaps in digital revascularization and replantation. J Reconstr Microsurg 1987;3:113-9.

8. Klein C. [Experiences with an arterialized venous flap for intraoral defect reconstruction]. Zentralbl Chir 2000;125:51-5.

9. Kovacs AF. Comparison of two types of arterialized venous forearm flaps for oral reconstruction and proposal of a reliable procedure. Journal of cranio-maxillo-facial surgery : official publication of the European Association for Cranio-Maxillo-Facial Surgery 1998;26:249-54.

10. Garlick JW, Goodwin IA, Wolter K, Agarwal JP. Arterialized venous flow-through flaps in the reconstruction of digital defects: case series and review of the literature. Hand (N Y) 2015;10:184-90.

11. Woon CY, Lee JY, Teoh LC. Flap resurfacing of postinfection soft-tissue defects of the hand. Plast Reconstr Surg 2007;120:1922-9.

12. Inoue G, Maeda N. Arterialized venous flap coverage for skin defects of the hand or foot. J Reconstr Microsurg 1988;4:259-66.

13. Brooks D. The "reliably unreliable" venous flap. J Hand Surg Am 2009;34:1361-2; author reply 2.

14. Yan H, Fan C, Zhang F, Gao W, Li Z, Zhang X. Reconstruction of large dorsal digital defects with arterialized venous flaps: our experience and comprehensive review of literature. Ann Plast Surg 2013;70:666-71.

15. Khouri RK, Cooley BC, Kunselman AR, Landis JR, Yeramian P, Ingram D, Natarajan N, Benes CO, Wallemark C. A prospective study of microvascular free-flap surgery and outcome. Plast Reconstr Surg 1998;102:711-21.

16. Bui DT, Cordeiro PG, Hu QY, Disa JJ, Pusic A, Mehrara BJ. Free flap reexploration: indications, treatment, and outcomes in 1193 free flaps. Plast Reconstr Surg 2007;119:2092-100.

17. Nakatsuka T, Harii K, Asato H, Takushima A, Ebihara S, Kimata Y, Yamada A, Ueda K, Ichioka S. Analytic review of 2372 free flap transfers for head and neck reconstruction following cancer resection. J Reconstr Microsurg 2003;19:363-8; discussion 9.

18. Nakayama Y, Soeda S, Kasai Y. Flaps nourished by arterial inflow through the venous system: an experimental investigation. Plastic and reconstructive surgery 1981;67:328-34.

19. Vaubel W. Indikationen und Technik des arterialisierten Lappens zur Deckung großer Defekte im Handbereich. Hefte Unfallheilkd 1975;126:381.

20. Casal D, Cunha T, Pais D, Videira P, Coloma J, Zagalo C, Angelica-Almeida M, O'Neill JG. Systematic Review and Meta-Analysis of Unconventional Perfusion Flaps in Clinical Practice. Plastic and reconstructive surgery 2016;138:459-79.

21. Wharton R, Creasy H, Bain C, James M, Fox A. Venous flaps for coverage of traumatic soft tissue defects of the hand: a systematic review. The Journal of hand surgery, European volume 2017:1753193417712879.

22. Voukidis T. An axial-pattern flap based on the arterialised venous network: an experimental study in rats. Br J Plast Surg 1982;35:524-9.

23. Germann GK, Eriksson E, Russell RC, Mody N. Effect of arteriovenous flow reversal on blood flow and metabolism in a skin flap. Plastic and reconstructive surgery 1987;79:375-80.

24. Miles DA, Crosby NL, Clapson JB. The role of the venous system in the abdominal flap of the rat. Plastic and reconstructive surgery 1997;99:2030-3.

25. Oksar HS, Coskunfirat OK, Ozgentas HE. Perforator-based flap in rats: a new experimental model. Plastic and reconstructive surgery 2001;108:125-31.

26. Ozgentas HE, Shenaq S, Spira M. Development of a TRAM flap model in the rat and study of vascular dominance. Plastic and reconstructive surgery 1994;94:1012-7; 25-6 discussion.

27. Petry JJ, Wortham KA. The anatomy of the epigastric flap in the experimental rat. Plastic and reconstructive surgery 1984;74:410-3.

28. Roberts AP, Cohen JI, Cook TA. The rat ventral island flap: a comparison of the effects of reduction in arterial inflow and venous outflow. Plastic and reconstructive surgery 1996;97:610-5.

29. Sano K, Hallock GG, Rice DC. The relative importance of the deep and superficial vascular systems for delay of the transverse rectus abdominis musculocutaneous flap as demonstrated in a rat model. Plastic and reconstructive surgery 2002;109:1052-7; discussion 8-9.

30. Strauch B, Murray DE. Transfer of composite graft with immediate suture anastomosis of its vascular pedicle measuring less than 1 mm. in external diameter using microsurgical techniques. Plastic and reconstructive surgery 1967;40:325-9.

31. Kayano S, Hallock GG, Rice DC, Nakagawa M. Instructional models for dissection techniques of perforator flaps. In: Blondeel P, Morris SF, Hallock GG, Neligan PC, eds. Perforator flaps: anatomy, technique and clinical applications Second ed. Italy: Quality medical publishing, Inc.; 2013:97-107.

32. Shurey S, Akelina Y, Legagneux J, Malzone G, Jiga L, Ghanem AM. The rat model in microsurgery education: classical exercises and new horizons. Archives of plastic surgery 2014;41:201-8.

33. Lee S. Historical events on development of experimental microsurgical organ transplantation. Yonsei Med J 2004;45:1115-20.

34. Siemionow MZ. Microsurgery models. In: Siemionow MZ, ed. Plastic and Reconstructive Surgery: Experimental models and research designs. First ed. London: Springer - Verlag; 2015:3-67.

35. Scultetus AH, Villavicencio JL, Rich NM. Facts and fiction surrounding the discovery of the venous valves. Journal of vascular surgery 2001;33:435-41.

36. Valdatta L, Congiu T, Thione A, Buoro M, Faga A, Dall'Orbo C. Do superficial epigastric veins of rats have valves? Br J Plast Surg 2001;54:151-3.

37. Wang Y, Chen SY, Gao WY, Ding J, Shi W, Feng XL, Tao XY, Wang L, Ling DS. Experimental study of survival of pedicled perforator flap with flow-through and flow-end blood supply. The British journal of surgery 2015;102:375-81.

38. Cavadas PC, Vera-Sempere FJ. Prefabrication of a vascularized nerve graft by vessel implantation: preliminary report of an experimental model. Microsurgery 1994;15:877-81.

39. Koyama T, Sugihara-Seki M, Sasajima T, Kikuchi S. Venular valves and retrograde perfusion. In: Swartz HM, Harrison DK, Bruley DF, eds. Oxygen transport to tissue XXXVI. First ed. New York, USA: Springer; 2014:317-23.

40. Casal D, Pais D, Iria I, Mota-Silva E, Almeida M-A, Alves S, Pen C, Farinho A, Mascarenhas-Lemos L, Ferreira-Silva J, Ferraz-Oliveira M, Vassilenko V, Videira PA, Gory O'Neill J. A Model of Free Tissue Transfer: The Rat Epigastric Free Flap. Journal of Visualized Experiments 2017;1:e55281.

41. Green CE. Anatomy of the Rat. First ed. New York: Hafner Publishing Company; 1968.

42. Fukui A. Microvascular anastomoses in the rat. In: Tamai S, Usui M, Yoshizu T, eds. Experimental and Clinical Reconstructive Microsurgery. First ed. Japan: Springer-Verlag; 2004:35-43.

43. Hirase Y. Skin and muscle flaps in the rat. In: Tamai S, Usui M, Yoshizu T, eds. Experimental and Clinical Reconstructive Microsurgery. First ed. Japan: Springer-Verlag; 2004:111-4.

44. Dunn RM, Mancoll J. Flap models in the rat: a review and reappraisal. Plastic and reconstructive surgery 1992;90:319-28.

45. Klein I, Steger U, Timmermann W, Thiede A, Gassel HJ. Microsurgical training course for clinicians and scientists at a German University hospital: a 10-year experience. Microsurgery 2003;23:461-5.

46. Matsumoto NM, Aoki M, Nakao J, Peng WX, Takami Y, Umezawa H, Akaishi S, Ohashi R, Naito Z, Ogawa R. Experimental Rat Skin Flap Model That Distinguishes between Venous Congestion and Arterial Ischemia: The Reverse U-Shaped Bipedicled Superficial Inferior Epigastric Artery and Venous System Flap. Plastic and reconstructive surgery 2017;139:79e-84e.

47. Ruby LK, Greene M, Risitano G, Torrejon R, Belsky MR. Experience with epigastric free flap transfer in the rat: technique and results. Microsurgery 1984;5:102-4.

48. Morain WD. Historical Perspectives. In: Mathes SJ, ed. Plastic Surgery. Second ed. Philadelphia: Saunders; 2006:27-34.

49. Tamai S. The history of microsurgery. In: Tamai S, Usui M, Yoshizu T, eds. Experimental and Clinical Reconstructive Microsurgery. First ed. Tokyo: Springer-Verlag; 2003:3-24.

50. Christoforou D, Alaia M, Craig-Scott S. Microsurgical management of acute traumatic injuries of the hand and fingers. Bull Hosp Jt Dis (2013) 2013;71:6-16.

51. Santoni-Rugiu P, Sykes PJ. Skin flaps. In: Santoni-Rugiu P, Sykes PJ, eds. A History of Plastic Surgery. First ed. Germany: Springer; 2007:79-119.

52. Bettencourt-Pires MA, Casal D, Arrobas-da-Silva F, Ritto IC, Furtado IA, Pais D, Goyri-O´Neill JE. ANATOMY AND GRAFTS – From Ancient Myths, to Modern Reality. Archives of Anatomy 2014;2:88-107.

53. Casal D, Gomez MM, Antunes P, Candeias H, Almeida MA. Defying standard criteria for digital replantation: A case series. International journal of surgery case reports 2013;4:597-602.

54. Gomez MM, Casal D. Reconstruction of large defect of foot with extensive bone loss exclusively using a latissimus dorsi muscle free flap: a potential new indication for this flap. The Journal of foot and ankle surgery : official publication of the American College of Foot and Ankle Surgeons 2012;51:215-7.

55. Weng W, Zhang F, Zhao B, Wu Z, Gao W, Li Z, Yan H. The complicated role of venous drainage on the survival of arterialized venous flaps. Oncotarget 2017;8:16414-20.

56. Ceylan R, Kaya B, Caydere M, Terzioglu A, Aslan G. Comparison of ischaemic preconditioning with surgical delay technique to increase the viability of single pedicle

island venous flaps: an experimental study. Journal of plastic surgery and hand surgery 2014;48:368-74.

57. Yan H, Brooks D, Jackson WD, Angel MF, Akdemir O, Zhang F. Improvement of prearterialized venous flap survival with delay procedure in rats. J Reconstr Microsurg 2010;26:193-200.

58. Pittet B, Quinodoz P, Alizadeh N, Schlaudraff KU, Mahajan AL. Optimizing the arterialized venous flap. Plastic and reconstructive surgery 2008;122:1681-9.

59. Casal D, Mota-Silva E, Pais D, Iria I, Videira PA, Tanganho D, Alves S, Mascarenhas-Lemos L, J. M-F, Ferraz-Oliveira M, Vassilenko V, Goyri-O'Neill J. Optimization of an arterialized venous fasciocutaneous flap in the abdomen of the rat. PRS Global Open 2017;in press.

60. Zasloff M. Antimicrobial peptides: do they have a future as therapeutics. In: Harder J, Schroder JM, eds. Antimicrobial peptides: role in human health and disease. First ed. London: Springer; 2016:147-54.

61. Costerton JW, Stewart PS, Greenberg EP. Bacterial Biofilms: A Common Cause of Persistent Infections. Science 1999;284:1318-22.

62. Barker JC, Khansa I, Gordillo GM. A Formidable Foe Is Sabotaging Your Results: What You Should Know about Biofilms and Wound Healing. Plastic and reconstructive surgery 2017;139:1184e-94e.

63. Kostakioti M, Hadjifrangiskou M, Hultgren SJ. Bacterial biofilms: development, dispersal, and therapeutic strategies in the dawn of the postantibiotic era. Cold Spring Harb Perspect Med 2013;3:a010306.

64. Desouches C, Alluin O, Mutaftschiev N, Dousset E, Magalon G, Boucraut J, Feron F, Decherchi P. [Peripheral nerve repair: 30 centuries of scientific research]. Revue neurologique 2005;161:1045-59.

65. Boyd KU, Fox IK. Nerve repair and grafting. In: Mackinnon SE, ed. Nerve surgery. First ed. New York: Thieme; 2015:75-100.

66. Wood MJ, Johnson PJ, Myckatyn TM. Anatomy and physiology for the peripheral nerve surgeon. In: Mackinnon SE, Yee A, eds. Nerve Surgery. First ed. New York: Thieme; 2015:1-40.

67. Dy CJ, Isaacs J. Preface. In: Dy CJ, Isaacs J, eds. American Society for Surgery of the Hand surgical anatomy: nerve reconstruction. First ed. Chicago, USA: American Society for Surgery of the Hand; 2017:xi.

68. Trehan SK, Model Z, Lee SK. Nerve Repair and Nerve Grafting. Hand clinics 2016;32:119-25.

69. Engin MS, Demirtas Y, Neimetzade T, Ayas B, Aksakal IA, Karacalar A. A vascularized nerve graft substitute generated in a chamber bioreactor-A preliminary report. Hand and Microsurgery 2016;5:62-9.

70. Donzelli R, Capone C, Sgulo FG, Mariniello G, Maiuri F. Vascularized nerve grafts: an experimental study. Neurological research 2016;38:669-77.

71. D'Arpa S, Claes KEY, Stillaert F, Colebunders B, Monstrey S, Blondeel P. Vascularized nerve "grafts": just a graft or a worthwhile procedure? Plastic and Aesthetic Research 2015;2:183-94.

72. Sabapathy SR, Venkatramani H. Harvest of extraplexal donor nerves for transfer or grafting. In: Dy CJ, Isaacs J, eds. American Society for Surgery of the Hand surgical anatomy: nerve reconstruction. First ed. Chicago, USA: American Society for Surgery of the Hand; 2017:161-86.

73. ANGÉLICA-ALMEIDA M, CASAL D, MAFRA M, MASCARENHAS-LEMOS L, SILVA E, FARINHO A, IRIA I, MARTINS FERREIRA J, FERRAZ-OLIVEIRA M, VIDEIRA P, VASSILENKO V, AMARANTE J, GOYRI-O'NEILL J. Evaluation of the efficacy of different conduits to bridge a 10 millimeter defect in the rat sciatic nerve in the presence of an axial blood supply. Archives of Anatomy 2014;2:8-30.

74. Giusti G, Lee JY, Kremer T, Friedrich P, Bishop AT, Shin AY. The influence of vascularization of transplanted processed allograft nerve on return of motor function in rats. Microsurgery 2016;36:134-43.

75. Giusti G, Willems WF, Kremer T, Friedrich PF, Bishop AT, Shin AY. Return of motor function after segmental nerve loss in a rat model: comparison of autogenous nerve graft, collagen conduit, and processed allograft (AxoGen). The Journal of bone and joint surgery American volume 2012;94:410-7.

76. Shin RH, Friedrich PF, Crum BA, Bishop AT, Shin AY. Treatment of a segmental nerve defect in the rat with use of bioabsorbable synthetic nerve conduits: a comparison of commercially available conduits. J Bone Joint Surg Am 2009;91:2194-204.

77. Rosberg HEeLD. Epidemiology of hand injuries in a middle-sized city in southern Sweden - a retrospective study with an 8-year interval. Scand J Plast Rec Surg Hand Surg 2004:347-55.

78. Angius D, Wang H, Spinner RJ, Gutierrez-Cotto Y, Yaszemski MJ, Windebank AJ. A systematic review of animal models used to study nerve regeneration in tissue-engineered scaffolds. Biomaterials 2012;33:8034-9.

79. Evans GR. Peripheral nerve injury: a review and approach to tissue engineered constructs. Anat Rec 2001;263:396-404.

80. Myckatyn TM, Mackinnon SE. A review of research endeavors to optimize peripheral nerve reconstruction. Neurol Res 2004;26:124-38.

81. Kilinc A, Ben Slama S, Dubert T, Dinh A, Osman N, Valenti P. [Results of primary repair of injuries to the median and ulnar nerves at the wrist]. Chirurgie de la main 2009;28:87-92.

82. Chan RK. Splinting for peripheral nerve injury in upper limb. Hand surgery : an international journal devoted to hand and upper limb surgery and related research : journal of the Asia-Pacific Federation of Societies for Surgery of the Hand 2002;7:251-9.

83. Casal D, Carvalho S, Pais D, Mota-Silva E, Iria I, Vieira P, Goyri-O'Neill J. Unconventional Perfusion Flaps. In: Casal D, ed. Flap Surgery: AvidScience; 2017:2-41.

84. Quain R. Anatomy of the Arteries of the Human Body. London: Taylor & Walton; 1844:326-37.

85. Hazlett JW. The superficial ulnar artery with reference to accidental intra-arterial injection. Can Med Assoc J 1949;61:289-93.

86. Williamson DG, Richards RS. Flexor tendon injuries and reconstruction. In: Mathes SJ, ed. Plastic Surgery. Philadelphia: Saunders; 2006:383-6.

87. Tang JB. Flexor tendons. In: Chung KC, Disa JJ, Gosain AK, Kinney BM, Rubin JP, eds. Plastic Surgery: Indications and Practice. 1st ed. China: Saunders; 2009:1124-5.

88. Brand PW. Tendon grafting. THE JOURNAL OF BONE AND JOINT SURGERY 1961;43B:444-53.

Chapter 15

CONCLUSION

I believe that is fair to say that we have generally achieved the goals established at this work's inception.

In particular, we thoroughly reviewed the clinical and experimental literature on the use of unconventional perfusion flaps (**UPFs**), verifying that UPF survival was not significantly different from that reported in conventional flaps.

We characterized an optimized experimental model of fasciocutaneous arterialized venous flaps (**AVF**) in the abdomen of the rat, after studying in detail the anatomy of this region, as well as the behavior of a typical conventional fasciocutaneous flap in this region.

We observed an increased survival of the optimized experimental model of AVF, after transducing this flap with the human beta defensin genes 2 and 3, in the presence of *Pseudomonas aeruginosa* infection and of a foreign body.

We assessed the efficacy of an arterialized neurovenous flap (**ANVF**) in the reconstruction of a 10-mm-long median nerve defect in an ischemic environment in a rat model. We observed better functional outcomes in ANVF comparatively to nerve grafts in this context.

We studied the surgical anatomy and histology of regions commonly used to harvest UPFs. This knowledge helped clarify important surgical anatomical features underlying UPF's dissection. Moreover, these data may prove valuable when deciding which flap to harvest for reconstructing specific defects.

Finally, we used some of the knowledge gathered during this set of reviews and experiments to successfully reconstruct a long combined ulnar artery and nerve defect in a teenager.

Overall, the experiments we performed in rat models and the anatomical and histological studies we made in the human cadaver proved instrumental for advancing knowledge of UPFs.

Chapter 16

FUTURE PERSPECTIVES

Although this thesis may have helped clarify some important aspects related to unconventional perfusion flap (**UPF**) use, many questions remain to be answered. Consequently, further research in this field is definitely warranted. Some of the lines of research I personally would like to pursue are:

1- To keep a continuously cumulating meta-analysis project on UPFs, systematically aggregating data from published experimental and/or clinical papers. This would potentially allow faster discovery of patterns associated with increased or decreased success in the use of these flaps.

2- To study the effect of using different gene delivery methods and antimicrobial peptides to treat *Pseudomonas aeruginosa* infection or other bacterial infections both in the fasciocutaneous model we used in this work, and in other models, potentially involving other clinically relevant tissues, such as bone.

3- To assess the efficacy of using arterialized neurovenous flaps (ANVFs) for bridging long nerve defects in the clinical context, particularly in circumstances of local ischemia. It would be of paramount importance to objectively and systematically compare the results

obtained with ANVFs with those obtained with nerve grafts, which are until now the gold standard worldwide for this type of reconstructions.[1]

4- Study the surgical anatomy of other regions of the body that could potentially be used as sources of UPFs, in order to expand the potential application of these flaps.

References

1. Sulaiman W, Gordon T. Neurobiology of peripheral nerve injury, regeneration, and functional recovery: from bench top research to bedside application. Ochsner J 2013;13:100-8.

APPENDIX 1

Chapter 1

Unconventional Perfusion Flaps

Diogo Casal[1,2]*, Sara Carvalho[2], Diogo Pais[1], Eduarda Mota Silva[3], Inês Iria[4], Paula Videira[5] and João Goyri O'Neill[1]

[1]Anatomy Department, NOVA Medical School, Universidade NOVA de Lisboa, Portugal
[2]Plastic and Reconstructive Surgery Department and Burn Unit, Centro Hospitalar de Lisboa Central – Hospital de São José, Portugal
[3]LIBPhys, Physics Department; Faculdade de Ciências e Tecnologias, Universidade NOVA de Lisboa, Portugal
[4]Molecular Microbiology and Biotechnology Unit|Drug Discovery Area; Faculdade de Farmácia, Universidade de Lisboa, Portugal
[5]UCIBIO, Life Sciences Department, Faculty of Sciences and Technology, Universidade NOVA de Lisboa, Portugal

*__Corresponding Author:__ Diogo Casal, Anatomy Department, NOVA Medical School, Universidade NOVA de Lisboa, Campo dos Mártires da Pátria, 130, 1169-056, Lisbon, Portugal, Email: diogo_bogalhao@yahoo.co.uk

First Published **July 24, 2017**

Abstract

Integumentary defects, either isolated or combined with loss of other tissues, are frequently encountered clinically, and their reconstruction is often vexing and imperfect.

Unconventional perfusion flaps (UPFs) are reconstructive options characterized by being perfused exclusively by veins. They were first introduced in the clinical literature by Vaubel in 1976 and further elaborated experimentally in 1981 by Nakayama. In UPFs at least one of the afferent veins of the flap is anastomosed to a feeding vessel. Usually, this feeding vessel is an artery, and the UPF is called an **arterialized venous flap (AVF)**. If the feeding vessel is a vein, the UPF is called a **venous flap** (VF). The efflux of blood is ensured in most cases by the continuity of one or more of the UPF's veins with neighboring veins.

UPFs present several potential advantages relatively to conventional perfusion flaps, namely: faster and easier dissection; thinness and pliability; minimal morbidity in

the donor zone; and can be harvested from most regions of the body.

Despite all these advantages, UPFs have rarely been mentioned in the clinical literature, probably because some authors report high necrosis rates, particularly in the presence of infection, and because the underlying physiologic mechanisms remain poorly understood.

Notwithstanding, there is considerable evidence to suggest the usefulness of these reconstructive options in integumentary reconstruction, particularly in regions where a thin and pliable covering is desirable. Moreover, UPFs may be useful for bridging nerve defects. However, further studies are needed to certify the efficacy of UPFs in this context.

Unconventional Perfusion Flaps in the Context of Plastic and Reconstructive Surgery

There has ample evidence that from the dawn of times human beings have sustained injuries to all regions of the body [1,2]. In fact, even human ancestors' remains show skeletal evidence of violent blows from as early as the beginning of the Paleolithic period [3]. From these injuries a wide variety of defects presumably resulted, the most well documented being fractures and fractures' complications, such as osteomyelitis [4].

When these injuries did not result in the death of those affected, functional disability and/or deformity resulted. The latter, in turn, devalued individuals both familiarly, socially, and economically, curtailing the potential of the individuals affected. Even today, apart from the obvious consequences of functional impairment, disfigurement has been shown to be associated with low self-esteem, to greatly depreciate one's value in society, and to exert a major toll in one's love life [5-9]. From another perspective, the importance attributed to beauty throughout times has led people from all parts of the world to seek numerous procedures to boost external appearance. The contemporary corollary of this prevailing trend is the hype for aesthetic surgery worldwide [10,11].

As a result of these ancestral worries, tales of body parts transfers between individuals, frequently from different species, are found in many of the most ancient civilizations from all over the globe [12]. More than three millennia ago, local flaps with reconstructive purposes were described in the Edwin Smith papyrus [12]. However, the strategies available to reconstruct faulty or missing parts of the body were limited for a great part of the human history by an insufficient knowledge of physiology [13-15].

It was only in 1628, when William Harvey provided an accurate description of the blood circulation in the human body, that was known that systemic arteries deliver blood rich in oxygen and nutrients to tissues for their

maintenance, while systemic veins drain carbon dioxide and metabolic wastes from these tissues back to the right atria of the heart [16]. This knowledge, published for the first time in "*Exercitatio Anatomica de Motu Cordis et Sanguinis in Animalibus*", commonly quoted as "*de Motu Cordis*", truly revolutionized all fields of Medicine. It laid the foundations for understanding tissue transfers, such as grafts and flaps, in what much later become known as Plastic and Reconstructive Surgery [13,17].

In contemporary times, integumentary defects, either isolated or combined with loss of other tissues, such as tendon, bone, vessels and/or nerve, can result from a great deal of situations such as trauma, including burns; tumor extirpation; infection; radiotherapy and/or auto-immune conditions [18]. These defects can thus be rather diverse in nature and clinical implications. However, in most circumstances optimal aesthetical and functional results are difficult to attain. Generally speaking, the following surgical options are available in increasing order of complexity: grafts, local flaps, regional flaps and free flaps [18].

A **graft** is defined as the transference of a tissue or a combination of tissues with no blood supply of their own initially to another place in the body. The potential viable volume and thickness of grafts are therefore limited, as during the first 2 to 3 days after grafting tissues will be forced to survive through a process of "plasmatic imbibition". This process consists in direct exchanges of oxygen, carbon dioxide, water, metabolites and catabolites

between the engrafted tissues and the wound bed through direct diffusion [18]. For this process to occur, it is mandatory that the wound bed and neighboring tissues are adequately perfused, until neoangiogenesis provides the graft with a blood supply of its own [19].

There are references to skin grafts being performed as far back as in ancient Indian scrolls more than 2500 years ago [20]. Apart from the anecdotal report of Leonardo Fioravanti replantation of an avulsed nasal tip of a Spanish soldier in 1570 as a skin graft, this technique was all but forgotten until the work of Barionio's work on skin grafts in sheep [21]. This work was published in 1804 with the title "*On grafting in animals*". Notwithstanding, skin grafting only became current clinical practice after the description of pinch skin grafts by Reverdin in 1869 [12]. Ollier and Thiersch further expanded the application of skin grafts by the introduction of partial thickness skin grafts in 1872 and 1886, respectively [22]. The introduction of large full-thickness skin grafts is generally attributed to Wolfe and Krause in 1875 and 1893, respectively [20]. In 1964, Tanner described the mesh skin graft, permitting the expansion of skin grafts up to nine times their original surface. Arguably, this further revolutionized plastic surgery, and in the particular the treatment of burned patients, saving countless lives [23,24]. Building on these milestones, numerous advances were made, leading to contemporary grafting procedures, now encompassing numerous structures besides the skin, such as mucosa,

tendon, bone, cartilage, nerve, and fat alone or in multiple combinations [12,25-30].

A **flap** is a composite block of tissues with a blood supply of its own. The flap can be **pedicled** if its original vascular connections are left in place. The flap's pedicle then becomes the pivotal point around each the tissue transfer can be performed. In a **free flap**, the original blood supply is sectioned and subsequently its vessels are microvascularly sutured to vessels in the recipient zone. In large and/or complex tissue defects, free flaps are frequently the only reconstructive option, allowing the replacement of vessels, nerves, tendons, ligaments, bone, cartilage, muscle and/or joints [18,31-35]. Despite the inherent technical difficulties in performing the microvascular anastomoses and the non-negligible risk of pedicle vessel thrombosis, free flaps have become increasingly common in the past decades, with numerous different flaps and variations of these flaps being described [17,36]. Nowadays, free flaps solve otherwise untreatable situations or cases whose prior treatment was clearly insufficient [31-35,37,38].

Most free flaps used in contemporary clinical practice are based on a vascular pedicle composed of, at least, one artery and one vein. These flaps can be considered **conventional flaps (CFs)** In order to obtain arteries of sufficient length and caliber to adequately perform vascular anastomoses at the recipient site, CFs arteries are usually painstakingly dissected below muscular fascias, often demanding a deep, technically challenging and time-con-

suming dissection. As a corollary, CFs tend to be relatively thick, even after debulking the flap, and the donor site morbidity is not always insignificant. Unfortunately, thick CFs are not always ideal to reconstruct regions where the integument is shallow, such as the head and neck regions, the dorsum of the hand, the foot or the external genitalia. Additionally, the harvesting of a CF demands the sacrifice of significant anatomical structures in the donor zone, as it entails at least the recruitment of a large enough deep artery and eventually of a deep vein, on which the CF is based [39].

In the past two decades, in an effort to minimize these shortcomings of CFs, some surgeons have advocated the resort to **supermicrosurgery** techniques, in which flaps are pedicled on very fine vessels, less than 1 mm in diameter, with resort to special surgical instruments and techniques [40]. Although, supermicrosurgery does preclude the need in many cases of dissecting and sacrificing CP vessels bellow muscular fascia, it has not gained widespread acceptance, as it is technically very demanding, requires special and expensive equipment, flaps' pedicles are often short and difficult to inset, and flaps are, according to many authors, prone to thrombosis, due to the tiny size of flaps' vessels [17,40,41].

Unconventional perfusion flaps (UPFs) are characterized by being perfused solely through their venous system. They were first introduced in the clinical literature in 1976 by Vaubel to reconstruct the dorsum of the

hand with a forearm fasciocutaneous flap [42,43]. In 1981, Nakayama *et al.* described a fasciocutaneous UPF in the ventrolateral aspect of the rat's abdomen [44]. In UPFs at least one of the afferent veins of the flap is anastomosed to a feeding vessel at the recipient site. Usually, this feeding vessel is an artery, and the UPF is called an **arterialized venous flap (AVF)**. If the feeding vessel is a vein, the UPF is called a **venous flap (VF)** [43]. In UPFs the efflux of blood is ensured in most cases by the continuity of one or more of the flap's veins with neighboring veins (Figure 1).

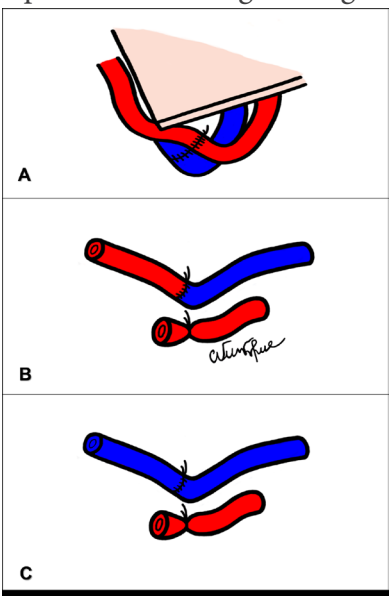

Figure 1: Schematic representation of the basic vascular architecture at the afferent side of the flap of a conventional perfusion flap (A), of a venous arterialized flap (B), and of a venous flap (C). Red vessels represent arteries and blue vessels symbolize veins.

A: In a conventional flap, here exemplified by a conventional free flap, the artery and vein that normally supply the three-dimensional block of tissues that compose the flap are anastomosed to a vein and artery at the reception zone. Blood perfusion through the flap occurs as in the rest of the body.

B: In an arterialized venous flap, the three-dimensional block of tissues that constitute the flap is completely deprived of any arteries and thus become entirely dependent on the venous system for blood flow. At least one of the flap's veins is connected to one recipient site's artery. One or more veins are usually anastomosed to recipient site's veins in order to permit flap outflow (not shown).

C: In venous flaps, the tissues that make up the flap also rely initially completely on perfusion through the venous system. Venous anastomoses are performed at the recipient site at the inflow and outflow regions of the flap (the latter are not shown).

In rare circumstances, the draining vein of the flap is surgically connected to an adjacent artery, usually to satisfy the double purpose of draining the UPFs blood efflux and to reconstruct a missing artery segment. These latter UPFs are called **flow through AVFs** [45,46].

Advantages of Unconventional Perfusion Flaps

Being based solely on the venous system, UPFs can be easily tailored around the superficial venous system. These

flaps can include any tissues neighboring veins. Hence, they can include skin, subcutaneous tissue, fascia, nerves, and even bone and/or cartilage in various combinations [43,47]. Consequently, UPFs present several potential advantages relatively to CFs, namely:

- UPFs have a faster and easier dissection, as the superficial venous system is readily observed and accessible above muscle fascia;
- UPFs avoid the need to resorting to ancillary image examinations, making them excellent options when expedite reconstruction is necessary, particularly in trauma cases
- UPFs can be very thin and pliable, being ideal to reconstruct similar regions of the integument;
- UPFs are associated with minimal morbidity in the donor zone, as their dissection does not require going deeper to the muscle fascia;
- UPFs can be harvested from most regions of the body, allowing to choose inconspicuous donor zones where the integument is redundant, such as in the anteromedial aspect of the limbs, in order to facilitate direct closure of the secondary defect [43,48,49].

For all these reasons, there has been some enthusiasm with the use of these flaps in the reconstruction of multiple types of defects, namely in deep burns [50-54], defects of the hands and fingers [49,50,55-60], including congeni-

tal or acquired defects of the nail complex [61,62], as well as in the reconstruction of other limb defects [63,64], and in defects resulting from the excision of head and neck tumors [48,65,66].

In the cases of burns to the face and hands, UPFs seem particularly promising, as they allow the reconstruction of aesthetic and functional areas with thin, pliable and homogenous skin. In this way, they reportedly ensure a better functional and aesthetical outcome compared to grafts in these burns [50,53].

Despite all these advantages, UPFs have been reported in relatively few papers, which describe in most cases small series of patients [43,67]. Three main reasons have been proposed to explain this limited use. One is that some authors report high necrosis rates with these flaps, particularly in the presence of infection [43,49]. Another reason is that the physiologic mechanisms that allow UPFs to survive are still poorly understood [48,49,68]. Finally, although a myriad of experimental models of UPFs has been described in various animal species, no one has stood out as ideal. Therefore, overall there is lack of uniformity in the literature on UPFs regarding the best methodologies to improve survival of these flaps [46,69,70].

Physiology of Unconventional Perfusion Flaps

There is no consensus in the literature regarding UPFs' mechanisms of survival, nor on the best vascular patterns

for their vascular design and transplantation [46,70,71].

Among the multiple mechanisms proposed to justify the early survival of UPFs, the following are repeatedly mentioned as being the most significant in the short term and are schematically illustrated in Figure 2.

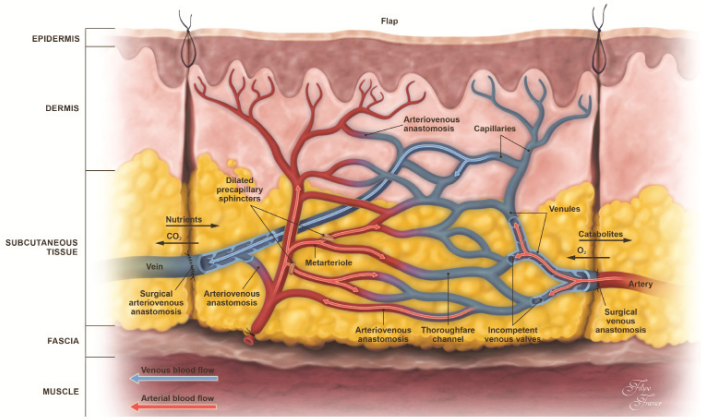

Figure 2: Schematic representation of an unconventional perfusion flap (arterialized venous flap) and its blood supply illustrating the putative physiologic mechanisms that allow its survival during the first 3 to 4 days after flap transfer. Plasmatic imbibition, venous valve incompetency, microvascular arterio-venous shunting, and the Bohr's effect are considered the main mechanisms. Red vessels represent the original arterial system of the flap. Blue vessels represent the original venous system of the flap. Red arrows indicate the direction of arterial blood flow. Blue arrows indicate the direction of venous blood flow. The drawing is not to scale.

- During the first 3 to 4 days, plasmatic imbibition from the wound bed and adjacent margins allows the diffusion of oxygen, water and metabolites

from the wound to the flap, as well as the elimination of carbon dioxide and catabolites in the opposite direction [72-78].

- The arterial blood flowing into the venous system renders most venous valves incompetent, allowing antidromic blood perfusion within the flap [48,49].
- The ischemic condition of the UPF promotes the relaxation of the precapillary sphincters and of the thick muscular walls of the arterio-venous anastomoses' permitting antidromical blood flow from the venous component of capillaries and from venules into the arterial component of capillary networks and into arterioles, respectively. From there blood percolates the proximal arterial tree, creating multiple microvascular shunts and functional arterio-venous shunts. For this mechanism to be efficient, a sufficiently extensive venous network must be present [48,49,68,79-83].
- The ischemic and acidic environment of the flap facilitates oxygen uptake from hemoglobin at the precapillary, capillary and postcapillary levels due to the Bohr's effect [73,84-88].

In the long term, the survival of UPFs seems to be mainly dependent on vertical neoangiogenesis from the wound bed into the flap, as well as on horizontal neoangiogenesis from the wound margins into the flap (Figure

3). Neoangiogenesis within the flap itself, increasing flap's collateral circulation, also seems to play a pivotal role [49,70,89,90].

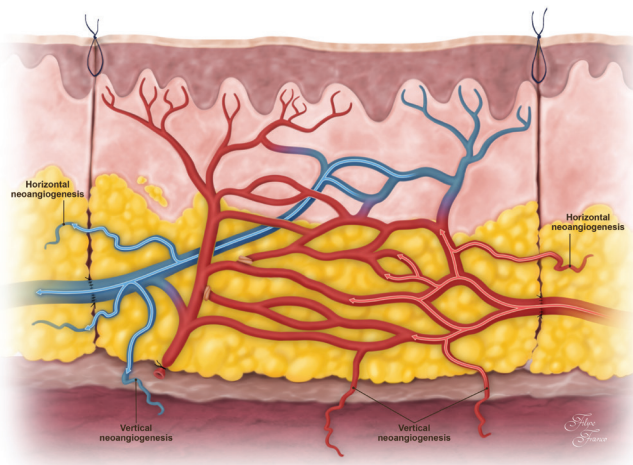

Figure 3: Schematic representation of an unconventional perfusion flap (arterialized venous flap) and its blood supply illustrating the putative physiologic mechanisms that allow its survival after the first 3 to 4 days after flap transfer. Vertical and horizontal neoangiogenesis are considered the prevailing mechanisms. Red vessels represent the arterial system of the flap (original arteries of the flap and the original veins that have suffered a process of arterialization). Blue vessels represent the venous system of the flap. Red arrows indicate the direction of arterial blood flow. Blue arrows indicate the direction of venous blood flow. The drawing is not to scale.

Despite intensive research in the mechanisms explaining the viability of unconventional perfusion, there are several reports of UPFs' high necrosis rates both experimentally and clinically [91-94]. Multiple strategies have been proposed to increase UPFs' viability, namely delay procedures [95-100], pre-arterialization [100-102], surgical expansion [51,75], growth factor application [103,104], arterio-venous shunt restriction (i.e., ligation of large and direct communications between the afferent and efferent sides of the flap, in order to force blood flow into the periphery of the flap) [105] and choice of specific vascular patterns [49,89,102]. Until now, there is no clear evidence of the efficacy of these measures.

Unconventional Perfusion Flaps and Nerve Repair

One of the main limitations in the reconstruction of extensive nerve defects, such as brachial plexus injuries, is the limited number of nerve sources available for nerve repair [106,107]. Moreover, there is growing experimental and clinical evidence that nerve flaps are superior to nerve grafts for bridging long and thick nerve defects [108]. However, currently, nerve grafts are the most commonly used options for bridging nerve defects in the clinical context [109-113].

Nerve flaps, having a blood supply of their own, have been shown experimentally to be more efficient than nerve grafts in promoting the invasion by macrophages, the re-

motion of myelin fragments in the degenerating nerve fibers, and the survival of Schwann cells [114,115]. Overall, nerve flaps are less prone to central necrosis, fibrosis and histological derangement relatively to nerve grafts, particularly in conditions of local ischemia [116,117]. In fact, nerve grafts are initially entirely dependent on plasmatic imbibition and diffusion from the local medium, until neoangiogenesis occurs. If the local environment is mostly deprived of oxygen and nutrients and/or too far from the inner portion of the graft, nerve graft necrosis and failure of nerve repair will ensue [109,118-121].

These experimental data have been supported by some empirical clinical data. In fact, it has been shown clinically that an adequate blood supply to the proximal and distal nerve stumps is associated with better functional results after peripheral nerve repair [122]. The influence of an adequate blood supply to the zone of peripheral nerve repair is particularly evident in cases of concomitant radiotherapy (as it happens in the context of tumor extirpation and administration of adjuvant therapy), or in areas of marked fibrosis, such as those present after extensive local trauma [111,112,123].

All the data mentioned above refers to "conventional nerve flaps" (CNFs), These can be defined as nerve segments with an arterial and venous blood supply. However, CNFs are seldom used clinically because there are only a few of dispensable nerve segments (i.e., whose extirpation will not result in a significant deficit in the donor zone)

that present a blood supply that allows harvesting them as CNFs [120]. The sural nerve, the saphenous nerve, the lateral cutaneous nerve of the thigh, and the sensory branch of the radial nerve to the dorsum of the hand are the most commonly used CNFs, while the ulnar nerve flap has been used in cases of extensive brachial plexus lesions [109,122,124,125].

Another reason that hinders the clinical application of CNFs is that they entail laborious harvesting dissections and technically vexing anastomoses of small sized vessels. Moreover, due to anatomical constraints, CNFs cannot always be raised [126]. To try to surpass these limitations of CNFs, Townsend and Taylor in 1984 proposed concept of "arterialized neurovenous flaps" (**ANVFs**) [127]. These flaps are composed of nerve segments pedicled exclusively on their accompanying veins. When insetted in the recipient zone, at least one of the ANVF's veins is connected to a local artery, whereas at least one of its veins is anastomosed to a recipient site's vein [127]. The use of these flaps greatly expands the choice of nerve flaps for reconstructing peripheral nerve defects. As peripheral nerves and the venous system develop in a synchronous fashion, with multiple levels of molecular cross-talk in their origin, differentiation, and elongation until reaching their target organs, they remain in close anatomical proximity since the end of the fetal period [128]. Consequently, there are numerous places where the superficial venous system is in the vicinity of expendable superficial nerves that thus can be raised as ANVFs [128,129].

However, since their original description, ANVFs use in the clinical context has been reported only rarely and these reports have been limited to case reports and small case series [43]. This may be partly justified by the fact that there are only two papers on the functional, histological and electrophysiological outcome of ANVFs in peripheral nerve repair in the experimental context [130,131]. These studies describe femoral nerve repairs in rats followed during relatively short periods of time. Therefore, further experimental and clinical studies with ANVFs are definitely warranted.

Contemporary Limitations in the Knowledge of Unconventional Perfusion Flaps

As alluded above, there are several significant hiatuses in the knowledge of UPFs, that have been deterring many surgeons to use them in the clinical context. From the authors' perspective, the following are among the most pressing questions to address in this context:

1. Systematically review and analyze the somewhat disperse and often contradictory literature on the experimental and clinical use of UPFs, in order to infer patterns that could maximize the efficacy of these flaps.
2. Establish standardized experimental models of UPFs in order to facilitate comparison of inter-

ventions, and results, as well as to allow surgical training by novices in the field.

3. Thoroughly evaluate the experimental and clinical usefulness of using ANVFs for bridging nerve defects in situations where local perfusion was preserved or compromised.
4. Assess the surgical anatomy of UPFs in different regions of the body, in order to facilitate the choice of particular vascular patterns of UPFs in specific clinical circumstances.

Conclusion

Despite some current limitations in the knowledge of UPFs, there is considerable experimental and clinical evidence to suggest the usefulness of these reconstructive options. Most frequently, these flaps have been used in integumentary reconstruction, particularly in regions where a thin and pliable covering is desirable. In these circumstances, UPFs seem to present several advantages compared to CPFs. Moreover, there is some evidence that UPFs may be useful for bridging nerve defects, especially when local ischemia is present. However, further studies are needed to certify the efficacy of UPFs in this context.

Acknowledgments

The authors would like to thank Mr. Nuno Folque for producing the drawings contained figure 1 and Mr. Filipe Franco for the drawings contained in figures 2 and 3.

References

1. Roberts C. Recording and analysis of data: palaeopathology. In: Roberts C, editor. Human remains in Archaeology: a handbook. Second edn. Great Britain: Council for British Archaelogy. 2012; 153-190.
2. Roberts C, Manchester K. Trauma. In: Roberts C, Manchester K, editors. The archaelogy of disease. Third edn. Great Britain: The History Press. 2010; 84-131.
3. ACA, Rogriguez-Martin C. Traumatic conditions. In: ACA, Rogriguez-Martin C, editors. The Cambridge encyclopedia of human paleopathology. 1st edn. United Kingdom: Cambridge University Press. 2011; 19-50.
4. ACA, Rogriguez-Martin C. Bacterial infections: osteomyelitis. In: AC A, Rogriguez-Martin C, editors. The Cambridge encyclopedia of human paleopathology. 1st edn. United Kingdom: Cambridge University Press. 2011; 172-181.
5. Etcoff N. Introduction: The nature of beauty. In: Etcoff N, editor. The survival of the prettiest: the science of beauty. 1. First ed. USA: Random house. 1999; 1-28.
6. Thompson A, Kent G. Adjusting to disfigurement: processes involved in dealing with being visibly

different. Clinical psychology review. 2001; 21: 663-682.

7. Cooke Macgregor F. Facial disfigurement: problems and management of social interaction and implications for mental health. Aesthetic plastic surgery. 1990; 14: 249-257.
8. Ellis K. A Brief Overview of the Effect of War Injuries on Sexual Health and Intimacy. Intimacy Post-Injury. Combat Trauma and Sexual Health. 2016; 1.
9. Low C, Fullarton M, Parkinson E, O'brien K, Jackson S, et al. Issues of intimacy and sexual dysfunction following major head and neck cancer treatment. Oral oncology. 2009; 45: 898-903.
10. Gilman SL. Judging by appearances. In: Gilman SL, editor. Making the body beautiful: a cultural hystory of aesthetic surgery. 1st edn. United Kingdom: Princeton Umiversity Press. 2001.
11. Teitelbaum S. Enthusiasm versus data: how does an aesthetic procedure become "hot"? . The Oxford University Press. 2006.
12. Bettencourt-Pires MA, Casal D, Arrobas-da-Silva F, Ritto IC, Furtado IA, et al. ANATOMY AND GRAFTS - From Ancient Myths, to Modern Reality. Archives of Anatomy. 2014; 1: 88-107.

13. Santoni-Rugiu P, Sykes PJ. The anatomical foundations of surgery. In: Schröder G, editor. A history of plastic surgery. 1st edn. Berlin: Springer-Verlag. 2007; 1-37.

14. Barker CF, Markmann JF. Historical overview of transplantation. Cold Spring Harb Perspect Med. 2013; 3: a014977.

15. Evans LA. A historical, clinical, and ethical overview of the emerging science of facial transplantation. Plast Surg Nurs. 2011; 31: 151-157.

16. Ribatti D. William Harvey and the discovery of the circulation of the blood. Journal of Angiogenesis Research. 2009; 1: 3.

17. Kocher MS. History of replantation: From miracle to microsurgery. World Journal of Surgery. 1995; 19: 462-467.

18. Mathes S, Hansen S. Flap Classification and Applications. In: Mathes S, Hentz V, editors. Plastic Surgery General Principles. Second edn. Philadelphia: Saunders Elsevier. 2006; 365-481.

19. Paletta C, Pokorny J, Rumbolo P. Skin Grafts. In: Mathes S, Hentz V, editors. Plastic Surgery General Principles. Second edn. Philadelphia: Saunders Elsevier. 2006; 293-316.

20. Johnson TM, Ratner D, Nelson BR. Soft tissue reconstruction with skin grafting. Journal of the

American Academy of Dermatology. 1992; 27: 151-165.

21. Miller PJ, Hertler C, Alexiades G, Cook TA. Replantation of the amputated nose. Archives of otolaryngology--head & neck surgery. 1998; 124: 907-910.

22. Smahel J. The healing of skin grafts. Clin Plast Surg. 1977; 4: 409-424.

23. Tanner JC Jr., Vandeput J, Olley JF. THE MESH SKIN GRAFT. Plastic and reconstructive surgery. 1964; 34: 287-292.

24. Singh M, Nuutila K, Collins KC, Huang A. Evolution of skin grafting for treatment of burns: Reverdin pinch grafting to Tanner mesh grafting and beyond. Burns: Journal of the International Society for Burn Injuries.2017.

25. Chick LR. Brief History and Biology of Skin Grafting. Annals of plastic surgery. 1988; 21: 358-365.

26. Hauben DJ, Baruchin A, Mahler D. On the History of the Free Skin Graft. Annals of plastic surgery. 1982; 9: 242-246.

27. Mahmoudi N, Eslahi N, Mehdipour A, Mohammadi M, Akbari M, et al. Temporary skin grafts based on hybrid graphene oxide-natural biopolymer nanofibers as effective wound healing substitutes: pre-clinical and pathological studies in ani-

mal models. Journal of materials science Materials in medicine. 2017; 28: 73.

28. Fox JD, Baquerizo-Nole KL, Van Driessche F, Yim E, Nusbaum B, et al. Optimizing Skin Grafting Using Hair-derived Skin Grafts: The Healing Potential of Hair Follicle Pluripotent Stem Cells. Wounds. 2016; 28: 109-111.
29. Achora S, Muliira JK, Thanka AN. Strategies to promote healing of split thickness skin grafts: an integrative review. J Wound Ostomy Continence Nurs. 2014; 41: 335-339.
30. van der Eerden PA, Verdam FJ, Dennis SC, Vuyk H. Free cartilage grafts and healing by secondary intention: a viable reconstructive combination after excision of nonmelanoma skin cancer in the nasal alar region. Arch Facial Plast Surg. 2009; 11: 18-23.
31. Morain WD. Historical Perspectives. In: Mathes SJ, editor. Plastic Surgery. Second edn. Philadelphia: Saunders. 2006; 27-34.
32. Christoforou D, Alaia M, Craig-Scott S. Microsurgical management of acute traumatic injuries of the hand and fingers. Bull Hosp Jt Dis. 2013; 71: 6-16.
33. Santoni-Rugiu P, Sykes PJ. Skin flaps. In: Santoni-Rugiu P, Sykes PJ, editors. A History of Plastic Sur-

gery. First edn. Germany: Springer. 2007; 79-119.

34. Tamai S. The history of microsurgery. In: Tamai S, Usui M, Yoshizu T, editors. Experimental and Clinical Reconstructive Microsurgery. First edn. Tokyo: Springer-Verlag. 2003; 3-24.

35. Bettencourt-Pires MA, Casal D, Arrobas-da-Silva F, Ritto IC, Furtado IA, et al. ANATOMY AND GRAFTS – From Ancient Myths, to Modern Reality. Archives of Anatomy. 2014; 2: 88-107.

36. Casal D, Pais D, Iria I, Mota-Silva E, Almeida M-A, lica, et al. A Model of Free Tissue Transfer: The Rat Epigastric Free Flap. Journal of Visualized Experiments. 2017; 119: e55281.

37. Casal D, Gomez MM, Antunes P, Candeias H, Almeida MA. Defying standard criteria for digital replantation: A case series. International journal of surgery case reports. 2013; 4: 597-602.

38. Gomez MM, Casal D. Reconstruction of large defect of foot with extensive bone loss exclusively using a latissimus dorsi muscle free flap: a potential new indication for this flap. J Foot Ankle Surg. 2012; 51: 215-217.

39. Wei F, Suominen S. Principles and Techniques in Microvascular Surgery. In: Mathes S, Hentz V, editors. Plastic Surgery General Principles. Second edn. Philadelphia: Saunders Elsevier. 2006; 507-538.

40. Park JE, Chang DW. Advances and Innovations in Microsurgery. Plastic and reconstructive surgery. 2016; 138: 915e-924e.

41. Shurey S, Akelina Y, Legagneux J, Malzone G, Jiga L, et al. The rat model in microsurgery education: classical exercises and new horizons. Archives of plastic surgery. 2014; 41: 201-208.

42. Hussmann J, Bahr C, Steinau HU, Vaubel E. [Indications for arterialization of tissue]. Langenbecks Arch Chir Suppl Kongressbd. 1996; 113: 1164-1166.

43. Casal D, Cunha T, Pais D, Videira P, Coloma J, et al. Systematic Review and Meta-Analysis of Unconventional Perfusion Flaps in Clinical Practice. Plastic and reconstructive surgery. 2016; 138: 459-479.

44. Nakayama Y, Soeda S, Kasai Y. Flaps nourished by arterial inflow through the venous system: an experimental investigation. Plastic and reconstructive surgery. 1981; 67: 328-334.

45. Fukui A, Inada Y, Maeda M, Tamai S, Mizumoto S, et al. Pedicled and "flow-through" venous flaps: clinical applications. J Reconstr Microsurg. 1989; 5: 235-243.

46. Goldschlager R, Rozen WM, Ting JW, Leong J. The nomenclature of venous flow-through flaps:

updated classification and review of the literature. Microsurgery. 2012; 32: 497-501.

47. Borumandi F, Higgins JP, Buerger H, Vasilyeva A, Benlidayi ME, et al. Arterialized Venous Bone Flaps: An Experimental Investigation. Scientific reports. 2016; 6.

48. Kovacs AF. Comparison of two types of arterialized venous forearm flaps for oral reconstruction and proposal of a reliable procedure. Journal of cranio-maxillo-facial surgery: official publication of the European Association for Cranio-Maxillo-Facial Surgery. 1998; 26: 249-254.

49. Woo SH, Kim KC, Lee GJ, Ha SH, Kim KH, et al. A retrospective analysis of 154 arterialized venous flaps for hand reconstruction: an 11-year experience. Plastic and reconstructive surgery. 2007; 119: 1823-1838.

50. Woo SH, Seul JH. Optimizing the correction of severe postburn hand deformities by using aggressive contracture releases and fasciocutaneous free-tissue transfers. Plastic and reconstructive surgery. 2001; 107: 1-8.

51. Woo SH, Seul JH. Pre-expanded arterialised venous free flaps for burn contracture of the cervicofacial region. Br J Plast Surg. 2001; 54: 390-395.

52. Agarwal P, Kumar A, Sharma D. Feasibility of type III venous flap in coverage of hand defects follow-

ing trauma and burns. J Clin Orthop Trauma. 2016; 7: 150-153.

53. Iglesias M, Butron P, Chavez-Munoz C, Ramos-Sanchez I, Barajas-Olivas A. Arterialized venous free flap for reconstruction of burned face. Microsurgery. 2008; 28: 546-550.

54. Ueda Y, Mizumoto S, Hirai T, Doi Y, Fukui A, et al. Two-stage arterialized flow-through venous flap transfer for third-degree burn defects on the dorsum of the hand. J Reconstr Microsurg. 1997; 13: 489-496.

55. Takeuchi M, Sakurai H, Sasaki K, Nozaki M. Treatment of finger avulsion injuries with innervated arterialized venous flaps. Plastic and reconstructive surgery. 2000; 106: 881-885.

56. Inoue G, Suzuki K. Arterialized venous flap for treating multiple skin defects of the hand. Plastic and reconstructive surgery. 1993; 91: 299-302.

57. Iwasawa M, Ohtsuka Y, Kushima H, Kiyono M. Arterialized venous flaps from the thenar and hypothenar regions for repairing finger pulp tissue losses. Plastic and reconstructive surgery. 1997; 99: 1765-1770.

58. Woo SH, Jeong JH, Seul JH. Resurfacing relatively large skin defects of the hand using arterialized venous flaps. J Hand Surg Br. 1996; 21: 222-229.

59. Yokoyama T, Tosa Y, Hashikawa M, Kadota S, Hosaka Y. Medial plantar venous flap technique for volar oblique amputation with no defects in the nail matrix and nail bed. Journal of plastic, reconstructive & aesthetic surgery. JPRAS. 2010; 63: 1870-1874.

60. Park JU, Kim K, Kwon ST. Venous Free Flaps for the Treatment of Skin Cancers of the Digits. Ann Plast Surg. 2014.

61. Nakayama Y, Iino T, Uchida A, Kiyosawa T, Soeda S. Vascularized free nail grafts nourished by arterial inflow from the venous system. Plastic and reconstructive surgery. 1990; 85: 239-245; discussion 46-47.

62. Patradul A, Ngarmukos C, Parkpian V, Kitidumrongsook P. Arterialized venous toenail flaps for treating nail loss in the fingers. J Hand Surg Br. 1999; 24: 519-524.

63. Koshima I, Soeda S, Nakayama Y, Fukuda H, Tanaka J. An arterialised venous flap using the long saphenous vein. Br J Plast Surg. 1991; 44: 23-26.

64. Chavoin JP, Rouge D, Vachaud M, Boccalon H, Costagliola M. Island flaps with an exclusively venous pedicle. A report of eleven cases and a preliminary haemodynamic study. Br J Plast Surg. 1987; 40: 149-154.

65. Safak T, Akyurek M. Cephalic vein-pedicled arterialized anteromedial arm venous flap for head and neck reconstruction. Ann Plast Surg. 2001; 47: 446-449.

66. Park SW, Heo EP, Choi JH, Cho HC, Kim SH, et al. Reconstruction of defects after excision of facial skin cancer using a venous free flap. Ann Plast Surg. 2011; 67: 608-611.

67. Jabir S, Frew Q, El-Muttardi N, Dziewulski P. A systematic review of the applications of free tissue transfer in burns. Burns: journal of the International Society for Burn Injuries. 2014; 40: 1059-1070.

68. Nichter LS, Jazayeri MA. The physiologic basis for nonconventional vascular perfusion. Plastic and reconstructive surgery. 1995; 95: 406-412.

69. Garlick JW, Goodwin IA, Wolter K, Agarwal JP. Arterialized venous flow-through flaps in the reconstruction of digital defects: case series and review of the literature. Hand (N Y). 2015; 10: 184-190.

70. Yan H, Brooks D, Ladner R, Jackson WD, Gao W, et al. Arterialized venous flaps: a review of the literature. Microsurgery. 2010; 30: 472-478.

71. Yan H, Zhang F, Akdemir O, Songcharoen S, Jones NI, et al. Clinical applications of venous flaps in

the reconstruction of hands and fingers. Arch Orthop Trauma Surg. 2011; 131: 65-74.

72. Ueda K, Harada T, Nagasaka S, Oba S, Inoue T, et al. An experimental study of delay of flow-through venous flaps. Br J Plast Surg. 1993; 46: 56-60.

73. Fukui A, Inada Y, Maeda M, Mizumoto S, Yajima H, et al. Venous flap-its classification and clinical applications. Microsurgery. 1994; 15: 571-578.

74. Inada Y, Fukui A, Tamai S, Maeda M, Mizumoto S. An experimental study of the venous flap: investigation of the recipient vein. J Reconstr Microsurg. 1990; 6: 123-128.

75. Mutaf M, Tasaki Y, Fujii T. Expansion of venous flaps: an experimental study in rats. Br J Plast Surg. 1998; 51: 393-401.

76. Hyza P, Vesely J, Novak P, Stupka I, Sekac J, et al. Arterialized venous free flaps - a reconstructive alternative for large dorsal digital defects. Acta Chir Plast. 2008; 50: 43-50.

77. Fukui A, Inada Y, Murata K, Tamai S. "Plasmatic imbibition" in the rabbit flow-through venous flap, using horseradish peroxidase and fluorescein. J Reconstr Microsurg. 1995; 11: 255-264.

78. Fukui A, Maeda M, Tamai S, Inada Y. "Plasmatic imbibition" in the rat musculocutaneous pedicled venous flap: enzymatic proof using horseradish peroxidase. Microsurgery. 1993; 14: 114-119.

79. Galumbeck MA, Freeman BG. Arterialized venous flaps for reconstructing soft-tissue defects of the extremities. Plastic and reconstructive surgery. 1994; 94: 997-1002.

80. Woo SH, Kim SE, Lee TH, Jeong JH, Seul JH. Effects of blood flow and venous network on the survival of the arterialized venous flap. Plastic and reconstructive surgery. 1998; 101: 1280-1289.

81. Roberts AP, Cohen JI, Cook TA. The rat ventral island flap: a comparison of the effects of reduction in arterial inflow and venous outflow. Plastic and reconstructive surgery. 1996; 97: 610-615. 82.

82. Inada Y, Fukui A, Tamai S, Mizumoto S. The arterialised venous flap: experimental studies and a clinical case. Br J Plast Surg. 1993; 46: 61-67.

83. Fukui A, Inada Y, Murata K, Ueda Y, Tamai S. A method for prevention of arterialized venous flap necrosis. J Reconstr Microsurg. 1998; 14: 67-74.

84. Dvir E, Hickey MJ, Hurley JV, Morrison WA. A histological and carbon perfusion study of cephalic and saphenous venous flaps in the dog. Br J Plast Surg. 1994; 47: 263-267.

85. Liu C, Lu K, Wu W. [The causes of necrosis of arteriovenous flap and its modification]. Zhonghua Zheng Xing Shao Shang Wai Ke Za Zhi. 1994; 10: 173-177.

86. Masquelet AC. [Venous return in the flap with retrograde arterial flow]. Annales de chirurgie plastique et esthetique. 1994; 39: 327-329.

87. Smith RJ, Fukuta K, Wheatley M, Jackson IT. Role of perivenous areolar tissue and recipient bed in the viability of venous flaps in the rabbit ear model. Br J Plast Surg. 1994; 47: 10-14.

88. Suzuki Y, Suzuki K, Ishikawa K. Direct monitoring of the microcirculation in experimental venous flaps with afferent arteriovenous fistulas. Br J Plast Surg. 1994; 47: 554-559.

89. Yan H, Zhang F, Akdemir O, Songcharoen S, Jones NI, et al. Clinical applications of venous flaps in the reconstruction of hands and fingers. Arch Orthop Trauma Surg. 2010.

90. Yan H, Kolkin J, Zhao B, Li Z, Jiang S, et al. The effect of hemodynamic remodeling on the survival of arterialized venous flaps. PloS one. 2013; 8: e79608.

91. Germann GK, Eriksson E, Russell RC, Mody N. Effect of arteriovenous flow reversal on blood flow and metabolism in a skin flap. Plastic and reconstructive surgery. 1987; 79: 375-380.

92. Sakai S. Arterialised venous groin flap: case report. Br J Plast Surg. 1996; 49: 90-92.

93. Yucel A, Bayramicli M. Effects of hyperbaric oxygen treatment and heparin on the survival of uni-

pedicled venous flaps: an experimental study in rats. Ann Plast Surg. 2000; 44: 295-303.

94. Atabey A, Gezer S, Vayvada H, Kirkali G, Menderes A, et al. Ischemia/reperfusion injury in flow-through venous flaps. Ann Plast Surg. 1998; 40: 612-616.

95. Cho BC, Byun JS, Baik BS. Dorsalis pedis tendocutaneous delayed arterialized venous flap in hand reconstruction. Plastic and reconstructive surgery. 1999; 104: 2138-2144.

96. Cho BC, Lee JH, Byun JS, Baik BS. Clinical applications of the delayed arterialized venous flap. Ann Plast Surg. 1997; 39: 145-157.

97. Lalkovic M, Kozarski J, Panajotovic L, Visnjic M, Djurdjevic D, et al. Surface enlargement of a new arterialised venous flap by the surgical delay method. Vojnosanitetski pregled Military-medical and pharmaceutical review. 2014; 71: 547-553.

98. Ueda K, Nuri T, Akamatsu J, Sugita N, Otani K. Clinical trial of delay of the venous island flap. Plastic and reconstructive surgery. 2010; 126: 104e-105e.

99. Ueda K, Nuri T, Akamatsu J, Sugita N, Otani K, et al. Delay of the reverse pedicled venous island flap: clinical applications. Journal of plastic surgery and hand surgery. 2013; 47: 350-354.

100. Yan H, Brooks D, Jackson WD, Angel MF, Akdemir O, et al. Improvement of prearterialized venous flap survival with delay procedure in rats. J Reconstr Microsurg. 2010; 26: 193-200.

101. Alexander G. Multistage type III venous flap or 'pre-arterialisation of an arterialised venous flap'. Br J Plast Surg. 2001; 54: 734.

102. Wungcharoen B, Santidhananon Y, Chongchet V. Pre-arterialisation of an arterialised venous flap: clinical cases. Br J Plast Surg. 2001; 54: 112-116.

103. Zhang F, Brooks D, Chen W, Mustain W, Chen MB, et al. Improvement of venous flap survival by application of vascular endothelial growth factor in a rat model. Ann Plast Surg. 2006; 56: 670-673.

104. Pittet B, Quinodoz P, Alizadeh N, Schlaudraff KU, Mahajan AL. Optimizing the arterialized venous flap. Plastic and reconstructive surgery. 2008; 122: 1681-1689.

105. Lin YT, Henry SL, Lin CH, Lee HY, Lin WN, et al. The shunt-restricted arterialized venous flap for hand/digit reconstruction: enhanced perfusion, decreased congestion, and improved reliability. J Trauma. 2010; 69: 399-404.

106. Kakinoki R, Ikeguchi R, Nakayama K, Nakamura T. Functioning transferred free muscle in-

nervated by part of the vascularized ulnar nerve connecting the contralateral cervical seventh root to themedian nerve: case report. J Brachial Plex Peripher Nerve Inj. 2007; 2: 18.

107. Engin MS, Demirtas Y, Neimetzade T, Ayas B, Aksakal IA, et al. A vascularized nerve graft substitute generated in a chamber bioreactor-A preliminary report. Hand and Microsurgery. 2016; 5: 62-69.

108. Friedman AH. An eclectic review of the history of peripheral nerve surgery. Neurosurgery. 2009; 65: A3-8.

109. Trehan SK, Model Z, Lee SK. Nerve Repair and Nerve Grafting. Hand clinics. 2016; 32: 119-125.

110. Wood MJ, Johnson PJ, Myckatyn TM. Anatomy and physiology for the peripheral nerve surgeon. In: Mackinnon SE, Yee A, editors. Nerve Surgery. First edn. New York: Thieme. 2015; 1-40.

111. Brandt J, Dahlin LB, Lundborg G. Autologous tendons used as grafts for bridging peripheral nerve defects. J Hand Surg Br. 1999; 24: 284-290.

112. Millesi H. Bridging defects: autologous nerve grafts. Acta Neurochir Suppl. 2007; 100: 37-38.

113. D'Arpa S, Claes KEY, Stillaert F, Colebunders B, Monstrey S, et al. Vascularized nerve "grafts": just a graft or a worthwhile procedure? Plastic and Aesthetic Research. 2015; 2: 183-194.

114. Koshima IH, K. Experimental studies on vascularized nerve grafts in rats. J Microsurg. 1981; 2: 225-226.

115. Donzelli R, Capone C, Sgulo FG, Mariniello G, Maiuri F. Vascularized nerve grafts: an experimental study. Neurological research. 2016; 38: 669-677.

116. Breindenbach WT, JK. The anatomy of free vascularized nerve grafts. Clin Plast Surg. 1984; 11: 65-71.

117. Burnett MG, Zager EL. Pathophysiology of peripheral nerve injury: a brief review. Neurosurgical focus. 2004; 16: 1-7.

118. Sinis N, Kraus A, Papagiannoulis N, Werdin F, Schittenhelm J, et al. Concepts and developments in peripheral nerve surgery. Clinical neuropathology. 2009; 28: 247-262.

119. Desouches C, Alluin O, Mutaftschiev N, Dousset E, Magalon G, et al. [Peripheral nerve repair: 30 centuries of scientific research]. Revue neurologique. 2005; 161: 1045-1059.

120. Terzis JK, Skoulis TG, Soucacos PN. Vascularized nerve grafts. A review. International angiology : a journal of the International Union of Angiology. 1995; 14: 264-277.

121. Taylor GI, Pan WR. The angiosome concept. In: Dodwell P, editor. The angiosome concept and tissue transfer. First edn. Florida: Quality Medical Publishing, Inc. 2014; 354-395.

122. Jabaley ME. Primary Nerve Repair. In: Slutsky DJ, Hentz VR, editors. Peripheral Nerve Surgery: Practical Applications in the Upper Extremity. Churchill Livingstone. 2006; 23-38.

123. Iida T, Nakagawa M, Asano T, Fukushima C, Tachi K. Free vascularized lateral femoral cutaneous nerve graft with anterolateral thigh flap for reconstruction of facial nerve defects. J Reconstr Microsurg. 2006; 22: 343-348.

124. Battiston B, Papalia I, Tos P, Geuna S. Chapter 1: Peripheral nerve repair and regeneration research: a historical note. International review of neurobiology. 2009; 87: 1-7.

125. Breidenbach WC, Terzis JK. Vascularized nerve grafts: an experimental and clinical review. Ann Plast Surg. 1987; 18: 137-146.

126. Hong MK, Taylor GI. Angiosome territories of the nerves of the upper limbs. Plastic and reconstructive surgery. 2006; 118: 148-160.

127. Townsend PL, Taylor GI. Vascularised nerve grafts using composite arterialised neurovenous systems. Br J Plast Surg. 1984; 37: 1-17.

128. Carmeliet P. Blood vessels and nerves: common signals, pathways and diseases. Nature Reviews Genetics. 2003; 4: 710-720.

129. Chuang DC. Adult brachial plexus reconstruction with the level of injury: review and personal experience. Plast Reconstr Surg. 2009; 124: e359-369.

130. Vargel I, Demirci M, Erdem S, Firat P, Surucu HS, et al. A comparison of various vascularization-perfusion venous nerve grafts with conventional nerve grafts in rats. J Reconstr Microsurg. 2009; 25: 425-437.

131. Vargel I. Impact of vascularization type on peripheral nerve microstructure. J Reconstr Microsurg. 2009; 25: 243-253.

APPENDIX 2

Systematic Review and Meta-Analysis of Unconventional Perfusion Flaps in Clinical Practice

Diogo Casal, M.D.
Teresa Cunha, M.Sc.
Diogo Pais, M.D., Ph.D.
Paula Videira, Ph.D.
Joana Coloma, R.N., M.S.P.H.
Carlos Zagalo, M.D., Ph.D.
Maria Angélica-Almeida, M.D.
João Goyri O'Neill, M.D., Ph.D.

Lisbon, Portugal

Background: Although unconventional perfusion flaps have been in clinical use since 1975, many surgeons are still deterred from using them, because of some reports of high necrosis rates.
Methods: The authors performed a systematic review and meta-analysis of all articles written in English, French, German, Spanish, and Portuguese on the clinical use of unconventional perfusion flaps and indexed to PubMed from 1975 until July 15, 2015.
Results: A total of 134 studies and 1445 patients were analyzed. The estimated survival rate of unconventional perfusion flaps was 89.5 percent (95 percent CI, 87.3 to 91.3 percent; $p < 0.001$). Ninety-two percent of unconventional perfusion flaps (95 percent CI, 89.9 to 93.7 percent; $p < 0.001$) presented complete or nearly complete survival. Most defects mandating unconventional perfusion flap reconstruction were caused by trauma (63.6 percent), especially of the hand and fingers (75.1 percent). The main complication of all types of flaps was a variable degree of necrosis (7.5 percent of all unconventional perfusion flaps presented marginal necrosis; 9.2 percent and 5.5 percent had significant and complete necrosis, respectively). There was a positive correlation between the rate of postoperative infection and the need for a new flap (Pearson coefficient, 0.405; $p = 0.001$). Flaps used to reconstruct the upper limb showed better survival than those transferred to the head and neck or to the lower limb ($p < 0.001$).
Conclusion: Unconventional perfusion flaps show high survival rates and should probably be used more liberally, particularly in the realm of upper limb reconstruction. (*Plast. Reconstr. Surg.* 138: 459, 2016.)
CLINICAL QUESTION/LEVEL OF EVIDENCE: Therapeutic, V.

Forty years have passed since Vaubel first executed an arterialized venous flap to cover a defect on the dorsum of the hand.[1] This marked the birth of so-called unconventional perfusion flaps. Unconventional perfusion flaps can be defined as composite blocks of tissues perfused solely through their venous system. They comprise arterialized venous flaps and venous flaps. Arterialized venous flaps receive an arterial inflow at one end of their venous system, and drain their blood through another portion of their venous system. Venous flaps receive venous blood through one end of their venous system and drain their blood into a venous outflow.[2–5]

Since Vaubel's first description in 1975, the use of unconventional perfusion flaps has

From the Plastic and Reconstructive Surgery Department and Burn Unit, Centro Hospitalar de Lisboa Central; the Anatomy Department, the Centre for Chronic Diseases, and Global Health and Tropical Medicine, Nova Medical School, Faculdade de Ciências Médicas; the Department of Life Sciences, Faculdade de Ciências e Tecnologia, da Universidade Nova de Lisboa; and the Head and Neck Surgery Department, Lisbon Delegation of the Portuguese Institute of Oncology.
Received for publication October 21, 2015; accepted March 22, 2016.

DOI: 10.1097/PRS.0000000000002390

Disclosure: *The authors have no financial or commercial interest to declare in relation to the content of this article.*

Supplemental digital content is available for this article. A direct URL citation appears in the text; simply type the URL address into any Web browser to access this content. A clickable link to the material is provided in the HTML text of this article on the *Journal*'s Web site (www.PRSJournal.com).

been mainly sporadic, largely because of some reported high necrosis rates,[6–10] and also because of a still incompletely understood physiology and ill-defined clinical indications.[2–5] In particular, various articles have described higher partial and complete necrosis rates when unconventional perfusion flaps are placed over chronically infected open wounds or ischemic wound beds, or when large flaps are used.[2,3,11–14] Moreover, several authors have advocated the use of particular vascular patterns for reconstructing specific types of defects.[2–4,11,12] However, these indications and vascular constructions have not been submitted to proper literature comparison and statistical scrutiny.

In spite of a few excellent narrative reviews regarding the use of unconventional perfusion flaps, no systematic reviews or meta-analyses are available.[2–4,15] Furthermore, the German literature has been largely neglected in these reviews. Finally, a literature-wide review and subsequent statistical analysis of the factors associated with unconventional perfusion flap success or failure are direly needed.

The primary objective of this work was to comprehensively review the literature on unconventional perfusion flaps to estimate the global survival rate of these flaps. The secondary aim of this study was to determine the relation between several patient and wound parameters and survival of unconventional perfusion flaps.

PATIENTS AND METHODS

On July 15, 2015, the authors searched the PubMed database regarding the clinical application of unconventional perfusion flaps (Fig. 1). The following terms were used: "arterialized venous flap," "arterialized venous flap," "unconventional flap," "unconventional perfusion flap," and "venous flap." The search terms were combined with the Boolean operators ''AND" and "OR." Only articles referring to human studies and written in English, French, Spanish, German, or Portuguese were selected. Studies written in different languages from those mentioned above or articles referring exclusively to animal or dissection studies were excluded.

The title and abstract of all identified studies were examined independently by two reviewers (D.C. and T.C.). In cases where suitability of a given study for inclusion in the review was unclear, the entire article was obtained and assessed for appropriateness. Next, the references contained in these articles were scanned by the two independent reviewers to obtain further articles that were missed in the first-round search. All articles were obtained in their full-text version and read independently by the two reviewers.

For each study, the following parameters were assessed: year of publication; nationality; patient age; gender proportion; defect location and cause; flap size; flap donor site; flap composition; flap insetting vascular architecture; percentage of flaps that presented complete survival (defined as 100 percent survival area or superficial necrosis with self-healing of the flap's surface within the first 15 days after surgery), nearly complete survival (considered 90 to 100 percent flap survival or unspecified inconsequential "marginal necrosis"), significant necrosis (>10 percent flap necrosis), and complete necrosis (100 percent flap necrosis or "nonsurviving flaps"); presence of infection before flap insetting; wound bed status before flap placement (well vascularized if the flap was placed over viable muscle, fascia, fat, synovial tissue, epitenon, or granulation tissue; poorly vascularized, if the flap was placed over an irradiated area, scar tissue or tendon; and nonvascularized, if the flap was placed over bone, cartilage or prosthetic material); and presence and nature of complications (epidermolysis, flap congestion, and venous insufficiency by themselves were not considered complications, as they were uniformly present in the first few days after surgery). Epidermolysis was considered to be present when there was evidence of the epidermis being only loosely attached to the dermis, readily exfoliating or forming blisters.[16] If the damage to the skin was deeper than the epidermis, flap necrosis was considered to be present, as described above.

The quality of evidence of each article was assessed using the modified Grades of Recommendation, Assessment, Development and Evaluation quality assessment criteria[17] (all series with fewer than three patients were considered to be composed of sparse data and to have a significant probability of reporting bias, and thus were attributed a very low quality of evidence score). When estimating effect sizes for the entire population, the authors included only studies with at least a low quality of evidence score according to the modified Grades of Recommendation, Assessment, Development and Evaluation quality assessment criteria.[17] Whenever individual patient data were present in articles, they were used for individual patient data meta-analysis. For the sake of individual case analysis, the data from the two articles by Hussmann et al., which referred to the same series, were considered coincidental.[18,19]

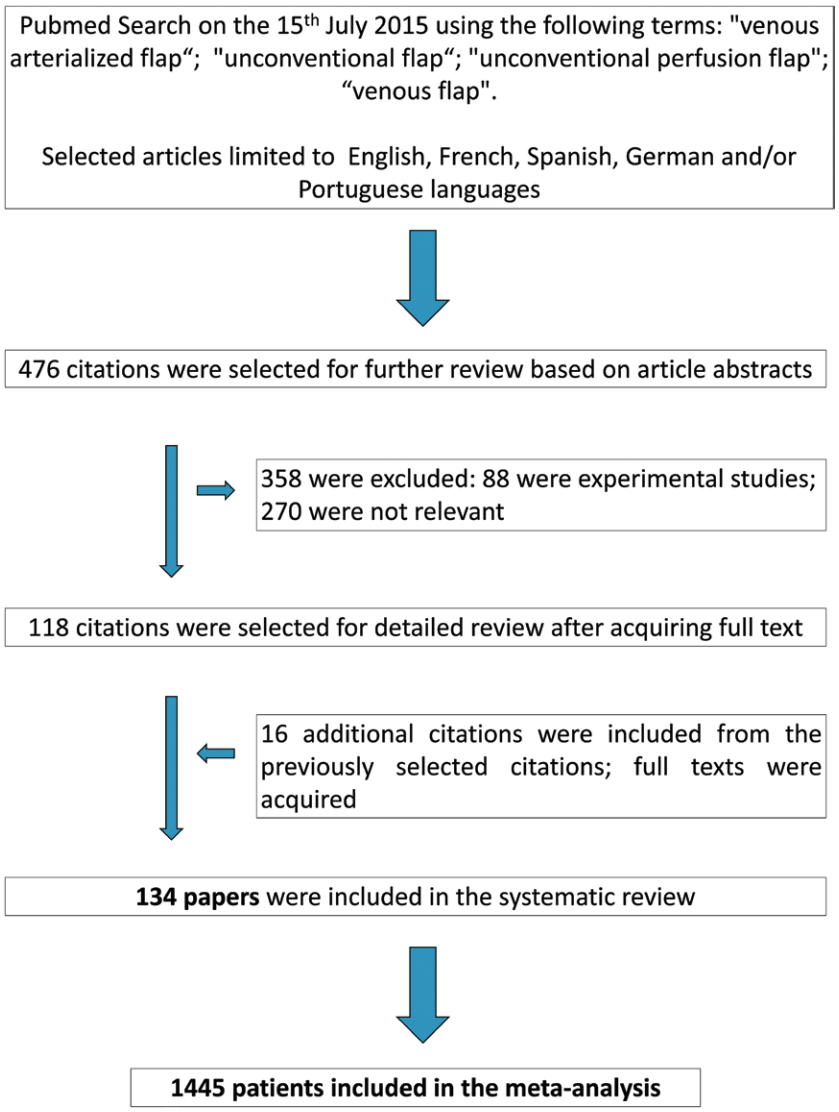

Fig. 1. Data collection from the literature. A total of 134 articles were obtained, corresponding to data from 1445 individual patients.

The data were retrieved from the available literature, each parameter at a time, from each report separately. Finally, the data were inserted into an Excel database (Microsoft Corp., Redmond, Wash.). When discrepancies were found in data retrieval, the articles were reanalyzed by the two reviewers independently.

Qualitative variables were expressed as percentages. Quantitative variables were expressed as means ± SD. The Comprehensive Meta-Analysis 2.0 software (Biostat, Englewood, N.J.) was used to estimate population summary effects and to produce forest plots using random-effects models. IBM SPSS Version 21.0 software (IBM Corp., Armonk, N.Y.) was used for descriptive and inferential statistical analysis. The Kolmogorov-Smirnov test was used to assess whether variables were distributed normally. Analysis of variance and t test were used to compare averages in normally distributed data. Kruskal-Wallis and Mann-Whitney tests were used to compare means in nonnormally distributed data. Proportions were analyzed with the chi-square test or Fisher's exact test. Dichotomous variables were compared with the binomial test. A two-tail value of $p < 0.05$ was considered to be statistically significant.

RESULTS

A total of 134 studies were found regarding the clinical application of unconventional perfusion flaps, encompassing(1445 patients Fig. 1). (**See Table, Supplemental Digital Content 1**,

Vascular patterns referred to in the literature	General description		First description	Classifications	Main clinical indications
Venous arterialized flaps	"Arterialized venous flow-through flaps" Orthodromic blood flow (blood flows in the same direction as venous valves open)	Straight venous pattern akin to a standard vein graft	Yoshimura 1987 (37)	IA (Woo) III (Chen)	Small, long and narrow defects (19) Can be used for simultaneous vascular reconstruction (19)
		Y-shaped pattern	Mimoun 1986 (34)	IB (Woo) III (Chen)	
	Antidromic blood flow (blood flows in the opposite direction of venous valves opening in the afferent vein)	Y-shaped pattern	Kovacs 1998 (6)	IIA (Woo)	Medium-sized defects (19) Can be used for simultaneous vascular reconstruction (19)
		H-shaped pattern	Chia 1988 (39)	IIB (Woo)	
	Anti and orthodromic blood flow (mixed pattern of through and against-valve blood flow)		Vaubel 1975 (1)	III (Woo)	Large defects (19) Can be used for simultaneous vascular reconstruction (19)
	Pedicled arterialized venous flap (blood enters the flap antidromically and leaves orthodromically through preserved efferente veins)		Kayikcioglu 1998 (84)	-	Medium-sized limb defects (84)
	Single vein arterialized venous flap (blood enters the flap through a single vessel; usually venous drainage is ensured by medical leeches)		Hussman 1996 (17)	-	Reported in cases of replantation of body parts in which a single vein can be used for vascular anastomosis (17, 18)

Fig. 2. (*Continued*).

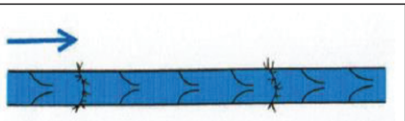	Venous flaps	Free venous flow through flap (the flap is nourished exclusively by venous blood flowing orthodromically)	Honda 1984 (31)	I (Chen)	Can be used for simultaneous vascular reconstruction (31)
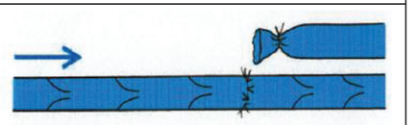		Distally pedicled based venous flap	Amarante 1988 (38)	IIA (Chen)	Upper and lower limb defects small and medium defects (38)
		Proximally pedicled venous flap	Chavoin 1987 (35)	IIB (Chen)	Upper and lower limb defects small and medium defects (35)
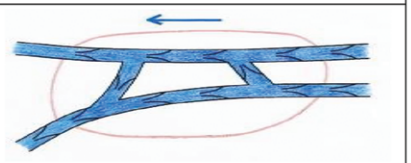		Sliding venous flap (the flap is transposed based exclusively on the dissected venous network)	Inada 1991 (50)	-	Useful for mobilizing adjacent tissues in areas where the superficial venous network is well developed, such as the dorsum of fingers and toes (50)
	Arterialized venous arterial flap	Arterialized venous arterial (AVA) flow through flap	Townsend 1984 (32)	IA (Woo) IV (Chen)	Can be used for simultaneous vascular reconstruction Can incorporate long nerve segments (32)
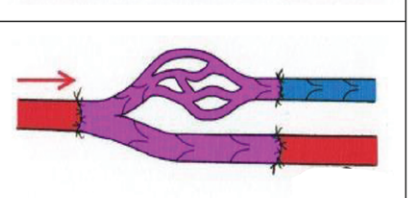		Arterialized venous arterial (AVA) flow through flap with ≥ 1 additional discontinuous efferent veins	Rozen 2012 (136)	IV (Chen)	Can be used for simultaneous vascular reconstruction (19)

Fig. 2. (*Continued*). Schematic representation of the different types of unconventional perfusion flaps described in the literature, their respective classification, and reported clinical applications. Unconventional perfusion flaps receive blood through one or more of their veins. This blood may be arterial or venous. Unconventional perfusion flap venous drainage occurs through one or more veins to adjacent veins and/or arteries. *Red area* represents arterial blood flow. *Blue* and *purple regions* represent venous and mixed arterial and venous blood, respectively. *Arrows* indicate the direction of blood flow. *Curved lines* inside the vessels represent venous valves. The drawings are not to scale. The classifications used were those proposed by Woo et al. (Woo SH, Kim KC, Lee GJ, et al. A retrospective analysis of 154 arterialized venous flaps for hand reconstruction: An 11-year experience. *Plast Reconstr Surg.* 2007;119:1823–1838.) and by Chen, Tang, and Noordhoff (Chen HC, Tang YB, Noordhoff MS. Four types of venous flaps for wound coverage: A clinical appraisal. *J Trauma* 1991;31:1286–1293).

which summarizes the information present in these studies,[1,2,6–8,10,11,13,15,16,18–22,31,32,36,38–152] ***http://links.lww.com/PRS/B785.***) All studies were clinical observational studies. The average number of patients included in each study was 11.3 ± 17.7. The most common countries where these studies were conducted were, in decreasing order of frequency, Japan (25.9 percent), United States (12.6 percent), China/Taiwan (10.4 percent), South Korea and Turkey (8.1 percent each), and Germany (6.7 percent). According to the Grades of Recommendation, Assessment, Development and Evaluation quality assessment criteria, the quality of these studies was low in 48.9 percent and very low in 50.4 percent of cases. The largest series was presented by Woo et al. in 2007, corresponding to 154 cases of arterialized venous flaps.[20] The different types of unconventional perfusion flaps and their main clinical applications are illustrated in Figure 2.

There were more male than female patients being submitted to unconventional perfusion flap reconstruction (76.26 percent versus 23.74 percent; $p < 0.001$). Patients' average age was 37.10 ± 16.69 years ($n = 629$), varying between 1 and 86 years. Flap size varied between 1.0 and 390.0 cm^2, presenting an average size of 27.36 ± 42.52 cm^2 ($n = 795$).

Most defects mandating unconventional perfusion flap reconstruction were caused by trauma (63.6 percent). However, defects also resulted from tumor extirpation (13.5 percent), burns (8.7 percent), congenital malformations (1.8 percent), infections (1.2 percent), Dupuytren's disease treatment and/or scar contracture release (4.6 percent), and venous ulcer coverage (0.1 percent). These defects were distributed by the following anatomical regions: head and neck (8.5 percent), arm and forearm (4.4 percent), hand and fingers (75.1 percent), leg (2.6 percent), trunk and genitals (4.7 percent), and foot (4.7 percent). As shown in Figure 3, type I arterialized venous flaps were the most commonly used unconventional perfusion flaps for reconstructing the head, neck, hand, fingers, and foot ($p < 0.05$). "Arterialized venous arterial" flow-through flaps were the most frequent unconventional perfusion flaps used in the reconstruction of the arm and forearm ($p < 0.05$). For reconstructing leg defects, venous flaps were preferred ($p < 0.05$).

The most common donor sites were, in decreasing frequency, the forearm (61.8 percent), the hand and fingers (18.9 percent), foot and toes (9.8 percent), lower leg (8.4 percent), thigh (0.4 percent), and groin (0.2 percent). Unconventional perfusion flap composition was rather heterogeneous: skin, skin appendages, and subcutaneous fat (87.3 percent); skin, subcutaneous fat, and subcutaneous nerves (8.1 percent); skin, subcutaneous fat, and tendon(s) (3.5 percent); skin, tendon(s), nerve(s), and bone (0.6 percent); skin and cartilage (0.3 percent); skin, subcutaneous fat, and bone (0.1 percent); and bone (0.1 percent).

Meta-analysis of the survival rate of unconventional perfusion flaps using the Comprehensive Meta-Analysis 2.0 software and a random effects model, estimated an overall survival rate of 89.5 percent (95 percent CI, 87.3 to 91.3; $p < 0.001$). Using the same methodology, 92.0 percent of unconventional perfusion flaps (95 percent CI, 89.9 to 93.7 percent; $p < 0.001$) were estimated to present complete or nearly complete survival, and only 7.5 percent (95 percent CI, 5.9 to 9.5 percent; $p < 0.001$) of unconventional perfusion flaps presented complete or nearly complete necrosis (Figs. 4 and 5). This pattern of most flaps presenting complete or nearly complete survival was observed in all types of unconventional perfusion flaps ($p \leq 0.003$).

The survival and complications of the different types of unconventional perfusion flaps is illustrated in Table 1 and in Figures 6 and 7. The main complication of all types of unconventional perfusion flaps was a variable degree of necrosis. Globally, 7.5 percent of flaps presented marginal necrosis; 9.2 percent and 5.5 percent had significant and complete necrosis, respectively. Less common complications included need for anastomoses revision (1.2 percent), infection (0.9 percent), and hematoma formation (0.5 percent) (Figs. 8 and 9).

Figure 6 illustrates the characteristics of the major types of unconventional perfusion flaps, and their main applications and results. Overall, there was a negative correlation between flap size and complete flap survival (Pearson coefficient, –0.354; $p < 0.001$). In addition, there was a positive correlation between average flap size and the following variables: presence of significant necrosis (Pearson coefficient, 0.263; $p = 0.028$), average rate of complications (Pearson coefficient, 0.441; $p < 0.001$), presence of epidermolysis (Pearson coefficient, 0.270; $p = 0.028$), rate of postoperative infection (Pearson coefficient, 0.663; $p < 0.001$), and need for a new flap (Pearson coefficient, 0.373; $p = 0.003$). Flaps with an area over 20 cm^2 were not correlated with higher necrosis rates than smaller flaps, after stratifying for flap type. No statistically significant differences were found

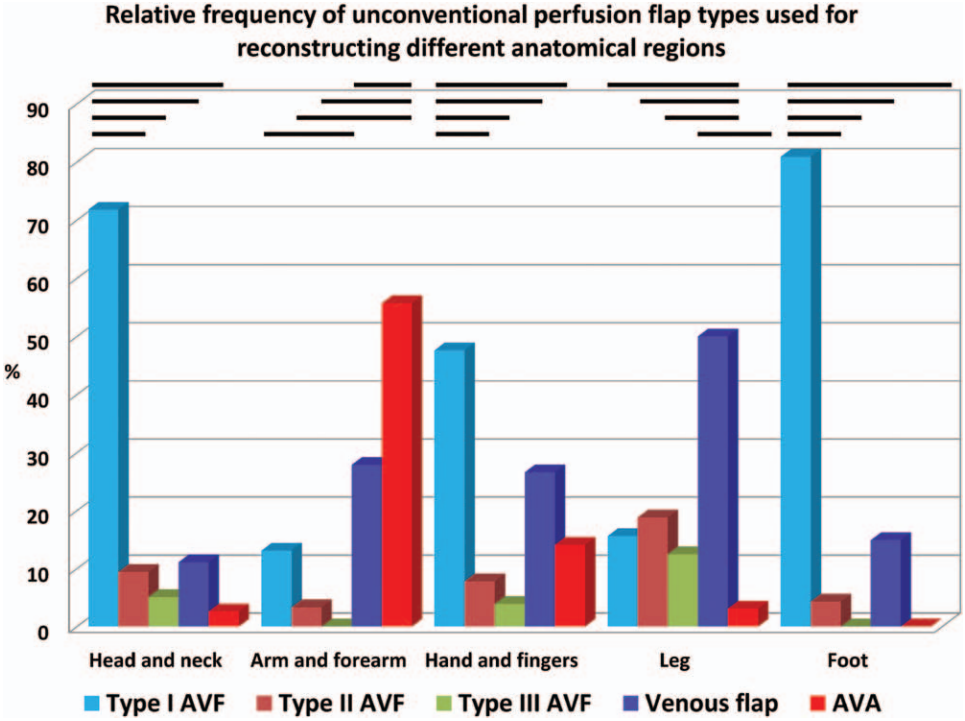

Fig. 3. Bar chart depicting the relative frequency of unconventional perfusion flap types used for reconstructing different anatomical regions. The *lines above the bars* indicate statistically significant differences in the relative frequency of major unconventional perfusion flap types ($p < 0.05$). *AVF*, arterialized venous flap; *AVA*, arterialized venous arterial flap.

among the different types of unconventional perfusion flaps regarding overall survival rates, categorical flap survival, or complications rates (Figs. 8 through 10).

The rate of postoperative infection was 3.79 ± 17.57 percent. The need for a new flap after an unconventional perfusion flap was observed in 7.90 ± 21.46 percent of cases. There was a positive correlation between the rate of postoperative infection and the need for a new flap (Pearson coefficient, 0.405; $p = 0.001$). When clinically significant postoperative infection was noted, unconventional perfusion flap loss requiring a new flap occurred in 50 percent of cases ($n = 4$; $p < 0.001$). No association was found between wound bed blood supply and unconventional perfusion flap survival.

Overall flap survival rates were 82.93 ± 37.86 percent in the head and neck ($n = 82$), 91.94 ± 27.45 percent in the arm and forearm ($n = 62$), 95.33 ± 21.10 percent in the hand and fingers ($n = 1050$), 84.85 ± 36.41 percent in the leg ($n = 33$), and 86.57 ± 34.36 percent in the foot ($n = 67$). Unconventional perfusion flaps used to reconstruct the upper limb showed better overall survival rates than those transferred to the head and neck or to the lower limb ($p < 0.001$) (Fig. 8). No difference was found in the survival rate of unconventional perfusion flaps used for reconstructing defects of different origin.

Digital replantation as arterialized venous flaps showed complete survival in all cases reported ($n = 3$).[19] The single-vein arterialized venous flap also showed a survival rate of 100 percent in three cases of ear replantation.[19,21,22]

Comparing study results before and after the 2007 article by Woo et al.,[20] several significant differences were noted: the average unconventional perfusion flap survival area increased from 91.10 ± 16.83 cm^2 to 97.65 ± 1.68 cm^2 ($p = 0.01$), the proportion of unconventional perfusion flaps with complete survival increased from 74.22 ± 29.48 percent to 87.85 ± 20.83 percent ($p = 0.16$), the percentage of unconventional perfusion flaps undergoing complete necrosis decreased from 6.24 ± 12.75 to 1.76 ± 3.87 ($p = 0.009$), and the proportion of flaps implanted on nonperfused wound beds increased from 43.84 ± 35.56 percent to 71.56 ± 35.61 percent ($p = 0.043$).

DISCUSSION

Some of the lingering questions behind the use of unconventional perfusion flaps are related

Flap survival rate; 95% CI

Study name	Event rate	Lower limit	Upper limit	Z-Value	p-Value	Relative weight
Honda 1984	0,917	0,378	0,995	1,623	0,105	0,50
Townsend 1984	0,938	0,461	0,996	1,854	0,064	0,51
Gu 1985	0,857	0,573	0,964	2,346	0,019	1,66
Chavoin 1987	0,958	0,575	0,997	2,170	0,030	0,52
Thatte 1987	0,833	0,194	0,990	1,039	0,299	0,45
Tsai 1987	0,733	0,467	0,896	1,733	0,083	2,59
Yoshimura 1987	0,964	0,616	0,998	2,289	0,022	0,52
Amarante 1988	0,833	0,194	0,990	1,039	0,299	0,45
Foucher 1988	0,957	0,748	0,994	3,023	0,003	0,99
Inoue 1988	0,800	0,530	0,934	2,148	0,032	2,20
Fukui 1989	0,958	0,575	0,997	2,170	0,030	0,52
Gu 1989	0,750	0,238	0,966	0,951	0,341	0,79
Nishi 1989	0,938	0,461	0,996	1,854	0,064	0,51
Rose 1989 (b)	0,967	0,634	0,998	2,341	0,019	0,52
Thatte 1989 (a)	0,875	0,463	0,983	1,820	0,069	0,91
Thatte 1989 (b)	0,875	0,463	0,983	1,820	0,069	0,91
Inoue 1990	0,955	0,739	0,994	2,975	0,003	0,99
Nakayama 1990	0,875	0,266	0,993	1,287	0,198	0,48
Chen 1991	0,964	0,786	0,995	3,236	0,001	1,00
Fukui 1991	0,938	0,461	0,996	1,854	0,064	0,51
Inada 1991	0,929	0,423	0,996	1,748	0,081	0,50
Inoue 1991 (a)	0,900	0,326	0,994	1,474	0,140	0,49
Inoue 1991 (b)	0,813	0,553	0,938	2,289	0,022	2,23
Koshima 1991	0,875	0,266	0,993	1,287	0,198	0,48
Fasika 1992	0,833	0,194	0,990	1,039	0,299	0,45
Fukui 1993	0,938	0,461	0,996	1,854	0,064	0,51
Inoue 1993	0,917	0,378	0,995	1,623	0,105	0,50
Kamei 1993	0,875	0,266	0,993	1,287	0,198	0,48
Chen 1994	0,875	0,266	0,993	1,287	0,198	0,48
Fukui 1994	0,963	0,779	0,995	3,197	0,001	1,00
Galumbeck 1994	0,900	0,326	0,994	1,474	0,140	0,49
karacala 1994	0,964	0,616	0,998	2,289	0,022	0,52
Nishi 1994	0,906	0,746	0,969	3,741	0,000	2,44
Vesely 1995	0,667	0,154	0,957	0,566	0,571	0,71
Xiu 1995	0,938	0,461	0,996	1,854	0,064	0,51
Cheng 1996 (a)	0,944	0,495	0,997	1,947	0,052	0,51
Hussman 1996	0,942	0,856	0,978	5,412	0,000	3,12
Woo 1996	0,962	0,597	0,998	2,232	0,026	0,52
Yilmaz 1996	0,917	0,378	0,995	1,623	0,105	0,50
Cho 1997	0,923	0,609	0,989	2,387	0,017	0,96
Iwasawa 1997	0,933	0,648	0,991	2,550	0,011	0,97
Klein 1997	0,724	0,538	0,856	2,323	0,020	4,19
Ueda 1997	0,900	0,326	0,994	1,474	0,140	0,49
Inoue 1998	0,842	0,608	0,948	2,661	0,008	2,30
Kantarci 1998	0,905	0,689	0,976	3,028	0,002	1,74
Kayikcioglu 1998	0,875	0,463	0,983	1,820	0,069	0,91
Kovács 1998	0,600	0,297	0,842	0,628	0,530	2,20
Ayad 1999	0,950	0,525	0,997	2,029	0,042	0,51
Cho 1999	0,833	0,194	0,990	1,039	0,299	0,45
Patradul 1999	0,955	0,552	0,997	2,103	0,035	0,52
Klein 2000	0,692	0,533	0,816	2,337	0,019	5,20
Reinoso 2000	0,919	0,777	0,974	4,031	0,000	2,46

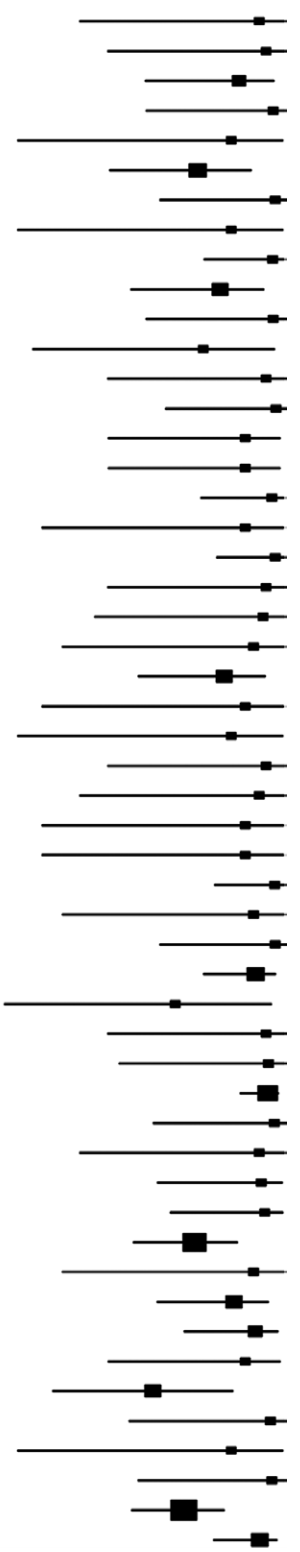

Fig. 4. (*Continued*).

Takeuchi 2000	0,833	0,194	0,990	1,039	0,299	0,45
Murata 2001	0,938	0,461	0,996	1,854	0,064	0,51
Woo 2001 (a)	0,900	0,326	0,994	1,474	0,140	0,49
Woo 2001 (b)	0,875	0,266	0,993	1,287	0,198	0,48
Wungcharoen 2001	0,944	0,495	0,997	1,947	0,052	0,51
DeLorenzi 2002	0,925	0,792	0,976	4,185	0,000	2,48
Kushima 2002	0,960	0,765	0,994	3,114	0,002	1,00
Hussman 2003	0,943	0,857	0,978	5,444	0,000	3,12
Zhu 2003	0,200	0,027	0,691	-1,240	0,215	0,84
Koch 2004 (a)	0,964	0,616	0,998	2,289	0,022	0,52
Kopp 2004 (b)	0,929	0,423	0,996	1,748	0,081	0,50
Lin 2004	0,974	0,690	0,998	2,519	0,012	0,53
Nakazawa 2004 (a)	0,900	0,326	0,994	1,474	0,140	0,49
Titley 2004	0,833	0,194	0,990	1,039	0,299	0,45
Pellini 2006	0,958	0,575	0,997	2,170	0,030	0,52
Yokoyama 2006	0,929	0,423	0,996	1,748	0,081	0,50
Woo 2007	0,981	0,941	0,994	6,721	0,000	2,59
Brooks 2008	0,944	0,495	0,997	1,947	0,052	0,51
Hyza 2008	0,964	0,616	0,998	2,289	0,022	0,52
Kakinoki 2008	0,686	0,548	0,798	2,594	0,009	6,01
Kim 2008	0,833	0,194	0,990	1,039	0,299	0,45
Kong 2008	0,886	0,755	0,952	4,324	0,000	3,51
Yokoyama 2008 (b)	0,944	0,495	0,997	1,947	0,052	0,51
Cil 2009 (a)	0,950	0,525	0,997	2,029	0,042	0,51
Cil 2009 (b)	0,938	0,461	0,996	1,854	0,064	0,51
Lin 2010	0,969	0,650	0,998	2,390	0,017	0,52
Yokoyama 2010	0,950	0,525	0,997	2,029	0,042	0,51
Park 2011	0,875	0,463	0,983	1,820	0,069	0,91
Davami 2012	0,974	0,690	0,998	2,519	0,012	0,53
Rozen 2012 (a)	0,917	0,378	0,995	1,623	0,105	0,50
Rosen 2012 (b)	0,972	0,678	0,998	2,479	0,013	0,53
Yan 2012	0,982	0,770	0,999	2,808	0,005	0,53
Yu 2012	0,929	0,423	0,996	1,748	0,081	0,50
Kawakatsu 2013	0,929	0,423	0,996	1,748	0,081	0,50
Lam 2013	0,978	0,732	0,999	2,662	0,008	0,53
Ueda 2013	0,950	0,525	0,997	2,029	0,042	0,51
Walle 2013	0,909	0,561	0,987	2,195	0,028	0,95
Yan 2013	0,962	0,597	0,998	2,232	0,026	0,52
Giesen 2014	0,929	0,630	0,990	2,472	0,013	0,97
Han 2014	0,984	0,794	0,999	2,907	0,004	0,53
Kayalar 2014 (a)	0,938	0,461	0,996	1,854	0,064	0,51
Kayalar 2014 (b)	0,927	0,796	0,976	4,234	0,000	2,48
Liu 2014	0,958	0,575	0,997	2,170	0,030	0,52
Sakamoto 2014	0,900	0,326	0,994	1,474	0,140	0,49
Garlick 2015	0,938	0,461	0,996	1,854	0,064	0,51
Park 2015	0,962	0,597	0,998	2,232	0,026	0,52
Zor 2015	0,950	0,525	0,997	2,029	0,042	0,51
	0,895	0,873	0,913	20,084	0,000	

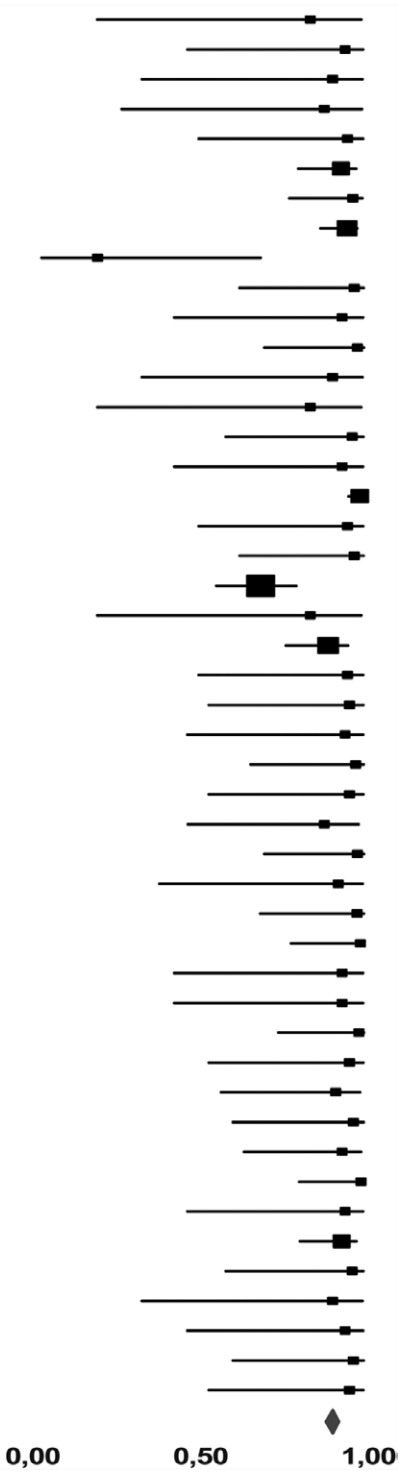

Fig. 4. (*Continued*). Forest plots of all case series reporting unconventional perfusion flaps reviewing survival rate. A random effects model was used. Meta-analysis of the survival rate of unconventional perfusion flaps, using the Comprehensive Meta-Analysis 2.0 software and random effects model, revealed an overall survival rate of 89.5 percent ($p < 0.001$; 95 percent CI, 87.3 to 91.3 percent). Using the same methodology, 92.0 percent (95 percent CI, 90.3 to 94.0 percent) of unconventional perfusion flaps showed complete or nearly complete survival ($p < 0.001$).

Proportion of complete and nearly complete survival *versus* complete or partial necrosis; 95% CI

Study name	Event rate	Lower limit	Upper limit	Z-Value	p-Value	Relative weight
Vaubel 1975	0,995	0,926	1,000	3,741	0,000	0,58
Mmoun 1986	0,995	0,926	1,000	3,741	0,000	0,58
Chavoin 1987	0,995	0,926	1,000	3,741	0,000	0,58
Thatte 1987	0,995	0,926	1,000	3,741	0,000	0,58
Tsai 1987	0,733	0,638	0,811	4,474	0,000	1,55
Yoshimura 1987	0,995	0,926	1,000	3,741	0,000	0,58
Chia 1988	0,995	0,926	1,000	3,741	0,000	0,58
Foucher 1988	0,913	0,840	0,955	6,626	0,000	1,46
Inoue 1988	0,666	0,569	0,752	3,263	0,001	1,56
Fukui 1989	0,750	0,656	0,825	4,757	0,000	1,55
Gu 1989	0,750	0,656	0,825	4,757	0,000	1,55
Nishi 1989	0,857	0,774	0,913	6,270	0,000	1,51
Rose 1989 (a)	0,995	0,926	1,000	3,741	0,000	0,58
Thatte 1989 (a)	0,875	0,795	0,927	6,435	0,000	1,50
Thatte 1989 (b)	0,750	0,656	0,825	4,757	0,000	1,55
Inoue 1990	0,772	0,680	0,844	5,111	0,000	1,54
Nakayama 1990	0,995	0,926	1,000	3,741	0,000	0,58
Chen 1991	0,892	0,815	0,940	6,546	0,000	1,48
Fukui 1991	0,713	0,617	0,793	4,109	0,000	1,55
Inada 1991	0,995	0,926	1,000	3,741	0,000	0,58
Inoue 1991 (a)	0,750	0,656	0,825	4,757	0,000	1,55
Inoue 1991 (b)	0,563	0,464	0,656	1,247	0,213	1,56
Ohtsuka 1992	0,995	0,926	1,000	3,741	0,000	0,58
Fasika 1992	0,995	0,926	1,000	3,741	0,000	0,58
Fukui 1993	0,714	0,618	0,794	4,140	0,000	1,55
Inoue 1993	0,800	0,710	0,867	5,545	0,000	1,53
Kamei 1993	0,995	0,926	1,000	3,741	0,000	0,58
Chen 1994	0,995	0,926	1,000	3,741	0,000	0,58
Fukui 1994	0,741	0,646	0,817	4,601	0,000	1,55
Galumbeck 1994	0,995	0,926	1,000	3,741	0,000	0,58
karacala 1994	0,847	0,763	0,905	6,170	0,000	1,52
Nishi 1994	0,665	0,566	0,752	3,187	0,001	1,56
Xiu 1995	0,995	0,926	1,000	3,741	0,000	0,58
Cheng 1996 (a)	0,995	0,926	1,000	3,741	0,000	0,58
Hussman 1996	0,827	0,740	0,889	5,926	0,000	1,53
Sakai 1996	0,005	0,000	0,074	-3,741	0,000	0,58
Woo 1996	0,995	0,926	1,000	3,741	0,000	0,58
Yilmaz 1996	0,800	0,710	0,867	5,545	0,000	1,53
Cho 1997	0,769	0,677	0,842	5,078	0,000	1,54
Iwasawa 1997	0,867	0,786	0,921	6,378	0,000	1,50
Klein 1997	0,721	0,626	0,800	4,270	0,000	1,55
Ueda 1997	0,995	0,926	1,000	3,741	0,000	0,58
Inoue 1998	0,520	0,427	0,612	0,417	0,676	1,57
Kantarci 1998	0,858	0,775	0,913	6,283	0,000	1,51
Kayikcioglu 1998	0,875	0,795	0,927	6,435	0,000	1,50
Kovács 1998	0,500	0,403	0,597	0,000	1,000	1,56
Ayad 1999	0,778	0,687	0,849	5,222	0,000	1,54
Cho 1999	0,995	0,926	1,000	3,741	0,000	0,58

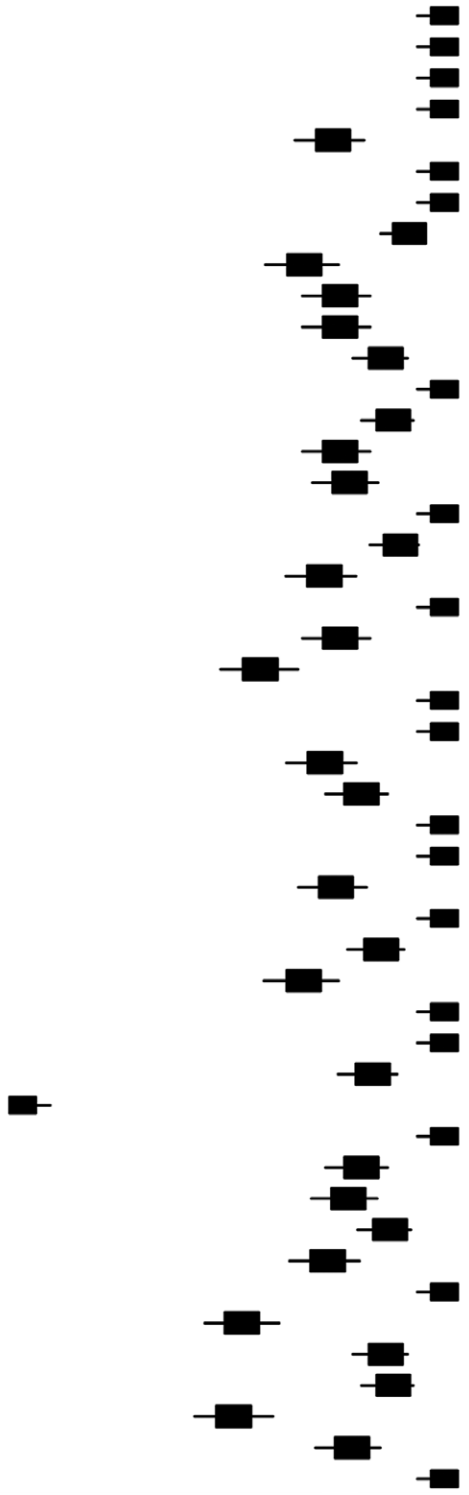

Fig. 5. (*Continued*).

Koch 1999	0,995	0,926	1,000	3,741	0,000	0,58
Cunha-Gomes 2000	0,995	0,926	1,000	3,741	0,000	0,58
Klein 2000	0,461	0,366	0,559	-0,780	0,435	1,56
Reinoso 2000	0,649	0,551	0,736	2,940	0,003	1,56
Takeuchi 2000	0,995	0,926	1,000	3,741	0,000	0,58
Chia 2001	0,995	0,926	1,000	3,741	0,000	0,58
Murata 2001	0,995	0,926	1,000	3,741	0,000	0,58
Safak 2001	0,995	0,926	1,000	3,741	0,000	0,58
Woo 2001 (b)	0,995	0,926	1,000	3,741	0,000	0,58
Wungcharoen 2001	0,995	0,926	1,000	3,741	0,000	0,58
Brooks 2002	0,995	0,926	1,000	3,741	0,000	0,58
DeLorenzi 2002	0,573	0,474	0,666	1,448	0,147	1,56
Kushima 2002	0,840	0,755	0,900	6,079	0,000	1,52
Hussman 2003	0,813	0,725	0,878	5,725	0,000	1,53
Zhu 2003	0,200	0,133	0,290	-5,545	0,000	1,53
Cheng 2004	0,995	0,926	1,000	3,741	0,000	0,58
Koch 2004 (a)	0,923	0,852	0,962	6,622	0,000	1,44
Lin 2004	0,945	0,879	0,976	6,482	0,000	1,38
Nakazawa 2004 (a)	0,995	0,926	1,000	3,741	0,000	0,58
Nakazawa 2004 (b)	0,995	0,926	1,000	3,741	0,000	0,58
Titley 2004	0,995	0,926	1,000	3,741	0,000	0,58
Hyza 2005	0,995	0,926	1,000	3,741	0,000	0,58
Yokoyama 2006	0,995	0,926	1,000	3,741	0,000	0,58
Woo 2007	0,961	0,900	0,985	6,204	0,000	1,31
Brooks 2008	0,995	0,926	1,000	3,741	0,000	0,58
Hyza 2008	0,770	0,678	0,842	5,085	0,000	1,54
Iglesias 2008	0,995	0,926	1,000	3,741	0,000	0,58
Kong 2008	0,612	0,513	0,703	2,222	0,026	1,56
Tang 2008	0,995	0,926	1,000	3,741	0,000	0,58
Trovato 2008 (a)	0,995	0,926	1,000	3,741	0,000	0,58
Trovato 2008 (b)	0,995	0,926	1,000	3,741	0,000	0,58
Yokoyama 2008 (b)	0,995	0,926	1,000	3,741	0,000	0,58
Cil 2009 (b)	0,995	0,926	1,000	3,741	0,000	0,58
Lin 2010	0,995	0,926	1,000	3,741	0,000	0,58
Yokoyama 2010	0,995	0,926	1,000	3,741	0,000	0,58
Kakinoki 2011	0,995	0,926	1,000	3,741	0,000	0,58
Rounds 2011	0,995	0,926	1,000	3,741	0,000	0,58
Davami 2012	0,995	0,926	1,000	3,740	0,000	0,58
Rozen 2012 (a)	0,995	0,926	1,000	3,741	0,000	0,58
Rosen 2012 (b)	0,995	0,926	1,000	3,741	0,000	0,58
Walle 2013	0,909	0,835	0,952	6,623	0,000	1,46
Yan 2013	0,995	0,926	1,000	3,741	0,000	0,58
Giesen 2014	0,930	0,860	0,966	6,595	0,000	1,42
Han 2014	0,871	0,790	0,924	6,397	0,000	1,50
Kayalar 2014 (a)	0,995	0,926	1,000	3,741	0,000	0,58
Kayalar 2014 (b)	0,927	0,857	0,964	6,611	0,000	1,43
Liu 2014	0,995	0,926	1,000	3,741	0,000	0,58
Momeni 2014	0,995	0,926	1,000	3,741	0,000	0,58
Sakamoto 2014	0,995	0,926	1,000	3,741	0,000	0,58
Garlick 2015	0,995	0,926	1,000	3,741	0,000	0,58
Park 2015	0,750	0,656	0,825	4,757	0,000	1,55
Zor 2015	0,770	0,678	0,842	5,085	0,000	1,54
	0,924	0,903	0,940	18,624	0,000	

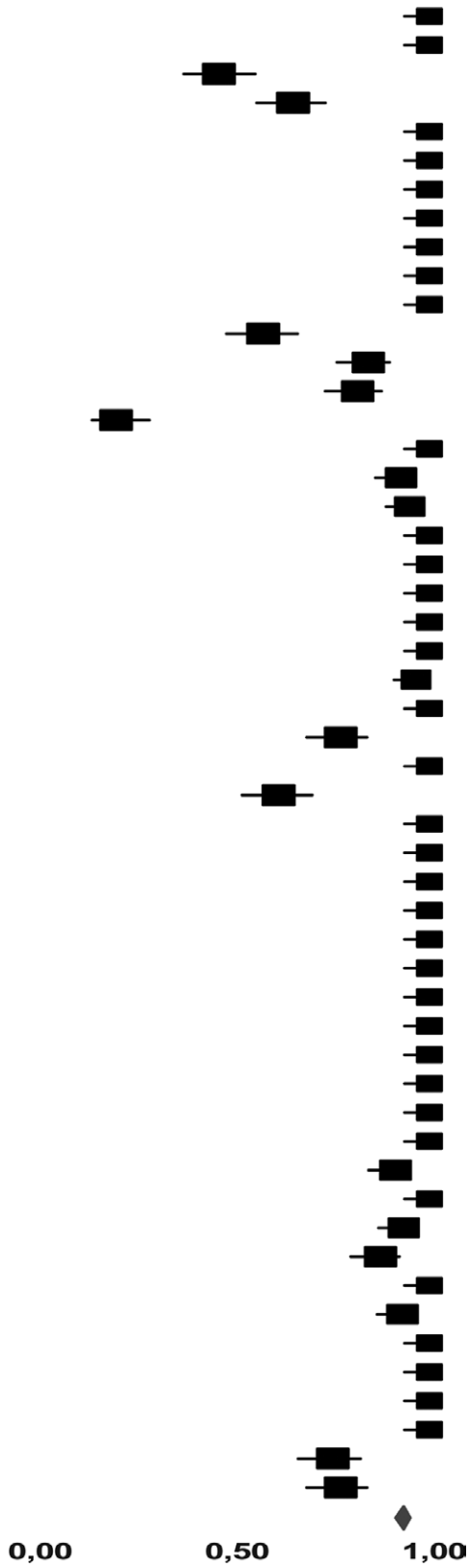

Fig. 5. (*Continued*). Forest plots of all case series reporting unconventional perfusion flaps reviewing proportion of complete and nearly complete survival versus complete or partial necrosis. A random effects model was used. Meta-analysis of the survival rate of unconventional perfusion flaps, using the Comprehensive Meta-Analysis 2.0 software and random effects model, revealed only 8.8 percent of unconventional perfusion flaps presented complete or nearly complete necrosis.

Table 1. Survival Rates and Complications of Different Unconventional Perfusion Flaps Calculated from Individual Patient Data Extracted from the Different Articles*

						Complications Other Than Necrosis			
Type of UPF	No.	Complete Survival (%)	Nearly Complete Survival (%)	Significant Necrosis (%)	Complete Necrosis (%)	None (%)	Infection (%)	Hematoma (%)	Need for Anastomosis Revision (%)
Type IA AVF	285	76.5 (218)	14 (4.9)	33 (11.6)	20 (7.0)	181 (72.4)	1 (0.4)	2 (0.8)	2 (0.8)
Type IB AVF	107	84 (78.5)	13 (12.1)	6 (5.6)	4 (3.7)	82 (76.6)	0 (0.0)	00 (0.0)	4 (3.7)
Type IIA AVF	24	24 (100.0)	0 (0.0)	0 (0.0)	0 (0.0)	23 (95.8)	0 (0.0)	0 (0.0)	0 (0.0)
Type IIB AVF	60	45 (75.0)	5 (8.3)	7 (11.7)	3 (5.0)	46 (73.0)	1 (1.6)	0 (0.0)	1 (1.6)
Type III AVF	31	26 (83.9)	4 (12.9)	0 (0.0)	1 (3.2)	26 (83.9)	1 (3.2)	0 (0.0)	0 (0.0)
Type I VF	127	88 (69.3)	19 (15.0)	8 (6.3)	12 (9.4)	93 (68.4)	3 (2.2)	0 (0.0)	3 (2.2)
Type IIA VF	40	38 (95.0)	1 (2.5)	0 (0.0)	1 (2.5)	18 (78.3)	0 (0.0)	0 (0.0)	1 (4.3)
Type IIB VF	73	46 (63.0)	12 (16.4)	13 (17.8)	2 (2.7)	34 (54.0)	0 (0.0)	2 (3.2)	0 (0.0)
Type IV AA P0	114	88 (77.2)	10 (8.8)	10 (8.8)	6 (5.3)	106 (79.1)	2 (1.5)	1 (0.8)	0 (0.0)
Type IV AA P1	17	16 (94.1)	1 (5.9)	0 (0.0)	0 (0.0)	16 (94.1)	0 (0.0)	0 (0.0)	0 (0.0)
Pedicled AVF	13	10 (76.9)	2 (15.4)	0 (0.0)	1 (7.7)	10 (76.9)	0 (0.0)	0 (0.0)	0 (0.0)
Sliding VF	7	5 (71.4)	2 (28.6)	0 (0.0)	0 (0.0)	5 (71.4)	0 (0.0)	0 (0.0)	0 (0.0)
Single vein AVF	3	3 (100.0)	0 (0.0)	0 (0.0)	0 (0.0)	3 (100.0)	0 (0.0)	0 (0.0)	0 (0.0)
Type I AVF (includes types IA AVF and IB AVF)	460	327 (76.0)	27 (6.3)	49 (11.4)	27 (6.3)	288 (72.9)	1 (0.3)	2 (0.5)	6 (1.5)
Type II AVF (includes types IIA AVF and IIB AVF)	84	69 (82.1)	5 (6.0)	7 (8.3)	3 (3.6)	69 (79.3)	1 (1.1)	0 (0.0)	1 (1.1)
Type III AVF	31	26 (83.9)	4 (12.9)	0 (0.0)	1 (3.2)	26 (83.9)	1 (3.2)	0 (0.0)	0 (0.0)
Venous flaps	247	177 (71.7)	34 (13.8)	21 (8.5)	15 (6.1)	150 65.5)	3 (1.3)	2 (0.9)	4 (1.7)
Type IV AA	131	104 (79.4)	11 (8.4)	10 (7.6)	6 (4.6)	122 (80.8)	2 (1.3)	1 (0.7)	0 (0.0)
Flap area <6 cm^2	114	100 (87.7)	5 (4.4)	8 (7.0)	1 (0.9)	89 (82.4)	2 (1.9)	1 (0.9)	1 (0.9)
Flap area 6–20 cm^2	374	306 (81.8)	23 (6.1)	20 (5.3)	25 (6.7)	198 (72.5)	2 (0.7)	1 (0.41)	3 (1.1)
Flap area >20 cm^2	242	174 (71.9)	33 (13.6)	19 (7.9)	16 (6.6)	134 (65.4)	3 (1.5)	2 (1.0)	3 (1.5)
All groups	1445	958 (77.8)	92 (7.5)	113 (9.2)	68 (5.5)	723 (71.2)	9 (0.9)	5 (0.5)	12 (1.2)

UPF, unconventional perfusion flap; AVF, arterialized venous flap; VF, venous flap; AA, arterialized venous arterial flap.
*Complete survival was defined as 100% survival area or superficial necrosis with self-healing of the flap's surface within the first 15 days after surgery. Nearly complete survival was defined as 90–100% flap survival or unspecified inconsequential "marginal necrosis." Significant necrosis was defined as >10% of flap necrosis. Complete necrosis was defined as 100% flap necrosis.

to their survival rate, their clinical efficacy, and their overall usefulness relative to the increasingly diverse, tailor-made, thin conventional flaps.[2–4,15] According to the present study, the estimated survival rate of unconventional perfusion flaps is 89.5 percent (95 percent CI, 87.3 to 91.3 percent; $p < 0.001$). Moreover, 92.2 percent (95 percent CI, 90.1 to 93.9; $p < 0.001$) of these flaps are estimated to present complete or nearly complete survival, whereas only 7.5 percent (95 percent CI, 5.9 to 9.5 percent; $p < 0.001$) will show complete or nearly complete necrosis. This means not only that unconventional perfusion flaps survive in most cases but, in most instances, that their survival is complete or nearly complete. However, in 7.90 ± 21.46 percent of cases, it was necessary to perform a new flap to reconstruct the defect not solved by the initial unconventional perfusion flap. In fact, it may be argued that the mentioned rate of 89.5 percent of unconventional perfusion flap survival is still lower than the frequently reported 95 to 100 percent survival rate of most conventional free flaps.[23–25] In addition, conventional flaps seldom present significant areas of necrosis, making them overall more reliable.[23–25] Notwithstanding, unconventional perfusion flaps still have unique advantages relative to conventional flaps, namely, their ease of dissection, not requiring the sacrifice of major arteries at the donor site, their thinness and pliability, and their potential to include missing tissues other than skin (i.e., tendons, nerves, and even bone).[23–25] As they can be fabricated from any combination of tissues abutting the venous system, they show remarkable versatility in the reconstruction of multiple defects, as summarized in Figure 2.

In addition, unconventional perfusion flaps are important options to consider in replantation of severed body parts (e.g., digits) for two distinct reasons. On the one hand, as stated above, completely avulsed digits, with no usable artery in the amputated segment that were replanted as purely arterialized venous flaps showed complete survival in all cases reported ($n = 3$).[19] On the other hand, according to the literature on digital replantation, unconventional perfusion flaps are frequently

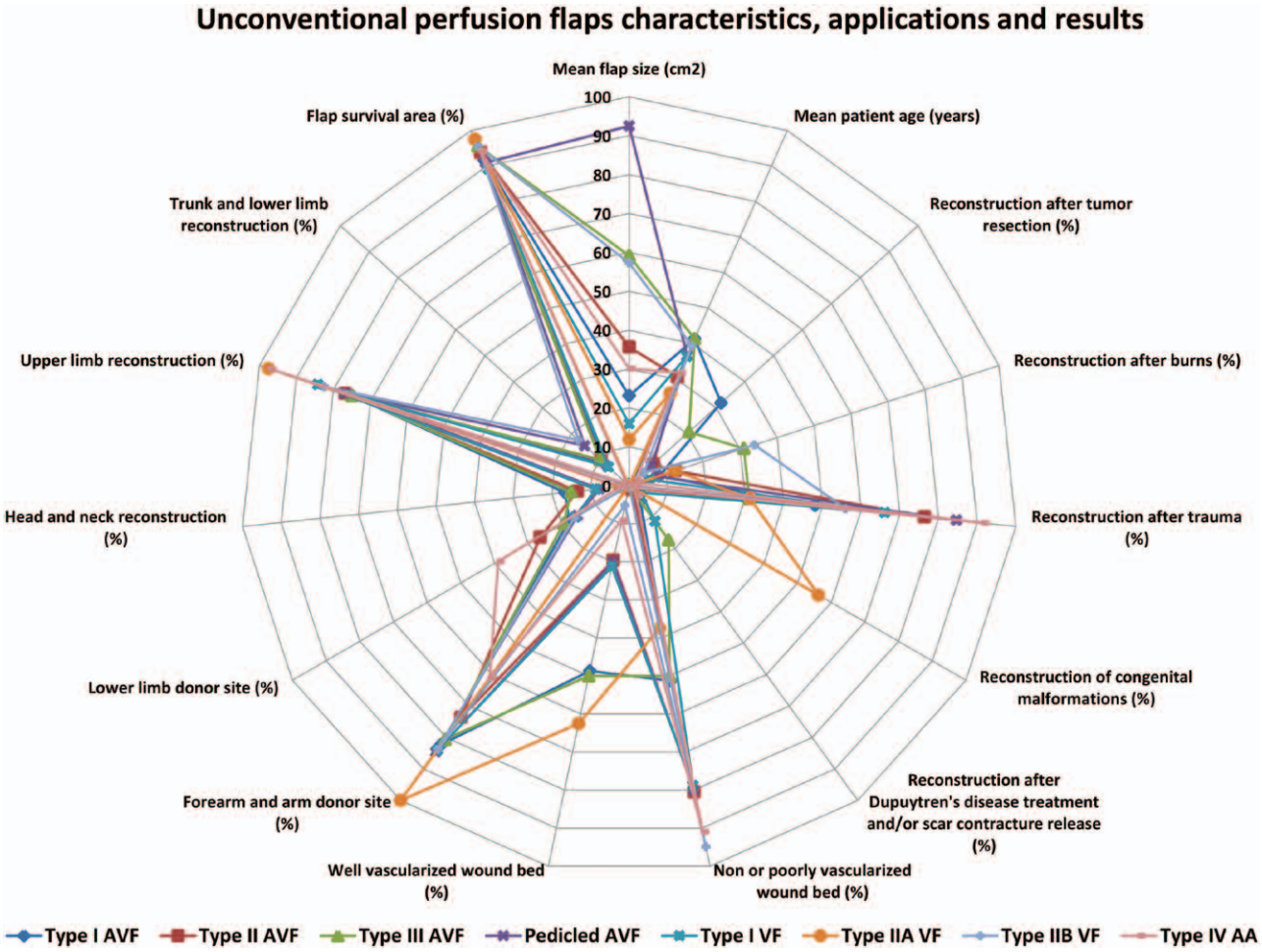

Fig. 6. Star plot illustrating unconventional perfusion flap characteristics, applications, and clinical results. *AVF*, arterialized venous flap; *VF*, venous flap; *AA*, arterialized venous arterial flap.

used to bridge skin defects in the amputation zone, fulfilling the double purpose of reconstructing vascular and skin defects in amputated segments that are otherwise replanted in a conventional fashion.[20,23–26] In summary, the literature suggests that even in the context of trauma and eventually prolonged ischemia commonly associated with digital amputation, unconventional perfusion flaps may be useful options to bear in mind.

Interestingly, the single-vein arterialized venous flap also showed a survival rate of 100 percent in three cases of ear replantation.[19,21,22] This latter finding is somewhat counterintuitive, because a necessary condition for blood to flow in any given capillary network is a pressure gradient between the afferent side and the efferent side. However, in two of the three studies referring to single-vein arterialized venous flap ear replantation, medical leeches were used, which probably created a venous outflow that allowed flap blood perfusion.[19,21,22]

Noteworthy is the fact that unconventional perfusion flaps used to reconstruct the upper limb showed better viability than those transferred to the head and neck or to the lower limb ($p < 0.001$). To the best of the authors' knowledge, this has not been reported before and thus deserves further study. One reason for this difference in the viability of unconventional perfusion flaps in distinct anatomical areas may be related to the diverse venous pressures in these areas.[27] One may argue that the relatively low venous pressure in the head and neck region may lead to rapid blood flow in the central veins of the flap, making the peripheral region of the flap more prone to critical ischemia and necrosis. In contrast, in the lower limb, the higher venous pressure may diminish the gradient between the inflow and outflow veins, making global flap perfusion less efficient. However, these hypotheses lack further experimental and clinical validation.

There was a positive correlation between average flap size and the following variables: presence

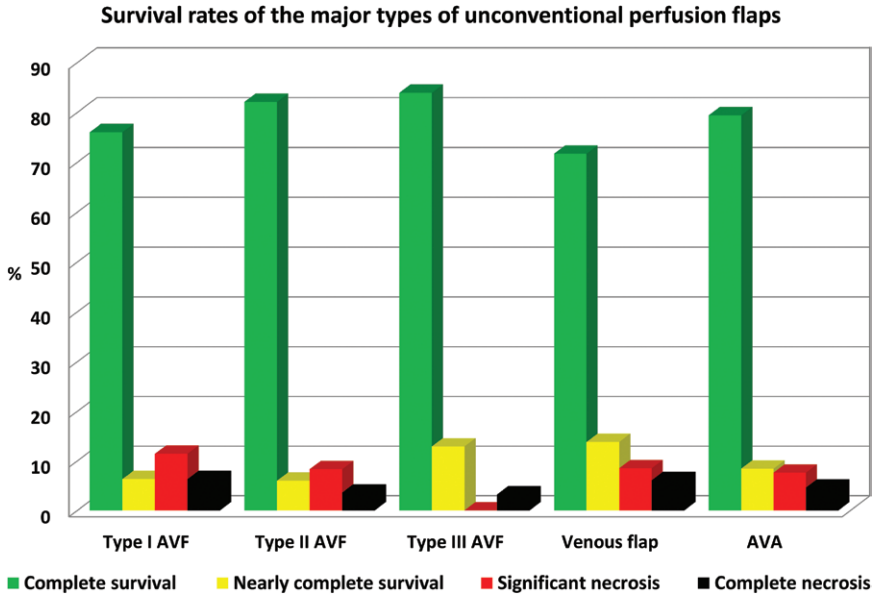

Fig. 7. Bar charts illustrating the survival of the most common types of unconventional perfusion flaps. *AVF*, arterialized venous flap; *AVA*, arterialized venous arterial flap. There were no statistically significant differences among the different types of unconventional perfusion flaps ($p < 0.05$).

of significant necrosis (Pearson coefficient, 0.263; $p = 0.028$), average rate of complications (Pearson coefficient, 0.441; $p < 0.001$), presence of epidermolysis (Pearson coefficient, 0.270; $p = 0.028$), rate of postoperative infection (Pearson coefficient, 0.663; $p < 0.001$), and need for a new flap (Pearson coefficient, 0.373; $p = 0.003$). This suggests that, as a general rule, unconventional perfusion flaps should be kept relatively small and thin, as has been proposed by several authors.[20,23–26] However, regarding categorical flap size, flaps with an area over 20 cm^2 were not correlated with higher complete necrosis rates. This may be partly explained by publication bias, as authors are less likely to

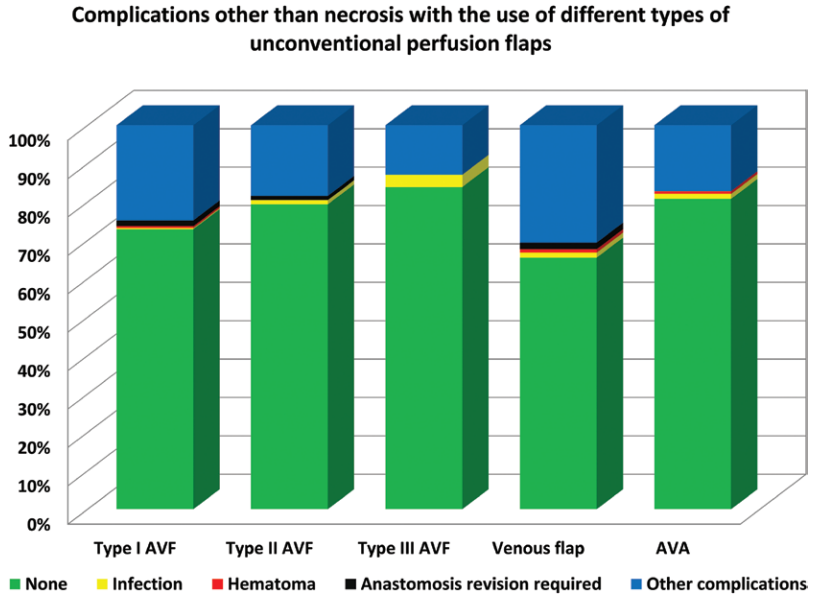

Fig. 8. Stacked column chart illustrating complications other than necrosis with the use of different types of unconventional perfusion flaps. Other complications include wound dehiscence, delayed healing, prolonged venous stasis, and significant flap congestion. *AVF*, arterialized venous flap; *AVA*, arterialized venous arterial flap.

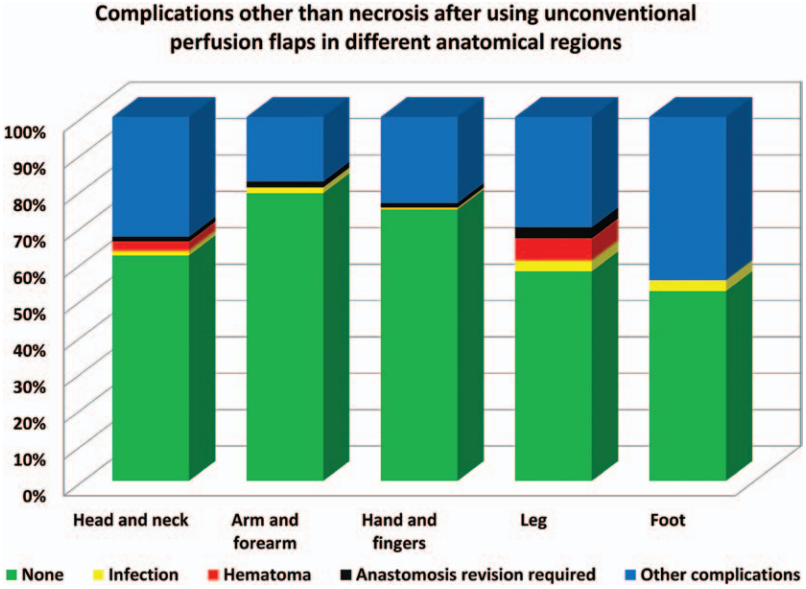

Fig. 9. Stacked column chart illustrating complications other than necrosis with the use of unconventional perfusion flaps in different anatomical regions. *AVF*, arterialized venous flap; *AVA*, arterialized venous arterial flap. Other complications include wound dehiscence, delayed healing, prolonged venous stasis, and significant flap congestion.

report large or very later unconventional perfusion flaps that suffered complete necrosis.

Contrary to what has been reported by some authors, no association was found between poorly perfused or nonperfused wound beds and flap failure. However, there was a positive correlation between the rate of postoperative infection and the need for a new flap (Pearson coefficient, 0.405; $p = 0.001$). Moreover, when clinically significant postoperative infection was noted,

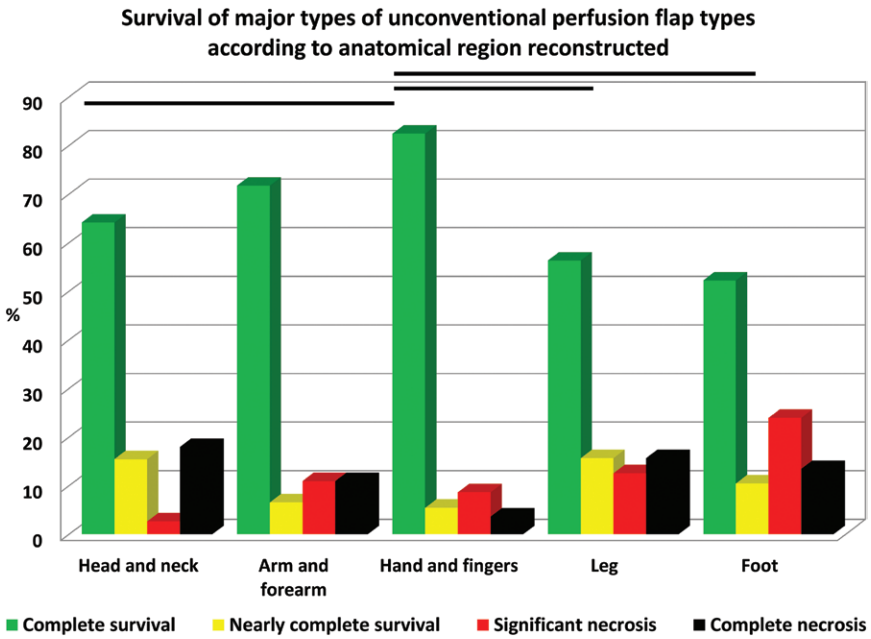

Fig. 10. Bar chart illustrating the survival of the major types of unconventional perfusion flaps according to anatomical region reconstructed. *AVF*, arterialized venous flap; *AVA*, arterialized venous arterial flap. The *lines above the bars* indicate statistically significant differences in the relative frequency of necrosis rates for each anatomical region ($p < 0.05$).

unconventional perfusion flap loss requiring a new flap occurred in 50 percent of cases ($n = 4$; $p < 0.001$). This may explain why several authors avoid using unconventional perfusion flaps when dealing with infected wound beds.[12]

It is interesting to note that the 2007 article published by Woo et al., based on their large experience of over 150 arterialized venous flaps, marks a turning point in the literature on unconventional perfusion flaps, probably by helping to clarify the physiology, vascular architecture, and clinical application of these flaps.[20] In fact, comparing study results before and after this seminal work, several differences were noted: the average unconventional perfusion flap survival area increased from 91.10 ± 16.83 cm^2 to 97.65 ± 1.68 cm^2 ($p = 0.01$), the proportion of unconventional perfusion flaps with complete survival increased from 74.22 ± 29.48 percent to 87.85 ± 20.83 percent ($p = 0.16$), the percentage of unconventional perfusion flaps undergoing complete necrosis decreased from 6.24 ± 12.75 to 1.76 ± 3.87 ($p = 0.009$), and the proportion of flaps implanted on nonperfused wound beds increased from 43.84 ± 35.56 percent to 71.56 ± 35.61 percent ($p = 0.043$). In this article, Woo et al. classified arterialized venous flaps into three major types, taking into account blood flow direction inside the venous system and its orientation relative to the venous valves, the venous architecture inside the flap, and the number of recipient veins (Fig. 2).[20] In addition, clear indications regarding the size and ideal clinical applications of each flap type were given in that article, which may have helped optimize their use.[20] A similar attempt at systematizing the various types of venous flaps has been made by Chen, Tang, Noordhoff, and Goldschlager (Fig. 2).[56]

It is noteworthy that 71.8 percent of all reported studies on unconventional perfusion flaps were conducted in seven countries alone (i.e., Japan, United States, People's Republic of China, Taiwan, Republic of Korea, Turkey, and Germany). These data suggest that these flaps are not yet routinely performed worldwide, and that they are probably more common in countries with a longer microsurgical tradition.

The authors concede that, as occurs in all systematic reviews, the present systematic review and meta-analysis may be affected by several types of bias, particularly publication bias.[28,29] The latter is related to the fact that positive results are much more likely than negative results to be published. The most effective way to minimize this type of error in meta-analysis is to perform a truly comprehensive review of the literature in a given period, as the authors did in the present study.[28,29] As far as we could determine, the present work is the most extensive review on the subject of unconventional perfusion flaps, including not only the English literature, but also the French, German, Spanish, and Portuguese literature. The inclusion of the German literature brought to light, for example, that, in contrast to what is frequently stated, it was not Nakayama et al. who described for the first time an arterialized venous flap in 1981.[30] In fact, in 1975, Vaubel had already reported an arterialized venous flap to reconstruct the integumentary defect resulting from the excision of a tumor on the dorsum of the hand.[1]

As in all meta-analyses, the data were retrieved from the available literature, each parameter at a time, from each report separately. As expected, not all articles provided information for all variables. Therefore, the data extracted from the individual articles and from the individual patient data were not coincidental for all variables. As a consequence, the statistical inferences made from these data using specific statistical techniques and software to extrapolate the values of each variable to the general population were not always completely overlapping.[31] This is the reason why, for example, we observed an apparent 2.5 percent discrepancy in the estimated overall survival of unconventional perfusion flaps and the proportion of unconventional perfusion flaps that presented complete or nearly complete survival. However, we would like to point out that the estimated survival rate of unconventional perfusion flaps was 89.5 percent, but the 95 percent confidence interval of this estimate was 87.3 to 91.3 percent. Furthermore, the estimated proportion of unconventional perfusion flaps that presented complete or nearly complete survival was 92.0 percent, but the 95 percent confidence interval of this estimate was 89.9 to 93.7 percent. Therefore, although these variables were not absolutely coincidental, there was an overlap in the estimated 95 percent confidence interval of 89.9 to 91.3 percent ($p < 0.001$). These confidence intervals reflect the inherent uncertainty in producing estimates for the general population, describing a range of values within which we can reasonably expect the true value to be.[32]

Another limitation of the present work is that all studies included are composed of case series and case reports, which are merely observational studies. According to the Grades of Recommendation, Assessment, Development and Evaluation

quality assessment criteria, the quality of evidence in these studies was low in 48.9 percent and very low in 50.4 percent of cases. This proportion is similar to proportions reported in many systematic reviews and meta-analyses in the field of plastic surgery.[33] To diminish the effect of biases caused by small series inclusion, when estimating the average flap survival rate and the proportion of complete and nearly complete survival versus complete or partial necrosis, the authors included only studies with a low quality of evidence score (Fig. 3). Figure 3 shows that the effect sizes are reasonably constant from study to study, which suggests that it is appropriate to compute summary effect sizes with these data for these two variables.[32,34]

Finally, it is well known that in technically demanding procedures, such as those involved in planning and executing unconventional perfusion flaps, heterogeneity of surgeons and patients alike, in different centers in various parts of the world, may yield substantially different results in apparently similar circumstances.[35] Thus, because of the possibility that the results presented in this article may be somewhat affected by these biases and limitations, prospective studies comparing conventional and unconventional perfusion flaps are still warranted to better assess the true survival rate and advantages of the latter.

According to the available literature, unconventional perfusion flaps, conventional free flaps, and local conventional flaps each present potential advantages and disadvantages (Table 2). For example, most unconventional perfusion flaps and all conventional free flaps require microsurgical skills and instruments. In addition, they are associated with longer operative times. Thus, these two types of flaps may be precluded in patients with significant comorbidities in whom prolonged surgery would be too risky. In this context, local pedicled flaps may be advantageous. Notwithstanding, it should be noted that the latter type of flap may be limited by the quality and quantity of local tissues. Moreover, because of frequent anatomical variations, local and free conventional flaps often require preoperative imaging and/or ultrasound evaluation.[36] In contrast, unconventional perfusion flaps can often be raised after visual inspection of the venous system, without the need for these ancillary examinations. In addition, unconventional perfusion flaps provide the significant advantage of allowing a natural thin, pliable covering of integumentary defects (i.e., in hands, feet, and genitalia).[3,37]

This systematic review shows that some degree of flap congestion and epidermolysis was invariably described with use of unconventional perfusion flaps. This may make the postoperative

Table 2. Comparison of the Advantages and Disadvantages of Unconventional Perfusion Flaps, Conventional Free Flaps, and Conventional Local Flaps in the Clinical Setting

Type of Flap	Unconventional Perfusion Flaps	Conventional Free Flaps	Conventional Local Flaps
Advantages	Thin and pliable; easy to plan and to harvest; can include different structures abutting the flap's venous system (e.g., tendons, nerves, cartilage, bone); can be easily tailored to reconstruct small to large vascular defects; minimal donor-site morbidity (often can be programmed to allow primary closure of the donor region; do not require sacrificing an arterial source); can be used as rescue flaps in the absence of arteries in amputated segments (e.g., digits or ear parts)	Can be tailored to include multiple tissues in various geometric arrangements; can be used to transfer distant tissues with high metabolic rates such as muscle and bowel; minimal or no necrosis in the majority of cases; easy and standardized postoperative monitoring in most cases	Usually do not require microsurgical skills; tissue transfer is relatively easy and fast, which is important in patients in whom prolonged surgery is not advisable; allow reconstruction with similar neighboring tissues; flap thickness is usually similar to that of the neighboring defect; minimal or no necrosis in the majority of cases; easy and standardized postoperative monitoring
Disadvantages	Difficult postoperative monitoring; some degree of unpredictability; frequent epidermolysis, congestion and marginal necrosis; more prone to necrosis in the presence of infection; often requires microsurgical skills; longer operating times than local flaps	Usually bulkier; thinning the flap through perforator dissection requires advanced microsurgical expertise; affected by unpredictable anatomical variation, often demanding preoperative imaging or ultrasound evaluation; greater donor-site morbidity (demands the sacrifice of a donor-site artery); always requires microsurgical skills; usually more laborious and time consuming to harvest than unconventional perfusion flaps	Choices limited by type, quality, and quantity of local tissues; add an additional injury to an already damaged body segment; when large local flaps are harvested, additional flaps or grafts are required to reconstruct the secondary defect; perforator flaps are based on perforator vessels, which are highly variable in number, location, caliber, and relationship with surrounding structures, often demanding preoperative imaging or ultrasound evaluation

surveillance of these flaps more difficult compared with conventional flaps.[2–4,15]

CONCLUSIONS

According to this meta-analysis, the estimated survival rate of unconventional perfusion flaps is 89.5 percent (95 percent CI, 87.3 to 91.3 percent; $p < 0.001$). Thus, these flaps are safe in most circumstances, and should probably be used more liberally, particularly in the realm of upper limb reconstruction.

Diogo Casal, M.D.
Anatomy Department
Nova Medical School
Campo dos Mártires da Pátria, 130
Lisbon 1169-056, Portugal
diogo_bogalhao@yahoo.co.uk

ACKNOWLEDGMENTS

Diogo Casal, M.D., received a grant from the Programme for Advanced Medical Education sponsored by Fundação Calouste Gulbenkian, Fundação Champalimaud, Ministério da Saúde and Fundação para a Ciência e Tecnologia, Portugal. The authors are very grateful to Nuno Folque for producing all the drawings contained in this article.

REFERENCES

1. Vaubel W. Indication and technic for arterialized grafts for the covering of large defects in the hand area (in German). *Hefte Unfallheilkd.* 1975;126:381–384.
2. Goldschlager R, Rozen WM, Ting JW, Leong J. The nomenclature of venous flow-through flaps: Updated classification and review of the literature. *Microsurgery* 2012;32:497–501.
3. Yan H, Brooks D, Ladner R, Jackson WD, Gao W, Angel MF. Arterialized venous flaps: A review of the literature. *Microsurgery* 2010;30:472–478.
4. Yan H, Zhang F, Akdemir O, et al. Clinical applications of venous flaps in the reconstruction of hands and fingers. *Arch Orthop Trauma Surg.* 2011;131:65–74.
5. Jabir S, Frew Q, El-Muttardi N, Dziewulski P. A systematic review of the applications of free tissue transfer in burns. *Burns* 2014;40:1059–1070.
6. Thatte RL, Thatte MR. The saphenous venous flap. *Br J Plast Surg.* 1989;42:399–404.
7. Zhu C, Zhang F, Lei MP, Oswald T, Lineaweaver WC. Clinical case experience using microsurgical venous flaps for soft-tissue coverage of the lower extremity. *J Reconstr Microsurg.* 2003;19:173–177.
8. Tsai TM, Matiko JD, Breidenbach W, Kutz JE. Venous flaps in digital revascularization and replantation. *J Reconstr Microsurg.* 1987;3:113–119.
9. Klein C. Experiences with an arterialized venous flap for intraoral defect reconstruction (in German). *Zentralbl Chir.* 2000;125:51–55.
10. Kovács AF. Comparison of two types of arterialized venous forearm flaps for oral reconstruction and proposal of a reliable procedure. *J Craniomaxillofac Surg.* 1998;26:249–254.
11. Garlick JW, Goodwin IA, Wolter K, Agarwal JP. Arterialized venous flow-through flaps in the reconstruction of digital defects: Case series and review of the literature. *Hand (NY)* 2015;10:184–190.
12. Woon CY, Lee JY, Teoh LC. Flap resurfacing of postinfection soft-tissue defects of the hand. *Plast Reconstr Surg.* 2007;120:1922–1929.
13. Inoue G, Maeda N. Arterialized venous flap coverage for skin defects of the hand or foot. *J Reconstr Microsurg.* 1988;4:259–266.
14. Brooks D. The "reliably unreliable" venous flap. *J Hand Surg Am.* 2009;34:1361–1362; author reply 1362.
15. Yan H, Fan C, Zhang F, Gao W, Li Z, Zhang X. Reconstruction of large dorsal digital defects with arterialized venous flaps: Our experience and comprehensive review of literature. *Ann Plast Surg.* 2013;70:666–671.
16. Epidermolysis. In: Werner B, ed. *Stedman's Medical Dictionary.* 27th ed. Baltimore, Md: Lippincott Williams & Wilkins; 2000:604.
17. Guyatt GH, Oxman AD, Vist GE, et al.; GRADE Working Group. GRADE: An emerging consensus on rating quality of evidence and strength of recommendations. *BMJ* 2008;336:924–926.
18. Hussmann J, Bahr C, Steinau HU, Vaubel E. Indications for arterialization of tissue. *Langenbecks Arch Chir Suppl Kongressbd.* 1996;113:1164–1166.
19. Hussmann J, Bahr C, Russell RC, Steinau HU, Vaubel E. Experimentelle und klinische Erfahrungen mit der Stromumkehr. *GMS Interdiscip Plast Reconstr Surg DGPW* 2003:15:24–29.
20. Woo SH, Kim KC, Lee GJ, et al. A retrospective analysis of 154 arterialized venous flaps for hand reconstruction: An 11-year experience. *Plast Reconstr Surg.* 2007;119:1823–1838.
21. Trovato MJ, Agarwal JP. Successful replantation of the ear as a venous flap. *Ann Plast Surg.* 2008;61:164–168.
22. Momeni A, Parrett BM, Kuri M. Using an unconventional perfusion pattern in ear replantation-arterialization of the venous system. *Microsurgery* 2014;34:657–661.
23. Khouri RK, Cooley BC, Kunselman AR, et al. A prospective study of microvascular free-flap surgery and outcome. *Plast Reconstr Surg.* 1998;102:711–721.
24. Bui DT, Cordeiro PG, Hu QY, Disa JJ, Pusic A, Mehrara BJ. Free flap reexploration: Indications, treatment, and outcomes in 1193 free flaps. *Plast Reconstr Surg.* 2007;119:2092–2100.
25. Nakatsuka T, Harii K, Asato H, et al. Analytic review of 2372 free flap transfers for head and neck reconstruction following cancer resection. *J Reconstr Microsurg.* 2003;19:363–368; discussion 369.
26. Casal D, Gomez MM, Antunes P, Candeias H, Almeida MA. Defying standard criteria for digital replantation: A case series. *Int J Surg Case Rep.* 2013;4:597–602.
27. Fukui A, Maeda M, Inada Y, Tamai S, Mine T. An investigation of venous pressure and oxygen tension in human extremities: An experimental study of survival in pedicled venous flaps. *J Reconstr Microsurg.* 1991;7:217–221; discussion 223.
28. Borenstein M, Hedges LV, Higgins JP, Rothstein HR. Publication bias. In: Borenstein M, ed. *Introduction to Meta-analysis.* Chichester, United Kingdom: Wiley; 2009:277–292.
29. Sterne JA, Egger M, Mother D. Addressing reporting biases. In: Higgins JP, Green S, eds. *Cochrane Handbook for Systematic Review of Interventions.* Chichester, United Kingdom: Wiley-Blackwell; 2009:297–333.
30. Nakayama Y, Soeda S, Kasai Y. Flaps nourished by arterial inflow through the venous system: An experimental investigation. *Plast Reconstr Surg.* 1981;67:328–334.
31. Higgins JPT, Deeks JJ. Selecting studies and collecting data. In: Higgins JP, Green S, eds. *Cochrane Handbook of Systematic Reviews of Interventions.* Chichester, United Kingdom: Wiley-Blackwell; 2009:151–185.

32. Schünemann HJ, Oxman AD, Vist GE, et al. Interpreting results and drawing conclusions. In: Higgins JP,, Green S, eds. *Cochrane Handbook of Systematic Reviews of Interventions*. Chichester, United Kingdom: Wiley-Blackwell; 2009:359–387.
33. Margaliot Z, Chung KC. Systematic reviews: A primer for plastic surgery research. *Plast Reconstr Surg.* 2007;120:1834–1841.
34. Borenstein M, Hedges LV, Higgins JPT, Rothstein HR. Why perform a meta-analysis. In: Borenstein M, ed. *Introduction to Meta-analysis*. Chichester, United Kingdom: Wiley; 2007:9–14.
35. Lu XW, Idu MM, Ubbink DT, Legemate DA. Meta-analysis of the clinical effectiveness of venous arterialization for salvage of critically ischaemic limbs. *Eur J Vasc Endovasc Surg.* 2006;31:493–499.
36. Cil Y, Yapici AK, Kocman AE, Ozturk S. Distally based venous flap for proximal phalangeal soft tissue burn defect and web space burn contracture. *J Burn Care Res.* 2009;30:643–647.
37. Yan H, Zhang F, Akdemir O, et al. Clinical applications of venous flaps in the reconstruction of hands and fingers. *Arch Orthop Trauma Surg.* 2011;131:65–74.
38. Honda T, Nomura S, Yamauchi S, Shimamura K, Yoshimura M. The possible applications of a composite skin and subcutaneous vein graft in the replantation of amputated digits. *Br J Plast Surg.* 1984;37:607–612.
39. Townsend PL, Taylor GI. Vascularised nerve grafts using composite arterialised neuro-venous systems. *Br J Plast Surg.* 1984;37:1–17.
40. Kakinoki R, Ikeguchi R, Nankaku M, Nakamua T. Factors affecting the success of arterialised venous flaps in the hand. *Injury* 2008;39(Suppl 4):18–24.
41. Mimoun M, Baux S, Kirsch JM, Fahed I. An original flap: The arterialized venous flap (in French). *Ann Chir Plast Esthet.* 1986;31:219–224.
42. Chavoin JP, Rouge D, Vachaud M, Boccalon H, Costagliola M. Island flaps with an exclusively venous pedicle: A report of eleven cases and a preliminary haemodynamic study. *Br J Plast Surg.* 1987;40:149–154.
43. Thatte RL, Thatte MR. Cephalic venous flap. *Br J Plast Surg.* 1987;40:16–19.
44. Yoshimura M, Shimada T, Imura S, Shimamura K, Yamauchi S. The venous skin graft method for repairing skin defects of the fingers. *Plast Reconstr Surg.* 1987;79:243–250.
45. Amarante J, Reis J. Reverse-flow island flap: Clinical report and venous drainage. *Plast Reconstr Surg.* 1988;81:137.
46. Chia SL, Cheng HH, Mao L. Free transplantation of venous network pattern skin flap. *Plast Reconstr Surg.* 1988;82:892–895.
47. Foucher G, Norris RW. The venous dorsal digital island flap or the "neutral" flap. *Br J Plast Surg.* 1988;41:337–343.
48. Fukui A, Inada Y, Maeda M, et al. Pedicled and "flow-through" venous flaps: Clinical applications. *J Reconstr Microsurg.* 1989;5:235–243.
49. Gu YD, Zhang GM, Chen DS, Yan JG, Cheng XM. Arterialized free flap: Report of four cases. *Chin Med J (Engl.)* 1989;102:140–144.
50. Nishi G, Shibata Y, Kumabe Y, Hattori S, Okuda T. Arterialized venous skin flaps for the injured finger. *J Reconstr Microsurg.* 1989;5:357–365.
51. Rose EH. Small flap coverage of hand and digit defects. *Clin Plast Surg.* 1989;16:427–442.
52. Rose EH, Kowalski TA, Norris MS. The reversed venous arterialized nerve graft in digital nerve reconstruction across scarred beds. *Plast Reconstr Surg.* 1989;83:593–604.
53. Thatte MR, Kumta SM, Purohit SK, Deshpande SN, Thatte RL. Cephalic venous flap: A series of 8 cases and a preliminary report on the use of 99mTc labelled RBCs to study the saphenous venous flap in dogs. *Br J Plast Surg.* 1989;42:193–198.
54. Inoue G, Maeda N, Suzuki K. Resurfacing of skin defects of the hand using the arterialised venous flap. *Br J Plast Surg.* 1990;43:135–139.
55. Nakayama Y, Iino T, Uchida A, Kiyosawa T, Soeda S. Vascularized free nail grafts nourished by arterial inflow from the venous system. *Plast Reconstr Surg.* 1990;85:239–245; discussion 246.
56. Chen HC, Tang YB, Noordhoff MS. Four types of venous flaps for wound coverage: A clinical appraisal. *J Trauma* 1991;31:1286–1293.
57. Inada Y, Fukui A, Tamai S, Kakihana T, Maeda M. The sliding venous flap for covering skin defects with poor blood supply on the lateral aspects of fingers. *Br J Plast Surg.* 1991;44:368–371.
58. Inoue G, Tamura Y. One-stage repair of both skin and tendon digital defects using the arterialized venous flap with palmaris longus tendon. *J Reconstr Microsurg.* 1991;7:339–343.
59. Inoue G, Maeda N, Suzuki K. Closure of big toe defects after wrap-around flap transfer using the arterialized venous flap. *J Reconstr Microsurg.* 1991;7:1–8.
60. Koshima I, Soeda S, Nakayama Y, Fukuda H, Tanaka J. An arterialised venous flap using the long saphenous vein. *Br J Plast Surg.* 1991;44:23–26.
61. Iwasawa M, Furuta S, Noguchi M, Hirose T. Reconstruction of fingertip deformities of the thumb using a venous flap. *Ann Plast Surg.* 1992;28:187–189.
62. Morris SF, MacGill KA, Taylor GI. Scalp replantation by arterialised venous network flow-through. *Br J Plast Surg.* 1992;45:187–192.
63. Ohtsuka H, Ohtani K. A free arterialized venous loop flap. *Plast Reconstr Surg.* 1992;89:965–967.
64. Fasika OM, Stilwell JH. Arterialized venous flap for covering and revascularizing finger injury. *Injury* 1993;24:67–68.
65. Fukui A, Maeda M, Tamai S, Inada Y. The pedicled venous flap: Clinical applications. *Br J Plast Surg.* 1993;46:68–71.
66. Inada Y, Fukui A, Tamai S, Mizumoto S. The arterialised venous flap: Experimental studies and a clinical case. *Br J Plast Surg.* 1993;46:61–67.
67. Inoue G, Suzuki K. Arterialized venous flap for treating multiple skin defects of the hand. *Plast Reconstr Surg.* 1993;91:299–302; discussion 303.
68. Kamei K, Ide Y. The pedicled arterialized venous flap. *J Reconstr Microsurg.* 1993;9:287–291.
69. Chen CL, Chiu HY, Lee JW, Yang JT. Arterialized tendocutaneous venous flap for dorsal finger reconstruction. *Microsurgery* 1994;15:886–890.
70. Fukui A, Inada Y, Maeda M, Mizumoto S, Yajima H, Tamai S. Venous flap: Its classification and clinical applications. *Microsurgery* 1994;15:571–578.
71. Galumbeck MA, Freeman BG. Arterialized venous flaps for reconstructing soft-tissue defects of the extremities. *Plast Reconstr Surg.* 1994;94:997–1002.
72. Karacalar A, Ozcan M. Free arterialized venous flap for the reconstruction of defects of the hand: New modifications. *J Reconstr Microsurg.* 1994;10:243–248.
73. Nishi G. Venous flaps for covering skin defects of the hand. *J Reconstr Microsurg.* 1994;10:313–319.
74. Webster HR, Inglefield CJ. Closure of the second toe transfer donor site without disruption of the deep transverse metatarsal ligament. *Microsurgery* 1994;15:802–804.
75. Xiu ZF, Chen ZJ. Clinical applications of venous flaps. *Ann Plast Surg.* 1995;34:518–522.
76. Yilmaz M, Menderes A, Karaca C, Barutçu A. Free arterialized venous forearm flap. *Ann Plast Surg.* 1995;34:88–91.
77. Veselý J, Kucera J. Immediate free flap reconstruction of traumatic defects. *Acta Chir Plast.* 1995;37:7–11.

78. Bolitho DG, Hudson DA. The superficial temporal venous island flap for eyebrow reconstruction. *Eur J Plast Surg.* 1996;19:103–104.
79. Cheng SL, Wong SS. Salvage of superficial palmar avulsion. *J Trauma* 1996;40:22–26.
80. Cheng TJ, Chen HC, Tang YB. Salvage of a devascularized digit with free arterialized venous flap: A case report. *J Trauma* 1996;40:308–310.
81. Inoue G, Tamura Y, Suzuki K. One-stage repair of skin and tendon digital defects using the arterialized venous flap with palmaris longus tendon: An additional four cases. *J Reconstr Microsurg.* 1996;12:93–97.
82. Sakai S. Arterialised venous groin flap: Case report. *Br J Plast Surg.* 1996;49:90–92.
83. Woo SH, Jeong JH, Seul JH. Resurfacing relatively large skin defects of the hand using arterialized venous flaps. *J Hand Surg Br.* 1996;21:222–229.
84. Yilmaz M, Menderes A, Karataş O, Karaca C, Barutçu A. Free arterialised venous forearm flaps for limb reconstruction. *Br J Plast Surg.* 1996;49:396–400.
85. Cho BC, Lee JH, Byun JS, Baik BS. Clinical applications of the delayed arterialized venous flap. *Ann Plast Surg.* 1997;39:145–157.
86. Iwasawa M, Ohtsuka Y, Kushima H, Kiyono M. Arterialized venous flaps from the thenar and hypothenar regions for repairing finger pulp tissue losses. *Plast Reconstr Surg.* 1997;99:1765–1770.
87. Klein C, Kovács A, Stuckensen T. Free arterialised venous forearm flaps for intraoral reconstruction. *Br J Plast Surg.* 1997;50:166–171.
88. Ueda Y, Mizumoto S, Hirai T, Doi Y, Fukui A, Tamai S. Two-stage arterialized flow-through venous flap transfer for third-degree burn defects on the dorsum of the hand. *J Reconstr Microsurg.* 1997;13:489–496.
89. Inoue G, Maeda N. Complications in wrap-around-flap donor sites after reconstruction using an arterialized venous flap. *J Reconstr Microsurg.* 1998;14:377–380; discussion 380.
90. Kantarci U, Cepel S, Gürbüz C. Venous free flaps for reconstruction of skin defects of the hand. *Microsurgery* 1998;18:166–169.
91. Kayikçioğlu A, Akyürek M, Safak T, Ozkan O, Keçik A. Arterialized venous dorsal digital island flap for fingertip reconstruction. *Plast Reconstr Surg.* 1998;102:2368–2372; discussion 2373.
92. Ayad H. Free arterialized venous flap. *Ann Burns Fire Disasters* 1999;12:158–163.
93. Cho BC, Byun JS, Baik BS. Dorsalis pedis tendocutaneous delayed arterialized venous flap in hand reconstruction. *Plast Reconstr Surg.* 1999;104:2138–2144.
94. Koch H, Moshammer H, Spendel S, Pierer G, Scharnagl E. Wrap-around arterialized venous flap for salvage of an avulsed finger. *J Reconstr Microsurg.* 1999;15:347–350.
95. Patradul A, Ngarmukos C, Parkpian V, Kitidumrongsook P. Arterialized venous toenail flaps for treating nail loss in the fingers. *J Hand Surg Br.* 1999;24:519–524.
96. Cunha-Gomes D, Bhathena H, Kavarana NM. Case report: A free arterialized venous flap for intraoral cancer reconstruction. *Acta Chir Plast.* 2000;42:13–15.
97. Klein C. Experiences with an arterialized venous flap for intraoral defect reconstruction (in German). *Zentralbl Chir.* 2000;125:51–55.
98. Reynoso R, Haddad JL, Sastré N. A few considerations regarding enhancement of arterialized skin flap survival. *Microsurgery* 2000;20:176–180.
99. Takeuchi M, Sakurai H, Sasaki K, Nozaki M. Treatment of finger avulsion injuries with innervated arterialized venous flaps. *Plast Reconstr Surg.* 2000;106:881–885.
100. Alexander G. Multistage type III venous flap or 'pre-arterialisation of an arterialised venous flap'. *Br J Plast Surg.* 2001;54:734.
101. Chia J, Lim A, Peng YP. Use of an arterialized venous flap for resurfacing a circumferential soft tissue defect of a digit. *Microsurgery* 2001;21:374–378.
102. Murata K, Inada Y, Fukui A, Tamai S, Takakura Y. Clinical application of the reversed pedicled venous flap containing perivenous areolar tissue and/or nerve in the hand. *Br J Plast Surg.* 2001;54:615–620.
103. Safak T, Akyürek M. Cephalic vein-pedicled arterialized anteromedial arm venous flap for head and neck reconstruction. *Ann Plast Surg.* 2001;47:446–449.
104. Woo SH, Seul JH. Optimizing the correction of severe postburn hand deformities by using aggressive contracture releases and fasciocutaneous free-tissue transfers. *Plast Reconstr Surg.* 2001;107:1–8.
105. Woo SH, Seul JH. Pre-expanded arterialised venous free flaps for burn contracture of the cervicofacial region. *Br J Plast Surg.* 2001;54:390–395.
106. Wungcharoen B, Santidhananon Y, Chongchet V. Pre-arterialisation of an arterialised venous flap: Clinical cases. *Br J Plast Surg.* 2001;54:112–116.
107. Brooks D, Buntic R, Buncke HJ. Use of a venous flap from an amputated part for salvage of an upper extremity injury. *Ann Plast Surg.* 2002;48:189–192.
108. De Lorenzi F, van der Hulst RR, den Dunnen WF, et al. Arterialized venous free flaps for soft-tissue reconstruction of digits: A 40-case series. *J Reconstr Microsurg.* 2002;18:569–574; discussion 575.
109. Kushima H, Iwasawa M, Maruyama Y. Recovery of sensitivity in the hand after reconstruction with arterialised venous flaps. *Scand J Plast Reconstr Surg Hand Surg.* 2002;36:362–367.
110. Aoki M, Watanabe K, Kura SJ, Yamashita T. Flag flap for coverage of a skin defect caused after debridement of chronic osteomyelitis of the proximal phalanx of the 5th toe. *Foot* 2003;13:171–173.
111. Cheng TJ, Chen YS, Tang YB. Use of a sequential two-in-one free arterialised venous flap for the simultaneous reconstruction of two separate defects on the foot. *Br J Plast Surg.* 2004;57:685–688.
112. Koch H, Scharnagl E, Schwarzl FX, Haas FM, Hubmer M, Moshammer HE. Clinical application of the retrograde arterialized venous flap. *Microsurgery* 2004;24:118–124.
113. Kopp J, Bach A, Loos B, et al. Use of vacuum therapy during defect coverage of the upper extremity with microsurgically grafted arterialized venous flaps (in German). *Zentralbl Chir.* 2004;129(Suppl 1):S82–S84.
114. Lin CH, Wei FC, Lin YT, Chen CT. Composite palmaris longus-venous flap for simultaneous reconstruction of extensor tendon and dorsal surface defects of the hand: Long-term functional result. *J Trauma* 2004;56:1118–1122.
115. Nakazawa H, Nozaki M, Kikuchi Y, Honda T, Isago T. Successful correction of severe contracture of the palm using arterialized venous flaps. *J Reconstr Microsurg.* 2004;20:527–531.
116. Nakazawa H, Kikuchi Y, Honda T, Isago T, Morioka K, Itoh H. Use of an arterialised venous skin flap in the replantation of an amputated thumb. *Scand J Plast Reconstr Surg Hand Surg.* 2004;38:187–191.
117. Titley OG, Chester DL, Park AJ. A-a type, arterialized, venous, flow-through, free flap for simultaneous digital

revascularization and soft tissue reconstruction-revisited. *Ann Plast Surg.* 2004;53:185–191.
118. Deune EG, Rodriguez E, Hatef D, Frassica F. Arterialized venous flow-through flap for simultaneous reconstruction of a radial artery defect and palmar forearm soft-tissue loss from sarcoma resection. *J Reconstr Microsurg.* 2005;21:85–91.
119. Hyza P, Vesely J, Stupka I, Cigna E, Monni N. The bilobed arterialized venous free flap for simultaneous coverage of 2 separate defects of a digit. *Ann Plast Surg.* 2005;55:679–683.
120. Kopp J, Bach AD, Kneser U, Loos B, Horch RE. Use of vacuum therapy in a huge arterialized venous flap to reconstruct a complete avulsion of a thumb (in German). *Zentralbl Chir.* 2006;131(Suppl 1):S3–S6.
121. Mureau MA, Flood SJ, Hofer SO. Total peroneal artery occlusion during fibula free flap harvesting: Salvage using the venous flow-through principle. *Plast Reconstr Surg.* 2006;117:101e–106e.
122. Pellini R, Pichi B, Ruggieri M, Ruscito P, Spriano G. Venous flow-through flap as an external monitor for buried radial forearm free flap in head and neck reconstruction *J Plast Reconstr Aesthet Surg* 2006;59:1217–1221.
123. Yokoyama T, Hosaka Y, Kusano T, Morita M, Takagi S. Finger palmar surface reconstruction using medial plantar venous flap: Possibility of sensory restoration without neurorrhaphy. *Ann Plast Surg.* 2006;57:552–556.
124. Brooks D, Buntic RF, Taylor C. Use of the venous flap for salvage of difficult ring avulsion injuries. *Microsurgery* 2008;28:397–402.
125. Hýza P, Veselý J, Novák P, Stupka I, Sekác J, Choudry U. Arterialized venous free flaps: A reconstructive alternative for large dorsal digital defects. *Acta Chir Plast.* 2008;50:43–50.
126. Iglesias M, Butrón P, Chávez-Muñoz C, Ramos-Sánchez I, Barajas-Olivas A. Arterialized venous free flap for reconstruction of burned face. *Microsurgery* 2008;28:546–550.
127. Kakinoki R, Ikeguchi R, Nankaku M, Nakamua T. Factors affecting the success of arterialised venous flaps in the hand. *Injury* 2008;39(Suppl 4):18–24.
128. Kim JS, Choi TH, Kim NG, et al. Flow-through arterialised venous free flap using the long saphenous vein for salvage of the upper extremity. *Scand J Plast Reconstr Surg Hand Surg.* 2008;42:218–223.
129. Kong BS, Kim YJ, Suh YS, Jawa A, Nazzal A, Lee SG. Finger soft tissue reconstruction using arterialized venous free flaps having 2 parallel veins. *J Hand Surg Am.* 2008;33:1802–1806.
130. Tang WR, Varkey P, Girotto R, Tan NC, Rose V, Chen HC. The venous flap: A safe alternative to the simple vein graft in a special situation. *J Plast Reconstr Aesthet Surg.* 2008;61:434–437.
131. Trovato MJ, Brooks D, Buntic RF, Buncke GM. Simultaneous coverage of two separate dorsal digital defects with a syndactylizing venous free flap. *Microsurgery* 2008;28:248–251.
132. Yokoyama T, Cardaci A, Hosaka Y, Revol M, d'Alcontres FS, Servant JM. Location of communicating veins for medial plantar venous flap. *Ann Plast Surg.* 2008;61:99–104.
133. Yokoyama T, Hosaka Y, Servant JM, Takagi S, Cardaci A. A simplification for harvesting medial plantar venous flap with communicating veins: Usefulness of preoperative ultrasound imaging. *Ann Plast Surg.* 2008;60:379–385.
134. Cil Y, Kocman AE, Yapici AK. Distally based venous flap: A new technique for the correction of syndactyly without skin graft in adult patients. *Chir Organi Mov.* 2009;93:123–129.
135. Ueda K, Nuri T, Akamatsu J, Sugita N, Otani K. Clinical trial of delay of the venous island flap. *Plast Reconstr Surg.* 2010;126:104e–105e.
136. Yokoyama T, Tosa Y, Hashikawa M, Kadota S, Hosaka Y. Medial plantar venous flap technique for volar oblique amputation with no defects in the nail matrix and nail bed. *J Plast Reconstr Aesthet Surg.* 2010;63:1870–1874.
137. Park SW, Heo EP, Choi JH, et al. Reconstruction of defects after excision of facial skin cancer using a venous free flap. *Ann Plast Surg.* 2011;67:608–611.
138. Rounds K, Buntic R, Brooks D. Artery-vein-artery venous flap for simultaneous soft-tissue repair and radial artery reconstruction: Case report. *J Hand Surg Am.* 2011;36:1339–1342.
139. Davami B, Arasteh E, Pourkhamene G. Versatility of venous flap for coverage of proximal and middle phalanges of fingers. *Tech Hand Up Extrem Surg.* 2012;16:23–26.
140. Rozen WM, Ting JW, Gilmour RF, Leong J. The arterialized saphenous venous flow-through flap with dual venous drainage. *Microsurgery* 2012;32:281–288.
141. Yan H, Gao W, Zhang F, Li Z, Chen X, Fan C. A comparative study of finger pulp reconstruction using arterialised venous sensate flap and insensate flap from forearm. *J Plast Reconstr Aesthet Surg.* 2012;65:1220–1226.
142. Kawakatsu M, Ishikawa K, Sawabe K. Free arterialised flow-through venous flap with venous anastomosis as the outflow (A-A-V flap) for reconstruction after severe finger injuries. *J Plast Surg Hand Surg.* 2013;47:66–69.
143. Lam W, Lin W, Bell D, Higgins J, Lin Y, Wei F. The physiology, microcirculation and clinical application of the shunt-restricted arterialized venous flaps for the reconstruction of digital defects. *J Hand Surg Eur Vol.* 2013;38:352–365.
144. Ueda K, Nuri T, Akamatsu J, Sugita N, Otani K, Yamada A. Delay of the reverse pedicled venous island flap: Clinical applications. *J Plast Surg Hand Surg.* 2013;47:350–354.
145. Walle L, Vollbach FH, Fansa H. Arterialized venous free flaps for resurfacing hand and finger defects (in German). *Handchir Mikrochir Plast Chir.* 2013;45:160–166.
146. Giesen T, Forster N, Künzi W, Giovanoli P, Calcagni M. Retrograde arterialized free venous flaps for the reconstruction of the hand: Review of 14 cases. *J Hand Surg Am.* 2014;39:511–523.
147. Han SK, Kim SY, Gu JH, Jeong SH, Kim WK. Influence of the pedicle orientation and length on viability of unipedicled venous island flaps. *Microsurgery* 2014;34:197–202.
148. Kayalar M, Levent K, Sugun TS, Gurbuz Y, Savran A, Kaplan I. Syndactylizing arterialized venous flaps for multiple finger injuries. *Microsurgery* 2014;34:527–534.
149. Kayalar M, Kucuk L, Sugun TS, Gurbuz Y, Savran A, Kaplan I. Clinical applications of free arterialized venous flaps. *J Plast Reconstr Aesthet Surg.* 2014;67:1548–1556.
150. Liu Y, Jiao H, Ji X, et al. A comparative study of four types of free flaps from the ipsilateral extremity for finger reconstruction. *PLoS One* 2014;9:e104014.
151. Sakamoto N, Matsumura H, Komiya T, Imai R, Niyaz A, Watanabe K. Syndactyly correction using a venous flap with the plantar cutaneous venous arch. *Ann Plast Surg.* 2014;72:643–648.
152. Park JU, Kim K, Kwon ST. Venous free flaps for the treatment of skin cancers of the digits. *Ann Plast Surg.* 2015;74:536–542.

APPENDIX 3

Plastic and Reconstructive Surgery

Unconventional perfusion flaps in the experimental setting: a systematic review and meta-analysis

--Manuscript Draft--

Manuscript Number:	
Article Type:	Original Article
Full Title:	Unconventional perfusion flaps in the experimental setting: a systematic review and meta-analysis
Corresponding Author:	Diogo Bogalhão Casal, M.D. Hospital de São José Lisbon, Portugal, Lisbon PORTUGAL
Order of Authors:	Diogo Bogalhão Casal, M.D.
	David Tanganho, M.D.
	Teresa Cunha, M.D.
	Eduarda Mota-Silva, M.Sci.
	Ines Iria, M.Sci.
	Diogo Pais, M.D., PhD
	Paula Antunes Videira, M.Sci.; PhD
	José Videira-Castro, M.D.
	João Goyri-O'Neill, M.D., PhD
Abstract:	Background: Unconventional perfusion flaps (UPFs) offer multiple potential advantages compared to traditional flaps. Although there are numerous experimental papers on UPFs, the multiple animal species involved, the myriad vascular constructions used, and the frequently conflicting data reported makes synthesis of this information challenging. The main aim of this paper was to perform a systematic review and meta-analysis of the literature on the experimental use of UPFs, in order to identify the best experimental models proposed, as well as to estimate their global survival rate. Methods: We performed a systematic review and meta-analysis of all the articles written in English, French, Italian, Spanish and Portuguese on the experimental use of UPFs and indexed to PubMed since 1981 until the 1st February 2017. Results: A total of 68 studies were found, corresponding to 86 optimized experimental models and to 1073 UPFs. Overall UPF survival rate was 90.8% (95% CI, 86.9% to 93.6%; p<0.001). The estimated proportion of experimental UPFs presenting complete survival or nearly complete survival was 74.4% (95% CI, 62.1% to 83.7%; p<0.001). The most commonly reported animal species in the literature were the rabbit (57.1%), the rat (26.4%), and the dog (14.3%). No significant differences were found in survival rates among these species, nor among the diverse vascular patterns used. Conclusions: These data do not differ significantly from those reported regarding the use of UPFs in human medicine, suggesting that rabbit, rat and canine experimental UPF models may adequately mimic the clinical application of UPFs.
Keywords:	Arterialized venous flaps; venous flaps; unconventional perfusion; meta-analysis; systematic review; flap survival; flap necrosis.
Manuscript Classifications:	Flap physiology; Flaps; Meta-analysis; Soft tissue injuries; Systematic review
Additional Information:	
Question	**Response**
Do you feel the manuscript qualifies as an outcomes study?	Yes

Please select: as follow-up to "Do you feel the manuscript qualifies as an outcomes study?"	Systematic review or meta-analysis: Summarizes existing literature with or without statistical analysis.
What should be the general public's take away from your research?	There are good experimental models of venous flaps

TITLE PAGE (AUTHORS, CORRESPONDING AUTHOR, AFFILIATION, FINANCIAL DISCLOSURE,

“Unconventional perfusion flaps in the experimental setting: a systematic review and meta-analysis.”

Author list:Diogo **Casal**,, M.D.[1,2,3], David **Tanganho**, M.D.[1,2], Teresa **Cunha**, M.D. [1,2], Eduarda **Mota-Silva**, M.Sci.[1,2,4], Inês **Iria**, M.Sci.[5], Diogo **Pais**, M.D., PhD[2], Paula **Videira**, PhD[3], José **Videira-Castro**, M.D.[1], João **Goyri-O’Neill**, M.D., PhD.[2]

1. Plastic and Reconstructive Surgery Department and Burn Unit; Centro Hospitalar de Lisboa Central, Lisbon, Portugal

2. Anatomy Department; Nova Medical School, Lisbon, Portugal

3. UCIBIO, Departamento de Ciências da Vida, Faculdade de Ciências e Tecnologias, Universidade NOVA de Lisboa, Caparica, Portugal

4. LIBPhys – Physics Department, Faculdade de Ciências e Tecnologias, Universidade NOVA de Lisboa, Caparica, Portugal

5. Molecular Microbiology and Biotechnology Unit|Drug Discovery Area; Faculdade de Farmácia, Universidade de Lisboa, Lisbon, Portugal

Corresponding author:

Diogo Casal, M.D.

Plastic and Reconstructive Surgery Department and Burn Unit, Centro Hospitalar de Lisboa Central, Lisbon, Portugal

diogo_bogalhao@yahoo.co.uk

Financial Disclosure Statement: Diogo Casal received a grant from “The Programme for Advanced Medical Education” sponsored by “Fundação Calouste Gulbenkian, Fundação Champalimaud, Ministério da Saúde and Fundação para a Ciência e Tecnologia, Portugal.”

The authors have no financial or commercial interest to declare in relation to the content of this article.

Title: Unconventional perfusion flaps in the experimental setting: a systematic review and meta-analysis

Short Title: Experimental unconventional perfusion flaps: a systematic review

Authors:

Diogo Casal, M.D.[1,2,3]

David Tanganho M.D.[1,2]

Teresa Cunha, M.D. [1,2]

Eduarda Mota-Silva, M.Sci.[1,2,4]

Inês Iria, M.Sci.[5]

Diogo Pais, M.D., PhD[2]

Paula Antunes Videira, PhD[3]

José Videira-Castro, M.D.[1]

João Goyri-O'Neill, M.D., PhD.[2]

Affiliations:

1- Plastic and Reconstructive Surgery Department and Burn Unit; Centro Hospitalar de Lisboa Central, Lisbon, Portugal
2- Anatomy Department; Nova Medical School, Lisbon, Portugal
3- UCIBIO, Departamento de Ciências da Vida, Faculdade de Ciências e Tecnologias, Universidade NOVA de Lisboa, Caparica, Portugal
4- LIBPhys – Physics Department, Faculdade de Ciências e Tecnologias, Universidade NOVA de Lisboa, Caparica, Portugal
5- Molecular Microbiology and Biotechnology Unit|Drug Discovery Area; Faculdade de Farmácia, Universidade de Lisboa, Lisbon, Portugal

Abstract:

Background: Unconventional perfusion flaps (UPFs) offer multiple potential advantages compared to traditional flaps. Although there are numerous experimental papers on UPFs, the multiple animal species involved, the myriad vascular constructions used, and the frequently conflicting data reported makes synthesis of this information challenging. The main aim of this paper was to perform a systematic review and meta-analysis of the literature on the experimental use of UPFs, in order to identify the best experimental models proposed as well as to estimate their global survival rate.

Methods: We performed a systematic review and meta-analysis of all the articles written in English, French, Italian, Spanish and Portuguese on the experimental use of UPFs and indexed to PubMed since 1981 until the 1st February 2017.

Results: A total of 68 studies were found, corresponding to 86 optimized experimental models and to 1073 UPFs. Overall UPF survival rate was 90.8% (95% CI, 86.9% to 93.6%; p<0.001). The estimated proportion of experimental UPFs presenting complete survival or nearly complete survival was 74.4% (95% CI, 62.1% to 83.7%; p<0.001). The most commonly reported animal species in the literature were the rabbit (57.1%), the rat (26.4%), and the dog (14.3%). No significant differences were found in survival rates among these species, nor among the diverse vascular patterns used.

Conclusions: These data do not differ significantly from those reported regarding the use of UPFs in human medicine, suggesting that rabbit, rat and canine experimental UPF models may adequately mimic the clinical application of UPFs.

Keywords: Arterialized venous flaps; venous flaps; unconventional perfusion; meta-analysis; systematic review; flap survival; flap necrosis.

Introduction:

Unconventional perfusion flaps (UPFs) have been increasingly used in the clinical setting for the past four decades, offering multiple advantages relatively to traditional flaps.(1) Being composite blocks of tissues perfused solely through their venous system, their dissection is relatively simple, expeditious and not associated with major donor site morbidity. Moreover, these flaps, which comprise arterialized venous flaps (AVFs) and venous flaps (VFs), are intrinsically thin and pliable. These last features are potentially highly advantageous for reconstructing shallow defects particularly in mobile regions where the integument is thin, namely in the upper limb, in the face and the external genitalia.(1-5) Finally, as they are usually tailored around the superficial venous system, which is often visible through the skin, their harvesting precludes the need of ancillary pre-operative tests. Consequently, UPFs are particularly useful for emergent reconstruction in the realm of trauma cases.

Even though there are several clinical and experimental papers on UPFs, the multiple animal species involved, the myriad vascular constructions used, and the frequently conflicting data reported makes synthesis of this information challenging. For this reason, even today many surgeons and researchers are discouraged from using these flaps in either the clinical or the experimental settings.(1-6) Thus, it would be of paramount importance to find patterns in the available literature on UPFs, with the goal to facilitate knowledge acquisition by novices in the field, and to aid in future experimental works.

Hence, the main aim of this paper was to perform a systematic review and meta-analysis of the literature on the experimental use of UPFs, in order to identify the best experimental models proposed as well as to estimate their global survival rate. Secondarily, this paper aimed at estimating the UPF survival rate for each animal species and vascular patterns used in these optimized experimental models.

Methods:

On the 1st February 2017, the authors searched the PubMed database concerning experimental animal models of UPFs (**Fig. 1**). The following terms were used: “arterialized venous flap”; “arterialised venous flap”; “unconventional flap”; “unconventional perfusion flap”; “non-conventional flap”; “non-conventional perfusion flap”; “venous flap” and “venous perfusion flap”. These search terms were combined with the Boolean operators ‘‘OR” and “AND”.

Inclusion Criteria

All articles reporting experimental animal studies, written in English, Spanish, Portuguese, French or Italian, and describing qualitatively and/or quantitatively flap survival and/or necrosis were selected.

Exclusion Criteria:

The following articles/experimental models were excluded from the analysis:

1 - Studies written in different languages from those mentioned above;

2- Articles referring exclusively to human or dissection studies;

3- Studies/experimental models addressing solely histological features or pharmacological and/or genetic manipulation of flaps with no information regarding quantitative or qualitative evaluation of flap necrosis or survival;

4- Studies/experimental models whose flap vascular network included total blood flow reversal at the expense of one major artery without apparent potential clinical benefit;

5- Studies/experimental models addressing revascularization of the extremities by reverse circulation;

6- Papers/experimental models describing exclusively pre-fabricated flaps with arteriovenous fistulas, since these flaps tend to behave similarly to conventional perfusion flaps.(7, 8)

In each paper included for analysis, individuals whose vascular anastomoses presented thrombosis were excluded from the analysis.

The title and abstract of all identified studies were examined independently by three reviewers (D.C., D.T. and T.C.). In cases where suitability of a given study for inclusion in the review was not clear, the entire article was obtained and evaluated for appropriateness. Furthermore, the references contained in the retrieved articles were scanned by the three independent reviewers, in order to obtain further articles that were missed in the first-round search. All articles were acquired in their full-text version and read independently by the three reviewers.

For each study, the following variables were recorded: year of publication; nationality; animal species, and strains used, as well as experimental animal gender. When a study reported more than one vascular construction, the one or ones with a better flap survival rate ($p<0.05$) was/were chosen as **optimized experimental models**. These models were used as individual units for the sake of subsequent statistical analysis.

For each experimental model, the following parameters were assessed: number of animals used; anatomical region of the UPF donor site; vascular pattern used to perfuse the flap (1) (when considering rabbit ears, the authors took into consideration that the largest veins [central vein, anterior marginal vein and posterior marginal vein] are devoid of venous valves (9, 10)); vascularization of the recipient wound bed (*well vascularized* if the flap was placed over viable muscle, fascia, fat, synovial tissue, epitenon or granulation tissue; and *non-vascularized*, if the flap was placed over bone, cartilage or prosthetic material); application of an impermeable barrier between the

flap and the recipient bed (to prevent diffusion of oxygen and nutrients and/or neoangiogenesis from the wound to the deep aspect of the flap); resort to flap delay procedures; flap composition; flap innervation; flap survival rate; percentage of flaps that presented *complete survival* (defined as 100% survival area or superficial necrosis with self-healing of the flap's surface at its latest evaluation), *nearly complete survival* (considered 85 to 100% flap survival or unspecified inconsequential "marginal necrosis"), *significant necrosis* (> 15% flap necrosis) and *complete necrosis* (100% flap necrosis or "non-surviving flaps"). If in doubt, a higher necrosis category was considered for each experimental model. The numeric values of necrosis considered were always those reported on the last day of the experiments described in each individual article.

The presence and nature of complications were also recorded (epidermolysis, flap congestion and venous insufficiency by themselves were not considered complications, as they were reportedly present in the first few days after surgery according to most authors). *Epidermolysis* was considered to be present when there was only evidence of the epidermis being loosely attached to the dermis, readily exfoliating or forming blisters.(11) If the damage to the skin extended deeper than the epidermis, flap necrosis was considered to be present, as described above.

When estimating effect sizes for the entire population, the authors only included studies with at least 3 animals, to minimize publication bias. Whenever individual animal data were present in papers, they were used for individual data meta-analysis. (12)

The data were retrieved from the available literature, each parameter at a time, from each paper in turn. Finally, the data were inserted into an Excel database (Microsoft Corp., Redmond, Wash.®). When discrepancies were found in data retrieval, the articles were reanalyzed by the three reviewers independently.

Statistical Analysis:

Quantitative variables were expressed as means ± standard deviation. Qualitative variables were expressed as percentages. IBM SPSS Version 21.0 software (IBM Corp., Armonk, N.Y.®) was used for descriptive and inferential statistical analysis.

The Kolmogorov-Smirnov test was used to assess whether variables were normally distributed. Analysis of variance and *t-student* tests were used to compare averages in normally distributed data. Kruskal-Wallis and Mann-Whitney tests were used to compare means in non-normally distributed data. Proportions were analyzed with the Chi-square test or Fisher's exact test. Dichotomous variables were compared with the binomial test. Association between numerical variables was assessed using Pearson's correlation coefficient.

The Comprehensive Meta-Analysis 2.0 software (Biostat, Englewood, N.J.®) was used to estimate population summary effects and to produce forest and funnel plots using random-effects models. Studies heterogeneity for each parameter was assessed using Cochran's Q test, I-squared and Tau-squared statistics.(13) Evidence of publication bias was investigated through evaluation of funnel plot symmetry and by application of the Egger's test.(14, 15)

A two-tail value of $p < 0.05$ was considered to be statistically significant.

Results:

The systematic review of the literature allowed the identification of 68 studies on the experimental use of UPFs in the experimental setting (**Fig. 1**). Overall, this corresponded to a total of 1073 flaps. Among these studies, it was possible to identify 86 optimized experimental models of UPFs. The features of these models are summarized in **Table 1**.

First Author	Year	Country	Optimized experimental animal model	Species	Strain	Gender	n	Flap donor site	Flap vascular pattern	Wound bed blood supply	Delayed flap	Flap composition	Flap innervation preserved	Flap survival rate (%)	Categorical flap survival (%)				Necrotic flap area (%)		
															CS	NCS	SN	CN	Average	Min.	Max.
Nakayama (16)	1981	Japan	1	Rat	n/a	M	5	T/A	6	WV	Yes	FC	n/a	100	100	0	0	0	0	0	0
			2	Rat	n/a	M	10	T/A	6	WV	No	FC	n/a	100	n/a	n/a	0	0	2	0	2.7
			3	Rat	n/a	M	20	T/A	4	WV	No	FC	n/a	100	n/a	n/a	n/a	0	7	0	21
Voukidis (17)	1982	UK	4	Rat	SD	M+F	10	A/G	3	IB	Yes	FC	No	100	n/a	n/a	n/a	0	n/a	n/a	n/a
Mundy (18)	1984	USA	5	Rabbit	n/a	n/a	5	E	1	B/C	Yes	FC	No	n/a	n/a	n/a	n/a	n/a	13	n/a	n/a
			6	Rabbit	n/a	n/a	5	E	1	B/C	No	FC	No	n/a	n/a	n/a	n/a	n/a	24	n/a	n/a
Ji (19)	1984	China	7	Rabbit	n/a	M+F	33	E	1	B/C	No	FC	No	100	90.9	0	9.1	0	n/a	0	n/a
Beehary (20)	1984	France	8	Rat	n/a	n/a	5	A/G	3	WV	No	FC	n/a	100	100	0	0	0	0	0	0
Baek (21)	1985	South Korea	9	Dog	M	n/a	36	H	10	WV	No	FC	No	100	100	0	0	0	0	0	0
			10	Dog	M	n/a	10	H	10	IB	No	FC	No	100	100	0	0	0	0	0	0
			11	Dog	M	n/a	2	H	7	WV	No	FC	No	100	100	0	0	0	0	0	0
Nichter (10)	1985	USA	12	Rabbit	NZ	M	10	E	2	SE	No	B/C	No	100	n/a	n/a	n/a	0	n/a	n/a	n/a
Thatte (22)	1987	India	13	Dog	M	M+F	14	H	10	WV	No	FC	No	91.7	n/a	n/a	n/a	8.33	n/a	n/a	100
Germann (23)	1987	Germany	14	Pig	Y	M	12	H	5	WV	No	FC	Yes	0	0	0	0	100	100	100	100
Amarante (24)	1988	Portugal	15	Dog	n/a	n/a	5	H	10	WV	No	FC	Yes	100	100	0	0	0	0	0	0
			16	Dog	n/a	n/a	5	H	9	WV	No	FC	Yes	100	100	0	0	0	0	0	0
			17	Dog	n/a	n/a	4	H	7	WV	No	FC	Yes	100	100	0	0	0	0	0	0
Fukui (25)	1988	Japan	18	Rabbit	n/a	n/a	20	E	10	B/C	No	FC	No	100	90	10	0	0	n/a	0	n/a
Sasa (26)	1988	USA	19	Dog	M	M+F	8	F	10	WV	No	FC	No	75	0	75	0	25	n/a	n/a	100
Inada (27)	1989	Japan	20	Rabbit	n/a	n/a	20	E	10	B/C	No	FC	No	100	90	0	10	0	n/a	0	n/a
			21	Rabbit	n/a	n/a	21	E	1	B/C	No	FC	No	100	85.7	0	14.3	0	n/a	0	n/a
Yuen (28)	1991	China	22	Rat	W	M	10	A/G	9	WV	No	FC	n/a	90	80	n/a	n/a	10	n/a	0	100
			23	Rat	W	M	10	A/G	9	IB	No	FC	n/a	100	90	n/a	n/a	0	n/a	0	n/a
Noreldin (29)	1992	USA	24	Rat	W	M	20	A/G	10	WV	No	FC	n/a	90	75	n/a	n/a	10	n/a	0	100
Takato (30)	1992	Canada	25	Rabbit	NZ	F	18	A/G	3	WV	No	FC	No	100	66.7	33.3	0	0	2.4	0	10
Chow (31)	1992	China	26	Rat	SD	n/a	20	A/G	3	WV	No	FC	n/a	n/a	n/a	n/a	n/a	n/a	39.6	n/a	n/a
Angel (32)	1992	USA	27	Dog	n/a	n/a	6	H	10	WV	No	FC	No	100	n/a	n/a	n/a	0	n/a	n/a	n/a
Inada (33)	1992	Japan	28	Rabbit	n/a	n/a	10	E	10	B/C	No	FC	Yes	100	0	0	100	0	56	30	78
Inada (34)	1993	Japan	29	Rabbit	J	n/a	18	E	1	B/C	No	FC	n/a	100	n/a	n/a	0	0	n/a	n/a	n/a
			30	Rabbit	J	n/a	17	E	2	B/C	No	FC	n/a	100	n/a	n/a	0	0	n/a	n/a	n/a
Matsushita (35)	1993	USA	31	Rabbit	NZ	M+F	6	T/A	10	WV	No	FC	Yes	100	83.3	n/a	n/a	0	n/a	0	n/a
Gençosmanoglu (36)	1993	Turkey	32	Rabbit	n/a	n/a	10	T/A	10	WV	No	FC	Yes	100	80	20	0	0	n/a	0	n/a
Ueda (37)	1993	Japan	33	Rabbit	n/a	n/a	15	E	10	SE	Yes	B/C	Yes	100	n/a	n/a	n/a	0	n/a	n/a	n/a
Fukui (38)	1993	Japan	34	Rat	F	M	28	D	10	WV	No	MFC	Yes	85.7	85.7	0	0	14.3	14.3	0	100
Takato (39)	1993	Japan	35	Rabbit	NZ	M	5	A/G	10	IB	No	FC	n/a	100	0	0	100	0	74.8	67.6	79.7
Thatte (40)	1993	India	36	Rat	W	M	5	A/G	10	WV	No	FC	n/a	100	n/a	n/a	n/a	0	n/a	n/a	n/a
Lenoble (41)	1993	France	37	Rat	W	M+F	15	A/G	10	WV	No	FC	Yes	26.7	0	20	6.7	73.3	77	10	100
Smith (42)	1994	USA	38	Rabbit	NZ	n/a	10	E	10	B/C	No	FC	n/a	100	70	n/a	n/a	0	18.1	0	n/a
Dvir (43)	1994	Australia	39	Dog	M	n/a	6	F	10	WV	No	FC	n/a	66.7	33.3	0	33.3	33.3	41.7	0	100
			40	Dog	M	n/a	6	F	1	WV	No	FC	n/a	66.7	33.3	16.7	16.7	33.3	41.7	0	100
			41	Dog	M	n/a	6	F	4	WV	No	FC	n/a	66.7	50	0	16.7	33.3	46.7	0	100
Suzuki(44)	1994	Japan	42	Rabbit	J	M	6	E	1	B/C	No	FC	Yes	100	n/a	n/a	n/a	0	n/a	n/a	n/a
Wolff (45)	1995	Germany	43	Rat	W	M	7	A/G	4	WV	No	FC	n/a	100	14.3	57.1	28.6	0	7	0	16
Byun (46)	1995	USA	44	Rabbit	NZ	M	8	E	3	SE	Yes	B/C	Yes	100	0	100	0	0	5.9	n/a	n/a
Xiu (47)	1996	China	45	Rabbit	n/a	n/a	20	T/A	10	WV	No	FC	n/a	n/a	n/a	n/a	n/a	n/a	7.68	n/a	n/a
Pittet (48)	1996	USA	46	Rabbit	NZ	n/a	16	E	1	B/C	No	FC	No	100	100	0	0	0	0	0	1
Adamo (49)	1996	Italy	47	Rat	W	n/a	10	T/A	10	WV	No	FC	n/a	100	n/a	n/a	40	0	n/a	n/a	n/a
			48	Rat	W	n/a	10	T/A	10	IB	No	FC	n/a	100	n/a	n/a	30	0	n/a	n/a	70
Xiu (50)	1996	China	49	Rabbit	n/a	n/a	40	T/A	10	WV	No	FC	No	n/a	n/a	n/a	n/a	n/a	31.3	0	100
Miles (51)	1997	Canada	50	Rat	SD	M	4	T/A	5	WV	No	FC	n/a	n/a	n/a	n/a	n/a	n/a	43	n/a	n/a
Yilmaz (52)	1997	Turkey	51	Rabbit	NZ	n/a	12	E	10	SE	No	B/C	No	83.3	41.7	n/a	n/a	16.7	24.2	0	100
Fukui (53)	1998	Japan	52	Rabbit	n/a	n/a	22	E	1	WV	Yes	FC	No	100	54.6	n/a	n/a	0	n/a	0	n/a
Woo (54)	1998	South Korea	53	Dog	M	M+F	12	H	4	IB	No	FC	n/a	n/a	n/a	n/a	n/a	n/a	3.8	n/a	n/a
Yuan (55)	1998	China	54	Rabbit	NZ	n/a	38	E	10	SE	No	B/C	No	100	n/a	n/a	n/a	0	n/a	n/a	n/a
Atabey (56)	1998	Turkey	55	Rabbit	NZ	n/a	10	T/A	10	WV	No	FC	No	30.0	30	0	0	70	30	0	100
Cho (57)	1998	South Korea	56	Rabbit	NZ	M	7	E	1	SE	Yes	B/C	Yes	100	0	0	100	0	40.3	22	56
Mutaf (58)	1998	Japan	57	Rat	L	n/a	10	T/A	10	IB	Yes	FC	n/a	n/a	n/a	n/a	n/a	n/a	37.4	n/a	n/a
Yilmaz (59)	1999	Turkey	58	Rabbit	NZ	n/a	12	E	1	IB	No	B/C	No	83.3	58.3	n/a	n/a	16.7	22	0	100
Murata (60)	1999	Japan	59	Rabbit	n/a	n/a	10	E	10	WV	No	FC	Yes	100	10	n/a	n/a	0	17.5	0	100
Yücel (61)	2000	Turkey	60	Rat	SD	M	32	A/G	10	WV	No	FC	No	0	0	0	0	100	100	100	100
Tang (62)	2000	Taiwan	61	Rabbit	NZ	n/a	30	T/A	10	WV	No	MFC	No	100	n/a	n/a	n/a	0	n/a	0	n/a
Wungcharoen (63)	2001	Thailand	62	Rat	W	M	9	T/A	3	IB	Yes	FC	No	n/a	n/a	n/a	n/a	n/a	2.5	n/a	n/a
Saray (64)	2002	Turkey	63	Rabbit	n/a	n/a	10	E	10	IB	No	FC	No	100	n/a	n/a	n/a	0	41.9	n/a	n/a
Chang (65)	2003	China	64	Rabbit	NZ	n/a	10	H	8	IB	No	FC	Yes	100	50	50	0	0	5.5	0	n/a
Coruh (66)	2004	Turkey	65	Rabbit	NZ	M	10	E	10	B/C	No	FC	No	100	0	0	100	0	40	26.0	77.6
			66	Rabbit	NZ	M	10	E	10	B/C	No	FC	No	100	0	0	100	0	42	19.7	55.4
Lin (67)	2004	Taiwan	67	Rabbit	NZ	n/a	13	E	10	SE	No	B/C	No	100	n/a	n/a	n/a	0	6.6	0	55.6
Baser (68)	2005	Turkey	68	Rat	SD	n/a	6	D	10	WV	Yes	FC	n/a	100	16.7	0	83.3	0	37.5	0	46
Zhang (69)	2006	USA	69	Rat	SD	M	10	A/G	10	WV	No	FC	No	n/a	n/a	n/a	n/a	n/a	61	n/a	n/a
Özyazgan (70)	2007	Turkey	70	Rabbit	NZ	n/a	7	E	10	B/C	No	FC	No	n/a	n/a	n/a	n/a	n/a	44	n/a	n/a
Özyazgan (71)	2007	Turkey	71	Rabbit	NZ	M	14	E	10	B/C	No	FC	No	n/a	n/a	n/a	n/a	n/a	39	n/a	n/a
Pittet (72)	2008	Switzerland	72	Rabbit	NZ	n/a	15	E	1	WV	No	FC	No	100	n/a	n/a	0	0	0.6	0	n/a
			73	Rabbit	NZ	n/a	19	E	1	WV	No	FC	No	100	n/a	n/a	6	0	5.3	n/a	n/a
			74	Rabbit	NZ	n/a	14	E	1	IB	No	FC	No	100	n/a	n/a	8	0	6.5	n/a	n/a
Tan (73)	2009	Singapore	75	Rabbit	NZ	M+F	10	T/A	3	IB	No	FC	No	80.0	40	0	40	20	55.5	0	100
Yan (74)	2010	USA	76	Rat	SD	M	8	A/G	4	WV	Yes	FC	n/a	100	0	100	0	0	2	n/a	n/a
Lalkovic (75)	2010	Serbia	77	Rabbit	BC	n/a	10	E	3	SE	No	B/C	No	100	n/a	n/a	n/a	0	1.7	n/a	n/a
Iglesias (76)	2013	Mexico	78	Rabbit	NZ	M+F	12	E	1	SE	No	B/C	n/a	100	91.7	8.3	0	0	1.2	0	15
Yan (77)	2013	China	79	Rabbit	J	M+F	6	T/A	3	WV	No	FC	n/a	100	0	n/a	n/a	0	40.8	n/a	n/a
Yan (78)	2013	China	80	Rabbit	J	M+F	12	T/A	3	WV	Yes	FC	n/a	100	0	n/a	n/a	0	40.8	n/a	n/a
Ceylan (79)	2014	Turkey	81	Rat	W	M	6	A/G	9	WV	No	FC	n/a	100	0	16.7	83.3	0	28.7	6.2	54.8
			82	Rat	W	M	6	A/G	9	WV	Yes	FC	n/a	100	0	83.3	16.7	0	12.1	8.0	18.2
Lalkovic (80)	2014	Serbia	83	Rabbit	BC	M	10	E	1	SE	Yes	B/C	No	100	0	100	0	0	8.7	4.1	15.4
Borumandi (81)	2016	Austria	84	Pig	n/a	n/a	6	H	4	WV	No	B/C	No	100	n/a	n/a	n/a	n/a	n/a	n/a	n/a
Weng (82)	2017	China	85	Rabbit	J	M+F	11	A/G	6	WV	No	FC	n/a	n/a	n/a	n/a	n/a	n/a	28.1	n/a	n/a
			86	Rabbit	J	M+F	12	A/G	5	WV	No	FC	n/a	n/a	n/a	n/a	n/a	n/a	26.7	n/a	n/a

Table 1. Summary of the studies on unconventional perfusion flaps in experimental animal models identified in the systematic review and included in the meta-analysis. For each study, the optimized experimental animal model is identified, as well as its characteristics. These experimental models were those which presented better flap survival rates in each published paper ($p<0.05$).

n, number of flaps in each optimized experimental model; **n/a**, information non-available; **Min.**, minimum; **Max.**, maximum

Categorical flap survival: CN, complete necrosis; **CS**, complete survival; **NCS**, nearly complete survival; **SN**, significant necrosis

Strain: BC, Big Chinchilla rabbit; **F**, Fischer rat; **J**, Japanese white rabbit; **L**, Lewis rat; **M**, Mongrel dog; **NZ**, New Zealand white rabbit; **SD**, Sprague Dawley rat; **W**, Wistar rat; **Y**, Yorkshire pig

Gender: F, female; **M**, male; **M + F**, both males and females

Flap donor site: A/G, abdomen and/or groin; **D**, dorsum; **E**, ear; **F**, forelimb; **H**, hindlimb; **T/A**, thorax and abdomen

Flap vascular pattern (1): "**1**", type Ia arterialized venous flap according to Woo classification; "**2**", type Ib arterialized venous flap according to Woo classification; "**3**", type IIa arterialized venous flap according to Woo classification; "**4**", type IIb arterialized venous flap according to Woo classification; "**5**", type III arterialized venous flap according to Woo classification; "**6**", pedicled arterialized venous flap; "**7**", type I venous flap according to Chen classification; "**8**", type IIa venous flap according to Chen classification; "**9**", type IIb venous flap according to Chen classification; "**10**", sliding venous flap

Wound bed blood supply: B/C, bone or cartilage; **IB**, impermeable barrier underneath the flap; **SE**, skeletonized ear; **WV**, well vascularized

Flap composition: B/C, includes bone and/or cartilage (other than skin with its appendages and subcutaneous tissue); **FC**, fasciocutaneous (skin with its appendages and subcutaneous tissue); **MFC**, myofasciocutaneous (skin with its appendages, subcutaneous tissue and muscle/portion of muscle)

Studies publication spanned from 1981 to 2017. Half of the identified papers were published until 1994, and three quarters of these were published until 2003. Studies were performed in 20 different countries (**Table 1**). By decreasing order of frequency, the countries with the greater number of studies were: Japan (19.8%), Turkey (14.3%), China and the USA (13.2% each), and Canada and South-Korea (both corresponding to 5.5%). The most commonly used animal species was the rabbit (57.1%), followed by the rat (26.4%), the dog (14.3%), and the pig (2.2%). Mice models were not reported in the literature. Amongst rabbits, the most commonly used strain was the White New Zealand rabbit (55.8%), followed by the White Japanese rabbit (9.6%), and the Big Chinchilla rabbit (3.8%). The most commonly strain of rat was the Wistar rat (45.8%), followed by the Sprague-Dawley rat (29.2%), and the Lewis and Fischer strains (4.2% each). Almost all the studies made in dogs were performed in mongrel dogs (96.2%). Concerning the two pig studies, one reported the use of the Yorkshire pig strain, while the other used an unspecified variety of pigs.

On average, each optimized experimental model was developed based on the dissection of 12.14 ± 8.01 UPFs (ranging from 2 to 40). Regarding animal gender, most studies were conducted on male animals (26.4%), or using both male and female animals (15.4%). Only 3.3% of studies reported studies exclusively on female animals. However, the majority of the studies did not specify the gender of experimental animals (54.9%). Concerning anatomical location, most UPFs models were performed in the ear (36.3%). In decreasing order of frequency, the next most common

anatomical regions used were the abdomen and/or groin (25.3%), the thorax and the abdomen (18.7%), the hindlimb (13.2%), the forelimb (4.4%), and the dorsum (2.2%). The most common anatomical regions used in each species to produce UPFs were as follows: the ear in the rabbit (63.5%), the abdomen and/or groin in the rat (58.3%), the hindlimb in the dog (69.2%), and in the pig (100%).

The different vascular patterns reported in the literature are detailed in **Figures 2** and **3**.

The most common vascular patterns were in decreasing order of frequency: sliding VFs (40.7%), type IA AVFs (20.9%), type IIA AVFs (8.8%), pedicled AVFs (6.6%), and both type IIB AVFs and proximally pedicled VFs (5.5% each). Infrequent vascular patterns included type IB AVFs (4.4%), type III AVFs (3.3%), free venous flow through (2.2%), and distally based VFs (1.1%).

Figure 4 shows the relative proportion of the different vascular patterns in the different animal species. This figure also highlights the main features of the optimized experimental models in the different animal species.

In the majority of cases (54.7%), flaps were placed over well-perfused wound beds. In 18.6% of cases, flaps were placed over bare bone or cartilage. In 15.6% of the models an impermeable barrier was placed under the UPF to prevent flap nutrition or gas exchanges from the wound bed. When rabbits were used, UPFs were frequently based on skeletonized ears or ear segments. In these cases (11.6% of all experimental models) the flap was also completely dependent on its own vascular pedicle, not being able to depend on a vascularized wound bed. In 18.7% of cases some sort of surgical delay procedure was performed prior to flap elevation to increase flap survival.

Concerning flap composition, most UPFs were fasciocutaneous (85.7%; $p<0.001$). Flaps included bone and/or cartilage in 13.2% of cases. There was only one study

reporting a myofasciocutaneous flap, corresponding to 1.1% of all optimized experimental models.(38) In almost all cases, UPFs were non-innervated (91.2%; p<0.001).

Meta-analysis of experimental UPFs using a random effects model estimated an overall flap survival rate of 90.8% (95% CI, 86.9% to 93.6%; p<0.001) [**Fig. 5**]. Study heterogeneity assessment for this parameter was as follows: Cochran-Q value 134.98; p<0.001; I-squared 47.40; Tau-squared 1.24. The funnel plot of the studies used to produce this estimate suggested there was evidence of publication bias regarding this parameter (**Supplementary figure 1**). Publication bias was further supported by Egger's test (p<0.001).

The estimated proportion of experimental UPFs presenting complete survival or nearly complete survival was 74.4% (95% CI, 62.1% to 83.7%; p<0.001) [**Fig. 6**]. Evaluation of studies heterogeneity regarding this variable was: Cochran-Q value 162.77; p<0.001; I-squared 71.74; Tau-squared 2.58. The funnel plot regarding the estimation of this parameter suggested the presence of publication bias (**Supplementary figure 2**). However, Egger's test failed to support this assumption (p=0.342).

In all animal species except the pig, most flaps presented complete or nearly complete survival (**Fig. 7**). In the pig, there was only one study using a type III AVF fasciocutaneous flap. In this model all flaps suffered complete necrosis.(23) No significant differences were found between UPFs necrosis rates among the other animal species. In the same way, no significant differences were found between survival rates of the different vascular patterns (**Fig. 7**). Similarly, no differences were found in UPFs survival rates regarding: gender; anatomical location where the flap was produced; wound bed blood supply, including the placement or not of an impermeable barrier underneath the flap; resort to surgical delay procedures; UPF histological composition and/or innervation.

All articles addressing UPF's clinical features described flap congestion, edema, venous engorgement, blister formation and/or epidermolysis as constant findings in the first days after surgery.

Discussion:

As far as the authors could determine, this paper is the first systematic review and meta-analysis on the experimental use of UPFs. Using a random effects model, the authors estimated UPF survival rate to be 90.8% (95% CI, 86.9% to 93.6%; p<0.001) [**Fig. 5**]. Moreover, using a similar methodology the estimated proportion of UPFs that survive completely or nearly completely was 74.4% (95% CI, 62.1% to 83.7%; p<0.001) [**Fig. 6**]. These data indicate that, according to the available literature, the majority of UPFs performed in the experimental setting survived, although a significant fraction of these flaps presented a variable degree of necrosis.

Interestingly, the estimated overall UPF survival rate in the experimental setting [90.8% (95% CI, 86.9% to 93.6%; p<0.001)] was similar to that reported by the authors on a previous meta-analysis addressing the clinical application of UPFs [89.%; 95% CI, 87.3 to 91.3; p < 0.001)].(1)

In contrast, the estimated proportion of UPFs presenting complete or nearly complete survival was 74.4% (95% CI, 62.1% to 83.7%; p<0.001) in the experimental setting, compared to 92.0% (95% CI, 89.9% to 93.7%; p<0.001) in the clinical context.(1) However, in both meta-analyses the majority of UPFs presented complete or nearly complete survival. The differences observed may be partially explained by the different vascular patterns used in the experimental and clinical contexts. In the experimental setting, the most common vascular constructs were in decreasing order of frequency: sliding VFs (40.7%), type IA AVFs (20.9%), and type IIA AVFs (8.8%). In the clinical context, the patterns most frequently reported were: type IA AVFs (33.5%), type IV arterialized venous arterial flaps (14.8%), and type I VF (12.5%).(1, 83)

The most commonly used animal species to produce UPFs was the rabbit (57.1%), followed by the rat (26.4%), the dog (14.3%), and the pig (2.2%). Mice were not used for this purpose. This contrasts with the majority of the literature on experimental flap surgery, which indicates the rat as the most widely used animal model.(84) This is certainly due to the fact that rabbits and rats are easy to obtain and keep, they are relatively inexpensive, and they have a large enough size to perform microvascular procedures.(84-86) Although dogs and pigs have larger-sized vessels, they are more expensive to obtain and to maintain. In addition, the use of these animal species has been submitted to increasingly stringent control by ethical committees and animal welfare bodies.(87-89) Noteworthily, there were no significant differences in UPF survival rates in the most commonly used animal species (rabbit, rat, and dog) [**Fig. 7**]. Regarding animal gender, most studies were conducted on male animals (26.4%), or on both male and female animals (15.4%). Only 3.3% of studies used exclusively female animals. Several authors defend the choice of male animals for experimental flap studies based on the lesser variability of the hormonal *milieu* in the latter gender, and based on the fact that female sex hormones are associated with increased proclivity to vascular anastomoses' thrombosis.(40) However, in the present meta-analysis, the authors failed to observe statistically significant differences in UPFs related to experimental animal gender.

Concerning flap composition, the majority of UPFs were fasciocutaneous (85.7%). Flaps included bone and/or cartilage in 13.2% of cases. It was possible to identify a single study reporting myofasciocutaneous flaps, corresponding to 1.1% of all experimental models.(38) This adds strength to the widely held belief that unconventional perfusion is most adequately suited to perfuse tissues with low metabolic needs, such as those composing the integument, cartilage and/or bone.(1-6)

The authors feel that care must be used when extrapolating the results of this meta-analysis for the clinical setting, since there are important differences between the UPFs performed experimentally and those performed in humans. For example, one of the main discrepancies relates to the disparate vessel and flap sizes across species.(1) Another important difference is that in almost experimental studies vascular anastomoses are performed locally between similarly sized vessels. In opposition, clinically, UPFs are mostly transferred to distant places.(1) This makes vessel caliber incongruence more probable in the latter setting. In addition, vessels' twisting or traction are more likely in distant tissue transfers. These, in turn, may potentiate vascular thrombosis.

Moreover, the blood supply to the integument of various experimental animals has been shown to vary substantially to that reported in humans.(90, 91) For example, Taylor *et al.* have shown that in loose-skinned animals, such as the rabbit, the rat or the dog, there is a preponderance of the direct cutaneous vessels, compared to the dominance of the musculocutaneous vessels in humans and pigs.(90, 91) Furthermore, experimental animals, particularly those with loosely draped skin possess a layer of smooth muscle in the deep aspect of the integument known as panniculus carnosus, which is associated with vascular plexuses of its own.(85, 92) In humans, this layer is virtually absent in the majority of the body, being represented mostly by the platysma and the palmaris longus muscles. In pigs, the panniculus carnosus layer is present in most of the integument. However, it is firmly adherent to overlying skin and to the underlying muscle fascia, making pig skin apparently a more suitable model for comparison with the human integument.(93, 94) Despite all these data, the only study conducted on the pig's hindlimb to produce a type III arterialized venous fasciocutaneous flap revealed complete necrosis of all flaps.(23) This may be explained by the larger thickness of the pig's integument relatively to that of the other

experimental animal species, and even to that of humans in the usual locations where these flaps are harvested in this latter species.(1, 93) In fact, according to most authors, UPFs depend, at least initially, on gas exchanges in the vicinity of the venous system of the flap, which could help explain why thin flaps present the best results in the clinical setting.(1, 95-97)

Table 2 summarizes the main features of the different animal species used to produce experimental UPFs.

	Rabbit	Rat	Dog	Pig
Availability	Easy to acquire	Easy to acquire	Requires special facilities and more stringent evaluation by ethical committees	Requires special facilities and more stringent evaluation by ethical committees
Acquisition cost	Moderate	Low	High	High
Maintenance cost	Low	Low	Moderate	High
Handling and maintenance facilities and skills	Requires special facilities and training	Commonly available	Requires special facilities and training	Requires special facilities and training
Integumentary similarity to the human integument	Significant differences in integument composition and blood supply	Significant differences in integument composition and blood supply Smaller vessels than those most commonly employed clinically	Significant differences in integument composition and blood supply	Similar to humans in terms of blood supply architecture and vessel sizes Differs from humans due to the presence of a well-developed panniculus carnosus and due to the relatively thick integument
Proportion of UPFs experimental models in the literature	57.1%	24.6%	14.3%	2.2%

Table 2. Comparison of the different animal species used for producing experimental unconventional perfusion flaps (UPFs.)

Study limitations

The present study may be affected by several types of bias, as happens in all meta-analyses, particularly retrospective meta-analysis, as this one.(98, 99)

One of the problems of including UPFs performed in different animal species using multiple vascular patterns is that there is a variable degree of inherent heterogeneity. In fact, this heterogeneity was confirmed for both population estimates using the Cochran-Q test ($p<0.001$). The authors tried to partially circumvent this problem by using random effects models for estimating population parameters.(13)

Another major potential caveat of the present study was the effect of publication bias. The latter bias reflects the observation that positive results are more likely to be published compared to neutral or negative ones. The Egger's test supported the presence of this type of bias for the estimate of overall UPF survival, while failing to support it in the estimation of the proportion of UPFs whose survival was complete or near complete. It is widely accepted that the most efficacious way to downplay the effect of publication bias is to perform a systematic and comprehensive review of the literature, as it was performed in the present study.(98, 99) Additionally, the authors have strictly adhered to the widely accepted PRISMA checklist for systematic reviews and meta-analysis, as shown in the ***Supplementary Table 1***, to minimize the risk of committing methodological mistakes.(100, 101)

Finally, the authors believe that although this paper has the significant merit of providing a synthesis of the available literature regarding the use of experimental UPFs, it contributes only modestly to understanding the mechanisms underlying the survival or necrosis of these flaps, making further studies in this field warranted. Ideally, a large animal study in primates could help to elucidate more

perfectly the mechanisms of UPF perfusion, viability, and overall survival in humans. However, such a study would be logistically vexing and expensive to conduct.

Conclusions:

According to the present data, the majority of UPFs performed in the experimental setting survive (90.8%; 95% CI, 86.9% to 93.6%; p<0.001). Furthermore, survival is complete or nearly complete in an estimated 74.4% of cases (95% CI, 62.1% to 83.7%; p<0.001). The rabbit, the rat and the dog were the most commonly used animal species for producing UPFs. No significant differences were found in survival rates among these species, nor among the diverse vascular patterns used.

These data do not differ significantly from those reported in a similar study performed on the UPFs in human medicine.(1) This suggests that the available rabbit, rat and canine experimental UPF models can adequately mimic the clinical application of UPFs.

Acknowledgments:

The authors are very grateful to Mr. Filipe Franco for producing all the drawings contained in this paper.

Financial Disclosure Statement: One of the authors (D.C.) received a grant from "The Programme for Advanced Medical Education" sponsored by "Fundação Calouste Gulbenkian, Fundação Champalimaud, Ministério da Saúde and Fundação para a Ciência e Tecnologia, Portugal."

The authors have no financial or commercial interests to declare in relation to the content of this article.

References

1. Casal, D., Cunha, T., Pais, D., et al. Systematic Review and Meta-Analysis of Unconventional Perfusion Flaps in Clinical Practice. *Plastic and reconstructive surgery* 2016;138:459-479.

2. Goldschlager, R., Rozen, W. M., Ting, J. W., Leong, J. The nomenclature of venous flow-through flaps: updated classification and review of the literature. *Microsurgery* 2012;32:497-501.

3. Yan, H., Brooks, D., Ladner, R., Jackson, W. D., Gao, W., Angel, M. F. Arterialized venous flaps: a review of the literature. *Microsurgery* 2010;30:472-478.

4. Yan, H., Zhang, F., Akdemir, O., et al. Clinical applications of venous flaps in the reconstruction of hands and fingers. *Arch Orthop Trauma Surg* 2011;131:65-74.

5. Jabir, S., Frew, Q., El-Muttardi, N., Dziewulski, P. A systematic review of the applications of free tissue transfer in burns. *Burns : journal of the International Society for Burn Injuries* 2014;40:1059-1070.

6. Weng, W., Zhang, F., Zhao, B., et al. The complicated role of venous drainage on the survival of arterialized venous flaps. *Oncotarget* 2017.

7. Guo, L., Pribaz, J. J. Clinical flap prefabrication. *Plastic and reconstructive surgery* 2009;124:e340-350.

8. Abbase, E. A., Shenaq, S. M., Spira, M., el-Falaky, M. H. Prefabricated flaps: experimental and clinical review. *Plastic and reconstructive surgery* 1995;96:1218-1225.

9. Haines, P., Nichter, L. S., Morgan, R. F., Horowitz, J. H., Edgerton, M. T. A digit replantation model. *Microsurgery* 1985;6:70-72.

10. Nichter, L. S., Haines, P. C. Arterialized venous perfusion of composite tissue. *Am J Surg* 1985;150:191-196.

11. Epidermolysis. In B. Werner ed., *Stedman's medical dictionary*, 27th ed. USA: Lippincott Williams and Wilkins, 2000:604.

12. Korevaar, D. A., Hooft, L., ter Riet, G. Systematic reviews and meta-analyses of preclinical studies: publication bias in laboratory animal experiments. *Laboratory animals* 2011;45:225-230.

13. Borenstein, M., Hedges, L. V., Higgins, J. P., Rothstein, H. R. Identifying and quantifying heterogeneity. In M. Borenstein, L. V. Hedges, J. P. Higgins, H. R. Rothstein eds., *Introduction to Meta-analysis*, First ed. United Kingdom: Wiley; 2009:107-125.

14. Sterne, J. A., Sutton, A. J., Ioannidis, J. P., et al. Recommendations for examining and interpreting funnel plot asymmetry in meta-analyses of randomised controlled trials. *BMJ* 2011;343:d4002.

15. Egger, M., Davey Smith, G., Schneider, M., Minder, C. Bias in meta-analysis detected by a simple, graphical test. *Bmj* 1997;315:629-634.

16. Nakayama, Y., Soeda, S., Kasai, Y. Flaps nourished by arterial inflow through the venous system: an experimental investigation. *Plastic and reconstructive surgery* 1981;67:328-334.

17. Voukidis, T. An axial-pattern flap based on the arterialised venous network: an experimental study in rats. *Br J Plast Surg* 1982;35:524-529.

18. Mundy, J. C., Panje, W. R. Creation of free flaps by arterialization of the venous system. *Arch Otolaryngol* 1984;110:221-223.

19. Ji, S. Y., Chia, S. L., Cheng, H. H. Free transplantation of venous network pattern skin flap: an experimental study in rabbits. *Microsurgery* 1984;5:151-159.

20. Beehary, S., Hoang, P., Foucher, G. L'artérialisation des lambeaux veineux. *Annales de chirurgie plastique et esthetique* 1985;30:95-97.

21. Baek, S. M., Weinberg, H., Song, Y., Park, C. G., Biller, H. F. Experimental studies in the survival of venous island flaps without arterial inflow. *Plastic and reconstructive surgery* 1985;75:88-95.

22. Thatte, R. L., Thatte, M. R. A study of the saphenous venous island flap in the dog without arterial inflow using a non-biological conduit across a part of the length of the vein. *Br J Plast Surg* 1987;40:11-15.

23. Germann, G. K., Eriksson, E., Russell, R. C., Mody, N. Effect of arteriovenous flow reversal on blood flow and metabolism in a skin flap. *Plastic and reconstructive surgery* 1987;79:375-380.

24. Amarante, J., Costa, H., Reis, J., Soares, R. Venous skin flaps: an experimental study and report of two clinical distal island flaps. *Br J Plast Surg* 1988;41:132-137.

25. Fukui, A., Inada, Y., Tamai, S., Mizumoto, S., Yajima, H., Sempuku, T. Skin graft including subcutaneous vein: experimental study and clinical applications. *J Reconstr Microsurg* 1988;4:223-231.

26. Sasa, M., Xian, W. Q., Breidenbach, W., Tsai, T. M., Shibata, M., Firrell, J. Survival and blood flow evaluation of canine venous flaps. *Plastic and reconstructive surgery* 1988;82:319-327.

27. Inada, Y., Fukui, A., Tamai, S., Masuhara, K. Experimental studies of skin flaps with subcutaneous veins. *J Reconstr Microsurg* 1989;5:249-261.

28. Yuen, Q. M., Leung, P. C. Some factors affecting the survival of venous flaps: an experimental study. *Microsurgery* 1991;12:60-64.

29. Noreldin, A. A., Fukuta, K., Jackson, I. T. Role of perivenous areolar tissue in the viability of venous flaps: an experimental study on the inferior epigastric venous flap of the rat. *Br J Plast Surg* 1992;45:18-22.

30. Takato, T., Zuker, R. M., Turley, C. B. Viability and versatility of arterialized venous perfusion flaps and prefabricated flaps: an experimental study in rabbits. *J Reconstr Microsurg* 1992;8:111-119.

31. Chow, S. P., Chen, D. Z., Gu, Y. D. A comparison of arterial and venous flaps. *J Hand Surg Br* 1992;17:359-364.

32. Angel, M. F., Knight, K. R., Dvir, E., Mellow, C. G., Morrison, W. A., O'Brien, B. M. Biochemical analysis of the venous flap in the dog. *J Surg Res* 1992;53:24-29.

33. Inada, Y., Hirai, T., Fukui, A., Omokawa, S., Mii, Y., Tamai, S. An experimental study of the flow-through venous flap: investigation of the width and area of survival with one flow-through vein preserved. *J Reconstr Microsurg* 1992;8:297-302.

34. Inada, Y., Fukui, A., Tamai, S., Mizumoto, S. The arterialised venous flap: experimental studies and a clinical case. *Br J Plast Surg* 1993;46:61-67.

35. Matsushita, K., Firrell, J. C., Ogden, L., Tsai, T. M. Blood flow and tissue survival in the rabbit venous flap. *Plastic and reconstructive surgery* 1993;91:127-135; discussion 136-127.

36. Gencosmanoglu, R., Ulgen, O., Yaman, C., Songur, E., Akin, Y., Cagdas, A. Mechanisms of viability in rabbit flank venous flaps. *Ann Plast Surg* 1993;30:60-66.

37. Ueda, K., Harada, T., Nagasaka, S., Oba, S., Inoue, T., Harashina, T. An experimental study of delay of flow-through venous flaps. *Br J Plast Surg* 1993;46:56-60.

38. Fukui, A., Tamai, S., Maeda, M., Inada, Y., Mii, Y., Mine, T. The pedicled venous flap. An experimental study. *Br J Plast Surg* 1993;46:116-121.

39. Takato, T., Komuro, Y., Yonehara, H., Zuker, R. M. Prefabricated venous flaps: an experimental study in rabbits. *Br J Plast Surg* 1993;46:122-126.

40. Thatte, M., Healy, C., McGrouther, D. Laser Doppler and microvascular pulsed Doppler studies of the physiology of venous flaps. *European Journal of Plastic Surgery* 1993;16:134-138.

41. Lenoble, E., Lavau, L., Foucher, G., Voisin, M. C., Goutallier, D. [Influence of the anatomy of the pedicle on the survival of venous vascularized flaps. Experimental study on the rat]. *Annales de chirurgie plastique et esthetique* 1993;38:612-620.

42. Smith, R. J., Fukuta, K., Wheatley, M., Jackson, I. T. Role of perivenous areolar tissue and recipient bed in the viability of venous flaps in the rabbit ear model. *Br J Plast Surg* 1994;47:10-14.

43. Dvir, E., Hickey, M. J., Hurley, J. V., Morrison, W. A. A histological and carbon perfusion study of cephalic and saphenous venous flaps in the dog. *Br J Plast Surg* 1994;47:263-267.

44. Suzuki, Y., Suzuki, K., Ishikawa, K. Direct monitoring of the microcirculation in experimental venous flaps with afferent arteriovenous fistulas. *Br J Plast Surg* 1994;47:554-559.

45. Wolff, K. D., Telzrow, T., Rudolph, K. H., Franke, J., Wartenberg, E. Isotope perfusion and infrared thermography of arterialised, venous flow-through and pedicled venous flaps. *Br J Plast Surg* 1995;48:61-70.

46. Byun, J. S., Constantinescu, M. A., Lee, W. P., May, J. W., Jr. Effects of delay procedures on vasculature and survival of arterialized venous flaps: an experimental study in rabbits. *Plastic and reconstructive surgery* 1995;96:1650-1659.

47. Xiu, Z. F., Chen, Z. J. The microcirculation and survival of experimental flow-through venous flaps. *Br J Plast Surg* 1996;49:41-45.

48. Pittet, B., Chang, P., Cederna, P., Cohen, M. B., Blair, W. F., Cram, A. E. The role of neovascularization in the survival of an arterialized venous flap. *Plastic and reconstructive surgery* 1996;97:621-629.

49. Adamo, C., Rubino, C. Venous flaps and perivenous areolar tissue: an experimental study in rats. *J Reconstr Microsurg* 1996;12:179-181.

50. Xiu, Z., Chen, Z. The effect of glutathione, superoxide dismutase and adenosine triphosphate on venous flap survival. *European Journal of Plastic Surgery* 1996;19:170-173.

51. Miles, D. A., Crosby, N. L., Clapson, J. B. The role of the venous system in the abdominal flap of the rat. *Plastic and reconstructive surgery* 1997;99:2030-2033.

52. Yilmaz, M., Menderes, A., Vayvada, H., Karaca, C., Barutcu, A. Effects of the number of pedicles on perfusion and survival of venous flaps: an experimental study in rabbits. *Ann Plast Surg* 1997;39:278-286.

53. Fukui, A., Inada, Y., Murata, K., Ueda, Y., Tamai, S. A method for prevention of arterialized venous flap necrosis. *J Reconstr Microsurg* 1998;14:67-74.

54. Woo, S.-H., Kim, S.-E., Lee, T.-H., Jeong, J.-H., Seul, J.-H. Effects of Blood Flow and Venous Network on the Survival of the Arterialized Venous Flap. *Plastic and reconstructive surgery* 1998;101:1280-1289.

55. Yuan, R., Shan, Y., Zhu, S. Circulating mechanism of the "pure" venous flap: direct observation of microcirculation. *J Reconstr Microsurg* 1998;14:147-152.

56. Atabey, A., Gezer, S., Vayvada, H., et al. Ischemia/reperfusion injury in flow-through venous flaps. *Ann Plast Surg* 1998;40:612-616.

57. Cho, B. C., Lee, M. S., Lee, J. H., Byun, J. S., Baik, B. S. The effects of surgical and chemical delay procedures on the survival of arterialized venous flaps in rabbits. *Plastic and reconstructive surgery* 1998;102:1134-1143.

58. Mutaf, M., Tasaki, Y., Fujii, T. Expansion of venous flaps: an experimental study in rats. *Br J Plast Surg* 1998;51:393-401.

59. Yilmaz, M., Menderes, A. Investigation of metabolism and perfusion in arterialized venous replantation: experimental study in rabbits. *Ann Plast Surg* 1999;43:67-73.

60. Murata, K., Tamai, S., Inada, Y., Fukui, A., Miyamoto, S. Transfer of a pedicled venous flap containing perivenous areolar tissue and nerve: an experimental study. *Br J Plast Surg* 1999;52:223-229.

61. Yucel, A., Bayramicli, M. Effects of hyperbaric oxygen treatment and heparin on the survival of unipedicled venous flaps: an experimental study in rats. *Ann Plast Surg* 2000;44:295-303.

62. Tang, Y. B., Simchon, S., Chen, H. C. Microcirculation of a venous flap: an experimental study with microspheres in rabbits. *Scand J Plast Reconstr Surg Hand Surg* 2000;34:207-212.

63. Wungcharoen, B., Pradidarcheep, W., Santidhananon, Y., Chongchet, V. Pre-arterialisation of the arterialised venous flap: an experimental study in the rat. *Br J Plast Surg* 2001;54:621-630.

64. Saray, A., Can, B., Sevin, K. Effects of methylprednisolone on the viability of experimental flow-through venous flaps. *J Reconstr Microsurg* 2002;18:615-622.

65. Chang, S. M., Gu, Y. D., Li, J. F. Comparison of different managements of large superficial veins in distally based fasciocutaneous flaps with a veno-neuro-adipofascial pedicle: an experimental study using a rabbit model. *Microsurgery* 2003;23:555-560.

66. Coruh, A., Abaci, K., Gunay, G. K. Effect of topical nitroglycerine on the survival of ischemic flow-through venous flaps in rabbits. *J Reconstr Microsurg* 2004;20:261-266.

67. Lin, C. H., Wei, F. C., Mardini, S., Ma, S. F. Microcirculation study of rabbit ear arterial and venous flow-through flaps using a window chamber model. *J Trauma* 2004;56:894-900.

68. Baser, N. T., Silistreli, O. K., Sisman, N., Oztan, Y. Effects of surgical or chemical delaying procedures on the survival of proximal predicled venous island flaps: an experimental study in rats. *Scand J Plast Reconstr Surg Hand Surg* 2005;39:197-203.

69. Zhang, F., Brooks, D., Chen, W., Mustain, W., Chen, M. B., Lineaweaver, W. C. Improvement of venous flap survival by application of vascular endothelial growth factor in a rat model. *Ann Plast Surg* 2006;56:670-673.

70. Ozyazgan, I., Tuncer, A., Yazici, C., Gunay, G. K. Reactive oxygen species in experimental ischemic flow-through venous flaps and effects of antioxidants on reactive oxygen species and flap survival. *Ann Plast Surg* 2007;58:661-666.

71. Ozyazgan, I., Ozkose, M., Baskol, G. Nitric oxide in flow-through venous flaps and effects of L-arginine and nitro-L-arginine methyl ester (L-NAME) on nitric oxide and flap survival in rabbits. *Ann Plast Surg* 2007;59:550-557.

72. Pittet, B., Quinodoz, P., Alizadeh, N., Schlaudraff, K. U., Mahajan, A. L. Optimizing the arterialized venous flap. *Plastic and reconstructive surgery* 2008;122:1681-1689.

73. Tan, M. P., Lim, A. Y., Zhu, Q. A novel rabbit model for the evaluation of retrograde flow venous flaps. *Microsurgery* 2009;29:226-231.

74. Yan, H., Brooks, D., Jackson, W. D., Angel, M. F., Akdemir, O., Zhang, F. Improvement of prearterialized venous flap survival with delay procedure in rats. *J Reconstr Microsurg* 2010;26:193-200.

75. Lalković, M., Kozarski, J., Panajotović, L., et al. The new experimental design of arterialized venous flap on the rabbit ear model. *Acta veterinaria* 2010;60:633-640.

76. Iglesias, M., Fonseca-Lazcano, J. A., Moran, M. A., Butron, P., Diaz-Morales, M. Revascularization of Arterialized Venous Flaps through a Total Retrograde Reverse

Blood Flow: Randomized Experimental Trial of Viability. *Plastic and reconstructive surgery Global open* 2013;1:e34.

77. Yan, H., Kolkin, J., Zhao, B., et al. The effect of hemodynamic remodeling on the survival of arterialized venous flaps. *PloS one* 2013;8:e79608.

78. Yan, H., He, Z., Li, Z., et al. Large prefabricated skin flaps based on the venous system in rabbits: a preliminary study. *Plastic and reconstructive surgery* 2013;132:372e-380e.

79. Ceylan, R., Kaya, B., Caydere, M., Terzioglu, A., Aslan, G. Comparison of ischaemic preconditioning with surgical delay technique to increase the viability of single pedicle island venous flaps: an experimental study. *Journal of plastic surgery and hand surgery* 2014;48:368-374.

80. Lalkovic, M., Kozarski, J., Panajotovic, L., et al. Surface enlargement of a new arterialised venous flap by the surgical delay method. *Vojnosanitetski pregled Military-medical and pharmaceutical review* 2014;71:547-553.

81. Borumandi, F., Higgins, J. P., Buerger, H., et al. Arterialized Venous Bone Flaps: An Experimental Investigation. *Scientific reports* 2016;6.

82. Weng, W., Zhang, F., Zhao, B., et al. The complicated role of venous drainage on the survival of arterialized venous flaps. *Oncotarget* 2017;8:16414-16420.

83. Chen, H. C., Tang, Y. B., Noordhoff, M. S. Four types of venous flaps for wound coverage: a clinical appraisal. *J Trauma* 1991;31:1286-1293.

84. Dunn, R. M., Mancoll, J. Flap models in the rat: a review and reappraisal. *Plastic and reconstructive surgery* 1992;90:319-328.

85. Casal, D., Pais, D., Iria, I., et al. A Model of Free Tissue Transfer: The Rat Epigastric Free Flap. *Journal of Visualized Experiments* 2017;1:e55281.

86. Mapara, M., Thomas, B. S., Bhat, K. M. Rabbit as an animal model for experimental research. *Dental Research Journal* 2012;9:111-118.

87. Swindle, M. M., Smith, A. C., Laber-Laird, K., Dungan, L. Swine in Biomedical Research: Management and Models. *ILAR Journal* 1994;36:1-5.

88. Tanaka, H., Kobayashi, E. Education and research using experimental pigs in a medical school. *Journal of Artificial Organs* 2006;9:136-143.

89. Hasiwa, N., Bailey, J., Clausing, P., et al. Critical evaluation of the use of dogs in biomedical research and testing in Europe. *Altex* 2011;28:326-340.

90. Taylor, G. I., Minabe, T. The angiosomes of the mammals and other vertebrates. *Plastic and reconstructive surgery* 1992;89:181-215.

91. Taylor, G. I., Pan, W. R. The angiosome concept. In P. Dodwell ed., *The angiosome concept and tissue transfer*, Vol. 1, First ed. Florida: Quality Medical Publishing, Inc.; 2014:354-395.

92. Pearl, R. M., Johnson, D. The vascular supply to the skin: an anatomical and physiological reappraisal--Part II. *Annals of plastic surgery* 1983;11:196-205.

93. Rose, E. H., Vistnes, L. M., Ksander, G. A. The panniculus carnosus in the domestic pig. *Plastic and reconstructive surgery* 1977;59:94-97.

94. Kerrigan, C. L., Zelt, R. G., Thomson, J. G., Diano, E. The pig as an experimental animal in plastic surgery research for the study of skin flaps, myocutaneous flaps and fasciocutaneous flaps. *Laboratory animal science* 1986;36:408-412.

95. Kovacs, A. F. Comparison of two types of arterialized venous forearm flaps for oral reconstruction and proposal of a reliable procedure. *Journal of cranio-maxillo-facial surgery : official publication of the European Association for Cranio-Maxillo-Facial Surgery* 1998;26:249-254.

96. Woo, S. H., Kim, K. C., Lee, G. J., et al. A retrospective analysis of 154 arterialized venous flaps for hand reconstruction: an 11-year experience. *Plastic and reconstructive surgery* 2007;119:1823-1838.

97. Wharton, R., Creasy, H., Bain, C., James, M., Fox, A. Venous flaps for coverage of traumatic soft tissue defects of the hand: a systematic review. *The Journal of hand surgery, European volume* 2017:1753193417712879.

98. Borenstein, M., Hedges, L. V., Higgins, J. P., Rothstein, H. R. Publication bias. In M. Borenstein ed., *Introduction to Meta-analysis*, First ed. United Kingdom: Wiley and Sons; 2009:277-292.

99. Sterne, J. A., Egger, M., Mother, D. Addressing reporting biases. In J. P. Higgins, S. Green eds., *Cochrane handbook for systematic review of interventions*, First ed. United Kingdom: Wiley-Blackwell; 2009:297-333.

100. Liberati, A., Altman, D. G., Tetzlaff, J., et al. The PRISMA statement for reporting systematic reviews and meta-analyses of studies that evaluate health care interventions: explanation and elaboration. *PLoS medicine* 2009;6:e1000100.

101. Panic, N., Leoncini, E., de Belvis, G., Ricciardi, W., Boccia, S. Evaluation of the endorsement of the preferred reporting items for systematic reviews and meta-analysis (PRISMA) statement on the quality of published systematic review and meta-analyses. *PloS one* 2013;8:e83138.

Figure Legends:

Figure 1. Data collection from the literature. A total of 68 studies were retrieved from the literature, corresponding to data from 1073 individual unconventional perfusion flaps.

Figures 2A, 2B and 2C. Schematic representation of the different types of arterialized venous flaps (AVFs) performed in experimental models according to the literature.

AVFs receive arterial blood through one or more of their veins. AVFs venous drainage occurs through one or more veins to neighboring veins and/or arteries.

Red areas represent arterial blood flow. *Blue* and *purple* regions denote venous and mixed arterial and venous blood, respectively. The *arrows* specify the direction of blood flow. The curved lines inside the vessels illustrate venous valves.

First description: in cases where the first description of the type of unconventional pattern was not performed in the experimental setting (**E**), the description in the clinical setting (**C**) is also indicated.

Classifications: The classifications used were those proposed by Woo (96), and by Chen, Tang, and Noordhoff (2).

The drawings are not to scale.

Figures 3A and 3B. Schematic representation of the different types of venous flaps (VFs) performed in experimental models according to the literature.

These flaps receive venous blood through one or more of their veins. VFs venous drainage occurs through one or more veins to neighboring veins.

Red areas represent arterial blood flow. *Blue* and *purple* regions denote venous and mixed arterial and venous blood, respectively. The *arrows* specify the direction of blood flow. The curved lines inside the vessels illustrate venous valves.

First description: in cases where the first description of the type of unconventional pattern was nor performed in the experimental setting (**E**), the description in the clinical setting (**C**) is also indicated.

Classifications: The classifications used were those proposed by Woo (96), and by Chen, Tang, and Noordhoff (2).

The drawings are not to scale.

Figure 4. Star plot illustrating unconventional perfusion flap models' features in different animal species.
AVF, arterialized venous flap; **VF**, venous flap; **UPF**, unconventional perfusion flap.

Figure 5. Forest plot of all studies reporting unconventional perfusion flap (UPFs) survival rates. Meta-analysis of experimental UPFs using a random effects model estimated an overall flap survival rate of 90.8% (95% CI, 86.9% to 93.6%; $p<0.001$)

CI, confidence interval.

Figure 6. Forest plot of all studies describing the proportion of unconventional perfusion flaps (**UPFs**) presenting complete survival or nearly complete survival

The estimated proportion of experimental UPFs presenting complete survival or nearly complete survival was 74.4% (95% CI, 62.1% to 83.7%; p<0.001).

CI, confidence interval.

Figure 7. Bar charts illustrating the survival of the most common types of unconventional perfusion flaps according to animal species and vascular pattern employed.

AVF, arterialized venous flap; **UPF**, unconventional perfusion flap.

There were no statistically significant differences between the different types of unconventional perfusion flaps ($p < 0.05$).

Supplementary Information:

Supplementary Figure 1. Funnel plot of the studies used to estimate the survival rate of the experimental unconventional perfusion flaps. This graphic suggests there is publication bias. This was confirmed by the application of the Egger's test ($p<0.001$).

Study heterogeneity assessment for this parameter was as follows: Cochran-Q value 134.98; $p<0.001$; I-squared 47.40; Tau-squared 1.24.

Supplementary Figure 2. Funnel plot of the studies used to estimate proportion of experimental UPFs that presented complete survival or nearly complete survival. This graphic might suggest there is publication bias. However, Egger's test failed to confirm this assumption ($p=0.342$).

Evaluation of studies heterogeneity regarding this variable was: Cochran-Q value 162.77; $p<0.001$; I-squared 71.74; Tau-squared 2.58.

Supplementary Table 1. Application of the PRISMA checklist in the present work, in order to minimize methodological mistakes. (100, 101)

Diogo Cesol
Enkwell Corresponding Author Last Name (Please Print)

PRS-D-__-_____
Enkwell Number

AUTHOR FORMS

Please complete and sign all three forms.

Form 1. Prior Publication Certification

This manuscript contains original material. Neither the article nor any part of its essential substance, Tables or figures has been or will be published elsewhere before appearing in PRS.

Signed: Diogo Cesol

2. Some of the material in this paper has been, or is being published elsewhere. Details are in the appended letter.

Signed: Diogo Cesol

Form 2. Assignment of any and all copyright

In consideration of the American Society of Plastic Surgeons, Inc. (ASPS) taking action in reviewing and editing my (our) submission, the author(s) undersigned hereby transfer, assign and otherwise convey all copyright ownership to ASPS in all languages, and in all forms of media now or hereafter known, including electronic media such as CD-ROM, Internet, and Intranet in the event that such work is published by the ASPS.

Must be signed by all Authors:

Signed: Diogo Cesol Date: 5-9-17

Signed: David Tanganho Date: 5-9-17

Signed: Teresa Cardoso Date: 05-09-2017

Signed: Eduarda Mota-Silva Date: 5-9-17

Signed: Inês Lúcia Date: 05-09-2017

Signed: Diogo Pais Date: 5/9/17

Signed: Paula Videira Date: 05-09-2017

José Videira e Castro 05-09-17

Joe Coyne O'Neill 05-09-2017

Form 3. Conflict of Interest Disclosure statement by an Author of a manuscript submitted to *Plastic and Reconstructive Surgery*

I, (We) Jiayu Cosel, have submitted for publication in ***Plastic and Reconstructive Surgery***® a manuscript entitled:
Unconventional perfusion flaps in the experimental setting: a systematic review and meta-analysis
I, (We) hereby certify, that:

No financial support or benefits have been received by me or any co-author, by any member of my (our) immediate family or any individual or entity with whom or with which I (we) have a relationship from any commercial source which is related directly or indirectly to the scientific work which is reported on in the article except as described below.

{I (we) understand an example of such a financial interest would be a consulting relationship or stock interest in any business entity which is included in the subject mater of the manuscript or which sells a product relating to the subject matter of the manuscript.}

In addition to filling out and signing this declaration, *I acknowledge that I (we) also made complete disclosure in the manuscript itself*, stating all sources of funds that have supported this work and also a statement of financial interest, if any. Each author on the manuscript has disclosed any commercial association or financial disclosure that might pose a conflict of interest with information presented in this manuscript. *If the authors have no financial interest or commercial association with any of the subject matter or products mentioned in our manuscript, that too will be indicated.* I (we) hereby agree that such disclosures will be printed with the manuscript if it is accepted.

Furthermore, I (we) understand that potential sanctions may be imposed by *Plastic and Reconstructive Surgery* for violation of this complete disclosure policy. I (we) understand that potential disciplinary actions may include warning letters, refusal to publish an article in question, retraction of a published paper, notification to our primary institution, and/or exclusion from publication in *Plastic and Reconstructive Surgery* for a specified time frame.

The corresponding author has the obligation of having any and all co-authors sign this form and date his or her signature.

On behalf of the authors

Jiayu Cosel
Signature and Date

Signature and Date

Signature and Date

Table 1

First Author	Year	Country	Optimized experimental animal model	Species	Strain	Gender	n	Flap donor site	Flap vascular pattern	Wound bed blood supply	Delayed flap	Flap composition	Flap innervation preserved	Flap survival rate (%)	Categorical flap survival (%)				Necrotic flap area (%)		
															CS	NCS	SN	CN	Average	Min.	Max.
Nakayama (17)	1981	Japan	1	Rat	n/a	M	5	T/A	6	WV	Yes	FC	n/a	100	100	0	0	0	0	0	0
			2	Rat	n/a	M	10	T/A	6	WV	No	FC	n/a	100	n/a	n/a	0	0	2	0	2.7
			3	Rat	n/a	M	20	T/A	4	WV	No	FC	n/a	100	n/a	n/a	n/a	0	7	0	21
Voukidis (18)	1982	UK	4	Rat	SD	M+F	10	A/G	3	IB	Yes	FC	No	100	n/a	n/a	n/a	0	n/a	n/a	n/a
Mundy (19)	1984	USA	5	Rabbit	n/a	n/a	5	E	1	B/C	Yes	FC	No	n/a	n/a	n/a	n/a	n/a	13	n/a	n/a
			6	Rabbit	n/a	n/a	5	E	1	B/C	No	FC	No	n/a	n/a	n/a	n/a	n/a	24	n/a	n/a
Ji (20)	1984	China	7	Rabbit	n/a	M+F	33	E	1	B/C	No	FC	No	100	90.9	0	9.1	0	n/a	0	n/a
Beehary (21)	1984	France	8	Rat	n/a	n/a	5	A/G	3	WV	No	FC	n/a	100	100	0	0	0	0	0	0
Baek (22)	1985	South Korea	9	Dog	M	n/a	36	H	10	WV	No	FC	No	100	100	0	0	0	0	0	0
			10	Dog	M	n/a	10	H	10	IB	No	FC	No	100	100	0	0	0	0	0	0
			11	Dog	M	n/a	2	H	7	WV	No	FC	No	100	100	0	0	0	0	0	0
Nichter (11)	1985	USA	12	Rabbit	NZ	M	10	E	2	SE	No	B/C	No	100	n/a	n/a	n/a	0	n/a	n/a	n/a
Thatte (23)	1987	India	13	Dog	M	M+F	14	H	10	WV	No	FC	No	91.7	n/a	n/a	n/a	8.33	n/a	n/a	100
Germann (24)	1987	Germany	14	Pig	Y	M	12	H	5	WV	No	FC	Yes	0	0	0	0	100	100	100	100
Amarante (25)	1988	Portugal	15	Dog	n/a	n/a	5	H	10	WV	No	FC	Yes	100	100	0	0	0	0	0	0
			16	Dog	n/a	n/a	5	H	9	WV	No	FC	Yes	100	100	0	0	0	0	0	0
			17	Dog	n/a	n/a	4	H	7	WV	No	FC	Yes	100	100	0	0	0	0	0	0
Fukui (26)	1988	Japan	18	Rabbit	n/a	n/a	20	E	10	B/C	No	FC	No	100	90	10	0	0	n/a	0	n/a
Sasa (27)	1988	USA	19	Dog	M	M+F	8	F	10	WV	No	FC	No	75	0	75	0	25	n/a	n/a	100
Inada (28)	1989	Japan	20	Rabbit	n/a	n/a	20	E	10	B/C	No	FC	No	100	90	0	10	0	n/a	0	n/a
			21	Rabbit	n/a	n/a	21	E	1	B/C	No	FC	No	100	85.7	0	14.3	0	n/a	0	n/a
Yuen (29)	1991	China	22	Rat	W	M	10	A/G	9	WV	No	FC	n/a	90	80	n/a	n/a	10	n/a	0	100
			23	Rat	W	M	10	A/G	9	IB	No	FC	n/a	100	90	n/a	n/a	0	n/a	0	n/a
Noreldin (30)	1992	USA	24	Rat	W	M	20	A/G	10	WV	No	FC	n/a	90	75	n/a	n/a	10	n/a	0	100
Takato (31)	1992	Canada	25	Rabbit	NZ	F	18	A/G	3	WV	No	FC	No	100	66.7	33.3	0	0	2.4	0	10
Chow (32)	1992	China	26	Rat	SD	n/a	20	A/G	3	WV	No	FC	n/a	n/a	n/a	n/a	n/a	n/a	39.6	n/a	n/a
Angel (33)	1992	USA	27	Dog	n/a	n/a	6	H	10	WV	No	FC	No	100	n/a	n/a	n/a	0	n/a	n/a	n/a
Inada (34)	1992	Japan	28	Rabbit	n/a	n/a	10	E	10	B/C	No	FC	Yes	100	0	0	100	0	56	30	78
Inada (35)	1993	Japan	29	Rabbit	J	n/a	18	E	1	B/C	No	FC	n/a	100	n/a	n/a	0	0	n/a	n/a	n/a
			30	Rabbit	J	n/a	17	E	2	B/C	No	FC	n/a	100	n/a	n/a	0	0	n/a	n/a	n/a
Matsushita (36)	1993	USA	31	Rabbit	NZ	M+F	6	T/A	10	WV	No	FC	Yes	100	83.3	n/a	n/a	0	n/a	0	n/a
Gençosmanoglu (37)	1993	Turkey	32	Rabbit	n/a	n/a	10	T/A	10	WV	No	FC	Yes	100	80	20	0	0	n/a	0	n/a
Ueda (38)	1993	Japan	33	Rabbit	n/a	n/a	15	E	10	SE	Yes	B/C	Yes	100	n/a	n/a	n/a	0	n/a	n/a	n/a
Fukui (39)	1993	Japan	34	Rat	F	M	28	D	10	WV	No	MFC	Yes	85.7	85.7	0	0	14.3	14.3	0	100
Takato (40)	1993	Japan	35	Rabbit	NZ	M	5	A/G	10	IB	No	FC	n/a	100	0	0	100	0	74.8	67.6	79.7
Thatte (41)	1993	India	36	Rat	W	M	5	A/G	10	WV	No	FC	n/a	100	n/a	n/a	n/a	0	n/a	n/a	n/a
Lenoble (42)	1993	France	37	Rat	W	M+F	15	A/G	10	WV	No	FC	Yes	26.7	0	20	6.7	73.3	77	10	100
Smith (43)	1994	USA	38	Rabbit	NZ	n/a	10	E	10	B/C	No	FC	n/a	100	70	n/a	n/a	0	18.1	0	n/a
Dvir (44)	1994	Australia	39	Dog	M	n/a	6	F	10	WV	No	FC	n/a	66.7	33.3	0	33.3	33.3	41.7	0	100
			40	Dog	M	n/a	6	F	1	WV	No	FC	n/a	66.7	33.3	16.7	16.7	33.3	41.7	0	100
			41	Dog	M	n/a	6	F	4	WV	No	FC	n/a	66.7	50	0	16.7	33.3	46.7	0	100
Suzuki(45)	1994	Japan	42	Rabbit	J	M	6	E	1	B/C	No	FC	Yes	100	n/a	n/a	n/a	0	n/a	n/a	n/a
Wolff (46)	1995	Germany	43	Rat	W	M	7	A/G	4	WV	No	FC	n/a	100	14.3	57.1	28.6	0	7	0	16
Byun (47)	1995	USA	44	Rabbit	NZ	M	8	E	3	SE	Yes	B/C	Yes	100	0	100	0	0	5.9	n/a	n/a
Xiu (48)	1996	China	45	Rabbit	n/a	n/a	20	T/A	10	WV	No	FC	n/a	n/a	n/a	n/a	n/a	n/a	7.68	n/a	n/a
Pittet (49)	1996	USA	46	Rabbit	NZ	n/a	16	E	1	B/C	No	FC	No	100	100	0	0	0	0	0	1
Adamo (50)	1996	Italy	47	Rat	W	n/a	10	T/A	10	WV	No	FC	n/a	100	n/a	n/a	40	0	n/a	n/a	n/a
			48	Rat	W	n/a	10	T/A	10	IB	No	FC	n/a	100	n/a	n/a	30	0	n/a	n/a	70
Xiu (51)	1996	China	49	Rabbit	n/a	n/a	40	T/A	10	WV	No	FC	No	n/a	n/a	n/a	n/a	n/a	31.3	0	100
Miles (52)	1997	Canada	50	Rat	SD	M	4	T/A	5	WV	No	FC	n/a	n/a	n/a	n/a	n/a	n/a	43	n/a	n/a
Yilmaz (53)	1997	Turkey	51	Rabbit	NZ	n/a	12	E	10	SE	No	B/C	No	83.3	41.7	n/a	n/a	16.7	24.2	0	100
Fukui (54)	1998	Japan	52	Rabbit	n/a	n/a	22	E	1	WV	Yes	FC	No	100	54.6	n/a	n/a	0	n/a	0	n/a
Woo (55)	1998	South Korea	53	Dog	M	M+F	12	H	4	IB	No	FC	n/a	n/a	n/a	n/a	n/a	n/a	3.8	n/a	n/a
Yuan (56)	1998	China	54	Rabbit	NZ	n/a	38	E	10	SE	No	B/C	No	100	n/a	n/a	n/a	0	n/a	n/a	n/a
Atabey (57)	1998	Turkey	55	Rabbit	NZ	n/a	10	T/A	10	WV	No	FC	No	30.0	30	0	0	70	30	0	100
Cho (58)	1998	South Korea	56	Rabbit	NZ	M	7	E	1	SE	Yes	B/C	Yes	100	0	0	100	0	40.3	22	56
Mutaf (59)	1998	Japan	57	Rat	L	n/a	10	T/A	10	IB	Yes	FC	n/a	n/a	n/a	n/a	n/a	n/a	37.4	n/a	n/a
Yilmaz (60)	1999	Turkey	58	Rabbit	NZ	n/a	12	E	1	IB	No	B/C	No	83.3	58.3	n/a	n/a	16.7	22	0	100
Murata (61)	1999	Japan	59	Rabbit	n/a	n/a	10	E	10	WV	No	FC	Yes	100	10	n/a	n/a	0	17.5	0	100
Yücel (62)	2000	Turkey	60	Rat	SD	M	32	A/G	10	WV	No	FC	No	0	0	0	0	100	100	100	100
Tang (63)	2000	Taiwan	61	Rabbit	NZ	n/a	30	T/A	10	WV	No	MFC	No	100	n/a	n/a	n/a	0	n/a	0	n/a
Wungcharoen (64)	2001	Thailand	62	Rat	W	M	9	T/A	3	IB	Yes	FC	No	n/a	n/a	n/a	n/a	n/a	2.5	n/a	n/a
Saray (65)	2002	Turkey	63	Rabbit	n/a	n/a	10	E	10	IB	No	FC	No	100	n/a	n/a	n/a	0	41.9	n/a	n/a
Chang (66)	2003	China	64	Rabbit	NZ	n/a	10	H	8	IB	No	FC	Yes	100	50	50	0	0	5.5	0	n/a
Coruh (67)	2004	Turkey	65	Rabbit	NZ	M	10	E	10	B/C	No	FC	No	100	0	0	100	0	40	26.0	77.6
			66	Rabbit	NZ	M	10	E	10	B/C	No	FC	No	100	0	0	100	0	42	19.7	55.4
Lin (68)	2004	Taiwan	67	Rabbit	NZ	n/a	13	E	10	SE	No	B/C	No	100	n/a	n/a	n/a	0	6.6	0	55.6
Baser (69)	2005	Turkey	68	Rat	SD	n/a	6	D	10	WV	Yes	FC	n/a	100	16.7	0	83.3	0	37.5	0	46
Zhang (70)	2006	USA	69	Rat	SD	M	10	A/G	10	WV	No	FC	No	n/a	n/a	n/a	n/a	n/a	61	n/a	n/a
Özyazgan (71)	2007	Turkey	70	Rabbit	NZ	n/a	7	E	10	B/C	No	FC	No	n/a	n/a	n/a	n/a	n/a	44	n/a	n/a
Özyazgan (72)	2007	Turkey	71	Rabbit	NZ	M	14	E	10	B/C	No	FC	No	n/a	n/a	n/a	n/a	n/a	39	n/a	n/a
Pittet (73)	2008	Switzerland	72	Rabbit	NZ	n/a	15	E	1	WV	No	FC	No	100	n/a	n/a	0	0	0.6	0	n/a
			73	Rabbit	NZ	n/a	19	E	1	WV	No	FC	No	100	n/a	n/a	6	0	5.3	n/a	n/a
			74	Rabbit	NZ	n/a	14	E	1	IB	No	FC	No	100	n/a	n/a	8	0	6.5	n/a	n/a
Tan (74)	2009	Singapore	75	Rabbit	NZ	M+F	10	T/A	3	IB	No	FC	No	80.0	40	0	40	20	55.5	0	100
Yan (75)	2010	USA	76	Rat	SD	M	8	A/G	4	WV	Yes	FC	n/a	100	0	100	0	0	2	n/a	n/a
Lalkovic (76)	2010	Serbia	77	Rabbit	BC	n/a	10	E	3	SE	No	B/C	No	100	n/a	n/a	n/a	0	1.7	n/a	n/a
Iglesias (77)	2013	Mexico	78	Rabbit	NZ	M+F	12	E	1	SE	No	B/C	n/a	100	91.7	8.3	0	0	1.2	0	15
Yan (78)	2013	China	79	Rabbit	J	M+F	6	T/A	3	WV	No	FC	n/a	100	0	n/a	n/a	0	40.8	n/a	n/a
Yan (79)	2013	China	80	Rabbit	J	M+F	12	T/A	3	WV	Yes	FC	n/a	100	0	n/a	n/a	0	40.8	n/a	n/a
Ceylan (80)	2014	Turkey	81	Rat	W	M	6	A/G	9	WV	No	FC	n/a	100	0	16.7	83.3	0	28.7	6.2	54.8
			82	Rat	W	M	6	A/G	9	WV	Yes	FC	n/a	100	0	83.3	16.7	0	12.1	8.0	18.2
Lalkovic (81)	2014	Serbia	83	Rabbit	BC	M	10	E	1	SE	Yes	B/C	No	100	0	100	0	0	8.7	4.1	15.4
Borumandi (82)	2016	Austria	84	Pig	n/a	n/a	6	H	4	WV	No	B/C	No	100	n/a	n/a	n/a	n/a	n/a	n/a	n/a
Weng (83)	2017	China	85	Rabbit	J	M+F	11	A/G	6	WV	No	FC	n/a	n/a	n/a	n/a	n/a	n/a	28.1	n/a	n/a
			86	Rabbit	J	M+F	12	A/G	5	WV	No	FC	n/a	n/a	n/a	n/a	n/a	n/a	26.7	n/a	n/a

Table 1. Summary of the studies on unconventional perfusion flaps in experimental animal models identified in the systematic review and included in the meta-analysis. For each study, the optimized experimental animal model is identified, as well as its characteristics. These experimental models were those which presented better flap survival rates in each published paper ($p<0.05$).

n, number of flaps in each optimized experimental model; **n/a**, information non-available; **Min.**, minimum; **Max.**, maximum

Categorical flap survival: CN, complete necrosis; **CS**, complete survival; **NCS**, nearly complete survival; **SN**, significant necrosis

Strain: BC, Big Chinchilla rabbit; **F**, Fischer rat; **J**, Japanese white rabbit; **L**, Lewis rat; **M**, Mongrel dog; **NZ**, New Zealand white rabbit; **SD**, Sprague Dawley rat; **W**, Wistar rat; **Y**, Yorkshire pig

Gender: F, female; **M**, male; **M + F**, both males and females

Flap donor site: A/G, abdomen and/or groin; **D**, dorsum; **E**, ear; **F**, forelimb; **H**, hindlimb; **T/A**, thorax and abdomen

Flap vascular pattern (1): "**1**", type Ia arterialized venous flap according to Woo classification; "**2**", type Ib arterialized venous flap according to Woo classification; "**3**", type IIa arterialized venous flap according to Woo classification; "**4**", type IIb arterialized venous flap according to Woo classification; "**5**", type III arterialized venous flap according to Woo classification; "**6**", pedicled arterialized venous flap; "**7**", type I venous flap according to Chen classification; "**8**", type IIa venous flap according to Chen classification; "**9**", type IIb venous flap according to Chen classification; "**10**", sliding venous flap

Wound bed blood supply: B/C, bone or cartilage; **IB**, impermeable barrier underneath the flap; **SE**, skeletonized ear; **WV**, well vascularized

Flap composition: B/C, includes bone and/or cartilage (other than skin with its appendages and subcutaneous tissue); **FC**, fasciocutaneous (skin with its appendages and subcutaneous tissue); **MFC**, myofasciocutaneous (skin with its appendages, subcutaneous tissue and muscle/portion of muscle)

	Rabbit	Rat	Dog	Pig
Availability	Easy to acquire	Easy to acquire	Requires special facilities and more stringent evaluation by ethical committees	Requires special facilities and more stringent evaluation by ethical committees
Acquisition cost	Moderate	Low	High	High
Maintenance cost	Low	Low	Moderate	High
Handling and maintenance facilities and skills	Requires special facilities and training	Commonly available	Requires special facilities and training	Requires special facilities and training
Integumentary similarity to the human integument	Significant differences in integument composition and blood supply	Significant differences in integument composition and blood supply Smaller vessels than those most commonly employed clinically	Significant differences in integument composition and blood supply	Similar to humans in terms of blood supply architecture and vessel sizes Differs from humans due to the presence of a well-developed panniculus carnosus and due to the relatively thick integument
Proportion of UPFs experimental models in the literature	57.1%	24.6%	14.3%	2.2%

Table 2. Comparison of the different animal species used for producing experimental unconventional perfusion flaps (UPFs.)

Figure 1

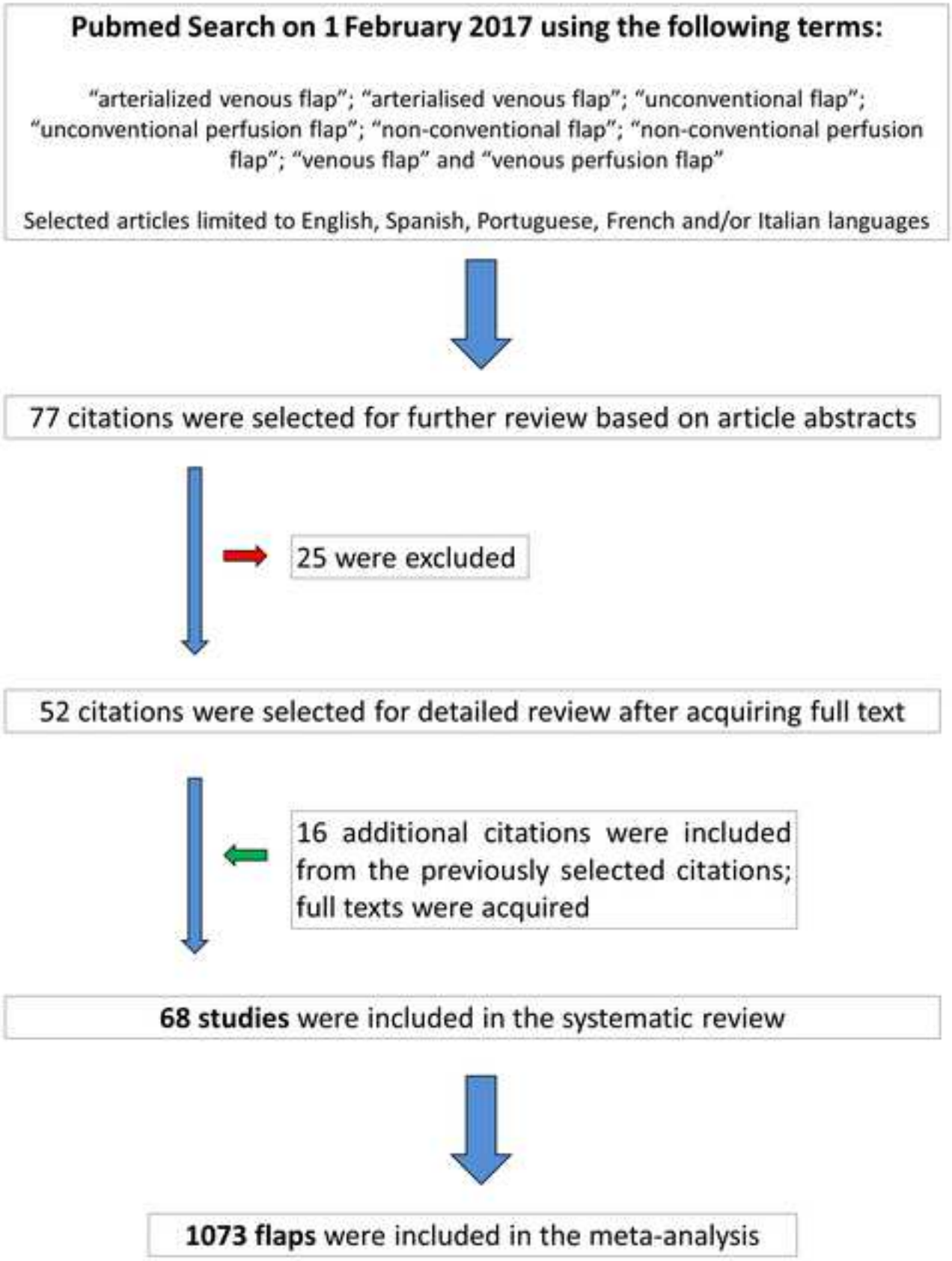

Figure 2A

Vascular patterns referred in the literature	General description			Additional Information
	"Arterialized venous flow-through flaps" Orthodromic blood flow (blood flows in the same direction as venous valves open)	Straight venous pattern akin to a sttandard vein graft	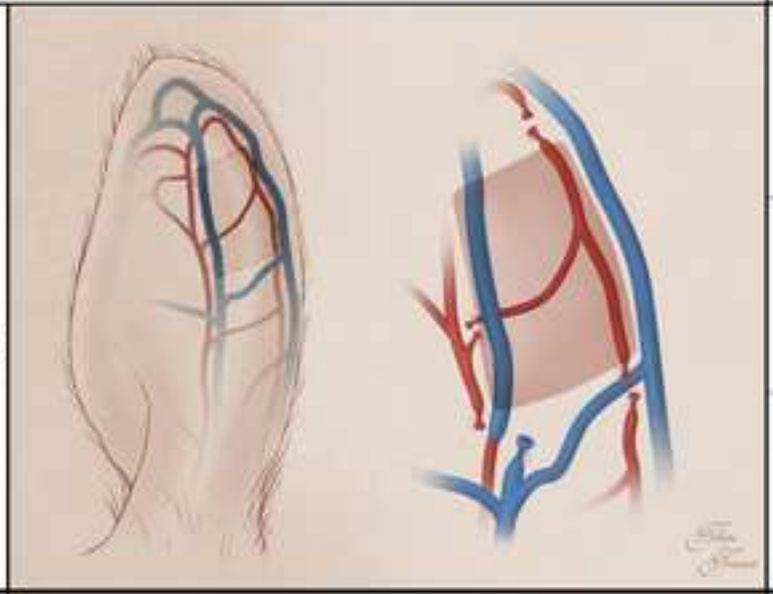	**First Discription** Mundy 1984 [18] **(E)** **Classifications** IA (Woo) III (Chen) **Number of papers and Flaps Analized** **Rabbits**: 12 papers; 215 flaps **Dog:** 1 paper; 6 flaps
		Y-shaped pattern	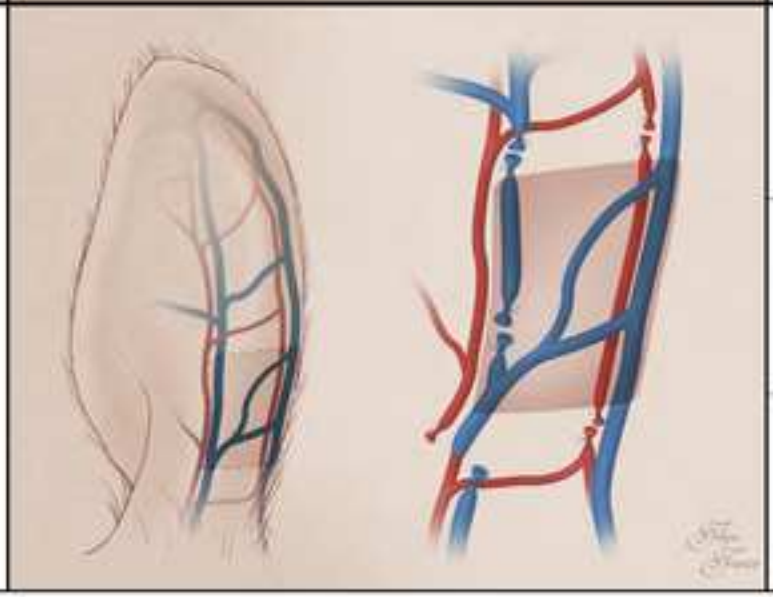	**First Discription** Nichter 1985 [10] **(E)** **Classifications** IB (Woo) III (Chen) **Number of papers and Flaps Analized** **Rabbits**: 2 papers; 27 flaps

Figure 2B

Vascular patterns referred in the literature	General description			Additional Information
	Antidromic blood flow (blood flows in the opposite direction of venous valves opening in the afferent vein)	Y-shaped pattern	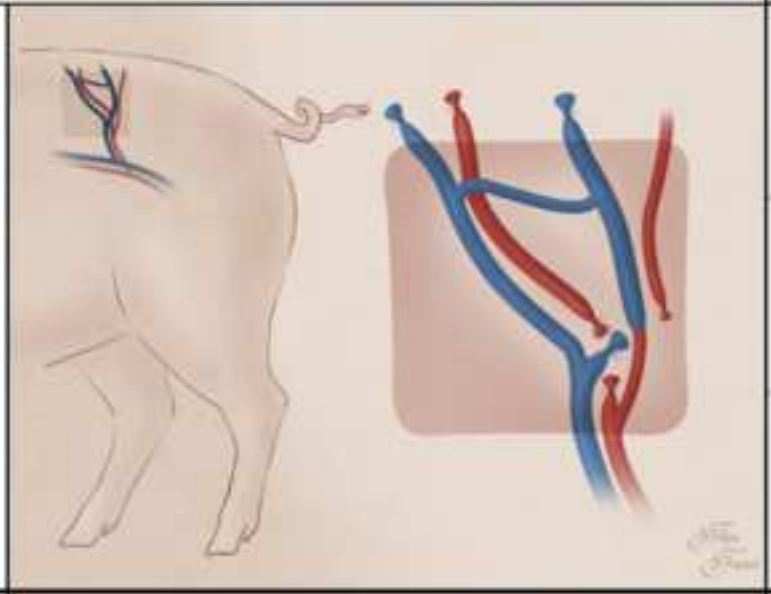	**First Discription** Voukidis 1982 [17] **(E)** **Classifications** IA (Woo) **Number of papers and Flaps Analized** **Rabbits**: 6 papers; 64 flaps **Rat:** 4 paper; 44 flaps
		H-shaped pattern	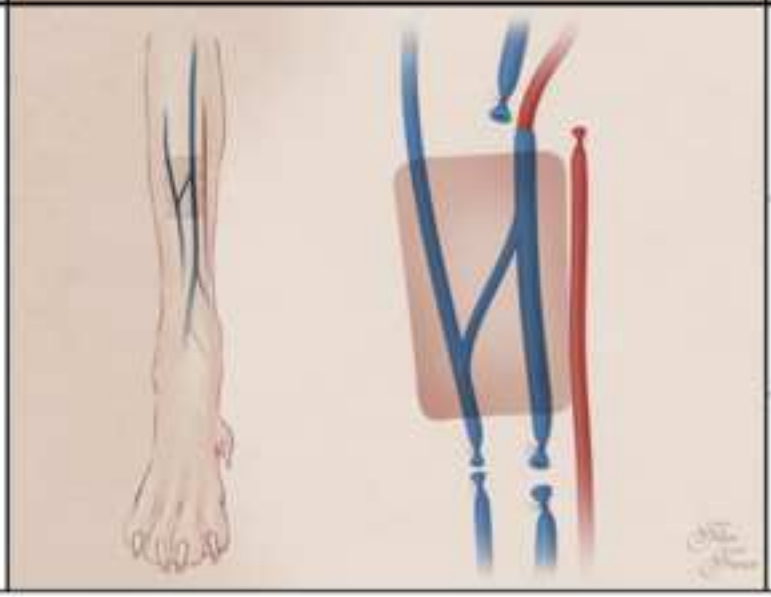	**First Discription** Nakayama 1981 [16] **(E)** **Classifications** IB (Woo) **Number of papers and Flaps Analized** **Rat**: 3 papers; 35 flaps **Dog**: 2 papers; 18 flaps; **Pig**: 1 paper; 6 flaps

Figure 2C

Vascular patterns referred in the literature	General description		Additional Information
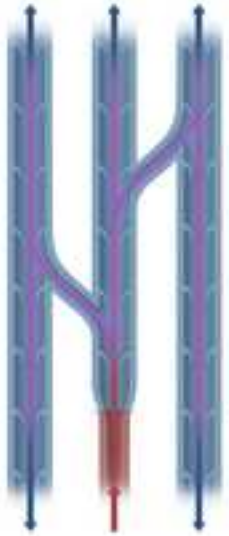	Anti and orthodromic blood flow (mixed pattern of through and against-valve blood flow)	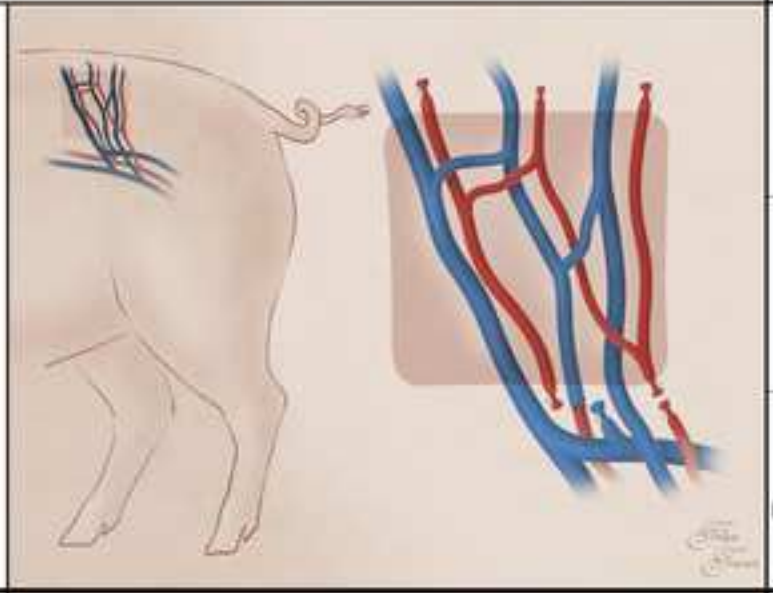	**First Discription** Germann 1987 [23] **(E)** **Classifications** III (Woo) **Number of papers and Flaps Analized** **Rabbits**: 1 paper; 12 flaps **Pig:** 1 paper; 12 flaps; **Rat:** 4 paper; 44 flaps
	Pedicled arterialized venous flap (blood enters the flap antidromically and leaves orthodromically through preserved efferent veins)	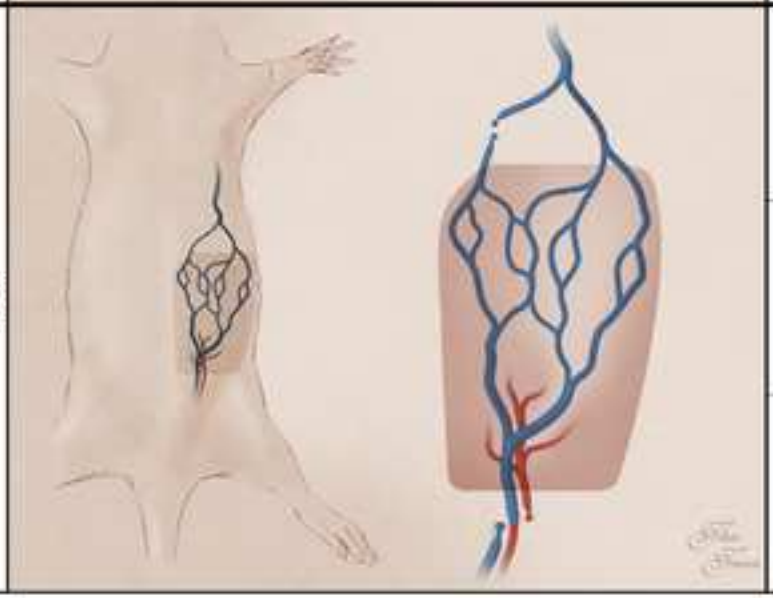	**First Discription** Nakayama 1981 [16] **(E)** **Classifications** - **Number of papers and Flaps Analized** **Rat**: 1 paper; 15 flaps **Rabbit:** 1 paper; 11 flaps

Figure 3A

Vascular patterns referred in the literature	General description		Additional Information
	Free venous flow through flap (the flap is nourished exclusively by venous blood flowing orthodromically)	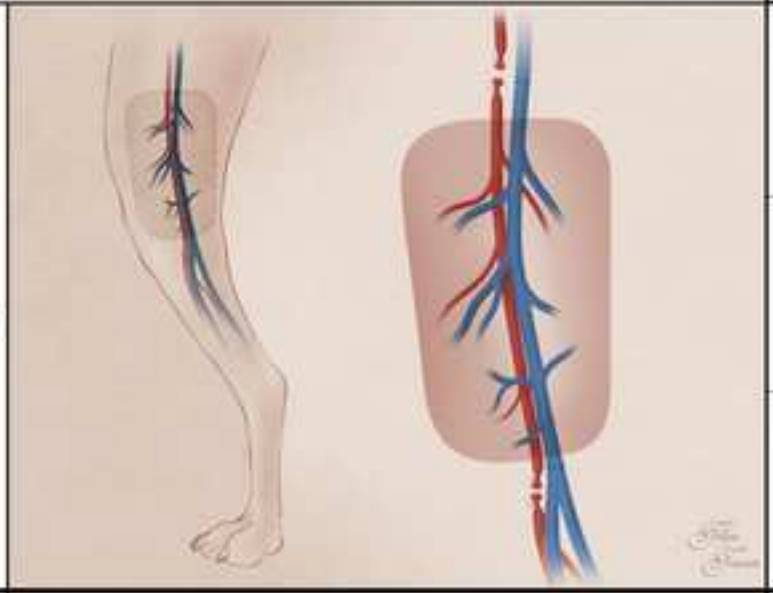	**First Discription** Baek 1985 [21] **(E)** Honda 1984-[95] **(C)** **Classifications** I (Chen) **Number of papers and Flaps Analized** **Dog:** 2 papers; 6 flaps
	Distally pedicled based venous flap	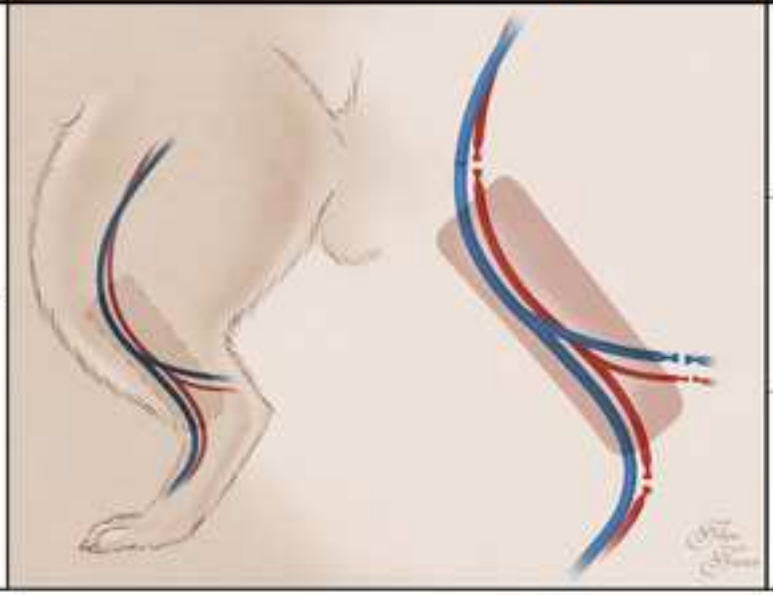	**First Discription** Chang 2003 [65] **(E)** Amarante 1988 [24] **(C)** **Classifications** IIA (Chen) **Number of papers and Flaps Analized** **Rabbit:** 1 paper; 10 flaps

Figure 3B

Vascular patterns referred in the literature	General description		Additional Information
	Proximally pedicled venous flap	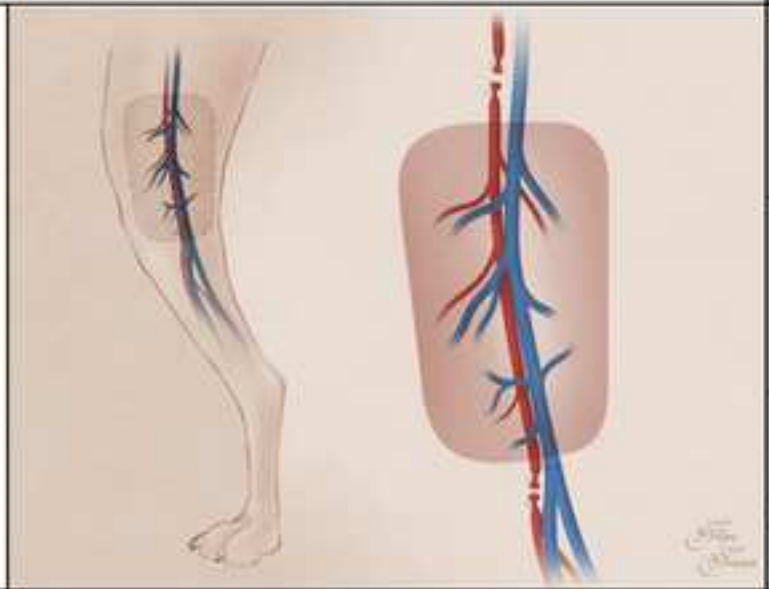	**First Discription** Amarante 1988 [24] **(E)** Chavoin 1987 [93] **(C)** **Classifications** IIB (Chen) **Number of papers and Flaps Analized** **Rabbit:** 2 papers; 32 flaps **Dog:** 1 paper; 5 flaps
	**Sliding venous flap** **(the flap is transposed based exclusively on the dissested venous network)**	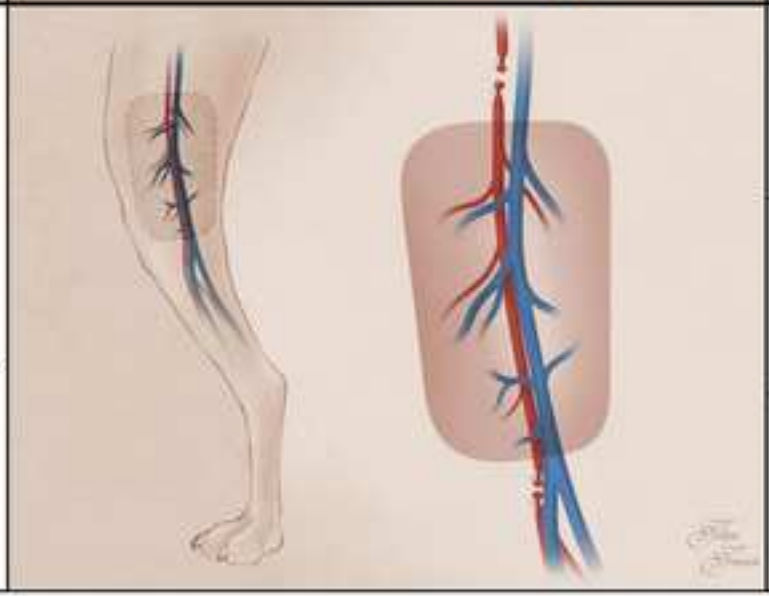	**First Discription** Baek 1985 [21] **(E)** **Classifications** - **Number of papers and Flaps Analized** **Rabbit:** 21 papers; 320 flaps **Rat:** 9 papers; 146 flaps **Dog:** 6 papers; 85 flaps

Figure 4

Click here to download Figure Figure 4.tif

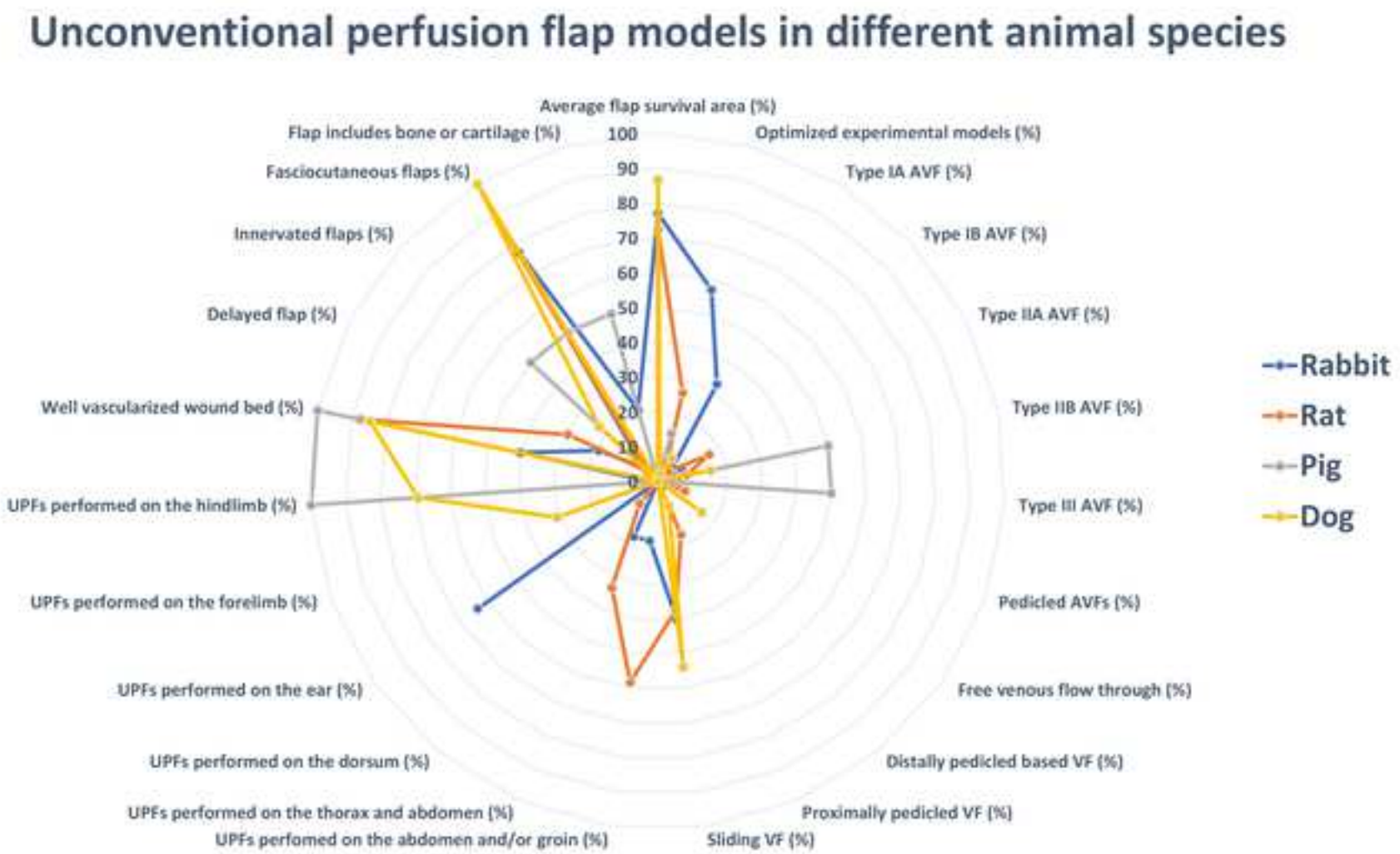

Figure 5

Click here to download Figure Figure 5.tif

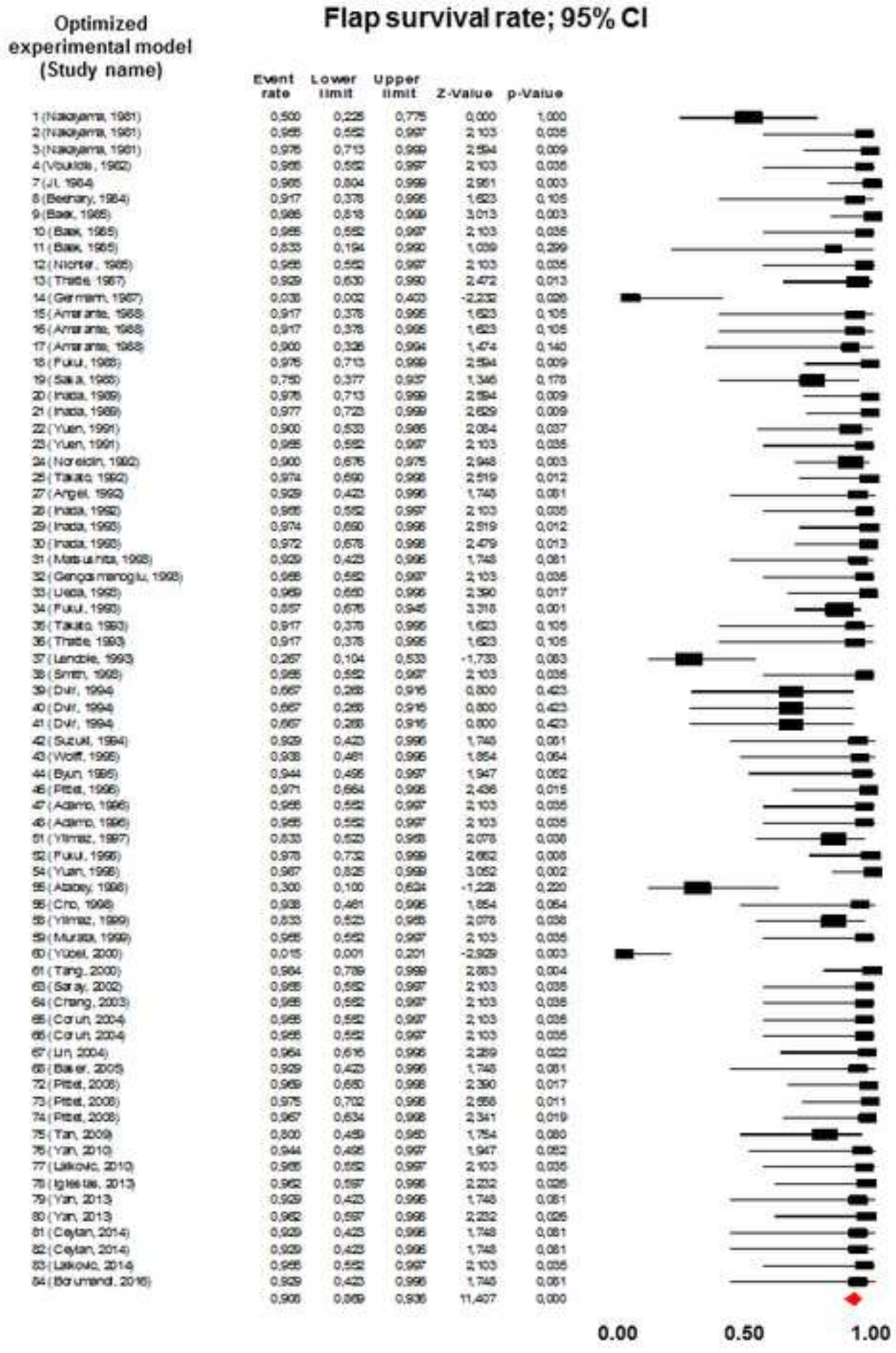

Figure 6

Click here to download Figure Figure 6.tif

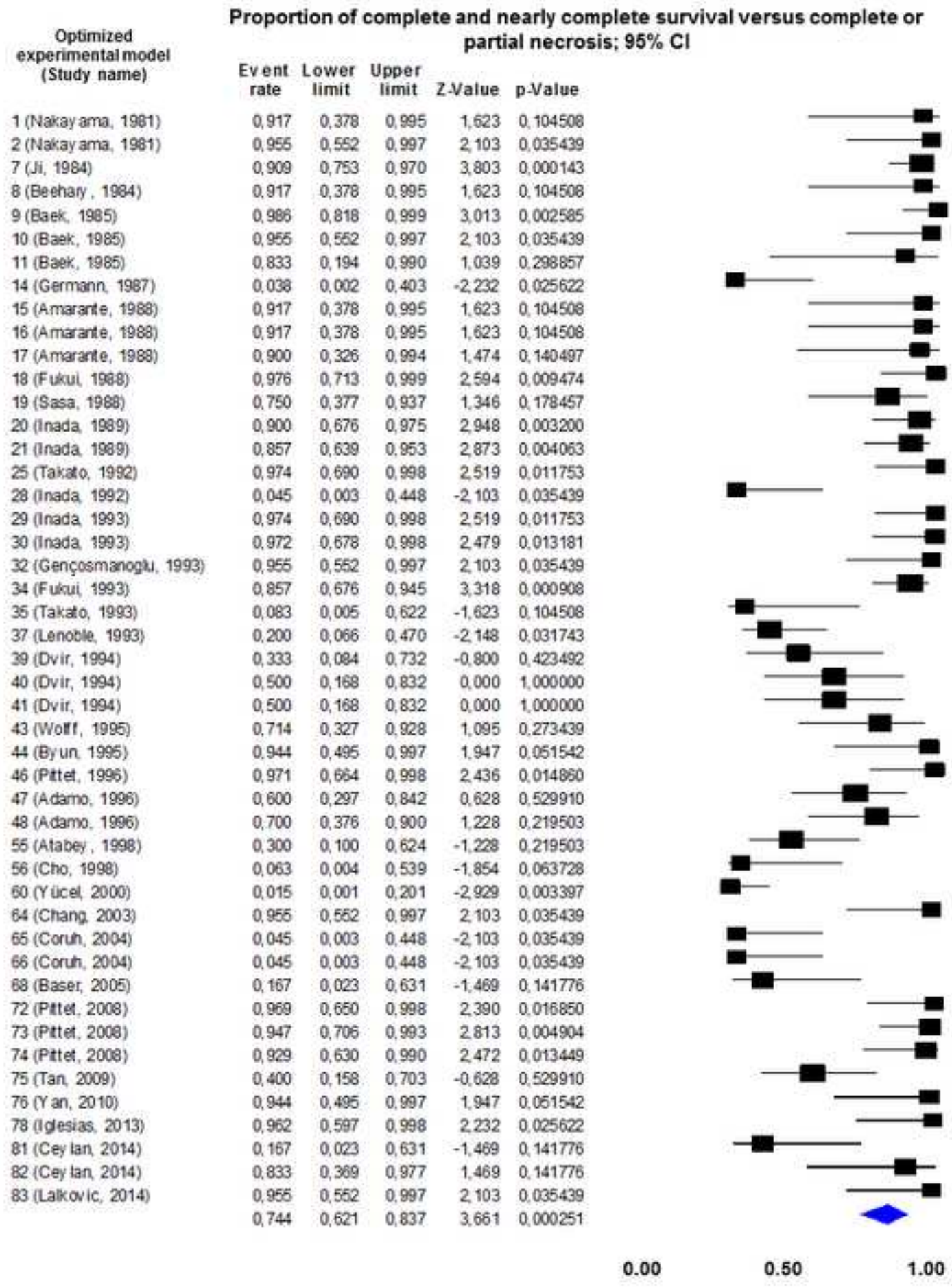

Figure 7

Click here to download Figure Figure 7.tif

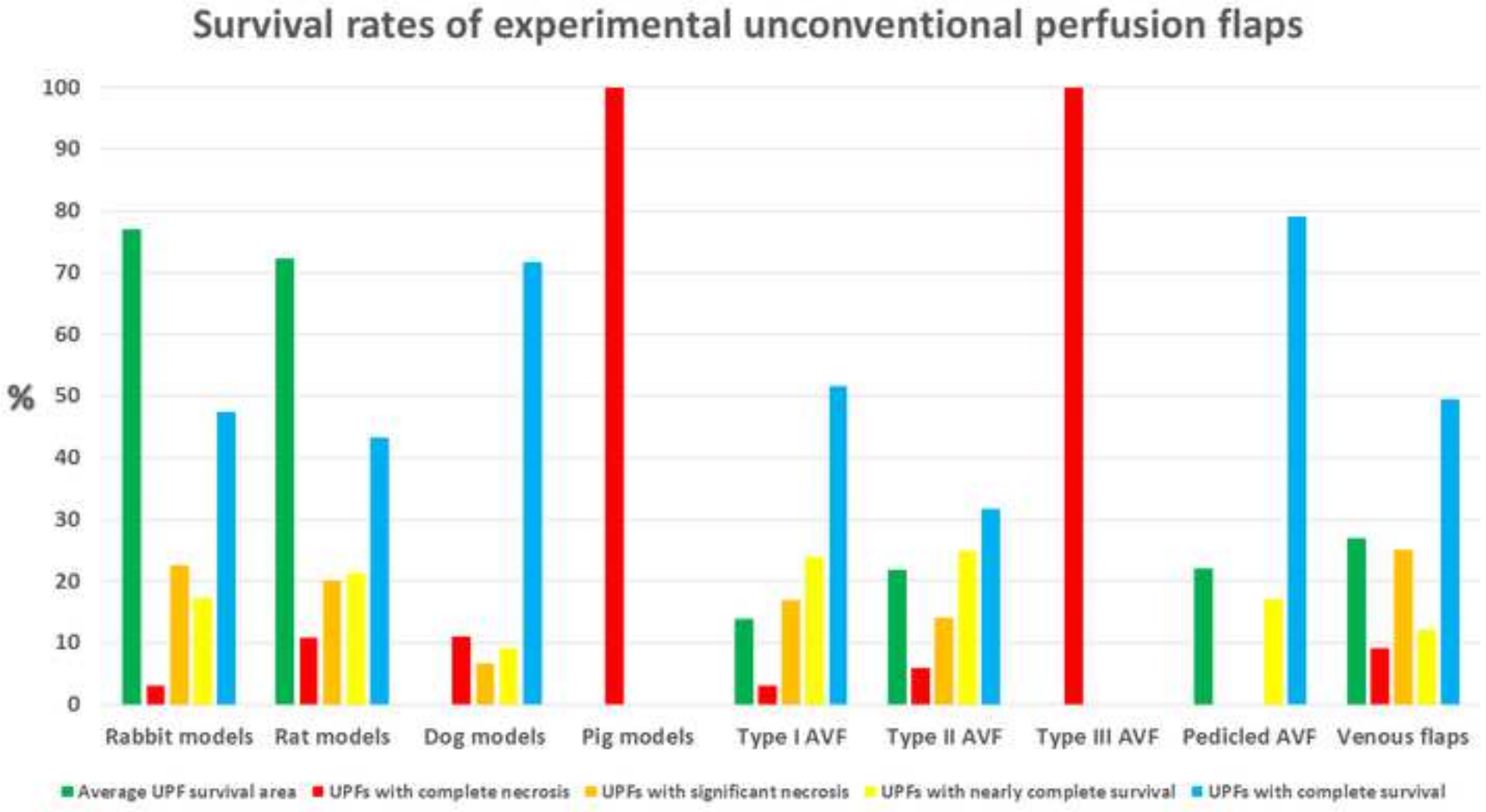

Supplementary Figure 1

Supplementary Figure 2

Supplemental Table 1

Dear Professor Rod Rohrich
Editor of the *Plastic and Reconstructive Surgery Journal*,

We take the liberty of submitting the manuscript of a paper entitled "***Systematic review and meta-analysis of unconventional perfusion flaps in the experimental setting***" for publication in the ***Plastic and Reconstructive Surgery Journal***. This study was performed in a methodologically adequate manner following the PRISMA checklist, as shown in the *Supplementary Table 1*.(1, 2)

For the past four decades, unconventional perfusion flaps (UPFs) have been increasingly used in the clinical setting, offering multiple advantages in comparison to traditional flaps.(3, 4) Their dissection is relatively simple, expeditious and not associated with major donor site morbidity. Moreover, these flaps are intrinsically thin and pliable, two highly advantageous features for reconstructing shallow defects particularly in mobile regions where the integument is thin, such as the face or the hands.(3, 5-8) Finally, as they are usually tailored around the superficial venous system, their harvesting precludes the need of ancillary pre-operative tests. Therefore, UPFs are particularly useful for emergent reconstruction in the realm of trauma cases.

Recently, we had the privilege of publishing in the journal a systematic review and meta-analysis on the clinical application of UPFs.(3) This helped to systematize the available information on the clinical application of these flaps.

However, the numerous experimental papers on UPFs, the multiple animal species involved, the myriad vascular constructions used, and the frequently conflicting data reported, with necrosis rates varying between 100% and 0%, makes synthesis of the information on the experimental use of UPFs challenging.(9-11)

Hence, **the main aim of this paper was to perform a systematic review and meta-analysis of the literature on the experimental use of UPFs, in order to identify the best experimental models proposed as well as to estimate their global survival rate.** Additionally, in the attempt to systematize all the scattered data available, we present professionally-drawn artworks that clearly illustrate all the vascular patterns reported in the experimental literature. This synthesis allows a rapid and sound grasp of the literature on experimental models of UPFs. Additionally, it may be used as a reference for trainees and researchers interested in the field.

We identified 68 studies on the experimental use of UPFs in the experimental setting, corresponding to a total of 1073 flaps. The rabbit, the rat and the dog were the most commonly used animal species for producing UPFs. Using a random effects model, the authors estimated UPF survival rate to be 90.8% (95% CI, 86.9% to 93.6%; p<0.001). Interestingly, the estimated overall UPF survival rate in the experimental setting was similar to that reported by us on the clinical application of UPFs [89.%; 95% CI, 87.3 to 91.3; p < 0.001)].(3) This suggests that the available rabbit, rat and canine experimental UPF models can adequately mimic the application of UPFs.

No doubt, this paper contributes to broaden the knowledge on the yet controversial literature on UPFs. Moreover, all this data is highly pertinent for anyone with an interest in reconstructive surgery, microsurgery and/or experimental models of ischemia. Hence, we strongly believe that this paper is of significant value and interest to the readership of ***Plastic and Reconstructive Surgery Journal*** and thus deserves publication.

If you have any doubts or queries, please do not hesitate to contact us.
Thank you so much for your kind attention.

The authors.

References

1. Liberati, A., Altman, D. G., Tetzlaff, J., et al. The PRISMA statement for reporting systematic reviews and meta-analyses of studies that evaluate health care interventions: explanation and elaboration. *PLoS medicine* 2009;6:e1000100.
2. Panic, N., Leoncini, E., de Belvis, G., Ricciardi, W., Boccia, S. Evaluation of the endorsement of the preferred reporting items for systematic reviews and meta-analysis (PRISMA) statement on the quality of published systematic review and meta-analyses. *PloS one* 2013;8:e83138.
3. Casal, D., Cunha, T., Pais, D., et al. Systematic Review and Meta-Analysis of Unconventional Perfusion Flaps in Clinical Practice. *Plastic and reconstructive surgery* 2016;138:459-479.
4. Wharton, R., Creasy, H., Bain, C., James, M., Fox, A. Venous flaps for coverage of traumatic soft tissue defects of the hand: a systematic review. *The Journal of hand surgery, European volume* 2017:1753193417712879.
5. Goldschlager, R., Rozen, W. M., Ting, J. W., Leong, J. The nomenclature of venous flow-through flaps: updated classification and review of the literature. *Microsurgery* 2012;32:497-501.
6. Yan, H., Brooks, D., Ladner, R., Jackson, W. D., Gao, W., Angel, M. F. Arterialized venous flaps: a review of the literature. *Microsurgery* 2010;30:472-478.
7. Yan, H., Zhang, F., Akdemir, O., et al. Clinical applications of venous flaps in the reconstruction of hands and fingers. *Arch Orthop Trauma Surg* 2011;131:65-74.
8. Jabir, S., Frew, Q., El-Muttardi, N., Dziewulski, P. A systematic review of the applications of free tissue transfer in burns. *Burns : journal of the International Society for Burn Injuries* 2014;40:1059-1070.
9. Nakayama, Y., Soeda, S., Kasai, Y. Flaps nourished by arterial inflow through the venous system: an experimental investigation. *Plastic and reconstructive surgery* 1981;67:328-334.
10. Voukidis, T. An axial-pattern flap based on the arterialised venous network: an experimental study in rats. *Br J Plast Surg* 1982;35:524-529.
11. Germann, G. K., Eriksson, E., Russell, R. C., Mody, N. Effect of arteriovenous flow reversal on blood flow and metabolism in a skin flap. *Plastic and reconstructive surgery* 1987;79:375-380.

PRISMA 2009 Checklist

Section/topic	#	Checklist item	Reported on page #
TITLE			
Title	1	Identify the report as a systematic review, meta-analysis, or both.	1
ABSTRACT			
Structured summary	2	Provide a structured summary including, as applicable: background; objectives; data sources; study eligibility criteria, participants, and interventions; study appraisal and synthesis methods; results; limitations; conclusions and implications of key findings; systematic review registration number.	3
INTRODUCTION			
Rationale	3	Describe the rationale for the review in the context of what is already known.	5
Objectives	4	Provide an explicit statement of questions being addressed with reference to participants, interventions, comparisons, outcomes, and study design (PICOS).	5
METHODS			
Protocol and registration	5	Indicate if a review protocol exists, if and where it can be accessed (e.g., Web address), and, if available, provide registration information including registration number.	6-9
Eligibility criteria	6	Specify study characteristics (e.g., PICOS, length of follow-up) and report characteristics (e.g., years considered, language, publication status) used as criteria for eligibility, giving rationale.	6
Information sources	7	Describe all information sources (e.g., databases with dates of coverage, contact with study authors to identify additional studies) in the search and date last searched.	6
Search	8	Present full electronic search strategy for at least one database, including any limits used, such that it could be repeated.	6,7
Study selection	9	State the process for selecting studies (i.e., screening, eligibility, included in systematic review, and, if applicable, included in the meta-analysis).	7-8
Data collection process	10	Describe method of data extraction from reports (e.g., piloted forms, independently, in duplicate) and any processes for obtaining and confirming data from investigators.	7-8
Data items	11	List and define all variables for which data were sought (e.g., PICOS, funding sources) and any assumptions and simplifications made.	7-8
Risk of bias in individual studies	12	Describe methods used for assessing risk of bias of individual studies (including specification of whether this was done at the study or outcome level), and how this information is to be used in any data synthesis.	9
Summary measures	13	State the principal summary measures (e.g., risk ratio, difference in means).	8-9
Synthesis of results	14	Describe the methods of handling data and combining results of studies, if done, including measures of consistency (e.g., I^2) for each meta-analysis.	8-9

PRISMA 2009 Checklist

Section/topic	#	Checklist item	Reported on page #
Risk of bias across studies	15	Specify any assessment of risk of bias that may affect the cumulative evidence (e.g., publication bias, selective reporting within studies).	8-9
Additional analyses	16	Describe methods of additional analyses (e.g., sensitivity or subgroup analyses, meta-regression), if done, indicating which were pre-specified.	8-9
RESULTS			
Study selection	17	Give numbers of studies screened, assessed for eligibility, and included in the review, with reasons for exclusions at each stage, ideally with a flow diagram.	10-13
Study characteristics	18	For each study, present characteristics for which data were extracted (e.g., study size, PICOS, follow-up period) and provide the citations.	10-13
Risk of bias within studies	19	Present data on risk of bias of each study and, if available, any outcome level assessment (see item 12).	15,16
Results of individual studies	20	For all outcomes considered (benefits or harms), present, for each study: (a) simple summary data for each intervention group (b) effect estimates and confidence intervals, ideally with a forest plot.	10-13
Synthesis of results	21	Present results of each meta-analysis done, including confidence intervals and measures of consistency.	10-13
Risk of bias across studies	22	Present results of any assessment of risk of bias across studies (see Item 15).	13,14
Additional analysis	23	Give results of additional analyses, if done (e.g., sensitivity or subgroup analyses, meta-regression [see Item 16]).	15,16
DISCUSSION			
Summary of evidence	24	Summarize the main findings including the strength of evidence for each main outcome; consider their relevance to key groups (e.g., healthcare providers, users, and policy makers).	17-21
Limitations	25	Discuss limitations at study and outcome level (e.g., risk of bias), and at review-level (e.g., incomplete retrieval of identified research, reporting bias).	22,23
Conclusions	26	Provide a general interpretation of the results in the context of other evidence, and implications for future research.	24
FUNDING			
Funding	27	Describe sources of funding for the systematic review and other support (e.g., supply of data); role of funders for the systematic review.	25

From: Moher D, Liberati A, Tetzlaff J, Altman DG, The PRISMA Group (2009). Preferred Reporting Items for Systematic Reviews and Meta-Analyses: The PRISMA Statement. PLoS Med 6(6): e1000097. doi:10.1371/journal.pmed1000097

MANUSCRIPT PREPARATION AUTHOR CHECKLIST

Copy this form or download from http://www.PRSJournal.com and www.editorialmanager.com/prs

Use this checklist to help you include all required elements of your submission. **Please complete the checklist and submit it with your manuscript.** Note: Although all items are necessary, authors must sign off on this checklist the items indicated in red.

- [x] Prepare manuscript following Instructions for Authors
- [x] Prepare all files necessary for submitting on PRS' enkwell electronic system
- [x] Cover letter to Editor with address, phone #, fax # and or e-mail address of corresponding author
- [x] Title page, including
  - Complete title of article
  - List of authors, including first names and highest academic degrees
  - All authors' affiliation(s) and full financial disclosures listed
  - A footnote listing date(s) and site(s) of presentation (if applicable)
- [x] Name and address of corresponding author
- [x] Listing of each author's role/participation in the authorship of the manuscript on the manuscript (on a separate page in the manuscript)
- [x] Statement of IRB Approval and/or statement of conforming to Helsinki Declaration
- [ ] Clinical Trial Registration information provided:
  - Name of Trial database registered_____
  - Registration Number and date registered_____
- [x] Structured abstract for original articles
- [ ] Summary for Case Reports and Ideas and Innovations
- [x] List of references
- [x] List of figure legends, including credit lines
- [ ] Copies of signed patient release forms for the use of all photographs in which patients can be identified. Forms can be found at: www.plasreconsurg.org
- [x] Tables, including credit lines
- [x] High quality color figures, properly prepared according to the above guidelines

Any manuscript that does not include this completed checklist or is missing essential elements may be returned to the corresponding author for additional information.

Declaration of Authorship for *(title)* "Conventional perfusion flaps in the experimental setting: a systematic review and meta-analysis" for *Plastic and Reconstructive Surgery*

Author Name	Substantial contributions to the conception or design of the work; or the acquisition, analysis, or interpretation of data for the work; (**initial here**)	Drafting the work or revising it critically for important intellectual content; (**initial here**)	Final approval of the version to be published; (**initial here**)	Agreement to be accountable for all aspects of the work in ensuring that questions related to the accuracy or integrity of any part of the work are appropriately investigated and resolved; (**initial here**)	By placing my **SIGNATURE** below I attest that I meet all four criteria of authorship for this article and am **legally responsible** for the content here-in.
Diogo Casal	D.C.	D.C.	D.C.	D.C.	Diogo Casal
David Tangonho	D.T.	D.T.	D.T	D.T.	David Tangonho
Teresa Cunha	T.C.	T.C.	T.C.	T.C.	Teresa Cunha
Eduarda Mota-Silva	EMS	EMS	EMS	EMS	Eduarda Mota-Silva
Inês Inia	I.I.	I.I	I.I.	I.I.	Inês Inia
Diogo Pais	DP	DP	DP	DP	Diogo Pais
Paula Videira	P.V.	P.V.	P.V	P.V	Paula Videira
José Videira e Castro	JVC	JVC	JVC	JVC	José Videira e Castro

Declaration of authorship

Declaration of Authorship for *Plastic and Reconstructive Surgery* (page 2)					
Author Name	Substantial contributions to the conception or design of the work; or the acquisition, analysis, or interpretation of data for the work; (**initial here**)	Drafting the work or revising it critically for important intellectual content; (**initial here**)	Final approval of the version to be published; (**initial here**)	Agreement to be accountable for all aspects of the work in ensuring that questions related to the accuracy or integrity of any part of the work are appropriately investigated and resolved; (**initial here**)	By placing my **SIGNATURE** below I attest that I meet all four criteria of authorship for this article and am **legally responsible** for the content here-in.
Lúa Gopi O'Neill	LO	LO	LO	LO	Lúa Gopi O'Neill

APPENDIX 4

OPEN

PRS GLOBAL OPEN EXPERIMENTAL

Blood Supply to the Integument of the Abdomen of the Rat: A Surgical Perspective

Diogo Casal, MD*†‡§
Diogo Pais, MD, PhD†
Inês Iria, MSci§¶
Paula A. Videira, PhD‡§‖
Eduarda Mota-Silva, MSci**
Sara Alves, MSci††
Luís Mascarenhas-Lemos, MD††
Cláudia Pen, MSci††
Valentina Vassilenko, PhD**
João Goyri-O'Neill, MD, PhD†

Background: Many fundamental questions regarding the blood supply to the integument of the rat remain to be clarified, namely the degree of homology between rat and humans. The aim of this work was to characterize in detail the macro and microvascular blood supply to the integument covering the ventrolateral aspect of the abdominal wall of the rat.
Methods: Two hundred five Wistar male rats weighing 250–350 g were used. They were submitted to gross anatomical dissection after intravascular colored latex injection (n = 30); conversion in modified Spalteholz cleared specimens (n=10); intravascular injection of a Perspex® solution, and then corroded, in order to produce vascular corrosion casts of the vessels in the region (n = 5); histological studies (n = 20); scanning electron microscopy of vascular corrosion casts (n = 10); surgical dissection of the superficial caudal epigastric vessels (n = 100); and to thermographic evaluation (n = 30).
Results: The ventrolateral abdominal wall presented a dominant superficial vascular system, which was composed mainly of branches from the superficial caudal epigastric artery and vein in the caudal half. The cranial half still received significant arterial contributions from the lateral thoracic artery in all cases and from large perforators coming from the intercostal arteries and from the deep cranial epigastric artery.
Conclusions: These data show that rats and humans present a great deal of homology regarding the blood supply to the ventrolateral aspect of the abdominal integument. However, there are also significant differences that must be taken into consideration when performing and interpreting experimental procedures in rats. *(Plast Reconstr SurgGlobOpen2017;5:;doi:10.1097/GOX.0000000000001454;Publishedonlinexxxxxx2017.)*

INTRODUCTION

The rat is arguably the most commonly used animal model for training and research in plastic surgery.[1–11] Its abdominal wall is frequently employed in tissue perfusion and transference studies.[12–18] Oddly, anatomical and histological studies concerning the blood supply to the integument over the ventrolateral aspect of the abdomen of the rat (IOVAAR) are scant and are based on small series of animals.[19] Hence, many fundamental questions remain to be clarified, namely the degree of homology between it and that of humans.[19] The aim of this work was to characterize in detail the macro and microvascular blood supply to the IOVAAR.

METHODS

This study focused on the blood supply to the IOVAAR, defined by the region ventral to the dorsal axillary lines. Two hundred five Wistar male rats weighing 250–350 g were used.

*From the *Plastic and Reconstructive Surgery Department and Burn Unit, Centro Hospitalar de Lisboa Central, Lisbon, Portugal; †Anatomy Department, Nova Medical School, Lisbon, Portugal; ‡UCIBIO, Departamento de Ciências da Vida, Faculdade de Ciências e Tecnologia, Universidade NOVA de Lisboa, Caparica, Portugal; §Glycoimmunology group, CEDOC, NOVA Medical School, Universidade NOVA de Lisboa, Lisbon, Portugal; ¶Molecular Microbiology and Biotechnology Group, iMed—Research Institute for Medicines, Faculdade de Farmácia Universidade Lisboa, Lisbon, Portugal; ‖CDG & Allies—Professionals and Patient Associations International Network (CDG & Allies—PPAIN), Caparica, Portugal; **LIBPhys, Physics Department, Faculdade de Ciências e Tecnologias, Universidade NOVA de Lisboa, Lisbon, Portugal; and ††Pathology Department, Centro Hospitalar de Lisboa Central, Lisbon, Portugal.*
Received for publication November 7, 2016; accepted July 7,2017.

DOI: 10.1097/GOX.0000000000001454

Disclosure: *Supported by a grant from "The Programme for Advanced Medical Education" (Dr. Casal), sponsored by "Fundação Calouste Gulbenkian, Fundação Champalimaud, Ministério da Saúde and Fundação para a Ciência e Tecnologia, Portugal." The Article Processing Charge was paid for by the authors.*

Supplemental digital content is available for this article. Clickable URL citations appear in the text.

All the animals were housed under standard environmental conditions and given nothing by mouth 6 hours before surgical procedures.

All in vivo studies were performed in strict accordance with the recommendations in the Guide for Proper Conduct of Animal Experiments and Related Activities in Academic Research and Technology, 2006.

The protocol was approved by the Institutional Animal Care and Use Committee and Ethical Committee at the authors' institution (08/2012/CEFCM).

Gross Anatomical Dissection

In 30 rats, a 22G catheter was introduced in the left ventricle and another in the right ventricle. A volume of 180–200 ml/Kg of a red colored latex solution (Robialac) was introduced in the left ventricle and a volume of 300–350 ml/Kg of a blue colored latex solution (Robialac) was introduced in the right ventricle, until good peripheral contrast perfusion was noted. Subsequently, the rats were submitted to abdominal wall dissection to characterize the origin of the supplying vessels. This technique allows to highlight the vessels as they are normally observed during surgical procedures.[20]

In 10 rats subjected to a similar procedure, the IOVAAR was converted into modified Spalteholz cleared specimens.[21] This technique creates transparent 3-dimensional specimens, while preserving vascular and perivascular structure.[22]

Five rats were submitted to a left ventricular injection of a Perspex solution, and then corroded, to produce vascular corrosion casts of the vessels in the IOVAAR. Vascular corrosion casts produce a faithful replica of vascular beds, allowing detailed 3-dimensional morphological analysis of even small vessels.[23]

All identified perforator vessels were plotted on a Cartesian grid centered on the pubic symphysis.

Microscopic Anatomical Study—Optical Microscopy

Ten rats were submitted to surgical collection of the IOVAAR, which was fixed in 10% paraformaldehyde and prepared for histological examination, using hematoxylin-eosin and Masson's trichrome stains, as well as immunohistochemistry for CD31 for staining the endothelium[24–26] and for neurofilaments for staining nerves.[27] Rats were submitted to axial sections in the caudal, middle, and cranial aspect of both sides of the abdomen. Ten additional rats were subjected to the preparation just described and their largest integumentary veins were sectioned longitudinally for evaluation of venous valves.

Microscopic Anatomical Study—Scanning Electron Microscopy of Vascular Corrosion Casts

Ten rats were submitted to intravascular injection of a resin cast (Mercox) and latter corroded.[28] The vascular casts were processed and examined using 2 scanning electron microscopes (acceleration voltage of 2–30 kV): a JEOL JSM-5410, for histomorphometric analysis, and a JEOL JSM-7001F, for obtaining high-quality images. Vascular casts were interpreted according to Aharinejad and Lametschwandtner.[28]

Surgical Anatomy of the Superficial Caudal Epigastric Vessels

In 100 rats used for surgical training and experiments, the origin of the superficial caudal epigastric vessels (SCEVs) was registered on the left side of the abdomen.

The specimens were photographed using adequate microscopes. Vessels' dimensions were determined using the ImageJ software.

Thermographic Evaluation

In 30 rats, thermographic assessment of the IOVAAR was performed with a FLIR E6 camera placed 25 cm above the abdomen. Evaluations were done after the rats were anesthetized intraperitoneally with a mixture of ketamine and diazepam and placed on their backs for 10 minutes. The day before the evaluation, animals were lightly anesthetized and the hair of the abdominal area removed using a depilatory cream. Evaluations were performed at a constant room temperature (22°C) and humidity (50%).[29]

Statistical Analysis

Qualitative variables were expressed as percentages. Quantitative variables were expressed as means ± SD. The SPSS 21.0 software was used for statistical analysis. The Kolmogorov-Smirnov test was used to assess normality. Analysis of variance and Student's t test were used to compare averages in normally distributed data. Kruskal-Wallis and Mann-Whitney tests were used to compare means in nonnormally distributed data. Proportions were analyzed with the chi-square test or Fisher's exact test.

A cluster analysis was performed using a 2-step clustering procedure based on the Schwarz Bayesian criteria to determine the overall distribution of all significant cutaneous perforators.

A 2-tailed $P < 0.05$ was considered to be statistically significant.

RESULTS

Gross Anatomy

Figure 1 summarizes the most common disposition found in the main vessels supplying the IOVAAR. This region presented a dominant superficial vascular system (Figs. 2–4; **see figure, Supplementary Digital Content 1**, which demonstrates lateral thoracic (LT) vessels and their anatomical relations, ***http://links.lww.com/PRSGO/A503***). In the caudal half, this system was composed mainly of branches from the superficial caudal epigastric artery (SIEA) and vein (SIEV), which are the equivalent to the human superficial inferior epigastric artery and vein. The cranial half also received significant arterial contributions from the LT artery in all cases, and from 1 (64.4%), 2 (26.7%), or 3 (8.9%) large perforators coming from the intercostal arteries, and from the deep cranial epigastric artery, forming, in this latter case, the superficial cranial epigastric artery (present in 95.6%

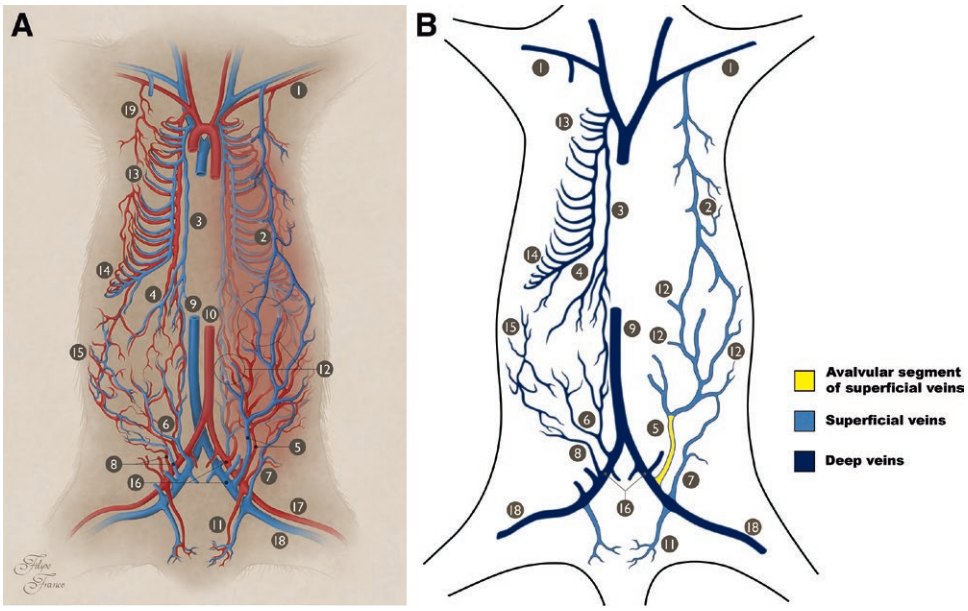

Fig. 1. Macrovascular blood supply to the IOVAAR. A, Schematic drawing illustrating the major vessels supplying IOVAAR. On the right side of the picture, the superficial vessels (superficial to the muscle fascia) are represented in full. On this side, the deeper vessels (deep to the muscle fascia) are represented in a lighter color. On the left side of the picture, only the deeper vessels (deep to the muscle fascia) are represented. Blue structures represent veins. Red structures represent arteries. B, Schematic drawing illustrating the major veins draining the IOVAAR, as represented in 1A. On the left side of the picture are represented the deep veins (deep to the muscle fascia), whereas on the right side of the picture are represented the superficial veins. The valvular and avalvular segments are shown. 1, Axillary artery and vein; 2, LT (thoracoepigastric) vein; 3, internal thoracic artery and vein; 4, cranial epigastric artery and vein; 5, SIEA and vein; 6, deep caudal epigastric artery and vein; 7, superficial circumflex iliac artery and vein; 8, deep circumflex iliac artery and vein; 9, caudal vena cava; 10, abdominal aorta; 11, superficial EPA and vein; 12, perforator arteries and veins; 13, cranial intercostal arteries and veins; 14, caudal intercostal arteries and veins; 15, lumbar (or iliolumbar) arteries and veins; 16, external iliac artery and vein; 17, femoral artery; 18, femoral vein; 19, LT artery.

of cases on the right side and 93.3% of cases on the left side). Most of the lateral and cranial aspects of the IOVAAR drained into the tributaries of the large LT vein (thoracoepigastric vein). In all cases, the lateral branch of the SIEV and the branches that originated the LT vein were anastomosed in the lateral aspect of the midportion of the abdomen (Figs. 3, 4).

The IOVAAR received relatively minor contributions from the comparatively diminutive deep inferior epigastric system, from the terminal branches of the last 6 intercostal vessels and lumbar/iliolumbar vessels, from the thoracodorsal vessels, from the deep and superficial circumflex iliac vessels, and from the external pudendal vessels.

The Angiosomes of the IOVAAR

The angiosomes of the IOVAAR are represented in Figure 2. The SCEVs presented numerous variations (**see figure, Supplementary Digital Content 2**, which demonstrates schematic representation of the variations in the origin, termination, and distribution of the SIEA and vein, respectively, and the external pudendal artery (EPA) and vein on the left side of the rat, ***http://links.lww.com/PRSGO/A504***). The frequency of each variation is shown at the top right hand corner of each drawing. The total number of rats analyzed was 185 (http://links.lww.com/PRSGO/A504). In most cases (71.7%), the SIEA and the EPA originated from a common trunk called pudendoepigastric arterial trunk. In only 28.3% of cases did the SIEA and the superficial EPA arise as isolated vessels. The SIEA and the EPA were each accompanied by a comitant vein that had a parallel course, draining either into the pudendoepigastric venous trunk or into the femoral vein.

After its origin, the SIEA moved obliquely in the direction of the axilla. In all cases, this artery divided into 2 branches, being followed in its trajectory toward the axilla by its lateral branch. The lateral branch of the SIEA was larger than its medial counterpart in nearly all cases (94.5% of cases on the right side and 95.6% on the left side). The lateral branch anastomosed with the terminal branches of the LT artery and with the dominant perforators originating from the intercostal vessels. The medial branch of the SIEA anastomosed with the superficial cranial epigastric artery and/or with perforators of the deep cranial epigastric artery (Figs. 2–4; **Supplementary Digital Content 1**, ***http://links.lww.com/PRSGO/A503***).

The large LT vein could be found in a line drawn from the rat's hip to the ipsilateral axilla (Figs. 3, 4; **Supple-**

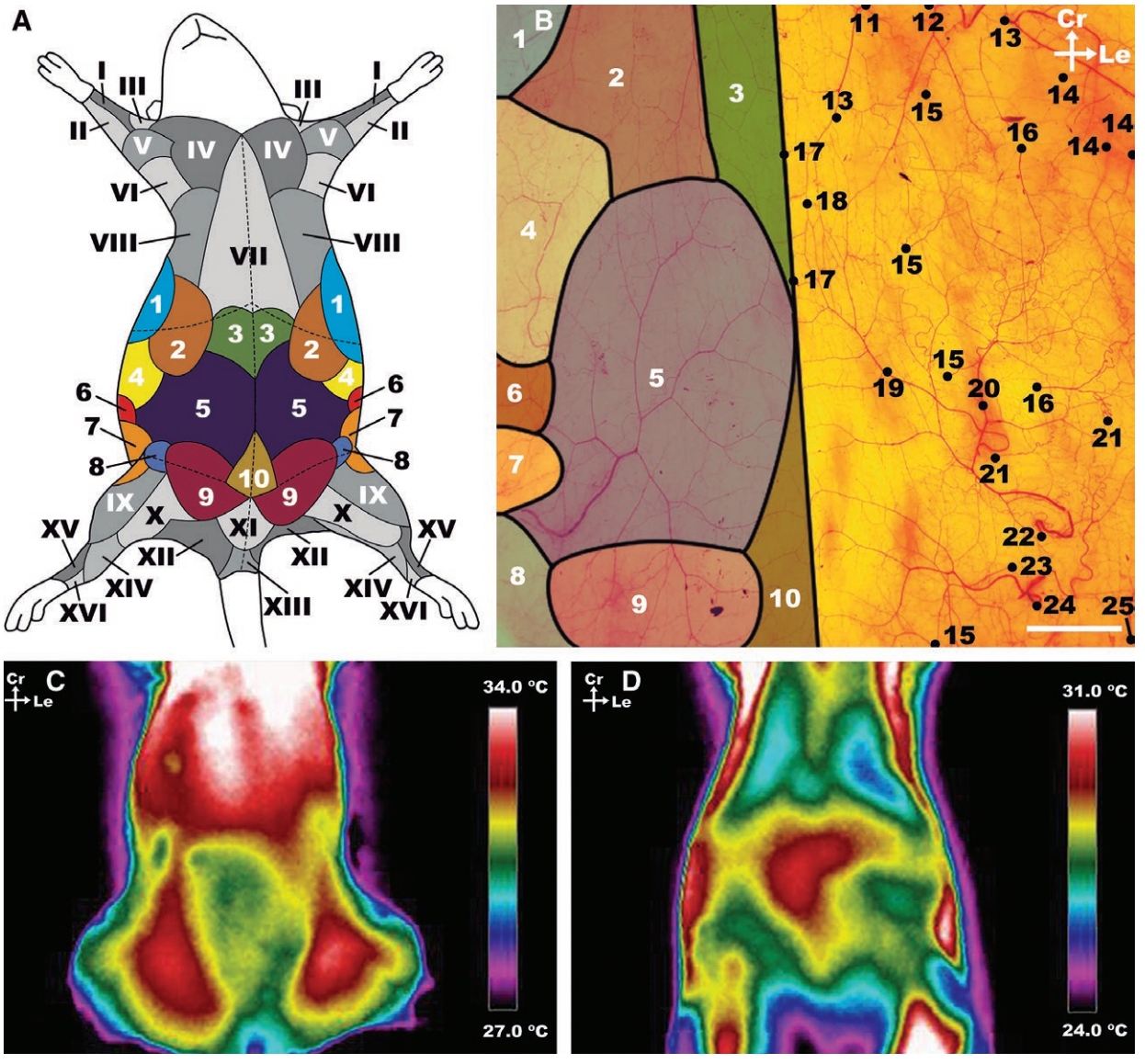

Fig. 2. Macrovascular blood supply to the ventrolateral aspect of the rat's abdominal wall. A, Schematic representation of the angiosomes of the ventrolateral aspect of the rat. The angiosomes of the abdomen studied in the present study are represented are numbered in Arabic numerals and represented in different colors. The adjacent angiosomes are numbered in roman numerals and highlighted in different levels of gray. These angiosomes have been represented according to Taylor et al.[32,33] and Kochi et al.[40] B, Photograph of the integument covering the ventrolateral aspect of the abdomen of the rat after processing by the modified Spalteholz technique showing the supplying vessels and respective angiosomes. The top limit of the photograph corresponds to the lower limit of the rib cage, the lower limit to a transverse line abutting the pubic symphysis; the lateral limits of the photograph correspond to the dorsal axillary lines. C and D, Representative infrared thermography images of the ventrolateral aspect of the abdomen of the rat. C, Direct infrared thermography with hotspots in the region of the dominant axial vessels (the caudal superficial epigastric vessels). D, Infrared thermography after cooling of the rat's surface, by placing a silicone gel bag at a temperature of approximately 21ºC for 2 minutes. This image shows the location of the dominant perforator vessels in the central and cranial aspect of the abdomen. The thermograms were taken for a period of 5 minutes with 30-second intervals. Ca, caudal; Cr, cranial; Le, left; La, lateral; M, medial. I, median angiosome; II, ulnar angiosome; III, deep brachial angiosome; IV, transverse cervical angiosome; V, dorsal circumflex humeral angiosome; VI, circumflex scapular angiosome; VII, internal thoracic angiosome; VIII, cranial intercostal perforators angiosome; IX, lateral circumflex femoral angiosome; X, medial circumflex femoral angiosome; XI, superficial external pudendal angiosome; XII, caudal gluteal angiosome; XIII, internal pudendal angiosome; XIV, saphenous angiosome; XV, fibular angiosome; XVI, anterior tibial angiosome. 1, thoracodorsal angiosome; 2, LT angiosome; 3, cranial epigastric angiosome; 4, caudal intercostal perforators angiosome; 5, superficial caudal epigastric angiosome; 6, lumbar (or iliolumbar) perforators angiosome; 7, deep circumflex iliac angiosome; 8, deep external pudendal angiosome; 9, superficial external pudendal angiosome; 10, deep caudal epigastric angiosome; 11, cranial deep epigastric artery perforator; 12, LT artery; 13, thoracodorsal artery perforator; 14, intercostal perforators; 15, perforators from the medial branch of the deep caudal and cranial epigastric arteries; 16, perforators from the lateral branch of the deep caudal and cranial epigastric arteries; 17, choke vessels between the two superficial caudal epigastric angiosomes; 18, anastomoses between the superficial caudal epigastric arteries and the LT arteries; 19, medial branch of the SIEA; 20, lateral branch of the SIEA; 21, lumbar perforators; 22, SIEA; 23, superficial EPA; 24, deep EPA; 25, deep circumflex iliac artery. Calibration bar = 10 mm.

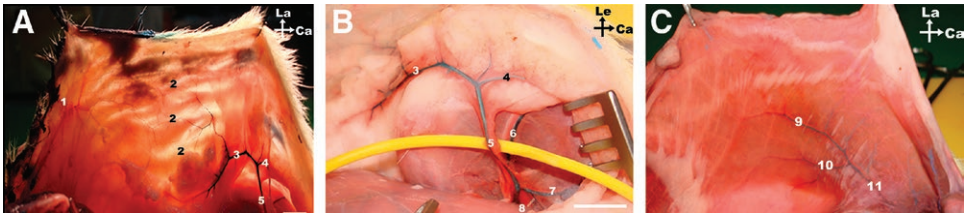

Fig. 3. Macrovascular blood supply to the ventrolateral aspect of the rat's abdominal wall. A, Photograph under transillumination of the integument covering the left side of the abdomen sowing its largest vessels. B, Photograph of the left groin region showing the origin of the SCEVs from the femoral vessels; C, Photograph of the deep surface of the left rectus abdominis muscle, showing the deep caudal epigastric vessels supplying this muscle; Ca, caudal; Cr, cranial; Le, left; La, lateral; M, medial. 1, LT artery; 2, anastomoses between the superficial caudal epigastric arteries and the LT arteries; 3, lateral branch of the SIEA; 4, medial branch of the SIEA; 5, SIEA; 6, femoral vessels and nerve; 7, Deep EPA; 8, superficial EPA; 9, medial branch of the deep caudal epigastric artery; 10, lateral branch of the deep caudal epigastric artery; 11, deep caudal epigastric vessels; 12, cranial deep epigastric artery perforator; 13, xyphoid process; 14, perforators from the medial branch of the deep caudal and cranial epigastric arteries; 15, intercostal perforators; 16, lumbar perforators. Calibration bar = 10 mm.

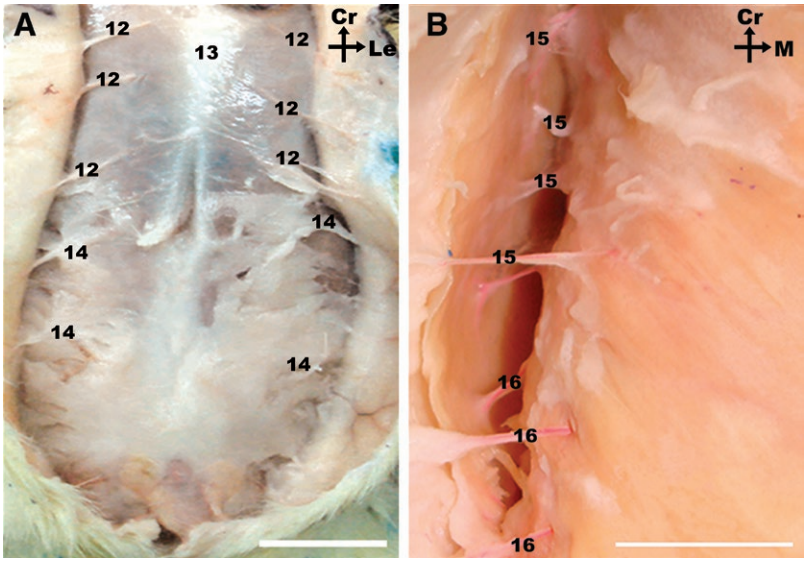

Fig. 4. A, Photograph of the integument of the ventral region of the abdomen of the rat, after midline incision and partial lateral retraction, showing multiple perforators supplying this region coming off the deep cranial and caudal epigastric vessels. B, Photograph of the right flank of the abdomen showing multiple lateral perforators supplying the lateral aspect of the integument of the rat in this region.

mentary Digital Content 1, ***http://links.lww.com/PRSGO/A503***). This vein originated at the level of the costal margin from the convergence of 3 veins that drained the medial, central, and lateral portion of the cranial aspect of the IOVAAR.

The SIEA and the SIEV were accompanied by a sizeable branch of the saphenous nerve—the caudal epigastric nerve (Fig. 5). At its origin, the diameter of this nerve was 0.33±0.17 mm. It divided into 2, 3, or 4 branches in the proximal third of the SIEA in 60.6%, 13.1%, and 26.2% of cases, respectively. These branches traveled with the SIEA from its origin and in turn provided multiple twigs throughout the territory of the SCEVs and also to the medial aspect of the thigh.

Musculocutaneous Perforators

Multiple sizeable perforator vessels were seen piercing the muscles and muscular fascia and supplying the IOVAAR (Figs. 2–4, 6; **Supplementary Digital Content 1**, ***http://links.lww.com/PRSGO/A503***). These perforators were most commonly seen arising from the rectus abdominis fascia in the central aspect of the abdomen (Fig. 7). In this region, the superficial vascular system was less dense (Fig. 2). The largest central abdominal perforators derived mainly from the deep epigastric vessels and particularly from the cranial deep epigastric vessels. On each side, there were on average 6.52±3.64 perforators on the right side and 6.56±3.67 perforators on the left side, ranging between 2 and 15.

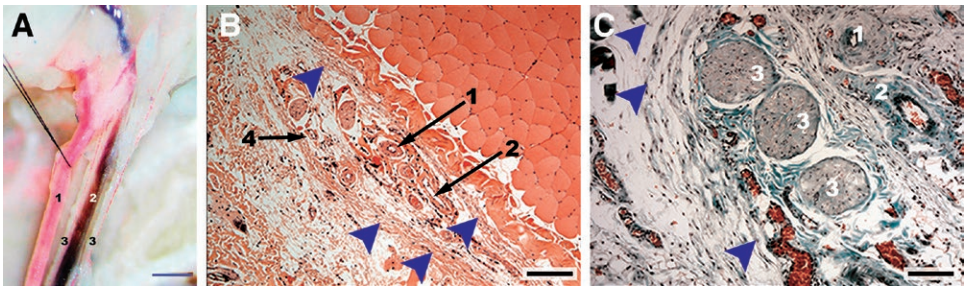

Fig. 5. Superficial caudal epigastric neurovascular bundle and its branches. A, Photograph of the superficial caudal epigastric neurovascular bundle after intraarterial and intravenous injection with a red and blue solution, respectively. B, Microphotograph of a hematoxylin-eosin–stained section of a transverse section of the caudal superficial epigastric neurovascular bundle. C, Microphotograph of a Masson's trichrome stained section of a transverse section of the caudal superficial epigastric neurovascular bundle. 1, SIEA; 2, superficial caudal epigastric vein; 3, branches of the caudal epigastric nerve; 4, superficial caudal epigastric lymphatic vessels. Arrow heads indicate the sheath involving the superficial caudal epigastric neurovascular bundle. Calibration bar in A = 1000 μm; calibration bars in B and C = 100 μm.

Overall, 79.1% of perforators originated in the deep epigastric system, whereas 28.1% originated in the segmental vessels that supplied the abdominal wall (last 6 intercostal, lumbar/iliolumbar, and the deep circumflex iliac vessels). This difference was statistically significant ($P < 0.05$). Perforators were more common in the cranial half of the abdomen, that is to say in the region were the axial vessels were inexistent or of a smaller caliber [$P < 0.05$; Fig. 7; **see figure, Supplementary Digital Content 3**, which demonstrates a dot plot graph drawn over a schematic drawing of the ventrolateral surface of the rat showing the location of the abdominal perforator arteries in the anterior and lateral aspect of the abdominal wall and their origin from the paramedian arteries (cranial and caudal deep epigastric arteries) and from the segmental vessels (intercostal, lumbar/iliolumbar arteries), ***http://links.lww.com/PRSGO/A505***]. A 2-step cluster analysis based on the Schwarz Bayesian criteria allowed the identification of 7 musculocutaneous perforator clusters on each side of the abdomen (Fig. 7).

Table 1 summarizes the main histomorphometric features of the largest vessels supplying the IOVAAR. No statistically significant differences were found between the right and left sides of the body.

Noteworthy is the large direct cutaneous vessels described above were present in areas where the integument was laxer, whereas the musculocutaneous perforators were placed more densely in the region where the IOVAAR was more adherent to the underlying muscle fascia. Moreover, the perforator vessels were longer in the lateral aspect of the abdomen compared with those that were more centrally placed in the region of the rectus abdominis muscles. Interestingly, on each side of the abdomen, there was a triangular region, lateral to the lateral branch of the SCEVs, where large vessels were absent (**see figure, Supplementary Digital Content 4**, which demonstrates a schematic diagram illustrating the safe zones (blue) for subcutaneous and intraperitoneal injections in the ventrolateral abdomen of the rat due to the relative scarcity of large vessels in these areas, ***http://links.lww.com/PRSGO/A506***).

Microscopic Anatomy

The IOVAAR was composed of multiple layers, including a sheath of loose connective tissue associated with white adipose tissue and smooth muscle known as panniculus carnosus (Fig. 6; **see figure, Supplementary Digital Content 5**, which displays a general view of the blood supply to the different layers of the ventrolateral aspect of the abdominal wall of the Wistar rat, ***http://links.lww.com/PRSGO/A507***). Soon after their origin, the large nominated vessels with an axial pattern were found in the panniculus adiposus, immediately superficial to the panniculus carnosus layer. These vessels gave ascending branches to all layers of the IOVAAR, including the panniculus carnosus. The musculocutaneous perforator vessels originated arterioles and received venules to and from the muscular subfascial, fascial, and epifascial plexuses. Additionally, in their ascending trajectory toward the skin, they gave branches to all the layers of the IOVAAR. Overall, integumentary vessels formed fine interconnecting meshworks of predominantly horizontal arrangement, establishing the following vascular plexuses: prefascial plexus, panniculus carnosus plexus, panniculus adiposus plexus, subdermal plexus, reticular dermal plexus, and subpappilary dermal plexus (Figs. 3–7; Supplementary Digital Content 1, 5, 6; **see figure, Supplementary Digital Content 6**, which shows details of the blood supply to the different layers of the ventrolateral aspect of the abdominal wall of the Wistar rat, ***http://links.lww.com/PRSGO/A508***).

At the subdermal and the subpapillary vascular plexuses, scattered and rare arteriovenous anastomoses were found. Precapillary sphincters were frequent findings at the subdermal and reticular dermis plexuses. Multiple venous valves were found in all layers of the integument, from the reticular dermis plexus until the major nominated veins. However, the first-order subdermal veins presented large segments devoid of valves. Venous valves were almost always bicuspid, although a few tricuspid valves were observed. All the nominated veins and their tributaries presented venous valves, with the exception of the SIEV itself, which presented no valves in all specimens studied (**see figure, Supplementary Digital Content**

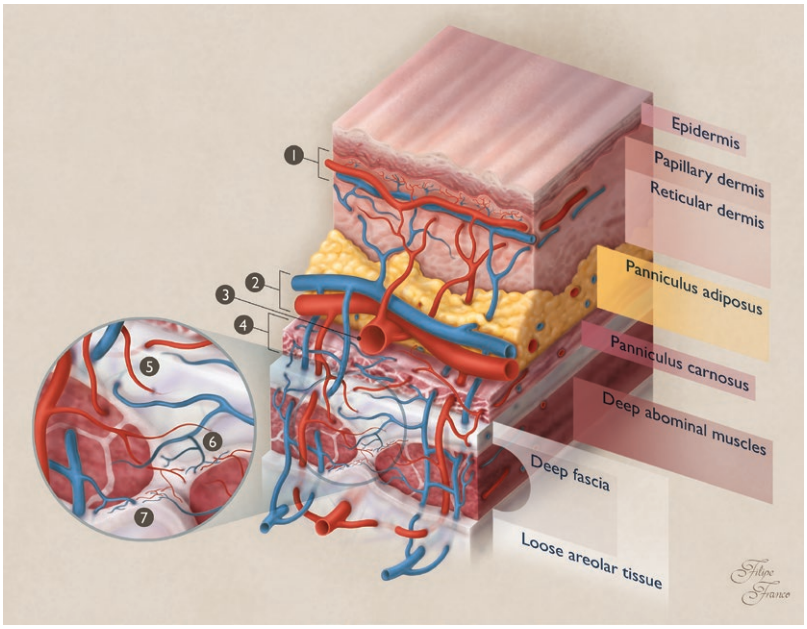

Fig. 6. Schematic drawing of the blood supply to the different layers of the integument of the ventrolateral aspect of the abdomen of the rat. The integument of the rat is composed of the skin, a fatty layer known as panniculus adiposus, and beneath this latter layer of a sheath of loose connective tissue associated with white adipose tissue and smooth muscle forming a layer known as panniculus carnosus. This layer is located just above the abdominal wall muscles and muscle fascias. There is a loose areolar tissue beneath the panniculus carnosus and the muscle fascia. The integument presented the following plexuses: a loose and thin prefascial plexus in the prefascial areolar tissue; a dense and thin panniculus carnosus plexus encompassing the entire thickness of this layer and mostly dependent on the direct cutaneous axial vessels. This plexus was mostly composed of third-order arterioles and venules, as well as capillaries; a loose panniculus adiposus plexus, mainly composed of obliquely disposed ascending and descending first-order arterioles and venules, respectively, supplying the overlying layers and the adjacent fatty tissue; a subdermal plexus at the upper portion of the panniculus adiposus, immediately beneath the skin, composed of second-order arterioles and venules with a horizontal orientation; a reticular dermal plexus composed of vertically arranged third-order ascending and descending arterioles and venules, respectively, as well as their terminal branches, which formed capillary networks around sebaceous dermal glands and the papillae of hair follicles; a subpappilary dermal plexus, at the dermal-epidermal interface, composed of capillary loops with a predominantly horizontal disposition interspersed with occasional vertical capillary loops. These capillaries were in continuity with the vertical arterioles and venules of the reticular plexus. Blue structures represent veins. Red structures represent arteries. 1, Subpapillary vascular plexus; 2, subdermal vascular plexus; 3, superficial arteriole in the panniculus adiposus; 4, panniculus carnosus vascular plexus; 5, arterioles and venules supplying the prefascial vascular plexus in the prefascial areolar tissue; 6, fascial vascular plexus; 7, subfascial vascular plexus.

7, which demonstrates a venous drainage of the integument of the ventrolateral abdomen of the rat, ***http://links.lww.com/PRSGO/A509***; **see figure, Supplementary Digital Content 8**, which demonstrates details of the microvascular blood supply to the integument covering the ventrolateral aspect of the abdomen of the rat, ***http://links.lww.com/PRSGO/A510***).

Each of the branches of the caudal epigastric nerve presented a monofascicular pattern (Fig. 5). The average number of nerve fibers in the proximal portion of this nerve was 1093.00 ± 88.32 on the right side and 1051.50 ± 107.39 on the left side, being overall 1072.20 ± 97.80. The difference between sides was not statistically significant.

Thermographic Results

Figure 2 illustrates the typical infra-red thermographic images of the IOVAAR obtained directly and post cooling of the rat's surface. In all cases, direct thermography showed a region of higher temperature corresponding to the territory of the SCEVs and the LT vessels. Post cooling thermography, used to highlight perforator vessels, showed a region of higher temperatures in the central and cranial aspect of the abdomen.

DISCUSSION

The IOVAAR has been used regularly for training and research purposes since at least 1967 when the rat

epigastric flap was described.[30] Surprisingly, few studies have addressed the macroscopic vascular anatomy of this region.[4,7,31–37] Furthermore, the literature on the microvascular blood supply to the rat's integument is even scarcer, being restricted to the paw and tail regions.[28,38] As far as the authors could determine, the present series, comprising 205 rats, is the largest on the macroscopic and microscopic anatomy of the vascular blood supply to the IOVAAR.

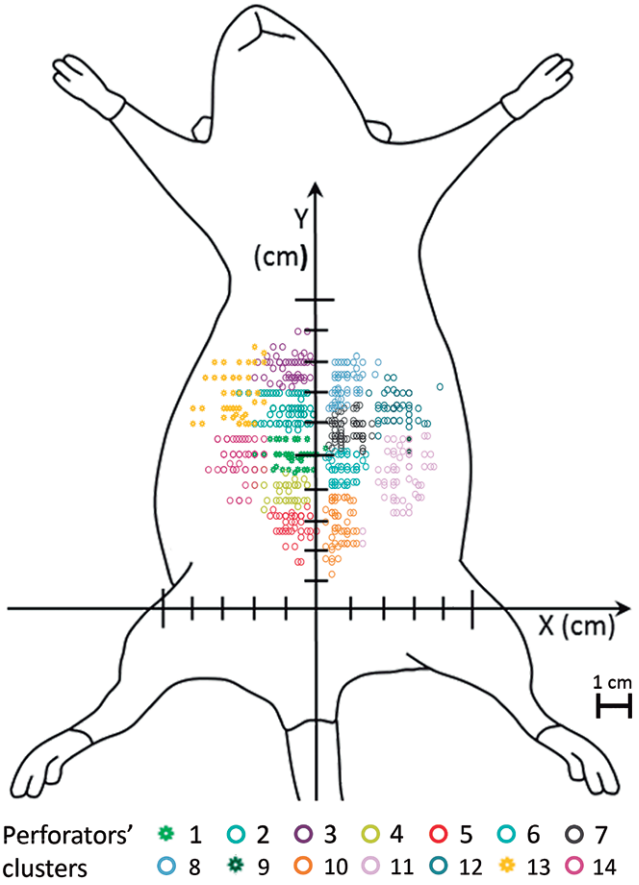

Fig. 7. Dot plot graph drawn over a schematic drawing of the ventrolateral surface of the rat showing the location of the abdominal perforator arteries in the anterior and lateral aspect of the abdominal wall. A two-step cluster analysis based on the Schwarz Bayesian criteria allowed the identification of 7 perforator clusters on each side of the abdomen.

Numerous doubts persist regarding the extent of similarity between the blood supply to this region in humans and rats. Some authors state that the blood supply is relatively similar,[31] whereas others argue that it is substantially different.[32] Table 2 summarizes the main differences found in the present study. Overall, although there are some strong analogies between rats and the humans, namely a common vascular framework (Figs. 1, 6), there are also some noteworthy differences.

The most striking difference refers to the preponderance of the direct cutaneous vessels in the rat, compared with the dominance of the musculocutaneous vessels in humans. Taylor[32,33] attributed this difference to the fact that in loose-skinned animals, like the rat, the integument is more mobile relative to the underlying muscles due to the presence of a loose areolar tissue layer between the muscular fascia and the panniculus carnosus (Fig. 6). The corollary of this is a greater dependence on direct cutaneous vessels in loose-skinned animals compared with humans.[32,33] Interestingly, in the present study, the greater number of perforators was in fact found close to the midline, an in particular in the cranial half of the abdomen, precisely where the integument of the rat was more adherent to the underlying muscle fascia (Fig. 7). In this region, the superficial vascular system was less dense (Fig. 1).

Another important difference found in this work relative to humans is that central abdominal perforators in the rat were derived mostly from the deep cranial epigastric artery and not from the deep inferior epigastric vessels as in the former species.[34] These findings are supported by the 2 other articles that systematically evaluated the number and location of musculocutaneous perforators of the rat's abdomen.[34,37] Hence, perforator flaps in the IOVAAR seem to be substantially different from those in humans, in terms of vascular homology.

An additional difference relative to humans is the importance of the vessels in the panniculus carnosus of the rat for integumentary perfusion. This had already been hinted by the greater survival of flaps that included this layer, comparatively to flaps that excluded it.[39] In fact, we observed that, soon after their origin, the major subcutaneous vessels coursed in the panniculus adiposus immedi-

Table 1. Histomorphometric Evaluation of the Major Arteries and Veins Supplying the Ventrolateral Region of the Integument of the Abdomen of the Rat

Vessel	Length* (cm)	Caliber† (mm)	Wall Thickness‡ (μm)
SIEA	1.45±0.22	0.32±0.13	479.07±27.37
SCEV	1.61±0.19	0.65±0.24	183.05±15.63
First divisions of the SIEA	0.72±0.16	0.13±0.08	288.19±31.72
First divisions of the SCEV	0.92±0.18	0.18±0.05	128.24±43.53
Second divisions of the SIEA	0.60±0.12	0.08±0.03	202.38±87.34
Second divisions of the SCEV	0.85±0.20	0.16±0.09	102.63±65.71
Thoracoepigastric vein	4.13±1.59	0.47±0.17	41.67±15.67
First divisions of the thoracoepigastric vein	1.63±0.47	0.17±0.04	0.11±0.09
Second divisions of the thoracoepigastric vein	0.96±0.54	0.14±0.05	0.09±0.08

Values are expressed as average values ± SD.
*Length determination was based on Spalteholz cleared specimens (n = 10).
†Caliber determination was based on Spalteholz cleared specimens (n = 10), on transverse histological sections stained with CD 31 (n = 10) and on the scanning electron microscopy observation of the vascular corrosion casts (n = 10).
‡Wall thickness determination was based on transverse histological sections stained with Masson's Trichrome (n = 10).

Sudharshini	August 12, 2017 6:15 PM	18:15	4 Color Fig(s): F1-8	Art: GOX-D-16-00632

Table 2. Main Differences between the Usual Blood Supply to the Integument of the Ventrolateral Aspect of the Abdomen of Humans[33,57] and Rats

Anatomical Structure(s)	Humans	Rat
Dominant arteries	Musculocutaneous (in particular the deep inferior epigastric artery)	Direct cutaneous (in particular the SIEA/superficial inferior epigastric artery)
Dominant veins	Superficial and deep veins (in particular the deep inferior epigastric veins and the superficial inferior epigastric vein)	Superficial veins (in particular the LT vein/thoracoepigastric vein and the SCEV/superficial inferior epigastric vein)
SIEV	Frequently absent or hypoplasic	Always present and with a sizeable caliber
Perforator vessels	Major role in the normal perfusion; more numerous; more abundant laterally and below the umbilicus	Less important role in integumentary perfusion; less numerous; mostly located in an area cranially to the umbilicus
Venous valves	Uniformly present in the superficial and deep venous systems	More abundant in the deep venous system and in the cranial aspect of the superficial venous system
Panniculus carnosus	Absent	Well-developed and associated with a vascular plexus
Nerves accompanying major vessels	Intercostal nerves 7–12 accompanying the homonymous vessels	Intercostal nerves 7–12 accompanying the homonymous vessels; caudal epigastric nerve/inferior epigastric nerve is a sizeable and constant nerve that is part of the superficial caudal epigastric neurovascular bundle

Fig. 8. Vascular pedicle of common flaps raised on the ventrolateral surface of the abdomen of the rat. Some of the most common flaps performed in this region are the TRAM flap based on the cranial epigastric vessels; the SCIA flap (also known as iliofemoral flap) based on the superficial circumflex iliac vessels; the DIEP flap based on the perforator vessels originating from the deep cranial epigastric vessels; the DSCI flap (also known as iliac osteocutaneous flap) based on the deep circumflex iliac vessels; the SIEA flap (also known as groin flap) based on the SCEVs; the EOMA perforator flap based on the perforators originating from the 6 last intercostal vessels or from the lumbar vessels; and the VRAM flap. 1, TRAM flap based on the cranial epigastric vessels; 2, SCIA or iliofemoral flap based on the superficial circumflex iliac vessels; 3, DIEP flap based on the perforator vessels originating from the deep cranial epigastric vessels; 4, DSCI or iliac osteocutaneous flap based on the deep circumflex iliac vessels; 5, SIEA or groin flap based on the SCEVs; 6, EOMA perforator flap based on the perforators originating from the last 6 caudal intercostal vessels or from the ilolumbar vessels; 7, VRAM flap. DIEP, deep inferior epigastric artery perforator; DSCI, deep circumflex iliac artery; EOMA, external oblique myocutaneous artery; SCIA, superficial circumflex iliac artery; TRAM, transverse rectus abdominis myocutaneous; VRAM, vertical rectus abdominis myocutaneous.

ately superficial to panniculus carnosus. In addition, the panniculus carnosus was provided with a vascular plexus of its own that was connected with the deep vascular system through anastomoses with branches of the musculocutaneous perforators (Fig. 6; see **Supplementary Digital Content 5,** ***http://links.lww.com/PRSGO/A507***, and **Supplementary Digital Content 6**, ***http://links.lww.com/PRSGO/A508***).

Interestingly, the SCEVs in the rat presented numerous anatomical variations (**Supplementary Digital Content 2**, ***http://links.lww.com/PRSGO/A504***). This had already been demonstrated in mice and humans.[40–42]

Our data showed that in nearly all cases, the lateral branch of the SIEA was dominant relative to its medial counterpart. This is in accordance with the observations of Petry and Wertham[4] who suggested that part of the survival variance of the rat epigastric flap could be explained by the inconsistent incorporation of this branch.

To the best of the authors' knowledge, the fascial envelope surrounding the superficial caudal epigastric neurovascular bundle and determining a specific compartment had not been described before. Notwithstanding, it is well known that when dissecting the superficial caudal epigastric pedicle, one has to tease away or to cut a delicate tissue sleeve that surrounds these structures. The superficial caudal epigastric fascia resembles the saphenous fascia that surrounds the saphenous veins in the lower limbs.[43] Acknowledging this fascial envelope may facilitate dissection of flaps in this region, particularly by novices in microsurgery.

An interesting information provided by this study was the identification of a triangular zone on each side of the IOVAAR where large vessels were absent (**Supplementary Digital Content 4**, ***http://links.lww.com/PRSGO/A506***). These zones are probably safer for performing abdominal injections. As far as the authors could determine, these safe zones had not been described before.

Our thermographic analysis suggested that the most important perforators physiologically were located in the central and cranial aspect of the abdomen (Fig. 2). This information concurred with the anatomical dissection studies performed in the present studies and with those described by other authors.[34,35] Moreover, our thermographic examination also favored the notion that in normal conditions the superficial vessels were more important for supplying blood to the integument in the caudal and lateral aspects of the IOVAAR, whereas the perforator vessels were more important in the central and cranial aspects. Additionally, these data lend support to the use of thermography as a good technique for evaluating the most important perforator vessels in rats, as it had already been shown in humans by other authors.[29]

The presence of valves in the veins of the IOVAAR has been a matter of debate.[19] Our data show that multiple venous valves are found in all layers of the integument, from the reticular dermis plexus until the major nominated veins (**Supplementary Digital Content 5,** ***http://links.lww.com/PRSGO/A507*****, Supplementary Digital Content 6,** ***http://links.lww.com/PRSGO/A508*****, Supplementary Digital Content 7,** ***http://links.lww.com/PRSGO/A509*****, Supplementary Digital Content 8,** ***http://links.lww.com/PRSGO/A510***). However, the subdermal first-order venules presented large segments devoid of valves, which probably facilitate oscillating or bidirectional blood flow.[44] All the nominated veins and their tributaries presented venous valves, with the exception of the SIEV (Fig. 1B). Valdatta et al.[19] also failed to observe valves inside this vein. Scanning electron microscopy of vascular corrosion casts of human tissues revealed valves in superficial veins as small as 20 μm in diameter in different regions of the integument, and in particular in the lower limb, the anterior and posterior walls of the trunk.[45] The major difference between humans and rats regarding venous valves in these regions is, thus, the relative paucity of venous valves in the caudal aspect of the dominant venous system of rats, namely in the SIEV. This difference should be born in mind, for example, when using rats in experimental studies of tissue perfusion, namely in unconventional perfusion flaps and in particular in arterialized venous flaps.[46,47]

Human microcirculatory studies have shown that the skin subpapillary plexus presents an abundance of vertically arranged capillary loops, coinciding with the dermal papillae. These loops are more pronounced and numerous in body regions were the skin is thicker and subject to intense forces, namely in weight-bearing regions or the palm of the hands.[48] However, in our study and contrarily to what has been described in the skin in the footpad of the rat,[48,49] vertical capillary loops in the subpapillary plexus were relatively scarce. Capillaries were more frequently disposed in a horizontal manner in this region. These findings may be due to the fact that this region of the skin of the rat is thinner, has fewer dermal papillae, and it is not usually submitted to intense vertical forces (see **Supplementary Digital Content 5,** ***http://links.lww.com/PRSGO/A507*****,** and **Supplementary Digital Content 6,** ***http://links.lww.com/PRSGO/A508***).

In concordance with other microcirculatory studies performed in the skin covering the abdomen of humans, the authors found that there were few arteriovenous anastomoses in the IOVAAR.[48,50] This suggests that this region probably does not play a primordial role in thermoregulation.[50]

This study also lends support to the use of the epigastric flap as sensate flap, as proposed by Hirigoyen et al.[51] (Fig. 5). This construction has a similar anatomical rationale to that of using the 12th intercostal nerve in the human species to tailor a neurosensible fasciocutaneous SIEA flap.[51] However, a major difference between rats and humans is that in the former the SIEA and the caudal epigastric nerve are proportionally larger and are always present. Additionally, it should be noted that there is no exact human equivalent to the caudal epigastric nerve.[51]

One of the main limitations of the present work is that the histomorphometric data presented probably underestimate vessels' size, because optical microscopy images, as well as scanning electron microscopy images are known to be associated with vessels' shrinking during processing, resulting in underestimation of vessels' size of up to 30%.[28,52]

Finally, we believe that the anatomical study herein described helps to better plan, execute, and interpret the evolution of the multiple flaps performed in the IOVAAR for teaching, training, and research purposes (Fig. 8; **see pdf, Supplementary Digital Content 9**, which displays photographs illustrating the surgical anatomy of a few common flaps made on the ventrolateral aspect of the abdomen of the rat based on nominated vessels, ***http://links.lww.com/PRSGO/A511***).[2,7,30,31,35,53–56]

CONCLUSIONS

The data presented in this article show that rats and humans present a great deal of homology regarding the blood supply to the ventrolateral aspect of the abdominal integument. However, there are also significant differences that must be taken into consideration when performing and interpreting experimental procedures in rats.

Diogo Casal, MD
Anatomy Department
NOVA Medical School
Universidade NOVA de Lisboa
Campo dos Mártires da Pátria, 130
1169-056, Lisbon
Portugal
E-mail: diogo_bogalhao@yahoo.co.uk

ACKNOWLEDGMENTS

The authors are very grateful to Mr. Filipe Franco and Mr. Nuno Folque for producing the drawings contained in this article.

The authors are very thankful to Professor Maria Angélica Almeida and Dr. José Videira e Castro for their advices in all steps of the research project. The authors also acknowledge the role of Mr. José Ferreira Silva and that of Dr. Mário Ferraz Oliveira in the supervision of the histological specimens.

REFERENCES

1. Miles DA, Crosby NL, Clapson JB. The role of the venous system in the abdominal flap of the rat. *Plast Reconstr Surg.* 1997;99:2030–2033.
2. Okşar HS, Coşkunfirat OK, Ozgentaş HE. Perforator-based flap in rats: a new experimental model. *Plast Reconstr Surg.* 2001;108:125–131.
3. Ozgentaş HE, Shenaq S, Spira M. Development of a TRAM flap model in the rat and study of vascular dominance. *Plast Reconstr Surg.* 1994;94:1012–7; 1025.
4. Petry JJ, Wortham KA. The anatomy of the epigastric flap in the experimental rat. *Plast Reconstr Surg.* 1984;74:410–413.
5. Roberts AP, Cohen JI, Cook TA. The rat ventral island flap: a comparison of the effects of reduction in arterial inflow and venous outflow. *Plast Reconstr Surg.* 1996;97:610–615.
6. Sano K, Hallock GG, Rice DC. The relative importance of the deep and superficial vascular systems for delay of the transverse rectus abdominis musculocutaneous flap as demonstrated in a rat model. *Plast Reconstr Surg.* 2002;109:1052–7; discussion 1058.
7. Strauch B, Murray DE. Transfer of composite graft with immediate suture anastomosis of its vascular pedicle measuring less than 1 mm. in external diameter using microsurgical techniques. *Plast Reconstr Surg.* 1967;40:325–329.
8. Kayano S, Hallock GG, Rice DC, et al. Instructional models for dissection techniques of perforator flaps. In: Blondeel P, Morris SF, Hallock GG, Neligan PC eds. *Perforator Flaps: Anatomy, Technique and Clinical Applications.* 2nd ed. Rome: Quality medical publishing, Inc.; 2013;1:97–107.
9. Shurey S, Akelina Y, Legagneux J, et al. The rat model in microsurgery education: classical exercises and new horizons. *Arch Plast Surg.* 2014;41:201–208.
10. Lee S. Historical events on development of experimental microsurgical organ transplantation. *Yonsei Med J.* 2004;45:1115–1120.
11. Siemionow MZ. Microsurgery models. In: Siemionow MZ, ed. *Plastic and Reconstructive Surgery: Experimental Models and Research Designs.* 1st ed. London, United Kingdom: Springer - Verlag; 2015:3–67.
12. Fukui A. Microvascular anastomoses in the rat. In: Tamai S, Usui M, Yoshizu T, eds. *Experimental and Clinical Reconstructive Microsurgery.* 1st ed. Tokyo: Springer-Verlag; 2004:35–43.
13. Hirase Y. Skin and muscle flaps in the rat. In: Tamai S, Usui M, Yoshizu T, eds. *Experimental and Clinical Reconstructive Microsurgery.* 1st ed. Tokyo: Springer-Verlag; 2004:111–114.
14. Morain WD. Historical perspectives. In: Mathes SJ, ed. *Plastic Surgery.* 2nd ed. Philadelphia, Pa.: Saunders; 2006;1:27–34.
15. Santoni-Rugiu P, Sykes PJ. Skin flaps. In: Santoni-Rugiu P, Sykes PJ, eds. *A History of Plastic Surgery.* 1st ed. Leipzig, Germany: Springer; 2007:79–119.
16. Tamai S. The history of microsurgery. In: Tamai S, Usui M, Yoshizu T, eds. *Experimental and Clinical Reconstructive Microsurgery.* 1st ed. Tokyo, Japan: Springer-Verlag; 2003:3–24.
17. Michaels J, 5th, Levine JP, Hazen A, et al. Biologic brachytherapy: ex vivo transduction of microvascular beds for efficient, targeted gene therapy. *Plast Reconstr Surg.* 2006;118:54–65; discussion 66.
18. Lao WW, Wang YL, Ramirez AE, et al. A new rat model for orthotopic abdominal wall allotransplantation. *Plast Reconstr Surg Glob Open.* 2014;2:e136.
19. Valdatta L, Congiu T, Thione A, et al. Do superficial epigastric veins of rats have valves? *Br J Plast Surg.* 2001;54:151–153.
20. Fukui A. Technique of microangiography. In: Tamai S, Usui M, Yoshizu T, eds. *Experimental and Clinical Reconstructive Microsurgery.* 1st ed. Tokyo: Springer-Verlag; 2004:55–56.
21. Sempuku T. Technique for making a Spalteholz cleared specimen. In: Tamai S, Usui M, Yoshizu T, eds. *Experimental and Clinical Reconstructive Microsurgery.* 1st ed. Tokyo: Springer-Verlag; 2004:59–60.
22. Steinke H, Wolff W. A modified Spalteholz technique with preservation of the histology. *Ann Anat.* 2001;183:91–95.
23. Sempuku T. Technique for making a vascular corrosion cast. In: Tamai S, Usui M, Yoshizu T eds. *Experimental and Clinical Reconstructive Microsurgery.* 1st ed. Tokyo: Springer-Verlag; 2004:57–58.
24. Fischer AH, Jacobson KA, Rose J, et al. Hematoxylin and eosin staining of tissue and cell sections. *CSH Protoc.* 2008;2008:pdb.prot4986.
25. Foot NC. The Masson trichrome staining methods in routine laboratory use. *Stain Technol.* 1933;8:101–110.
26. Pusztaszeri MP, Seelentag W, Bosman FT. Immunohistochemical expression of endothelial markers CD31, CD34, von Willebrand factor, and Fli-1 in normal human tissues. *J Histochem Cytochem.* 2006;54:385–395.
27. Raimondo S, Fornaro M, Di Scipio F, et al. Chapter 5: methods and protocols in peripheral nerve regeneration experimental research: part II-morphological techniques. *Int Rev Neurobiol.* 2009;87:81–103.
28. Aharinejad SH, Lametschwandtner A. Identification and interpretation of cast vessel structures. In: Aharinejad SH, Lametschwandtner A, eds. *Microvascular Corrosion Casting in Scanning Electron Microscopy: Techniques and Applications.* 1st ed. New York, N.Y.: Springer-Verlag; 1992:103–115.
29. Sheena Y, Jennison T, Hardwicke JT, et al. Detection of perforators using thermal imaging. *Plast Reconstr Surg.* 2013;132:1603–1610.
30. Gurunluoglu R, Siemionow MZ. The microsurgical groin skin flap in the rat model. In: Siemionow MZ, ed. *Plastic and Reconstructive Surgery: Experimental Models and Research Designs.* 1st ed. London, United Kingdom: Spronger; 2015:53–62.
31. Dunn RM, Mancoll J. Flap models in the rat: a review and reappraisal. *Plast Reconstr Surg.* 1992;90:319–328.
32. Taylor GI, Minabe T. The angiosomes of the mammals and other vertebrates. *Plast Reconstr Surg.* 1992;89:181–215.
33. Taylor GI, Pan WR. The angiosome concept. In: Dodwell P, ed. *The Angiosome Concept and Tissue Transfer.* 1st ed. Saint Louis, Missouri: Quality Medical Publishing, Inc.; 2014;1:354–395.
34. Hallock GG, Rice DC. Physiologic superiority of the anatomic dominant pedicle of the TRAM flap in a rat model. *Plast Reconstr Surg.* 1995;96:111–118.
35. Hallock GG, Rice DC. Cranial epigastric perforator flap: a rat model of a true perforator flap. *Ann Plast Surg.* 2003;50:393–397.
36. Ozkan O, Coşkunfirat OK, Ozgentaş HE, et al. New experimental flap model in the rat: free flow-through epigastric flap. *Microsurgery.* 2004;24:454–458.

37. Ozkan O, Koshima I, Gonda K. A supermicrosurgical flap model in the rat: a free true abdominal perforator flap with a short pedicle. *Plast Reconstr Surg.* 2006;117:479–485.
38. Aharinejad SH, Lametschwandtner A. The peripheral sense organs. The integument. In: Aharinejad SH, Lametschwandtner A, eds. *Microvascular Corrosion Casting in Scanning Electron Microscopy: Techniques and Applications.* 1st ed. New York, N.Y.: Springer-Verlag; 1992:354–360.
39. Pearl RM, Johnson D. The vascular supply to the skin: an anatomical and physiological reappraisal—Part II. *Ann Plast Surg.* 1983;11:196–205.
40. Kochi T, Imai Y, Takeda A, et al. Characterization of the arterial anatomy of the murine hindlimb: functional role in the design and understanding of ischemia models. *PLoS One.* 2013;8:e84047.
41. Gagnon A, Blondeell P. Deep and superficial inferior epigastric artery perforator flaps. *Cirugía Plástica Ibero-Latinoamericana.* 2006;32:7–13.
42. Fathi M, Hatamipour E, Fathi HR, et al. The anatomy of superficial inferior epigastric artery flap. *Acta Cir Bras.* 2008;23:429–434.
43. Abu-Hijleh MF, Roshier AL, Al-Shboul Q, et al. The membranous layer of superficial fascia: evidence for its widespread distribution in the body. *Surg Radiol Anat.* 2006;28:606–619.
44. Blondeel PN, Morris NJ, Hallock GG, et al. Vascular territories of the integument. In: Blondeel PN, Morris NJ, Hallock GG, Neligan PC, eds. *Perforator Flaps: Anatomy, Technique and Clinical Implications.* 2nd ed. St. Louis, MO: Quality Medical Publishing, Inc.; 2013;1:26–52.
45. Caggiati A, Phillips M, Lametschwandtner A, et al. Valves in small veins and venules. *Eur J Vasc Endovasc Surg.* 2006;32:447–452.
46. Casal D, Cunha T, Pais D, et al. Systematic review and meta-analysis of unconventional perfusion flaps in clinical practice. *Plast Reconstr Surg.* 2016;138:459–479.
47. Koyama T, Sugihara-Seki M, Sasajima T, et al. Venular valves and retrograde perfusion. In: Swartz HM, Harrison DK, Bruley DF, eds. *Oxygen Transport to Tissue XXXVI.* New York, N.Y.: Springer; 2014;1:317–323.
48. Aharinejad SH, Lametschwandtner A. Microangioarchitecture of selected organ systems: the integument. In: Aharinejad SH, Lametschwandtner A, eds. *Microvascular Corrosion Casting in Scanning Electron Microscopy: Techniques and Applications.* 1st ed. New York, N.Y.: Springer-Verlag; 1992:354–360.
49. Imayama S. Scanning and transmission electron microscope study on the terminal blood vessels of the rat skin. *J Invest Dermatol.* 1981;76:151–157.
50. Walløe L. Arterio-venous anastomoses in the human skin and their role in temperature control. *Temperature (Austin).* 2016;3:92–103.
51. Hirigoyen MB, Rhee JS, Weisz DJ, et al. Reappraisal of the inferior epigastric flap: a new neurovascular flap model in the rat. *Plast Reconstr Surg.* 1996;98:700–705.
52. Millington PF, Wilkinson R. The skin in depth: dermal vasculature. In: Harrison RJ, McMinn RM, eds. *Biologic Structure and Function of the Skin: Skin.* 1st ed. London: Cambridge University Press; 1983;1:69–72.
53. Syed SA, Tasaki Y, Fujii T, et al. A new experimental model: the vascular pedicle cutaneous flap over the dorsal aspect (flank and hip) of the rat. *Br J Plast Surg.* 1992;45:23–25.
54. Ozkan O, Akyürek M, Safak T, et al. A new flap model in rats: iliac osteomusculocutaneous flap. *Ann Plast Surg.* 2001;47:161–167.
55. Nasır S. New modification of the oldest flap in rats to increase antigenicity of transplanted skin: The Extended Groin Flap Model. *Plas Reconstr Surg.* 2015;1:227–236.
56. Dunn RM, Huff W, Mancoll J. The rat rectus abdominis myocutaneous flap: a true myocutaneous flap model. *Ann Plast Surg.* 1993;31:352–357.
57. Taylor GI, Watterson PA, Zelt RG. The vascular anatomy of the anterior abdominal wall: the basis for flap design. *Perspect Plast Surg.* 1991;5:1–28.

APPENDIX 5

Video Article

A Model of Free Tissue Transfer: The Rat Epigastric Free Flap

Diogo Casal[1,4], Diogo Pais[1], Inês Iria[3,4], Eduarda Mota-Silva[5], Maria-Angélica Almeida[2], Sara Alves[6], Cláudia Pen[6], Ana Farinho[4], Luís Mascarenhas-Lemos[1,6], José Ferreira-Silva[6], Mário Ferraz-Oliveira[6], Valentina Vassilenko[5], Paula A. Videira[3,4], João Gory O'Neill[1,5]

[1]Anatomy Department, NOVA Medical School, Universidade NOVA de Lisboa

[2]Plastic and Reconstructive Surgery Department and Burn Unit, Centro Hospitalar de Lisboa Central - Hospital de São José

[3]UCIBIO, Life Sciences Department, Faculty of Sciences and Technology, Universidade NOVA de Lisboa

[4]CEDOC, NOVA Medical School, Universidade NOVA de Lisboa

[5]Physics Department, Faculty of Sciences and Technology, LIBPhys

[6]Pathology Department, Centro Hospitalar de Lisboa Central – Hospital de São José

Correspondence to: Diogo Casal at diogo_bogalhao@yahoo.co.uk

URL: https://www.jove.com/video/55281
DOI: doi:10.3791/55281

Keywords: Medicine, Issue 119, Flap, Free Tissue Transfer, Free Flap, Rats, Epigastric Artery, Anatomy, Physiology, Animal Experimentation, Surgical Procedures, Teaching, Learning

Date Published: 1/15/2017

Citation: Casal, D., Pais, D., Iria, I., Mota-Silva, E., Almeida, M.A., Alves, S., Pen, C., Farinho, A., Mascarenhas-Lemos, L., Ferreira-Silva, J., Ferraz-Oliveira, M., Vassilenko, V., Videira, P.A., Gory O'Neill, J. A Model of Free Tissue Transfer: The Rat Epigastric Free Flap. *J. Vis. Exp.* (119), e55281, doi:10.3791/55281 (2017).

Abstract

Free tissue transfer has been increasingly used in clinical practice since the 1970s, allowing reconstruction of complex and otherwise untreatable defects resulting from tumor extirpation, trauma, infections, malformations or burns. Free flaps are particularly useful for reconstructing highly complex anatomical regions, like those of the head and neck, the hand, the foot and the perineum. Moreover, basic and translational research in the area of free tissue transfer is of great clinical potential. Notwithstanding, surgical trainees and researchers are frequently deterred from using microsurgical models of tissue transfer, due to lack of information regarding the technical aspects involved in the operative procedures. The aim of this paper is to present the steps required to transfer a fasciocutaneous epigastric free flap to the neck in the rat.

This flap is based on the superficial epigastric artery and vein, which originates from and drain into the femoral artery and vein, respectively. On average the caliber of the superficial epigastric vein is 0.6 to 0.8 mm, contrasting with the 0.3 to 0.5 mm of the superficial epigastric artery. Histologically, the flap is a composite block of tissues, containing skin (epidermis and dermis), a layer of fat tissue (*panniculus adiposus*), a layer of striated muscle (*panniculus carnosus*), and a layer of loose areolar tissue.

Succinctly, the epigastric flap is raised on its pedicle vessels that are then anastomosed to the external jugular vein and to the carotid artery on the ventral surface of the rat's neck. According to our experience, this model guarantees the complete survival of approximately 70 to 80% of epigastric flaps transferred to the neck region. The flap can be evaluated whenever needed by visual inspection. Hence, the authors believe this is a good experimental model for microsurgical research and training.

Video Link

The video component of this article can be found at https://www.jove.com/video/55281/

Introduction

Free tissue transfer has been increasingly used in clinical practice for reconstructing missing tissues since the 1970s[1-5]. This has allowed reconstruction of complex and otherwise untreatable defects resulting from tumor extirpation, trauma, infections, malformations or burns[1-7]. Free flaps of this kind are particularly useful for reconstructing highly complex anatomical regions, like those of the head and neck, the hand, the foot, and the perineum[1,4].

However, even today surgical trainees are frequently daunted by the complexity of several steps involved in raising, transferring and insetting a free flap with the use of microsurgical techniques and instruments[8,9]. In addition, it is widely accepted that to become a proficient microsurgeon, extensive experimental practice in an animal model is mandatory[4,8-13].

Moreover, basic and translational research in the area of free tissue transfer is of great clinical potential[8,14-16]. Notwithstanding, researchers are frequently deterred from using microsurgical models of tissue transfer due to lack of information regarding the technical aspects involved in the operative procedures[4,8-14]. The rat is a good animal model for microsurgical research and training, as it is relatively inexpensive, easy to keep, and amenable to frequent manipulation[8,11,13,14,17,18].

Although several free bone, muscle and skin flaps have been described in the rat[18-24], the free epigastric fasciocutaneous flap is the most widely used for teaching purposes[9,12,13,18,25]. This free flap was first described in 1967 by Strauch and Murray and has gained increasing popularity ever

since, due to several factors, namely constant vascular anatomy, relative ease of dissection, sizeable nutrient vessels, and redundancy of skin in the donor zone, which allows primary closure of the defect resulting from flap's elevation[4,9-11,13,17,18,25-28].

Flap Anatomy and Histology
The epigastric flap is supplied by the superficial epigastric artery and vein (**Figure 1**). These vessels originate from and drain into the femoral artery and vein, respectively. On average the caliber of the superficial epigastric vein is 0.6 to 0.8 mm, contrasting with the 0.3 to 0.5 mm of the superficial epigastric artery (**Figure 2**)[17,18]. The superficial epigastric artery gives off two main branches: a lateral and a medial branch that in turn divide multiple times, originating capillary networks that supply most of the integument of the epigastric region. These capillaries drain into the tributaries of the superficial epigastric veins that have a parallel course to the arterial tree (**Figure 2**)[13,17,18]. The diagram in **Figure 3** represents the region of the ventrolateral abdominal wall supplied by the superficial epigastric vessels that can be mobilized in the epigastric flap. This flap can be up to 5 cm in length and 3 cm in width[13,17,18].

Histologically, the flap is composed of the integument that covers the ventrolateral abdominal wall muscles **(Figure 4)**[13,17,18]. It contains a superficial layer of skin, formed by the dermis and epidermis. Beneath the skin there is a layer of fat tissue named *panniculus adiposus*. Below this layer there is another layer of striated muscle known as *panniculus carnosus*[18,28,29]. Below the *panniculus carnosus* there is loose areolar tissue which is superficial to the deep fascia that covers the larger abdominal muscles. Hence, the flap is a composite block of tissues, containing all these layers, except for the deep muscle fascia (**Figure 5**)[13,17,18,27-31].

Protocol

All procedures involving animal subjects were approved by the Institutional Animal Care and Use Committee and Ethical Committee at Nova University Medical School, Lisbon, Portugal (08/2012/CEFCM).

1. Surgical Procedure Set-up Notes

1. Use adult Wistar rats weighing 250 to 350 g.
2. Keep the rats with food and water *ad libitum* with 12 hr light-dark cycles 7 days prior to surgery.
3. Weigh the rat in order to determine the amount of anesthetic required.
4. Autoclave all surgical instruments before surgery.
5. Layout all the surgical supplies and instruments needed for the procedure (see the Table of Materials).
6. Perform the surgery under an operating microscope using conventional and microsurgical instruments.
7. Position the homeothermic blanket, rectal probe, and heat lamp.
8. Place one 20 ml sterilized vial containing 0.9% saline in a water bath warmed to 37 ºC.
9. Wear sterilized gloves to disinfect all surfaces of the operating setting with an alcoholic solution. Remove the gloves.
10. Place a scrub cap and mask.
11. Disinfect hands with water and soap and wear another pair of sterilized gloves.
12. Wear a sterile surgical gown.

2. Anesthesia and Skin Preparation

NOTE: Have an assistant help with the following four steps, as a sterile gown and gloves are worn.

1. Anesthetize the rat with a mixture of Ketamine and Diazepam given intraperitoneally. The dose is 5 mg/kg ketamine and 0.25 mg/kg diazepam. Judge the depth of anesthesia by toe pinch and by observance of respiration rate throughout the entire procedure[8,14,15,32].
2. Apply an ophthalmic gel over the anterior surface of the eyes to avoid corneal abrasion.
3. Remove the hair over the ventral surface of the abdomen with a depilatory cream. After hair removal, remove the depilatory cream with warm saline.
4. Spray a substantial amount of alcoholic solution over the operative site. Leave the product on the operative site and do not wipe it off. Wait at least 15 sec. Repeat the application 3 times. Leave a contact time of at least 2 min before proceeding with the surgery. Other research units use other protocols to prevent surgical site infection.
5. Wearing sterilized gloves, place 2 surgical drapes on both sides of the rat.

3. Donor Site Surgical Procedure

1. **Set the boundaries of an epigastric flap ranging approximately 5 cm in length and 3 cm width.**
    1. Using a surgical skin marker, draw a line from the xiphoid process of the sternum to the pubic symphysis, in order to mark the midline over the ventral surface of the rat's abdomen.
    2. On the left side of the rat, using a surgical skin marker, draw two perpendicular lines to the first line: one crossing immediately caudal to the thoracic cage, and another one, parallel to the latter and just cranial to the groin fold (**Figures 3** and **6**).
    3. Mark the lateral incision with a surgical skin marker with a line parallel to the midline and around 3 cm apart from it.

2. **Flap harvesting**
    1. Incise the skin with a number 15 scalpel blade until reaching the *panniculus carnosus* layer.
    2. Deeper to the *panniculus carnosus* plane, make the incision with an electric cautery until reaching the muscle fascia.
    3. Raise the flap from medial to lateral and from cranial to caudal, exposing the flap's pedicle.
    4. Carefully ligate and divide the perforating vessels coming up from the deep muscle layer and going into the flap's deep surface.
    5. Place a retractor in the caudal aspect of the flap and dissect the flap's pedicle cautiously by gently teasing away the loose surrounding tissues (**Figure 7**).

6. Ligate and divide the lateral femoral circumflex artery and vein using 9/0 Nylon for the ligatures.
7. Isolate the femoral artery and vein. When present, ligate (using 9/0 Nylon) and divide branches of these vessels to adjacent muscles.
8. Firstly, use a double vascular clamp to clamp the proximal aspect of the femoral vein. Subsequently clamp its distal aspect. Then, clamp the distal aspect of the femoral artery and finally its proximal aspect.
9. Clamp the distal aspect of the femoral artery and finally its proximal aspect.
10. Place a single vascular clamp in the superficial epigastric vein and another one in the superficial epigastric artery. Use a pair of straight microsurgery scissors to cut the superficial epigastric artery and vein at their origin and termination, respectively.
11. Copiously irrigate the lumen of these vessels with heparinized normal saline 10 IU/ml, until no blood or debris are seen inside the vessels' lumen[33].
12. Pull and trim a cuff of adventitia close to the vascular section sites.
13. Transfer the epigastric flap to the neck using Addison's forceps (**Figure 8**).
14. Close the donor site with subcuticular interrupted 5/0 absorbable stitches.
15. Close the skin with interrupted 5/0 Nylon stitches.

4. Recipient Site Surgical Procedure

1. **Exposure of Recipient Site Vessels**
    1. Using a surgical skin marker, draw a line over the medial border of the left sternocleidomastoid (SCM) muscle.
    2. Using a surgical skin marker, draw another line immediately cranial and parallel to the left clavicle. These two lines must converge at the left sternoclavicular joint.
    3. Incise the skin using a number 15 scalpel blade.
    4. Use an electric cautery to cut through the subcutaneous tissue.
    5. Use a pair of dissecting scissors to skeletonize the external jugular vein lateral to the SCM muscle.
    6. Isolate and ligate the tributaries of the external jugular in this (**Figure 9**).
    7. Ligate the external jugular vein just below the mandible with a 9/0 Nylon suture.
    8. Place a single venous clamp beneath the latter ligation and cut the external jugular vein using a pair of straight microsurgery scissors.
    9. Wash the lumen of the vein with heparinized normal saline in a concentration of 10 IU/ml.
    10. Isolate the medial margin of the SCM muscle and retract this muscle laterally, thus exposing the carotid artery and the vagus nerve (**Figure 10**).
    11. Make a transverse incision in the middle third of the SCM muscle using the electric cautery.
    12. Place a retractor between the deep surface of the SCM muscle and the strap muscles.
    13. Tease away the vagus nerve from the carotid artery, taking care not to damage these structures.

2. **Vascular anastomoses**
    1. Position a double arterial clamp in the carotid artery.
    2. Place a 9/0 Nylon stitch in the lateral aspect of the carotid artery, and use this stitch to pull this part of the vessel wall.
    3. Use a pair of straight microsurgery scissors to produce an opening in this region of vessel wall.
    4. Using interrupted 10/0 Nylon sutures perform a termino-lateral anastomosis between the superficial epigastric artery of the flap and the carotid artery at the level of the recently created carotid opening.
    5. Approach the proximal stump of the external jugular vein and the superficial epigastric vein and inspect the caliber of these two veins.
        1. If the discrepancy in size is slight to moderate, dilate the lumen of the cut end of the superficial epigastric vein using dilation forceps.
        2. If the caliber difference is very pronounced, in addition to forceps dilation, bevel the end of the superficial epigastric vein in a 30 to 45° angle.
        3. Perform the venous anastomosis, using interrupted 11/0 Nylon sutures.
    6. Remove the single clamps placed onto the flap's vessels.
    7. Remove the double clamp positioned in the femoral vein.
    8. Remove the double clamp placed in the femoral artery.

3. **Assess patency and competency of anastomoses**
    1. Verify if the flap's artery and vein are fully dilated and no significant bleeding is observed after 3 min of removing the vascular clamps (**Figure 11**).
        1. If there is bleeding during this period place a moist saline gauze over the anastomosis and apply gentle pressure.
        2. If bleeding from anastomoses does not stop after 3 min, add additional 11/0 Nylon interrupted sutures, after vascular clamp placement, as needed.
    2. Wait 10 min with the flap connected to the neck vessels and wrapped by a gauze moistened in warm saline.
    3. Assess flap's perfusion and neck wound hemostasis. Inspect the anastomoses for signs of hemorrhage, thrombosis or excessive traction.
    4. Secure the flap in the recipient site starting with 5/0 subcuticular interrupted sutures.
    5. Close the skin with 5/0 Nylon interrupted sutures (**Figure 12**).

5. Post-operative Care

1. Leave the rat to recover inside its individual cage in the right lateral decubitus position. Keep the cage warm by placing an electric heat pad set on low beneath. Place a light cloth between the cage and the electric heat pad to avoid hyperthermia.

2. Watch the animal continuously turning it to the opposite lateral decubitus every 5 min, until it resumes sternal recumbency and it is able to ambulate.
3. House the rats individually until removing the surgical stitches two weeks after the surgical procedure.
4. Give an anti-inflammatory drug 1 mg/kg subcutaneously once a day for the 3 days following surgery, for postoperative analgesia.

6. Flap Assessment

1. Present a food treat over the head of the rat and assess flap's viability by visual inspection.
2. If exposure is insufficient using the previous step, have an assistant applying gentle touch over the interscapular region of the rat, while examining the flap.
3. Use digital photography and ImageJ software to quantitatively evaluate the areas of wound dehiscence, flap epidermolysis, hyperemia, congestion and/or necrosis, as explained in detail by Trujillo *et al.*[15].

Representative Results

According to the authors' experience of more than ten years using the epigastric free flap as a model of free tissue transfer both in the context of microsurgery courses and for research purposes, the rate of flap survival depends somewhat on the dexterity and experience of the surgeon. Generally speaking, if the technical aspects described above are taken into consideration, a nearly complete survival rate (<10% of flap necrosis) of around 70% of flaps is to be expected. Around 10% of flaps present partial necrosis (10 to 50%). About 20% of flaps suffer complete necrosis. An 80% nearly complete survival rate was obtained in the last 20 procedures performed by the first author (D.C.) (**Figure 13**).

During the first two days postoperatively, the free epigastric flap is often edematous and presents some degree of venous congestion. These usually both subside gradually between 3 and 5 days after surgery. Typically, during the first week, the rat removes most external stitches and part of the subcuticular sutures, often resulting in scattered areas of slight wound dehiscence (**Figure 14**). After day 10, the hair slowly starts to grow on the flap's surface. At the end of the first month after surgery, the flap is usually covered with slightly shorter hair than the adjacent skin. Two months postoperatively, the presence of the flap is heralded by a slight lump, and by a relatively inconspicuous scar around the flap's margins (**Figure 14**). Auto cannibalism of the flap is an infrequent finding that, in the authors' experience, occurs almost exclusively in cases of total flap necrosis.

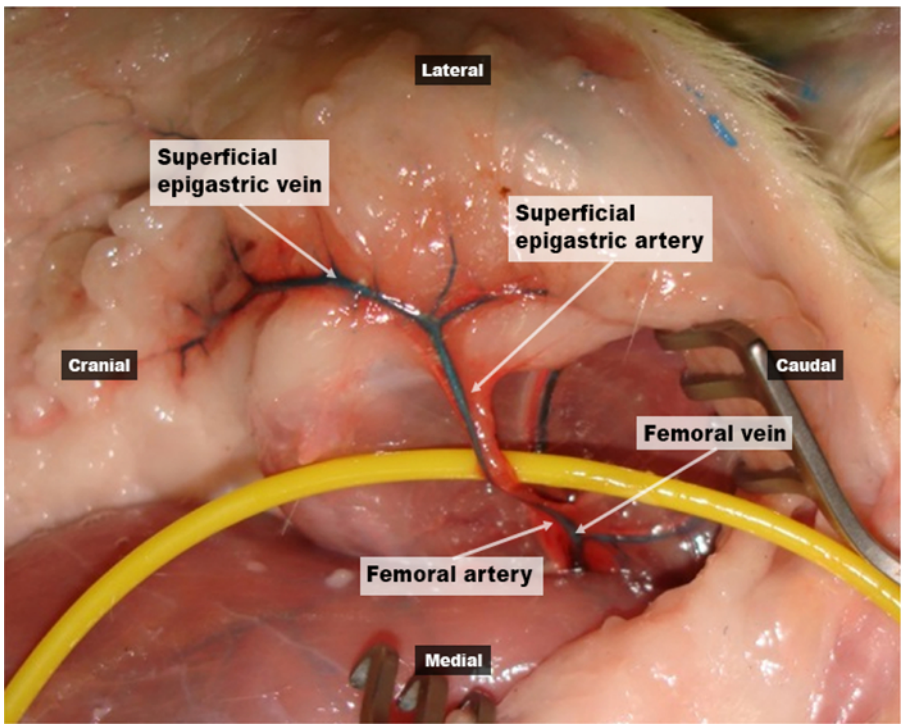

Figure 1: Vascular anatomy of the epigastric free flap.
This photograph shows the left epigastric region of a rat previously injected with a red latex solution in the arterial system and with a blue latex solution in the venous system. It is possible to observe that the epigastric region receives an axial blood supply from the superficial epigastric artery and vein. These vessels originate from and drain into the femoral artery and vein, respectively. Please click here to view a larger version of this figure.

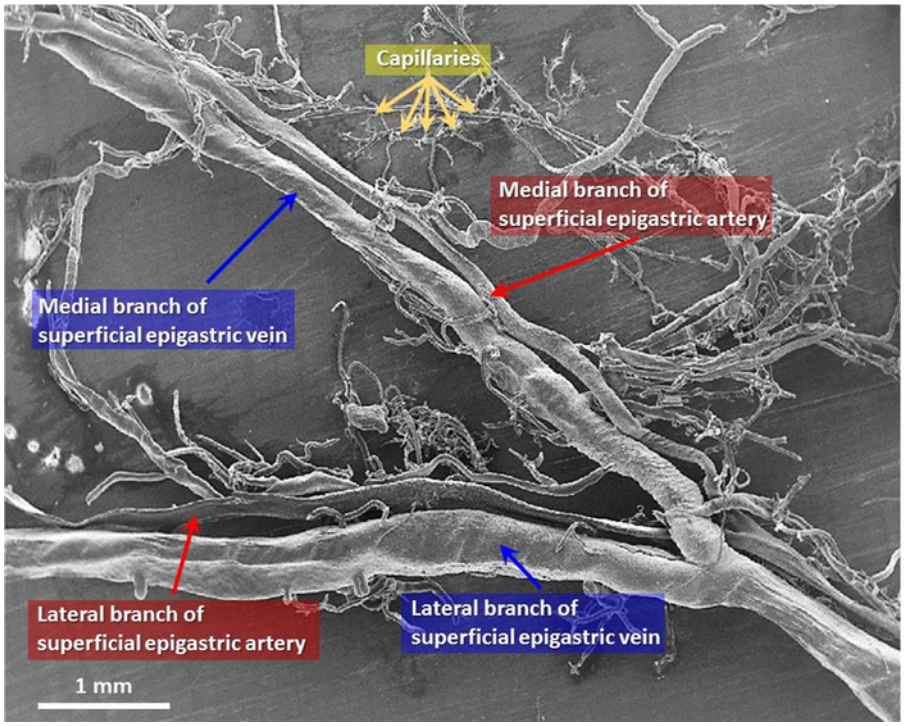

Figure 2: Scanning electron microscopy image of a corrosion cast of the superficial epigastric vessels showing the microscopic vascular blood supply to the epigastric free flap.
This scanning electron microscopy image of a corrosion cast of the superficial epigastric vessels of the rat shows that the vein has a larger caliber that the artery. On average the caliber of the superficial epigastric vein is 0.6 to 0.8 mm, compared with the 0.3 to 0.5 mm of the superficial epigastric artery. This image also shows that the superficial epigastric artery originates two main branches: a lateral and a medial branch that in turn divide multiple times, originating capillary networks that supply most of the epigastric region. These capillaries drain into the tributaries of the superficial epigastric vein that have a parallel course to the arterial tree. Please click here to view a larger version of this figure.

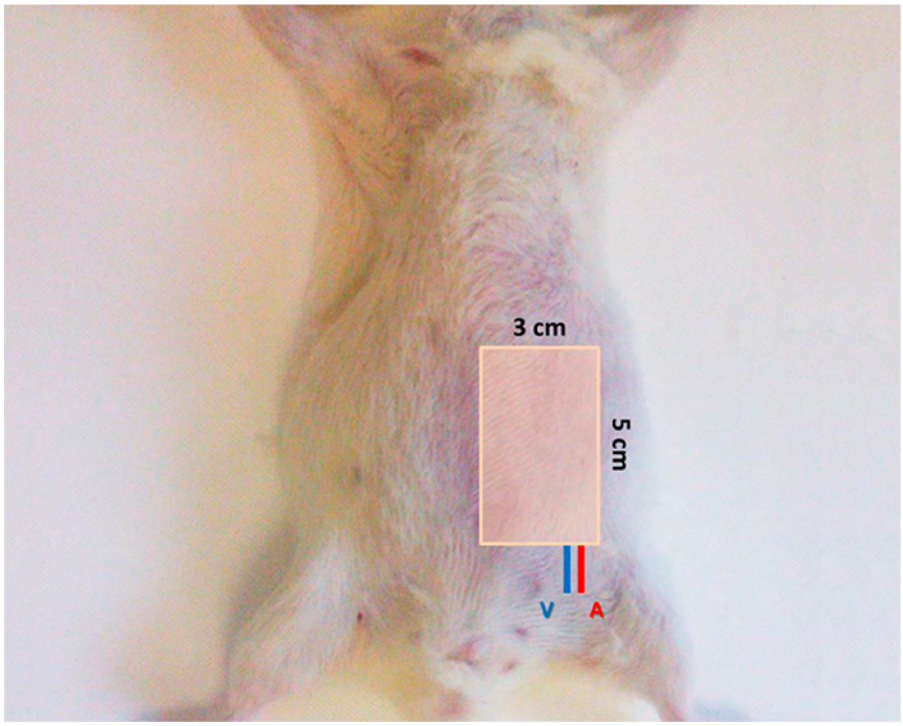

Figure 3: Potential area of a left epigastric free flap in the rat.
This diagram represents the region of the abdominal wall supplied by the superficial epigastric vessels and that can be mobilized in the epigastric flap. This flap can be up to 5 cm in length and 3 cm in width. Please click here to view a larger version of this figure.

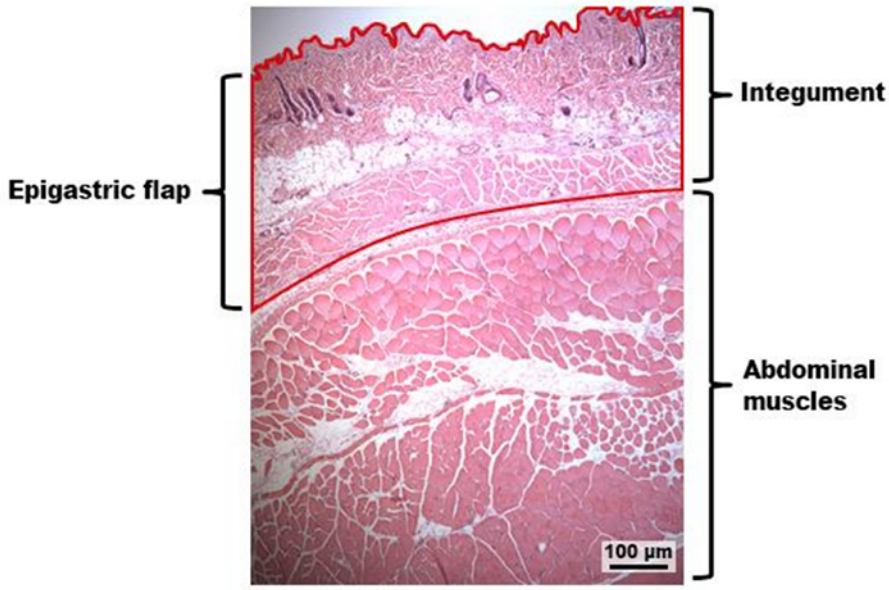

Figure 4: Photograph of a hematoxilin-eosin stained section of the epigastric flap.
This hematoxilin-eosin stained section of the epigastric region shows that the epigastric flap is composed of the integument of this region that covers the abdominal wall muscles. Please click here to view a larger version of this figure.

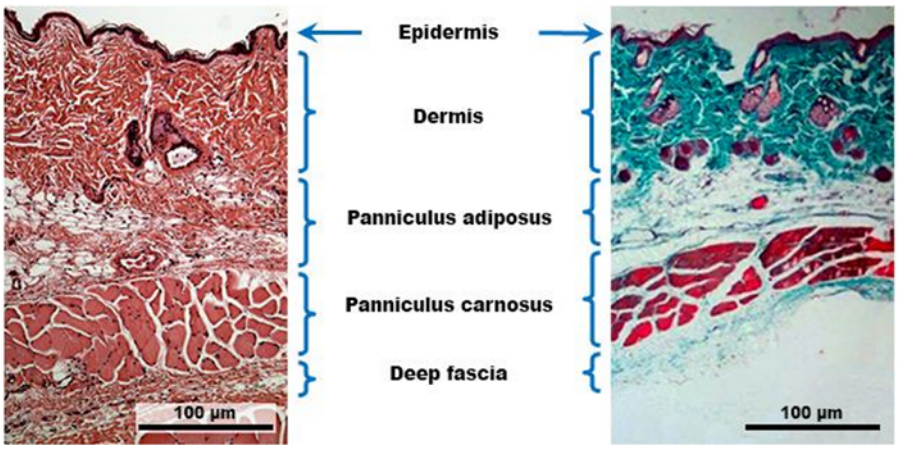

Figure 5: Histological composition of the epigastric flap.
The photograph on the left side represents a hematoxilin-eosin stained section of an epigastric flap, whereas the photograph on the right side was obtained from a Masson's trichrome section of this flap. These two pictures illustrate that the epigastric flap of the rat is a composite block of tissues. It contains a superficial layer of skin, formed by the dermis and epidermis. Beneath the skin there is a layer of fat tissue named *panniculus adiposus*. Below this layer there is layer of striated muscle known as *panniculus carnosus*. Below the *panniculus carnosus* there is a deep fascia that covers the larger and deeper abdominal muscles. Please click here to view a larger version of this figure.

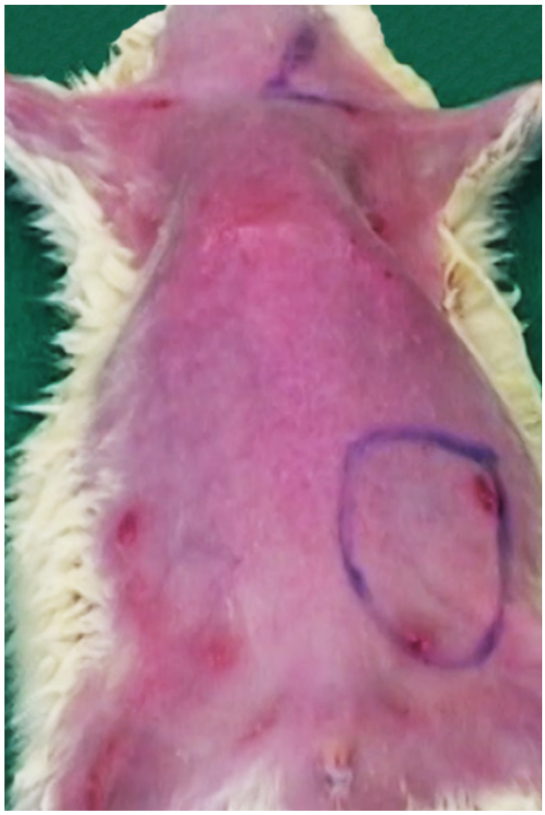

Figure 6. Pre-operative skin markings on the ventral surface of the rat prior to surgery.
This photograph illustrates the skin markings for the incisions used to raise the left epigastric flap and subsequently to inset this flap in the ventral aspect of the left cervical region.

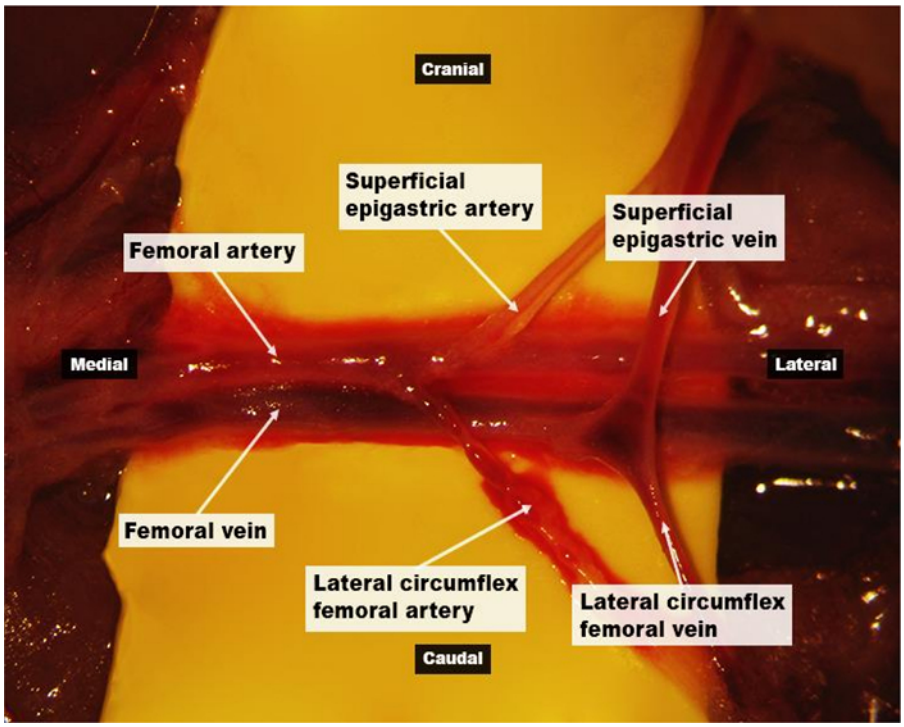

Figure 7. Surgical anatomy of the epigastric flap's nutrient vessels under the operating microscope (10X magnification).
This photograph shows the superficial epigastric artery and vein originating from and draining into the femoral artery and vein, respectively. The lateral femoral circumflex artery usually arises from the caudal aspect of the superficial epigastric artery. The lateral femoral circumflex vein has a similar path and usually terminates into the superficial epigastric vein. Please click here to view a larger version of this figure.

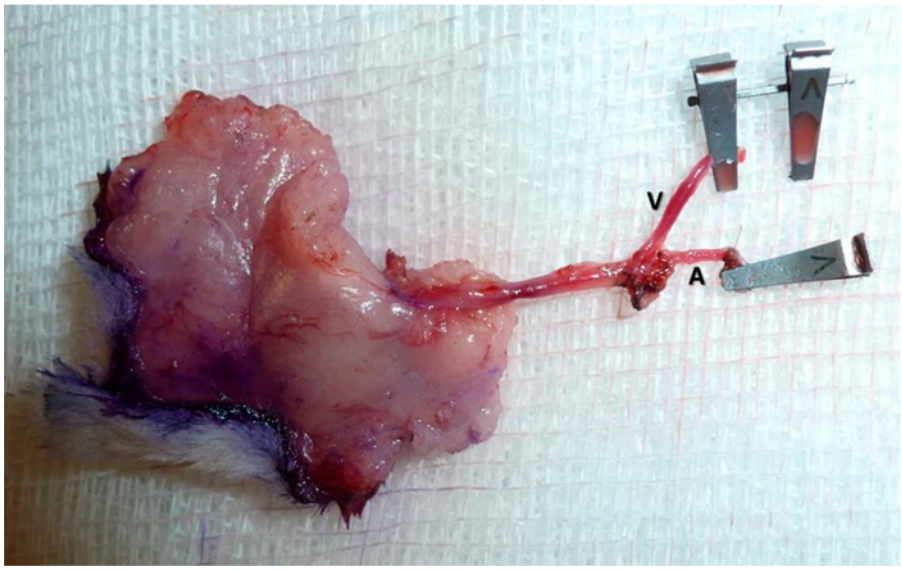

Figure 8. The epigastric flap *ex vivo* pedicled on its nutrient vessels (the superficial epigastric artery and vein - A, V, respectively). Please click here to view a larger version of this figure.

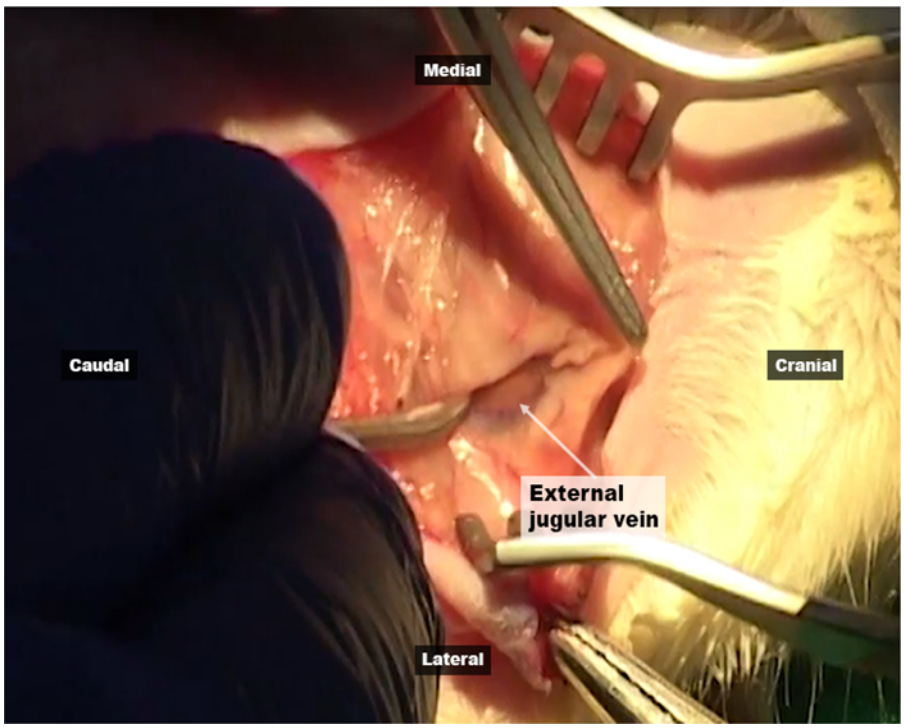

Figure 9. Operating view of the dissection of the recipient vein, i.e., the external jugular vein, on the left side of the neck (6x magnification).
It is possible to observe the subcutaneous course of the external jugular vein lateral to the sternocleidomastoid muscle. Please click here to view a larger version of this figure.

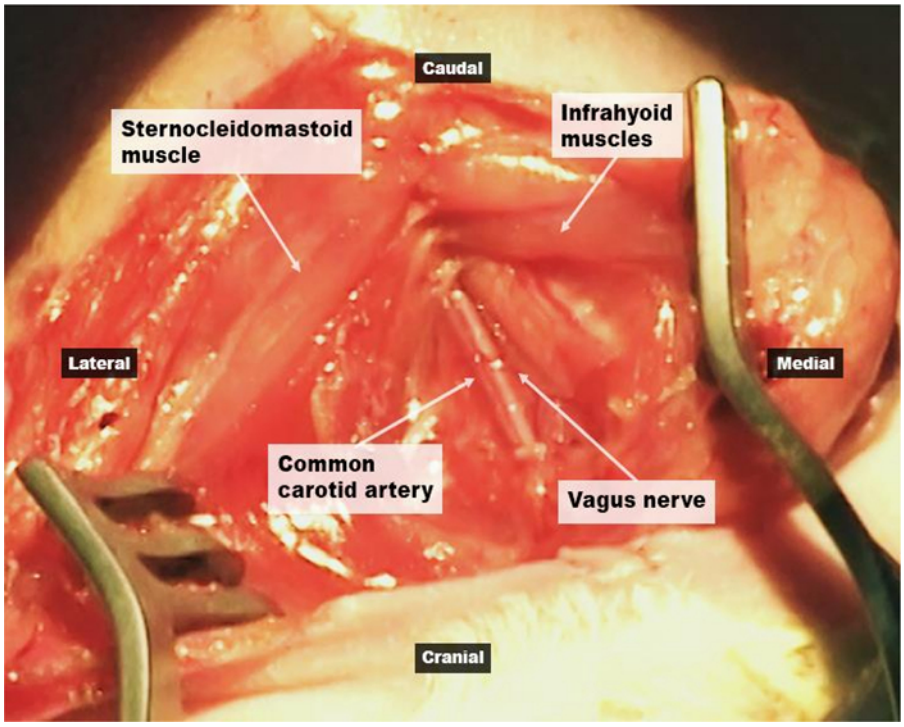

Figure 10. Operating view of the dissection of the donor artery, i.e., the common carotid, on the left side of the neck (10x magnification).
The artery and accompanying vagus nerve are exposed after retracting the sternocleidomastoid and the infrahyoid muscles, as shown. Please click here to view a larger version of this figure.

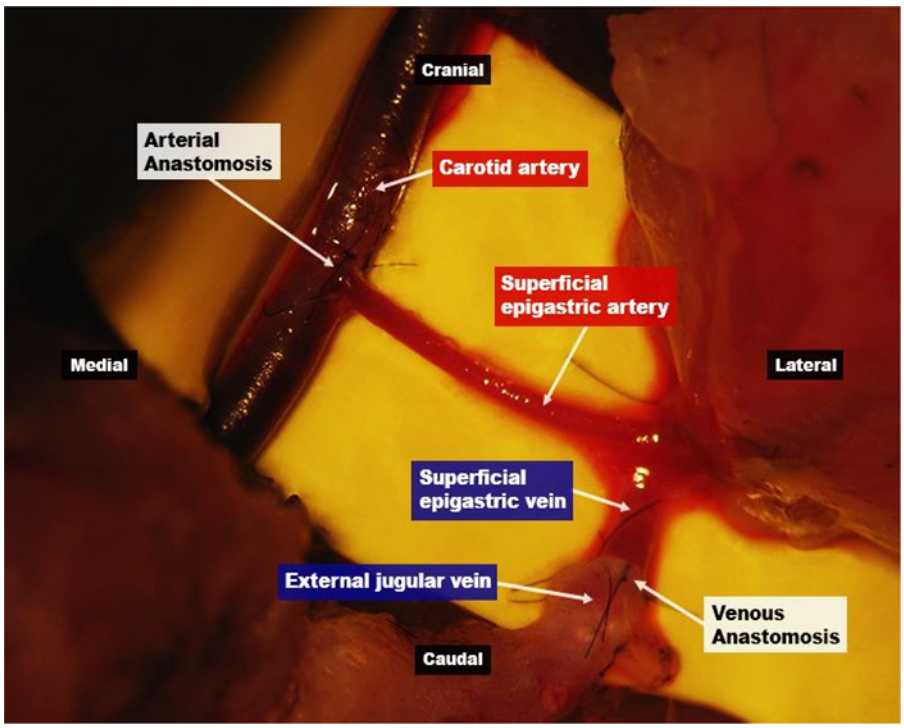

Figure 11. Photograph of the vascular anastomoses between the flap's vessels and the recipient vessels in the neck, as seen under the operating microscope (10x magnification).
This photograph shows the termino-lateral anastomosis between the common carotid and the superficial epigastric arteries. It is also possible to observe the termino-terminal anastomosis between the superficial epigastric and the external jugular veins. Please click here to view a larger version of this figure.

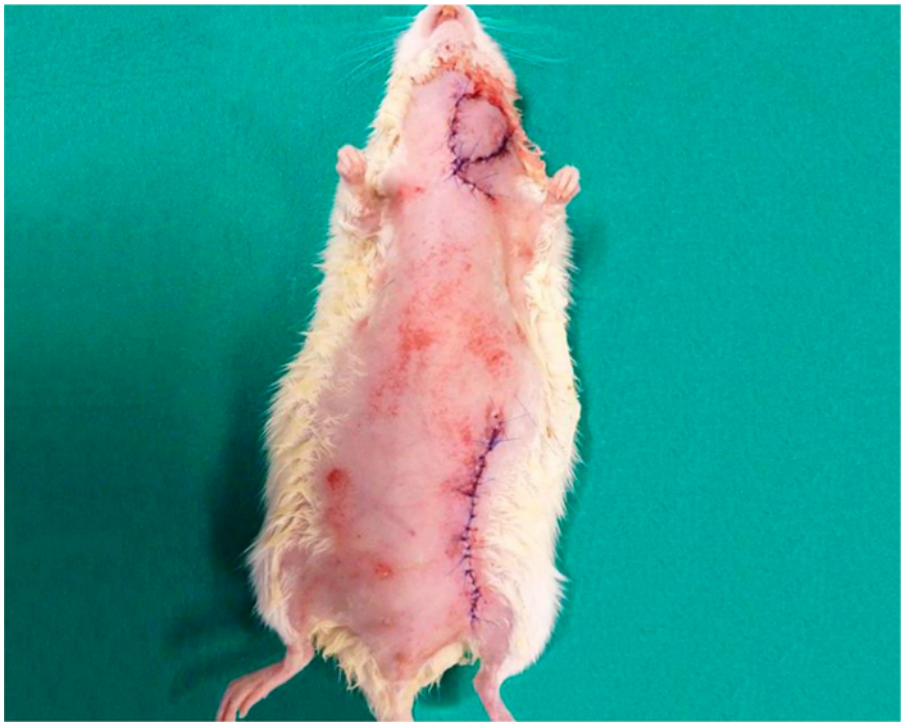

Figure 12. Photograph of ventral aspect of the rat immediately after the surgery.
Notice that the donor zone is easily closed primarily. Please click here to view a larger version of this figure.

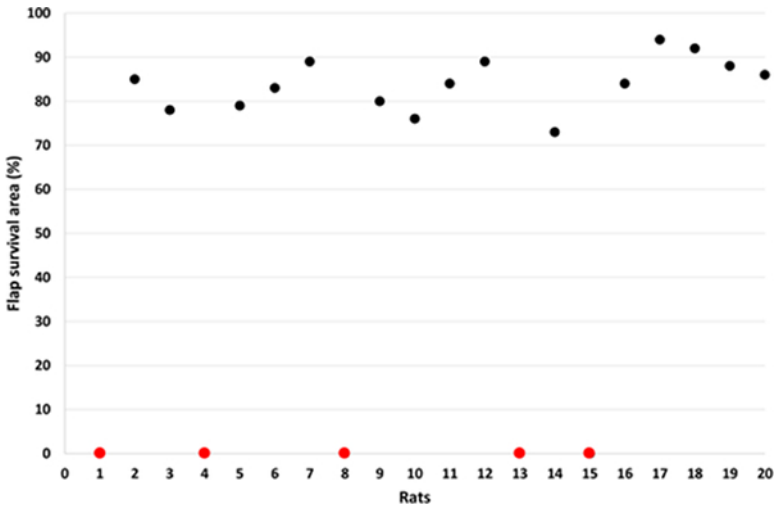

Figure 13. Epigastric free flap survival in 20 consecutive rats operated on by the first author (D.C.).
Five rats (20%) presented complete flap necrosis (cases 1, 4, 8, 13 and 15, represented by the red dots). Areas of flap necrosis were determined using the free software ImageJ, as explained in detail by Trujillo et al.[15]. Please click here to view a larger version of this figure.

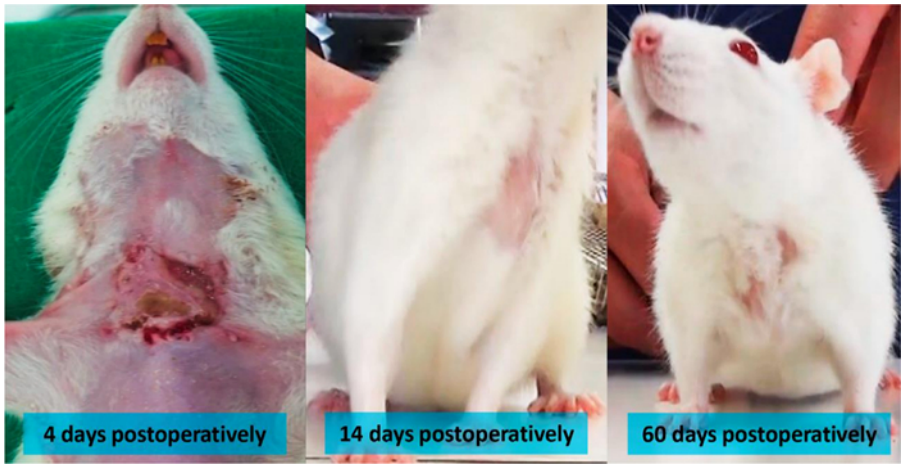

Figure 14. Photographs of the epigastric flap placed on the ventral aspect of the neck 4, 14 and 60 days postoperatively. Four days after surgery, there is typically some wound dehiscence, as the rat removes the stitches. However, the flap usually remains in place. It is possible to examine the flap daily by simple visual inspection. Please click here to view a larger version of this figure.

Discussion

The most important aspect to obtain consistent flap survival is paying attention to detail in various steps of the microsurgical technique. For example, to obtain good visualization of the vessels, of the surgical instruments and of the fine suture lines, it is very helpful to place underneath the vessels, a sterilized colored plastic background. As many researchers, we prefer to use sterilized fragments of yellow or green balloons (**Figures 7** and **11**). This background provides the additional advantage of minimizing adherence of suture lines to the adjacent structures, which sometimes leads to the need of pulling the suture line with too much tension, which may in turn lead to vascular tearing. Finally, the use of a background has the additional advantage of decreasing the probability of inadvertently dragging potential thrombogenic tissue debris to the anastomosis site.

Considering that the flap's vessels are very fine and fragile, it is important not to pinch the entire width of the vessels, in order to avoid intimal lesion that, in turn, will lead to intravascular thrombosis and flap failure. To prevent inadvertent injury to both the flap's vessels and to the recipient site's vessels, it is safer to liberally ligate and divide neighboring tributaries, which will allow an easier manipulation of these vessels.

Before starting the anastomoses, it is vital to place the vessels in their definitive position, striving to prevent vascular kinking or torsion of the flap's pedicle. Given the small caliber and delicate consistency of the vessels, these are often difficult to exclude unequivocally. One helpful trick is to secure the flap in its final position with 3 stitches placed away from the site of the anastomoses. Next, if in doubt, temporarily open the vascular clamps placed at the flap's pedicle, and fill the vessels' lumen with heparinized normal saline in a concentration of 10 IU/mL until they become engorged. This leads vessels to assume the configuration they will present after being perfused by blood, as when the clamps are removed after anastomoses completion.

Moreover, it is of paramount importance to detect any air bubbles, even if small, inside the vessels during the entire procedure and particularly before tying the final stitches. If these bubbles are distant from the vascular section, the vessels can be milked gently with microsurgical forceps. If they are located close to the anastomotic sites, simple irrigation leads the less dense bubbles to be easily expelled from the vascular lumen. Failure to acknowledge the presence of air bubbles can cause irreversible flap ischemia and necrosis, no doubt due to the fine caliber of the flap vessels.

Additionally, it cannot be overemphasized the need for meticulous care while passing and tying the stitches, in order to: include the three layers of the vessels (intima, media and adventitia); obtain good vessel eversion to ensure adequate intimal contact, which is vital to anastomosis sealing and endothelial regrowth; avoid loose vascular contact, which will result in anastomotic incompetence, i.e., bleeding; and avoid grabbing too much vascular tissue, which will lead to anastomosis stenosis and proclivity to thrombosis, which in turn will result in venous congestion or poor flap perfusion, if the vein or artery are involved, respectively.

Finally, it is essential to ensure perfect hemostasis, during the entire procedure, especially when raising the flap in its deep surface. Otherwise hematoma formation and rat death are likely to ensue.

Modifications and troubleshooting of the technique

The authors observed that making a transverse incision in the middle portion of the SCM using an electric cautery, not only allows a better exposure of the carotid artery, but also minimizes the risk of undue tension over the future arterial anastomosis.

Another important technical tip is to start the anastomosis from the vessels' back wall, in order to minimize the risk of unwillingly catching this wall when placing the stitches in the more easily exposed front wall. If the back wall is sutured to the anterior aspect of the anastomosis, lack of vascular patency will almost invariably result either immediately due to mechanical reasons or after only a few hours as a result of thrombosis[8].

If the anastomoses of the epigastric vessels of the rat are considered too technically challenging due to the small caliber of these vessels, the femoral vessels can be ligated distal to the origin of the epigastric vessels and used as the vascular pedicle of the epigastric flap. In this way, larger vessels will be used (the femoral artery has a caliber of 1.0 to 1.2 mm; and the femoral vein has a caliber of 1.2 to 1.5 mm). Moreover, by

dissecting and ligating the other tributaries of the femoral vessels, a vascular pedicle length of over 2 cm can be obtained, which will facilitate flap insetting[18,34,35].

Reproducibility

Our experience of more than ten years of using this flap for teaching and research purposes strongly suggests that the rat epigastric flap is a reproducible model of free tissue transfer[11,13,17,18,26]. It can be easily incorporated in microsurgical courses, as it is a good teaching and training model for microsurgery trainees[11,13,17,18,26]. In our experience, although technically challenging in the beginning for the novice in microsurgery, after some training, the free epigastric flap can be successfully transferred to the neck of the rat with minimal to no subsequent necrosis in 70 to 80% of cases. These results concur with those generally reported in the literature[13,18,36].

Significance with respect to existing methods

Numerous free flaps have been described in the rat[10,16,18,37-39]. The most commonly used for teaching and research purposes have been the transverse *rectus abdominis* myocutaneous flap, the *latissimus dorsi* and *serratus anterior* muscle flaps, the hind limb replantation model, and the epigastric (groin) flap[18,35]. These flaps have been favored, due to their consistent anatomy and sizeable vascular pedicle. The epigastric flap is arguably the one associated with lesser donor site morbidity, as it dissected above the muscle fascia[18]. Moreover, the epigastric flap, described in 1967, was the first flap to be described in rats[34,35]. This occurred only 4 years after the first description of an experimental flap in an animal by Goldwyn. Interestingly, this flap was a groin flap in the dog[34].

Limitations of the technique

The two main limitations of this model are the need for microsurgical skills in order to carry out the surgery, and the presence of significant necrosis in 20 to 25% of cases, according to different authors[13,18,36]. Another potential limitation of the model herein presented is the auto cannibalism of the flap. However, as the authors above, this is an infrequent finding that almost only occurs in cases of total flap necrosis.

Future applications of the technique

The rat epigastric free flap can be used in experimental studies of tissue perfusion, tissue repair and surgical wound infection[40,41]. Its nutrient vessels are particularly suitable for intravascular injection of solutions containing substances of interest, namely drugs, viral vectors or liposomes, that will mostly produce a local or regional effect[30,31]. In addition, beneath the flap, pathogens, foreign bodies, radioactive seeds or chemicals can also be placed, mimicking several disease processes and potential treatments[30,31].

Disclosures

The authors have nothing to disclose.

Acknowledgements

One of the authors (Diogo Casal) received a grant from The Program for Advanced Medical Education, which is sponsored by Fundação Calouste Gulbenkian, Fundação Champalimaud, Ministério da Saúde e Fundação para a Ciência e Tecnologia, Portugal.

The authors would like to thank the technical help of Mr. Alberto Severino in filming and editing the video. The authors are also grateful to Mr. Octávio Chaveiro, Mr. Marco Costa and Mr. Carlos Lopes for their help in preparing the animal specimens presented in this paper.

Finally, the authors would like to thank Ms. Gracinda Menezes for her help in all the logistical aspects pertaining to animal acquisition and maintenance.

References

1. Morain, W. D. in *Plastic Surgery.* Vol. 1 (ed S.J. Mathes) 27-34 Saunders, (2006).
2. Christoforou, D., Alaia, M., & Craig-Scott, S. Microsurgical management of acute traumatic injuries of the hand and fingers. *Bull Hosp Jt Dis (2013).* **71** (1), 6-16 (2013).
3. Santoni-Rugiu, P., & Sykes, P. J. in *A History of Plastic Surgery.* eds P. Santoni-Rugiu & P.J. Sykes) Ch. 3, 79-119 Springer, (2007).
4. Tamai, S. in *Experimental and Clinical Reconstructive Microsurgery.* eds S. Tamai, M. Usui, & T. Yoshizu) Ch. 1, 3-24 Springer-Verlag, (2003).
5. Bettencourt-Pires, M. A. *et al.* Anatomy and grafts - From Ancient Myths, to Modern Reality. *Arch Anat.* **2** (1), 88-107 (2014).
6. Casal, D., Gomez, M. M., Antunes, P., Candeias, H., & Almeida, M. A. Defying standard criteria for digital replantation: A case series. *Int J Surg Case Rep.* **4** (7), 597-602 (2013).
7. Gomez, M. M., & Casal, D. Reconstruction of large defect of foot with extensive bone loss exclusively using a latissimus dorsi muscle free flap: a potential new indication for this flap. *J Foot Ankle Surg.* **51** (2), 215-217 (2012).
8. Plenter, R. J., & Grazia, T. J. Murine heterotopic heart transplant technique. *J Vis Exp.* (89) (2014).
9. Pichierri, A. *et al.* How to set up a microsurgical laboratory on small animal models: organization, techniques, and impact on residency training. *Neurosurg Rev.* **32** (1), 101-110; discussion 110 (2009).
10. Klein, I., Steger, U., Timmermann, W., Thiede, A., & Gassel, H. J. Microsurgical training course for clinicians and scientists at a German University hospital: a 10-year experience. *Microsurgery.* **23** (5), 461-465 (2003).
11. Fukui, A. in *Experimental and Clinical Reconstructive Microsurgery.* eds S. Tamai, M. Usui, & T. Yoshizu) Ch. 1, 35-43 Springer-Verlag, (2004).
12. Ad-El, D. D., Harper, A., & Hoffman, L. A. Digital replantation teaching model in rats. *Microsurgery.* **20** (1), 42-44 (2000).

13. Ruby, L. K., Greene, M., Risitano, G., Torrejon, R., & Belsky, M. R. Experience with epigastric free flap transfer in the rat: technique and results. *Microsurgery.* **5** (2), 102-104 (1984).
14. Edmunds, M. C., Wigmore, S., & Kluth, D. In situ transverse rectus abdominis myocutaneous flap: a rat model of myocutaneous ischemia reperfusion injury. *J Vis Exp.* (76) (2013).
15. Trujillo, A. N., Kesl, S. L., Sherwood, J., Wu, M., & Gould, L. J. Demonstration of the rat ischemic skin wound model. *J Vis Exp.* (98) (2015).
16. Siemionow, M. Z. in *Plastic and Reconstructive Surgery: Experimental models and research designs.* (ed M.Z. Siemionow) Ch. 1-7, 3-67 Springer - Verlag, (2015).
17. Petry, J. J., & Wortham, K. A. The anatomy of the epigastric flap in the experimental rat. *Plast Reconstr Surg.* **74** (3), 410-413 (1984).
18. Hirase, Y. in *Experimental and Clinical Reconstructive Microsurgery.* eds S. Tamai, M. Usui, & T. Yoshizu) Ch. 6, 111-114 Springer-Verlag, (2004).
19. Zhang, F. *et al.* Microvascular transfer of the rectus abdominis muscle and myocutaneous flap in rats. *Microsurgery.* **14** (6), 420-423 (1993).
20. Tonken, H. P. *et al.* Microvascular transplant of the gastrocnemius muscle in rats. *Microsurgery.* **14** (2), 120-124 (1993).
21. Miyamoto, S. *et al.* Free pectoral skin flap in the rat based on the long thoracic vessels: a new flap model for experimental study and microsurgical training. *Ann Plast Surg.* **61** (2), 209-214 (2008).
22. Nasir, S., Aydin, A., Kayikcioglu, A., Sokmensuer, C., & Cobaner, A. New experimental composite flap model in rats: gluteus maximus-tensor fascia lata osteomuscle flap. *Microsurgery.* **23** (6), 582-588 (2003).
23. Coskunfirat, O. K., Islamoglu, K., & Ozgentas, H. E. Posterior thigh perforator-based flap: a new experimental model in rats. *Ann Plast Surg.* **48** (3), 286-291 (2002).
24. Ozkan, O. *et al.* A new flap model in rats: iliac osteomusculocutaneous flap. *Ann Plast Surg.* **47** (2), 161-167 (2001).
25. Padubidri, A. N., & Browne, E., Jr. Modification in flap design of the epigastric artery flap in rats--a new experimental flap model. *Ann Plast Surg.* **39** (5), 500-504 (1997).
26. Strauch, B., & Murray, D. E. Transfer of composite graft with immediate suture anastomosis of its vascular pedicle measuring less than 1 mm. in external diameter using microsurgical techniques. *Plast Reconstr Surg.* **40** (4), 325-329 (1967).
27. Green, C. E. *Anatomy of the Rat.* First edn, 124-153 Hafner Publishing Company, (1968).
28. Greene, E. C. *Anatomy of the rat.* New York, Hafner. (1959).
29. Langworthy, O. R. A morphological study of the panniculus carnosus and its genetical relationship to the pectoral musculature in rodents. *Am J Anat.* **35** (2), 283-302 (1925).
30. Popesko, P., Ratjová, V., & Horák, J. in *A Colour Atlas of the Anatomy of Small Laboratory Animals.* Vol. 2 13-104 Saunders, (1992).
31. Brown, S. H., Banuelos, K., Ward, S. R., & Lieber, R. L. Architectural and morphological assessment of rat abdominal wall muscles: comparison for use as a human model. *J Anat.* **217** (3), 196-202 (2010).
32. Harder, Y. *et al.* Ischemic tissue injury in the dorsal skinfold chamber of the mouse: a skin flap model to investigate acute persistent ischemia. *J Vis Exp.* (93), e51900 (2014).
33. Cox, G. W., Runnels, S., Hsu, H. S., & Das, S. K. A comparison of heparinised saline irrigation solutions in a model of microvascular thrombosis. *Br J Plast Surg.* **45** (5), 345-348 (1992).
34. Gurunluoglu, R., & Siemionow, M. Z. in *Plastic and Reconstructive Surgery: Experimental models and research designs.* (ed M.Z. Siemionow) Ch. 6, 53-62 Spronger, (2015).
35. Nasır, S. in *Plast Reconstr Surg.* 227-236 Springer, (2015).
36. Parsa, F. D., & Spira, M. Evaluation of anastomotic techniques in the experimental transfer of free skin flaps. *Plast Reconstr Surg.* **63** (5), 696-699 (1979).
37. Dunn, R. M., Huff, W., & Mancoll, J. The Rat Rectus Abdominis Myocutaneous Flap: A True Myocutaneous Flap Model. *Ann Plast Surg.* **31** (4), 352-357 (1993).
38. Özkan, Ö., et al. A new flap model in rats: iliac osteomusculocutaneous flap. *Ann Plast Surg.* **47** (2), 161-167 (2001).
39. Ozkan, O., Koshima, I., & Gonda, K. A supermicrosurgical flap model in the rat: a free true abdominal perforator flap with a short pedicle. *Plast Reconstr Surg.* **117** (2), 479-485 (2006).
40. Dorsett-Martin, W. A. Rat models of skin wound healing: a review. *Wound Repair Regen.* **12** (6), 591-599 (2004).
41. Ghali, S. *et al.* Treating chronic wound infections with genetically modified free flaps. *Plast Reconstr Surg.* **123** (4), 1157-1168 (2009).

APPENDIX 6

OPEN

PRS GLOBAL OPEN

EXPERIMENTAL

Optimization of an Arterialized Venous Fasciocutaneous Flap in the Abdomen of the Rat

Diogo Casal, MD*†‡
Eduarda Mota-Silva, MSc§
Diogo Pais, MD, PhD†
Inês Iria, MSc¶
Paula A. Videira, PhD¶
David Tanganho, MD*†
Sara Alves, MSc‖
Luís Mascarenhas-Lemos, MD‖
José Martins Ferreira, BSc‖
Mário Ferraz-Oliveira, MD‖
Valentina Vassilenko, PhD§
João Goyri O'Neill, MD, PhD†

Background: Although numerous experimental models of arterialized venous flaps (AVFs) have been proposed, no single model has gained widespread acceptance. The main aim of this work was to evaluate the survival area of AVFs produced with different vascular constructs in the abdomen of the rat.

Methods: Fifty-three male rats were divided into 4 groups. In group I (n = 12), a 5-cm-long and 3-cm-wide conventional epigastric flap was raised on the left side of the abdomen. This flap was pedicled on the superficial caudal epigastric vessels caudally and on the lateral thoracic vein cranially. In groups II, III, and IV, a similar flap was raised, but the superficial epigastric artery was ligated. In these groups, AVFs were created using the following arterial venous anastomosis at the caudal end of the flap: group II (n = 13) a 1-mm-long side-to-side anastomosis was performed between the femoral artery and vein laterally to the ending of the superficial caudal epigastric vein. In group III (n = 14), in addition to the procedure described for group II, the femoral vein was ligated medially. Finally, in group IV (n = 14), the superficial caudal epigastric vein was cut from the femoral vein with a 1-mm-long ellipse of adjacent tissue, and an end-to-side arterial venous anastomosis was established between it and the femoral artery.

Results: Seven days postoperatively, the percentage of flap survival was 98.89 ± 1.69, 68.84 ± 7.36, 63.84 ± 10.38, 76.86 ± 13.67 in groups I–IV, respectively.

Conclusion: An optimized AVF can be produced using the vascular architecture described for group IV. *(Plast Reconstr Surg Glob Open 2017;5:e1436; doi: 10.1097/GOX.0000000000001436; Published online 17 August 2017.)*

INTRODUCTION

More than 30 years have passed since Vaubel's 1975 description of an arterialized venous flap (AVF) to reconstruct the dorsum of the hand and the highly cited Nakayama's 1981 article on the creation of an experimental AVF model in the abdomen of the rat.[1,2] Initially, there was great enthusiasm with AVFs, since they allowed the transference from composite blocks of tissues based exclusively on the venous system. This in turn allowed the creation of thin, pliable, and versatile flaps, that could be tailored rapidly and with minimal morbidity in the donor zone.[3] However, reports of high necrosis rates and a poorly understood physiology have been deterring many surgeons of using AVFs in clinical practice.[3–8]

Although numerous experimental models of AVFs have been proposed, no model has gained widespread acceptance, which hinders comparison of observations on the physiology and interventions on these flaps. Additionally, lack of a standardized model of AVF can be an obstacle for the novice in microsurgery while preparing to execute these flaps in a training environment.[9] Therefore, the main aim of this work was to evaluate the flap survival area of AVFs produced with different vascular constructs in the abdomen of the rat. Secondary endpoints were determina-

*From the *Plastic and Reconstructive Surgery Department and Burn Unit, Centro Hospitalar de Lisboa Central, Lisbon, Portugal; †Anatomy Department, Nova Medical School, Lisbon, Portugal; ‡Glycoimmunology, CEDOC, NOVA Medical School, Lisbon, Portugal; §LIBPhys, Physics Department, Faculdade de Ciências e Tecnologias, Universidade NOVA de Lisboa, Caparica, Portugal; ¶Department of Life Sciences, Faculdade de Ciências e Tecnologias, Universidade NOVA de Lisboa, Caparica, Portugal; and ‖Pathology Department, Centro Hospitalar de Lisboa Central, Lisbon, Portugal.*

Received for publication April 6, 2017; accepted June 14, 2017.

DOI: 10.1097/GOX.0000000000001436

Disclosure: *Supported by a grant from "The Programme for Advanced Medical Education" (D.C.) sponsored by "Fundação Calouste Gulbenkian, Fundação Champalimaud, Ministério da Saúde and Fundação para a Ciência e Tecnologia, Portugal." The Article Processing Charge was paid for by the authors.*

Supplemental digital content is available for this article. Clickable URL citations appear in the text.

tion of the time required to produce the flap, animal mortality, and surgical complications, as well as thermographic, histological, and microvascular characterization of the different constructs. The ultimate goal of all these evaluations was to define an optimized model of AVF that could be easily replicated for research and teaching purposes.

METHODS

Fifty-three male rats weighing 250–350 g were used. Only male rats were used to prevent potential confounding effects of cyclical hormonal changes in female rats.[10] All the animals were housed under standard environmental conditions and given nothing by mouth 6 hours before surgical procedures. No antibiotic prophylaxis was given.

Rats were anesthetized with a mixture of ketamine (5 mg/kg) and diazepam (0.25 mg/kg) given intraperitoneally. The depth of anesthesia was evaluated by toe pinch and by observance of respiration rate throughout the entire procedure. Supplementary doses of the anesthetic mixture were provided as needed.[11]

After shaving the abdomen and placing the animals on the operation table, the skin was disinfected with an antiseptic solution (Cutasept, Hartmann, Heidenheim, Germany). Hypothermia was avoided by placing the rat over a heating pad for the duration of the surgery.

Under a surgical operating microscope, a 5-cm-long and 3-cm-wide fasciocutaneous flap was raised on the left side of the rat's abdomen immediately deep to the panniculus carnosus layer (Fig. 1). This flap was initially pedicled on the superficial caudal vessels caudally and on the lateral thoracic vein cranially. All other vessels were carefully ligated.[9,11]

Rats were then randomly assigned to the following groups (Fig. 2):

In group I (n = 12), a conventional perfusion flap (CPF) was raised as described above.

In groups II, III, and IV, the superficial epigastric artery was ligated with an 8/0 nylon suture. In these groups, AVFs were created using the following arterial venous anastomosis (AVA) at the caudal end of the flap:

In group II (n = 13), a 1-mm-long side-to-side anastomosis was performed between the femoral artery and vein laterally to the ending of the superficial caudal epigastric vein (SCEV) in the femoral vein. The AVA was performed after making a 1-mm-long ostium in adjacent flanks of the femoral artery and vein. A monofilament nylon 11/0–interrupted suture was used for the vascular anastomosis.[12]

In group III (n = 14), in addition to the procedure described for group II, the femoral vein was ligated immediately medial to the ending of the SCEV, to increase blood flow through the AVA.

Finally, in group IV (n = 14), the SCEV was cut from the femoral vein with a 1-mm-long ellipse of adjacent femoral vein tissue. The ostium in the femoral vein was closed with a monofilament nylon 11/0 continuous suture. The same suture line was used to perform a side-to-end AVA between the SCEV and the ventral flank of the femoral artery through a 1-mm-long ostium previously created in the latter vessel. Interrupted stitches were used for this anastomosis.

Surgical wounds were closed with 5/0 nylon stitches. No anticoagulants were administered pre-, intra-, or postoperatively.

After surgery, rats were kept in solitary rat cages and offered rat chow and water ad libitum.

Seven days after the surgery, rats were anesthetized as described above and AVA patency was noted. Only animals with patent AVAs were included in the study.

All surgical procedures were performed under aseptic conditions by the same microsurgeon (D.C.), to minimize intersurgeon variability. The operative time was registered in all animals by a blinded observer.

One hour postoperatively, 2 rats in each group were submitted to infrared thermography with a FLIR E6 camera (FLIR Systems, Wilsonville, Or.) placed 25 cm above the abdomen. Rats were placed on their backs for 10 minutes before this evaluation. Thermographic measurements were made at a constant room temperature (22 ± 0.05°C) and humidity (50%).[13]

Rats were assessed daily by the same researcher, to reduce interobserver bias and variability.[8] The following parameters were evaluated: animal wellbeing, flap viability, flap ischemia, and presence of complications. Objective measurement of flap survival was performed on the third and seventh days postoperatively based on digital photographs, which were later analyzed by a blinded observer using the free Image J software (National Institutes of Health, Bethesda, Md.).[11] AVF survival was expressed as a percentage of the total flap surface area.[14]

Half of the rats in each group were prepared for conventional histological examination, whereas the other half was submitted to processing to obtain vascular corrosion casts for scanning electron microscopy (SEM) evaluation. For histological processing, rats were submitted to axial sections in the caudal, middle, and cranial aspect of the AVF that were later stained using hematoxylin–eosin and Masson's trichrome. These rats were euthanized by exsanguination after dividing the neck vessels under sedation.

The rats destined to SEM analysis were submitted to intravascular injection of a resin cast (Mercox, Ladd Research, Williston, Vt.) and latter processed.[15] SEM images were obtained using a JEOL JSM-7001F with an acceleration voltage of 2–30 kV. Vascular cast interpretation of microvascular findings was made according to Aharinejad and Lametschwandtner.[15] These rats were euthanized by exsanguination after left and right ventricular catheterization.

All in vivo studies involving rats were carried out in strict accordance with the recommendations in the Guide for Proper Conduct of Animal Experiments and Related Activities in Academic Research and Technology.[16]

The protocol was approved by the Institutional Animal Care and Use Committee and Ethical Committee at the authors' institution (CEFCM/08/2012).

Statistical Analysis

Qualitative variables were expressed as percentages. Quantitative variables were expressed as means ± SD. IBM SPSS Version 21.0 software (Armonk, N.Y.) was used for descriptive and inferential statistical analysis. The Kolmogorov-

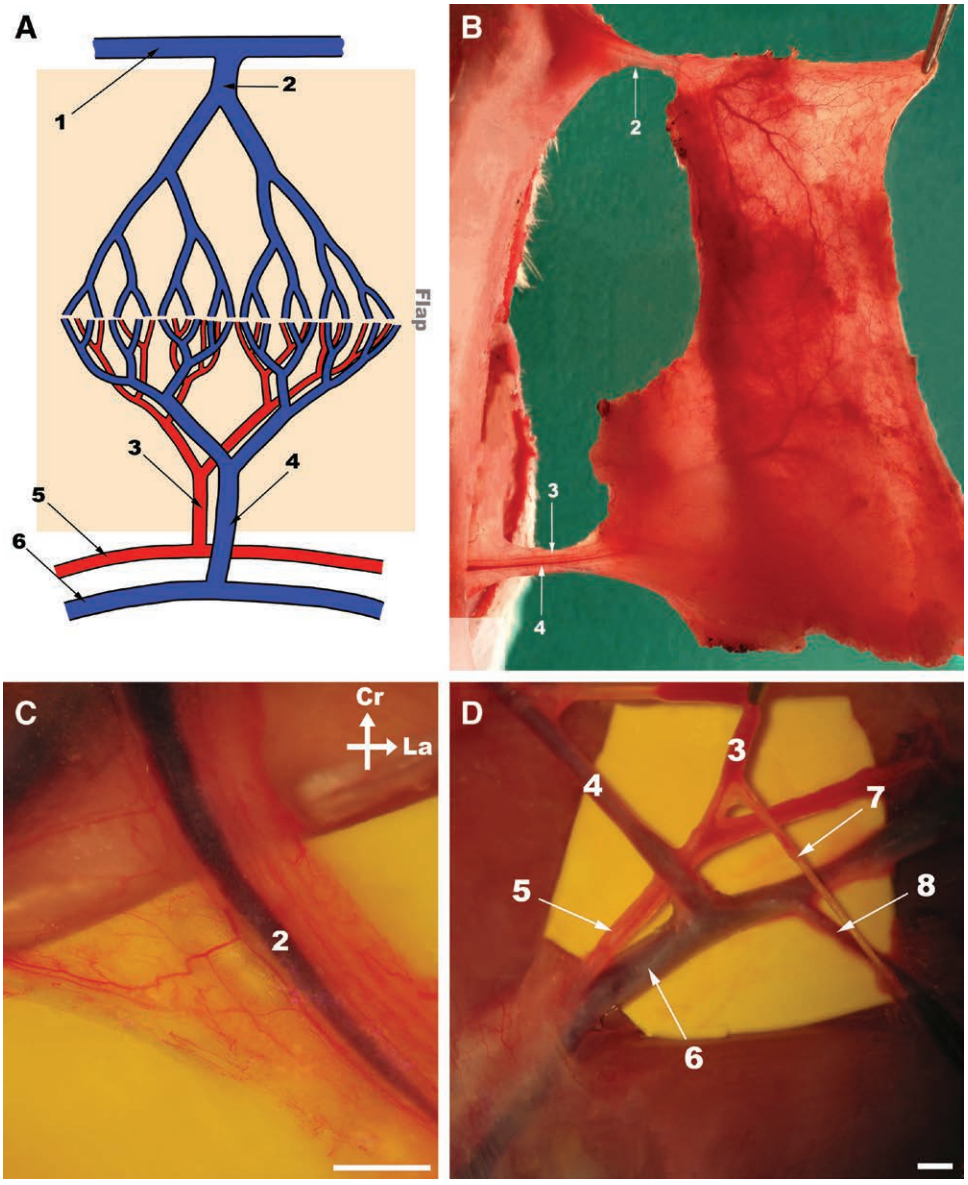

Fig. 1. Epigastric flap surgical anatomy. A, Schematic drawing of the blood supply to the rat's epigastric flap. The shaded area represents the flap. B, Photograph under transillumination of the flap's deeps surface raised on the left side of the abdomen showing its largest vessels. C, High amplification photograph of the lateral thoracic vein before being dissected from the surrounding loose areolar tissue. D, Photograph showing the origin of the superficial caudal epigastric vessels from the femoral vessels. Cr, cranial; La, lateral; 1, axillary vein; 2, lateral thoracic vein; 3, superficial caudal epigastric artery; 4, SCEV; 5, femoral artery; 6, femoral vein; 7, superficial external pudendal artery; 8, superficial external pudendal vein. Calibration bar = 1 mm.

Smirnov test was used to assess whether variables were distributed normally. Analysis of variance and *t* test were used to compare averages in normally distributed data. Kruskal-Wallis and Mann-Whitney tests were used to compare means in nonnormally distributed data. Proportions were analyzed with the chi-square test or Fisher's exact test. Kaplan Meier survival analysis was performed to identify differences in mortality between groups.

A 2-tail value of $P < 0.05$ was considered to be statistically significant.

RESULTS

Contrarily to CPFs (group I), all AVFs presented venous congestion, marked edema, epidermolysis, and areas of necrosis (**see figure,** Supplemental Digital Content 1, which shows representative photographs of CPFs and AVFs from the end of surgery to the seventh postoperative day, ***http://links.lww.com/PRSGO/A494***).

Most of the necrotic areas were clearly defined on the third day after surgery (Fig. 3; **see figures, Supplemental Digital Content 1**, ***http://links.lww.com/PRSGO/A494***

and Supplemental Digital Content 2, which shows box plot graphics illustrating flap survival in the different experimental groups 3 days postoperatively. Horizontal lines over boxplots indicate statistically significant differences, ***http://links.lww.com/PRSGO/A495***). On this day, the percentage of flap survival was 99.16±1.46, 71.48±7.80, 68.01±12.39, and 83.21±11.36 for groups I, II, III, and IV, respectively. Seven days postoperatively, the percentage of flap survival in these groups was 98.89±1.69, 68.84±7.36, 63.84±10.38, 76.86±13.67. Necrotic areas were more extensive in the caudal third of the flap (**Supplemental Digital Content 1**, ***http://links.lww.com/PRSGO/A494***). Flap survival was higher in the CPF group than in any of the AVF groups ($P < 0.01$). Among AVFs, group IV presented a higher flap survival than groups II and III ($P < 0.05$). There were no statistically significant differences between groups II and III.

Average operating time was increasing longer in groups I, II, III, and IV (Table 1; $P < 0.0001$). On average, it took twice the time to produce a group IV AVF compared with a CPF (group I).

There were no statistically significant differences in rat mortality rates among the different groups (Table 1).

The most common complication was hematoma, which occurred in 8.3%, 23.1%, 21.4%, and 14.3% of cases of groups I, II, III, and IV, respectively. Five rats (35.7%) in group III developed venous congestion and a swollen left hind limb. Four of these rats died within the first 48 hours after surgery. At the end of the experiment, surgical inspection of the AVA revealed an aneurysm in 1 of the rats in group III and thrombosis in 1 of the rats in group IV. No infections were noted. Overall, complications were more common in group III, although this difference was not statistically significant.

Thermographic evaluation revealed that all flaps, including CPFs, presented a lower temperature than the contralateral nonoperated region (Fig. 4). However, the temperature difference was higher in the AVFs, being of at least of 2°C in these flaps. In all AVFs, temperature was lower in the caudal third of the flap. No significant difference was found among the different AVF groups.

Histological and SEM evaluation of vascular corrosion casts revealed great morphological homogeneity among the different AVFs (**see figure,** Supplemental Digital Content 3, which displays a comparison of the histological features of AVFs compared with the CPFs controls, ***http://links.lww.com/PRSGO/A496***; **see figure,** Supplemental Digital Content 4, which displays a comparison of the microvasculature of the conventional flap and the AVF using scanning electron microscope images of vascular corrosion casts, ***http://links.lww.com/PRSGO/A497***). In fact, the authors were not able to identify distinctive morphological patterns for any of the AVFs groups, based on qualitative and/or quantitative features. Nevertheless, from a histological standpoint, comparatively to CPFs, AVFs presented greater flap edema, epidermolysis, loss of skin appendages, venous congestion and rupture, subcutaneous hematoma, and necrosis. In AVFs, there were regions of necrosis scattered throughout all integumentary layers. These histological features were more prominent in sections taken from the caudal third of AVFs. Moreover, all AVFs presented signs of SCEV arterialization and significant increment of the lumen diameter of the lateral thoracic vein (**Supplemental Digital Content 3**, ***http://links.lww.com/PRSGO/A496***).

The study of the microvasculature through SEM vascular corrosion casts revealed higher vascular density in AVFs. In addition, these flaps also presented loss of venular valves and/or venous valve incompetency particularly in the caudal half of the flap. Signs of sprouting angiogenesis were present in both CPFs and AVFs, although more markedly in the latter group. In AVFs, capillary vessels sprouted more commonly from venules, whereas in CPFs, new capillary vessels sprouted mostly from neighboring capillaries. In AVFs, it was also frequent to find evidence of intussusceptive angiogenesis (**Supplemental Digital Content 4**, ***http://links.lww.com/PRSGO/A497***).

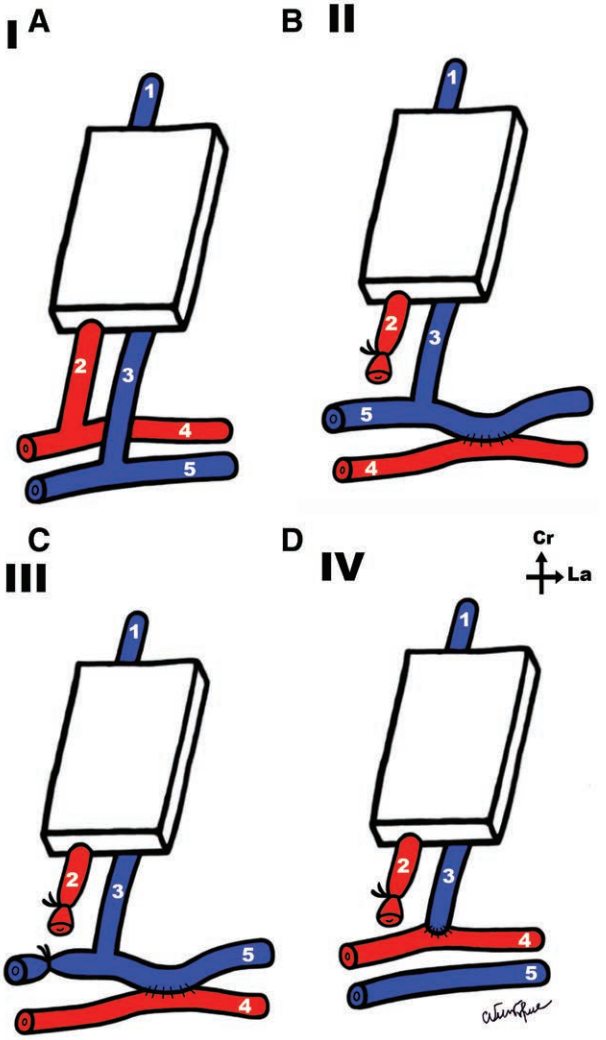

Fig. 2. A,B,C,D, Schematic representation of the vascular patterns in the different experimental groups. A, Group I (CPF). B, Group II (AVF produced by femoral side-to-side anastomosis). C, Group III (AVF produced by femoral side-to-side anastomosis and proximal ligation of the femoral vein). D, Group IV (AVF produced by terminal-lateral anastomosis of the epigastric vein to the femoral artery). Cr, cranial; La, lateral.

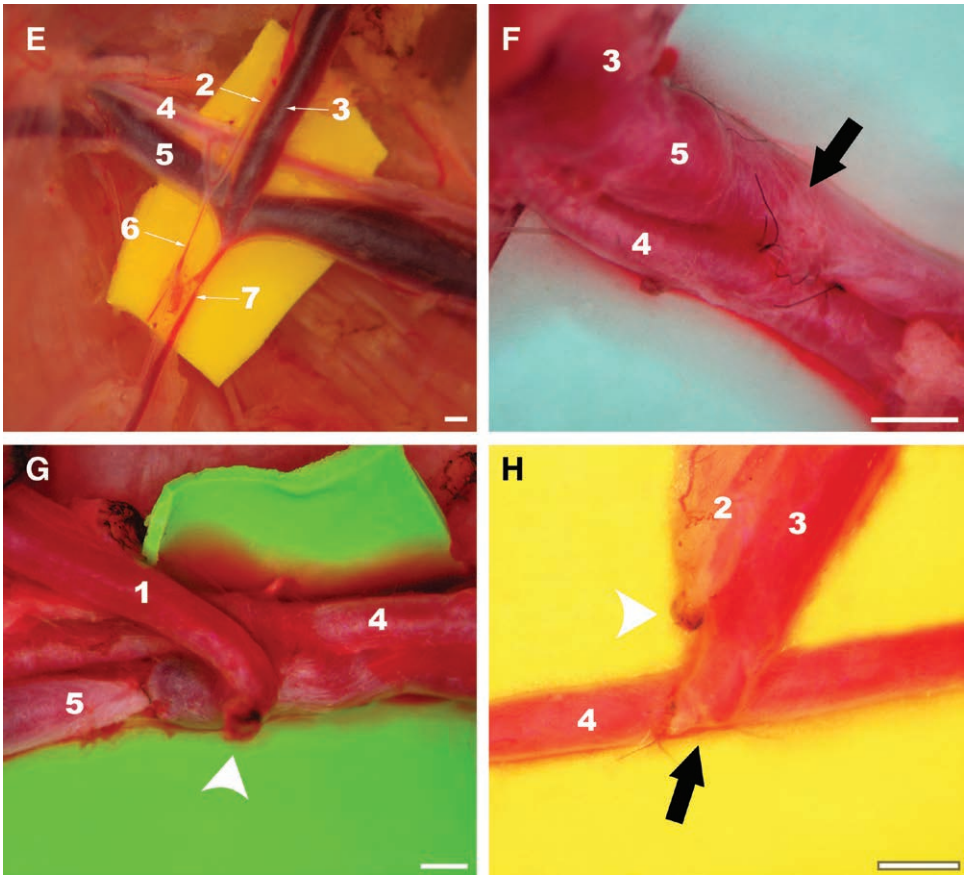

Fig. 2. *(Continued)*. E, F, G, H, Surgical operating view of the inflow vessels of the flap in groups I, II, III, and IV, respectively. Arrows indicate place of arteriovenous anastomosis. Arrow heads indicate vessel ligation. Calibration bar = 1 mm.

DISCUSSION

Average flap survival area of the best AVF model in this work (group IV) was 76.86±13.67%. This value is slightly inferior to that reported on a recent systematic review and meta-analysis on the clinical application of AVFs. In fact, it was estimated that the survival area of unconventional perfusion flaps used in the clinical context varies between 87.30% and 91.30% ($P<0.001$).[3] However, as the cited authors mention, this estimation may be affected by several biasses associated with any meta-analysis, namely publication bias, which tend to overestimate positive outcomes.[3]

AVF survival in the present work was worse than that described in the early description of Nakayama et al.[2] These authors described a mean area of survival of 98% in nondelayed AVFs. However, they left a superior skin pedicle that no doubt contributed arterial axial and random perfusion to the flap.[2] Nevertheless, the results herein presented concerning AVF survival are similar to those reported by other authors in the rat.[17–20]

The impact of different anastomotic layouts in flap survival had already been tested in CPFs.[21,22] In these flaps, it was shown that side-to-end and end-to-end arterial anastomoses of similarly sized arteries guaranteed comparable survivals.[21] However, as far as the authors could determine, this is the first time that the impact of microvascular anastomotic type on the survival of AVFs is studied. In the present work, the vascular layout used in group IV (side-to-end AVA) proved to be superior regarding AVF survival than that used in groups II and III (side-to-side AVAs). Many authors have used side-to-side AVAs of the femoral rats to obtain AVFs of the rat's abdomen. In this way, they avoid the technical challenging AVAs of very small vessels such as the SCEV and the homonymous artery, which are considerably prone to thrombosis.[12] Moreover, Nakayama et al.[2] had already demonstrated in a pilot study that direct end-to-end AVA of the femoral artery and SCEV was associated with significant hemodynamic disturbance and death of 13 of 15 rats.

The data herein presented suggest that the incorporation of a 1-mm-ellipse of the femoral vein adjacent to the draining point of the SCEV (group IV) allows a safe AVA. This pattern probably ensures a more direct blood flow into the SCEV and thus greater venous valves' incompetency, in comparison with AVAs in groups II and III. Furthermore, it is reasonable to expect that after removing the vascular clamps, the AVA in group IV is pulled by the distension of walls of the femoral artery, resulting in radial distraction of the SCEV. This, in turn, will further lead to venous valve incompetency in the later vessel, thus facilitating the entry of blood through the afferent vein of the group IV AVF.

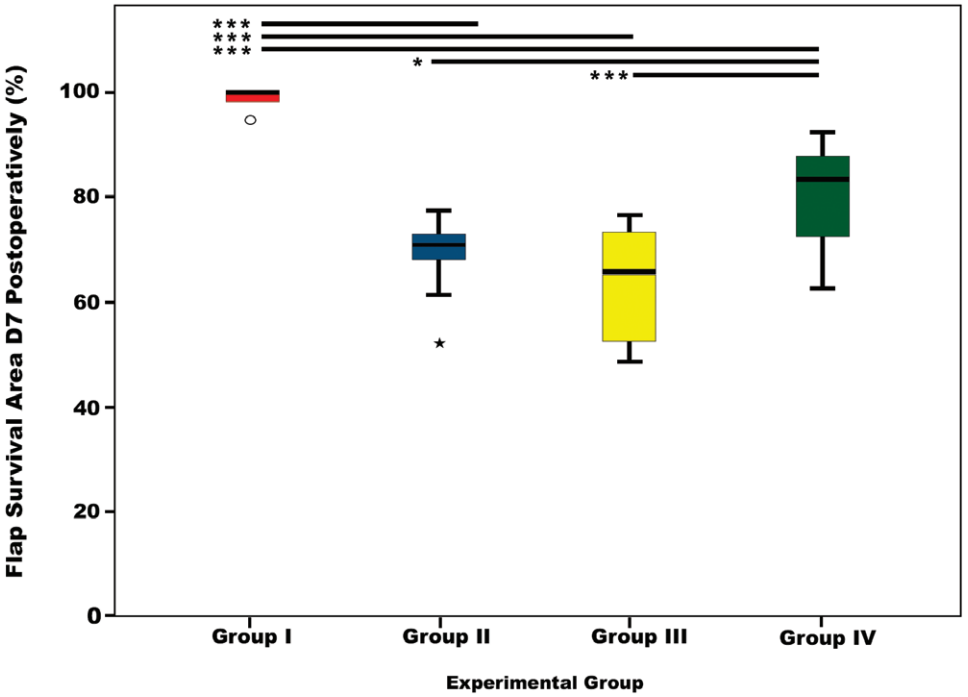

Fig. 3. Box plots graphics illustrating flap survival in the different experimental groups 7 days postoperatively. Horizontal lines over boxplots indicate statistically significant differences. *$P < 0.05$; **$P < 0.01$; ***$P < 0.001$.

Table 1. Comparison of the Different Vascular Constructs for Producing Arterialized Venous Fasciocutaneous Epigastric Flaps in the Rat

Assessed Parameters	Group I, CPF (n = 12)	Group II, AVF Produced by Side-to-Side Anastomosis (n = 13)	Group III AVF Produced by Side-to-Side Anastomosis and Femoral Vein Ligation (n = 14)	Group IV, AVF Produced by Terminal-Lateral Anastomosis (n = 14)	Statistically Significant Differences
Average operating time (min)	43.0 ± 5.4	72.2 ± 10.0	75.1 ± 9.4	89.9 ± 10.1	I < II < III < IV ($P < 0.0001$)
Rat mortality (%)	16.7	23.1	28.6	21.4	None
Surgical complications (%)					
Arteriovenous anastomosis thrombosis	0	0	0	7.1	None
Arteriovenous anastomosis aneurysm	0	0	7.1	0	None
Hematoma	8.3	23.1	21.4	14.3	None
Hind limb ischemia	0	0	35.7	0	Larger in group III ($P = 0.002$)
Complications other than necrosis	8.3	23.1	42.8	21.4	None
Technical difficulty	Easy	Moderate	Moderate	Challenging	N/A

A 2-tail value of $P < 0.05$ was considered to be statistically significant.
N/A, not applicable.

Interestingly, mathematical modeling using Laplace's law has suggested that the fine structure of venules under 100 μm in diameter renders the valves in these vessels readily incompetent in the presence of venous arterialization of ischemic lower limbs in humans.[23] Our SEM data give empirical support to this assertion in the rat model, as in all AVFs groups there were signs of loss valve competency particularly in venules located in the afferent half of the flap (**Supplemental Digital Content 4**, ***http://links.lww.com/PRSGO/A497***). Similar findings have been reported by other authors.[12]

Multiple examples of intussusceptive angiogenesis in the vascular molds of AVFs were observed in the present study. These may be justified by the fact that increases in blood pressure inside small vessels have been shown to be associated with transluminal tissue pillar formation and subsequent vascular splitting and neovessel formation.[24] This mechanism has been largely neglected in the literature and may have a pivotal role in AVF hemodynamic adaptation.[12]

To the best of the authors' knowledge, thermography imaging had never been employed before to study

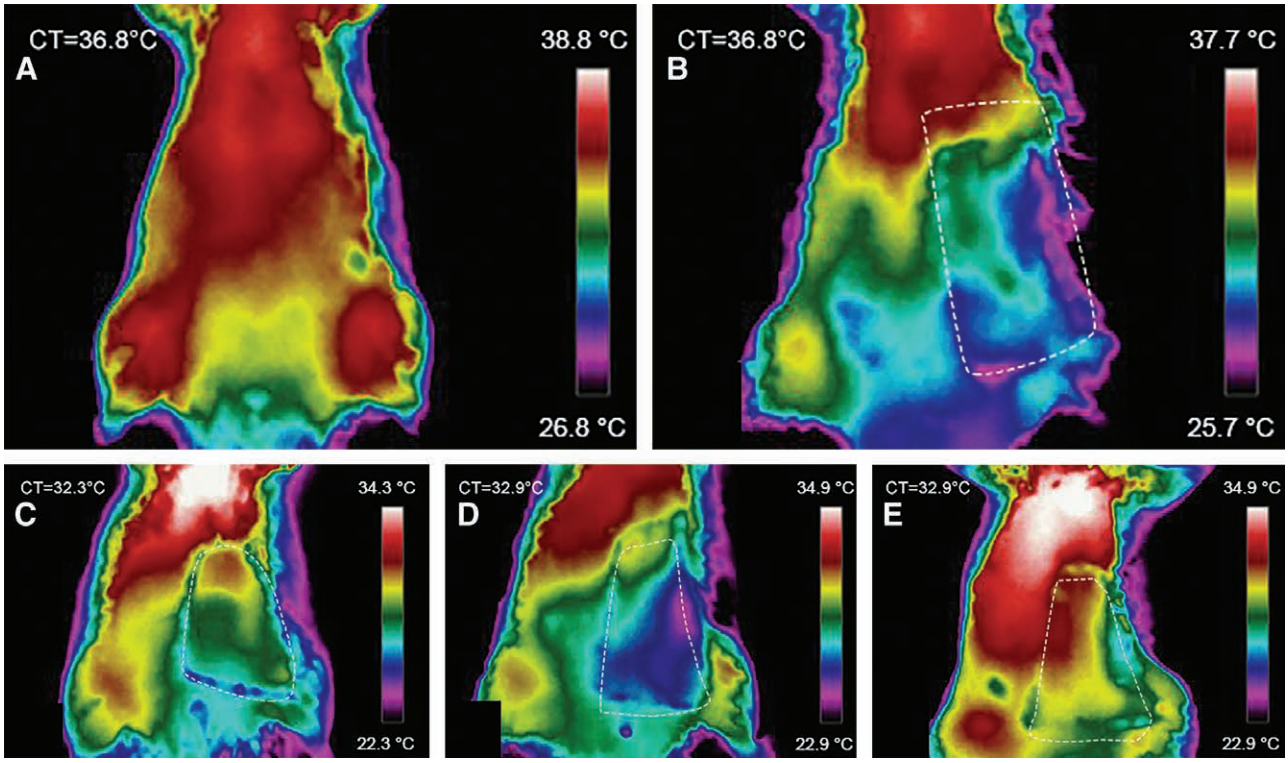

Fig. 4. Representative direct infrared thermography images of the ventrolateral aspect of the abdomen of the rat 1 hour postoperatively. Flap boundaries are highlighted with the interrupted lines. A, Rats before surgery. This image shows the location of the dominant perforator vessels in the central and cranial aspect of the abdomen. B, Group I (conventional flap). C, Group II (AVF produced by femoral lateral-lateral anastomosis). D, Group III (AVF produced by femoral latero-lateral anastomosis and proximal ligation of the femoral vein). E, Group IV (AVF produced by terminal-lateral anastomosis of the epigastric vein to the femoral artery). CT, rat core temperature.

perfusion of AVFs. Notwithstanding, skin temperature has been used as surrogate marker of perfusion in hind limb vein arterialization in rats. The rationale for this is that skin temperature is proportional to integumentary perfusion.[25] Our study lends support to the use of infrared thermography imaging for AVF perfusion evaluation, because it confirmed an inferior temperature in these flaps comparatively to CPFs and to the contralateral side of the abdomen. Additionally, in all AVFs, temperature was lower in the caudal third of the flap, where necrosis was more commonly found.

Recently, it has been shown that this region of the abdomen of the rat can be used to produce axial flaps simulating arterial ischemia or venous congestion, readily observed macroscopically by a pale and dark violet color, respectively.[14] Remarkably, in the present study, all AVFs groups presented a dark bluish color suggestive of venous congestion (**Supplemental Digital Content 1**, ***http://links.lww.com/PRSGO/A494***). Another common finding in these 2 studies was that necrotic areas were clearly defined in both CPFs and AVFs on the third postoperative day.[14] This information may be of great interest for future research works using similar flaps in this region of the rat.

Rats were chosen in the present study because they have been the most widely used animal model in the realm of experimental flap surgery.[26] This is certainly due to the fact they are readily available in most countries, they are easy to keep, and they are among the cheapest animals to obtain and to maintain.[26] Nonetheless, it should be noted that AVFs performed in humans are usually based on vessels of a larger caliber.[3] Hence, extrapolation of data obtained with the AVFs used in this article to humans must be done with this limitation in mind. In fact, it would be interesting to study the various vascular constructions described in these articles in other animal species, where larger flaps could be produced.

Furthermore, it is well known that in loose-skinned animals, the well-developed panniculus carnosus in the deep aspect of the integument leads to significant contraction of wounds and flaps.[27] To tackle this problem, multiple strategies have been devised, namely choosing anatomical sites where the integument is firmly adherent to the deep structures (e.g., rabbit ear) or using various devices or splints to fixate the integumentary layer and the surgical flaps.[27] Despite these limitations, in plastic surgery experimental research, it is customary to consider flap's survival and necrosis as a percentage of flap's total area, as the authors did in the present article.[9,11,14,26] However, this difference in flap and wound behavior between rodents and humans should be taken into consideration when generalizing the data presented in this article to the clinical scenario.

Finally, the authors believe that the AVFs in group IV represent an optimized model of unconventional perfu-

sion flap that can be easily replicated for research and teaching purposes. However, further studies are warranted to confirm or dismiss their usefulness in these contexts.

CONCLUSIONS

An optimized AVF can be reliably produced in the ventrolateral aspect of the abdomen of the rat by performing an end-to-side AVA between the femoral artery and the SCEV including the adjacent portion of the femoral vein, to produce a 1-mm-wide afferent vein. This model presented an average flap survival area of 76.86% ± 13.67%.

Diogo Casal, MD
Anatomy Department
NOVA Medical School
Campo dos Mártires da Pátria, 130
1169-056, Lisbon
Portugal
E-mail: diogo_bogalhao@yahoo.co.uk

ACKNOWLEDGMENTS

The authors are very grateful to Mr. Carlos Lopes and Mr. Octávio Chaveiro for their help in producing and observing the scanning electron microscope specimens. The authors also thank Mr. Nuno Folque for producing all the drawings contained in this article.

REFERENCES

1. Vaubel, W. Indikationen und Technik des arterialisierten Lappens zur Deckung großer Defekte im Handbereich. *Hefte Unfallheilkd.* 1975;126:381.
2. Nakayama Y, Soeda S, Kasai Y. Flaps nourished by arterial inflow through the venous system: an experimental investigation. *Plast Reconstr Surg.* 1981;67:328–334.
3. Casal D, Cunha T, Pais D, et al. Systematic review and meta-analysis of unconventional perfusion flaps in clinical practice. *Plast Reconstr Surg.* 2016;138:459–479.
4. Goldschlager R, Rozen WM, Ting JW, et al. The nomenclature of venous flow-through flaps: updated classification and review of the literature. *Microsurgery.* 2012;32:497–501.
5. Yan H, Brooks D, Ladner R, et al. Arterialized venous flaps: a review of the literature. *Microsurgery.* 2010;30:472–478.
6. Yan H, Zhang F, Akdemir O, et al. Clinical applications of venous flaps in the reconstruction of hands and fingers. *Arch Orthop Trauma Surg.* 2011;131:65–74.
7. Yan H, Fan C, Zhang F, et al. Reconstruction of large dorsal digital defects with arterialized venous flaps: our experience and comprehensive review of literature. *Ann Plast Surg.* 2013;70:666–671.
8. Weng W, Zhang F, Zhao B, et al. The complicated role of venous drainage on the survival of arterialized venous flaps. *Oncotarget.* 2017;8:16414–16420.
9. Hirase Y. Skin and muscle flaps in the rat. In: Tamai S, Usui M, Yoshizu T, eds. *Experimental and Clinical Reconstructive Microsurgery.* Vol. 1, 1st ed. Japan: Springer-Verlag; 2004:111–114.
10. Thatte M, Healy C, McGrouther D. Laser Doppler and microvascular pulsed Doppler studies of the physiology of venous flaps. *Eur J Plast Surg.* 1993;16:134–138.
11. Casal D, Pais D, Iria I, et al. A model of free tissue transfer: the rat epigastric free flap. *J Vis Exp.* 2017;1:e55281.
12. Wungcharoen B, Pradidarcheep W, Santidhananon Y, et al. Prearterialisation of the arterialised venous flap: an experimental study in the rat. *Br J Plast Surg.* 2001;54:621–630.
13. Sheena Y, Jennison T, Hardwicke JT, et al. Detection of perforators using thermal imaging. *Plast Reconstr Surg.* 2013;132:1603–1610.
14. Matsumoto NM, Aoki M, Nakao J, et al. Experimental rat skin flap model that distinguishes between venous congestion and arterial ischemia: the reverse U-shaped bipedicled superficial inferior epigastric artery and venous system flap. *Plast Reconstr Surg.* 2017;139:79e–84e.
15. Aharinejad SH, Lametschwandtner A. Identification and interpretation of cast vessel structures. In: Aharinejad SH, Lametschwandtner A, eds. *Microvascular Corrosion Casting in Scanning Electron Microscopy: Tecnhiques and Applications.* 1st ed. New York, N.Y.: Springer-Verlag; 1992:103–115.
16. National Research Council (U.S.). Committee for the update of the guide for the care and use of laboratory animals., Institute for Laboratory Animal Research (U.S.), National Academies Press (U.S.). *Guide for the Care and Use of Laboratory Animals.* 8th ed. Washington, D.C.: National Academies Press; 2011:xxv:220.
17. Başer NT, Silistreli OK, Sişman N, et al. Effects of surgical or chemical delaying procedures on the survival of proximal pedicled venous island flaps: an experimental study in rats. *Scand J Plast Reconstr Surg Hand Surg.* 2005;39:197–203.
18. Chow SP, Chen DZ, Gu YD. A comparison of arterial and venous flaps. *J Hand Surg Br.* 1992;17:359–364.
19. Miles DA, Crosby NL, Clapson JB. The role of the venous system in the abdominal flap of the rat. *Plast Reconstr Surg.* 1997;99:2030–2033.
20. Mutaf M, Tasaki Y, Fujii T. Expansion of venous flaps: an experimental study in rats. *Br J Plast Surg.* 1998;51:393–401.
21. Miyamoto S, Takushima A, Okazaki M, et al. Relationship between microvascular arterial anastomotic type and area of free flap survival: comparison of end-to-end, end-to-side, and retrograde arterial anastomosis. *Plast Reconstr Surg.* 2008;121:1901–1908.
22. Parsa FD, Spira M. Evaluation of anastomotic techniques in the experimental transfer of free skin flaps. *Plast Reconstr Surg.* 1979;63:696–699.
23. Koyama T, Sugihara-Seki M, Sasajima T, et al. Venular valves and retrograde perfusion. In: Swartz HM, Harrison DK, Bruley DF, eds. *Oxygen Transport to Tissue XXXVI.* 1st ed. New York, N.Y.: Springer; 2014;1:317–323.
24. Makanya AN, Hlushchuk R, Djonov VG. Intussusceptive angiogenesis and its role in vascular morphogenesis, patterning, and remodeling. *Angiogenesis.* 2009;12:113–123.
25. Sasajima T, Kikuchi S, Ishikawa N, et al. Skin temperature in lower hind limb subjected to distal vein arterialization in rats. In: Swartz HM, Harrison DK, Bruley DF eds. *Oxygen Transport to Tissue XXXVI.* 1st ed. New York, N.Y.: Springer; 2014;1:361–368.
26. Dunn RM, Mancoll J. Flap models in the rat: a review and reappraisal. *Plast Reconstr Surg.* 1992;90:319–328.
27. Davidson JM, Yu F, Opalenik SR. Splinting strategies to overcome confounding wound contraction in experimental animal models. *Adv Wound Care (New Rochelle).* 2013;2:142–148.

APPENDIX 7

PLOS Pathogens

BD-2 and BD-3 increase skin flap survival in a rat model of ischemia and Pseudomonas aeruginosa infection in the presence of a foreign body

--Manuscript Draft--

Manuscript Number:	
Full Title:	BD-2 and BD-3 increase skin flap survival in a rat model of ischemia and Pseudomonas aeruginosa infection in the presence of a foreign body
Short Title:	BD-2 and BD-3 increase skin flap survival in a rat model of infection
Article Type:	Research Article
Section/Category:	Bacteriology
Keywords:	Surgical wound infection; Pseudomonas aeruginosa; Foreign body; β-defensins; Antimicrobial infection; Genetic transduction; Lentivirus; Bacterial infections; Innate immunity; Scanning electron microscopy; Bacterial load; Skin flap survival
Corresponding Author:	Diogo Casal, M.D. Universidade Nova de Lisboa Faculdade de Ciencias Medicas Lisbon, PORTUGAL
Corresponding Author's Institution:	Universidade Nova de Lisboa Faculdade de Ciencias Medicas
First Author:	Diogo Casal, M.D.
Order of Authors:	Diogo Casal, M.D.
	Ines Iria
	Jose Ramalho
	Sara Alves
	Eduarda Mota-Silva
	Luis Mascarenhas-Lemos
	Carlos Pontinha
	Maria Guadalupe-Cabral
	Jose Ferreira-Silva
	Mario Ferraz-Oliveira
	Valentina Vassilenko
	João Goyri-O'Neill
	Diogo Pais
	Paula Alexandra Videira
Abstract:	Pseudomonas aeruginosa is one of the major culprits of nosocomial infections, particularly of prosthetic material, due to its ability to produce biofilms, and to thrive in poorly perfused tissues. The main aim of this work was to study the usefulness of human β-defensins 2 (BD-2) and 3 (BD-3) in the treatment of infected ischemic skin flaps. We investigated the effect of transducing rat ischemic skin flaps with lentiviral vectors encoding human BD-2, BD-3, or both BD-2+BD-3, to increase flap survival in the context of a P. aeruginosa infection associated with a foreign body. The secondary endpoints assessed were: bacterial counts, and biofilm formation on the surface of the foreign body. Arterialized venous flaps of the left epigastric region of rats were intentionally infected by placing two catheters under the flap with 105 CFU of P. aeruginosa before the surgical wound was hermetically closed. Flap biopsies were performed 3 and 7 days post-operatively, and the specimens

	submitted to immunohistochemical analysis for BD-2 and BD-3, as well as bacterial quantification. Subsequently, the catheter segments were analyzed with scanning electron microscopy (SEM). Ischemia and infection development were successfully confirmed by thermography and bacterial counting. Flaps transduced with BD-2 and BD-3 showed a successful expression of these defensins and presented increased flap survival. Moreover, rats transduced with BD-3 presented a net reduction in the number of P. aeruginosa on the surface of the foreign body and lesser biofilm formation. Flap survival was better correlated with SEM findings on the surface of the foreign body than with other bacterial quantification methods. This study demonstrates for the first time a model of ischemic flaps with infection and the usefulness of human BD-2 and BD-3 lentiviral vectors to clear infection in this context. Defensin gene therapy may be a suitable approach to treat nosocomial surgical infections.
Suggested Reviewers:	Judith Raschig University Hospital Tuebingen, Tuebingen, Germany jan.wehkamp@med.uni-tuebingen.de Experience with antimicrobial peptides' biology and potential clinical applications.
	Gayle Gordillo, M.D., PhD Researcher and physician, Ohio State University gayle.gordillo@osumc.edu This author has published on the importance of biofilms in wound physiology.
	Michael Zasloff, MD, PhD Georgetown University School of Medicine, Washington, DC maz5@georgetown.edu This author has published extensively on defensin biology and potential clinical applications.
	Guillermo Ramos-Gallardo, M.D., PhD Vallarta Medical Center guiyermoramos@hotmail.com This author has published on the importance of biofilms in mammalian wounds.
Opposed Reviewers:	
Additional Information:	
Question	**Response**
Financial Disclosure Please describe all sources of funding that have supported your work. **This information is required for submission and will be published with your article, should it be accepted.** A complete funding statement should do the following: Include **grant numbers and the URLs** of any funder's website. Use the full name, not acronyms, of funding institutions, and use initials to identify authors who received the funding. **Describe the role** of any sponsors or funders in the study design, data collection and analysis, decision to publish, or preparation of the manuscript. If the funders had **no role** in any of the above, include this sentence at the end of your statement: "*The funders had no role*	One of the authors (DC) received a grant from “The Programme for Advanced Medical Education” sponsored by “Fundação Calouste Gulbenkian, Fundação Champalimaud, Ministério da Saúde and Fundação para a Ciência e Tecnologia, Portugal.” The authors have no financial or commercial interests to declare in relation to the content of this article.

in study design, data collection and analysis, decision to publish, or preparation of the manuscript." However, if the study was **unfunded**, please provide a statement that clearly indicates this, for example: "*The author(s) received no specific funding for this work*." * typeset	
Competing Interests You are responsible for recognizing and disclosing on behalf of all authors any competing interest that could be perceived to bias their work, acknowledging all financial support and any other relevant financial or non-financial competing interests. Do any authors of this manuscript have competing interests (as described in the PLOS Policy on Declaration and Evaluation of Competing Interests)? **If yes**, please provide details about any and all competing interests in the box below. Your response should begin with this statement: *I have read the journal's policy and the authors of this manuscript have the following competing interests:* **If no** authors have any competing interests to declare, please enter this statement in the box: "*The authors have declared that no competing interests exist*." * typeset	The authors have declared that no competing interests exist.
Data Availability PLOS journals require authors to make all data underlying the findings described in their manuscript fully available, without restriction and from the time of publication, with only rare exceptions to address legal and ethical concerns (see the PLOS Data Policy and FAQ for further details). When submitting a manuscript, authors must provide a Data Availability Statement that describes where the data	Yes - all data are fully available without restriction

underlying their manuscript can be found. Your answers to the following constitute your statement about data availability and will be included with the article in the event of publication. **Please note that simply stating 'data available on request from the author' is not acceptable.** ***If, however, your data are only available upon request from the author(s), you must answer "No" to the first question below, and explain your exceptional situation in the text box provided.*** Do the authors confirm that all data underlying the findings described in their manuscript are fully available without restriction?	
Please describe where your data may be found, writing in full sentences. **Your answers should be entered into the box below and will be published in the form you provide them, if your manuscript is accepted.** If you are copying our sample text below, please ensure you replace any instances of XXX with the appropriate details. If your data are all contained within the paper and/or Supporting Information files, please state this in your answer below. For example, "All relevant data are within the paper and its Supporting Information files." If your data are held or will be held in a public repository, include URLs, accession numbers or DOIs. For example, "All XXX files are available from the XXX database (accession number(s) XXX, XXX)." If this information will only be available after acceptance, please indicate this by ticking the box below. If neither of these applies but you are able to provide details of access elsewhere, with or without limitations, please do so in the box below. For example: "Data are available from the XXX Institutional Data Access / Ethics Committee for researchers who meet the criteria for access to confidential data." "Data are from the XXX study whose authors may be contacted at XXX." * typeset	All relevant data are within the paper and its Supporting Information files
Additional data availability information:	

Cover Letter

Dear Professor Grant McFadden

Editor-in-Chief of *PLOS Pathogens*,

We take the liberty of submitting the manuscript of an original research entitled “BD-2 and BD-3 increase skin flap survival in a rat model of ischemia and *Pseudomonas aeruginosa* infection in the presence of a foreign body” for publication in the ***PLOS Pathogens.***

It is well known that *Pseudomonas aeruginosa* is one of the major culprits of nosocomial infections, particularly of prosthetic material, due to its ability to produce biofilms, and to thrive in poorly perfused tissues. Moreover, it is frequently resistant to conventional antibiotics. Despite some papers suggesting the efficacy of two antimicrobial peptides [human beta defensins 2 (BD-2) and 3 (BD-3)] against *P. aeruginosa in vitro*, as far as we could determine, no studies have been performed *in vivo*.

Hence, the main aim of this work was to study the usefulness of transducing an ischemic skin flap in the rat with BD-2, BD-3, and BD-2 + BD-3, to increase skin flap survival in the context of a *P. aeruginosa* infection associated with a foreign body. The secondary endpoints assessed were: bacterial counts, and biofilm formation on the surface of the foreign body, as well as rat survival.

An arterialized venous flap of the left epigastric region of the rat measuring 5 X 3 cm was used to mimic local ischemia.[1] Under the flap two 1-cm long 14 gauge catheters were placed and 10^5 CFU of *P. aeruginosa* were inoculated. The surgical wound was hermetically closed.

Rats were followed for 7 days. Flap biopsies were performed on the 3 and 7 days post-operatively. Flap transduction was confirmed with Real-Time and immunohistochemical evaluation of BD-2 and BD-3 in flap biopsies. These biopsies also allowed bacterial quantification by culture and Real Time PCR. At the end of the experiment the catheter segments were quantitatively analyzed regarding the presence of bacteria resorting to scanning electron microscopy (SEM).

Interestingly, we observed that BD-2 and BD-3 transduction increased skin flap survival in our model. Moreover, rats transfected with BD-3 presented a net reduction in the number of *P. aeruginosa* on the surface of the foreign body and lesser biofilm formation. There was no impact on rat survival. Finally, flap survival was better correlated with SEM findings on the surface of the foreign body than with other bacterial quantification methods.

We believe that this study is particularly suited for publication in *PLOS Pathogens*, for the following reasons:

1- This is the **first description of transduction of BDs genes to treat a *P. aeruginosa* infection *in vivo***.[2]

2- It is also the **first time that the transduction of an antimicrobial peptide (AMP) is performed with the intent to treat an infection**

developing in a poorly perfused region, simulating local ischemia. These scenarios are frequent in the clinical setting, occurring after trauma, radiotherapy or in ischemic regions of the body, namely in the lower limbs of atherosclerotic and/or diabetic patients.

3- As far as we could determine, **this paper analyzes in detail for the first time in the literature the morphometric features of the bacteria on the surface of a foreign body and thoroughly compares them with the clinical evaluation of the overlying skin flap,** and with bacterial quantification using microbiological cultures of tissue biopsy, and Real-Time PCR.

4- The fact that the **groups treated with BDs presented less biofilm, suggest that *in vivo* these AMPs are able to prevent the formation of biofilms,** which are one of the most common and important causes of clinical persistent infection.[3, 4] This undoubtedly adds to the knowledge of BD physiology, as most papers in this field refer to the action of AMPs *in vitro*, not addressing the role of these substances *in vivo*.[5]

5- **The methodology employed in this paper appears to adequately mimic clinically relevant wounds and bacterial infections associated with foreign bodies and local ischemia**. This will certainly be of great use to other researchers who intend to study bacterial infections in these circumstances.

6- Finally, **this study raises many possibilities, that may boost similar works in the field**, namely for testing the superiority of other

vectors, and other AMPs, as well as the susceptibility of other bacteria species, particularly bacteria resistant to conventional antibiotics.

In summary, for all the reasons we have just alluded to, it is our firm conviction that this study contributes substantially to the advancement of bacterial infection treatment and pathogenesis. Hence, we strongly believe that this paper is of significant value and interest to the readership of ***PLOS Pathogens*** and thus deserves publication.

If you have any doubts or queries, please do not hesitate to contact us.

Thank you so much for your kind attention.

Lisbon, 4th September 2017

(The authors)

References

1. Casal D, Mota-Silva E, Pais D, Iria I, Videira PA, Tanganho D, et al. Optimization of an arterialized venous fasciocutaneous flap in the abdomen of the rat. PRS Global Open. 2017;in press.

2. Zasloff M. Antimicrobial peptides: do they have a future as therapeutics. In: Harder J, Schroder JM, editors. Antimicrobial peptides: role in human health and disease. First ed. London: Springer; 2016. p. 147-54.

3. Costerton JW, Stewart PS, Greenberg EP. Bacterial Biofilms: A Common Cause of Persistent Infections. Science. 1999;284(5418):1318-22. doi: 10.1126/science.284.5418.1318.

4. Barker JC, Khansa I, Gordillo GM. A Formidable Foe Is Sabotaging Your Results: What You Should Know about Biofilms and Wound Healing. Plastic and reconstructive surgery. 2017;139(5):1184e-94e. Epub 2017/04/27. doi: 10.1097/prs.0000000000003325. PubMed PMID: 28445380; PubMed Central PMCID: PMCPMC5407389.

5. Kostakioti M, Hadjifrangiskou M, Hultgren SJ. Bacterial biofilms: development, dispersal, and therapeutic strategies in the dawn of the postantibiotic era. Cold Spring Harb Perspect Med. 2013;3(4):a010306. doi: 10.1101/cshperspect.a010306. PubMed PMID: 23545571; PubMed Central PMCID: PMCPMC3683961.

Full title: BD-2 and BD-3 increase skin flap survival in a rat model of ischemia and *Pseudomonas aeruginosa* infection in the presence of a foreign body

Short title: BD-2 and BD-3 increase skin flap survival in a rat model of infection

Authors:

Diogo Casal[1-4 ¶ *], Inês Iria[3,4,#a,#b ¶], José S. Ramalho[4], Sara Alves[5], Eduarda Mota-Silva[6], Luís Mascarenhas-Lemos[1,5], Carlos Pontinha[1,5], Maria Guadalupe-Cabral[4], José Ferreira-Silva[5], Mário Ferraz-Oliveira[5], Valentina Vassilenko[6], João Goyri-O'Neill[1], Diogo Pais[1], Paula A. Videira[3,4]

Affiliations:

1- Anatomy Department, NOVA Medical School, Universidade NOVA de Lisboa, Lisbon, Portugal

2- Plastic and Reconstructive Surgery Department and Burn Unit, Centro Hospitalar de Lisboa Central – Hospital de São José, Lisbon, Portugal

3- UCIBIO, Departamento de Ciências da Vida, Faculdade de Ciências e Tecnologia, Universidade NOVA de Lisboa, Caparica, Portugal

4- CEDOC, NOVA Medical School, Faculdade de Ciências Médicas, Universidade NOVA de Lisboa, Lisbon, Portugal

5- Pathology Department, Centro Hospitalar de Lisboa Central – Hospital de São José, Lisbon, Portugal

6- LIBPhys, Physics Department, Faculdade de Ciências e Tecnologias, Universidade NOVA de Lisboa, Caparica, Portugal

#a- Molecular Microbiology and Biotechnology Unit, iMed, ULisboa, Faculty of Pharmacy, Universidade de Lisboa, Lisbon, Portugal

#b- INESC, MN – Microsystems and Nanotechnologies, Instituto Superior Técnico, Universidade de Lisboa, Lisbon, Portugal

* Corresponding authors

E-mail: diogo_bogalhao@yahoo.co.uk (DC)

p.videira@fct.unl.pt (PAV)

¶ These authors contributed equally to this work.

Abstract

Pseudomonas aeruginosa is one of the major culprits of nosocomial infections, particularly of prosthetic material, due to its ability to produce biofilms, and to thrive in poorly perfused tissues. The main aim of this work was to study the usefulness of human β-defensins 2 (BD-2) and 3 (BD-3) in the treatment of infected ischemic skin flaps. We investigated the effect of transducing rat ischemic skin flaps with lentiviral vectors encoding human BD-2, BD-3, or both BD-2+BD-3, to increase flap survival in the context of a *P. aeruginosa* infection associated with a foreign body. The secondary endpoints assessed were: bacterial counts, and biofilm formation on the surface of the foreign body.

Arterialized venous flaps of the left epigastric region of rats were intentionally infected by placing two catheters under the flap with 10^5 CFU of *P. aeruginosa* before the surgical wound was hermetically closed.

Flap biopsies were performed 3 and 7 days post-operatively, and the specimens submitted to immunohistochemical analysis for BD-2 and BD-3, as well as bacterial quantification. Subsequently, the catheter segments were analyzed with scanning electron microscopy (SEM).

Ischemia and infection development were successfully confirmed by thermography and bacterial counting. Flaps transduced with BD-2 and BD-3 showed a successful expression of these defensins and presented increased flap survival. Moreover, rats transduced with BD-3 presented a net reduction in the number of *P. aeruginosa* on the surface of the foreign body and lesser biofilm formation. Flap survival was better correlated with SEM findings on the surface of the foreign body than with other bacterial quantification methods.

This study demonstrates for the first time a model of ischemic flaps with infection and the usefulness of human BD-2 and BD-3 lentiviral vectors to clear infection in this context. Defensin gene therapy may be a suitable approach to treat nosocomial surgical infections.

Keywords: Surgical wound infection; *Pseudomonas aeruginosa*; Foreign body; β-defensins; Antimicrobial infection; Genetic transduction; Lentivirus; Bacterial infections; Innate immunity; Scanning electron microscopy; Bacterial load; Skin flap survival

Author Summary

Pseudomonas aeruginosa is responsible for many serious, antibiotic-resistant infections in hospital patients, particularly in those implanted with prosthetic material. Additionally, *P. aeruginosa* tend to adhere to surfaces forming biofilms, being particularly troublesome when local tissues are poorly perfused. It has been known that skin naturally produces and secretes antimicrobial peptides (AMPs) that continuously help fight off the multiple bacteria to which it is exposed.

In this work, we induced the expression of two AMPs, the human β-defensins 2 and 3 (BD-2 and BD-3), in an ischemic, *P. aeruginosa*-infected skin flap. Arterialized venous flaps of the epigastric region of the rat in which blood circulation was deficient were used. In the undersurface of these flaps, two foreign bodies were placed and a 1-ml solution of 10^5 CFU of *P. aeruginosa* was inoculated. Rats were followed for 7 days after surgery. Flaps showed persistent ischemia and infection, as demonstrated by thermography and bacterial counts.

Rats transduced with BD-2 and BD-3 presented better flap survival compared to controls. Additionally, BD-3 transduced flaps presented less bacteria and biofilms on the surface of the foreign bodies.

This work highlights the potential of human defensins as an alternative to conventional antibiotics to treat complex infections.

All relevant data are within the paper and its Supporting Information files.

Introduction

Multi-resistant bacteria are on the rise all over the world, leading many to proclaim an imminent post-antibiotic era, in which common infections and surgeries could become life threatening conditions.[1-3] For instance, several authors have shown that a leg ulcer lasting for one month will have on average at least one isolated multi-drug resistant organism at that time.[4] Hence, it comes as no surprise that multiple new strategies to tackle bacterial infections are actively being sought [1-3, 5] and alternatives to conventional antibiotics are direly needed.[6]

In this context, antimicrobial peptides (AMPs) become particularly appealing as a new way to target one of the last “Achilles’ heels” of bacteria.[5, 7-13] AMPs are small cationic peptides that have pleotropic bactericidal effects. They are divided in multiple chemical classes, of which the most studied and populated are the cathelicidins, the defensins, the histatins, and the dermcidins.[5] Defensins have been indicated as one of the most promising AMP classes for potential therapeutic used based on *in vitro* essays.[13-15] Defensins, similarly to other AMPs, act mainly by disrupting the structure of gram-positive and gram-negative bacterial cell membrane. These AMPs also inhibit bacterial DNA replication, transduction and translation, disturbing bacterial homeostasis (**Fig 1**). The resulting byproducts trigger the activation of the complement system and inflammatory processes that further help clearing bacterial infections (**Figs 1** and **2**).[7, 10, 16] Moreover, it has been shown that due to its peculiar action in the cell membrane, seldom are bacteria able to develop resistance to defensins.[5, 17, 18]

Defensins, of which 15 isoforms are currently identified in humans, are remarkably widely secreted in multiple epithelia, leucocytes and platelets (**Fig 2**).[14, 19, 20] Apart

from their role in the innate immunity, it has been recognized that they are instrumental in immune regulation and to initiate, mobilize, and amplify acquired immunity.[5]

Among the most commonly encountered multi-resistant bacteria, *Pseudomonas aeruginosa* stands out as one of the major culprits of nosocomial infections worldwide, being associated with significant morbidity, mortality, and increased health costs. *P. aeruginosa* frequently causes antibiotic-refractory infections of prosthetic material, due to its ability to produce biofilms, and to its intrinsic, acquired and adaptive resistance mechanisms to multiple antibiotics.[2, 21, 22] Noteworthy, *P. aeruginosa* is known to thrive in poorly perfused tissues, as in ischemic wounds or limbs, such as those of many diabetic patients, as well as in chronic wounds or around prosthetic material.[4, 6, 23, 24]

Although numerous AMPs have shown microbicidal activity against *P. aeruginosa in vitro* [16, 25-27], as far as the authors could determine, there are no studies using β-defensins (BDs) to treat *P. aeruginosa* infections in *in vivo* models.[26, 27] This is unfortunate, since BDs have shown to be efficient against multi-resistant *P. aeruginosa in vitro*.[26, 27] Moreover, amongst BDs, BD-2 has been shown to be particularly effective against Gram-negative bacteria and some fungi, although relatively less potent against Gram-positive bacteria. Furthermore, BD-3 is reportedly a powerful antimicrobial agent with a broad range of activity toward yeast, Gram-negative and Gram-positive bacteria, including the vancomycin-resistant *Enterococcus faecium*.[25, 26]

Despite these interesting *in vitro* results, there are several reports stating that defensins, being cationic, have hampered bactericidal activity *in vivo* due to the presence of neutralizing anionic compounds in living tissues.[26, 28, 29]

Hence, the main aim of this work was to study the usefulness of transducing an ischemic skin flap in the rat with two human BDs (BD-2 and BD-3) to increase skin flap survival in the context of a *P. aeruginosa* infection in the presence of a foreign body. The secondary endpoints assessed were: reduction in bacterial counts, reduction in biofilm formation, and increase in rat survival rates. Interestingly, we observed that BD-2 and BD-3 increased skin flap survival in our model. Moreover, rats transduced with BD-3 presented a net reduction in the number of *P. aeruginosa* on the surface of the foreign body and lesser biofilm formation.

Materials and Methods

Figs 3 and **4** summarize the experiments done in this work.

Bacterial growth.

All bacteria were inoculated in Luria-Bertani (LB) broth and grown at 37 °C on a rotary shaker at 250 rpm, overnight. Exceptions were performed and are properly indicated.

Plasmids production. Competent *Escherichia coli* DH5α were transformed by heat-shock with pMD2.G and psPAX vectors, while competent *E. coli* Stbl3 were transformed with pLenti6.BD-2 and pLenti6.BD-3. Posteriorly, bacteria were grown in LB media, at optimal temperature in ampicillin presence, at 37 and 30 °C, respectively.

***Pseudomonas aeruginosa* – infection model.** *P. aeruginosa* CECT 110^{+} strain, that was kindly provided by Professor Isabel Sá Correia (Instituto Superior Técnico, Lisbon, Portugal), was grown until the mid-exponential phase and it was serially diluted in 0.01 M PBS at a OD_{600nm} of 0.0001 corresponding at $1.0x10^5$ CFU/ml. At all times, to confirm the *P. aeruginosa* CFUs, spreadings of bacteria were performed in LB agar dishes and colonies were counted after overnight incubation at 37 °C.

Before performing the antimicrobials assays in the animal model of ischemia, tests were conducted to determine the ideal bacterial concentration. The concentrations initially used were: 10^3; 10^4; 10^5; 10^6 and 10^7 CFU/ml. We selected the concentration of 10^5

CFU/ml, since this concentration systematically resulted in clinically significant infection and partial flap necrosis in our model. Higher concentrations led to complete or nearly complete flap necrosis (10^6 CFU/ml; n=2) and animal's death (10^7 CFU/ml; n=3), whereas lower concentrations (10^3 and 10^4 CFU/ml; n=3 for each concentration) did not produce clinically recognizable infection.

Lentivirus preparation

The defensin beta 4A (*DEFB4A*) and defensin beta 103A (*DEFB103A*) cDNA sequences, which code for the BD-2 and BD-3 proteins, respectively, were synthetized by GenScript Corporation® (New Jersey, USA) and cloned into pcDNA ENTR BP, using *Xho*I/*EcoR*I (*DEFB4A*) and *Sal*I/*Kpn*I (*DEFB103A*). This expression vector was generated by inserting a polylinker, previously chemically synthetized, containing several restriction sites into pcDNA6.2GW/Em-GFP, a mammalian expression Gateway® (Invitrogen) previously digested with DraI/XhoI. The defensins coding sequences were transferred into pLenti6 (Invitrogen®) by LR recombination.[30]

Lentivirus particles were produced according to ViraPower™ Lentiviral Expression Systems (ThermoFisher®) recommendations, using HEK293 cells. Recombinant BD-2 and BD-3 expression in HEK293 was confirmed by RT-PCR. The total RNA of cells lines was extracted using the GenElute™ Mammalian Total RNA Miniprep Kit (Sigma-Aldrich®), according to the manufacturer's instructions. In order to remove any genomic DNA contamination, a RNase-Free DNase Set (Qiagen®) was used. The SuperScript® III First-Strand Synthesis System (Invitrogen™) was used to perform the reverse transcription, following the manufacturer's instructions. PCR amplification was performed

using primers for each gene *DEFB4A* (*sense* – ATGAGGGTCTTGTATCTCCT, *antisense* – TCATGGCTTTTTGCAGCATT), *DEFB103A* (*sense* – TCATGGCTTTTTGCAGCATT, *antisense* – TTATTTCTTTCTTCGGCAGC) and *HPRT1* (encoding HPRT (hypoxanthine phosphoribosyltransferase)) (sense – ATCACAT TGTAGCCCTCTGTGTGCTCAAGG, antisense – GTCTGGAATTTCAAATCCAACAAA GTCTGGC).

Ethics statement

All procedures involving animal subjects were approved by the Institutional Animal Care and Use Committee and Ethical Committee at our institution (08/2012/CEFCM). All *in vivo* studies involving rats were carried according or exceeding the recommendations in the Guide for Proper Conduct of Animal Experiments and Related Activities in Academic Research and Technology.[31]

Animals

One hundred and two male adult Wistar rats weighing 250 to 350 grams were used. All the animals were housed under standard environmental conditions and given nothing by mouth six hours before surgical procedures. No antibiotic prophylaxis was given.

Rats were anesthetized with a mixture of ketamine (5 mg/kg) and diazepam (0.25 mg/kg) given intraperitoneally. The depth of anesthesia was evaluated by toe pinch and by observance of respiration rate throughout the entire procedure.[32-35] Supplementary doses of the anesthetic mixture were provided throughout the surgical procedures as needed.[36] An ophthalmic gel was applied over the anterior surface of the eyes to avoid

corneal abrasion. The hair over the ventral surface of the abdomen was removed with a depilatory cream (Veet®). After hair removal, the depilatory cream was cleaned from the abdomen with warm saline. After shaving the abdomen and placing the animals on the operation table, body temperature was recorded with a rectal thermometer and the rats were kept on a heating pad (Skaldo, Ardes ™), in order to maintain a constant body temperature. A substantial amount of an alcoholic solution (Cutasept F®, Hartmann ™) was sprayed over the operative site. The product was left in the operative site for at least 15 seconds. Application was repeated 3 times. After the last application, the disinfectant solution was left in contact with the operating field for at least 2 min before proceeding with the surgery. All surgical procedures were performed in strict sterility conditions.

Surgical Model

Succinctly, a variant of the rat abdominal arterialized venous flap was used as model of ischemic flap (**Fig 4**).[37, 38] This flap was transduced with an *ex vivo* infusion of a 100 µl solution containing approximately $4.7x10^9$ plaque-forming-units of recombinant lentiviruses coding for Green Fluorescent Protein (GFP) or BD-2 and/or BD-3.[39, 40] This model was combined with an adapted version of the rat foreign body infection model (**Fig 3**).[41]

In all animals, under a surgical operating microscope, a 5 cm long and 3 cm wide fasciocutaneous flap was raised on the left side of the rat's abdomen.[38] Cranially, the flap was connected exclusively to the skeletonized lateral thoracic vein. This vein was temporarily clamped. Caudally, the superficial caudal epigastric artery was ligated with an 8/0 Nylon suture. The superficial caudal epigastric vein (SCEV) was cannulated with

a 27-gauge ophthalmic cannula (BD Bioscience™). It was then perfused with a 100-µl solution whose composition varied amongst the experimental groups (**Figs 3** and **4**). In all cases the solution contained 5 µg of recombinant rat Vascular Endothelial Growth Factor A (VEGF; Immunotools®) in DMEM, in order to increase transduction efficiency. [39] The composition of the solution injected in the flap's venous system was as follows: **NaCl Group** (VEGF); **PA Group** (VEGF); **GFP Group** (VEGF + GFP coding lentivirus); **BD-2 Group** (VEGF + BD-2 coding lentivirus); **BD-3 Group** (VEGF + BD-3 coding lentivirus); **BD-2 + BD-3 Group** (VEGF + BD-2 + BD-3 coding lentivirus) (**Fig 3**). After injection, SCEV was immediately clamped for 90 min, in order to leave the injected solution in contact with the flap's vascular system.[39]

Subsequently, vascular clamps were removed and the SCEV was arterialized by connecting it to the femoral artery. In order to achieve this, the SCEV was cut from the femoral vein with a 1-mm long cuff of adjacent femoral vein tissue. The ostium in the femoral vein was closed with a continuous Nylon 11/0 suture. The same suture line was used to perform a side-to-end arteriovenous anastomosis between the SCEV and the ventral flank of the femoral artery through a 1-mm long ostium previously created in the latter vessel. Interrupted stitches were used for this anastomosis. The lateral thoracic vein was preserved cranially to ensure outflow from this arterialized venous flap.[38]

Two 1-cm segments of sterile 14-gauge silicone catheters (Mediplus™) were placed in the central aspect of the surgical wound. Surgical wounds were closed with a running 5/0 Nylon suture. Just before closing the lateral aspect of the skin wound, 1-ml of a 0.9% sodium chloride solution was instilled under the flap into the vicinity of the silicone catheter segments using an 18-gauge silicone catheter (Mediplus™). In all groups except

the NaCl group, the latter solution contained 10^5 CFU of *P. aeruginosa*. The running suture was closed immediately after injection, in order to avoid any spilling to the area adjacent to the flap (**Fig 4**).

No anticoagulants were administered pre, intra or postoperatively. All surgical procedures were performed by the same surgeon (D.C.), in order to minimize inter-surgeon variability.

Thermography

One hour after flap reperfusion, the rat abdomen was submitted to infrared thermography with a FLIR® E6 camera placed 25 cm above the abdomen. This evaluation intended to confirm the flap's relative ischemia compared to the contralateral side. Rats were placed on their backs for 10 min prior to this evaluation. Thermographic measurements were made at a constant room temperature (22 ºC) and humidity (50%).[38, 42]

Post-operative care and assessment

After thermographic evaluation was completed, a transparent Tegaderm™ (3M Deustschland GmbH®) transparent film dressing was applied over the flap and adjacent skin. Following surgery, rats were kept in solitary rat cages and offered rat chow and water *ad libitum*.

Rats were assessed daily by the same blinded researcher, in order to reduce inter observer bias and variability.[43] The following parameters were evaluated: animal wellbeing, flap viability, and presence of complications.

On the third and seventh days postoperatively, rats were anesthetized as described above. Objective measurement of flap survival was performed on these days based on digital photographs, which were later analyzed by a blinded observer using the free Image J® software.[36, 44] Flap survival was expressed as a percentage of the total flap surface area.

After disinfecting the rat's abdomen as described above, on the third postoperative day, a sample measuring approximately 1 cm in length and 0.5 cm in width was surgically excised from the most lateral aspect of the caudal third of the viable flap. These specimens were subjected to histological analysis, as well as bacterial counts by both culture and real-time PCR. The integumentary defect created by the biopsy was submitted to hemostasis and closure with a continuous 5/0 Nylon suture taking part of the integumentary redundancy in this region. A transparent Tegaderm™ (3M Deustschland GmbH®) transparent film dressing was again applied over the flap and adjacent skin.

On the seventh day after the first surgery, the lateral aspect of the flap was elevated, thus exposing the underlying catheter segments. These were then carefully removed, taking care not to touch the rat's skin and immediately immersed in the fixative solution.

The flap was then removed for histological analysis, as well as bacterial counts by culture and real-time PCR.

Evaluation of flap transduction by fluorescence microscopy

Four rats were submitted to the procedures described above for the GFP group with the exception that no bacteria were instilled. Seven days after the surgery, the skin

flap was harvested, fresh-frozen and observed under the fluorescence microscope. Two rats were submitted to an analogous the procedure, but no lentiviruses were used to transduce the flaps in these animals.

Quantification of BD-2 and BD-3 expression by quantitative real-time PCR

Total RNA from flap biopsies weighing (45- 50 mg) collected on the 7th day postoperatively was extracted using the GenElute^{TM} Mammalian Total RNA Miniprep Kit (Sigma-Aldrich). The RNase-Free DNase Set (Qiagen®) was used to eliminate genomic DNA, according to the manufacturer's instructions. RNA concentrations were measured and only samples with A260/A280 ratios between 1.8 and 2.1 were considered further. Five hundred nanograms of total RNA was reverse transcribed with random primers using the High Capacity cDNA Reverse Transcription Kit (Applied Biosystems^{TM}), according to the manufacturer's instructions. Real-time PCR was performed in a Rotor-Gene 6000 (Corbett Life Science) using TaqMan® Fast Universal PCR Master Mix (Applied Biosystems^{TM}). The assay IDs were provided by the manufacturer, being the following: *β-actin* (4352931E); *DEFB4B* (Hs00175474_m1) and *DEFB103A* (Hs00218678_m1) (Applied Biosystems^{TM}). Each reaction was performed in triplicate. Thermal cycling conditions were 95 for 20 seconds followed by 55 cycles of 95 for 3 seconds and 60 for 30 seconds. The gene expression was normalized to the endogenous control β-actin, which is known to have significant basal expression.[45] Gene relative expression was calculated using the $2^{-\Delta CT}\times 1000$ formula, an adaptation of the $2^{-\Delta\Delta Ct}$ method described by Livak and Schmittgen.[46-48] This allows us to calculate the number of mRNA molecules of the gene of interest per 1000 molecules of the endogenous control (β-actin).

Viable bacterial cell counts

Biopsies were collected in sterility and cut in small pieces (between 0.05 and 0.10 mm of maximum diameter). Next, they were macerated in 0.9 %(w/v) NaCl (Merck®) at 100 mg/mL concentration for 5 min with a Pellet pestle (Sigma-Aldrich®). Serial dilutions were performed from the supernatant in 0.9 %(w/v) NaCl (between 10^{-1} and 10^{-5}) and were spread on LB dishes in duplicated. The dishes were incubated at 37 °C during 14 h followed by quantification of CFUs. The CFUs counted were verified by running a series of tests, namely, Gram stain (Merck®); MacConkey growth (Carl Roth®) and *Oxidase* test (BioMérieux®) according to the manufacturers' instructions.

P. aeruginosa quantification by real-time PCR

Biopsies were collected in sterility, were immediately immersed in RNAlater® (Sigma-Aldrich®), and incubated overnight at 4 °C. On the following day, the biopsies were cut in small pieces (between 0.05 and 0.10 mm) and stored at -80 °C.

Forty-five to 50 mg of excised tissue was used to extract genomic DNA by NZY Tissue gDNA Isolation Kit (Nzytech®) according to the manufacturer's instructions.

Universal primers were used for 16S rDNA: *forward* 5'-GTGSTGCAYGGYTGTCGTCA and *reverse* 5´-ACGTCRTCCMCACCTTCCTC [49], to quantify *P. aeruginosa*. The real-time PCR was performed using Applied Biosystems 7500 real-time PCR System (Thermo Fisher Scientific®). The reaction mixture (10 µl) contained 2x SYBR Green PCR Master Mix (Thermo Fisher Scientific®), 0.1 nmol/µl of *forward* and *reverse* primers each and 5 ng/µl of *P. aeruginosa* gDNA.

Thermo-cycling program was 40 cycles of 95 °C for 20 s, 60 °C for 30 s and 72 °C for 40 s with an initial cycle at 50 °C for 2 min and 95 °C for 10 min. Next, a dissociation curve was performed at 95°C for 15 s and a range between 60 to 95 °C.

Histological processing

Flap biopsies were collected from the lateral aspect of the surgical flap of the rat 3 and 7 days postoperatively, as described above. Specimens were incubated in 10% (v/v) Formalin. After paraffinization (VWR®), specimens were cut on the microtome (Leica®) as 3 µm thick slices. These slices were stained with Hematoxylin-Eosin (HE) and Masson's Trichrome (MT), according to the manufacturers' indications.[50, 51] For immunohistochemical staining with anti-BD-2 and -BD-3, slices were obtained in the same manner, although for this purpose slices were 4 µm thick.

Immunohistochemistry processing for BD-2 and BD-3. Imunohistochemistry was performed by BenchMark ULTRA - Automated IHC/ISH slide staining system (Ventana®, Roche®). Summarily, the slides were heated at 80 °C for 15 min, deparaffinized with EZ prep (Ventana®, Roche®) for 8 min. Antigen retrieval was performed with a ULTRA CC2 (Ventana®, Roche®) at 95 °C for 8 min (for BD2 staining) and ULTRA CC1 (Ventana®, Roche®) at 95 °C for 20 min (for BD3 staining). Endogenous peroxidase was blocked with 3% (v/v) Hydrogen Peroxide (UltraView Universal DAB Inhibitor, Ventana®, Roche®) for 4 min. The following primary monoclonal antibodies were used at 37 °C: anti-BD-2 (β-defensin 4 (L13-10-D1): sc-59496; Santa Cruz Biotechnology, inc.®) [1:50] for 40 min; and anti-BD-3 (BD-3 human (SRP4524), Sigma Aldrich®) [1:2], for 32 min. Amplification

was accomplished with the UltraView Universal HRP Multimer (Ventana®, Roche®) for 8 min. Revelation was performed with the UltraView Universal DAB Chromogen and the UntraView Universal DAB H_2O_2 for 8 min (Ventana®, Roche®) followed by intensification with the UltraView Universal DAB Copper (Ventana®, Roche®) for 4 min. The nuclear contrast was performed with Hematoxylin and Bluing (Ventana®, Roche®) for 4 min each.

Finally, the slides were washed in water and detergent, dehydrated with increasing concentrations of Ethanol (75, 90 and 99% (v/v)) for 1 min each, cleared in Xylene (VWR®) and mounted with Synthetic Mounting Medium (Quick-D M-Klinipath®).

Catheter processing for SEM

The catheters were introduced in mounting pins to incubate at 4 °C, overnight in a solution of 2 %(v/v) Glutaraldehyde (Sigma-Aldrich®) in 0.05 M Sodium Phosphate Buffer (pH = 7.4) (Merck®) to fixate the specimens. Catheters were washed 3 times in 0.15 M Sodium Phosphate Buffer (pH = 7.4). Post fixation was performed in a solution of 1 %(v/v) Osmium Tetroxide (Sigma®) in 0.12 M sodium cacodylate Buffer (pH = 7.4) (Merck®) during 2 h at room temperature. The catheters were rinsed in deionized water and were dehydrated in increasing concentrations of ethanol for analysis (10, 25, 40, 60, 95, 100 %) (Merck®) for 20 min for each incubation. Next, they were maintained in Acetone Pro-Analise (Merck®) overnight. Critical Point (Polaron® E3100) was executed within a range of pressure and temperature of 78-80 Bar and 28-30 °C, respectively. Three purges using CO_2 (Gains®) were performed with an interval of 1 h between each. SPI Flash-Dry™ Silver Paint (SPI Supplies®) was used to mount the catheters to the stubs (Agar Scientific®). Catheters were metalized (Polaron® SC502) with Gold in the presence of

Argon (Airliquide®) at a pressure between 1 and 4 Pa and a current of 0.015 A. Four metallization cycles were performed. The specimens were examined with two scanning electron microscopes: a JEOL JSM-5410, with acceleration voltage of 0.015-0.030 V, for quantification purposes, and a JEOL JSM-7001F, with acceleration voltage of 0.015-0.030 V, for obtaining high quality images of selected specimens.

Histological and immunohistochemistry analysis

Each sample was independently reviewed by two blinded researchers. HE and MT staining were used to evaluate epidermolysis and necrosis. BD-2 and BD-3 expression was semi quantitatively assessed by a staining intensity score (0, negative; 1, weak; 2, moderate; 3, strong) in the skin and perivascular regions.[52] When differences were found, specimens were again reviewed by the two researchers until a consensus was reached.

SEM analysis of catheters' surface

Bacteria, leucocytes and phagocytes were identified on the surface of catheters as described by van Gennip *et al*, Polliack and Saint-Guillain *et al*, respectively.[53-55] Only catheters whose rats had survived the entire experiment (7 days) were used for counting purposes. Average bacterial density on the surface of the catheter was based on manual counting in 20 random SEM fields at a 7500X magnification on each of the two catheter segments in each rat by a blinded researcher. When only one catheter segment could be retrieved, average bacterial density was done analogously using 40 random SEM fields at 7500X magnification. When more than 300 bacteria were found in a given SEM field,

bacteria were considered uncountable. Using the same methodology, the disposition of bacteria in each SEM field was recorded as planktonic, biofilm or mixed.

Average leucocyte density on the surface of the catheter was performed in a similar fashion, with the exception that SEM fields used were obtained at 750X magnification. The average phagocyte density on the surface of catheters was determined in the same way. Phagocytes were defined as those leucocytes that showed evidence of pseudopods in direct contact with bacteria and/or biofilm.

Bacteria and leucocyte were included in counts only if the top upper edge of the cell was in the SEM field.[56, 57] SEM fields with clots or largely occupied by biofilms were discarded, as bacteria were not accessible to counting using the methodology employed.

Statistical analysis

Qualitative variables were expressed as percentages. Quantitative variables were expressed as means ± standard deviation. The SPSS 21.0 ® software was used for descriptive and inferential statistical analysis. The Kolmogorov-Smirnov test was used to assess if variables were normally distributed. ANOVA and t-Student test were used to compare averages in normally distributed data. Kruskal-Wallis and Mann-Whitney tests were used to compare means in non-normally distributed data. Wilcoxon rank-sum test was used to compare ordinal data. Proportions were analyzed with the Chi-square test or Fisher's exact test. Association between numerical variables was assessed using Pearson's correlation coefficient. Relationship between ordinal variables was evaluated with resort to Spearman Rank Correlation Coefficient. Differences in survival in the

different experimental groups was tested with the log rank test. A two-tailed $p<0.05$ was considered to be statistically significant.

Results

Inoculation of arterialized venous flaps results in a model of persistent ischemic flap infection

In order to obtain a rat model of ischemia and *P. aeruginosa* infection in the presence of a foreign body, we followed the steps summarized in **Fig 4**. Ischemia was obtained by using a variant of the rat abdominal arterialized venous flap, established by our group.[38] Infection was obtained by inoculating *P. aeruginosa* and two 1-cm segments of sterile 14-gauge silicone catheters were used to simulate foreign body.

Serial *P. aeruginosa* concentrations (10^3; 10^4; 10^5; 10^6 and 10^7 CFU/ml) were tested in the mentioned model. A target concentration of 10^5 CFU/ml was selected, since it caused no rat mortality within 7 days and systematically resulted in clinically significant infection and partial flap necrosis. Higher concentrations led to complete or nearly complete flap necrosis (10^6 CFU/ml; n=2) and animal's death (10^7 CFU/ml; n=3), whereas lower concentrations (10^3 and 10^4 CFU/ml; n=3 for each concentration) did not produce identifiable infection.

By thermography analysis, one hour after surgery, the average difference between the flap surface's temperature and the temperature of the surface of the homologous contralateral region was 2.34 ± 1.06 ºC ($p<0.001$). **Fig 5** shows the typical thermographic appearance of the flap one hour after surgery, illustrating the lower temperature of the flap compared to the contralateral side.

Overall our data shows that a model of ischemia, infection and foreign body can be successfully obtained by adapting our previous established model of the rat abdominal

arterialized venous flap, following inoculation with *P. aeruginosa* and introduction of silicone catheters.

BD-2 and BD-3 increase flap survival rates

We then assessed whether overexpression of BDs in the flaps could improve survival and reduce infection. For this purpose, we performed a set of experiments in rats that included flaps' transduction with lentiviruses containing the BD-2 and BD-3 genes, as represented in **Figs 3** and **4**.

Of the 102 operated rats, 19 died in the immediate postoperative period (<24 hours), and were not included in the study. The following number of rats was included in each experimental group: 12 in the NaCl control group; 13 in the *P. aeruginosa* group; 14 in the GFP group; 15 in the BD-2 transduced group; 15 in the BD-3 transduced group, and 14 in the BD-2 + BD-3 transduced group. There were no statistically significant differences between the different experimental groups regarding survival throughout the experiment. To certify the inoculation dose of *P. aeruginosa*, the effective average bacterial inoculation dose under the flap was determined by bacterial growth and found to be $(9.735 \pm 0.120) \times 10^4$ CFU, which was similar to the initial inoculation concentration of 10^5 CFU/ml. There were no statistically significant differences between the initial bacterial inoculum in the different experimental groups.

To confirm transduction efficiency, seven days after surgery, flaps from rats transduced with GFP were analyzed by fluorescence microscopy. As shown in **Fig 6**, flaps from GFP lentivirus-transduced rats showed GFP expression. The expression was greater in endothelia and in the epidermis (**Fig 6**). Quantification of BD-2 mRNA

expression by real-time PCR seven days after transduction, revealed 591.12x10^{6}% ± 894.00x10^{6}% relative expression of BD-2 in transduced flaps versus 3.53x10^{6}% ± 11.35x10^{6}% relative expression in non-transduced flaps (p=0.014) (**Fig 7**). Analogously, the relative BD-3 expression determined in a similar fashion was 253.09x10^{6}% ± 354.61x10^{6}% in transduced flaps and 25.94x10^{6}% ± 87.44x10^{6}% for non-transduced flaps (p=0.018) (**Fig 7**). Using the same methodology, no statistically significant differences were found in the relative expression of BD-2 in the BD-2 and in the BD-2 + BD-3 groups, nor in the relative expression of BD-3 in the BD-3 and in the BD-2 + BD-3 groups.

Fig 8 summarizes the main clinical, optical microscopy and SEM findings in the different experimental groups. On the third postoperative day, the average area of necrotic flap was higher in the *P. aeruginosa* (61.98% ± 18.52%) and GFP (67.39% ± 20.67%) groups than in the groups BD-2 (37.16% ± 9.04%), BD3 (17.79% ± 5.48%) and BD-2 + BD-3 (35.09% ± 9.43%) (p≤0.001). The necrotic area was the smallest in the NaCl (11.07% ± 5.72%) and in the BD-3 groups. There was no statistically significant difference between these two groups (p=0.836) (**Fig 9**).

On the seventh postoperative day, lower average flap necrosis rates were also found in the NaCl (20.88% ± 9.94%), BD-2 (42.81% ± 13.56%), BD-3 (25.39% ± 8.50%) and BD-2 + BD-3 (49.97% ± 11.37%) groups than in the *P. aeruginosa* (74.30% ± 16.43%) and GFP (82.53% ± 19.73%) groups (p<0.001). Although slightly higher, the average necrosis rates of groups BD-2 and BD3 was not significantly different from that of the NaCl group. However, the average necrosis rate of BD-2 + BD-3 was higher than that of the NaCl group (p=0.049) (**Fig 10**).

In summary, our results demonstrate that transduction of flaps with BD-2 or BD-3 improves infected flap survival at day 7 following surgery, by decreasing tissue necrosis.

Evidence of flap ischemia and defensin expression by histology and immunohistochemistry

Histological analysis of the flaps revealed signs of venous congestion, marked edema, epidermolysis and areas of necrosis in all experimental groups. However, these changes were more pronounced in the *P. aeruginosa* and GFP groups (**Fig 8**). Immunohistochemistry confirmed expression of BD-2 and BD-3 in the transduced rats (**Fig 8**). BD-2 expression occurred mainly in endothelia and perivascular tissues, although it was also observed in fibroblasts and in the epidermis. BD-3 expression was strongest in the epidermis and skin appendages (**Fig 8**). Using the mentioned semi-quantitative score for immunohistochemistry staining [52], BD-2 expression was as follows: 0.25 ± 0.45 for the NaCl group; 0.23 ± 0.44 for the PA group; 0.36 ± 0.50 for the GFP group; 2.07 ± 0.59 for the BD-2 group; 0.13 ± 0.35 for the BD-3 group; 1.64 ± 0.50 for the BD2 + BD-3 group. Proceeding in a similar way, BD-3 expression in the different experimental groups was the following: 0.67 ± 0.49 for the NaCl group; 0.69 ± 0.48 for the PA group; 0.79 ± 0.70 for the GFP group; 0.27 ± 0.59 for the BD-2 group; 2.80 ± 0.41 for the BD-3 group; 2.50 ± 0.52 for the BD2 + BD-3 group. BD-3 expression was stronger than BD-2 expression. However, this difference did not reach statistically significance.

BD-2 and BD-3 decrease bacterial numbers and biofilms on the surface of foreign bodies

We then assessed the number of bacteria on the surface of the foreign body in the different experimental groups. At the end of the experiment, it was possible to retrieve 56 catheters that were distributed as follows: 8 in the NaCl group, 6 in the PA group, 12 in

the GFP group, 9 in the BD-2 group, 11 in the BD-3 group, and 10 in the BD-2 + BD-3 group.

In all rats, infection was confirmed by growth in *P. aeruginosa* MacConkey agar, Gram stain and positive oxidase reaction. **Table 1** summarizes bacterial counts determined by different methods on the 7^{th} day postoperatively in the different experimental groups.

Table 1. Average values of bacterial counts determined by different methods on the 7th day postoperatively in the different experimental groups.

Experimental Group	Viable bacteria cultured from skin flap biopsy (CFU/mg)	Real-time PCR from skin flap biopsy (ng/µl)	Bacteria on the surface of the foreign body (n/SEM field)
NaCl	$2.42x10^{5} \pm 5.87x10^{5}$	$1.23x10^{-5} \pm 2.06x10^{-5}$	7.74 ± 8.18
PA	$6.98x10^{6} \pm 1.17x10^{7}$	$1.26x10^{-1} \pm 1.17x10^{7}$	71.70 ± 47.4
GFP	$9.46x10^{5} \pm 6.46x10^{5}$	$7.22x10^{0} \pm 1.36x10^{1}$	92.75 ± 35.9
BD-2	$8.06x10^{5} \pm 8.59x10^{5}$	$5.52x10^{-1} \pm 7.97x10^{-1}$	67.08 ± 42.4
BD-3	$2.51x10^{5} \pm 5.88x10^{5}$	$1.13x10^{-5} \pm 1.39x10^{-5}$	19.37 ± 16.3
BD-2 + BD-3	$3.55x10^{5} \pm 4.52x10^{5}$	$1.94x10^{-3} \pm 2.92x10^{-3}$	54.04 ± 41.6
Statistical analysis summary	No significant differences were found	No significant differences were found	NaCl < PA; p=0.013 NaCl < GFP; p<0.001 NaCl < BD-2; p=0.010 PA > BD-3; p=0.042 GFP > BD-3; p<0.001 BD-2 > BD-3; p=0.035

For each rat, the average number of bacteria on the surface of catheters was based on manual counting bacterial cells on 20 SEM fields at 7500X magnification on each of the two catheter segments, or, when only one catheter segment could be retrieved, on counts performed on 40 SEM fields of that catheter segment. A scanning electron microscopes JEOL JSM-5410, with acceleration voltage of 0.015-0.030 V, was used for quantification purposes.

Values are expressed as average ± standard deviation.

553 CFU, colony forming units; SEM, Scanning electron microscopy

554

555 As shown in **Table 1**, significant differences were found in the number of bacteria
556 on the surface of the foreign body (**Fig 11**). The number of bacteria on the surface of
557 catheters was lower in the NaCl, BD-3, and BD-2 + BD-3 groups. There were no
558 statistically significant differences between these 3 groups. The BD-3 group presented a
559 smaller number of bacteria on the surface of catheters than the *P. aeruginosa* ($p<0.042$),
560 GFP ($p<0.001$) and BD-2 ($p=0.035$) groups.

561 Concerning the distribution of bacteria on the surface of catheters (**Figs 12** to **14**),
562 the NaCl group presented the largest percentage of SEM fields without bacteria (42.81%
563 ± 28.36%; $p<0.001$), followed by the BD-3 group (12.72% ± 17.87%), the BD-2 group
564 (6.39% ± 12.32%), and the BD-2 + BD-3 group (2.75% ± 6.17%) (**Fig 13**). The percentage
565 of SEM fields without evidence of biofilm formation were also more numerous in the NaCl
566 (99.06% ± 1.86%), BD-2 (74.44% ± 22.63%), BD-3 (88.59% ± 12.40%), and BD-2 + BD-
567 3 (73.50% ± 17.72%) groups compared to the control groups *P. aeruginosa* (50.83% ±
568 23.06%) and GFP (39.38% ± 25.30%). This difference in biofilm presence of the former
569 four groups compared to the GFP control group was statistically very significant ($p\leq0.002$)
570 (**Fig 13**).

571 Numerous leucocytes could be observed on the surface of catheters in all groups.
572 (**Figs 8, 11** and **15**). Apart from the average number of leucocytes being superior in the
573 GFP group (4.92 ± 3.68 leucocytes/SEM field) than in the NaCl group (0.75 ± 0.93
574 leucocytes/SEM field; $p=0.016$), no other statistically significant differences were found in
575 leucocytes' and phagocytes' numbers on the surface of catheters in the remaining
576 experimental groups (**Fig 11**).

Bacterial contamination with cocci were observed in 8.92% ± 22.21% of SEM fields (**Fig 13**). There were no statistically significant differences between the different experimental groups.

Overall, data shows that in the model used the surface of foreign bodies presents significant numbers of bacteria. Flap transduction with either BD-2 or BD-3, and in particular with the latter, remarkably lowers bacterial numbers on the surface of foreign bodies.

Bacterial counts and biofilms on the surface of the foreign body were correlated with flap necrosis

We then assessed whether bacteria accumulation on the surface of the foreign body was correlated with flap necrosis. **Table 2** synthetizes the most relevant correlations in the data obtained in this study.

Table 2. Synthesis of the most relevant correlations in the data obtained in this study.

Variable	Variable	Pearson's correlation factor	P value
Flap necrosis rate on the 3rd postoperative day	**Flap necrosis rate on the 7th day**	0.922	p<0.001
	Average number of bacteria per SEM field	0.609	p<0.001
	Percentage of SEM fields with biofilm	0.596	p<0.001
	Percentage of SEM fields with planktonic bacteria	- 0.409	p=0.004
	Percentage of SEM fields without bacteria	- 0.426	p=0.003
	Percentage of SEM fields without biofilm	- 0.681	p<0.001
	***P. aeruginosa* counts on the 3rd postoperative day determined by culture of flap biopsies**	0.287	p=0.041
Flap necrosis rate on the 7th postoperative day	**Average number of bacteria per SEM field**	0.626	p<0.001
	Percentage of SEM fields with biofilm	0.563	p=0.001
	Percentage of SEM fields with planktonic bacteria	- 0.379	p=0.03
	Percentage of SEM fields without bacteria	- 0.462	p=0.007
	Percentage of SEM fields without biofilm	- 0.674	p<0.001
	***P. aeruginosa* counts on the 3rd postoperative day determined by culture of flap biopsies**	0.395	p=0.016
Average number of bacteria per SEM field	**Average number of leucocytes per SEM field**	0.276	p=0.041
	Average number of phagocytes per SEM field	0.401	p=0.002

SEM, scanning electron microscopy

Flap necrosis rates on the 3rd and 7th day postoperatively were highly correlated (Pearson's correlation factor = 0.922; p<0.001). Flap necrosis was also correlated with several features of catheters' surface. In fact, flap necrosis rate on the third postoperative day was positively correlated with the average number of bacteria per SEM field and the percentage of SEM fields with biofilm (Pearson's correlation factor = 0.609; p<0.001 and 0.596; p<0.001, respectively). It was negatively correlated with the following variables: percentage of SEM fields with planktonic bacteria. In percentage of SEM fields without bacteria; percentage of SEM fields without biofilm (Pearson's correlation factor = - 0.409, p=0.004; - 0.426, p=0.003 and - 0.681; p<0.001, respectively).

Analogously, flap necrosis on the seventh day postoperatively was positively correlated with the following findings: average number of bacteria per SEM field (Pearson's correlation factor = 0.626; p<0.001) and the percentage of SEM fields with biofilm (Pearson's correlation factor = 0.563; p=0.001). Moreover, flap necrosis rate on the seventh day after surgery was significantly negatively correlated with the percentage of SEM fields with planktonic bacteria, without bacteria and without biofilm (Pearson's correlation factor = - 0.379, p=0.03; - 0.462, p=0.007; - 0.674, p<0.001, respectively).

The average number of bacteria per SEM field was also positively correlated with the number of leucocytes (Pearson's correlation factor = 0.276; p=0.041); and phagocytes per SEM field (Pearson's correlation factor = 0.401; p=0.002).

P. aeruginosa counts on the 3rd postoperative day determined by culture of flap biopsies, were correlated with flap necrosis on that day (Pearson's correlation factor = 0.287; p=0.041) and on the seventh day after surgery (Pearson's correlation factor = 0.395; p=0.016) (**Fig 16**). However, there were no statistically significant correlations between

P. aeruginosa counts after flap biopsy on the seventh day after surgery and flap necrosis either on the 3rd or 7th postoperative days. (**Fig 17**).

There were no statistically significant correlations between bacterial quantification after flap biopsy and culture or real-time PCR, on the one hand, and SEM bacterial counts on the other hand.

In conclusion, our data shows that the bacterial counts on the surface of the foreign body and biofilm formation were correlated with flap necrosis.

Discussion

Our study showed that transducing an ischemic skin flap in the rat with human β-defensins, the BD-2 and BD-3 genes, increased skin flap survival in the context of a *P. aeruginosa* infection in the presence of a foreign body. In addition, BD-2 and particularly BD-3 transduction reduced *P. aeruginosa* numbers and biofilm formation on the surface of the foreign body. Other authors had already shown that BD-2 and BD-3 are overexpressed in the presence of *P. aeruginosa* keratitis in mice and that overexpression was associated with diminished *P. aeruginosa* numbers in the eyes of affected mice.[14, 58]

However, as far as the authors could determine, this is the first description of the transduction of BDs genes to treat a *P. aeruginosa* infection *in vivo*.[13] It is also the first time that the transduction of an AMP gene is performed with the intent to treat an infection taking place in a poorly perfused region, simulating local ischemia. This scenario is frequent in the clinical setting, occurring after trauma, radiotherapy or in ischemic regions of the body, namely in the lower limbs of atherosclerotic and/or diabetic patients.[59, 60] This study describes for the first time the morphometric features of the bacteria on the surface of a foreign body and thoroughly compares them with the clinical evaluation of the overlying skin flap, and with bacterial quantification using microbiological cultures of skin biopsy and real-time PCR. Other authors had already shown the possibility of treating a *Staphylococcus aureus* infection transducing a normally perfused flap with the AMP cathelicidin LL-37.[39]

The fact that the groups treated with BDs presented less biofilm, suggest that *in vivo* these AMPs are able to prevent the formation of biofilms, which are one of the most

common causes of clinical persistent infection.[61-66] This adds to the knowledge of BD physiology, as most papers in this field refer to the action of AMPs *in vitro*, not addressing the role of these substances *in vivo*.[67]

Flap necrosis rates on the 3rd and 7th day postoperatively were highly correlated (Pearson's correlation factor = 0.922; p<0.001). This suggests that, in this rodent model, the ongoing *P. aeruginosa* infection associated with the foreign body led to continuous breakdown of the overlying integument.[62] This had already been amply observed in clinical practice.[62, 68] Interestingly, in this work, flap necrosis was significantly correlated with several features of catheters' surface, namely bacterial numbers and biofilm presence. In opposition, in the present study, flap necrosis rates in the different groups was not correlated with bacterial determination by real-time PCR of flap biopsies. Moreover, only bacterial counts of microbiological cultures of biopsies of the flap performed on the third post-operative day correlated, and even then only poorly, with flap necrosis rates on the third (Pearson's correlation factor = 0.287; p=0.041) and seventh (Pearson's correlation factor = 0.395; p=0.016) days after surgery. This lends support to the notion that in bacteria capable of producing biofilms, such as *P. aeruginosa*, the protracted release of bacterial cells from the biofilm medium is one of the main determinants of continuous tissue damage to the overlying tissues.[41, 53, 62-64] In fact, a recent meta-analysis demonstrated that biofilms are present in more than three quarters of chronic wounds, increasing their extension or preventing their closure.[63]

All these data suggest that the model herein used adequately mimics clinically relevant skin ulcers and infections. Noteworthy, a similar model had already been described by Van Wijngaerden *et al*, who introduced a catheter in the back of the rat to

test antibiotic efficacy. Furthermore, other authors, have also placed a catheter under a well perfused flap in the groin region of the rat. Notwithstanding, these authors did not used SEM to evaluate the surface of the catheter used as a foreign body. It was only recently that van Gennip *et al.* emphasized the potential advantages of studying the morphology and interaction of bacteria and immune cells on the surface of foreign bodies with SEM. However, these latter authors placed the foreign body inside the peritoneal cavity.[53]

We believe that our model presents the additional advantage of simulating an ischemic environment surrounding the foreign body. In fact, as shown in **Fig 5**, one hour after surgery, the average temperature difference between the flap and the contralateral side was 2.34 ± 1.06 ºC ($p<0.001$). These data confirm that the surgical skin flap placed over the foreign body was ischemic, since skin temperature is known to be proportional to integumentary perfusion.[69]

One of the limitations of the present methodology was the impossibility to precisely differentiate between leucocytes types.[53, 70-74] Although immunological methods have been proposed to distinguish leucocyte types using SEM, it has been shown that these methods may significantly affect leucocyte adhesion and morphology, making interpretation of data difficult.[75] In future works, it would be interesting to characterize with other techniques leucocyte numbers and cell types both on the surface of the foreign body and in the surrounding tissues.

Another limitation of this study was the presence of contamination of the wound by bacteria other than *P. aeruginosa*, namely by cocci, in 8.92 ± 22.21% of SEM fields (**Fig 13**). This contamination affected all experimental groups equally. It is no doubt related to

the ischemic nature of the skin flap used, leading to partial flap necrosis, surgical wound dehiscence and contamination with saprophytic flora. Hence, studies similar to this one but with normally perfused flaps are, therefore, warranted, in order to minimize contamination with other bacterial species.

The authors must concede that multiple other delivery methods of the BDs genes could have been employed.[76, 77] Many of the other available vectors have potential advantages and disadvantages. For example, it has been shown that intradermal delivery of the transgenes might be superior to intravascular perfusion using lentivirus vectors in skin flaps.[78] Consequently, further studies are warranted in this field, namely to test the superiority of other vectors, as well as the susceptibility of other bacteria species, particularly bacteria resistant to conventional antibiotics. Furthermore, it would be interesting to assess if BDs could be used to reverse established biofilm on the surface of foreign bodies.

Finally, the authors would like to note that although the potential clinical merits of AMPs have been extoled for the past two decades, their clinical application has been tardy and incipient, due to potential systemic toxicity, susceptibility to proteases, and high cost of peptide production.[9, 10, 12, 13, 79, 80] Controlled local production of a specific AMP by a flap placed over a difficult wound (for example, osteomyelitis in a mangled extremity) may theoretically allow to eradicate a bacterial infection and thus allow wound closure.[39] If the introduction of the AMP sequence was to cause oncogenesis, the flap could be simply removed and replaced by another flap or eventually by a skin graft.[39, 81]

Acknowledgments

The authors would like to thank Mr. Filipe Franco for the drawings contained in this article.

The authors are deeply thankful to the unfaltering help of Mr. Octávio Xaveiro in the acquisition of the thousands SEM images.

Financial Disclosure Statement:

One of the authors (DC) received a grant from “The Programme for Advanced Medical Education” sponsored by “Fundação Calouste Gulbenkian, Fundação Champalimaud, Ministério da Saúde and Fundação para a Ciência e Tecnologia, Portugal.”

The authors have no financial or commercial interests to declare in relation to the content of this article.

References

1. Alanis AJ. Resistance to antibiotics: are we in the post-antibiotic era? Archives of medical research. 2005;36(6):697-705.

2. Falagas ME, Bliziotis IA. Pandrug-resistant Gram-negative bacteria: the dawn of the post-antibiotic era? International journal of antimicrobial agents. 2007;29(6):630-6.

3. Aminov RI. A brief history of the antibiotic era: lessons learned and challenges for the future. Frontiers in microbiology. 2010;1:134.

4. Mendes JJ, Marques-Costa A, Vilela C, Neves J, Candeias N, Cavaco-Silva P, et al. Clinical and bacteriological survey of diabetic foot infections in Lisbon. Diabetes research and clinical practice. 2012;95(1):153-61. Epub 2011/10/25. doi: 10.1016/j.diabres.2011.10.001. PubMed PMID: 22019426.

5. Peters BM, Shirtliff ME, Jabra-Rizk MA. Antimicrobial peptides: primeval molecules or future drugs? PLoS pathogens. 2010;6(10):e1001067. Epub 2010/11/10. doi: 10.1371/journal.ppat.1001067. PubMed PMID: 21060861; PubMed Central PMCID: PMC2965748.

6. Lipsky BA. Diabetic foot infections: Current treatment and delaying the 'post-antibiotic era'. Diabetes/metabolism research and reviews. 2016;32(S1):246-53.

7. Zasloff M. Antimicrobial peptides of multicellular organisms. Nature. 2002;415(6870):389-95. Epub 2002/01/25. doi: 10.1038/415389a. PubMed PMID: 11807545.

8. Fjell CD, Hiss JA, Hancock RE, Schneider G. Designing antimicrobial peptides: form follows function. Nature reviews Drug discovery. 2012;11(1):37-51.

9. Seo M-D, Won H-S, Kim J-H, Mishig-Ochir T, Lee B-J. Antimicrobial peptides for therapeutic applications: a review. Molecules. 2012;17(10):12276-86.

10. Nakatsuji T, Gallo RL. Antimicrobial peptides: old molecules with new ideas. The Journal of investigative dermatology. 2012;132(3 Pt 2):887-95. Epub 2011/12/14. doi: 10.1038/jid.2011.387. PubMed PMID: 22158560; PubMed Central PMCID: PMC3279605.

11. Sweeney IR, Miraftab M, Collyer G. A critical review of modern and emerging absorbent dressings used to treat exuding wounds. International wound journal. 2012;9(6):601-12. Epub 2012/01/18. doi: 10.1111/j.1742-481X.2011.00923.x. PubMed PMID: 22248337.

12. Shang D, Li X, Sun Y, Wang C, Sun L, Wei S, et al. Design of potent, non-toxic antimicrobial agents based upon the structure of the frog skin peptide, temporin-1CEb from Chinese brown frog, Rana chensinensis. Chemical biology & drug design. 2012;79(5):653-62. Epub 2012/02/22. doi: 10.1111/j.1747-0285.2012.01363.x. PubMed PMID: 22348663.

13. Zasloff M. Antimicrobial peptides: do they have a future as therapeutics. In: Harder J, Schroder JM, editors. Antimicrobial peptides: role in human health and disease. First ed. London: Springer; 2016. p. 147-54.

14. Gordon YJ, Romanowski EG, McDermott AM. A review of antimicrobial peptides and their therapeutic potential as anti-infective drugs. Current eye research. 2005;30(7):505-15. Epub 2005/07/16. doi: 10.1080/02713680590968637. PubMed PMID: 16020284; PubMed Central PMCID: PMC1497874.

15. Marr AK, Gooderham WJ, Hancock RE. Antibacterial peptides for therapeutic use: obstacles and realistic outlook. Current opinion in pharmacology. 2006;6(5):468-72. Epub 2006/08/08. doi: 10.1016/j.coph.2006.04.006. PubMed PMID: 16890021.

16. Wiesner J, Vilcinskas A. Antimicrobial peptides: the ancient arm of the human immune system. Virulence. 2010;1(5):440-64. Epub 2010/12/24. doi: 10.4161/viru.1.5.12983. PubMed PMID: 21178486.

17. Peschel A, Sahl H-G. The co-evolution of host cationic antimicrobial peptides and microbial resistance. Nature Reviews Microbiology. 2006;4(7):529-36.

18. Yeaman MR, Yount NY. Mechanisms of antimicrobial peptide action and resistance. Pharmacological reviews. 2003;55(1):27-55. Epub 2003/03/05. doi: 10.1124/pr.55.1.2. PubMed PMID: 12615953.

19. Hemshekhar M, Anaparti V, Mookherjee N. Functions of Cationic Host Defense Peptides in Immunity. Pharmaceuticals. 2016;9(3):40. doi: 10.3390/ph9030040. PubMed PMID: PMC5039493.

20. Yamaguchi Y, Ouchi Y. Antimicrobial peptide defensin: identification of novel isoforms and the characterization of their physiological roles and their significance in the pathogenesis of diseases. Proceedings of the Japan Academy Series B, Physical and biological sciences. 2012;88(4):152-66. Epub 2012/04/14. PubMed PMID: 22498979; PubMed Central PMCID: PMC3406309.

21. Breidenstein EB, de la Fuente-Nunez C, Hancock RE. Pseudomonas aeruginosa: all roads lead to resistance. Trends in microbiology. 2011;19(8):419-26. Epub 2011/06/15. doi: 10.1016/j.tim.2011.04.005. PubMed PMID: 21664819.

22. Chatterjee M, Anju CP, Biswas L, Anil Kumar V, Gopi Mohan C, Biswas R. Antibiotic resistance in Pseudomonas aeruginosa and alternative therapeutic options. International journal of medical microbiology : IJMM. 2016;306(1):48-58. Epub 2015/12/22. doi: 10.1016/j.ijmm.2015.11.004. PubMed PMID: 26687205.

23. Ge Y, MacDonald D, Hait H, Lipsky B, Zasloff M, Holroyd K. Microbiological profile of infected diabetic foot ulcers. Diabetic medicine : a journal of the British Diabetic Association. 2002;19(12):1032-4. Epub 2003/03/22. PubMed PMID: 12647846.

24. Schirmer S, Ritter R-G, Fansa H. Vascular surgery, microsurgery and supramicrosurgery for treatment of chronic diabetic foot ulcers to prevent amputations. PloS one. 2013;8(9):e74704.

25. Pazgier M, Hoover DM, Yang D, Lu W, Lubkowski J. Human beta-defensins. Cellular and molecular life sciences : CMLS. 2006;63(11):1294-313. Epub 2006/05/20. doi: 10.1007/s00018-005-5540-2. PubMed PMID: 16710608.

26. Maisetta G, Batoni G, Esin S, Florio W, Bottai D, Favilli F, et al. In vitro bactericidal activity of human beta-defensin 3 against multidrug-resistant nosocomial strains. Antimicrobial agents and chemotherapy. 2006;50(2):806-9. Epub 2006/01/27. doi: 10.1128/AAC.50.2.806-809.2006. PubMed PMID: 16436752; PubMed Central PMCID: PMC1366902.

27. Tai KP, Kamdar K, Yamaki J, Le VV, Tran D, Tran P, et al. Microbicidal effects of α- and θ-defensins against antibiotic-resistant Staphylococcus aureus and Pseudomonas aeruginosa. Innate immunity. 2015;21(1):17-29. doi: 10.1177/1753425913514784. PubMed PMID: PMC4062604.

28. Huang LC, Redfern RL, Narayanan S, Reins RY, McDermott AM. In vitro activity of human β-defensin 2 against Pseudomonas aeruginosa in the presence of tear fluid. Antimicrobial agents and chemotherapy. 2007;51(11):3853-60.

29. Raschig J, Mailander-Sanchez D, Berscheid A, Berger J, Stromstedt AA, Courth LF, et al. Ubiquitously expressed Human Beta Defensin 1 (hBD1) forms bacteria-entrapping nets in a redox dependent mode of action. PLoS pathogens. 2017;13(3):e1006261. Epub 2017/03/23. doi: 10.1371/journal.ppat.1006261. PubMed PMID: 28323883; PubMed Central PMCID: PMCPMC5376342.

30. Casalou C, Seixas C, Portelinha A, Pintado P, Barros M, Ramalho JS, et al. Arl13b and the non-muscle myosin heavy chain IIA are required for circular dorsal ruffle formation and cell migration. Journal of cell science. 2014;127(Pt 12):2709-22. Epub 2014/04/30. doi: 10.1242/jcs.143446. PubMed PMID: 24777479.

31. National Research Council (U.S.). Committee for the Update of the Guide for the Care and Use of Laboratory Animals., Institute for Laboratory Animal Research (U.S.), National Academies Press (U.S.). Guide for the care and use of laboratory animals. Washington, D.C.: National Academies Press,; 2011. Available from: http://www.ncbi.nlm.nih.gov/books/NBK54050.

32. Edmunds MC, Wigmore S, Kluth D. In situ transverse rectus abdominis myocutaneous flap: a rat model of myocutaneous ischemia reperfusion injury. Journal of visualized experiments : JoVE. 2013;(76). Epub 2013/06/19. doi: 10.3791/50473. PubMed PMID: 23770929.

33. Harder Y, Schmauss D, Wettstein R, Egana JT, Weiss F, Weinzierl A, et al. Ischemic tissue injury in the dorsal skinfold chamber of the mouse: a skin flap model to

investigate acute persistent ischemia. Journal of visualized experiments : JoVE. 2014;(93):e51900. Epub 2014/12/10. doi: 10.3791/51900. PubMed PMID: 25489743.

34. Plenter RJ, Grazia TJ. Murine heterotopic heart transplant technique. Journal of visualized experiments : JoVE. 2014;(89). Epub 2014/07/22. doi: 10.3791/51511. PubMed PMID: 25046118.

35. Trujillo AN, Kesl SL, Sherwood J, Wu M, Gould LJ. Demonstration of the rat ischemic skin wound model. Journal of visualized experiments : JoVE. 2015;(98). Epub 2015/04/14. doi: 10.3791/52637. PubMed PMID: 25866964.

36. Casal D, Pais D, Iria I, Mota-Silva E, Almeida M-A, Alves S, et al. A Model of Free Tissue Transfer: The Rat Epigastric Free Flap. Journal of Visualized Experiments. 2017;1(119):e55281. doi: doi:10.3791/55281.

37. Wungcharoen B, Pradidarcheep W, Santidhananon Y, Chongchet V. Pre-arterialisation of the arterialised venous flap: an experimental study in the rat. Br J Plast Surg. 2001;54(7):621-30. Epub 2001/10/05. doi: 10.1054/bjps.2001.3675. PubMed PMID: 11583500.

38. Casal D, Mota-Silva E, Pais D, Iria I, Videira PA, Tanganho D, et al. Optimization of an arterialized venous fasciocutaneous flap in the abdomen of the rat. PRS Global Open. 2017;in press.

39. Ghali S, Bhatt KA, Dempsey MP, Jones DM, Singh S, Aarabi S, et al. Treating chronic wound infections with genetically modified free flaps. Plastic and reconstructive surgery. 2009;123(4):1157-68. Epub 2009/04/02. doi: 10.1097/PRS.0b013e31819f25a4. PubMed PMID: 19337084.

40. Ghali S, Dempsey MP, Jones DM, Grogan RH, Butler PE, Gurtner GC. Plastic surgical delivery systems for targeted gene therapy. Ann Plast Surg. 2008;60(3):323-32. Epub 2008/04/30. doi: 10.1097/SAP.0b013e31806917b0. PubMed PMID: 18443515.

41. Van Wijngaerden E, Peetermans WE, Vandersmissen J, Van Lierde S, Bobbaers H, Van Eldere J. Foreign body infection: a new rat model for prophylaxis and treatment. The Journal of antimicrobial chemotherapy. 1999;44(5):669-74. Epub 1999/12/20. PubMed PMID: 10552984.

42. Sheena Y, Jennison T, Hardwicke JT, Titley OG. Detection of perforators using thermal imaging. Plastic and reconstructive surgery. 2013;132(6):1603-10.

43. Weng W, Zhang F, Zhao B, Wu Z, Gao W, Li Z, et al. The complicated role of venous drainage on the survival of arterialized venous flaps. Oncotarget. 2017. doi: 10.18632/oncotarget.14845. PubMed PMID: 28145882.

44. Trujillo AN, Kesl SL, Sherwood J, Wu M, Gould LJ. Demonstration of the rat ischemic skin wound model. Journal of visualized experiments : JoVE. 2015;(98):e52637. Epub 2015/04/14. doi: 10.3791/52637. PubMed PMID: 25866964; PubMed Central PMCID: PMCPMC4401402.

45. Bas A, Forsberg G, Hammarstrom S, Hammarstrom ML. Utility of the housekeeping genes 18S rRNA, beta-actin and glyceraldehyde-3-phosphate-dehydrogenase for normalization in real-time quantitative reverse transcriptase-polymerase chain reaction analysis of gene expression in human T lymphocytes. Scandinavian journal of immunology. 2004;59(6):566-73. Epub 2004/06/09. doi: 10.1111/j.0300-9475.2004.01440.x. PubMed PMID: 15182252.

46. Livak KJ, Schmittgen TD. Analysis of relative gene expression data using real-time quantitative PCR and the 2(-Delta Delta C(T)) Method. Methods (San Diego, Calif). 2001;25(4):402-8. Epub 2002/02/16. doi: 10.1006/meth.2001.1262. PubMed PMID: 11846609.

47. Silva M, Fung RKF, Donnelly CB, Videira PA, Sackstein R. Cell-Specific Variation in E-Selectin Ligand Expression among Human Peripheral Blood Mononuclear Cells: Implications for Immunosurveillance and Pathobiology. J Immunol. 2017;198(9):3576-87. Epub 2017/03/24. doi: 10.4049/jimmunol.1601636. PubMed PMID: 28330896; PubMed Central PMCID: PMCPMC5426364.

48. Carrascal MA, Severino PF, Guadalupe Cabral M, Silva M, Ferreira JA, Calais F, et al. Sialyl Tn-expressing bladder cancer cells induce a tolerogenic phenotype in innate and adaptive immune cells. Molecular oncology. 2014;8(3):753-65. Epub 2014/03/25. doi: 10.1016/j.molonc.2014.02.008. PubMed PMID: 24656965; PubMed Central PMCID: PMCPMC5528624.

49. Maeda H, Fujimoto C, Haruki Y, Maeda T, Kokeguchi S, Petelin M, et al. Quantitative real-time PCR using TaqMan and SYBR Green for Actinobacillus actinomycetemcomitans, Porphyromonas gingivalis, Prevotella intermedia, tetQ gene and total bacteria. FEMS Immunology & Medical Microbiology. 2003;39(1):81-6.

50. Fischer AH, Jacobson KA, Rose J, Zeller R. Hematoxylin and eosin staining of tissue and cell sections. Cold Spring Harbor Protocols. 2008;2008(5):pdb. prot4986.

51. Foot NC. The Masson trichrome staining methods in routine laboratory use. Stain Technology. 1933;8(3):101-10.

52. Kesting MR, Stoeckelhuber M, Holzle F, Mucke T, Neumann K, Woermann K, et al. Expression of antimicrobial peptides in cutaneous infections after skin surgery. The British journal of dermatology. 2010;163(1):121-7. Epub 2010/03/30. doi: 10.1111/j.1365-2133.2010.09781.x. PubMed PMID: 20346023.

53. van Gennip M, Christensen LD, Alhede M, Qvortrup K, Jensen PO, Hoiby N, et al. Interactions between polymorphonuclear leukocytes and Pseudomonas aeruginosa biofilms on silicone implants in vivo. Infection and immunity. 2012;80(8):2601-7. Epub 2012/05/16. doi: 10.1128/IAI.06215-11. PubMed PMID: 22585963; PubMed Central PMCID: PMC3434577.

54. Polliack A. The contribution of scanning electron microscopy in haematology: its role in defining leucocyte and erythrocyte disorders. Journal of microscopy. 1981;123(Pt 2):177-87. PubMed PMID: 7035677.

55. Saint-Guillain ML, Vray B, Hoebeke J, Leloup R. SEM morphological studies of phagocytosis by rat macrophages and rabbit polymorphonuclear leukocytes. Scanning electron microscopy. 1980;(Pt 2):205-12. Epub 1980/01/01. PubMed PMID: 6999599.

56. West MJ. Estimating object number. In: West MJ, editor. Basic stereology for biologists and neuroscientists. 1. First ed. New York: Cold Spring Harbor Laboratory Press; 2012. p. 31-58.

57. Geuna S. The revolution of counting "tops": two decades of the disector principle in morphological research. Microscopy research and technique. 2005;66(5):270-4. Epub 2005/06/09. doi: 10.1002/jemt.20167. PubMed PMID: 15940681.

58. Wu M, McClellan SA, Barrett RP, Zhang Y, Hazlett LD. β-defensins 2 and 3 together promote resistance to Pseudomonas aeruginosa keratitis. The Journal of Immunology. 2009;183(12):8054-60.

59. Morton LM, Phillips TJ. Wound healing and treating wounds: Differential diagnosis and evaluation of chronic wounds. Journal of the American Academy of Dermatology. 2016;74(4):589-605; quiz -6. Epub 2016/03/17. doi: 10.1016/j.jaad.2015.08.068. PubMed PMID: 26979352.

60. Armstrong DG, Lipsky BA. Diabetic foot infections: stepwise medical and surgical management. International wound journal. 2004;1(2):123-32. Epub 2006/05/26. doi: 10.1111/j.1742-4801.2004.00035.x. PubMed PMID: 16722884.

61. Costerton JW, Stewart PS, Greenberg EP. Bacterial Biofilms: A Common Cause of Persistent Infections. Science. 1999;284(5418):1318-22. doi: 10.1126/science.284.5418.1318.

62. Barker JC, Khansa I, Gordillo GM. A Formidable Foe Is Sabotaging Your Results: What You Should Know about Biofilms and Wound Healing. Plastic and reconstructive surgery. 2017;139(5):1184e-94e. Epub 2017/04/27. doi: 10.1097/prs.0000000000003325. PubMed PMID: 28445380; PubMed Central PMCID: PMCPMC5407389.

63. Malone M, Bjarnsholt T, McBain AJ, James GA, Stoodley P, Leaper D, et al. The prevalence of biofilms in chronic wounds: a systematic review and meta-analysis of published data. J Wound Care. 2017;26(1):20-5. doi: 10.12968/jowc.2017.26.1.20. PubMed PMID: 28103163.

64. Mihai MM, Holban AM, Giurcaneanu C, Popa LG, Oanea RM, Lazar V, et al. Microbial biofilms: impact on the pathogenesis of periodontitis, cystic fibrosis, chronic wounds and medical device-related infections. Curr Top Med Chem. 2015;15(16):1552-76. PubMed PMID: 25877092.

65. Ramos-Gallardo G. Chronic Wounds in Burn Injury: A Case Report on Importance of Biofilms. World J Plast Surg. 2016;5(2):175-80. PubMed PMID: 27579274; PubMed Central PMCID: PMCPMC5003954.

66. Scali C, Kunimoto B. An update on chronic wounds and the role of biofilms. J Cutan Med Surg. 2013;17(6):371-6. doi: 10.2310/7750.2013.12129. PubMed PMID: 24138971.

67. Kostakioti M, Hadjifrangiskou M, Hultgren SJ. Bacterial biofilms: development, dispersal, and therapeutic strategies in the dawn of the postantibiotic era. Cold Spring Harb Perspect Med. 2013;3(4):a010306. doi: 10.1101/cshperspect.a010306. PubMed PMID: 23545571; PubMed Central PMCID: PMCPMC3683961.

68. Snyder RJ, Bohn G, Hanft J, Harkless L, Kim P, Lavery L, et al. Wound Biofilm: Current Perspectives and Strategies on Biofilm Disruption and Treatments. Wounds. 2017;29(6):S1-s17. Epub 2017/07/07. PubMed PMID: 28682297.

69. Sasajima T, Kikuchi S, Ishikawa N, Koyama T. Skin temperature in lower hind limb subjected to distal vein arterialization in rats. In: Swartz HM, Harrison DK, Bruley DF, editors. Oxygen transport to tissue XXXVI. 1. First ed. New York, USA: Springer; 2014. p. 361-8.

70. POLLIACK A. Surface Features of Normal and leukemic lymphocytes by SEM. Clinical Immunology and Immunopathology. 1975;3:412-30.

71. Polliack A, Lampen N, Clarkson BD, De Harven E, Bentwich Z, Siegal FP, et al. Identification of human B and T lymphocytes by scanning electron microscopy. The Journal of experimental medicine. 1973;138(3):607-24. Epub 1973/09/01. PubMed PMID: 4542254; PubMed Central PMCID: PMC2139412.

72. Mian R, Westwood D, Stanley P, Marshall JM, Coote JH. Acute systemic hypoxia and the surface ultrastructure and morphological characteristics of rat leucocytes. Experimental physiology. 1993;78(6):839-42. Epub 1993/11/01. PubMed PMID: 8311950.

73. Pugh CW, MacPherson GG, Steer HW. Characterization of nonlymphoid cells derived from rat peripheral lymph. The Journal of experimental medicine. 1983;157(6):1758-79. Epub 1983/06/01. PubMed PMID: 6854208; PubMed Central PMCID: PMC2187049.

74. MacRae EK, Pryzwansky KE, Cooney MH, Spitznagel JK. Scanning electron microscopic observations of early stages of phagocytosis of E. coli by human neutrophils. Cell and tissue research. 1980;209(1):65-70. Epub 1980/01/01. PubMed PMID: 7000363.

75. Marino F, Schembri L, Rasini E, Pinoli M, Scanzano A, Luini A, et al. Characterization of human leukocyte-HUVEC adhesion: Effect of cell preparation methods. Journal of immunological methods. 2017;443:55-63. Epub 2017/02/09. doi: 10.1016/j.jim.2017.01.013. PubMed PMID: 28167274.

76. Kim TK, Eberwine JH. Mammalian cell transfection: the present and the future. Analytical and bioanalytical chemistry. 2010;397(8):3173-8. Epub 2010/06/16. doi:

10.1007/s00216-010-3821-6. PubMed PMID: 20549496; PubMed Central PMCID: PMC2911531.

77. Warnock JN, Daigre C, Al-Rubeai M. Introduction to viral vectors. In: Merten OW, Al-Rubeai M, editors. Viral vectors for gene therapy. 1. First ed. London: Humana Press; 2011. p. 1-25.

78. Leto Barone AA, Zhou ZY, Hughes MW, Park R, Schulman RM, Lee S, et al. Lentiviral transduction of face and limb flaps: implications for immunomodulation of vascularized composite allografts. Plastic and reconstructive surgery. 2012;129(2):391-400. Epub 2012/01/31. doi: 10.1097/PRS.0b013e31823aeaeb. PubMed PMID: 22286422.

79. Yang D, Chertov O, Bykovskaia SN, Chen Q, Buffo MJ, Shogan J, et al. Beta-defensins: linking innate and adaptive immunity through dendritic and T cell CCR6. Science. 1999;286(5439):525-8. Epub 1999/10/16. PubMed PMID: 10521347.

80. Stanfield RL, Westbrook EM, Selsted ME. Characterization of two crystal forms of human defensin neutrophil cationic peptide 1, a naturally occurring antimicrobial peptide of leukocytes. The Journal of biological chemistry. 1988;263(12):5933-5. Epub 1988/04/25. PubMed PMID: 3356711.

81. C Rennert R, Sorkin M, W Wong V, C Gurtner G. Organ-level tissue engineering using bioreactor systems and stem cells: implications for transplant surgery. Current stem cell research & therapy. 2014;9(1):2-9.

82. Sorensen OE. Antimicrobial peptides in cutaneous wound healing. In: Harder J, Schroder JM, editors. Antimicrobial peptides: rele in human health and disease. First ed. London: Springer; 2016. p. 1-15.

1021

1022

Figure Legends:

Fig 1. Schematic representation of some of the known effects of human β-defensins 2 and 3 on bacteria. Typical gram-negative bacteria are represented by the pink-red rod. Typical gram-positive bacteria are depicted by the violet coccus. Defensins intercalate into bacterial cell membrane and form pores through bacteria walls promoting osmotic imbalance and bacterial membrane rupture. This, in turn, promotes activation of the alternative pathway of the complement system leading to the formation of membrane attack complexes that further promote bacterial lysis and complement activation. Byproducts of complement activation and bacterial cell rupture act as chemotactic factors promoting the recruitment of inflammatory cells that will enhance bacterial clearance.[7, 82] Intracellularly, defensins inhibit bacterial DNA replication, transduction and translation, disturbing bacterial homeostasis.

BD-2, human β-defensin 2; BD-3, human β-defensin 3; hBD, human β-defensin

Fig 2. Schematic representation of some of the known effects of human β-defensin 2 and 3 on the immune system and their role in the destruction of bacteria. Gram-negative bacteria are represented by pink-red rods, whereas gram-positive bacteria are depicted by violet cocci.

Antimicrobial peptides, including defensins, are part of the innate resistance against bacterial invasion. Defensins are secreted by multiple epithelia, namely those lining skin, endothelia, gut, airways and the genitourinary tract, as well as by leucocytes and platelets. Microbial components, such as lipopolysaccharide, and other pro-inflammatory

stimuli are strong inducers of the expression and secretion of defensins. Defensins, in turn, act as potent chemotactic agents, activate the complement system, promote opsonization and phagocytosis of bacteria, and concomitantly lead to the release of oxygen reactive species and of further pro-inflammatory factors. All these phenomena lead to positive feedback mechanisms that collectively facilitate resolution of bacterial infections.[19, 82]

BD-2, human β-defensin2; BD-3, human β-defensin3; hBD, human β-defensin

Fig 3. Diagram illustrating the experimental groups used in this work.

NaCl group - In this group, flaps were intravascularly injected with a 100-µl solution of recombinant rat Vascular Endothelial Growth Factor-A that was left to act for 90 min. Before closing the surgical wounds, one milliliter of a 0.9% sodium chloride solution was instilled under the flap into the vicinity of the silicone catheter segments.

PA group - In this group, flaps were intravascularly injected with a 100-µl solution of recombinant rat Vascular Endothelial Growth Factor-A that was left to act for 90 min. Before closing the surgical wounds, one milliliter of a 0.9% sodium chloride solution containing 10^5 CFU *Pseudomonas aeruginosa* was instilled under the flap into the vicinity of the silicone catheter segments.

GFP group - In this group, flaps were intravascularly injected with a 100-µl milliliter solution of recombinant rat Vascular Endothelial Growth Factor-A and a Green Fluorescent Protein coding lentivirus. This solution was left to act for 90 min. Before closing the surgical wounds, one milliliter of a 0.9% sodium chloride solution containing

10^5 CFU *P. aeruginosa* was instilled under the flap into the vicinity of the silicone catheter segments.

BD-2 group - In this group, flaps were intravascularly injected with a 100-µl solution of recombinant rat Vascular Endothelial Growth Factor-A and a human β-defensin 2 coding lentivirus. This solution was left to act for 90 min. Before closing the surgical wounds, one milliliter of a 0.9% sodium chloride solution containing 10^5 CFU *P. aeruginosa* was instilled under the flap into the vicinity of the silicone catheter segments.

BD-3 group - In this group, flaps were intravascularly injected with a 100-µl solution of recombinant rat Vascular Endothelial Growth Factor-A and a human β-defensin 3 coding lentivirus. This solution was left to act for 90 min. Before closing the surgical wounds, one milliliter of a 0.9% sodium chloride solution containing 10^5 CFU *P. aeruginosa* was instilled under the flap into the vicinity of the silicone catheter segments.

BD-2 + BD-3 group - In this group, flaps were intravascularly injected with a 100-µl solution of recombinant rat Vascular Endothelial Growth Factor-A and human β-defensin 2 and 3 coding lentivirus. This solution was left to act for 90 min. Before closing the surgical wounds, one milliliter of a 0.9% sodium chloride solution containing 10^5 CFU *P. aeruginosa* was instilled under the flap into the vicinity of the silicone catheter segments.

Fig 4. Diagram illustrating the main steps in the production of the rodent model of ischemia, *Pseudomonas aeruginosa* infection associated with a foreign body, lentiviral delivery of antimicrobial peptides, and evaluation of flap progression. From (A1) to (A7), a summary of the steps involved in the model of foreign body infection underneath an ischemic fasciocutaneous flap is represented.

(A1) A variant of the rat abdominal arterialized venous flap was used as model of ischemic flap.[37, 38] In all animals, under a surgical operating microscope, a 5 cm long and 3 cm wide fasciocutaneous flap was raised on the left side of the rat's abdomen. Cranially, the flap was connected exclusively to the skeletonized lateral thoracic vein. This vein was temporarily clamped. Caudally, the superficial caudal epigastric artery was ligated.

(A2) The superficial caudal epigastric vein (SCEV) was cannulated with a 27-gauge ophthalmic cannula.

(A3) The SCEV was perfused with 100 µl solution of the following solutions: **NaCl Group** (VEGF); **PA Group** (VEGF); **GFP Group** (VEGF + GFP coding lentivirus); **BD-2 Group** (VEGF + BD-2 coding lentivirus); **BD-3 Group** (VEGF + BD-3 coding lentivirus); **BD-2 + BD-3 Group** (VEGF + BD-2 + BD-3 coding lentivirus). The SCEV was then immediately clamped for 90 min, in order to leave the injected solution in contact with the flap's vascular system.

(A4) Clamps were removed and the SCEV was arterialized by connecting it to the femoral artery. In order to achieve this the SCEV was cut from the femoral vein with a 1-mm long cuff of adjacent femoral vein tissue. The ostium in the femoral vein was closed with a continuous Nylon 11/0 suture. The same suture line was used to perform a side-to-end arteriovenous anastomosis between the SCEV and the ventral flank of the femoral artery through a 1-mm long ostium previously created in the latter vessel. Interrupted stitches were used for this anastomosis. The lateral thoracic vein was preserved cranially to ensure outflow from the arterialized venous flap.

(A5) Two 1-cm segments of sterile 14-gauge silicone catheters (Mediplus™) were placed in the central aspect of the surgical wound, underneath the flap.

(A6) Surgical wounds were closed with a running 5/0 Nylon suture.

(A7) Immediately before closing the lateral aspect of the skin wound, a 1-ml of a 0.9% sodium chloride solution was instilled under the flap into the vicinity of the silicone catheter segments using a 18-gauge silicone catheter (Mediplus™). In all groups except the NaCl group, the injected solution also contained 10^5 CFU *Pseudomonas aeruginosa*. The running suture was closed immediately after injection, in order to avoid any spilling to the area adjacent to the flap. A transparent Tegaderm™ transparent film dressing was applied over the flap and adjacent skin.

(B), Flap biopsies were collected on the third and seventh day postoperatively to determine bacterial counts after bacterial culture.

(C), Flap survival and perfusion was assessed by clinical inspection and with resort to direct infrared thermography.

(D), Bacterial numbers and disposition were assessed on the surface of foreign bodies using scanning electron microscopy.

(E), Flap transduction with the human β-defensin 2 (BD-2) and/or β-defensin 3 (BD-3) genes was evaluated by immunohistochemical evaluation of flap biopsies 3 and 7 days after surgery.

VEGF, Vascular Endothelial Growth Factor

Fig 5. Representative direct infrared thermography image of the ventrolateral aspect of the abdomen of the rat 1 hour postoperatively. Flap boundaries are highlighted with the interrupted lines. This image illustrates that the temperature of the

flap's surface is inferior to the contralateral side, due to the flap's relative ischemia, which results from its unconventional pattern of perfusion.

CT, rat's core temperature.

Fig 6. Typical fluorescence image photographs of the skin and hypodermis of the flap of a rat transduced with a Green Fluorescent Protein coding lentivirus (**LV-GFP**) and those of the flap of a non-transduced rat (**Control**) seven days after surgery. These photographs demonstrate transduction of flaps by the virus.

Calibration bar = 100 μm

Fig 7. Analysis of the BD-2 and BD-3 mRNA expression in rat flaps. Box plots represent the relative mRNA expression level of human β-defensins 2 and 3 (BD-2 and 3) analyzed in transduced flaps compared to non-transduced flaps on the seventh post-operative day relatively to the expression of the β-actin in these flaps using real-time PCR. The relative mRNA levels of each gene are expressed as the percentage of the β-actin mRNA levels.

Horizontal lines in the upper portion of the figure indicate statistically significant differences between groups ($p<0.05$).

Fig 8. Typical macroscopic and microscopic features of flaps in the different experimental groups. Macroscopic images were taken on the third day post-operatively (D3 Post-op), and seven days post-operatively (D7 Post-op). Microscopic images were taken with immunohistochemical staining with anti-BD-2 (BD-2 IH), or anti-BD-3 (BD-3

IH) antibodies of flap biopsies performed on the seventh day after the surgery. Scanning electron microscopy images (SEM) were taken at 750X or 7500X amplification,

Calibration bar = 100 µm (M, N, P-T, V-X); 25 µm (O, U); 10 µm (Y-D'); 1 µm (E' - J')

Fig 9. Bar graphs representing the skin flap necrosis rate on the third postoperative day in the different experimental groups. Horizontal lines in the upper portion of the figure indicate statistically significant differences between groups ($p<0.05$).

Error bars indicate 95% confidence intervals.

**, $p<0.01$. ***, $p<0.001$

Fig 10. Bar graphs representing the skin flap necrosis rate on the seventh postoperative day in the different experimental groups. Horizontal lines in the upper portion of the figure indicate statistically significant differences between groups ($p<0.05$).

Error bars indicate 95% confidence intervals.

***, $p<0.001$

Fig 11. Bar graphs representing the average number of bacteria, leucocytes and phagocytes on the surface of the catheter segments placed underneath the flaps per scanning electron microscopy (SEM) field. For each rat, the average number of bacteria on the surface of catheters was based on manual counting bacterial cells on 20 SEM fields at 7500X magnification on each of the two catheter segments, or, when only one catheter segment could be retrieved, on counts performed on 40 SEM fields of that catheter segment. Average leucocyte and phagocyte density on the surface of the

catheter was performed in a similar way, with the exception that SEM fields used were at obtained 750X magnification. A scanning electron microscope JEOL JSM-5410, with acceleration voltage of 0.015-0.030 V, was used for quantification purposes.

Horizontal lines in the upper portion of the figure indicate statistically significant differences between groups ($p<0.05$).

Error bars indicate 95% confidence intervals.

***, $p<0.001$

Fig 12. Morphological features of bacteria on the surface of the foreign body in increasing magnifications by scanning electron microscopy. (A and B) Flat biofilm on the surface of a catheter segment. (C) Magnification of the large rectangular area in the center of (B) showing *Pseudomonas aeruginosa* and associated biofilm. (D) Magnification of the small rectangular area in the center of (B) showing *Pseudomonas aeruginosa* bacterial cells dividing in the biofilm. (E) Mushroom-shaped biofilm with uncountable bacterial cells. (F) Higher magnification view of the rectangular dotted area in the center of (E) showing bacterial division and adherence to the surface of the catheter (arrow heads). (G) Biofilm covering most of *P. aeruginosa* cells. (H) High magnification view of a *P. aeruginosa* cell dividing on the surface of the catheter. (I) High magnification image of a single *P. aeruginosa* cell on the surface of the biofilm showing the irregularities of the bacterial wall surface.

Calibration bar = 100 μm (A); 10 μm (B, E); 1 μm (C, D, F to I)

Fig 13. Typical scanning electron microscopy images of the surface of catheters showing the variable distribution of bacteria. (A) *Pseudomonas aeruginosa* in the planktonic form; (B) *P. aeruginosa* are seen forming a large flat biofilm in the central portion of the image; (C) Small cocci (contamination) are seen on the surface of an hair shaft that contaminated the surgical wound; the box represents an higher amplification view of the middle portion of the hair shaft (D) *P. aeruginosa* cells are seen scattered on the surface of the catheter; some of these cells are dividing; amongst *P. aeruginosa*, it is possible to observe cocci; (E) Diplococcus; (F) Staphylococcus.

Calibration bar = 1 μm (A, D, E, F); 10 μm (B, C)

Fig 14. Bar graphs representing the proportion of scanning electron microscopy (SEM) fields in the different experimental groups with no bacteria, with planktonic bacteria, with both planktonic bacteria and biofilm, and only with biofilm. For each rat, observations were made on 20 random SEM fields at 7500X magnification on each of the two catheter segments, or, when only one catheter segment could be retrieved, on 40 random SEM fields of that catheter segment.

Horizontal lines in the upper portion of the figure indicate statistically significant differences between groups ($p<0.05$).

Error bars indicate 95% confidence intervals.

**, $p<0.01$

***, $p<0.001$

Fig 15. Typical scanning electron microscopy images of the surface of catheters showing multiple features of leucocyte morphology and interaction with the surrounding environment. (A) Low magnification view of the surface of the catheter showing giant leucocytes interspersed with smaller leucocytes. (B) Leucocyte engulfing a *Pseudomonas aeruginosa* cell in the area highlighted with the interrupted line box; on the top right corner of the picture there is a higher amplification view of this interaction. (C) Leucocyte adhering to the catheter's surface. (D) A leucocyte phagocytosing a region with biofilm. (E) and (F) leucocytes interacting on the surface of the catheter (dotted boxes highlight amplified views of these interactions). (G) Large leucocyte engulfing adjacent biofilm. (H) In the central portion of the image there is a large leucocyte extending a pseudopod into adjacent *P. aeruginosa*. (I) Three leucocytes with multiple vesicles on their surface.

Calibration bar = 100 μm (A); 1 μm (B); 10 μm (C to I).

Fig 16. Graphic representation of the relation between the proportion of flap necrosis (expressed as percentage of flap's initial area) and bacterial counts after flap biopsy on the third day after surgery in the different experimental groups.

On the third postoperative day, flap necrosis and bacterial counts were lower in the animals expressing human β-defensins 2 and 3.

Error bars indicate 95% confidence intervals.

Fig 17. Graphic representation of the relation between the proportion of flap necrosis (expressed as percentage of flap's initial area) and bacterial counts after flap biopsy on the seventh day after surgery in the different experimental groups.

On the seventh postoperative day, flap necrosis and bacterial counts were lower in the animals expressing human β-defensins 2 and 3.

Error bars indicate 95% confidence intervals.

Figure 1

Click here to download Figure Figure 1.tif

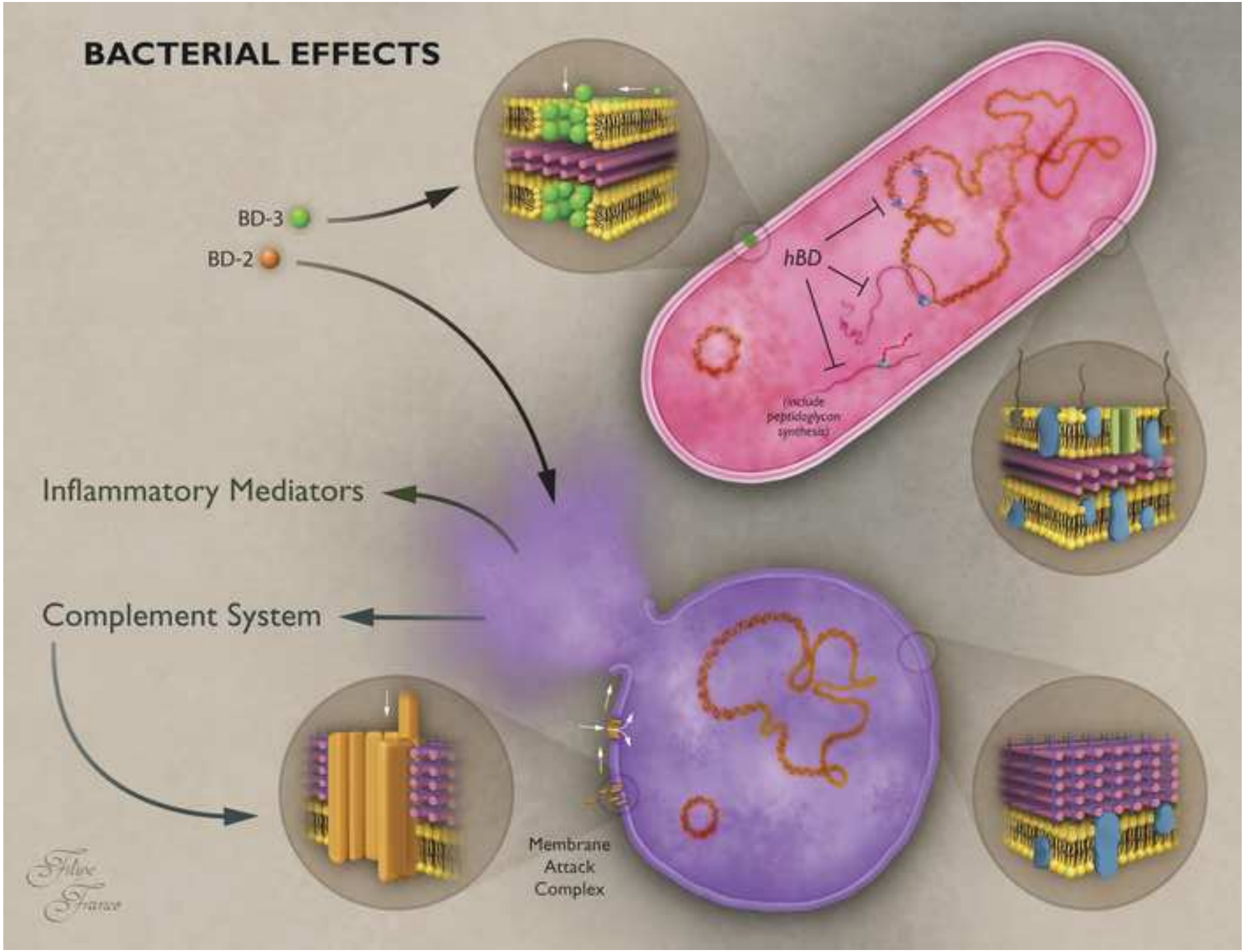

Figure 2

Click here to download Figure Figure 2.tif

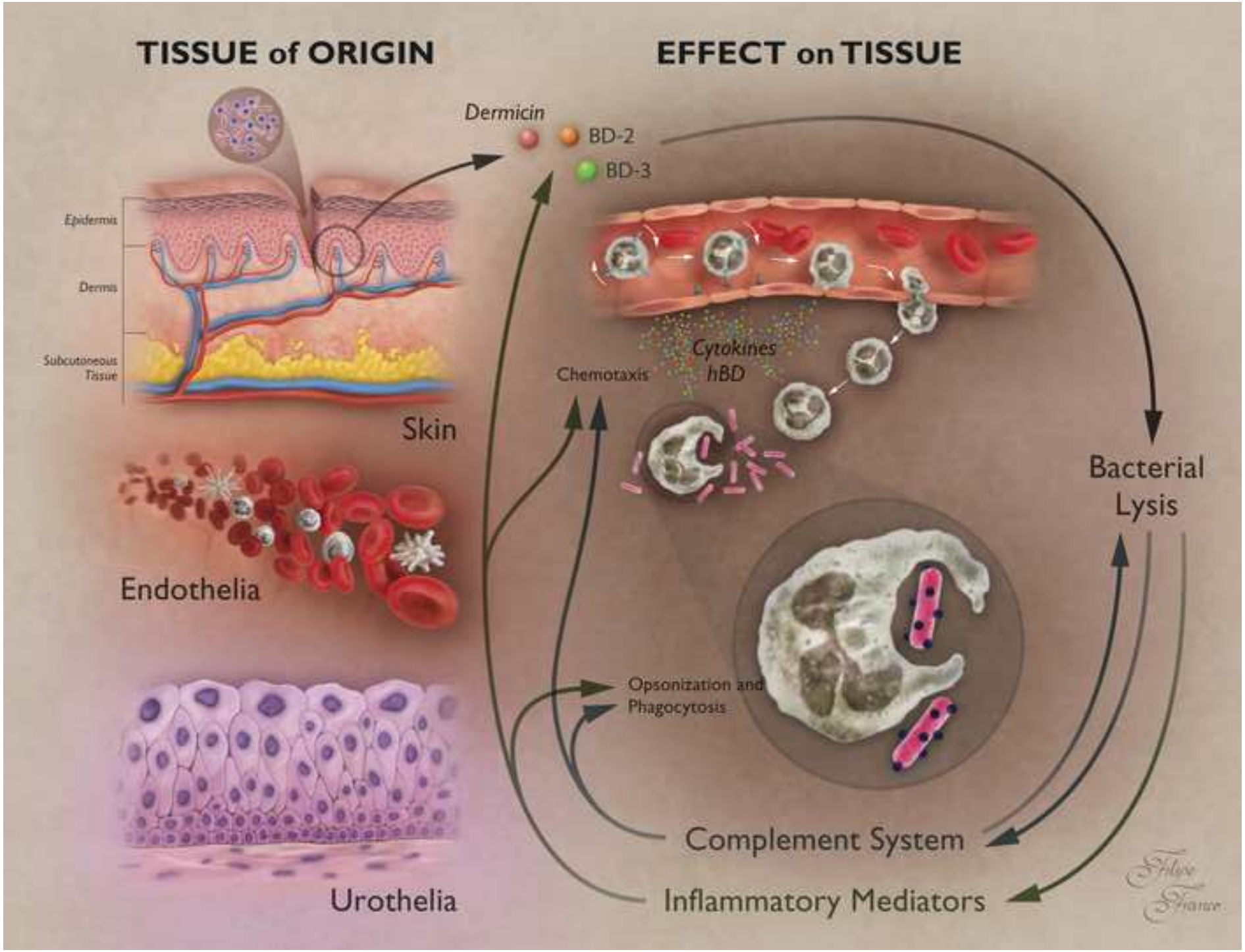

Figure 3

Click here to download Figure Figure 3.tif

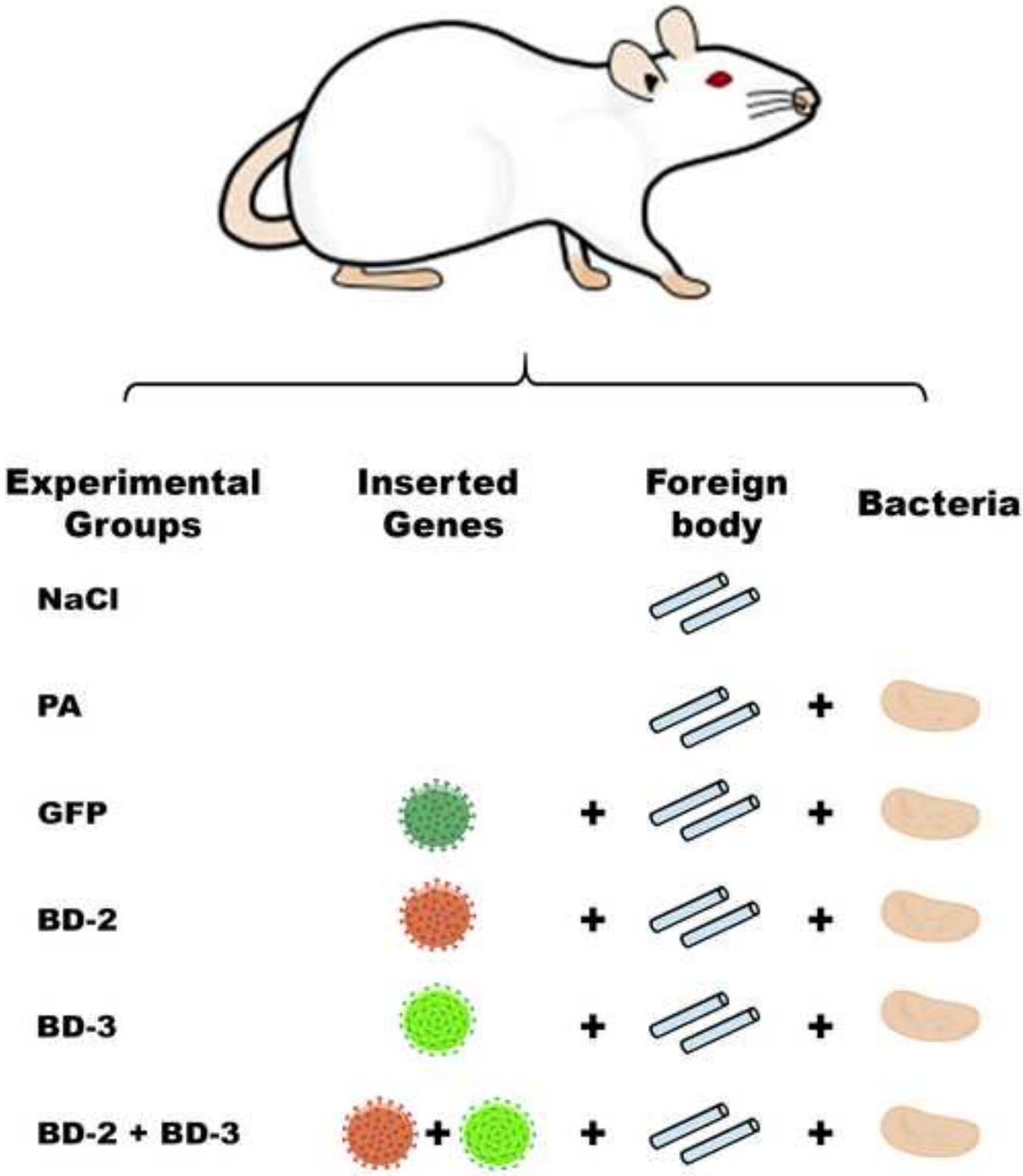

Figure 4

Click here to download Figure Figure 4.tif

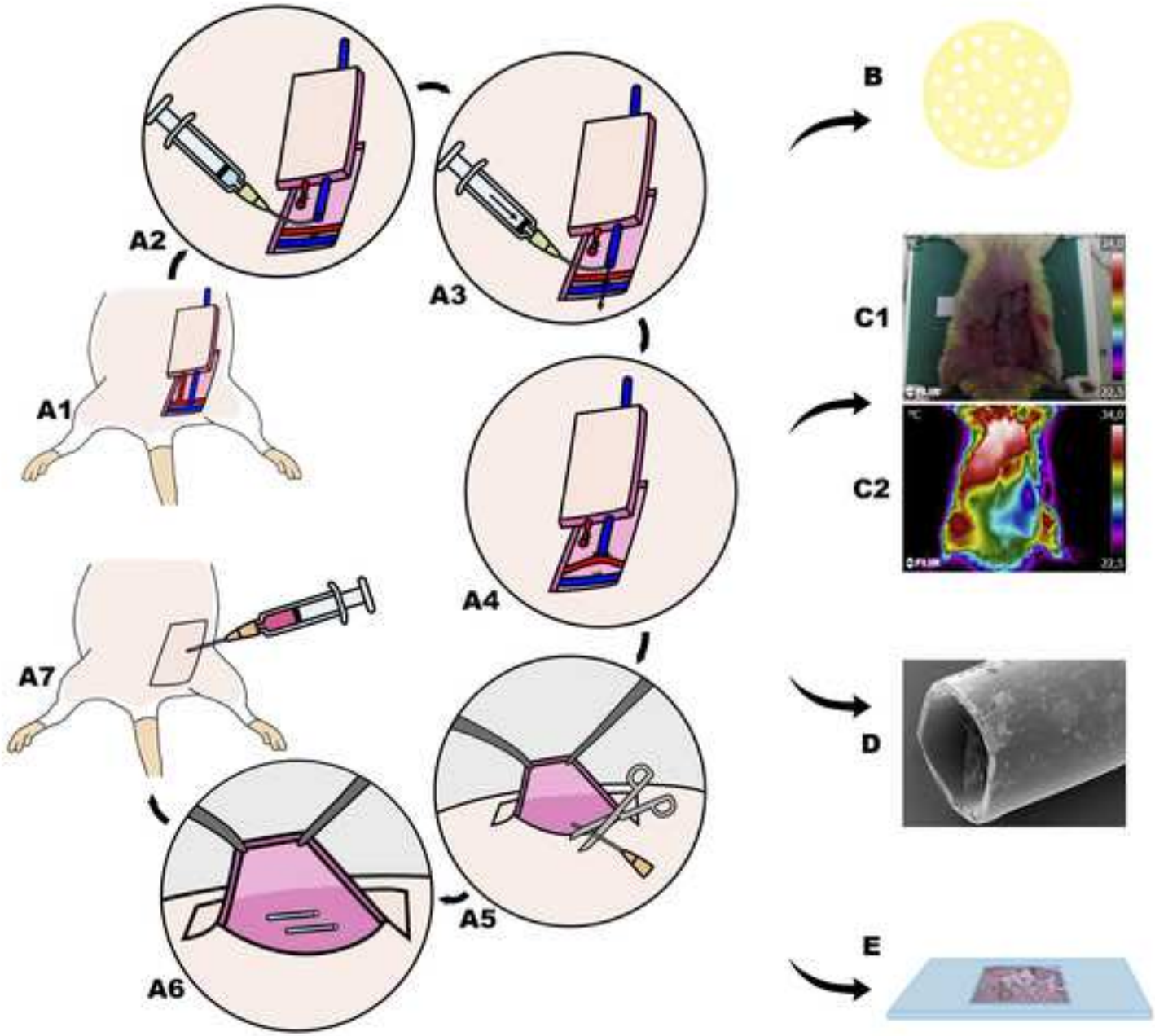

Figure 5

Click here to download Figure Figure 5.tif

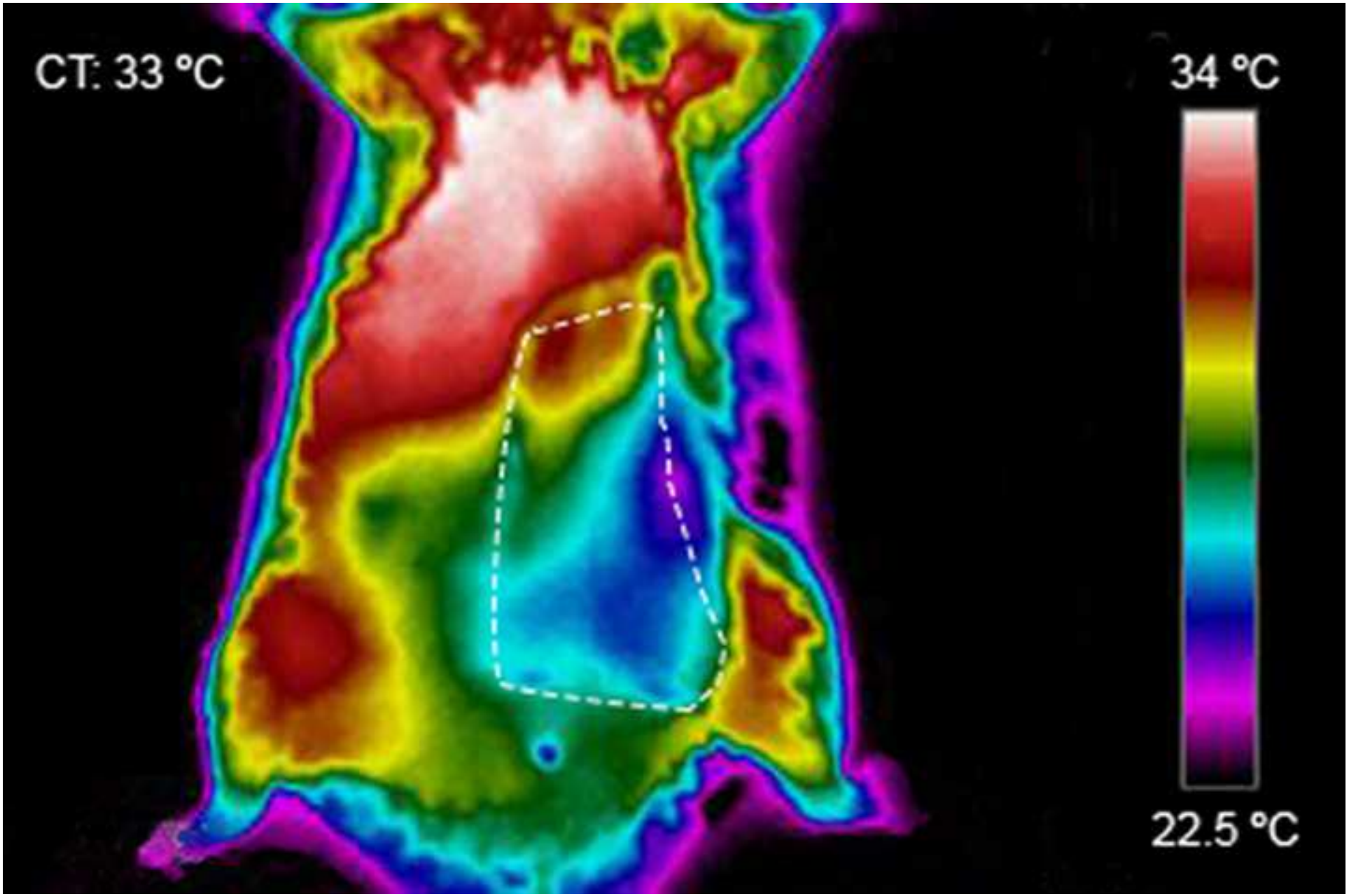

Figure 6

Click here to download Figure Figure 6.tif

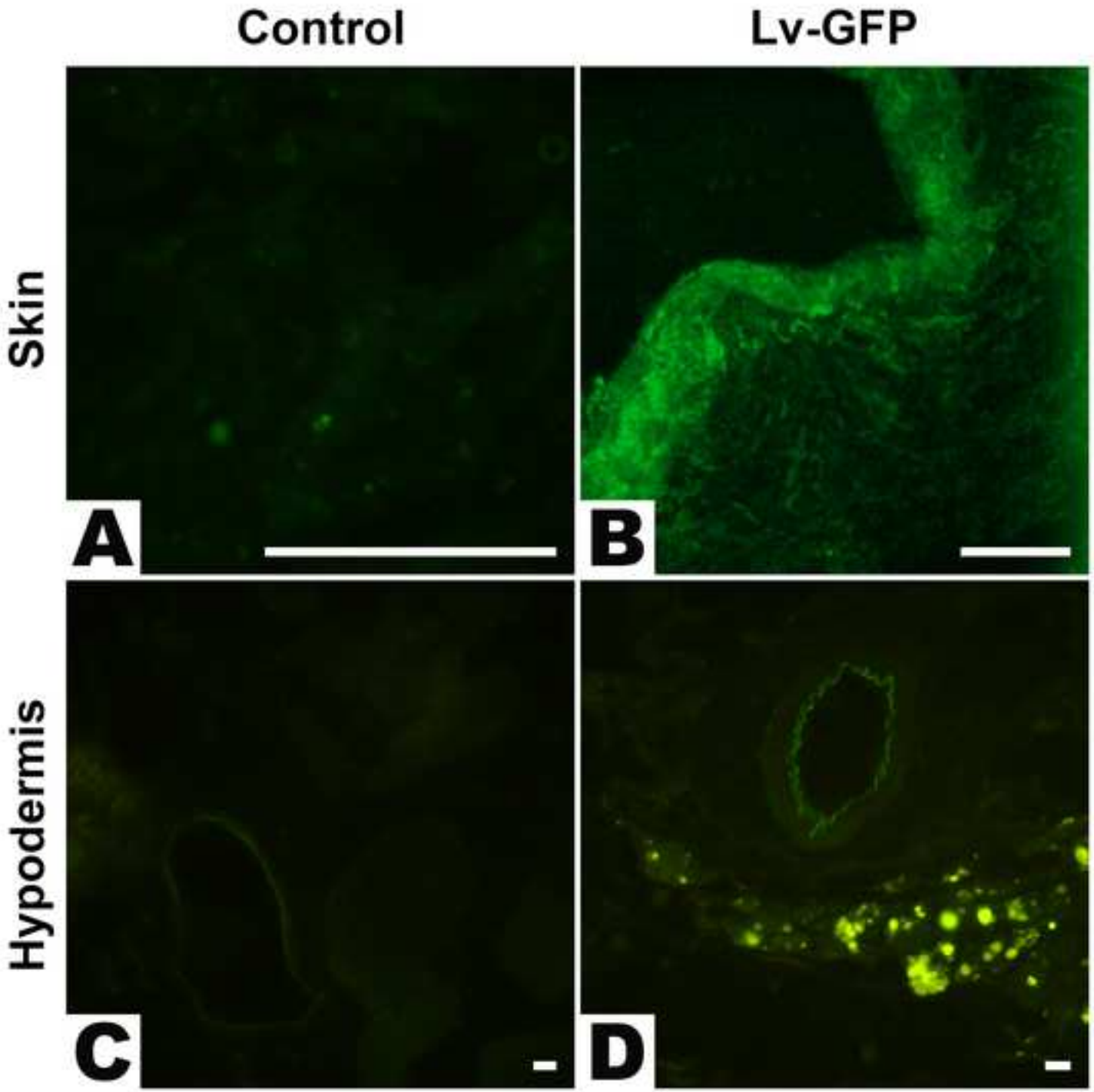

Figure 7

Click here to download Figure Figure 7.tif

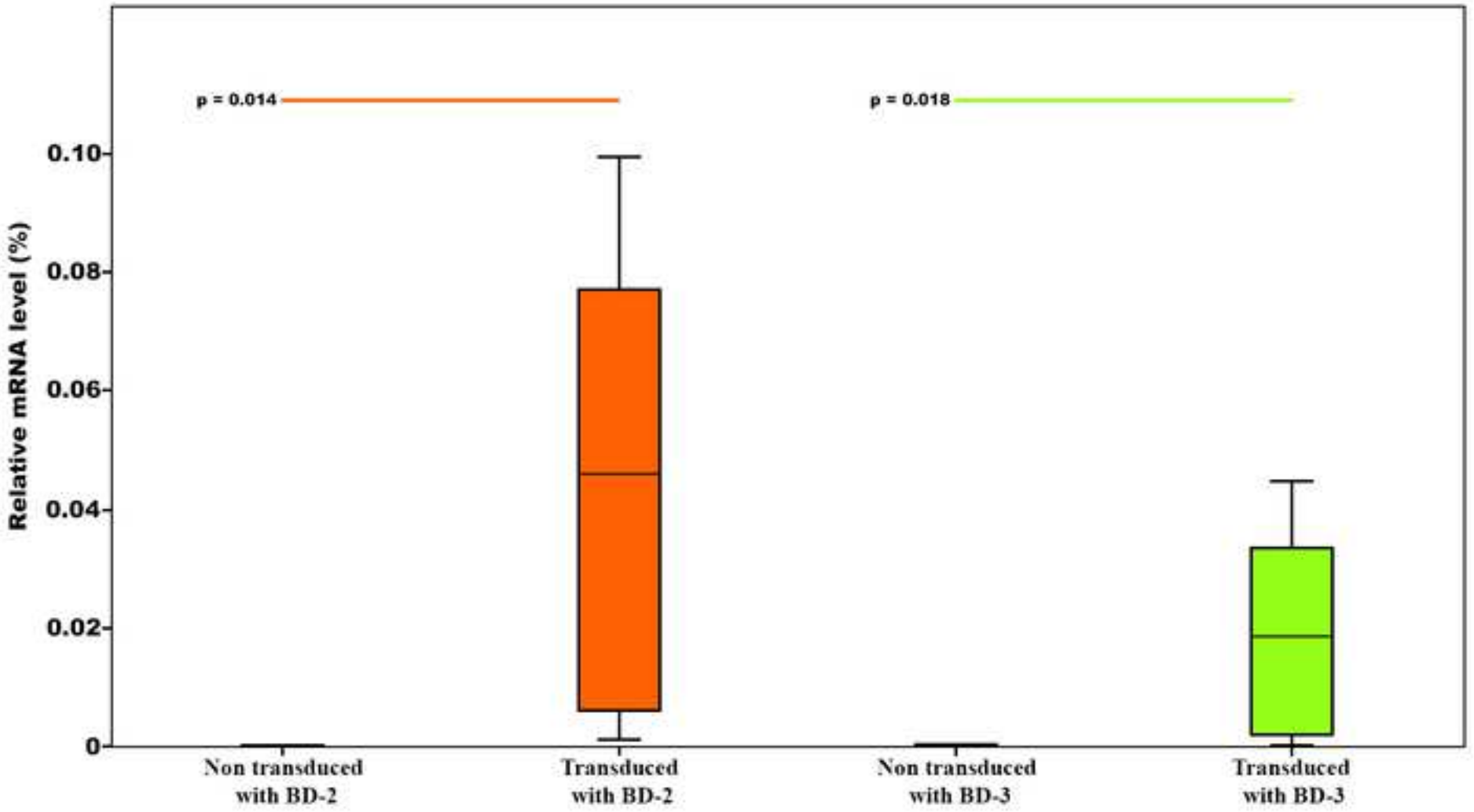

Figure 8

Click here to download Figure Figure 8.tif

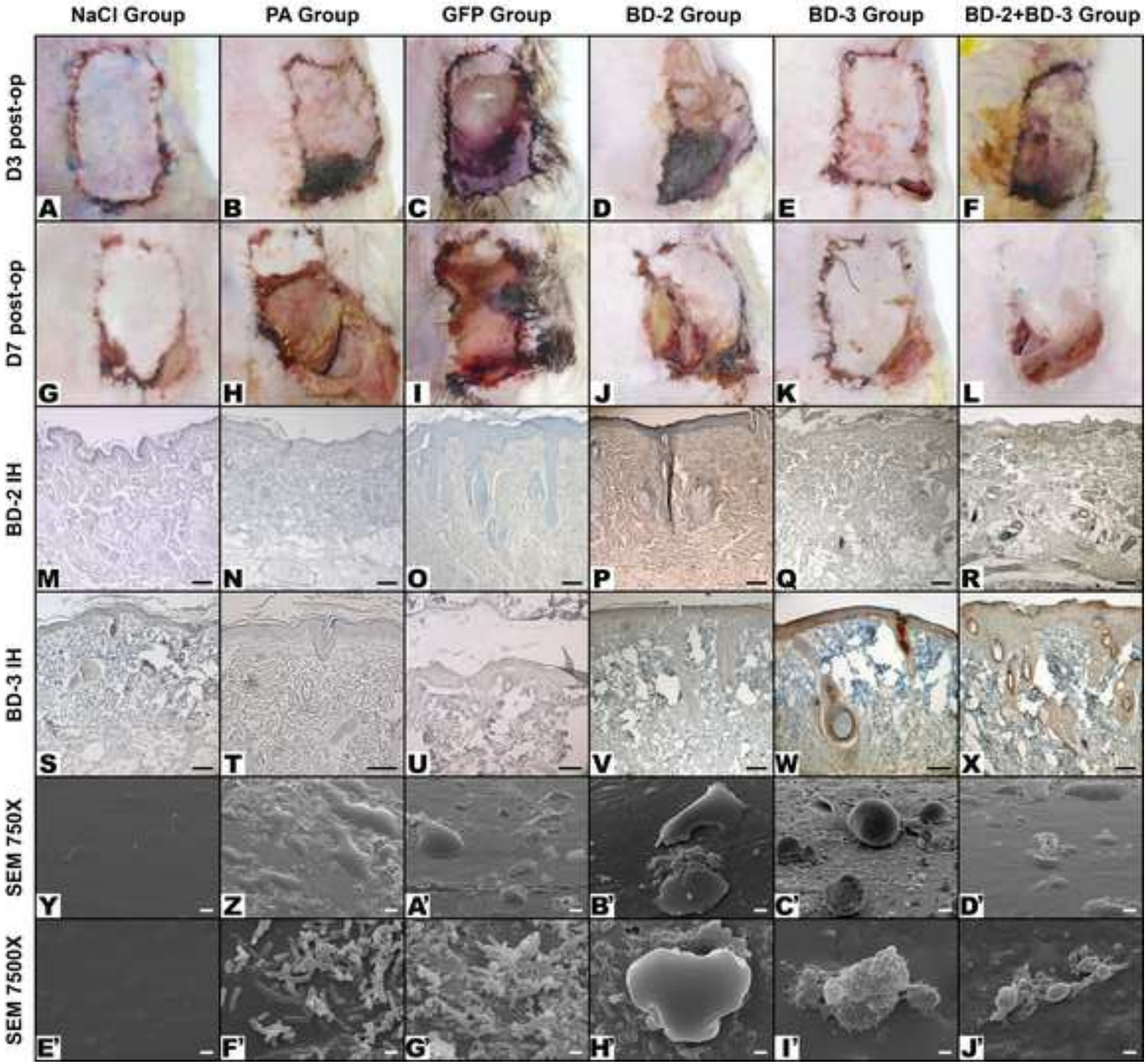

Figure 9

Click here to download Figure Figure 9.tif

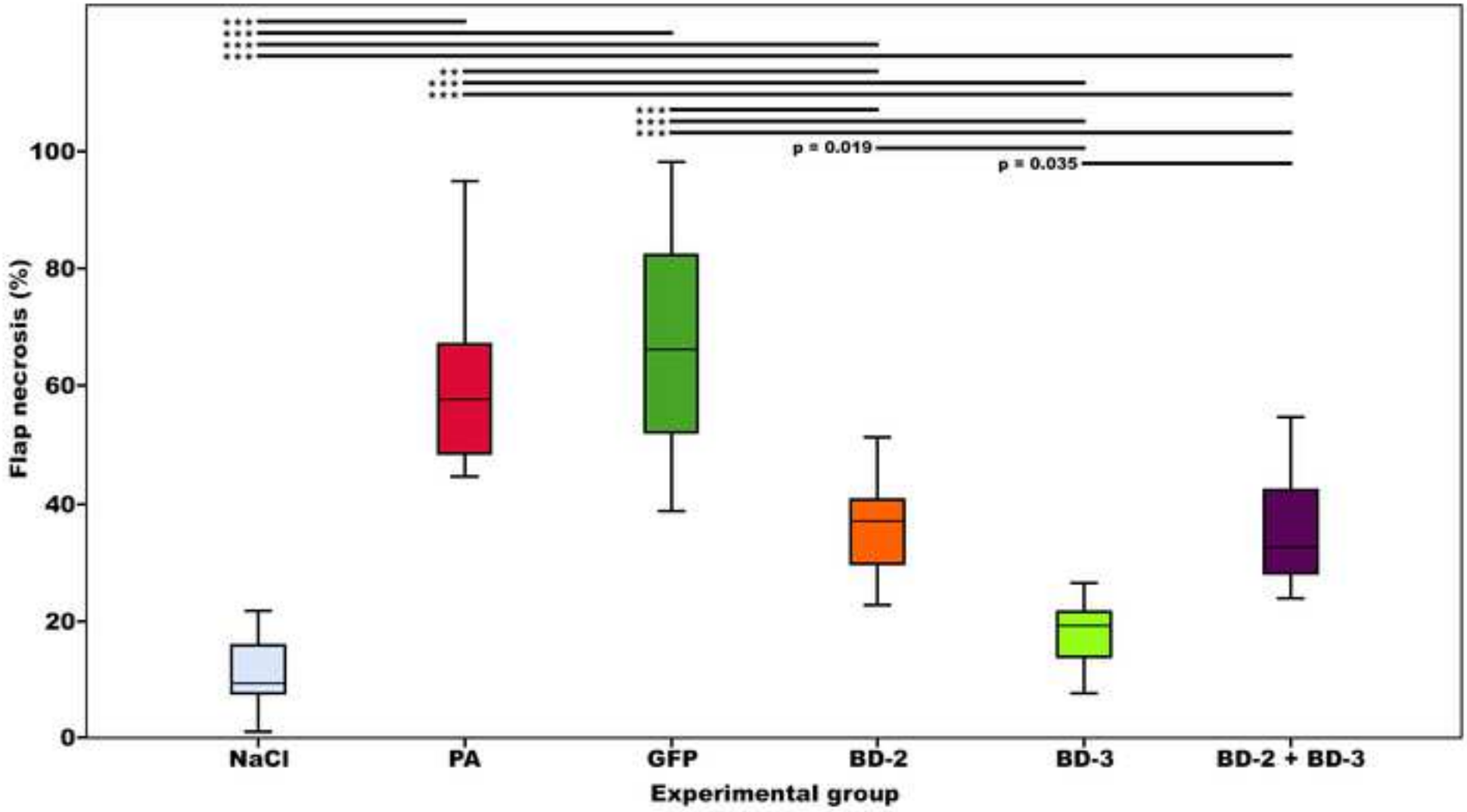

Figure 10

Click here to download Figure Figure 10.tif

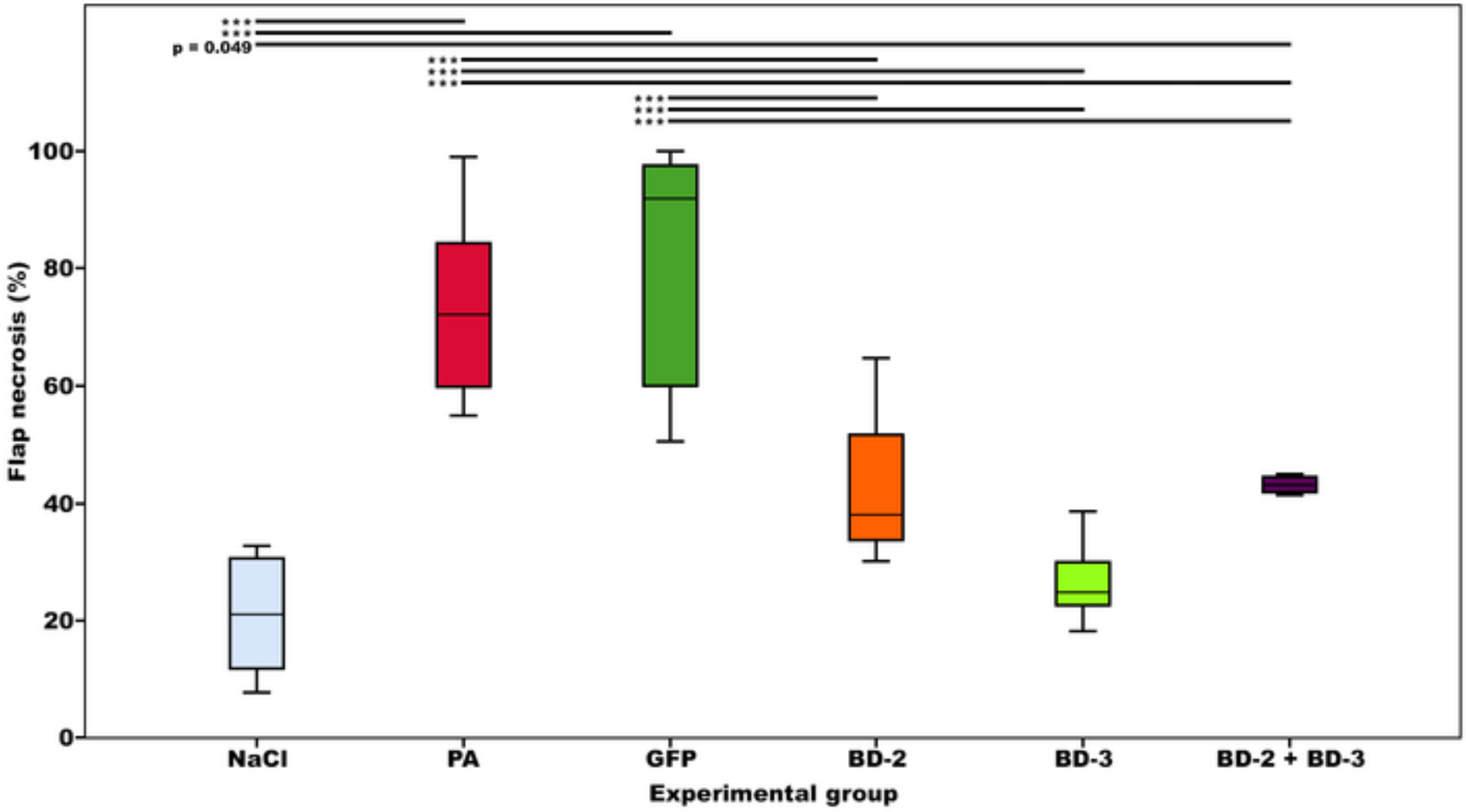

Figure 11

Click here to download Figure Figure 11.tif

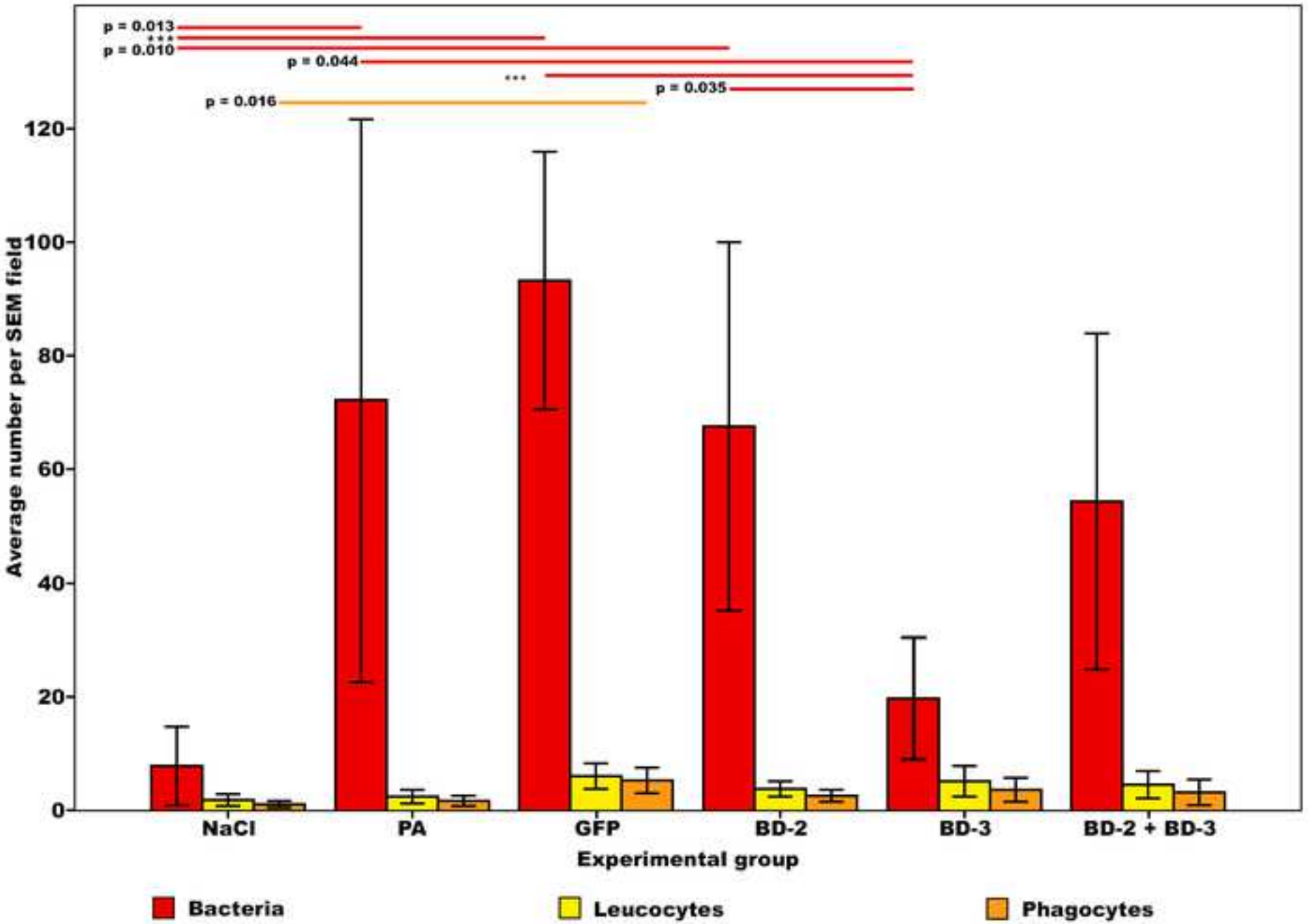

Figure 12

Click here to download Figure Figure 12.tif

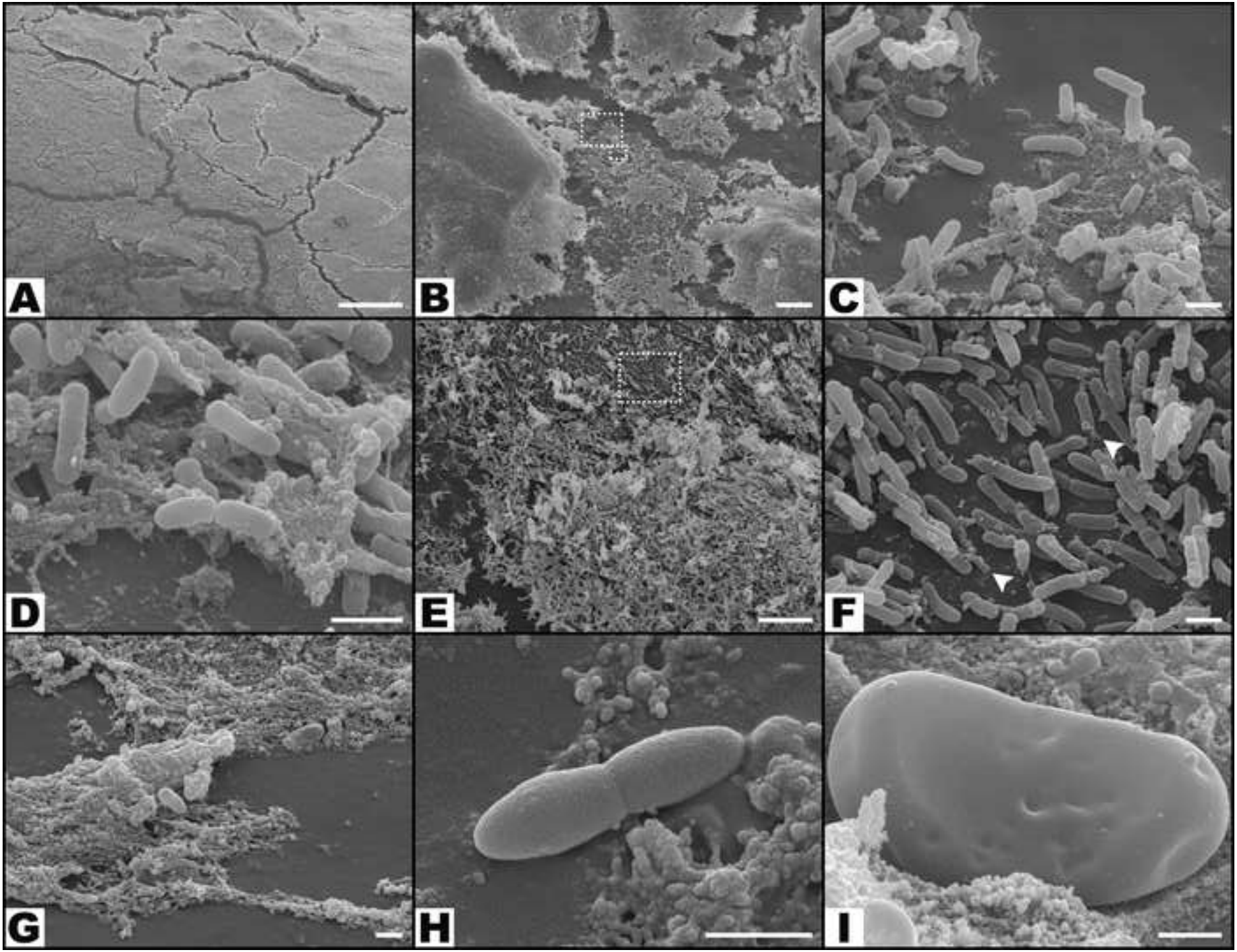

Figure 13

Click here to download Figure Figure 13.tif

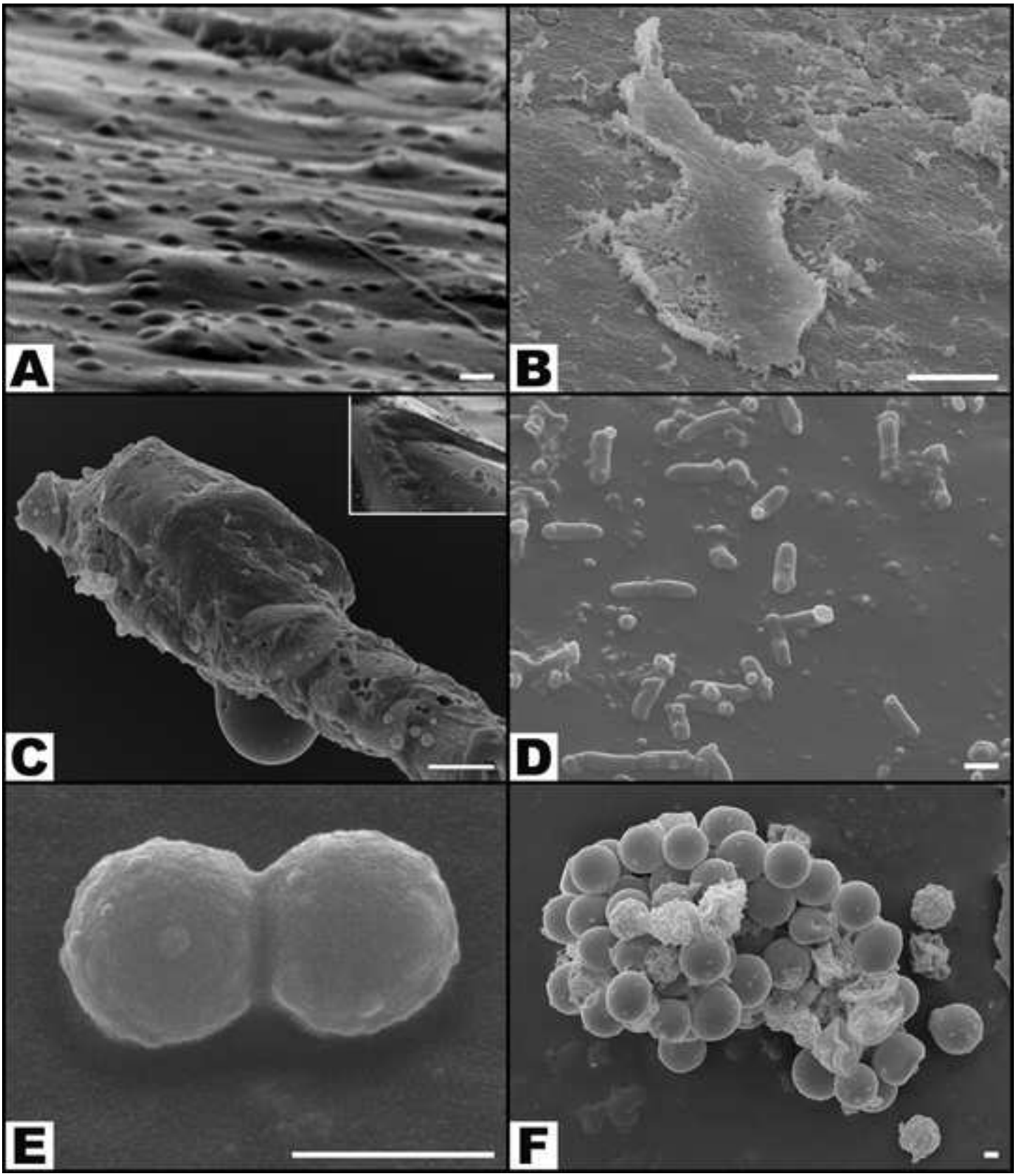

Figure 14

Click here to download Figure Figure 14.tif

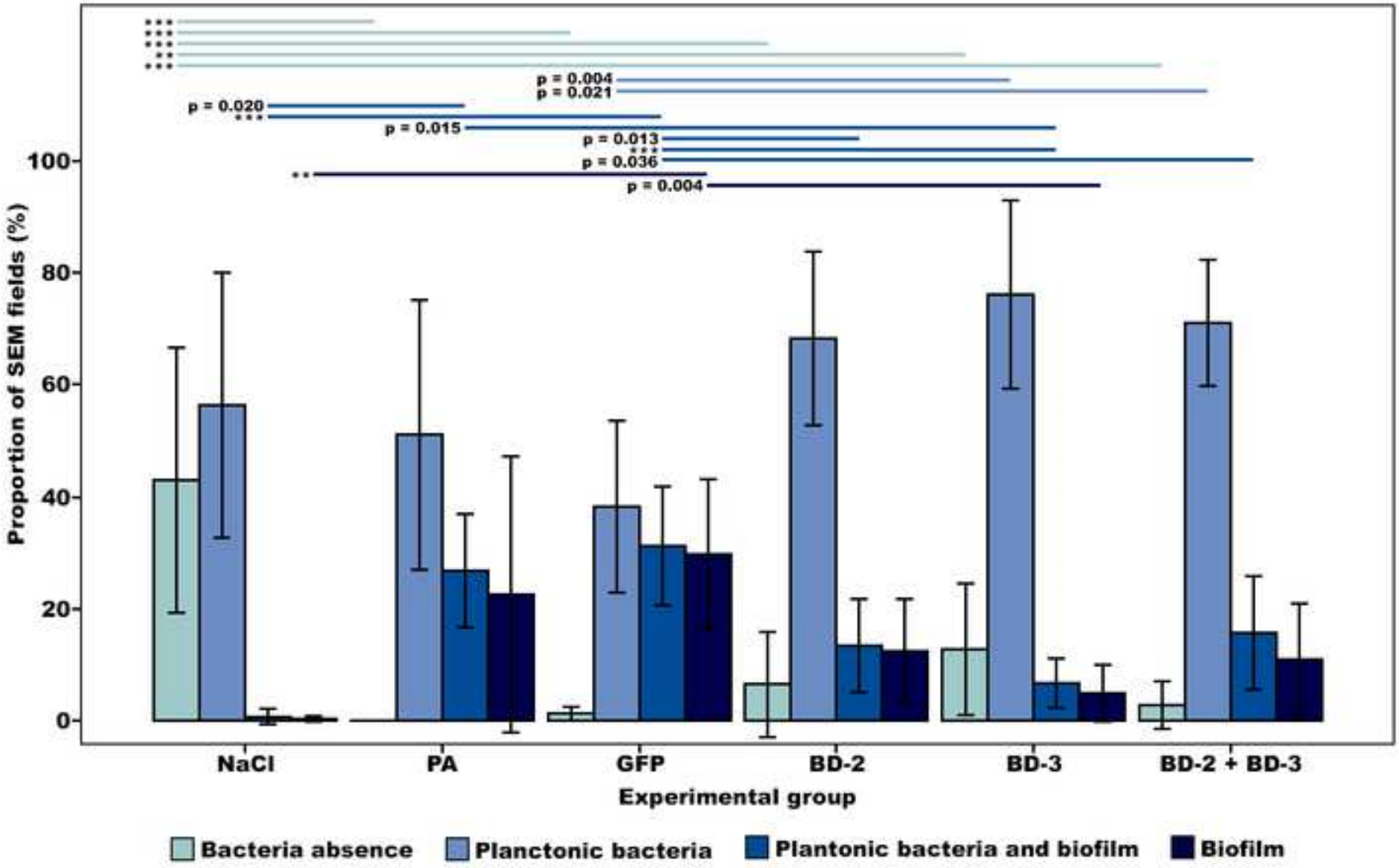

Figure 15

Click here to download Figure Figure 15.tif

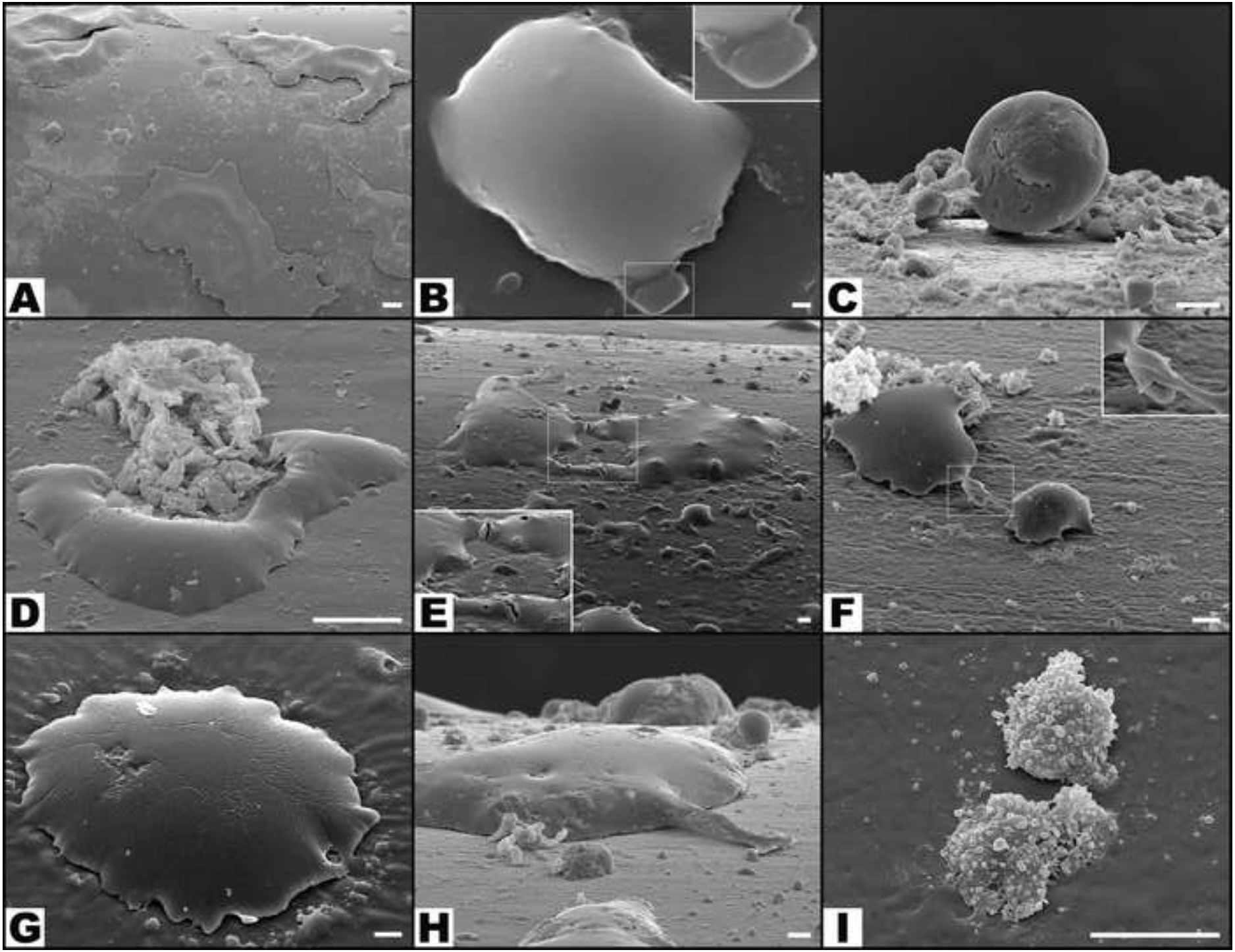

Figure 16

Click here to download Figure Figure 16.tif

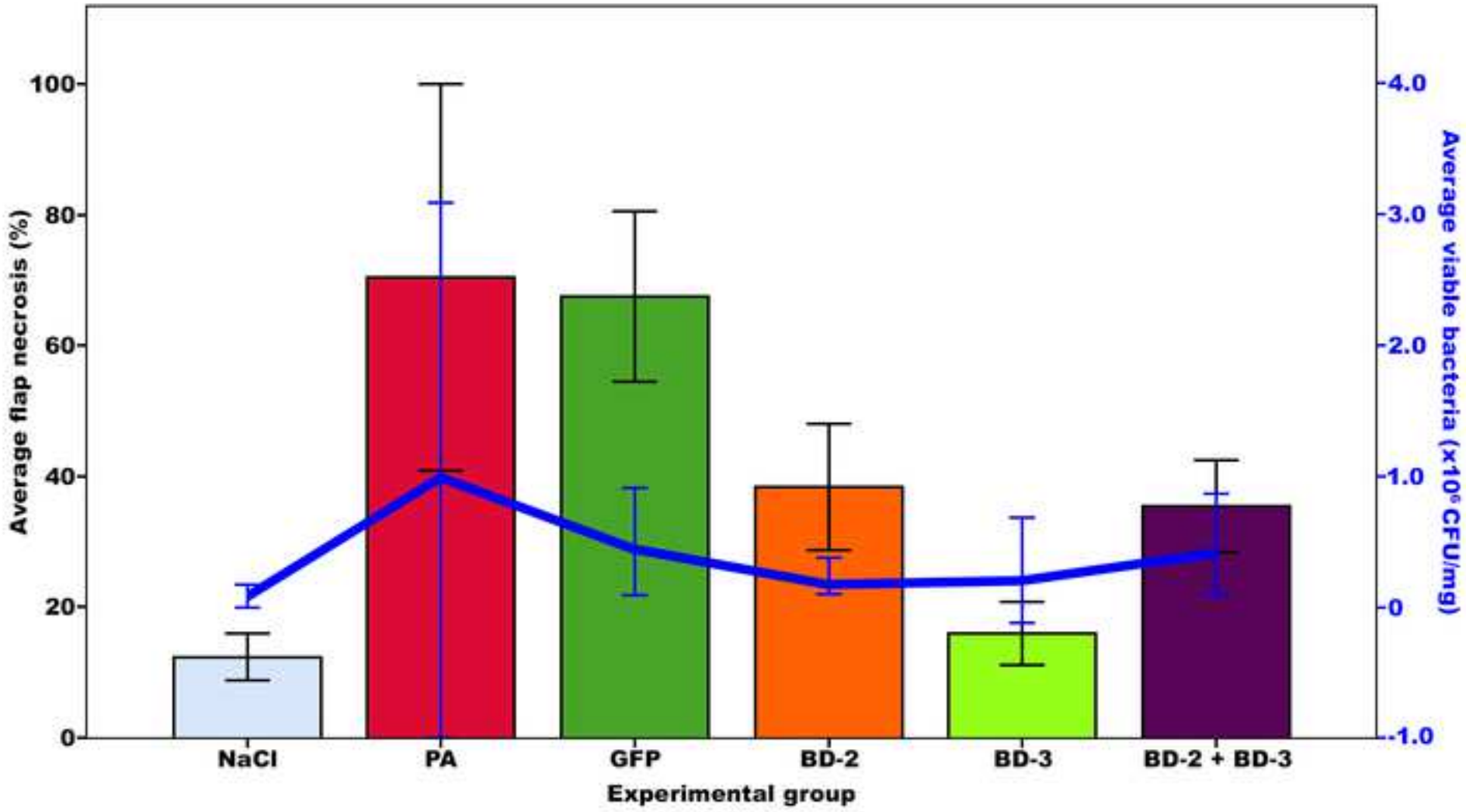

Figure 17

Click here to download Figure Figure 17.tif

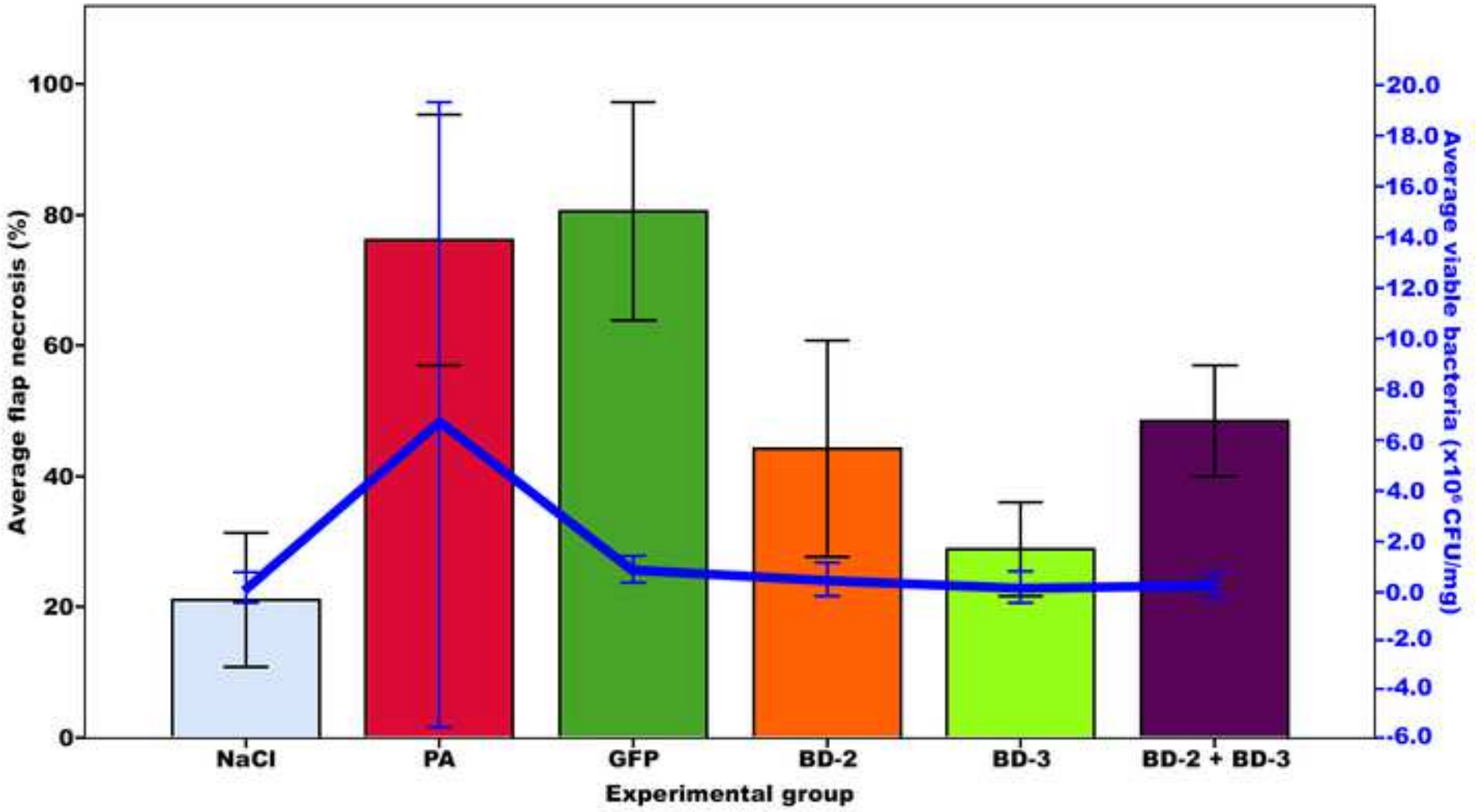

APPENDIX 8

PLOS ONE

Reconstruction of a 10-mm-long median nerve gap in an ischemic environment using autologous conduits with different patterns of blood supply: a comparative study in the rat

--Manuscript Draft--

Manuscript Number:	
Article Type:	Research Article
Full Title:	Reconstruction of a 10-mm-long median nerve gap in an ischemic environment using autologous conduits with different patterns of blood supply: a comparative study in the rat
Short Title:	Median nerve reconstruction in an ischemic environment
Corresponding Author:	Diogo Casal, M.D. Universidade Nova de Lisboa Faculdade de Ciencias Medicas Lisbon, PORTUGAL
Keywords:	Peripheral nerve; injury; surgery; reconstruction; repair; graft; flap; ischemia; blood supply.
Abstract:	The aim of this study was to evaluate in the Wistar rat the efficacy of various autologous nerve conduits with various forms of blood supply in reconstructing a 10-mm-long gap in the median nerve (MN) under conditions of local ischemia. A 10-mm-long median nerve defect was created in the right arm. A loose silicone tube was placed around the nerve gap zone, in order to simulate a local ischemic environment. Rats were divided in the following experimental groups (each with 20 rats): the nerve Graft (NG) group, in which the excised MN segment was reattached; the conventional nerve flap (CNF) and the arterialized neurovenous flap (ANVF) groups in which the gap was bridged with homonymous median nerve flaps; the prefabricated nerve flap (PNF) group in which the gap was reconstructed with a fabricated flap created by leaving an arteriovenous fistula in contact with the sciatic nerve for 5 weeks; and the two control groups, Sham and Excision groups. In the latter group, the proximal stump of the MN nerve was ligated and no repair was performed. The rats were followed for 100 days. During this time, they did physiotherapy. Functional, electroneuromyographic and histological studies were performed. The CNF and ANVF groups presented better results than the NG group in the following assessments: grasping test, nociception, motor stimulation threshold, muscle weight, and histomorphometric evaluation. Radial deviation of the operated forepaw was more common in rats that presented worse results in the other outcome variables. Overall, CNFs and ANVFs produced a faster and more complete recovery than NGs in the reconstruction of a 10-mm-long median nerve gap in an ischemic environment in the Wistar rat. Although, results obtained with CNFs were in most cases were better than ANVFs, these differences were not statistically significant for most of the outcome variables.
Order of Authors:	Diogo Casal, M.D.
	Eduarda Mota-Silva
	Inês Iria
	Sara Alves
	Ana Farinho
	Cláudia Pen
	Nuno Lourenço-Silva
	Luis Mascarenhas-Lemos
	Jose Silva-Ferreira
	Mário Ferraz-Oliveira

	Valentina Vassilenko
	Paula Alexandra Videira
	João Goyri-O'Neill
	Diogo Pais
Opposed Reviewers:	
Additional Information:	
Question	**Response**
Financial Disclosure Please describe all sources of funding that have supported your work. **This information is required for submission and will be published with your article, should it be accepted.** A complete funding statement should do the following: Include **grant numbers and the URLs** of any funder's website. Use the full name, not acronyms, of funding institutions, and use initials to identify authors who received the funding. **Describe the role** of any sponsors or funders in the study design, data collection and analysis, decision to publish, or preparation of the manuscript. If the funders had **no role** in any of the above, include this sentence at the end of your statement: "*The funders had no role in study design, data collection and analysis, decision to publish, or preparation of the manuscript*." However, if the study was **unfunded**, please provide a statement that clearly indicates this, for example: "*The author(s) received no specific funding for this work*." * typeset	One of the authors (D.C.) received a grant from “The Programme for Advanced Medical Education” sponsored by “Fundação Calouste Gulbenkian, Fundação Champalimaud, Ministério da Saúde and Fundação para a Ciência e Tecnologia, Portugal.” The authors have no financial or commercial interests to declare in relation to the content of this article.
Competing Interests You are responsible for recognizing and disclosing on behalf of all authors any competing interest that could be perceived to bias their work, acknowledging all financial support and any other relevant financial or non-financial competing interests. Do any authors of this manuscript have competing interests (as described in the PLOS Policy on Declaration and	The authors have declared that no competing interests exist.

Evaluation of Competing Interests)? **If yes**, please provide details about any and all competing interests in the box below. Your response should begin with this statement: *I have read the journal's policy and the authors of this manuscript have the following competing interests:* **If no** authors have any competing interests to declare, please enter this statement in the box: "*The authors have declared that no competing interests exist.*" * typeset	
Ethics Statement You must provide an ethics statement if your study involved human participants, specimens or tissue samples, or vertebrate animals, embryos or tissues. All information entered here should **also be included in the Methods section** of your manuscript. Please write "N/A" if your study does not require an ethics statement. **Human Subject Research (involved human participants and/or tissue)** All research involving human participants must have been approved by the authors' Institutional Review Board (IRB) or an equivalent committee, and all clinical investigation must have been conducted according to the principles expressed in the Declaration of Helsinki. Informed consent, written or oral, should also have been obtained from the participants. If no consent was given, the reason must be explained (e.g. the data were analyzed anonymously) and reported. The form of consent (written/oral), or reason for lack of consent, should be indicated in the Methods section of your manuscript. Please enter the name of the IRB or Ethics Committee that approved this study in the space below. Include the approval number and/or a statement indicating approval of this research.	All in vivo studies involving rats were carried out in strict accordance with or exceeding the recommendations in the Guide for Proper Conduct of Animal Experiments and Related Activities in Academic Research and Technology. The experimental protocol was approved by the Institutional Animal Care and Use Committee and Ethical Committee at the authors' institution (CEFCM/08/2012).

Animal Research (involved vertebrate animals, embryos or tissues) All animal work must have been conducted according to relevant national and international guidelines. If your study involved non-human primates, you must provide details regarding animal welfare and steps taken to ameliorate suffering; this is in accordance with the recommendations of the Weatherall report, "The use of non-human primates in research." The relevant guidelines followed and the committee that approved the study should be identified in the ethics statement. If anesthesia, euthanasia or any kind of animal sacrifice is part of the study, please include briefly in your statement which substances and/or methods were applied. Please enter the name of your Institutional Animal Care and Use Committee (IACUC) or other relevant ethics board, and indicate whether they approved this research or granted a formal waiver of ethical approval. Also include an approval number if one was obtained. **Field Permit** Please indicate the name of the institution or the relevant body that granted permission.	
Data Availability PLOS journals require authors to make all data underlying the findings described in their manuscript fully available, without restriction and from the time of publication, with only rare exceptions to address legal and ethical concerns (see the PLOS Data Policy and FAQ for further details). When submitting a manuscript, authors must provide a Data Availability Statement that describes where the data underlying their manuscript can be found. Your answers to the following constitute your statement about data availability and will be included with the article in the event of publication. **Please note that simply stating 'data available on request from the author' is not acceptable.** ***If,***	Yes - all data are fully available without restriction

however, your data are only available upon request from the author(s), you must answer "No" to the first question below, and explain your exceptional situation in the text box provided. Do the authors confirm that all data underlying the findings described in their manuscript are fully available without restriction?	
Please describe where your data may be found, writing in full sentences. **Your answers should be entered into the box below and will be published in the form you provide them, if your manuscript is accepted.** If you are copying our sample text below, please ensure you replace any instances of XXX with the appropriate details. If your data are all contained within the paper and/or Supporting Information files, please state this in your answer below. For example, "All relevant data are within the paper and its Supporting Information files." If your data are held or will be held in a public repository, include URLs, accession numbers or DOIs. For example, "All XXX files are available from the XXX database (accession number(s) XXX, XXX)." If this information will only be available after acceptance, please indicate this by ticking the box below. If neither of these applies but you are able to provide details of access elsewhere, with or without limitations, please do so in the box below. For example: "Data are available from the XXX Institutional Data Access / Ethics Committee for researchers who meet the criteria for access to confidential data." "Data are from the XXX study whose authors may be contacted at XXX." * typeset	All data is fully availabe in the manuscriot.
Additional data availability information:	

Dear Professor Hagen Andruszkow
Editor of the *PLOS One*,

We take the liberty of submitting the manuscript of a paper entitled "***Reconstruction of a 10-mm-long median nerve gap in an ischemic environment using autologous conduits with different patterns of blood supply: a comparative study in the rat***" for publication in the ***PLOS One***.

To this day, few injuries create as much angst in both patients and doctors as the loss of neurological function. The patient must deal with paralysis, paresthesias, pain, and a prolonged and uncertain recovery. In fact, despite numerous surgical and technical developments, the results with peripheral nerve repair are still disappointing.[1-3] The available therapeutic options are complex, technically demanding, often unfulfilling, and frustratingly unpredictable.[4] Results are particularly unsatisfactory in cases of long nerve defects and in the presence of local ischemia. In these circumstances, it is frequent not to obtain useful recovery in the involved nerve territory.[1-3] **One of the longest debates in this field is the role of vascularized nerve grafts (i.e. nerve flaps) in the context of peripheral nerve defects associated with ischemia**.[5-8] Apparently, nerve flaps would be superior to nerve grafts. However, they are difficult to raise, adding substantially to the technically difficulty of the surgery.[9] Moreover, only a few options for tailoring nerve flaps exist.[5, 6, 8] Furthermore, while some authors have reported better results with nerve grafts than nerve flaps [8, 10, 11], others have found no significant differences.[7, 8]

Overall, no conclusive evidence exists to settle this debate. This is due to the fact that different researchers have used different animal species, anatomical regions, reconstructive strategies and follow-up times. Furthermore, authors have also used variable outcome variables to assess nerve regeneration. These methodological differences make information synthesis difficult.[7] Finally, even though there are a few side-to-side comparisons of different gap reconstruction methods in the rat hindlimb, using the sciatic nerve, as far as the authors could determine, there is no similar study using the rat forelimb.[10, 12, 13] This is unfortunate, since clinically most peripheral nerve lesions occur in the upper extremity.[3, 7, 14]

Therefore, **the aim of this study was to evaluate in the Wistar rat the efficacy of various autologous nerve conduits with various forms of blood**

supply in reconstructing a 10-mm-long gap in the median nerve (MN) under conditions of local ischemia.

A 10-mm-long median nerve defect was created in the right arm. A loose silicone tube was placed around the nerve gap zone, in order to simulate a local ischemic environment. Rats were divided in the following experimental groups (each with 20 rats): nerve Graft (**NG**) group, in which the excised MN segment was reattached; conventional nerve flap (**CNF**) and arterialized neurovenous flap (**ANVF**) groups in which the gap was bridged with homonymous median nerve flaps; prefabricated nerve flap (**PNF**) group in which the gap was reconstructed with a fabricated flap created by leaving an arteriovenous fistula in contact with the sciatic nerve for 5 weeks; and the two control groups, **Sham** and **Excision** groups. In the latter group, the proximal stump of the MN nerve was ligated and no repair was performed. The rats were followed for 100 days. During this time, a series of devices were used to simulate physiotherapy. A thorough battery of functional, electroneuromyographic and histological studies was performed.

Overall, CNFs and ANVFs produced a faster and more complete recovery than NGs in the reconstruction of a 10-mm-long median nerve gap in an ischemic environment in the Wistar rat. Although results obtained with CNFs were in most cases better than those of ANVFs, these differences were not statistically significant for most of the outcome variables.

Additionally, to the best of the authors' knowledge, this is the largest series in the literature comparing different autologous techniques of MN gap reconstruction in the rat, in the presence of local ischemia.[15-17]

All this data suggest that **nerve flaps may be superior options to the traditionally used NGs for bridging peripheral nerve defects in the upper limb in the presence of local ischemia**, as occurs after major trauma, and/or radiotherapy, and/or in the presence of limb ischemia. This information is unquestionably of great clinical interest.

Another interesting finding of this study was the identification of radial deviation in forepaw prints of the rats with poorer outcomes in the following variables: FCR, maximal isometric flexion force, MN cross section area, total number of MN nerve fibers, and number of peripherin stained fibers. **Thus, radial deviation of forepaws imprints may be of interest as a surrogate marker of MN lesion.** The underlying mechanism for radial deviation may be the denervation of the intrinsic

muscles of the forepaw of the rat innervated by the MN, generating a situation similar to the median claw hand observed in humans.[18, 19] However, further studies are required to confirm or dismiss this hypothesis.

For all the these reasons, no doubt, this paper contributes to broaden the knowledge on peripheral nerve repair. Moreover, all this data is highly pertinent for anyone with an interest in upper limb surgery, neurosurgery, reconstructive surgery and/or peripheral nerve repair.

Hence, we strongly believe that this paper is of significant value to a broad audience including the readership of ***PLOS One*** and thus deserves publication.

If you have any doubts or queries, please do not hesitate to contact us.
Thank you so much for your kind attention.

The authors

References

1. Desouches C, Alluin O, Mutaftschiev N, Dousset E, Magalon G, Boucraut J, et al. [Peripheral nerve repair: 30 centuries of scientific research]. Revue neurologique. 2005;161(11):1045-59. Epub 2005/11/17. PubMed PMID: 16288170.
2. Boyd KU, Fox IK. Nerve repair and grafting. In: Mackinnon SE, editor. Nerve surgery. 1. First ed. New York: Thieme; 2015. p. 75-100.
3. Wood MJ, Johnson PJ, Myckatyn TM. Anatomy and physiology for the peripheral nerve surgeon. In: Mackinnon SE, Yee A, editors. Nerve Surgery. 1. First ed. New York: Thieme; 2015. p. 1-40.
4. Dy CJ, Isaacs J. Preface. In: Dy CJ, Isaacs J, editors. American Society for Surgery of the Hand surgical anatomy: nerve reconstruction. 1. First ed. Chicago, USA: American Society for Surgery of the Hand; 2017. p. xi.
5. Trehan SK, Model Z, Lee SK. Nerve Repair and Nerve Grafting. Hand clinics. 2016;32(2):119-25. Epub 2016/04/21. doi: 10.1016/j.hcl.2015.12.002. PubMed PMID: 27094885.
6. Engin MS, Demirtas Y, Neimetzade T, Ayas B, Aksakal IA, Karacalar A. A vascularized nerve graft substitute generated in a chamber bioreactor-A preliminary report. Hand and Microsurgery. 2016;5(2):62-9.
7. Donzelli R, Capone C, Sgulo FG, Mariniello G, Maiuri F. Vascularized nerve grafts: an experimental study. Neurological research. 2016;38(8):669-77. doi: 10.1080/01616412.2016.1198527. PubMed PMID: 27349271.
8. D'Arpa S, Claes KEY, Stillaert F, Colebunders B, Monstrey S, Blondeel P. Vascularized nerve "grafts": just a graft or a worthwhile procedure? Plastic and Aesthetic Research. 2015;2(4):183-94.
9. Sabapathy SR, Venkatramani H. Harvest of extraplexal donor nerves for transfer or grafting. In: Dy CJ, Isaacs J, editors. American Society for Surgery of the Hand surgical anatomy: nerve reconstruction. 1. First ed. Chicago, USA: American Society for Surgery of the Hand; 2017. p. 161-86.
10. ANGÉLICA-ALMEIDA M, CASAL D, MAFRA M, MASCARENHAS-LEMOS L, SILVA E, FARINHO A, et al. Evaluation of the efficacy of different conduits to bridge a 10 millimeter defect in the rat sciatic nerve in the presence of an axial blood supply. Archives of Anatomy. 2014;2:8-30.
11. Giusti G, Lee JY, Kremer T, Friedrich P, Bishop AT, Shin AY. The influence of vascularization of transplanted processed allograft nerve on return of motor function in rats. Microsurgery. 2016;36(2):134-43. Epub 2015/01/06. doi: 10.1002/micr.22371. PubMed PMID: 25557845.
12. Giusti G, Willems WF, Kremer T, Friedrich PF, Bishop AT, Shin AY. Return of motor function after segmental nerve loss in a rat model: comparison of autogenous nerve graft, collagen conduit, and processed allograft (AxoGen). The Journal of bone and joint surgery American volume. 2012;94(5):410-7. Epub 2012/03/09. doi: 10.2106/jbjs.k.00253. PubMed PMID: 22398734.
13. Shin RH, Friedrich PF, Crum BA, Bishop AT, Shin AY. Treatment of a segmental nerve defect in the rat with use of bioabsorbable synthetic nerve conduits: a comparison of commercially available conduits. J Bone Joint Surg Am. 2009;91(1):2194-204.
14. Rosberg HEeLD. Epidemiology of hand injuries in a middle-sized city in southern Sweden - a retrospective study with an 8-year interval. Scand J Plast Rec Surg Hand Surg. 2004;(38):347-55.

15. Angius D, Wang H, Spinner RJ, Gutierrez-Cotto Y, Yaszemski MJ, Windebank AJ. A systematic review of animal models used to study nerve regeneration in tissue-engineered scaffolds. Biomaterials. 2012;33(32):8034-9. Epub 2012/08/15. doi: 10.1016/j.biomaterials.2012.07.056. PubMed PMID: 22889485; PubMed Central PMCID: PMCPMC3472515.
16. Evans GR. Peripheral nerve injury: a review and approach to tissue engineered constructs. Anat Rec. 2001;263(4):396-404.
17. Myckatyn TM, Mackinnon SE. A review of research endeavors to optimize peripheral nerve reconstruction. Neurol Res. 2004;26(1):124-38.
18. Kilinc A, Ben Slama S, Dubert T, Dinh A, Osman N, Valenti P. [Results of primary repair of injuries to the median and ulnar nerves at the wrist]. Chirurgie de la main. 2009;28(2):87-92. Epub 2009/02/28. doi: 10.1016/j.main.2009.01.001. PubMed PMID: 19246233.
19. Chan RK. Splinting for peripheral nerve injury in upper limb. Hand surgery : an international journal devoted to hand and upper limb surgery and related research : journal of the Asia-Pacific Federation of Societies for Surgery of the Hand. 2002;7(2):251-9. Epub 2003/02/22. PubMed PMID: 12596288.

Title: Reconstruction of a 10-mm-long median nerve gap in an ischemic environment using autologous conduits with different patterns of blood supply: a comparative study in the rat

Authors:

Diogo Casal[1-4*], Eduarda Mota-Silva[5*], Inês Iria[4], Sara Alves[6], Ana Farinho[4], Cláudia Pen[6], Nuno Lourenço-Silva[4], Luís Mascarenhas-Lemos[1,6], José Silva-Ferreira[6], Mário Ferraz-Oliveira[6], Valentina Vassilenko[5], Paula Alexandra Videira[3,4], João Goyri-O'Neill[1], Diogo Pais[1]

1- Anatomy Department, NOVA Medical School, Universidade NOVA de Lisboa, Lisbon, Portugal

2- Plastic and Reconstructive Surgery Department and Burn Unit, Centro Hospitalar de Lisboa Central – Hospital de São José, Lisbon, Portugal

3- UCIBIO, Life Sciences Department, Faculty of Sciences and Technology, Universidade NOVA de Lisboa, Caparica, Portugal

4- CEDOC, NOVA Medical School, Universidade NOVA de Lisboa, Lisbon, Portugal

5- LIBPhys, Physics Department, Faculdade de Ciências e Tecnologias, Universidade NOVA de Lisboa, Lisbon, Portugal

6- Pathology Department, Centro Hospitalar de Lisboa Central – Hospital de São José, Lisbon, Portugal

- DC and EMS contributed equally

Abstract:

The aim of this study was to evaluate in the Wistar rat the efficacy of various autologous nerve conduits with various forms of blood supply in reconstructing a 10-mm-long gap in the median nerve (**MN**) under conditions of local ischemia.

A 10-mm-long median nerve defect was created in the right arm. A loose silicone tube was placed around the nerve gap zone, in order to simulate a local ischemic environment. Rats were divided in the following experimental groups (each with 20 rats): the nerve Graft (**NG**) group, in which the excised MN segment was reattached; the conventional nerve flap (**CNF**) and the arterialized neurovenous flap (**ANVF**) groups in which the gap was bridged with homonymous median nerve flaps; the prefabricated nerve flap (**PNF**) group in which the gap was reconstructed with a fabricated flap created by leaving an arteriovenous fistula in contact with the sciatic nerve for 5 weeks; and the two control groups, Sham and Excision groups. In the latter group, the proximal stump of the MN nerve was ligated and no repair was performed. The rats were followed for 100 days. During this time, they did physiotherapy. Functional, electroneuromyographic and histological studies were performed.

The CNF and ANVF groups presented better results than the NG group in the following assessments: grasping test, nociception, motor stimulation threshold, muscle weight, and histomorphometric evaluation. Radial deviation of the operated forepaw was more common in rats that presented worse results in the other outcome variables.

Overall, CNFs and ANVFs produced a faster and more complete recovery than NGs in the reconstruction of a 10-mm-long median nerve gap in an ischemic environment in the Wistar rat. Although, results obtained with CNFs were in most cases were better than ANVFs, these differences were not statistically significant for most of the outcome variables.

Short title:

Median nerve reconstruction in an ischemic environment

Keywords: Peripheral nerve; injury; surgery; reconstruction; repair; graft; flap; ischemia; blood supply.

Author Summary:

Sometimes, people lose part of their nerves as a result of trauma or during tumor removal surgeries. Consequently, patients are often faced with chronic paralysis, numbness, pain, and disfigurement in the territory of the affected nerve. To make things worse, the available options to reconstruct nerve gaps lead to a prolonged and uncertain recovery. Options are particularly less efficient when the tissues around the nerve gap have a poor blood supply.

In this work, we created a 10-mm-long gap in one the nerves of the arm of the rat. To simulate bad perfusion to the region around the nerve gap, a silicone barrier was placed around it. We then tried different forms of bridging the nerve gap. In one group, we just placed the nerve segment we had excised and applied it as a nerve graft. This nerve segment had no blood supply of its own initially. In two other groups, we used the same strategy, but kept some form of blood supply, creating a nerve flap.

Nerve flaps led to better results. This suggests that in people who have lost a part of nerve, a nerve flap should be used, particularly if the surrounding tissues are poorly vascularized.

Introduction:

Although bold surgeons such as Paul d'Argine were reportedly performing nervous sutures 600 AD, even today, despite numerous surgical and technical developments, the results with peripheral nerve repair are still disappointing.[1-3] Results are particularly unsatisfactory in cases of long nerve defects, being frequent not to obtain useful recovery in the involved nerve territory.[1-3] In 1870, Philipeaux and Vulpian proposed the use of nerve grafts (**NGs**) (devoid of intrinsic blood flow until neoangiogenesis from neighboring tissues occurs) to promote axonal regeneration through nerve defects.[4] Since then, NGs have become the gold standard for the reconstruction of peripheral nerve defects.[5] Even today, the multiple modern techniques of tubulization, using artificial nerve conduits, are generally discouraged for reconstructing defects over 5 to 6 cm in length.[1-3, 6-9] Additionally, experimental data suggests that autologous NG may yield superior motor recovery compared to nerve conduits, and to processed nerve allografts.[10]

From their inception, it was realized that the results obtained with NGs were far from perfect. Consequently, in 1921, Ney proposed the use of vascularized nerve segments, based on a conventional blood supply with an arterial and venous blood supply.[11] These conventional nerve flaps (**CNF**s) were further developed by Strange and Seddon in 1947.[12, 13] However, all these authors described pedicled CNFs, whose usefulness was limited because they could only be mobilized locally. Only in 1976 was the concept of free CNF

introduced by Taylor.[14] Still, these free CNFs are based on very small-sized nourishing vessels, making their dissection laborious and the vascular anastomoses at the recipient site difficult. Additionally, due to anatomical variations, they cannot always be raised.[15] Finally, there is a limited number of available CNFs.[16-18]

In order to circumvent these problems, in 1984, Taylor and Townsend proposed the use of arterialized neurovenous flaps (**ANVFs**).[19] These nerve flaps are based on the anatomical proximity of the venous system to multiple nerves, particularly in the subcutaneous tissue.[20, 21] ANVFs are thus composed of expendable nerve segments and adjoining veins.[20] Usually, one end of the vein is anastomosed to a recipient site artery and the other end is connected to a recipient site vein.[21] ANVFs can be harvested easily from multiple places of the body, particularly from the limbs, having a relatively expedite dissection. Furthermore, superficial veins have a large enough caliber to allow relatively easy vascular anastomoses.[19] Occasionally, the vascular architecture of ANVFs can be used to simultaneously reconstruct adjacent vascular and nerve defects.[21]

CNFs seem to guarantee better functional results than NGs for bridging nerve defects, particularly in conditions of local ischemia or fibrosis, as they are less likely to undergo central necrosis and histological disorganization.[22-24] In fact, contrarily to NGs, CNFs do not depend on plasmatic imbibition during the first 3 to 4 days after transfer for survival.[24-29]. Other authors argue that nerve flaps are not necessarily advantageous, as nerve grafts rapidly regain a new blood supply in several experimental models.[30] Some authors add that,

although recovery tends to be faster with CNFs, the end functional results are similar with CNFs and NGs.[24, 30]

Currently, as far as the authors could determine, the evidence of the efficacy of ANVFs for bridging nerve defects is limited to two articles on the reconstruction of femoral nerve defects in the rat.[28, 29]

Cavadas *et al.* suggested prefabrication of nerve flaps by placing an arteriovenous fistula in contact with nerve segments.[31] Theoretically, this could allow the creation of nerve flaps in virtually any place of the body, solving many of the problems with CNFs. Additionally, there is one study reporting that these prefabricated nerve flaps (**PNFs**) present superior results than NGs in the reconstruction of nerve defects in conditions of local compromise of circulation.[32] Yet, PNFs are not routinely used in clinical practice, in great part due to lack of supporting evidence of their usefulness.[33]

One of the reasons why conclusive evidence is difficult to obtain in the realm of peripheral nerve gap reconstruction is that different researchers have used different animal species, anatomical regions, reconstructive strategies and follow-up times. Furthermore, authors have also used variable outcome variables to assess nerve regeneration. These methodological differences make information synthesis challenging.[30] Finally, even though there are a few side-to-side comparisons of different gap reconstruction methods in the rat hindlimb, using the sciatic nerve, as far as the authors could determine, there is no similar study using the rat forelimb.[10, 22, 34] This is unfortunate, since clinically most peripheral nerve lesions occur in the upper extremity.[3, 35]

Therefore, the aim of this study was to evaluate in the Wistar rat the efficacy of various autologous nerve conduits with various forms of blood supply in reconstructing a 10-mm-long gap in the median nerve (**MN**) under conditions of local ischemia.

Methods:

Animal well-being and ethical committee's approval

All *in vivo* studies involving rats were carried out in strict accordance with or exceeding the recommendations in the Guide for Proper Conduct of Animal Experiments and Related Activities in Academic Research and Technology.[36, 37]

The experimental protocol was approved by the Institutional Animal Care and Use Committee and Ethical Committee at the authors' institution (CEFCM/08/2012).

Pre-operative training and accommodation

Three weeks before the surgery, rats were accustomed to being handled by the researchers. In addition, they were familiarized with the different functional tests used in the postoperative assessment that are described below. During this period the rats were manipulated daily.[38, 39] Pre and post-operatively the rats were maintained in an enriched environment. They were kept in customized cages of 60 X 30 X 90 cm, each with four stages, three ladders, a suspended rope and a training wheel. Each cage contained 5 to 6 rats. This environment intended to mimic the usual physiotherapy that peripheral nerve patients are typically offered postoperatively.[40]

Perioperative care of experimental animals

All the animals were housed under standard environmental conditions and fasted six hours before surgical procedures. No antibiotic prophylaxis was given.

Rats were anesthetized with a mixture of ketamine (5 mg/kg) and diazepam (0.25 mg/kg) given intraperitoneally. The depth of anesthesia was evaluated by toe pinch and by observance of respiration rate throughout the entire procedure. Supplementary doses of the anesthetic solution were provided as needed.[41]

After shaving the surgical sites and placing the animals on the operation table, the surgical field was disinfected with an antiseptic solution (Cutasept®), and draped. All surgical procedures were performed under strict antiseptic procedures. Surgeries were performed by the same author (D.C.), in order to avoid inter-surgeon variability. Surgical procedures were performed under a stereotaxic operating microscope (Leica® M651) and using microsurgical instruments. Hypothermia was avoided by placing the rat over a heating pad during surgical procedures and in the postoperative period.

Surgical model of nerve gap and ischemia in the rat's forelimb

A surgical model of ischemia surrounding a 10-mm-long median nerve defect was used (**Fig 1**).[29, 39, 42-45] As other authors, we have used a loose silicone tube with a 5-mm-wide inner diameter, and of 15-mm-length (Fortune Medical Inst. Corp.®; Reference 2011-0035) around the nerve repair zone, in order to simulate a local ischemic environment.[29, 42] This tube was sectioned longitudinally, so that it could be opened and subsequently be used to isolate the region of the

reconstructed nerve segment (**Fig 1H**). When vascularized nerve segments were used, the longitudinal opening in the silicone tube was left wide enough to accommodate the *vasa nervorum* supplying the nerve conduit, while isolating the reconstructed nerve segment from the surrounding vascularized tissues. At the end of the procedure a simple 5/0 Nylon stitch was placed at each end of the tube, passing both sides of the slit, to prevent migration of the silicone tube.

One hundred and twenty female Wistar rats, aged 4 to 6 months, and weighing between 200 and 250 grams, were randomly allocated in one of the following experimental groups in equal numbers (n=20):

Sham group: a longitudinal incision was made until the subfascial plane throughout the entire medial aspect of the right arm. A myotomy of the lateral portion of the sternal head of the pectoralis major muscle was then performed, in order to expose the MN. This nerve was gently teased away from the surrounding structures in the arm region, becoming pedicled in its segmental blood supply from the brachial vessels.[46] The mentioned 15-mm-long silicone tube was placed around the nerve preserving its local feeding branches. The skin wound was sutured with interrupted 5/0 Nylon stitches in all the experimental groups (**Fig 1A, G** and **H**).

Excision group: After exposing the right median nerve as detailed above, a 10-mm-long segment in the central portion of the MN in the arm was marked with a surgical ruler and a surgical marker. The region of the median nerve

proximal and distal to this marked region was tagged with 10/0 Nylon stitches. The marked region was cut sharply with a pair of straight microsurgery scissors. The excised segment was discarded. The proximal stump of the median nerve was ligated with an 8/0 Nylon stitch. The stumps of the median nerve were place inside both endings of the silicone tube (**Fig 1B** and **I**).[47]

Nerve graft (NG) group: Following the excision of the 10-mm-long segment of the right MN as described above, the nerve segment was placed in its original. The nerve segment was not placed in an inverted position, as it is normally recommended, to facilitate comparison with the remaining experimental groups (**Fig 1C** and **J**). Nerve repair was performed using four to six interrupted 10/0 epineural Nylon stitches in all the experimental groups using conduits.[48]

Conventional nerve flap (CNF) group: The 10-mm-long nerve segment was dissected and excised as detailed above, leaving it pedicled on its epineural arteries and veins in the brachial region (**Fig 1D, K, L** and **M**).[42]

Arterialized neurovenous flap (ANVF) group: After isolating and cutting the 10-mm-long nerve segment as described for the CNF group, all epineural arteries were carefully cauterized, leaving the nerve conduit pedicled solely on the epineural veins in the brachial region. Immediately proximally to the terminal division of the brachial artery, the brachial artery and accompanying vein were

anastomosed lateral-laterally after performing a 1.5-mm-long incision the adjoining flanks of these two vessels. The anastomosis was performed with interrupted 12/0 Nylon stitches. Consequently, an arterial venous anastomosis was created in the distal aspect of the arm, leading to the creation of an arterialized neurovenous conduit, which was used to bridge the MN gap (**Fig 1E, N, O** and **P**).

Pre-fabricated nerve flap (PNF) group: In this group, a conventional nerve flap was fabricated around the left sciatic nerve of the rat using the technique described by Cavadas and Vera-Sempere (**Figs 1F, Q** and **R**).[31] Succinctly, an arterial-venous fistula is created in the ventral aspect of the left thigh using the superficial caudal epigastric veins, which are connected to the femoral artery (**Fig 2**). This fistula was maintained in contact with the left sciatic nerve for 5 weeks. This leads to the fabrication of a conventional perfusion flap including a segment of the left sciatic nerve. Subsequently, this PNF was transferred to the right arm to reconstruct the median nerve defect (**Figs 1F, Q** and **R**; and **Fig 2**). The arterial end of the arterial-venous fistula was terminal-laterally anastomosed to the distal portion of the brachial artery and the venous end of the fistula was terminal-laterally anastomosed to the proximal aspect of the brachial vein using interrupted 12/0 Nylon stitches (**Fig 2B**).

Postoperative Evaluation

Rats were assessed daily regarding general activity, grooming, signs of wound infections or dehiscence, as well as for signs of autotomy.[49-51] They were maintained in the recommended cycles of light and darkness. Animals were provided food and water *ad libitum*.[40]

Rats were followed for 100 days (**D**) after MN reconstruction.

Every 15 days (D15, D30, D45, D60, D75, D90), they were submitted to the following evaluations: grasping test; nociception evaluation; running velocity; walking track analysis. On D90, after being subjected to these evaluations, they were anesthetized as described above, and submitted to injection of retrogradely labelling neuronal markers. On D100, rats were submitted to infra-red thermography (**IRT**) of the palmar aspect of the forepaws, electroneuromyography (**ENMG**), and strength evaluation after direct MN stimulation. Subsequently, a median ventral thoracotomy was performed, and the left and right ventricles were catheterized with 20G silicone catheters. The rats were submitted to exsanguination and replacement of blood volume by heparinized saline injected through the left ventricle, followed by 300 ml of 4% paraformaldehyde in 0.1M PBS (pH 7.40).[52] Finally, both flexor carpis radialis muscles were harvested and weighted, and nerve tissue was collected for histomorphometrical analysis using conventional stains, immunohistochemistry and fluorescence microscopy.[45]

Grasping Test: This test was used to assess motor recovery of the muscles controlled by the MN.[53] The rat was suspended by its tail over a grid, which it reflexively tried to grab. The rat was gently pulled by its tail with increasing strength until it loosened its grip. The rat was able to grab the grid only if the MN was functioning. Grasping strength was graded as follows: 0 – no grasping movement; 1- slight flexion of fingers, but with no significant grasping strength; 2- minimal grasping strength; 3- significant grasping strength but still inferior to the unaffected contralateral side; 4- normal grasping strength (equal to the contralateral, non-affected, limb).[53, 54]

Pin prick test: This test was used to evaluate nociception.[49, 55] In this test, the rats were placed on an elevated plastic platform with a 4x4 mm square grid pattern with 1.9 mm of length each. This grid was supported by a metallic frame that was 21-cm-tall. The grid was covered with a transparent plastic box with the following dimensions of 15.5x15.5x11cm.[49, 55] For each rat and evaluation point, rats were left on the platform covered by the plastic box for a few minutes until the exploratory and major grooming activities subsided. Subsequently, a number 4 Von Frey hair (bending force of 25g) was inserted through the mesh to poke the palmar aspect of the forepaw in its radial aspect, corresponding to the skin territory of the MN. The evaluation was considered correct only if the Von Frey filament bended.[56] Forepaws were evaluated in turn, when the rat was stationary and standing on the four paws. A few seconds mediated each evaluation to minimize apparent behavioral responses to the previous stimulus. Ambulation and biting the filament were considered ambiguous responses, and

in such cases the stimuli were repeated. Five measurements were made for each paw. Each time the following score was used: 0 – no response; 1 – the rat slowly takes the paw away from the Von Frey hair; 2 – the rat vigorously removes the forepaw from the Von Frey hair and/or licks the paw. Consequently, for each rat and time point, a nociceptive score was calculated as the sum of the responses to the five stimuli. This originated a value that ranged from 0 (no response for all noxious stimuli) to 10 (high response for all noxious stimuli).[39, 47, 49, 57-60]

Ladder rung walking test: This test was used to assess forelimb strength, stepping, placing, and co-ordination.[61] Rats were trained to run an inclined ladder of 120x9x2cm dimensions with 18 steps, of 1.5-cm-thickness and spaced 4 cm. The ladder was positioned with and inclination of approximately 10 degrees and led to a 13.20x11cm opening on a dark wooden box with 31.5x35x35cm of internal dimensions.

The rats were conditioned to run the ladder and enter the dark box on several training sessions that consisted of 5 trials each. In the first trials, the rats were positioned close to the box's door and guided in. For the subsequent 3 sessions, rats were progressively positioned further away from the box opening in each trial and persuaded to get in the box by gentle touching and/or pulling of tail's tip. Once inside the box, the sliding door closed the entrance and the rat was given a food treat. For the last trials, rats would only receive a snack, if they walked through the ladder without stopping or hesitating. Finally, for the last 5 sessions performed before surgery, the time to complete the task was recorded. The

examiner started the timer (precision of 1/100sec JUNSD®) once the animal started walking at the beginning of the ladder and stopped the timer when the rat's snout crossed the box's entrance. The test was considered valid, if the animal did not stop and did not hesitate during the task. After surgery, each evaluation session consisted of five trials, each separated by at least a one-minute interval. The time taken to complete each run was recorded.[45, 49, 55, 62]

Walking track analysis: This test was used to evaluate forelimb motor recovery.[63, 64] The experimental apparatus consisted of a confined walkway with 16.5 cm in height, 8.7 cm in width and 43 cm in length. This walkway lead to a rectangular opening with 8.8x8.2cm in one of the walls of a black wooden box with the dimensions of 23x36x28 cm. The box's entrance could be closed rapidly by a vertical sliding door. The box had a removable top that could be used to retrieve the rat. [63, 64]

Before the surgery, rats were trained to walk through the walkway until reaching the inside of the box. Particular attention was given to familiarize the rats with the noise of closing the sliding door. To positively condition rats, a food treat was given once the task was completed successfully. For the evaluations, the floor of the walkway was paved with graph paper (Ambar®). Rats forepaws were stained with methylene blue 1% W/V (Merck ®) with a painting brush. The rats were then led into the corridor. This test was done on every evaluation day and repeated as many times as needed until a representative print of both forepaws was obtained. [63, 64]

The following parameters were assessed for typical consecutive imprints of both forepaws (**Fig 3**) [63]:

Stance factor: paw impression area on the paper sheet.

Print length factor: longest length of the paw impression.

Finger spread factor: widest width of the paw impression.

Intermediate finger spread factor: widest width between the second and third fingers.

Additionally, the following parameters were assessed in the two pairs of representative sequential bilateral paw impressions (**Fig 3**) [63]:

Stride length: distance between homologous points of sequential paw impressions on a given side.

Base of support: perpendicular distance between the central portion of the paw impression and the direction of movement.[39, 49, 63]

Walking track analysis parameters were measured using the free software FIJI®.

Infra-red thermography (IRT) of the cutaneous territory of the median nerve: Thermography was used as a non-invasive surrogate marker of cutaneous denervation in the territory of the MN.[65-67] This assessment method was performed in the plantar territory of the MN on D100 after anesthetizing the rat.

The following aspects were taken into consideration before performing IRT:

- A room with a constant temperature, between 18ºC to 25ºC and without significant heat sources (such as computers or refrigerators). The room

temperature and humidity was registered using a normal digital hydro-thermometer (TFA®) with a thermal resolution of 0.1º C.

- The animals were brought to the room where the acquisitions were going to be performed 2 hours prior to the evaluation to allow acclimatization to occur. After being anesthetized, rats were placed on a clean and stable surface away from reflective materials and other possible sources of artefacts. The rat's central temperature was also monitored during all evaluation using a digital thermometer (Electro® DH SA) with a thermal resolution of 0.1º C inserted 2 cm inside the rectum.

The temperature was assessed using a FLIR® E6 camera, which has an accuracy of ± 2º C within the ambient temperature range and a thermal sensitivity of <0.06° C. An IR resolution of 160 x 120 pixels interpolated on 320 x 240 resolution within the camera electronics. The camera was switched on 15 minutes before acquisition and was not switched off during the experiment. The emissivity parameter was set on the camera for that of the skin, ε=0.98.

Each rat was gently laid on its dorsum on a polyethylene sponge, and its forepaws carefully fixed in supination with double face glue tape. After 3 minutes, the camera was held at 90º angle and 30 cm distance from the rat, focusing the animal's body on the camera. Then, three acquisitions were made, spaced 30 seconds apart. In the end, the rectal thermometer was removed.

The acquired thermograms were transferred to a computer and analyzed using the free software FLIR Tools+ ®. The temperature of the plantar surface of both forepaws was measured defining a rectangular region of interest of 9 X 11

pixels in the plantar territory of the MN. The mean, maximum and minimal temperature values were exported to a ".CSV" document and later added to an Excel (Microsoft Office®) and SPSS 21.0 (IBM Statistics®) databases.

ENMG: This assessment was performed on D100 on both forelimbs. The authors ensured that rats were deeply anesthetized before starting the acquisition, to minimize variability associated with voluntary and/or involuntary movements autonomously produced by the experimental animal.[68] The evaluations were always performed by the two senior authors (D.C. and E.M.S), in the same room, and under the same controlled environmental conditions.[7, 68, 69]

The experimental setting was composed of BIOPAC MP35® hardware and a BSLM Stimulator®. The electrodes used for stimulation and recording were made by taping a pair of disposable acupuncture needles (0.25x25 mm Shenzhou® Acupuncture Needles) with a distance of 25 mm between them. The Compound Muscle Action Potentials (CMAPs) were recorded using the BSL PRO 3.7® software, adjusting settings to create an optimized template. The stimulator and electrodes were connected to the BIOPAC MP35. The channels were set up as follows: CH1 - Stimulator BSLSM to 0-10Volts); and CH2 - EMG to 30-1000 Hz. The signal was acquired at a sample rate of 50 kHz, at a duration of 40.000 ms, amplified 1000X and filtered using a 30-1000 Hz band. The stimulation output was set for a single pulse with a duration of 1 ms.[7, 68, 69]

Under the surgical microscope and with the rat in dorsal decubitus, the MN was dissected free from the silicone rod and from the surrounding tissues. The flexor digitorum sublimis muscle was exposed on both forearms with a ventral longitudinal incision. The signal ground plug was connected by inserting the ground needle in the quadriceps femoris muscle of the left hindlimb. Starting with the right forepaw, the recording electrodes were put into the flexor digitorum sublimis muscle belly and the stimulation electrode hold proximally in the MN. Both electrodes were moistened with saline (Basi®). Initially, a stimulation amplitude of 10 mV was chosen by adjusting the stimulator knot and the CMPA was recorded. During the evaluation, the amplitude of stimulation was increased gradually in 10 mV steps until reaching 2000 mV. The same procedure was then repeated on the left forepaw.[7, 68, 69]

The following parameters were measured from CMPAs using measurement tools from the BSLPro 3.7® software:

- **Neurological Stimulation Threshold** - the minimum stimulus amplitude value to evoke a reproducible, stimulus correlated CMAP.

- **Motor Stimulation Threshold** - the minimum stimulus amplitude value to evoke a reproducible, stimulus correlated muscle contraction.

These last two parameters evaluate nerve regeneration, as there is a minimal number of nerve fibers required to produce either a CMAP or a visible muscle contraction.[70]

A minimal value of stimulation voltage after which the amplitude of CMAP did not increase further was registered for each rat. This value was increased by

20%, resulting in the supramaximal stimulation value. After this value was determined and the correspondent stimulus applied, the next CMAPs parameters were recorded:

- **Latency** – the time interval from the time of the electric stimulus to the first deviation from the baseline; assesses nerve conduction velocity in the fastest nerve fibers, that is to say the largest myelinated fibers.[69]

- **Neuromuscular transduction velocity** – the quotient between electrode distance and latency

- **CMAP Amplitude** – the highest difference between the largest CMAP oscillation and baseline. This value evaluates the number of reinnervated motor units [64]

- **CMAP duration** - the interval of time during which the CMPA occurs. It assesses synchrony of muscle innervation, which is dependent on the degree of muscle reinnervation and myelination of the innervating motor fibers.[69, 71]

Wrist Flexion Strength Assessment: As wrist flexion is predominantly dependent on the MN, this evaluation was used on D100 to assess strength in this nerve's territory. To assess wrist flexion strength the mentioned BIOPAC MP35®, BSLMA stimulator software® and stimulation electrodes were used to stimulate the MN. Using BSL PRO 3.7® software, the following parameters were adjusted to create a template for stimulation: the input channel CH1 was set as

Stimulator-BSLSTM (0-10 Volts) and the output settings were selected for stimuli duration of 30 seconds with pulses of 1 ms duration and 1 Hz frequency. The amplitude of the pulses was adjusted on the stimulator knot for 1.5 V or 3 V according to the evaluation moment. A dynamometer, Sauter® FH 5, with a resolution of d=0.001 N was linked to a computer. The AFH-01® software was installed on the computer and linked to FH 5 dynamometer allowing real time visualization of data by building a plot of force per time (N/sec). This data was later imported to an excel sheet (Microsof Office®) for analysis.[62]

With the rat anesthetized, a silk 5/0 stitch was passed through the second interosseous space. This stitch was associated with a 5-cm-long loop. The rat was put on its back and a self-retaining retractor used to expose the nerve. Starting with the right forepaw, the suture loop was placed in the dynamometer's hook and the forepaw aligned with the dynamometer, without putting too much strain on the suture line. The contralateral paw was fixed with tape to avoid extra movement interferences in the dynamometer readings. The stimulating electrodes were put proximally in the MN and wetted with saline (Basi®). The dynamometer was set to zero and the stimulator adjusted to a supramaximal amplitude stimulation of 1.5 V for 30 seconds. The same steps were done on the left forepaw. The data thus recorded with the AHF1 software® were imported into an Excel® (Microsoft Office™) datasheet. Maximum and average force values and the area under the curve (AUC) for the strength X time graph were calculated for each evaluation.

Flexor carpi radialis (FCR) muscle weight: Being innervated exclusively by the MN, this muscle's weight was used to assess motor reinnervation in the territory of the MN. After euthanizing the rats as described above, the muscle was harvested on both sides from its origin until its distal tendon insertion. Both muscles were weighed using a precision scale, KERN770®, which had a precision of 0.1 mg.[45, 47]

Histological evaluation: The MN distally to the repair site and the middle portion of the nerve conduit used to bridge the defect were harvested after euthanasia. The specimens were fixed in 10% paraformaldehyde, and prepared for histological examination, using hematoxylin-eosin and Masson's trichrome stains, as well as immunohistochemistry for neurofilaments, peripherin and acetylcholinesterase (**Table 1**).[72-75]

Nerve fiber		Numerical classification of nerve fibers	Innervated structures / function	Nerve fiber diameter (µm)	Myelination	Conduction velocity (m/s)[76]
type	subtype					
A	α	Ia	Muscle spindle annulospiral receptor (main responsible for proprioception) Extrafusal skeletal muscle fibers (voluntary motor control)	12 - 22	Thickly myelinated	70 - 120
A		Ib	Golgi tendon organ (contractile force)	12 - 22	Thickly myelinated	70 - 120
A	β	II	Pressure, touch and vibration receptors of the skin (cutaneous mechanoreceptors sensibility) Muscle spindle flower spray receptors (secondary responsible for proprioception)	5 - 12	Thickly myelinated	30 - 70
A	γ	II	Intrafusal skeletal muscle fibers (muscle tone control)	2 - 8	Thickly myelinated	15 - 30
A	δ	III	Some nociceptors (sharp pain), cold receptors, most hair receptors (touch and pressure), some visceral receptors	1 - 5	Thinly myelinated	5 - 30
B	-	-	Preganglionic autonomic efferents	< 3	Thinly myelinated	3 - 15
C	-	IV	Most nociceptors (dull, aching pain), warmth receptors, some mechanoreceptors, itch receptors, some visceral receptors, postganglionic autonomic efferents	0.1-1.3	Nonmyelinated	0.6 - 2.0

Table 1. Staining of the different types of nerve fibers using immunohistochemistry for neurofilaments (blue areas), acetylcholinesterase (red areas) and peripherin (brown areas).[49, 77-80] Neurofilament staining marks virtually all nerve fibers. Acetylcholinesterase staining highlights mostly motor nerve fibers.[81] Most sympathetic nerve fibers are marked by peripherin staining. Fibers that do not stain by acetylcholinesterase and peripherin are predominantly myelinated sensory fibers.[79]

The combination of these immunohistochemical methods roughly allows to functionally dissect peripheral nerves.[72]

Histomorphometric evaluation was performed independently by two blinded observers, using the software Fiji®. In cases of discrepancies superior to 5%, the histological sections were reviewed by the two observers. The following parameters were determined in the MN section immediately distal to the repaired nerve gap: cross section area in a transverse section, total number of nerve fibers (neurofilament positive), number of acetylcholinesterase positive nerve fibers, number of peripherin positive nerve fibers, number of acetylcholinesterase – and peripherin negative fibers. Furthermore, the vascular density in the middle of the reconstructed segment was also determined. Vascular density inside the reconstructed median nerve segment was determined based on counts of the vessels inside the epineurium, as the vessels over the epineurium mixed with the surrounding tissues in an indistinct manner, making the establishment of boundaries between the epineurium and surrounding tissues frequently impossible. [72, 82]

The number of structures inside nerve segments was calculated by the product of the cross-section area of the respective nerve segment (assessed on 4X amplification) and of the density of the structure of interest. Density was determined by counting the average number of structures in 3 random 20X amplification fields and dividing this value by the area of that field. To avoid under or overestimation of structures number, structures included in counts only if the top upper edge of the structure was included in the microscopic field.[83, 84]

Retrograde neuron marking and fluorescence microscopy evaluation: On D90, after performing the functional examinations described above, and with the rat under anesthesia, 12 µl of 5% True Blue Diaceturate (TB, Sigma®) e 12 µl of 3% of Lucifer Yellow Dilithium salt (LY, Sigma®) were injected intradermally in the skin territory of the MN in the right hand (at the level of the radial hand pads) and in the right flexor carpis radialis muscle, respectively, using 27-gauge intradermic needles (BD Bioscience™).[40, 52, 85] This allowed to morphologically evaluate the sensory and motor reconstruction of the MN across the nerve gap.[40, 47, 86, 87]

On D100, after euthanizing the rat, the following structures were removed: MN proximal to the reconstructed MN, the C7 spinal cord segment in continuity with the dorsal and ventral C7 spinal nerve roots, and including the C7 dorsal root ganglion (DRG) on both sides. A left parasagittal section was made in the ventral surface of the spinal cord segment, in order to convey information on laterality. These nerve structures were immersed in 4% paraformaldehyde and 10% sucrose in 0.1 M phosphate buffered saline (PBS) at pH 7.4 for 48 hours for fixation. After fixation, the specimens were transferred into increasing concentrations of sucrose in PBS for at least 15 hours for each concentration (15% and 30%). The specimens were then frozen in liquid nitrogen. Subsequently, transverse cryostat sections were cut at 20 µm for the DRG and the MN and at 50 µm for the spinal cord segments. These sections were then thaw-mounted on polylysine-coated glass slides.[88, 89]

Specimens were observed by epifluorescence under a fluorescence microscope.

The number of marked nerve fibers in the proximal aspect of the MN was assessed as described above. For each DRG, the number of True Blue labelled cells was semi quantitatively assessed by counting the fluorescent cells on what appears to be the largest cross section. For each C7 spinal cord, the region with greatest fluorescence in the ventral horn was searched with a 4X amplification. In this area, the average number of Lucifer Yellow stained cells was determined based on counts done in 3 random 20X-amplification fields.[40, 44]

Statistical analysis

Qualitative variables were expressed as percentages. Quantitative variables were expressed as means ± SD. IBM SPSS Version 21.0® software was used for descriptive and inferential statistical analysis. The Kolmogorov-Smirnov test was used to assess whether variables were distributed normally. Analysis of variance and t test were used to compare averages in normally distributed data. Kruskal-Wallis and Mann-Whitney tests were used to compare means in non-normally distributed data. Proportions were analyzed with the chi-square test or Fisher's exact test. Association between numerical variables was investigated using Pearson's correlation coefficient. Relationship between ordinal variables was evaluated with resort to Spearman Rank Correlation Coefficient. Kaplan Meier survival analysis was performed to identify differences between groups regarding time to recovery of a positive grasping test.

A two-tail value of $p<0.05$ was considered to be statistically significant.

Results:

Rat mortality was higher in the PNF group

The total number of rats reaching the end of the experiment was 87. These animals were distributed in the experimental groups as follows: 17 in the Sham group; 17 in the Excision group; 10 in the NG group; 20 in the CNF group; 15 in the ANVF group; and 8 in the PNF group (**Table 2**). All rats died in the perioperative period (<48 hours after surgery). Mortality rate was higher in the PNF group than in the remaining experimental groups (60% versus 21%; $p<0.05$). In the former group, 10 deaths occurred in the first 24 hours after the first surgery, and the remaining 2 deaths in the day after the second surgery. In all the deceased animals in all experimental groups, necropsy examination revealed signs of hematoma and hypovolemia.

Daily observation of rats did not reveal signs of distress

General health and behavior of the experimental animals was adequate throughout the experiment. All rats presented moderate to high levels of activity, grooming themselves regularly. None of the animals presented autophagy or self-mutilation. The surgical wounds healed uneventfully. Skin ulcers were not observed on the operated paws.

Animal weight gain did not vary significantly among the experimental groups

At the end of the experiment, the average weight gain was 79.4% ± 4.9% for the Sham group; 74.2% ± 3.8% for the Excision group; 83.3% ± 6.2% for the NG group; 74.0% ± 6.8% for the CNF group; 75.3% ± 7.6% for the ANVF group; and 79.9% ± 6.1% for the PNF group. These differences were not statistically significant (**Table 2**).

Parameter		Sham group	Excision group	NG group	CNF group	ANVF group	PNF group	Relevant findings
Mortality		15%	15%	50%	0%	25%	60%	Mortality rate was higher in the NG and the PNF groups than in the remaining experimental groups ($p<0.05$)
Animal weight gain (%)		79.4 ± 4.9	74.2 ± 3.8	83.3 ± 6.2	74.0 ± 6.8	75.3 ± 7.6	79.9 ± 6.1	No significant differences
Time to recovery of grasping (days)		0 (immediately after surgery)	87.31 ± 4.41	75.00 ± 5.86	45.75 ± 2.98	34.00 ± 2.30	97.50 ± 1.53	Fastest recovery of grasping was observed in the CNF and ANVF groups ($p<0.001$)
Average grasping strength	**D30**	4.00 ± 0.00	0.00 ± 0.00	0.00 ± 0.00	0.60 ± 0.82	0.67 ± 0.62	0.00 ± 0.00	On D90, grasping strength was greater in the CFN and ANVF than in the Excision, Nerve graft and PNF groups
	D45	4.00 ± 0.00	0,06 ± 0.24	0.00 ± 0.00	1.10 ± 1.02	1.60 ± 0.51	0.00 ± 0.00	
	D60	4.00 ± 0.00	0.18 ± 0.39	0.60 ± 0.70	2.30 ± 1.13	2.60 ± 1.05	0.00 ± 0.00	
	D75	4.00 ± 0.00	0.29 ± 0.47	0.80 ± 0.63	3.00 ± 1.01	2,80 ± 1.01	0.00 ± 0.00	
	D90	4.00 ± 0.00	0.35 ± 0.49	1.30 ± 0.95	3.80 ± 0.41	3.80 ± 0.41	1.50 ± 1.20	
Running Velocity in the ladder (cm/s)	**D30**	57.17 ± 31.02	21.10 ± 6.17	15.29 ± 13.14	32.06 ± 13.30	31.81 ± 9.93	15.51 ± 6.24	On D90 there were no statistical significant differences between sham and the CNF, the ANVF and the PNF groups
	D45	58.74 ± 37.33	21.65 ± 6.57	15.32 ± 4.76	29.54 ± 7.22	34.12 ± 4.80	28.08 ± 9.85	
	D60	60.26 ± 39.96	21.56 ± 4.85	29.42 ± 12.97	40.96 ± 10.60	35.76 ± 8.62	39.66 ± 17.53	
	D75	64.63 ± 36.08	23.48 ± 4.86	30.91 ± 22.98	43.13 ± 8.36	48.88 ± 11.61	35.06 ± 7.23	
	D90	63.34 ± 31.58	23.30 ± 5.05	39.83 ± 14.33	54.46 ± 19.13	56.71 ± 10.21	39.23 ± 14.05	
Pin Prick test (%)	**D30**	97.05 ± 4.70	5.88 ± 9.39	21.71 ± 12.10	39.18 ± 44.54	75.06 ± 18.74	2.50 ± 4.63	On D90, the best results were observed in the Sham, CNF and the ANVF groups ($p<0.001$)
	D45	107.67 ± 9.12	18.69 ± 21.89	19.11 ± 16.82	69.86 ± 27.93	82.17 ± 13.80	24.17 ± 22.51	
	D60	102.21 ± 4.91	13.33 ± 4.46	20.44 ± 6.73	93.89 ± 20.12	83.33 ± 14.80	35.07 ± 3.17	
	D75	93.33 ± 5.09	16.74 ± 7.90	40.00 ± 29.06	93.00 ± 4.70	94.01 ± 8.28	37.57 ± 27.04	
	D90	100.20 ± 6.47	7.84 ± 10.95	42.00 ± 18.14	87.24 ± 17.63	107.03 ± 29.20	48.21 ± 29.81	

Table 2. Mortality, weight gain, grasping test, ladder running test and pin prick test results throughout the experiment.

NG, nerve graft; **CNF**, conventional nerve flap; **ANVF**, arterialized neurovenous flap; **PNF**, prefabricated nerve flap

D, day after the beginning of the experiment

Average grasping strength was evaluated semi quantitatively using a scale of 0 to 4 (0, no grasping; 1, flexes fingers only without opposition; 2, flexes fingers against minimal opposition; 3, flexes fingers against opposition but with less strength than the contralateral limb; 4, flexes fingers with the same strength as the contralateral limb.

Pin prick test results are expressed as percentages of the average contralateral values.

Numeric variables are expressed as average ± standard deviation.

The Grasping Test revealed faster and more complete motor recovery in the CNF and in the ANVF groups than in the NG group

Recovery of grasping occurred in the immediate postoperative period in all rats in the Sham Group. In all other groups, no grasping was observed immediately after surgery (**Fig. 4**). Fastest recovery of grasping was observed in the CNF and ANVF groups ($p<0.001$). At the end of the experiment, grasping strength was greater in the CFN and ANVF than in the Excision, Nerve graft and PNF groups (**Fig. 5**). In fact, on D90, there were no statistically significant differences between the CNF, ANVF and the Sham groups (**Fig. 5**).

Running Ladder Test revealed comparable velocities at the end of the experiment between the Sham group and the CNF, the ANVF, and the PNF

On D15, the average velocity in the running ladder test was greater in the Sham group than in all other groups ($p<0.01$; **Fig 6**; **Table 2**). The superiority of this group was maintained until D60. From this time on, there was no statistical difference between this group and the CNF and PNF groups. On D90 there were no statistical significant differences between sham and the CNF, the ANVF and the PNF groups. At the end of the experiment, the CNF and ANVF groups presented better average velocities than the NG group but these differences were not statistically significant (**Fig. 6**).

Pin prick test revealed better nociceptive recovery in the CNF and ANVF groups

Thirty days after surgery, the ANVF group presented the best average sensory recovery in the Pin Prick test, showing no statistical significant difference relatively to the Sham group (**Fig. 7**; **Table 2**). On D60 and D90, the best results were observed in the Sham, CNF and the ANVF groups. The latter two groups presented average scores significantly superior to those observed in the NG and PFN groups ($p<0.001$; **Fig. 7**).

Walking Track Analysis revealed that the rate of radial deviation was lower in groups in which a vascularized nerve conduit was used

On D30 the CNF group presented a better normalized stance factor than the excision, NG and PNF groups ($p<0.001$; **Fig. 8A**; **Table 3**). Subsequently, no statistically significant differences were found between groups. The average normalized print length in the operated limb was higher in the CNF, ANVF and PNF than in the NG on D30. On D60 no differences were found between groups. On D90, CNF and PNF presented better results than the ANVF group regarding the normalized print length (**Fig. 8B**). Pertaining to normalized finger spread and intermediate finger spread, on D30, better results were observed in the groups using vascularized conduits compared to the NG group ($p<0.05$; **Figs. 8C** and **D**). However, at the end of the experiment these differences were no longer visible. Finally, stride analysis failed to reveal meaningful differences between the different groups (**Figs. 8E** and **8F**).

Parameter		Sham group	Excision group	NG group	CNF group	ANVF group	PNF group	Relevant findings
Stance factor (%)	D30	97.02 ± 20.42	70.57 ± 18.01	70.91 ± 18.64	103.34 ± 22.69	88.72 ± 19.44	72.39 ± 40.35	On D30 the CNF group presented a better normalized stance factor than the excision, NG and PNF groups ($p<0.001$)
	D45	100.65 ± 14.18	120.18 ± 40.80	77.85 ± 28.34	114.91 ± 21.08	100.93 ± 15.61	106.07 ± 10.93	
	D60	95.37 ± 14.98	87.47 ± 20.83	88.79 ± 16.99	88.79 ± 16.99	81.82 ± 22.12	86.66 ± 14.66	
	D75	98.75 ± 16.03	92.59 ± 24.66	77.08 ± 35.73	77.08 ± 35.73	87.24 ± 25.43	86.70 ± 17.38	
	D90	104.56 ± 11.47	85.63 ± 27.23	102.87 ± 19.10	85.77 ± 16.12	94.79 ± 15.80	112.55 ± 38.97	
Print length (%)	D30	98.24 ± 2.95	94.41 ± 3.31	88.18 ± 3.84	97.45 ± 3.45	93.38 ± 5.19	94.35 ± 5.19	On D30 print length was higher in the CNF, ANVF and PNF groups than in the NG group on D30 ($p<0.01$)
	D45	99.19 ± 5.21	97.15 ± 5.36	91.11 ± 2.19	96.59 ± 3.02	95.52 ± 13.62	99.56 ± 4.00	
	D60	100.16 ± 4.44	98.45 ± 2.45	96.40 ± 2.85	97.46 ±4.39	94.79 ± 12.94	92.72 ± 4.55	
	D75	99.98 ± 5.19	97.21 ± 5.10	95.64 ± 3.21	95.29 ± 2.86	88.66 ± 16.80	98.93 ± 4.21	
	D90	100.00 ± 4.00	97.18 ± 4.49	93.63 ± 2.80	94.51 ± 1.92	88.70 ± 10.85	97.88 ± 2.13	
Finger spread (%)	D30	96.16 ± 10.83	85.58 ± 8.05	66.72 ± 8.75	94.71 ± 4.20	99.98 ± 14.70	89.15 ± 3.24	On D30 the CNF, ANVF, and PNF groups presented better results than the NG group ($p<0.05$)
	D45	94.21 ± 4.06	90.20 ± 9.69	79.64 ± 7.01	87.96 ± 7.68	95.87 ± 21.38	98.35 ± 10.43	
	D60	95.61 ± 5.28	89.70 ± 9.74	78.94 ± 11.59	89.99 ± 10.54	87.75 ± 19.14	91.37 ± 3.60	
	D75	111.47 ± 38.51	106.03 ± 45.96	86.89 ± 5.78	87.87 ± 7.67	86.31 ± 26.29	95.13 ± 5.03	
	D90	102.07 ± 10.52	93.57 ± 10.37	84.57 ± 12.18	88.11 ± 6.71	80.42 ± 23.16	99.63 ± 6.74	
Intermediate finger spread (%)	D30	94.58 ± 12.14	89.42 ± 14.37	76.13 ± 18.89	89.09 ± 10.04	93.15 ± 13.70	81.21 ± 9.56	On D30 the CNF, ANVF, and PNF groups presented better results than the NG group ($p<0.05$)
	D45	89.93 ± 8.65	88.23 ± 14.16	77.92 ± 15.33	87.89 ± 14.93	91.15 ± 24.47	96.22 ± 8.38	
	D60	95.61 ± 5.28	89.70 ± 9.74	78.94 ± 11.59	89.99 ± 10.54	78.22 ± 24.92	88.14 ± 10.83	
	D75	102.32 ± 10.46	80.44 ± 26.49	85.18 ± 7.51	87.74 ± 15.62	78.67 ± 31.31	94.30 ± 12.43	
	D90	102.07 ± 10.52	93.57 ± 10.37	84.57 ± 12.18	88.11 ± 6.71	93.63 ± 6.34	91.53 ± 6.37	

Parameter		Sham group	Excision group	NG group	CNF group	ANVF group	PNF group	Relevant findings
Stride length (%)	**D30**	102.11 ± 6.80	102.86 ± 9.79	102.93 ± 8.39	109.47 ± 10.52	95.86 ± 4.09	106.26 ± 29.08	No significant differences between experimental groups
	D45	105.44 ± 12.32	103.59 ± 10.12	109.39 ± 14.56	116.24 ± 13.17	111.60 ± 32.18	101.15 ± 5.96	
	D60	100.66 ± 10.50	101.05 ± 9.82	105.18 ± 7.52	100.69 ± 3.95	105.63 ± 6.43	114.53 ± 26.66	
	D75	100.14 ± 7.62	95.74 ± 12.45	100.67 ± 15.26	102.40 ± 12.81	99.84 ± 8.70	111.28 ± 11.85	
	D90	100.40 ± 10.31	97.58 ± 12.05	95.74 ± 9.62	107.22 ± 10.75	100.37 ± 10.35	114.25 ± 17.68	
Base of support (%)	**D30**	82.16 ± 38.70	77.42 ± 39.42	91.22 ± 23.90	149.03 ± 10.49	99.97 ± 56.78	87.93 ± 18.65	No significant differences between experimental groups
	D45	74.38 ± 26.77	131.15 ± 58.52	82.24 ± 13.51	123.14 ± 47.25	108.52 ± 25.71	105.10 ± 47.60	
	D60	108.78 ± 42.96	108.13 ± 20.38	107.00 ± 22.48	109.57 ± 18.87	75.00 ± 33.74	112.26 ± 64.79	
	D75	87.68 ± 32.12	70.16 ± 26.24	138.07 ± 75.83	84. 88 ± 20.40	173.19 ± 87.47	135.91 ± 84.45	
	D90	100.63 ± 24.07	106.52 ± 27.14	111.80 ± 67.69	135.57 ± 53.80	95.20 ± 28.02	127.17 ± 61.37	
Presence of radial deviaion (%)	**D30**	0	94.1	100	40	13.3	0	For each time point, the rate of radial deviation was lower in groups in which a vascularized nerve conduit was used compared to the NG group ($p<0.001$)
	D45	0	100	100	20	13.3	0	
	D60	0	100	100	0	20	0	
	D75	0	100	70	0	20	0	
	D90	0	100	30	0	20	0	

Table 3. Walking track analysis results throughout the experiment.

NG, nerve graft; **CNF**, conventional nerve flap; **ANVF**, arterialized neurovenous flap; **PNF**, prefabricated nerve flap

D, day after the beginning of the experiment

Numeric variables are expressed as average ± standard deviation.

Radial deviation of the operated forepaw print was present on D30 in 94.1% of the rats in the Excision group, 100% of the rats in the NG group, 40% of those in the CNF group, and 13.3% in ANVF (**Figs. 9A** and **9B**). On D60, 100% of the rats in the Excision and the NG groups presented radial deviation, while only 20% of the rats in the ANVF group presented radial deviation. From D60 on, no radial deviation was observed in the CNF group. On D90, radial deviation was observed in 100% of the Excision group, 30% of the NG group, and 20% of the ANVF group (**Fig. 9C**). Radial deviation was never observed in the animals in the Sham and in the PNF groups. For each assessment day, the rate of radial deviation was lower in the groups in which a vascularized nerve conduit was used compared to the NG group ($p<0.001$).

Thermographic assessment failed to show differences between groups

IRT of the skin of the MN territory in the right forepaw revealed an average normalized temperature of 99.4% ± 5.9%; 101.7% ± 7.1%; 104.9% ± 13.7%; 101.8% ± 8.0%; 103.6% ± 7.2%; and 109.0% ± 10.8% in the Sham, Excision, NG, CNF, and PNF groups, respectively, compared to the contralateral side (**Fig. 10; Table 4**). These

differences were not statistically significant. Analogously, no differences were found pertaining to the maximal and minimal temperatures on the surface of the forepaws (**Table 4**).

Parameter	Sham group	Excision group	NG group	CNF group	ANVF group	PNF group	Relevant findings
Forepaw average temperature (%)	99.4 ± 5.9	101.7 ± 7.1	104.9 ± 13.7	101.8 ± 8.0	103.6 ± 7.2	109.0 ± 10.8	No significant differences between experimental groups
Forepaw minimal temperature (%)	100.45 ± 5.49	102.25 ± 7.04	105.47 ± 14.34	102.45 ± 8.39	104.36 ± 7.83	108.61 ± 11.58	No significant differences between experimental groups
Forepaw maximal temperature (%)	98.86 ± 6.43	99.97 ± 6.41	101.44 ± 6.94	100.42 ± 6.74	100.63 ± 3.17	107.03 ± 5.04	No significant differences between experimental groups

Table 4. Infra-red thermography evaluation of the region of the forepays innervated by the median nerve 90 days postoperatively.

NG, nerve graft; **CNF**, conventional nerve flap; **ANVF**, arterialized neurovenous flap; **PNF**, prefabricated nerve flap

D, day after the beginning of the experiment

Numeric variables are expressed as average ± standard deviation.

Electroneuromyographic assessment revealed a lower motor stimulation threshold in the CNF and ANVF than in the NG group

On D90, the normalized neurological stimulation threshold was significantly higher in the Excision group than in the remaining groups ($p<0.001$; **Fig 11A; Table 5**). In fact, no reproducible CAMP was obtained in the former group. No other differences were found relatively to normalized neurological stimulation threshold in the other groups. However, regarding the normalized motor stimulation threshold, the lowest values were obtained in the Sham group ($p<0.01$; **Fig 11B**). Lower values were obtained in the CNF and the ANVF groups than in the NG group ($p<0.001$; **Fig 11B**). No statistically significant differences were found in the latency and neuromuscular transduction parameters between the Sham group and the groups submitted to nerve gap reconstruction (**Figs 11 C** and **D**). Pertaining to the CMAP amplitude, higher values were obtained in the Sham group (110.63% ± 45.66%) than in the other groups submitted to nerve gap reconstruction ($p<0.05$; **Fig 11E**). These values were higher in the CNF group (69.53% ± 13.80%), in the ANVF group (73.34% ±22.86%) and the PNF group (71.68% ± 23.56%) than in the NG group (41.60% ± 24.4%). However, these differences did not meet statistical significance. Apart from a longer CMAP duration in the CNF group compared to the ANVF ($p<0.001$), no other significant differences were found between groups (**Fig 11F**). **Figure 12** shows the typical morphology of the CMAPs in the different experimental groups. The ENMG pattern in the NG group tended to be similar to that of the Sham group or to that of the contralateral non-operated side of all rats, apart from having a smaller amplitude (**Figs 12 A** and **B**). The ENMG pattern in the CNF, ANVF and in the PNF groups was invariably polyphasic,

and showed a tendency to be of a longer duration but of a slightly lesser amplitude compared to the non-operated side (**Figs 12 C** to **E**). In the Excision group, no CMAPs were observed after applying an electrical stimulus to the MN.

Parameter	Sham group	Excision group	NG group	CNF group	ANVF group	PNF group	Relevant findings
Neurological stimulation threshold (%)	281.63 ± 271.65	5359.98 ± 3466.52	2108.12 ± 2115.13	428.45 ± 472.87	1063.00 ± 807.61	1270.30 ± 482.72	On D90, this parameter was significantly higher in the Excision group than in the remaining groups (p<0.001)
Motor stimulation threshold (%)	462.52 ± 118.91	1694.10 ± 503.24	1249.50 ± 503.24	535.38 ± 253.15	619.46 ± 264.36	948.57 ± 592.41	Lower values were obtained in the CNF and the ANVF groups than in the NG group (p<0.001
Latency (%)	113.55 ± 25.04	N/A	132.80 ± 69.95	72.82 ± 84.87	105.28 ± 52.41	131.97 ± 56.46	No significant differences between experimental groups
Neuromuscular transduction velocity (%)	92.01 ± 20.88	N/A	91.30 ± 26.51	100.06 ± 31.26	94.05 ± 26.33	88.15 ± 34.77	No significant differences between experimental groups
CMAPs amplitude (%)	110.63 ±45.66	N/A	41.60 ± 24.84	69.53 ± 13.80	73.34 ± 22.86	71.68 ± 23.56	No significant differences between experimental groups
CMAPs duration (%)	101.12 ± 23.92	N/A	151.06 ± 54.52	242.17 ± 185.97	82.87 ± 36.69	103.13 ± 31.24	Longer CMAP duration in the CNF group compared to the ANVF group (p<0.001)

Table 5. Electroneuromyographic assessment at the end of the experiment

NG, nerve graft; **CNF**, conventional nerve flap; **ANVF**, arterialized neurovenous flap; **PNF**, prefabricated nerve flap

CMAPs, compound muscle action potential.

N/A, non-applicable

All parameters are expressed as percentages of the average contralateral values.

Numeric variables are expressed as average ± standard deviation.

Muscle Strength was inferior in the NG group, although the differences did not meet statistically significance

Normalized maximum isometric tetanic wrist flexion on the operated limb on D90 was 141.00% ± 75.55% in the Sham group, 35.67% ± 46.51% in the NG, 60.56% ± 27.59% in the CNF group, 63.05% ± 12.95% in the ANVF group, and 52.61% ± 18.73% in the PNF group. This value was significantly higher in the Sham group than in the other groups ($p<0.001$; **Fig. 13A**). The normalized area under the curve during a 30-second interval and supra-tetanic stimulation was 112.54% ± 19.43% in the Sham group, 58.81% ± 29.63% in the NG group, 63.12% ± 12.43% in the CNF, 69.80% ± 31.67% in the ANVF group, and 93.61% ± 34.91% in the PNF group. Once again, the Sham group presented a better result in this parameter than all the other experimental groups, except for the PNF group ($p<0.001$; **Fig. 13B**).

Muscle Weight was inferior in the NG and in the PNF groups

The normalized results for FCR muscle weight at the end of the experiment were 101.15% ± 8.14% for the Sham group, 30.24% ± 7.23% for the Excision group, 47.14% ±14.72 for the NG group, 80.29 ± 14.29% for the CNF group, 82.24% ±10.64% for the ANVF group, and 62.71% ± 11.12% for the PNF group (**Figs 14** and **15**). The Sham group presented a higher muscle weight than any of the other experimental groups ($p<0.001$). Among the groups using nerve conduits the CNF and the ANVF presented a better muscle weight than the NG and the PNF ($p<0.01$). The difference between these latter two groups was not statistically significant, although the PNF presented a higher average value.

Histomorphometrical evaluation of the distal aspect of the median nerve showed a tendency to worse results in the NG group

Histological examination of the median nerve distally to the reconstructed nerve segment revealed an inferior average cross section area in the Excision group (**Figs 16 A**, and **17**; **Table 6**). Among the groups using nerve conduits, the NG presented an inferior area. However, this difference was statistically significant only between the NG and the PNF groups ($p<0.05$).

Parameter	Sham group	Excision group	NG group	CNF group	ANVF group	PNF group	Relevant findings
Cross section area (%)	106.59 ± 27.45	54.67 ± 26.55	72.42 ± 30.28	93.38 ± 10.87	82.44 ± 15.77	109.42 ± 19.86	Higher in the PNF group than in the NG group ($p<0.05$)
Total number of fibers (%)	101.76 ± 5.30	N/A	56.88 ± 17.85	97.91 ± 50.72	67.71 ± 18.58	70.33 ± 9.31	Higher in the CNF group than in the NG group ($p<0.01$)
Acetylycholinesterase positive nerve fibers (%)	106.94 ± 17.65	N/A	40.90 ± 5.54	49.67 ± 8.61	49.67 ± 8.61	47.07 ± 10.82	No significant differences between experimental groups
Peripherin positive nerve fibers (%)	101.64 ± 5.53	N/A	56.90 ± 17.83	101.45 ± 49.23	101.45 ± 49.23	73.03 ± 11.49	Numbers of peripherin positive and acethyl-cholinesterase negative and peripherin negative fibers were higher in the CNF and in the Sham groups than in the NG group ($p<0.001$)
Acethylcholinesterase negative and peripherin negative nerve fibers (%)	95.58 ± 10.76	N/A	61.02 ± 21.59	126.28 ± 78.51	73.20 ± 22.36	75.03 ± 11.61	
Vascular density in the middle portion of the reconstructed nerve segment (%)	335.98 ± 155.89	N/A	126.70 ± 50.92	249.67 ± 62.73	310.51 ± 188.86	385.04 ± 225.80	Higher in the PNF group than in the NG group ($p<0.05$)

Table 6. Histomorphometric evaluation of the right median nerve distally to the repair zone and of the vascular density in the middle portion of the reconstructed nerve defect in the different experimental groups

NG, nerve graft; **CNF**, conventional nerve flap; **ANVF**, arterialized neurovenous flap; **PNF**, prefabricated nerve flap

N/A, non-applicable

All parameters are expressed as percentages of the average contralateral values.

Numeric variables are expressed as average ± standard deviation.

Regarding the internal structure of the distal portion of the MN, the total number of nerve fibers was significantly higher in the CNF than in the NG ($p<0.01$; **Fig 16 B**). No other differences were found between the groups using conduits. The number of acetylcholinesterase positive fibers was higher in the Sham control group than in the remaining experimental groups ($p<0.001$; **Fig 16C**). Concerning this type of fibers, no differences were found in the latter groups. The average number of peripherin positive fibers was higher in the CNF and in the Sham groups than in the NG group ($p<0.001$; **Fig 16D**). Finally, the average number of acetylcholinesterase negative and peripherin negative fibers was once again higher in the CNF group than in the NG group ($p<0.001$; **Fig 16E**). Vascular density in the reconstructed nerve segment was lower in the NG group than in either the Sham or the PNF groups ($p<0.05$; **Fig 16 F**). No statistically significant differences were found between the CNF, ANVF and the PNF groups.

Histological characterization of the nerve conduits revealed greater architectural disorganization in the nerve graft conduit

Histological examination of the nerve conduits used to bridge the MN defect revealed preservation of the normal nerve architecture in the Sham group (**Figs 17A** to **17J**). In the Excision group, the distal stump of the MN showed clear signs of Wallerian degeneration in all the rats, as well as a proximal stump neuroma (**Figs 17K** to **17T**). In all rats in the NG group, there was a significant degree of fibrosis among the reconstituted nerve fibers. These fibrous septa divided the nerve structure in irregular bundles (**Figs 17P** to **17T**). In the CNF, the ANVF and the PNF groups, the reconstructed segment presented a single

nerve fascicle (CNF and ANVF groups) or two nerve fascicles (PNF) whose fibers were disposed in a cohesive fashion (**Figs 17T** to **I'**). In all the histological specimens in the ANVF group the brachial vein showed clear signs of arterialization. In addition, large tortuous veins could be seen in the proximity of the nerve segment (**Figs 17Z** and **17A'**). No clear signs of thrombosis were observed in the vein supplying flap in the ANVF group. In the histological sections of the PNF group it was also possible to observe arterialization of the venous fistula used to recruit the sciatic nerve segment (**Fig 17E'**). There was a greater density of large sized arterioles and venules in the epineurial region of these nerve segments than in any of the nerve conduits used in the other groups (**Fig 17F'**). Analogously, there is no evidence of vascular thrombosis of the vascular construct used to mobilize the nerve conduit. The primitive internal structure of the sciatic nerve was preserved until the most distal aspect of the nerve conduit in the PNF group (**Figs 17G'** to **I'**).

Retrograde axonal tracing using fluorescent markers showed anatomical restoration in all the groups using conduits

Lucifer Yellow and True Blue were seen reaching the proximal MN, the C7 dorsal root ganglion and the ventral horn of the C7 spinal cord segment in all rats in the Sham, NG, CNF, ANVF and PNF groups (**Figs 18** and **19**). In the Excision group, although there was some degree of auto fluorescence, no clear intracytoplasmic markers were observed. Semi quantitative evaluation revealed a higher number of stained cells in the Sham group in all the regions studied (**Fig 20A** to **D; Table 7**). The CNF group presented a higher

expression of fluorescent markers at all these locations than the NG group. However, this difference was statistically significant only for the Lucifer Yellow staining of the cells in the ventral horn of the spinal cord (p=0.045; **Fig 20D**). There were no significant differences between the NG group and the ANVF and the PNF groups regarding fluorescence staining.

Parameter	Sham group	NG group	CNF group	ANVF group	PNF group	Relevant findings
True Blue stained axons in the median nerve	96.10 ± 30.70	44.00 ± 14.29	55.58 ± 30.06	61.93 ± 40.55	77.25 ± 18.50	Higher average value in the Sham group than in the NG and CNF groups (p<0.05)
Diamidino Yellow stained axons in the median nerve	115.70 ± 28.49	45.10 ± 14.40	63.58 ± 21.88	63.07 ± 33.22	78.12 ± 24.19	No significant differences in the experimental groups
Stained ganglion cells	48.20 ± 13.95	19.60 ± 6.36	29.92 ± 5.19	20.13 ± 8.49	20.38 ± 12.47	No significant differences in the experimental groups
Stained ventral horn cells	6.50 ± 2.59	3.20 ± 1.23	5.25 ± 1.14	3.80 ± 1.47	4.12 ± 1.25	The CNF group presented a higher average value than the NG group (p=0.045)

Table 7. Evaluation of retrograde marking of the right median nerve proximally to the lesion site, of the right C7 dorsal ganglion and of the right ventral horn of the spinal cord at the C7 level.

NG, nerve graft; **CNF**, conventional nerve flap; **ANVF**, arterialized neurovenous flap; **PNF**, prefabricated nerve flap; **N/A**, non-applicable

All parameters are expressed as percentages of the average contralateral values.

Numeric variables are expressed as average ± standard deviation.

Multiple correlations were found between functional motor variables and neurophysiological and histomorphometric variables

Time to recovery of grasping in the operated limb was positively correlated with the neurological threshold (Pearson's correlation coefficient = 0.484; $p<0.001$), and with the motor threshold (Pearson's correlation coefficient = 0.735; $p<0.001$). Time to recovery of grasping was negatively correlated with the following parameters: CMAP Amplitude (Pearson's correlation coefficient = -0.611; $p<0.001$); FCR weight (Pearson's correlation coefficient = -0.769; $p<0.001$); maximal isometric wrist flexion strength (Pearson's correlation coefficient = -0.571; $p<0.001$); AUC in the strength x time graph (Pearson's correlation coefficient = -0.324; $p=0.003$); number of MN nerve fibers (Pearson's correlation coefficient = -0.464; $p<0.001$); number of MN acetylcholinesterase positive fibers (Pearson's correlation coefficient = -0.718; $p<0.001$); number of MN peripherin positive fibers (Pearson's correlation coefficient = -0.393; $p=0.004$); number of Lucifer Yellow positive fibers in the MN (Pearson's correlation coefficient = -0.409; $p=0.002$); number of True Blue marked DRG cells (Pearson's correlation coefficient = -0.511; $p<0.001$); and number of Lucifer Yellow marked neurons in the ventral horn of the spinal cord (Pearson's correlation coefficient = -0.393; $p=0.004$).

Similarly, FCR weight was positively correlated with the following variables: maximal isometric wrist flexion strength (Pearson's correlation coefficient = 0.548; p<0.001); AUC in the strength x time graph (Pearson's correlation coefficient = 0.288; p=0.009); CMAP amplitude (Pearson's correlation coefficient = 0.724; p<0.001); MN nerve area cross sectional area (Pearson's correlation coefficient = 0.486; p<0.001); number of MN nerve fibers (Pearson's correlation coefficient = 0.644; p<0.001); number of MN acetylcholinesterase positive fibers (Pearson's correlation coefficient = 0.624; p<0.001); number of MN peripherin positive fibers (Pearson's correlation coefficient = 0.454; p=0.001); number of MN acetylcholinesterase negative and peripherin negative fibers (Pearson's correlation coefficient = 0.294; p=0.038); vascular density in the reconstructed nerve gap (Pearson's correlation coefficient = 0.337; p=0.019); number of Lucifer Yellow positive fibers in the MN (Pearson's correlation coefficient = 0.356; p=0.008); number of True Blue stained DRG cells (Pearson's correlation coefficient = 0.418; p=0.002); and number of Lucifer Yellow marked neurons in the ventral horn of the spinal cord (Pearson's correlation coefficient = 0.352; p=0.008)

In opposition, FCR weight was negatively correlated with the neurological threshold (Pearson's correlation coefficient = -0.617; p<0.001), and with the motor threshold (Pearson's correlation coefficient = -0.803; p<0.001).

Additionally, maximal isometric wrist flexion strength was positively correlated with the following variables: CMAP Amplitude (Pearson's correlation coefficient = 0.434; p<0.001); MN area cross sectional area (Pearson's correlation coefficient = 0.292; p=0.024); number of MN nerve fibers (Pearson's correlation coefficient = 0.378; p=0.003); number

of MN acetylcholinesterase positive fibers (Pearson's correlation coefficient = 0.639; p<0.001); number of Lucifer Yellow stained fibers in the MN (Pearson's correlation coefficient = 0.357; p=0.007); number of True Blue marked DRG cells (Pearson's correlation coefficient = 0.396; p=0.003); and number of Lucifer Yellow positive neurons in the ventral horn of the spinal cord (Pearson's correlation coefficient = 0.521; p<0.001).

Maximal isometric wrist flexion strength was negatively correlated with the neurological threshold (Pearson's correlation coefficient = -0.324; p=0.003); and with the motor threshold (Pearson's correlation coefficient = -0.511; p<0.001).

AUC in the strength x time graph was positively correlated with CMAP Amplitude (Pearson's correlation coefficient = 0.428; p<0.001); the number of MN acetylcholinesterase positive fibers (Pearson's correlation coefficient = 0.458; p=0.001); the number of Lucifer Yellow stained fibers in the MN (Pearson's correlation coefficient = 0.305; p=0.023), and with the number of True Blue marked DRG cells (Pearson's correlation coefficient = 0.312; p=0.021).

AUC in the strength evaluation graph was negatively correlated with the motor threshold (Pearson's correlation coefficient = -0.321; p=0.003).

Velocity in the inclined ladder on D90 was positively correlated with the following assessments: FCR weight (Pearson's correlation coefficient = 0.547; p<0.001); Maximal isometric wrist flexion strength (Pearson's correlation coefficient = 0.248; p<0.024); CMAP Amplitude (Pearson's correlation coefficient = 0.428; p<0.001); MN cross sectional area (Pearson's correlation coefficient = 0.302; p=0.012); number of MN nerve fibers

(Pearson's correlation coefficient = 0.474; p<0.001); number of MN acetylcholinesterase positive fibers (Pearson's correlation coefficient = 0.434; p=0.002); number of MN peripherin positive fibers (Pearson's correlation coefficient = 0.334; p=0.012); and number of True Blue positive fibers in the MN (Pearson's correlation coefficient = 0.305; p=0.012)

Rats that did not present radial deviation in the walking tracks fared better that rats did present radial deviation in the following parameters: FCR weight (37.59% ± 16.27% vs. 84.25% ± 18.72%; p<0.001), maximal isometric flexion force (87.75% ± 62.36% vs. 27.47% ± 13.35%; p<0.001), MN cross section area (98.79% ± 22.10% vs. 66.79% ± 29.42%; p<0.001), total number of MN nerve fibers (87.43% ± 33.14% vs. 23.40% ± 37.77%; p<0.001); and number of peripherin stained fibers (88.08% ± 33.03% vs. 53.57% ± 41.28%; p=0.021).

Multiple correlations were found between nociception assessment and functional motor, neurophysiological and histomorphometric variables

Nociception evaluation by the pin prick test on D90 was positively correlated with velocity in the inclined ladder on D90 (Pearson's correlation coefficient = 0.550; p<0.001); with CMAP Amplitude (Pearson's correlation coefficient = 0.589; p<0.001); with MN cross section area (Pearson's correlation coefficient = 0.422; p=0.001); with the number of MN nerve fibers (Pearson's correlation coefficient = 0.614; p<0.001); with the number of MN

acetylcholinesterase positive fibers (Pearson's correlation coefficient = 0.316; p=0.011); with the number of MN peripherin positive fibers (Pearson's correlation coefficient = 0.348; p=0.012); with the number of True Blue stained fibers in the MN (Pearson's correlation coefficient = 0.295; p=0.029); with the number of Lucifer Yellow stained fibers in the MN (Pearson's correlation coefficient = 0.293; p=0.030); with the number of stained DRG cells (Pearson's correlation coefficient = 0.274; p=0.043); and even with the number of Lucifer Yellow positive neurons in the ventral horn of the spinal cord (Pearson's correlation coefficient = 0.339; p=0.011).

Finally, nociception evaluation by the pin prick test on D90 was negatively correlated the neurological threshold (Pearson's correlation coefficient = -0.561; p=0.003).

Discussion:

The authors believe that of the main merits of the present work was to apply in a same model of peripheral nerve gap and local ischemia, various autologous reconstructive techniques, in order to obtain more homogenous results. In fact, it is commonly accepted that it is difficult to conciliate the highly diverse experimental evidence, due to the various animal species tested, the multiple anatomical regions used, the inclusion or not of local ischemia, the different parameters evaluated, and the heterogenous follow-up time.[30] Additionally, to the best of the authors' knowledge, this is the largest series in the literature comparing different autologous techniques of MN gap reconstruction in the rat, in the presence of local ischemia.[90-92]

Overall, the results of this article seem to lend to support to the notion that vascularized nerve conduits in an ischemic environment lead to a more rapid and complete recovery. In fact, for all the parameters assessed, the groups using vascularized nerve conduits presented at least as good result of NG, and, in many circumstances, they ensured a better result that the latter option. For example, the Grasping Test revealed faster and more complete motor recovery in the CNF and in the ANVF groups than in the NG group. Likewise, the Pin prick test showed better nociceptive recovery in the CNF and ANVF groups than in the NG group. Walking Track Analysis revealed that the rate of radial deviation was lower in groups in which a vascularized nerve conduit was used. ENMG assessment revealed a lower motor stimulation threshold in the CNF and ANVF than in the NG group. Moreover, CNF and the ANVF presented better FCR muscle weight than

the NG group. Additionally, histomorphometric evaluation of the distal aspect of the MN showed a tendency to worse results in the NG group. In fact, CNF presented a higher MN cross section area, higher total number of nerve fibers, as well as higher number of peripherin positive and acetylcholinesterase negative and peripherin negative nerve fibers. Finally, histological characterization of the nerve conduits revealed greater architectural disorganization in the nerve graft conduit. The CNF group presented a higher expression of fluorescent markers at all these locations than the NG group.

Koshima *et al.* in 1985 had demonstrated that in the sciatic nerve of rats, CNFs yielded better results than NGs in reconstructing nerve defects in scarred regions after previous burns.[93, 94] Gu *et al.* in 1985 presented a study on New Zealand rabbits showing that CNFs were superior to nerve grafts for reconstructing a 20-mm MN defect even in favorable local conditions.[95] These data were soon validated in experiments performed in the same species by different authors.[96] However, subsequently, other authors concluded that nerve flaps did not benefit in reconstructing nerve defects in the context of normal perfusion in a rabbit model, suggesting that nerve flap reconstruction may be more beneficial in conditions of local ischemia.[30]

Notwithstanding, there is experimental evidence that CNFs, having a blood supply of its own, guarantee a better survival of Schwann cells, and are more efficiently permeated by macrophages, which will remove myelin fragments from degenerated axons.[97] Overall, these processes maintain a better architecture of the nerve conduit, promoting nerve regeneration.[22, 96-98] Blood supply to nerve conduits seems to be particularly critical in conditions of local ischemia, namely in regions of intense fibrosis, or prior

radiotherapy.[22, 96-98] These experimental findings have been corroborated clinically. In fact, it is well established that good perfusion of the nerve repair zone is mandatory to ensure a good functional outcome. [2, 3, 99, 100]

Interestingly, in this work, CNFs and ANVFs were, for most of the assessed variables, comparable.[95] Vargel *et al.* using a femoral nerve model of ischemia in the rat showed that ANVFs presented superior results to NGs in nerve gap reconstruction.[28, 29] In fact, Townsend *et al.* had already demonstrated a faster rate of axonal elongation in ANVFs executed in the hindlimb of 15 greyhound dogs compared to NGs.[19]

The PNF group did not present as good results as the CNF and the ANVF groups. This may be due to the fact that the sciatic nerve not only is larger than the MN, but it is also polyfascicular, composed of motor, sensory and mixed fascicles.[46, 47, 101] The MN of the rat is, at the arm level, monofascicular (**Fig 17**).[102] These morphometric differences may have led to a poor correspondence between motor and sensory axons, which, in turn, may have been responsible for inferior results in the PNF group comparatively to the other groups using vascularized nerve conduits.[103] These data contrast with those presented in the report of Karcher *et al.*, in which an arteriovenous fistula was used to produce a PNF involving the femoral nerve of the rat. This PFN provided better results in the reconstruction of a fascicle of the sciatic nerve of the rat than those obtained with an homologous NG.[32]

No significant differences were observed in the thermographic pattern of the different experimental groups 100 days after surgery (**Fig 10**). Several authors have reported higher skin temperature in the territory of recently severed nerves, putatively related to the loss of activity of the sympathetic fibers contained in these nerves, leading to cutaneous vasodilation and consequently local increase in blood supply and, ultimately higher temperature.[67, 104, 105] However, this association has not been demonstrated in cases of longstanding lesions.[106] For example, Sacharuk *et al.* have demonstrated a normalization of skin temperature in the hindlimb 21 days after a crush injury to the sciatic nerve.[106]

Interestingly, in this work multiple correlations were found between functional tests and neurophysiological and histomorphometric variables. In particular, an interesting finding of this study was the identification of radial deviation in forepaw prints of the rats with poorer outcomes in the following variables: FCR, maximal isometric flexion force, MN cross section area, total number of MN nerve fibers, and number of peripherin stained fibers. Thus, radial deviation of forepaws imprints may be of interest as surrogate marker of MN lesion. The underlying mechanism for radial deviation may be the denervation of the intrinsic muscles of the forepaw of the rat innervated by the MN, generating a situation similar to the median claw hand observed in humans.[107, 108] However, further studies are required to confirm or dismiss this hypothesis. In particular, it would have been interesting to study the histology of the muscles of rats presenting radial deviation and comparing these findings with those of rats without radial deviation.

Study Limitations Section

The trends in motor and sensory recovery between the different experimental groups were not homogenous for all the outcome variables assessed. However, the underlying mechanisms of peripheral nerve recovery are known to be complex and time-dependent, involving many issues affecting neuron survival, proximal axon regeneration, synaptogenesis, recovery of the denervated motor and sensory targets, as well as cerebral plasticity.[10, 100, 109, 110]

Apart from radial deviation, walking track analysis failed to provide consistent differences between groups. However, other authors have also found that single MN lesions in the rat frequently do not produce consistent changes in the walking pattern.[44] Moreover, other authors have argued that pawprint analysis is more useful for crushing nerve lesions than for segmental nerve defect reconstruction.[10] Moreover, it has also been shown that walking track analysis do not always correlate with muscle recovery.[111]

Regarding the choice of animal model, the rat sciatic nerve is arguably the most used nerve in peripheral nerve research.[112, 113] Notwithstanding, in this work the authors decided to use the rat MN, as the latter may present various advantages relatively to the former.[44, 45] In fact, MN lesions seem to be associated with lesser incidence of joint contractures and auto-mutilation of the affected limb.[44] Overall, rat welfare is more preserved with MN lesions than with sciatic nerve lesions.[113, 114] In addition, as the MN is shorter than the sciatic nerve, nerve recovery is observed sooner.[44, 112, 115-118] On top of this, most peripheral nerve lesions in the human species occur in the upper limb, further validating the use of this nerve in the rat.[3, 35, 119] Moreover, fine movement coordination in hand and finger movements is remarkably similar in rats and

humans.[113, 120] Finally, recently, multiple standardized strategies have been introduced to assess motor and sensory recovery in the rat MN model, permitting an easier comparison of results.[38, 39, 43, 45, 46, 62, 111, 113, 121]

Regarding the induction of a local ischemic environment, other authors have used a silicone barrier around the nerve repair zone in order to simulate a local ischemic medium.[29, 42] However, it may be argued that this model is not perfect, as silicone rods have been successfully used to reconstruct nerve defects in substitution of autologous conduits.[122, 123]

Also, the authors must concede that a major caveat of the present work is that rat peripheral nerves have much smaller cross-sectional areas than the homologous human structures. Theoretically, this should facilitate nerve revascularization, and promote better overall results in rats comparatively to humans.[29] In this sense, it would be useful to try to replicate the study herein described in larger animals. Furthermore, it is well established that reinnervation and functional recovery is more likely when nerve targets are closer to the repair zone.[109] The reasons for these are multiple: atrophy and fatty replacement of chronically denervated muscle, chronically denervated Schwann cells being less able to support regenerating axons, distal nerve histological disorganization increasing the likelihood of regenerating axons going into inappropriate endoneurial tubes and target organs (e.g. motor axons growing into endoneurial tubes connected to skin sensory organs or sensory axons growing into endoneurial tubes destined to motor plates).[109, 124] Moreover, under optimal conditions, in mammals, axonal elongation occurs at a rate of approximately 1-3 mm/day, limited by slow anterograde axonal

transport.[3, 100, 109] This means that rats and humans have similar nerve regeneration speeds. However, rat's nerves end organs are much closer to the place of nerve repair than in Man. Hence, the results of nerve repair are much faster in rats, which is convenient from an experimental point of view.[7, 93, 125, 126] Nevertheless, nerve recovery will probably be more complete than that observed in humans in similar circumstances.[3, 100, 127] To curb these biases, in the present study, the authors have restricted follow-up to 100 days. In fact, such follow-up time is used by most other researchers, in order to mitigate the effect of the exceptional neuroregenerative potential of rats.[90, 92] However, for all these reasons, the extrapolation of our results to the clinical setting should be made with caution. It would therefore be useful to try to replicate our findings in larger animals.

Another technical aspect that should be born in mind when comparing the results presented in this paper with those of other authors is that in the present work the excised MN segment was not inverted, as it is customary.[44, 48] The inversion of the nerve segment minimizes distal dispersion of the growing axons, maximizing the odds of these axons reaching their target organs, and ultimately leading to better functional recovery.[44, 48] In spite of this, the need of obtaining vascularized nerve conduits in this work precluded MN inversion. However, this variable was the same in all experimental groups, maintaining internal consistency of results.

Additionally, rat sexual dimorphism in nerve regeneration should be taken into account.[113] Female rats present better nerve regeneration, presumably because of the beneficial effects of sex hormones.[113, 128-130] This fact leads many researchers to

use female rats in peripheral nerve regeneration to maximize differences between experimental groups.[113] However, in humans, most injuries occur in males.[35, 131]

As other authors, in the present work we have used a morphological assessment of the blood supply to the reconstructed nerve segment, which was the *vasa nervorum* density.[132] However, it would be interesting to precisely evaluate the perfusion in each of the nerve conduits used using other methods in future studies.[133] Quantitative microelectrode hydrogen clearance polarography, laser doppler flowmetry, autoradiography employing radionuclides, and microsphere embolization would be viable alternatives.[132]

The arterio-venous fistula used to produce PNFs could have been applied in the contralateral forelimb, to produce a PNF involving a MN segment homologous to the nerve defect. This could potentially have facilitated comparison of the different vascular patterns used in nerve flaps. However, this option was not favored in the present study, as it would be technically vexing, and it would cause a major motor limitation in both forepaws, potentially compromising rats' abilities to conduct their daily activities, such as feeding or grooming.

In this study, only the most commonly described unconventional perfusion nerve flap was used, the ANVF. However, venous flow-through NFs have been shown to yield similar results to those obtained with ANVFs in a rat femoral nerve model.[28, 29] Further studies are warranted to confirm or dismiss this findings in the model used in the present study. Finally, it would have been interesting to include in this work a group using a rat MN allograft, as these conduits have been gaining increasing popularity in clinical practice.[9,

10, 23, 123] Noteworthily, Giusti *et al.* have recently demonstrated in a rat sciatic nerve model that blocking allograft vascularization from surrounding tissues was detrimental for motor recovery.[23] Thus, further studies are warranted in this field.

Conclusion:

CNFs and ANVFs produced a faster and more complete recovery than NGs in the reconstruction of a 10-mm-long median nerve gap in an ischemic environment in the Wistar rat. Although results obtained with CNFs were in most cases better than those of ANVFs, these differences were not statistically significant for most of the outcome variables.

Acknowledgments:

The authors would like to thank Mr. Filipe Franco and Mr. Nuno Folque for the drawings contained in this article.

Financial Disclosure Statement: One of the authors (D.C.) received a grant from “The Programme for Advanced Medical Education” sponsored by “Fundação Calouste Gulbenkian, Fundação Champalimaud, Ministério da Saúde and Fundação para a Ciência e Tecnologia, Portugal.”

The authors have no financial or commercial interests to declare in relation to the content of this article.

References

1. Desouches C, Alluin O, Mutaftschiev N, Dousset E, Magalon G, Boucraut J, et al. [Peripheral nerve repair: 30 centuries of scientific research]. Revue neurologique. 2005;161(11):1045-59. Epub 2005/11/17. PubMed PMID: 16288170.

2. Boyd KU, Fox IK. Nerve repair and grafting. In: Mackinnon SE, editor. Nerve surgery. 1. First ed. New York: Thieme; 2015. p. 75-100.

3. Wood MJ, Johnson PJ, Myckatyn TM. Anatomy and physiology for the peripheral nerve surgeon. In: Mackinnon SE, Yee A, editors. Nerve Surgery. 1. First ed. New York: Thieme; 2015. p. 1-40.

4. Philipeaux J, Vulpian A. Note sur des essais de greffe d'un troncon du nerf lingual entre les deux bouts du nerf hypoglosse, apres excision d'un segment de ce dernier nerf. Arch Physiol Norm Pathol. 1870;3:618-20.

5. Friedman AH. An eclectic review of the history of peripheral nerve surgery. Neurosurgery. 2009;65(4 Suppl):A3-8. Epub 2009/12/16. doi: 10.1227/01.NEU.0000346252.53722.D3. PubMed PMID: 19927076.

6. Geuna S, Tos P, Titolo P, Ciclamini D, Beningo T, Battiston B. Update on nerve repair by biological tubulization. Journal of brachial plexus and peripheral nerve injury. 2014;9(1):3. Epub 2014/03/13. doi: 10.1186/1749-7221-9-3. PubMed PMID: 24606921; PubMed Central PMCID: PMC3953745.

7. M.A. F, Wilbourn AJ. The electrodiagnostic examination with peripheral nerve injuries. In: Mackinnon SE, editor. Nerve surgery. 1. First ed. New York: Thieme; 2015. p. 59-74.

8. Rinker B, Zoldos J, Weber RV, Ko J, Thayer W, Greenberg J, et al. Use of Processed Nerve Allografts to Repair Nerve Injuries Greater Than 25 mm in the Hand. Ann Plast Surg. 2017;78(6S Suppl 5):S292-s5. Epub 2017/03/23. doi: 10.1097/sap.0000000000001037. PubMed PMID: 28328632.

9. Safa B, Buncke G. Autograft Substitutes: Conduits and Processed Nerve Allografts. Hand clinics. 2016;32(2):127-40. Epub 2016/04/21. doi: 10.1016/j.hcl.2015.12.012. PubMed PMID: 27094886.

10. Giusti G, Willems WF, Kremer T, Friedrich PF, Bishop AT, Shin AY. Return of motor function after segmental nerve loss in a rat model: comparison of autogenous nerve graft, collagen conduit, and processed allograft (AxoGen). The Journal of bone and joint surgery American volume. 2012;94(5):410-7. Epub 2012/03/09. doi: 10.2106/jbjs.k.00253. PubMed PMID: 22398734.

11. Ney KW. TECHNIC OF NERVE SURGERY. Annals of surgery. 1921;74(1):37-60. Epub 1921/07/01. PubMed PMID: 17864490; PubMed Central PMCID: PMCPMC1399588.

12. Seddon H. The use of autogenous grafts for the repair of large gaps in peripheral nerves. British Journal of Surgery. 1947;35(138):151-67.

13. Strange F. An operation for nerve pedicle grafting. Preliminary communication. British Journal of Surgery. 1947;34(136):423-5.

14. Taylor GI, Ham FJ. The free vascularized nerve graft. A further experimental and clinical application of microvascular techniques. Plastic and reconstructive surgery. 1976;57(4):413-26. Epub 1976/04/01. PubMed PMID: 1273122.

15. Hong MK, Taylor GI. Angiosome territories of the nerves of the upper limbs. Plastic and reconstructive surgery. 2006;118(1):148-60. Epub 2006/07/04. doi: 10.1097/01.prs.0000221075.91038.08. PubMed PMID: 16816688.

16. Breidenbach WC, Terzis JK. The blood supply of vascularized nerve grafts. J Reconstr Microsurg. 1986;3(1):43-58. Epub 1986/10/01. doi: 10.1055/s-2007-1007038. PubMed PMID: 3795195.

17. Chuang DC. Adult brachial plexus reconstruction with the level of injury: review and personal experience. Plast Reconstr Surg. 2009;124(6 Suppl):e359-69. Epub 2010/01/09. doi: 10.1097/PRS.0b013e3181bcf16c

00006534-200912001-00010 [pii]. PubMed PMID: 19952704.

18. Kakinoki R, Ikeguchi R, Nakayama K, Nakamura T. Functioning transferred free muscle innervated by part of the vascularized ulnar nerve connecting the contralateral cervical seventh root to themedian nerve: case report. J Brachial Plex Peripher Nerve Inj. 2007;2:18. Epub 2007/09/22. doi: 1749-7221-2-18 [pii]

10.1186/1749-7221-2-18. PubMed PMID: 17883873; PubMed Central PMCID: PMC2080628.

19. Townsend PL, Taylor GI. Vascularised nerve grafts using composite arterialised neuro-venous systems. Br J Plast Surg. 1984;37(1):1-17. Epub 1984/01/01. PubMed PMID: 6692051.

20. Casal D, Carvalho S, Pais D, Mota-Silva E, Iria I, Vieira P, et al. Unconventional Perfusion Flaps. 2017. In: Flap Surgery [Internet]. AvidScience; [2-41]. Available from:

http://www.avidscience.com/wp-content/uploads/2017/08/unconventional-perfusion-flaps.pdf.

21. Casal D, Cunha T, Pais D, Videira P, Coloma J, Zagalo C, et al. Systematic Review and Meta-Analysis of Unconventional Perfusion Flaps in Clinical Practice. Plastic and reconstructive surgery. 2016;138(2):459-79. doi: 10.1097/PRS.0000000000002390. PubMed PMID: 27465169.

22. ANGÉLICA-ALMEIDA M, CASAL D, MAFRA M, MASCARENHAS-LEMOS L, SILVA E, FARINHO A, et al. Evaluation of the efficacy of different conduits to bridge a 10 millimeter defect in the rat sciatic nerve in the presence of an axial blood supply. Archives of Anatomy. 2014;2:8-30.

23. Giusti G, Lee JY, Kremer T, Friedrich P, Bishop AT, Shin AY. The influence of vascularization of transplanted processed allograft nerve on return of motor function in rats. Microsurgery. 2016;36(2):134-43. Epub 2015/01/06. doi: 10.1002/micr.22371. PubMed PMID: 25557845.

24. D'Arpa S, Claes KEY, Stillaert F, Colebunders B, Monstrey S, Blondeel P. Vascularized nerve "grafts": just a graft or a worthwhile procedure? Plastic and Aesthetic Research. 2015;2(4):183-94.

25. Brandt J, Dahlin LB, Lundborg G. Autologous tendons used as grafts for bridging peripheral nerve defects. J Hand Surg Br. 1999;24(3):284-90. Epub 1999/08/05. doi: 10.1054/jhsb.1999.0074

S0266-7681(99)90074-8 [pii]. PubMed PMID: 10433437.

26. Millesi H. Bridging defects: autologous nerve grafts. Acta Neurochir Suppl. 2007;100:37-8. Epub 2007/11/08. PubMed PMID: 17985542.

27. Hems TEJ, Glasby MA. Comparison of different methods of repair of long peripheral nerve defects: an experimental study. British journal of plastic surgery. 1992;45(7):497-502. doi: http://dx.doi.org/10.1016/0007-1226(92)90141-J.

28. Vargel I. Impact of vascularization type on peripheral nerve microstructure. J Reconstr Microsurg. 2009;25(4):243-53. Epub 2008/12/17. doi: 10.1055/s-0028-1104557. PubMed PMID: 19085817.

29. Vargel I, Demirci M, Erdem S, Firat P, Surucu HS, Tan E, et al. A comparison of various vascularization-perfusion venous nerve grafts with conventional nerve grafts in rats. J Reconstr Microsurg. 2009;25(7):425-37. Epub 2009/05/28. doi: 10.1055/s-0029-1223852. PubMed PMID: 19472105.

30. Donzelli R, Capone C, Sgulo FG, Mariniello G, Maiuri F. Vascularized nerve grafts: an experimental study. Neurological research. 2016;38(8):669-77. doi: 10.1080/01616412.2016.1198527. PubMed PMID: 27349271.

31. Cavadas PC, Vera-Sempere FJ. Prefabrication of a vascularized nerve graft by vessel implantation: preliminary report of an experimental model. Microsurgery. 1994;15(12):877-81. Epub 1994/01/01. PubMed PMID: 7535881.

32. Karcher H, Kleinert R. Regeneration in vascularized and free nerve grafts. A comparative morphological study in rats. Journal of maxillofacial surgery. 1986;14(6):341-3. Epub 1986/12/01. PubMed PMID: 3467003.

33. Guo L, Pribaz JJ. Clinical flap prefabrication. Plastic and reconstructive surgery. 2009;124(6 Suppl):e340-50. Epub 2010/01/09. doi: 10.1097/PRS.0b013e3181bcf094. PubMed PMID: 19952702.

34. Shin RH, Friedrich PF, Crum BA, Bishop AT, Shin AY. Treatment of a segmental nerve defect in the rat with use of bioabsorbable synthetic nerve conduits: a comparison of commercially available conduits. J Bone Joint Surg Am. 2009;91(1):2194-204.

35. Rosberg HEeLD. Epidemiology of hand injuries in a middle-sized city in southern Sweden - a retrospective study with an 8-year interval. Scand J Plast Rec Surg Hand Surg. 2004;(38):347-55.

36. National Research Council (U.S.). Committee for the Update of the Guide for the Care and Use of Laboratory Animals., Institute for Laboratory Animal Research (U.S.), National Academies Press (U.S.). Guide for the care and use of laboratory animals. Washington, D.C.: National Academies Press,; 2011. Available from: http://www.ncbi.nlm.nih.gov/books/NBK54050.

37. Havenaar Rea. Biology and husbrandry of laboratoy animals. In: Principles of Laboratory Animal Science. Editores: Van Zutphen, L.F.M.; Baumans, V.; Beynen, A.C.. Elsevier. 2001:29-32.

38. Bertelli JAM, J.C. Behavioural evaluating methods in the objective clinical assessment of motor function after experimental brachial plexus reconstruction in the rat. Journal of neuroscience methods. 1993;46:203-8.

39. Dijkstra JR, et al. . Methods to evaluate functional nerve recovery in adult rats: walking track analysis, video analysis and the withdrawal reflex. Journal of neuroscience methods. 2000;96(2):89-96.

40. Rupp A, Dornseifer U, Rodenacker K, Fichter A, Jutting U, Gais P, et al. Temporal progression and extent of the return of sensation in the foot provided by the saphenous nerve after sciatic nerve transection and repair in the rat - implications for nociceptive assessments. Somatosensory & motor research. 2007;24(1-2):1-13. Epub 2007/06/15. doi: 10.1080/08990220601116329. PubMed PMID: 17558918.

41. Casal D, Pais D, Iria I, Mota-Silva E, Almeida M-A, Alves S, et al. A Model of Free Tissue Transfer: The Rat Epigastric Free Flap. Journal of Visualized Experiments. 2017;1(119):e55281. doi: doi:10.3791/55281.

42. Matsumine H, Sasaki R, Takeuchi Y, Miyata M, Yamato M, Okano T, et al. Vascularized versus nonvascularized island median nerve grafts in the facial nerve regeneration and functional recovery of rats for facial nerve reconstruction study. Journal of reconstructive microsurgery. 2014;30(02):127-36.

43. Bertelli JAM, J.C. The grasping test: a simple behavioral method for objective quantitative assessment of peripherla nerve regeneration in the rat. Journal of neuroscience methods. 1995;58(1-2):151-5.

44. Bontioti EKM, Dahlin LB. Regeneration and functional recovery in the upper extermity of rats after various types of nerve injuries. Journal of the Peripheral Nervous System. 2003;8:159-68.

45. Galtrey CM, Fawcett JW. Characterization of tests of functional recovery after median and ulnar nerve injury and repair in the rat forelimb. J Peripher Nerv Syst. 2007;12(1):11-27. Epub 2007/03/22. doi: 10.1111/j.1529-8027.2007.00113.x. PubMed PMID: 17374098.

46. Angelica-Almeida M, Casal D, Mafra M, Mascarenhas-Lemos L, Martins-Ferreira J, Ferraz-Oliveira M, et al. Brachial plexus morphology and vascular supply in the wistar rat. Acta Med Port. 2013;26(3):243-50. Epub 2013/07/03. PubMed PMID: 23815839.

47. Bertelli JA, Taleb M, Saadi A, Mira JC, Pecot-Dechavassine M. The rat brachial plexus and its terminal branches: an experimental model for the study of peripheral nerve regeneration. Microsurgery. 1995;16(2):77-85. Epub 1995/01/01. PubMed PMID: 7783609.

48. Yanase Y. Micronerve suture and graft in the rat. In: Tamai S, Usui M, Yoshizu T, editors. Experimental and Clinical Reconstructive Microsurgery. First ed. Japan: Springer-Verlag; 2004. p. 44-51.

49. Geuna S, Varejao AS. Evaluation methods in the assessment of peripheral nerve regeneration. Journal of neurosurgery. 2008;109(2):360-2; author reply 2. Epub 2008/08/02. doi: 10.3171/JNS/2008/109/8/0360. PubMed PMID: 18671655.

50. Ronchi G, Nicolino S, Raimondo S, Tos P, Battiston B, Papalia I, et al. Functional and morphological assessment of a standardized crush injury of the rat median nerve. Journal of neuroscience methods. 2009;179(1):51-7. Epub 2009/05/12. doi: 10.1016/j.jneumeth.2009.01.011. PubMed PMID: 19428511.

51. Ronchi G, Raimondo S, Varejao AS, Tos P, Perroteau I, Geuna S. Standardized crush injury of the mouse median nerve. Journal of neuroscience methods. 2010;188(1):71-5. Epub 2010/01/29. doi: 10.1016/j.jneumeth.2010.01.024. PubMed PMID: 20105442.

52. Kobbert C, Apps R, Bechmann I, Lanciego JL, Mey J, Thanos S. Current concepts in neuroanatomical tracing. Progress in neurobiology. 2000;62(4):327-51. Epub 2000/06/17. PubMed PMID: 10856608.

53. Bertelli JAM, J.C. The grasping test: a simple behavioral method for objective quantitative assessment of peripheral nerve regeneration in the rat. Journal of neuroscience methods. 1995;58(1-2):151-5.

54. Papalia I, Tos P, Stagno d'Alcontres F, Battiston B, Geuna S. On the use of the grasping test in the rat median nerve model: a re-appraisal of its efficacy for quantitative assessment of motor function recovery. Journal of neuroscience methods. 2003;127(1):43-7. Epub 2003/07/17. PubMed PMID: 12865147.

55. Costa LM, Simoes MJ, Mauricio AC, Varejao AS. Chapter 7: Methods and protocols in peripheral nerve regeneration experimental research: part IV-kinematic gait analysis to quantify peripheral nerve regeneration in the rat. International review of neurobiology. 2009;87:127-39. Epub 2009/08/18. doi: 10.1016/s0074-7742(09)87007-4. PubMed PMID: 19682636.

56. Howard RF, Hatch DJ, Cole TJ, Fitzgerald M. Inflammatory pain and hypersensitivity are selectively reversed by epidural bupivacaine and are developmentally regulated. Anesthesiology. 2001;95(2):421-7. PubMed PMID: 11506116.

57. de Sousa MV, Ferraresi C, de Magalhaes AC, Yoshimura EM, Hamblin MR. Building, testing and validating a set of home-made von Frey filaments: A precise, accurate and cost effective alternative for nociception assessment. Journal of

neuroscience methods. 2014;232:1-5. Epub 2014/05/06. doi: 10.1016/j.jneumeth.2014.04.017. PubMed PMID: 24793398.

58. Lambert GA, Mallos G, Zagami AS. Von Frey's hairs--a review of their technology and use--a novel automated von Frey device for improved testing for hyperalgesia. Journal of neuroscience methods. 2009;177(2):420-6. Epub 2008/12/02. doi: 10.1016/j.jneumeth.2008.10.033. PubMed PMID: 19041344.

59. Blackburn-Munro G. Pain-like behaviours in animals - how human are they? Trends in pharmacological sciences. 2004;25(6):299-305. Epub 2004/05/29. doi: 10.1016/j.tips.2004.04.008. PubMed PMID: 15165744.

60. Pitcher GM, Ritchie J, Henry JL. Paw withdrawal threshold in the von Frey hair test is influenced by the surface on which the rat stands. Journal of neuroscience methods. 1999;87(2):185-93. Epub 2001/03/07. PubMed PMID: 11230815.

61. Metz GA, Whishaw IQ. Cortical and subcortical lesions impair skilled walking in the ladder rung walking test: a new task to evaluate fore-and hindlimb stepping, placing, and co-ordination. Journal of neuroscience methods. 2002;115(2):169-79.

62. Hadlock TA, et al. A comparison of assessments of functional recovery in the rat. J Peripher Nerv Syst. 1999;4(3-4):258-64.

63. Brown CJ, Mackinnon SE, Evans PJ, Bain JR, Makino AP, Hunter DA, et al. Self-evaluation of walking-track measurement using a Sciatic Function Index. Microsurgery. 1989;10(3):226-35. Epub 1989/01/01. PubMed PMID: 2796719.

64. Hruska RE, Kennedy S, Silbergeld EK. Quantitative aspects of normal locomotion in rats. Life sciences. 1979;25(2):171-9.

65. Ludwig N, Formenti D, Gargano M, Alberti G. Skin temperature evaluation by infrared thermography: Comparison of image analysis methods. Infrared Physics & Technology. 2014;62:1-6.

66. Bennett GJ, Ochoa J. Thermographic observations on rats with experimental neuropathic pain. Pain. 1991;45(1):61-7.

67. Wakisaka S, Kajander KC, Bennett GJ. Abnormal skin temperature and abnormal sympathetic vasomotor innervation in an experimental painful peripheral neuropathy. Pain. 1991;46(3):299-313.

68. Wu Y, Martínez MÁM, Balaguer PO. Overview of the Application of EMG Recording in the Diagnosis and Approach of Neurological Disorders. In: Turker H, editor. Electrodiagnosis in New Frontiers of Clinical Research. Rijeka: InTech; 2013. p. Ch. 01.

69. Werdin F, Grussinger H, Jaminet P, Kraus A, Manoli T, Danker T, et al. An improved electrophysiological method to study peripheral nerve regeneration in rats. Journal of neuroscience methods. 2009;182(1):71-7. Epub 2009/06/10. doi: 10.1016/j.jneumeth.2009.05.017. PubMed PMID: 19505504.

70. Manoli T, Werdin F, Gruessinger H, Sinis N, Schiefer JL, Jaminet P, et al. Correlation analysis of histomorphometry and motor neurography in the median nerve rat model. Eplasty. 2014;14:e17. Epub 2014/06/07. PubMed PMID: 24904711; PubMed Central PMCID: PMC3984537.

71. Navarro X, Udina E. Chapter 6: Methods and protocols in peripheral nerve regeneration experimental research: part III-electrophysiological evaluation.

International review of neurobiology. 2009;87:105-26. Epub 2009/08/18. doi: 10.1016/s0074-7742(09)87006-2. PubMed PMID: 19682635.

72. Raimondo S, Fornaro M, Di Scipio F, Ronchi G, Giacobini-Robecchi MG, Geuna S. Chapter 5: Methods and protocols in peripheral nerve regeneration experimental research: part II-morphological techniques. International review of neurobiology. 2009;87:81-103. Epub 2009/08/18. doi: 10.1016/s0074-7742(09)87005-0. PubMed PMID: 19682634.

73. World I. Neurofilament Antibody Staining Protocol for Immunohistochemistry [16/09/2017]. Available from: http://www.ihcworld.com/_protocols/antibody_protocols/neurofilament_chemicon.htm.

74. Holland SK, Hessler RB, Reid-Nicholson MD, Ramalingam P, Lee JR. Utilization of peripherin and S-100 immunohistochemistry in the diagnosis of Hirschsprung disease. Mod Pathol. 2010;23(9):1173-9.

75. Rakonczay Z, Brimijoin S. Monoclonal antibodies to rat brain acetylcholinesterase: comparative affinity for soluble and membrane-associated enzyme and for enzyme from different vertebrate species. Journal of neurochemistry. 1986;46(46).

76. Ikeda M, Oka Y. The relationship between nerve conduction velocity and fiber morphology during peripheral nerve regeneration. Brain and Behavior. 2012;2(4):382-90. doi: 10.1002/brb3.61. PubMed PMID: PMC3432961.

77. Afifi AK, Bergman RA. Neurohistology. In: Afifi AK, Bergman RA, editors. Functional Neuroanatomy: text and atlas. Second ed. United States of America: McGraw-Hill; 2005. p. 3-23.

78. Nolte J. Sensory receptors and the peripheral nervous system. In: Nolte J, editor. The human brain: an introduction to its functional anatomy. Fifth ed. Tucson, Arizon: Mosby; 2002. p. 197-222.

79. Riley DA, Sanger JR, Matloub HS, Yousif NJ, Bain JLW, Moore GH. Identifying motor and sensory myelinated axons in rabbit peripheral nerves by histochemical staining for carbonic anhydrase and cholinesterase activities. Brain Research. 1988;453(1):79-88. doi: http://dx.doi.org/10.1016/0006-8993(88)90145-X.

80. Zochodne DW. The intact peripheral nerve tree. In: Zochodne DW, editor. Neurobiology of peripheral nerve regeneration. 1. First ed. United Kingdom: Cambridge; 2008. p. 8-38.

81. Szabolcs MJ, Windisch A, Koller R, Pensch M. Axon typing of rat muscle nerves using a double staining procedure for cholinesterase and carbonic anhydrase. The journal of histochemistry and cytochemistry : official journal of the Histochemistry Society. 1991;39(12):1617-25. Epub 1991/12/01. doi: 10.1177/39.12.1719070. PubMed PMID: 1719070.

82. Geuna S, Tos P, Guglielmone R, Battiston B, Giacobini-Robecchi MG. Methodological issues in size estimation of myelinated nerve fibers in peripheral nerves. Anatomy and embryology. 2001;204(1):1-10. Epub 2001/08/17. PubMed PMID: 11506429.

83. West MJ. Estimating object number. In: West MJ, editor. Basic stereology for biologists and neuroscientists. 1. First ed. New York: Cold Spring Harbor Laboratory Press; 2012. p. 31-58.

84. Geuna S. The revolution of counting "tops": two decades of the disector principle in morphological research. Microscopy research and technique. 2005;66(5):270-4. Epub 2005/06/09. doi: 10.1002/jemt.20167. PubMed PMID: 15940681.

85. Puigdellivol-Sanchez A, Prats-Galino A, Molander C. On regenerative and collateral sprouting to hind limb digits after sciatic nerve injury in the rat. Restorative neurology and neuroscience. 2005;23(2):97-107. Epub 2005/07/02. PubMed PMID: 15990416.

86. Daly WT, Yao L, Abu-rub MT, O'Connell C, Zeugolis DI, Windebank AJ, et al. The effect of intraluminal contact mediated guidance signals on axonal mismatch during peripheral nerve repair. Biomaterials. 2012;33(28):6660-71. doi: 10.1016/j.biomaterials.2012.06.002. PubMed PMID: 22738778.

87. Sarikcioglu L, Oguz N. Exercise training and axonal regeneration after sciatic nerve injury. The International journal of neuroscience. 2001;109(3-4):173-7. Epub 2001/11/09. PubMed PMID: 11699329.

88. Jivan S, Novikova LN, Wiberg M, Novikov LN. The effects of delayed nerve repair on neuronal survival and axonal regeneration after seventh cervical spinal nerve axotomy in adult rats. Experimental brain research Experimentelle Hirnforschung Experimentation cerebrale. 2006;170(2):245-54. Epub 2005/12/06. doi: 10.1007/s00221-005-0207-7. PubMed PMID: 16328277.

89. Rupp A. Functional, electrophysioologic and morphometric evaluation of peripheral nerve regeneration after bridging a 14 mm gap in the rat sciatic nerve. Munich: Ludwig-Maximilians; 2007.

90. Angius D, Wang H, Spinner RJ, Gutierrez-Cotto Y, Yaszemski MJ, Windebank AJ. A systematic review of animal models used to study nerve regeneration in tissue-engineered scaffolds. Biomaterials. 2012;33(32):8034-9. Epub 2012/08/15. doi: 10.1016/j.biomaterials.2012.07.056. PubMed PMID: 22889485; PubMed Central PMCID: PMCPMC3472515.

91. Evans GR. Peripheral nerve injury: a review and approach to tissue engineered constructs. Anat Rec. 2001;263(4):396-404.

92. Myckatyn TM, Mackinnon SE. A review of research endeavors to optimize peripheral nerve reconstruction. Neurol Res. 2004;26(1):124-38.

93. Koshima I, Harii K. Experimental study of vascularized nerve grafts: Multifactorial analyses of axonal regeneration of nerves transplanted into an acute burn wound. The Journal of hand surgery. 1985;10(1):64-72. doi: http://dx.doi.org/10.1016/S0363-5023(85)80249-5.

94. Koshima I, Harii K. Experimental study of vascularized nerve grafts: multifactorial analyses of axonal regeneration of nerves transplanted into an acute burn wound. The Journal of hand surgery. 1985;10(1):64-72. Epub 1985/01/01. PubMed PMID: 3968406.

95. Gu YD, Wu MM, Zheng YL, Li HR, Xu YN. Arterialized venous free sural nerve grafting. Ann Plast Surg. 1985;15(4):332-9. Epub 1985/10/01. PubMed PMID: 4083733.

96. Breidenbach WC, Terzis JK. Vascularized nerve grafts: an experimental and clinical review. Ann Plast Surg. 1987;18(2):137-46. Epub 1987/02/01. PubMed PMID: 3566101.

97. Koshima IH, K. Experimental studies on vascularized nerve grafts in rats. J Microsurg. 1981;2:225-6.

98. Breindenbach WT, JK. The anatomy of free vascularized nerve grafts. Clin Plast Surg. 1984;11:65-71.

99. Jabaley ME. Primary Nerve Repair. In: Peripheral Nerve Surgery: Practical Applications in the Upper Extremity. Editores: Slutsky, D.J.; Hentz, V.R. Churchill Livingstone. 2006:23-38.

100. Dahlin LB. Nerve injury and repair: from molecule to Man. In: Slutsky DJ, Hentz VR, editors. Peripheral Nerve Surgery: Practical Applications in the Upper Extremity. Philadelphia: Elsevier; 2006. p. 1-22.

101. ANGÉLICA-ALMEIDA M, CASAL D, MAFRA M, MASCARENHAS-LEMOS L, MARTINS-FERREIRA J, FERRAZ-OLIVEIRA M, et al. Angiomorphological comparison of the sciatic nerve of the rat and the human median nerve: implications in experimental procedures. Archives of Anatomy. 2014;2:31-51.

102. Santos AP, Suaid CA, Fazan VP, Barreira AA. Microscopic anatomy of brachial plexus branches in Wistar rats. Anat Rec (Hoboken). 2007;290(5):477-85. doi: 10.1002/ar.20519. PubMed PMID: 17436315.

103. Nichols CM, Brenner MJ, Fox IK, Tung TH, Hunter DA, Rickman SR, et al. Effects of motor versus sensory nerve grafts on peripheral nerve regeneration. Experimental neurology. 2004;190(2):347-55. doi: http://dx.doi.org/10.1016/j.expneurol.2004.08.003.

104. Bennett K, Heywood W, Di WL, Harper J, Clayman GL, Jayakumar A, et al. The identification of a new role for LEKTI in the skin: The use of protein 'bait' arrays to detect defective trafficking of dermcidin in the skin of patients with Netherton syndrome.

Journal of proteomics. 2012;75(13):3925-37. Epub 2012/05/17. doi: 10.1016/j.jprot.2012.04.045. PubMed PMID: 22588119.

105. Ochoa JL, Yarnitsky D, Marchettini P, Dotson R, Cline M. Interactions between sympathetic vasoconstrictor outflow and C nociceptor-induced antidromic vasodilatation. Pain. 1993;54(2):191-6. Epub 1993/08/01. PubMed PMID: 8233533.

106. Sacharuk VZ, Lovatel GA, Ilha J, Marcuzzo S, Pinho ASd, Xavier LL, et al. Thermographic evaluation of hind paw skin temperature and functional recovery of locomotion after sciatic nerve crush in rats. Clinics. 2011;66(7):1259-66.

107. Kilinc A, Ben Slama S, Dubert T, Dinh A, Osman N, Valenti P. [Results of primary repair of injuries to the median and ulnar nerves at the wrist]. Chirurgie de la main. 2009;28(2):87-92. Epub 2009/02/28. doi: 10.1016/j.main.2009.01.001. PubMed PMID: 19246233.

108. Chan RK. Splinting for peripheral nerve injury in upper limb. Hand surgery : an international journal devoted to hand and upper limb surgery and related research : journal of the Asia-Pacific Federation of Societies for Surgery of the Hand. 2002;7(2):251-9. Epub 2003/02/22. PubMed PMID: 12596288.

109. Sulaiman W, Gordon T. Neurobiology of peripheral nerve injury, regeneration, and functional recovery: from bench top research to bedside application. Ochsner J. 2013;13(1):100-8. PubMed PMID: 23531634; PubMed Central PMCID: PMCPMC3603172.

110. Vincent R. Adult and obstetrical brachial plexus injuries. In: Peripheral Nerve Surgery: Practical applications in the upper extremity. Editores: Slutsky DJ, Hentz VR. Churchill Livingstone. 2006:299-317.

111. Urbancheck MSea. Rat walking tracks do not reflect maximal muscle force capacity. J Reconstr Microsurg. 1999;15(2):143-9.

112. Bontioti E. End-to-side nerve repair. A study in the forelimb of the rat. Tese de Doutoramento. Faculdade de Medicina da Universidade de Lund. Suécia. 2005:36-41.

113. Tos P, Ronchi G, Papalia I, Sallen V, Legagneux J, Geuna S, et al. Chapter 4: Methods and protocols in peripheral nerve regeneration experimental research: part I-experimental models. International review of neurobiology. 2009;87:47-79. Epub 2009/08/18. doi: 10.1016/s0074-7742(09)87004-9. PubMed PMID: 19682633.

114. Papalia I, Tos P, Scevola A, Raimondo S, Geuna S. The ulnar test: a method for the quantitative functional assessment of posttraumatic ulnar nerve recovery in the rat. Journal of neuroscience methods. 2006;154(1-2):198-203. Epub 2006/02/10. doi: 10.1016/j.jneumeth.2005.12.012. PubMed PMID: 16466801.

115. Bodine-Fowler SCea. Inaccurate projection of rat soleus motoneurons: a comparison of nerve repair techniques. Muscle & nerve. 1997;20(1):29-37.

116. Valero-Cabre AN, X. H reflex restitution and facilitation after different types of peripheral nerve injury and repair. Brain Res. 2001;919(2):302-12.

117. Wall PD, et al. Autotomy following peripheral nerve lesions: experimental anaesthesia dolorosa. Pain. 1979;7(2):103-11.

118. Bertelli JAS, A; Pecot-Dechavassine, M. The rat brachial plexus an its terminal branches: an experimental model for the study of peripheral nerve regeneration. Microsurgery. 1995;16:77-85.

119. Murovic JA. Upper-extremity peripheral nerve injuries: a Louisiana State University Health Sciences Center literature review with comparison of the operative

outcomes of 1837 Louisiana State University Health Sciences Center median, radial, and ulnar nerve lesions. Neurosurgery. 2009;65(4 Suppl):A11-7. Epub 2009/12/16. doi: 10.1227/01.neu.0000339130.90379.89. PubMed PMID: 19927055.

120. Nichols CM, Myckatyn TM, Rickman SR, Fox IK, Hadlock T, Mackinnon SE. Choosing the correct functional assay: a comprehensive assessment of functional tests in the rat. Behavioural brain research. 2005;163(2):143-58. Epub 2005/06/28. doi: 10.1016/j.bbr.2005.05.003. PubMed PMID: 15979168.

121. Bertelli JAG, M.F. Concepts of Nerve Regeneration and Repair Applied to the Brachial Plexus Reconstruction. Microsurgery. 2006;26:230-44.

122. Battiston B, Geuna S, Ferrero M, Tos P. Nerve repair by means of tubulization: literature review and personal clinical experience comparing biological and synthetic conduits for sensory nerve repair. Microsurgery. 2005;25(4):258-67. Epub 2005/06/04. doi: 10.1002/micr.20127. PubMed PMID: 15934044.

123. Isaacs J, Browne T. Overcoming short gaps in peripheral nerve repair: conduits and human acellular nerve allograft. Hand (N Y). 2014;9(2):131-7. doi: 10.1007/s11552-014-9601-6. PubMed PMID: 24839412; PubMed Central PMCID: PMCPMC4022952.

124. Fu SY, Gordon T. Contributing factors to poor functional recovery after delayed nerve repair: prolonged denervation. The Journal of neuroscience : the official journal of the Society for Neuroscience. 1995;15(5 Pt 2):3886-95. Epub 1995/05/01. PubMed PMID: 7751953.

125. Guth L. Regeneration in the mammalian peripheral nervous system. Physiological reviews. 1956;36(4):441-78. Epub 1956/10/01. PubMed PMID: 13370345.

126. Strasberg JE, Strasberg S, Mackinnon SE, Watanabe O, Hunter DA, Tarasidis G. Strain differences in peripheral-nerve regeneration in rats. J Reconstr Microsurg. 1999;15(4):287-93. Epub 1999/06/11. doi: 10.1055/s-2007-1000103. PubMed PMID: 10363552.

127. Kaplan HM, Mishra P, Kohn J. The overwhelming use of rat models in nerve regeneration research may compromise designs of nerve guidance conduits for humans. Journal of materials science Materials in medicine. 2015;26(8):226. Epub 2015/08/25. doi: 10.1007/s10856-015-5558-4. PubMed PMID: 26296419; PubMed Central PMCID: PMCPMC4545171.

128. Melcangi RC, Giatti S, Calabrese D, Pesaresi M, Cermenati G, Mitro N, et al. Levels and actions of progesterone and its metabolites in the nervous system during physiological and pathological conditions. Progress in neurobiology. 2014;113:56-69. Epub 2013/08/21. doi: 10.1016/j.pneurobio.2013.07.006. PubMed PMID: 23958466.

129. Roglio I, Bianchi R, Gotti S, Scurati S, Giatti S, Pesaresi M, et al. Neuroprotective effects of dihydroprogesterone and progesterone in an experimental model of nerve crush injury. Neuroscience. 2008;155(3):673-85. Epub 2008/07/16. doi: 10.1016/j.neuroscience.2008.06.034. PubMed PMID: 18625290.

130. Kovacic U, Sketelj J, Bajrovic FF. Sex-related difference in collateral sprouting of nociceptive axons after peripheral nerve injury in the rat. Experimental neurology. 2003;184(1):479-88. Epub 2003/11/26. PubMed PMID: 14637117.

131. Frazier WH, et al. Hand injuries: incidence and epidemiology in an emergency service. Jacep. 1978;7(7):265-8.

132. Zochodne DW. Regeneration and the vasa nervorum. In: Zochodne DW, editor. Neurobiology of peripheral nerve regeneration. 1. First ed. United Kingdom: Cambridge; 2008. p. 153-69.

133. Wang Y, Tang P, Zhang L, Guo Y, Wan W. Quantitative evaluation of the peripheral nerve blood perfusion with high frequency contrast-enhanced ultrasound. Academic radiology. 2010;17(12):1492-7.

Figure Legends:

Figure 1. Experimental groups' schematic representation and representative photographs. A to F, Schematic drawings of the different methods of bridging the median nerve gap in the various experimental groups. G to R, photographs of representative intra-operative images. All images represent the right forelimb with the exception of Q, which represents the left groin region.

1, median nerve; 2, distal stump of the median nerve; 3, proximal stump of the median nerve; 4, autologous median nerve graft; 5, median nerve conventional flap; 6, arterialized neurovenous flap; 7, brachial artery; 8, arterio-venous anastomosis; 9, brachial vein; 10, prefabricated nerve flap; 11, arterio-venous fistula used to produce the prefabricated nerve flap; 12, medial antebrachial nerve; 13, ulnar nerve; 14, silicone rod place around the nerve gap to simulate an ischemic environment; 15, *vasa nervorum* to median nerve flap; 16, *vena nervorum*; 17, arteriovenous loop; 18, femoral vein; 19, femoral artery

Ca, Caudal; Cr, Cranial; La, Lateral; Me, Medial.

Calibration bar = 1 mm

Figure 2. Conventional flap pre-fabrication and transfer.

A. Prefabrication of the flap in the left thigh.

B. Insetting of the flap in the recipient area in the right arm.

1. An inverted “T” incision is performed in the most caudal aspect of the ventral region of the abdomen of the rat, with the axial portion crossing immediately cranial to the pubic symphysis and with the longitudinal component extending from this point cranially for 3 cm.

2. The right superficial caudal epigastric vein is dissected from the homonymous artery and the caudal epigastric nerve during its entire length, including also part of the its lateral afferent vein.

3. The venous segment is harvested and its origin and termination sites are ligated with interrupted 9/0 Nylon stitches.

4. The venous conduit is inverted and its terminal-laterally anastomosed to the left femoral artery using an interrupted 11/0 Nylon suture.

5. The two epigastric veins are terminal-terminally anastomosed with interrupted 11/0 Nylon stitches, producing and arterial-venous fistula;

6. The left sciatic nerve is exposed through a ventral approach in the medial aspect of the thigh, in the space between the gracilis muscle, placed laterally, and the semimembranosus muscle, located medially. The medial femoral circumflex vessels are ligated and divided. The arterial-venous fistula is placed over the ventrally exposed left sciatic nerve. A silicon sheath is placed around the nerve and the arterial-venous fistula.

7. The silicone sheath is folded on itself and maintained in place with interrupted 5/0 Nylon stitches. The surgical wounds are closed with interrupted 5/0 Nylon stitches.

8. The sciatic nerve and fistula are maintained in contact for 5 weeks, allowing the development of vascular connections between the fistula and the sciatic nerve.

9. After five weeks, a conventional flap including a segment of the sciatic nerve measuring approximately 15 mm has been fabricated.

10. A 10-mm-long segment of the right median nerve is excised.

12. The prefabricated nerve flap is inset in the region of the median nerve defect. Excessive neural tissue is trimmed at both ends. The arterial end of the arterial-venous fistula was terminal-laterally anastomosed to the distal portion of the brachial artery and the venous end of the fistula was terminal-laterally anastomosed to the proximal aspect of the brachial vein using interrupted 12/0 Nylon stitches. Neural anastomoses were performed using interrupted epineural 11/0 Nylon sutures.

Figure 3. Walking tracks measurements using forepaw impressions.

A. Photograph of a typical print of the left forepaw (uninjured).

B. Contrast-enhanced image of the photograph in Figure 3A, using the software Fiji®. Similar images were used for measurement purposes, namely of determination of the stance factor (paw impression area on the paper sheet)

C. Typical forepaw prints of a rat in the nerve graft group.

1, Intermediate finger spread factor: widest width between the second and third fingers; 2, Finger spread factor: widest width of the paw impression; 3, Print length factor: longest

length of the paw impression; 4, Stride length: distance between homologous points of successive paw impressions on a given side; 5, Base of support: perpendicular distance between the central portion of the paw impression and the direction of movement.

Figure 4. Time to recovery of grasping in the operated limb.

Fastest recovery of grasping was observed in the CNF and ANVF groups ($p<0.001$).

Figure 5. Qualitative assessment of grasping strength in the operated limb in the different experimental groups 30, 60 and 90 days after the reconstruction of the median nerve gap. Vertical bars represent 95% confidence intervals.

Horizontal lines in the upper portion of the figure indicate statistically significant differences between groups ($p<0.05$).

*, $p<0.05$; **, $p<0.01$; ***, $p<0.001$

Figure 6. Average velocity in the ladder running test in the different experimental groups during the experiment.

Vertical bars represent 95% confidence intervals.

Horizontal lines in the upper portion of the figure indicate statistically significant differences between groups on the 90^{th} day postoperatively ($p<0.05$).

*, p<0.05; **, p<0.01; ***, p<0.001

Figure 7. Nociceptive evaluation using cumulative pin prick test results in the operated forelimb normalized to the contralateral limb in the different experimental groups throughout the experiment. Vertical bars represent 95% confidence intervals.

Horizontal lines in the upper portion of the figure indicate statistically significant differences between experimental groups (p<0.05).

**, p<0.01; ***, p<0.001.

Figure 8. Walking track analysis of the right forelimb (operated paw) of rats in the different experimental groups throughout the experience. Values are expressed as percentages of averages normalized to the contralateral side.

A, Stance factor. B, Print length; C, Finger spread factor; D, Intermediate finger spread factor; E, Stride length; F, Base of support.

Vertical bars represent 95% confidence intervals.

Horizontal lines in the upper portion of the figure indicate statistically significant differences between experimental groups (p<0.05).

*, p<0.05; **, p<0,01; ***, p<0.001

Figure 9. Presence of radial deviation in the walking tracks of the operated forepaws in the different experimental groups at the end of the experiment. A, Left forepaw print of a rat in the nerve graft group, showing a normal impression. B, Right forepaw print of the same rat, showing radial deviation of the paw. C, Bar graph showing the proportion of rats with radial deviation of the operated forepaws at the end of the experiment.

Figure 10. Temperature on the surface of the skin territory of the median nerve.

A. Boxplot graphic illustrating the average temperature in the skin territory of the right median nerve relatively to that of the contralateral side. Temperature measurements were made using infra-red thermography.

B. Typical thermography image. C. Image resulting from the overlap of the thermography image and of the digital photographic image. This allows to evaluate the temperature in the territory of the median nerve.

Figure 11. Electroneuromyographic assessment of the right forelimb (operated paw) of rats in the different experimental groups throughout the experience. Values are expressed as percentages of averages normalized to the homologous contralateral side average values.

A, Neurological stimulation threshold; B, Motor stimulation threshold; C, Latency; D, Neuromuscular transduction velocity; E, Compound muscle action potentials (CMAPs) amplitude; F, CMAPs duration.

Vertical lines represent 95% confidence intervals.

Horizontal lines in the upper portion of the figure indicate statistically significant differences between experimental groups ($p<0.05$).

*, $p<0.05$; **, $p<0,01$; ***, $p<0.001$

Figure 12. Typical compound muscle action potentials patterns in the different experimental groups.

A. Sham group and left paw of the rats in the other experimental groups.

B. Nerve graft group.

C. Conventional nerve flap group.

D. Arterialized neurovenous flap group.

E. Prefabricated nerve flap group.

Figure 13. Muscle strength evaluation at the end of the experiment in the operated forelimb in the different experimental groups.

A. Maximal isometric wrist flexion force after tetanic stimulation.

B. Area under the curve (AUC) during a 30-second interval and supratetanic stimulation

Values are expressed as percentages of averages normalized to the homologous contralateral side average values.

Vertical lines represent 95% confidence intervals.

Horizontal lines in the upper portion of the figure indicate statistically significant differences between experimental groups ($p<0.05$).

**, p<0,01; ***, p<0.001

Figure 14. Flexor carpis radialis muscle weight of the right forelimb (operated paw) of rats in the different experimental groups. Values are expressed as percentages of averages normalized to the homologous contralateral side average values.

Vertical lines represent 95% confidence intervals.

Horizontal lines in the upper portion of the figure indicate statistically significant differences between experimental groups ($p<0.05$).

p<0,01; ***, p<0.001

Figure 15. Photographs of the flexor carpis radialis muscle illustrating muscle gross appearance in the different experimental groups on the operated side (R, right) and on the non-operated side (L, left).

A. Excision group.

B. Nerve graft group.

C. Conventional nerve flap group.

D. Arterialized neurovenous flap group.

E. Prefabricated nerve flap group.

Figure 16. Histomorphometric evaluation of the right median nerve distally to the repair zone in the different experimental groups. Results are expressed as a percentage of the normal, contralateral side

and are given as the mean.

A. Median nerve cross section area distally to the repair zone.

B. Total number of fibers (stained for neurofilaments) distally to the repair zone.

C. Acetylcholinesterase positive (+) nerve fibers distally to the repair zone.

D. Peripherin positive (+) nerve fibers distally to the repair zone.

E. Acetylcholinesterase negative (-) and peripherin negative (-) nerve fibers distally to the repair zone.

F. Vascular density in a cross section of the middle portion of the reconstructed nerve defect.

Vertical lines represent 95% confidence intervals.

Horizontal lines in the upper portion of the figure indicate statistically significant differences between experimental groups ($p<0.05$).

*, $p<0.05$; **, $p<0,01$; ***, $p<0.001$

Figure 17. Representative histological features of the different experimental groups.

HE, hematoxylin-eosin staining; MT, Masson's trichrome staining; NF, neurofilament immunohistochemical staining; Per, peripherin immunohistochemical staining; ACHE, acetylcholinesterase immunohistochemical staining.

Calibration bar (A to E) = 10 µm

Calibration bar (F to I') = 100 µm

Figure 18. Fluorescence microscopy photographs of cross sections of the right median nerve proximally to the lesion, of the C7 spinal cord segment, and of the C7 the right dorsal root ganglion in the different experimental groups.

Dor, dorsal; R, right

Red calibration bar = 1 mm

White calibration bar = 100 µm

Figure 19. Typical high amplification fluorescence microscopy photographs of cross sections of the C7 the right dorsal root ganglion (**A** and **C**) showing ganglion cells stained with the True Blue® tracer and of motoneurons in the ventral horn of the spinal cord stained with the lucifer yellow (LY) ® tracer (**B** and **D**). Intracytoplasmic inclusions of these two markers are clearly visible in a rat of the Sham group.

Calibration bar = 100 µm

Figure 20. Semi quantitative evaluation of retrograde marking of the right median nerve proximally to the lesion site, of the right C7 dorsal ganglion and of the right ventral horn of the spinal cord at the C7 level in the different experimental groups.

A. Average number of True Blue diaceturate stained fibers in the right median nerve proximally to the repair site.

B. Average number of Lucifer Yellow CH dilithium stained fibers in the right median nerve proximally to the repair site.

C. Average number of True Blue diaceturate stained ganglion cells in the right C/ dorsal ganglion.

D. Average number of Lucifer Yellow CH dilithium stained cells in the ventral horn of the C7 spinal cord segment.

Vertical lines represent 95% confidence intervals.

Horizontal lines in the upper portion of the figure indicate statistically significant differences between experimental groups ($p<0.05$).

*, $p<0.05$; **, $p<0,01$; ***, $p<0.001$

Figure 1

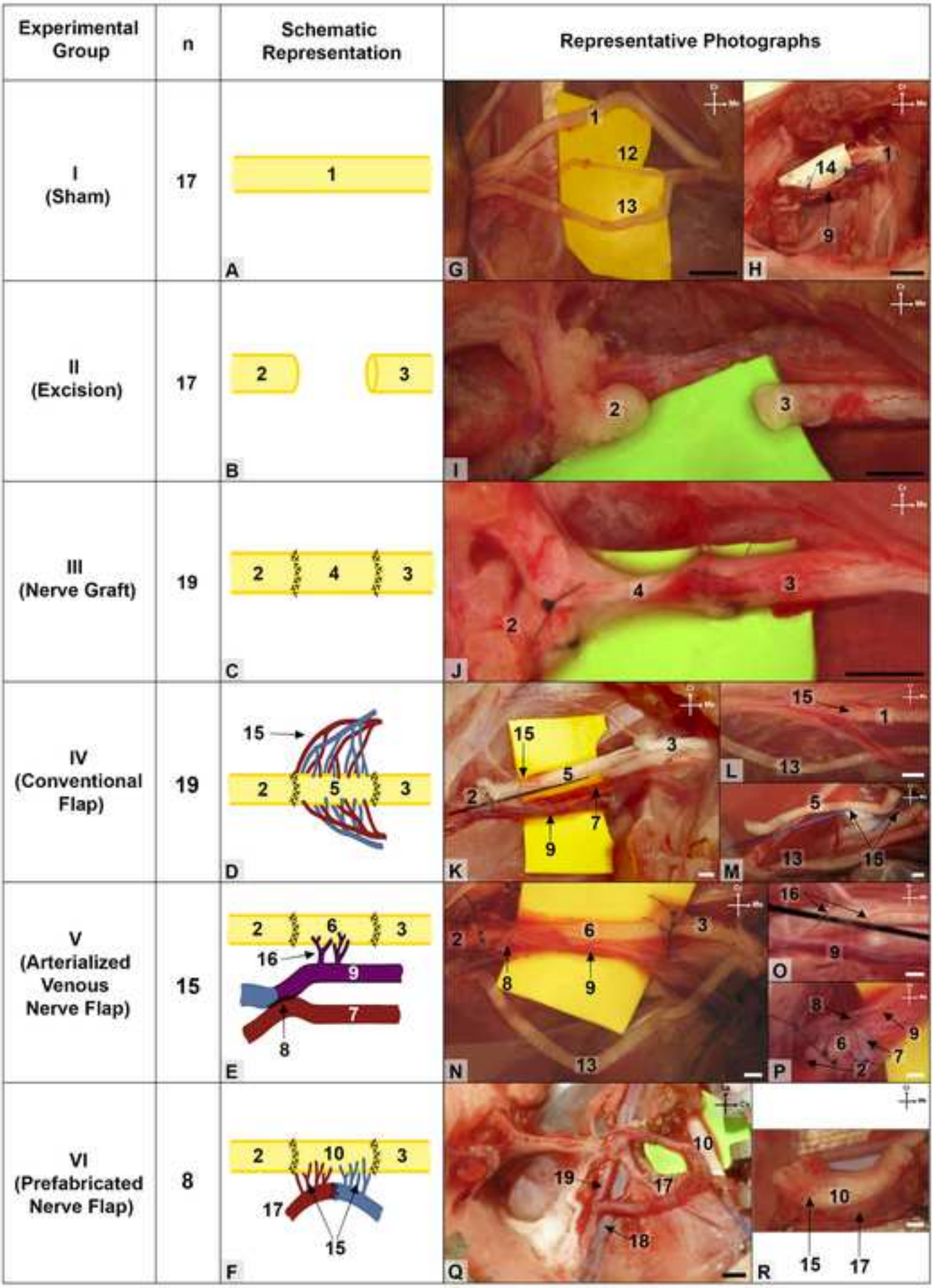

Figure 2

Click here to download Figure Figure 2.tif

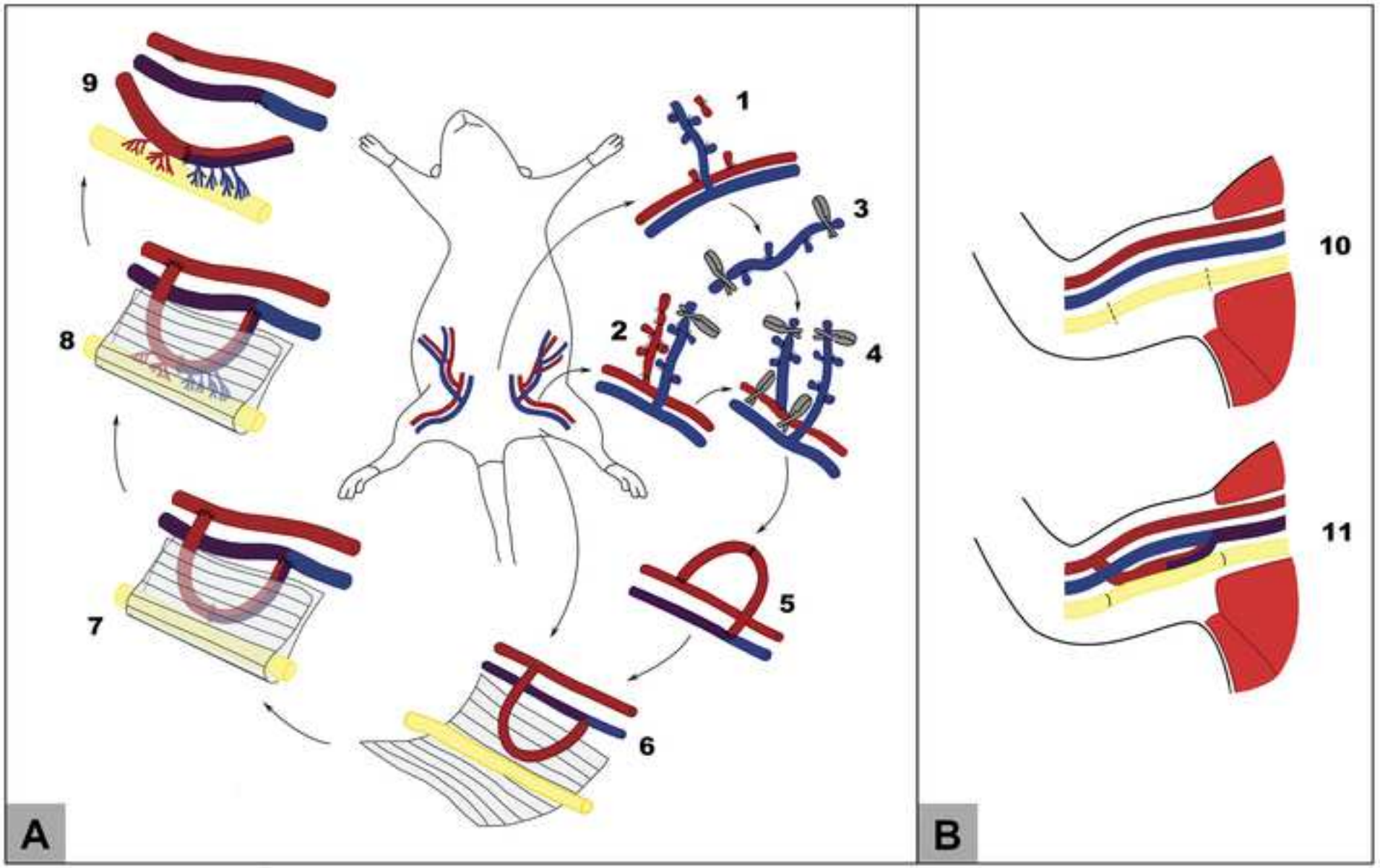

Figure 3

Click here to download Figure Figure 3.tif

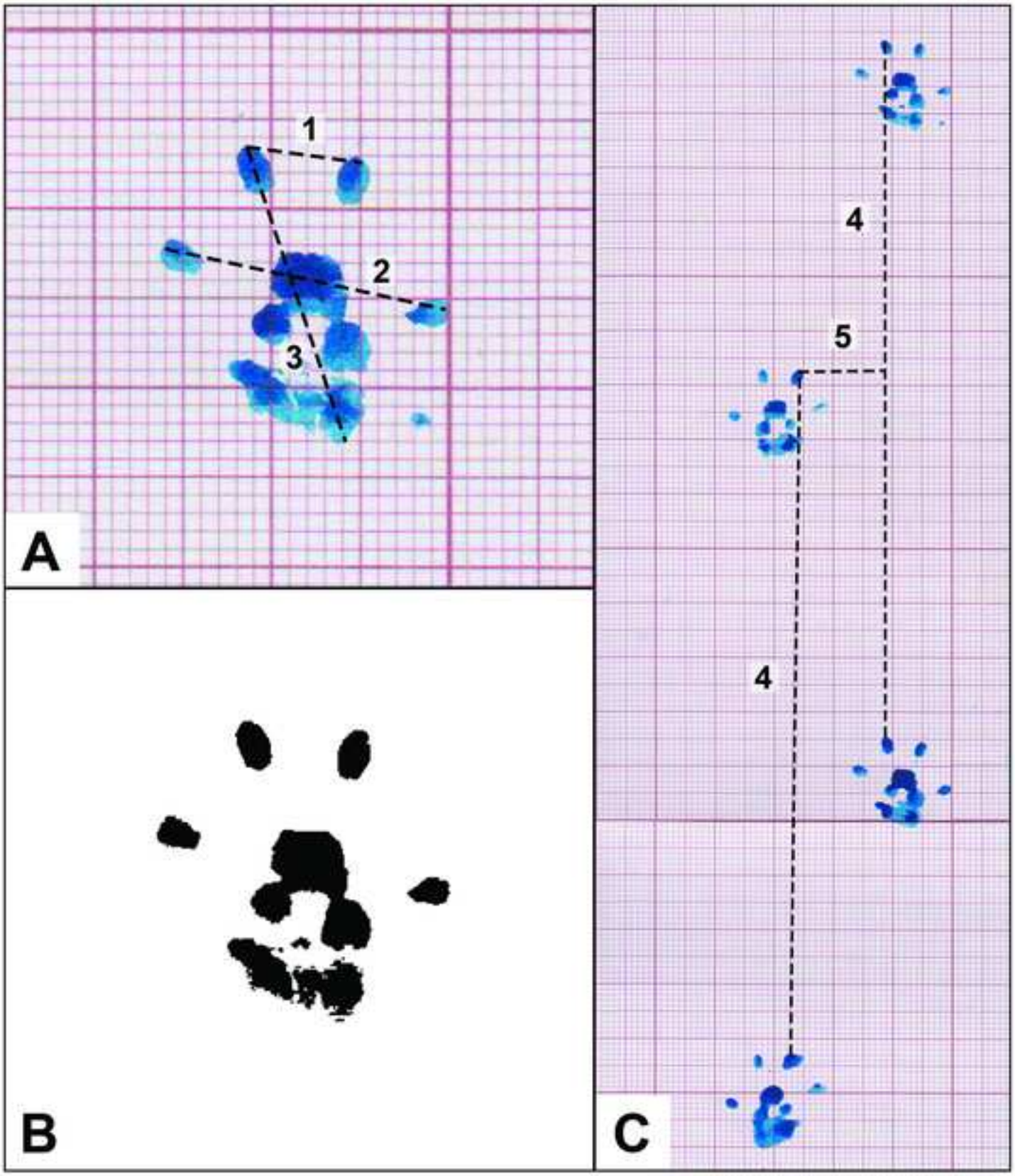

Figure 4

Click here to download Figure Figure 4.tif

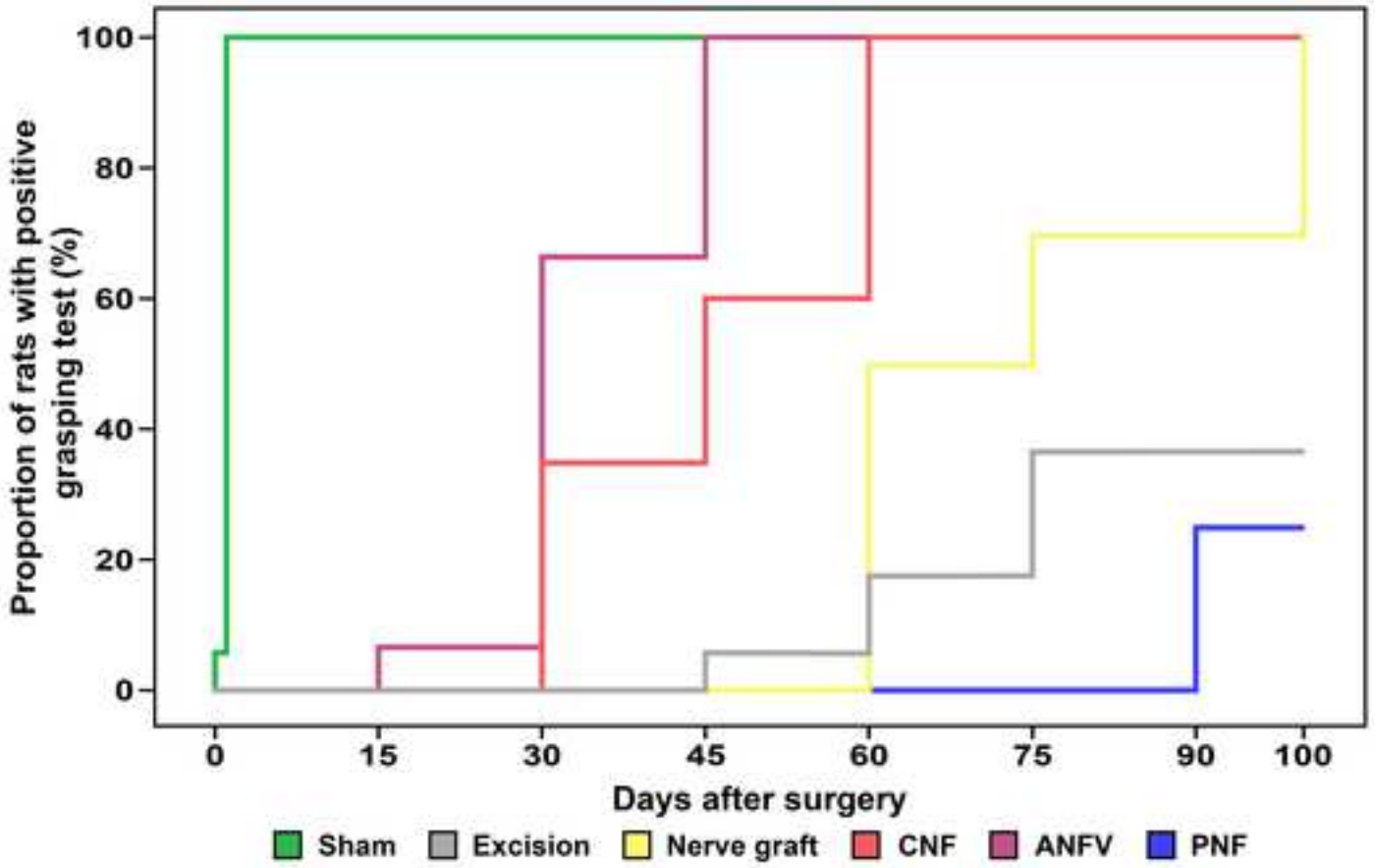

Experimental Group	Time to recovery of grasping in days (average ± standard deviation)
Sham	0 (immediately after surgery)
Excision	87.31 ± 4.41
Nerve Graft	75.00 ± 5.86
Conventional Nerve Flap (CNF)	45.75 ± 2.98
Arterialized Neurovenous Flap (ANF)	34.00 ± 2.30
Prefabricated Nerve Flap (PNF)	97.50 ± 1.53

Figure 5

Click here to download Figure Figure 5.tif

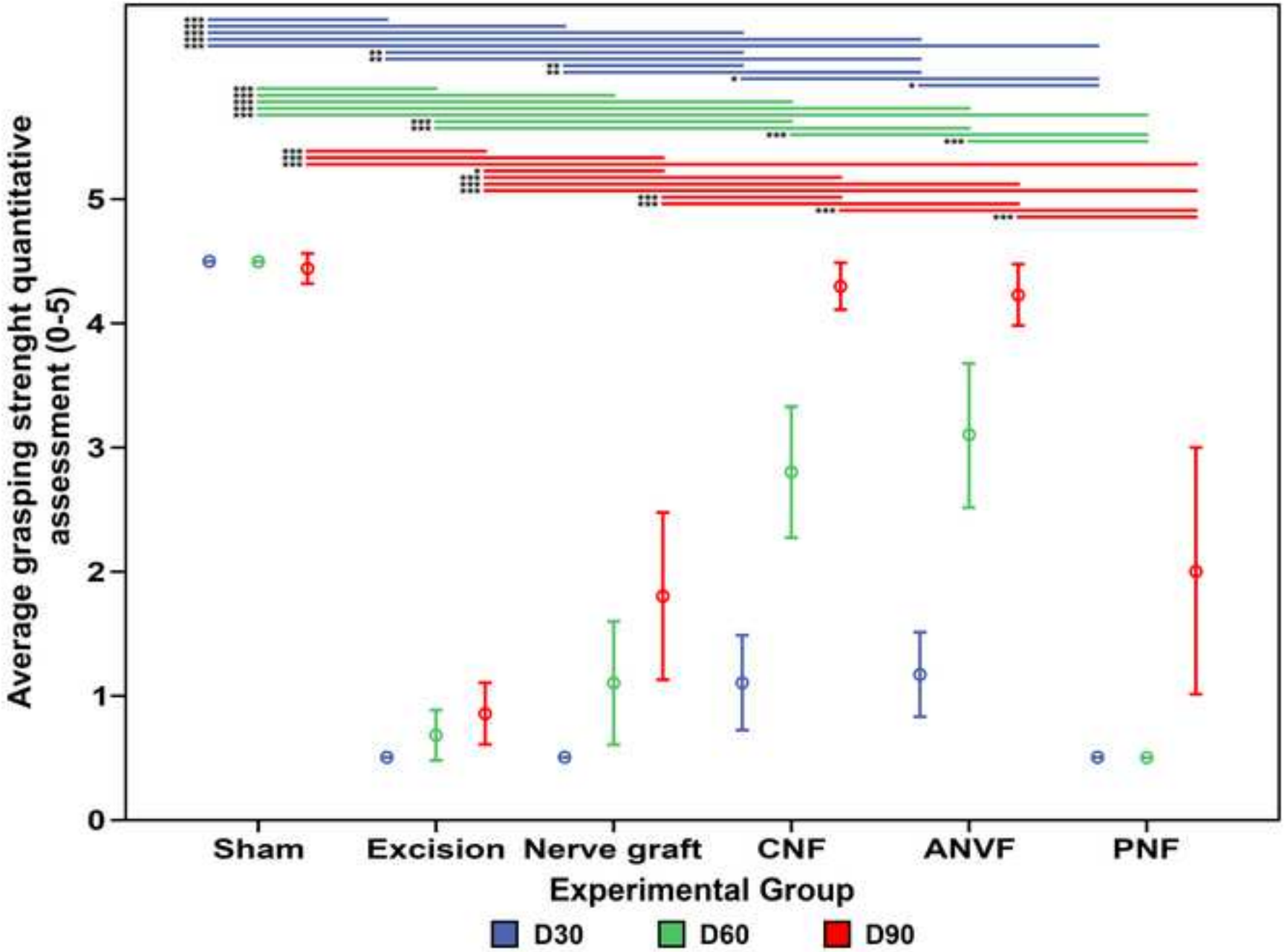

Figure 6

Click here to download Figure Figure 6.tif

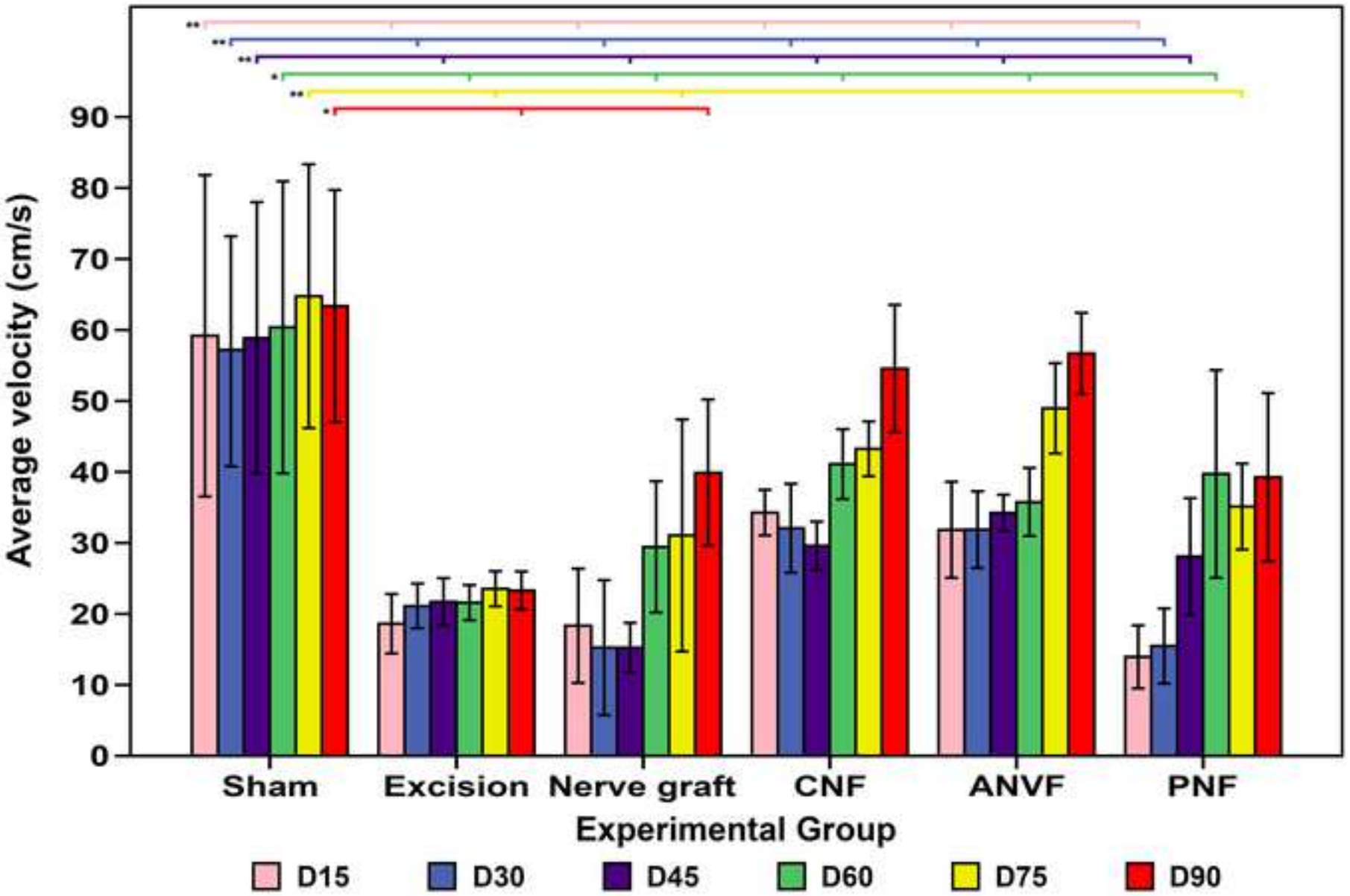

Figure 7

Click here to download Figure Figure 7.tif

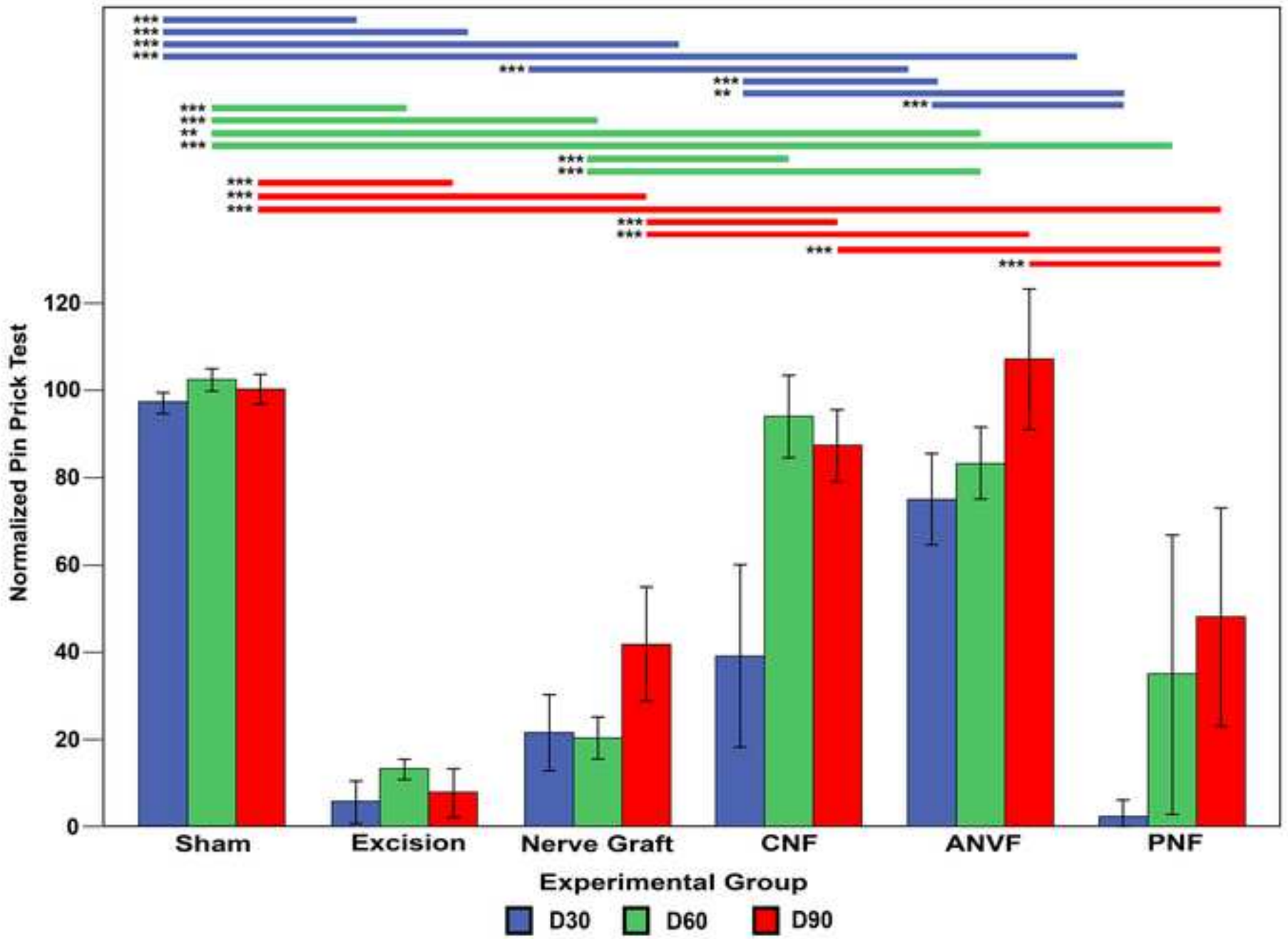

Figure 8

Click here to download Figure Figure 8.tif

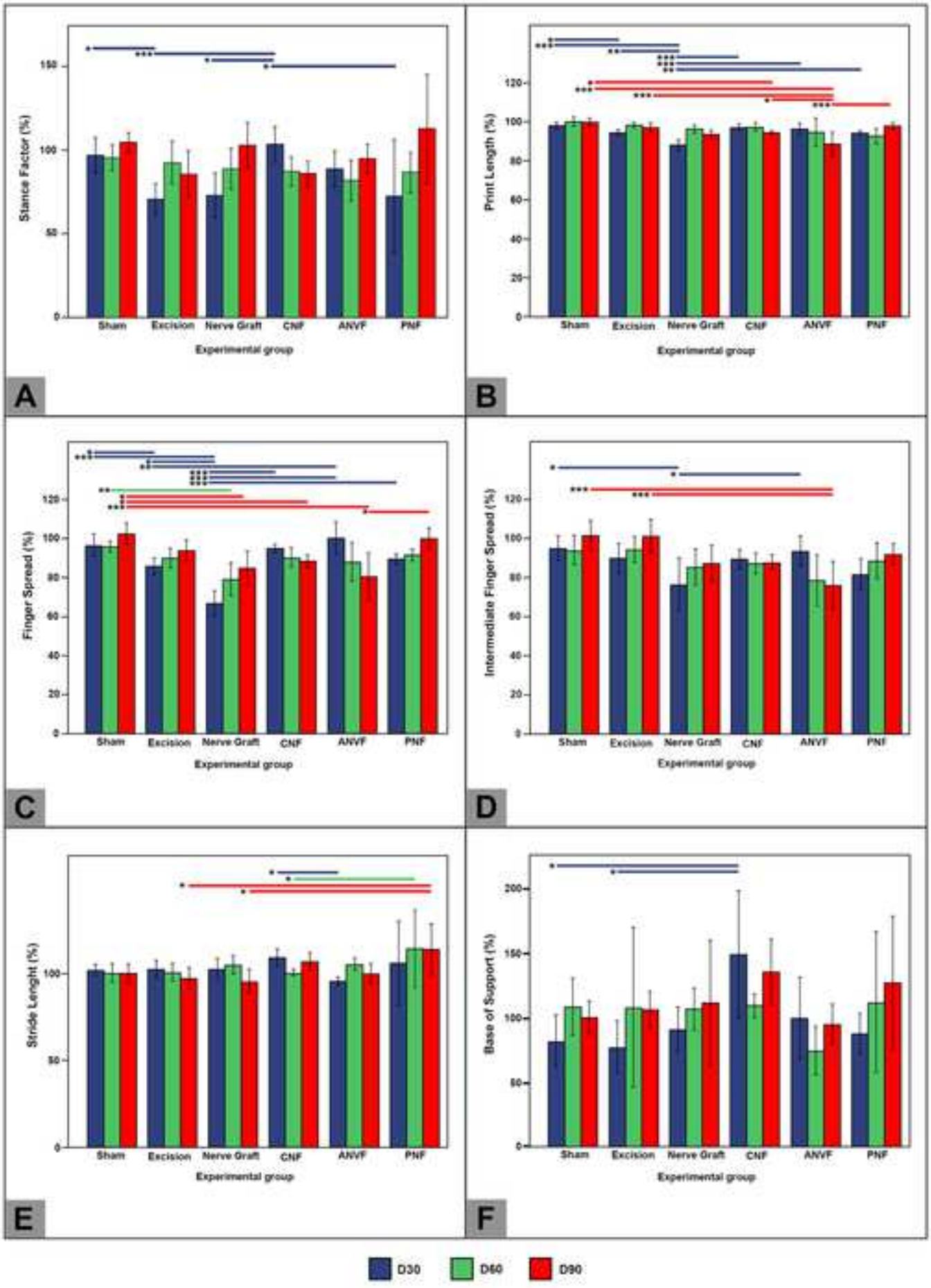

Figure 9

Click here to download Figure Figure 9.tif

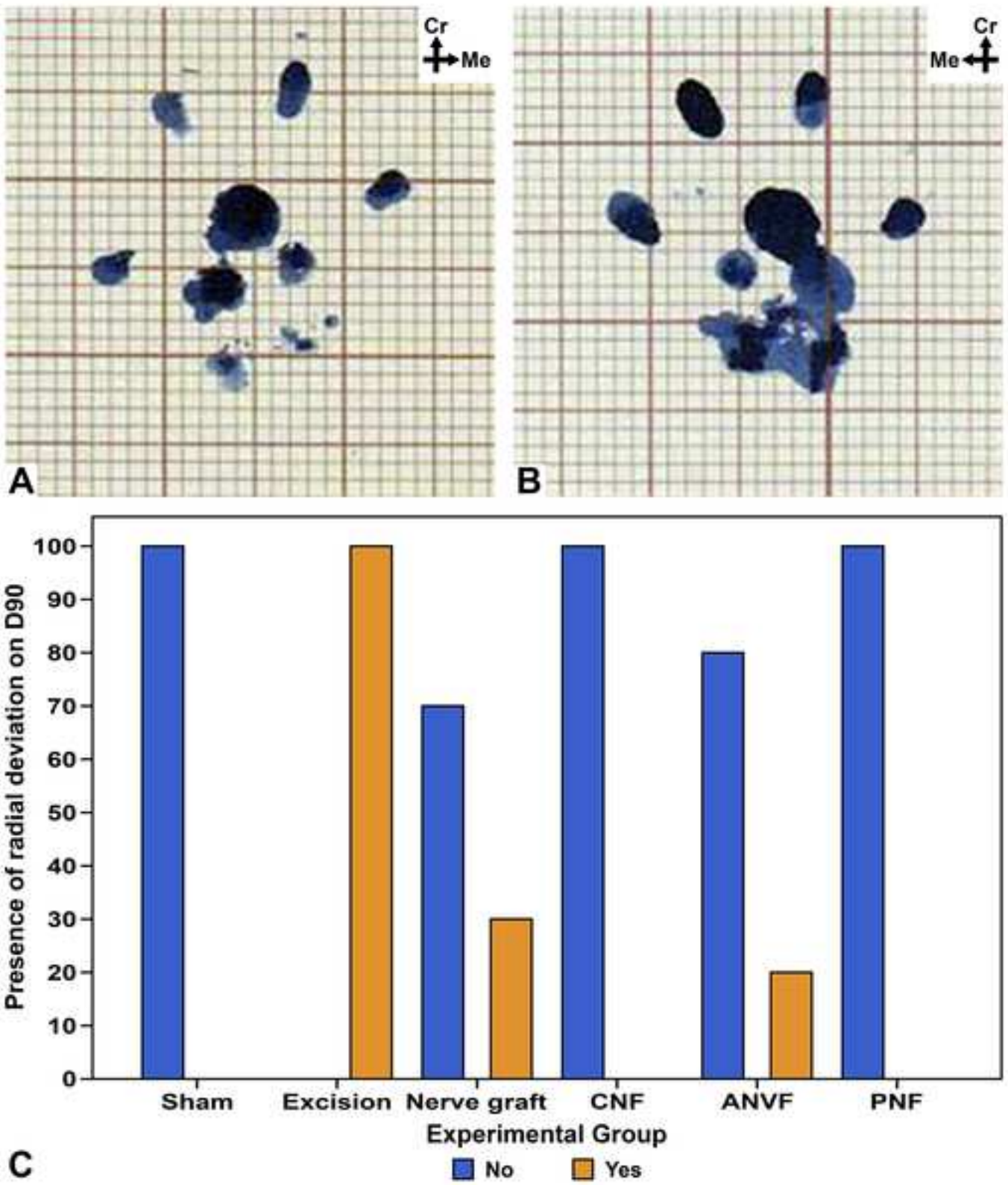

Figure 10

Click here to download Figure Figure 10.tif

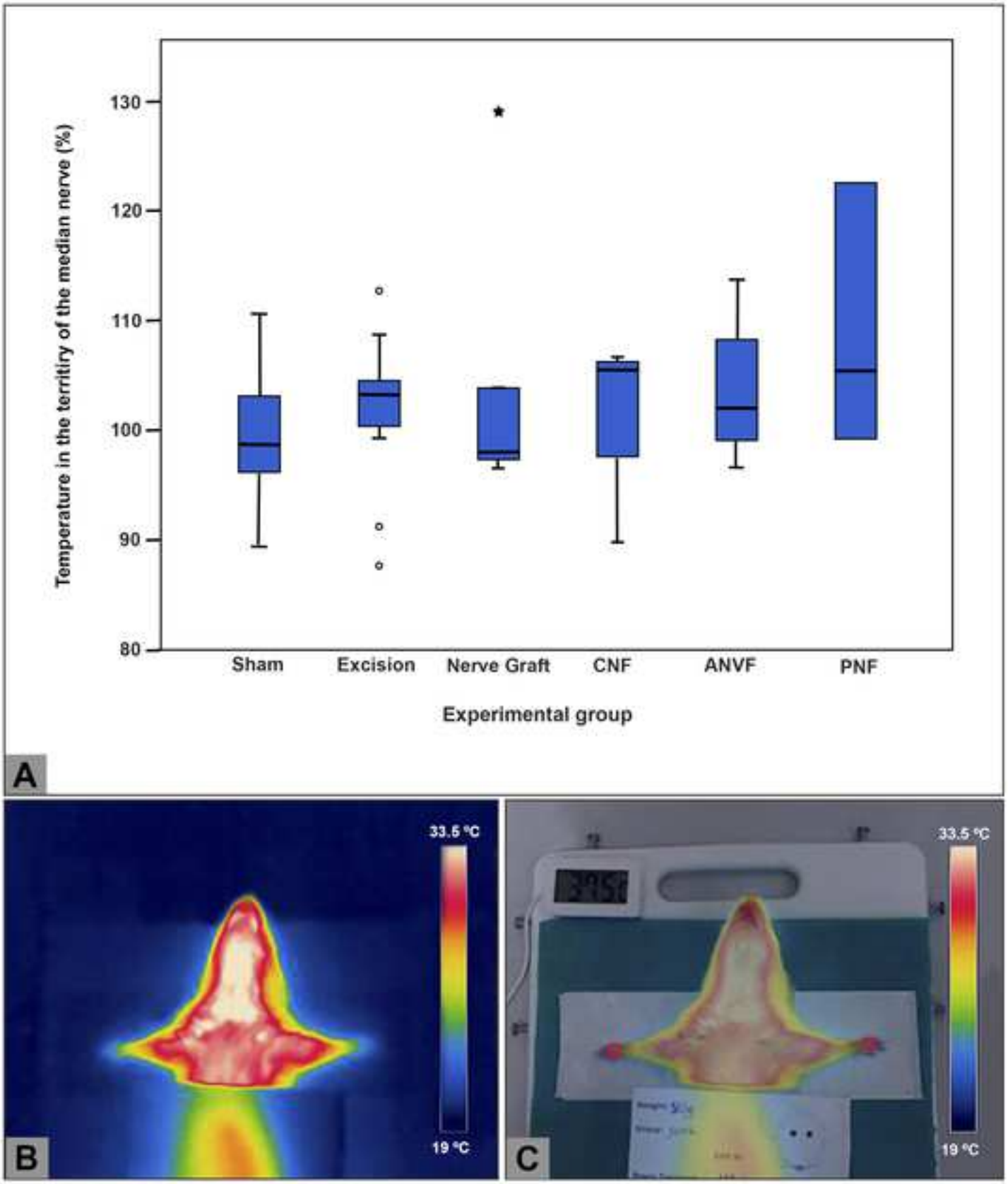

Figure 11

Click here to download Figure Figure 11.tif

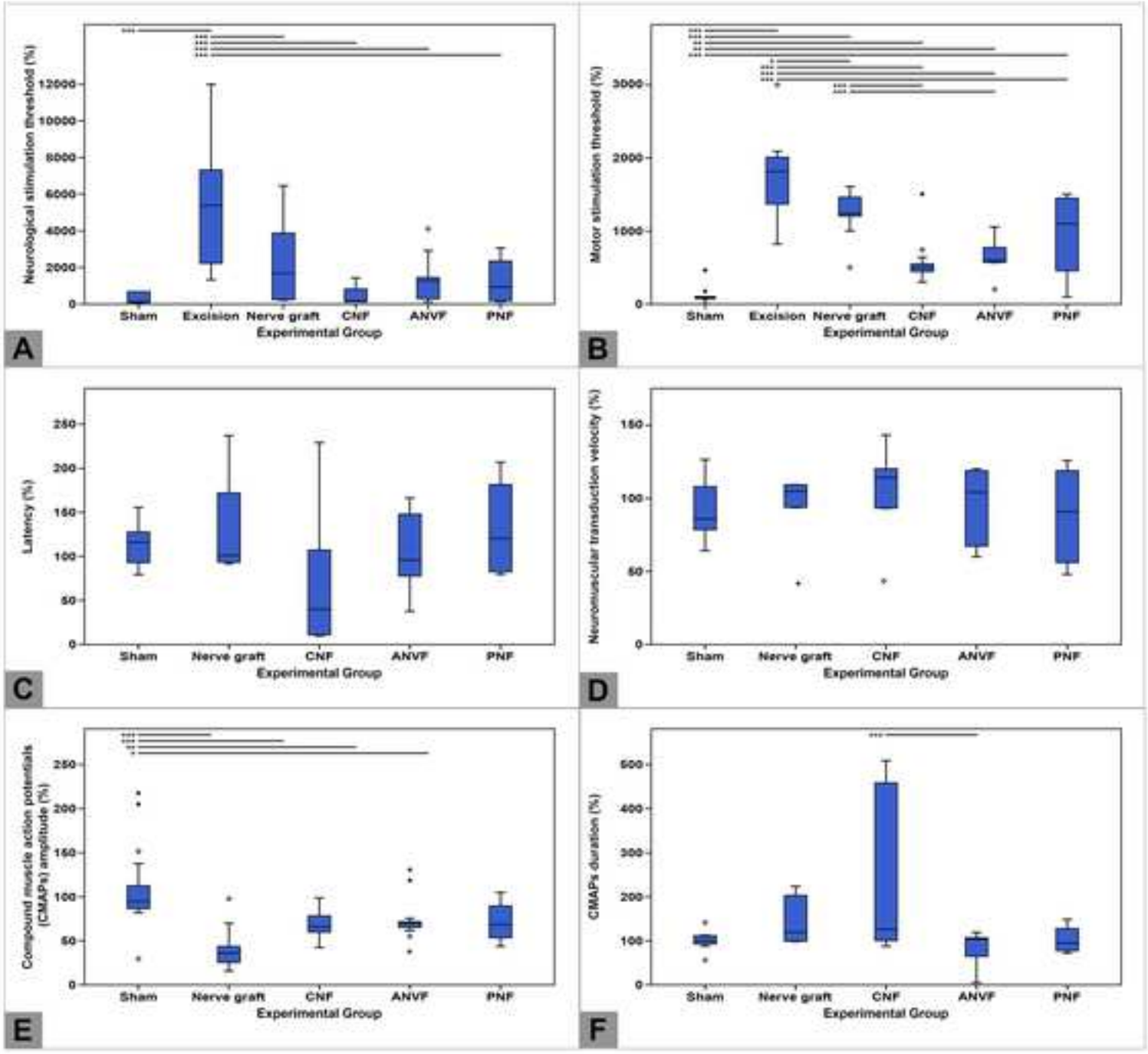

Figure 12

Click here to download Figure Figure 12.tif

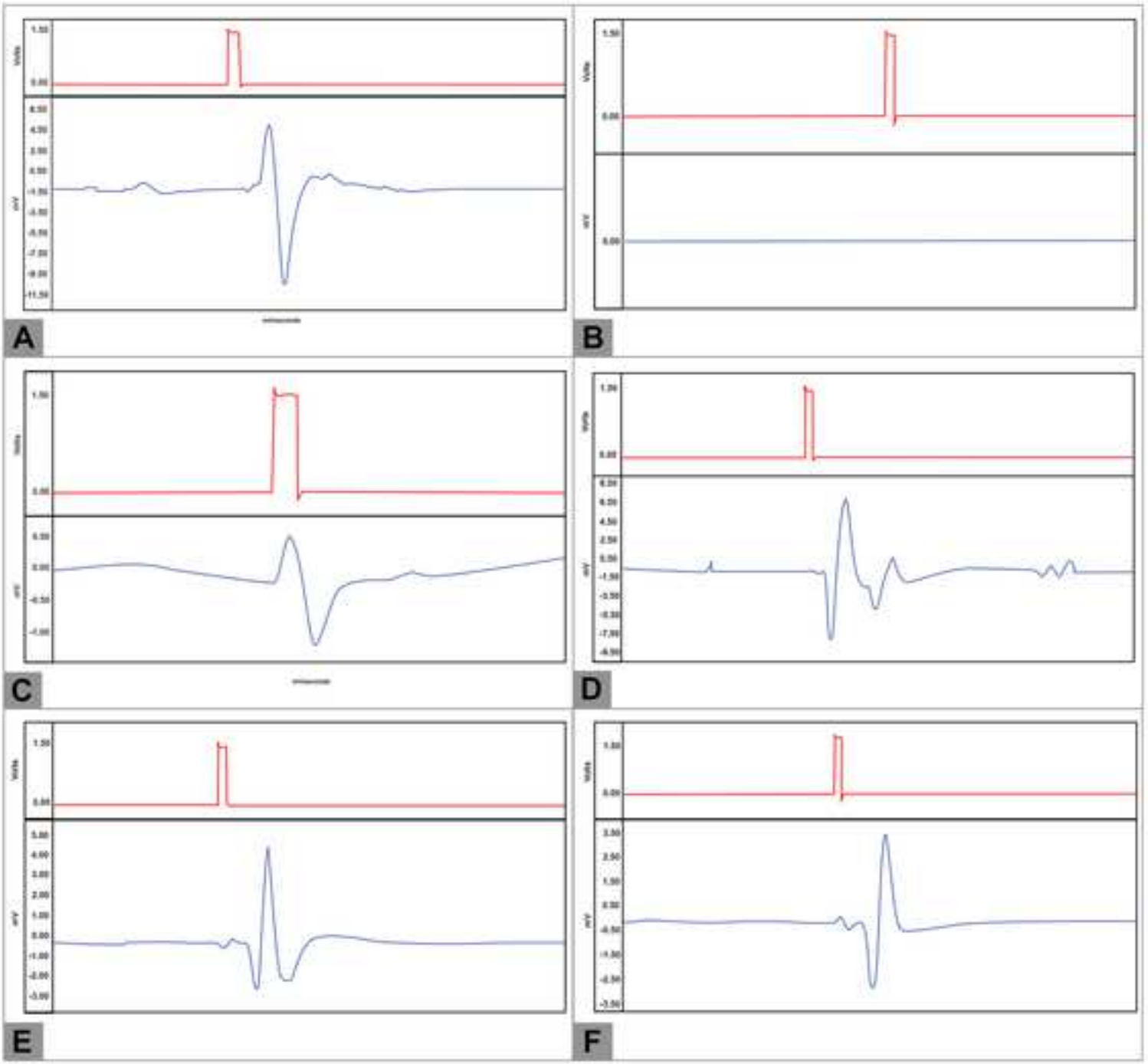

Figure 13

Click here to download Figure Figure 13.tif

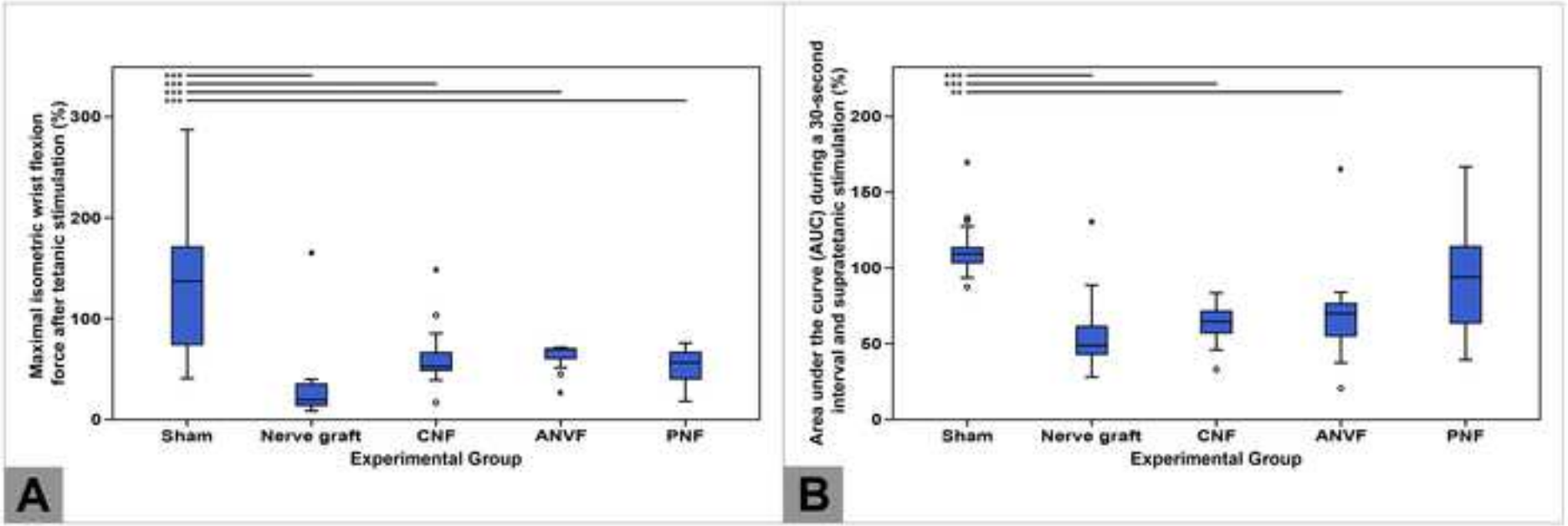

Figure 14

Click here to download Figure Figure 14.tif

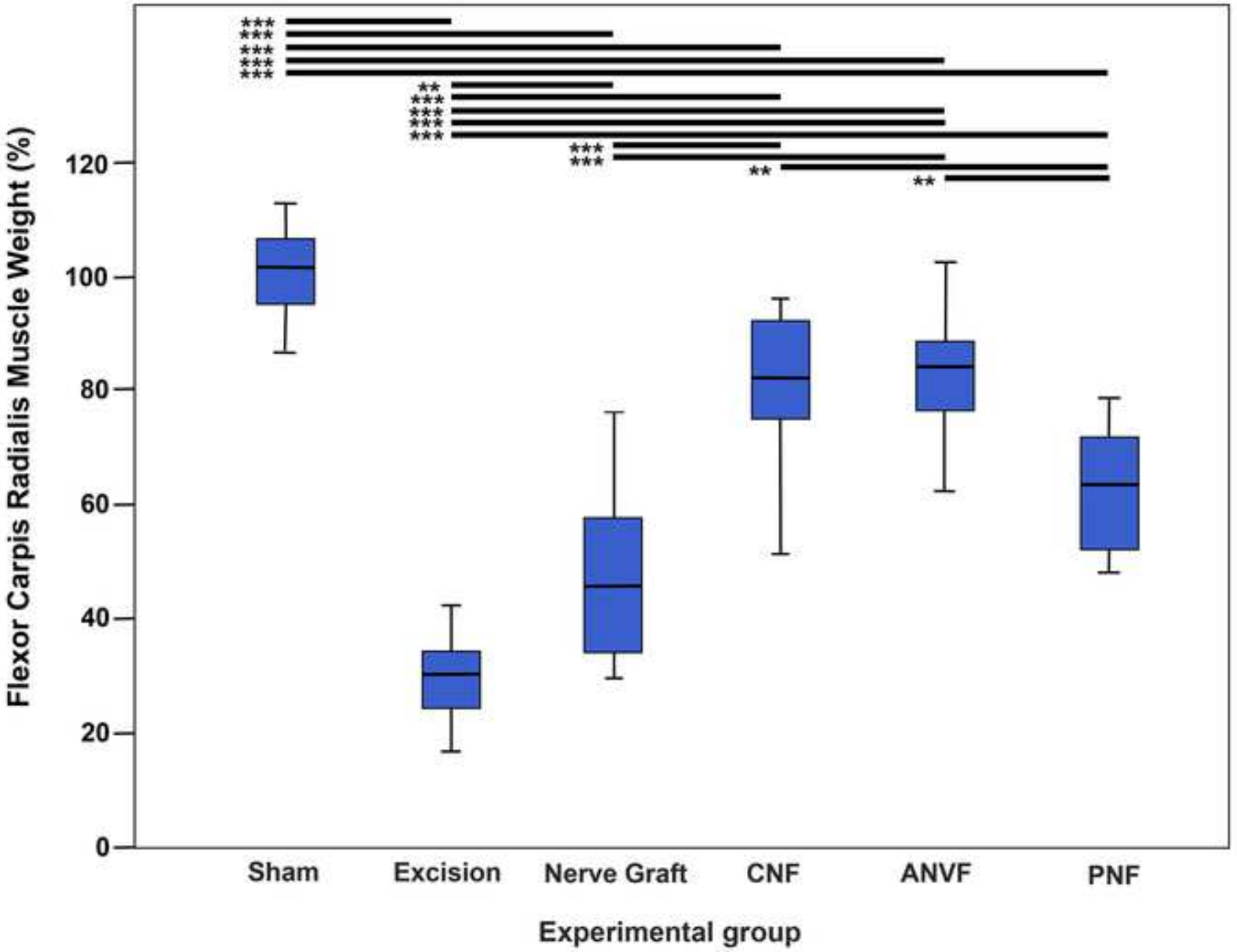

Figure 15

Click here to download Figure Figure 15.tif

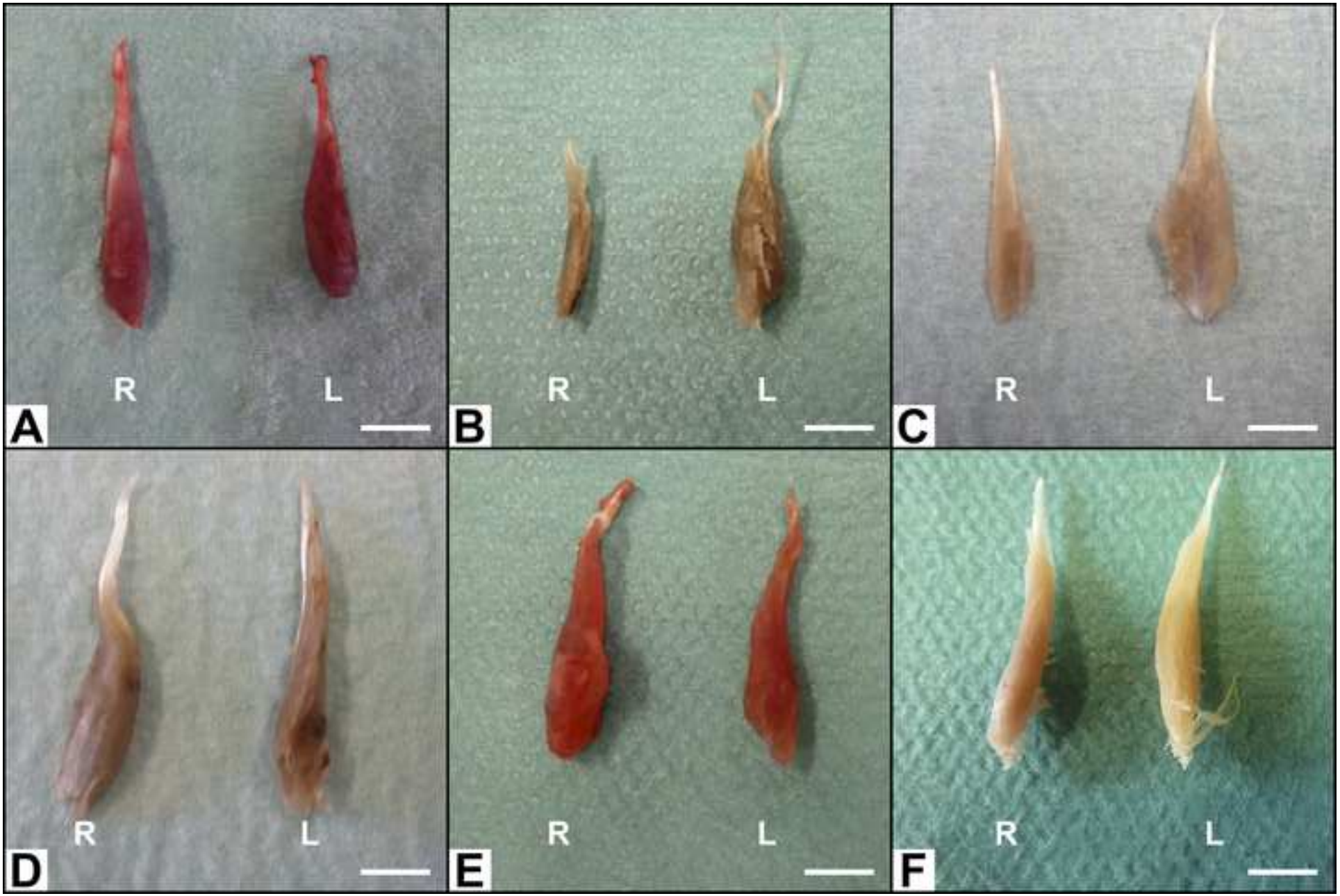

Figure 16

Click here to download Figure Figure 16.tif

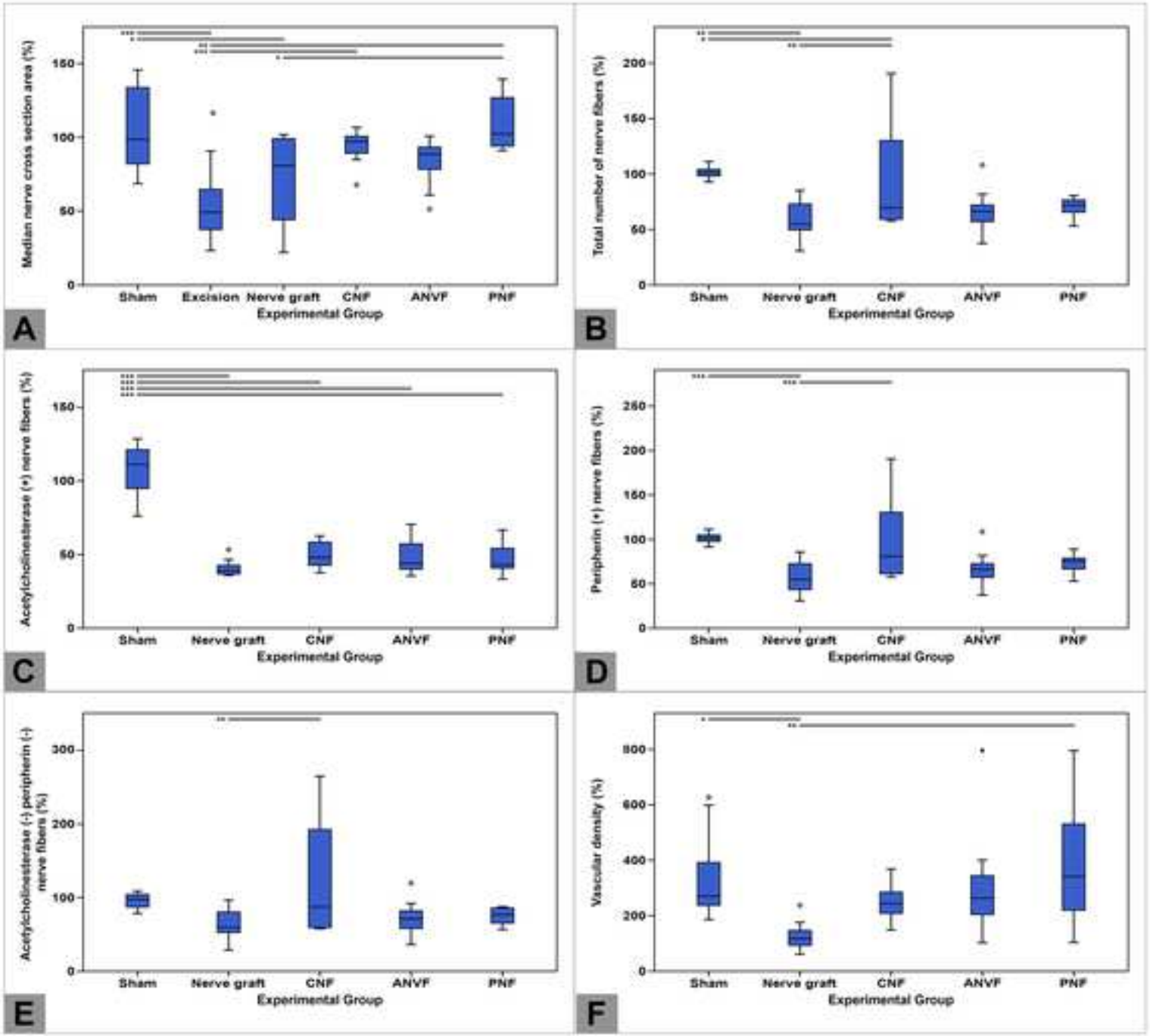

Figure 17

Click here to download Figure Figure 17.tif

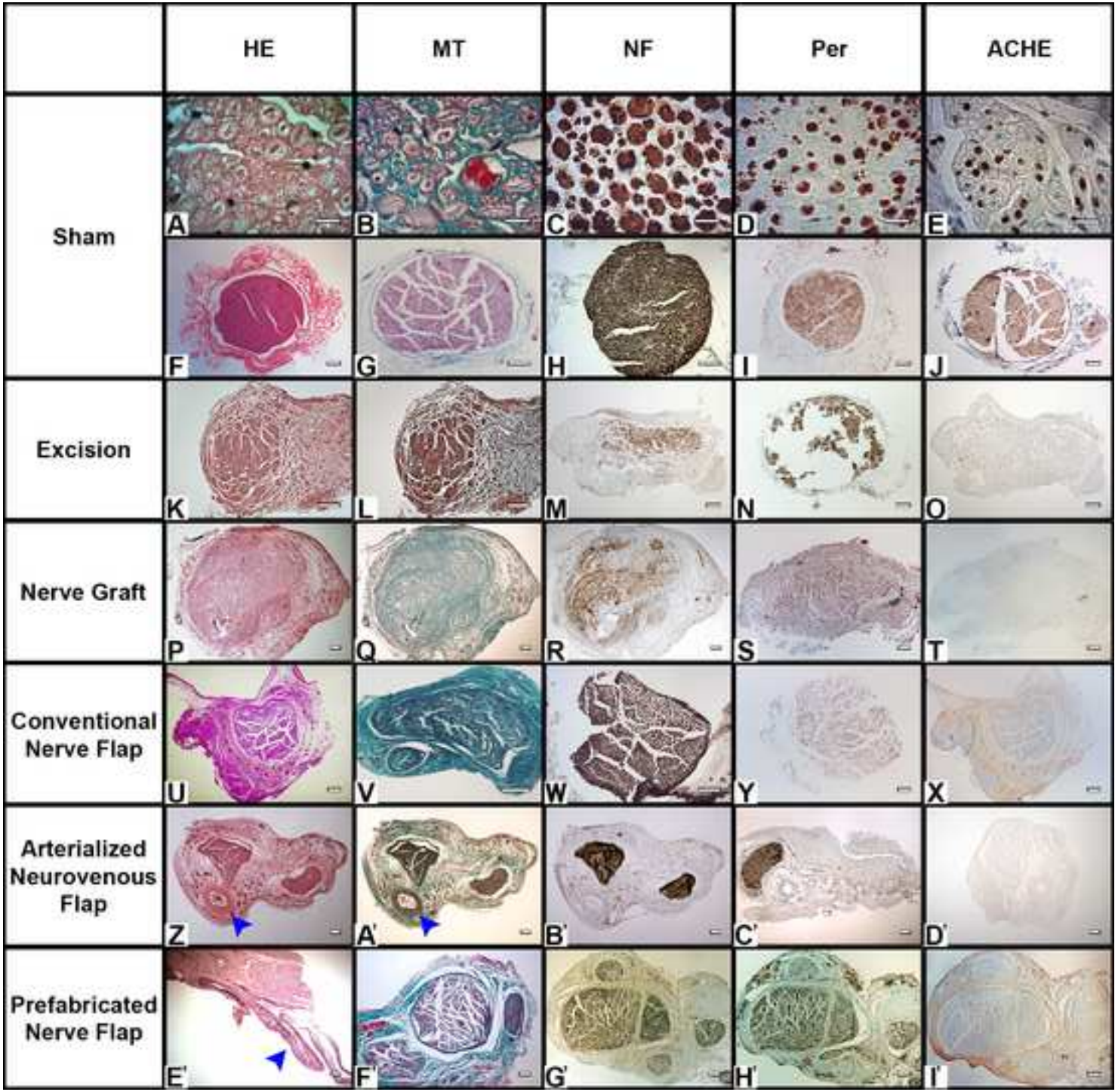

Figure 18

Click here to download Figure Figure 18.tif

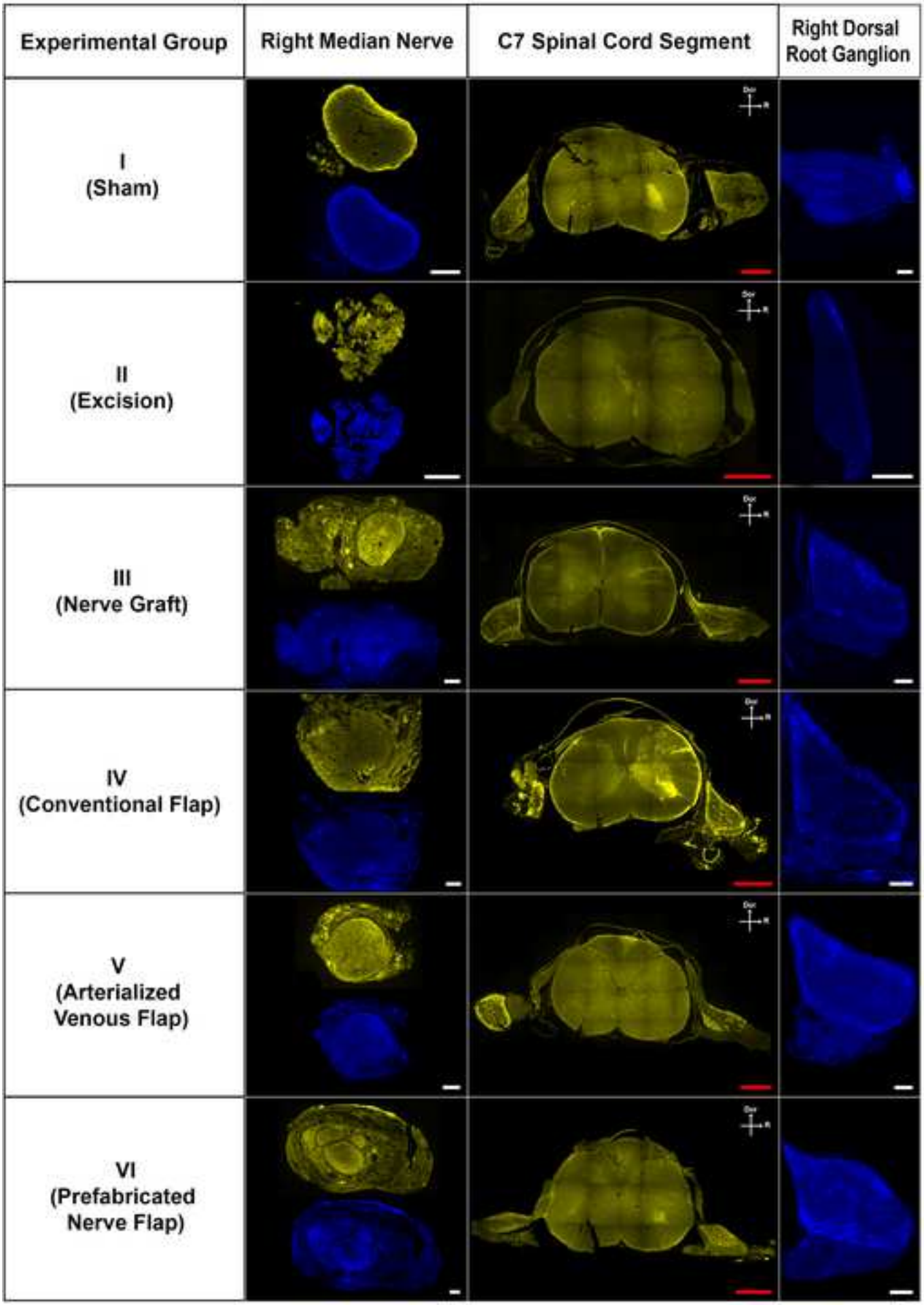

Figure 19

Click here to download Figure Figure 19.tif

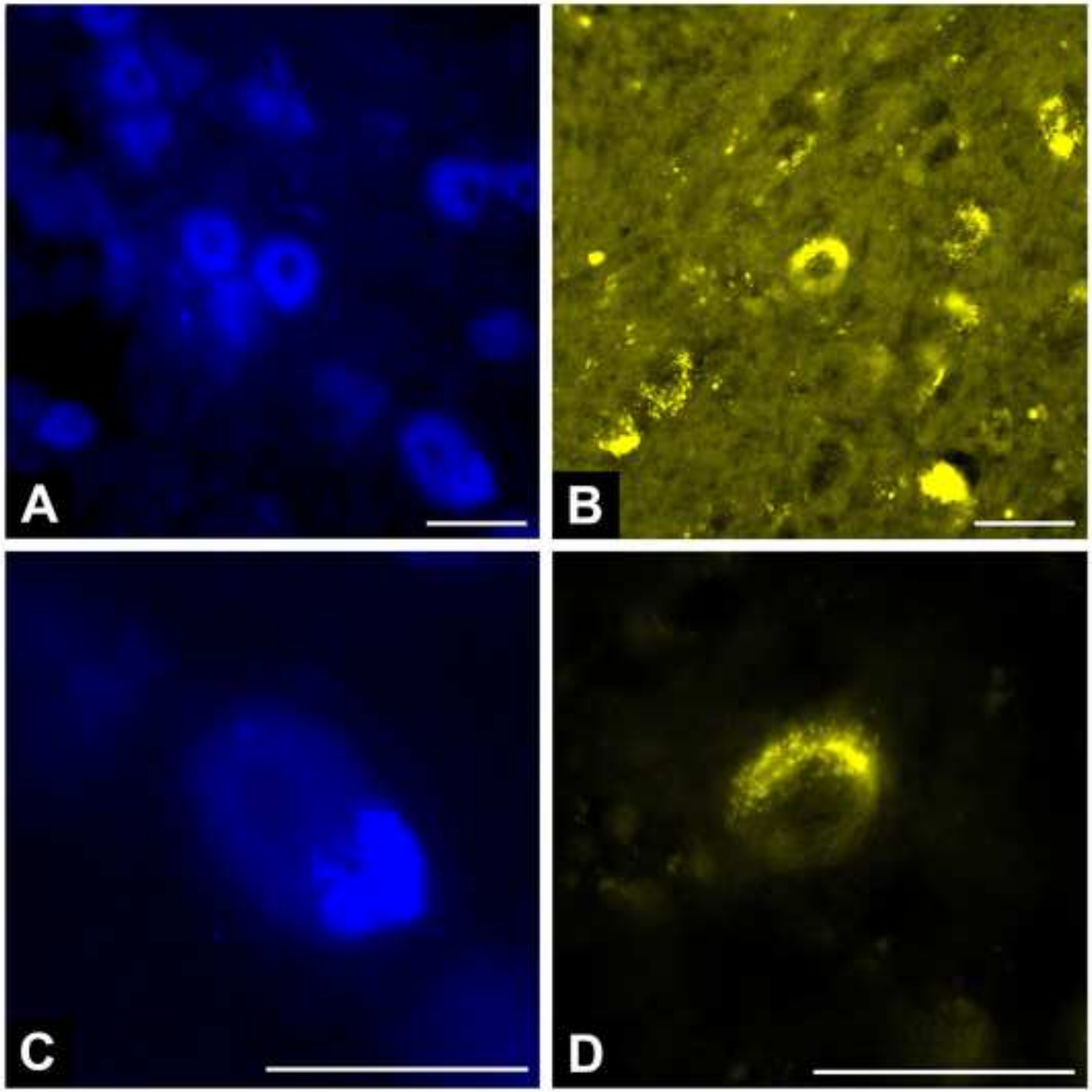

Figure 20

Click here to download Figure Figure 20.tif

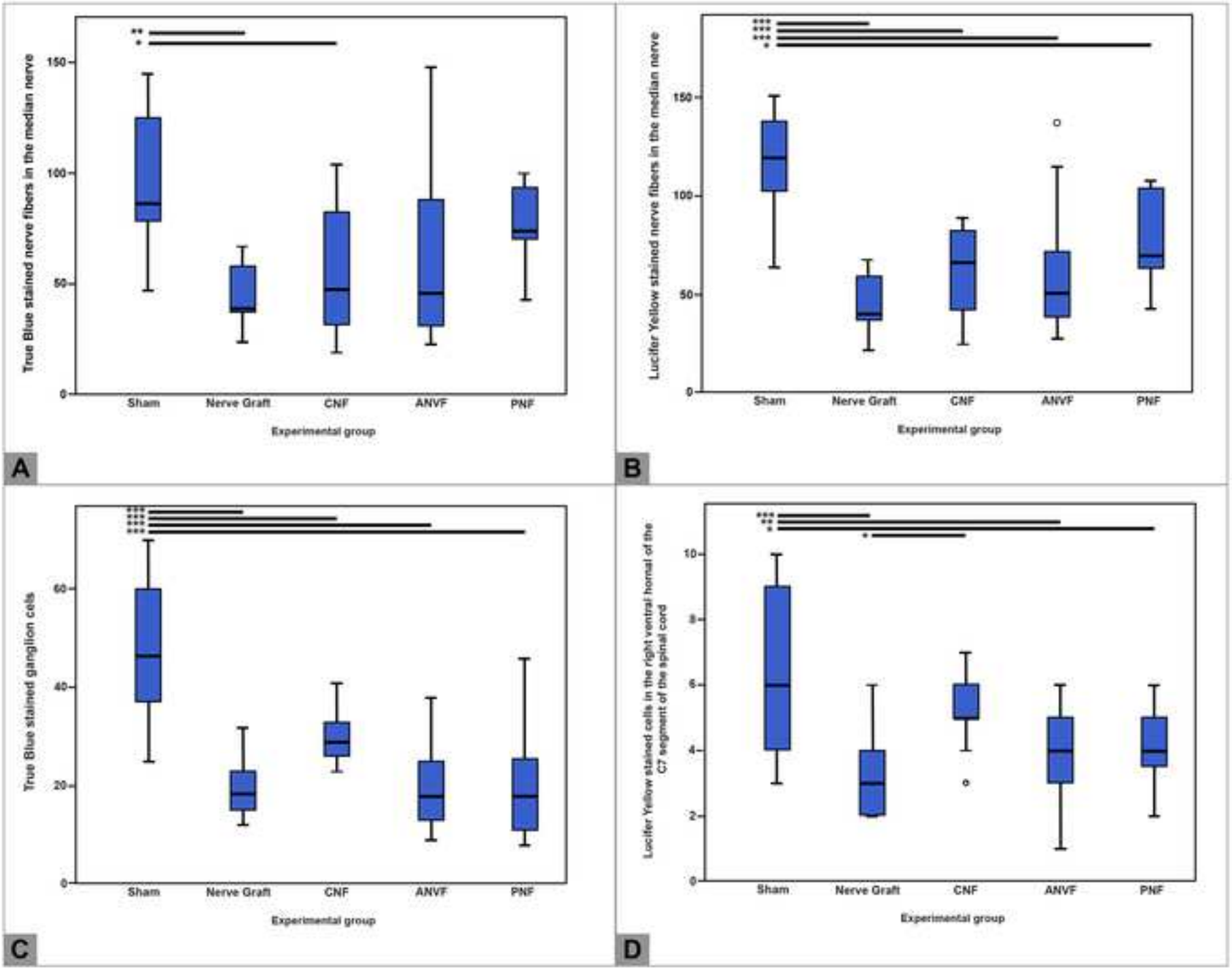

APPENDIX 9

PLOS ONE

Surgical anatomy of common regions used to harvest unconventional perfusion flaps: a cadaveric dissection study

--Manuscript Draft--

Manuscript Number:	
Article Type:	Research Article
Full Title:	Surgical anatomy of common regions used to harvest unconventional perfusion flaps: a cadaveric dissection study
Short Title:	Surgical anatomy of unconventional perfusion flaps
Corresponding Author:	Diogo Casal, M.D. Universidade Nova de Lisboa Faculdade de Ciencias Medicas Lisbon, PORTUGAL
Keywords:	Anatomy; Flaps; Cadavers; Surgery; Blood supply; Reconstruction
Abstract:	Background: Unconventional perfusion flaps (UPFs) have shown promising results for the reconstruction of otherwise difficult to treat defects. The literature is particularly scant regarding articles specifically addressing the surgical anatomy of UPFs. Hence the main aim of this paper was to perform a cadaveric dissection study to characterize the relevant anatomy and histology of these areas, from the point of view of the surgeon interested in harvesting UPFs. Methods: Twenty-six freshly frozen adult human cadavers were used for anatomical and histological studies. Results: In all the regions studied the superficial cutaneous nerves were closer to sizeable superficial veins than to arteries of significant caliber and to their respective comitante veins. The largest veins in each region were placed deeper than smaller veins. The largest veins were enveloped by relatively thick doublings of the superficial fascia, which formed fascial sheaths around these superficial veins. The thinnest flaps were the dorsal foot (2.97 ± 1.69 mm), and the anterior antebrachial flaps (4.76 ± 0.73 mm). These UPFs presented an integumentary thickness similar to that of the eyelid and that of the penis. The sural flap was the one associated with a larger single nerve (4.32 ± 0.83 mm) followed by the saphenous (3.89 ± 1.53 mm), and the medial brachial (2.87 ± 0.49) flaps. Conclusions: In multiple anatomical regions, the superficial venous system was consistently found in close proximity to expendable superficial nerves, tendons, and even bone segments. This knowledge helps to set the ground to tailor composite UPFs for different purposes.
Order of Authors:	Diogo Casal, M.D.
	Diogo Pais
	Eduarda da Mota-Silva
	Ines Iria
	Sara Alves
	Luis Mascarenhas-Lemos
	Claudia Pen
	Mario Ferraz-Oliveira
	Paula Alexandra Videira
	Joao Goyri-O'Neill
Opposed Reviewers:	
Additional Information:	

Question	Response
Financial Disclosure Please describe all sources of funding that have supported your work. **This information is required for submission and will be published with your article, should it be accepted.** A complete funding statement should do the following: Include **grant numbers and the URLs** of any funder's website. Use the full name, not acronyms, of funding institutions, and use initials to identify authors who received the funding. **Describe the role** of any sponsors or funders in the study design, data collection and analysis, decision to publish, or preparation of the manuscript. If the funders had **no role** in any of the above, include this sentence at the end of your statement: "*The funders had no role in study design, data collection and analysis, decision to publish, or preparation of the manuscript.*" However, if the study was **unfunded**, please provide a statement that clearly indicates this, for example: "*The author(s) received no specific funding for this work.*" * typeset	One of the authors (DC) received a grant from “The Programme for Advanced Medical Education” sponsored by “Fundação Calouste Gulbenkian, Fundação Champalimaud, Ministério da Saúde and Fundação para a Ciência e Tecnologia, Portugal.” The authors have no financial or commercial interests to declare in relation to the content of this article. The funders had no role in study design, data collection and analysis, decision to publish, or preparation of the manuscript.
Competing Interests You are responsible for recognizing and disclosing on behalf of all authors any competing interest that could be perceived to bias their work, acknowledging all financial support and any other relevant financial or non-financial competing interests. Do any authors of this manuscript have competing interests (as described in the PLOS Policy on Declaration and Evaluation of Competing Interests)? **If yes**, please provide details about any and all competing interests in the box below. Your response should begin with this statement: *I have read the journal's policy and the authors of this manuscript have the following competing interests:*	The authors have declared that no competing interests exist

If no authors have any competing interests to declare, please enter this statement in the box: "*The authors have declared that no competing interests exist.*" * typeset	
Ethics Statement You must provide an ethics statement if your study involved human participants, specimens or tissue samples, or vertebrate animals, embryos or tissues. All information entered here should **also be included in the Methods section** of your manuscript. Please write "N/A" if your study does not require an ethics statement. **Human Subject Research (involved human participants and/or tissue)** All research involving human participants must have been approved by the authors' Institutional Review Board (IRB) or an equivalent committee, and all clinical investigation must have been conducted according to the principles expressed in the Declaration of Helsinki. Informed consent, written or oral, should also have been obtained from the participants. If no consent was given, the reason must be explained (e.g. the data were analyzed anonymously) and reported. The form of consent (written/oral), or reason for lack of consent, should be indicated in the Methods section of your manuscript. Please enter the name of the IRB or Ethics Committee that approved this study in the space below. Include the approval number and/or a statement indicating approval of this research. **Animal Research (involved vertebrate animals, embryos or tissues)** All animal work must have been conducted according to relevant national and international guidelines. If your study involved non-human primates, you must provide details regarding animal welfare	It was approved by the Ethical Committee at the authors' institution (08/2012/CEFCM).

and steps taken to ameliorate suffering; this is in accordance with the recommendations of the Weatherall report, "The use of non-human primates in research." The relevant guidelines followed and the committee that approved the study should be identified in the ethics statement. If anesthesia, euthanasia or any kind of animal sacrifice is part of the study, please include briefly in your statement which substances and/or methods were applied. Please enter the name of your Institutional Animal Care and Use Committee (IACUC) or other relevant ethics board, and indicate whether they approved this research or granted a formal waiver of ethical approval. Also include an approval number if one was obtained. **Field Permit** Please indicate the name of the institution or the relevant body that granted permission.	
Data Availability PLOS journals require authors to make all data underlying the findings described in their manuscript fully available, without restriction and from the time of publication, with only rare exceptions to address legal and ethical concerns (see the PLOS Data Policy and FAQ for further details). When submitting a manuscript, authors must provide a Data Availability Statement that describes where the data underlying their manuscript can be found. Your answers to the following constitute your statement about data availability and will be included with the article in the event of publication. **Please note that simply stating 'data available on request from the author' is not acceptable.** ***If, however, your data are only available upon request from the author(s), you must answer "No" to the first question below, and explain your exceptional situation in the text box provided.*** Do the authors confirm that all data underlying the findings described in their manuscript are fully available without restriction?	Yes - all data are fully available without restriction

Please describe where your data may be found, writing in full sentences. **Your answers should be entered into the box below and will be published in the form you provide them, if your manuscript is accepted.** If you are copying our sample text below, please ensure you replace any instances of XXX with the appropriate details. If your data are all contained within the paper and/or Supporting Information files, please state this in your answer below. For example, “All relevant data are within the paper and its Supporting Information files.” If your data are held or will be held in a public repository, include URLs, accession numbers or DOIs. For example, “All XXX files are available from the XXX database (accession number(s) XXX, XXX)." If this information will only be available after acceptance, please indicate this by ticking the box below. If neither of these applies but you are able to provide details of access elsewhere, with or without limitations, please do so in the box below. For example: “Data are available from the XXX Institutional Data Access / Ethics Committee for researchers who meet the criteria for access to confidential data.” “Data are from the XXX study whose authors may be contacted at XXX.” * typeset	All relevant data are within the paper and its Supporting Information files.
Additional data availability information:	

Dear Professor Hagen Andruszkow

Editor of the *PLOS One*,

We take the liberty of submitting the manuscript of a paper entitled "***Surgical anatomy of common regions used to harvest unconventional perfusion flaps: a cadaveric dissection study***" for publication in the ***PLOS One***.

As it is known, loss of significant amounts of tissue occurs frequently after trauma, tumor excision, infections, radiotherapy and/or auto-immune diseases.[1] Unconventional perfusion flaps (**UPFs**) have shown promising results for the reconstruction of otherwise difficult to treat defects.[2-4] Among the most prominent potential advantages of UPFs, are the fact that they can potentially include nerve segments, allowing the reconstruction of nerve defects with vascularized nerve segments.[2, 3, 5] This could be potentially very advantageous, as nerve flaps have been associated experimentally to better results than the traditional nerve grafts.[6-9] Moreover, the number of conventional nerve flaps (**CNF**), that is nerve segments with at least one artery and one vein of their own, is limited. Furthermore, frequently, it is technically difficult to isolate the feeding vessels of CNFs.[10, 11]

It has been largely assumed that, being UPFs usually based on the visible superficial venous system, anatomical and histological studies of these flaps are not necessary. In fact, the literature is particularly scant regarding articles specifically addressing the surgical anatomy of UPFs. Arguably, this is one of the main factors that has been limiting the clinical application of these flaps.[2] Another limiting factor is the significant inconsistency in the surgical literature regarding the terminology used to nominate the superficial veins on which these flaps are based.[2, 12-16]

Therefore, **the main aim of this paper was to perform a cadaveric dissection study to characterize the relevant anatomy and histology of these areas, from the point of view of the surgeon interested in harvesting UPFs**.

Secondarily, the authors present professionally drawn schematic representations of the most commonly encountered superficial veins in these regions, in order to facilitate planning and execution of UPFs.

Twenty-six freshly frozen adult human cadavers were used for anatomical and histological studies. **This series represents by far the largest series on the anatomy and histology of UPFs.**

Some of the **main findings of this study** were:

- Large **subcutaneous veins were surrounded by doublings of the superficial fascia**.
- Subcutaneous **veins were placed at different depths**, with the largest being deeply placed and the smallest more superficially placed.
- The **superficial cutaneous nerves, routinely used as autologous nerve grafts, were closer to sizeable superficial veins than to arteries and respective *comitante* veins of significant caliber**. Thus, to harvest a nerve segment as a conventional nerve flap (**CNF**), a deeper dissection would be required than to harvest a homologous UPF. Moreover, CNFs would tend to be bulkier than the corresponding UPFs.
- The **UPF associated with the great saphenous vein could include a portion of corticocancellous bone** from the medial aspect of the tibia. The

inclusion of bone in UPFs, eventually associated with a skin paddle, and nerve segments, may further increase the potential use of these flaps for reconstruction of complex head and neck and limb defects, further increasing the reconstructive surgeon's armamentarium.

In order to systematize these important findings, in addition to the **schematic drawings and illustrative cadaveric dissection and histology photographs**, the authors have added a **table synthetizing the main anatomical and morphometric features of each flap**. This table will certainly be of great use for anyone deciding what UPF to use to reconstruct a given defect.

For all these reasons, no doubt, this paper significantly contributes to broaden the knowledge on reconstructive surgery. Moreover, all this data is also highly pertinent for anyone with an interest in limb surgery, neurosurgery, burn surgery and/or peripheral nerve repair.

Hence, we strongly believe that this paper is of significant value to a broad audience including the readership of ***PLOS One*** and thus deserves publication.

If you have any doubts or queries, please do not hesitate to contact us.

Thank you so much for your kind attention.

The authors

References

1. Pomahac B, Hirsch T, Eriksson E. Wound management. In: Chung KC, Disa JJ, Gosain AK, Kinney BM, Rubin JP, editors. Plastic Surgery Indications and Practice. 1. First ed. Chicago, USA: Saunders Elsevier; 2009. p. 27-32.

2. Casal D, Carvalho S, Pais D, Mota-Silva E, Iria I, Vieira P, et al. Unconventional Perfusion Flaps. 2017. In: Flap Surgery [Internet]. AvidScience; [2-41]. Available from: http://www.avidscience.com/wp-content/uploads/2017/08/unconventional-perfusion-flaps.pdf.

3. Casal D, Cunha T, Pais D, Videira P, Coloma J, Zagalo C, et al. Systematic Review and Meta-Analysis of Unconventional Perfusion Flaps in Clinical Practice. Plastic and reconstructive surgery. 2016;138(2):459-79. doi: 10.1097/PRS.0000000000002390. PubMed PMID: 27465169.

4. Wharton R, Creasy H, Bain C, James M, Fox A. Venous flaps for coverage of traumatic soft tissue defects of the hand: a systematic review. The Journal of hand surgery, European volume. 2017:1753193417712879. Epub 2017/06/14. doi: 10.1177/1753193417712879. PubMed PMID: 28605949.

5. Townsend PL, Taylor GI. Vascularised nerve grafts using composite arterialised neuro-venous systems. Br J Plast Surg. 1984;37(1):1-17. Epub 1984/01/01. PubMed PMID: 6692051.

6. ANGÉLICA-ALMEIDA M, CASAL D, MAFRA M, MASCARENHAS-LEMOS L, SILVA E, FARINHO A, et al. Evaluation of the efficacy of different conduits to bridge a 10 millimeter defect in the rat sciatic nerve in the presence of an axial blood supply. Archives of Anatomy. 2014;2:8-30.

7. Giusti G, Lee JY, Kremer T, Friedrich P, Bishop AT, Shin AY. The influence of vascularization of transplanted processed allograft nerve on return of motor function in rats. Microsurgery. 2016;36(2):134-43. Epub 2015/01/06. doi: 10.1002/micr.22371. PubMed PMID: 25557845.

8. D'Arpa S, Claes KEY, Stillaert F, Colebunders B, Monstrey S, Blondeel P. Vascularized nerve "grafts": just a graft or a worthwhile procedure? Plastic and Aesthetic Research. 2015;2(4):183-94.

9. Iida T, Nakagawa M, Asano T, Fukushima C, Tachi K. Free vascularized lateral femoral cutaneous nerve graft with anterolateral thigh flap for reconstruction of facial nerve defects. J Reconstr Microsurg. 2006;22(5):343-8. Epub 2006/07/18. doi: 10.1055/s-2006-946711. PubMed PMID: 16845615.

10. Brandt J, Dahlin LB, Lundborg G. Autologous tendons used as grafts for bridging peripheral nerve defects. J Hand Surg Br. 1999;24(3):284-90. Epub 1999/08/05. doi: 10.1054/jhsb.1999.0074

S0266-7681(99)90074-8 [pii]. PubMed PMID: 10433437.

11. Millesi H. Bridging defects: autologous nerve grafts. Acta Neurochir Suppl. 2007;100:37-8. Epub 2007/11/08. PubMed PMID: 17985542.

12. Reich-Schupke S, Stucker M. Nomenclature of the veins of the lower limbs - current standards. Journal der Deutschen Dermatologischen Gesellschaft = Journal of the German Society of Dermatology : JDDG. 2011;9(3):189-94. Epub 2010/11/10. doi: 10.1111/j.1610-0387.2010.07548.x. PubMed PMID: 21059172.

13. Kachlik D, Pechacek V, Musil V, Baca V. Information on the changes in the revised anatomical nomenclature of the lower limb veins. Biomedical papers of the Medical Faculty of the University Palacky, Olomouc, Czechoslovakia. 2010;154(1):93-7. Epub 2010/05/07. PubMed PMID: 20445717.

14. Kachlik D, Pechacek V, Baca V, Musil V. The superficial venous system of the lower extremity: new nomenclature. Phlebology. 2010;25(3):113-23. Epub 2010/05/21. doi: 10.1258/phleb.2009.009046. PubMed PMID: 20483860.

15. Kachlik D, Baca V, Bozdechova I, Cech P, Musil V. Anatomical terminology and nomenclature: past, present and highlights. Surgical and radiologic anatomy : SRA. 2008;30(6):459-66. Epub 2008/05/20. doi: 10.1007/s00276-008-0357-y. PubMed PMID: 18488135.

16. Caggiati A, Bergan JJ, Gloviczki P, Eklof B, Allegra C, Partsch H. Nomenclature of the veins of the lower limb: extensions, refinements, and clinical application. Journal of vascular surgery. 2005;41(4):719-24. Epub 2005/05/06. doi: 10.1016/j.jvs.2005.01.018. PubMed PMID: 15874941.

Title: “Surgical anatomy of common regions used to harvest unconventional perfusion flaps: a cadaveric dissection study”

Author List: Diogo **Casal**, MD[1,2,3,4]; Diogo **Pais**, MD, PhD[2]; Eduarda **Mota-Silva**, MSci.[5]; Inês **Iria**, MSci[6]; Sara **Alves**, MSci[7]; Luís **Mascarenhas-Lemos**, MD[7]; Cláudia **Pen**, MSci[7]; Mário **Ferraz-Oliveira**, MD[7]; Paula A. **Videira**, PhD[3,4,8]; João **Goyri-O’Neill**, MD, PhD[2]

1. Plastic and Reconstructive Surgery Department and Burn Unit; Centro Hospitalar de Lisboa Central, Lisbon, Portugal
2. Anatomy Department; NOVA Medical School, Lisbon, Portugal
3. UCIBIO, Departamento de Ciências da Vida, Faculdade de Ciências e Tecnologia, Universidade NOVA de Lisboa, Caparica, Portugal
4. CEDOC, NOVA Medical School, Universidade NOVA de Lisboa, Lisbon, Portugal
5. LIBPhys, Physics Department, Faculdade de Ciências e Tecnologias, Universidade NOVA de Lisboa, Lisbon, Portugal
6. iMed - Research Institute for Medicines, Faculdade de Farmácia Universidade Lisboa, Lisbon, Portugal
7. Pathology Department; Centro Hospitalar de Lisboa Central, Lisbon, Portugal
8. CDG & Allies – Professionals and Patient Associations International Network (CDG & Allies – PPAIN), Caparica, Portugal

Short running head: Surgical anatomy of unconventional perfusion flaps

Corresponding Author:

Diogo Casal, M.D.

Anatomy Department, NOVA Medical School, Universidade NOVA de Lisboa

Campo dos Mártires da Pátria, 130

1169-056, Lisbon, Portugal

diogo_bogalhao@yahoo.co.uk

Financial Disclosure Statement:

One of the authors received a grant from “The Programme for Advanced Medical Education” sponsored by “Fundação Calouste Gulbenkian, Fundação Champalimaud, Ministério da Saúde and Fundação para a Ciência e Tecnologia, Portugal.”

The authors have no financial or commercial interest to declare in relation to the content of this article.

Authors' contributions:

DC, DP, II, PAV, EMS, and JO participated in all steps of the research project, as well as in the interpretation and discussion of the results and drafting of the manuscript.

SA, LM and MFO participated in the production of all histological specimens, as well as in the photographing and analysis of these specimens. These authors also collaborated in the interpretation and discussion of the histological data.

All authors have read and approved the manuscript.

Abstract:

Background: Unconventional perfusion flaps (**UPFs**) have shown promising results for the reconstruction of otherwise difficult to treat defects. The literature is particularly scant regarding articles specifically addressing the surgical anatomy of UPFs. Hence the main aim of this paper was to perform a cadaveric dissection study to characterize the relevant anatomy and histology of these areas, from the point of view of the surgeon interested in harvesting UPFs.

Methods: Twenty-six freshly frozen adult human cadavers were used for anatomical and histological studies.

Results: In all the regions studied the superficial cutaneous nerves were closer to sizeable superficial veins than to arteries of significant caliber and to their respective *comitante* veins. The largest veins in each region were placed deeper than smaller veins. The largest veins were enveloped by relatively thick doublings of the superficial fascia, which formed fascial sheaths around these superficial veins. The thinnest flaps were the dorsal foot (2.97 ± 1.69 mm), and the anterior antebrachial flaps (4.76 ± 0.73 mm). These UPFs presented an integumentary thickness similar to that of the eyelid and that of the penis. The sural flap was the one associated with a larger single nerve (4.32 ± 0.83 mm) followed by the saphenous (3.89 ± 1.53 mm), and the medial brachial (2.87 ± 0.49) flaps.

Conclusions: In multiple anatomical regions, the superficial venous system was consistently found in close proximity to expendable superficial nerves, tendons, and even bone segments. This knowledge helps to set the ground to tailor composite UPFs for different purposes.

Clinical Question/Level of Evidence: Experimental

Keywords: Anatomy; Flaps; Cadavers; Surgery; Blood supply; Surgery; Reconstruction.

Introduction:

Loss of significant amounts of tissue occurs frequently after trauma, tumor excision, infections, radiotherapy and/or auto-immune diseases.[1] Unconventional perfusion flaps (**UPFs**) have shown promising results for the reconstruction of otherwise difficult to treat defects.[2-4] UPFs can be defined as blocks of tissues transferred solely on their venous system.[2, 3] If at the recipient site, one side of the venous system of this type of flaps is connected to an artery, the flap is called “arterialized venous flap” (**AVF**). If both sides of the flap are connected to recipient site’s veins, the flap receives the name of “venous flap” (**VF**).[2, 3, 5]

Among the most prominent potential advantages of UPFs, are the fact that they can potentially include nerve segments, allowing the reconstruction of nerve defects with vascularized nerve segments.[2, 3, 6] This could be potentially very advantageous, as nerve flaps have been associated experimentally to better results than the traditional nerve grafts.[7-10] Moreover, the number of conventional nerve flaps (**CNF**), that is nerve segments with at least one artery and one vein of their own, is limited. Furthermore, frequently, it is technically difficult to isolate the feeding vessels of CNFs.[11, 12]

It has been largely assumed that, being UPFs usually based on the visible superficial venous system, anatomical and histological studies of these flaps are not necessary. In fact, the literature is particularly scant regarding articles specifically addressing the surgical anatomy of UPFs. Arguably, this is one of the main factors that has been limiting the clinical application of these flaps.[2] Another limiting factor is the significant inconsistency in the surgical literature regarding the terminology used to nominate the superficial veins on which these flaps are based.[2, 13-17]

According to a recent systematic review and meta-analysis on UPFs, clinically the most common donor sites of these flaps are, in decreasing frequency, the forearm and arm (61.8%), the foot (9.8%), and the lower leg (8.4%). Hence the main aim of this paper was to perform a cadaveric dissection study to characterize the relevant anatomy and histology of these areas, from the point of view of the surgeon interested in harvesting UPFs.

Secondarily, the authors present schematic representations of the most commonly encountered superficial veins in these regions, in order to facilitate planning and execution of UPFs.

Methods:

Twenty-six freshly frozen adult human cadavers, embalmed according to a technique developed at our institution, were used.[18] Sixteen cadavers were female (61.5%), and 10 were male (38.5%). The average age of the specimens was 75.1 ± 10.5 years. Cadavers had no prior history or evidence of lower limb pathology.

In 15 cadavers, a tourniquet was placed at the proximal aspect of each thigh and upper arm. Subsequently, each cadaver was submitted to intravenous injection of a blue latex solution (Robbialac ®) in the superficial dorsal digital veins of the toes and fingers, using 22-gauge catheters. The injection was stopped when all the superficial veins in a given segment became engorged. In another cadaver, in addition to the procedure just described, a red latex solution (Robbialac ®) was injected in the common femoral arteries, until subungual perfusion of toes was noted. Cadavers were then kept at 4º C temperature for 24 hours. [19]

After this period, each region of interest was carefully dissected using 6X-magnification operating loupes (Design for Vision®). Relevant structures were measured and photographed. Their position was registered relatively to constant landmarks (joints and bone extremities).

The middle portion of each flap's region was biopsied and submitted to histological processing.

In 10 other cadavers subjected to a similar procedure, flap regions were converted into modified Spalteholz cleared specimens.[20] This technique creates transparent three-dimensional specimens, while preserving vascular and perivascular structure.[21]

In order to compare the nerve components of flaps with frequently injured nerves, the following nerves were retrieved from two cadavers: facial nerve at the posterior aspect of the parotid gland; hypoglossal nerve at the base of the tongue; masseteric nerve at the sigmoid notch; collateral digital nerve of the index finger at the proximal phalanx level; median nerve at the distal third of the arm; anterior division of the C7 spinal nerve.[22-25]

To compare the thickness of the integument of two regions considered difficult to reconstruct with the thickness of UPFs, in two male cadavers, biopsies were performed of the upper eyelid and of the penis.[2, 3]

Specimens were prepared for histological observation using hematoxylin-eosin and Masson's trichrome stains, as well as immunohistochemistry for neurofilaments for staining nerves.[26-29] Histological sections were observed and photographed using a Leica DM LB2® microscope. Representative images were selected for histomorphometric evaluation using the Fiji® software.

This study's protocol was approved by the Ethical Committee at the authors' institution (08/2012/CEFCM).

Statistical analysis

Qualitative variables were expressed as percentages. Quantitative variables were expressed as means ± SD. IBM SPSS Version 21.0® software was used for descriptive and inferential statistical analysis. The Kolmogorov-Smirnov test was used to assess whether variables were distributed normally. Analysis of variance and t test were used to compare averages in normally distributed data. Kruskal-Wallis and Mann-Whitney tests were used to compare means in non-normally distributed data. Proportions were analyzed with the chi-square test or Fisher's exact test. A two-tail value of $p<0.05$ was considered to be statistically significant.

Results:

Common anatomical and histological features of all anatomical regions studied

In all the regions studied the superficial cutaneous nerves were closer to sizeable superficial veins than to arteries of significant caliber and to their respective *comitante* veins (**Fig 1**). Of interest, sizeable superficial veins of the limbs were not placed at the same depth. In fact, the largest veins in each region were placed deeper than smaller veins. Intermediate-sized veins were placed at an intermediate depth (**Figs 2, 3** and **4**). The largest veins, namely the great saphenous vein, the short saphenous vein, the cephalic and basilic veins travelled close to the muscle fascia and they were enveloped by relatively thick doublings of the superficial fascia, which formed fascial sheaths around these superficial veins. Although the largest veins and superficial nerves shared common sheaths, histologically they were separated by fascial septa (**Fig. 2**).

In all the regions studied, the superficial fascia was readily identifiable, although it was significantly thinner than the muscle fascia. The superficial fascial divided the subcutaneous fat into a superficial and a deep fatty layer. The former layer was significantly thinner than the latter (**Fig. 2**).

Medial brachial flap

In the distal half of the medial region of the arm, the basilic vein was the dominant superficial vein (**Fig. 5**). This vein was accompanied by the medial antebrachial cutaneous nerve which pierced the muscle fascia through the same foramen through which the basilic vein reached the vasculo nervous bundle of the arm. In the most superficial portion of this flap's region, there were branches of the medial

antebrachial cutaneous nerve that supplied the skin of this region. In the deeper aspect, soon after reaching the subcutaneous compartment, the medial antebrachial cutaneous nerve divided into a larger anterior branch that escorted the basilic vein and a smaller posterior branch that travelled to the posteromedial aspect of the forearm. The basilic vein and the anterior branch of the medial antebrachial cutaneous nerve could be raised as a unit in all the specimens dissected. The nerve was placed deep to the vein in all cases.

Anterior antebrachial flap

The distal third of the anterior aspect of the forearm was covered with a thin and pliable integument (**Fig 6**). In this region, the dominant veins were the affluent veins of the median antebrachial veins, which were interconnected by oblique and transverse anastomoses (**Fig 6B**). There were small branches to the skin originating from the anterior branches of the medial antebrachial cutaneous nerve and from the lateral antebrachial cutaneous nerve. The palmaris longus tendon was present in this region in 88% of cases. The muscle fascia was placed relatively close to the superficial veins and skin, suggesting that these tissues could easily be mobilized *en bloc* as an UPF (**Fig 6C**).

Sural flap

In the inferior three quarters of the posterior aspect of the leg, the sural nerve and the short saphenous vein were in close proximity and presented a significant caliber in all cadavers (**Fig 7**). These structures followed a line that crossed from the space between the two bellies of the gastrocnemius muscle to the lateral aspect of the calcaneal tendon in all cases. In all specimens, both the sural nerve(s) and the short saphenous vein presented a significant diameter and could be harvested as a flap

for a length of at least 25 cm (**Fig 7B**). The sural nerve abandoned the posterior compartment of the leg in the transition between the upper third and the lower three quarters of the leg. In two cadavers (8%) the two roots of the sural nerve remained distinct throughout the entire usual course of the nerve originating two sural nerves. In the remaining cases, the sural nerve originated from two main roots derived from the common fibular and from the tibial nerves, being the latter root the dominant one. In all cases, the sural nerve(s) divided in its terminal branches in the vicinity of the lateral malleolus' tip. In 68% of cases, there was a superficial accessory small saphenous vein in the lateral aspect of the distal two thirds of the leg, travelling superficially and laterally to the short saphenous vein, until ending as one of the tributaries of the latter vein (**Fig. 4B**). The short saphenous vein penetrated the muscular fascia in the popliteal space. This vein was anastomosed with the posterior thigh circumflex vein (also known as Giacomini vein) and with the posterior accessory great saphenous vein in 72% and 52% of cases (**Fig. 4B**). The integument of this region was significantly thicker in the upper third of the leg than in the remaining lower two thirds (**Fig. 7C** to **7E**).

Saphenous flap

The great saphenous vein was located deep in the thick subcutaneous fat in the thigh. In this region, this vein was located at a significant distance from the subcutaneous nerves, namely from the saphenous nerve, which was sub aponeurotic throughout much of the thigh. This nerve became superficial only after leaving the adductor canal in the distal fifth of the thigh. Therefore, in the thigh, the great saphenous vein did not show an anatomy favorable to the elaboration of UPFs.

Below the knee, the great saphenous vein and the saphenous nerve presented a parallel path from the posterior aspect of the medial condyle of the femur to the anterior aspect of the medial malleolus (**Fig. 8**). The vein presented a sizeable caliber in all cases. In the lower leg, an anterior accessory great saphenous vein was observed superficially and laterally to the great saphenous vein on both sides in 3 cadavers (12%; **Fig. 4A**). The former vein presented a fascial sheath of its own similar to that of the great saphenous vein, until terminating in the latter vein in the thigh. In all circumstances, either through the anterior accessory great saphenous vein or through a direct tributary of the great saphenous vein, the distal two thirds of the medial aspect of the tibial bone presented venous effluents to the great saphenous vein system (**Fig. 8C**). The saphenous nerve gave off several branches to the anterior and posterior aspects of the inner side of the leg, becoming composed of multiple thin branches in the distal aspect of the leg.

In all the cutaneous nerves analyzed, including the saphenous and the sural nerves, a well-developed epineurial venous plexus was observed. This venous plexus drained into multiple small veins and venules that joined the adjacent superficial veins (**Fig. 9**).

Dorsal foot flap

This flap's region was dominated by two large venous structures: the medial and lateral marginal veins (**Fig. 10**). These two veins were interconnected by the dorsal venous arch of the foot, which, in turn, received in its distal convexity the superficial dorsal digital veins. From the concavity of the dorsal venous arch of the foot there was a variable number of veins that drained most frequently into the territory of the great saphenous vein or less frequently to the anterior accessory great saphenous vein (12%). There were multiple venous anastomoses between all the major

superficial veins of the dorsum of the foot (**Fig. 10 F**). Beneath the major veins, the medial dorsal and the intermediate dorsal cutaneous nerves of the foot could be found in all cases. Beneath these nerves, the relatively thin dorsal fascia of the foot covered the underlying extensor tendons, namely the accessory extensor hallucis longus tendon, and the extensor hallucis brevis tendon, which were present in 88% and 100% of cadavers, respectively. The integument in this region was very thin and pliable, particularly close to the proximal aspect of the toes (**Fig. 10**).

Medial plantar flap

This region presented a well-developed venous plexus surrounding the scaphoid tubercule (**Figs. 4D** and **11**). This plexus drained into the calcaneal veins, which, in turn, drained into the medial marginal vein. This region received numerous diminutive nerve branches from the terminal portion of the saphenous nerve.

The integumentary layer presented some noteworthy specificities. The skin was relatively thick and ridged, being similar to that found in the palmar aspect of the hand. The subcutaneous tissue was relatively scant and presented numerous fibrous septa connecting the underlying muscle fascia to the deep aspect of the reticular dermis (**Fig. 11C**).

Morphometric features of the UPFs

The thinnest flaps were the dorsal foot (2.97 ± 1.69 mm), and the anterior antebrachial flaps (4.76 ± 0.73 mm) [**Table 1**].

Unconventional Perfusion Flap	Potential composition	Maximal thickness (mm)	Diameter of dominant structures (mm)		Some potential specific clinical applications based on anatomical features
			Veins (v)	Nerves (n)	
Medial brachial	Skin + fat + nerve	10.72 ± 1.90	Basilic v.:	Medial antebrachial n.	• Flow-through flap • Intermediate-sized nerve reconstruction
			9.02 ± 1.68	2.87 ± 0.49	
Anterior antebrachial	Skin + fat + tendon + nerve	4.76 ± 0.73	Lateral antebrachial v.	Anterior branch of the lateral antebrachial n.	• Coverage of regions where the integument is thin • Small nerve reconstruction • Tendon or ligament reconstruction
			2.48 ± 0.79	0.79 ± 0.33	
			Median antebrachial v.	Anterior branch of the medial antebrachial n.	
			1.87 ± 0.57	0.83 ± 0.47	
Sural	Skin + fat + nerve	12.62 ± 2.18	Small saphenous v.	Sural n.	• Flow-through flap • Large nerve reconstruction
			6.44 ± 0.89	4.32 ± 0.83	
Saphenous	Skin + fat + nerve + bone	11.68 ± 3.06	Great saphenous v.	Saphenous n.	• Flow-through flap • Intermediate-sized nerve reconstruction • Bone reconstruction
			8.94 ± 1.48	3.89 ± 1.53	
Dorsal foot	Skin + fat + nerve + tendon	2.97 ± 1.69	Medial marginal v.	Medial dorsal cutaneous n. of the foot:	• Ideal for types II and III AVFs[3] • Coverage of regions where the integument is thin, such as digits • Tendon and/or ligament reconstruction • Small nerve reconstruction
			4.70 ± 1.15	1.16 ± 0.67	
			Lateral marginal v.	Intermediate dorsal cutaneous n. of the foot:	
			2.89 ± 0.74	1.01 ± 0.53	
Medial plantar	Skin + fat + nerve	5.79 ± 1.97	Medial marginal v. diameter	Branches of the saphenous nerve	• Coverage of palmar skin (sturdy and sensitive skin)
			4.98 ± 1.27	0.89 ± 0.37	

Table 1. Synthesis of surgical pertinent morphometric features of the unconventional perfusion flaps studied and their clinical corollary.

Values are expressed as averages ± standard deviation.

The thickest UPFs were the medial brachial (10.72 ± 1.90mm), the sural (12.62 ± 2.18 mm), the saphenous (11.68 ± 3.06 mm), and the medial plantar (5.79 ± 1.97 mm) flaps. The thinnest UPFs presented an integumentary thickness similar to that of the eyelid and that of the penis (**Fig 12**).

The flaps with the largest associated veins were in decreasing order: the medial brachial (9.02 ± 1.68 mm), the saphenous (8.94 ± 1.48 mm), and the sural (6.44 ± 0.89 mm) flaps.

The sural flap was the one associated with a larger single nerve (4.32 ± 0.83 mm; **Fig. 13**), followed by the saphenous (3.89 ± 1.53 mm), and the medial brachial (2.87 ± 0.49) flaps.

Discussion:

The description of the surgical anatomy of the veins draining the integument has been performed by other authors, namely by Ian Taylor's group.[30, 31]

However, as far as the authors could determine, the study herein presented, being composed of 26 cadaveric dissections, represents by far the largest series on the anatomy and histology of UPFs. Townsend and Taylor, in 1984, wrote a seminal paper on the subject, succinctly describing the anatomical proximity between the sural nerve and the short saphenous vein, and between the saphenous nerve and the great saphenous vein.[4, 6, 32-35] These anatomical studies set the basis for the clinical application of arterialized neurovenous flaps (**ANVFs**). However, they were based exclusively on 13 cadaveric dissections, not including the histological characterization of these regions. Subsequently, Taylor's group described in great detail the venossomes of the nerves of the upper and lower limbs, based on very meticulous dissections of 2 and 3 cadavers, respectively.[30, 36-38] Recently, Taylor *et al* amplified their series with an additional studying involving 20 lower limb cadaveric dissections.[39]

In 1999, Caggiati and Ricci recognized that the great saphenous vein and some of its tributaries were enclosed by the superficial fascia. This, in fact, explained the typical "Egyptian eye" sign observed on ultrasound examination of these structures. Therefore, they coined the term saphenous fascia, which was validated at a consensus meeting in Rome in 2002.[17, 40-42] In 2006, Abu-Hijleh *et al* noted that this pattern of distribution of the superficial fascia around superficial veins, forming vasculo nervous sheaths could be found in other parts the body.[43] However, their study was based exclusively on the dissection and histological characterization of six

embalmed adult cadavers, along with ultrasound imaging on four living subjects. Our data further lend support to their findings.

Additionally, in the present study, it was clearly noted that superficial veins were placed at different depths in the subcutaneous tissue. This knowledge is often neglected in many anatomy and surgery textbooks.[2, 31, 34, 35, 44] However, it is of potential great clinical interest when designing UPFs, as the use of more superficial veins allows the elaboration of thinner flaps. Besides the obvious morphometric implications, thinner flaps may be associated with greater survival of certain types of UPFs.[2, 4, 32-35]

This work has shown that in multiple anatomical regions the superficial venous system is consistently found in close proximity to expendable superficial nerves, tendons, and even bone segments. This information helps to set the ground to fabricate composite UPFs for different purposes (**Fig 4**; **Table 1**). The strong tendency for colocalization of superficial veins and nerves may be explained by the fact that these structures develop synchronically, with multiple levels of cross-talk in their origin, differentiation, and elongation until reaching their target organs. As a consequence, they remain in close anatomical proximity since the end of the fetal period.[31, 45] The practical corollary is that there are numerous places where the superficial venous system is in the vicinity of expendable superficial nerves that thus could be raised as ANVFs.[36, 45, 46] Interestingly, in all the regions studied, the superficial cutaneous nerves were closer to sizeable superficial veins than to arteries and respective *comitante* veins of significant caliber (**Fig 1**). Thus, to harvest a nerve segment as a conventional nerve flap (**CNF**) a deeper dissection would be required than to harvest a homologous ANVF. Moreover, CNFs would tend to be bulkier than the corresponding ANVFs.

However, although there is some evidence that ANVFs may be superior to nerve grafts, ANVFs and their anatomy are frequently neglected even in contemporary textbooks.[47, 48] Notwithstanding, it should also be noted that experimental studies in rats have shown that sensory nerves used as a grafts have yielded inferior motor recovery compared with autologous motor or mixed (sensory and motor) nerve grafts.[49, 50] This may theoretically limit the usefulness of ANVFs incorporating sensory nerves as the ones described in this article for reconstructing motor nerves in the clinical context. However, presently, sensory autologous nerve grafts remain the gold standard for peripheral nerve reconstruction in the clinical context.[51-53]

The present study suggests it is anatomically possible to include a bone segment of the medial aspect of the tibial bone in a AVF or in ANVF tailored around the great saphenous vein. As far as the authors could determine, an osteocutaneous AVF involving the medial aspect of the tibia has been performed in the clinical setting only once.[3] This flap was executed by Koshima *et al.* to successfully reconstruct a defect of the carpal region associated with osteomyelitis. This flap's design was based on the intra-operative observation that the tibial bone cortex was draining its blood to the great saphenous vein.[54] The present study lends support to this architecture of the saphenous UPF. Interestingly, recently, in a pig model, it was shown that large pieces of corticocancellous bone were kept viable on an arterialized venous type perfusion, showing better viability than equivalent bone grafts.[55]

The inclusion of bone in UPFs, eventually associated with a skin paddle, and nerve segments, may further increase the potential use of these flaps for reconstruction of complex head and neck and limb defects, further increasing the reconstructive surgeon's armamentarium.

The authors believe that the anatomical data herein presented may help to decide the best region to use for UPF harvesting in specific circumstances (**Table 1**).

Venous caliber and morphological pattern, flap thickness, skin quality, nerve disposition and caliber, as well as the potential for including other structures, such as bone and/or tendon are some of the factors to take in consideration in the decision process.

For example, the dorsal venous flap of the foot is a potential good candidate for digital reconstruction, namely for ring finger avulsion. In fact, its venous pattern make it a preferred option for tailoring antidromic AVFs, which seem to be most suited to cover large areas.[3] Moreover, its integument is thin and pliable, such as that of the fingers (Table 1). Finally, it can easily include the accessory extensor hallucis longus tendon which was found in the majority of cases, as well as the extensor hallucis brevis tendon, allowing for simultaneous skin, nerve, and tendon/ligament reconstruction.[56]

Study limitations section:

The illustrations of the most common disposition of the superficial veins and nerves of the superior and inferior limbs (**Figs 3** and **4**) do not take into the account the multiple possible variations of these structures.[31, 57-61] However, in the present work the authors strove to show the most common patterns encountered, rather than focusing on anatomical variations of specific structures that are addressed in detail elsewhere.[31, 57-61]

Although in the present study the authors did not find any large superficial arteries, these anatomical variants, particularly in the upper limb, should always be born in mind, in order to avoid iatrogeny when raising UPFs.[62-64]

The morphometric data presented in this paper may be underestimating the true size of the structures, since histological processing is known to lead to around 20% of volume shrinking.[65, 66]

Another limitation of this work is that it focussed on the regions that, according to the literature, are the more frequently used to raise UPFs.[2, 3, 32, 34, 35] Other regions should be studied.

Finally, the theoretical considerations formulated in the discussion section, although plausible, need empirical validation.

Conclusions:

In multiple anatomical regions, the superficial venous system is consistently found in close proximity to expendable superficial nerves, tendons, and even bone segments. This knowledge helps to set the ground to tailor composite UPFs for different purposes.

Acknowledgments

The authors would like to thank Mr. Filipe Franco for the drawings contained in this article.

Financial Disclosure Statement:

One of the authors (DC) received a grant from “The Programme for Advanced Medical Education” sponsored by “Fundação Calouste Gulbenkian, Fundação Champalimaud, Ministério da Saúde and Fundação para a Ciência e Tecnologia, Portugal.”

The authors have no financial or commercial interests to declare in relation to the content of this article.

References

1. Pomahac B, Hirsch T, Eriksson E. Wound management. In: Chung KC, Disa JJ, Gosain AK, Kinney BM, Rubin JP, editors. Plastic Surgery Indications and Practice. 1. First ed. Chicago, USA: Saunders Elsevier; 2009. p. 27-32.

2. Casal D, Carvalho S, Pais D, Mota-Silva E, Iria I, Vieira P, et al. Unconventional Perfusion Flaps. 2017. In: Flap Surgery [Internet]. AvidScience; [2-41]. Available from: http://www.avidscience.com/wp-content/uploads/2017/08/unconventional-perfusion-flaps.pdf.

3. Casal D, Cunha T, Pais D, Videira P, Coloma J, Zagalo C, et al. Systematic Review and Meta-Analysis of Unconventional Perfusion Flaps in Clinical Practice. Plastic and reconstructive surgery. 2016;138(2):459-79. doi: 10.1097/PRS.0000000000002390. PubMed PMID: 27465169.

4. Wharton R, Creasy H, Bain C, James M, Fox A. Venous flaps for coverage of traumatic soft tissue defects of the hand: a systematic review. The Journal of hand surgery, European volume. 2017:1753193417712879. Epub 2017/06/14. doi: 10.1177/1753193417712879. PubMed PMID: 28605949.

5. Casal D, Mota-Silva E, Pais D, Iria I, Videira PA, Tanganho D, et al. Optimization of an arterialized venous fasciocutaneous flap in the abdomen of the rat. PRS Global Open. 2017;in press.

6. Townsend PL, Taylor GI. Vascularised nerve grafts using composite arterialised neuro-venous systems. Br J Plast Surg. 1984;37(1):1-17. Epub 1984/01/01. PubMed PMID: 6692051.

7. ANGÉLICA-ALMEIDA M, CASAL D, MAFRA M, MASCARENHAS-LEMOS L, SILVA E, FARINHO A, et al. Evaluation of the efficacy of different conduits to bridge

a 10 millimeter defect in the rat sciatic nerve in the presence of an axial blood supply. Archives of Anatomy. 2014;2:8-30.

8. Giusti G, Lee JY, Kremer T, Friedrich P, Bishop AT, Shin AY. The influence of vascularization of transplanted processed allograft nerve on return of motor function in rats. Microsurgery. 2016;36(2):134-43. Epub 2015/01/06. doi: 10.1002/micr.22371. PubMed PMID: 25557845.

9. D'Arpa S, Claes KEY, Stillaert F, Colebunders B, Monstrey S, Blondeel P. Vascularized nerve "grafts": just a graft or a worthwhile procedure? Plastic and Aesthetic Research. 2015;2(4):183-94.

10. Iida T, Nakagawa M, Asano T, Fukushima C, Tachi K. Free vascularized lateral femoral cutaneous nerve graft with anterolateral thigh flap for reconstruction of facial nerve defects. J Reconstr Microsurg. 2006;22(5):343-8. Epub 2006/07/18. doi: 10.1055/s-2006-946711. PubMed PMID: 16845615.

11. Brandt J, Dahlin LB, Lundborg G. Autologous tendons used as grafts for bridging peripheral nerve defects. J Hand Surg Br. 1999;24(3):284-90. Epub 1999/08/05. doi: 10.1054/jhsb.1999.0074

S0266-7681(99)90074-8 [pii]. PubMed PMID: 10433437.

12. Millesi H. Bridging defects: autologous nerve grafts. Acta Neurochir Suppl. 2007;100:37-8. Epub 2007/11/08. PubMed PMID: 17985542.

13. Reich-Schupke S, Stucker M. Nomenclature of the veins of the lower limbs - current standards. Journal der Deutschen Dermatologischen Gesellschaft = Journal of the German Society of Dermatology : JDDG. 2011;9(3):189-94. Epub 2010/11/10. doi: 10.1111/j.1610-0387.2010.07548.x. PubMed PMID: 21059172.

14. Kachlik D, Pechacek V, Musil V, Baca V. Information on the changes in the revised anatomical nomenclature of the lower limb veins. Biomedical papers of the

Medical Faculty of the University Palacky, Olomouc, Czechoslovakia. 2010;154(1):93-7. Epub 2010/05/07. PubMed PMID: 20445717.

15. Kachlik D, Pechacek V, Baca V, Musil V. The superficial venous system of the lower extremity: new nomenclature. Phlebology. 2010;25(3):113-23. Epub 2010/05/21. doi: 10.1258/phleb.2009.009046. PubMed PMID: 20483860.

16. Kachlik D, Baca V, Bozdechova I, Cech P, Musil V. Anatomical terminology and nomenclature: past, present and highlights. Surgical and radiologic anatomy : SRA. 2008;30(6):459-66. Epub 2008/05/20. doi: 10.1007/s00276-008-0357-y. PubMed PMID: 18488135.

17. Caggiati A, Bergan JJ, Gloviczki P, Eklof B, Allegra C, Partsch H. Nomenclature of the veins of the lower limb: extensions, refinements, and clinical application. Journal of vascular surgery. 2005;41(4):719-24. Epub 2005/05/06. doi: 10.1016/j.jvs.2005.01.018. PubMed PMID: 15874941.

18. Goyri-O'Neill J, Pais D, Freire de Andrade F, Ribeiro P, Belo A, O'Neill A, et al. Improvement of the embalming perfusion method: the innovation and the results by light and scanning electron microscopy. Acta Med Port. 2013;26(3):188-94. Epub 2013/07/03. PubMed PMID: 23815830.

19. Fukui A. Tecnhique of microangiography. In: Tamai S, Usui M, Yoshizu T, editors. Experimental and Clinical Reconstructive Microsurgery. First ed. Japan: Springer-Verlag; 2004. p. 55-6.

20. Sempuku T. Technique for making a Spalteholz cleared specimen. In: Tamai S, Usui M, Yoshizu T, editors. Experimental and Clinical Reconstructive Microsurgery. First ed. Japan: Springer-Verlag; 2004. p. 59-60.

21. Steinke H, Wolff W. A modified Spalteholz technique with preservation of the histology. Ann Anat. 2001;183(1):91-5. doi: 10.1016/S0940-9602(01)80020-0. PubMed PMID: 11206989.

22. Murovic JA. Upper-extremity peripheral nerve injuries: a Louisiana State University Health Sciences Center literature review with comparison of the operative outcomes of 1837 Louisiana State University Health Sciences Center median, radial, and ulnar nerve lesions. Neurosurgery. 2009;65(4 Suppl):A11-7. Epub 2009/12/16. doi: 10.1227/01.neu.0000339130.90379.89. PubMed PMID: 19927055.

23. Rosberg HEeLD. Epidemiology of hand injuries in a middle-sized city in southern Sweden - a retrospective study with an 8-year interval. Scand J Plast Rec Surg Hand Surg. 2004;(38):347-55.

24. Kouyoumdjian JA. Peripheral nerve injuries: a retrospective survey of 456 cases. Muscle & nerve. 2006;34(6):785-8. doi: 10.1002/mus.20624. PubMed PMID: 16881066.

25. Ciaramitaro P, Mondelli M, Logullo F, Grimaldi S, Battiston B, Sard A, et al. Traumatic peripheral nerve injuries: epidemiological findings, neuropathic pain and quality of life in 158 patients. J Peripher Nerv Syst. 2010;15(2):120-7. Epub 2010/07/16. doi: 10.1111/j.1529-8027.2010.00260.x. PubMed PMID: 20626775.

26. Raimondo S, Fornaro M, Di Scipio F, Ronchi G, Giacobini-Robecchi MG, Geuna S. Chapter 5: Methods and protocols in peripheral nerve regeneration experimental research: part II-morphological techniques. International review of neurobiology. 2009;87:81-103. Epub 2009/08/18. doi: 10.1016/S0074-7742(09)87005-0. PubMed PMID: 19682634.

27. Fischer AH, Jacobson KA, Rose J, Zeller R. Hematoxylin and eosin staining of tissue and cell sections. Cold Spring Harbor Protocols. 2008;2008(5):pdb. prot4986.

28. Foot NC. The Masson trichrome staining methods in routine laboratory use. Stain Technology. 1933;8(3):101-10.

29. Pusztaszeri MP, Seelentag W, Bosman FT. Immunohistochemical expression of endothelial markers CD31, CD34, von Willebrand factor, and Fli-1 in normal human tissues. Journal of Histochemistry & Cytochemistry. 2006;54(4):385-95.

30. Taylor GI, Caddy CM, Watterson PA, Crock JG. The Venous Territories (Venosomes) of the Human Body: Experimental Study and Clinical Implications. Plastic and reconstructive surgery. 1990;86(2):185-213. PubMed PMID: 00006534-199008000-00001.

31. Sangari SK. Veins of the lower limb. In: Tubbs RS, Shoja MM, Loukas M, editors. Bergman's comprehensive encyclopedia of human anatomic variation. 1. First ed. New Jersey: Wiley Blackwell; 2016. p. 900-9.

32. Garlick JW, Goodwin IA, Wolter K, Agarwal JP. Arterialized venous flow-through flaps in the reconstruction of digital defects: case series and review of the literature. Hand (N Y). 2015;10(2):184-90. Epub 2015/06/03. doi: 10.1007/s11552-014-9684-0. PubMed PMID: 26034428.

33. Giesen T, Forster N, Kunzi W, Giovanoli P, Calcagni M. Retrograde arterialized free venous flaps for the reconstruction of the hand: review of 14 cases. The Journal of hand surgery. 2014;39(3):511-23. Epub 2014/02/25. doi: 10.1016/j.jhsa.2013.12.002. PubMed PMID: 24559628.

34. Goldschlager R, Rozen WM, Ting JW, Leong J. The nomenclature of venous flow-through flaps: updated classification and review of the literature. Microsurgery. 2012;32(6):497-501. Epub 2012/03/22. doi: 10.1002/micr.21965. PubMed PMID: 22434451.

35. Yan H, Brooks D, Ladner R, Jackson WD, Gao W, Angel MF. Arterialized venous flaps: a review of the literature. Microsurgery. 2010;30(6):472-8. Epub 2010/03/20. doi: 10.1002/micr.20769 [doi]. PubMed PMID: 20238385.

36. Taylor GI, Pan WR. The angiosome concept. In: Dodwell P, editor. The angiosome concept and tissue transfer. 1. First ed. Florida: Quality Medical Publishing, Inc.; 2014. p. 354-95.

37. Hong MK, Taylor GI. Angiosome territories of the nerves of the upper limbs. Plastic and reconstructive surgery. 2006;118(1):148-60. Epub 2006/07/04. doi: 10.1097/01.prs.0000221075.91038.08. PubMed PMID: 16816688.

38. Suami H, Taylor GI, Pan WR. Angiosome territories of the nerves of the lower limbs. Plastic and reconstructive surgery. 2003;112(7):1790-8. Epub 2003/12/10. doi: 10.1097/01.PRS.0000091161.95599.D8. PubMed PMID: 14663222.

39. Gascoigne AC, Ian Taylor G, Corlett RJ, Briggs C, Ashton MW. The Relationship of Superficial Cutaneous Nerves and Interperforator Connections in the Leg: A Cadaveric Anatomical Study. Plastic and reconstructive surgery. 2017;139(4):994e-1002e. Epub 2017/03/30. doi: 10.1097/prs.0000000000003157. PubMed PMID: 28350683.

40. Caggiati A. The saphenous venous compartments. Surgical and radiologic anatomy : SRA. 1999;21(1):29-34. PubMed PMID: 10370990.

41. Caggiati A. Fascial relations and structure of the tributaries of the saphenous veins. Surgical and radiologic anatomy : SRA. 2000;22(3-4):191-6. PubMed PMID: 11143312.

42. Caggiati A, Bergan JJ, Gloviczki P, Jantet G, Wendell-Smith CP, Partsch H, et al. Nomenclature of the veins of the lower limbs: an international interdisciplinary consensus statement. Journal of vascular surgery. 2002;36(2):416-22. PubMed PMID: 12170230.

43. Abu-Hijleh MF, Roshier AL, Al-Shboul Q, Dharap AS, Harris PF. The membranous layer of superficial fascia: evidence for its widespread distribution in the

body. Surgical and radiologic anatomy : SRA. 2006;28(6):606-19. Epub 2006/10/25. doi: 10.1007/s00276-006-0142-8. PubMed PMID: 17061033.

44. Woo SH, Kim KC, Lee GJ, Ha SH, Kim KH, Dhawan V, et al. A retrospective analysis of 154 arterialized venous flaps for hand reconstruction: an 11-year experience. Plastic and reconstructive surgery. 2007;119(6):1823-38. Epub 2007/04/19. doi: 10.1097/01.prs.0000259094.68803.3d [doi]

00006534-200705000-00029 [pii]. PubMed PMID: 17440363.

45. Carmeliet P. Blood vessels and nerves: common signals, pathways and diseases. Nature Reviews Genetics. 2003;4(9):710-20.

46. Chuang DC. Adult brachial plexus reconstruction with the level of injury: review and personal experience. Plast Reconstr Surg. 2009;124(6 Suppl):e359-69. Epub 2010/01/09. doi: 10.1097/PRS.0b013e3181bcf16c

00006534-200912001-00010 [pii]. PubMed PMID: 19952704.

47. Sabapathy SR, Venkatramani H. Harvest of extraplexal donor nerves for transfer or grafting. In: Dy CJ, Isaacs J, editors. American Society for Surgery of the Hand surgical anatomy: nerve reconstruction. 1. First ed. Chicago, USA: American Society for Surgery of the Hand; 2017. p. 161-86.

48. Boyd KU, Fox IK. Nerve repair and grafting. In: Mackinnon SE, editor. Nerve surgery. 1. First ed. New York: Thieme; 2015. p. 75-100.

49. Nichols CM, Brenner MJ, Fox IK, Tung TH, Hunter DA, Rickman SR, et al. Effects of motor versus sensory nerve grafts on peripheral nerve regeneration. Experimental neurology. 2004;190(2):347-55. doi: http://dx.doi.org/10.1016/j.expneurol.2004.08.003.

50. Moradzadeh A, Borschel GH, Luciano JP, Whitlock EL, Hayashi A, Hunter DA, et al. The impact of motor and sensory nerve architecture on nerve

regeneration. Experimental neurology. 2008;212(2):370-6. doi: http://dx.doi.org/10.1016/j.expneurol.2008.04.012.

51. Siemionow M, Uygur S, Ozturk C, Siemionow K. Techniques and materials for enhancement of peripheral nerve regeneration: a literature review. Microsurgery. 2013;33(4):318-28. Epub 2013/04/10. doi: 10.1002/micr.22104. PubMed PMID: 23568681.

52. Sulaiman W, Gordon T. Neurobiology of peripheral nerve injury, regeneration, and functional recovery: from bench top research to bedside application. Ochsner J. 2013;13(1):100-8. PubMed PMID: 23531634; PubMed Central PMCID: PMCPMC3603172.

53. Sinis N, Kraus A, Papagiannoulis N, Werdin F, Schittenhelm J, Meyermann R, et al. Concepts and developments in peripheral nerve surgery. Clinical neuropathology. 2009;28(4):247-62. Epub 2009/08/01. PubMed PMID: 19642504.

54. Koshima I, Soeda S, Nakayama Y, Fukuda H, Tanaka J. An arterialised venous flap using the long saphenous vein. Br J Plast Surg. 1991;44(1):23-6. Epub 1991/01/01. doi: 0007-1226(91)90171-F [pii]. PubMed PMID: 1993230.

55. Borumandi F, Higgins JP, Buerger H, Vasilyeva A, Benlidayi ME, Sencar L, et al. Arterialized Venous Bone Flaps: An Experimental Investigation. Scientific reports. 2016;6.

56. Casal D, Pais D, Angélica-Almeida M, Bilhim T, Santos A, Goyri-O'Neill J. Morphometric analysis of the extensor tendons of the hallux and potential implications for tendon grafting. European Journal of Anatomy. 2010;1(14):11-8.

57. Vazquez T, Sanudo J. Veins of the upper limb. In: Tubbs RS, Shoja MM, Loukas M, editors. Bergman's comprehensive encyclopedia of human anatomic variation. 1. First ed. New Jersey: Wiley Blackwell; 2016. p. 826-31.

58. Eid EM, Hegazy AM. Anatomical variations of the human sural nerve and its role in clinical and surgical procedures. Clin Anat. 2011;24(2):237-45. Epub 2010/10/16. doi: 10.1002/ca.21068. PubMed PMID: 20949489.

59. Ramakrishnan PK, Henry BM, Vikse J, Roy J, Saganiak K, Mizia E, et al. Anatomical variations of the formation and course of the sural nerve: A systematic review and meta-analysis. Annals of anatomy = Anatomischer Anzeiger : official organ of the Anatomische Gesellschaft. 2015;202:36-44. Epub 2015/09/06. doi: 10.1016/j.aanat.2015.08.002. PubMed PMID: 26342158.

60. Mahan MA, Spinner RJ. Nerves of the upper extremity. In: Tubbs RS, Shoja MM, Loukas M, editors. Bergman's comprehensive encyclopedia of human anatomic variation. 1. First ed. New Jersey: Wiley Blackwell; 2016. p. 1068-112.

61. Apaydin N. Lumbosacral plexus. In: Tubbs RS, Shoja MM, Loukas M, editors. Bergman's comprehensive encyclopedia of human anatomic variation. 1. First ed. New Jersey: Wiley Blackwell; 2016. p. 1113-29.

62. Casal D, Pais D, Toscano T, Bilhim T, Rodrigues L, Figueiredo I, et al. A rare variant of the ulnar artery with important clinical implications: a case report. BMC Res Notes. 2012;5:660. doi: 10.1186/1756-0500-5-660. PubMed PMID: 23194303; PubMed Central PMCID: PMCPMC3529700.

63. Rodriguez-Niedenfuhr M, Vazquez T, Nearn L, Ferreira B, Parkin I, Sanudo JR. Variations of the arterial pattern in the upper limb revisited: a morphological and statistical study, with a review of the literature. J Anat. 2001;199(Pt 5):547-66. Epub 2002/01/05. PubMed PMID: 11760886; PubMed Central PMCID: PMCPMC1468366.

64. Patel A. Lower limb arteries. In: Tubbs RS, Shoja MM, Loukas M, editors. Bergman's comprehensive encyclopedia of human anatomic variation. 1. First ed. New Jersey: Wiley Blackwell; 2016. p. 741-51.

65. Millington PF, Wilkinson R. The skin in depth: dermal vasculature. In: Harrison RJ, McMinn RM, editors. Biologic structure and function of the skin: Skin. 1. First ed. United Kingdom: Cambridge University Press; 1983. p. 69-72.

66. Chatterjee S. Artefacts in histopathology. J Oral Maxillofac Pathol. 2014;18(Suppl 1):S111-6. doi: 10.4103/0973-029X.141346. PubMed PMID: 25364159; PubMed Central PMCID: PMCPMC4211218.

Figure Legends:

Figure 1 - Photograph of an axial section through the upper third of a left leg showing the thickness of a sural nerve flap raised as a conventional flap (red dotted line) or as an unconventional perfusion flap (blue dotted line). The cadaver was injected with a red latex solution in the arterial system and with a blue latex solution in the venous system.

1, tibial bone; 2, fibula; 3, small saphenous vein; 4, sural nerve; 5, fibular artery; 6, fibular vein

Figure 2 - Relationship between the superficial veins and nerves and the superficial fascia.

(A) Photograph an axial section of the upper third of a left leg in a cadaver previously injected with colored latex solutions showing the relative disposition of the superficial veins to adjoining fascial sheaths. (box on the right) Higher magnification view of the area highlighted in the dotted region of (A), exemplifying the position of superficial veins in different depths. (B) Microphotograph of a hematoxylin-eosin stained axial section of an anterior antebrachial flap illustrating the relation of an anterior median antebrachial vein with the surrounding fascias. (C) Photograph of a Masson's Trichrome stained axial section of a saphenous flap illustrating the relation of superficial veins in this region with the superficial fascias. (D) Schematic representation of the location of the different superficial veins.

1, tibia; 2, fibula; 3, muscle fascia; 4, great saphenous vein; 5, other superficial veins; 6, deep veins; 7, deep fatty layer of the subcutaneous tissue; 8, superficial fatty layer of the subcutaneous tissue; 9, skin paddle; 10, median antebrachial vein; 11, superficial fascia; 12, palmaris longus muscle; 13, communicating vein; 14, saphenous nerve

Sup, Superior; Med, Medial

Arrow heads indicate the superficial fascia; the asterisk indicates the fascial septum that separates the great saphenous vein from the saphenous nerve.

Calibration bar = 1 mm

Figure 3 - Graphical representation of the most common disposition of the superficial veins of the upper limbs and their main anatomical relations with neighboring superficial nerves. These veins are placed at different depths.

1, cephalic vein; 2, accessory cephalic vein; 3, basilic vein; 4, median antebrachial vein; 5, lateral median antebrachial vein; 6, medial median antebrachial vein; 7, dorsal venous arch of the hand; 8, dorsal metacarpal veins; 9, dorsal digital veins; 10, intercapitular veins; 11, cephalic vein of the thumb; 12, lateral antebrachial nerve; 13, medial antebrachial nerve; 14, superficial palmar venous network

Figure 4 - Graphical representation of the most common disposition of the superficial veins of the lower limbs and their main anatomical relations with neighboring superficial nerves. These veins are placed at different depths.

1, great saphenous vein; 2, small saphenous vein; 3, medial marginal vein; 4, lateral marginal vein; 5, dorsal venous arch of the foot; 6, superficial dorsal metatarsal veins; 7, superficial dorsal digital veins; 8, anterior accessory great saphenous vein; 9, posterior accessory great saphenous vein; 10, cranial extension of the small saphenous vein; 11, posterior thigh circumflex vein or Giacomini vein; 12, intercapitular veins; 13, intersaphenous veins; 14, anterior thigh circumflex vein; 15, lateral venous plexus of the thigh; 16, lateral venous plexus of the leg; 17, superficial accessory great saphenous vein; 18, superficial external pudendal vein; 19, superficial epigastric vein; 20, superficial circumflex iliac vein; 21, saphenous nerve; 22, sural nerve; 23, anterior femoral cutaneous nerve; 24, superficial fibular nerve; 25, medial branch of the deep fibular nerve; 26, lateral malleolar vein; 27, medial malleolar vein; 28, lateral femoral cutaneous nerve of the thigh; 29, calcaneal veins; 30, peri-scaphoid venous circle; 31, superficial venous network of the plant of the foot; 32, superficial accessory small saphenous vein

Figure 5 - Anatomy and histology of the medial brachial flap.

(A) Schematic representation of the medial venous brachial flap; (B) Photograph of a Masson's trichrome stained axial section of the middle portion of the flap; (C and D) Photographs of the flap after processing by the modified Spalteholz technique showing the venous network.

1, basilic vein; 2, medial antebrachial nerve; 3, medial median antebrachial vein; 4, medial antebrachial vein; 5, muscle fascia; 6, superficial fatty layer of the subcutaneous tissue; 7, deep fatty layer of the subcutaneous tissue; 8, skin paddle

Ant, Anterior; Inf, Inferior

Arrow heads indicate the superficial fascia

Calibration bar = 1 cm

Figure 6 - Anterior forearm flap anatomy and histology.

(A) Schematic representation of the flap observed from its deep aspect; (B) Photograph of the anterior venous flap after processing by the modified Spalteholz technique showing the venous network and the palmaris longus tendon; (C) Photograph of a Masson's trichrome stained axial section of the middle third of the flap showing the flap's histology.

1, median antebrachial veins; 2, anterior branch of the medial cutaneous antebrachial nerve; 3, anterior branch of the lateral cutaneous antebrachial nerve; 4, palmaris longus tendon; 5, muscle fascia; 6, superficial fatty layer of the subcutaneous tissue; 7, deep fatty layer of the subcutaneous tissue; 8, skin paddle

Sup, Superior; Lat, Lateral

Arrow heads indicate the superficial fascia

Calibration bar = 1 cm

Figure 7 - Sural flap anatomy and histology.

(A) Schematic representation of the sural venous flap; (B) Photograph of a cadaveric dissection of the lateral aspect of a right leg showing the flap's neurovenous pedicle;

(C) Photograph of a Masson's trichrome stained axial section of the upper third of the leg showing the flap's histology; (D) Photograph of a Masson's trichrome-stained axial section of the middle third of the leg showing the flap's histology; (E) Photograph of a Masson's trichrome stained axial section of the lower third of the leg showing the flap's histology.

1, short saphenous vein; 2, sural nerve; 3, epineurial veins; 4, perineurial veins; 5, endoneurial veins; 6, skin paddle; 7, superficial fatty layer of the subcutaneous tissue; 8, deep fatty layer of the subcutaneous tissue; 9, muscle fascia

Sup, Superior; Ant, Anterior

Arrow heads indicate the superficial fascia

Calibration bar = 5 mm

Figure 8 - Saphenous flap anatomy and histology.

(A) Schematic representation of the saphenous venous flap; (B) Photograph of a cadaveric dissection of the medial aspect of a right leg showing the flap's neurovenous pedicle; (C and D) Photographs of the flap after processing by the modified Spalteholz technique showing the venous network over the medial aspect of the tibial bone (C) and that under the skin paddle (D); (E) Photograph of a Masson's trichrome stained axial section of the upper third of the leg showing the flap's histology; (F) Photograph of a Masson's trichrome stained axial section of the distal third of the leg showing the flap's histology.

1, great saphenous vein; 2, anterior accessory great saphenous vein; 3, saphenous nerve branches; 4, skin paddle; 5, superficial fatty layer of the subcutaneous tissue; 6, deep fatty layer of the subcutaneous tissue; 7, muscle fascia; 8, medial cortex of the tibial bone

Sup, Superior; Pos, Posterior

Arrow heads indicate the superficial fascia

Black calibration bar in B,C = 1 cm

Black calibration bar in D = 5 cm

White calibration bar = 5 mm

Figure 9 - Anatomical relationship between superficial veins and adjacent superficial nerves.

(A) Photograph of a cadaveric dissection of the inferior portion of a left saphenous venous flap, showing the proximity of the great saphenous vein and the saphenous nerve branches, as well as the venous branches coming from the epineurial venous plexus to the tributaries of the great saphenous vein. The cadaver had been previously injected with a blue latex solution in the venous system and with a red latex solution in the arterial system. (B) Photograph of the great saphenous vein and accompanying saphenous nerve in the lower leg after processing by the modified Spalteholz technique of a lower limb previously injected with a blue latex solution in the venous system. It is possible to observe multiple small tributary veins originating in the region of the saphenous nerve and draining into the great saphenous vein. (C) Schematic representation of the blood supply to superficial nerves from adjacent superficial arteries and veins.

1, great saphenous vein; 2, saphenous nerve branches; 3, skin paddle of the saphenous venous flap; 4, epineurial veins; 5, perineural veins; 6, endoneurial veins

Sup, Superior; Pos, Posterior

Arrow heads indicate veins draining the epineurial venous plexus in the adjoining superficial vein.

Figure 10 - Anatomy and histology of the dorsal flap of the foot.

(A) Schematic representation of the dorsal venous flap of the foot; (B to C) Photographs of cadaveric dissections of the dorsum of the left foot. In (B) it is possible to observe the inclusion of the extensor hallucis brevis tendon. In (C) it is possible to observe the intimate relation of the deep aspect of the flap with the accessory extensor hallucis longus tendon and with the extensor hallucis brevis tendon. In (D) it is possible to observe the medial and intermediate dorsal nerves of the foot that can be included in the flap. (E and F) Photograph of the dorsal venous flap of the foot after processing by the modified Spalteholz technique showing the venous network from a superficial perspective. In (E) it is possible to observe the affluents and effluents of the dorsal venous arch of the foot. In (F) the intimate connection between the extensor hallucis brevis and the dorsal venous arch of the foot can be appreciated. (G and H) Photograph of a Masson's trichrome stained axial section of the proximal and distal half of the flap, respectively. It is possible to observe that the flap is significantly thinner close to the toes.

1, medial marginal vein; 2, lateral marginal vein; 3, medial dorsal cutaneous nerve of the foot; 4, intermediate dorsal cutaneous nerve of the foot; 5, superficial dorsal

digital veins; 6, accessory extensor hallucis longus tendon; 7, extensor hallucis brevis tendon; 7´, extensor hallucis brevis muscle belly; 8, skin paddle; 9, subcutaneous fat; 10, muscle fascia; 11,dorsal venous arch of the foot; 12 extensor hallucis longus tendon, 13, superficial dorsal metatarsal veins;

Pos, Posterior; Me, Medial; La, Lateral.

Calibration bar = 1 cm

Figure 11 - Anatomy and histology of the medial plantar flap.

(A) Schematic representation of the medial plantar flap; (B) Photograph of a dissection of the medial plantar flap; (C) Masson's trichrome-stained microphotograph showing medial plantar flap's histology.

1, medial marginal vein; 2, great saphenous vein; 3, saphenous nerve branches; 4, skin paddle; 5, subcutaneous fat; 6, muscle fascia; 7, calcaneal veins; 8, peri-scaphoid veins; 9, superficial fatty layer of the subcutaneous tissue; 10, deep fatty layer of the subcutaneous tissue

Sup, Superior; Pos, Posterior

Arrow heads indicate the superficial fascia

Calibration bar = 1 cm

Figure 12 - Comparison of the integument thickness in the upper eyelid, in the penis, in the dorsal venous flap, and in the anterior forearm venous flap using photographs of histological sections.

(A) Photograph of a Masson's trichrome stained axial section of the left half of a penis; (B) photograph of a Masson's trichrome stained parasagittal section of an upper eyelid; (C) photograph of a Masson's trichrome stained axial section of an anterior antebrachial venous flap; (D) photograph of a hematoxylin-eosin stained axial section of the venous flap of the dorsum of the foot.

1, integumentary layer; 2, dermis; 3, epidermis; 4, deep penile fascia; 5, albuginea layer of the penis; 6, corpus cavernosum; 7, corpus spongiosum; 8, orbicularis oculi muscle; 9, tarsal plate; 10, conjuntiva; 11, superficial fatty layer of the subcutaneous tissue of the limbs; 12, deep fatty layer of the subcutaneous tissue of the limbs; 13, superficial vein; 14, muscle fascia;
Ant, anterior; Sup, superior; Dor, dorsal; Lat, lateral
Arrow heads indicate the superficial fascia of the limbs

Calibration bar = 1 cm

Figure 13 - Optical microscopy photographs with the same magnification showing the relative size and internal structure of commonly injured nerves (A to F), and of potential nerve components of arterialized venous flaps (**ANVFs**).

(A), facial nerve at the posterior aspect of the parotid gland; (B), hypoglossal nerve at the base of the tongue; (C), masseteric nerve at the sigmoid notch; (D), collateral radial digital nerve of the index finger at the proximal phalanx level; (E), median nerve at the distal third of the arm; (F), anterior division of the C7 spinal nerve; (G), anterior branch of the medial antebrachial cutaneous nerve at the elbow crease

(medial brachial flap); (H), sural nerve in the middle third of the leg (sural flap); (I), saphenous nerve in the proximal third of the leg (saphenous flap); (J), medial dorsal cutaneous nerve of the foot (dorsal foot flap).

Calibration bar = 1 cm

Figure 1

Click here to download Figure Figure 1.tif

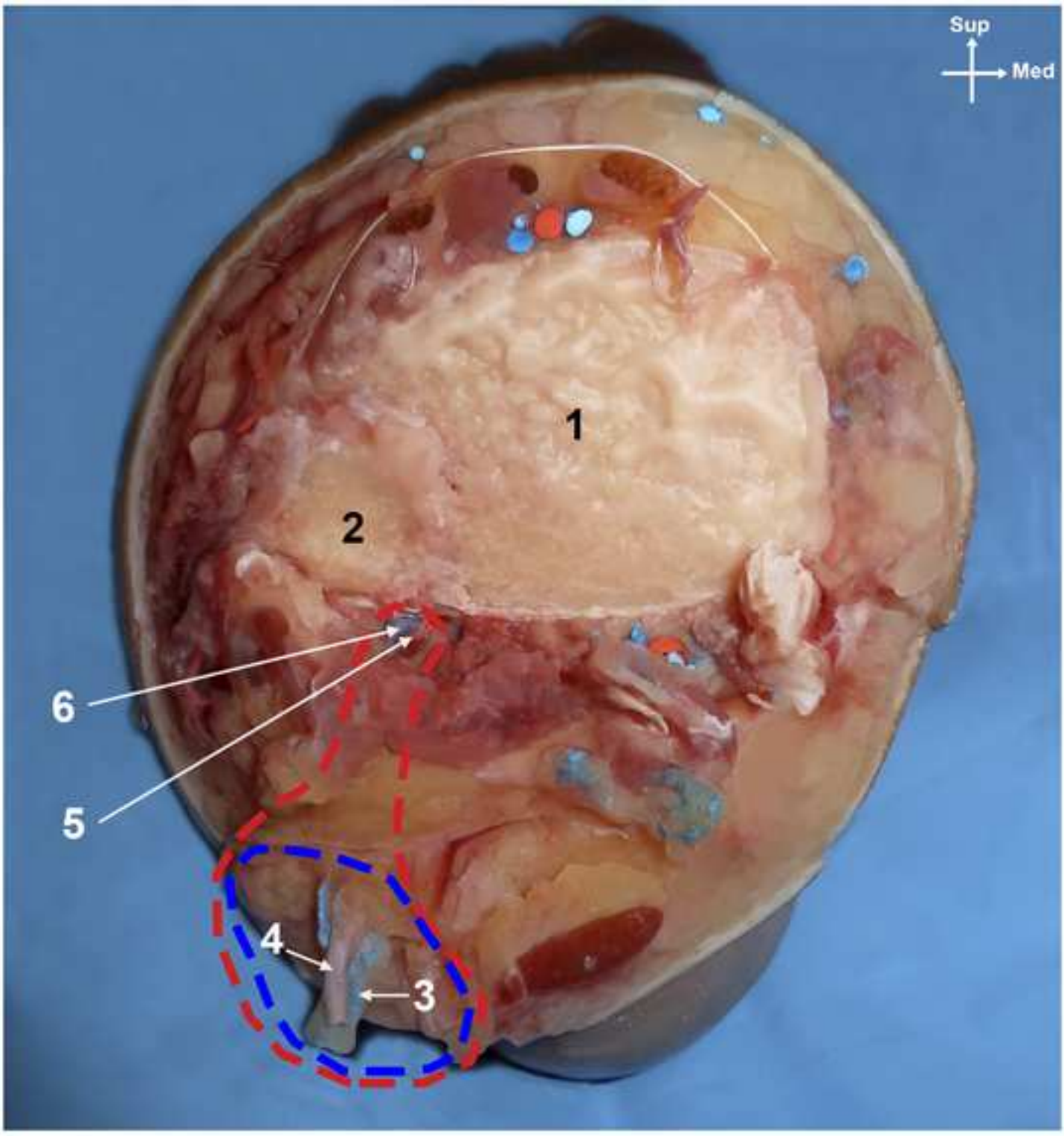

Figure 2

Click here to download Figure Figure 2.tif

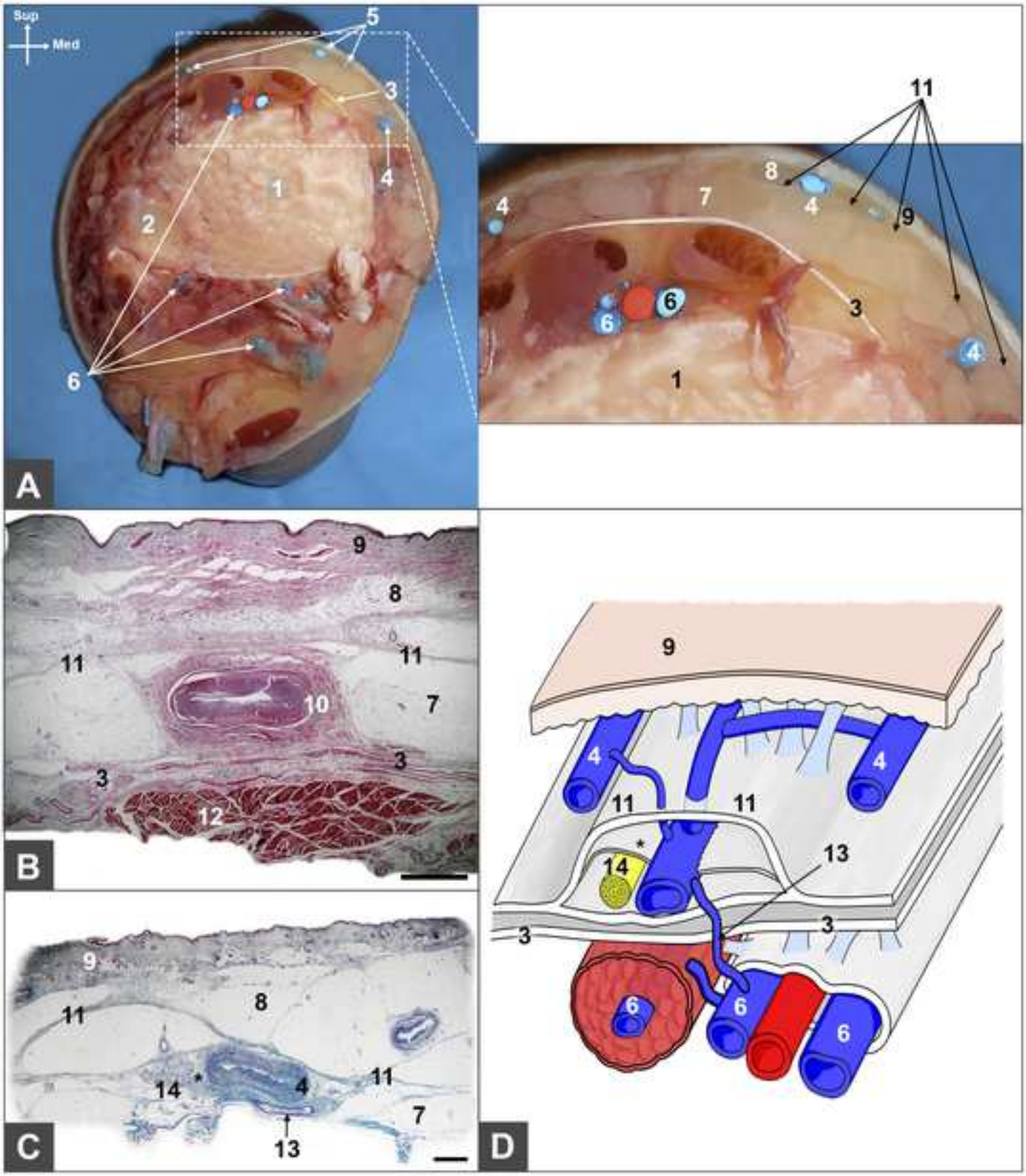

Figure 3

Click here to download Figure Figure 3.tif

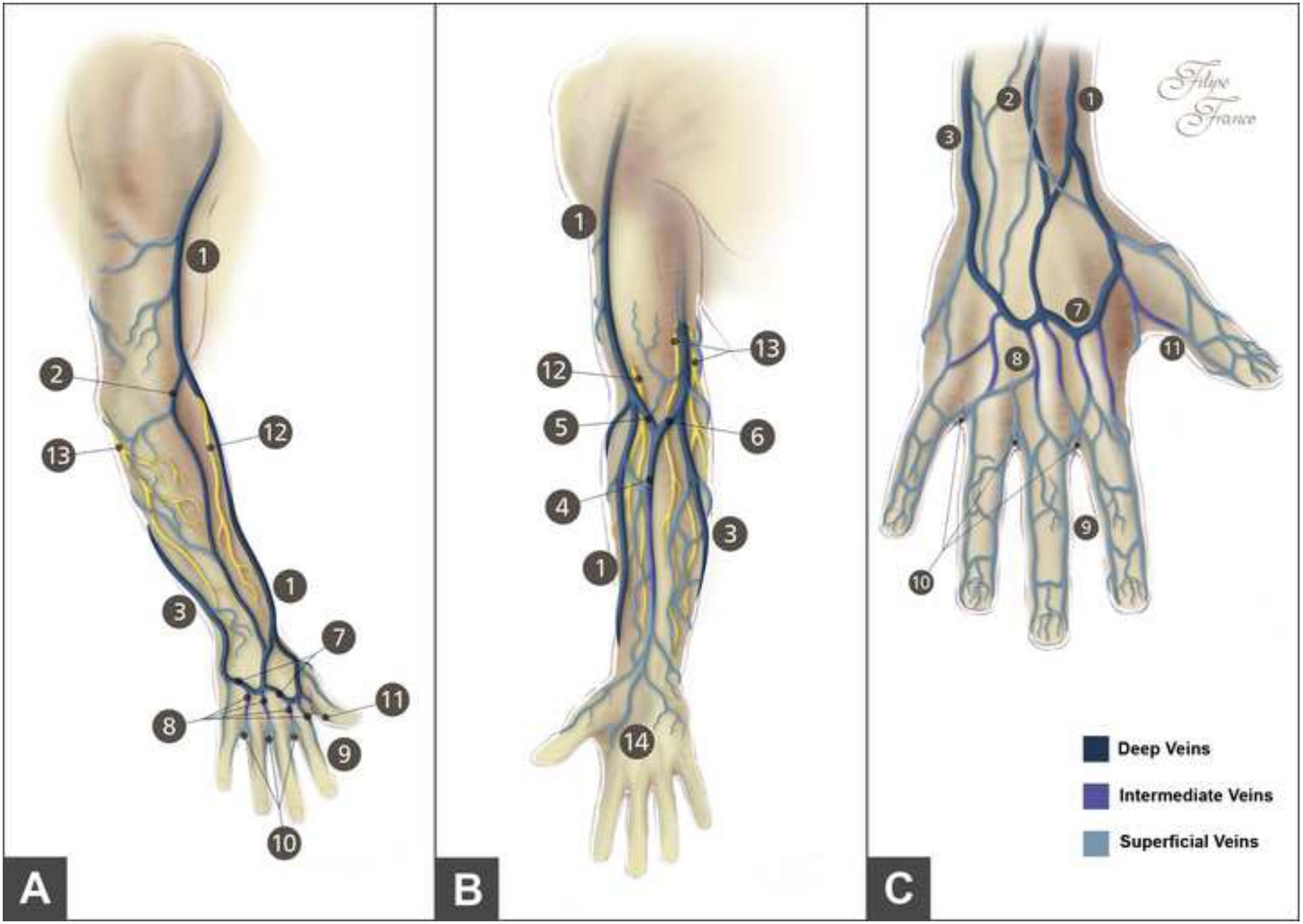

Figure 4

Click here to download Figure Figure 4.tif

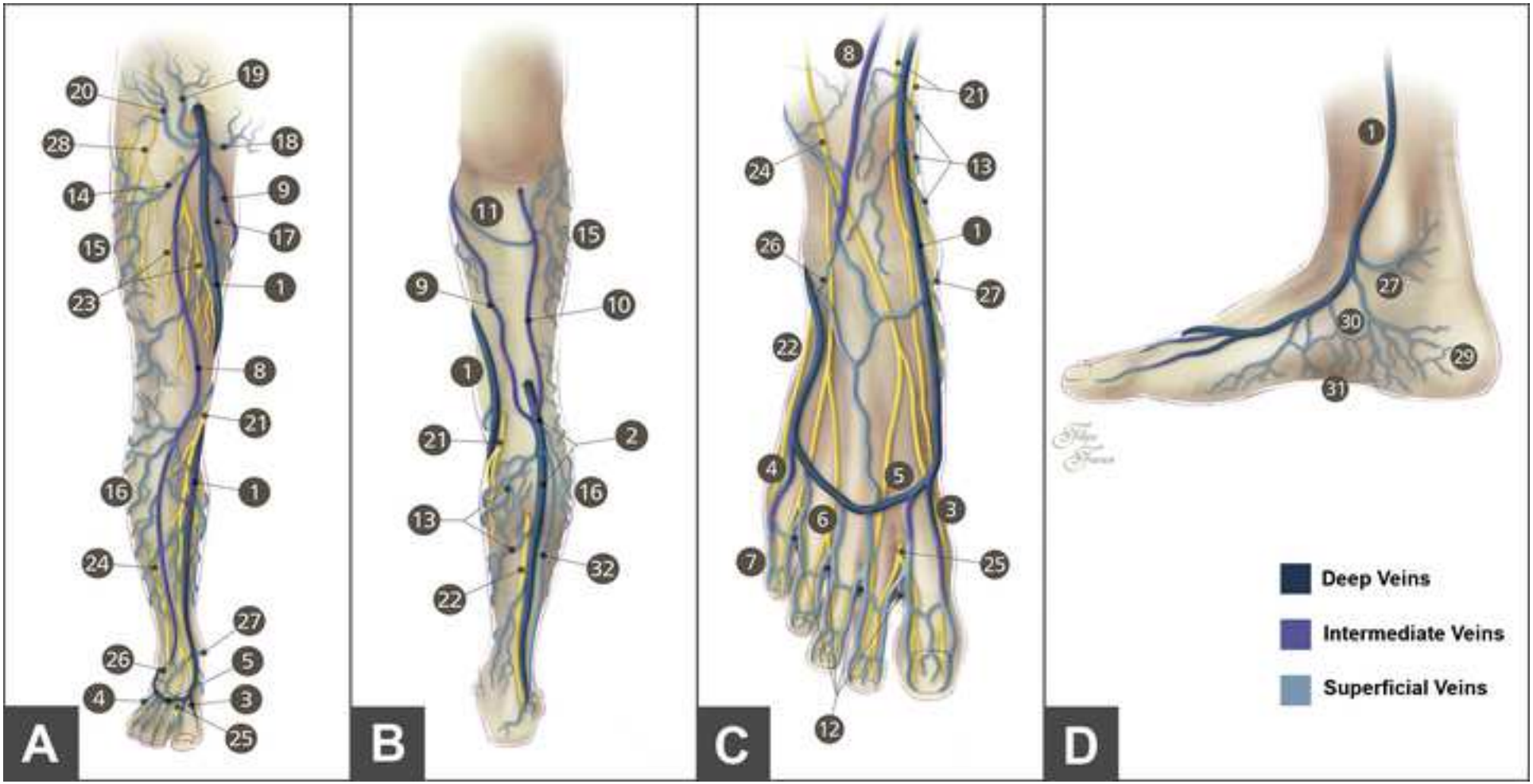

Figure 5

Click here to download Figure Figure 5.tif

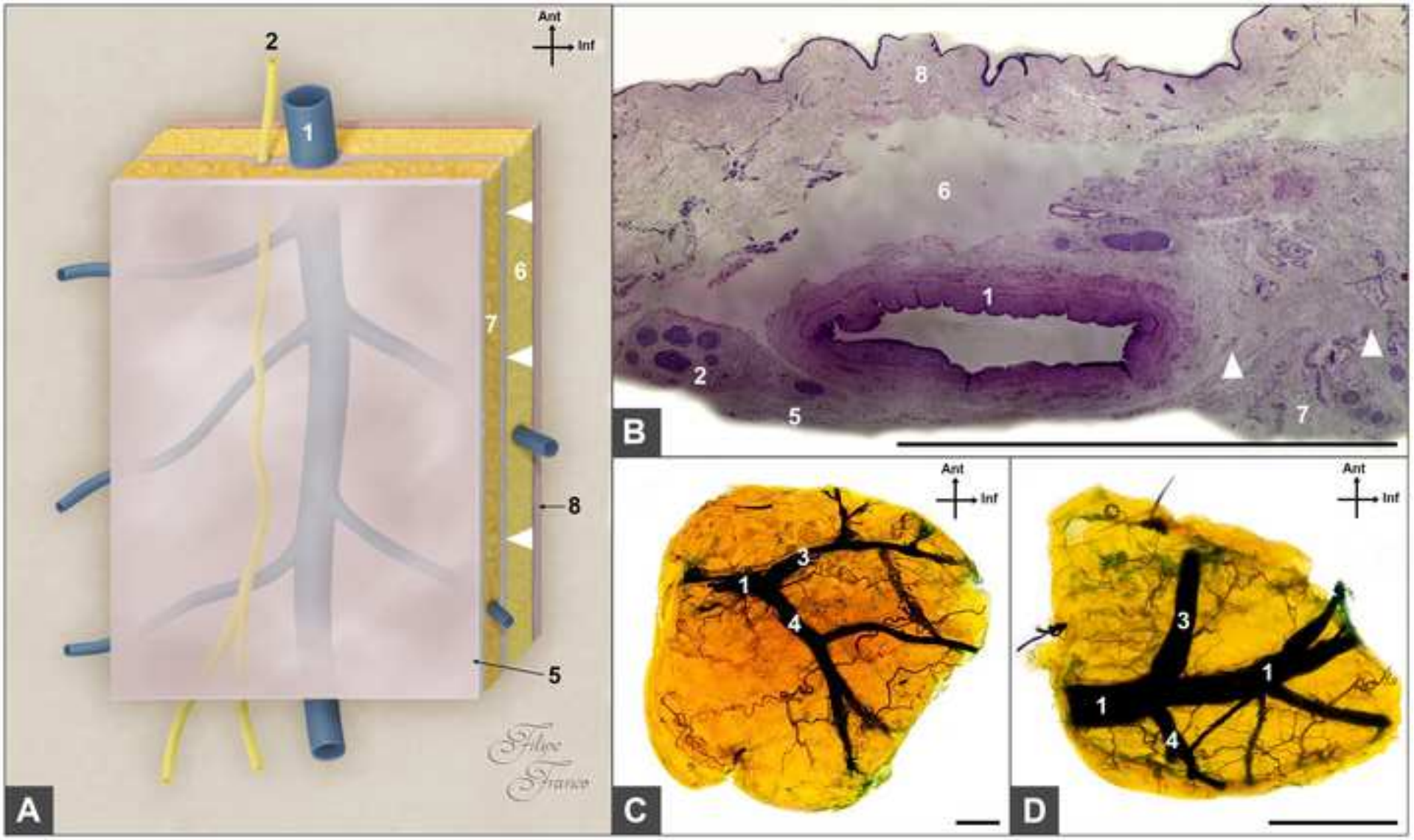

Figure 6

Click here to download Figure Figure 6.tif

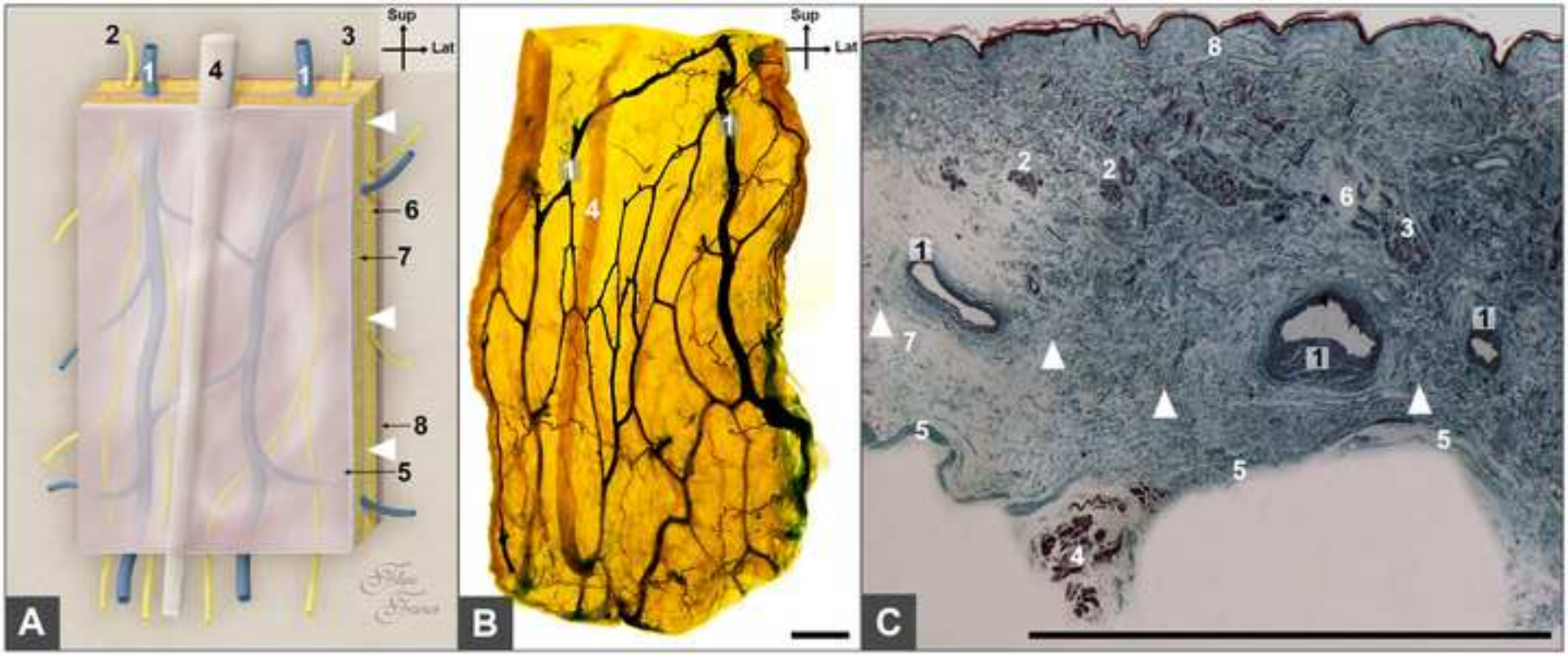

Figure 7

Click here to download Figure Figure 7.tif

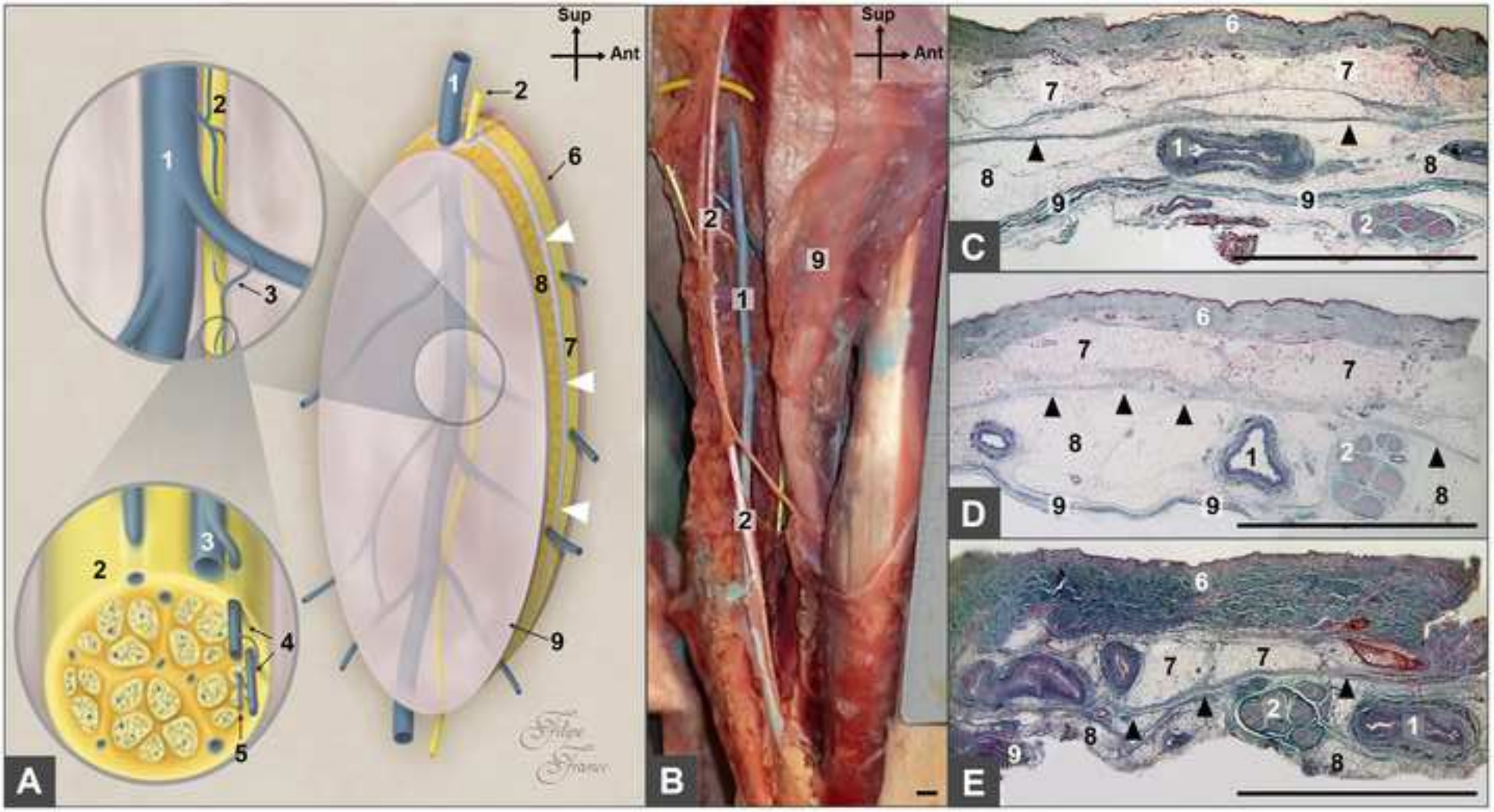

Figure 8

Click here to download Figure Figure 8.tif

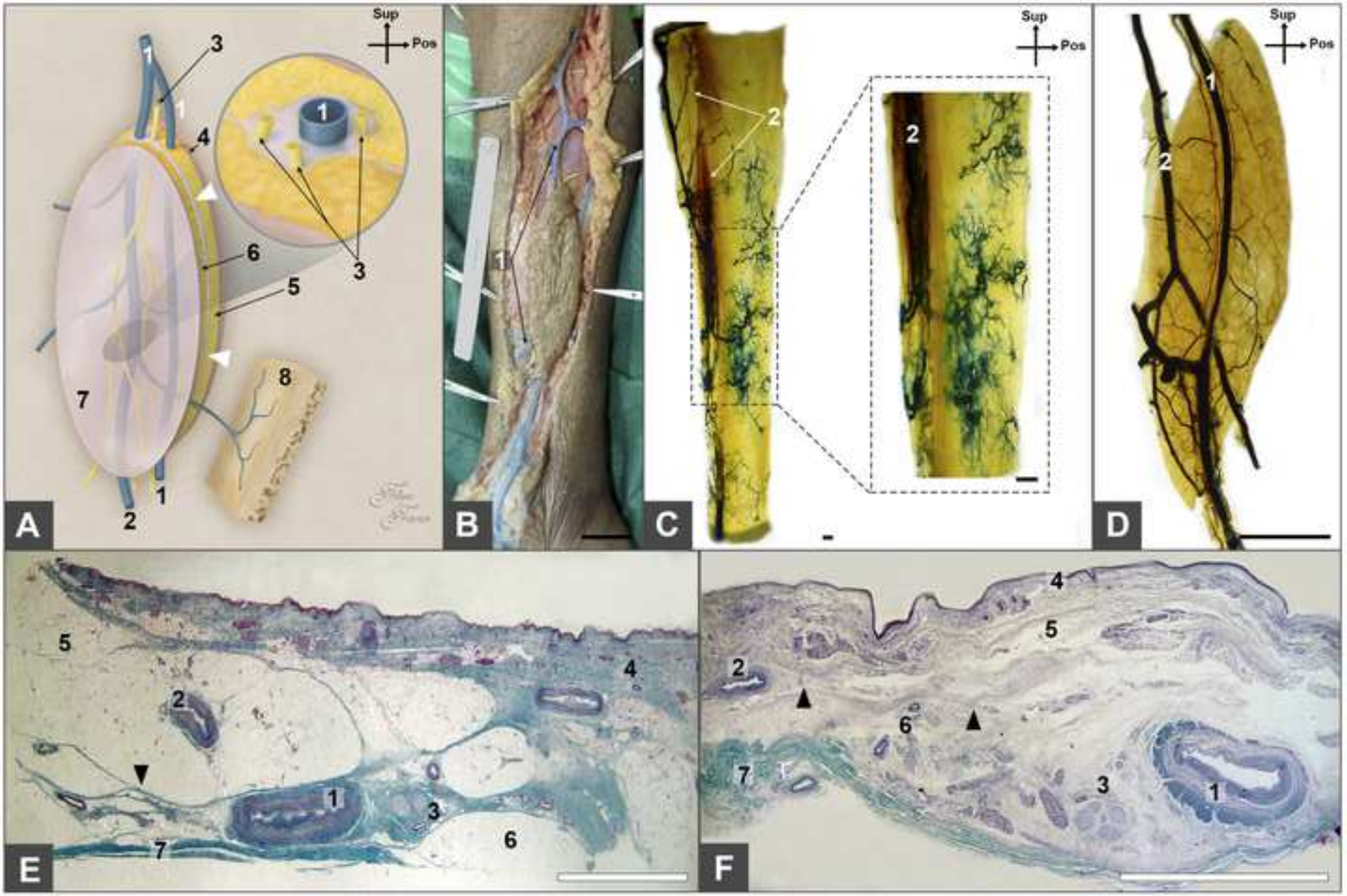

Figure 9

Click here to download Figure Figure 9.tif

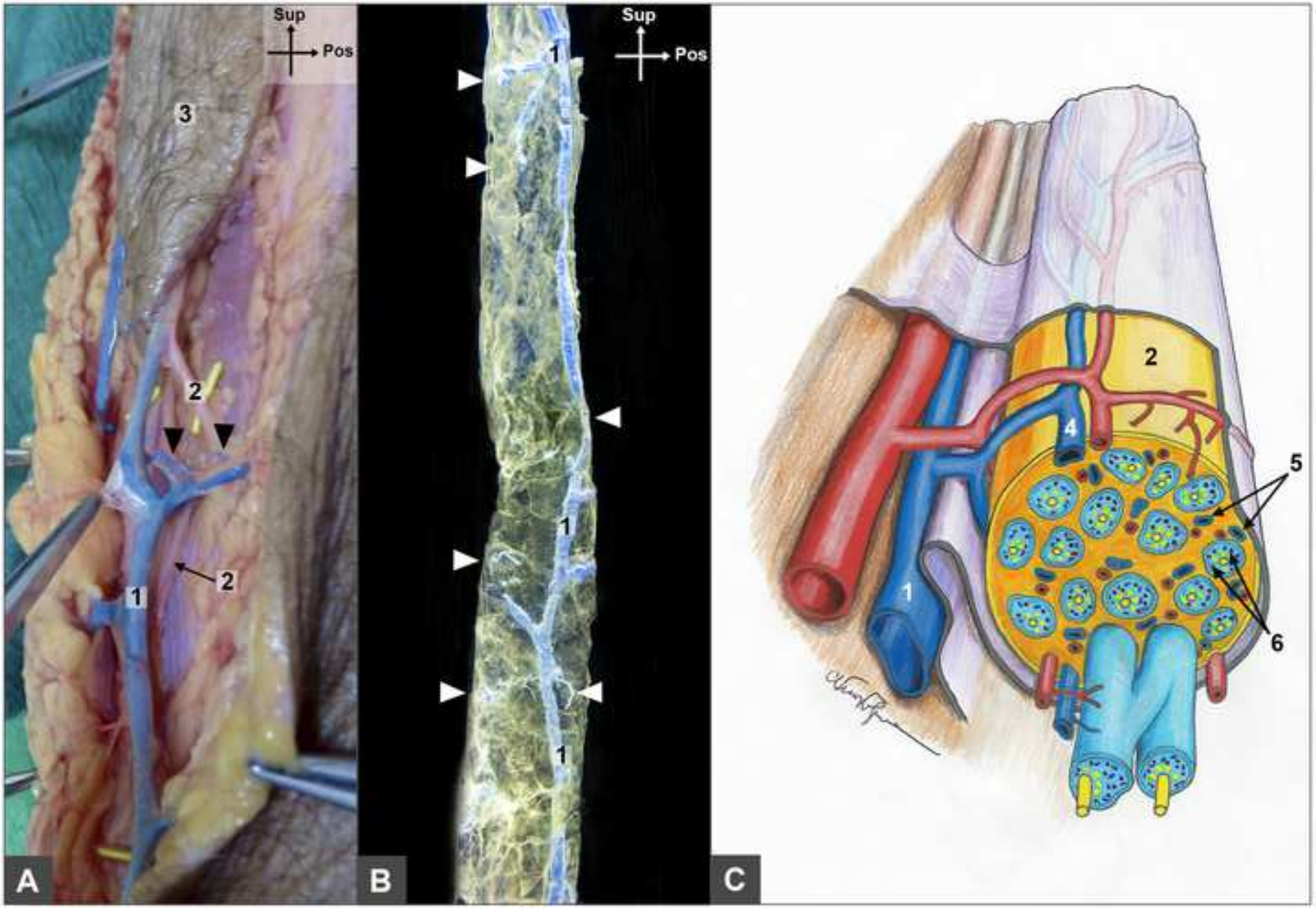

Figure 10

Click here to download Figure Figure 10.tif

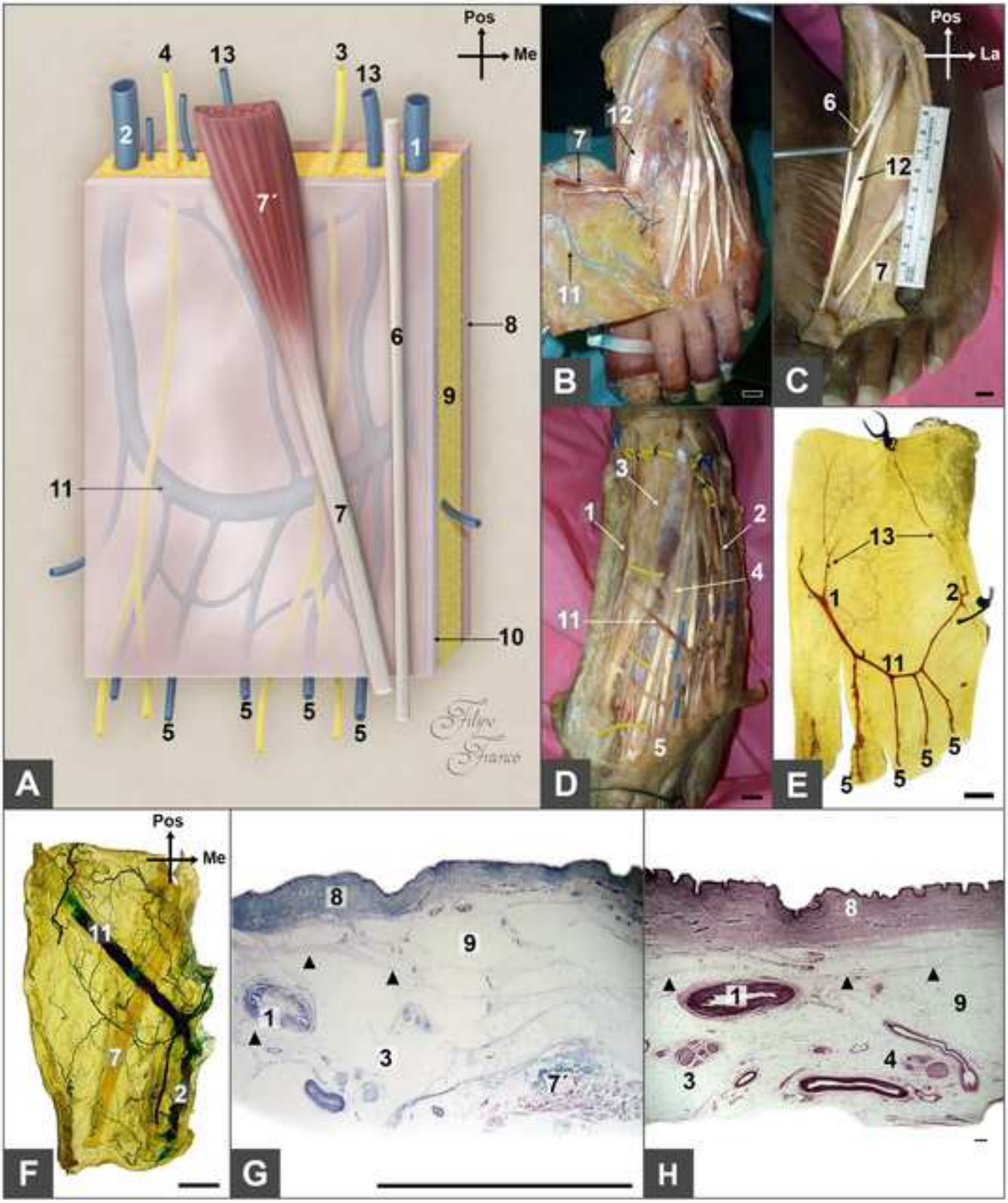

Figure 11

Click here to download Figure Figure 11.tif

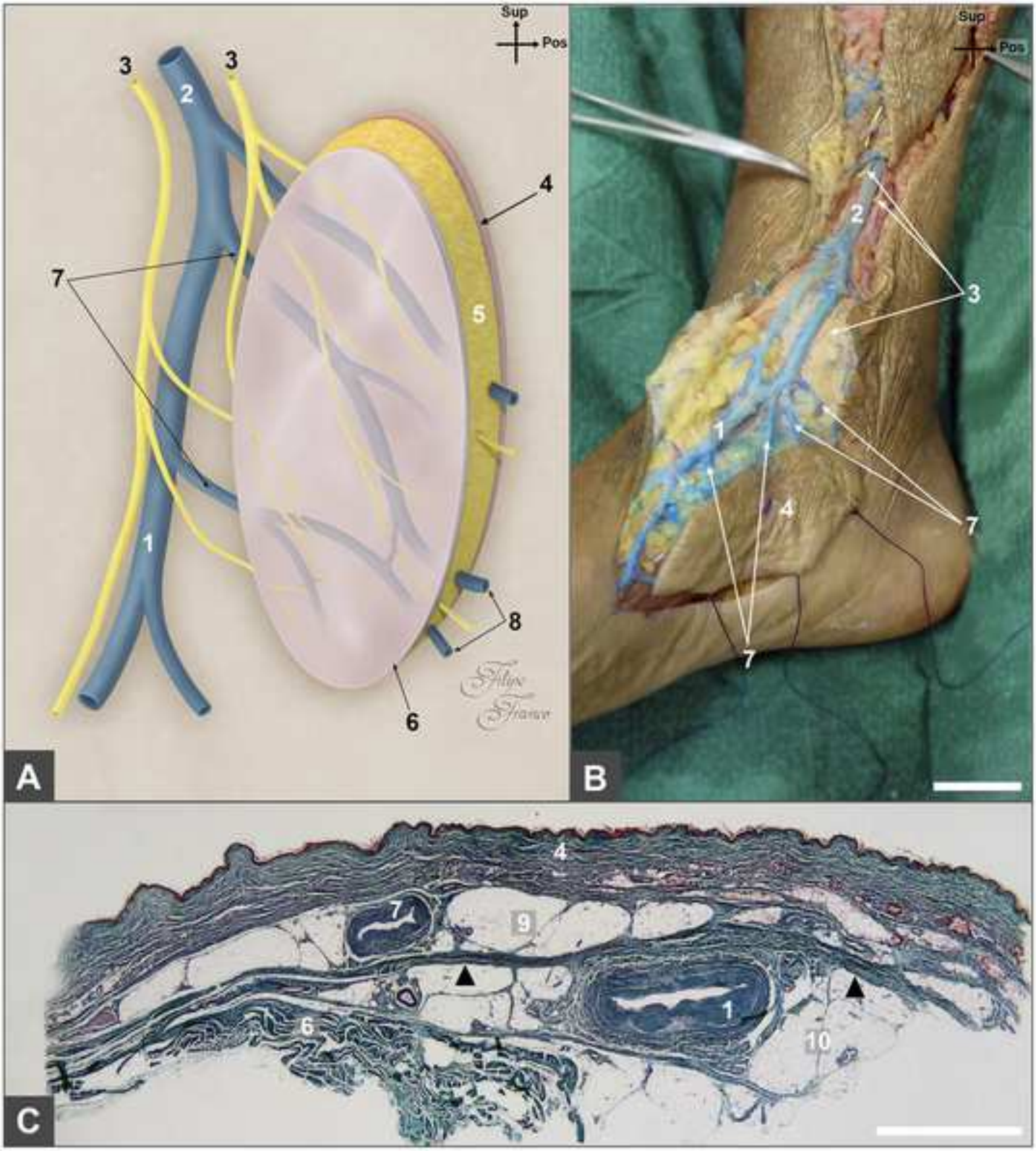

Figure 12

Click here to download Figure Figure 12.tif

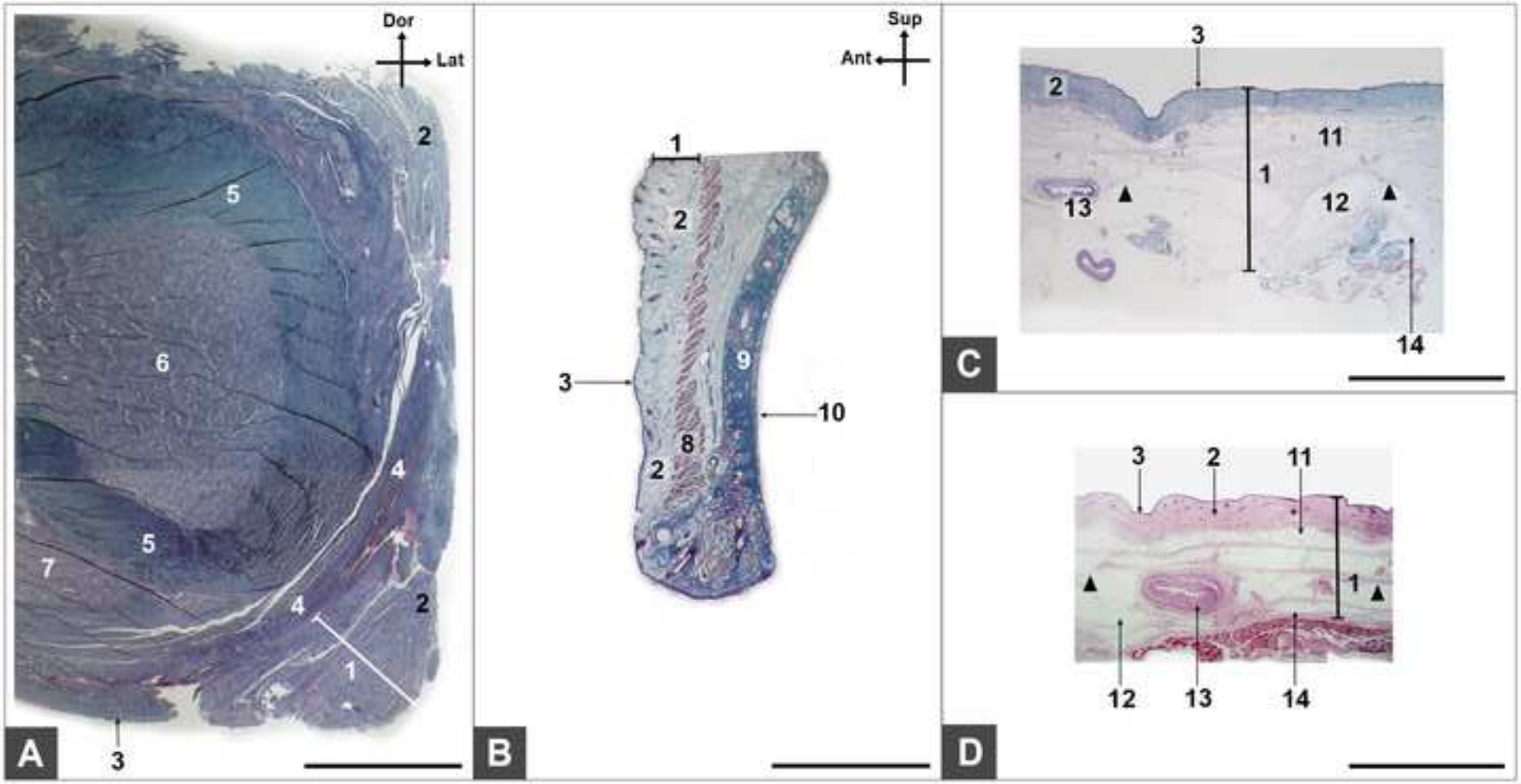

Figure 13

Click here to download Figure Figure 13.tif

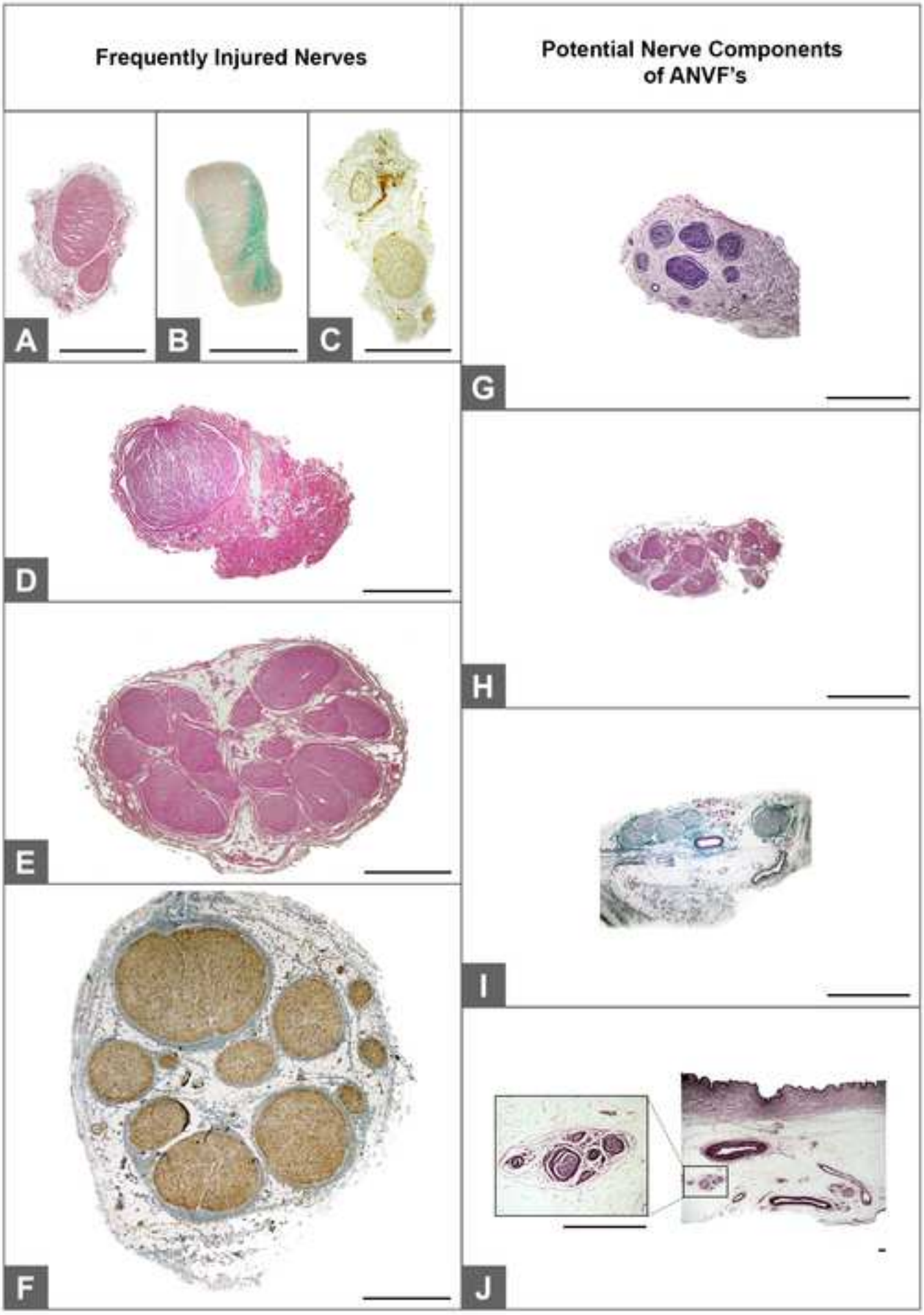

APPENDIX 10

Casal et al. BMC Research Notes 2012, 5:660
http://www.biomedcentral.com/1756-0500/5/660

BMC Research Notes

CASE REPORT Open Access

A rare variant of the ulnar artery with important clinical implications: a case report

Diogo Casal[1,2*], Diogo Pais[3], Tiago Toscano[4], Tiago Bilhim[5], Luís Rodrigues[3], Inês Figueiredo[3], Sónia Aradio[3], Maria Angélica-Almeida[6] and João Goyri-O'Neill[3]

Abstract

Background: Variations in the major arteries of the upper limb are estimated to be present in up to one fifth of people, and may have significant clinical implications.

Case presentation: During routine cadaveric dissection of a 69-year-old fresh female cadaver, a superficial brachioulnar artery with an aberrant path was found bilaterally. The superficial brachioulnar artery originated at midarm level from the brachial artery, pierced the brachial fascia immediately proximal to the elbow, crossed superficial to the muscles that originated from the medial epicondyle, and ran over the pronator teres muscle in a doubling of the antebrachial fascia. It then dipped into the forearm fascia, in the gap between the flexor carpi radialis and the palmaris longus. Subsequently, it ran deep to the palmaris longus muscle belly, and superficially to the flexor digitorum superficialis muscle, reaching the gap between the latter and the flexor carpi ulnaris muscle, where it assumed is usual position lateral to the ulnar nerve.

Conclusion: As far as the authors could determine, this variant of the superficial brachioulnar artery has only been described twice before in the literature. The existence of such a variant is of particular clinical significance, as these arteries are more susceptible to trauma, and can be easily confused with superficial veins during medical and surgical procedures, potentially leading to iatrogenic distal limb ischemia.

Keywords: Blood supply, Anatomy, Surgery, Arteries, Arm, Forearm, Cadaver, Dissection

Background

A sound knowledge of the vascular anatomy of the upper limb is of paramount importance, since this is a site of frequent injury and of various surgical and invasive procedures [1,2]. Normally, the arterial supply to the upper limb is provided by the axillary artery that originates the brachial artery, which, in turn, at the elbow originates the ulnar and radial arteries [3]. These two are placed between the forearm muscles, and give rise at the wrist level to the arteries that form the superficial and deep arterial palmar arches [3]. Usually, the ulnar artery gives off the common interosseous artery that divides into the anterior and posterior interosseous arteries [3].

It has been increasingly recognized that variations in the major arteries of the upper limb are common, being found in up to one fifth of individuals [1,4,5]. Among these, variants of the ulnar and radial arteries are the most common [1,3,4]. Particularly, the presence of superficial radial or ulnar arteries is of utmost clinical significance, as these arteries are most susceptible to trauma, and can be easily confused with superficial veins [1,2]. One variant of superficial ulnar arteries is the superficial brachioulnar artery (SuBUA), which is defined as an ulnar artery with a high origin in the arm that progresses over the superficial muscles of the forearm. The prevalence of the SuBUA varies widely in different studies [3]. For example, Adachi, in 1928, in an impressive series of 1198 upper limb dissections, identified only 8 cases of SuBUA, corresponding to a 0,7% prevalence of this variant [6]. In contrast, in 1844, Quain, had found 7% of SuBUA in 429 specimens dissected [7]. According to a recent review by Rodriguez-Niedenfuhr et al., the

* Correspondence: diogo_bogalhao@yahoo.co.uk
[1]Department of Anatomy, Faculty of Medical Sciences, New University of Lisbon, Lisbon, Portugal
[2]Plastic and Reconstructive Surgery, São José Hospital, Lisbon 1150-199, Portugal
Full list of author information is available at the end of the article

overall prevalence of this variant in the literature is estimated to be around 2,7% [3].

The authors report the case of a cadaver in which a bilateral SuBUA with an unusual path was identified bilaterally. The clinical implications of this anatomical variation are undoubtedly of great significance [3,5,8], and are described briefly in the Discussion Section.

Case presentation

During routine dissection of a 69-year-old fresh female cadaver at the Department of Anatomy at our institution, variations in the arterial system of both upper limbs were noted. There was no history or evidence of any invasive procedure in the upper limbs of that person.

On both sides, the brachial artery in the middle third of the arm originated a SuBUA (Figures 1 and 2). This artery penetrated the brachial fascia in the lower third of the arm, crossed anteriorly to the bicipital aponeurosis and to the muscles that originated from the medial epicondyle, and ran over the pronator teres muscle in a doubling of the antebrachial fascia (Figure 2). In the elbow region, the SuBUA was in intimate contact with the superficial structures, namely the medial antebrachial nerve and the subcutaneous veins (Figure 1). It then dipped into the forearm fascia, passed through a gap between the palmaris longus and the flexor carpi radialis, ran deep to the palmaris longus muscle belly, and superficially to the flexor digitorum superficialis muscle, reaching the gap between the latter and flexor carpi ulnaris muscle (Figure 2). In the middle third of the forearm the SuBUA was positioned lateral to the ulnar nerve.

The brachial artery continued through the radial artery (RA), which followed its usual course. In the upper third of the forearm, the RA gave off the common interosseous artery. This latter artery branched into the anterior and the posterior interosseous arteries (Figure 1). The anterior interosseous artery had a large caliber and originated branches to most of the anterior compartment muscles. The radial recurrent artery emanated from the radial artery, and the anterior ulnar recurrent artery was a branch of the common interosseous trunk.

In the distal third of the forearm and in the wrist region, the RA and the SuBUA divided in the same manner as the radial and ulnar arteries usually distribute [3], originating the superficial and deep palmar arterial arches. Figure 3 schematically portrays the distribution of the RA and the SuBUA in the cadaver herein described.

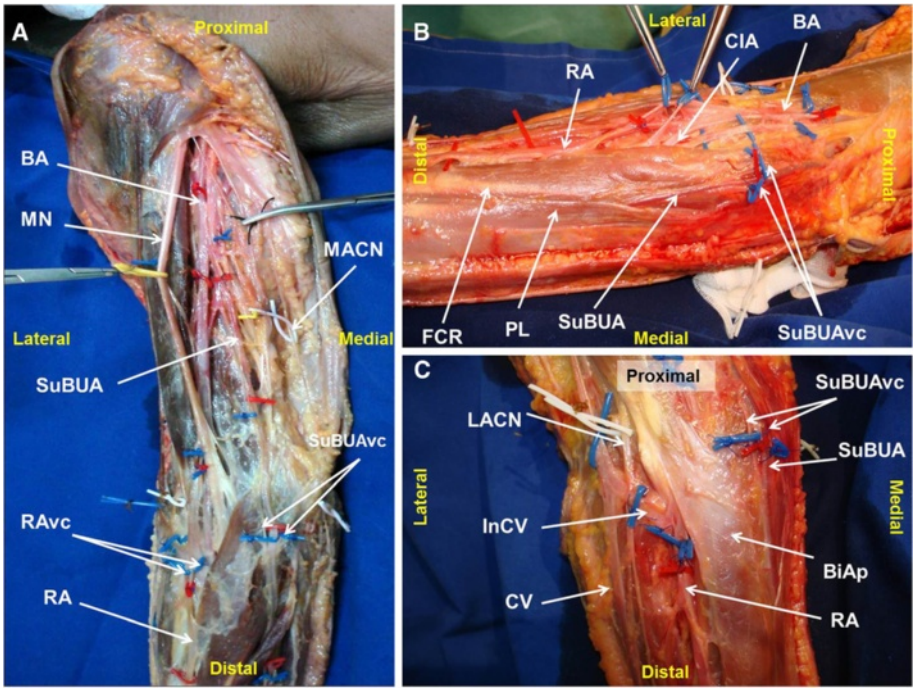

Figure 1 Right upper limb dissection photographs showing the origin and path of the superficial brachioulnar artery, and their neighbor structures at the arm and elbow. A – Upper arm and proximal forearm; **B** – Medial aspect of the elbow region; **C** – Anterior aspect of the elbow region. RA radial artery; SuBUA superficial brachioulnar artery; BA brachial artery; CIA common interosseous artery; CV cephalic vein; InCV Intermediate cephalic vein; RAvc radial artery venae comitantes; SuBUAvc superficial brachioulnar artery venae comitantes; LACN lateral antebrachial cutaneous nerve; MACN medial antebrachial cutaneous nerve; MN median nerve; PL palmaris longus muscle; FCR flexor carpi radialis muscle; BiAp bicipital aponeurosis.

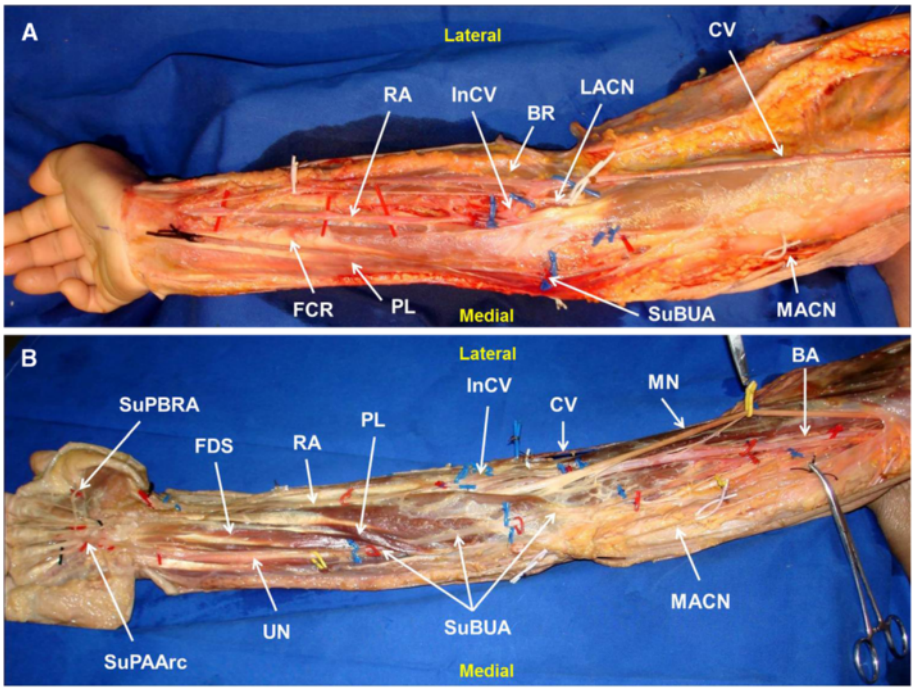

Figure 2 Right upper limb showing the anomalous course of the superficial brachioulnar artery in an above fascia (A) and a deeper to fascia (B) dissection. RA radial artery; SuBUA superficial brachioulnar artery; BA brachial artery; CIA common interosseous artery; CV cephalic vein; InCV Intermediate cephalic vein; RAvc radial artery venae comitantes; LACN lateral antebrachial cutaneous nerve; MACN medial antebrachial cutaneous nerve; MN median nerve; PL palmaris longus muscle; FCR flexor carpi radialis muscle; FDS flexor digitorum superficialis muscle.

Discussion

Rodriguez-Niedenfuhr et al., have recently proposed a system of classification of upper limb arterial variations, based on their extensive experience of almost 400 upper limb dissections, and based on a thorough literature review on the subject [3,8,9]. This terminology, which recently has been taken up by several authors [5], considers each arterial variation as an individual entity along its full extension in the upper limb [3]. Furthermore, this classification divides upper limb arterial variants in three broad groups based on their location in the arm, the arm and forearm, or the forearm. These three groups are further subdivided in several different categories, depending on the absence or duplication of arteries, and on whether these variants adopt a superficial or usual course in the forearm [3].

The variations found exclusively in the forearm are the superficial brachial artery and the accessory brachial artery. The former represents a brachial artery coursing in front of the median nerve, instead of being placed behind it. The accessory brachial artery is characterized by the existence of 2 brachial arteries that rejoin before giving off the forearm arteries. The accessory brachial artery originates from the main brachial artery [3].

The variations located at the level of both the arm and forearm are the superficial brachioulnar (SuBUA), the brachioulnar, the brachioradial, the superficial brachioradial, the brachiointerosseous, the superficial brachiomedian, and the superficial brachioulnoradial arteries [3].

The SuBUA is characterized by an ulnar artery that originates higher than usual and that courses over the forearm flexor muscles. In this setting, there is a whole arterial pattern, with a brachial or superficial brachial artery branching into the radial and common interosseous arterial trunk, or more rarely into the radial and ulnar arteries [3].

The brachioulnar artery corresponds to a high origin of the ulnar artery from the brachial artery, with the latter branching into the radial artery and the common interosseous arterial trunk [3].

The brachioradial artery represents a high origin of the radial artery from the brachial or superficial brachial artery that in turn branches into the ulnar artery and the common interosseous arterial trunk [3].

The superficial brachioradial artery consists of a high origin of the radial artery coursing over the brachioradialis muscle or the tendons that limit the snuffbox. In these circumstances the brachial artery usually originates the ulnar artery and the common interosseous arterial trunk [3].

The brachiointerosseous artery is defined by a high origin of the interosseous arterial trunk, in the context

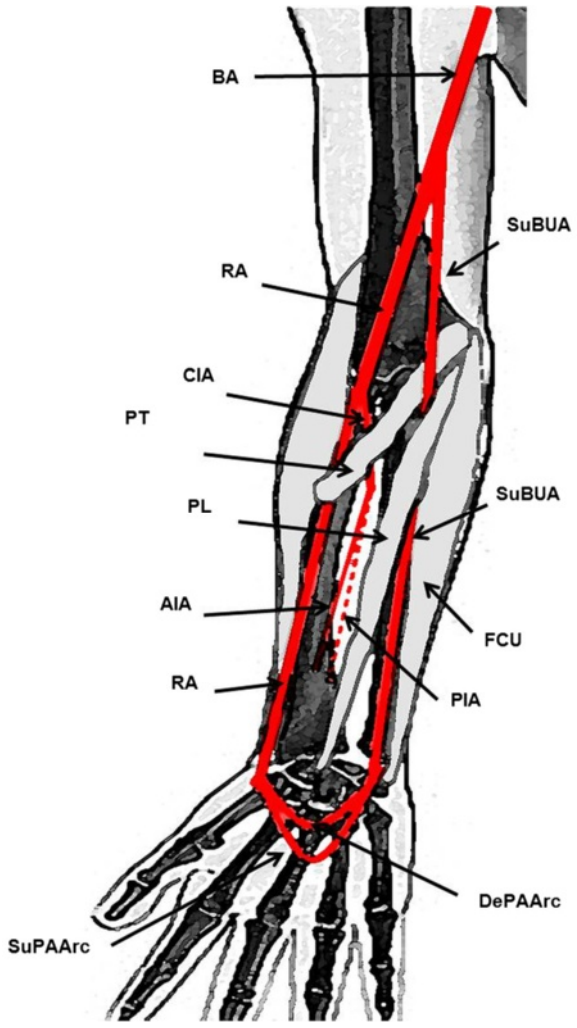

Figure 3 Schematic drawing of the origin and distribution of the superficial brachioulnar artery and its relation with the medial epicondyle muscles. RA radial artery; SuBUA superficial brachioulnar artery; BA brachial artery; CIA common interosseous artery; AIA anterior interosseous artery; PIA posterior interosseous artery; SUPAArch superficial palmar arterial arch; DePAArc deep palmar arterial arch; PL palmaris longus muscle; BR brachioradialis muscle; PT pronator teres muscle; FCU flexor carpi ulnaris muscle; PL palmaris longus muscle.

of a whole arterial pattern of the upper limb, with a brachial artery that divides into the radial and ulnar arteries [3].

The superficial brachiomedian artery is characterized by a high origin of the median artery that courses above the superficial flexor muscles and by a brachial artery that divides into the radial and ulnar arteries [3].

Finally, the superficial brachioulnoradial artery represents a superficial brachial artery that at the level of the elbow branches into the radial and ulnar arteries, which in turn will course over the superficial forearm flexor muscles. In this variant, the superficial brachial artery coexists with a normal brachial artery that ends in the common interosseous arterial trunk [3].

The variations found exclusively at the forearm level include the superficial radial artery, the duplication of the radial arteries, and the absence of the radial or ulnar arteries [3].

The superficial radial artery consists of a radial artery coursing above the tendons limiting the snuffbox. The absence of either the radial or ulnar arteries is considered very rare, as is the true duplication of the radial artery [3].

Therefore, considering Rodriguez-Niedenfuhr's classification, our case most closely resembles a SuBUA variant [3]. This variant corresponds to a brachial artery originating a superficial ulnar artery high up in the arm, whereas the radial artery is a continuation of the brachial artery [3]. The origin of the interosseous arteries from the radial artery, as recorded in the present case, is considered common in cases of ulnar arteries arising in the arm [3].

According to most authors, the SuBUA most frequently courses posteriorly to the bicipital aponeurosis, and not anteriorly as it was observed in our dissection (Figures 1C and 2A) [3]. In addition, in the work conducted by Rodriguez-Niedenfuhr et al., in all cases the SuBUA coursed anteriorly to all the flexor muscles of the forearm, and then placed itself in the lateral border of the flexor carpi ulnaris to adopt its position in the lateral aspect of the ulnar nerve at the level of the middle third of the forearm [3]. As far as the authors could determine, a SuBUA variant similar to the one we observed, with a path deep to the palmaris longus muscle, has just been reported twice in the literature. Quain found it in 2 cases while dissecting 429 upper limbs [7], and Hazlet once in 188 limbs [10].

Upper limb vascular variations are presently thought to result from a stochastic process of persistence, enlargement and differentiation of parts of the initial capillary network which would normally remain as capillaries or even regress [5,11]. The precise mechanisms that lead to the higher frequency of certain variants over others, remain to be elucidated [5,11]. Interestingly, Rodriguez-Niedenfuhr et al., identified a SuBUA in 4,7% of 150 upper limbs of embryos, which is a value superior to that reported by most authors in the general adult population [11].

The clinical importance of the superficial variations of the arteries of the upper limb are increasingly being recognized [1]. For example, by being superficial, they can be easily mistaken for subcutaneous veins, leading to inadvertent artery cannulation, with the potential risk of distal limb ischemia [1,12,13]. In addition, the superficial position of the radial or ulnar arteries makes them more vulnerable to trauma [1]. Moreover, the possibility

of a SBUR variant should always be born in mind when using the arm or forearm as a source or as a recipient of microvascular flaps, or when using the radial artery as vascular graft [14-16].

Clinically, the presence of superficial forearm arteries can be suspected in the absence of palpable ulnar or radial pulses in their usual location, when superficial pulsatile vessels are found, or when patients complain of intermittent forearm or hand pain [1].

Conclusion

The ulnar artery can present several anatomical variations. In this paper we describe a bilateral superficial brachioulnar artery that, instead of travelling over the anterior aspect of the forearm muscles, as is usually the case in this variant of the ulnar artery, coursed under the palmaris longus muscle, before reaching the lateral aspect of the flexor carpi ulnaris muscle and becoming part of the ulnar neurovascular bundle. This rare variant of the ulnar artery should always be born in mind when addressing the vessels of this region clinically.

Consent

Written informed consent was obtained from the person who donated the cadaver dissected, prior to her death, for all teaching and academic purposes, namely for publication of relevant findings in scientific reports, including images. A copy of the written consent is available for review by the Editor-in-Chief of this journal.

Competing interests

The authors declare that they have no competing interests.

Authors' contributions

All authors have read and approved the final manuscript. DC performed the dissection, played a major role in writing the manuscript, and analyzed the patient's data. DP played a major role in writing the manuscript, and analyzed the patient's data. TT aided in the editing of the manuscript, and analyzed the patient's data. TB aided in the editing of the manuscript, and analyzed the patient's data. LR performed the dissection, aided in the editing of the manuscript, and analyzed the patient's data. IF performed the dissection, aided in the editing of the manuscript, and analyzed the patient's data. SA performed the dissection, aided in the editing of the manuscript, and analyzed the patient's data. MA played a major role in writing the manuscript, and analyzed the patient's data. JGO played a major role in writing the manuscript, and analyzed the patient's data.

Acknowledgments

Part of this work was funded by "The Programme for Advanced Medical Education" sponsored by "Fundação Calouste Gulbenkian, Fundação Champalimaud, Ministério da Saúde and Fundação para a Ciência e Tecnologia, Portugal."

Author details

[1]Department of Anatomy, Faculty of Medical Sciences, New University of Lisbon, Lisbon, Portugal. [2]Plastic and Reconstructive Surgery, São José Hospital, Lisbon 1150-199, Portugal. [3]Department of Anatomy, Faculty of Medical Sciences, New University of Lisbon, Campo dos Mártires da Pátria, 30, 1169-056 Lisbon, Portugal. [4]Plastic and Reconstructive Surgery, Santa Maria Hospital, Avenida Professor Egas Moniz, 1649-035 Lisbon, Portugal. [5]Faculty of Medical Sciences, New University of Lisbon, Campo dos Mártires da Pátria, 30, 1169-056 Lisbon, Portugal. [6]Plastic and Reconstructive Surgery Department and Burn Unit, São José Hospital, Lisbon 1150-199, Portugal.

Received: 12 July 2012 Accepted: 26 November 2012
Published: 30 November 2012

References

1. Claassen H, Schmitt O, Werner D, Schareck W, Kroger JC, Wree A: **Superficial arm arteries revisited: brother and sister with absent radial pulse.** *Ann Anat* 2010, **192:**151–155.
2. Jacquemin G, Lemaire V, Medot M, Fissette J: **Bilateral case of superficial ulnar artery originating from axillary artery.** *Surg Radiol Anat* 2001, **23:**139–143.
3. Rodriguez-Niedenfuhr M, Vazquez T, Nearn L, Ferreira B, Parkin I, Sanudo JR: **Variations of the arterial pattern in the upper limb revisited: a morphological and statistical study, with a review of the literature.** *J Anat* 2001, **199:**547–566.
4. Claassen H, Schmitt O, Wree A: **Large patent median arteries and their relation to the superficial palmar arch with respect to history, size consideration and clinic consequences.** *Surg Radiol Anat* 2008, **30:**57–63.
5. Shen S, Hong MK: **A rare case of bilateral variations of upper limb arteries: brief review of nomenclature, embryology and clinical applications.** *Surg Radiol Anat* 2008, **30:**601–603.
6. Adachi B: *In Das Arteriensystem der Japaner. Volume 1*. Kyoto: Maruzen; 1928:285–356.
7. Quain R: *In Anatomy of the Arteries of the Human Body*. London: Taylor & Walton; 1844:326–337.
8. Rodriguez-Baeza A, Nebot J, Ferreira B, Reina F, Perez J, Sanudo JR, Roig M: **An anatomical study and ontogenetic explanation of 23 cases with variations in the main pattern of the human brachio-antebrachial arteries.** *J Anat* 1995, **187**(Pt 2):473–479.
9. Rodriguez-Niedenfuhr M, Sanudo JR, Vazquez T, Nearn L, Logan B, Parkin I: **Median artery revisited.** *J Anat* 1999, **195**(Pt 1):57–63.
10. Hazlett JW: **The superficial ulnar artery with reference to accidental intra-arterial injection.** *Can Med Assoc J* 1949, **61:**289–293.
11. Rodriguez-Niedenfuhr M, Burton GJ, Deu J, Sanudo JR: **Development of the arterial pattern in the upper limb of staged human embryos: normal development and anatomic variations.** *J Anat* 2001, **199:**407–417.
12. Mayhew JF, Mohiuddin S: **Inadvertent median artery cannulation.** *Paediatr Anaesth* 2005, **15:**1149. author reply 1149–1150.
13. Dearlove OR, Perkins R: **Inadvertent median artery cannulation.** *Paediatr Anaesth* 2005, **15:**439–440.
14. Porter CJ, Mellow CG: **Anatomically aberrant forearm arteries: an absent radial artery with co-dominant median and ulnar arteries.** *Br J Plast Surg* 2001, **54:**727–728.
15. Acarturk TO, Tuncer U, Aydogan LB, Dalay AC: **Median artery arising from the radial artery: its significance during harvest of a radial forearm free flap.** *J Plast Reconstr Aesthet Surg* 2008, **61:**e5–e8.
16. Kumar MR: **Multiple arterial variations in the upper limb of a South Indian female cadaver.** *Clin Anat* 2004, **17:**233–235.

doi:10.1186/1756-0500-5-660
Cite this article as: Casal *et al.*: A rare variant of the ulnar artery with important clinical implications: a case report. *BMC Research Notes* 2012 **5**:660.

APPENDIX 11

Morphometric analysis of the extensor tendons of the hallux and potential implications for tendon grafting

Diogo Casal[1,2], Diogo Pais[1], Maria Angélica-Almeida[2], Tiago Bilhim[1], António Santos[1], João Goyri-O'Neill[1]

1- Anatomy Department; Medical Sciences Faculty, New University of Lisbon, Portugal
2- Plastic and Reconstructive Surgery Department, São José Hospital, Lisbon, Portugal

SUMMARY

Although several tendon sources are available for reconstructive surgical procedures, all have one or more shortcomings. The aim of this work was to evaluate if the extensor tendons of the hallux showed anatomical characteristics that could make them an additional source for tendon grafting procedures.

The authors performed a detailed morphometric analysis of the extensor tendons of the hallux in 26 lower limbs in order to evaluate the putative association of anatomical variants with hallux valgus, and to attempt to assess the feasibility of using part of the extensor apparatus of the hallux as a source of tendon for grafting procedures.

An accessory extensor hallucis longus tendon was found in 92.3% of cases. The extensor hallucis brevis tendon length was 10.5 ± 0.6 cm; its width was 0.5 ± 0.1 cm, and its thickness varied between 1-2 mm, making it a potentially good candidate as a source of tendon grafts. Several anatomical variations were observed, namely the fusion of the tendons of the extensor hallucis brevis and the accessory extensor hallucis longus muscles in the distal part of the foot.

This new therapeutic option, if implemented, would possibly increase the supply of autogenous donor tissue for reconstructive procedures, thereby enhancing the reconstructive surgeon's armamentarium.

Key words: Extensor hallucis longus – Extensor hallucis brevis – Variation – Tendon injuries – Tissue graft

INTRODUCTION

Tendon grafts are often needed in reconstructive surgery and in the realms of Orthopedics, Plastic Surgery, Maxillofacial Surgery, Burn Surgery, and even in Heart Surgery (Wehbe, 1994; Schenk et al., 2009; Terzis and Kyere, 2008). These tendon grafts can be used to reconstruct tendon or ligament defects, stabilize joints and maintain soft tissues in position (Breek et al., 1989). Recently, the use of the plantaris tendon has been proposed for atrioventricular valve repair (Shuhaiber and Shuhaiber, 2003).

Redundancy in the function of certain tendons has been known for decades (Brand, 1961), allowing several alternatives for tendon harvesting to become perfectly established. However, when a patient sustains extensive injuries, it is not uncommon for autologous tendons to be insufficient to reconstruct all

Submitted: February 22, 2010
Accepted: March 30, 2010

Correspondence to:
Diogo Casal. Rua Luís Pastor de Macedo, N 32, 5D, 1750-159 Lisbon, Portugal. E-mail: diogo_bogalhao@yahoo.co.uk

the missing structures (Williamson and Richards, 2006). In addition, all tendon options currently in use for grafting procedures have one or more several limitations, namely: inconstancy; their removal results in a variable deficit in the donor region; and the surgical incisions required to perform their extirpation are located in body areas where healing is known to be suboptimal and thus results in conspicuous scars (Williamson and Richards, 2006; Tang, 2009). Therefore, any new alternative that might increase the supply of autologous tendons for reconstructive procedures would be invaluable.

Supernumerary tendons in the hallucal extensor apparatus have been well documented for more than 125 years (Macalister, 1875; Gray, 1918; Gruber, 1875; Sarrafian and Topouzian, 1969). In 1976, Tate and Pachnik described an accessory tendon of the extensor hallucis longus in the majority of individuals (Tate and Pachnik, 1976). In the 1980s Kaneff, Andreev and Stephanoff studied in detail the extensor tendons in the first ray of the foot, reporting several accessory tendons and over 20 different variations (Kaneff, 1986a, b; Kaneff and Andreev, 1983; Kaneff and Stephanoff, 1982). More recently, these findings have been reproduced by several authors (Denk et al., 2002; Bibbo et al., 2004; Hill and Gerges, 2008; Al-Saggaf, 2003; Bergman et al., 1988; Boyd et al., 2006; Aktekin et al., 2008).

Notwithstanding the reported high frequency of these accessory tendons, their clinical importance has been considered relatively minor, and their description is even omitted from many modern, comprehensive clinical anatomy textbooks (Hill and Gerges, 2008; Moore and Dalley, 2006). Moreover, the extensor tendons of the foot have not been used, as far as the authors know, as sources of tendon grafts (Chang, 2006; Tang, 2009).

Furthermore, certain authors have associated certain variations in the extensor apparatus of the hallux to hallux valgus (Al-Saggaf, 2003), which is a common condition in which there is lateral deviation of the big toe, at the metatarso-phalangeal joint (Prosche et al., 2004). However, these findings have not been replicated by others and are still a matter of debate (Bibbo et al., 2004).

Thus in this work we studied the extensor tendons of the hallux from human cadavers in order to evaluate the potential of any of these tendons as a source of tendon grafts, and to assess whether there might be any association between the morphometric features of these tendons and the presence of hallux valgus.

Materials and Methods

The study was performed on 26 lower extremities of freshly frozen adult human cadavers used for routine gross anatomical dissections at the Medical Sciences Faculty in Lisbon, Portugal. Age at death was mostly between 60 and 85 (average 72.3) years. There were 7 men (53.8%) and 6 women (46.2%). They had had no prior surgical procedures in the leg or foot regions.

The dorsum of the foot and lower leg were carefully dissected, exposing the extensor tendons of the hallux from their origin to their insertion. Their origin, length, width, thickness and type of insertion were recorded, as well as the occurrence of hallux valgus. The mean width of each tendon was calculated based on the average of the widths measured at three points: tendon origin, middle portion of the tendon, and immediately before insertion, in the most distal place where it would be surgically possible to section the tendon for harvesting.

This research required no specific permission from the ethics committee of our institution, and conformed to the provisions of the Declaration of Helsinki (1995, revised 2000).

Statistical analyses were performed using the PASWO 18.0 (IBM®) Statistical Analysis Software. The Chi-Square test was used to compare proportions, while Student's t test and ANOVA were used for comparing means. A p value below 0.05 was considered statistically significant. Mean values are represented by their numerical value ± standard deviation.

Results

In all cases, the extensor apparatus of the hallux was composed of the extensor hallucis longus tendon (EHLp) and the extensor hallucis brevis tendon (EHB). An accessory extensor hallucis longus tendon (EHLa) was found in 92.3% of cases. Figure 1 portrays the usual composition of the extensor tendons of the hallux. The EHLa originated from the same muscular belly as the EHLp in all cases (Fig. 1). When present, the EHLa was placed medially to the EHLp (91.7%) since its origin to its termination. Only in two feet, in

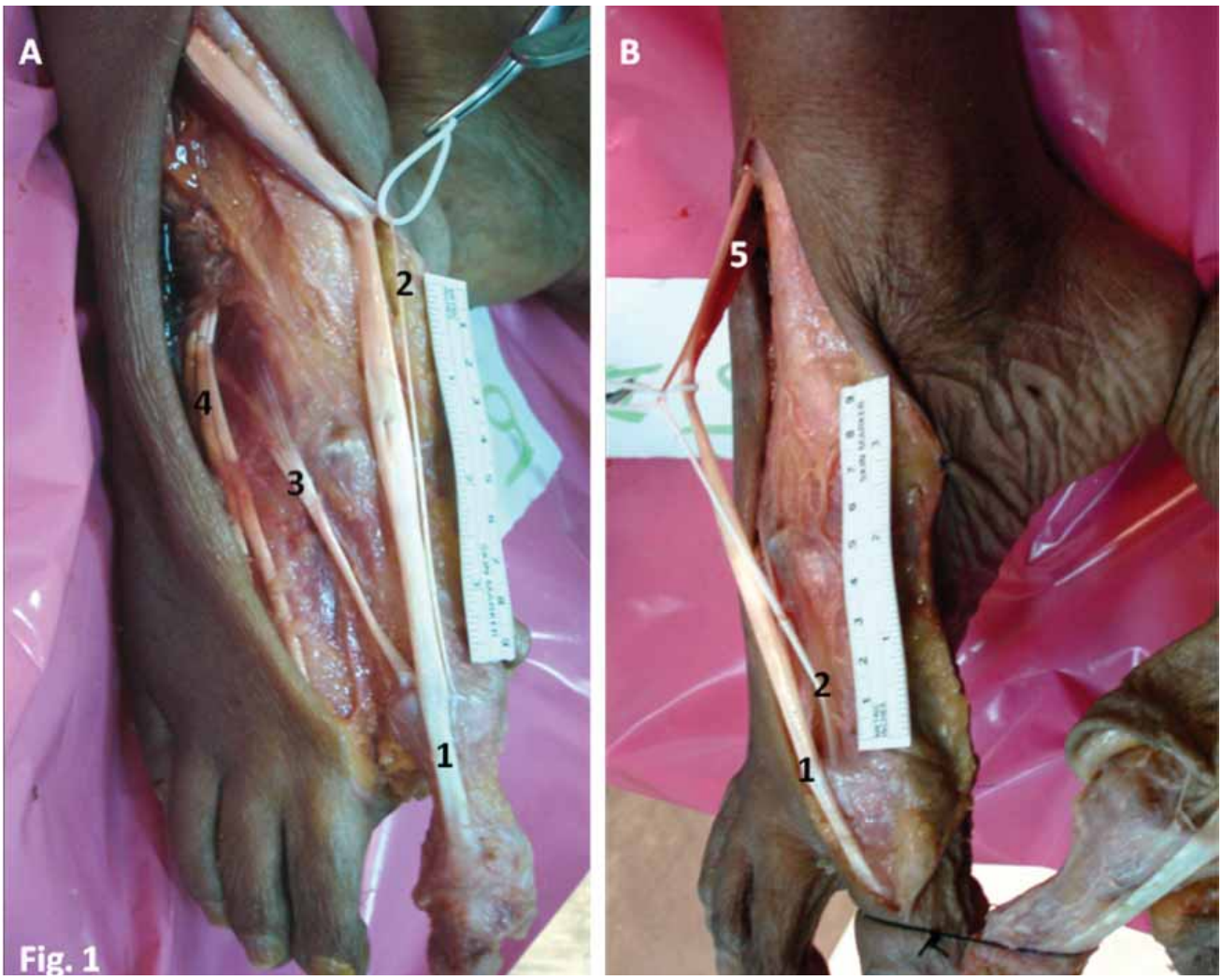

Figure 1. Dorsal (A) and medial (B) views of the right foot showing the extensor tendons of the hallux. 1- Extensor hallucis longus tendon; 2- Accessory extensor hallucis longus tendon; 3- Extensor hallucis brevis tendon; 4- Extensor digitorum longus tendons; 5- Common muscle belly of the extensor hallucis longus muscle giving off the extensor hallucis longus tendon and its accessory tendon.

the same cadaver, was the EHLa absent (Fig. 2A). In both feet of one cadaver (8.3%) the EHLa was placed laterally to the EHLp and terminated in the medial portion of the EHB (Fig. 2B). In one foot, there were two separate EHLa, one of them with a normal diameter but the other much thinner, that inserted separately at the base of the distal phalanx. These two separate EHLa were placed laterally to the EHLp.

Table 1 summarizes the results obtained globally, as well as those obtained after stratifying for sex and height. The EHLa mean width (0.3 ± 0.1 cm) was significantly lower than that of the EHLp (1.0 ± 0.2 cm), corresponding to approximately one third. However, in one cadaver this EHLa had a mean width of 0.5 mm bilaterally; i.e., half of the mean width of the EHLp itself in that case. There were no statistically significant differences between tendon length and width on the right and left sides.

The mean EHB length was 10.5 ± 0.6 cm, and its mean width was 0.5 ± 0.1 cm; i.e., half of the EHLp. The average thickness of the EHLp, EHLa, and of the EHB were remarkably constant, being approximately 3-4 mm, 0.5-1 mm, and 1-2 mm, respectively.

The EHB terminated in the dorsal and medial aspect of the base of the proximal phalanx of the hallux in all cases. The pattern of insertion of the EHLp and the EHLa, by contrast, was variable. In most cases (92.3%), the tendons terminated separately: the EHLp at the base of the distal phalanx of the hallux and the EHLa in the medial aspect of the dorsum of the base of the proximal phalanx of the big toe. In the only cadaver in which there was no EHLa, the EHLp terminated in the usual fashion at the

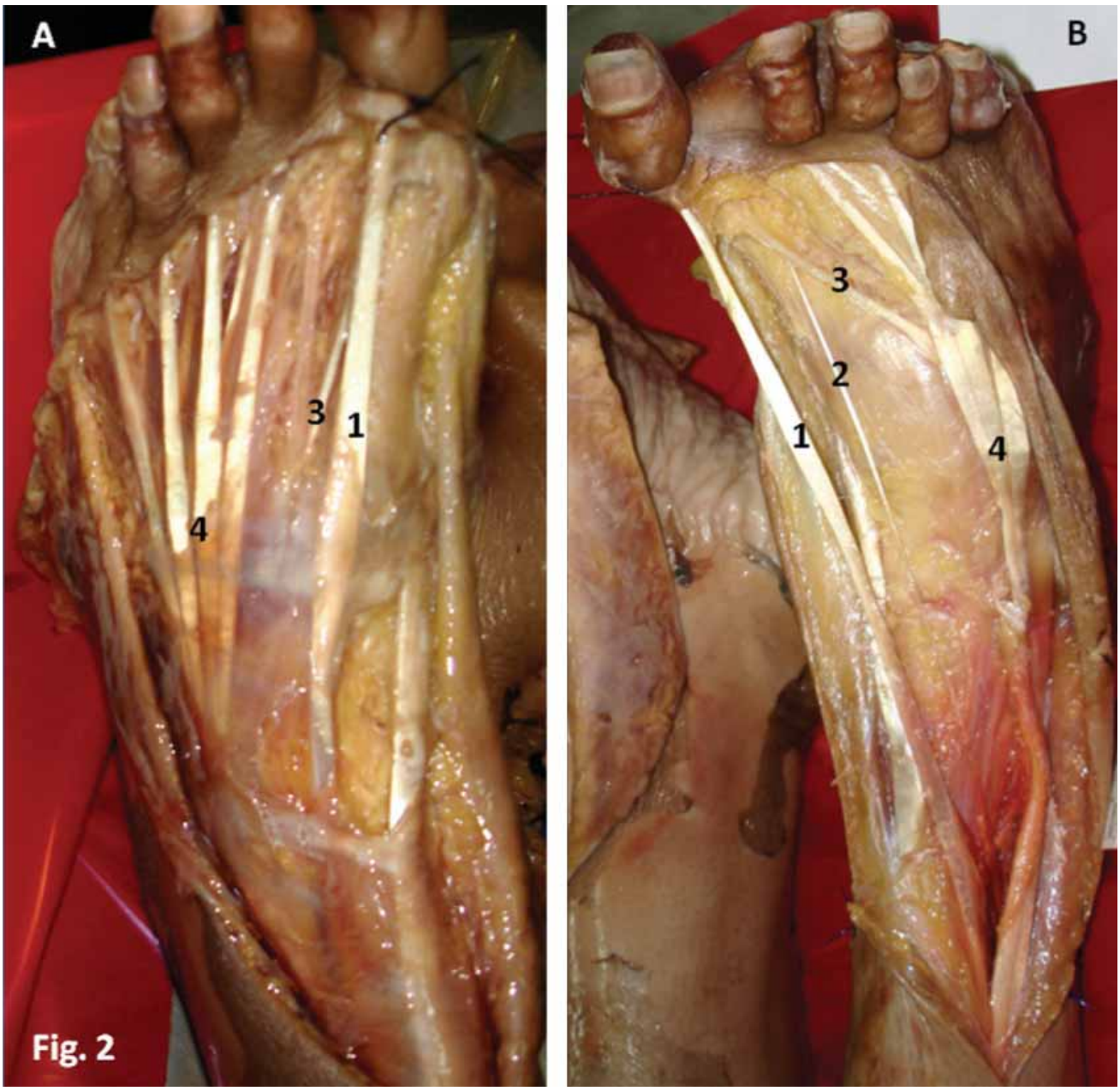

Figure 2. Dorsal view of the left (A) and right (B) feet of two different cadavers, showing anatomical variations in the extensor tendons of the hallux. In Figure 2A there is no accessory extensor hallucis longus tendon. In Figure 2B the accessory extensor hallucis longus tendon is placed laterally to the main extensor hallucis longus tendon and fuses with the extensor hallucis brevis tendon. 1- Extensor hallucis longus tendon; 2- Accessory extensor hallucis longus tendon; 3- Extensor hallucis brevis tendon; 4- Extensor digitorum longus tendons.

base of the distal phalanx. In one case in which there were two EHLa, these two tendons and the EHLp terminated isolatedly at the base of the proximal and distal phalanx, respectively. Thus, according to the Al-Sagaff classification of the insertion of the extensors of the hallux, the type I pattern was found in 92.4% of cases, whereas patterns I and III were found in 3.8% each (Al-Saggaf, 2003).

Hallux valgus was more frequent in females (72.7%) than in males (27.3%), this difference being statistically significant ($p = 0.02$). No other associations between the presence of hallux valgus and other parameters, namely type of insertion, were found.

Discussion

The composition of the extensor tendons of the hallux in our series did not differ significantly from what has been described in the literature, except for the prevalence of EHLa, which was 92.3% in our series; that is to say, much higher than that described originally by

			<1,75 m in Height (n=13)		>1,75 m in Height (n=13)		Overall
			Male n=3	Female n=10	Male n=11	Female n=2	n=26
EHLp	Length (cm)		24,5 ± 1,3 [23,5-26,0]	23,6 ± 0,6 [23,0-24,5]	26,5 ± 1,1 [25,0-28,0]	23,5 ± 0,1 [23,4-23,6]	24,9 ± 1,7 [23,0-28,0]
	Mean Width (cm)		0,9 ± 0,1 [0,8-1,1]	0,9 ± 0,1 [0,8-1,1]	1,1 ± 0,2 [0,7-1,3]	1,0 ± 0,1 [0,9-1,1]	1,0 ± 0,2 [0,7-1,3]
EHLa	Frequency		100%	90%	90,9%	100%	92,3% (24/26)
	Length (cm)		22,3 ± 1,9 [21,0-24,5]	21,4 ± 0,6 [21,0-22,5]	23,9 ± 0,7 [23,0-25,0]	22,0 ± 0,0 [22,0-22,1]	22,6 ± 1,4 [21,0-25,0]
	Mean Width (cm)		0,2 ± 0,0 [0,2-0,3]	0,3 ± 0,1 [0,2-0,4]	0,3 ± 0,1 [0,2-0,5]	0,3 ± 0,0 (0,3)	0,3 ± 0,1 [0,2-0,5]
	Position relatively to EHLp when present	Medial	100%	100%.	80%	100%	91,7%
		Lateral	0%	0%	20%	0%	8,3%
EHB	Length (cm)		10,3 ± 0,8 [9,5-11,0]	10,1 ± 0,7 [9,0-11,0]	10,9 ± 0,2 [10,5-11,0]	10,0 ± 0,1 [9,9-10,1]	10,5 ± 0,6 [9,0-11,0]
	Mean Width (cm)		0,5 ± 0,1 [0,4-0,5]	0,4 ± 0,1 [0,4-0,6]	0,5 ± 0,1 [0,4-0,6]	0,4 ± 0,1 [0,4-0,6]	0,5 ± 0,1 [0,4-0,6]
Pattern of Insertion	I		0%	0%	9,1%	0%	3,8% (1/26)
	II		100%	90%	90,9%	100%	92,3% (24/26)
	III		0%	10%	0%	0%	3,8% (1/26)
Frequency of Hallux Valgus			100%	60%	27,3%	100%	42,3%

Table 1. Morphometric features of the extensor tendons of the hallux in 26 feet. EHLp- extensor hallux longus proprius tendon; EHLa - extensor hallux longus accessorius tendon; EHB - extensor hallux brevis tendon. Pattern of insertion of the extensor apparatus is divided into three classes according Al-sagaff (2003). Values between [ ] represent the limits of variation of each variable.

Author(s)	Number of specimens studied
(Sarrafian and Topouzian, 1969)	30
(Kaneff, 1986a)	151
(Denk et al., 2002)	63
(Al-saggaf, 2003)	60
(Bibbo et al., 2004)	32
(Boyd et al., 2006)	81
(Aktekin et al., 2008)	90

Table 2. Sample sizes of the largest studies on the extensor hallux tendons published in the last 40 years.

Kaneff and Al-Sagaff, who reported values of 48.88% and 35%, respectively (Kaneff, 1986b; Al-Saggaf, 2003). However, our value is not significantly higher than that described recently by other authors, who described an EHLa in 70-87% of cases (Tate and Pachnik, 1976; Denk et al., 2002; Bibbo et al., 2003; Hill and Gerges, 2008). It is plausible that the differences found among the different authors may be due to population differences. However, given that our series of 26 specimens is relatively small (Table 2), we believe that further studies are warranted to test this hypothesis.

Al-Saggaf postulated that the presence of a supernumerary tendon of the extensor hallucis longus could be a predisposing factor for the development of hallux valgus (Al-Saggaf, 2003). However, this association was not replicated in subsequent investigations (Bibbo et al., 2004). Similarly, we also failed to identify any statistically significant association between the presence of EHLa or any other morphometric feature and the presence of hallux valgus.

We found several anatomical variations regarding the EHLa. In 7.7% of cases this supernumerary tendon was absent. In addition, although it was almost always located medially to the EHLp (91.7%) it was also placed lateral to it (8.3%). Interestingly, in one case the EHLa was placed laterally to the EHLp and terminated in the medial portion of the EHB, which in turn terminated in the usual fashion: in the dorsal and medial aspect of the base of the proximal phalanx of the hallux. This variation has been described for the first time by Denk et al. (2002) and corresponds, as far as the authors know, to the second case reported in the literatur.

By performing a morphometric analysis of the extensor tendons of the hallux, we observed that the EHLa and the EHB had, on average, a width that was one third and one half of that of the EHLp, respectively. This observation was not mentioned in the literature review we conducted, and may be of great interest for a better understanding of the functional aspects of the foot and their correlation with clinical findings. This knowledge could, for example, help explain why conservative treatment may suffice in a substantial number of cases of EHLp section or rupture, since the EHB and the EHLa will probably maintain the cut ends of the EHLp tendon close together, allowing tendon repair to occur spontaneously and thereby avoiding the need for surgery (Scaduto and Cracchiolo, 2000).

In addition, this study unequivocally suggests that the relatively large width and thickness of the EHB, as well as its significant length and constancy, would make EHB an excellent candidate as a source of tendon grafts. Moreover, this tendon fulfills all the other criteria currently accepted for donor tendons for tendon or ligament repair. In this sense, it is not situated too deeply, and hence would facilitate harvesting; no significant donor site loss would result from its harvesting, and its cross sectional diameter is not too large to hamper revascularization, while still being sufficient to provide enough autologus

material for reconstruction (Williamson and Richards, 2006). Another potential advantage of using this tendon as a graft would be that the surgical incision necessary to harvest it would be placed in the dorsum of the forefoot, which corresponds to a place of the body where wounds usually heal inconspicuously and where scars are not easily visible (Parkhouse et al., 2006). This is a major advantage relative to other donor sites, such as the forearm and leg, where scars are frequently more noticeable (Parkhouse et al., 2006).

Functionally, there is strong evidence to suggest that harvesting this tendon would not result in any significant clinical deficit, since the tendon is routinely incorporated in the dorsalis pedis flap with no resulting impairment of the extension of the hallux (Furlow, 2009). Indeed, it is unanimously accepted that the main function of the EHB is only to aid the EHLp in extending the big toe at the metatarso-phalangeal joint (Moore and Dalley, 2006).

Additionally, the EHB compares favorably with the tendons commonly used in clinical practice in terms of certain anatomical characteristics. The palmaris longus tendon, for example, which is the most commonly used donor tendon in Hand Surgery (Williamson and Richards, 2006), is only slighter longer (10 to 12 cm), and has a similar width and thickness: 3-5 mm and 1-2 mm, respectively (Chui and Edgerton, 1990). Moreover, whereas the EHB is generally considered to be constant, the palmaris longus muscle is known to be absent in up to 12 to 25% of limbs (Williamson and Richards, 2006; Neumeister and Wilhelmi, 2006; Moore and Dalley, 2006). The plantaris tendon, which is also commonly used in reconstructive procedures, is also absent in 18% of limbs (Williamson and Richards, 2006).

In spite of all these potential advantages, the use of the EHB has been overlooked as a potential tendon donor site in Reconstructive Surgery (Chang, 2006; Williamson and Richards, 2006; Tang, 2009; Neumeister and Wilhelmi, 2006). We believe this is rather unfortunate, since the EHB would be particularly well suited for the repair of torn ligaments of the hand, such as the collateral ligaments of the metacarpal-phalangeal joint of the thumb (Breek et al., 1989); the reconstruction of the A2 and A4 pulleys associated with the flexor tendons of the hand (Pederson et al., 2006) and, eventually, in some facial reconstructive procedures, to contribute to soft tissue suspension (Terzis and Kyere, 2008). This proposal, if implemented, would increase the supply of autologous donor tissue for reconstructive procedures, thereby enhancing the surgeon's arsenal.

Acknowledgments

The authors appreciate the proficiency of all Technical Staff members of the Department of Anatomy, in particular of Mr. Carlos Lopes and of Mr. Marco Costa.

References

Aktekin M, Uzmansel D, Kurtoglu Z, Sanli EC, Kara AB (2008). Examination of the accessory tendons of extensor hallucis longus muscle in fetuses. *Clin Anat,* 21: 713-717.

Al-Saggaf S (2003). Variations in the insertion of the extensor hallucis longus muscle. *Folia Morphol,* 62: 147-155.

Bergman RA, Afiri AK, Miyauchi R (1988). Illustrated encyclopedia of human anatomic variations.

Bibbo C, Anderson RB, Davis WH (2003). Injury characteristics and the clinical outcome of subtalar dislocations: a clinical and radiographic analysis of 25 cases. *Foot Ankle Int,* 24: 158-163.

Bibbo C, Arangio G, Patel DV (2004). The accessory extensor tendon of the first metatarsophalangeal joint. *Foot Ankle Int,* 25: 387-390.

Boyd N, Brock H, Meier A, Miller R, MLADY G, Firoozbakhsh K (2006). Extensor hallucis capsularis: frequency and identification on MRI. *Foot Ankle Int,* 27: 181-184.

Brand PW (1961). Tendon grafting. *J Bone Joint Surg,* 43B: 444-453.

Breek JC, Tan AM, Van Thiel TP, Daantje CR (1989). Free tendon grafting to repair the metacarpophalangeal joint of the thumb. Surgical techniques and a review of 70 patients. *J Bone Joint Surg Br,* 71: 383-387.

Chang P (2006). Repair and grafting of tendon. *In:* Mathes SJ (ed.) *Plastic Surgery.* 2nd ed. Saunders, Philadelphia.

Chui DTW, Edgerton BW (1990). Repair and grafting of tendon. In: McCarthy JG (ed.) *Plastic Surgery.* 1st ed. Saunders, Philadelphia.

Denk CC, Oznur A, Surucu HS (2002). Double tendons at the distal attachment of the extensor hallucis longus muscle. *Surg Radiol Anat,* 24: 50-52.

Furlow LT (2009). Dorsalis Pedis Flap. In: Strauch B, Vasconez LO, Hall-Findlay EJ, Lee BT (eds.). *Encyclopedia of Flaps.* 3rd ed. Lippincott Williams and Wilkins, Philadelphia.

Gray H (1918). *Anatomy of the Human Body.* Lea & Febiger, Philadelphia.

Gruber W (1875). Über die Varietäten des Musculus extensor hallucis longus. *Arch Anat Physiol Wissen Med,* 565-589.

Hill RV, Gerges L (2008). Unusual accessory tendon connecting the hallucal extensors. *Anat Sci Int,* 83: 298-300.

Kaneff A (1986a). Die Aufrichtung des Menschen und die morphologische Evolution der Musculi extensores digitorum pedis unter dem Gesichtspunkt der evolutiven Myologie. Teil I. *Gegenbaurs Morphol Jahrb,* 132: 375-419.

KANEFF A (1986b). Die Aufrichtung des Menschen und die morphologische Evolution der Musculi extensores digitorum pedis unter dem Gesichtspunkt der evolutiven Myologie. Teil III. *Gegenbaurs Morphol Jahrb,* 132: 681-722.

KANEFF A, ANDREEV D (1983). Über die organogenetische Entwicklung des M. extensor hallucis longus beim Menschen. *Anat Anz,* 154: 237-244.

KANEFF A, STEPHANOFF A (1982). Vergleichend-anatomische Untersuchung des M. extensor hallucis longus beim Menschen. *Gegenbaurs Morphol Jahrb,* 128: 690-701.

MACALISTER A (1875). Additional observations on muscular anomalies in human anatomy. *Trans R Ir Acad Sci,* 25: 1-130.

MOORE KL, DALLEY AF (2006). Lower Limb. *Clinically Oriented Anatomy.* 5th ed. Lippincott Williams and Wilkins, Philadelphia.

NEUMEISTER MW, WILHELMI BJ (2006). Flexor Tendon Repair. In: MCCARTHY JG, GALIANO RD, BOUTROS SG (eds). *Current Therapy in Plastic Surgery.* 1st ed. Saunders, Philadelphia.

PARKHOUSE N, CUBISON TCS, HUMZAH MD (2006). Scar Revision. In: MATHES SJ, HENTZ VR (eds). *Plastic Surgery.* 2nd ed. Saunders, Philadelphia.

PEDERSON WC, STEVANOVIC M, ZALAVRAS CL, SHERMAN R (2006). Reconstructive Surgery: Extensive Surgery to the Upper Limb. In: MATHES SJ (ed). *Plastic Surgery.* 2nd ed. Saunders, Philadelphia.

PROSCHE H, FUHRMANN R, LINB W, FRÖBER R (2004). The postoperative stability of the first metatarsal. *Eur J Anat,* 8: 55-59.

SARRAFIAN SK, TOPOUZIAN LK (1969). Anatomy and physiology of the extensor apparatus of the toes. *J Bone Joint Surg Am,* 51: 669-679.

SCADUTO AA, CRACCHIOLO A (2000). Lacerations and ruptures of the flexor or extensor hallucis longus tendons. *Foot Ankle Clin,* 5: 725-736.

SCHENK S, MEIZER R, KRAMER R, AIGNER N, LANDSIEDL F, STEINBOECK G (2009). Resection arthroplasty with and without capsular interposition for treatment of severe hallux rigidus. *Int Orthop,* 33: 145-150.

SHUHAIBER JH, SHUHAIBER HH (2003). Plantaris tendon graft for atrioventricular valve repair: a novel hypothetical technique. *Tex Heart Inst J,* 30: 42-44.

TANG JB (2009). Flexor tendons. In: CHUNG KC, DISA JJ, GOSAIN AK, KINNEY BM, RUBIN JP (eds). *Plastic Surgery: Indications and Practice.* 1st ed. Saunders, China.

TATE R, PACHNIK RL (1976). The accessory tendon of extensor hallucis longus: its occurrence and function. *J Am Podiatry Assoc,* 66: 899-907.

TERZIS JK, KYERE SA (2008). Minitendon graft transfer for suspension of the paralyzed lower eyelid: our experience. *Plast Reconstr Surg,* 121: 1206-1216.

WEHBE MA (1994). Tendon graft anatomy and harvesting. *Orthop Rev,* 23: 253-256.

WILLIAMSON DG, RICHARDS RS (2006). Flexor tendon injuries and reconstruction. In: MATHES SJ (ed). *Plastic Surgery.* Saunders, Philadelphia.

APPENDIX 12

MICROSURGERY

Reconstruction of a long defect of the ulnar artery and nerve with an arterialized neurovenous free flap in a teenager: a case report and literature review

Journal:	*Microsurgery*
Manuscript ID	MICR-17-0124.R2
Wiley - Manuscript type:	Case Report
Date Submitted by the Author:	n/a
Complete List of Authors:	Casal, Diogo; Nova Medical School, Anatomy; Centro Hospitalar de Lisboa Central EPE, Plastic Surgery Pais, Diogo; Nova Medical School, Anatomy Department Mota-Silva, Eduarda; Faculdade de Ciências e Tecnologia, Physics Department Pelliccia, Giovanni; Centro Hospitalar de Lisboa Central EPE Iria, Ines; Faculdade de Farmácia, Universidade de Lisboa Videira, Paula; Universidade Nova de Lisboa Faculdade de Ciencias e Tecnologia, UCIBIO, Life Sciences Department Mendes, Maria; Centro Hospitalar de Lisboa Central EPE, Plastic Surgery Goyri-O'Neill, João; Nova Medical School, Anatomy Mouzinho, Maria; Centro Hospitalar de Lisboa Central EPE
Keywords:	Trauma, Ulnar nerve, Peripheral nerve repair, Nerve graft, Venous arterialized flap

TITLE PAGE

Title: Reconstruction of a long defect of the ulnar artery and nerve with an arterialized neurovenous free flap in a teenager: a case report and literature review

Authors: Diogo Casal, M.D.[1,2]; Diogo Pais, M.D., PhD[1,2]; Eduarda Mota-Silva[3], M.Sci.; Giovanni Pelliccia, M.D. [1;2]; Inês Iria, M.Sci.[4]; Paula A. Videira, M.Sci., PhD[5]; Maria Manuel Mendes, M.D.[1]; João Goyri-O'Neill, M.D., PhD[2]; Maria Manuel Mouzinho, M.D.[1]

1. Plastic and Reconstructive Surgery Department and Burn Unit; Centro Hospitalar de Lisboa Central, Lisbon, Portugal
2. Anatomy Department; NOVA Medical School, Universidade NOVA de Lisboa, Lisbon, Portugal
3. LIBPhys, Physics Department, Faculdade de Ciências e Tecnologia, Caparica, Portugal
4. Molecular Microbiology and Biotechnology Unit|Drug Discovery Area; Faculdade de Farmácia, Universidade de Lisboa, Portugal
5. UCIBIO, Life Sciences Department, Faculdade de Ciências e Tecnologia, Universidade NOVA de Lisboa, Caparica, Portugal

The authors have no conflicts of interest to declare.

Corresponding author: Diogo Casal, M.D., Anatomy Department, Nova Medical School, Campo dos Mártires da Pátria, 130, 1169-056, Lisbon, Portugal;
e-mail address: diogo_bogalhao@yahoo.co.uk

Title: Reconstruction of a long defect of the ulnar artery and nerve with an arterialized neurovenous free flap in a teenager: a case report and literature review

ABSTRACT

There is evidence that nerve flaps are superior to nerve grafts for bridging long nerve defects. Moreover, arterialized neurovenous flaps (**ANVFs**) have multiple potential advantages over traditional nerve flaps in this context. This paper describes a case of reconstruction of a long defect of the ulnar artery and nerve with an arterialized neurovenous free flap and presents a literature review on this subject.

A 16-year-old boy sustained a stab wound injury to the medial aspect of the distal third of his right forearm. The patient was initially observed and treated at another institution where the patient was diagnosed with a flexor carpis ulnaris muscle and an ulnar artery section. The artery was ligated and the muscle was sutured. Four months later, the patient was referred to our institution with complaints of ulnar nerve damage, as well as hand pain and cold intolerance. Physical examination and ancillary tests supported the diagnosis of ulnar artery and nerve complete section. Surgery revealed an 8-cm hiatus of the ulnar artery and a 5-cm defect of the ulnar nerve. These gaps were bridged with a flow through ANVF containing the sural nerve and the lesser saphenous vein. The postoperative course was uneventful. Two years postoperatively, the patient had regained normal trophism and M5 strength in all previously paralyzed muscles according to the Medical Research Council Scale. Thermography revealed good perfusion in the right ulnar angiosome.

The ANVF may be an expedite, safe and efficient option to reconstruct a long ulnar nerve and artery defect.

Keywords:

Trauma; Ulnar nerve; Peripheral nerve repair; Nerve graft; Venous arterialized flap; Case report.

INTRODUCTION

Vascular and nerve injuries to the upper limb are relatively frequent.[1-5] However, functional results after peripheral nerve repair are far from perfect, especially for late repairs or in cases of long nerve defects.[1,5,6] This, in turn, often results in permanent and significant social and economic devaluation of those affected.[3,6-8]

There is mounting experimental and clinical evidence that nerve flaps are superior to nerve grafts for bridging long nerve defects.[5,9] In fact, nerve flaps, having a blood supply of their own since the moment of nerve transfer, are less prone to central necrosis, fibrosis and histological disorganization compared to nerve grafts, which depend initially on diffusion and subsequently on neoangiogenesis for survival.[5,10-13]

Most literature refers to “conventional nerve flaps” (**CNFs**), that is to say to nerve segments pedicled on a given arterial and venous pedicle. However, CNFs entail laborious dissections, and sometimes cannot be raised due to local anatomical constraints.[14] To circumvent these limitations, in 1984, Townsend and Taylor suggested a new way of transferring nerve segments pedicled exclusively on their accompanying veins. In these nerve flaps, at least one of the veins was connected to a recipient site’s artery, whereas at least one of the other veins drained the flap’s venous blood. These flaps were named “arterialized neurovenous flaps” (**ANVFs**).[15] However, since then, ANVFs have been reported clinically only a few times in case reports or small case series.[16]

In this paper, the authors describe a case report in which deferred reconstruction of a composite long arterial and nervous defect was performed with an ANVF in a teenage boy with an excellent functional outcome. Furthermore, the authors conducted a literature review on the use of ANVFs employed in the reconstruction of similar defects.

CASE REPORT

A 16-year-old right-handed Portuguese teenage boy sustained a broken glass injury to the medial aspect of the distal third of his right forearm when the patient was inadvertently pushed against a window at school. The patient was initially observed and treated at another institution where the patient was diagnosed with a flexor carpis ulnaris muscle and an ulnar artery section. The artery was ligated and the muscle was sutured with horizontal 3/0 Vicryl® mattress sutures.

Four months later, the patient was referred to our institution for observation in the Plastic and Reconstructive Surgery outpatient clinic. The patient complained of hypoesthesia and paresthesia in the territory of the right ulnar nerve. Moreover, the patient referred exertional pain, as well as cold intolerance in the affected hand. Physical examination, revealed an ulnar claw, with paralysis and wasting of the intrinsic hand muscles dependent on the ulnar nerve (**Fig. 1**). Allen's test revealed a poorly perfused hand when pressing the radial artery at wrist level. Electroneuromyography was consistent with chronic ulnar neurotmesis at the distal forearm.

Surgical exploration of the lesion under tourniquet control, revealed interruption of the ulnar nerve and artery (**Fig. 2A**). After debriding the fibrous tissue and removing the proximal stump's neuroma using surgical magnifying loops, there was an 8-cm hiatus of the ulnar artery and a 5-cm defect of the ulnar nerve (**Fig. 2A**).

These gaps were bridged with a flow through ANVF raised from the left lower leg (**Fig 2B**). This flap was composed of the sural nerve and of the lesser saphenous vein (**Fig. 2C**). The flap comprised two branches of the sural nerve that were used to reconstruct the ulnar nerve according to its internal topographical anatomy at the distal forearm level (**Figs. 2D and Fig. 3**). It was assumed that the motor component is medially placed whereas the sensory component is in the lateral aspect of the nerve.[9,17] The ulnar artery hiatus was

reconstructed with an inverted segment of the lesser saphenous vein included in the flap. Hence, blood flow in the ANVF was orthodromic. Vascular and neural anastomoses were performed with interrupted 9/0 Nylon stitches under the operating microscope.

In the flap's donor zone, the proximal stump of the sural nerve was stitched with a 6/0 Nylon suture to the belly of the lateral gastrocnemius muscle after creating a small window in the muscle fascia. The surgical wounds were closed in anatomical layers. The surgery's duration was 242 minutes.

After surgery, the patient's wrist was splinted for 15 days to prevent maximal extension and thus excessive tension on the vascular and nerve repairs. The patient was allowed to ambulate and freely use the patient's fingers immediately after surgery. The patient was discharged home 3 days after surgery. Postoperatively, the patient underwent an intensive physiotherapy program for one year. The patient was followed regularly at the outpatient clinic for 2 years. Five months after surgery, Tinel's sign could be observed at the wrist level. Intrinsic muscles innervated by the ulnar nerve started to show voluntary contraction at 8 months post-operatively. The patient referred gain of sensibility in the ulnar aspect of his hand 6 months after the surgical procedure. At the last follow up visit, the patient had regained normal trophism and M5 strength in all previously paralyzed muscles according to the Medical Research Council Scale, i.e. muscle strength was no different from that observed in the opposite side (**Figs. 4A, 4C** and **4D**). Furthermore, according to this scale, his sensory recovery was S3 in the territory of the ulnar nerve, i.e. return of superficial cutaneous pain and tactile sensibility without over-response.[18] Two years after the last surgery, two-point discrimination in the hypothenar region was 5 mm and 7 mm in the palmar aspect of the fifth finger. At this time, the patient presented a relatively inconspicuous scar in the donor zone, as well as absence of limb edema (**Fig. 4E**).

Since the last surgery, the patient denied either cold intolerance or exertional fatigue in the affected hand. Two years after this surgery, thermographic examination of the upper limbs was performed with a FLIR® E6 camera placed 25 cm above the hands.[19] This exam

revealed a symmetrical pattern with good perfusion throughout, including in the territory of the right ulnar angiosome (**Fig. 4A**).

Two years after the last surgery, electroneuromyography confirmed reinnervation in the territory of the ulnar nerve.

DISCUSSION

Oddly, although potentially advantageous, the reconstruction of nerve defects using ANVFs is rarely mentioned in the literature (**Table 1**).[16] Townsend *et al* pioneered this field in 1984 with a seminal paper describing 13 lower limb cadaveric dissections, an histological study in the greyhound dog comparing axonal elongation in nerve grafts and ANVFs, and 7 clinical cases.[15] In this series, 5 combined nerve and arterial defects of the upper limb and 2 facial nerve lesions were successfully reconstructed using ANVFs.[15] The next year, Gu *et al* described 14 clinical cases in which upper limb nerve defects over 10 cm in length associated with vascular injuries were reconstructed using ANVFs.[20] Most of these patients presented good results, although there were 2 vascular thrombosis of the ANVFs and there were 2 cases of absence of neurological recovery in patients with longstanding lesions.[20] Since 1989, there were multiple papers describing the simultaneous reconstruction of nerve and skin defects using ANVFs associated with a skin paddle.[16,21-23] In that same year, Rose *et al* presented a series of 14 ANVFs fabricated from the medial fibular nerve and from the dorsalis pedis venae comitantes that were effectively used to bridge digital nerve defects associated with significant local fibrosis.[24]

Since then, multiple papers have been published describing the use of ANVFs in virtually all anatomical regions. The largest of these series describe the use of several ANVFs to simultaneous reconstruct composite vascular and nerve defects of the upper limb, either occurring proximally at the arm level, or distally at the finger level.[25-27] Multiple variations in the composition of ANVFs were introduced, including tendon[25,28], deep fascia[29], bone[23,30] and/or the nail complex[30]. However, only a few authors have reported the use of ANVFs similar to that described in this paper for the reconstruction of arterial and nerve defects at the forearm level.[15,16,25,31] Moreover, all these reconstructions were performed in adults. Consequently, as far as the authors could determine, this is the first report of an ANVF being used to reconstruct a composite long nerve and arterial defect in a pediatric patient.

One reason to justify this may be that extensive vascular and nerve damage is increasingly rare in children and teenagers in most countries.[32,33] Moreover, these lesions are frequently associated with damage to other structures, namely the integumentary system, mandating reconstruction of concomitant tissue injuries with flaps containing muscle and/or skin paddles. Finally, having an incompletely understood physiology, ANVFs are often not the first reconstructive option for most surgeons.[5,16]

Comparatively to CNFs, ANVFs, as the one used in this patient, have the significant merit of being easy to raise and tailor due to the constant proximity of superficial veins to superficial nerves.[5,13] Furthermore, the architecture of the ANVF used in this case, also allowed the simultaneous reconstruction of the ulnar artery and nerve (**Fig. 3).** The inclusion of two terminal branches of the sural nerve made possible to reconstruct the ulnar nerve in a somatotopic fashion. It is well established that in the distal aspect of the forearm, the ulnar nerve is composed of a motor branch centrally located between the ulnarly-placed dorsal cutaneous branch and the radially-placed palmar sensory component.[17] This topographical nerve reconstruction may have played a significant role in the full recovery presented by the patient. This is stark contrast with the poor results generally observed with ulnar nerve reconstruction even in the distal portion of the upper limb.[5,13,34,35] Nevertheless, the authors must concede that one of the factors responsible for the good functional outcome was the young age of the patient.[5]

The patient presented a positive Tinnel's sign at the wrist level five months after surgery. Roughly, this corresponded to an average axonal growth of 1.3 mm/day (i.e., the fastest axons elongated around 200 mm in approximately 150 days). This value is similar to that generally reported in ideal conditions with nerve grafts and conventional nerve flaps at the patient's age.[36-38] In fact, it has been estimated that in optimal repair conditions axonal growth can occur at a speed of 1 to 3 mm per day.[36-38]

Similarly to what has been described by other authors, no significant donor site morbidity

was observed in this patient.

CNFs are generally considered superior to nerve grafts for reconstructing long and thick nerve defects, particularly in regions of relative ischemia, such after radiotherapy, intense fibrosis subsequent to extensive trauma or in the particular case of prior deep burns.[5,9,13,39] However, the utility of ANVFs in these situations is still based on scarce experimental data, anecdotal case reports and small case series. The good results obtained in this case report lend support to the use of ANVFs for reconstructing long nerve defects in teenagers. Notwithstanding, further experimental and clinical studies are warranted to confirm or dismiss these findings.

Overall, this case report suggests that the arterialized sural nerve/lesser saphenous neurovenous flap may be an expedite, safe and efficient option to reconstruct a long ulnar nerve and artery defect in the forearm of teenagers.

ABBREVIATIONS:

ANVF, arterialized neurovenous flap; **CNF**, conventional nerve flap.

DECLARATIONS

Consent for publication:

Written informed consent was obtained from the patient for publication of this case report and any accompanying images. A copy of the written consent is available for review by the Editor-in-Chief of this journal.

Competing interests:

The authors declare that they have no competing interests.

Funding:

One of the authors (Diogo Casal) received a grant from The Program for Advanced Medical Education, which is sponsored by Fundação Calouste Gulbenkian, Fundação Champalimaud, Ministério da Saúde e Fundação para a Ciência e Tecnologia, Portugal

Authors' contributions:

DC, MMendes and MMouzinho participated in the care of the patient. DC, DP, EMS, II, GP and JGO collected the data and drafted the manuscript. All authors have read and approved the manuscript.

Acknowledgments:

The authors are very grateful to Mr. Filipe Franco for the illustrative drawing in Figure 3.

References

1. Slutzky DJH, V.R. Peripheral Nerve Surgery: Practical Applications in the Upper Extremity. Churchill Livingstone. Elsevier. 2006.
2. Rosberg HEeLD. Epidemiology of hand injuries in a middle-sized city in southern Sweden - a retrospective study with an 8-year interval. Scand J Plast Rec Surg Hand Surg 2004(38):347-355.
3. Rosberg HE, et al. Injury to the human median and ulnar nerves nerves in the forearms - analysis of costs for treatment and rehabilitation of 69 patients in southern Sweden. J Hand Surg [Br] 2005;1(30):35-39.
4. Jabaley ME. Primary Nerve Repair. In: Peripheral Nerve Surgery: Practical Applications in the Upper Extremity. Editores: Slutsky, D.J.; Hentz, V.R. Churchill Livingstone. 2006:23-38.
5. Trehan SK, Model Z, Lee SK. Nerve Repair and Nerve Grafting. Hand clinics 2016;32(2):119-125.
6. Dahlin LB. Nerve injury and repair: from molecule to Man. In: Slutsky DJ, Hentz VR, editors. Peripheral Nerve Surgery: Practical Applications in the Upper Extremity. Philadelphia: Elsevier; 2006. p 1-22.
7. Broback LG, et al. Clinical and socio-economical aspects of hand injuries. Acta Chir Scand 1978;7-8(144):455-461.
8. Rosberg HESCDLB. Prospective analysis of costs, arm function and health status using DASH and SF36 in patients with and forearm trauma of varying severity (HISS). Scand J Plast Rec Surg Hand Surg 2004:2004.
9. Wood MJ, Johnson PJ, Myckatyn TM. Anatomy and physiology for the peripheral nerve surgeon. In: Mackinnon SE, Yee A, editors. Nerve Surgery. First ed. Volume 1. New York: Thieme; 2015. p 1-40.
10. Sinis N, Kraus A, Papagiannoulis N, Werdin F, Schittenhelm J, Meyermann R,

Haerle M, Geuna S, Schaller HE. Concepts and developments in peripheral nerve surgery. Clinical neuropathology 2009;28(4):247-262.

11. Desouches C, Alluin O, Mutaftschiev N, Dousset E, Magalon G, Boucraut J, Feron F, Decherchi P. [Peripheral nerve repair: 30 centuries of scientific research]. Revue neurologique 2005;161(11):1045-1059.

12. Terzis JK, Skoulis TG, Soucacos PN. Vascularized nerve grafts. A review. International angiology : a journal of the International Union of Angiology 1995;14(3):264-277.

13. Taylor GI, Pan WR. The angiosome concept. In: Dodwell P, editor. The angiosome concept and tissue transfer. First ed. Volume 1. Florida: Quality Medical Publishing, Inc.; 2014. p 354-395.

14. Hong MK, Taylor GI. Angiosome territories of the nerves of the upper limbs. Plastic and reconstructive surgery 2006;118(1):148-160.

15. Townsend PL, Taylor GI. Vascularised nerve grafts using composite arterialised neuro-venous systems. Br J Plast Surg 1984;37(1):1-17.

16. Casal D, Cunha T, Pais D, Videira P, Coloma J, Zagalo C, Angelica-Almeida M, O'Neill JG. Systematic Review and Meta-Analysis of Unconventional Perfusion Flaps in Clinical Practice. Plastic and reconstructive surgery 2016;138(2):459-479.

17. Davidge KM, Boyd KU. Ulnar nerve entrapment and injury. In: Mackinnon SE, editor. Nerve surgery. First ed. Volume 1. New York: Thieme; 2015. p 251-288.

18. Wang Y, Sunitha M, Chung KC. How to measure outcomes of peripheral nerve surgery. Hand clinics 2013;29(3):349-361.

19. Sheena Y, Jennison T, Hardwicke JT, Titley OG. Detection of perforators using thermal imaging. Plastic and reconstructive surgery 2013;132(6):1603-1610.

20. Gu YD, Wu MM, Zheng YL, Li HR, Xu YN. Arterialized venous free sural nerve grafting. Ann Plast Surg 1985;15(4):332-339.

21. Gu YD, Zhang GM, Chen DS, Yan JG, Cheng XM. Arterialized free flap. Report of four cases. Chin Med J (Engl) 1989;102(2):140-144.
22. Rose EH. Small flap coverage of hand and digit defects. Clin Plast Surg 1989;16(3):427-442.
23. Hussmann J, Bahr C, Steinau HU, Vaubel E. [Indications for arterialization of tissue]. Langenbecks Arch Chir Suppl Kongressbd 1996;113:1164-1166.
24. Rose EH, Kowalski TA, Norris MS. The reversed venous arterialized nerve graft in digital nerve reconstruction across scarred beds. Plastic and reconstructive surgery 1989;83(4):593-604.
25. Woo SH, Kim KC, Lee GJ, Ha SH, Kim KH, Dhawan V, Lee KS. A retrospective analysis of 154 arterialized venous flaps for hand reconstruction: an 11-year experience. Plastic and reconstructive surgery 2007;119(6):1823-1838.
26. Hussmann J, Bahr C, Russell RC, Steinau HU, Vaubel E. Experimentelle und klinische Erfahrungen mit der Stromumkehr. Journal der Deutschen Gesellschaft für Plastische und Wiederherstellungschirurgie 2003:24.
27. Yan H, Gao W, Zhang F, Li Z, Chen X, Fan C. A comparative study of finger pulp reconstruction using arterialised venous sensate flap and insensate flap from forearm. Journal of plastic, reconstructive & aesthetic surgery : JPRAS 2012;65(9):1220-1226.
28. Karacalar A, Ozcan M. Free arterialized venous flap for the reconstruction of defects of the hand: new modifications. J Reconstr Microsurg 1994;10(4):243-248.
29. Liu Y, Jiao H, Ji X, Liu C, Zhong X, Zhang H, Ding X, Cao X. A comparative study of four types of free flaps from the ipsilateral extremity for finger reconstruction. PloS one 2014;9(8):e104014.
30. Patradul A, Ngarmukos C, Parkpian V, Kitidumrongsook P. Arterialized venous toenail flaps for treating nail loss in the fingers. J Hand Surg Br 1999;24(5):519-524.

31. Bullocks J, Naik B, Lee E, Hollier L, Jr. Flow-through flaps: a review of current knowledge and a novel classification system. Microsurgery 2006;26(6):439-449.

32. Lad SP, Nathan JK, Schubert RD, Boakye M. Trends in median, ulnar, radial, and brachioplexus nerve injuries in the United States. Neurosurgery 2010;66(5):953-960.

33. Ciaramitaro P, Mondelli M, Logullo F, Grimaldi S, Battiston B, Sard A, Scarinzi C, Migliaretti G, Faccani G, Cocito D. Traumatic peripheral nerve injuries: epidemiological findings, neuropathic pain and quality of life in 158 patients. J Peripher Nerv Syst 2010;15(2):120-127.

34. Meek MF, Coert JH, Robinson PH. Poor results after nerve grafting in the upper extremity: Quo vadis? Microsurgery 2005;25(5):396-402.

35. Barrios C, Amillo S, de Pablos J, Canadell J. Secondary repair of ulnar nerve injury. 44 cases followed for 2 years. Acta orthopaedica Scandinavica 1990;61(1):46-49.

36. Sulaiman W, Gordon T. Neurobiology of peripheral nerve injury, regeneration, and functional recovery: from bench top research to bedside application. Ochsner J 2013;13(1):100-108.

37. M.A. F, Wilbourn AJ. The electrodiagnostic examination with peripheral nerve injuries. In: Mackinnon SE, editor. Nerve surgery. First ed. Volume 1. New York: Thieme; 2015. p 59-74.

38. Boyd KU, Fox IK. Nerve repair and grafting. In: Mackinnon SE, editor. Nerve surgery. First ed. Volume 1. New York: Thieme; 2015. p 75-100.

39. D'Arpa S, Claes KEY, Stillaert F, Colebunders B, Monstrey S, Blondeel P. Vascularized nerve "grafts": just a graft or a worthwhile procedure? Plastic and Aesthetic Research 2015;2(4):183-194.

Figure Legends:

Figure 1. Photographs showing the preoperative appearance.

A. A scar in the medial aspect of the distal third of the right forearm was visible (arrow) corresponding to the site of injury.

B. Comparison of the hands showed marked atrophy of the right hand intrinsic muscles, particularly in the medial palmar region.

C. An ulnar claw was evident due to atrophy of the intrinsic muscles supplied by the ulnar nerve.

Figure 2. Photographs of the surgery.

Scale bar = 1 cm

Pr, Proximal; Lat, Lateral; An, Anterior

1, Proximal stump of the ulnar artery; 2, Distal stump of the ulnar artery; 3, Proximal stump of the ulnar nerve; 4, Distal stump of the ulnar nerve; 5, Flexor carpis ulnaris muscle.

The yellow vessel loops were placed around two terminal branches of the sural nerve. The blue vessel loops were placed around the lesser saphenous vein.

A, Intraoperative view of the ulnar neurovascular bundle after removing the fibrotic tissue and the proximal stump neuroma; B, View of the lesser saphenous/sural neurovenous flap *in situ* after dissection; C, Detailed *ex vivo* view of the lesser saphenous/sural neurovenous flap prior to insetting into the defect; D, View of the arterialized neurovenous flap after insetting the flap and performing the neural and vascular anastomoses.

Figure 3. Schematic representation of the composition and vascular architecture of the lesser saphenous/sural neurovenous flap used to bridge the long arterial and nerve defect. The arrows indicate the direction of blood flow.

1, Proximal segment of the ulnar artery; 2, Distal segment of the ulnar artery; 3, Lesser

saphenous vein in an inverted position used to bridge the vascular gap; 4, Proximal stump of the ulnar nerve; 5, Distal stump of the ulnar nerve; 6, Sural nerve cables used for the somatotopic reconstruction of the ulnar nerve.

Figure 4. Appearance of the recipient and donor zones two years after surgery.

A. Anterior view of the distal aspect of the upper limbs showed no evidence of atrophy of hand muscles.

B. Infra-red thermography of the anterior aspect of the forearms and hands showed good perfusion of the ulnar aspect of the right hand.

C. Posterior view of the forearms and hands showed absence of ulnar claw in the right hand, as well as good finger abduction.

D. Posterior view of the hands demonstrated adequate finger adduction.

E. Posterior view of the lower legs and feet showed a relatively inconspicuous scar in the donor zone (arrow), as well as absence of limb edema.

Author	Year	n	Age (years)		M:F	Defect location	Defect origin	Flap(s) donor site(s)	Flap composition	Outcomes	Complications
			mean	min-max							
Townsend [15]	1984	7	33.2	20-54	4:3	HN; F; HF	Tu; B; Tr	L	nv	Five combined nerve and arterial defects of the upper limb and 2 facial nerve lesions were reconstructed with good results	0
Gu [20]	1985	14	30.8	20-54	10:4	F	Tr	L	nv	Fourteen clinical cases of upper limb nerve defects over 10 cm in length associated with vascular injuries were successfully reconstructed; 12 patients presented significant neurological recovery	14.2% vascular anastomosis thrombosis
Gu [21]	1989	4	29.8	17-54	3:1	F; L; HF	SC	F; L	S; sne	Skin and nerve hand defects were reconstructed with success in 3 out of 4 cases	25% FTN
Rose [22]	1989	1	38	38	1:0	HF	SC	n/a	S; sne	Skin and nerve digital defects were reconstructed with success in one patient	0
Rose [23]	1989	14	29	18-55	9:1	HF	Tr	Ft	nv	Fourteen digital nerve defects in poorly vascularized tissues were reconstructed with good results in 10 patients	0
Karacalar [24]	1994	13	23.9	12-35	11:2	HF	n/a	F	S; st; sne	Three skin and sensory digital defects were successfully reconstructed with innervated AVFs	15.4% FTN
Hussman [25]	1996	69	47	n/a	n/a	HN; F; L; HF	B; CM; Tr; Tu	F; L; Ft	S; stnb; sc	Multiple cases involving integumentary and nerve defects were successfully reconstructed with AVFs	18.8% FTN
Woo [26]	1996	12	36.2	18-59	11:1	HF	B; Tr; SC	F; L	S; sne	Nine cases of complex hand defects were successfully reconstructed in 9 patients with AVFs	25% FTN
Kayikcioglu [27]	1998	8	28.4	19-41	8:0	HF	Tr	HF	S; sne	Seven out of eight digital pulp defects were successfully reconstructed including two cases of simultaneous skin and nerve reconstruction	12.5% FTN
Patradul [28]	1999	10	25.3	6-47	4:5	HF	Tr	Ft	S; stnb	Successful distal finger reconstruction, including the nail complex, in 9 out of 10 patients. There was a case of simultaneous skin, tendon, bone and nerve reconstruction	10% FTN
Takeuchi [29]	2000	2	23.5	21-26	2:0	HF	Tr	Ft	Sne	Two innervated AVFs from the dorsum of the foot were successfully used to provide a sensate covering of degloved fingers in two patients. Nearly full range of motion of the fingers was obtained	0
Murata [30]	2001	7	39	20-57	6:0	HF	Tr	HF	S; sne	Seven venous flaps from the dorsum of the hand, including 3 sensate flaps, were successfully used to reconstruct digits	14.2% SpN
Hussmann [31]	2003	70	47.4	7-78	n/a	HN; F; L; HF	Tu; B; Tr; CM	F; L; Ft	S; stnb; sc	Multiple cases involving integumentary and nerve defects were successfully reconstructed with AVFs	18.6% FTN
Nakazawa [32]	2004	4	41	20-71	n/a	L	CM	L	S; sne	Four cases of extensive contractures of the palm were successful reconstructed using large AVFs, including a sensate flap	0
Woo [33]	2007	154	35.7	16-65	112:40	HF	B; Tr	F; L; Ft; HF	S; st; sne	154 cases of AVFs were used successfully in 92.9% of cases to reconstruct upper limb defects, including 8 sensate flaps. Innervated AVFs allowed an average static two-point discrimination of 10 mm, ranging from 8 to 15 mm	7.1% FTN
Davami [34]	2012	18	30.6	15-40	18:0	HF	Tr	HF	Sne	Sensate AVFs were used successfully in 18 patients to reconstruct the dorsum of the fingers	5.6% SpN
Yan [35]	2012	27	n/a	n/a	n/a	HF	Tr	F	S; sne	Twenty-seven AVFs were successfully used in the reconstruction of finger pulp defects in 23 patients, including 15 sensate flaps and 12 insensate flaps. Almost all the flaps in the sensate group obtained normal sensation, while most cases of the insensate group only achieved protective sensation.	0
Yu [36]	2012	6	24.5	n/a	5:1	HF; Ft	B; Tr	Ft	S; sne	Five skin defects of the hands, and one defect of the dorsum of the foot were successfully reconstructed with AVFs, including a sensate flap	0
Giesen [37]	2014	14	37.1	16-58	11:3	HF	Tu; Tr; I; O	F	S; st; sne	Fourteen defects of the hand were reconstructed with AVFs including 5 innervated flaps; one of the latter suffered complete necrosis	14.2% FTN; 7.1% AR
Liu [38]	2014	11	31	17-44	7:4	HF	Tr	F	Sne	Eleven innervated AVFs were used to successfully reconstruct digital defects. In 4 cases, AVF's vascular pedicle was used to effectively revascularize fingers	0

Table 1 Summary of the studies reporting unconventional perfusion flaps including nerves for reconstructive purposes.

Legend:

n, number of patients in each series

M, male; **F**, female

AVF, arterialized venous flap

Defect location and flap donor site: F, forearm; L, leg; Ft, foot; HN, head and neck; HF, hand and fingers; T, thigh.

Defect origin: B, burn and its sequelae; I, infection; CM, congenital malformation; SC, scar contracture; Tr, trauma; Tu, tumor; O, others.

Flap composition: nv, nerve and vein; s, skin with its appendages and subcutaneous tissue; sb, skin and bone; sc, skin and cartilage; sne, skin and nerve; st, skin and tendon; stnb, skin, tendon, nerve and bone.

Complications: AR, anastomosis revision; FTN, full thickness necrosis; I, infection; MN, marginal necrosis; SpN, superficial necrosis.

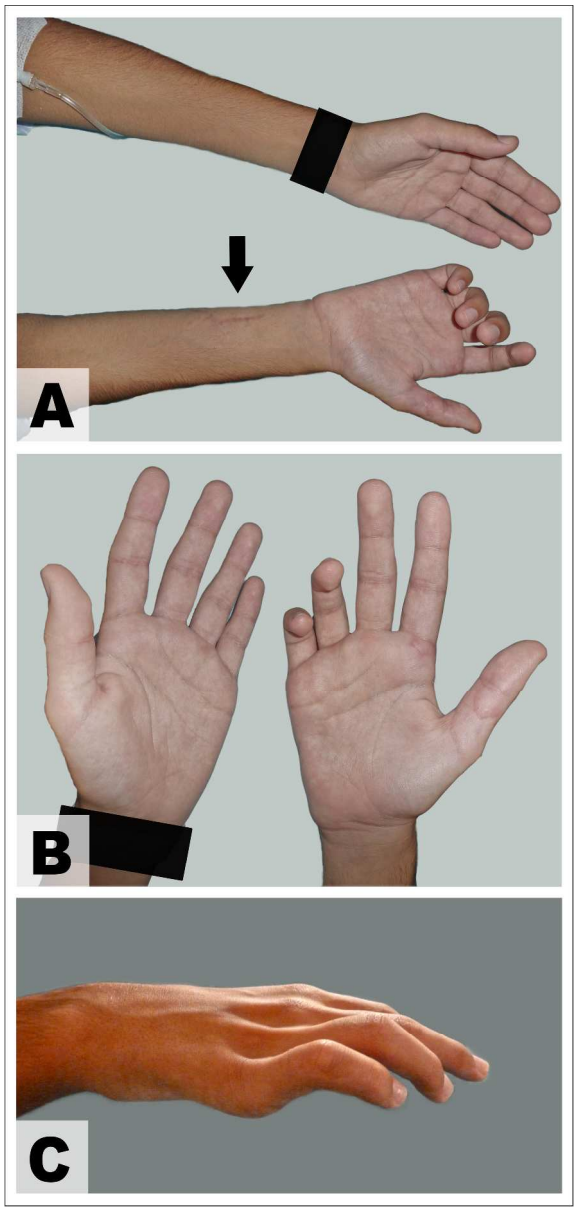

Figure 1. Photographs showing the preoperative appearance.
A. A scar in the medial aspect of the distal third of the right forearm was visible (arrow) corresponding to the site of injury.
B. Comparison of the hands showed marked atrophy of the right hand intrinsic muscles, particularly in the medial palmar region.
C. An ulnar claw was evident due to atrophy of the intrinsic muscles supplied by the ulnar nerve.

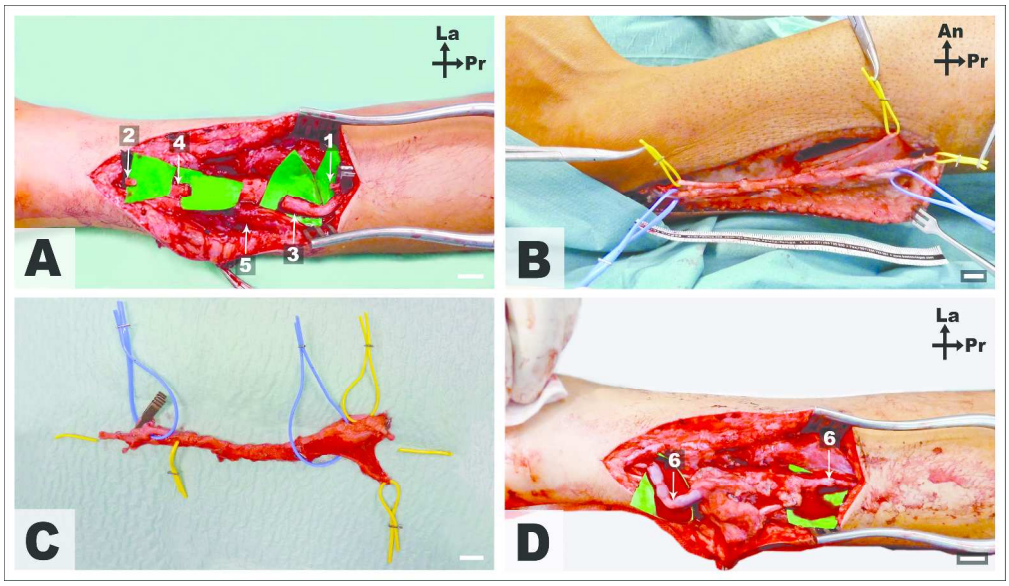

Figure 2. Photographs of the surgery.
Scale bar = 1 cm
Pr, Proximal; Lat, Lateral; An, Anterior
1, Proximal stump of the ulnar artery; 2, Distal stump of the ulnar artery; 3, Proximal stump of the ulnar nerve; 4, Distal stump of the ulnar nerve; 5, Flexor carpis ulnaris muscle.
The yellow vessel loops were placed around two terminal branches of the sural nerve. The blue vessel loops were placed around the lesser saphenous vein.
A, Intraoperative view of the ulnar neurovascular bundle after removing the fibrotic tissue and the proximal stump neuroma; B, View of the lesser saphenous/sural neurovenous flap in situ after dissection; C, Detailed ex vivo view of the lesser saphenous/sural neurovenous flap prior to insetting into the defect; D, View of the arterialized neurovenous flap after insetting the flap and performing the neural and vascular anastomoses.

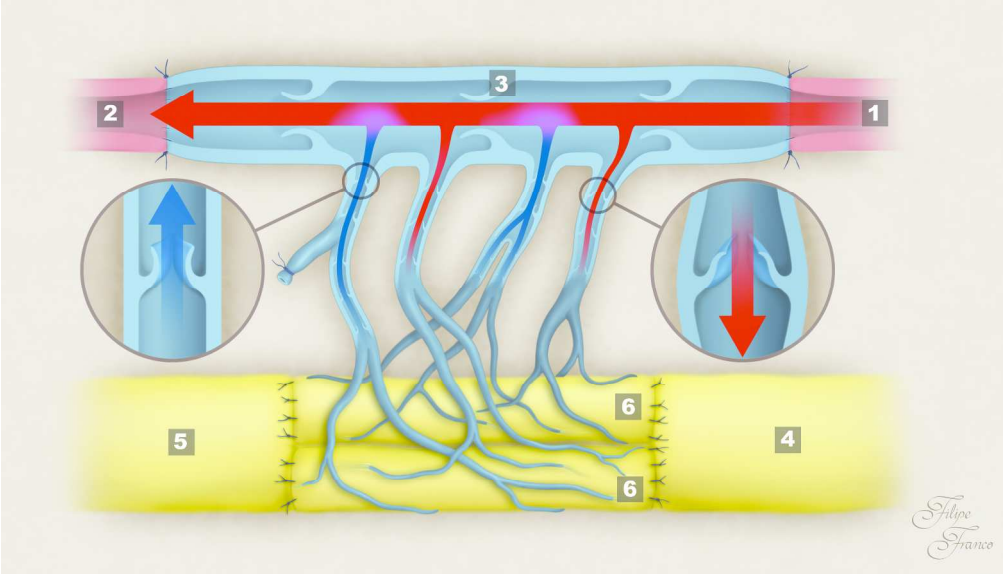

Figure 3. Schematic representation of the composition and vascular architecture of the lesser saphenous/sural neurovenous flap used to bridge the long arterial and nerve defect. The arrows indicate the direction of blood flow.
1, Proximal segment of the ulnar artery; 2, Distal segment of the ulnar artery; 3, Lesser saphenous vein in an inverted position used to bridge the vascular gap; 4, Proximal stump of the ulnar nerve; 5, Distal stump of the ulnar nerve; 6, Sural nerve cables used for the somatotopic reconstruction of the ulnar nerve.

322x185mm (300 x 300 DPI)

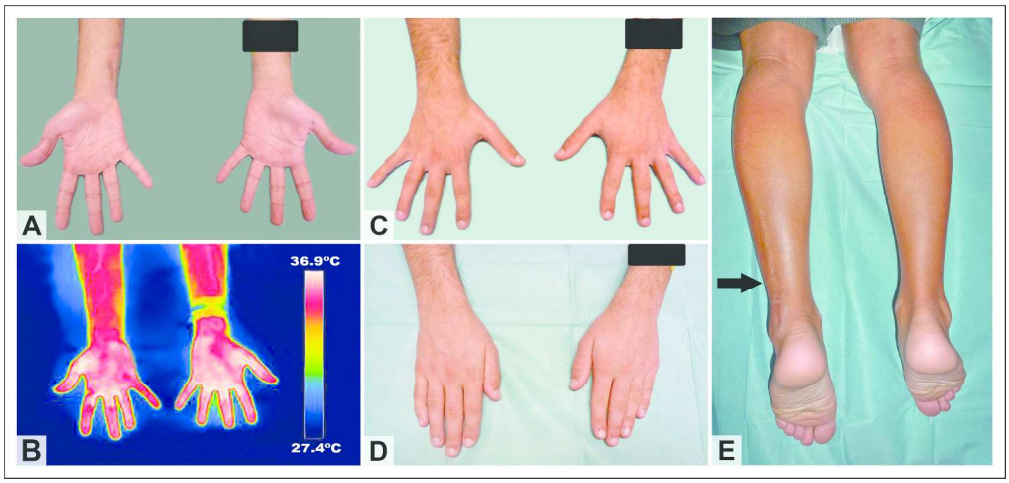

Figure 4. Appearance of the recipient and donor zones two years after surgery.
A. Anterior view of the distal aspect of the upper limbs showed no evidence of atrophy of hand muscles.
B. Infra-red thermography of the anterior aspect of the forearms and hands showed good perfusion of the ulnar aspect of the right hand.
C. Posterior view of the forearms and hands showed absence of ulnar claw in the right hand, as well as good finger abduction.
D. Posterior view of the hands demonstrated adequate finger adduction.
E. Posterior view of the lower legs and feet showed a relatively inconspicuous scar in the donor zone (arrow), as well as absence of limb edema.

286x135mm (300 x 300 DPI)